Physics-based rendering and its applications in computational photography and imaging

Adithya Pediredla

Dartmouth College

adithya.k.pediredla@dartmouth.com

Ioannis Gkioulekas

Carnegie Mellon University

igkioule@andrew.cmu.edu

computer vision

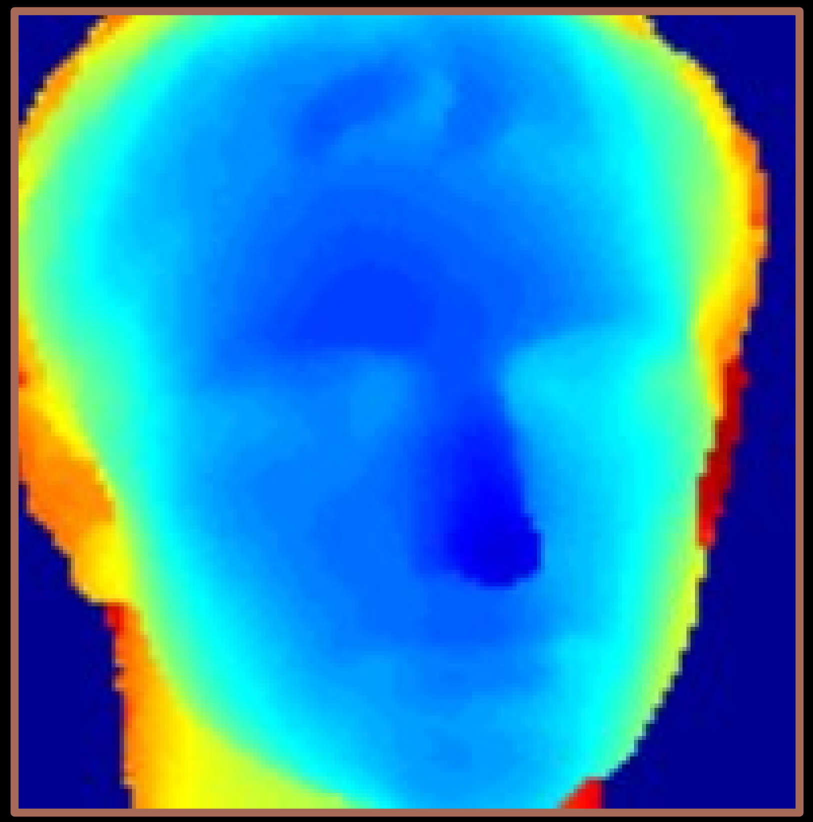

computer graphics

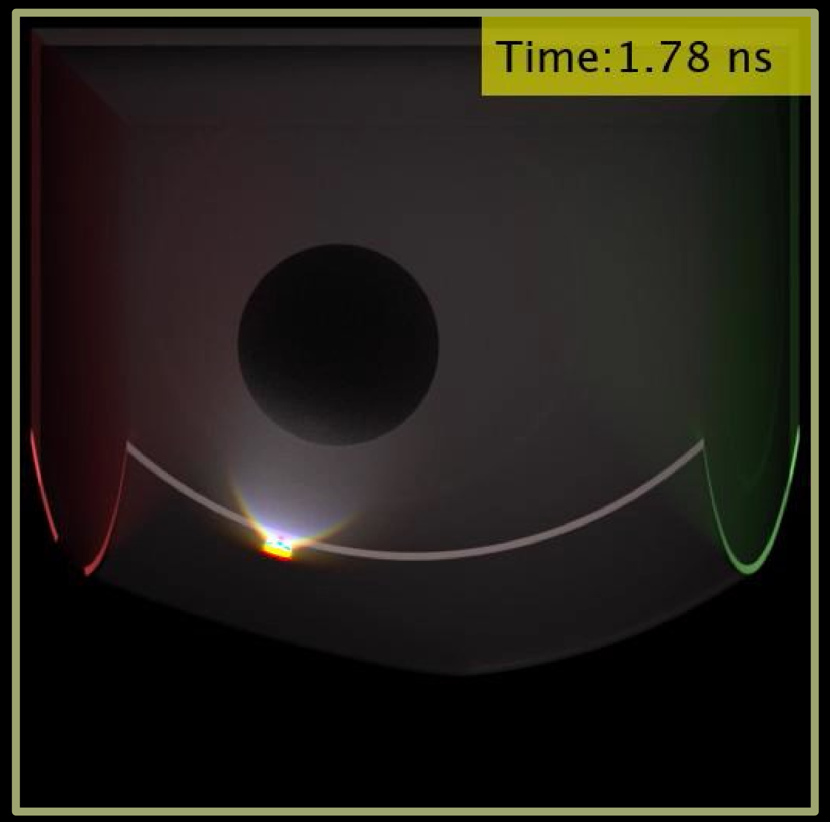

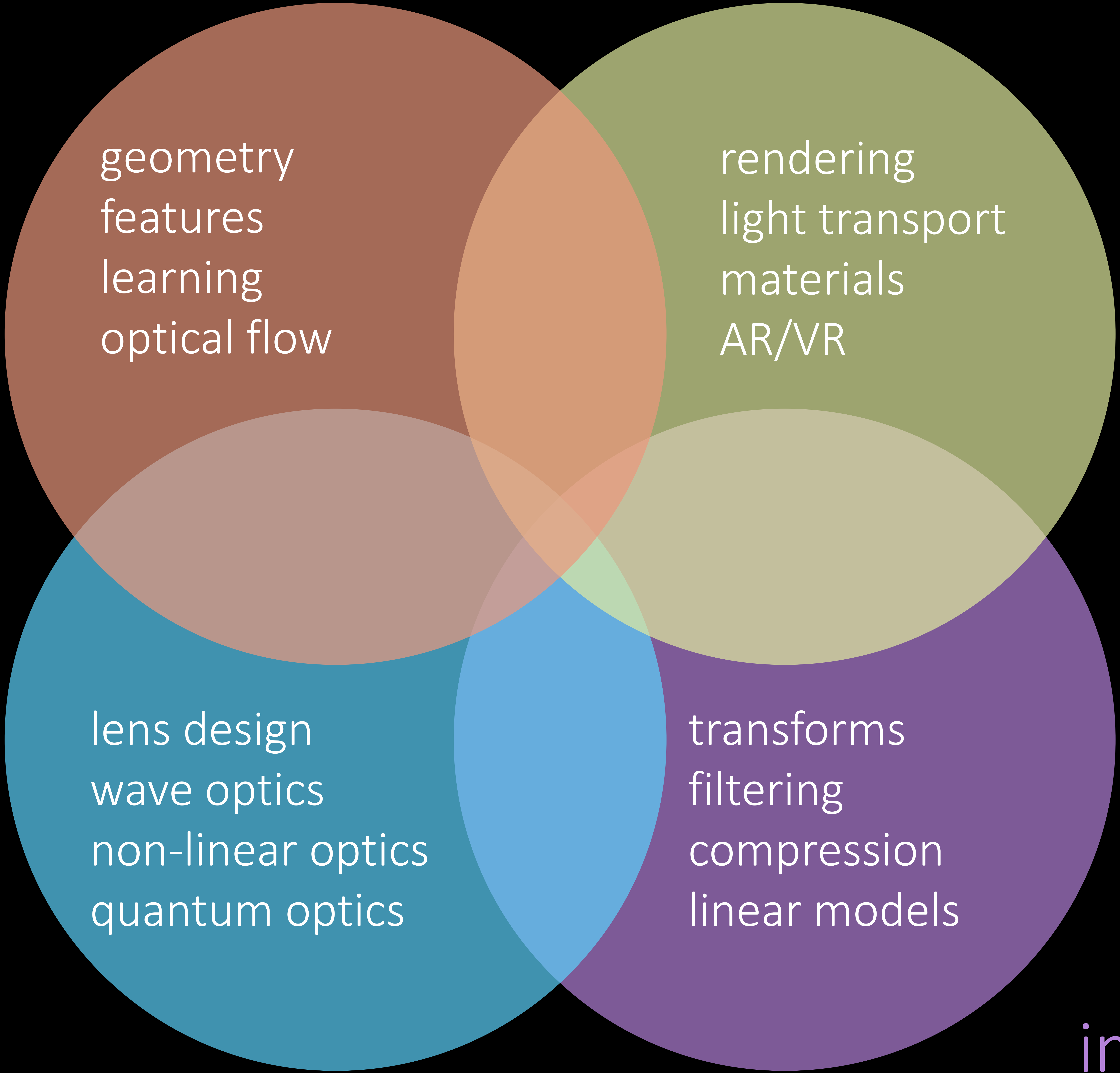

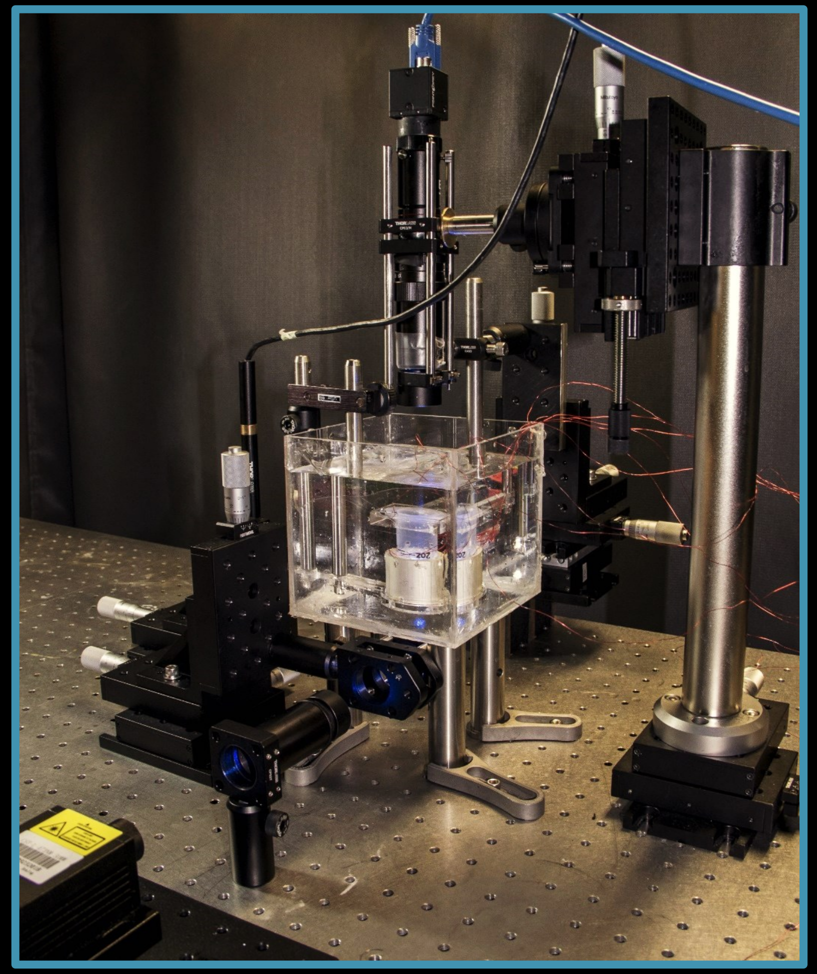

optics

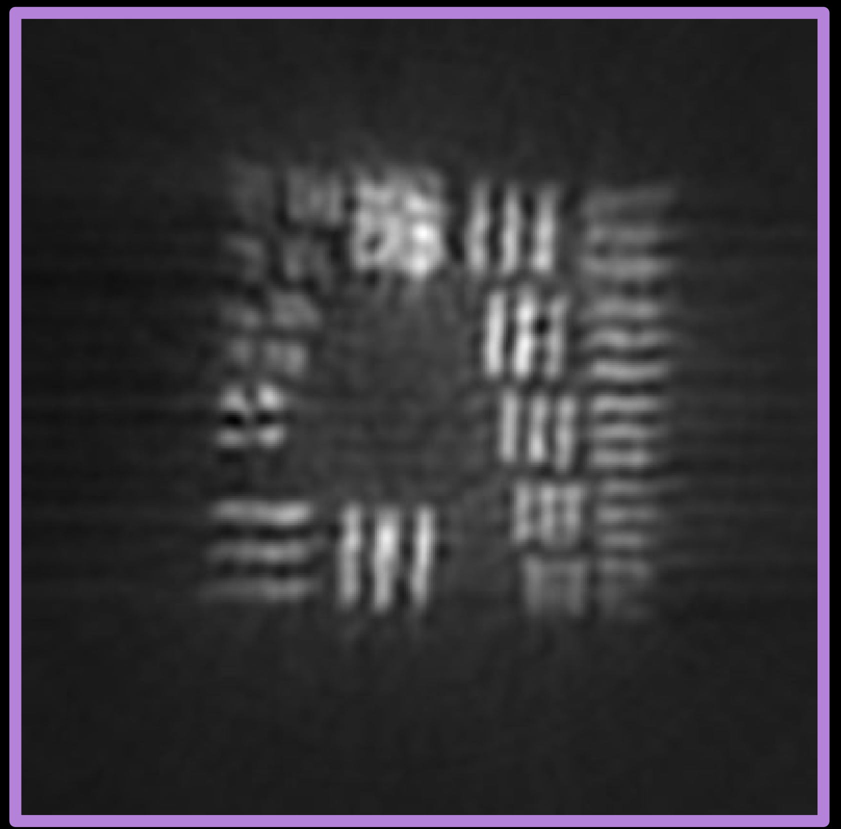

image processing


computer vision
computer graphics
Time:1.78 ns
geometry
features
learning
optical flow
rendering
light transport
materials
AR/VR
computational imaging
lens design
wave optics
non-linear optics
quantum optics
transforms
filtering
compression
linear models
optics
image processing


computer vision
computer graphics
geometry
features
learning
optical flow
rendering
light transport
materials
AR/VR
Time:1.78 ns
computational imaging
lens design
wave optics
non-linear optics
quantum optics
transforms
filtering
compression
linear models
optics
image processing


computer vision
geometry
features
learning
optical flow
computer graphics
rendering
light transport
materials
AR/VR
Time:1.78 ns
computational imaging
optics
lens design
wave optics
non-linear optics
quantum optics
image processing
transforms
filtering
compression
linear models

Physics-based rendering and its applications to computational imaging

Physics-based rendering and its applications to computational imaging

forward rendering

- accurate and efficient simulation
- virtually design sensors, optics, and algorithms

Physics-based rendering and its applications to computational imaging

forward rendering

- accurate and efficient simulation
- virtually design sensors, optics, and algorithms

inverse rendering

- accurate and efficient differentiable simulation
- tractably solve general inverse problems

Physics-based rendering and its applications to computational imaging

forward rendering

- accurate and efficient simulation
- virtually design sensors, optics, and algorithms

inverse rendering

- accurate and efficient differentiable simulation
- tractably solve general inverse problems

Physics-based rendering and its applications to computational imaging

forward rendering

- accurate and efficient simulation
- virtually design sensors, optics, and algorithms

inverse rendering

- accurate and efficient differentiable simulation
- tractably solve general inverse problems

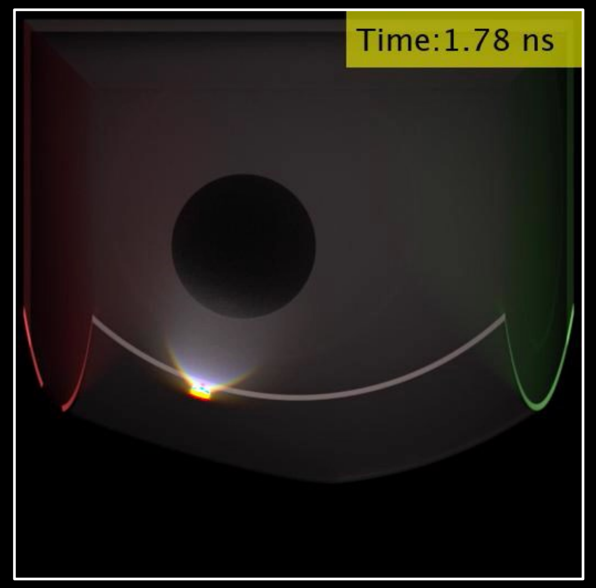

time-of-flight imaging

Physics-based rendering and its applications to computational imaging

forward rendering

- accurate and efficient simulation
- virtually design sensors, optics, and algorithms

inverse rendering

- accurate and efficient differentiable simulation
- tractably solve general inverse problems

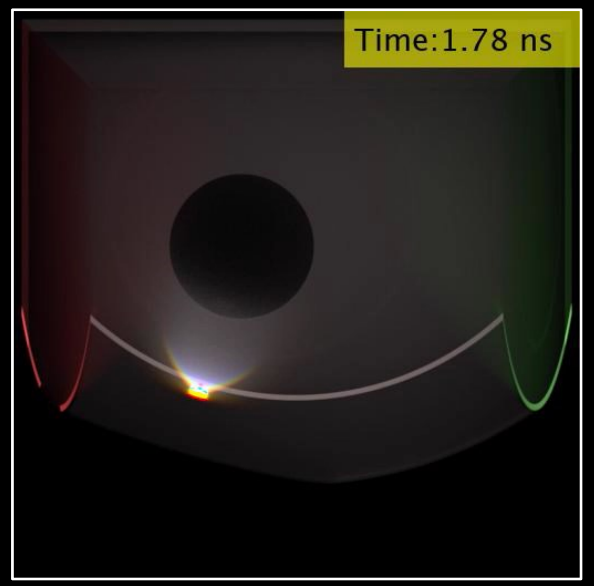

time-of-flight imaging

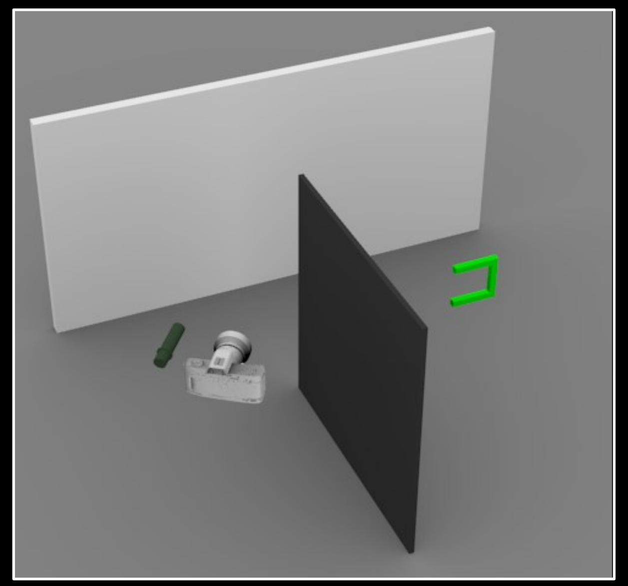

non-line-of-sight imaging

Physics-based rendering and its applications to computational imaging

forward rendering

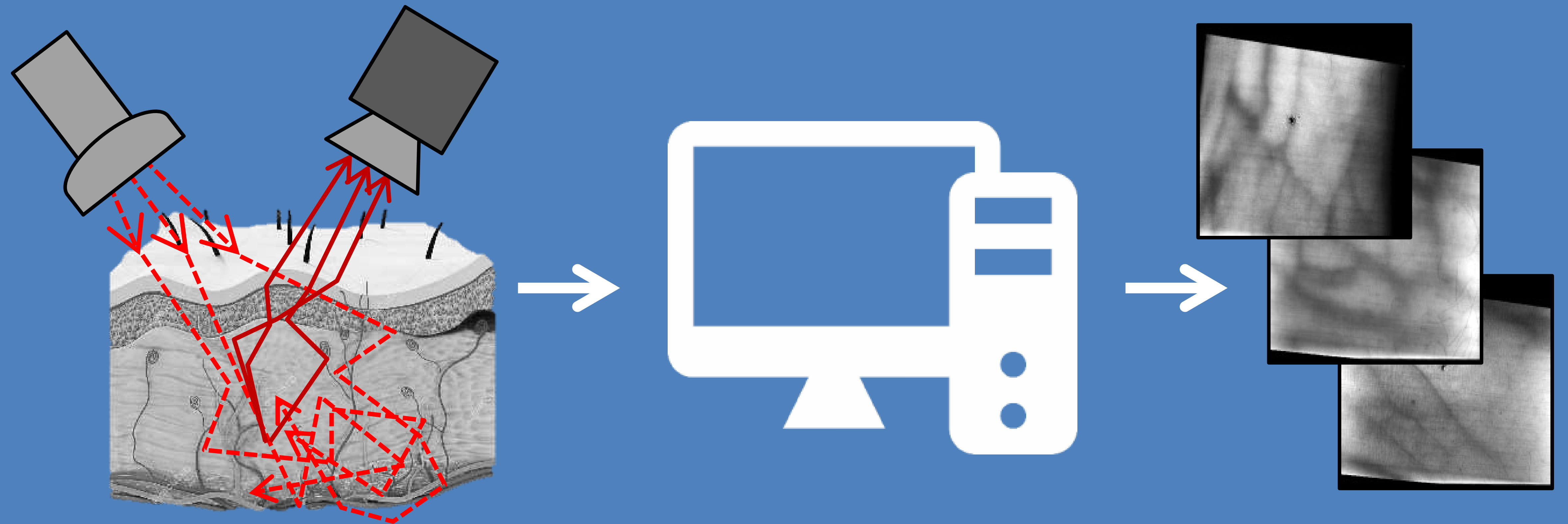

- accurate and efficient simulation
- virtually design sensors, optics, and algorithms

inverse rendering

- accurate and efficient differentiable simulation
- tractably solve general inverse problems

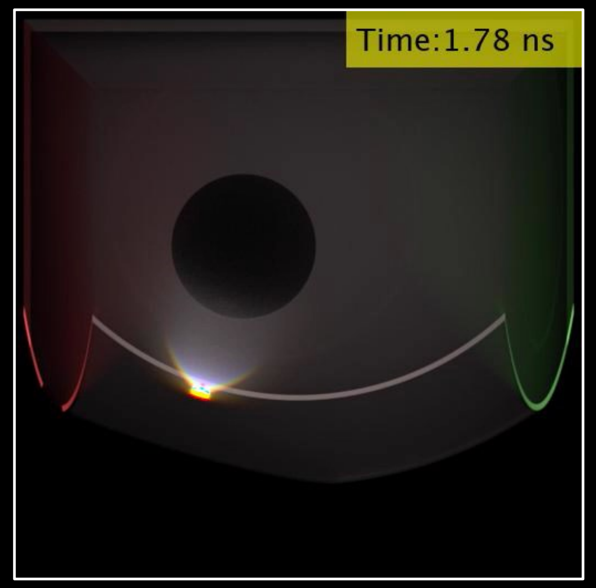

time-of-flight imaging

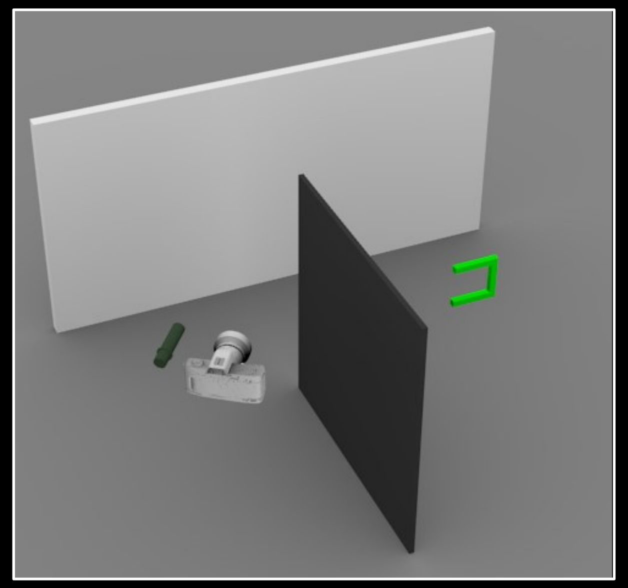

non-line-of-sight imaging

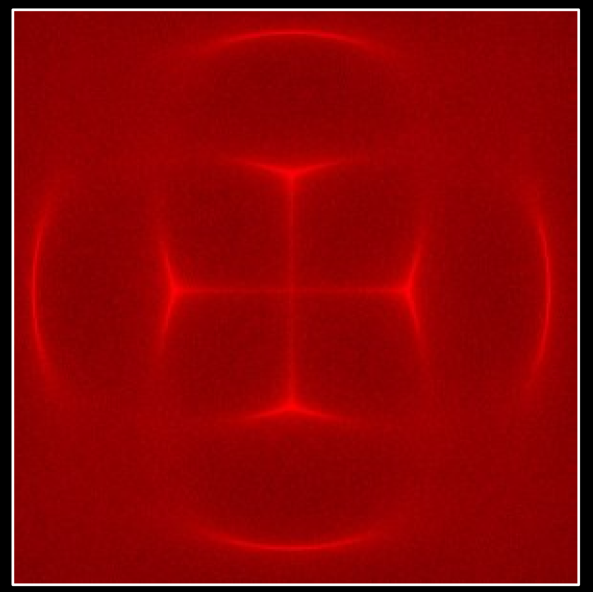

acousto-optic lensing

Physics-based rendering and its applications to computational imaging

forward rendering

- accurate and efficient simulation
- virtually design sensors, optics, and algorithms

inverse rendering

- accurate and efficient differentiable simulation
- tractably solve general inverse problems

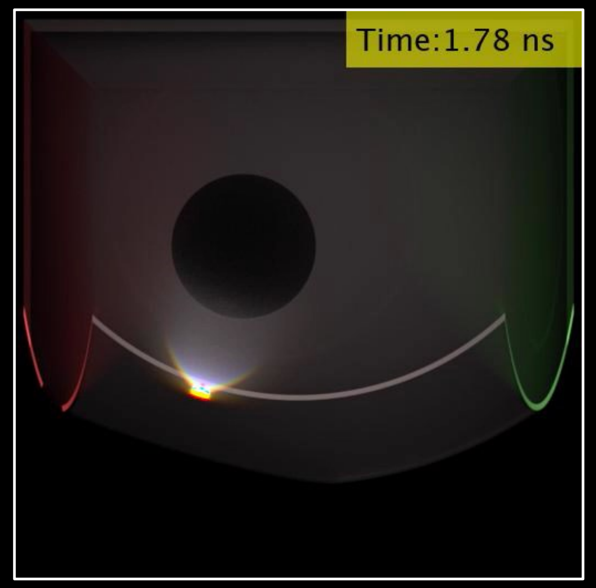

time-of-flight imaging

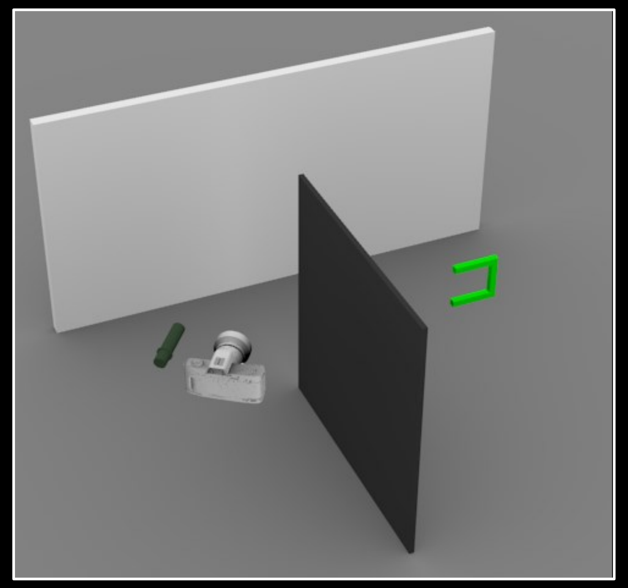

non-line-of-sight imaging

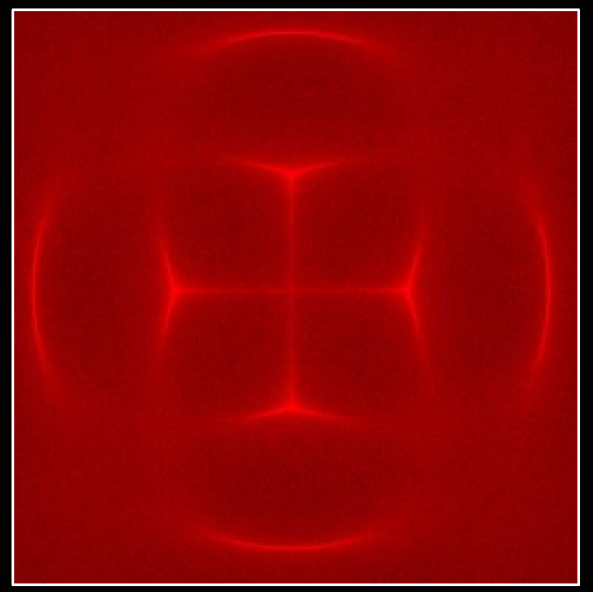

acousto-optic lensing

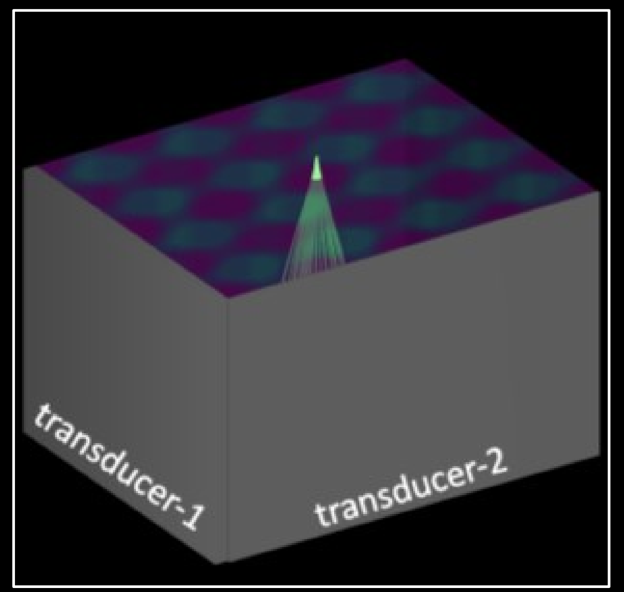

ultrafast light scanning

Physics-based rendering and its applications to computational imaging

forward rendering

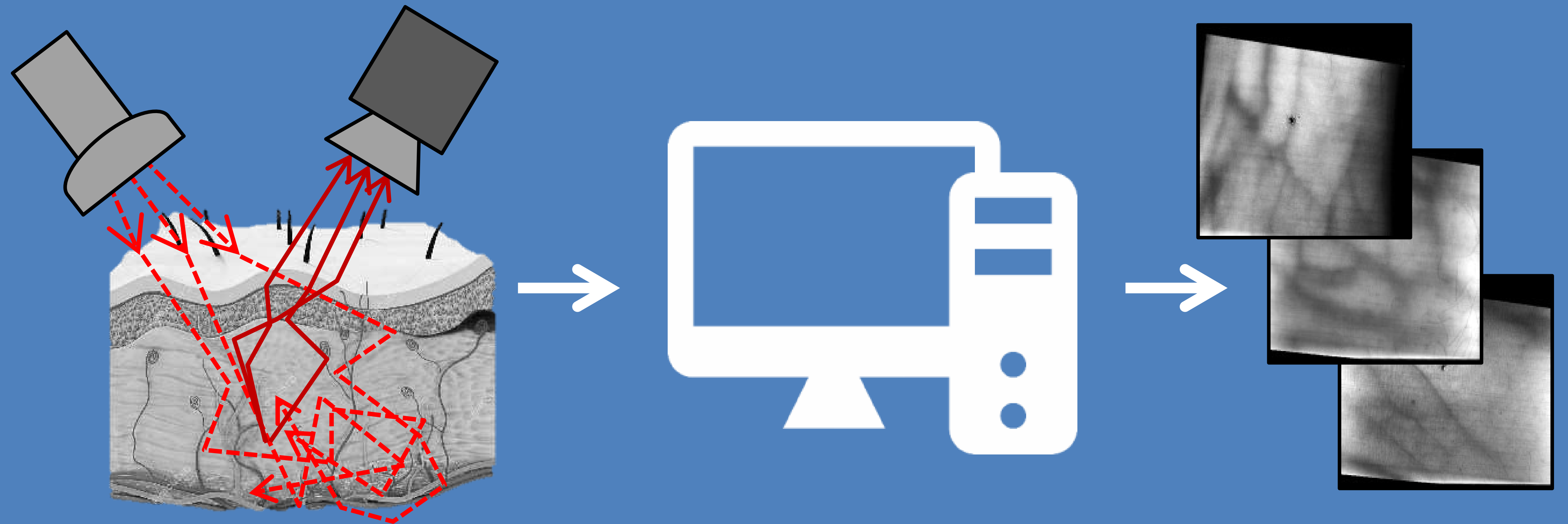

- accurate and efficient simulation
- virtually design sensors, optics, and algorithms

inverse rendering

- accurate and efficient differentiable simulation
- tractably solve general inverse problems

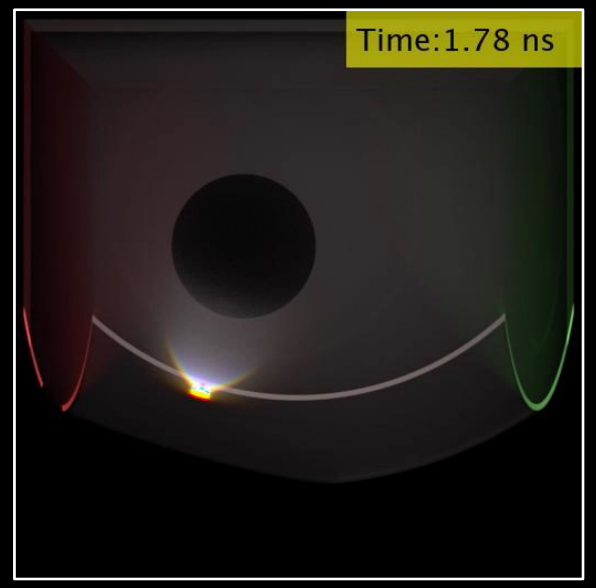

time-of-flight imaging

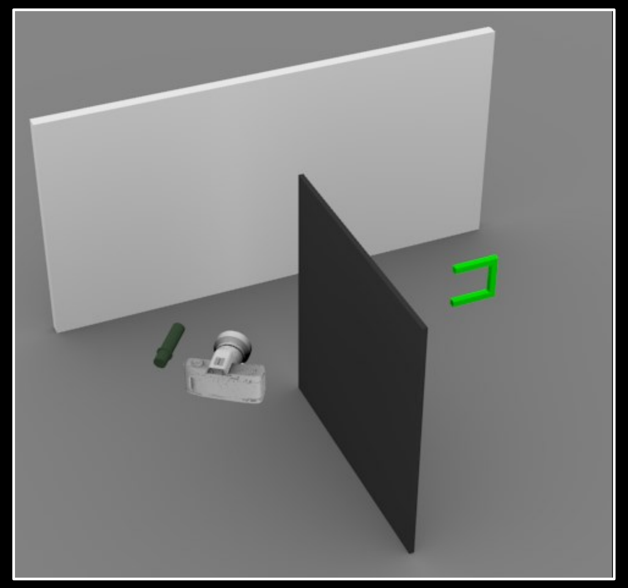

non-line-of-sight imaging

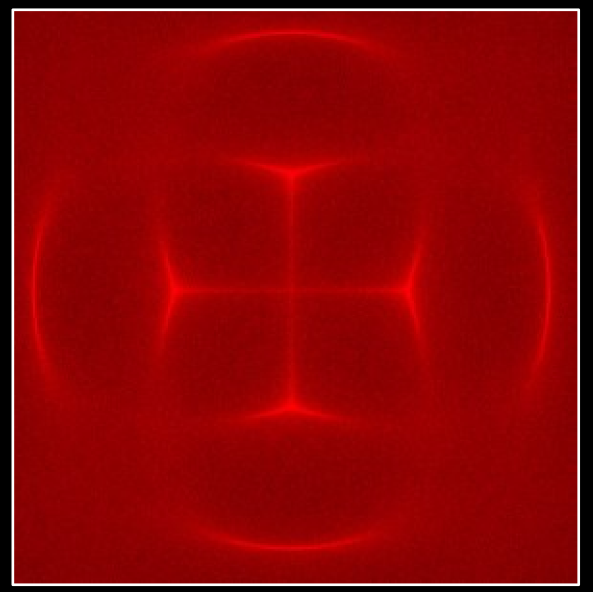

acousto-optic lensing

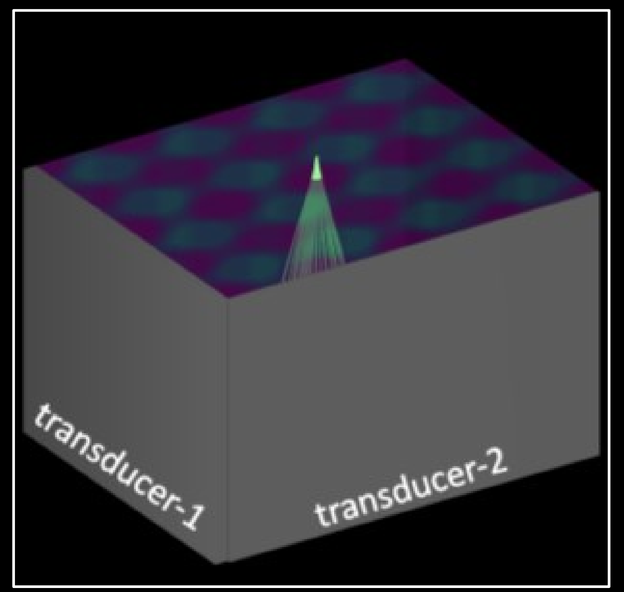

ultrafast light scanning

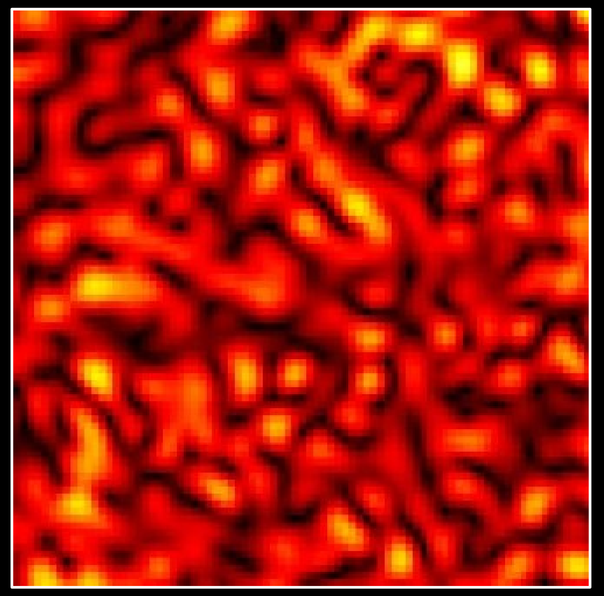

speckle imaging

Physics-based rendering and its applications to computational imaging

forward rendering

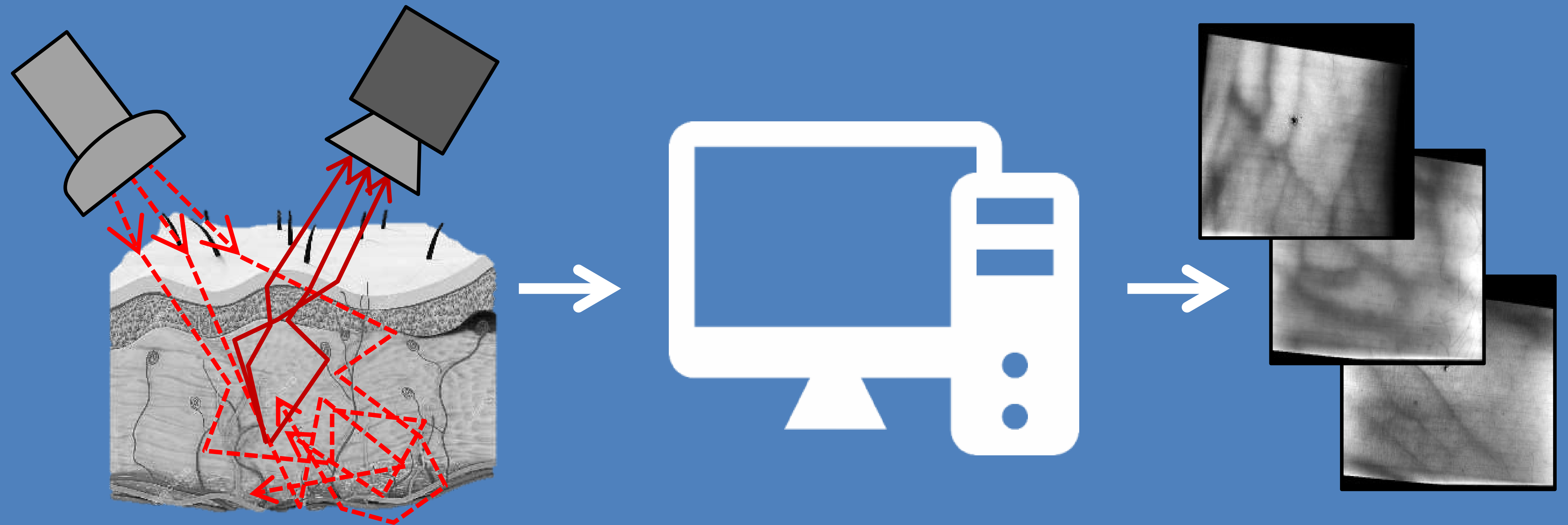

- accurate and efficient simulation
- virtually design sensors, optics, and algorithms

inverse rendering

- accurate and efficient differentiable simulation
- tractably solve general inverse problems

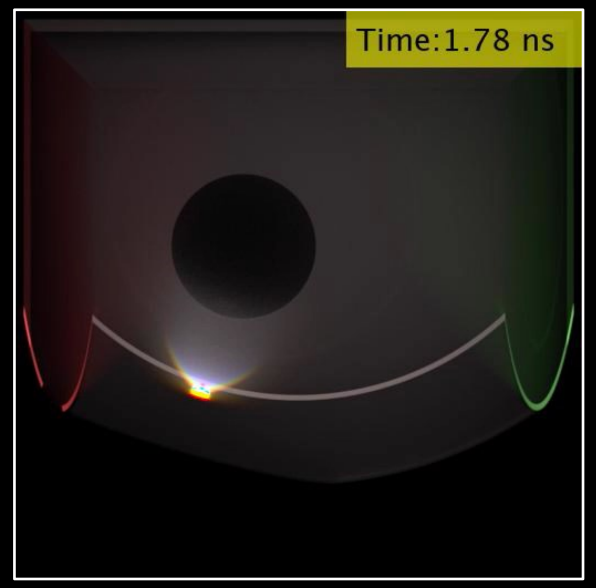

time-of-flight imaging

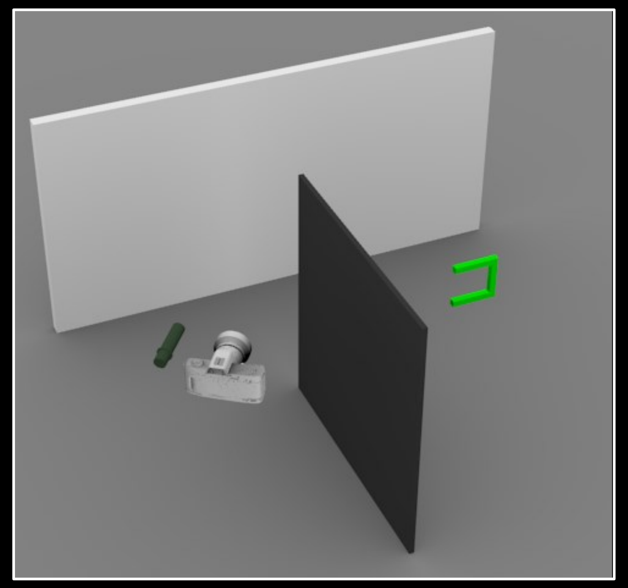

non-line-of-sight imaging

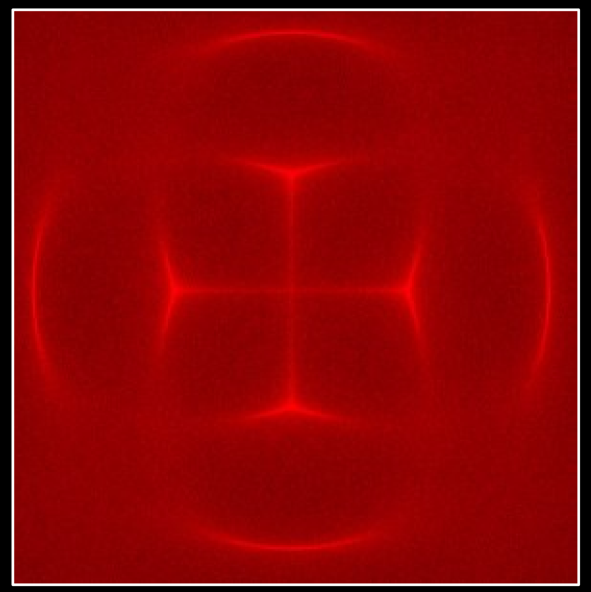

acousto-optic lensing

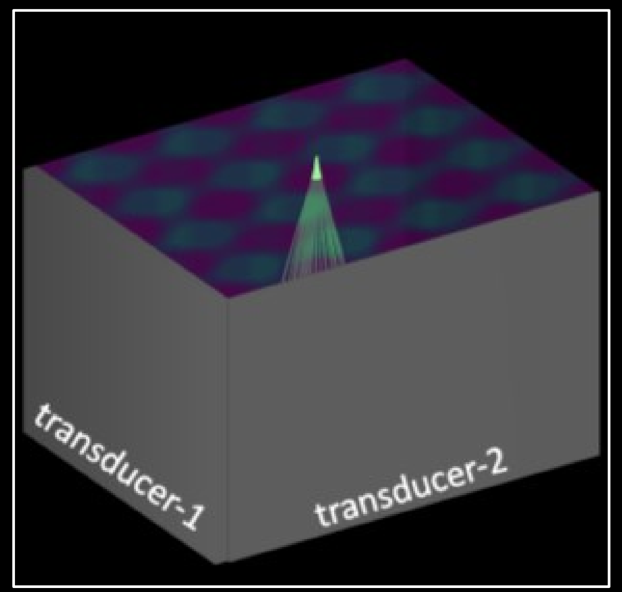

ultrafast light scanning

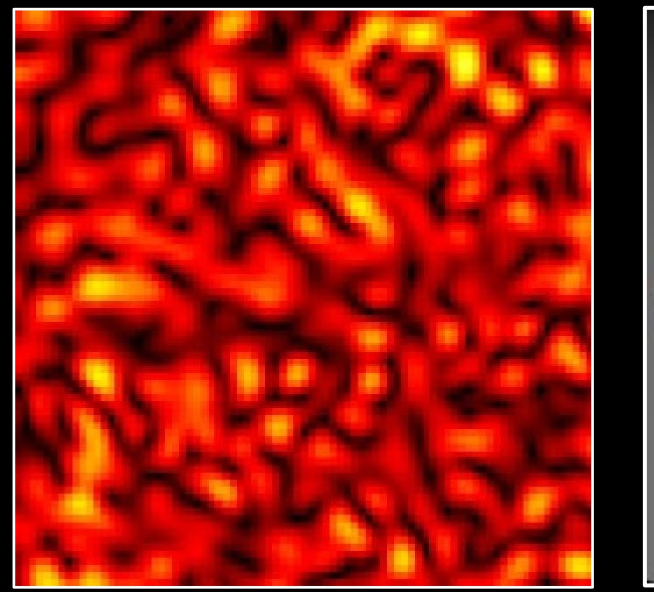

speckle imaging

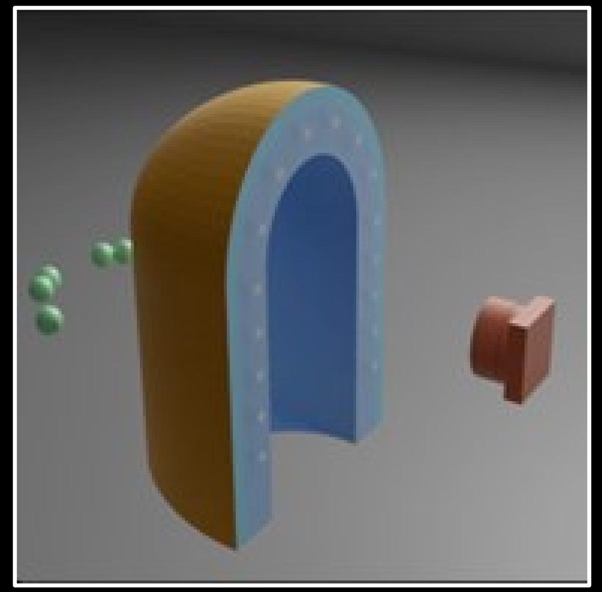

tactile sensor design

Physics-based rendering and its applications to computational imaging

forward rendering

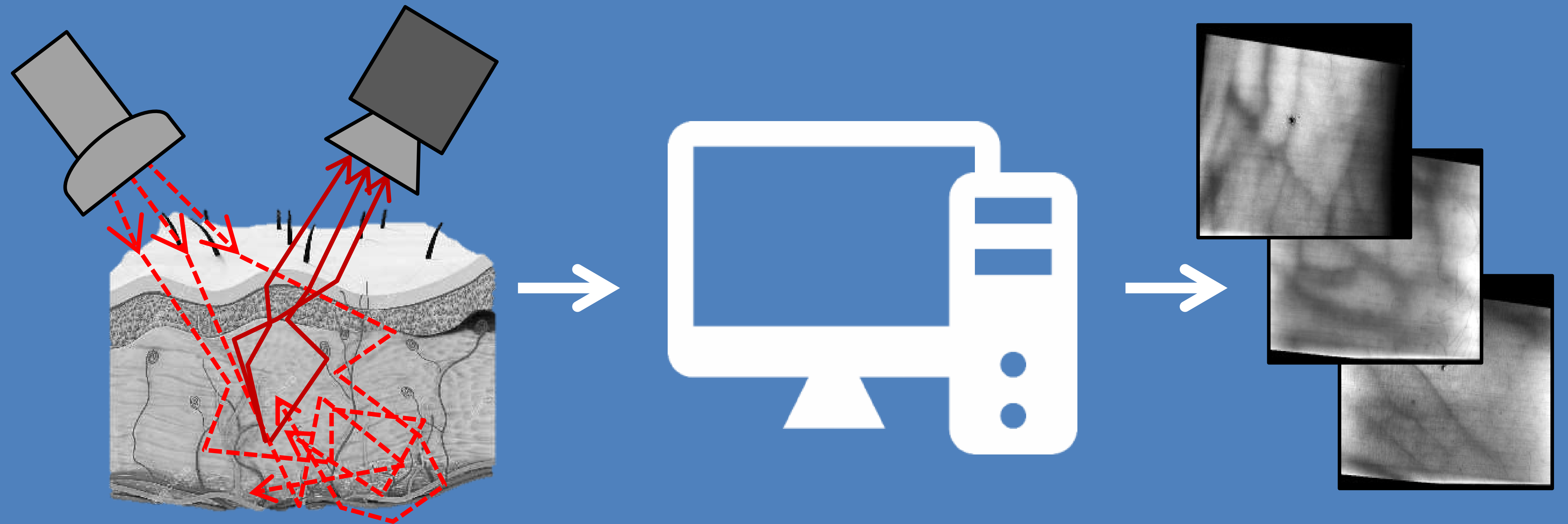

- accurate and efficient simulation
- virtually design sensors, optics, and algorithms

inverse rendering

- accurate and efficient differentiable simulation
- tractably solve general inverse problems

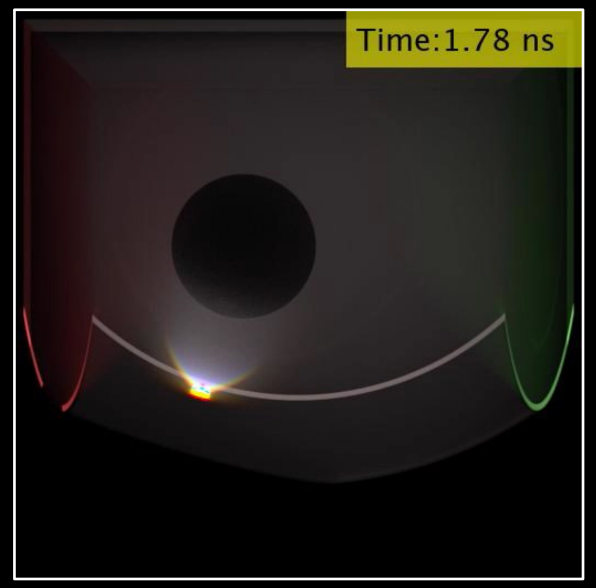

time-of-flight imaging

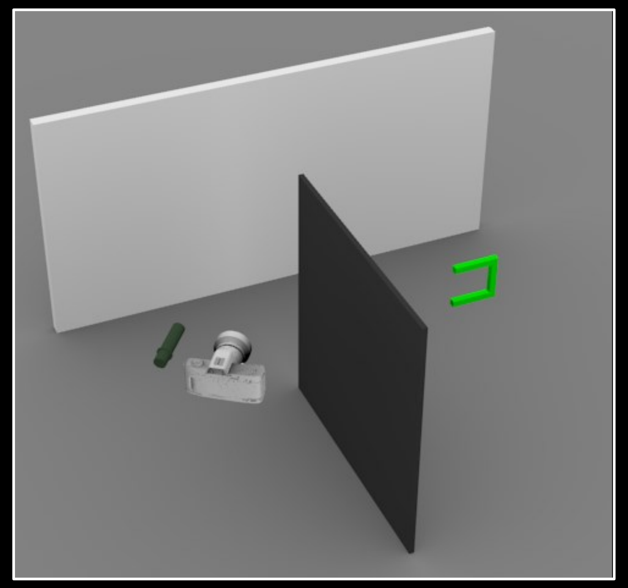

non-line-of-sight imaging

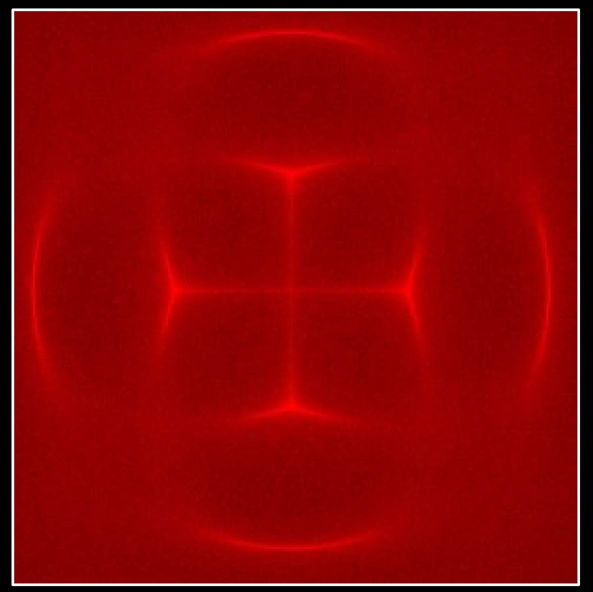

acousto-optic lensing

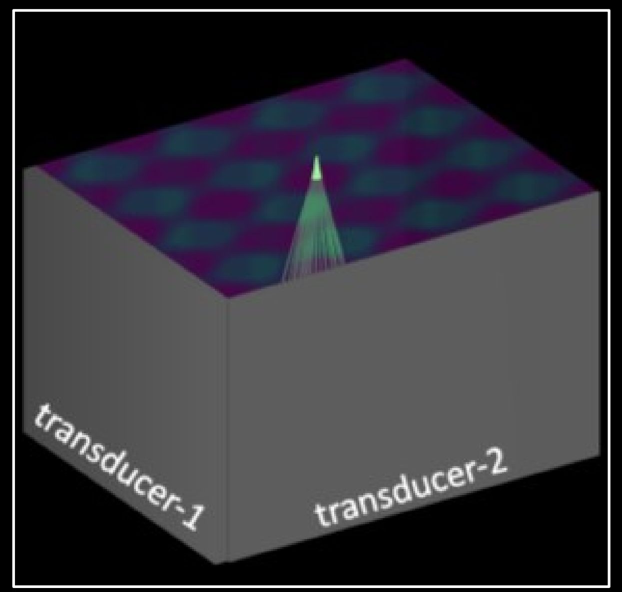

ultrafast light scanning

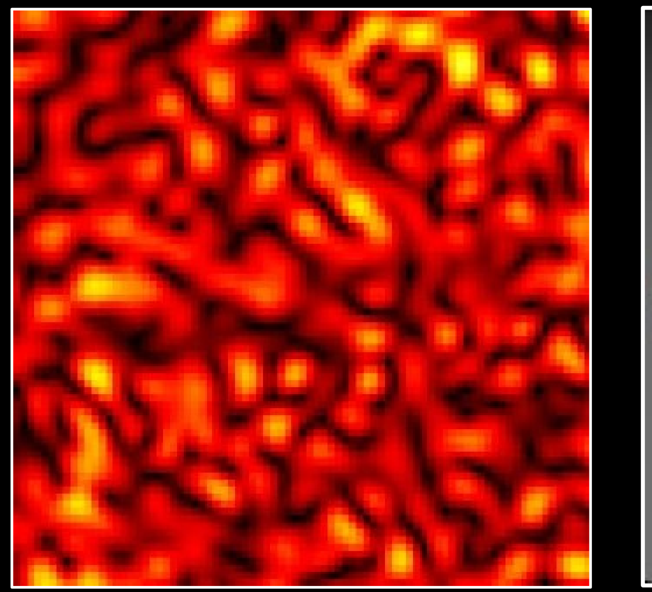

speckle imaging

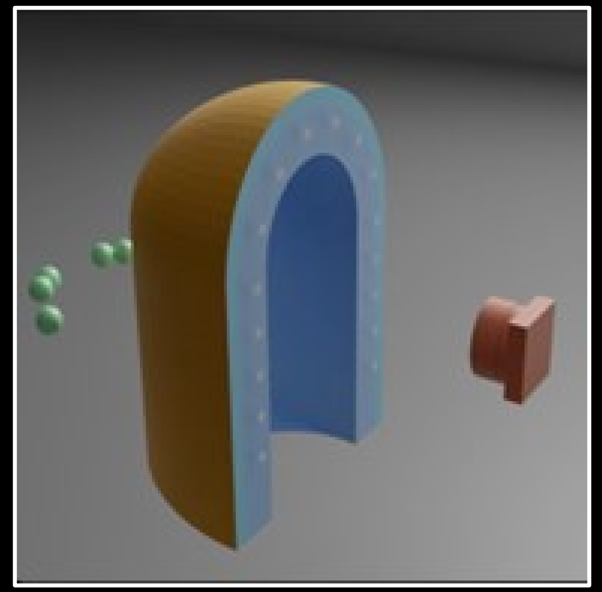

tactile sensor design

Physics-based rendering and its applications to computational imaging

forward rendering

- accurate and efficient simulation
- virtually design sensors, optics, and algorithms

inverse rendering

- accurate and efficient differentiable simulation
- tractably solve general inverse problems

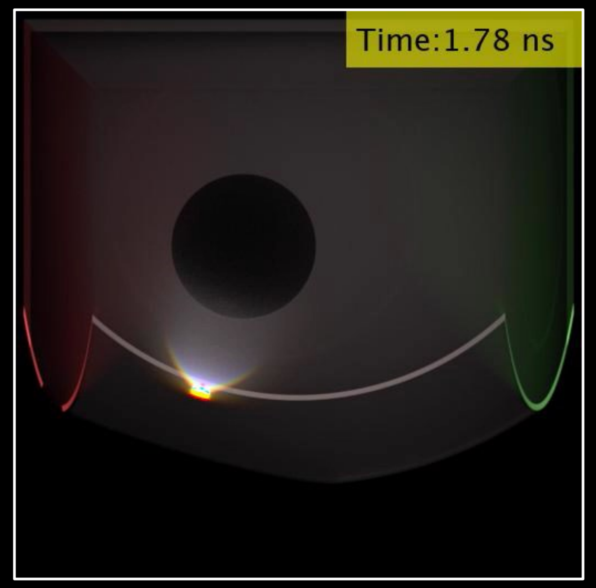

time-of-flight imaging

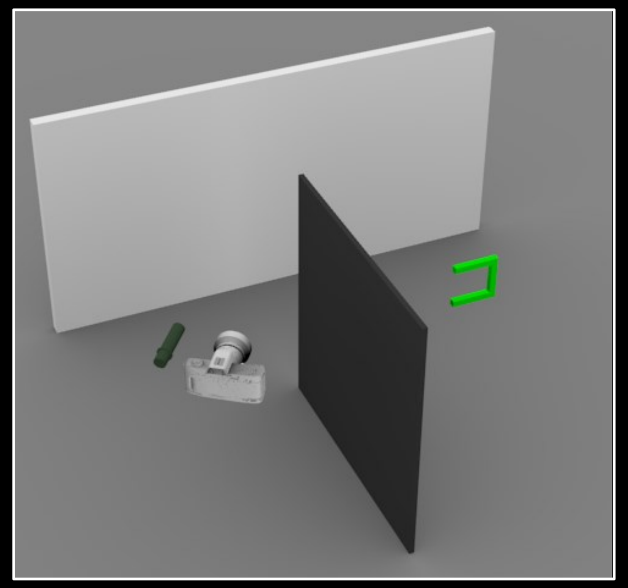

non-line-of-sight imaging

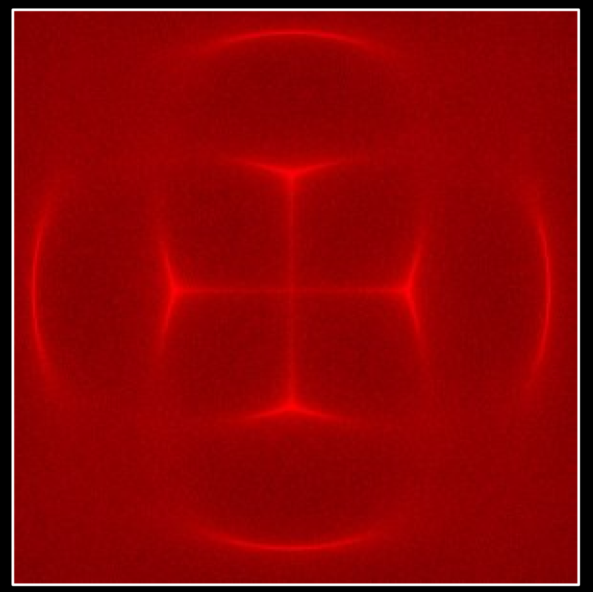

acousto-optic lensing

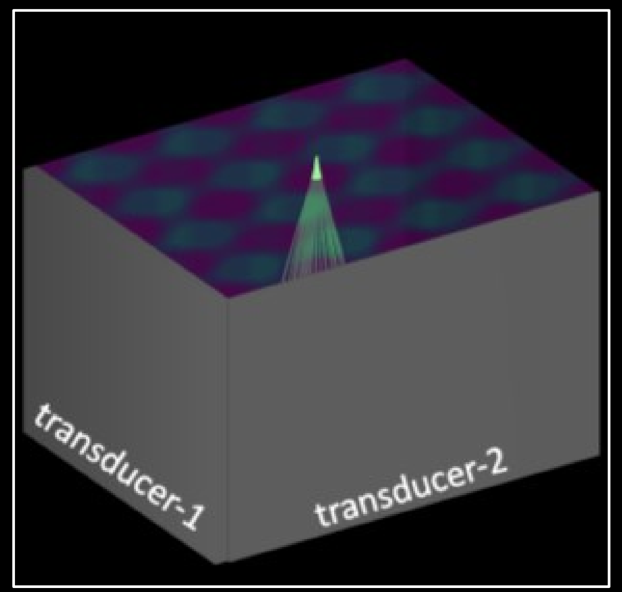

ultrafast light scanning

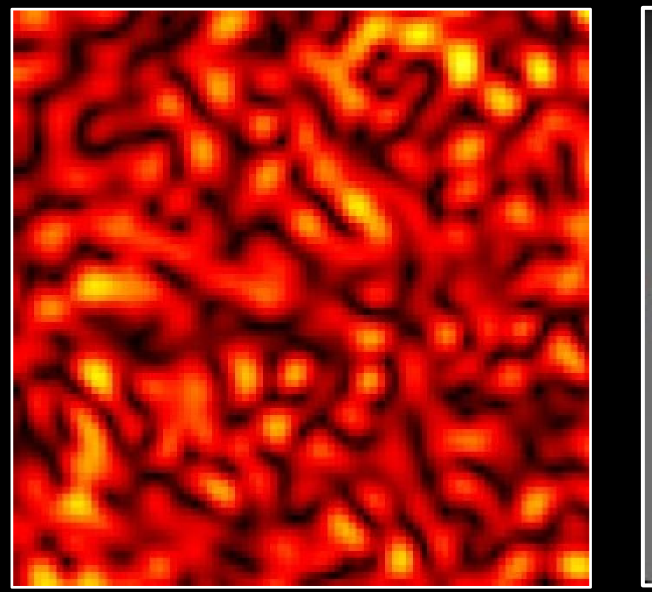

speckle imaging

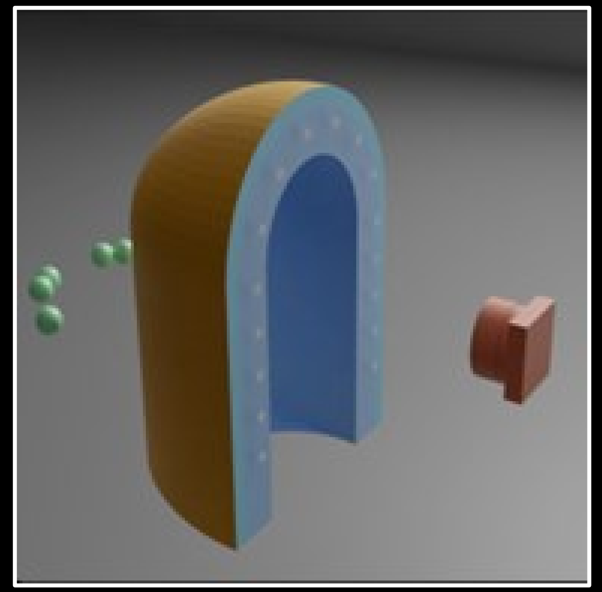

tactile sensor design

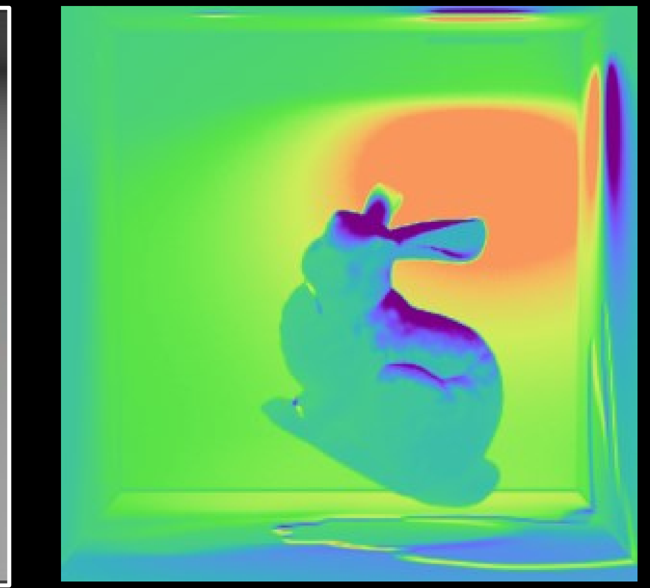

differentiable rendering

Physics-based rendering and its applications to computational imaging

forward rendering

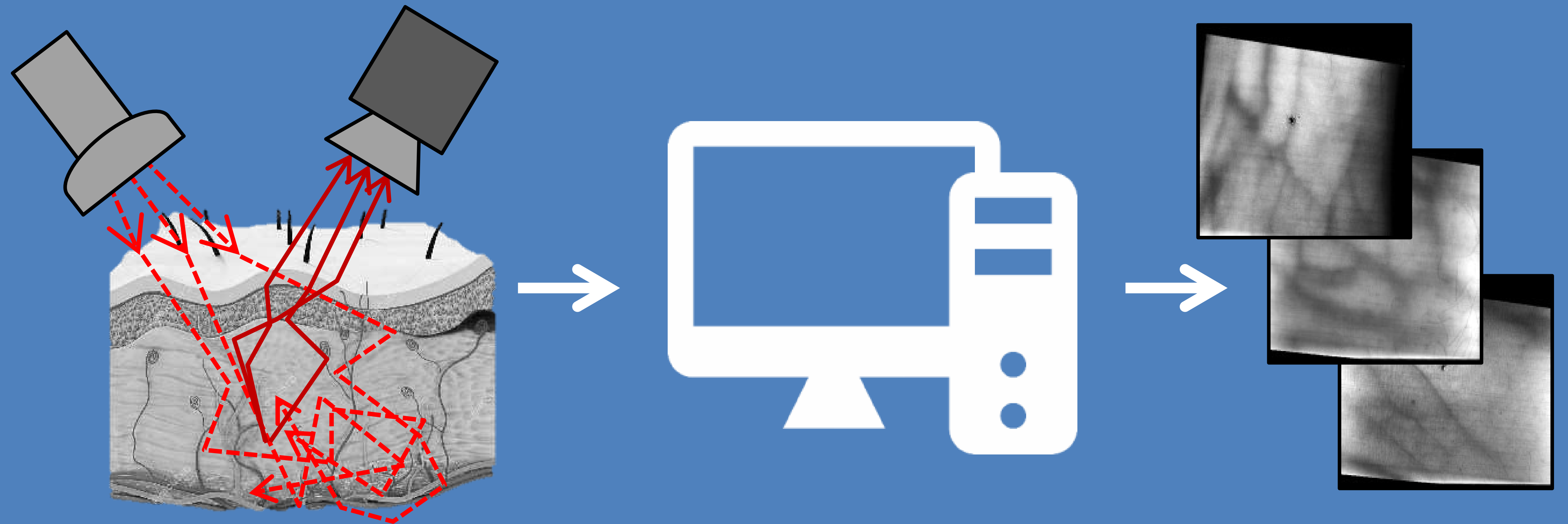

- accurate and efficient simulation
- virtually design sensors, optics, and algorithms

inverse rendering

- accurate and efficient differentiable simulation
- tractably solve general inverse problems

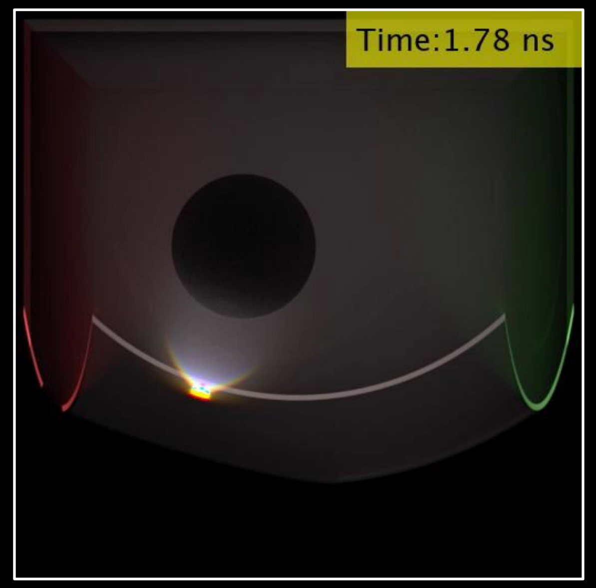

time-of-flight imaging

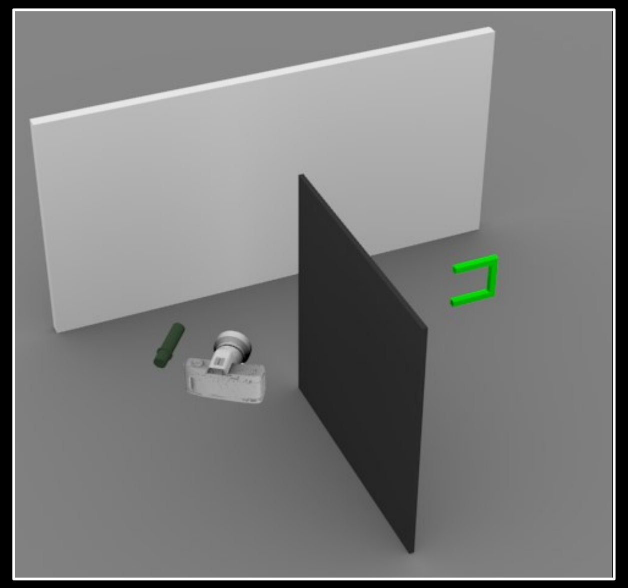

non-line-of-sight imaging

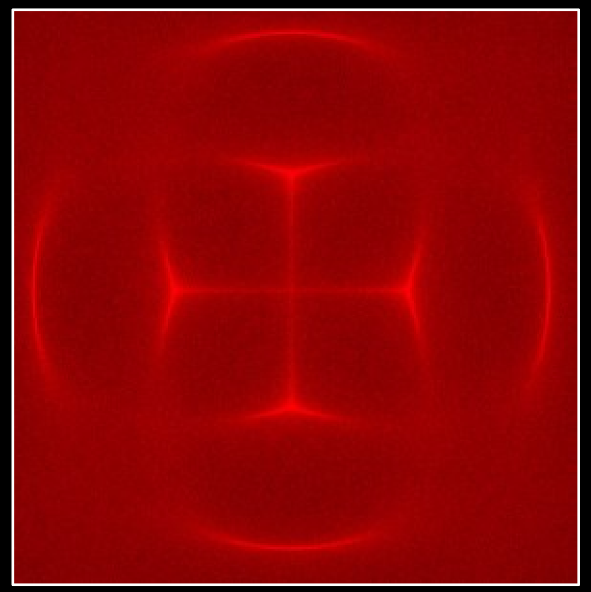

acousto-optic lensing

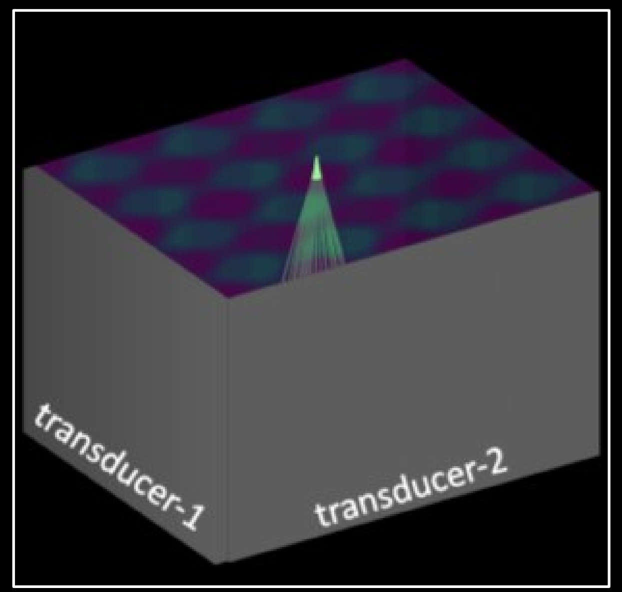

ultrafast light scanning

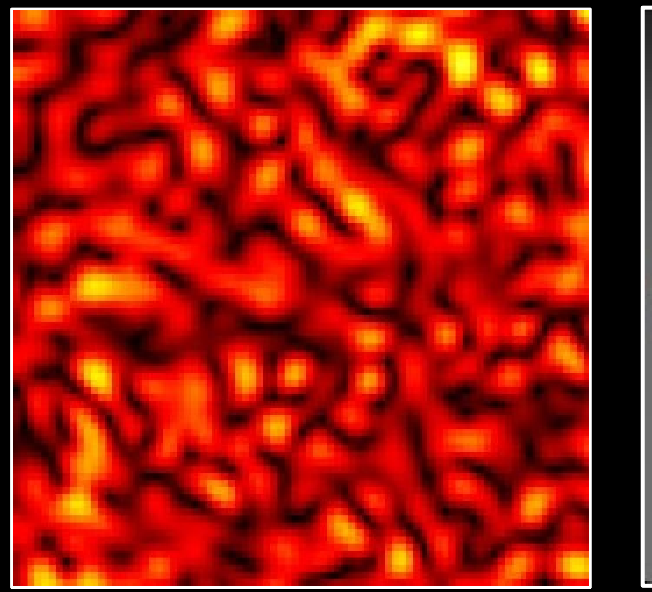

speckle imaging

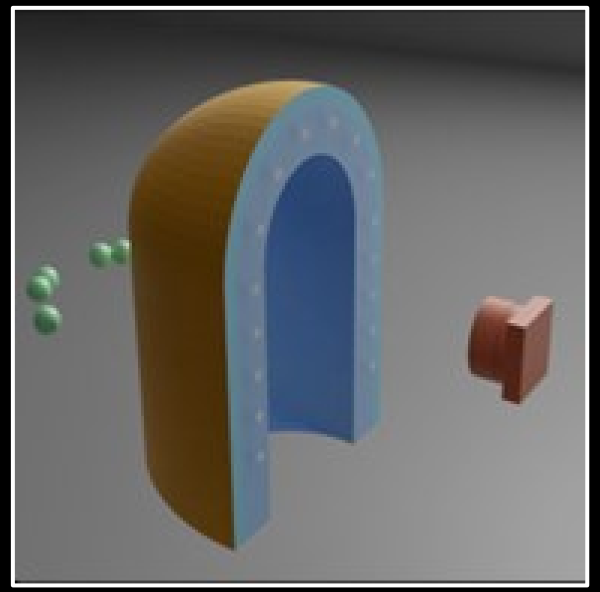

tactile sensor design

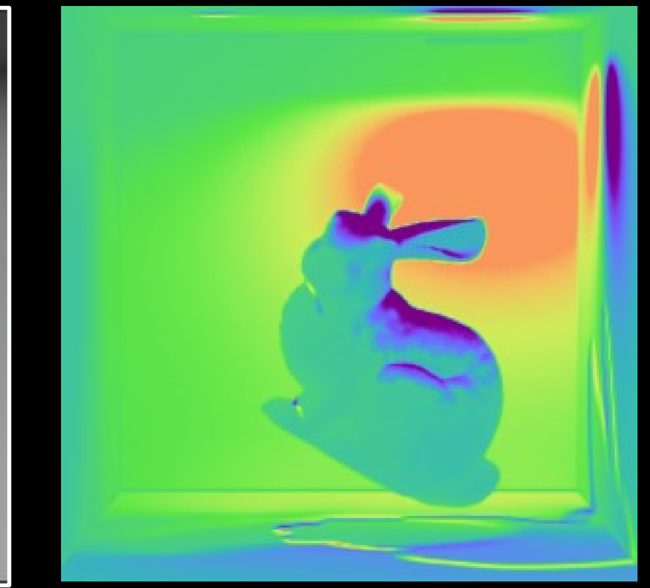

differentiable rendering

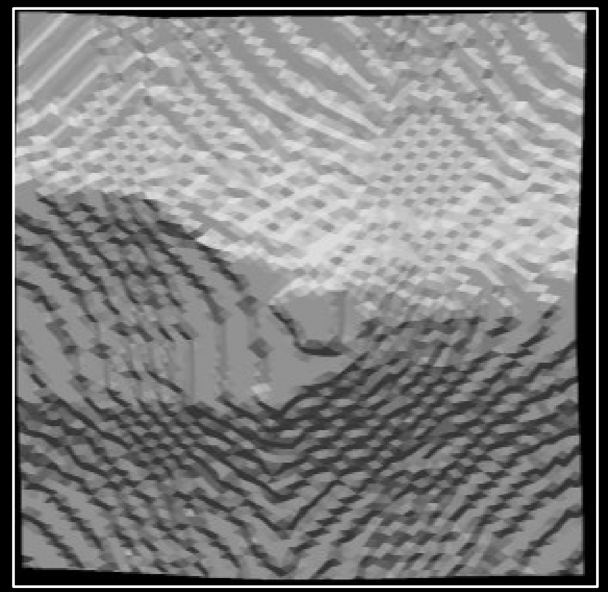

inverse problems

Complex light transport

After [Ritschel et al 2011]

Complex light transport

After [Ritschel et al 2011]

Complex light transport

After [Ritschel et al 2011]

Complex light transport

After [Ritschel et al 2011]

Complex light transport

After [Ritschel et al 2011]

Complex light transport

After [Ritschel et al 2011]

Complex light transport

After [Ritschel et al 2011]

Path integral form of light transport

$$\text{image} \quad I = \int_{\mathcal{P}} W_e(\mathbf{x}_0, \mathbf{x}_1) L_e(\mathbf{x}_k, \mathbf{x}_{k-1}) T(\bar{\mathbf{x}})\, d\bar{\mathbf{x}}$$

Path integral form of light transport

image $\quad I = \int_{\mathcal{P}} W_e(\mathbf{x}_0, \mathbf{x}_1) L_e(\mathbf{x}_k, \mathbf{x}_{k-1}) T(\bar{\mathbf{x}})\, d\bar{\mathbf{x}}$ light path

space of all light paths

Path integral form of light transport

sensor
weight

image $\quad I = \int_{\mathcal{P}} W_e(\mathbf{x}_0, \mathbf{x}_1) L_e(\mathbf{x}_k, \mathbf{x}_{k-1}) T(\bar{\mathbf{x}})\, d\bar{\mathbf{x}}$ light path

space of all light paths

Path integral form of light transport

sensor weight

source weight

image $I = \int_{\mathcal{P}} W_e(\mathbf{x}_0, \mathbf{x}_1) L_e(\mathbf{x}_k, \mathbf{x}_{k-1}) T(\bar{\mathbf{x}})\, d\bar{\mathbf{x}}$ light path

space of all light paths

Path integral form of light transport

sensor weight

source weight

image $\quad I = \int_{\mathcal{P}} W_e(\mathbf{x}_0, \mathbf{x}_1) L_e(\mathbf{x}_k, \mathbf{x}_{k-1}) T(\bar{\mathbf{x}})\, d\bar{\mathbf{x}}$ light path

path throughput

space of all light paths

$$T(\bar{\mathbf{x}}) = G(\mathbf{x}_0, \mathbf{x}_1) \prod_{j=1}^{k-1} f(\mathbf{x}_j, \mathbf{x}_{j+1}, \mathbf{x}_{j-1}) G(\mathbf{x}_j, \mathbf{x}_{j+1})$$

Path integral form of light transport

sensor weight

source weight

image $$I = \int_{\mathcal{P}} W_e(\mathbf{x}_0, \mathbf{x}_1) L_e(\mathbf{x}_k, \mathbf{x}_{k-1}) T(\bar{\mathbf{x}})\, d\bar{\mathbf{x}}$$ light path

space of all light paths

path throughput

$$T(\bar{\mathbf{x}}) = G(\mathbf{x}_0, \mathbf{x}_1) \prod_{j=1}^{k-1} f(\mathbf{x}_j, \mathbf{x}_{j+1}, \mathbf{x}_{j-1}) G(\mathbf{x}_j, \mathbf{x}_{j+1})$$

BSDF

Path integral form of light transport

sensor weight

source weight

image $$I = \int_{\mathcal{P}} W_e(\mathbf{x}_0, \mathbf{x}_1) L_e(\mathbf{x}_k, \mathbf{x}_{k-1}) T(\bar{\mathbf{x}}) \, d\bar{\mathbf{x}}$$ light path

path throughput

space of all light paths

$$T(\bar{\mathbf{x}}) = G(\mathbf{x}_0, \mathbf{x}_1) \prod_{j=1}^{k-1} f(\mathbf{x}_j, \mathbf{x}_{j+1}, \mathbf{x}_{j-1}) G(\mathbf{x}_j, \mathbf{x}_{j+1})$$

BSDF

geometry

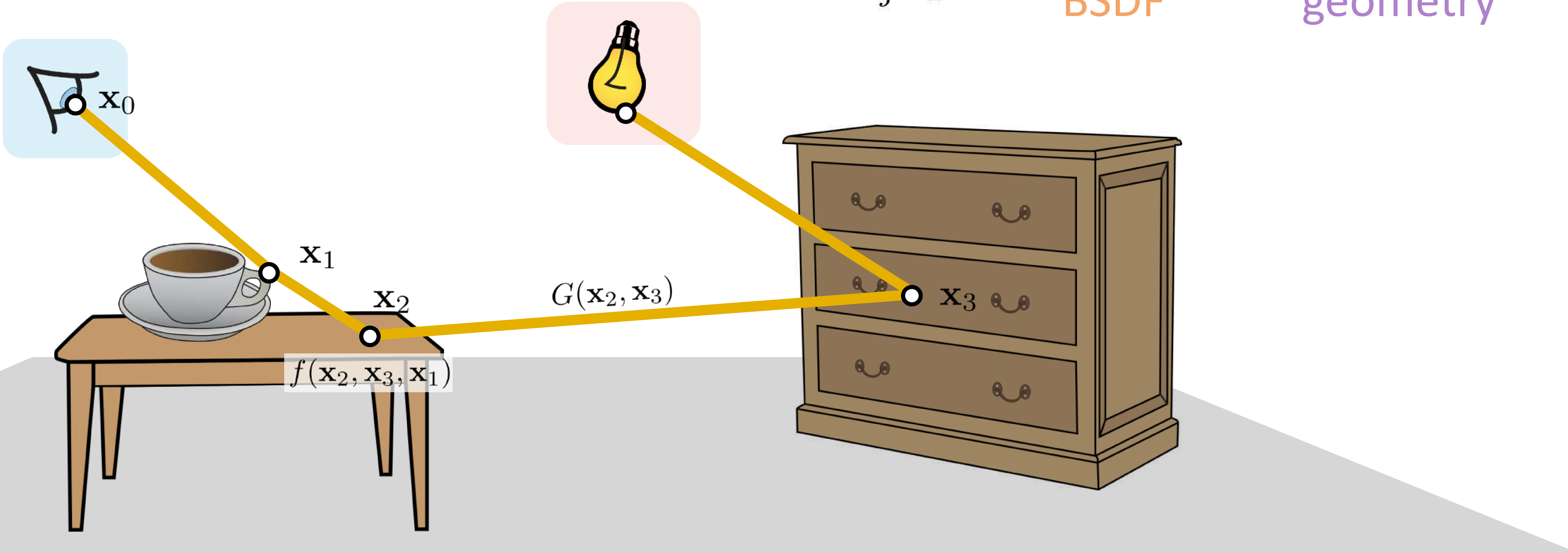

Monte Carlo rendering

approximate image as $I \approx \frac{1}{N}\sum_{i=1}^{N}\frac{W_e(\mathbf{x}_{i,0},\mathbf{x}_{i,1})L_e(\mathbf{x}_{i,k},\mathbf{x}_{i,k-1})T(\bar{\mathbf{x}}_i)}{p(\bar{\mathbf{x}}_i)}$

Monte Carlo rendering

approximate image as $I \approx \frac{1}{N} \boxed{\sum_{i=1}^{N}} \frac{W_e(\mathbf{x}_{i,0}, \mathbf{x}_{i,1}) L_e(\mathbf{x}_{i,k}, \mathbf{x}_{i,k-1}) T(\bar{\mathbf{x}}_i)}{p(\bar{\mathbf{x}}_i)}$

sum over *randomly* sampled paths

Monte Carlo rendering

sensor weight source weight path throughput

approximate image as $I \approx \frac{1}{N} \sum_{i=1}^{N} \frac{W_e(\mathbf{x}_{i,0}, \mathbf{x}_{i,1}) L_e(\mathbf{x}_{i,k}, \mathbf{x}_{i,k-1}) T(\bar{\mathbf{x}}_i)}{p(\bar{\mathbf{x}}_i)}$

sum over *randomly* sampled paths

Monte Carlo rendering

approximate image as $I \approx \frac{1}{N}\sum_{i=1}^{N} \frac{W_e(\mathbf{x}_{i,0}, \mathbf{x}_{i,1}) L_e(\mathbf{x}_{i,k}, \mathbf{x}_{i,k-1}) T(\bar{\mathbf{x}}_i)}{p(\bar{\mathbf{x}}_i)}$

sensor weight — $W_e(\mathbf{x}_{i,0}, \mathbf{x}_{i,1})$

source weight — $L_e(\mathbf{x}_{i,k}, \mathbf{x}_{i,k-1})$

path throughput — $T(\bar{\mathbf{x}}_i)$

PDF of random path — $p(\bar{\mathbf{x}}_i)$

sum over *randomly* sampled paths — $\sum_{i=1}^{N}$

Monte Carlo rendering

approximate image as $I_j \approx \frac{1}{N}\boxed{\sum_{i=1}^{N}}\frac{W_e(\mathbf{x}_{i,0},\mathbf{x}_{i,1})L_e(\mathbf{x}_{i,k},\mathbf{x}_{i,k-1})T(\bar{\mathbf{x}}_i)}{\boxed{p(\bar{\mathbf{x}}_i)}}$

sum over *randomly* sampled paths

PDF of random path

Path tracing: sample path starting from sensor

Monte Carlo rendering

approximate image as $I_j \approx \frac{1}{N} \sum_{i=1}^{N} \frac{W_e(\mathbf{x}_{i,0}, \mathbf{x}_{i,1}) L_e(\mathbf{x}_{i,k}, \mathbf{x}_{i,k-1}) T(\bar{\mathbf{x}}_i)}{p(\bar{\mathbf{x}}_i)}$

sum over *randomly* sampled paths

PDF of random path

Path tracing: sample path starting from sensor

Monte Carlo rendering

approximate image as $I_j \approx \frac{1}{N} \sum_{i=1}^{N} \frac{W_e(\mathbf{x}_{i,0}, \mathbf{x}_{i,1}) L_e(\mathbf{x}_{i,k}, \mathbf{x}_{i,k-1}) T(\bar{\mathbf{x}}_i)}{p(\bar{\mathbf{x}}_i)}$

sum over *randomly* sampled paths

PDF of random path

Light tracing: sample path starting from source

Monte Carlo rendering

approximate image as $I_j \approx \frac{1}{N} \boxed{\sum_{i=1}^{N}} \frac{W_e(\mathbf{x}_{i,0}, \mathbf{x}_{i,1}) L_e(\mathbf{x}_{i,k}, \mathbf{x}_{i,k-1}) T(\bar{\mathbf{x}}_i)}{\boxed{p(\bar{\mathbf{x}}_i)}}$

sum over *randomly* sampled paths

PDF of random path

Light tracing: sample path starting from source

Monte Carlo rendering

approximate image as $I_j \approx \dfrac{1}{N} \boxed{\sum_{i=1}^{N}} \dfrac{W_e(\mathbf{x}_{i,0}, \mathbf{x}_{i,1}) L_e(\mathbf{x}_{i,k}, \mathbf{x}_{i,k-1}) T(\bar{\mathbf{x}}_i)}{\boxed{p(\bar{\mathbf{x}}_i)}}$

sum over *randomly* sampled paths

PDF of random path

Bidirectional path tracing: sample path starting from both source and sensor

Monte Carlo rendering

approximate image as $I_j \approx \frac{1}{N} \sum_{i=1}^{N} \frac{W_e(\mathbf{x}_{i,0}, \mathbf{x}_{i,1}) L_e(\mathbf{x}_{i,k}, \mathbf{x}_{i,k-1}) T(\bar{\mathbf{x}}_i)}{p(\bar{\mathbf{x}}_i)}$

sum over *randomly* sampled paths

PDF of random path

Bidirectional path tracing: sample path starting from both source and sensor

Monte Carlo rendering

approximate image as $I_j \approx \frac{1}{N}\sum_{i=1}^{N}\frac{W_e(\mathbf{x}_{i,0},\mathbf{x}_{i,1})L_e(\mathbf{x}_{i,k},\mathbf{x}_{i,k-1})T(\bar{\mathbf{x}}_i)}{p(\bar{\mathbf{x}}_i)}$

sum over *randomly* sampled paths

PDF of random path

Bidirectional path tracing: sample path starting from both source and sensor

Monte Carlo rendering

approximate image as $I_j \approx \frac{1}{N} \sum_{i=1}^{N} \frac{W_e(\mathbf{x}_{i,0}, \mathbf{x}_{i,1}) L_e(\mathbf{x}_{i,k}, \mathbf{x}_{i,k-1}) T(\bar{\mathbf{x}}_i)}{p(\bar{\mathbf{x}}_i)}$

sum over *randomly* sampled paths

PDF of random path

Bidirectional path tracing: sample path starting from both source and sensor

Physics-based rendering and its applications to computational imaging

forward rendering

- accurate and efficient simulation
- virtually design sensors, optics, and algorithms

inverse rendering

- accurate and efficient differentiable simulation
- tractably solve general inverse problems

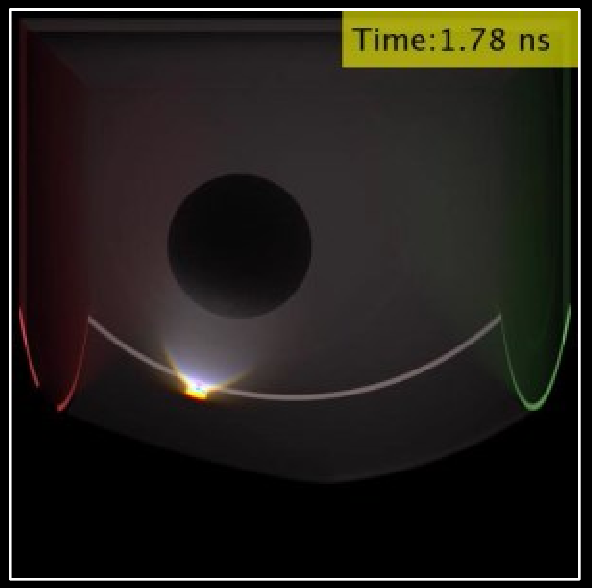

time-of-flight imaging

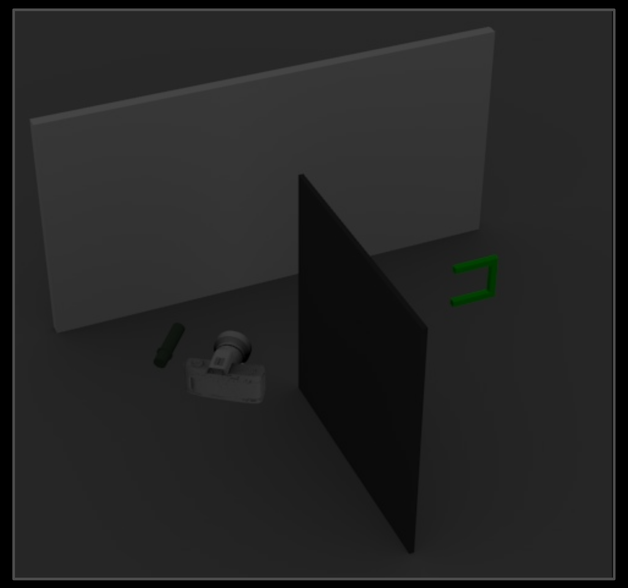

non-line-of-sight imaging

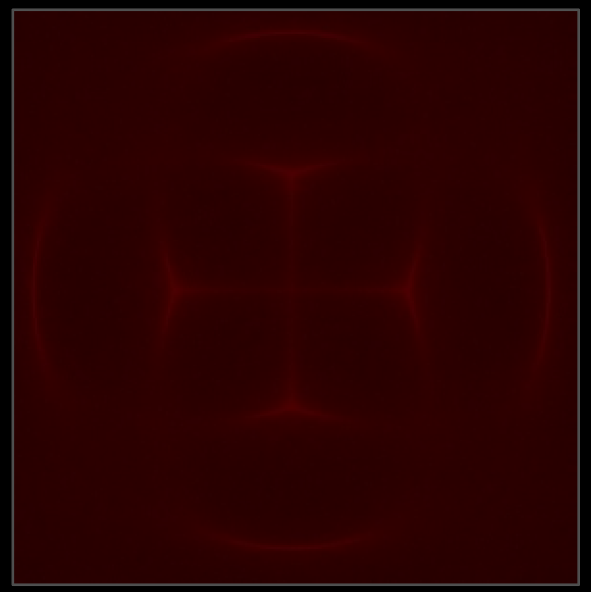

acousto-optic lensing

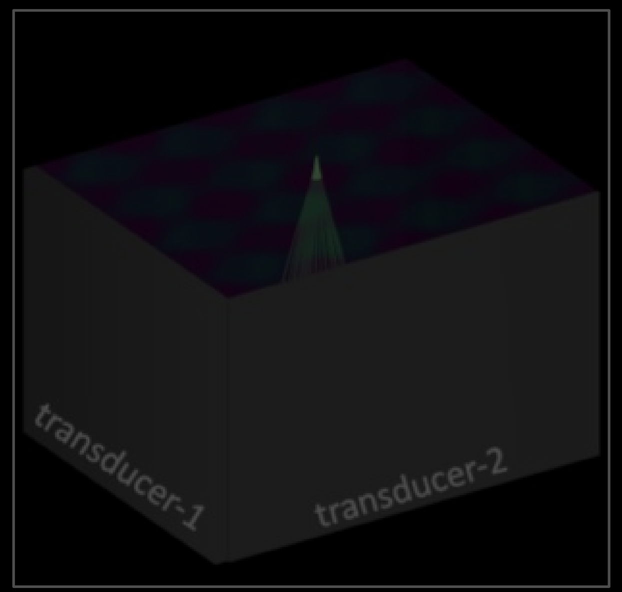

ultrafast light scanning

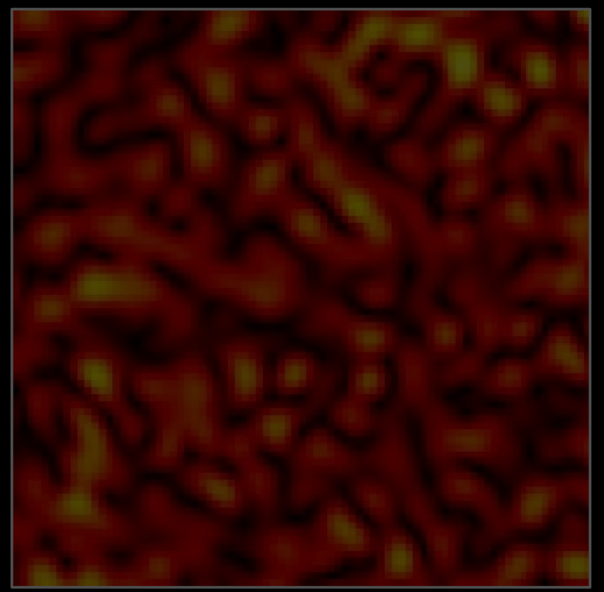

speckle imaging

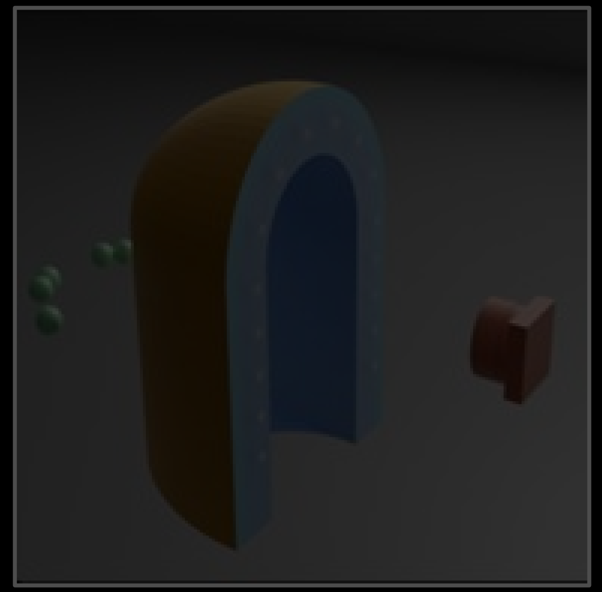

tactile sensor design

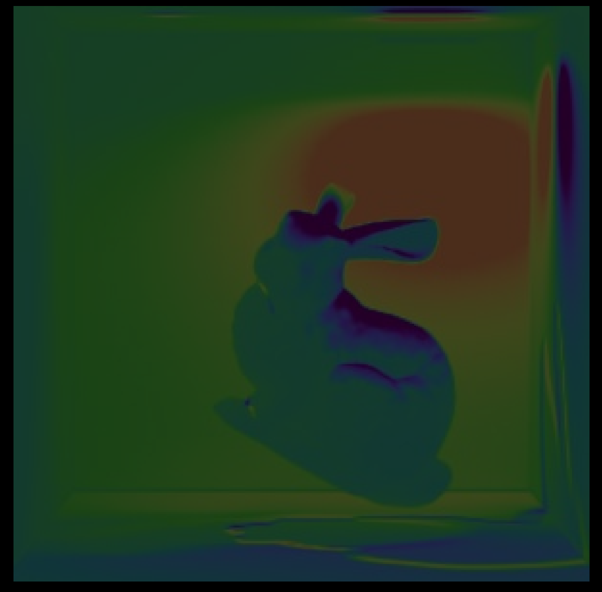

differentiable renderer

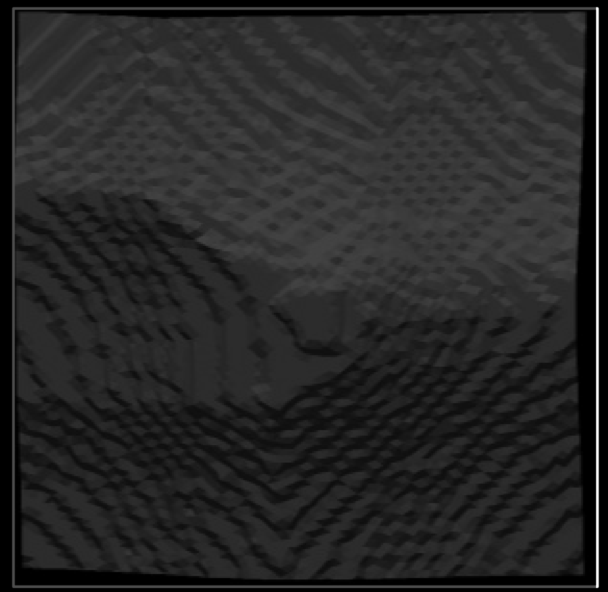

inverse problems

Time-of-flight cameras

[Velten et al. ToG, 2013]

Time-of-flight cameras

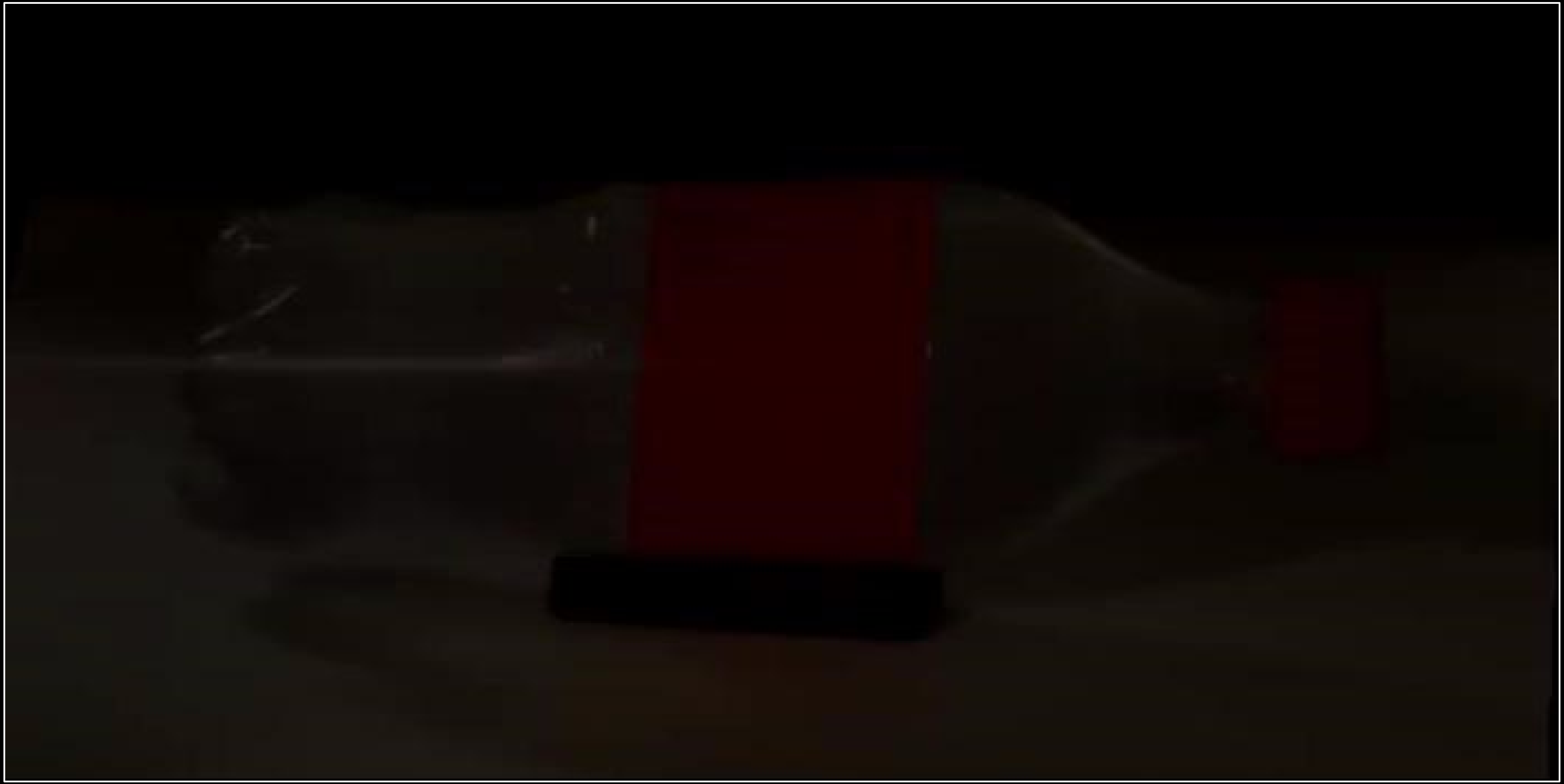

[Velten et al. ToG, 2013]

Time-of-flight cameras

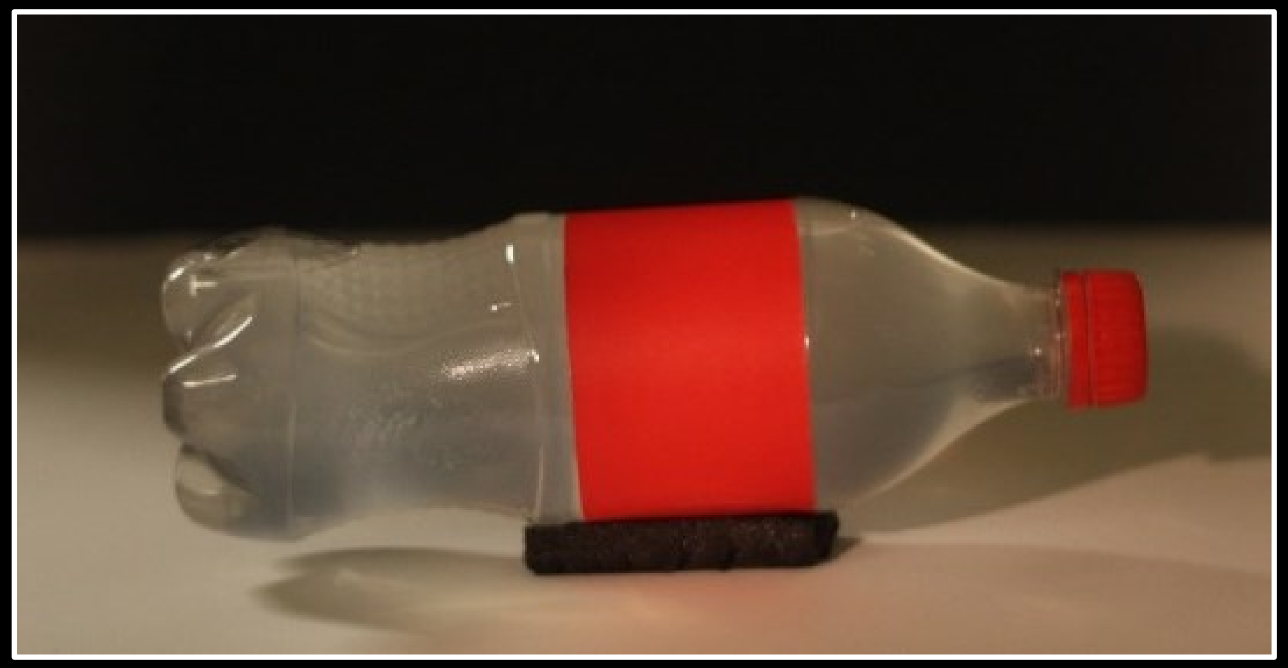

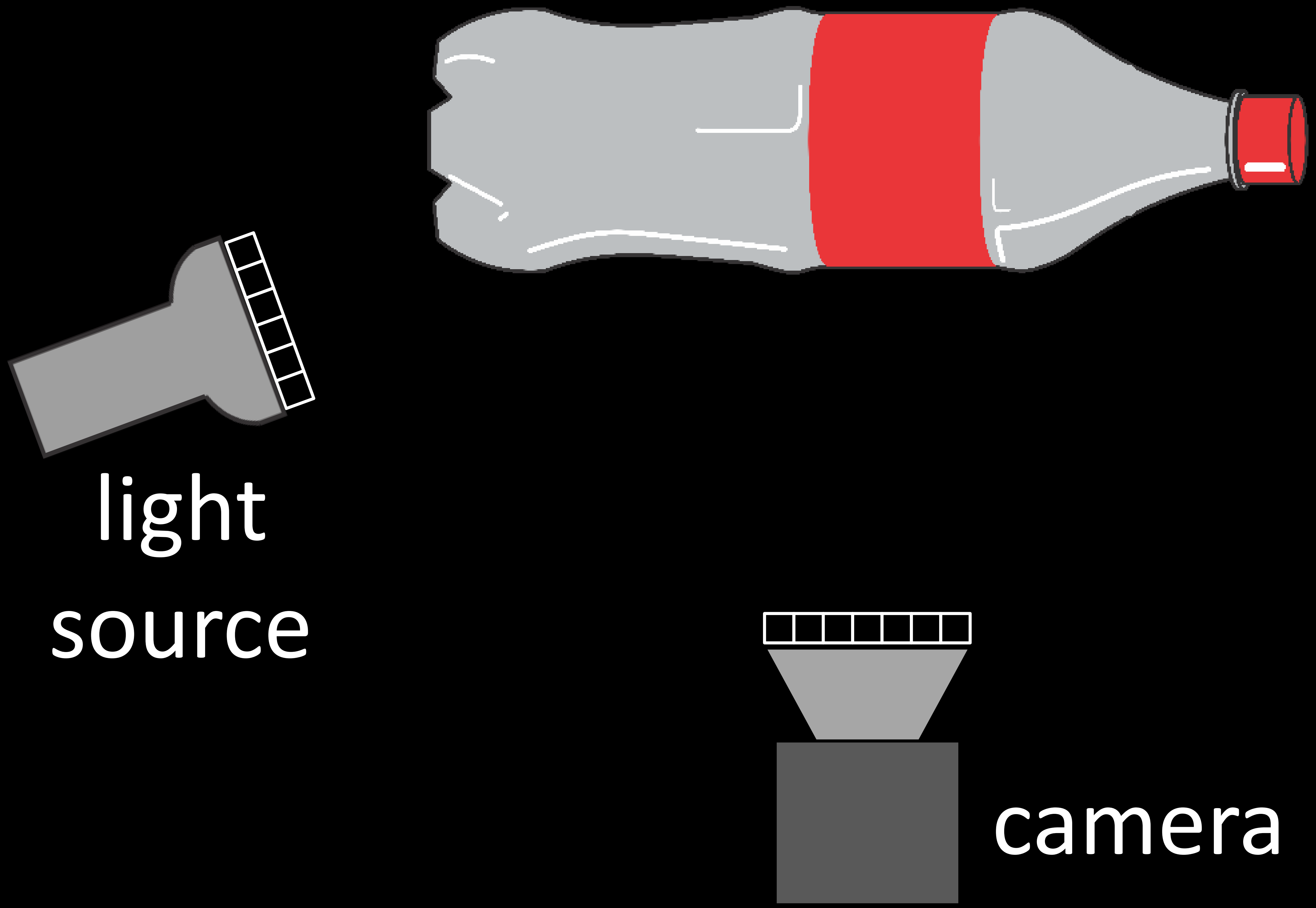

[Velten et al. ToG, 2013]

Time-of-flight cameras

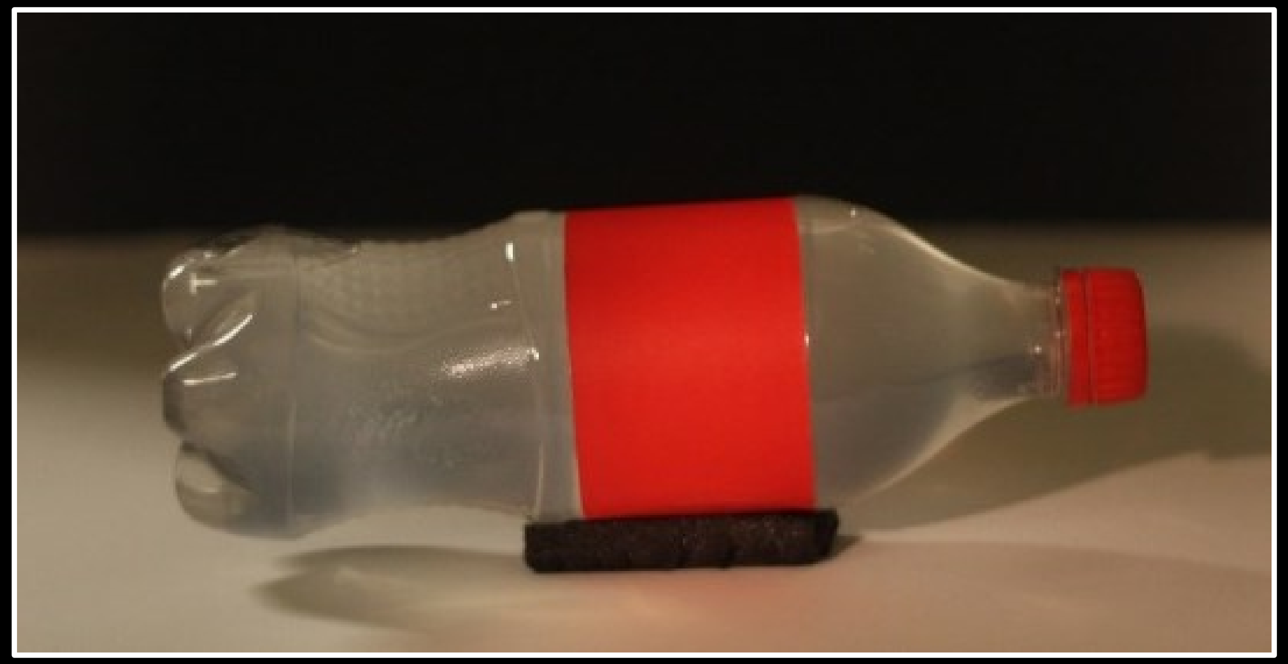

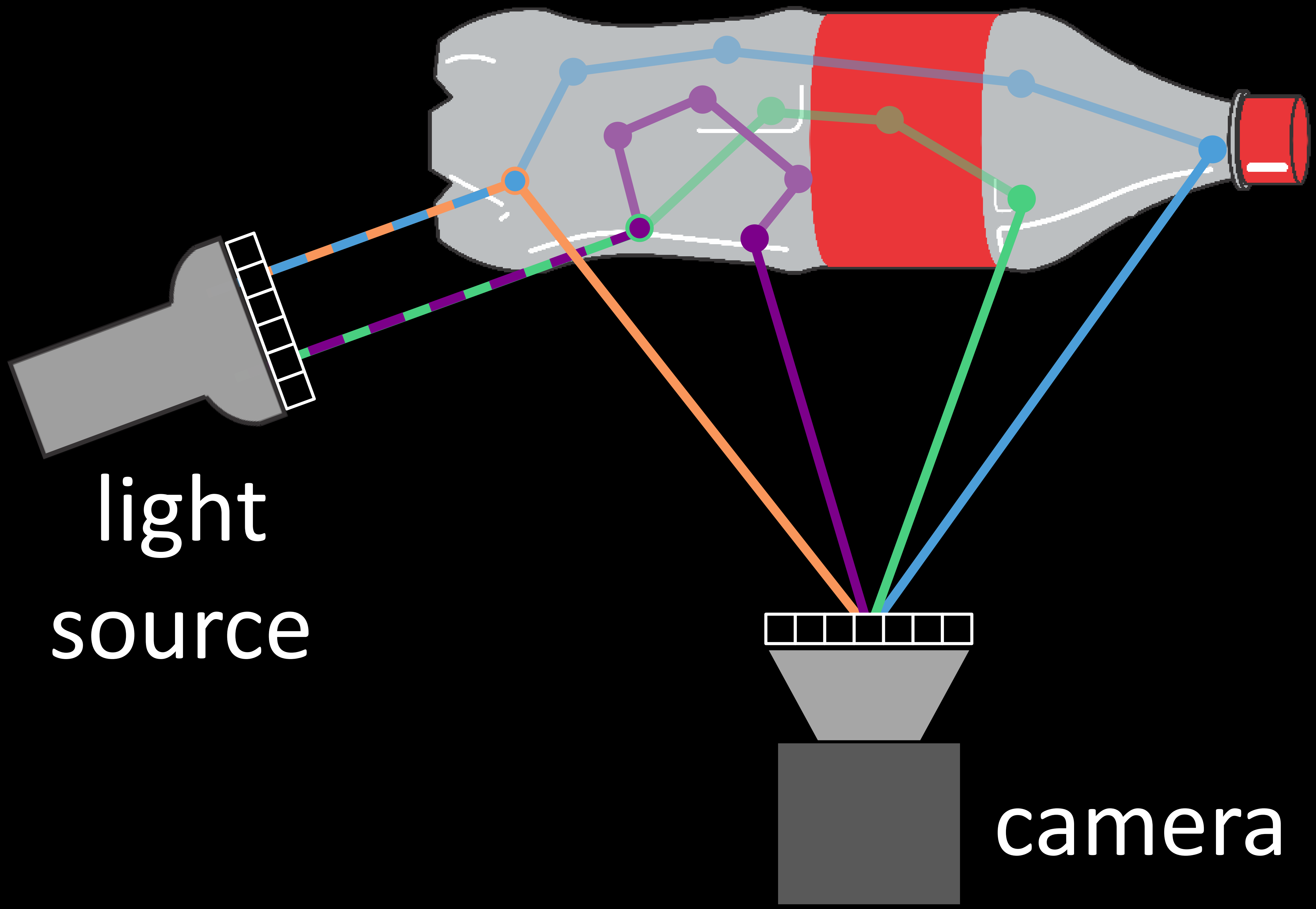

[Velten et al. ToG, 2013]

Time-of-flight cameras

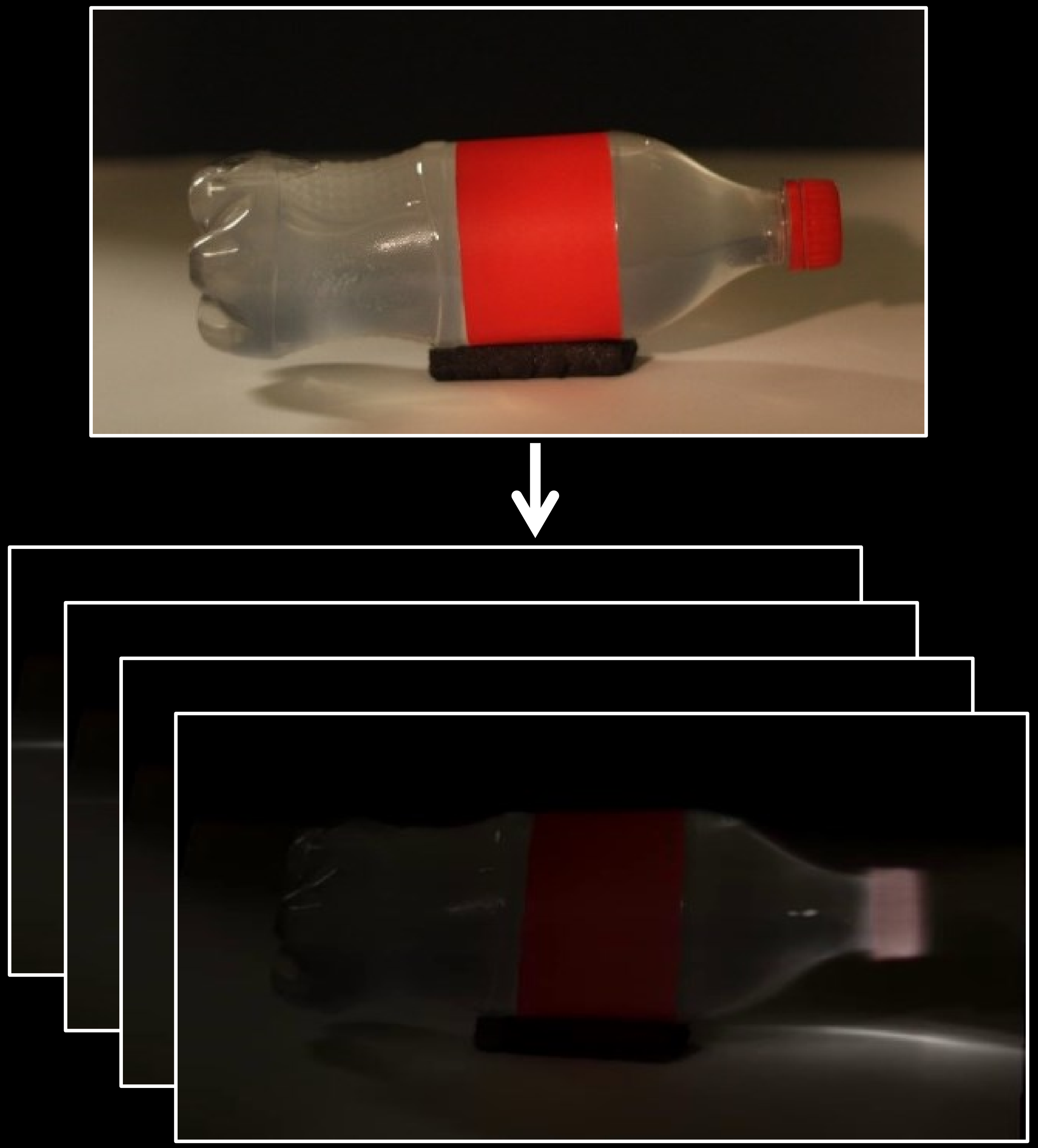

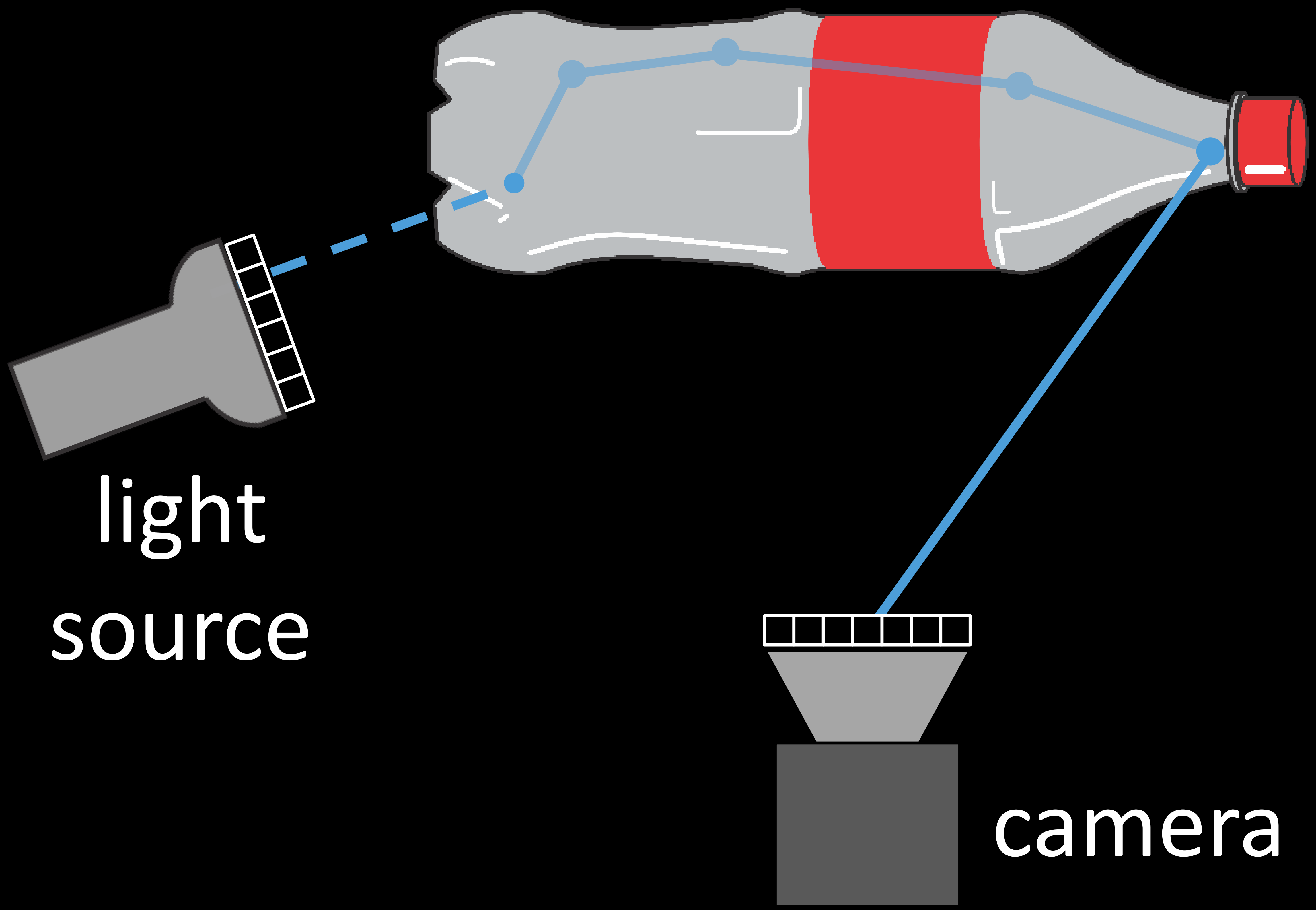

[Velten et al. ToG, 2013]

Time-of-flight cameras

SwissRanger SR4000

Hamamatsu streak

Brightway VISDOM

Microsoft Kinect

MPD SPAD

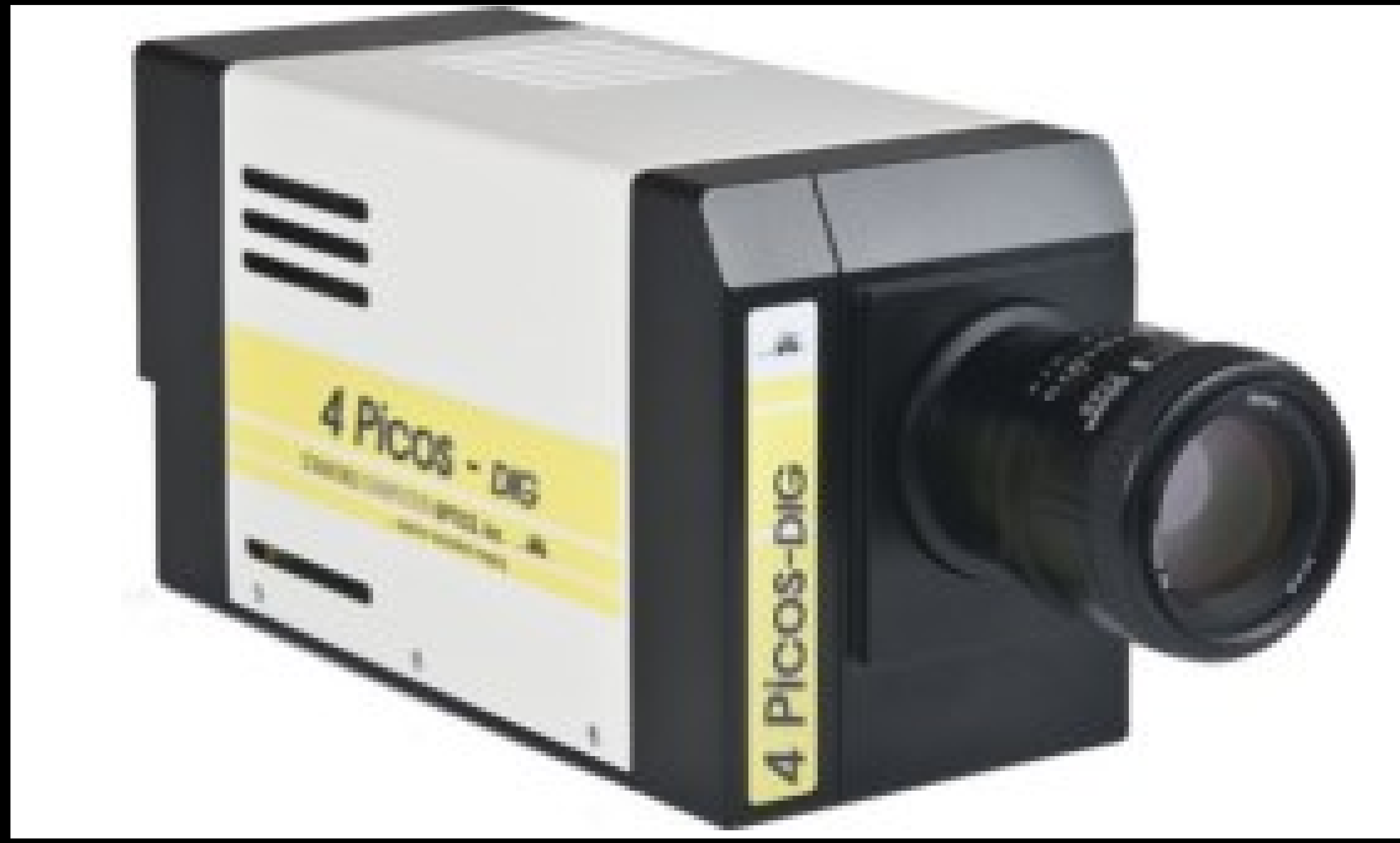

Stanford ICCD

Time-of-flight cameras

SwissRanger SR4000

Hamamatsu streak

Brightway VISDOM

Microsoft Kinect

MPD SPAD

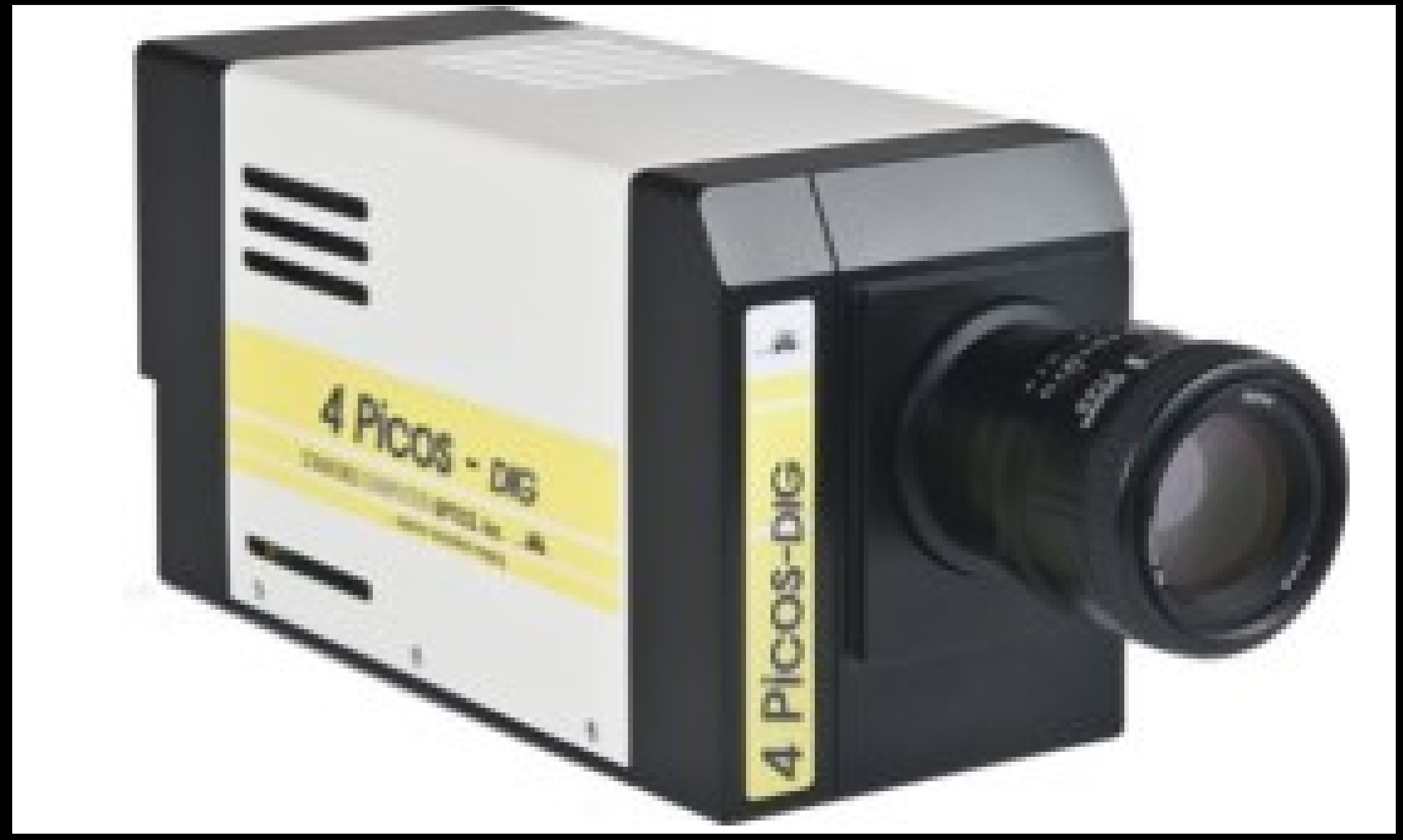

Stanford ICCD

continuous-wave

transient

time-gated

Time-of-flight cameras

intensity

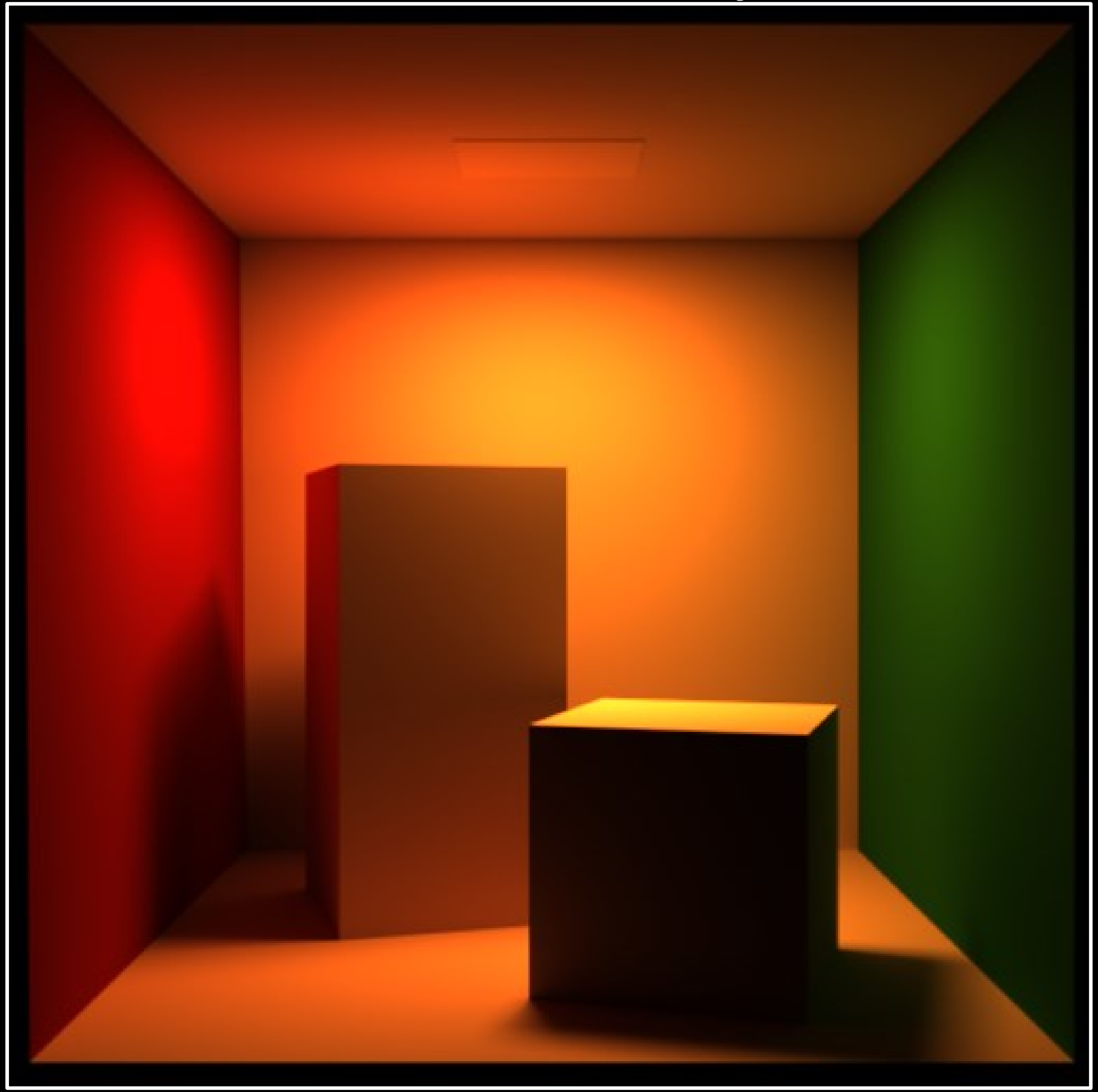

continuous wave

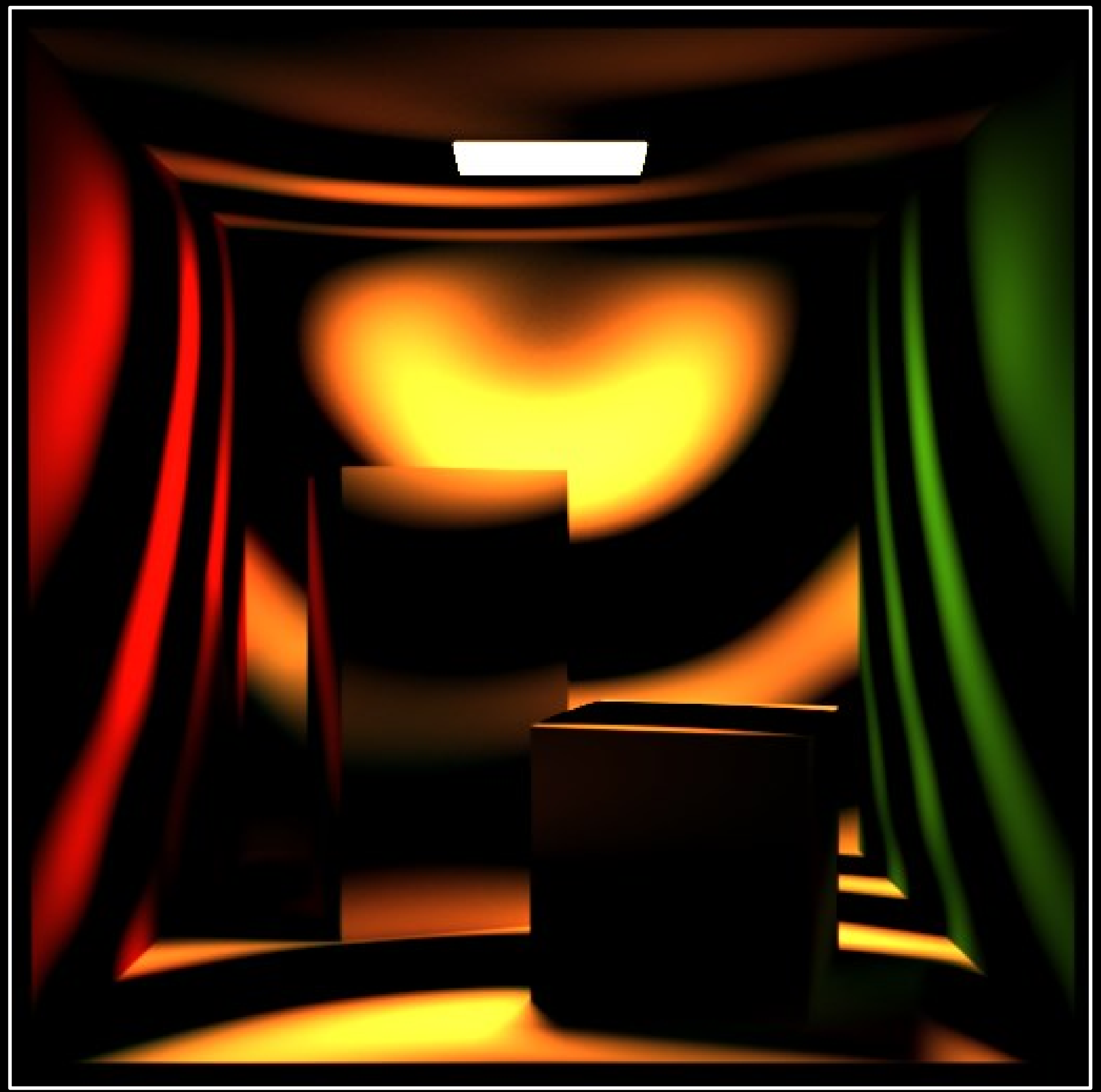

transient

time-gated

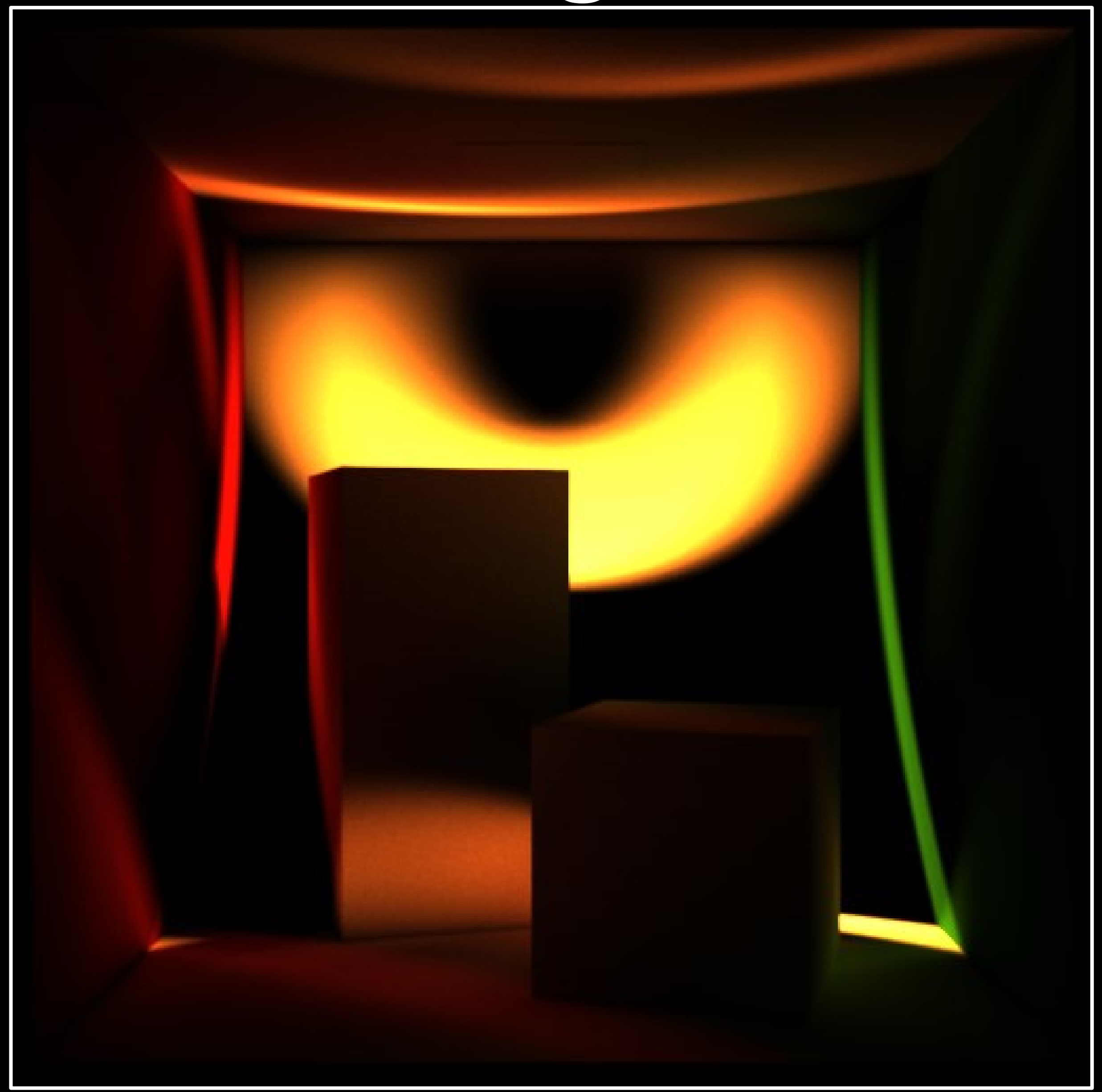

Time-of-flight cameras

intensity

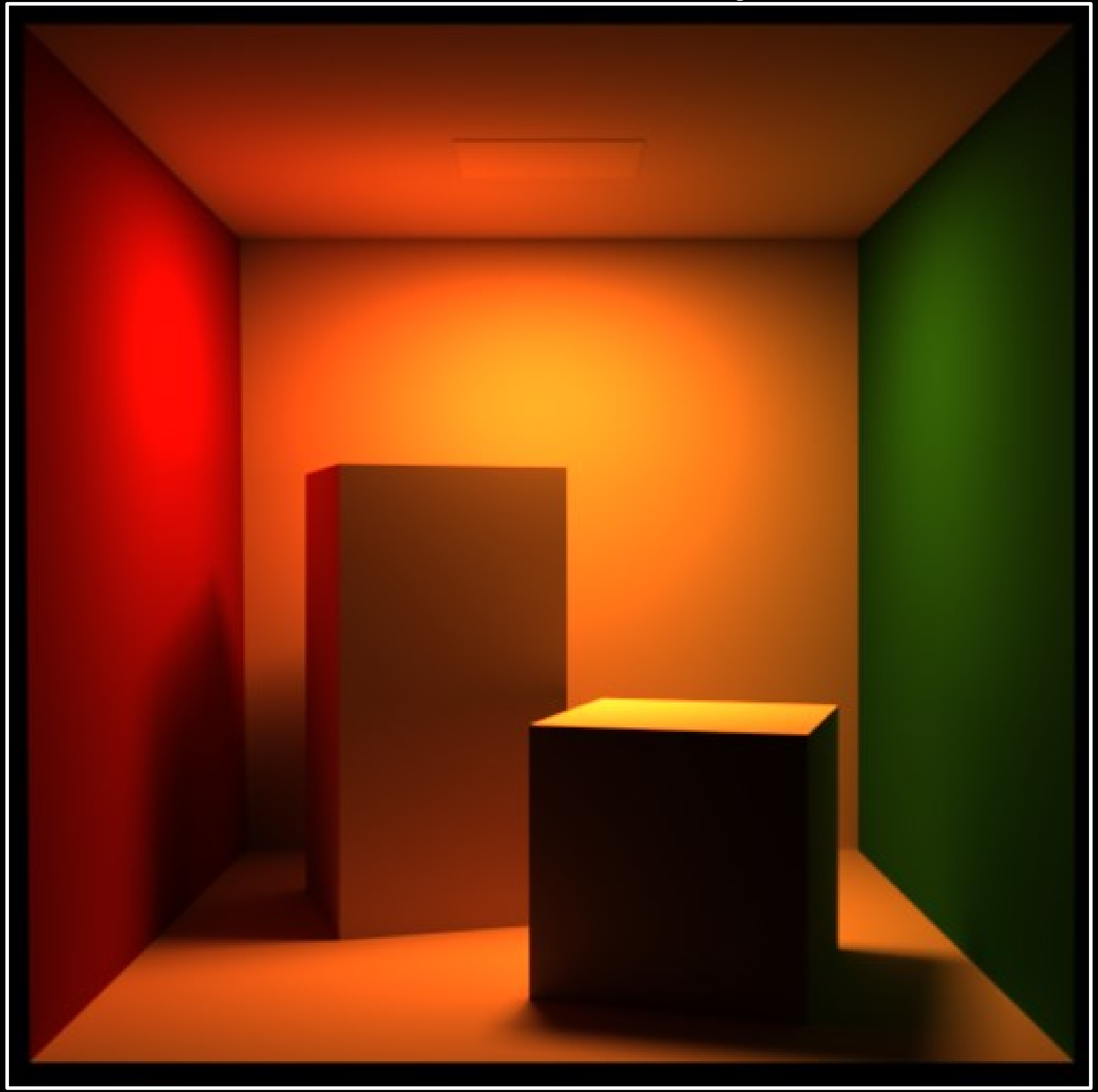

continuous wave

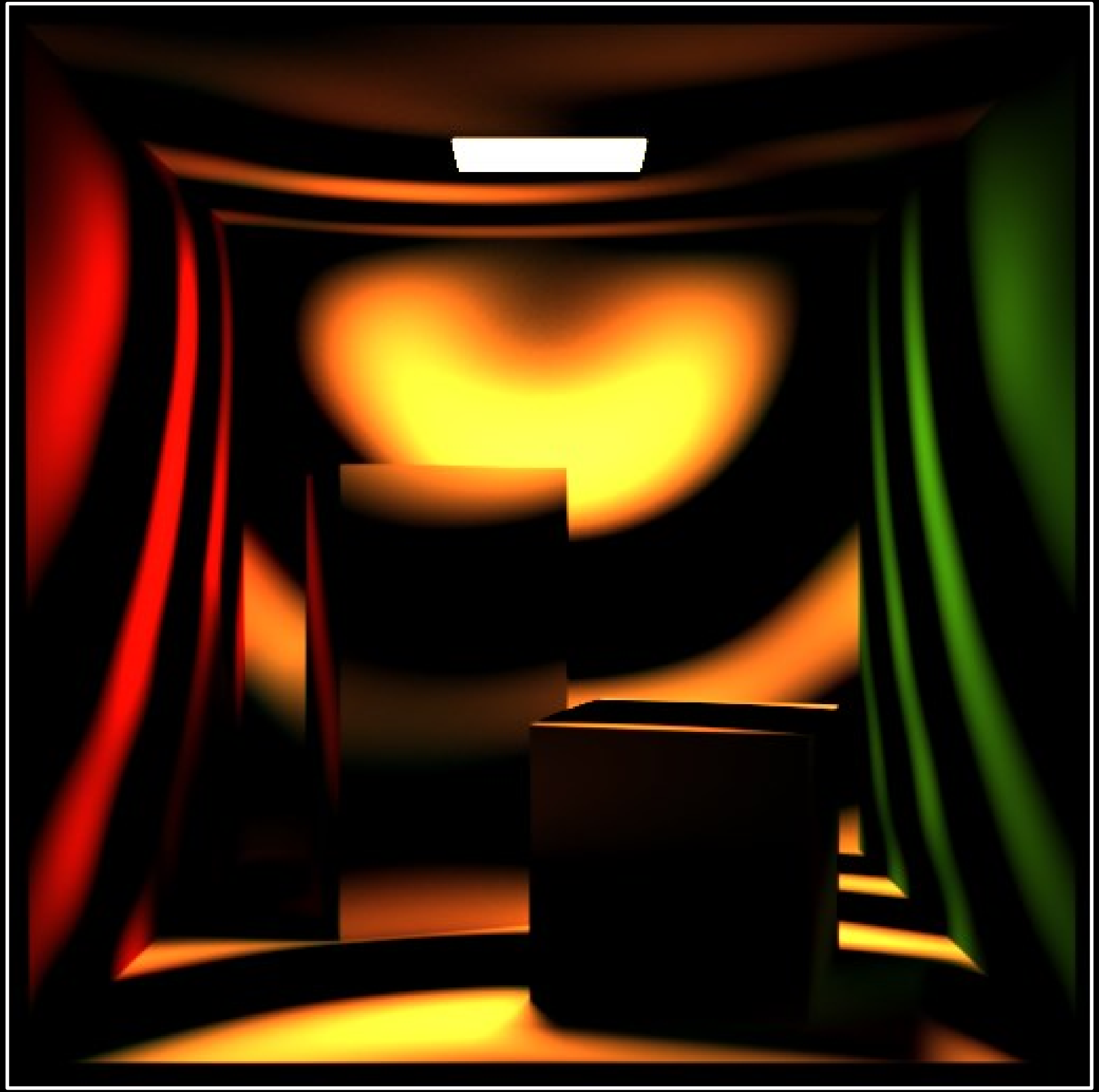

transient

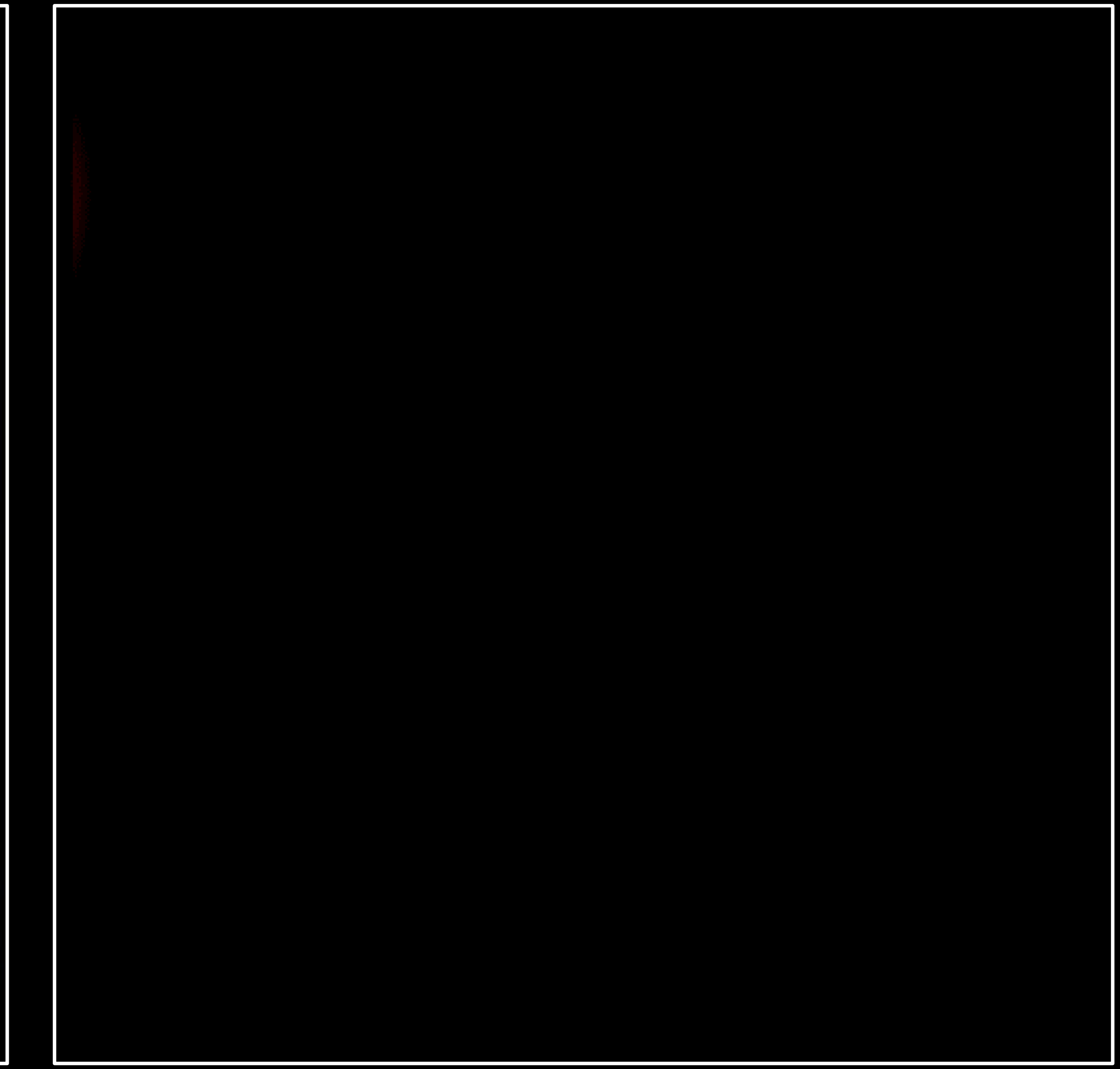

time-gated

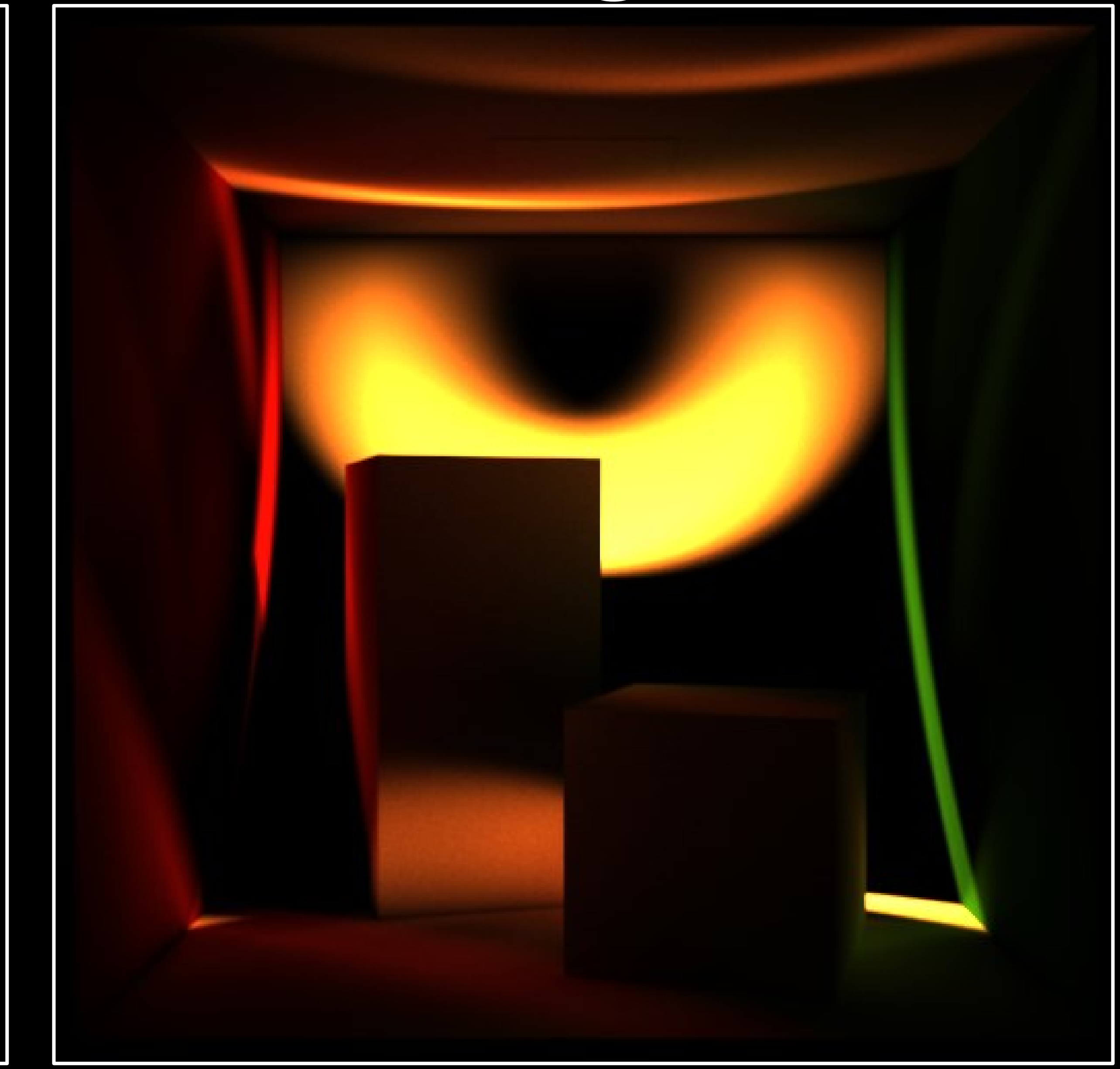

Rendering time-of-flight cameras: Path space integral

$$\text{image} = \int_{\text{light paths}} \mathrm{f}(\text{path})$$

path contribution, depends on scene properties, light source, and sensor

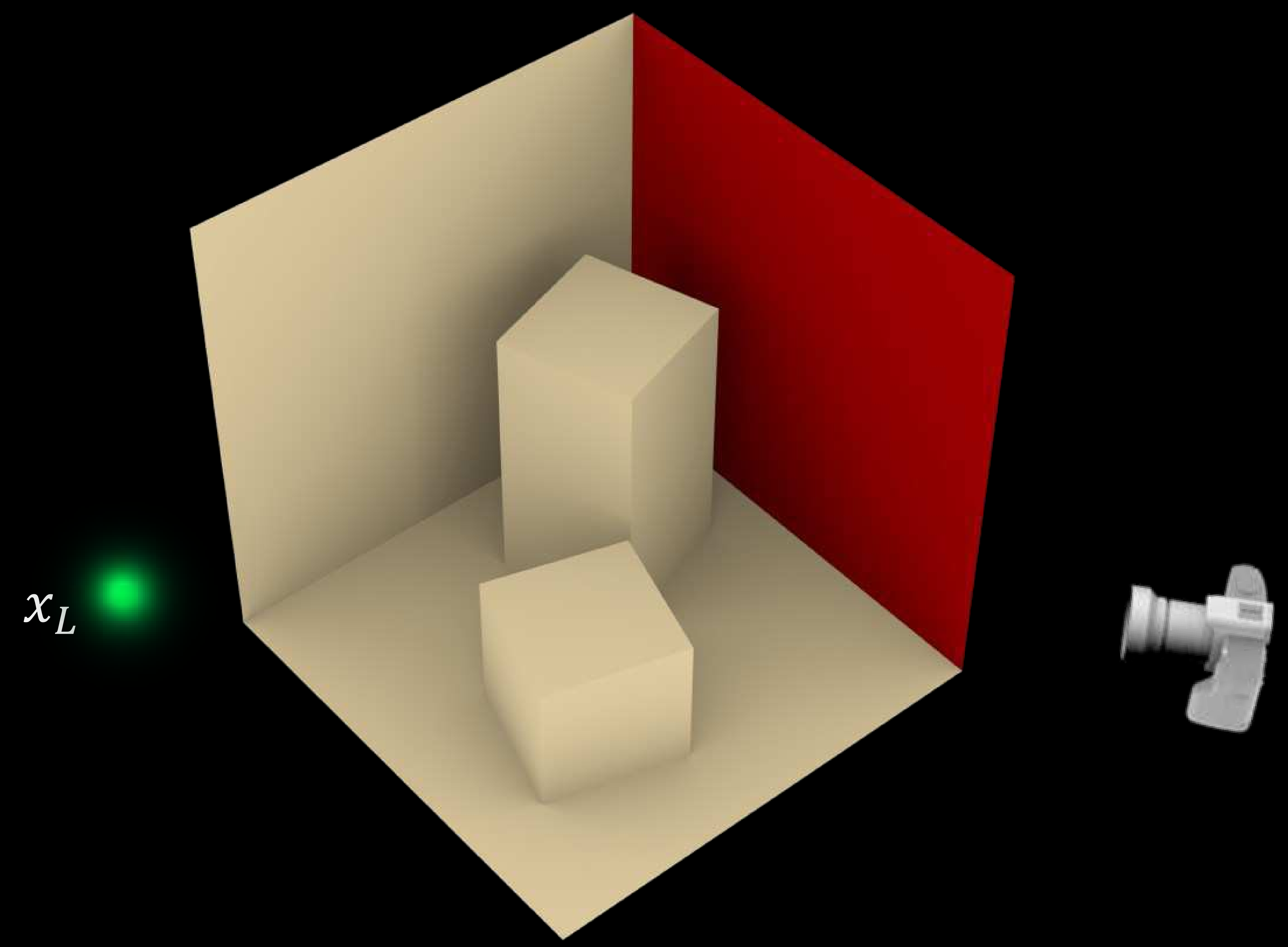

Rendering time-of-flight cameras: Path space integral

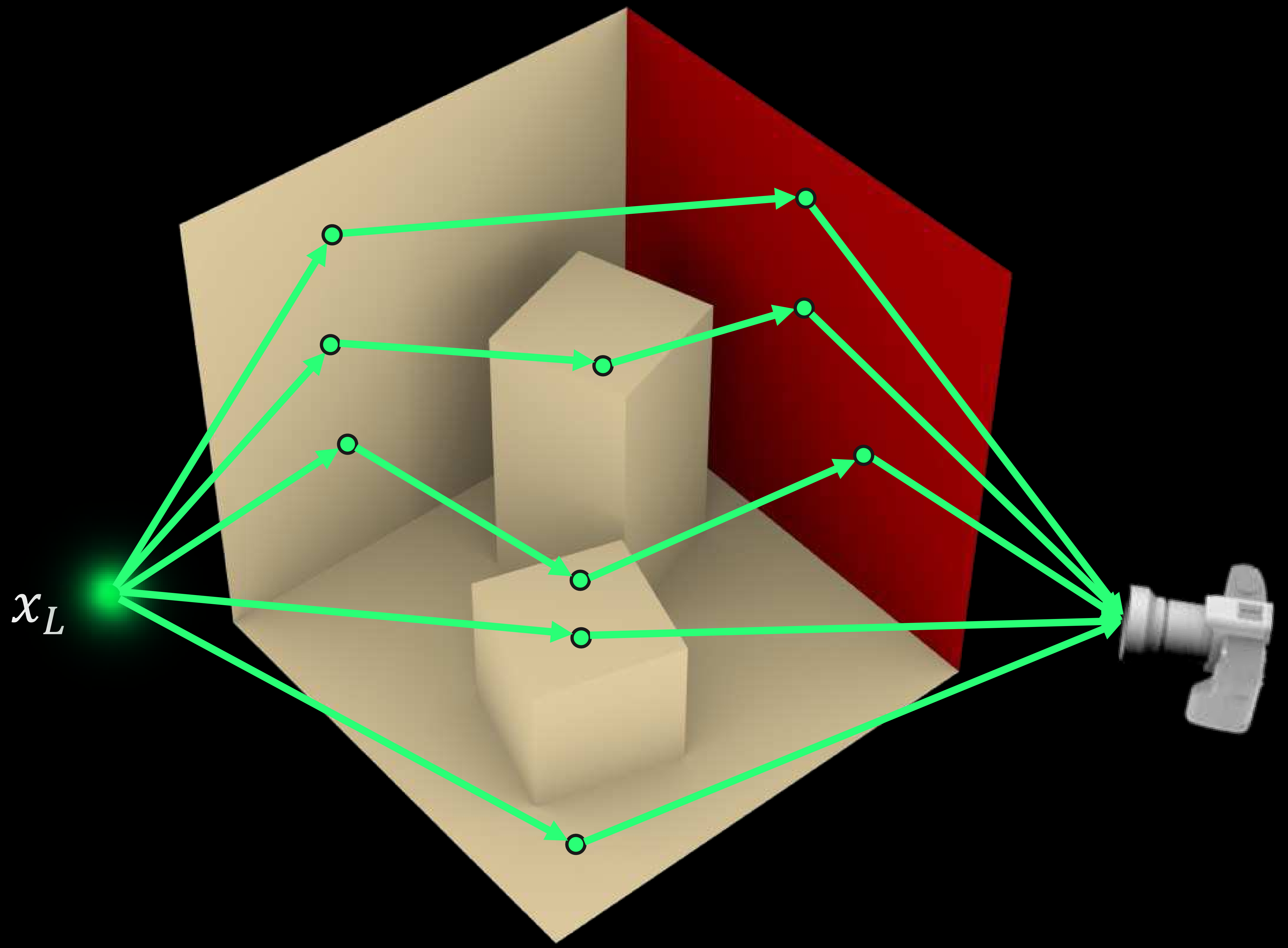

$$\text{image} = \int_{\text{light paths}} f(\text{path})$$

path contribution, depends on scene properties, light source, and sensor

Monte Carlo rendering:

- randomly <u>sample</u> paths: path_1, path_2, …, path_N
- approximate image as:

$$\text{image} \approx \sum_n \frac{f(\text{path}_n)}{\text{prob}(\text{path}_n)}$$

Rendering time-of-flight cameras: Path space integral

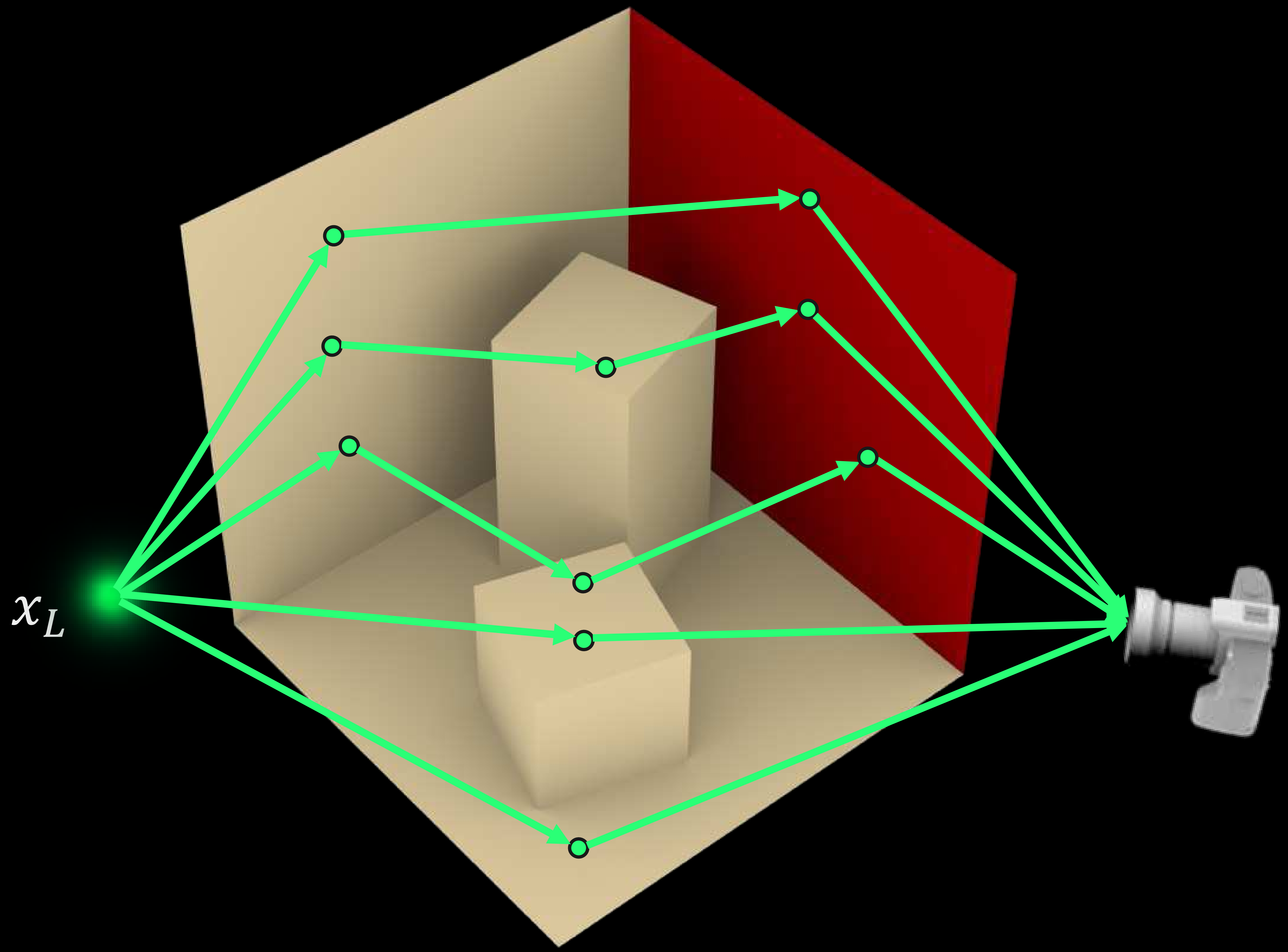

$$\text{image} = \int_{\text{light paths}} f(\text{path})\, W(|\text{path}|)$$

path length weight depends only on sensor

Monte Carlo rendering:

- randomly sample paths: path_1, path_2, ..., path_N
- approximate image as:

$$\text{image} \approx \sum_n \frac{f(\text{path}_n)}{\text{prob}(\text{path}_n)}$$

Rendering time-of-flight cameras: Path space integral

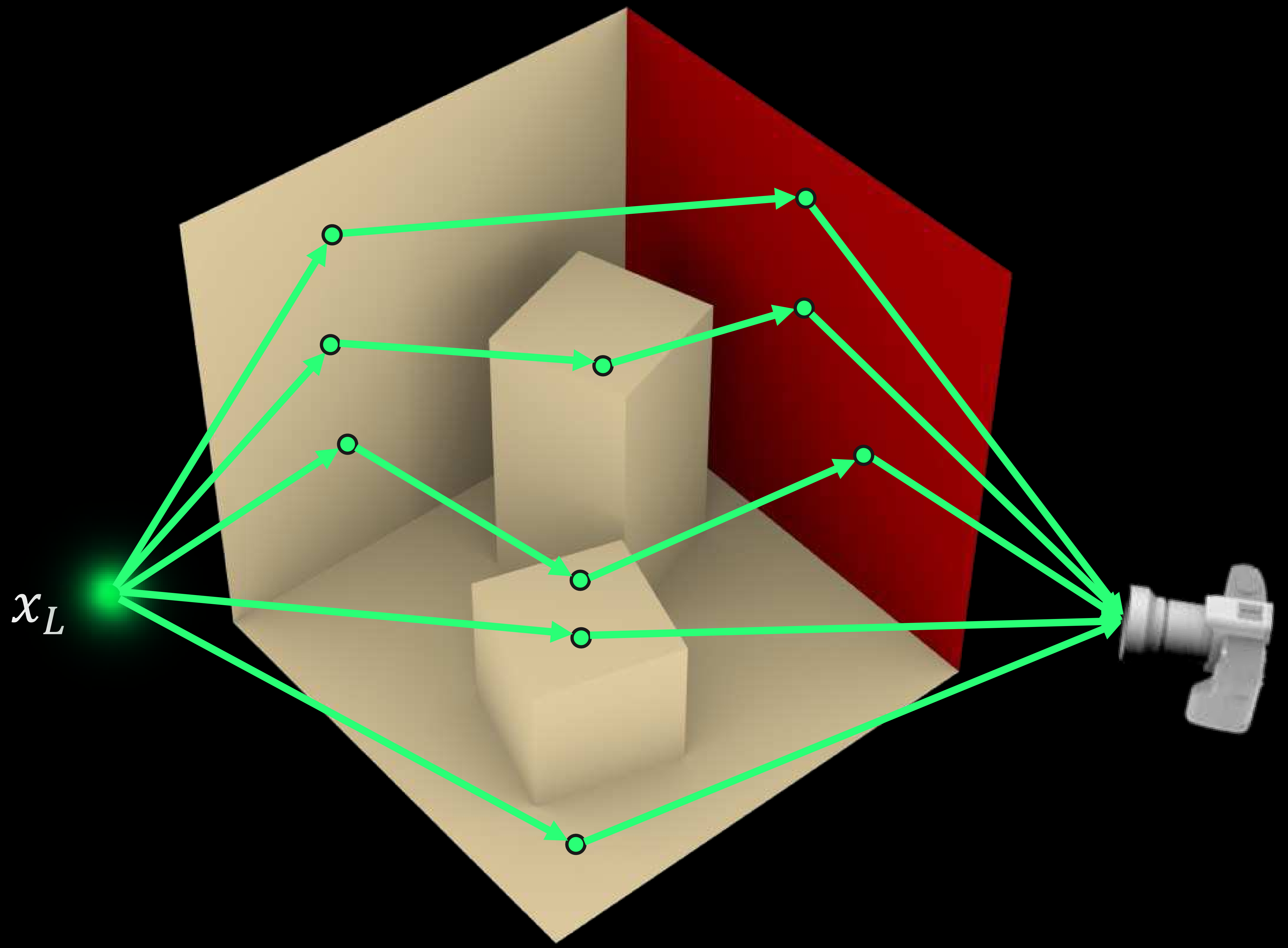

$$\text{image} = \int_{\substack{\text{light}\\\text{paths}}} f(\text{path})\, W(|\text{path}|)$$

path length weight depends only on sensor

Monte Carlo rendering:

- randomly <u>sample</u> paths: path_1, path_2, ..., path_N
- approximate image as:

$$\text{time-of-flight image} \approx \sum_n \frac{f(\text{path}_n)}{\text{prob}(\text{path}_n)} W(|\text{path}_n|)$$

Rendering continuous wave time-of-flight camera

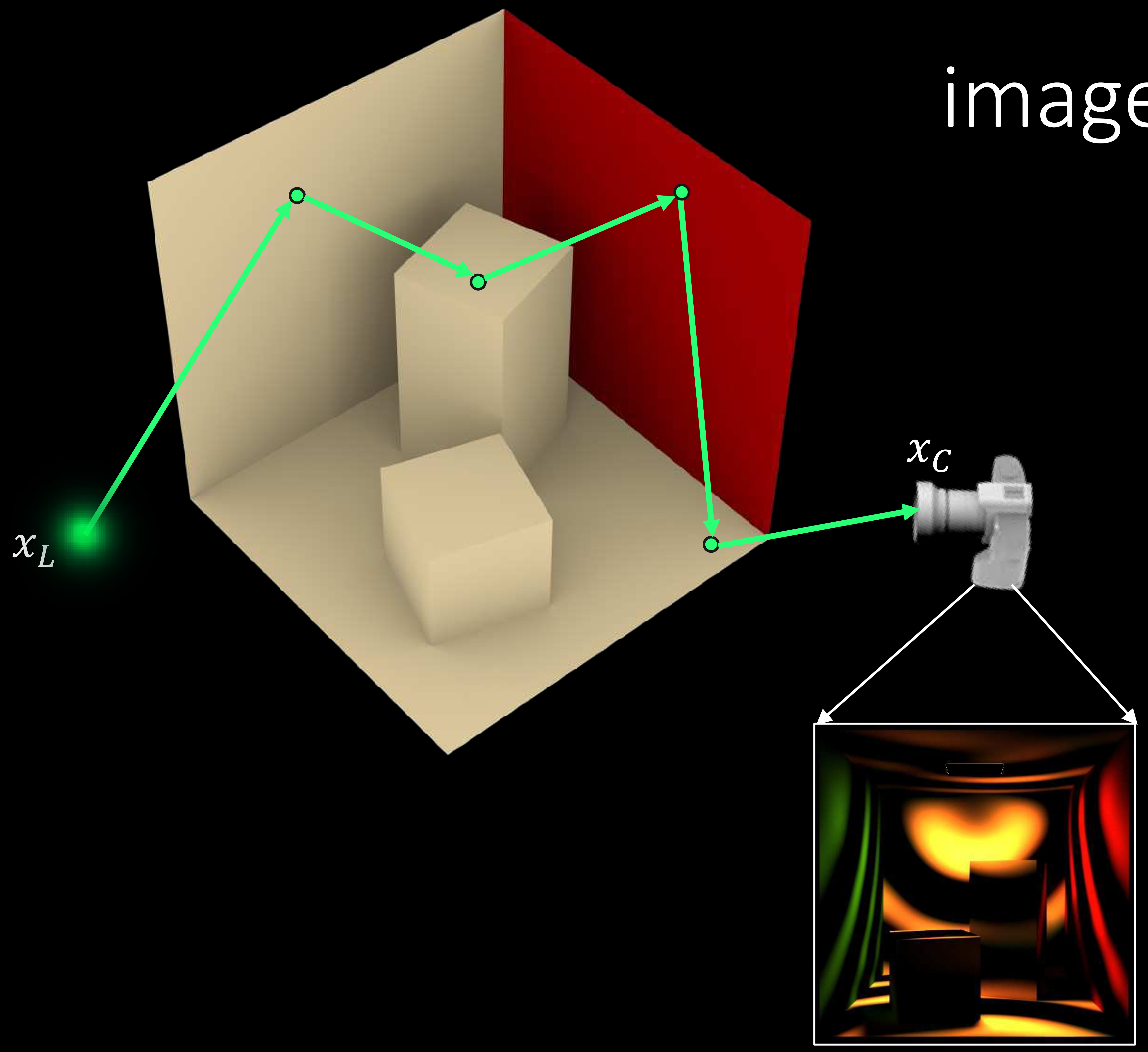

$$\text{image} = \int_{\text{light paths}} f(\text{path})\,W(|\text{path}|)$$

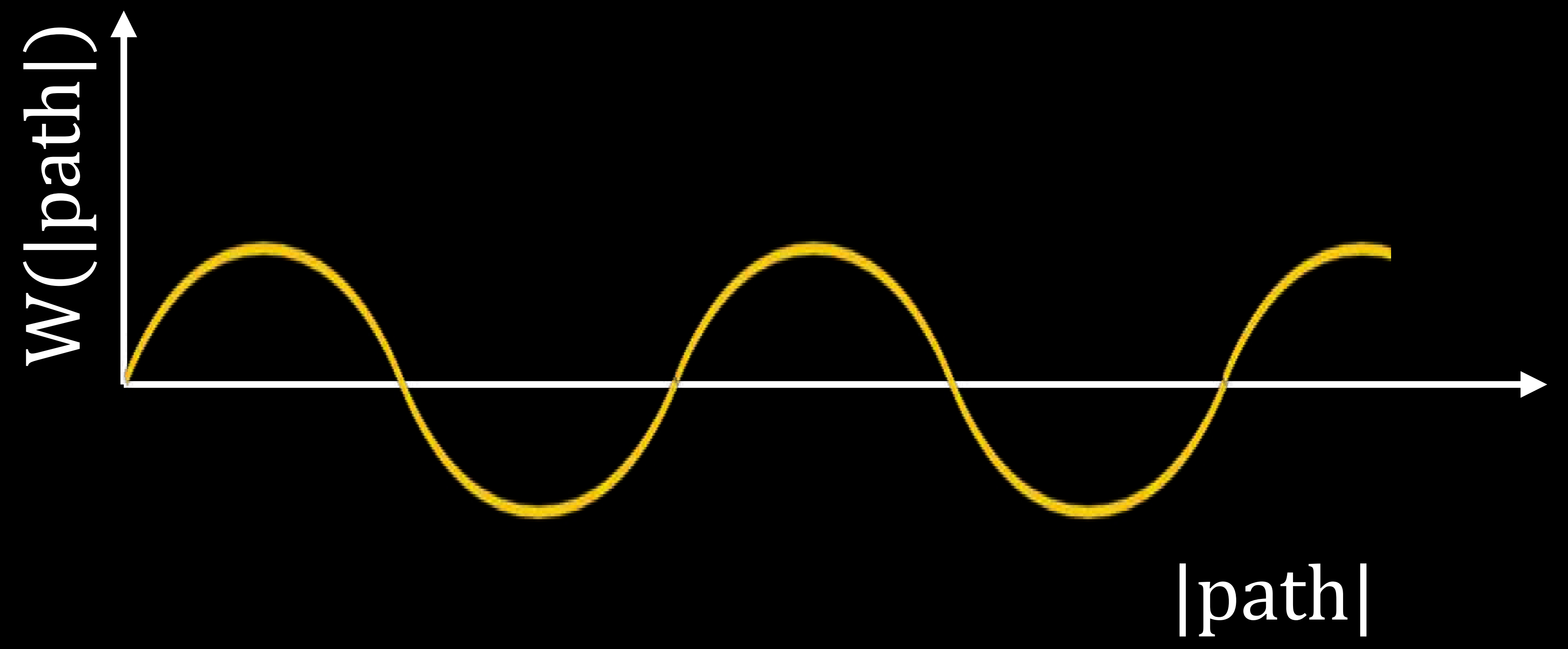

Classification: time-gated camera

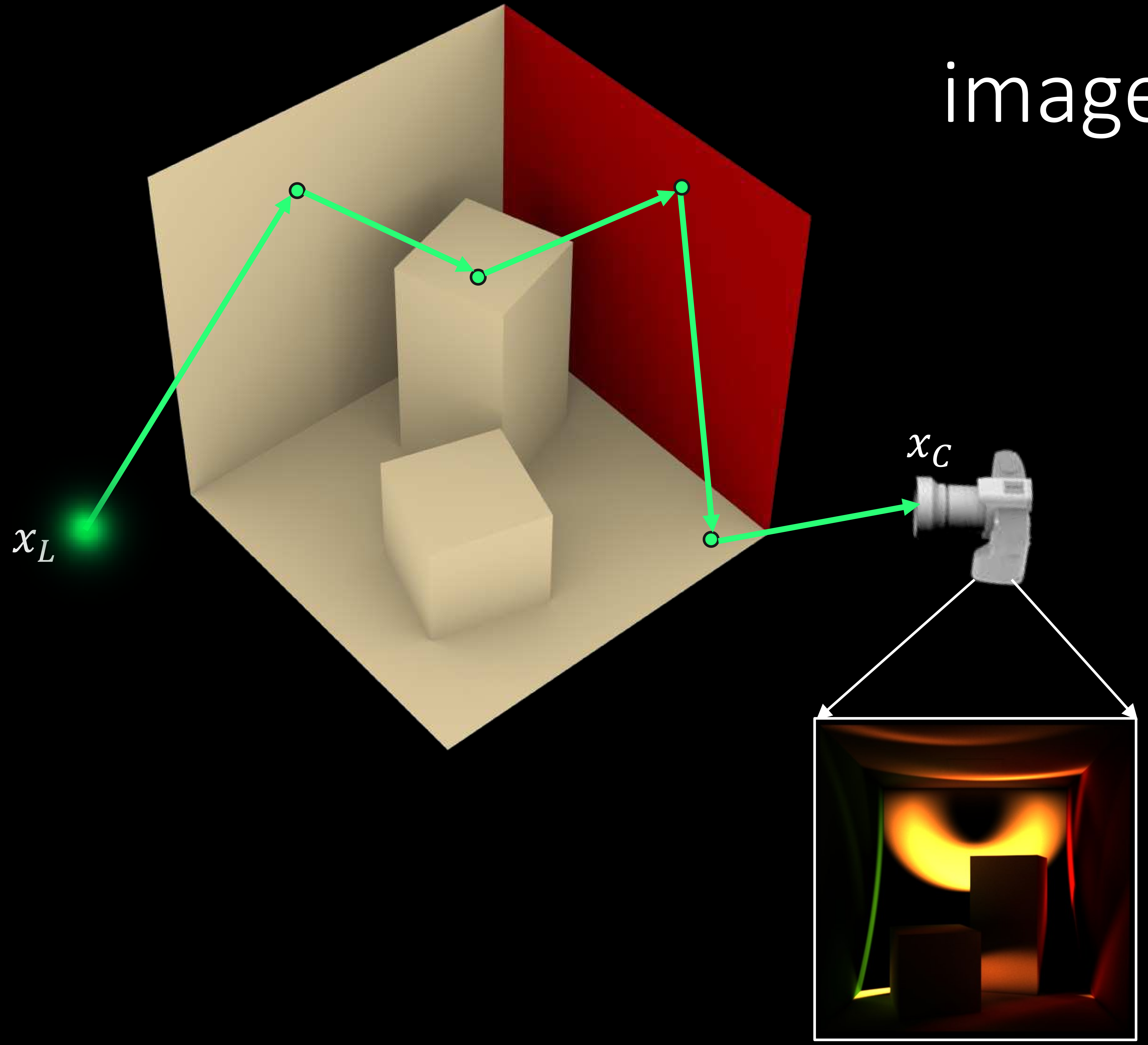

$$\text{image} = \int_{\substack{\text{light}\\\text{paths}}} f(\text{path})W(|\text{path}|)$$

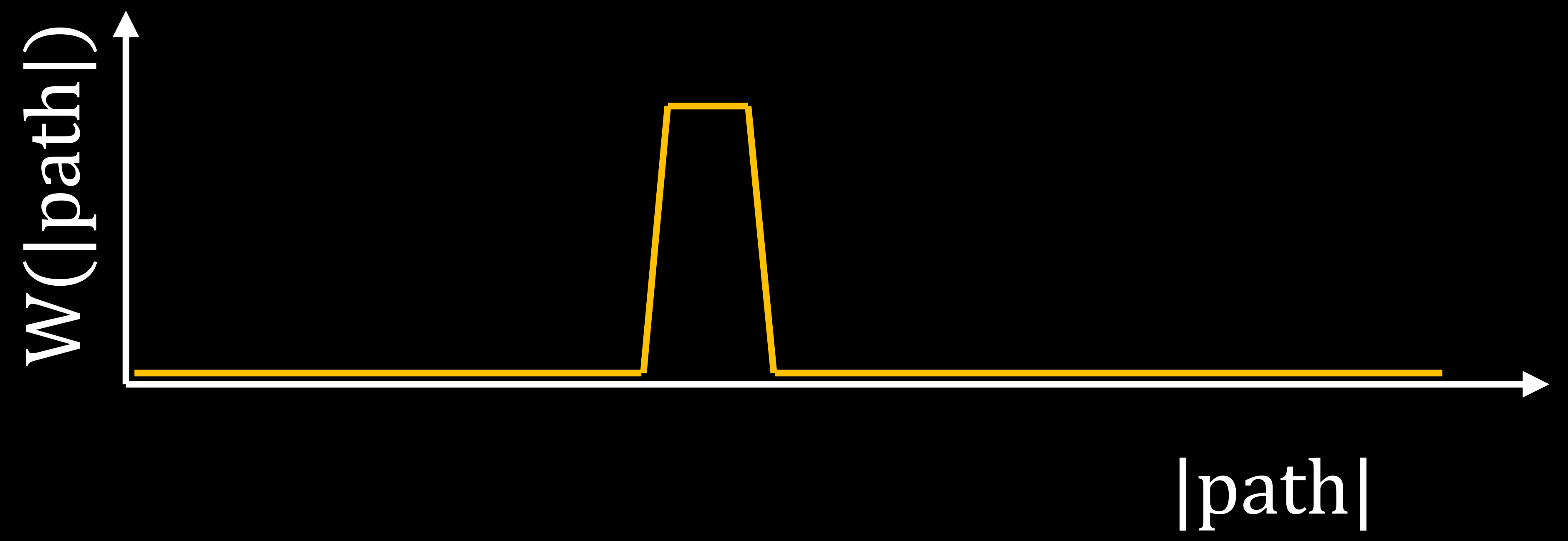

Rendering transient camera

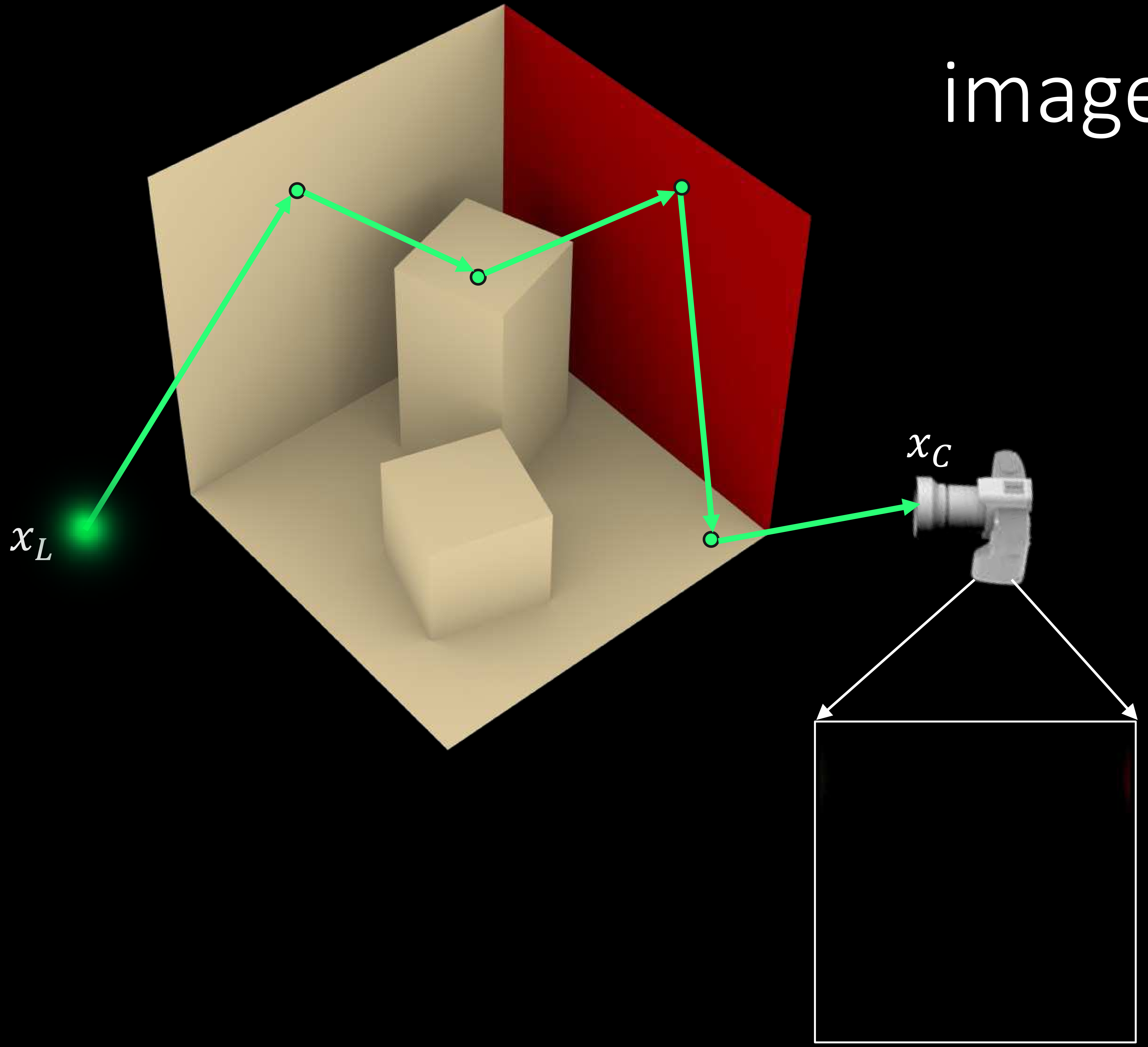

$$\text{image} = \int_{\text{light paths}} f(\text{path})\,W(|\text{path}|)$$

Path space integral for time-of-flight cameras

$$\text{image} = \int_{\text{light paths}} f(\text{path})W(|\text{path}|)$$

intensity

BDPT, PT, PM, KDE, etc

continuous-wave

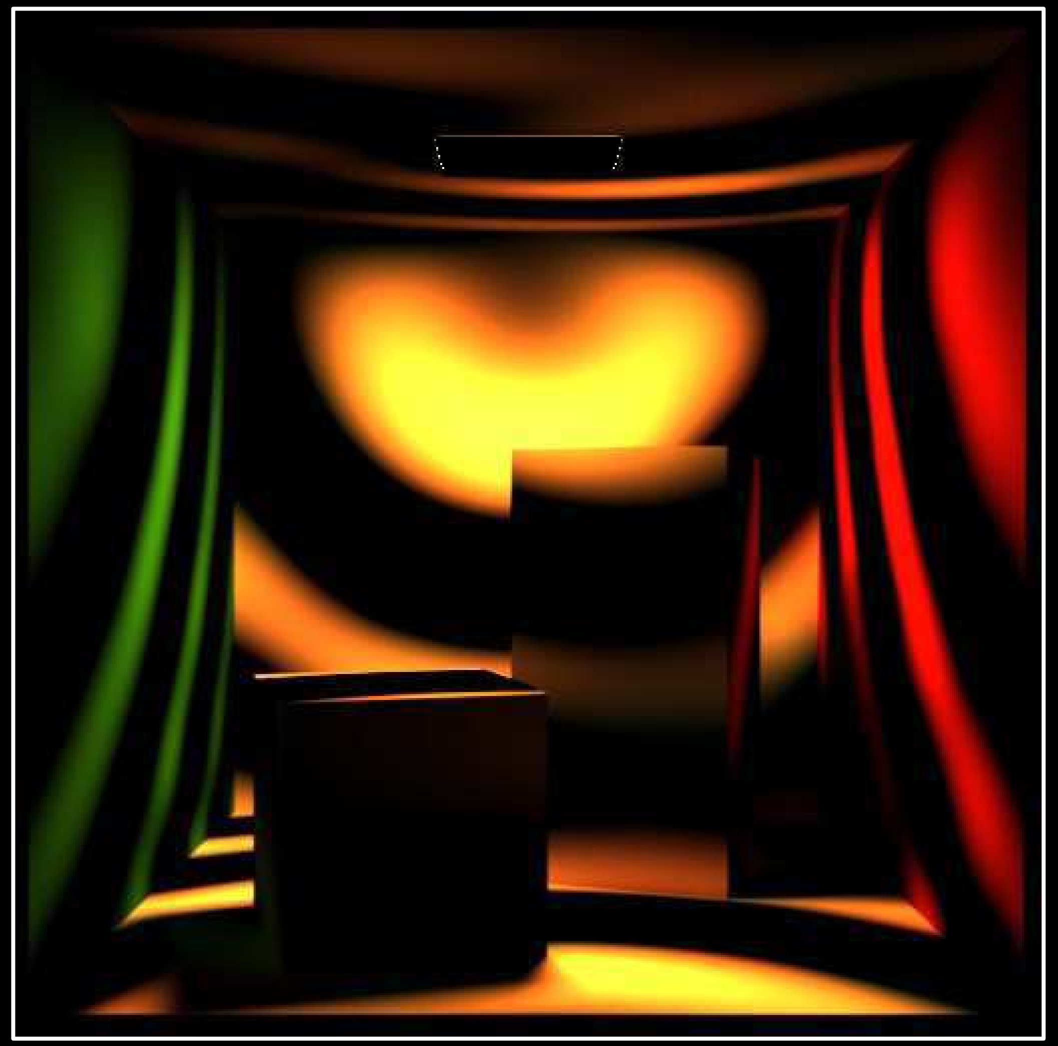

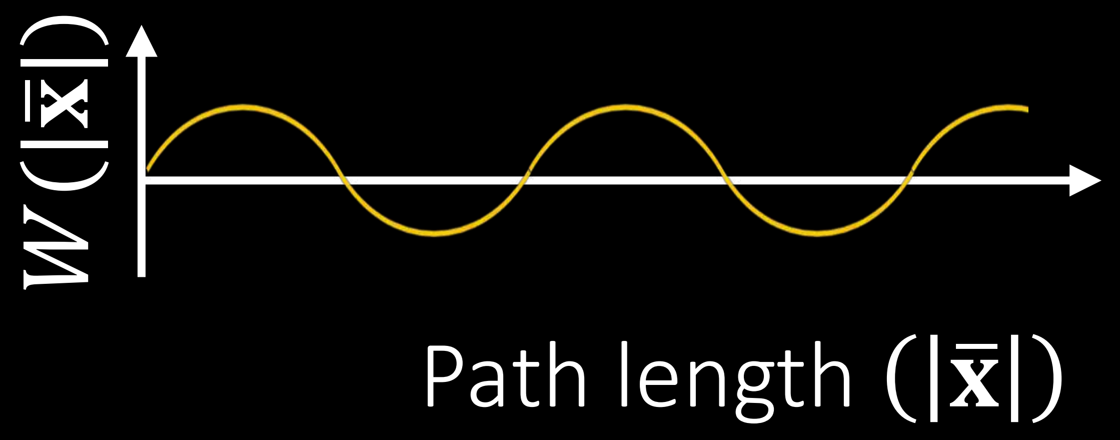

BDPT, PT, PM, KDE, etc

transient

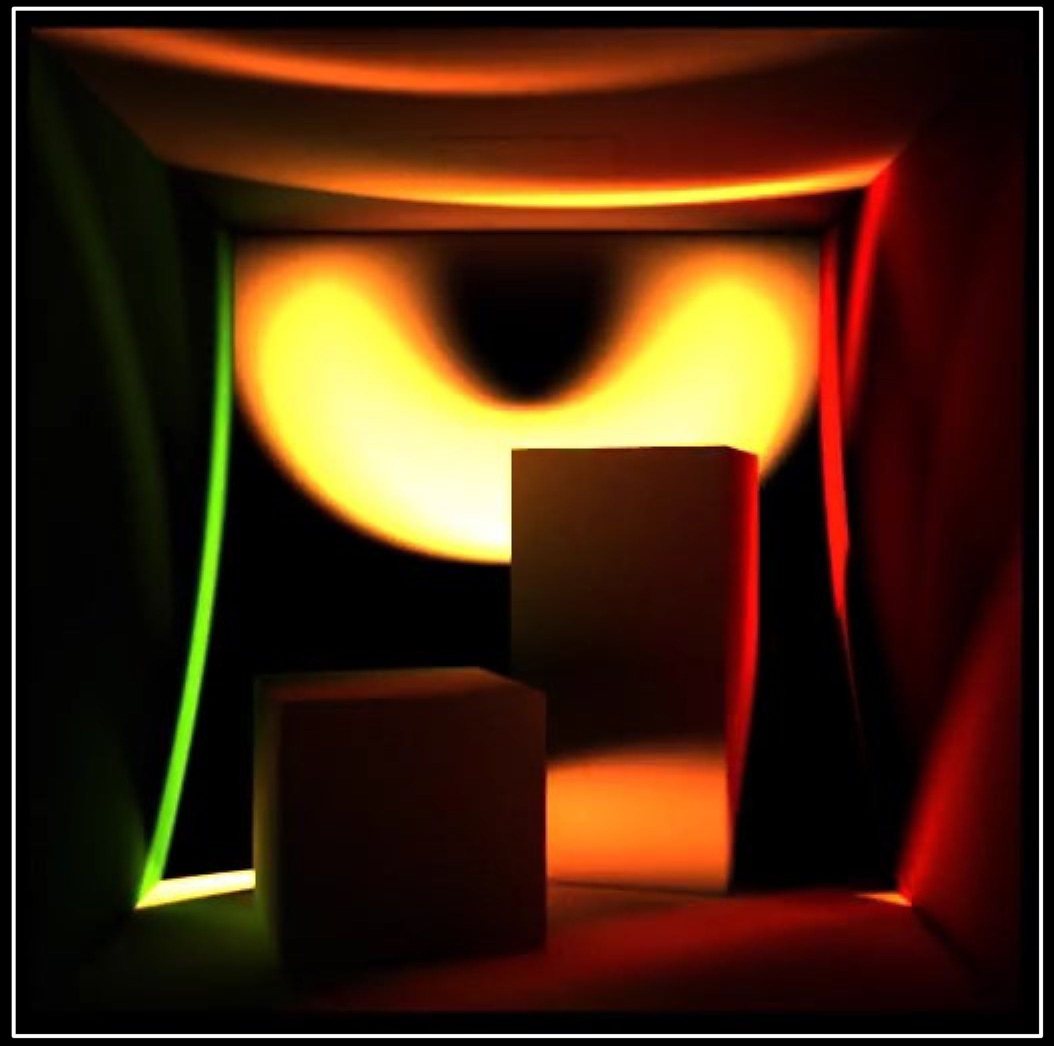

BDPT, PT, PM, KDE, etc
[Jarabo et al., 2014, 2017]
[Marco et al. 2017, 2018]

time-gated

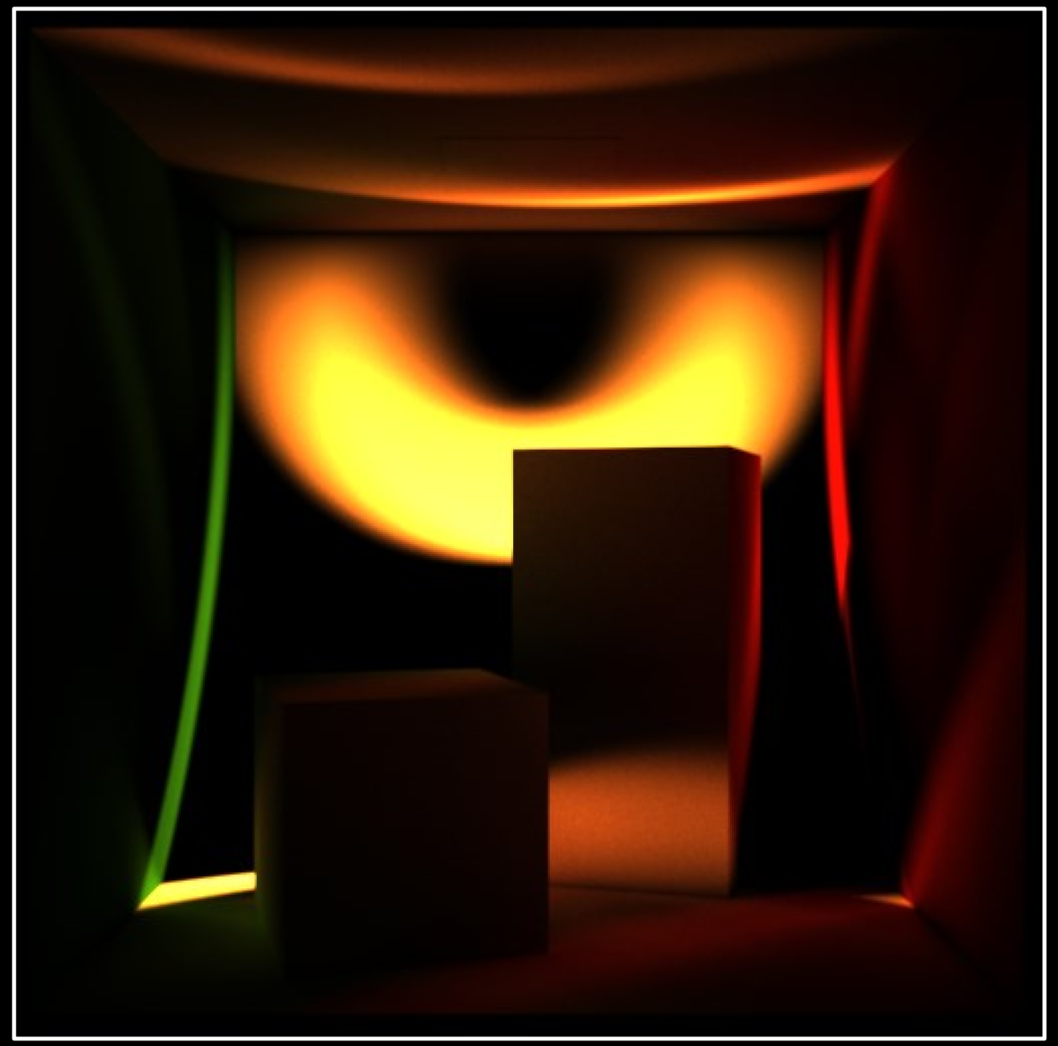

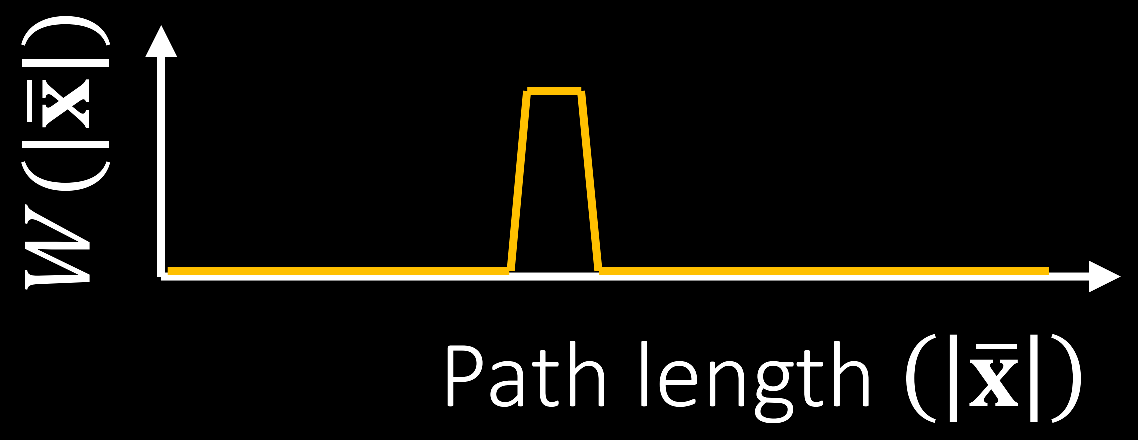

no efficient renderer

Path sampling for time-gated rendering is challenging

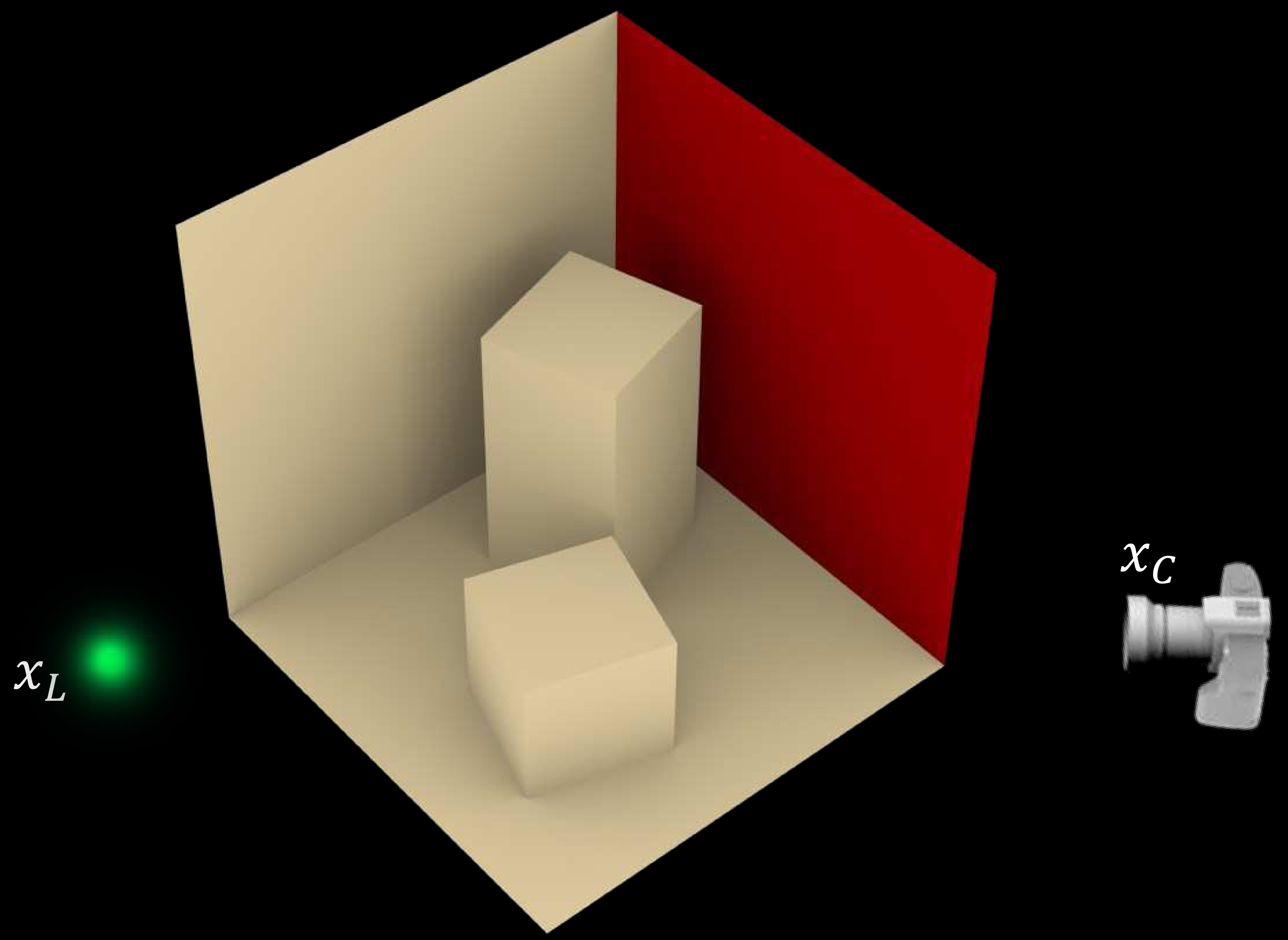

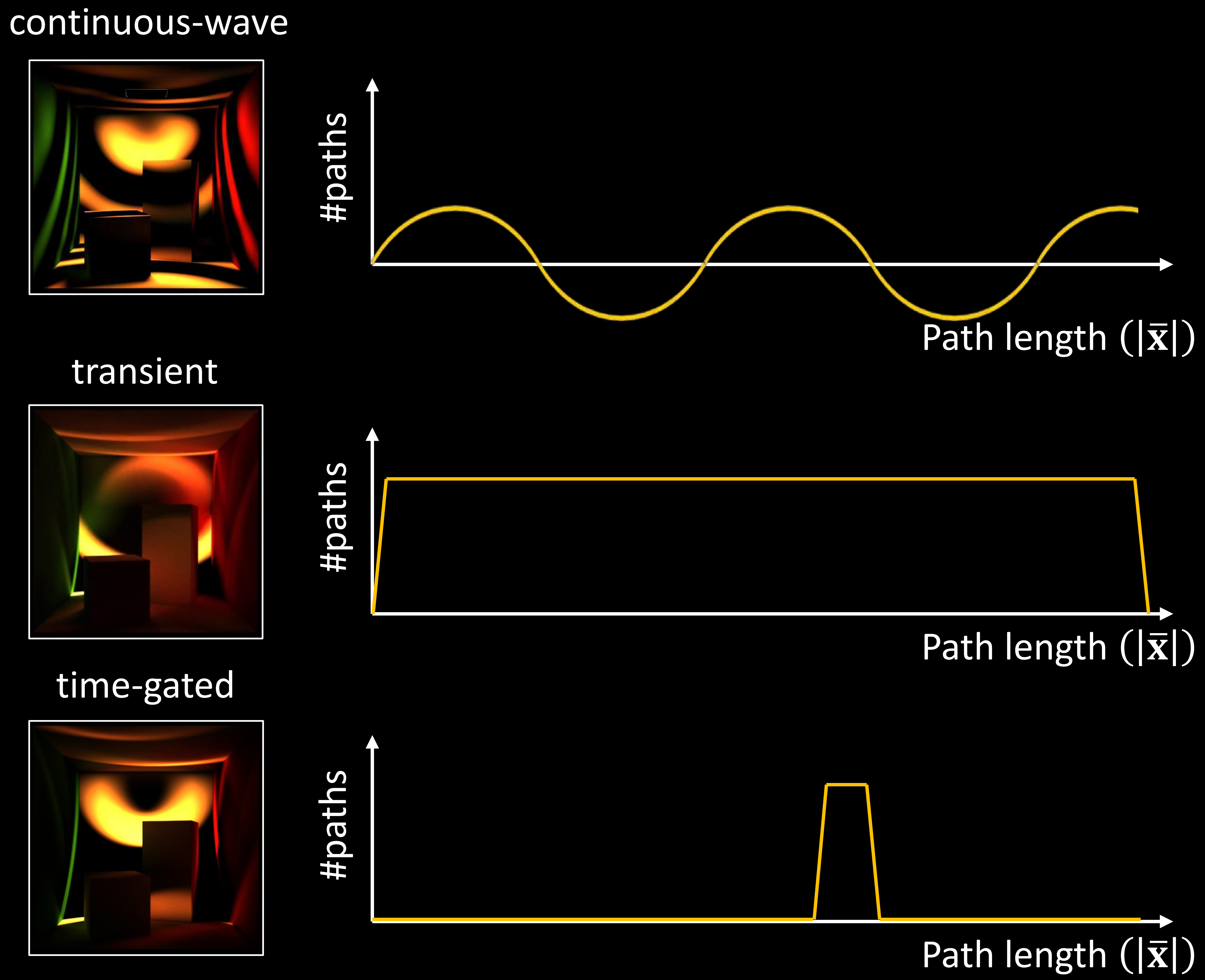

No control over path length

Path sampling for time-gated rendering is challenging

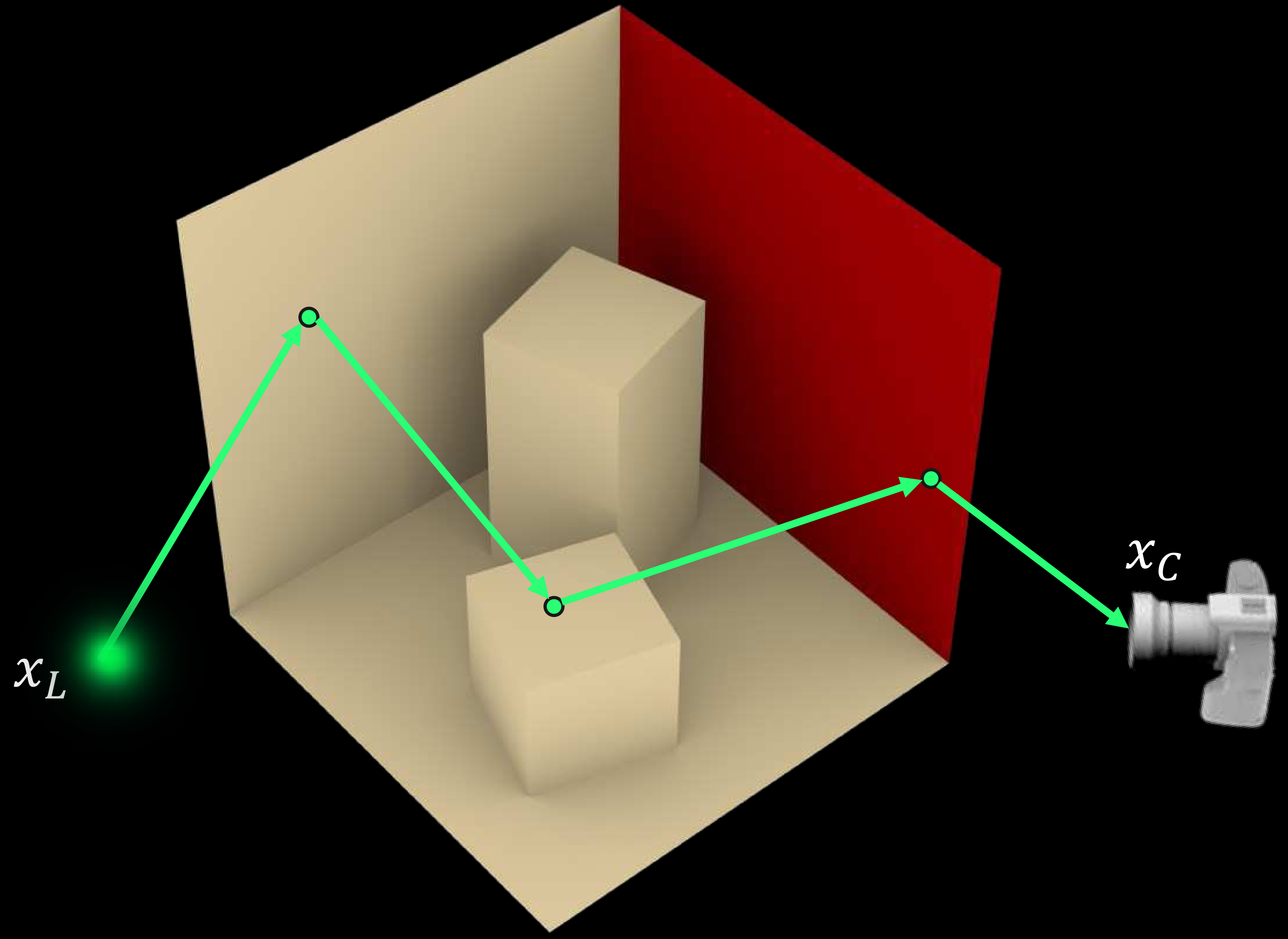

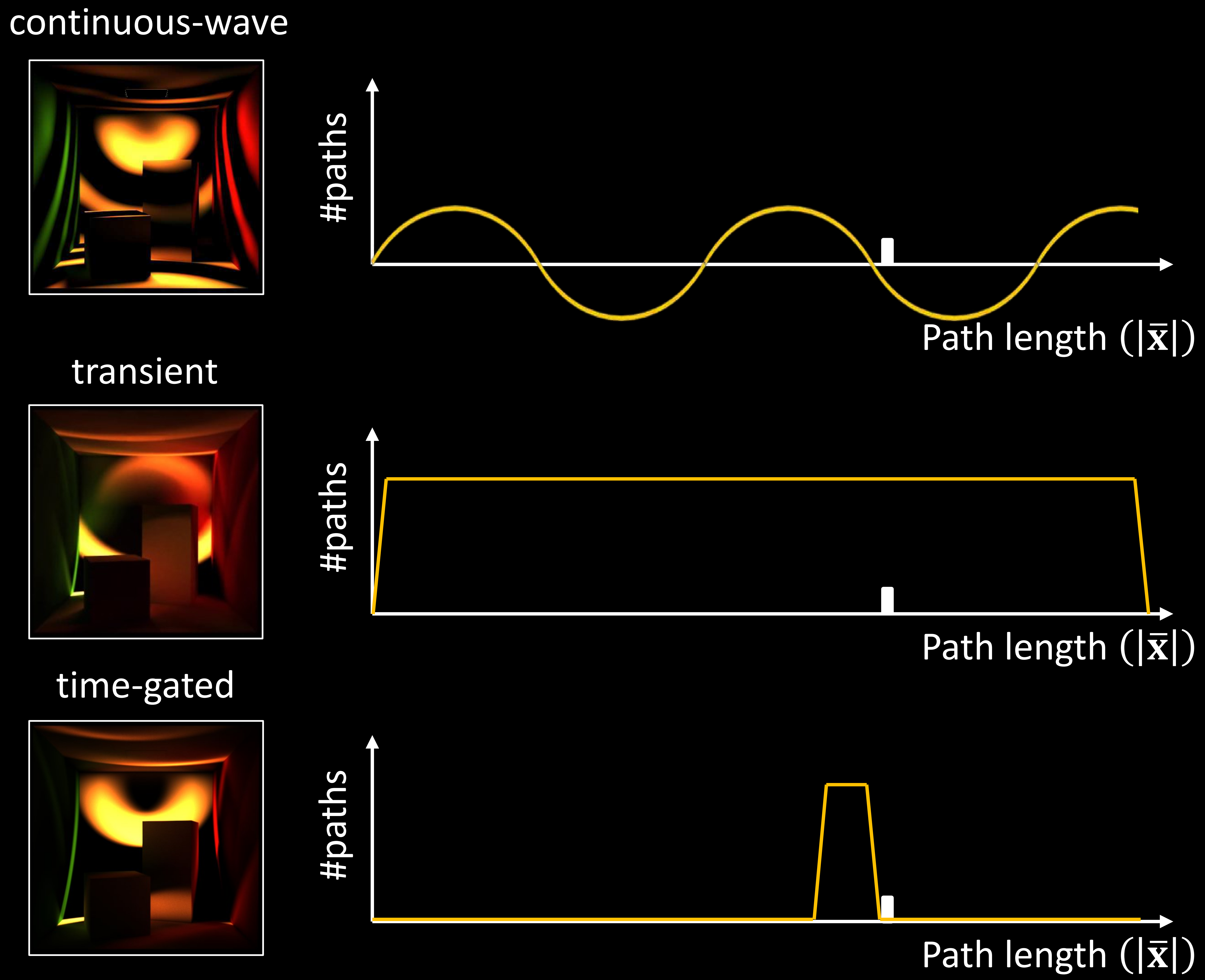

No control over path length

Path sampling for time-gated rendering is challenging

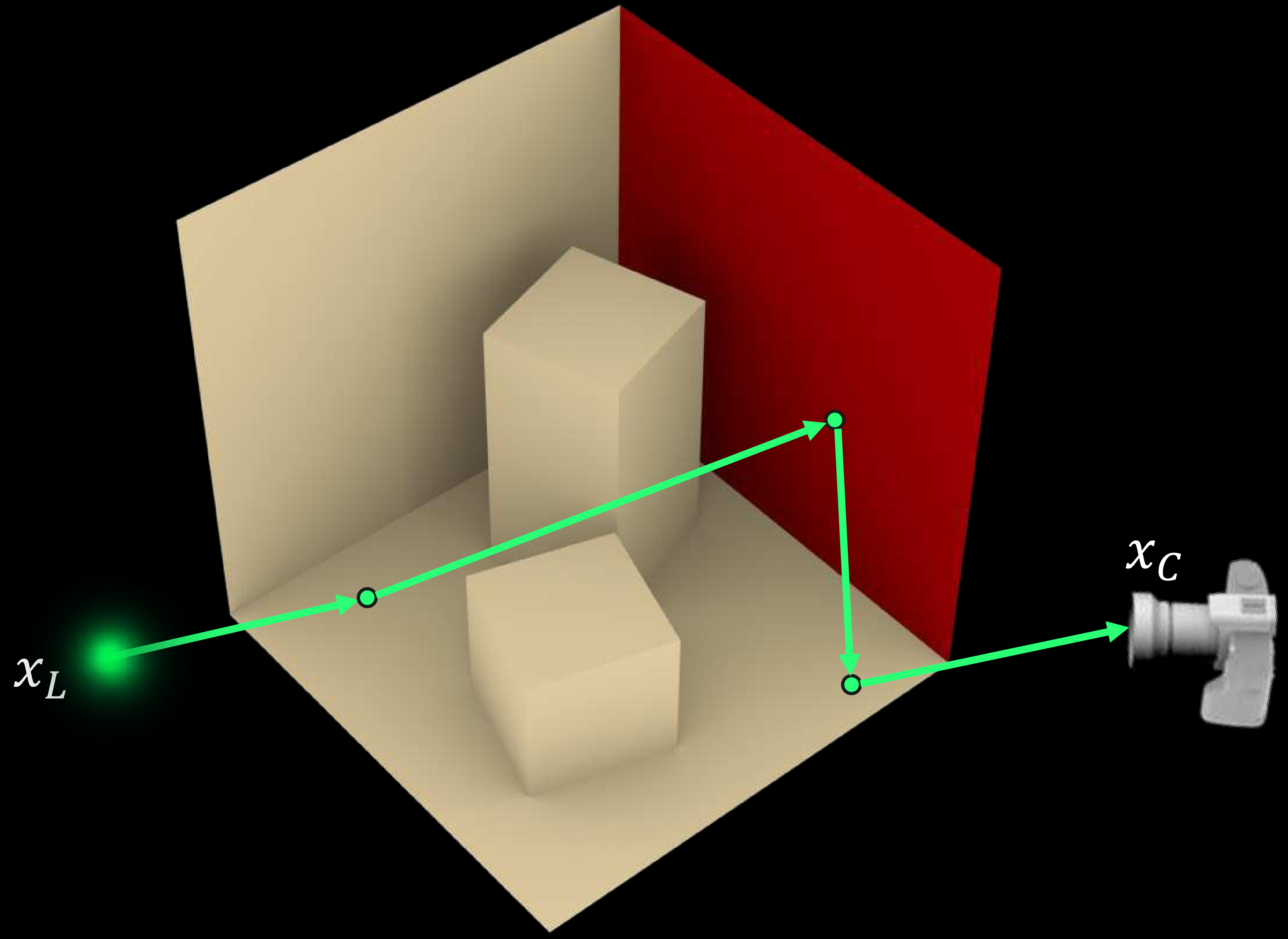

No control over path length

continuous-wave

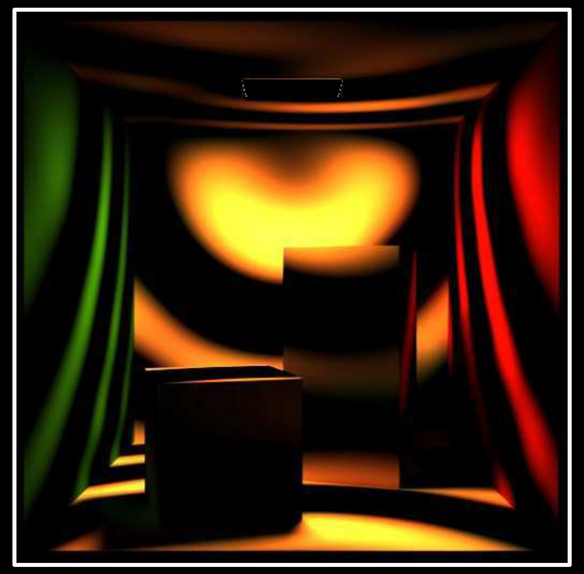

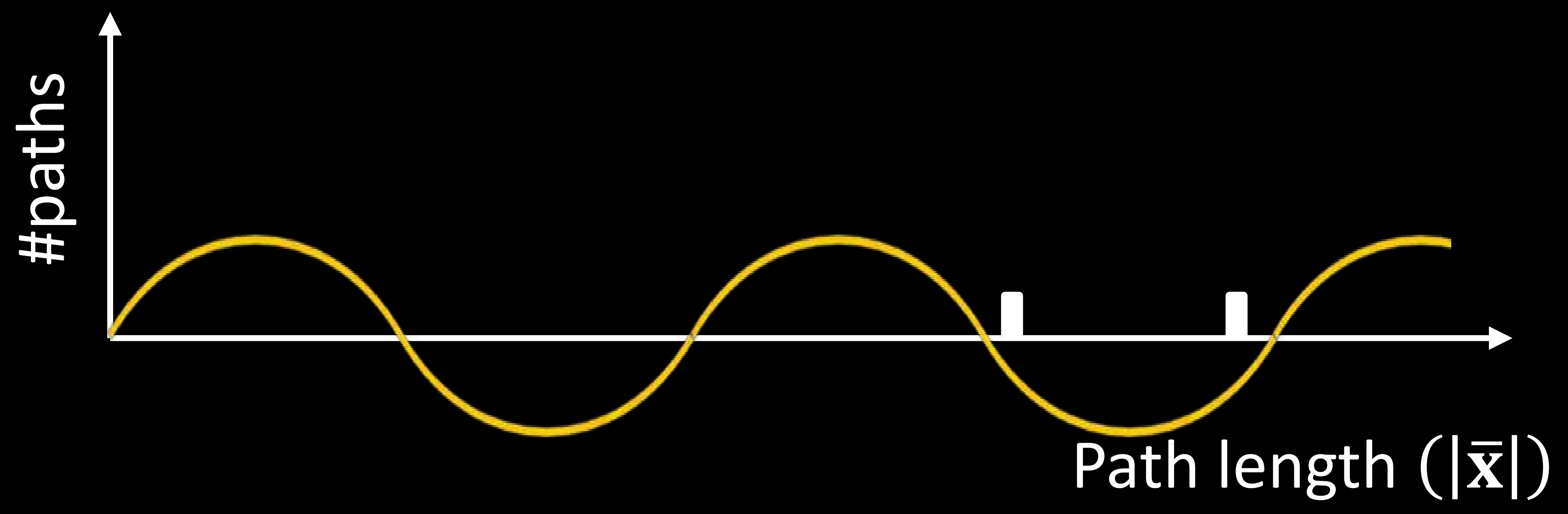

transient

time-gated

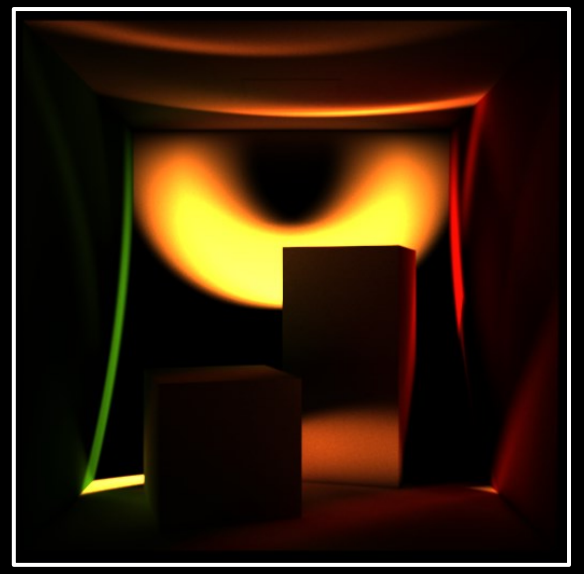

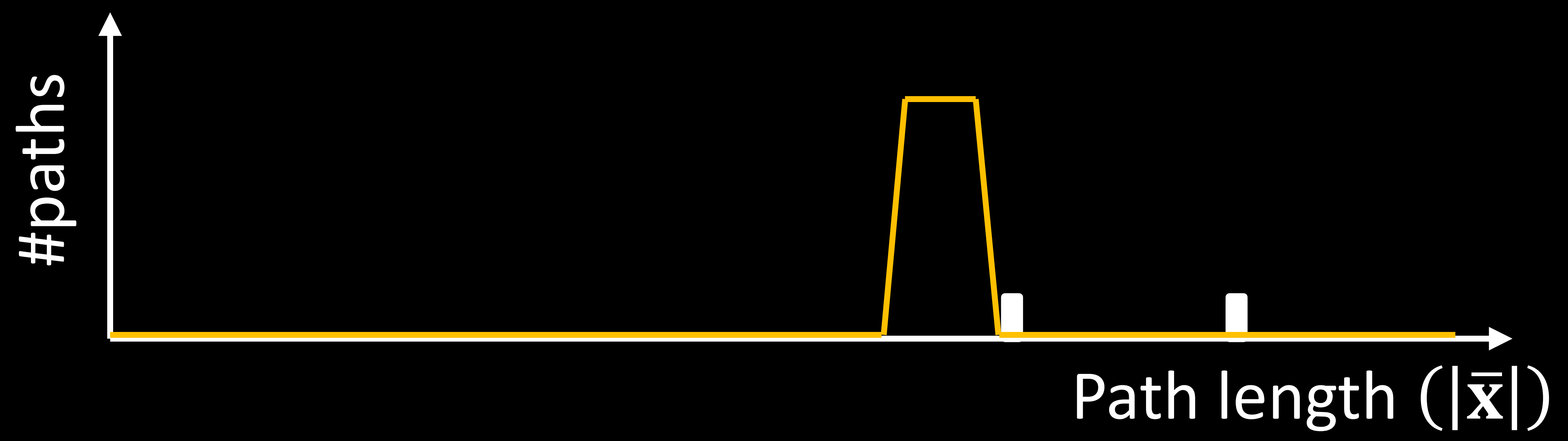

Path sampling for time-gated rendering is challenging

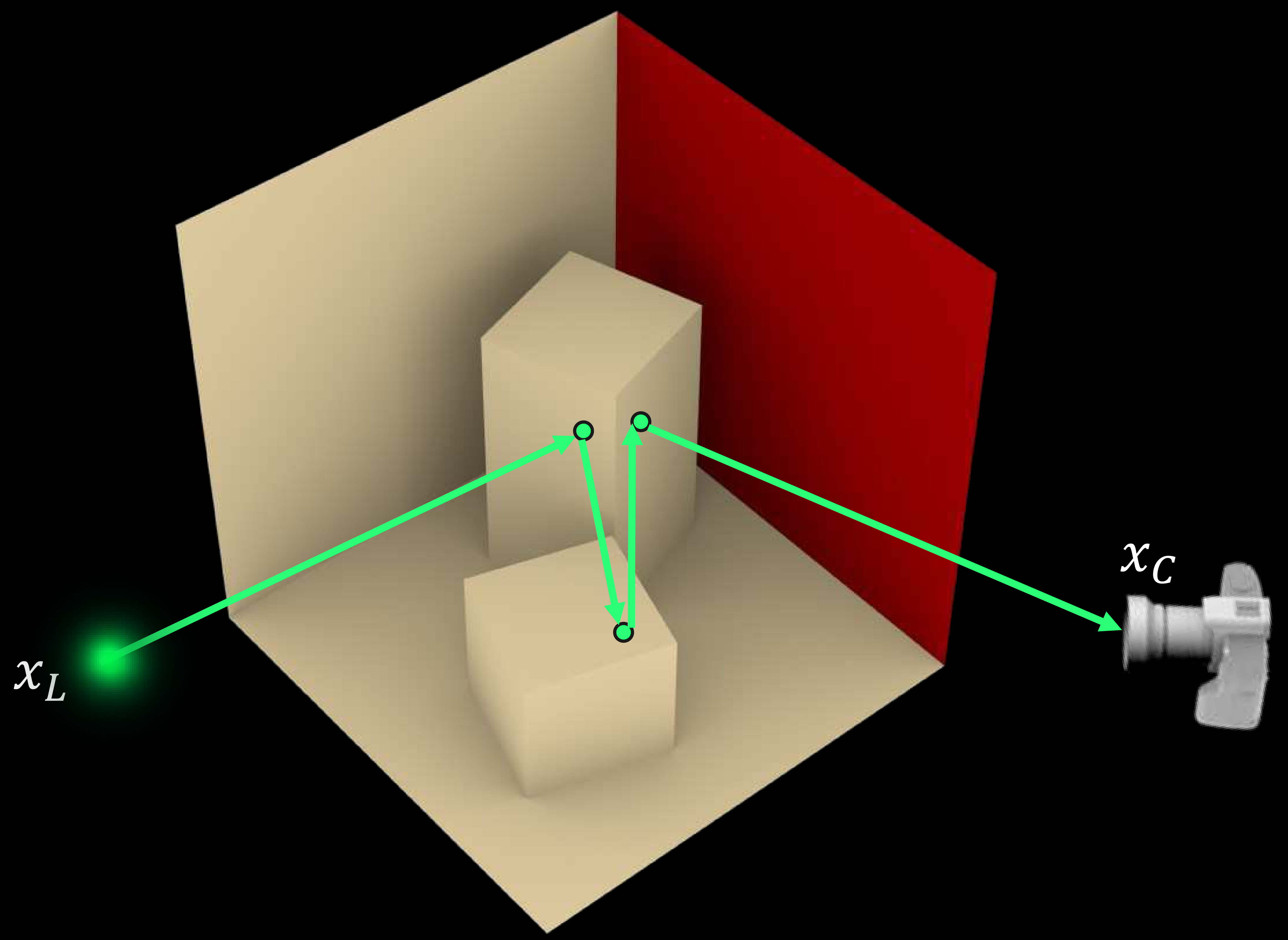

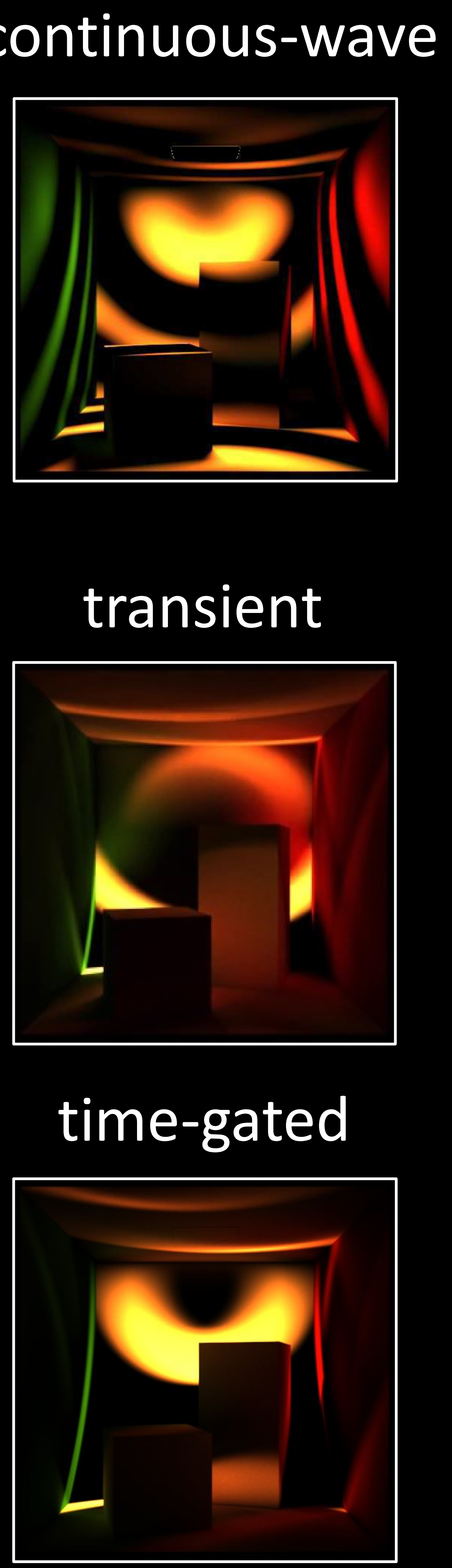

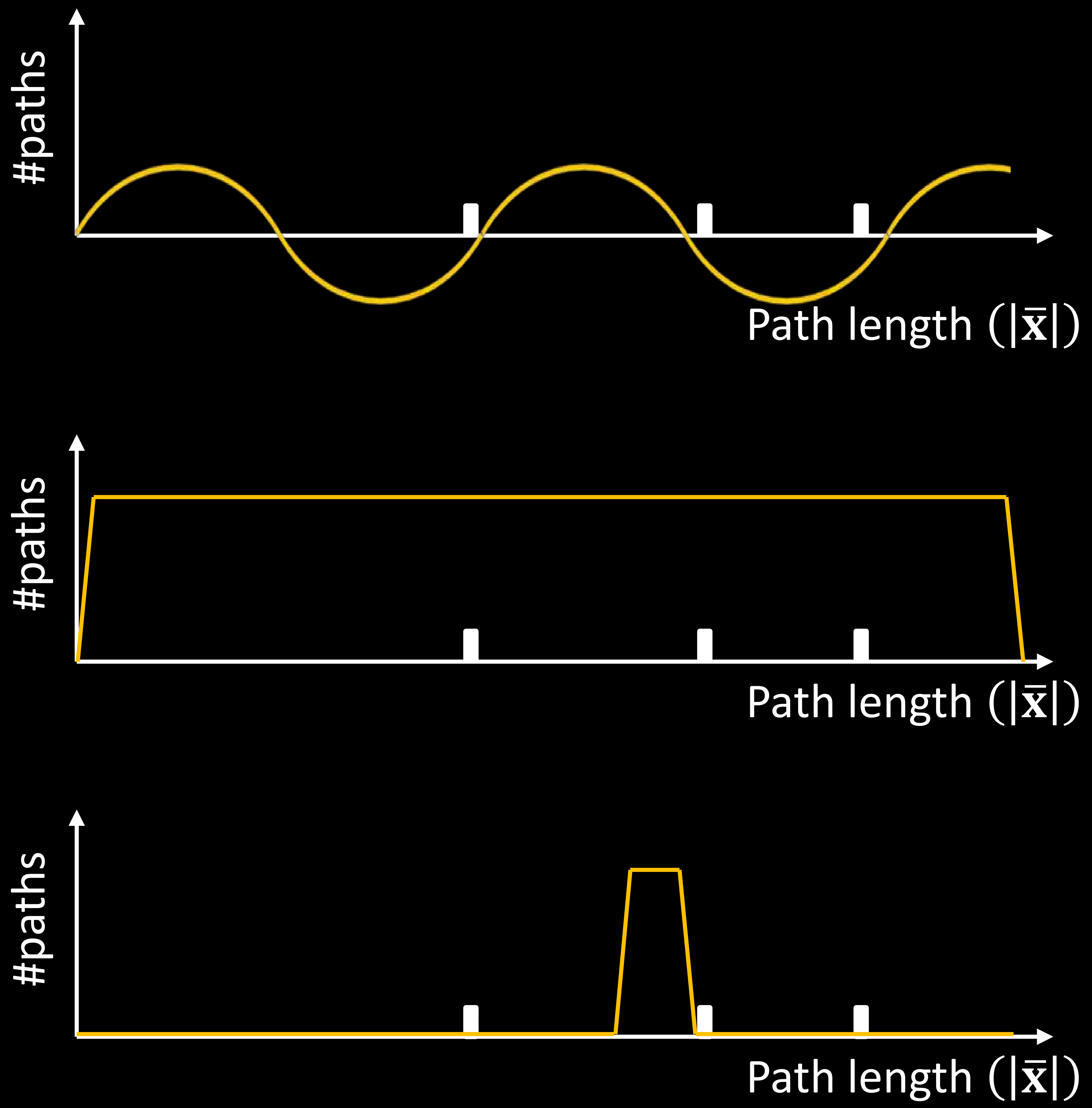

No control over path length

Path sampling for time-gated rendering is challenging

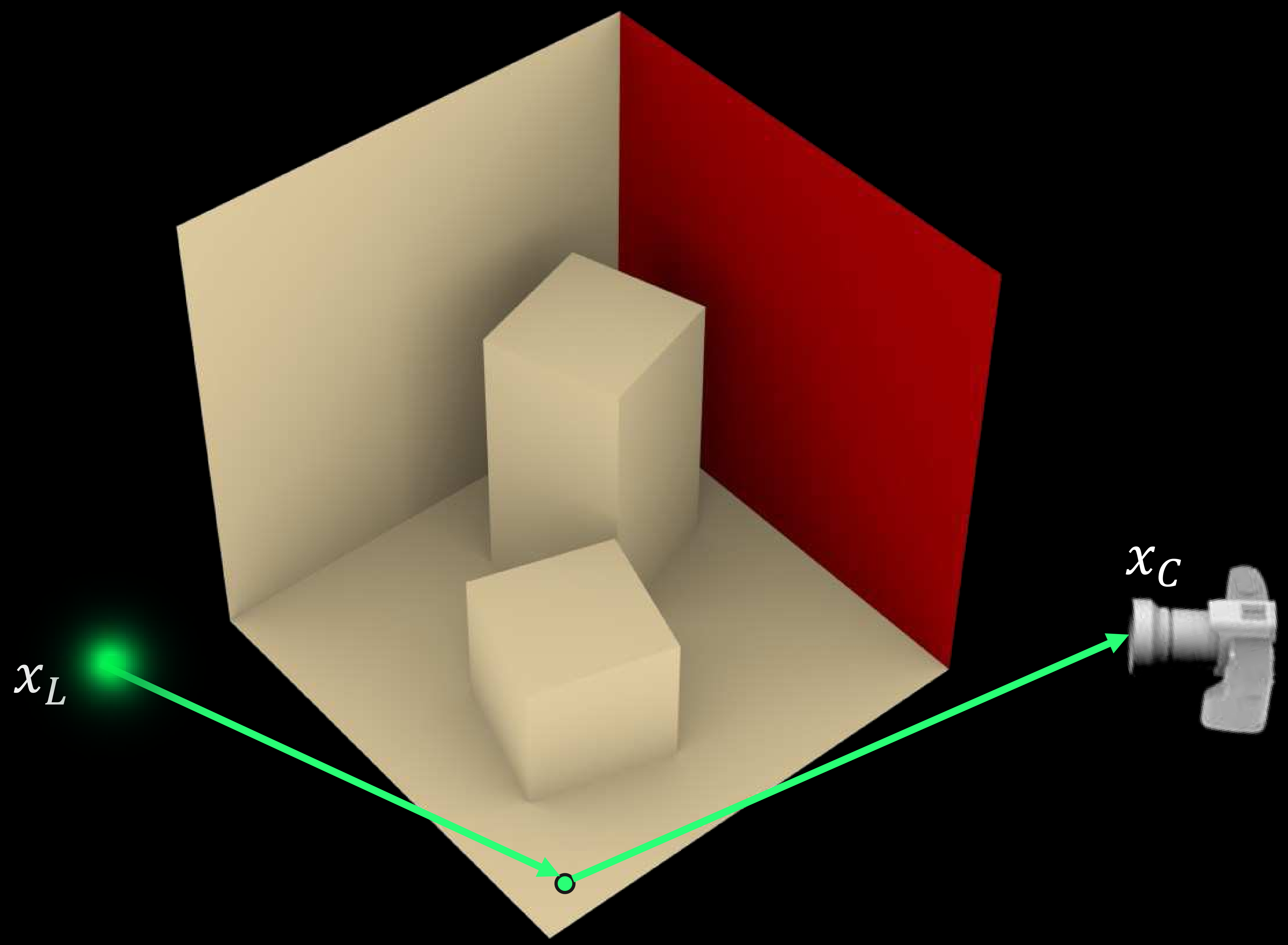

No control over path length

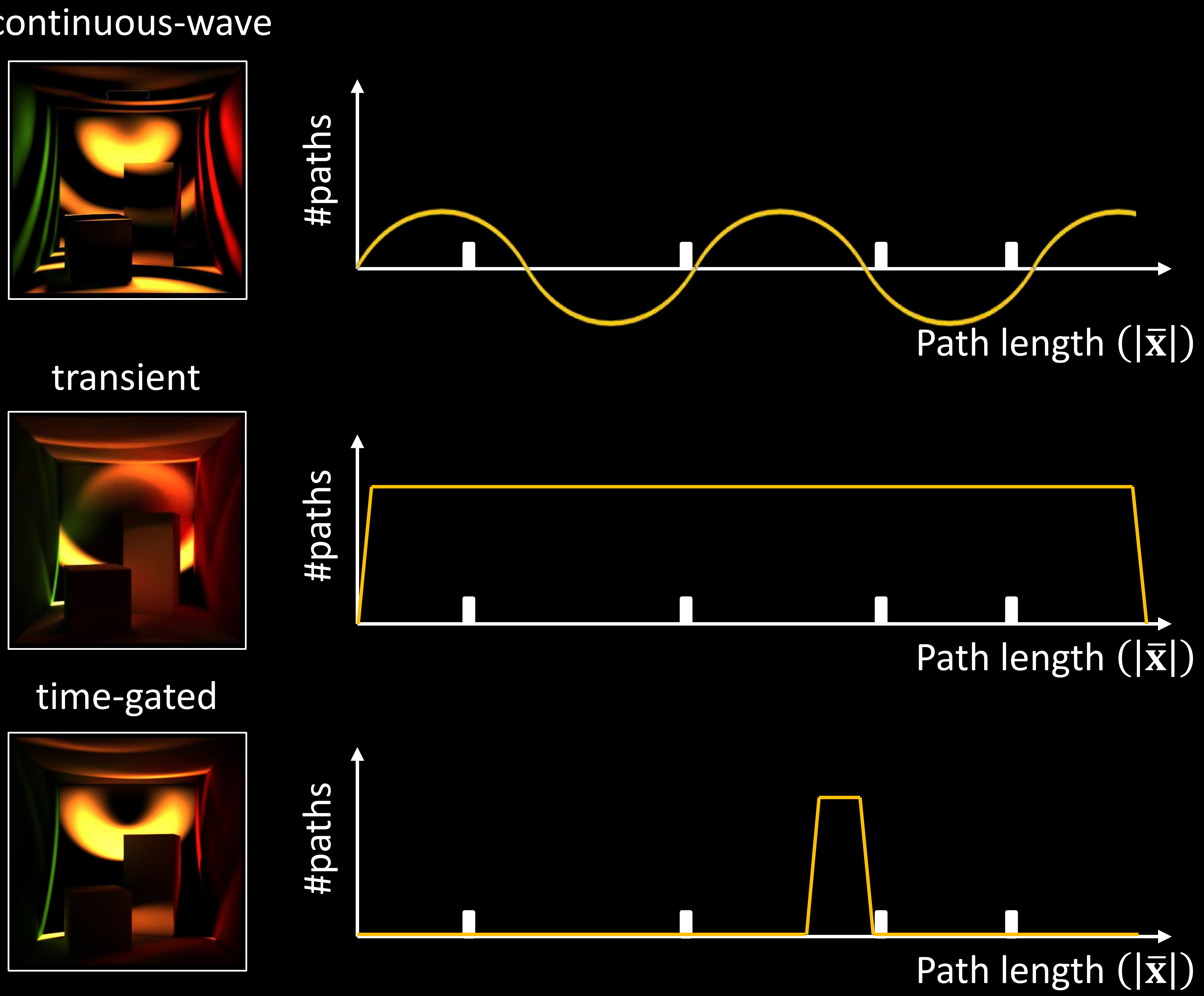

Path sampling for time-gated rendering is challenging

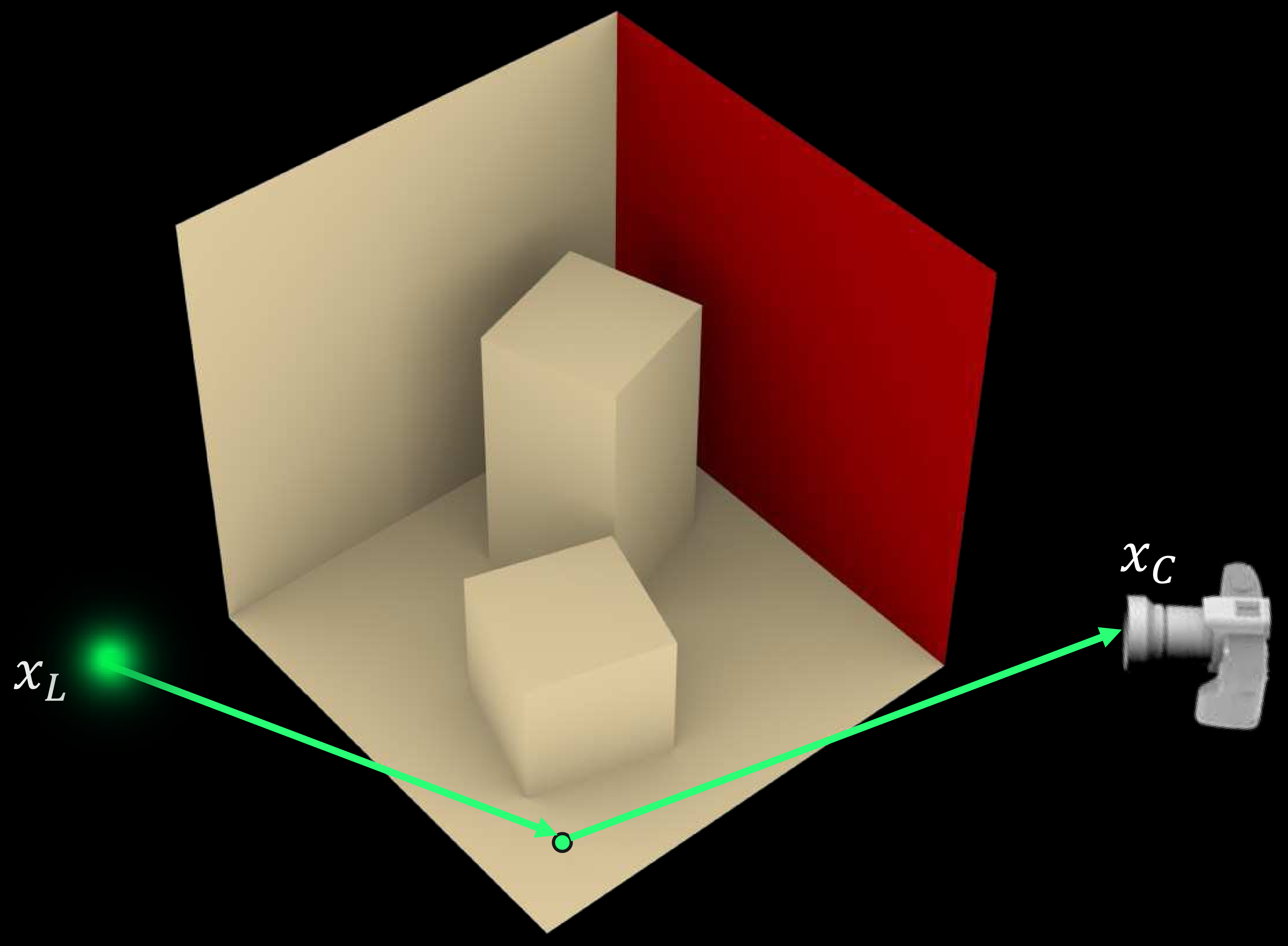

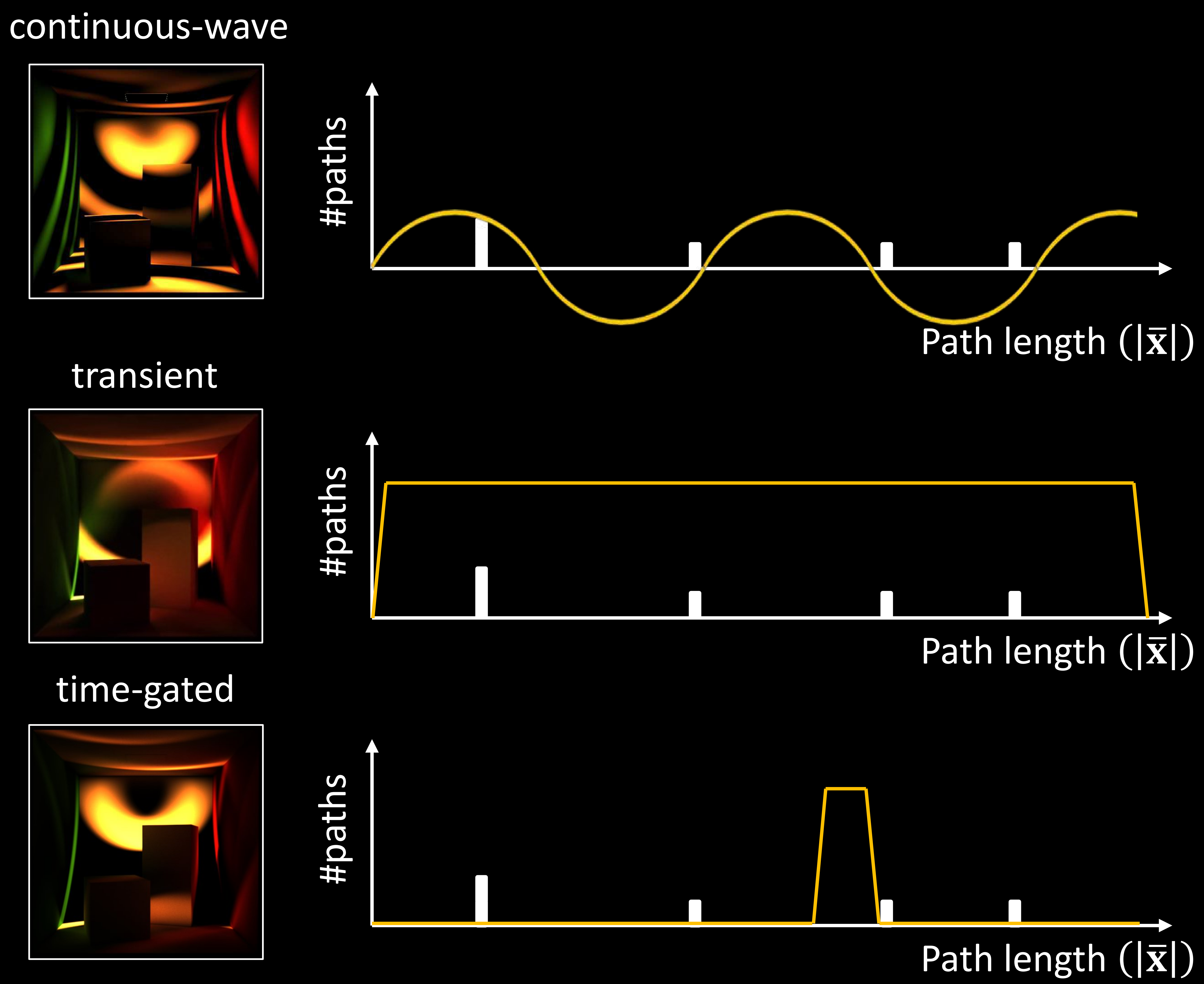

No control over path length

Path sampling for time-gated rendering is challenging

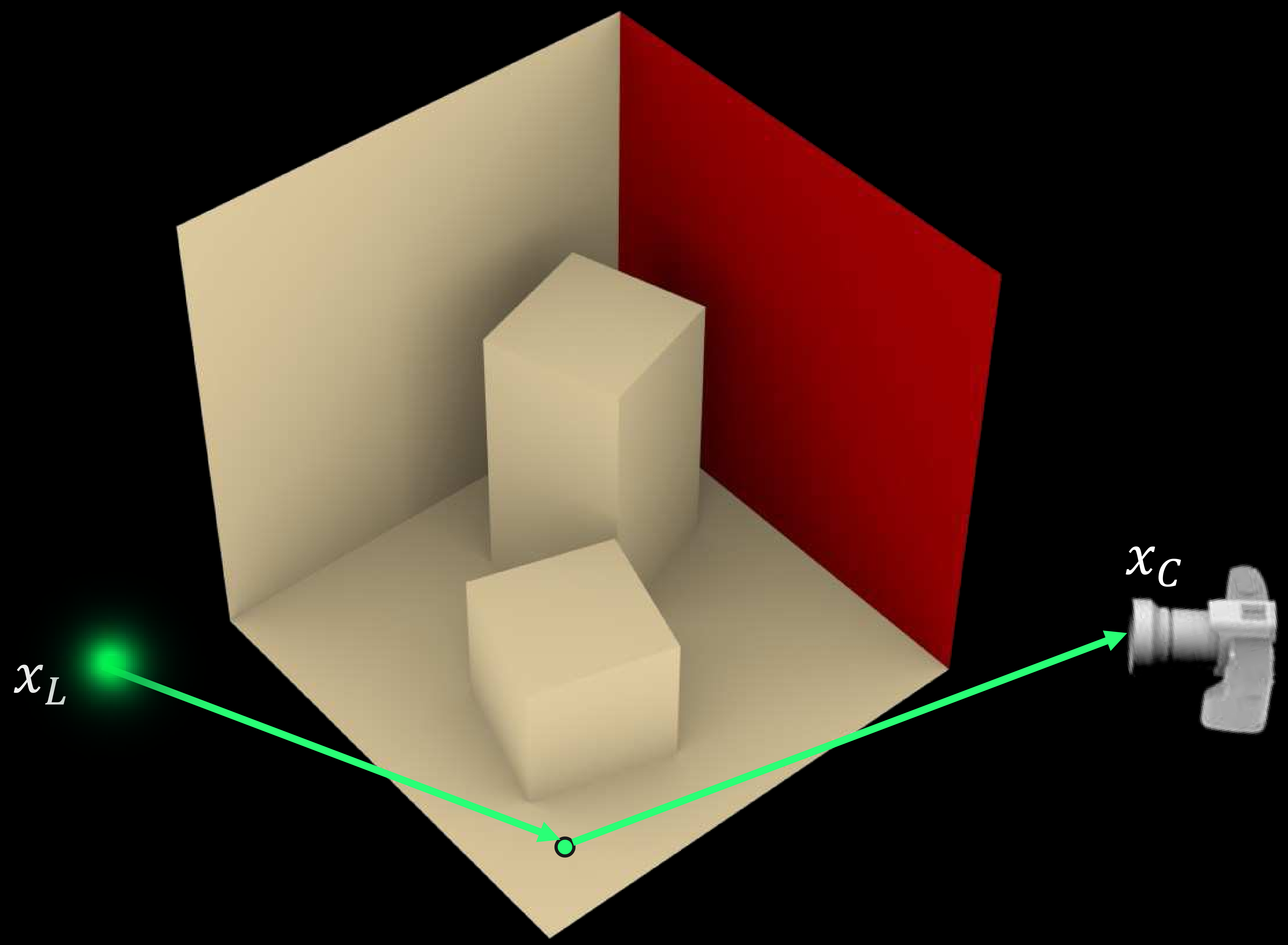

continuous-wave

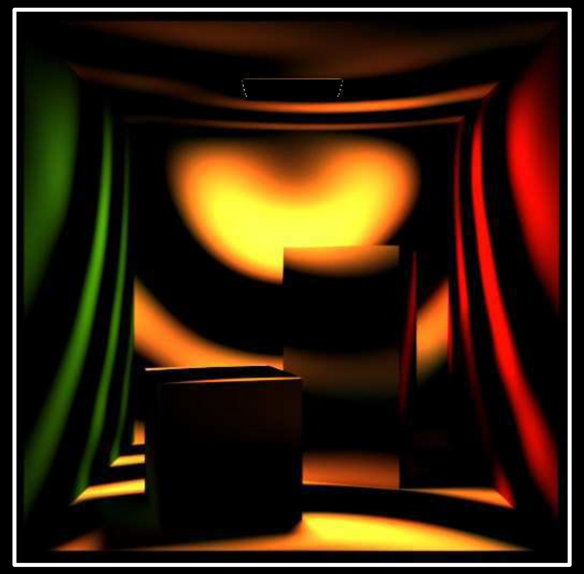

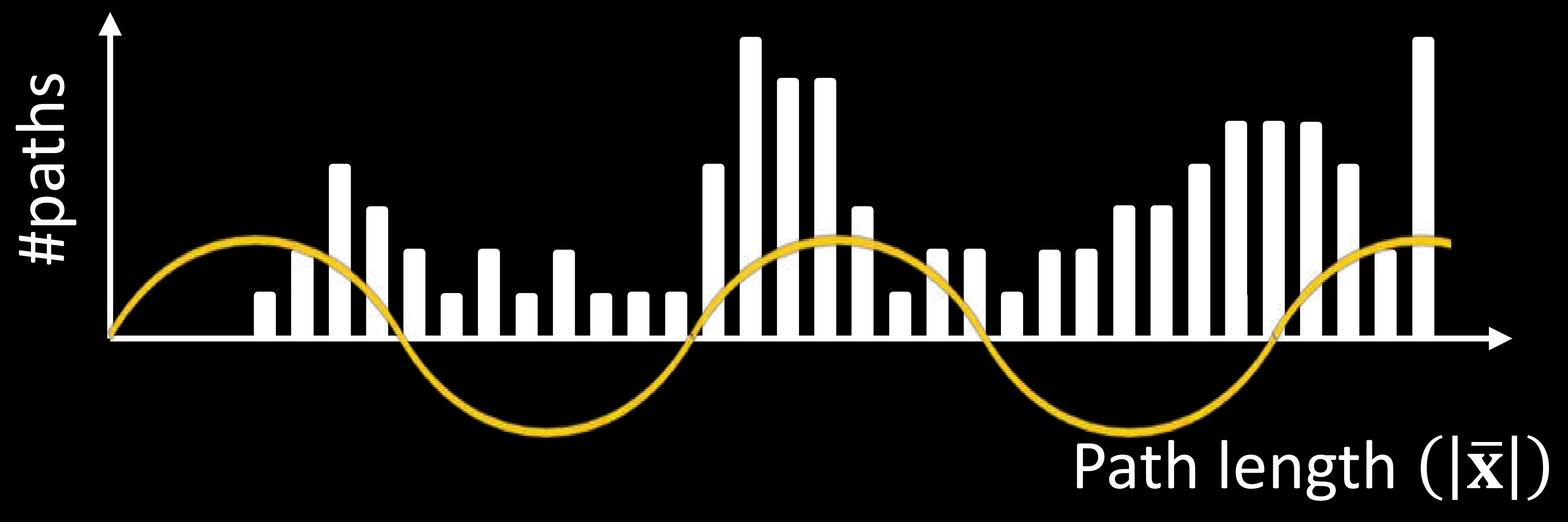

transient

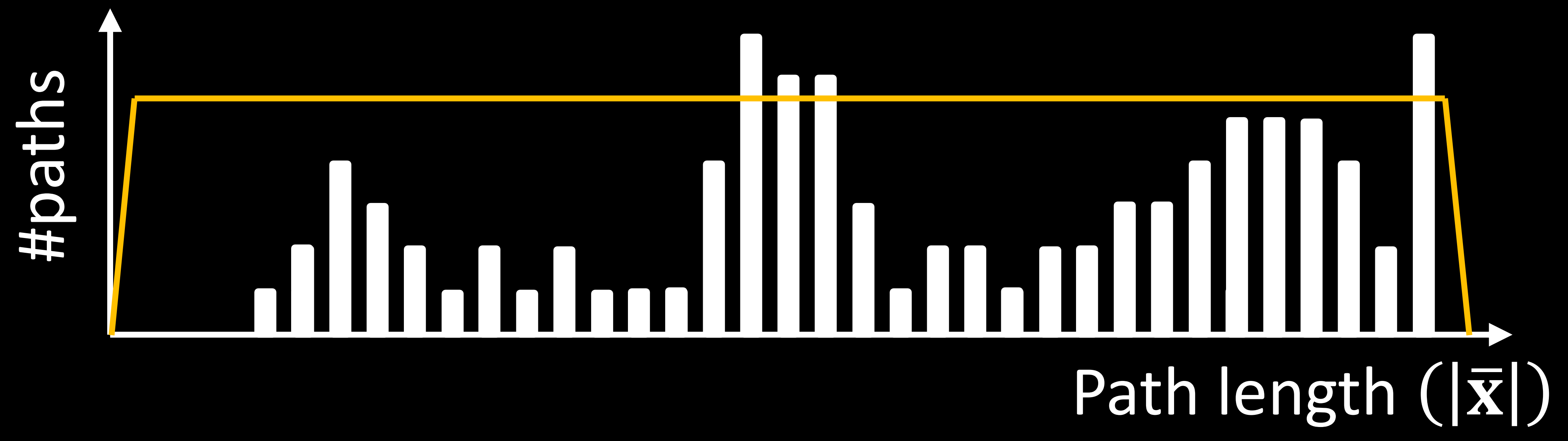

time-gated

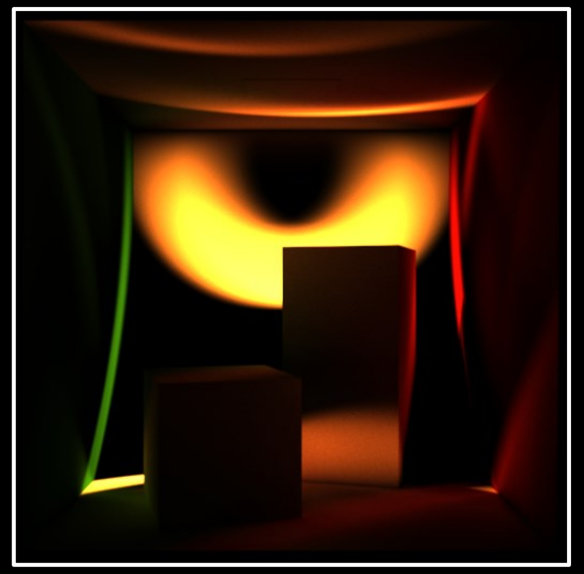

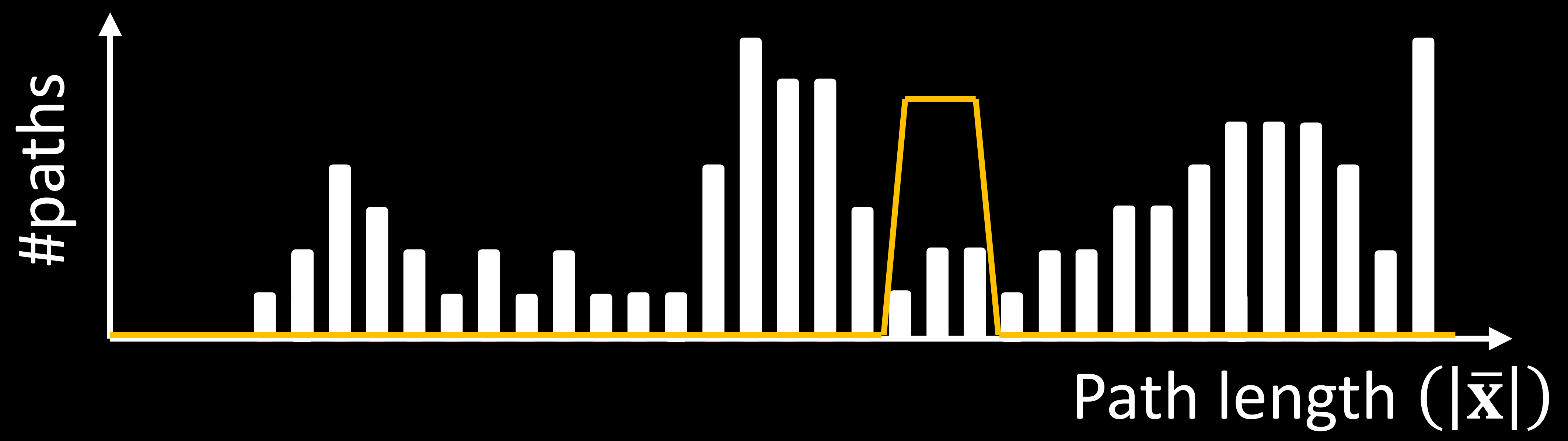

No control over path length

Path sampling for time-gated rendering is challenging

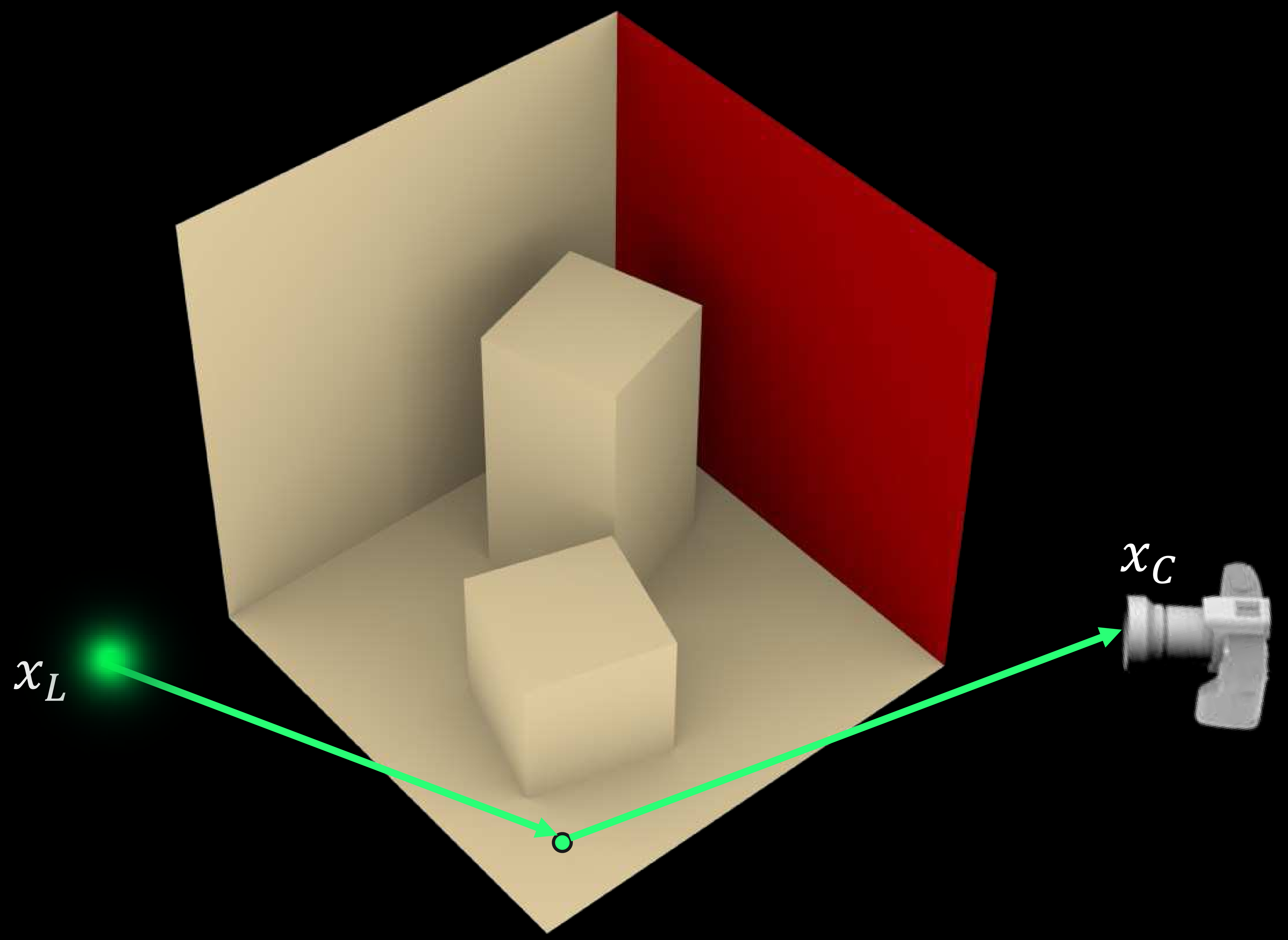

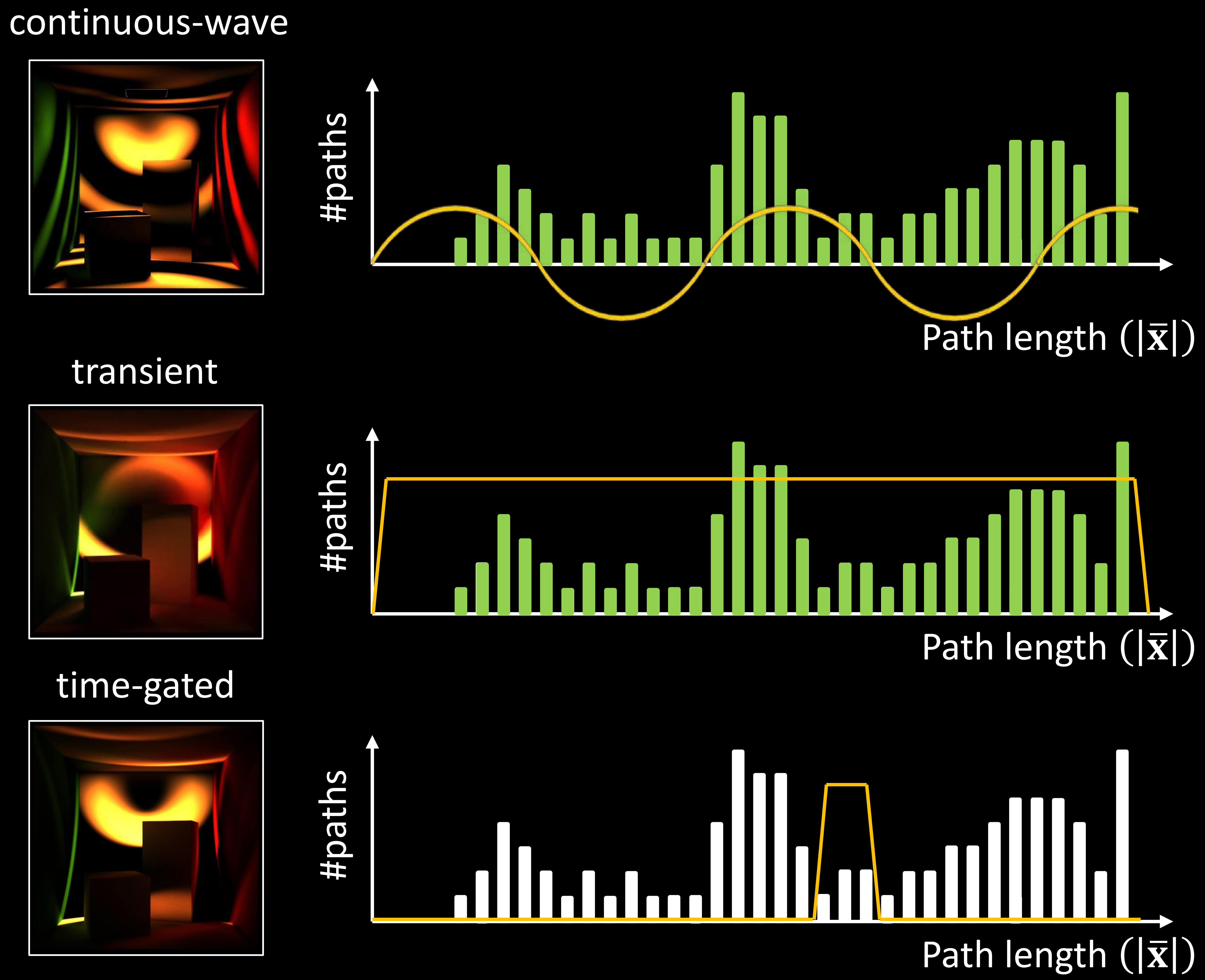

No control over path length

Path sampling for time-gated rendering is challenging

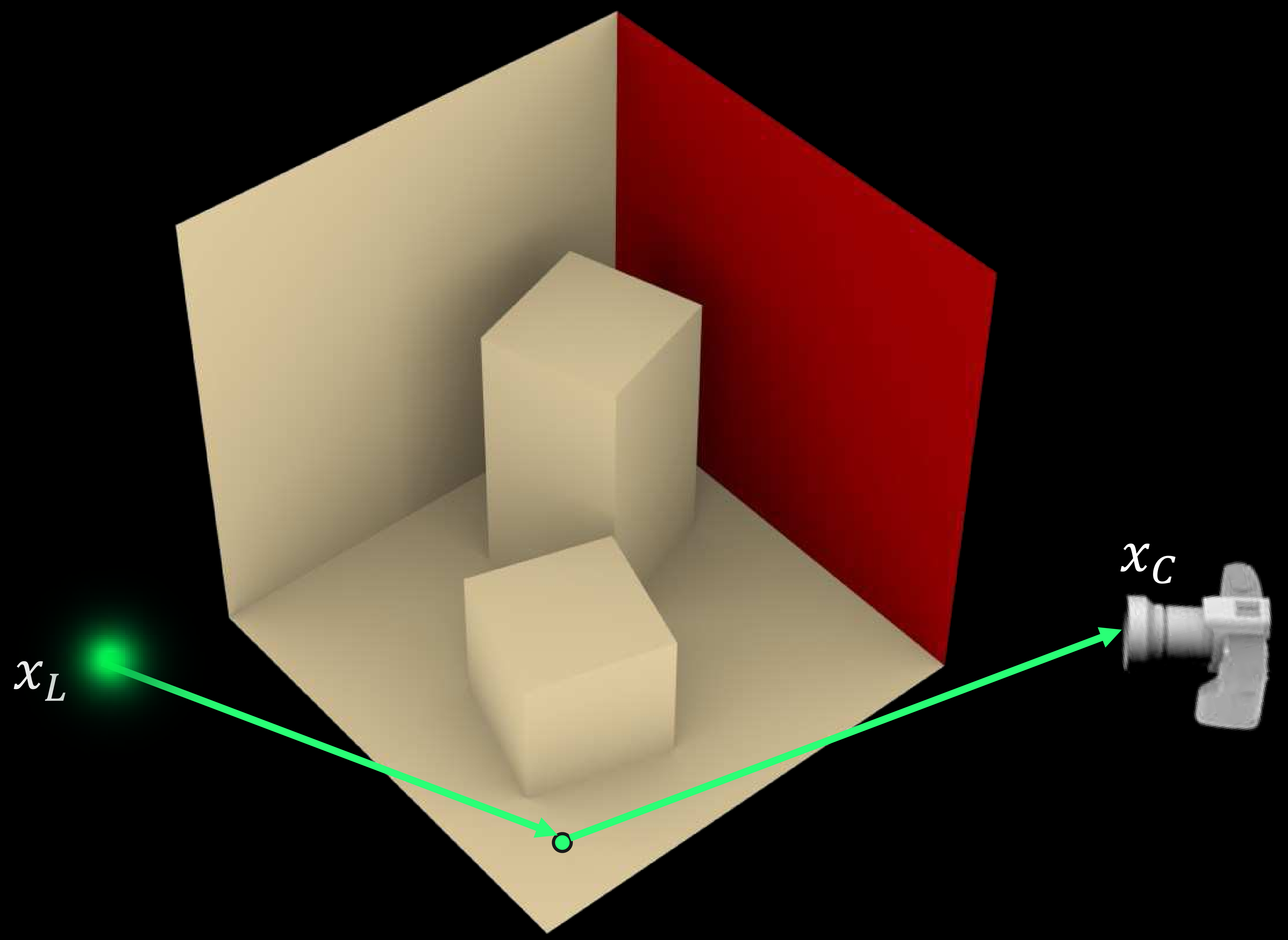

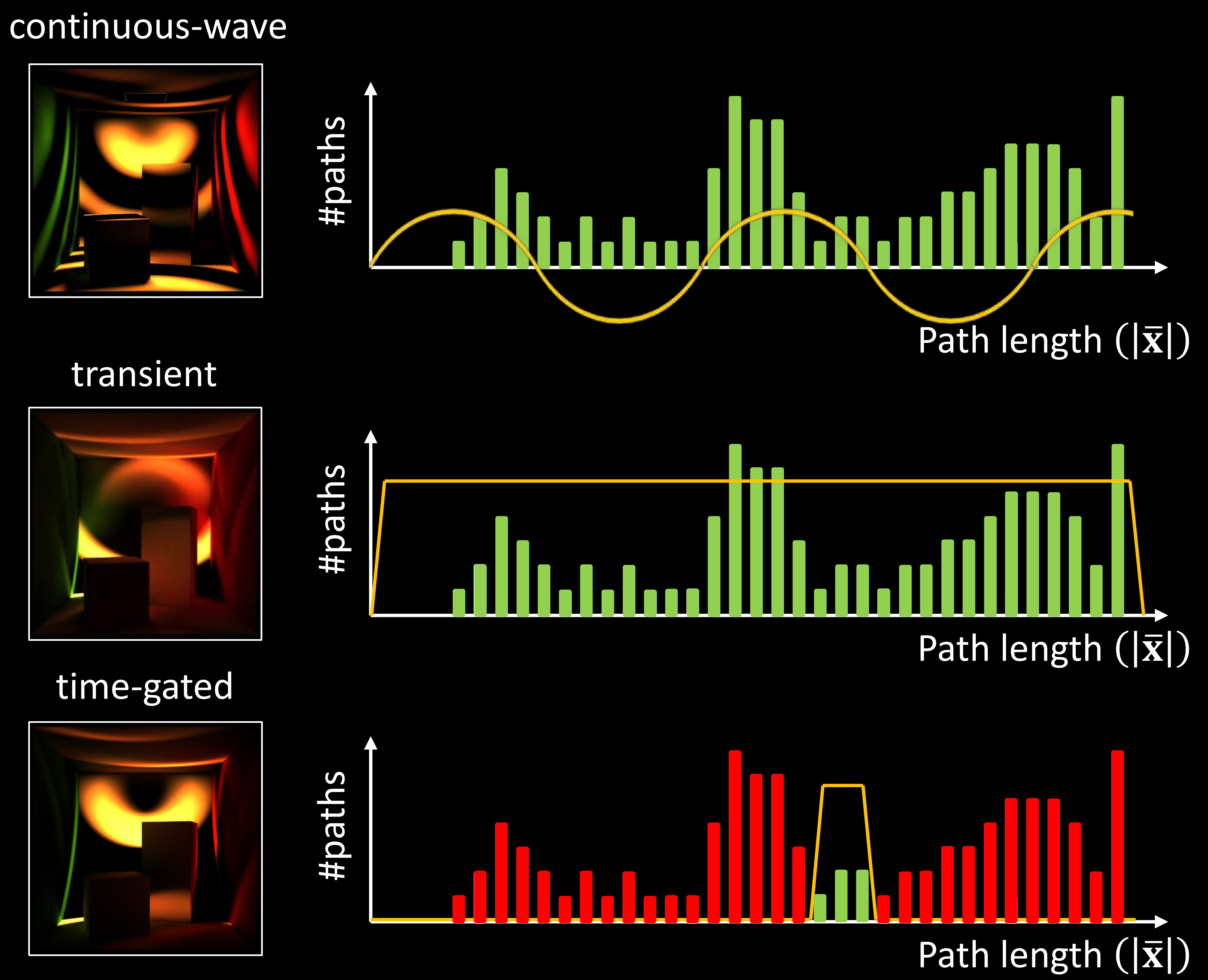

No control over path length

Path sampling for time-gated rendering is challenging

No control over path length

Path sampling for time-gated case

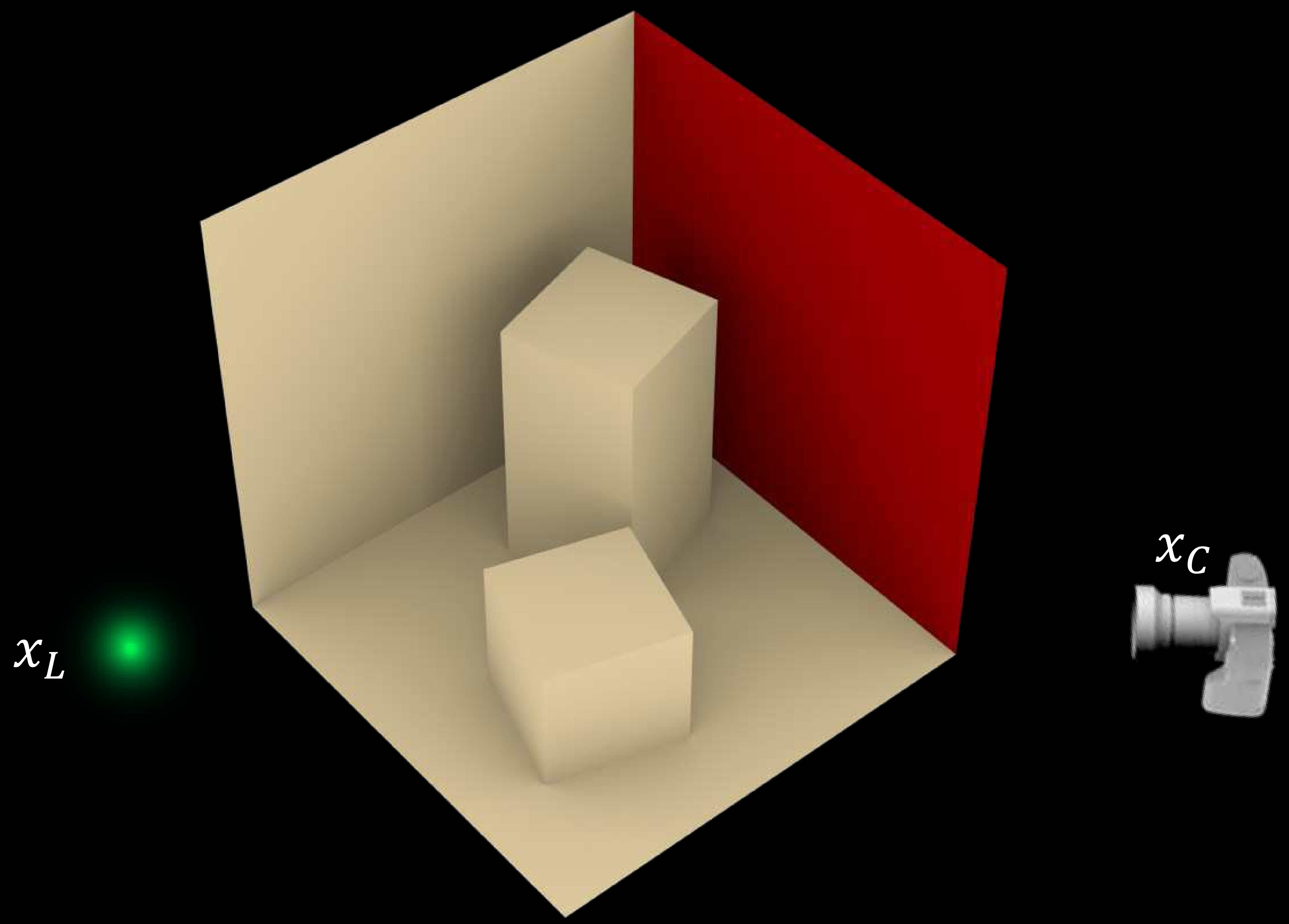

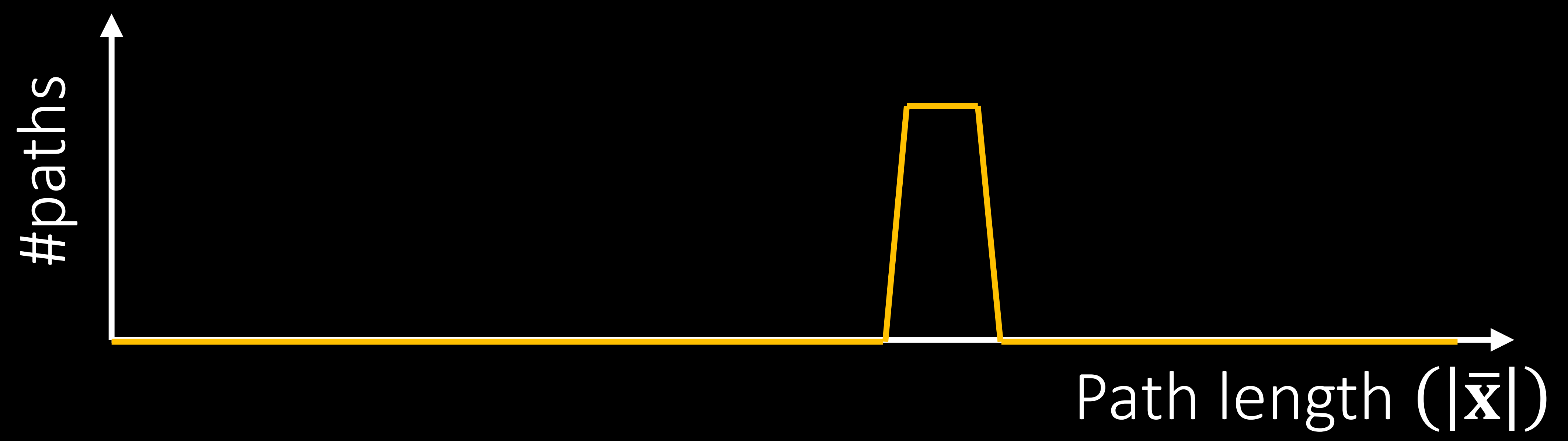

Path sampling for time-gated case

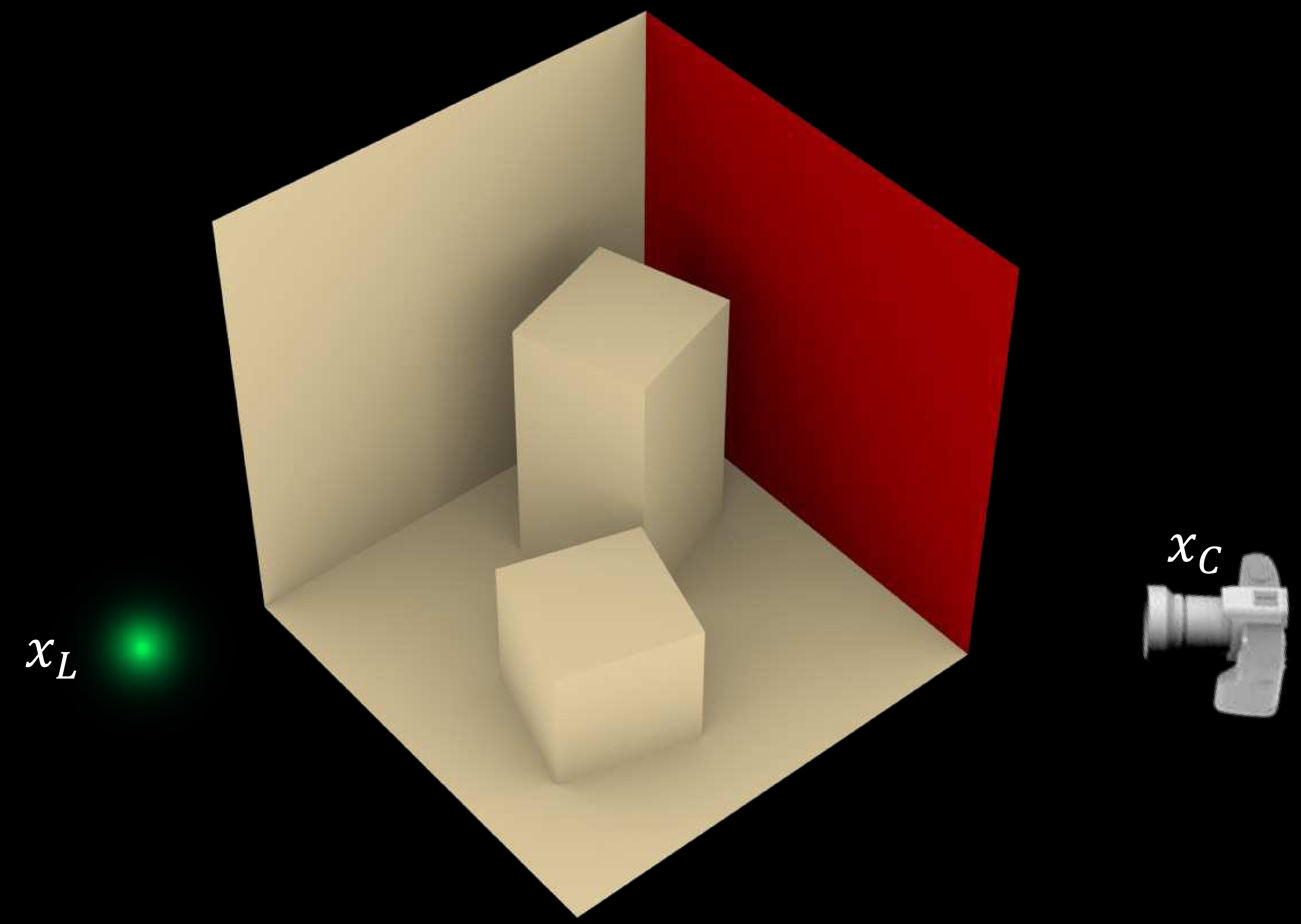

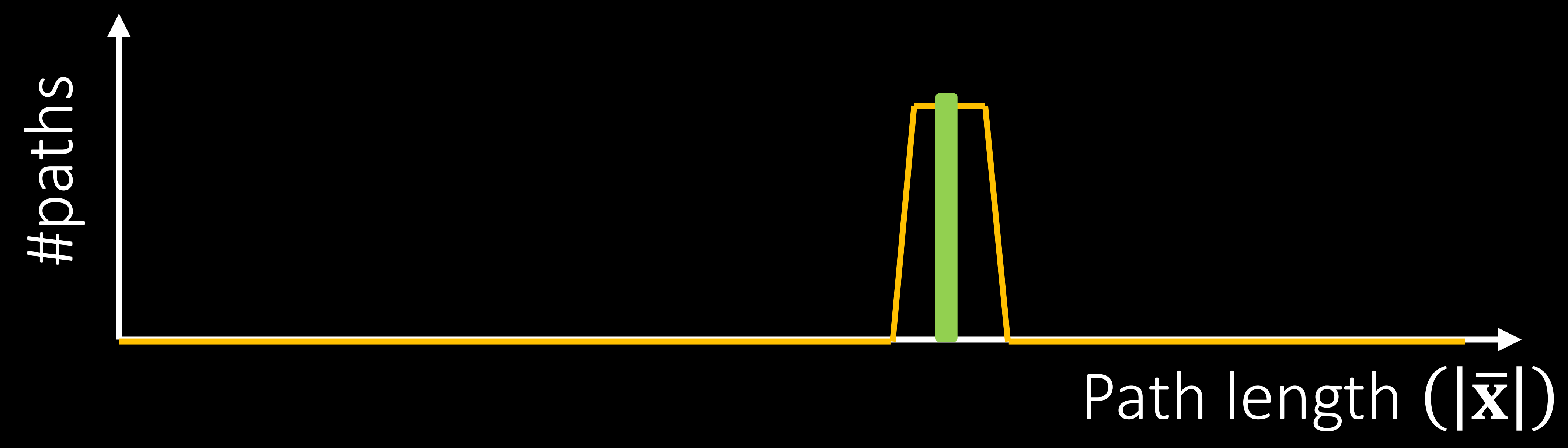

step 1: sample path length $|\bar{\mathbf{x}}|$

Path sampling for time-gated case

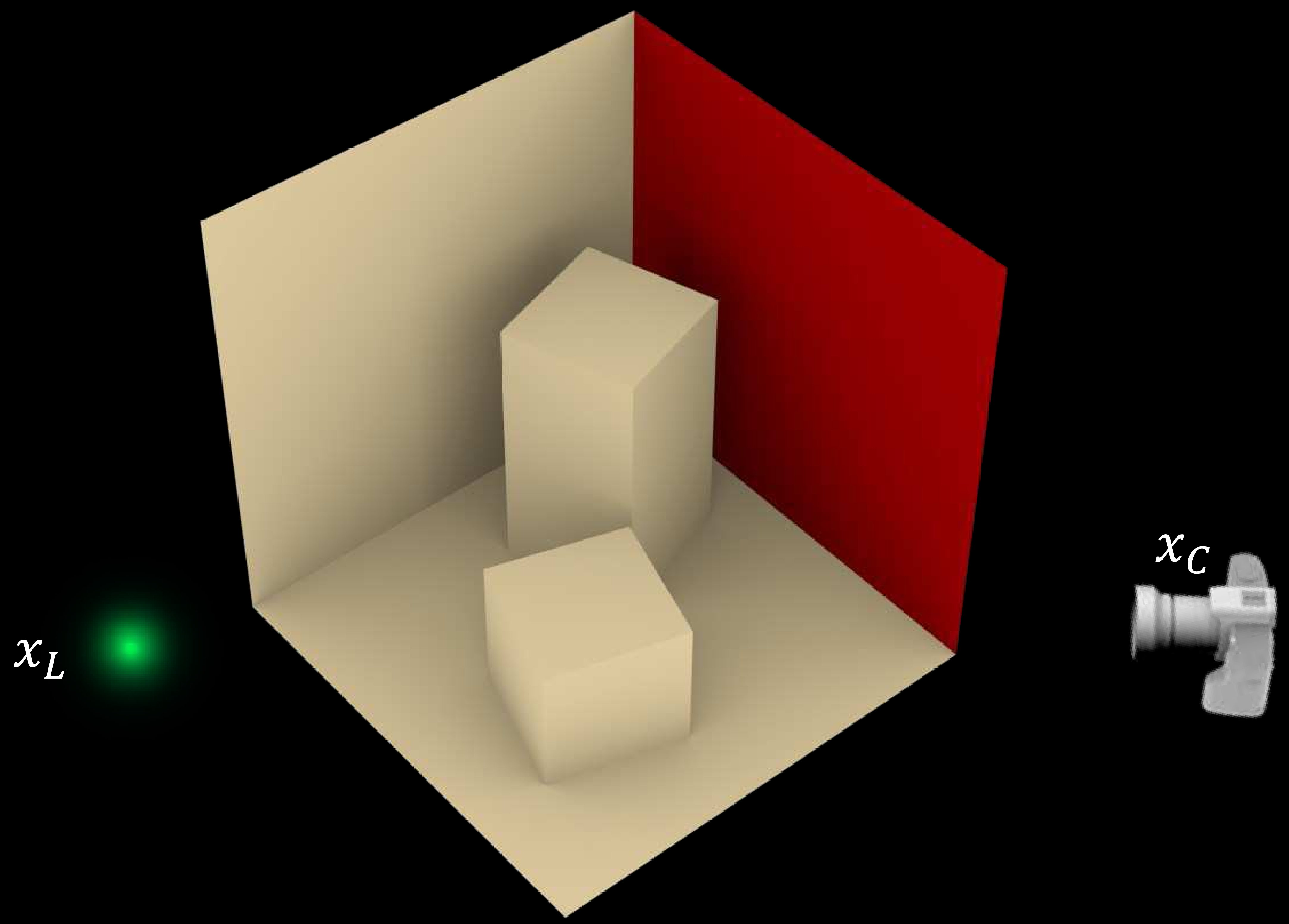

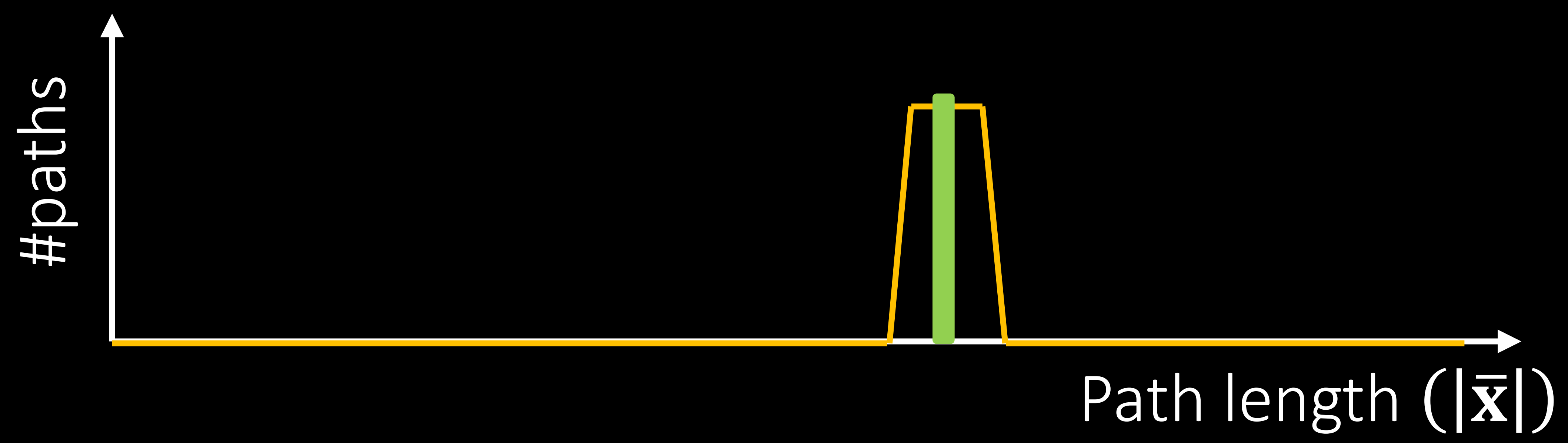

step 1: sample path length $|\bar{\mathbf{x}}|$

step 2: generate path with target length $|\bar{\mathbf{x}}|$

Path sampling for time-gated case

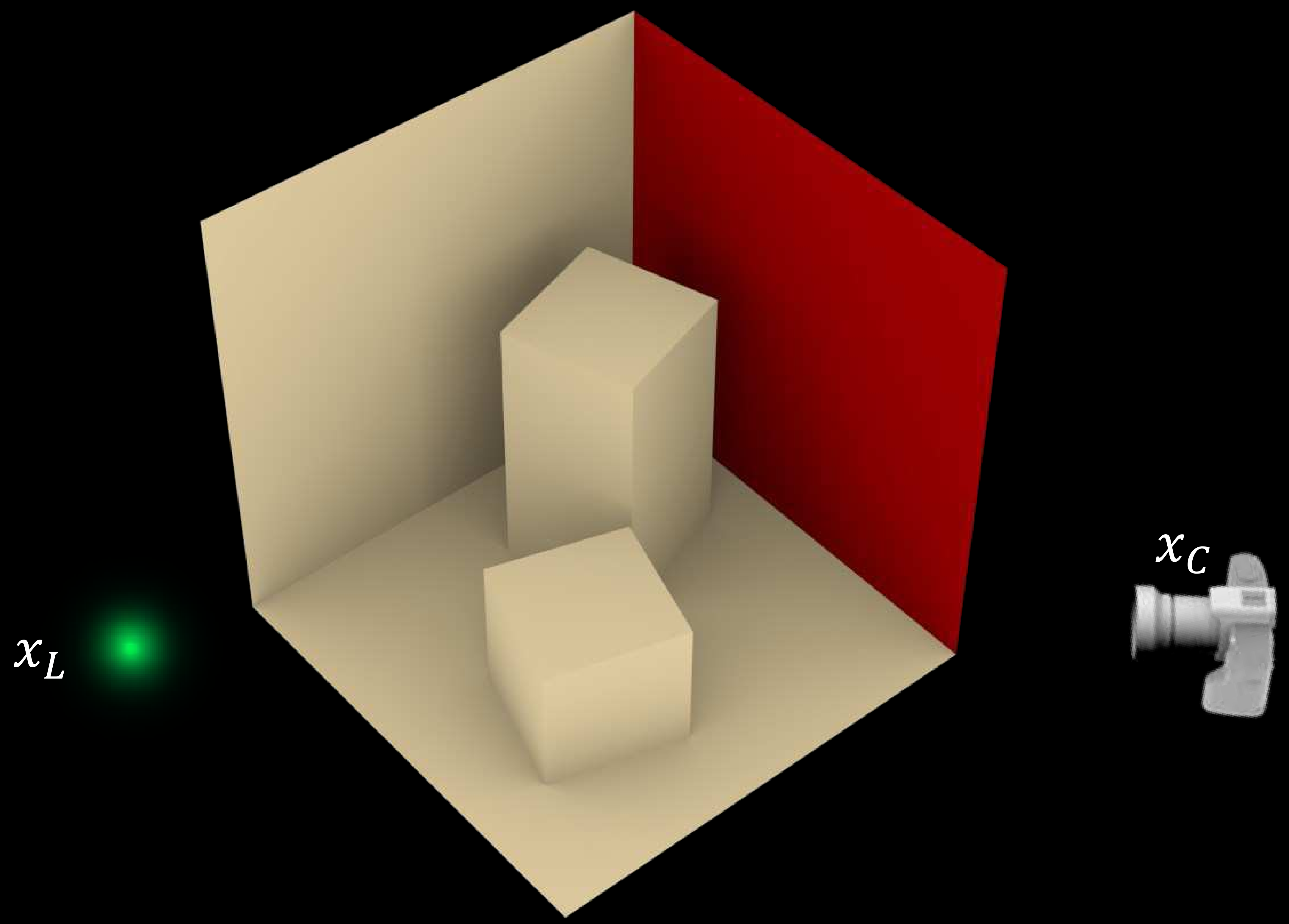

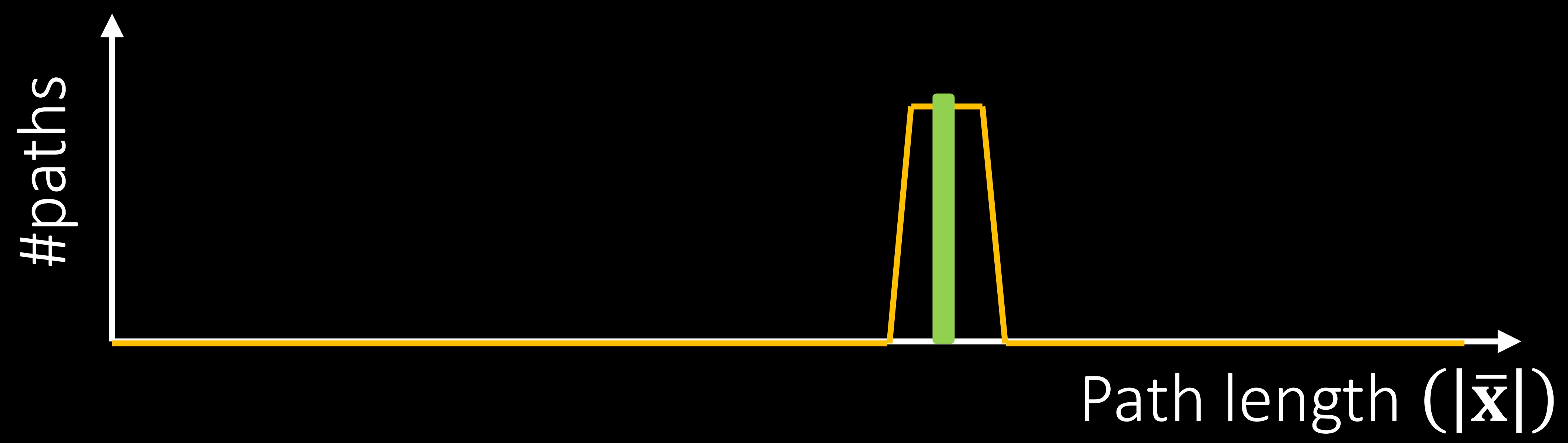

step 1: sample path length $|\bar{\mathbf{x}}|$

step 2: generate path with target length $|\bar{\mathbf{x}}|$

bidirectional path tracing (BDPT)

Path sampling for time-gated case

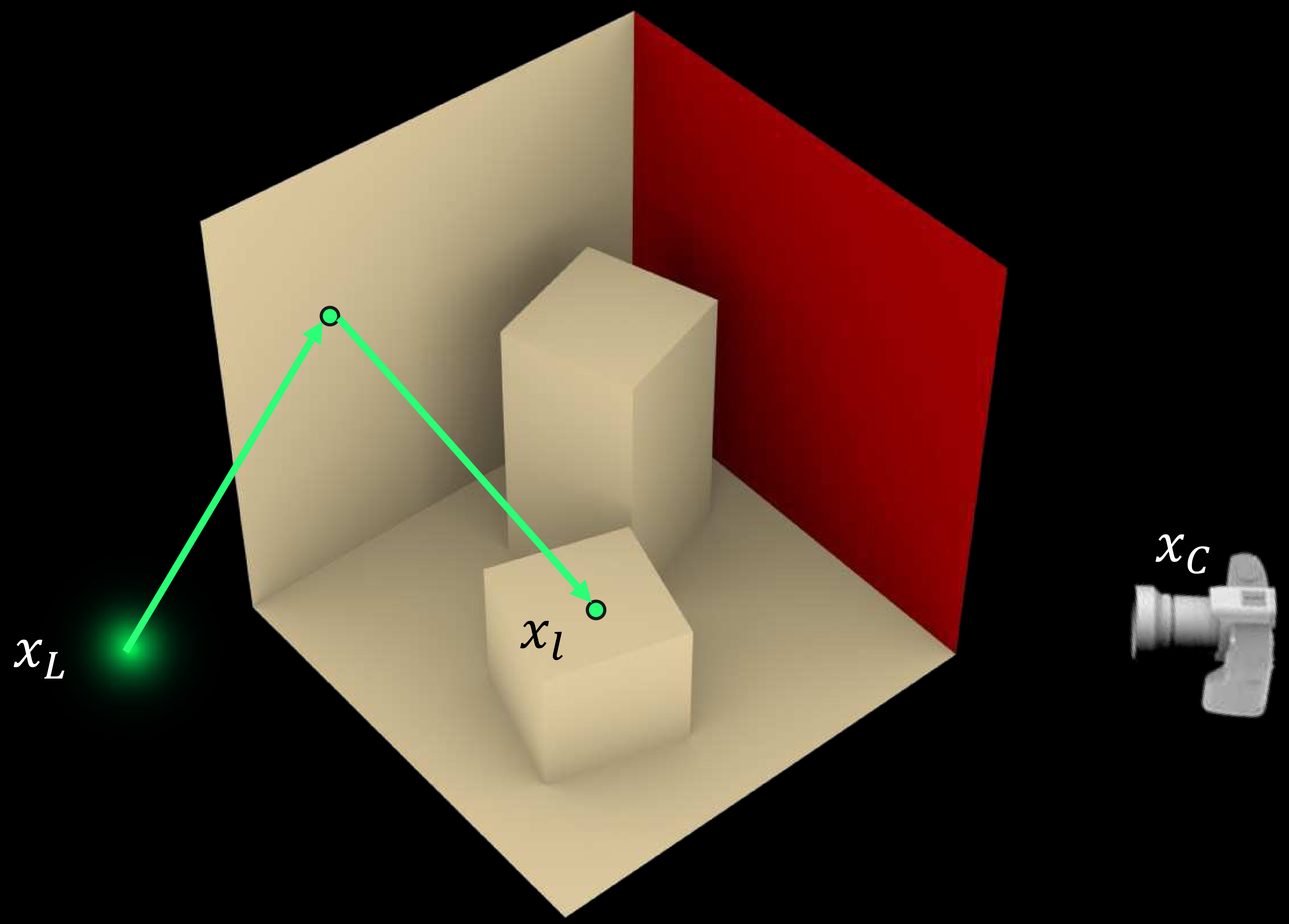

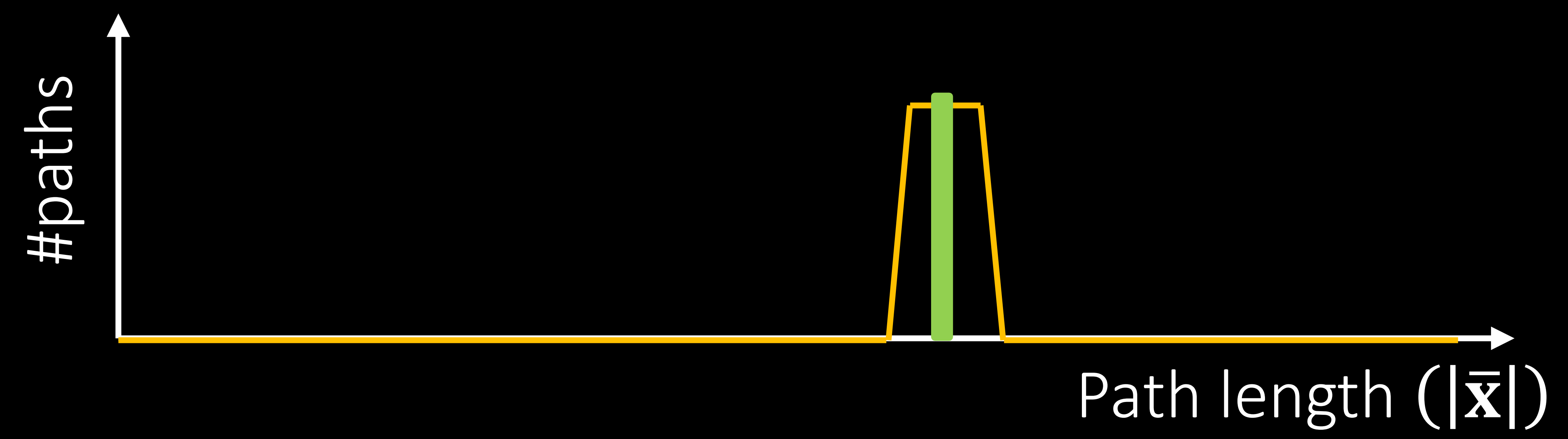

step 1: sample path length $|\bar{\mathbf{x}}|$

step 2: generate path with target length $|\bar{\mathbf{x}}|$

bidirectional path tracing (BDPT)

generate light sub-path, camera sub-path

Path sampling for time-gated case

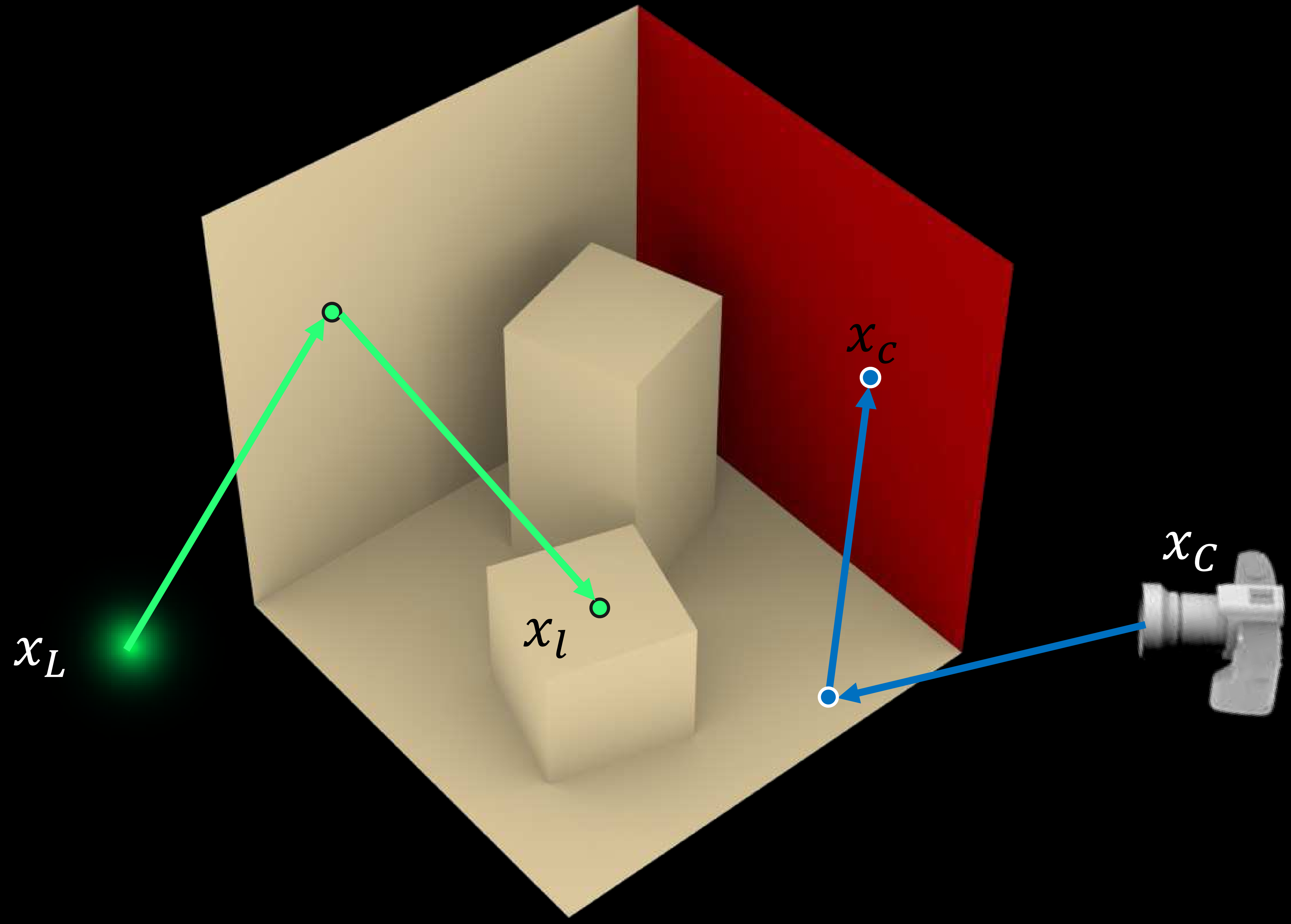

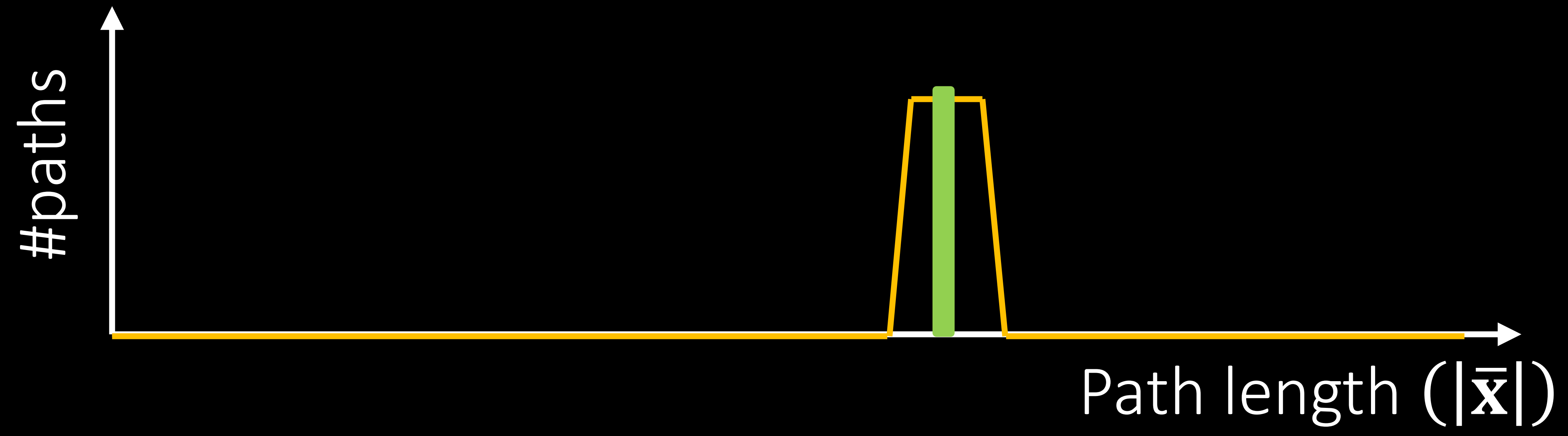

step 1: sample path length $|\bar{\mathbf{x}}|$

step 2: generate path with target length $|\bar{\mathbf{x}}|$

bidirectional path tracing (BDPT)

generate light sub-path, camera sub-path

Path sampling for time-gated case

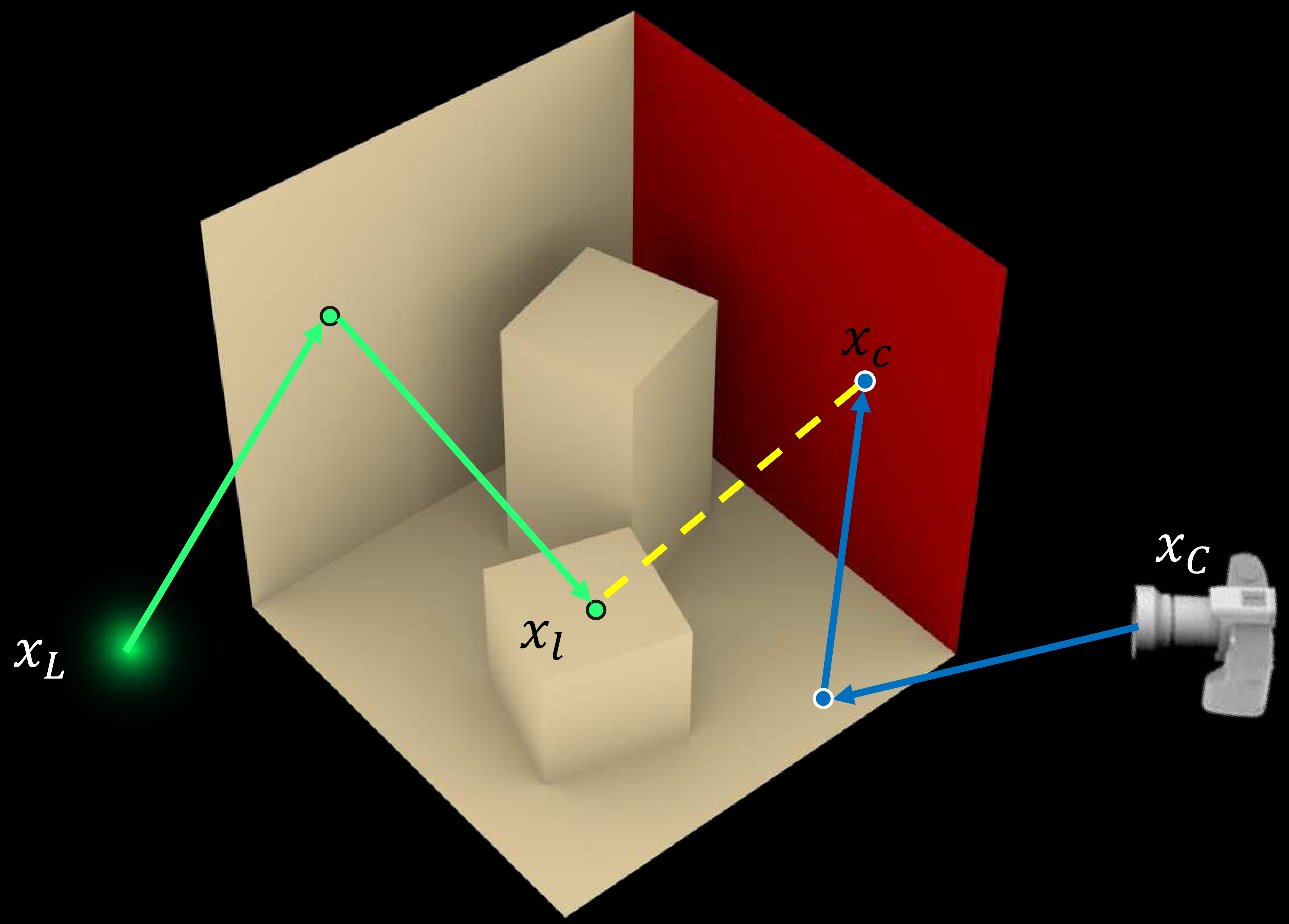

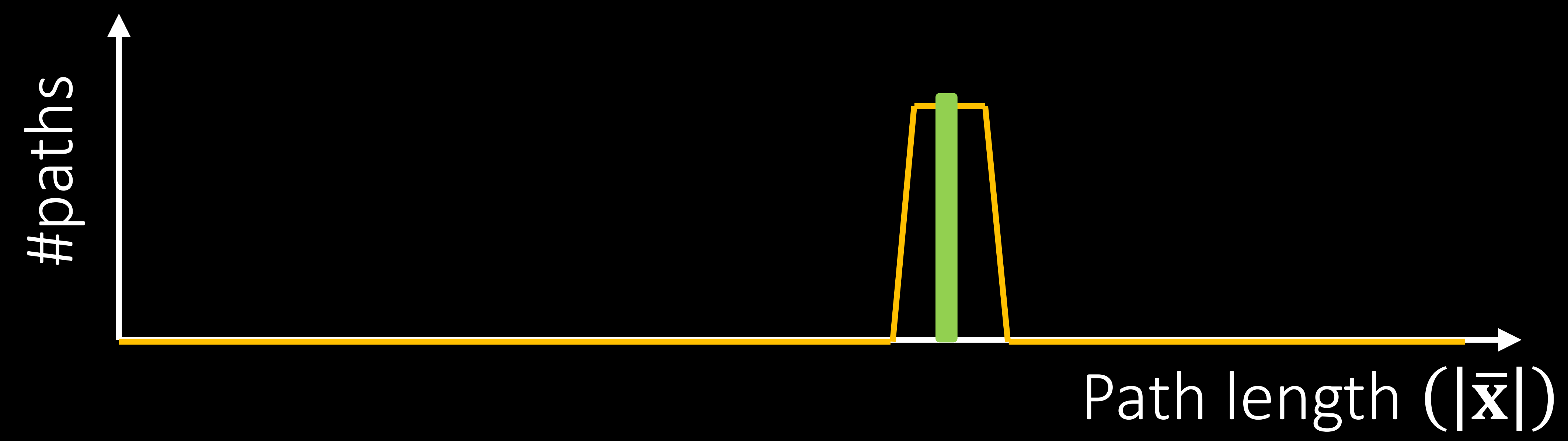

step 1: sample path length $|\bar{\mathbf{x}}|$

step 2: generate path with target length $|\bar{\mathbf{x}}|$

bidirectional path tracing (BDPT)

generate light sub-path, camera sub-path

join source sub-path end x_s and camera sub-path end x_c

Path sampling for time-gated case

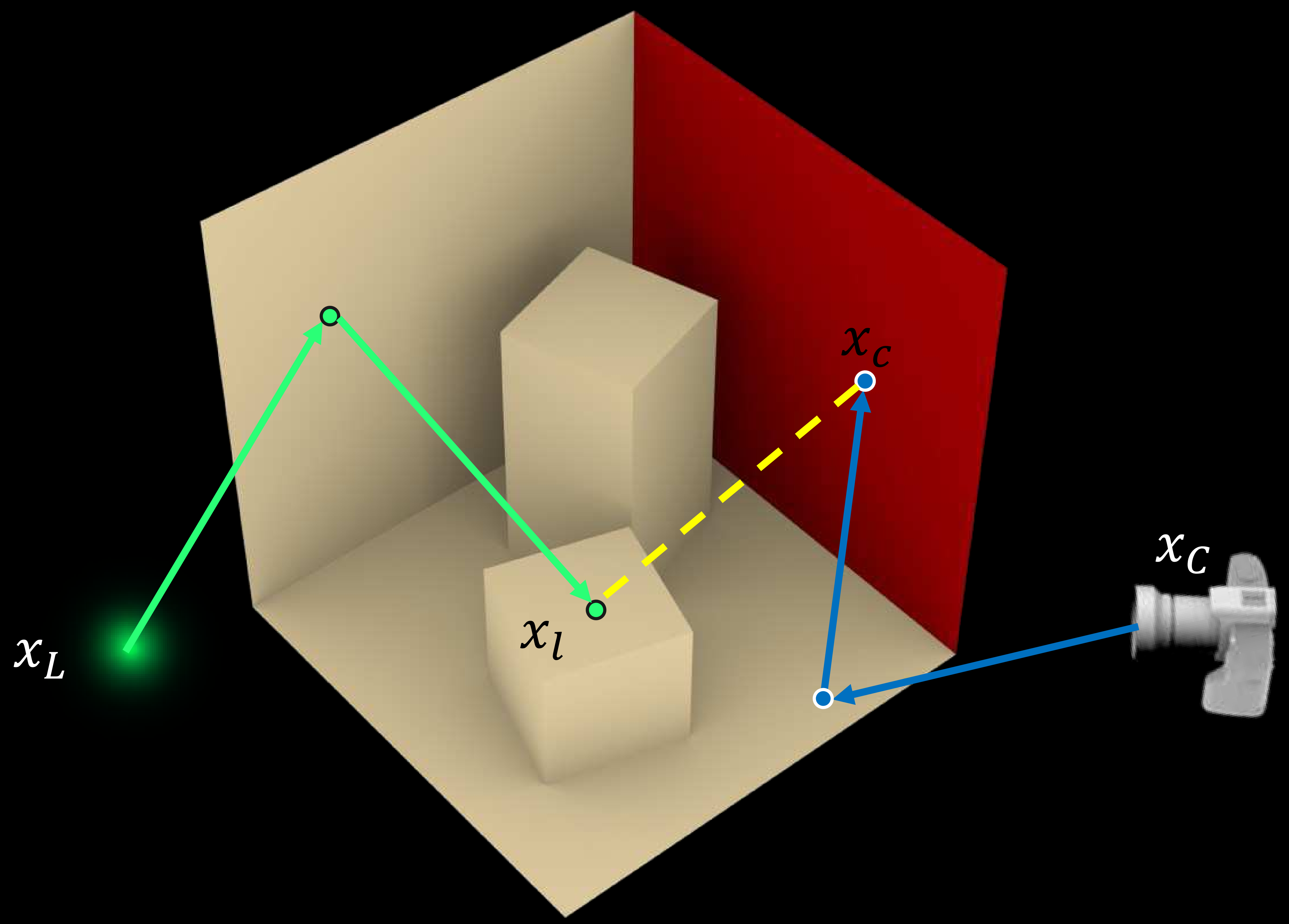

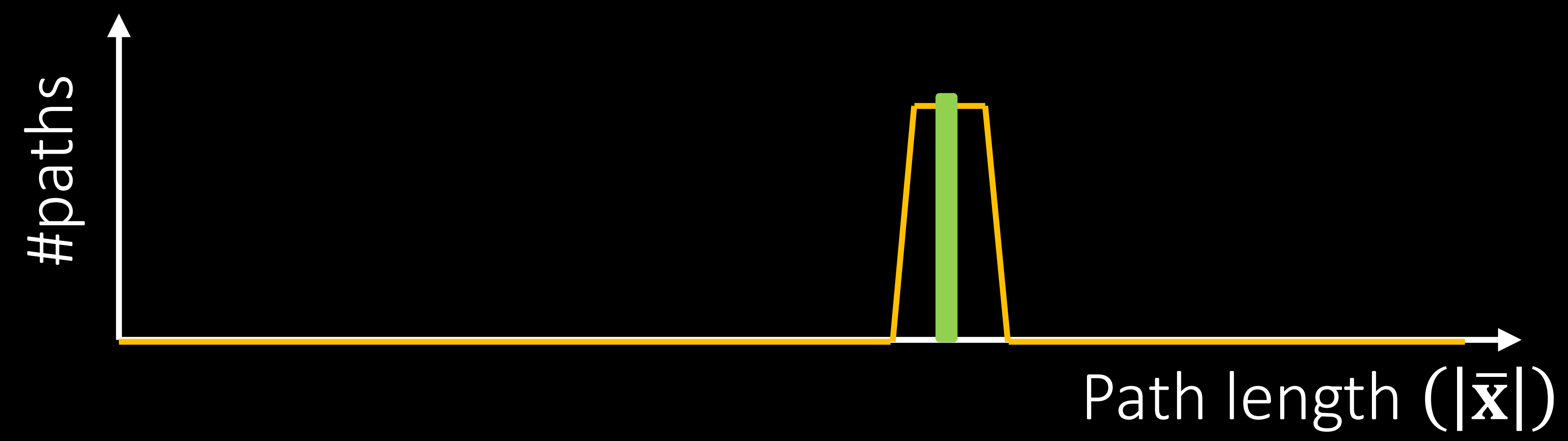

step 1: sample path length $|\bar{\mathbf{x}}|$

step 2: generate path with target length $|\bar{\mathbf{x}}|$

bidirectional path tracing (BDPT)

generate light sub-path, camera sub-path

~~join source sub-path end x_s and camera sub-path end x_c~~

Path sampling for time-gated case

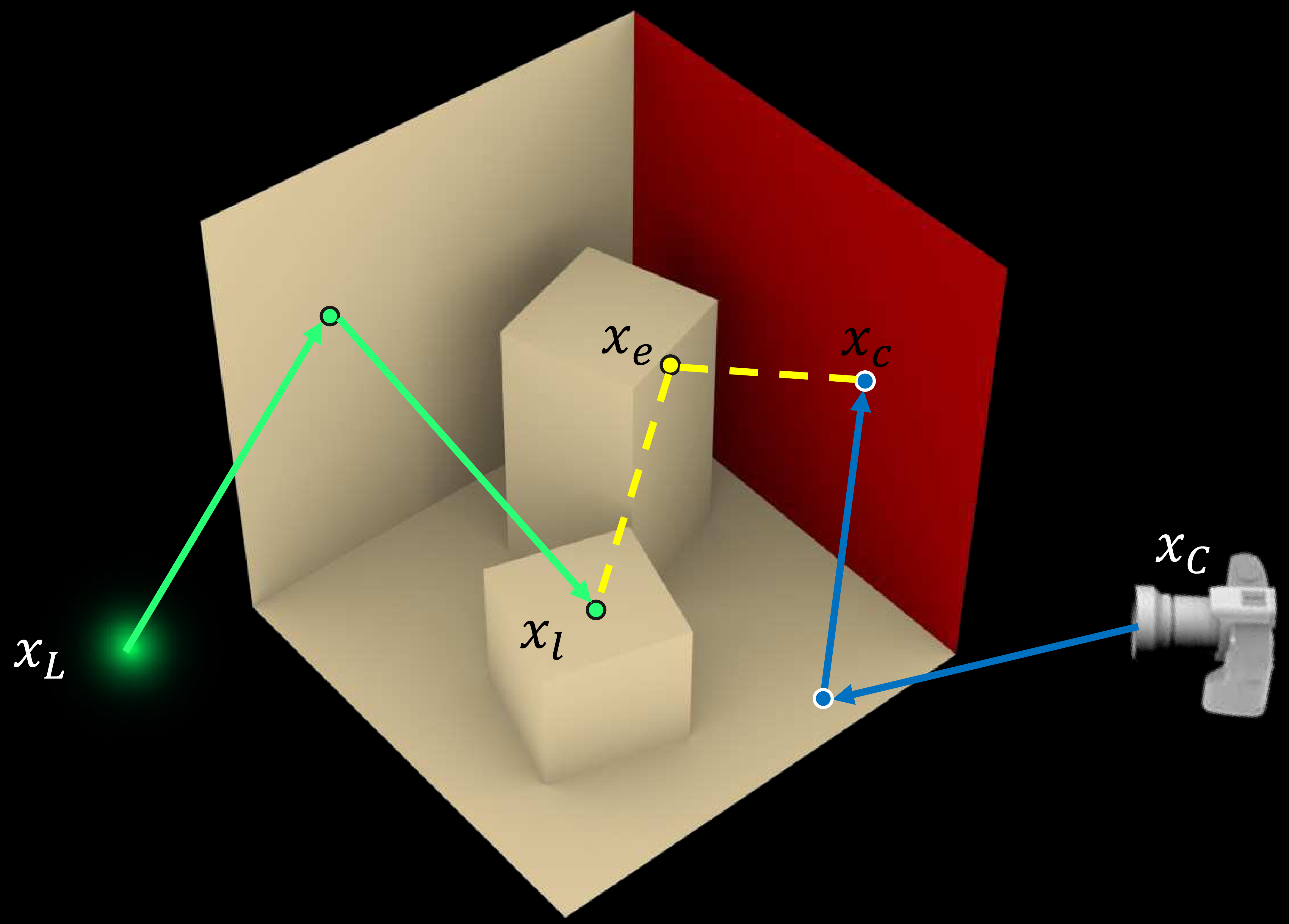

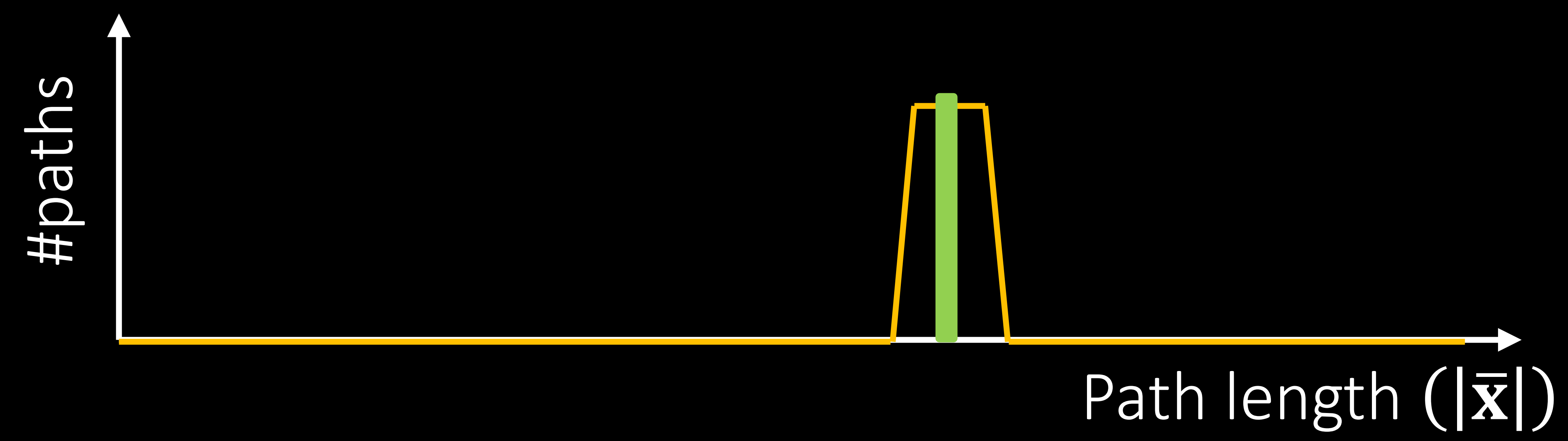

step 1: sample path length $|\bar{\mathbf{x}}|$

step 2: generate path with target length $|\bar{\mathbf{x}}|$

bidirectional path tracing (BDPT)

generate light sub-path, camera sub-path

join x_l and x_c via connecting vertex (x_e)

Path sampling for time-gated case

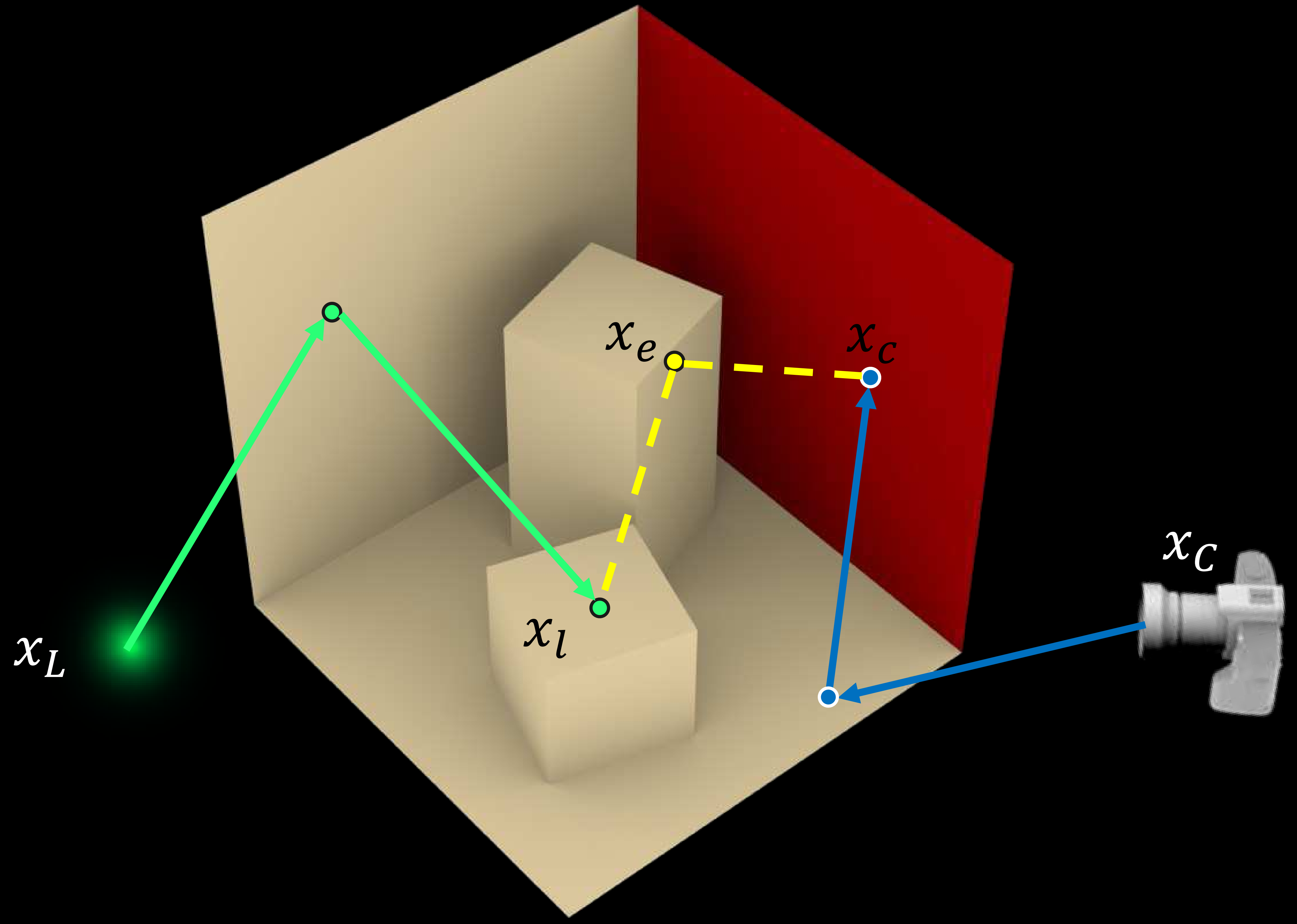

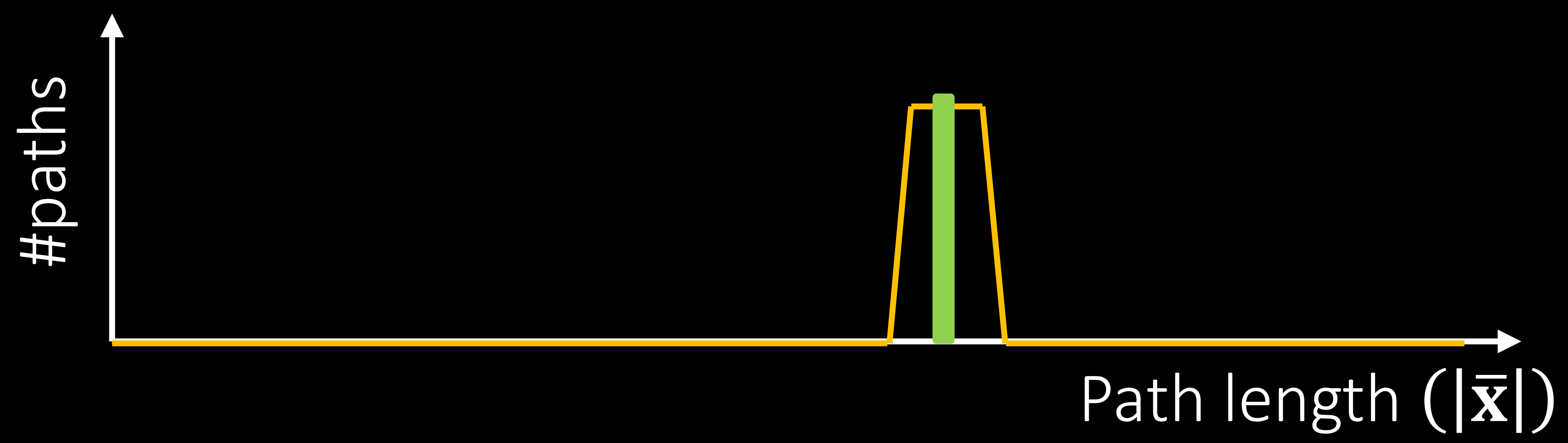

step 1: sample path length $|\bar{\mathbf{x}}|$

step 2: generate path with target length $|\bar{\mathbf{x}}|$

bidirectional path tracing (BDPT)

generate light sub-path, camera sub-path

join x_l and x_c via connecting vertex (x_e)

$$\left.\begin{array}{r}\text{source sub−path length} + \\ \text{sensor sub−path length} + \\ |x_e \to x_l| + |x_e \to x_c|\end{array}\right\} = |\bar{\mathbf{x}}|$$

Path sampling for time-gated case

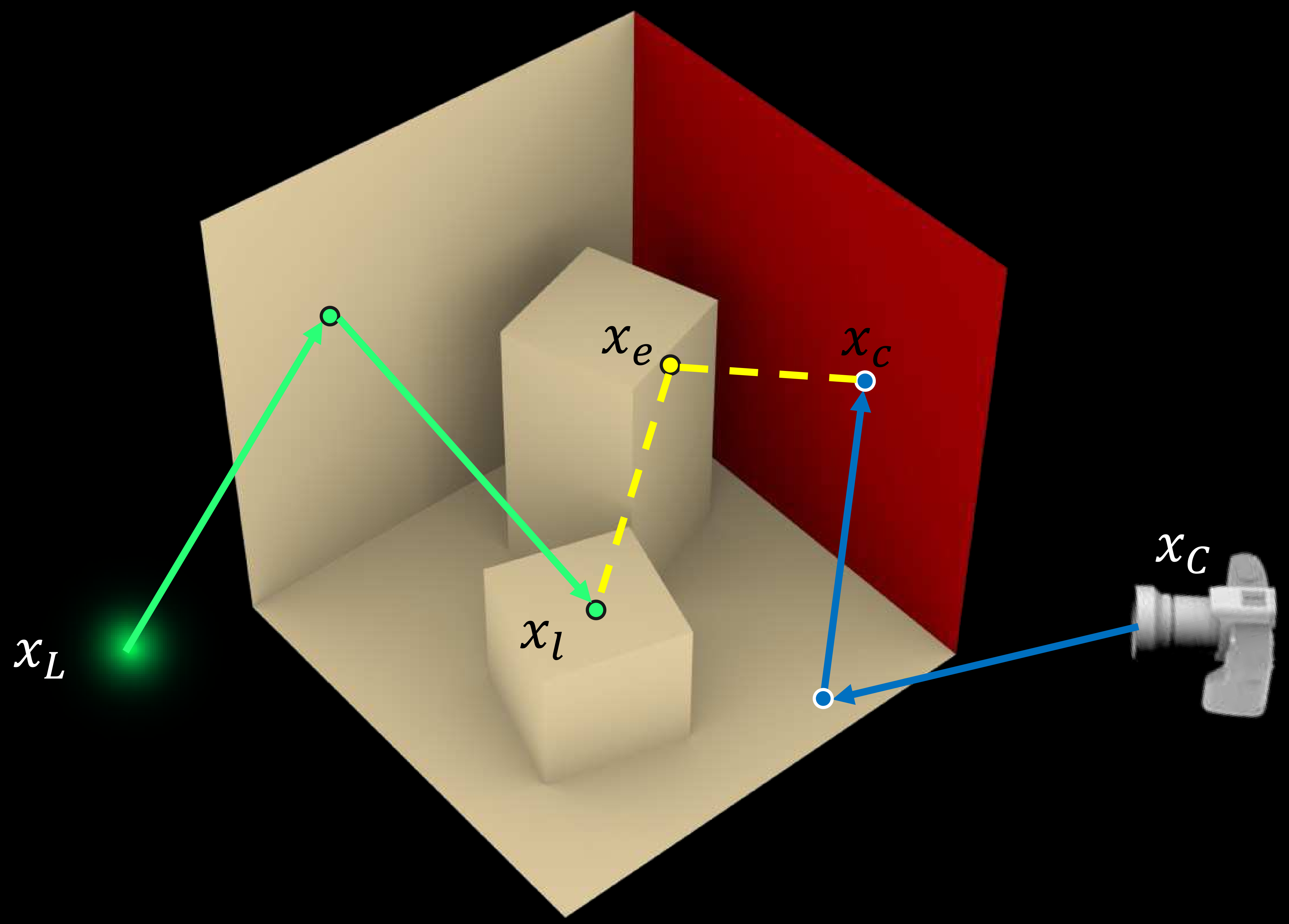

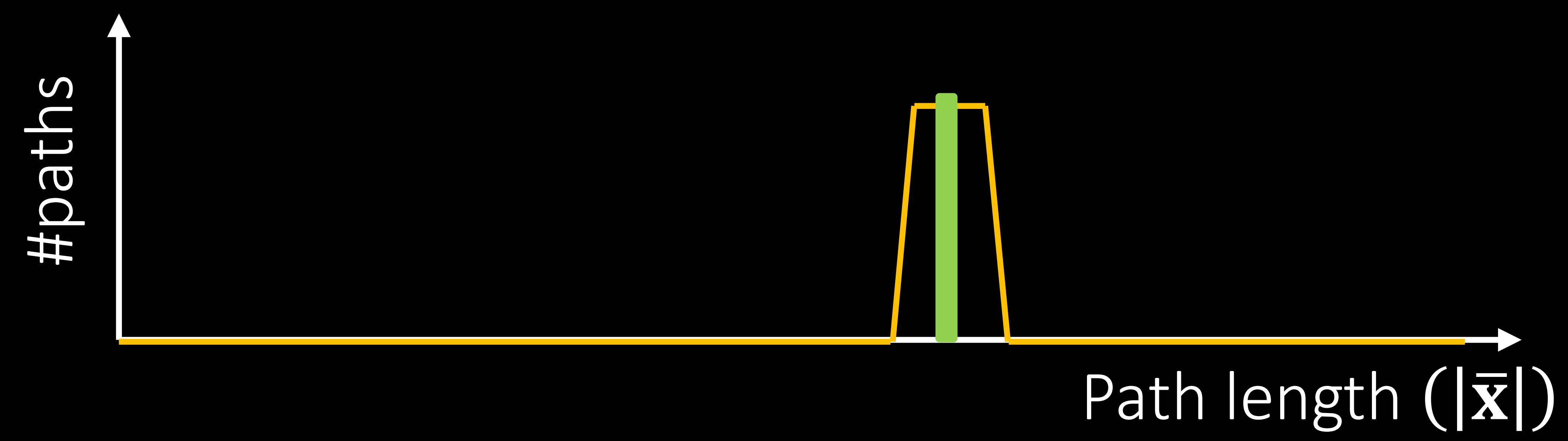

step 1: sample path length $|\bar{\mathbf{x}}|$

step 2: generate path with target length $|\bar{\mathbf{x}}|$

bidirectional path tracing (BDPT)

generate light sub-path, camera sub-path

join x_l and x_c via connecting vertex (x_e)

$$|x_e \rightarrow x_l| + |x_e \rightarrow x_c| = |\bar{\mathbf{x}}| - \text{source + sensor sub-path lengths}$$

Path sampling for time-gated case

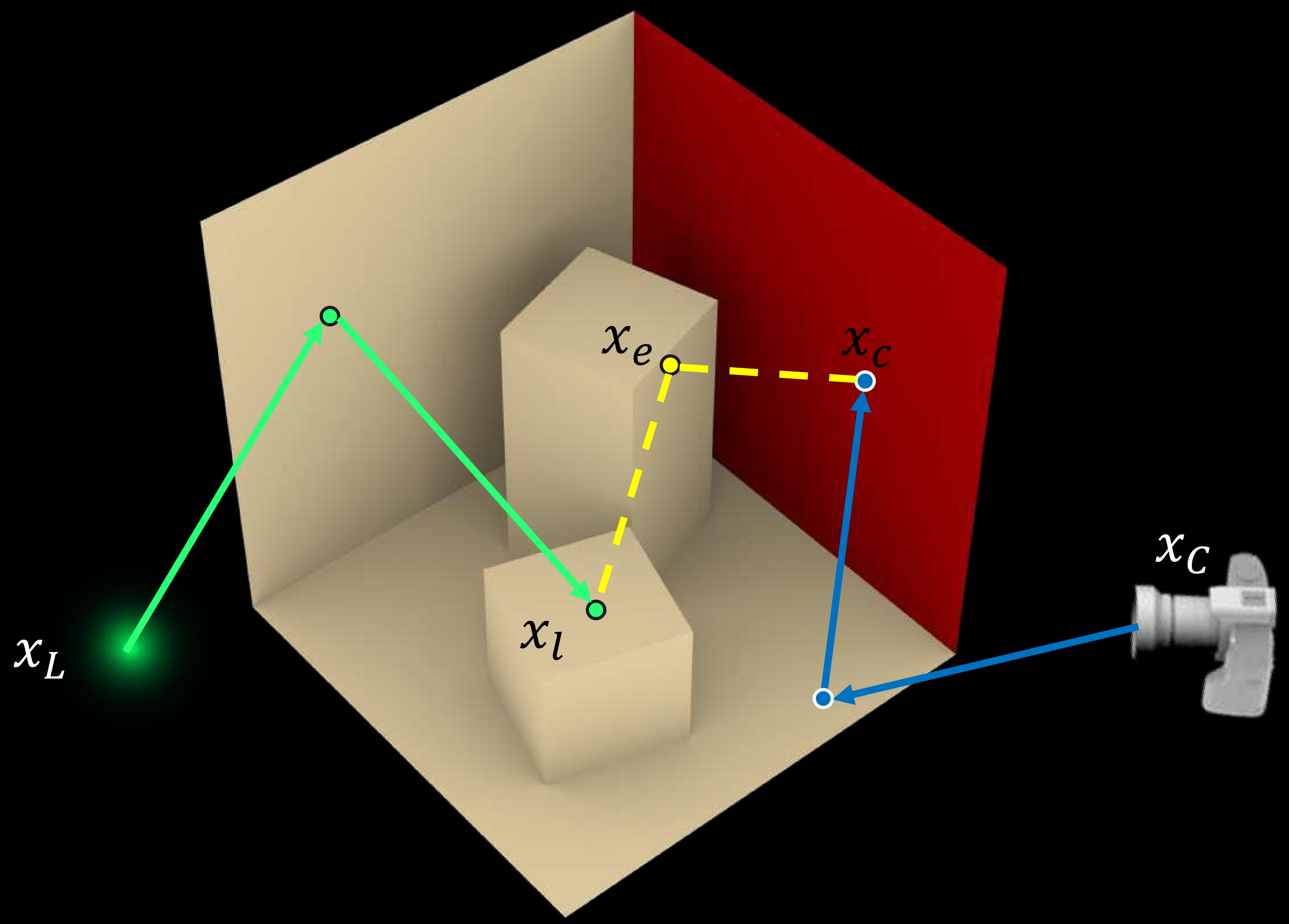

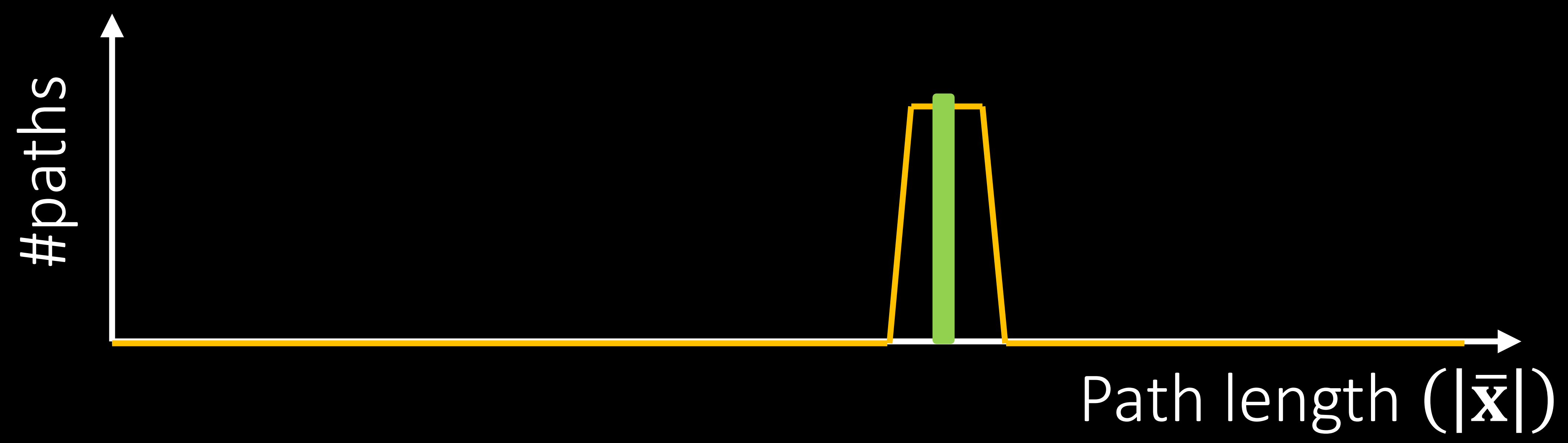

step 1: sample path length $|\bar{\mathbf{x}}|$

step 2: generate path with target length $|\bar{\mathbf{x}}|$

bidirectional path tracing (BDPT)

generate light sub-path, camera sub-path

join x_l and x_c via connecting vertex (x_e)

Definition of an ellipsoid: $|x_e \rightarrow x_l| + |x_e \rightarrow x_c| = |\bar{\mathbf{x}}| -$ source + sensor sub–path lengths

Path sampling for time-gated case

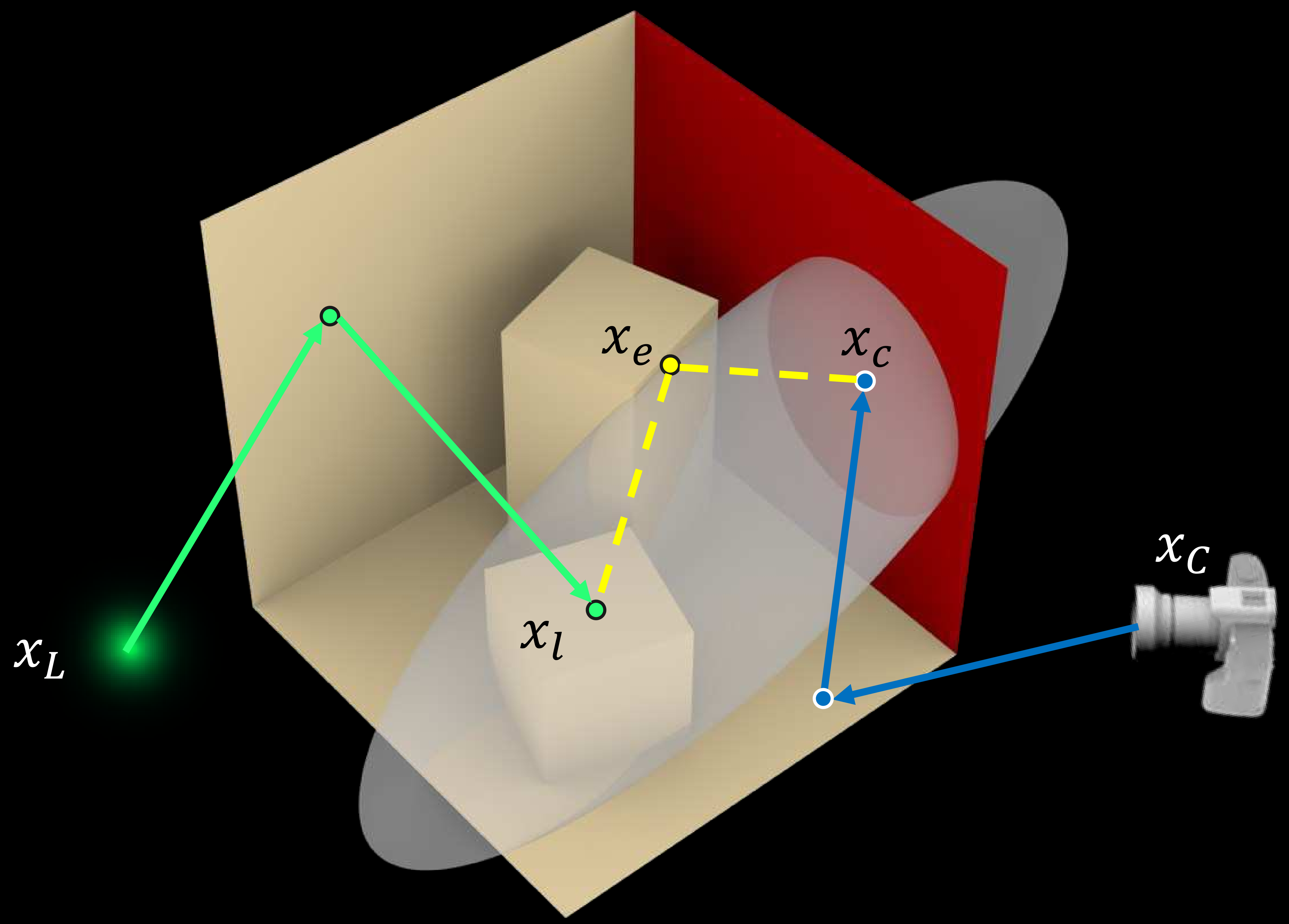

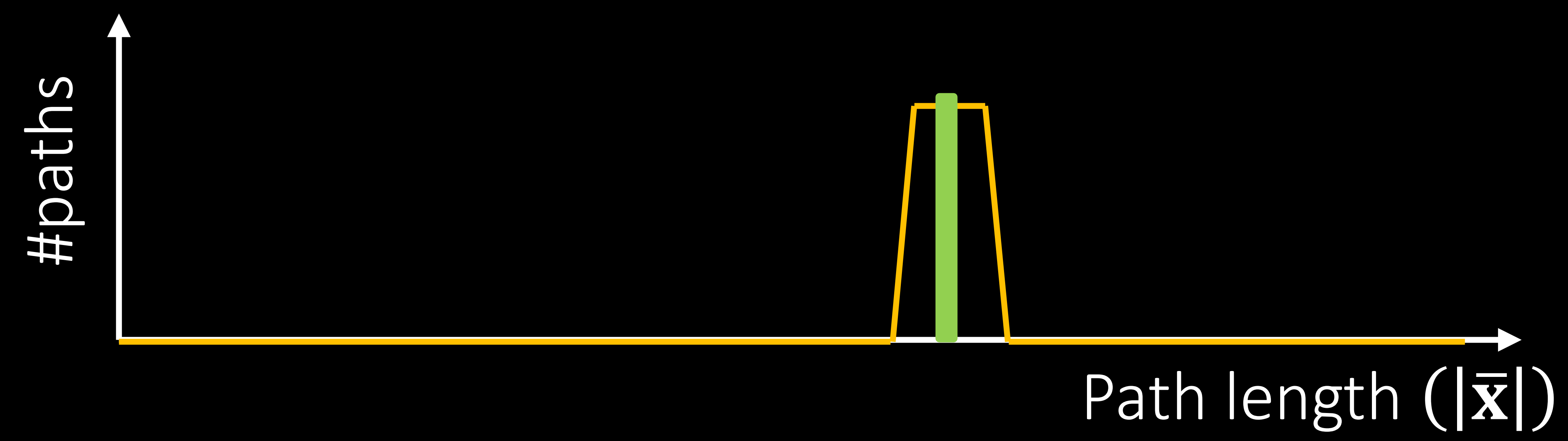

step 1: sample path length $|\bar{\mathbf{x}}|$

step 2: generate path with target length $|\bar{\mathbf{x}}|$

bidirectional path tracing (BDPT)

generate light sub-path, camera sub-path

join x_l and x_c via connecting vertex (x_e)

Definition of an ellipsoid: $|x_e \rightarrow x_l| + |x_e \rightarrow x_c| = |\bar{\mathbf{x}}| -$ source + sensor sub–path lengths

Path sampling for time-gated case

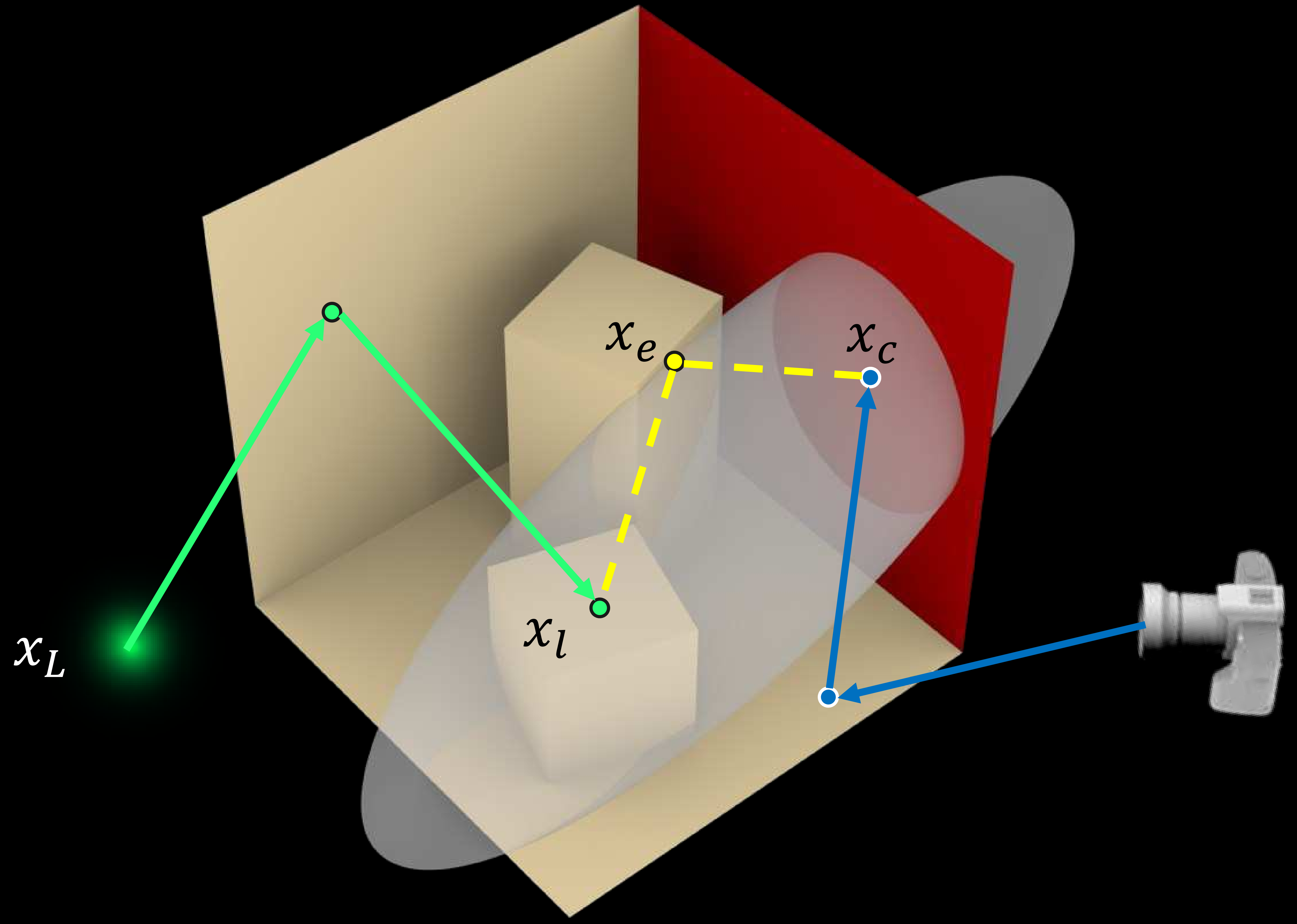

surface case

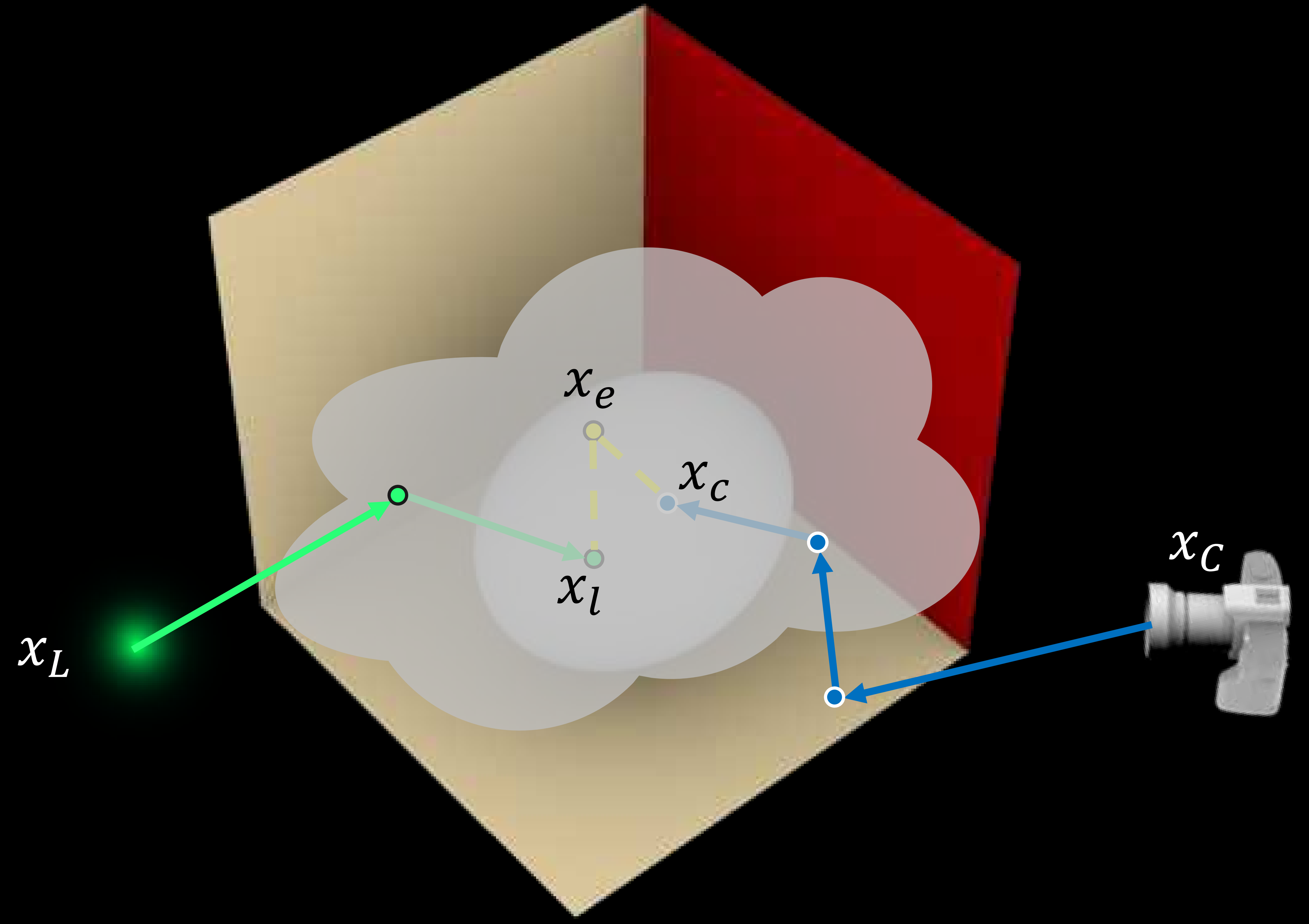

volumetric case

Path sampling for time-gated case

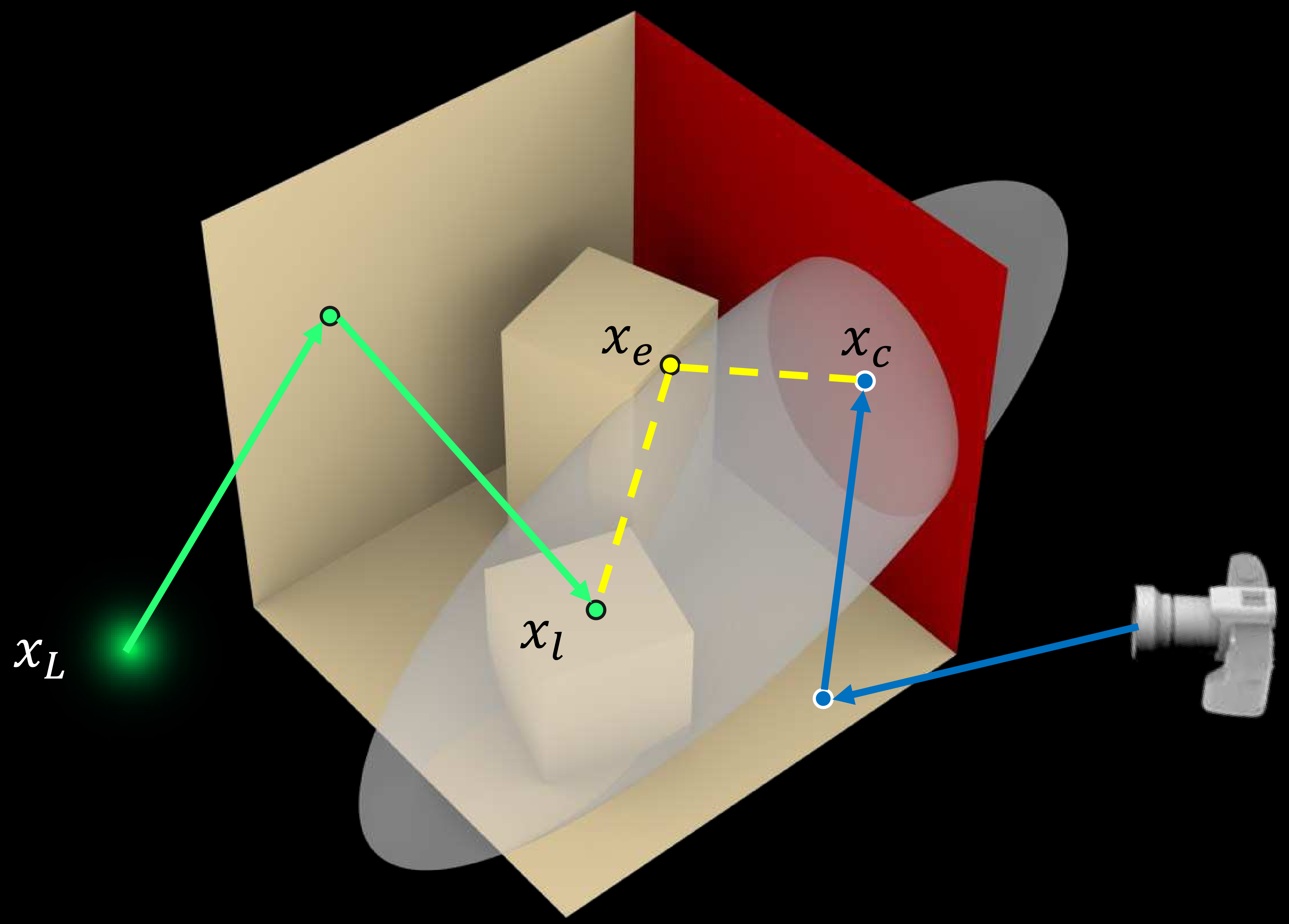

surface case

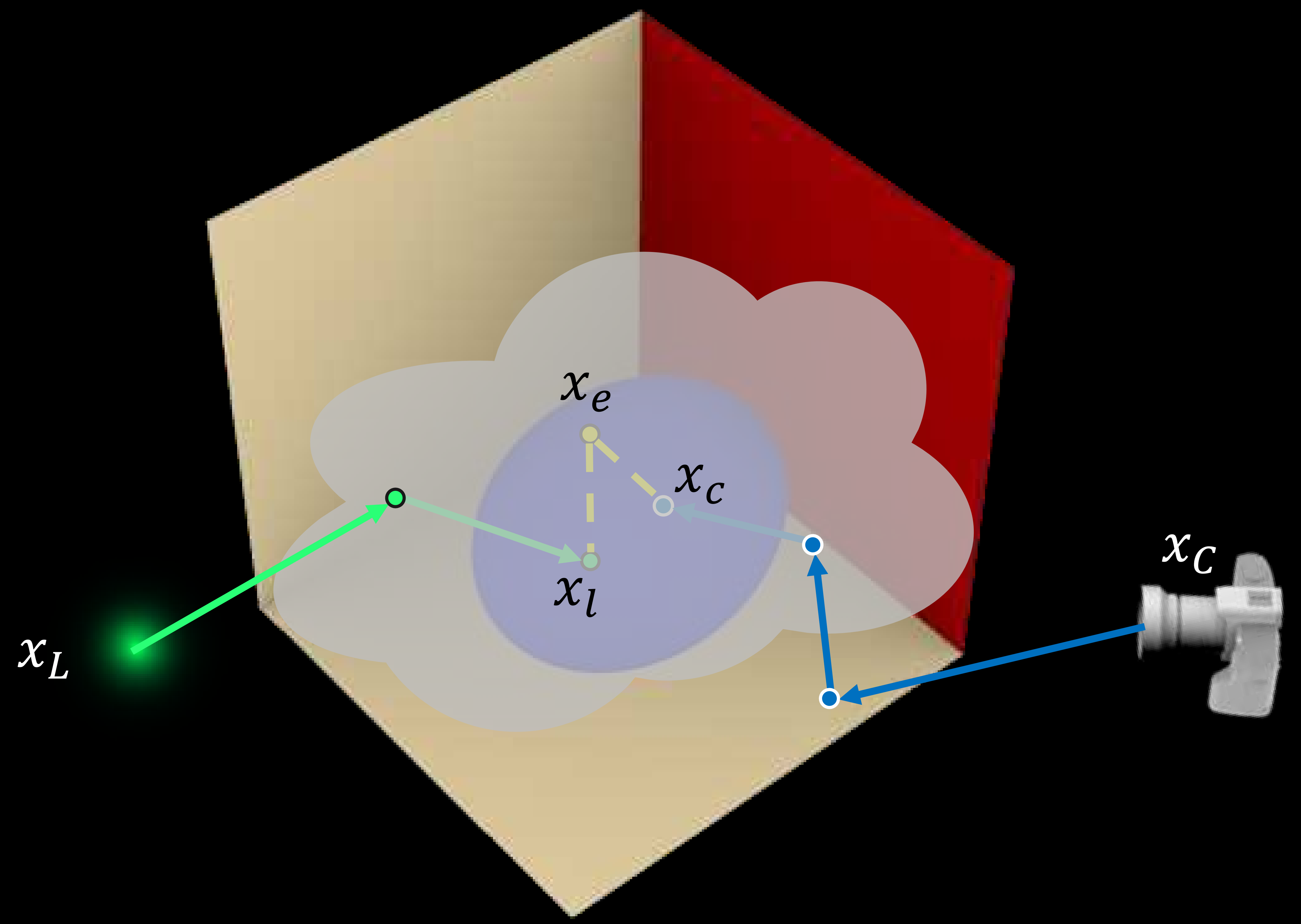

volumetric case

Path sampling for time-gated case

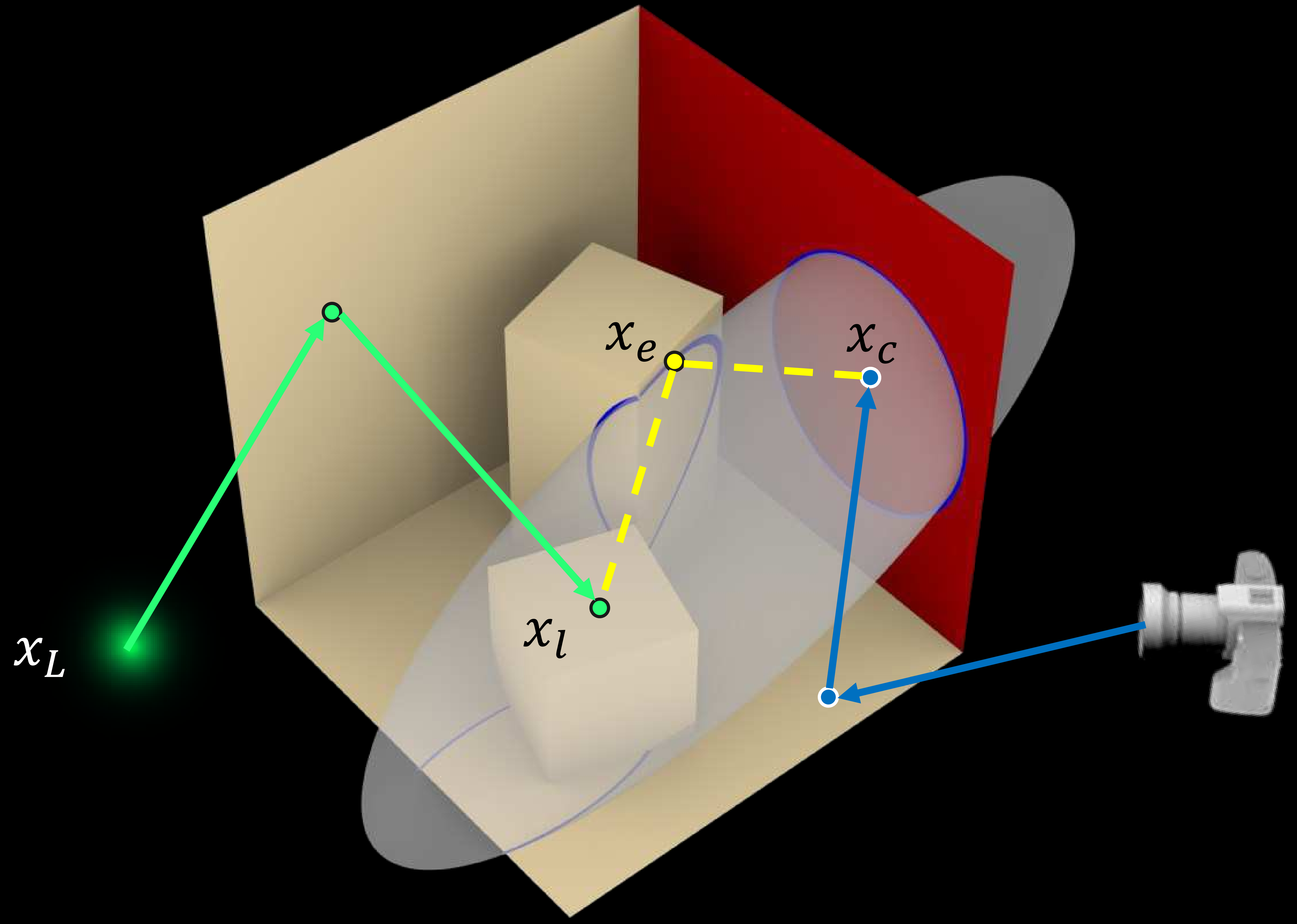

surface case

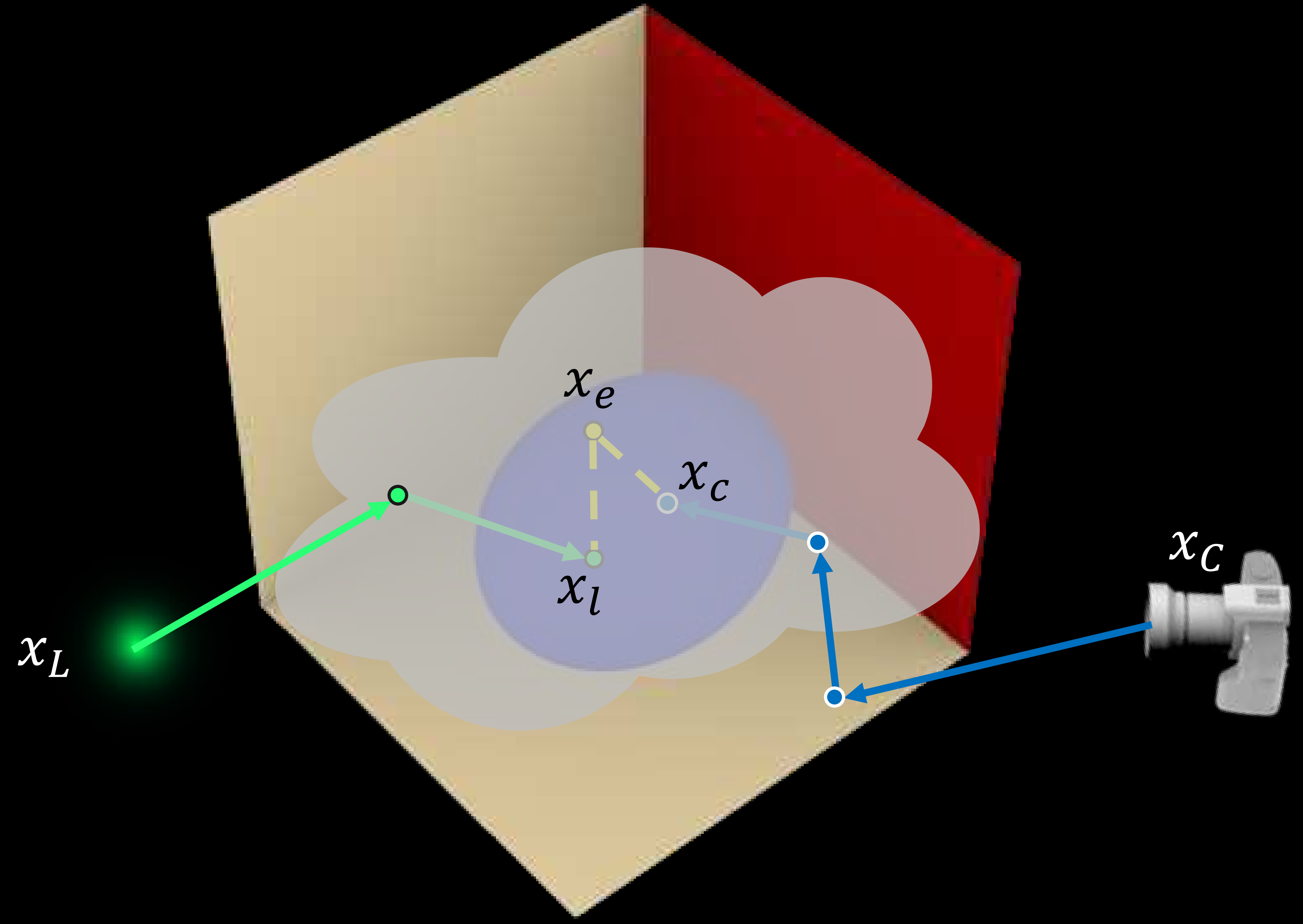

volumetric case

Application: proximity detector for cars

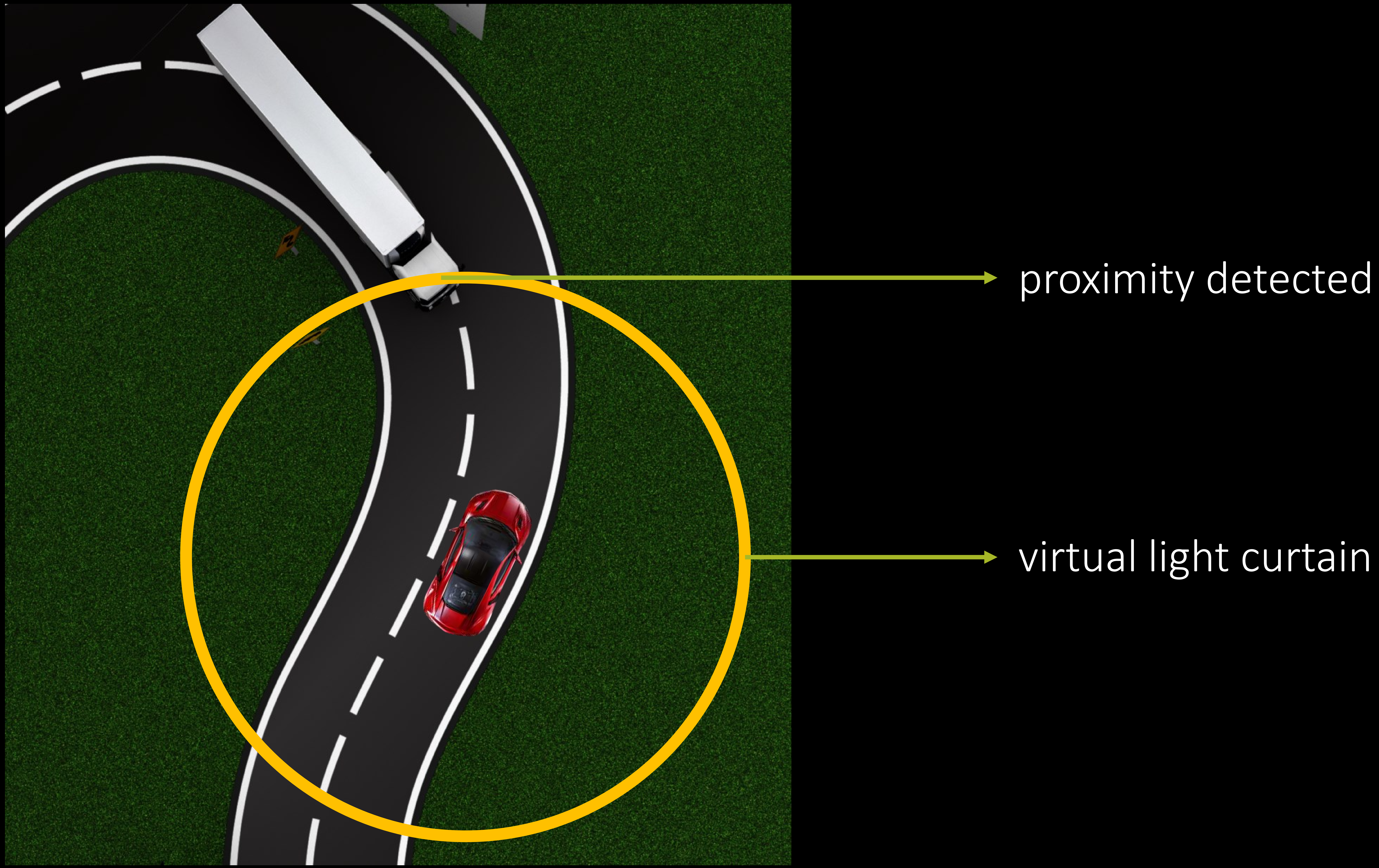

Application: proximity detector for cars

road scene

standard BDPT

BDPT w/ ellipsoidal connections

Gate width: 200 ps (1.14% scene)
Rendering time: 10s per frame

Application: proximity detector for cars

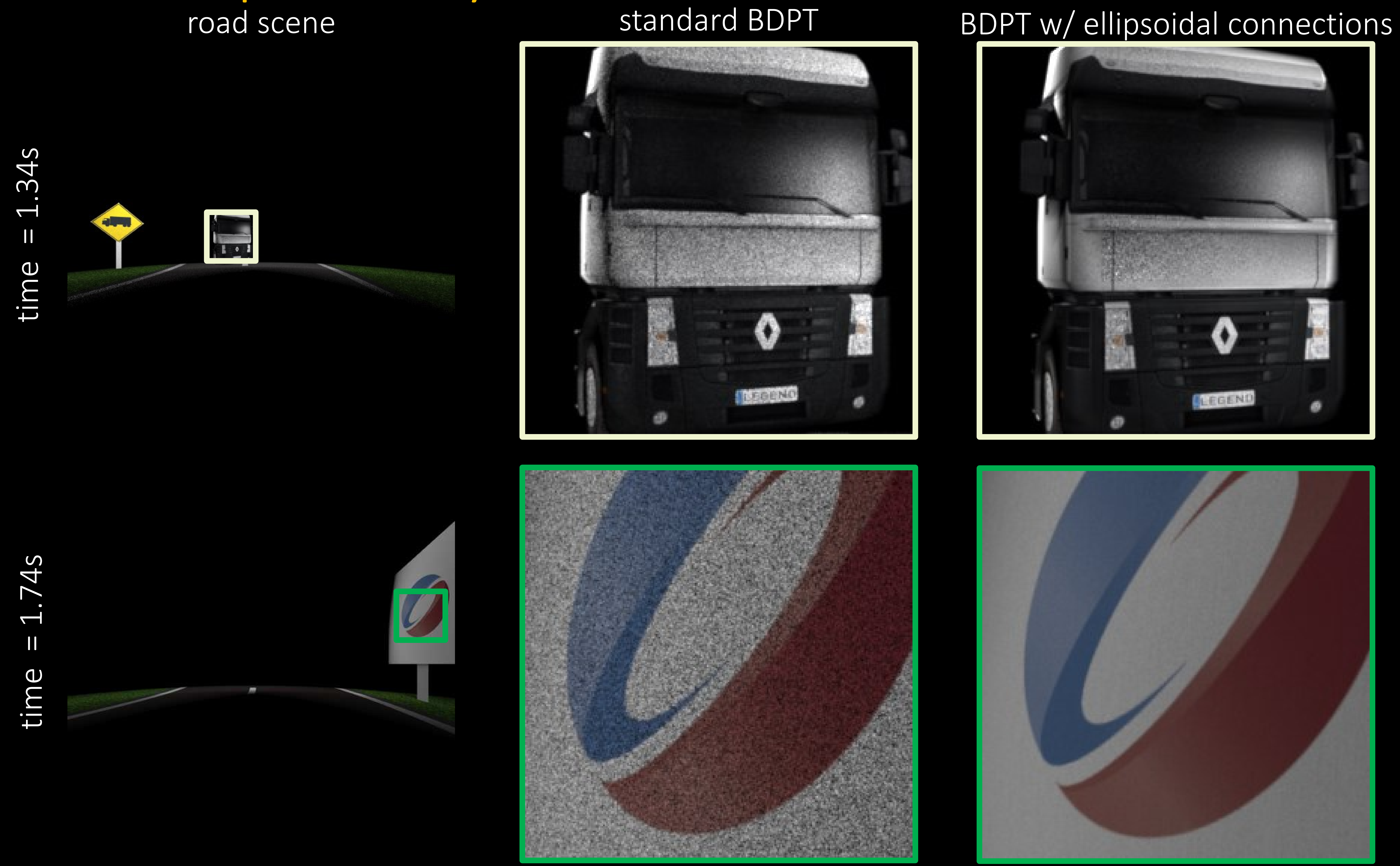

Imaging projects using this renderer

Mitsuba based
open source implementation

http://bit.ly/32Uzm1m

non-line-of-sight

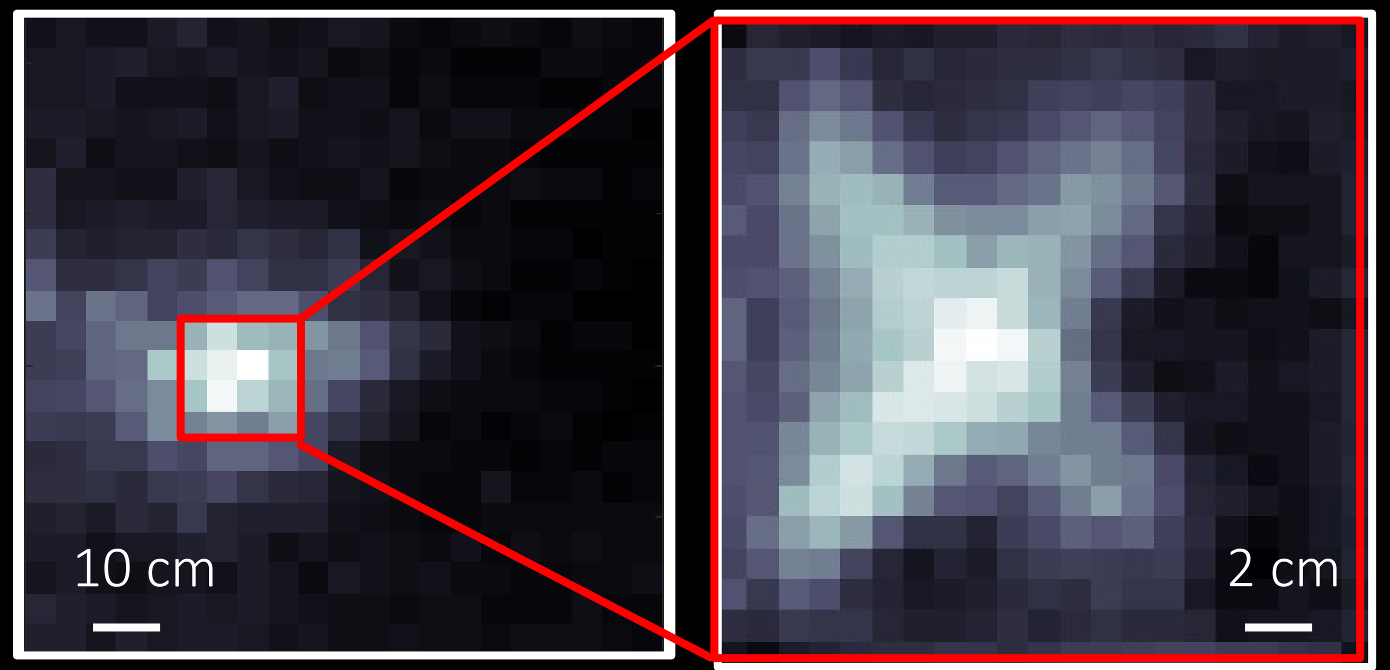

depth sensing

tissue imaging

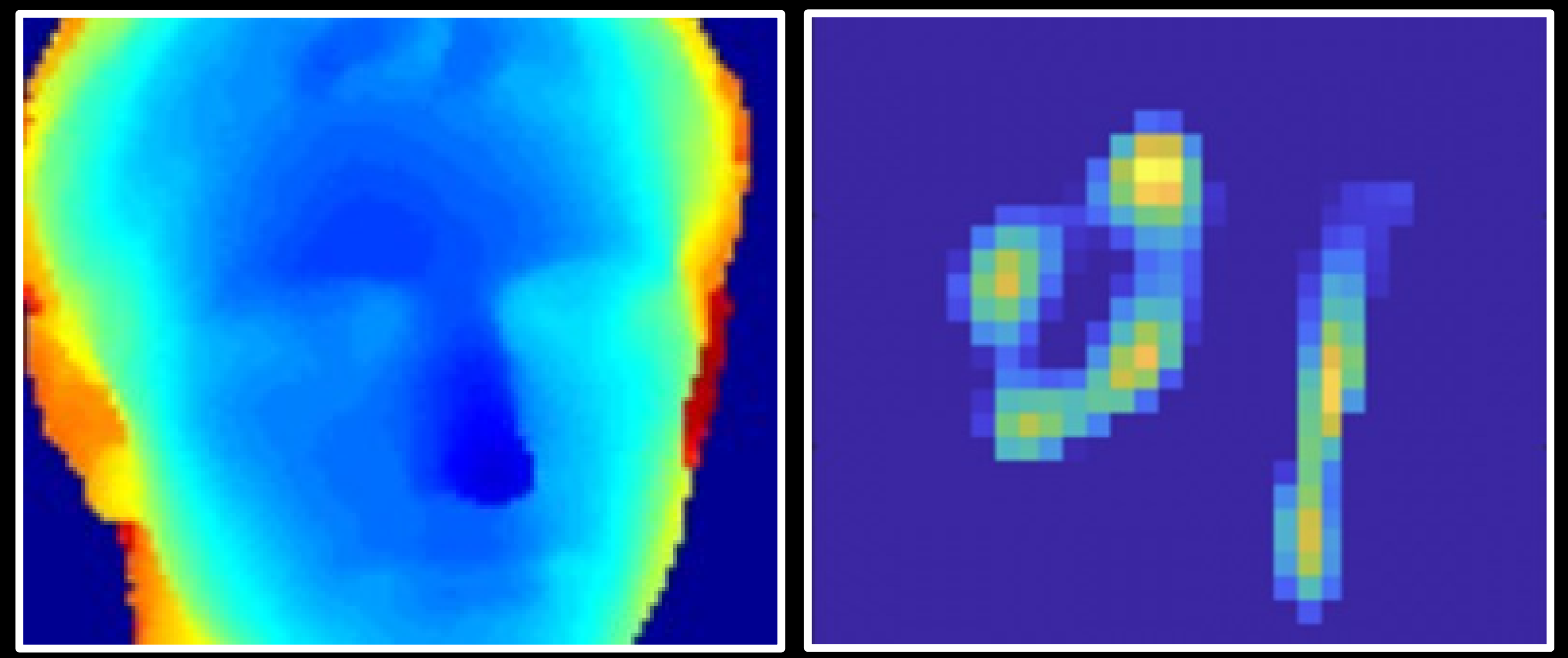

sensor design [White et al. 2022]]

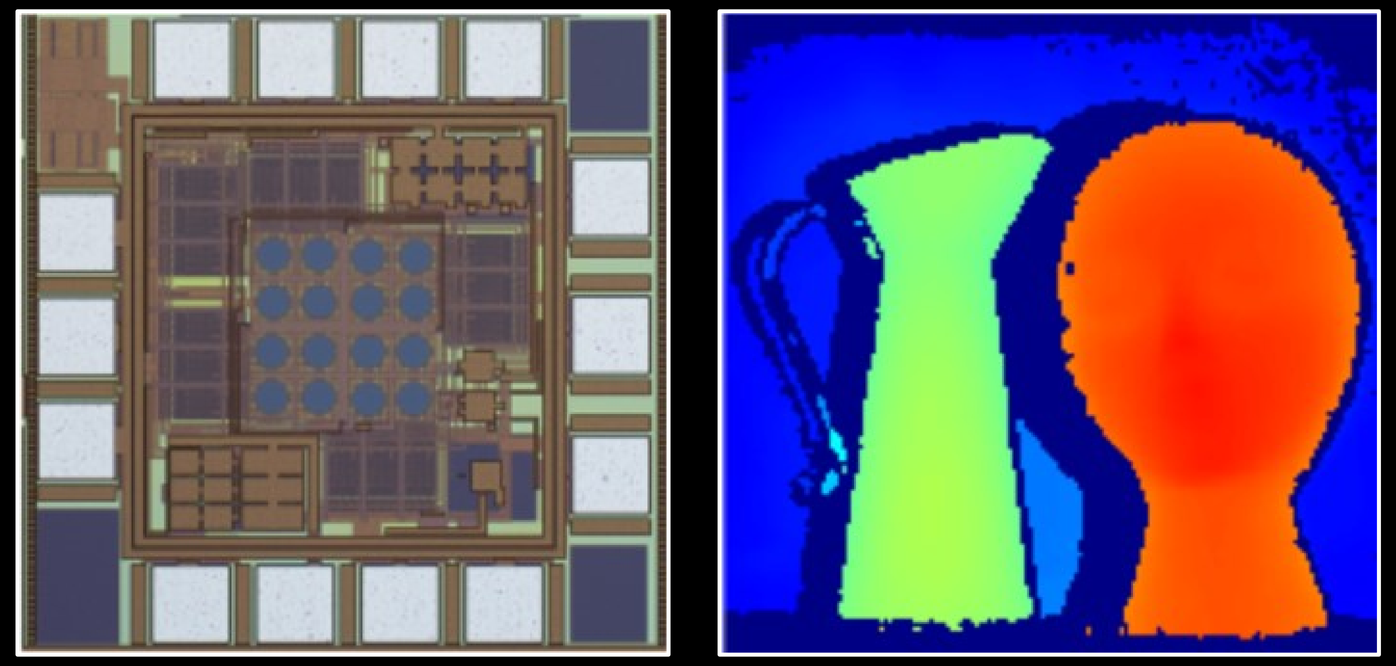

deep learning [Barragan et al. 2021]

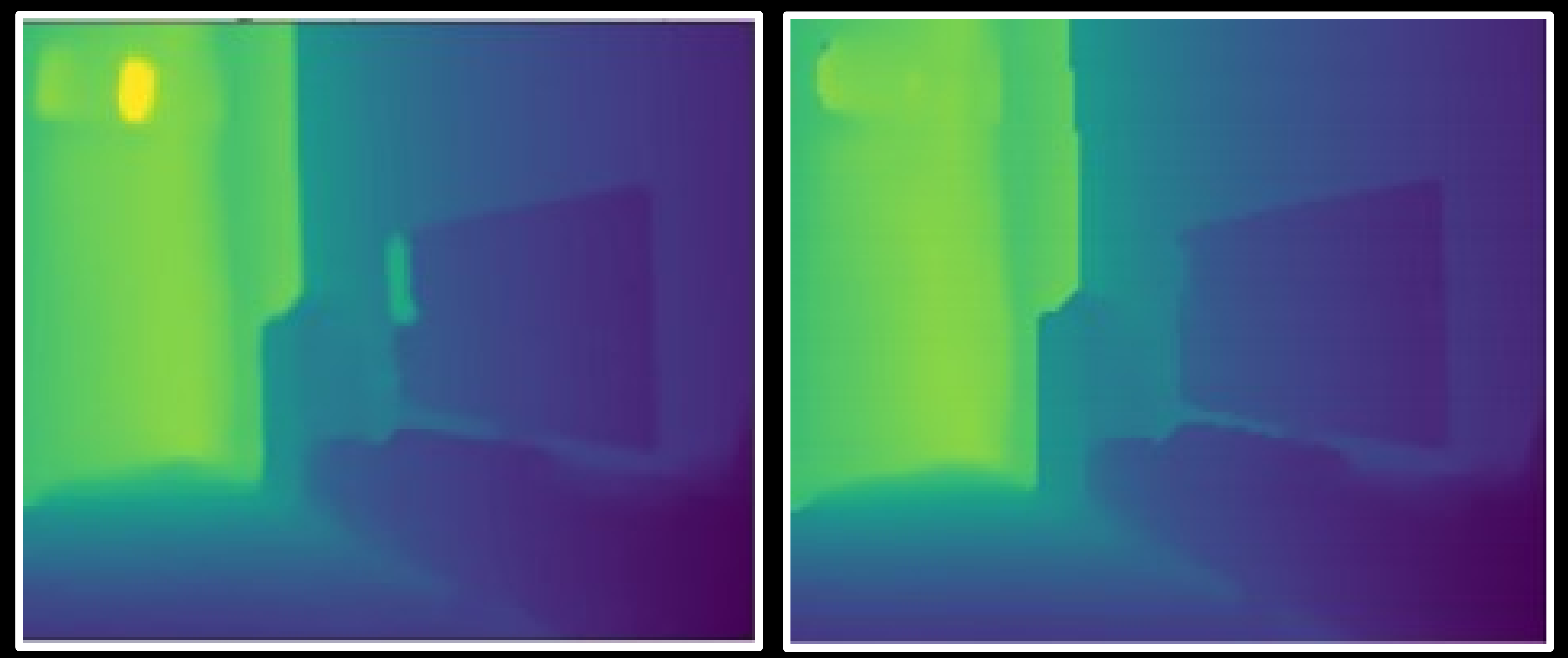

inverse rendering [Wu et al. 2021]

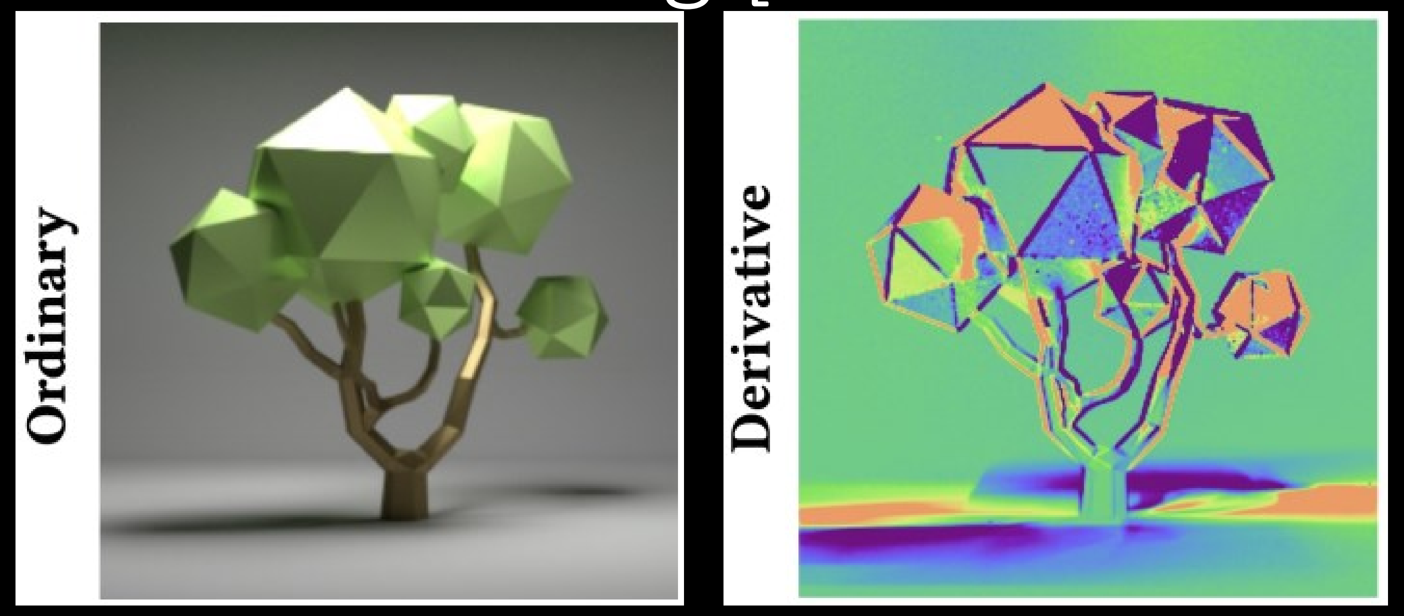

SONAR [Reed et al. 2023]

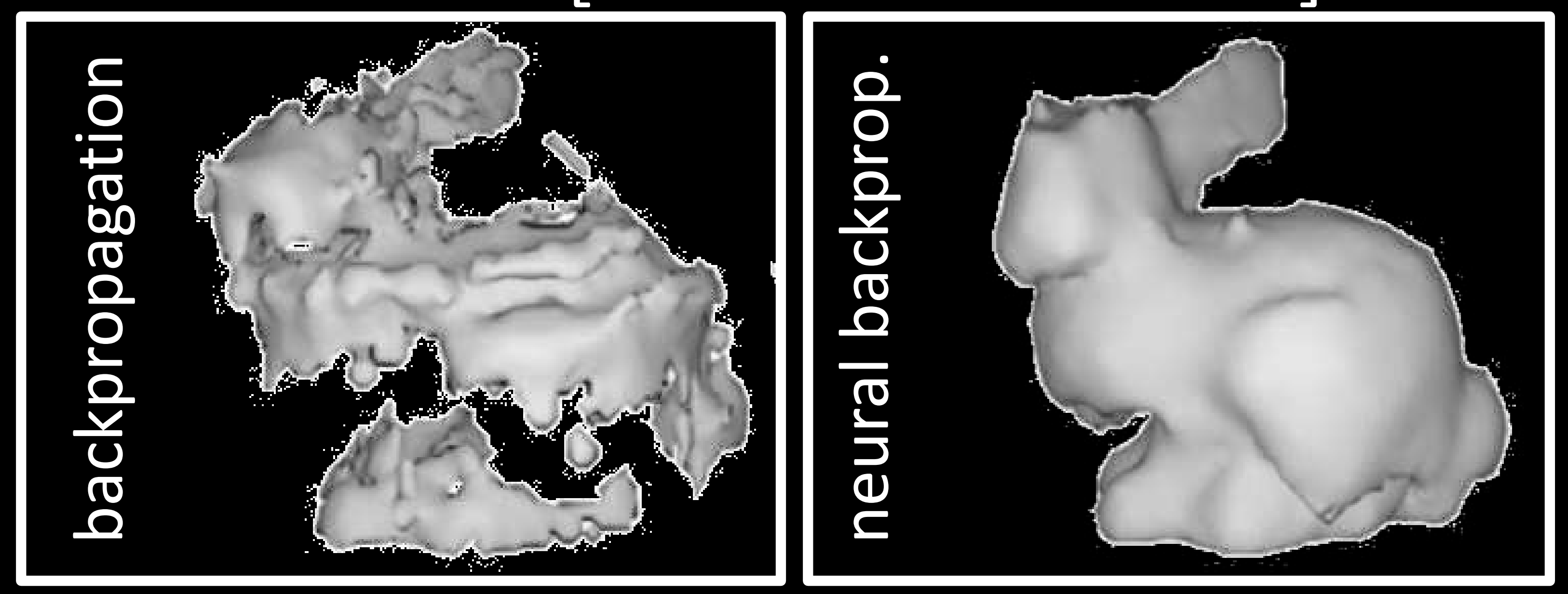

Imaging projects using this renderer

Mitsuba based
open source implementation

http://bit.ly/32Uzm1m

non-line-of-sight

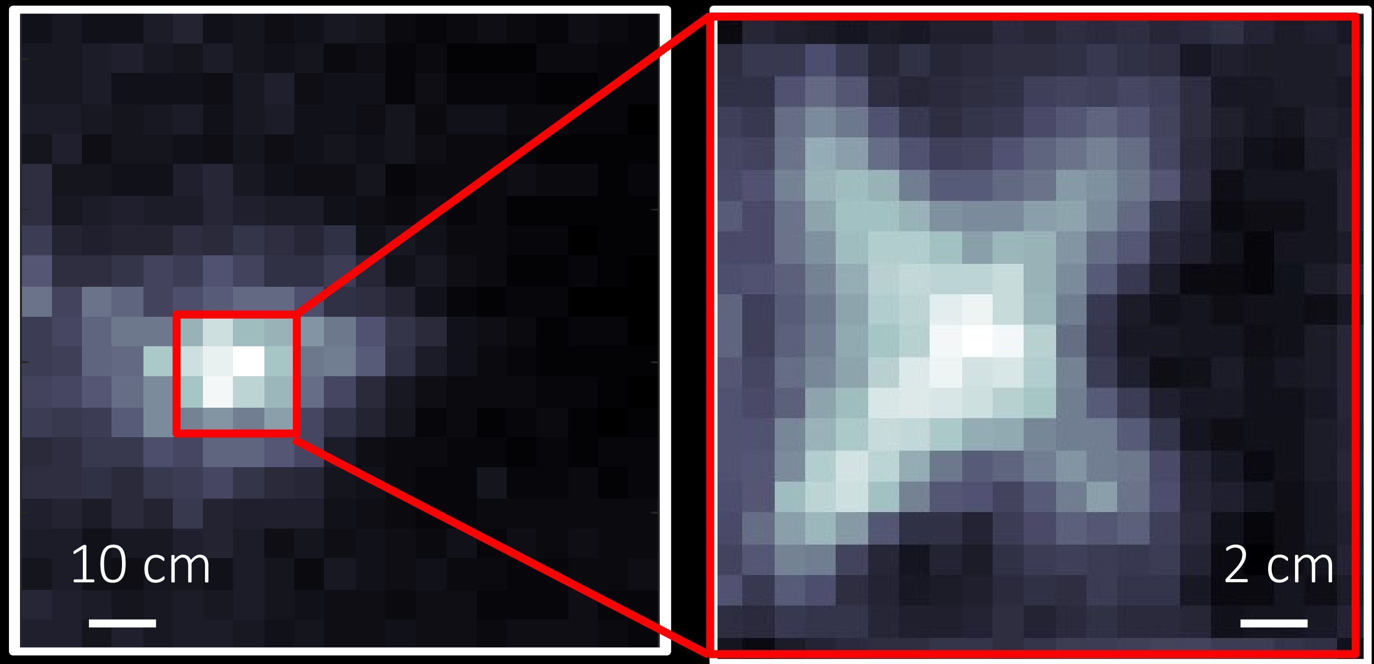

depth sensing

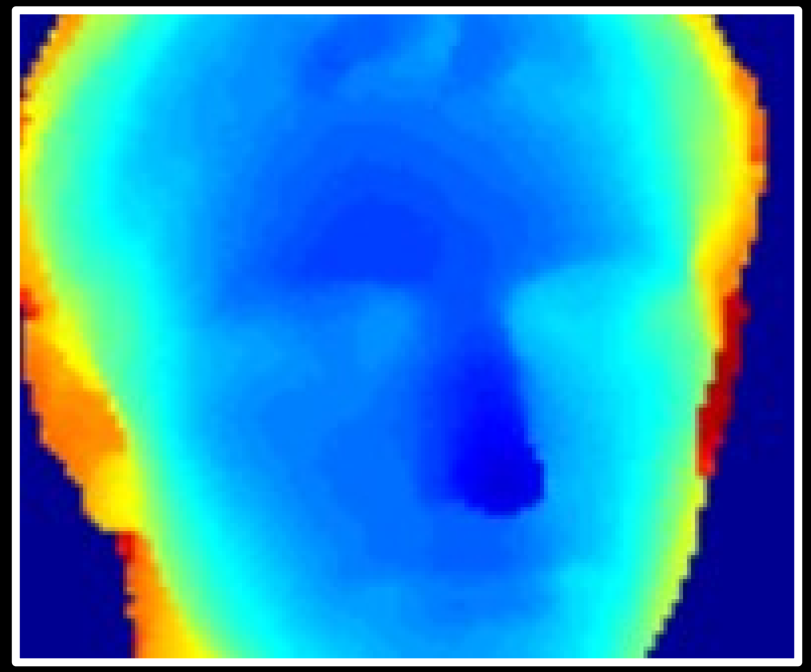

tissue imaging

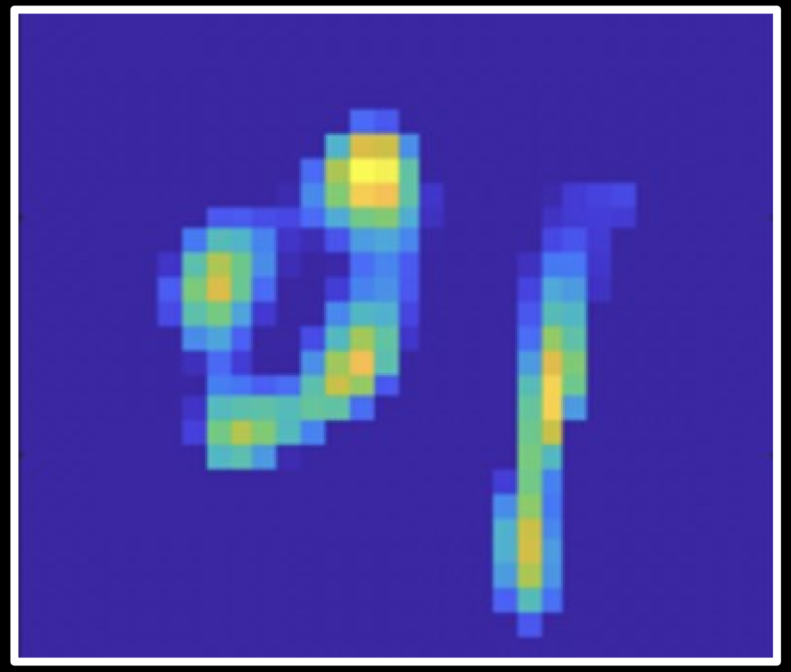

sensor design [White et al. 2022]]

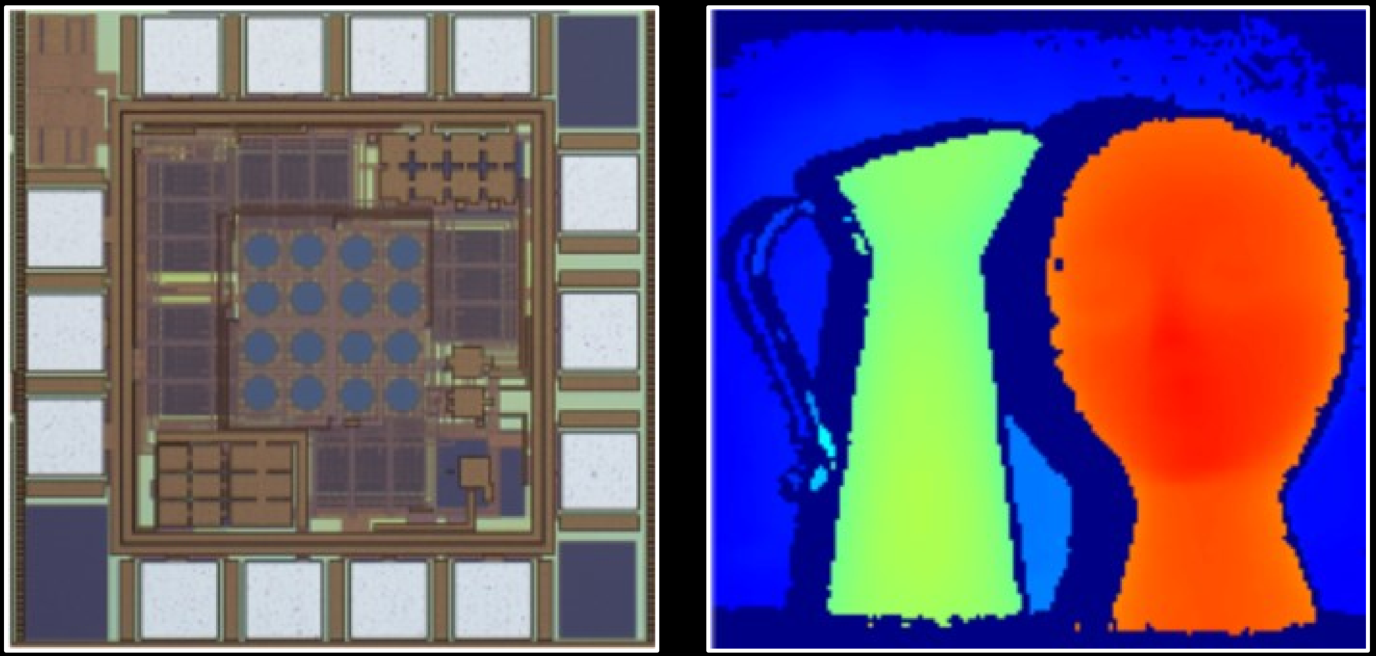

deep learning [Barragan et al. 2021]

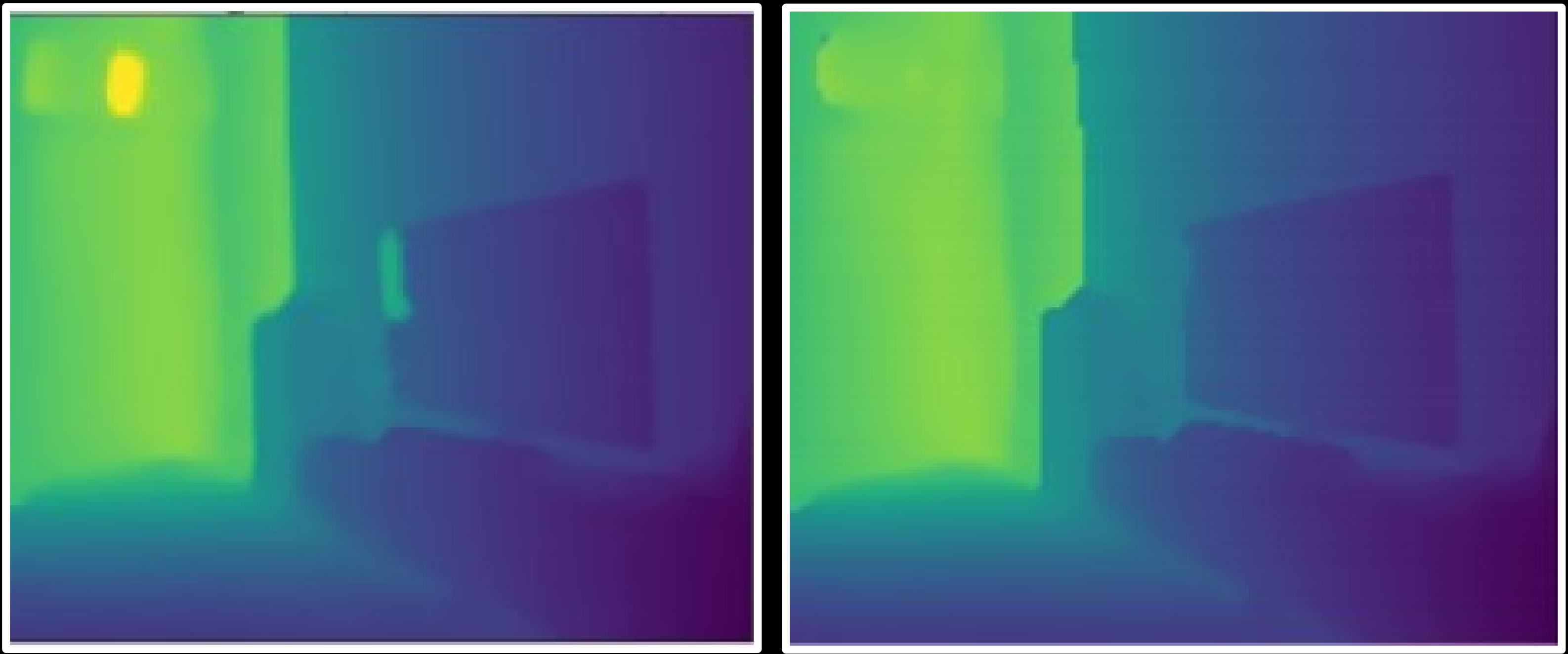

inverse rendering [Wu et al. 2021]

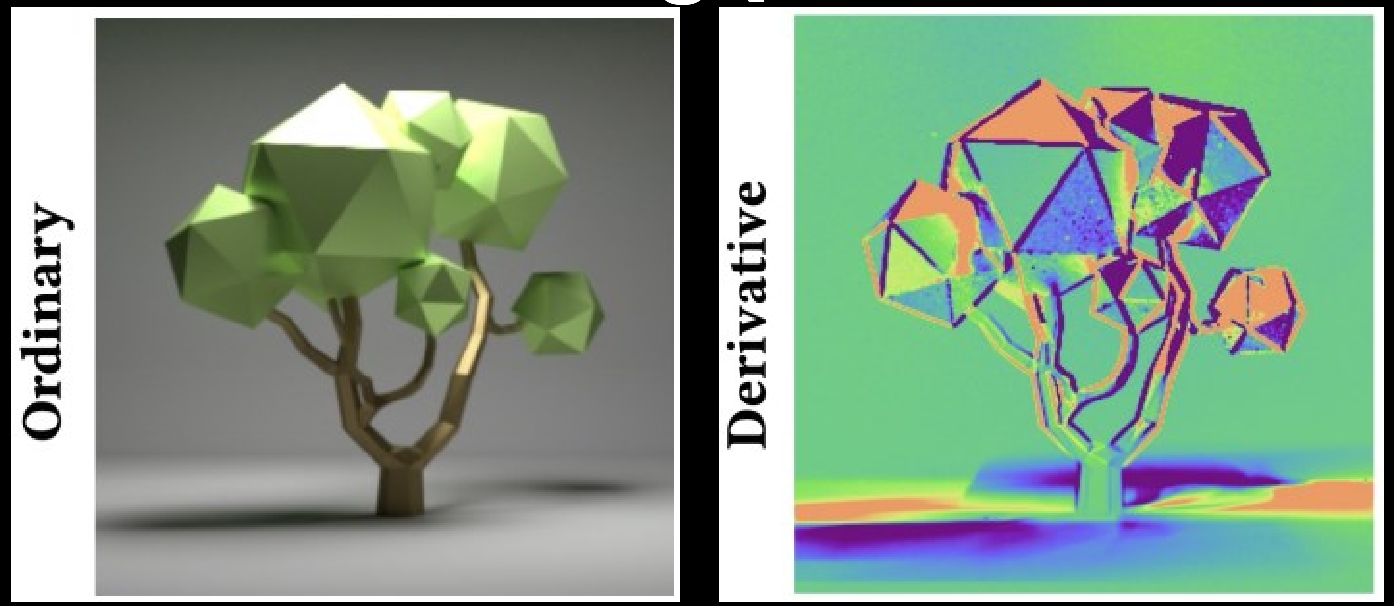

SONAR [Reed et al. 2023]

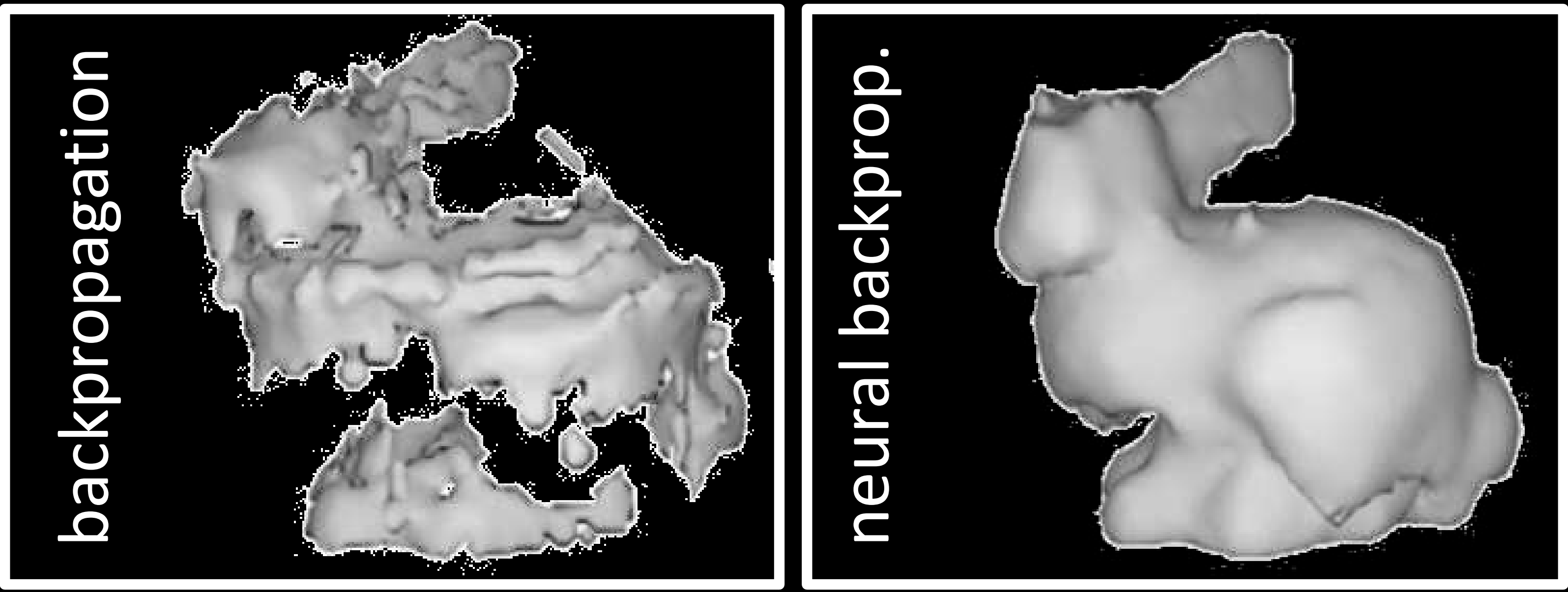

Physics-based rendering and its applications to computational imaging

forward rendering

- accurate and efficient simulation
- virtually design sensors, optics, and algorithms

inverse rendering

- accurate and efficient differentiable simulation
- tractably solve general inverse problems

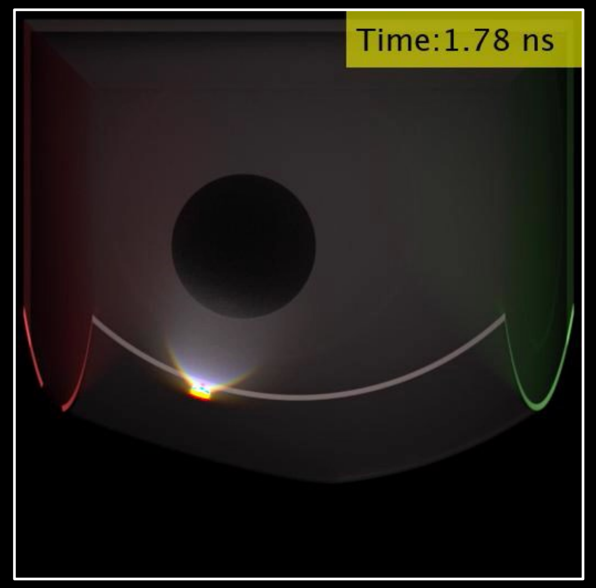

time-of-flight imaging

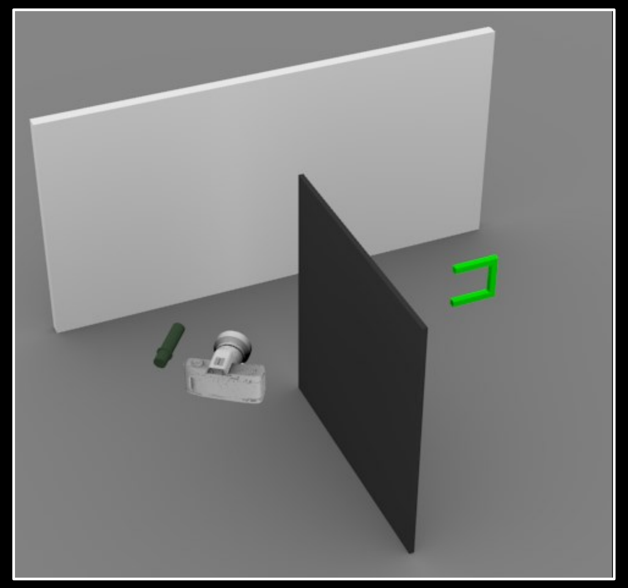

non-line-of-sight imaging

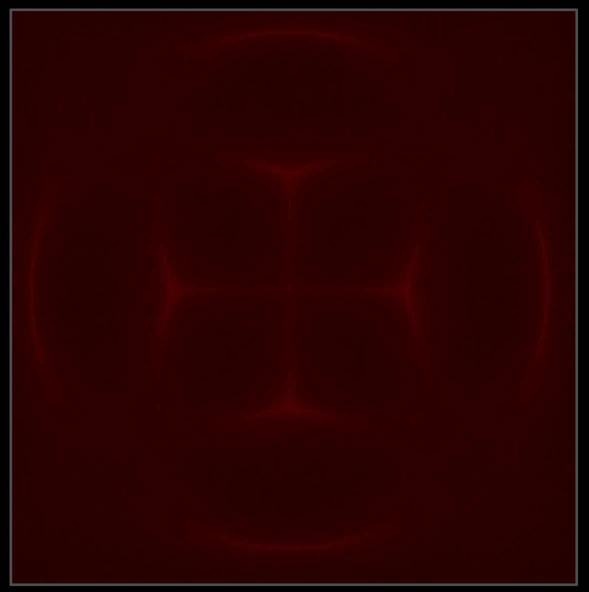

acousto-optic lensing

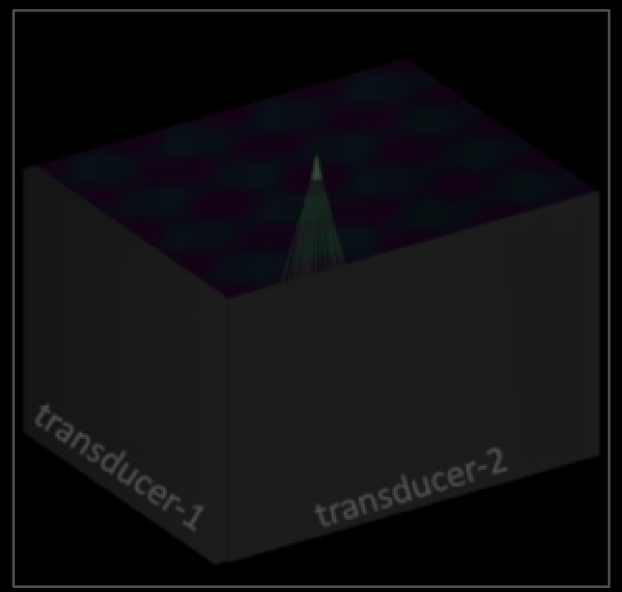

ultrafast light scanning

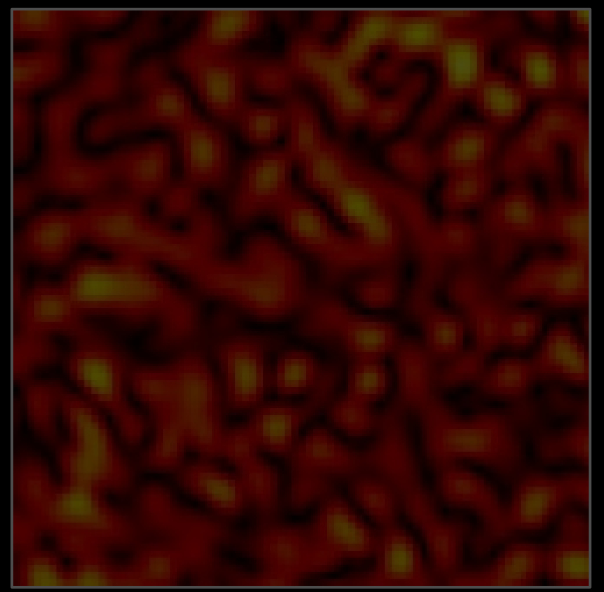

speckle imaging

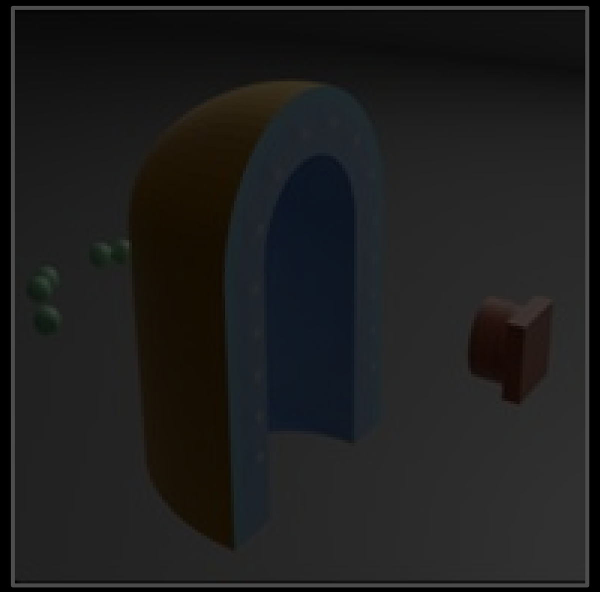

tactile sensor design

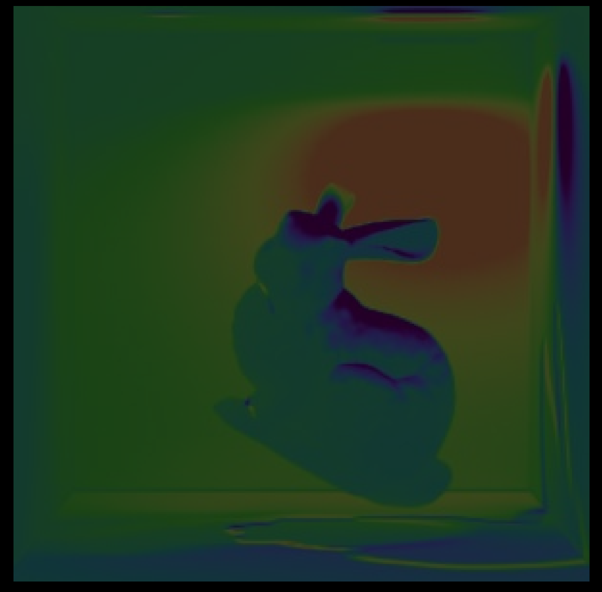

differentiable renderer

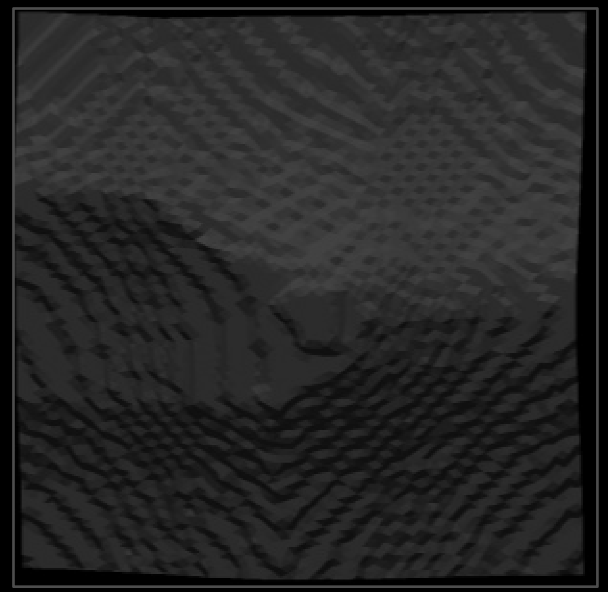

inverse problems

Non-line-of-sight imaging

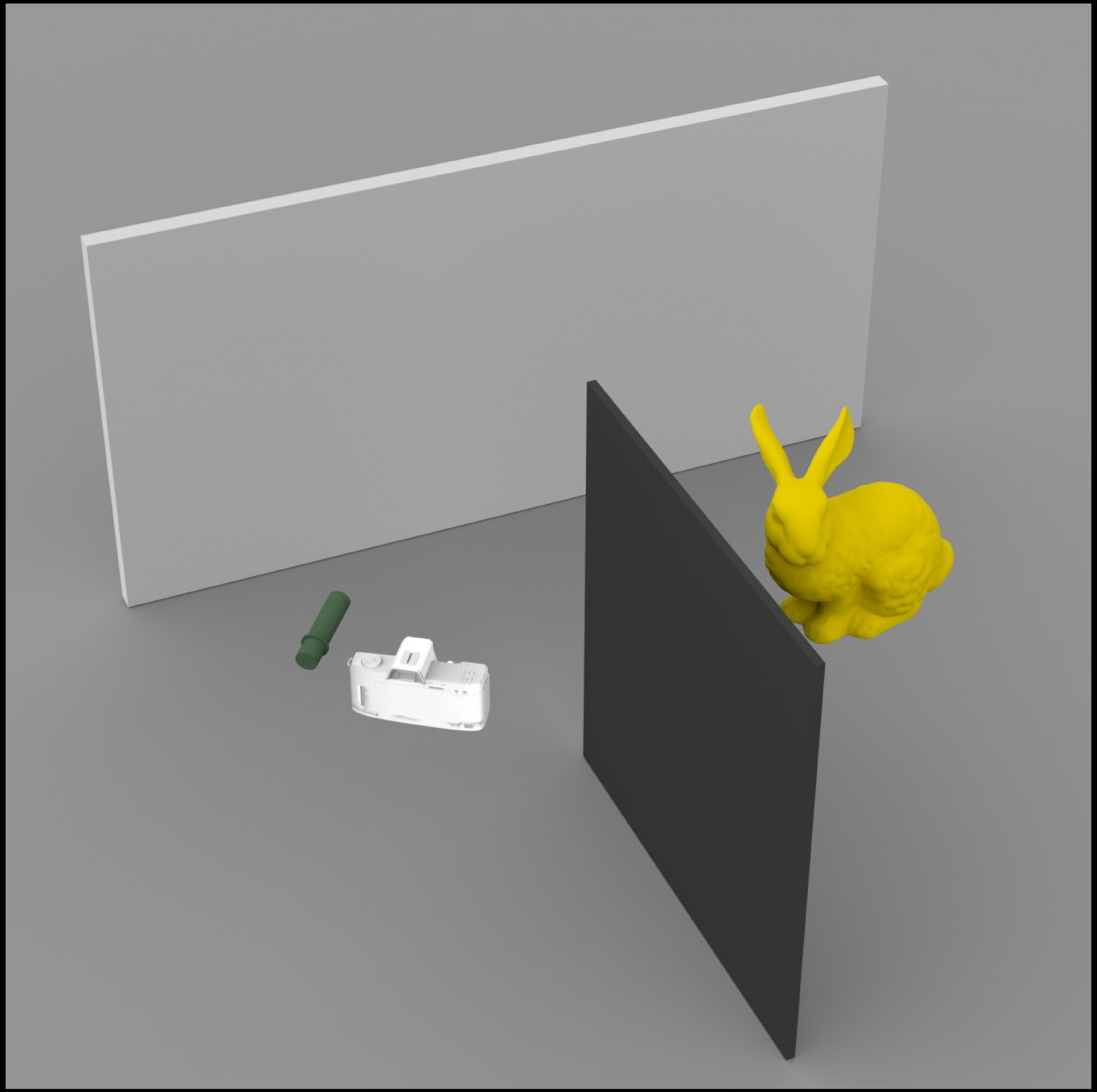

Applications

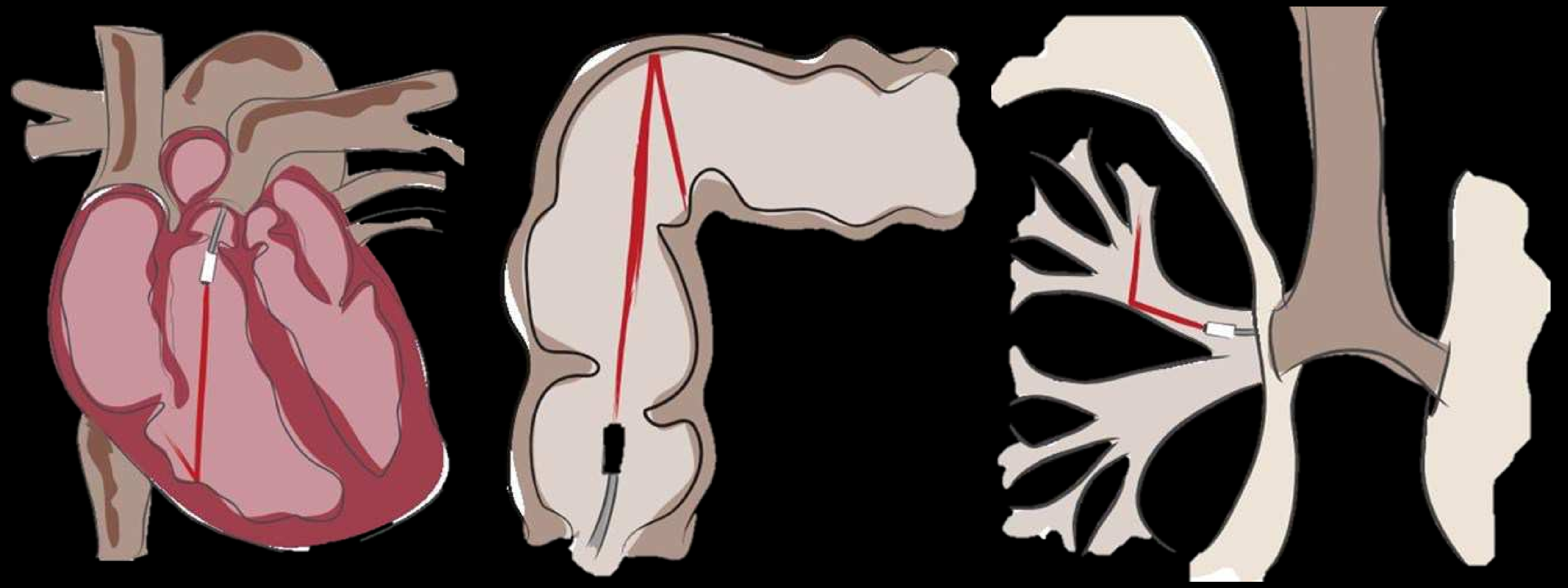

https://web.media.mit.edu/~raskar/cornar/

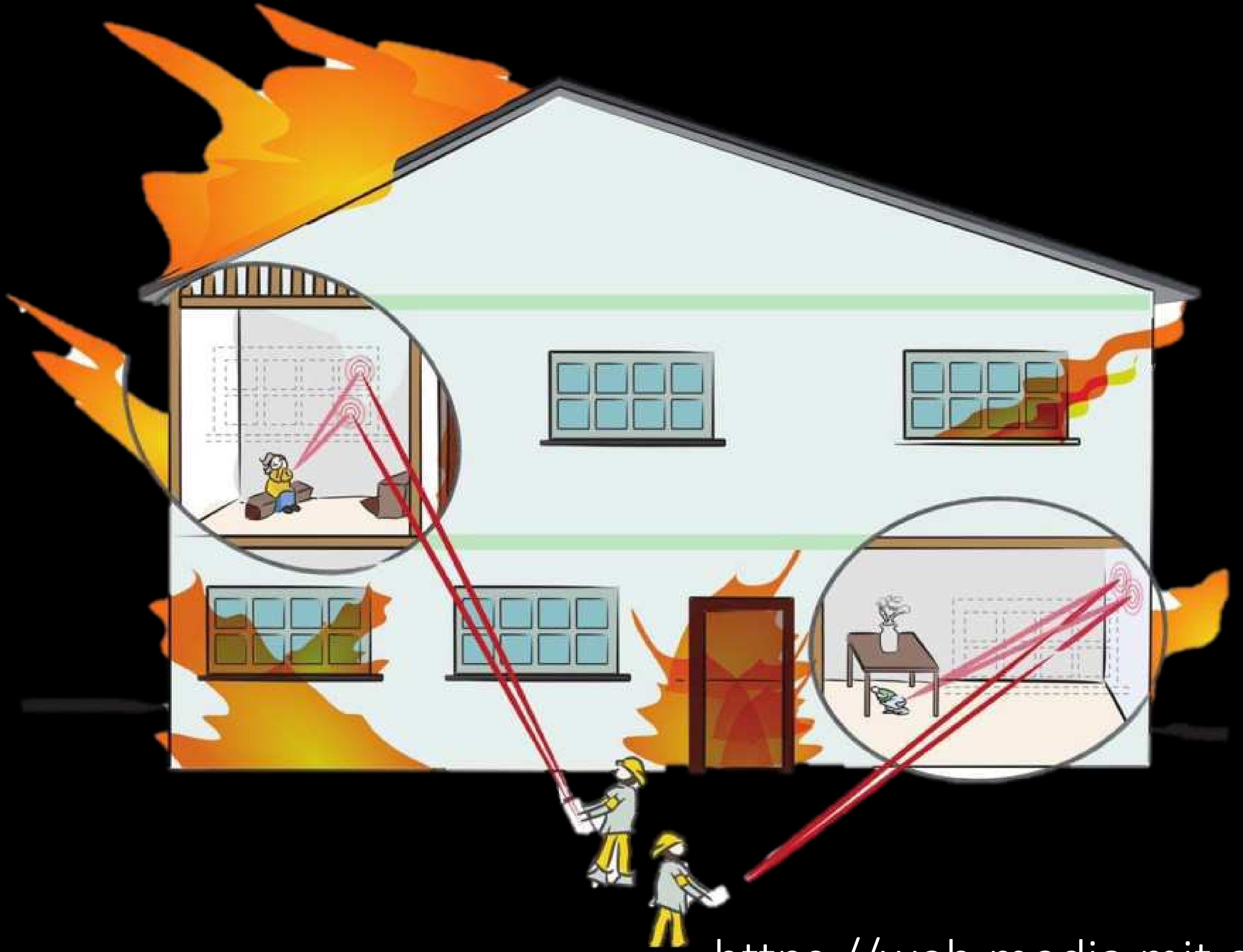

https://web.media.mit.edu/~raskar/cornar/

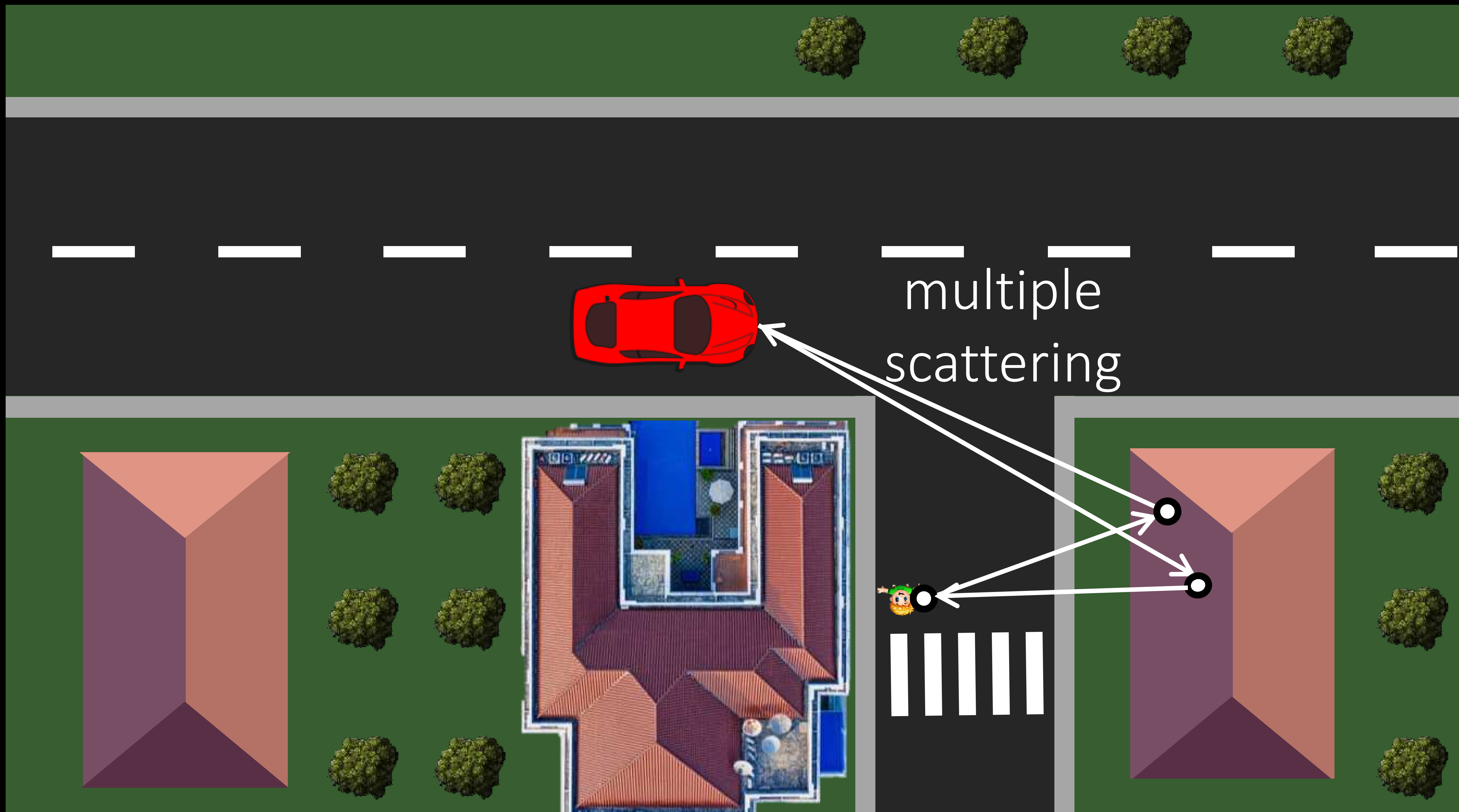

A lot of research on non-line-of-sight imaging

intensity imaging

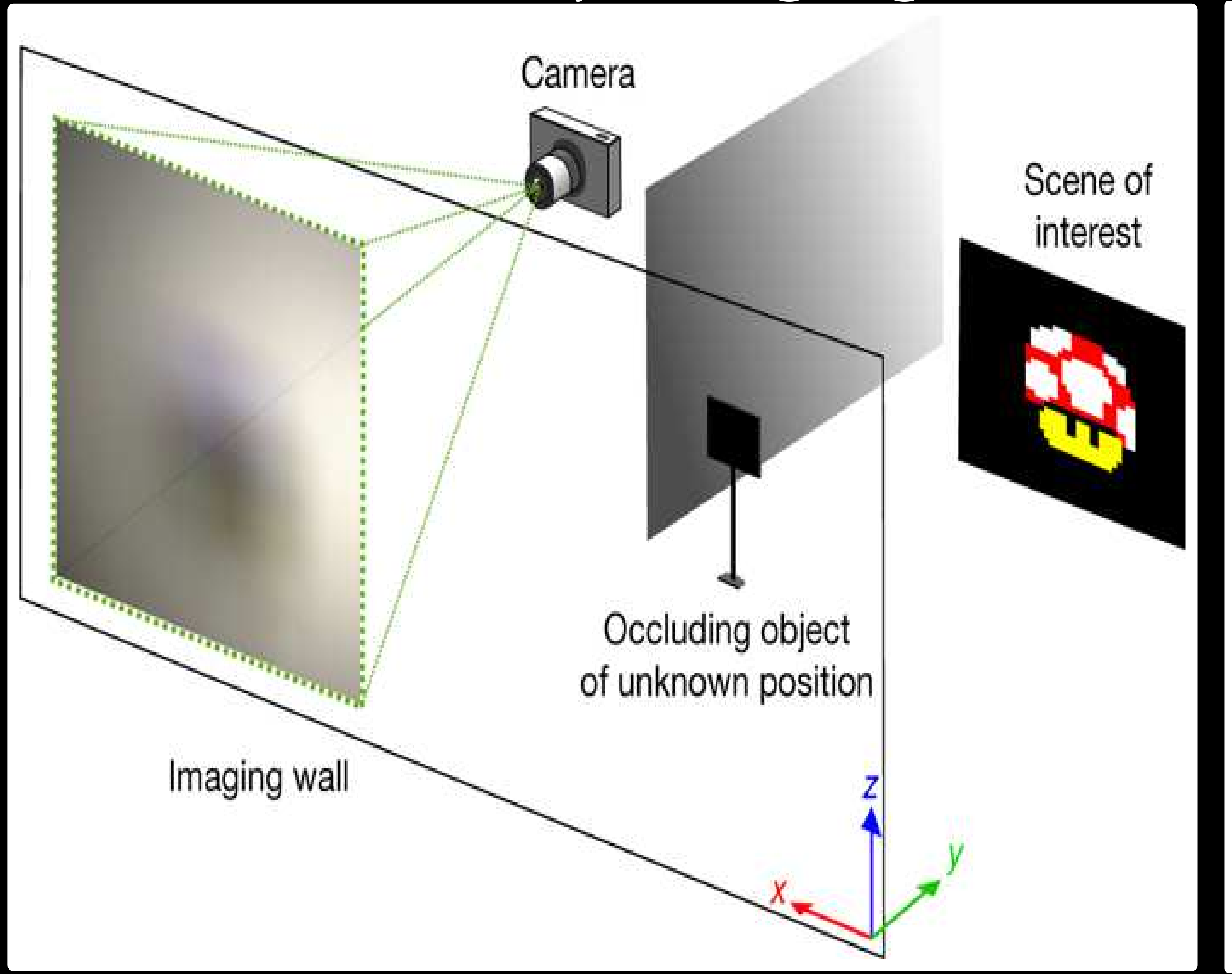

Bouman et al., ICCV 2017
Saunders et al., Nature 2019
Saunders et al., COSI 2019
Maeda et al., ICCP 2019
Lin et al., COSI 2020
Sharma, ICCV 2021

coherence imaging

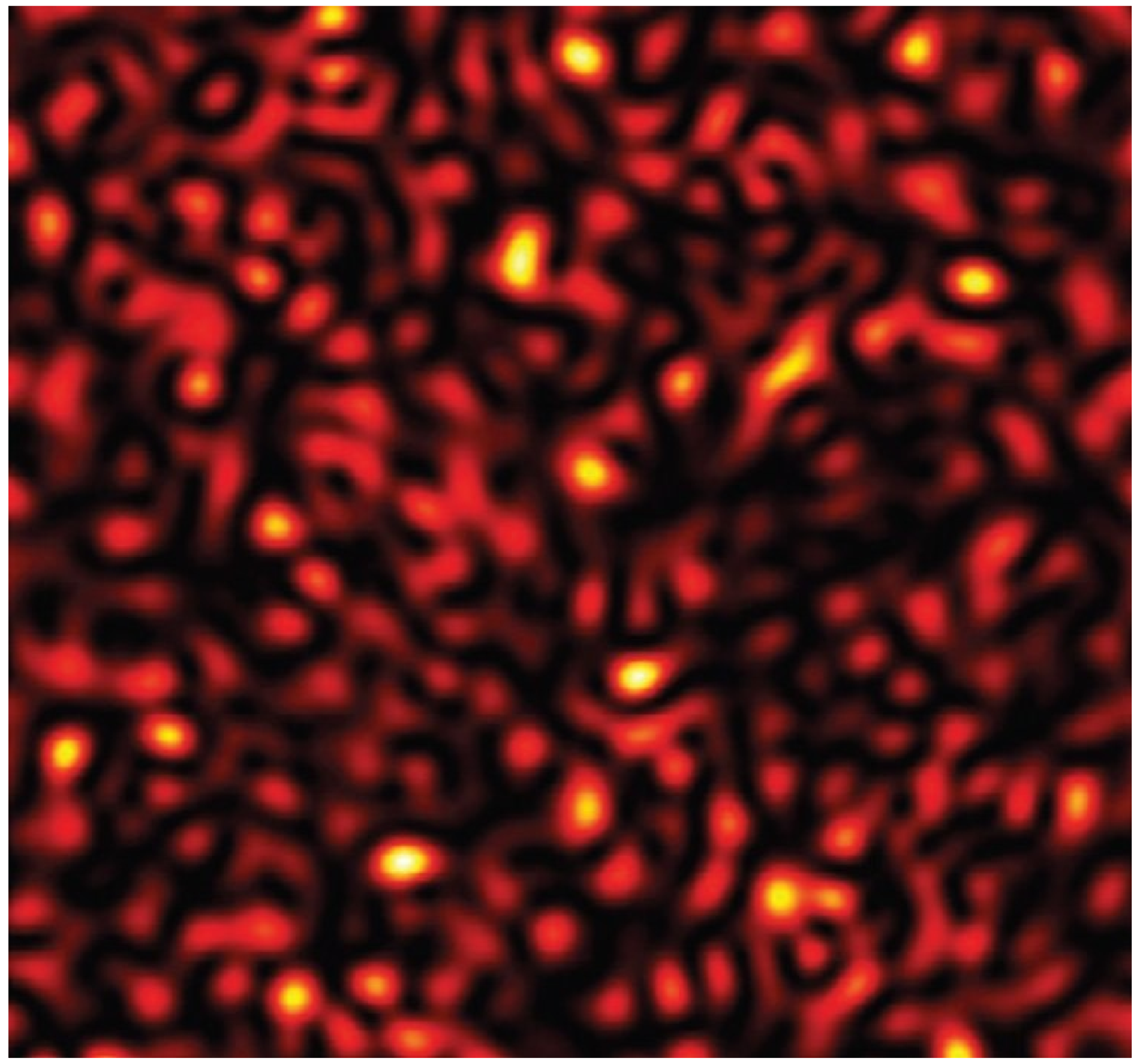

Katz et al., Nat. Photonics 2014
Lei et al., CVPR, 2019
Boger-Lombard, Nat. Com. 2019
Metzler et al., Optica 2020
Willomitzer et al., Nat. Com. 2021
Chen et al. SPIE 2022

time-of-flight imaging

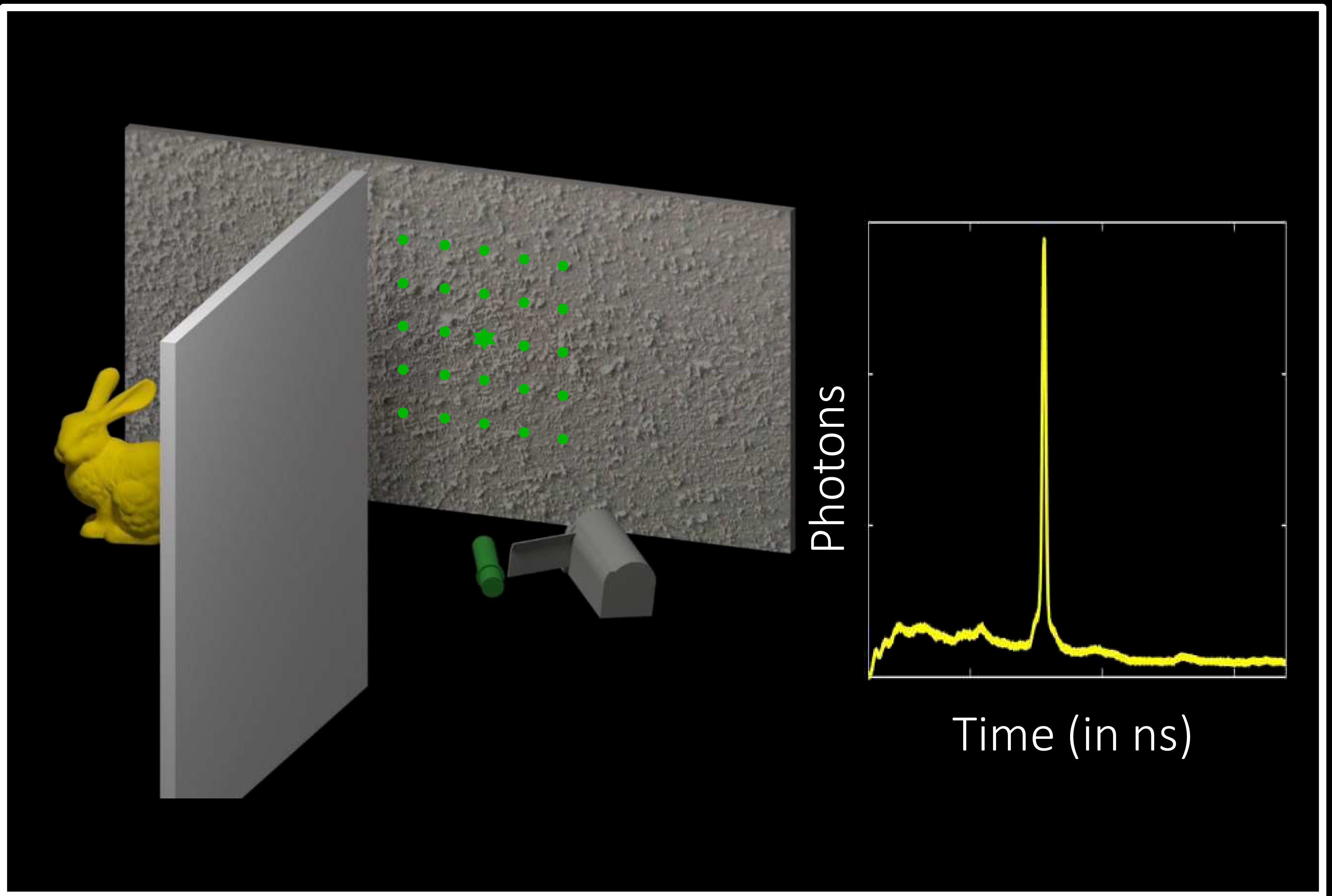

Velten et al., Nat. comm. 2012
Toole et al., Nature 2018
Liu et al., Nature 2019, Nat. comm. 2020
Rapp et al. Nat. comm. 2020
Xin et al., CVPR 2019
Nam et al., Nat. comm. 2021

How do we image in line-of-sight?

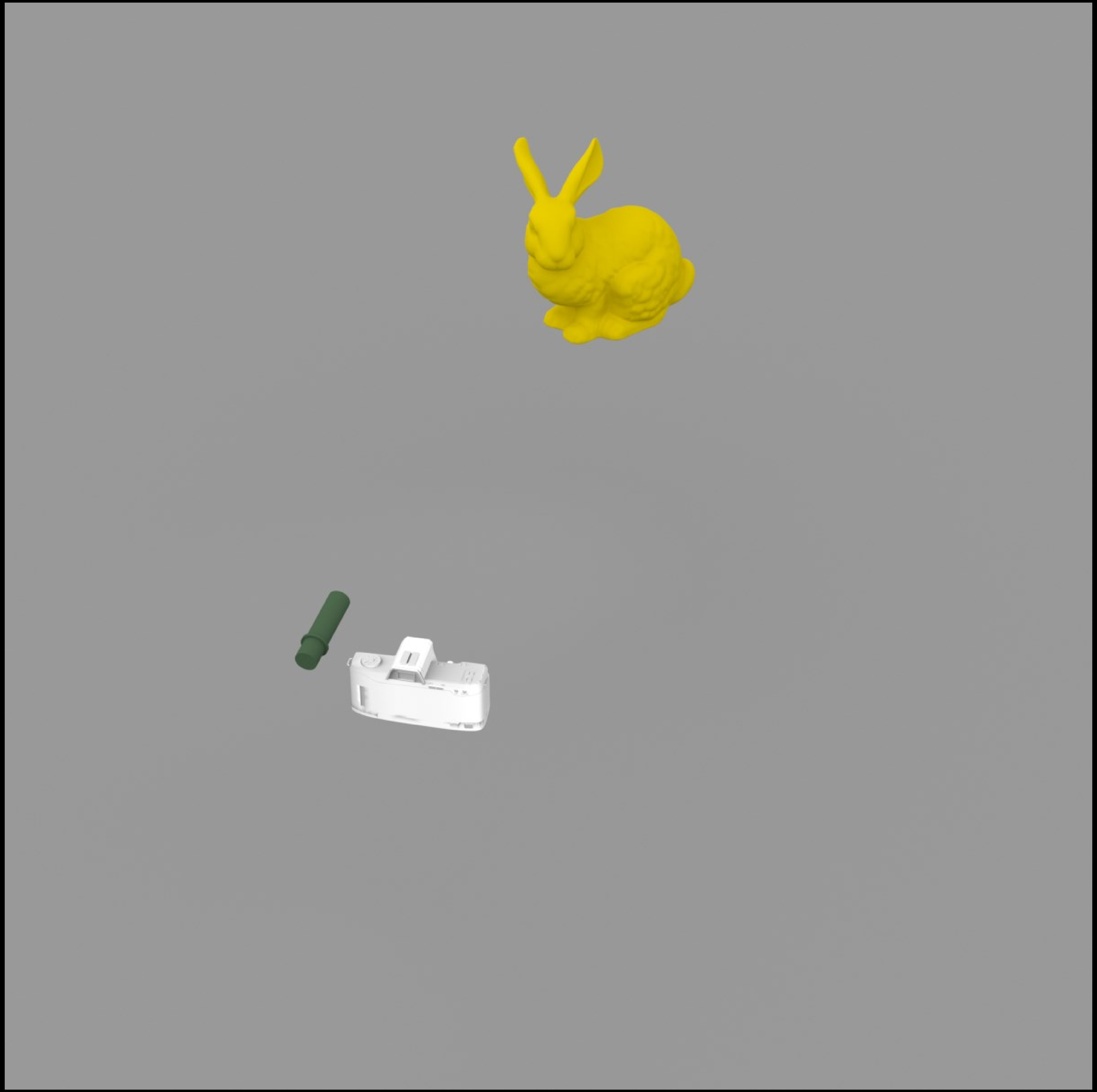

How do we image in line-of-sight?

How do we image in non-line-of-sight?

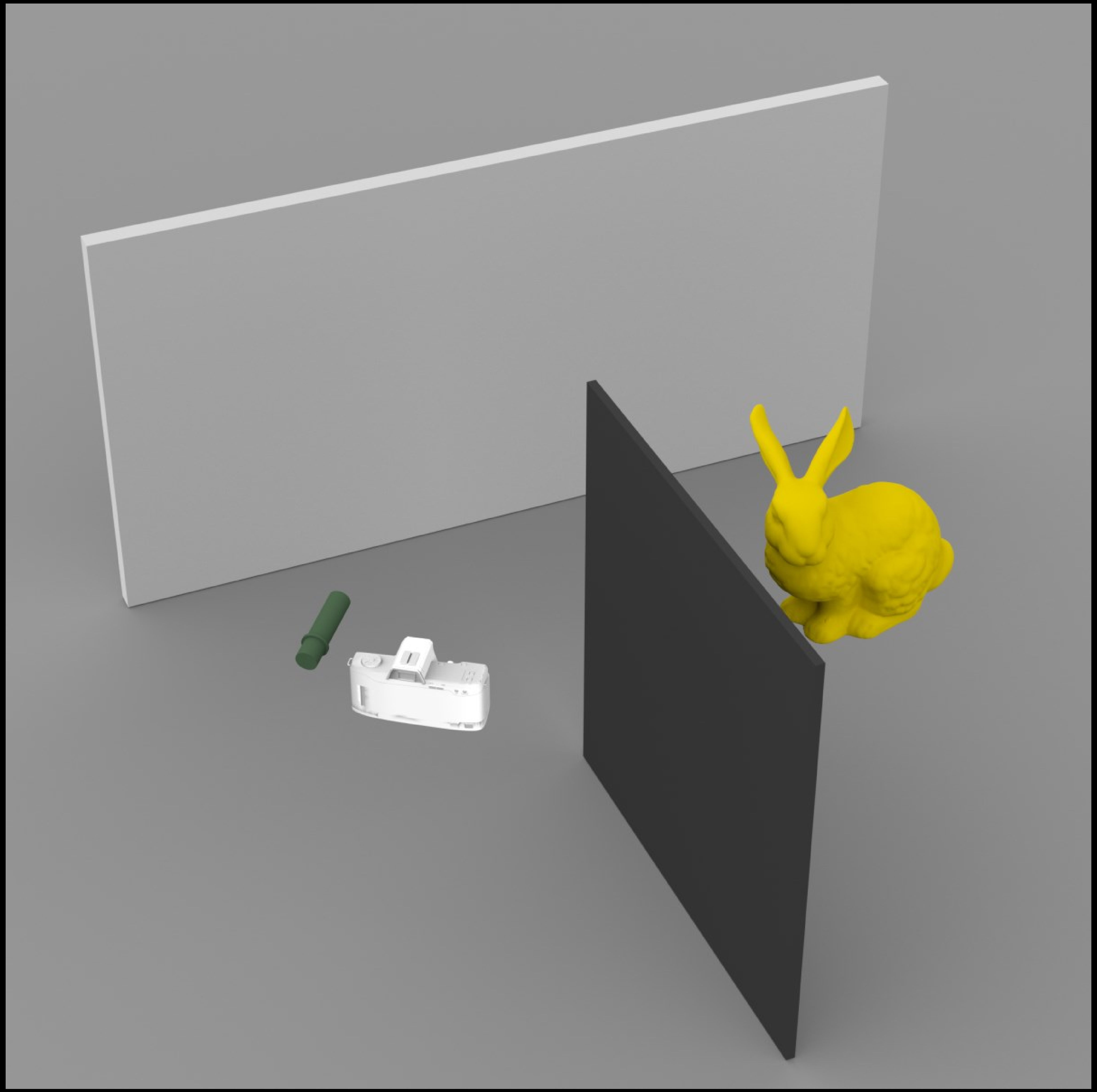

How do we focus on a voxel?

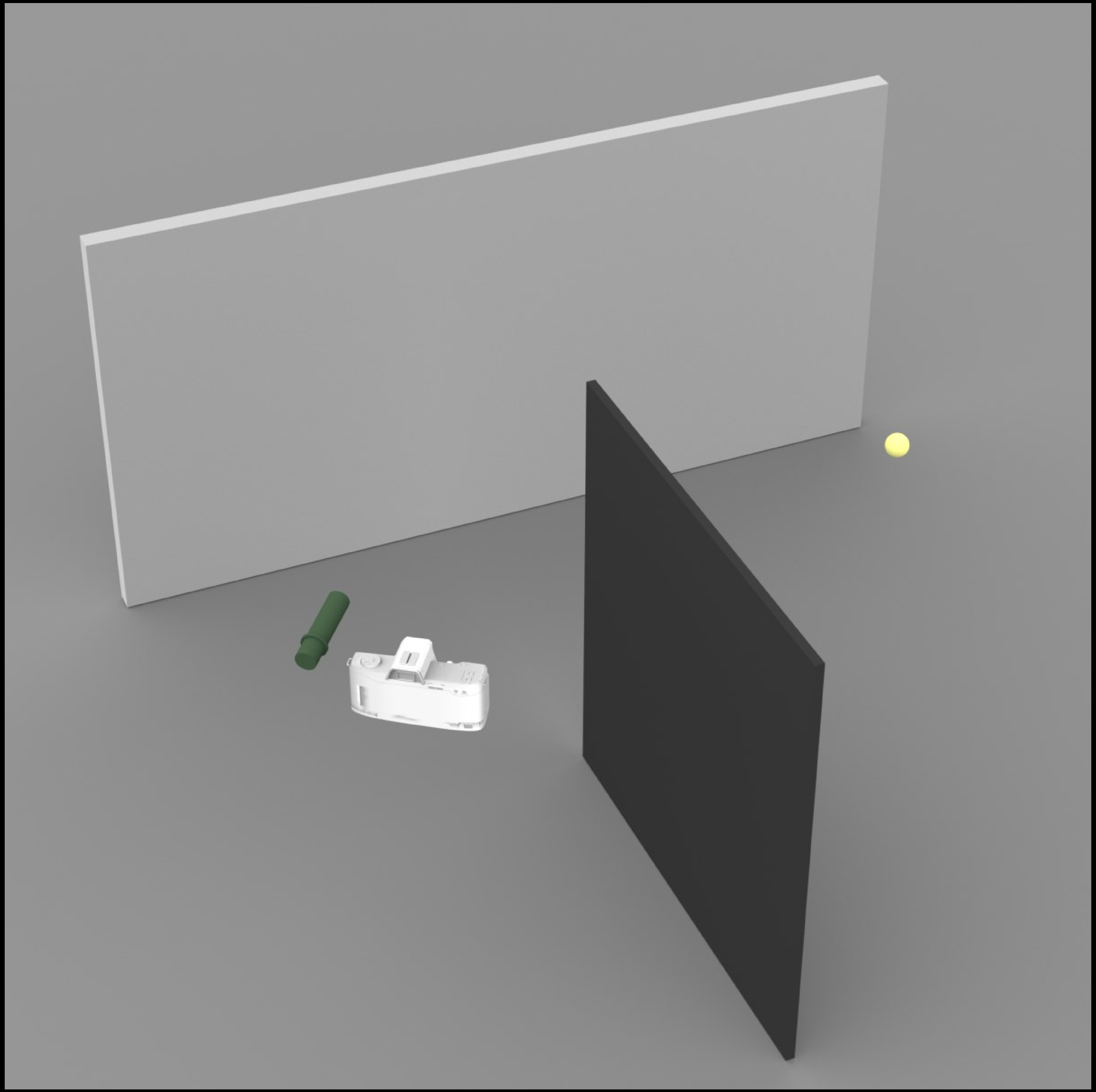

How do we focus on a voxel?

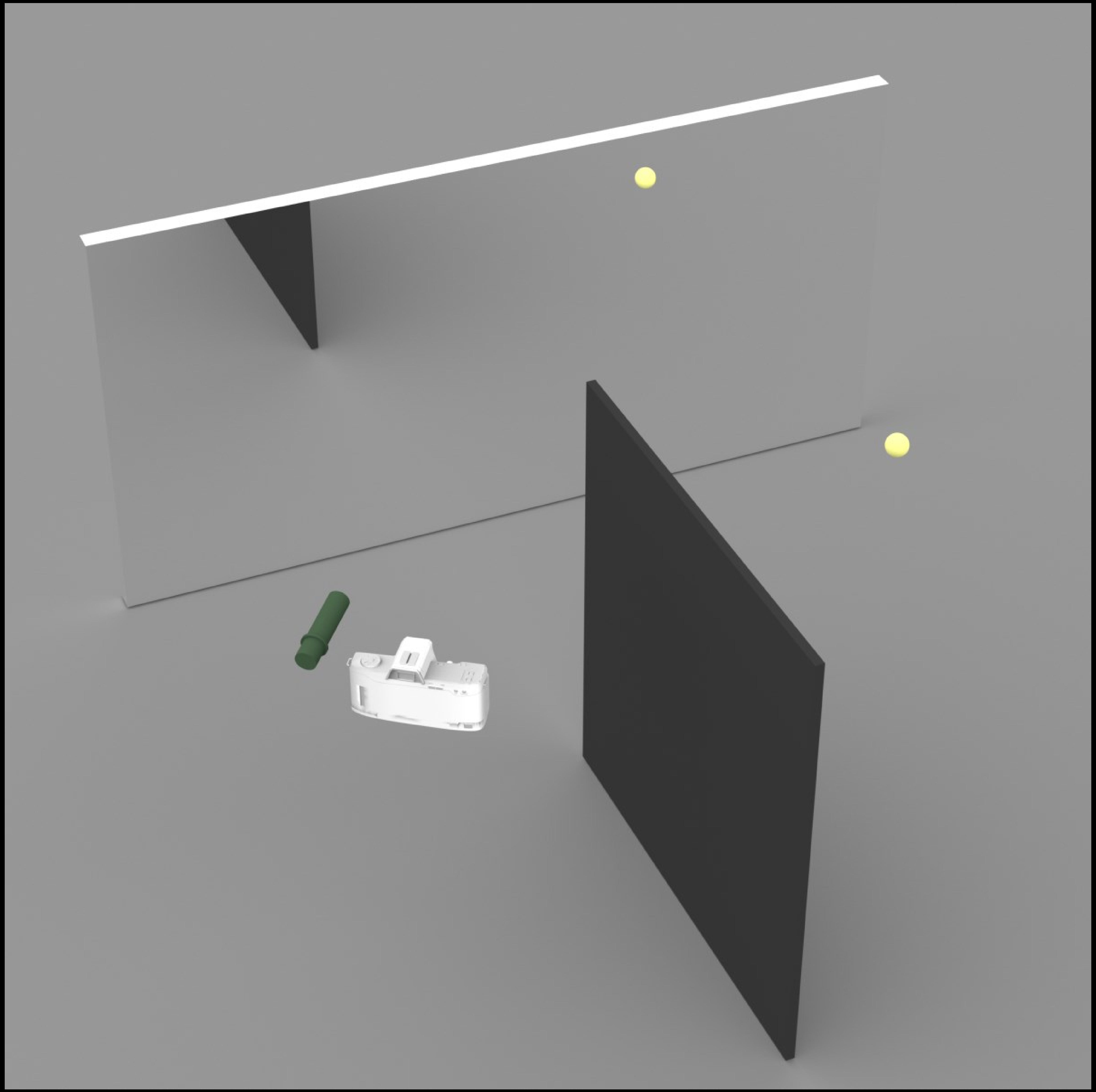

How do we focus on a voxel?

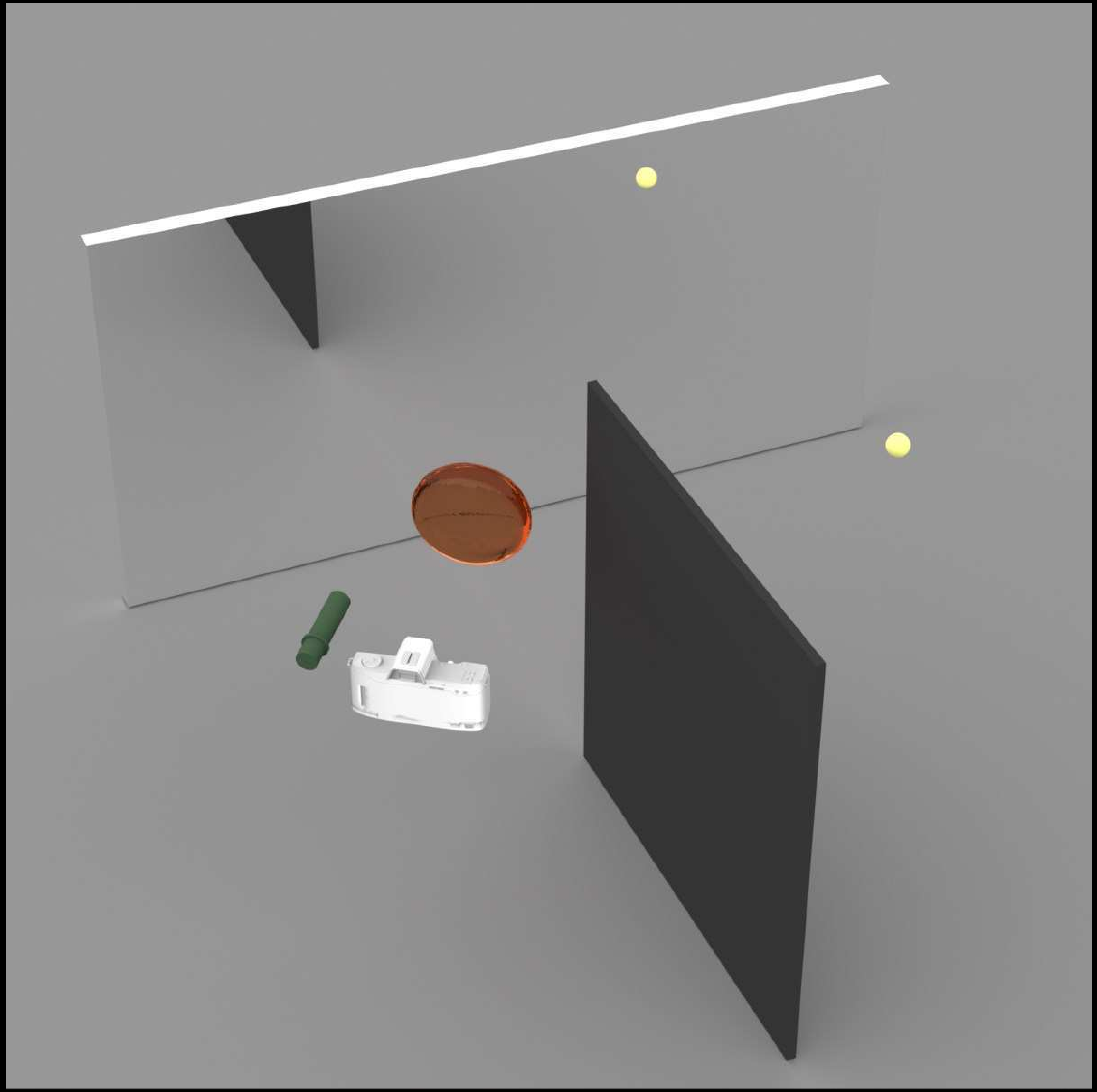

How do we focus on a voxel?

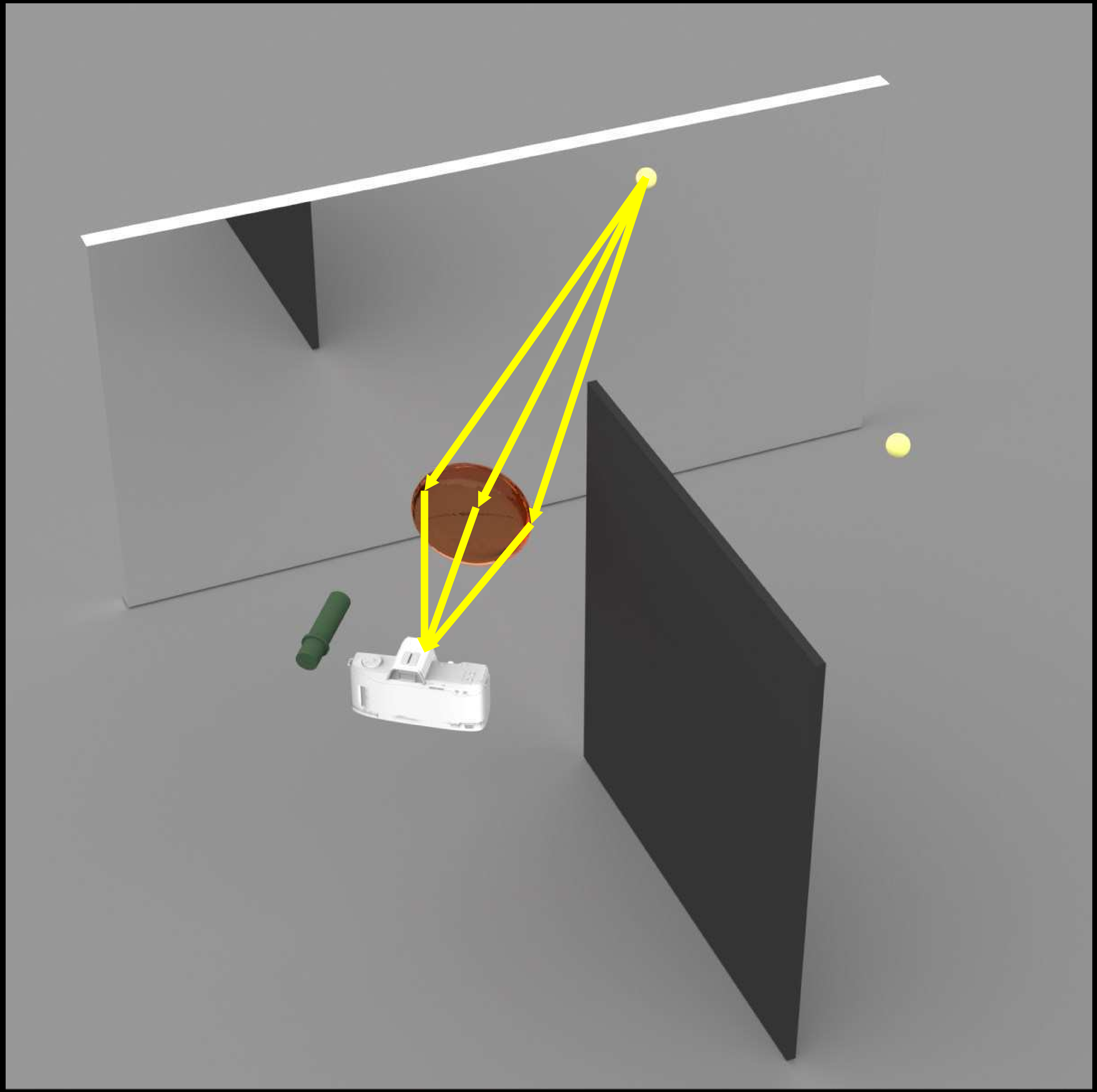

How do we focus on a voxel?

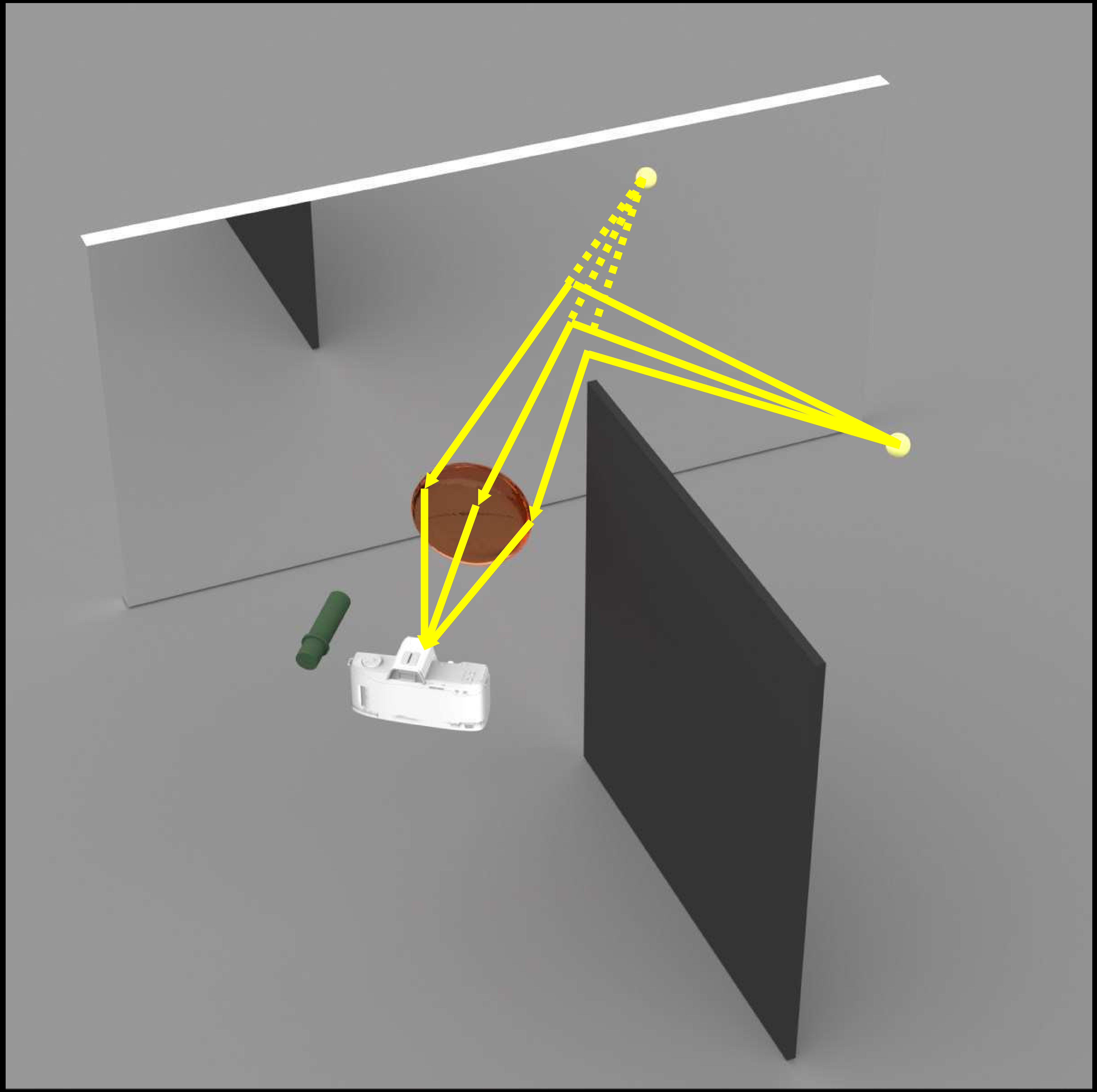

How do we focus on a voxel?

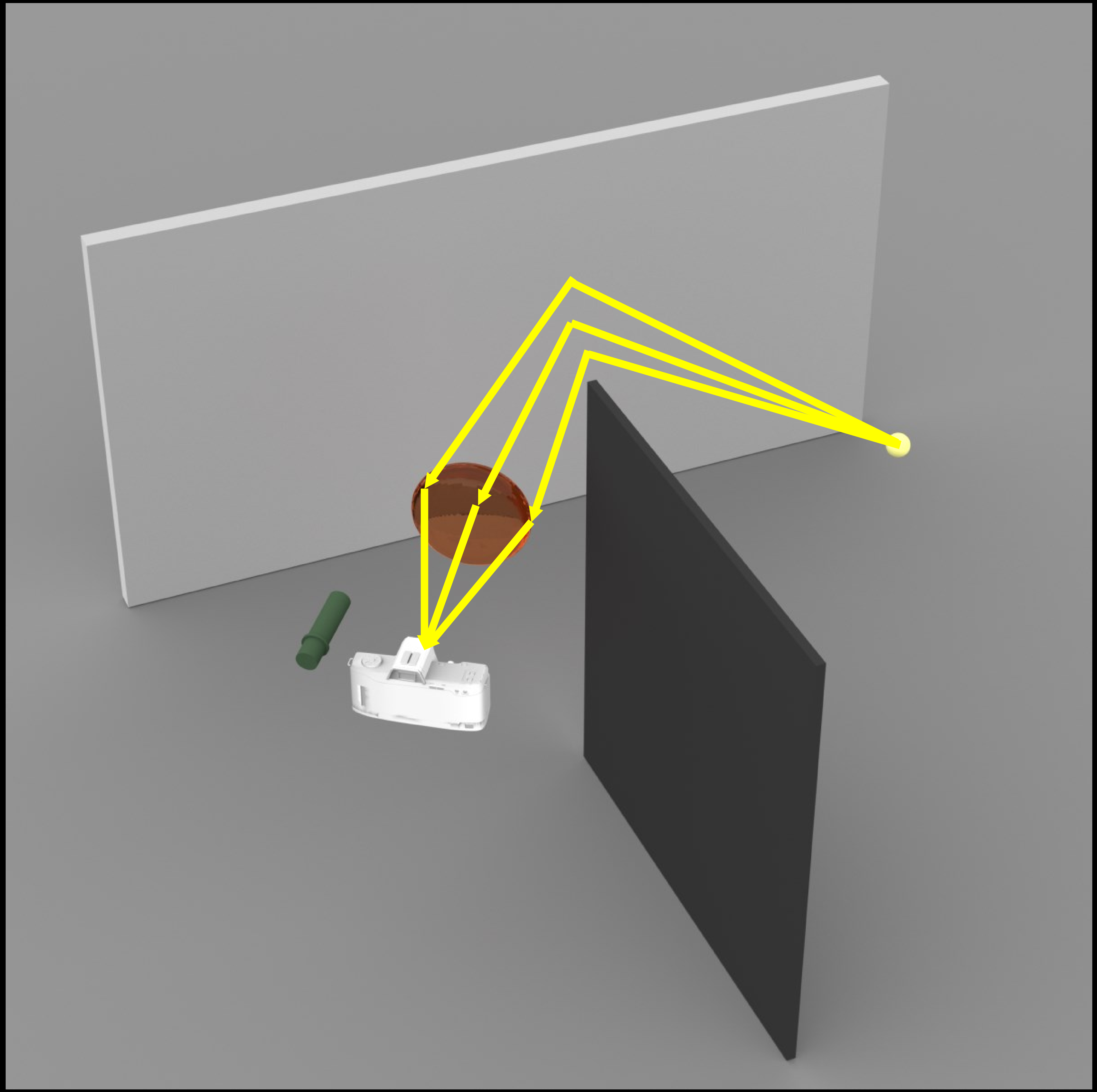

How do we focus on a voxel?

challenge:

out of focus voxels

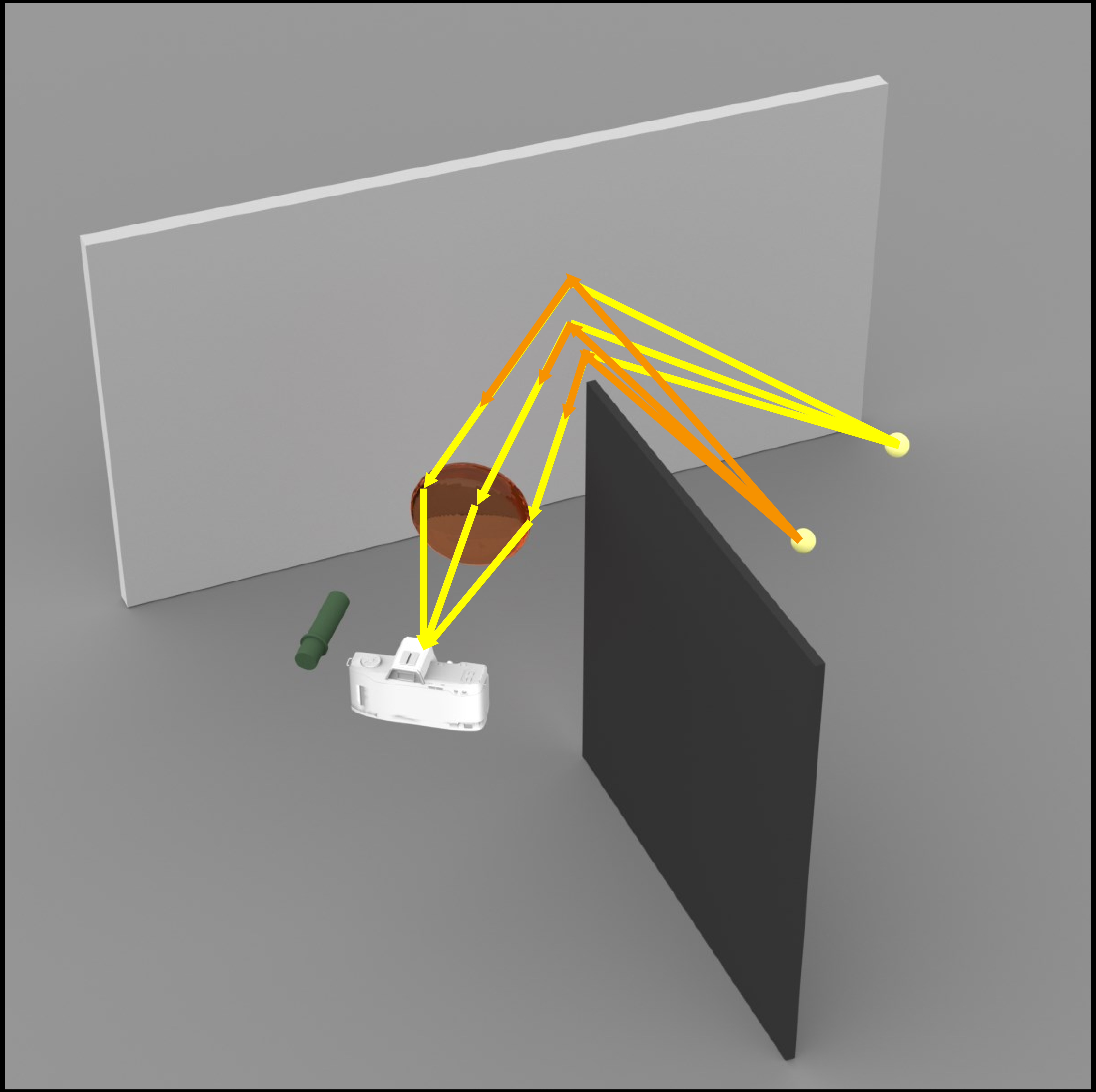

How do we focus on a voxel?

challenge:

out of focus voxels

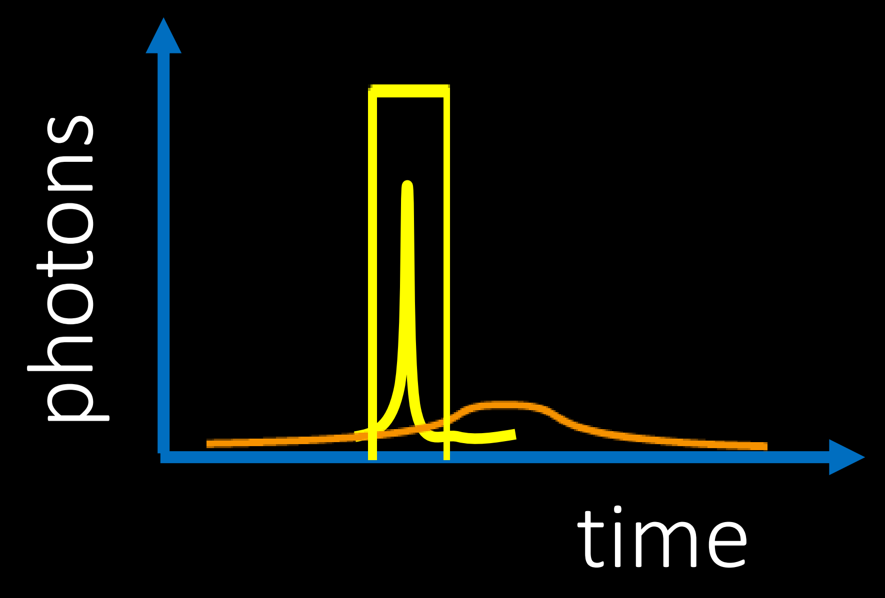

solution:

time-gate photons

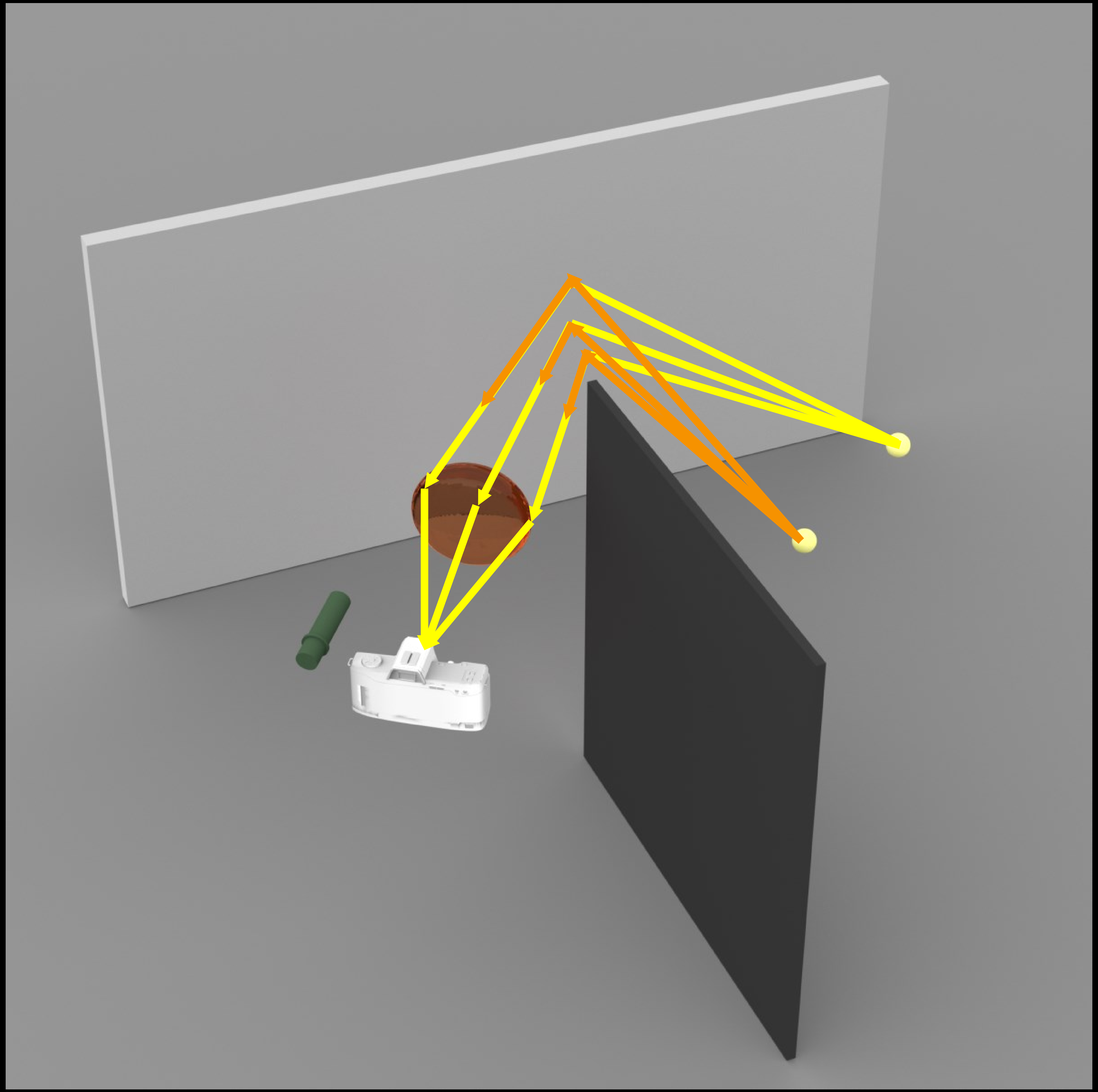

How do we focus on a voxel?

challenge:

non-specular photons

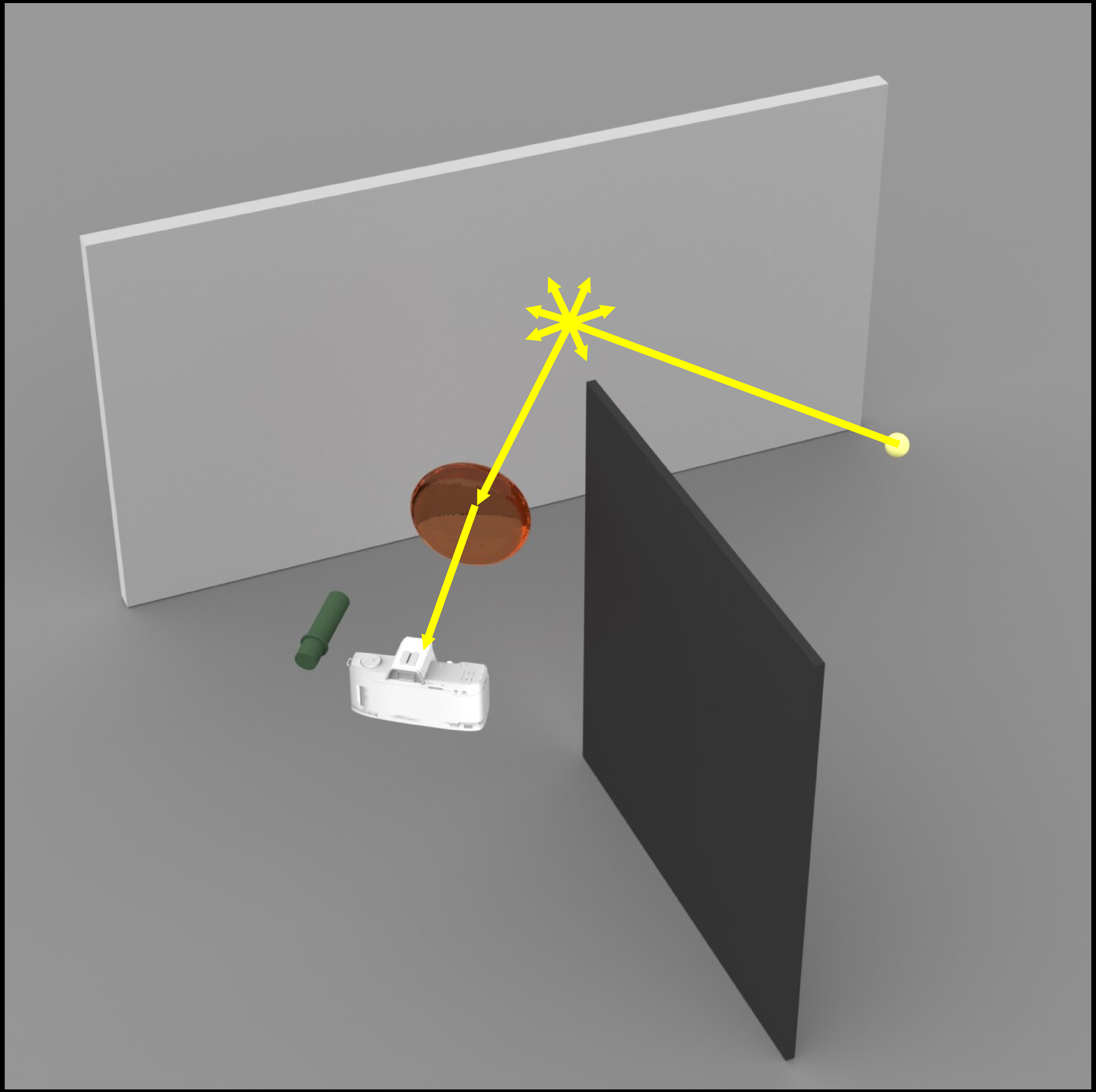

How do we focus on a voxel?

challenge:

non-specular photons

solution:

use a large lens?
expensive !!

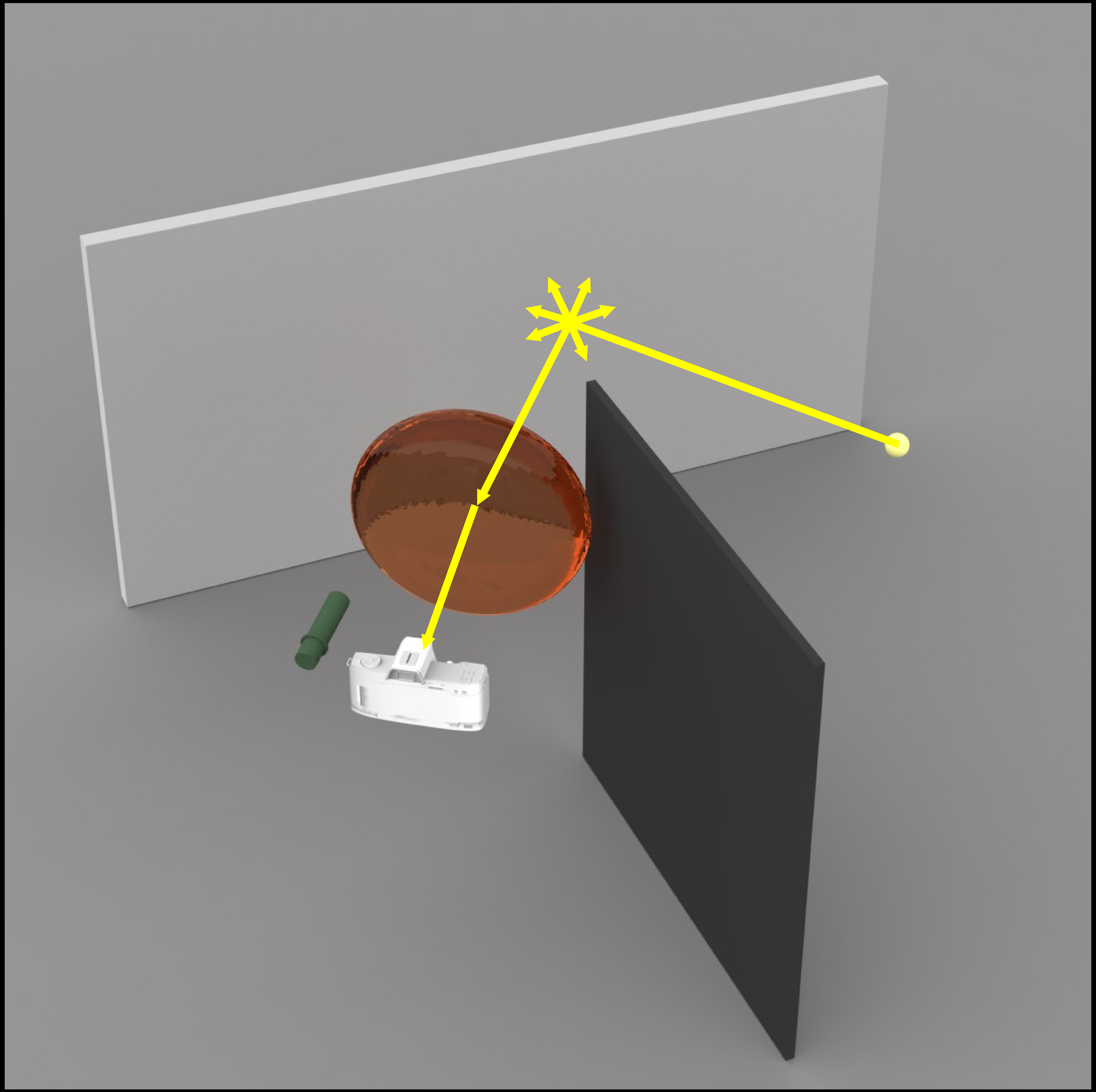

How do we focus on a voxel?

challenge:

non-specular photons

solution:

use a large lens?
expensive !!

what does a lens do?
delays rays such that they reach detector at same time instant

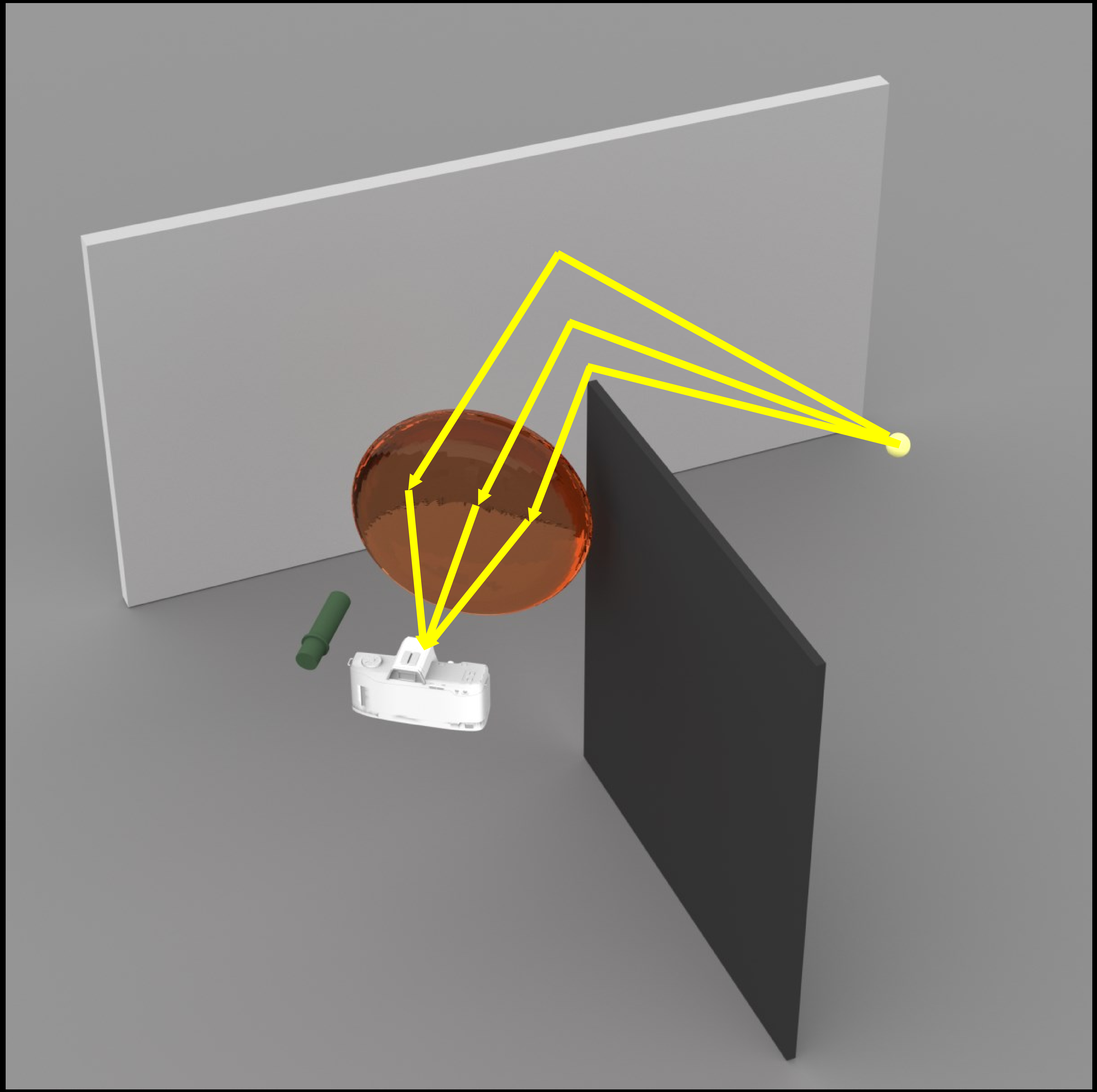

Temporal focusing: imitate the lens

challenge:

non-specular photons

solution:

use a large lens?
expensive !!

temporal focusing:
imitate large lens

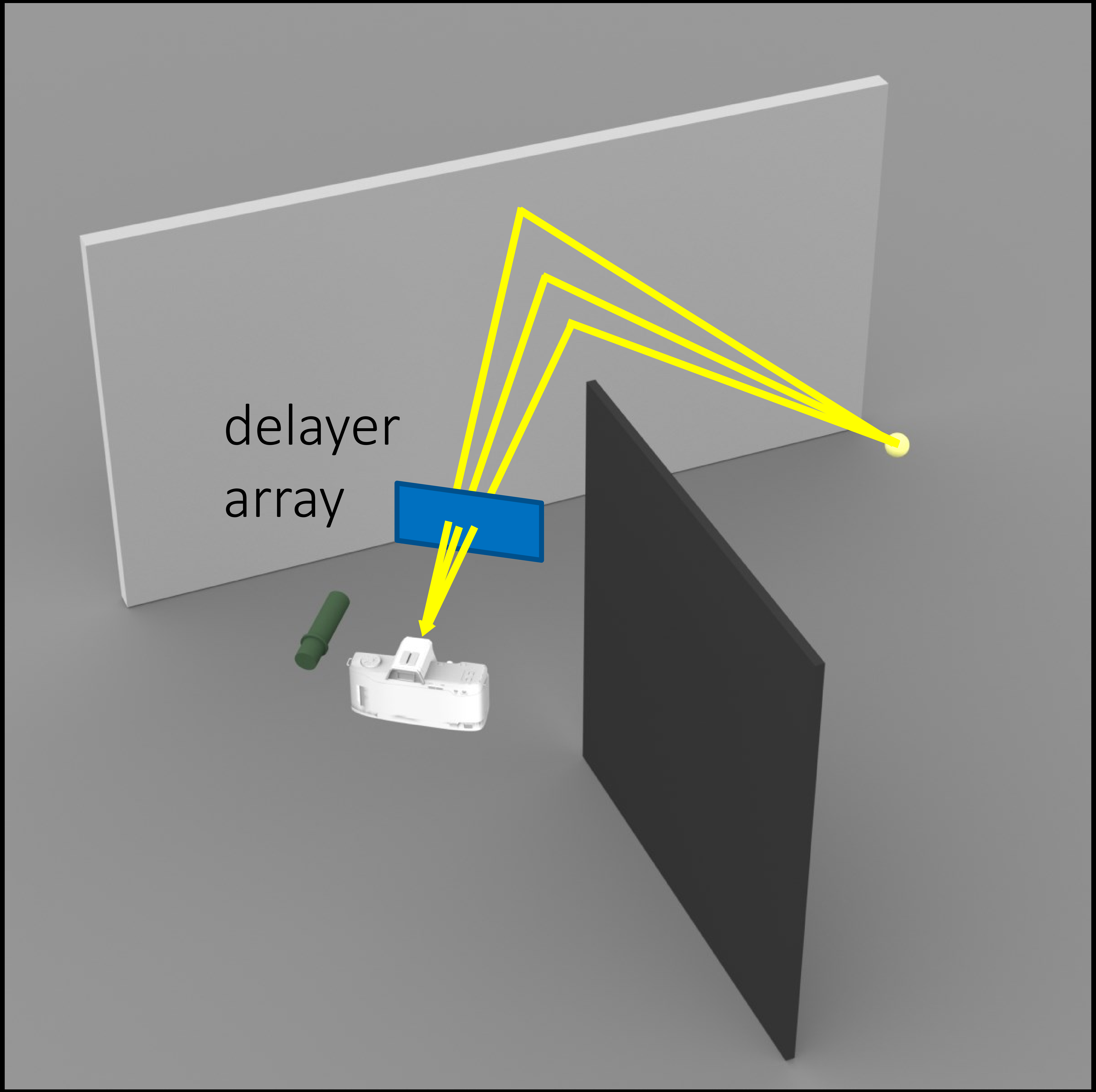

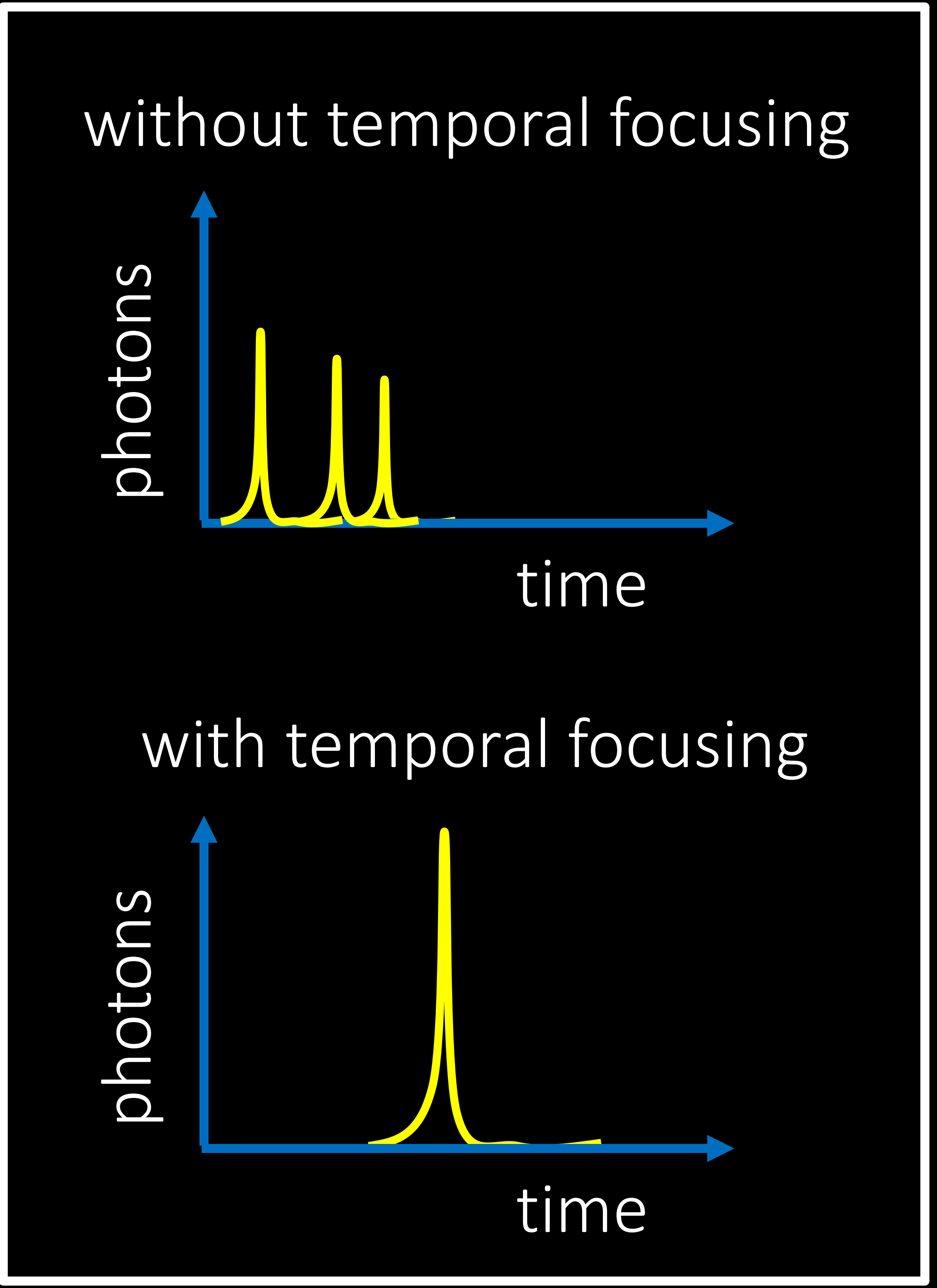

Temporal focusing: imitate the lens

challenge:

non-specular photons

solution:

use a large lens?
expensive !!

temporal focusing:
imitate large lens

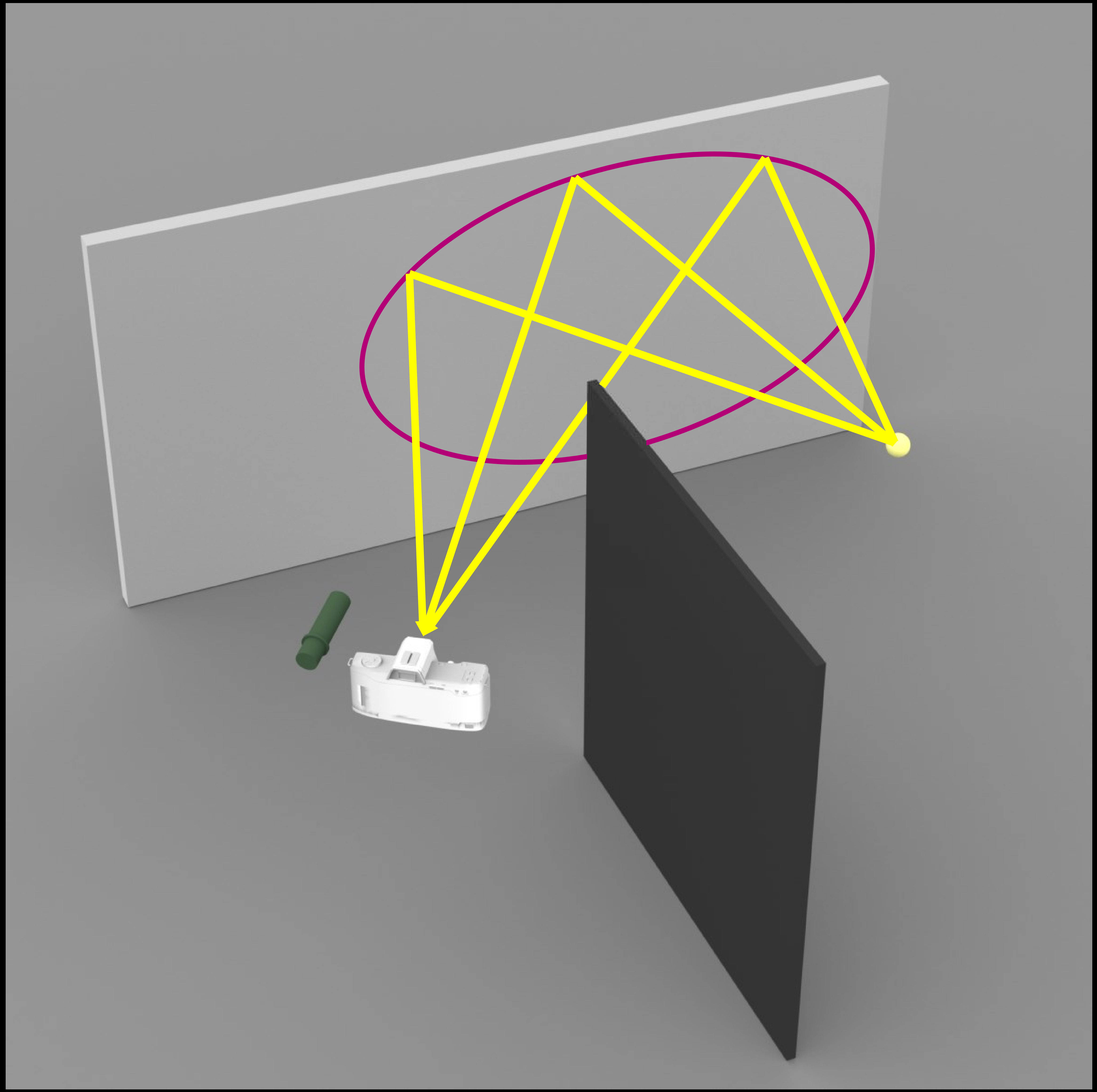

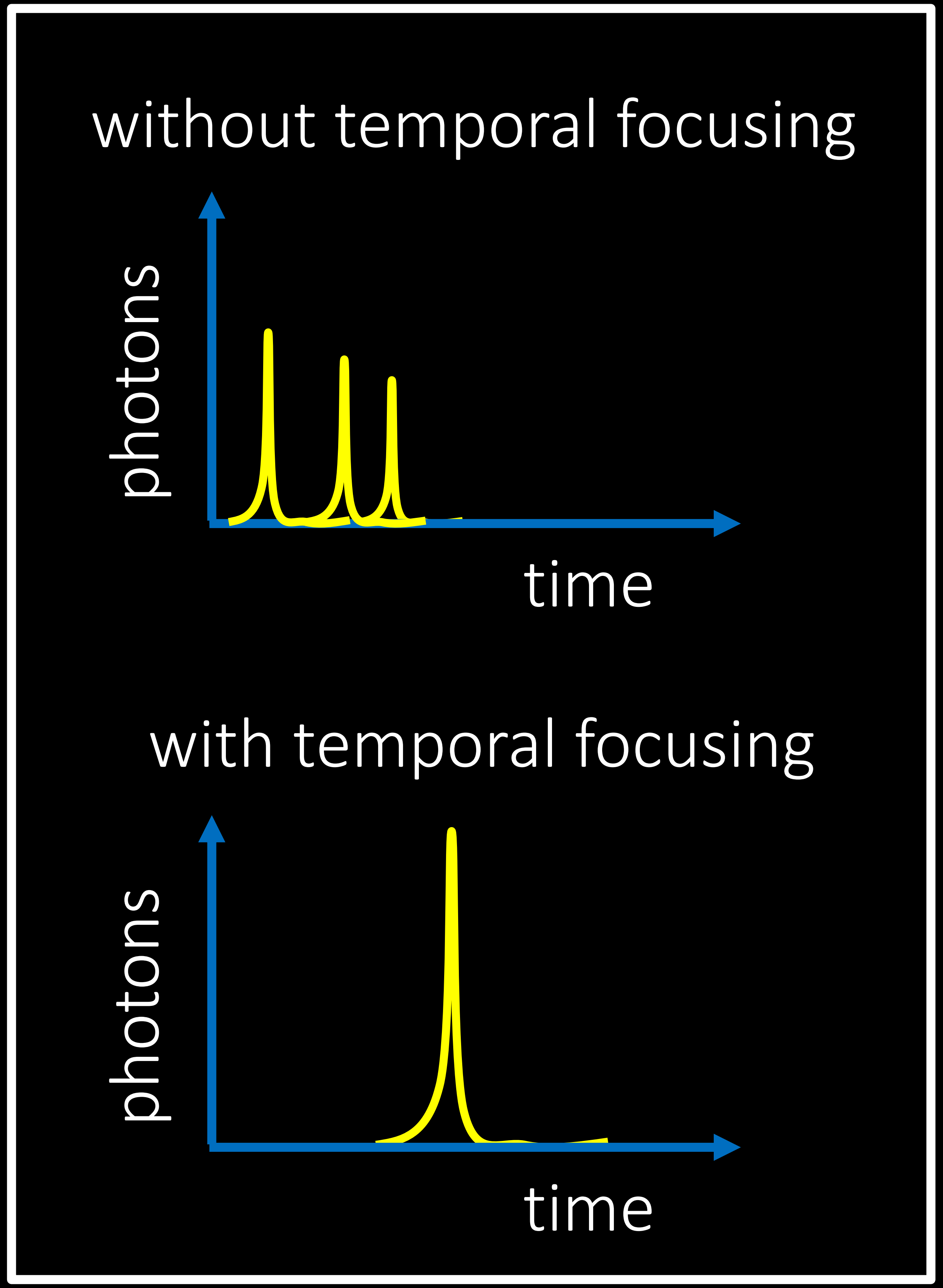

Temporal focusing: Illumination should also be an ellipse

challenge:

non-specular photons

solution:

use a large lens?
expensive !!

temporal focusing:
imitate large lens

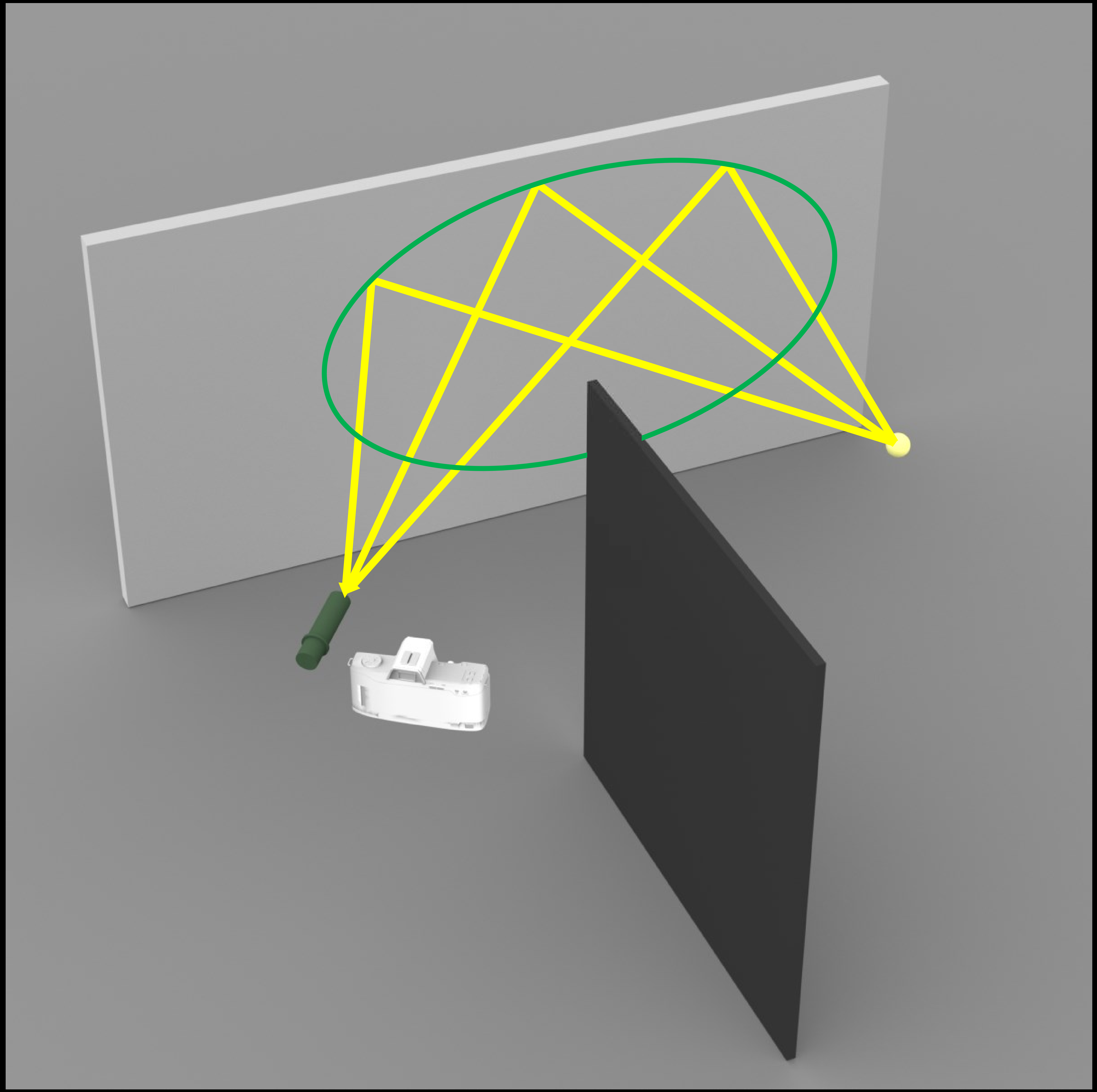

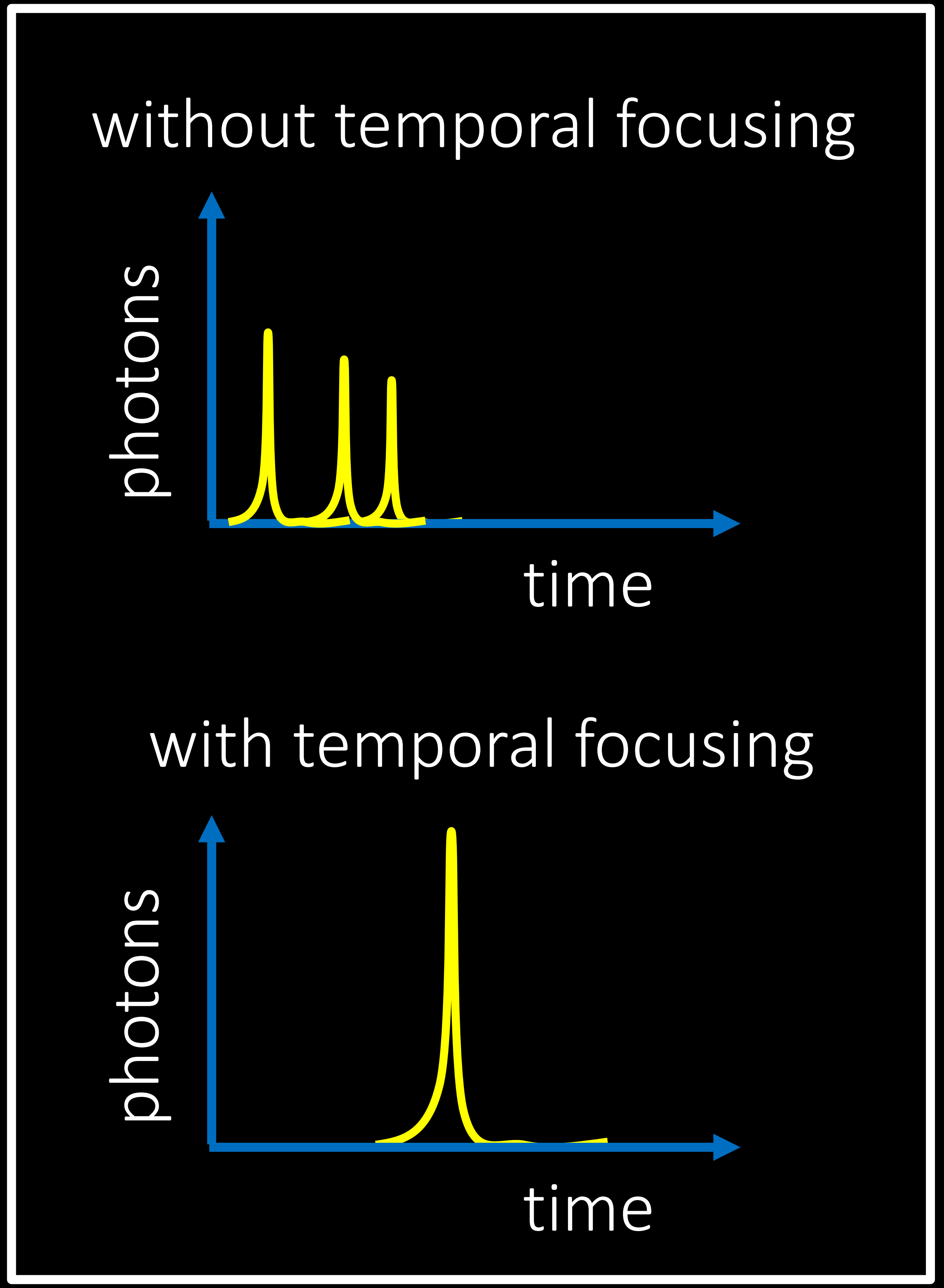

Design choices for temporal focusing

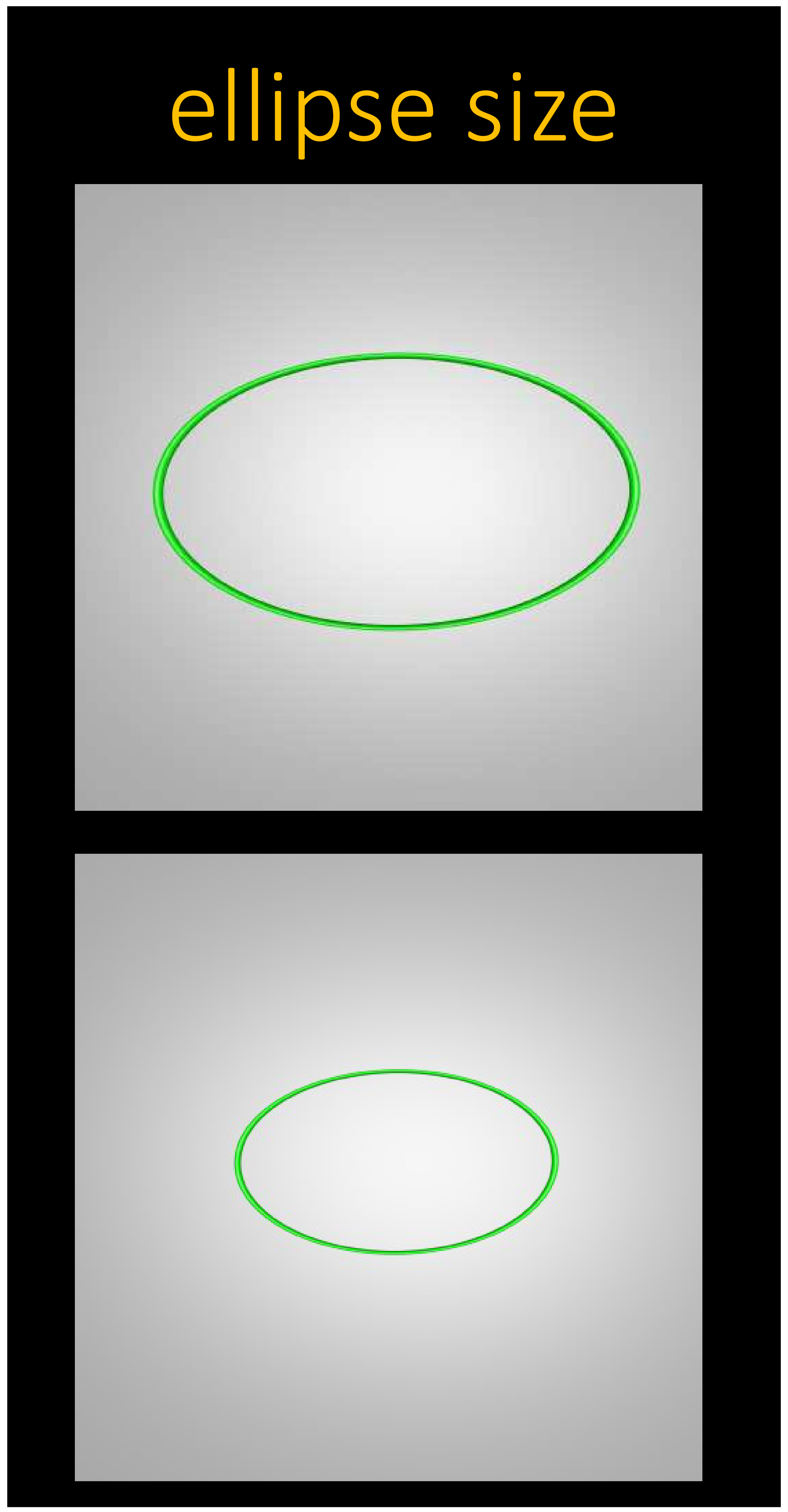

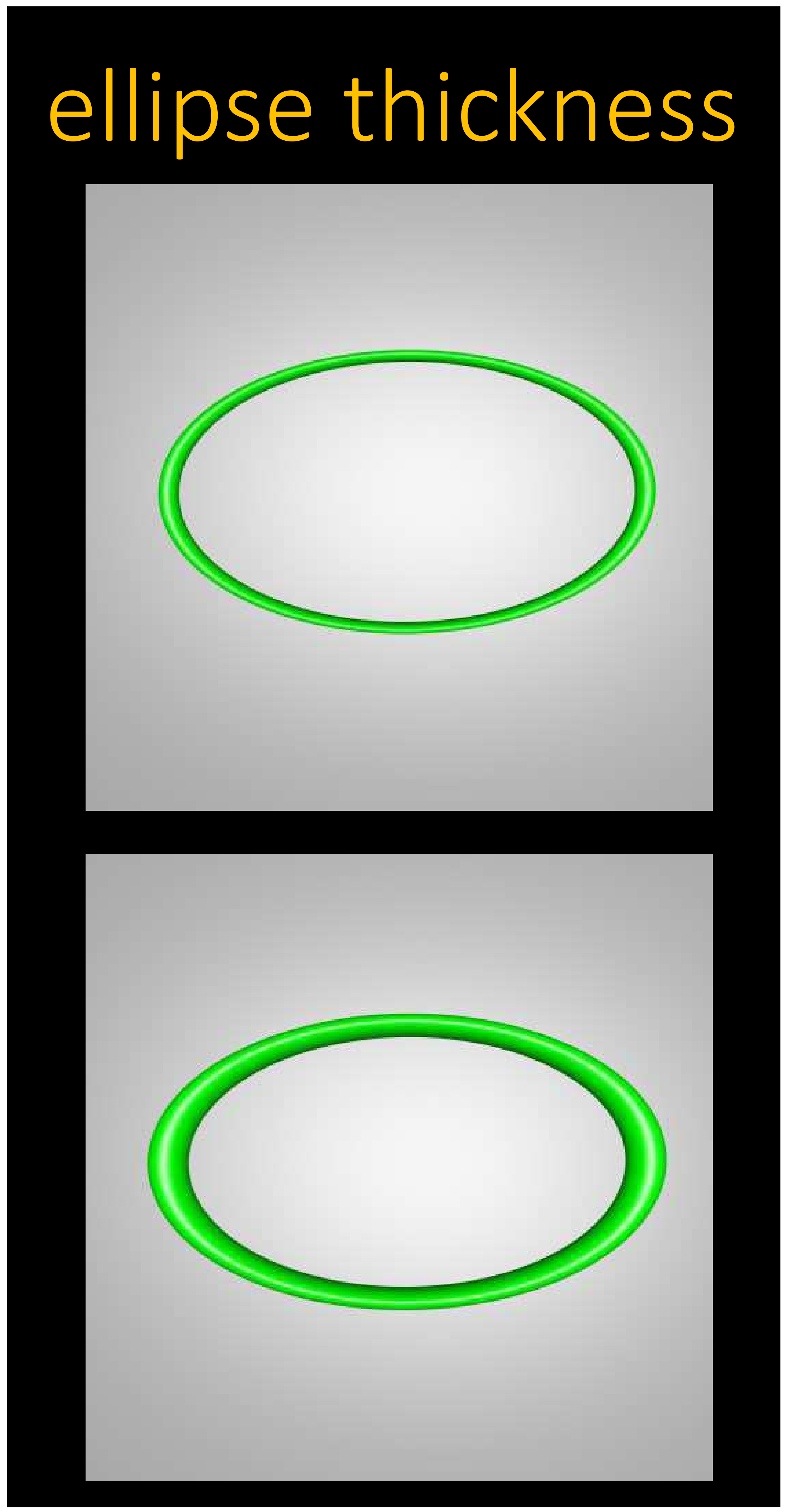

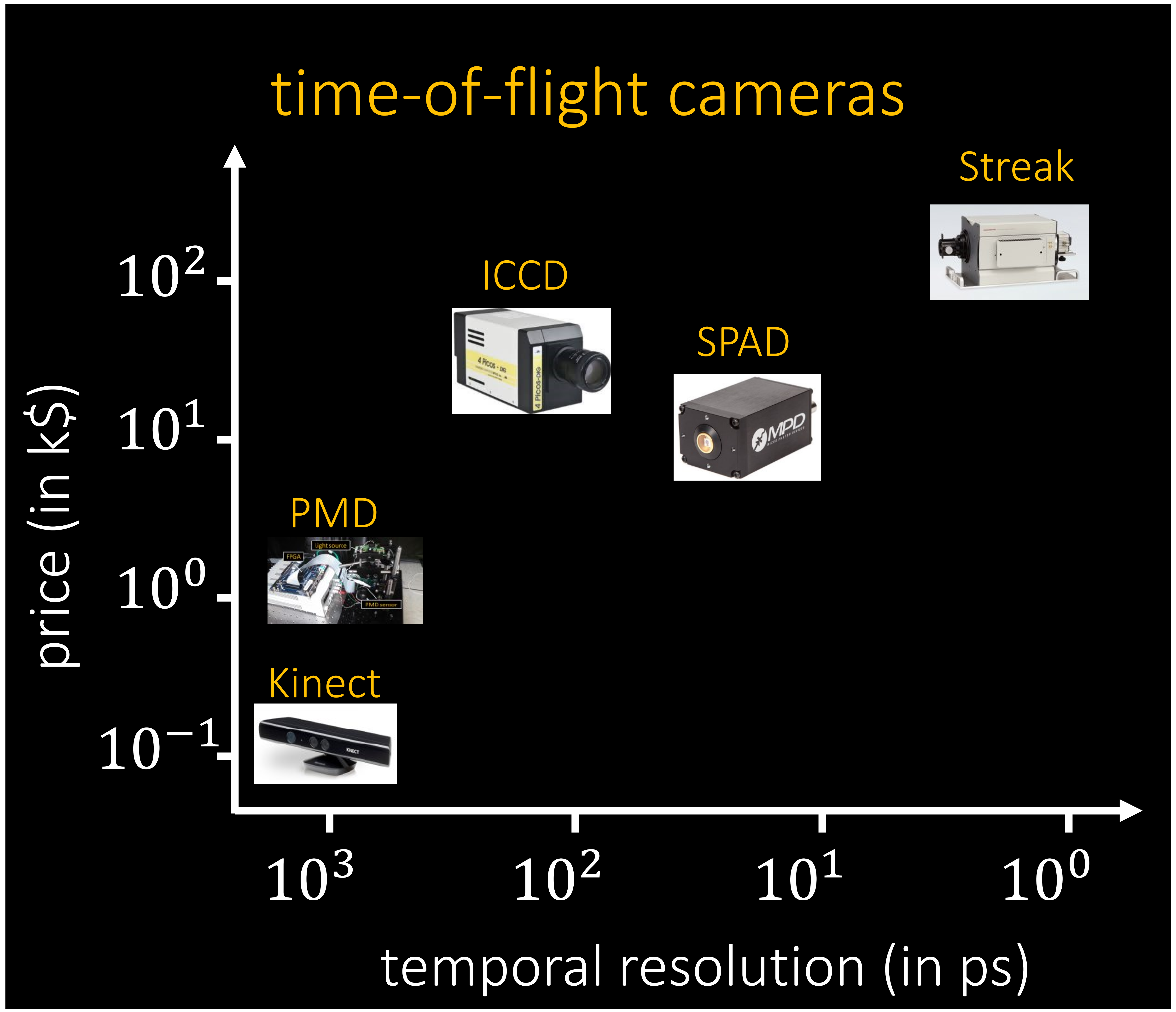

Pediredla et al. ICCP 2019.

Rendering non-line-of-sight imaging by temporal focusing

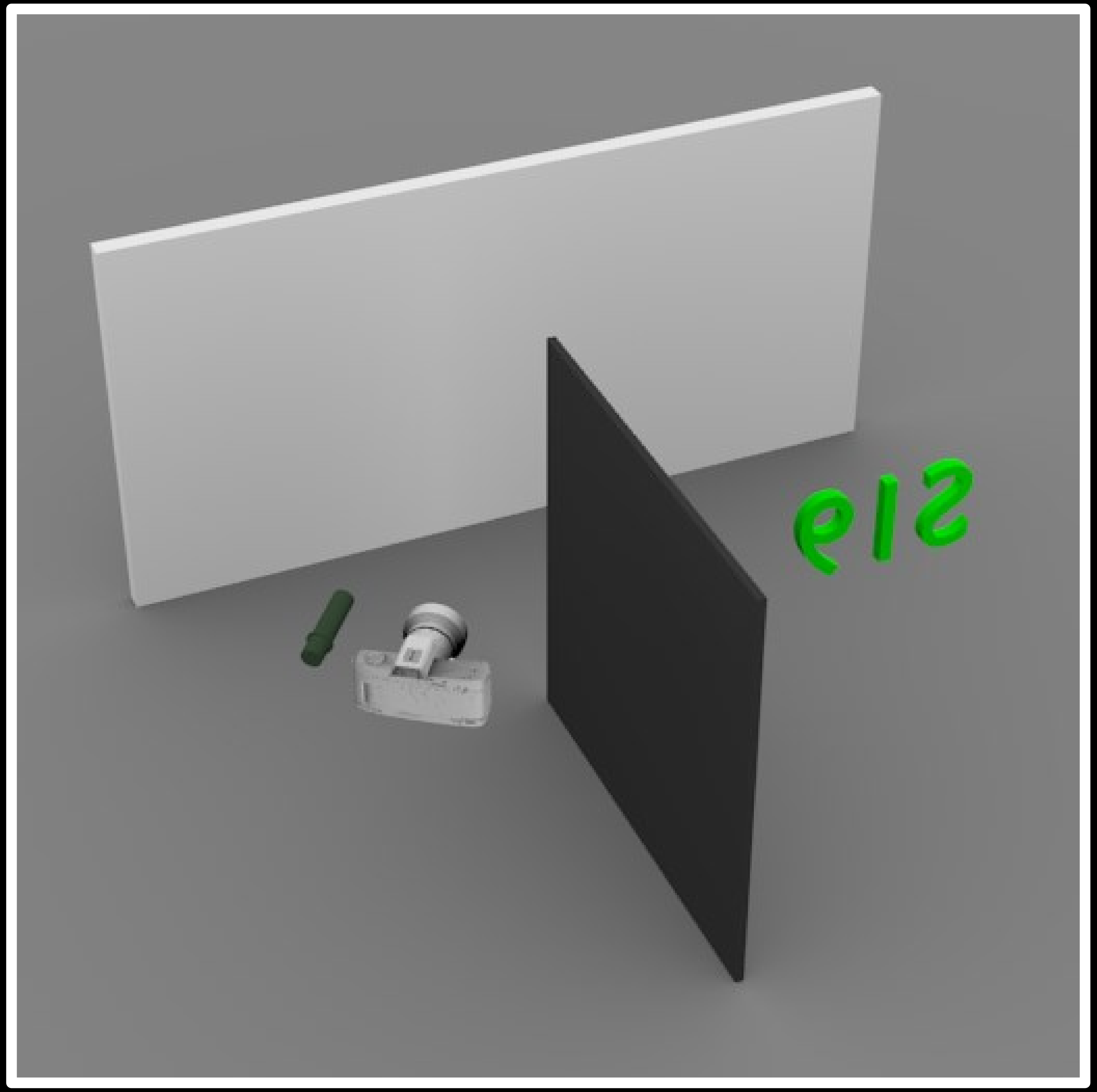

scene

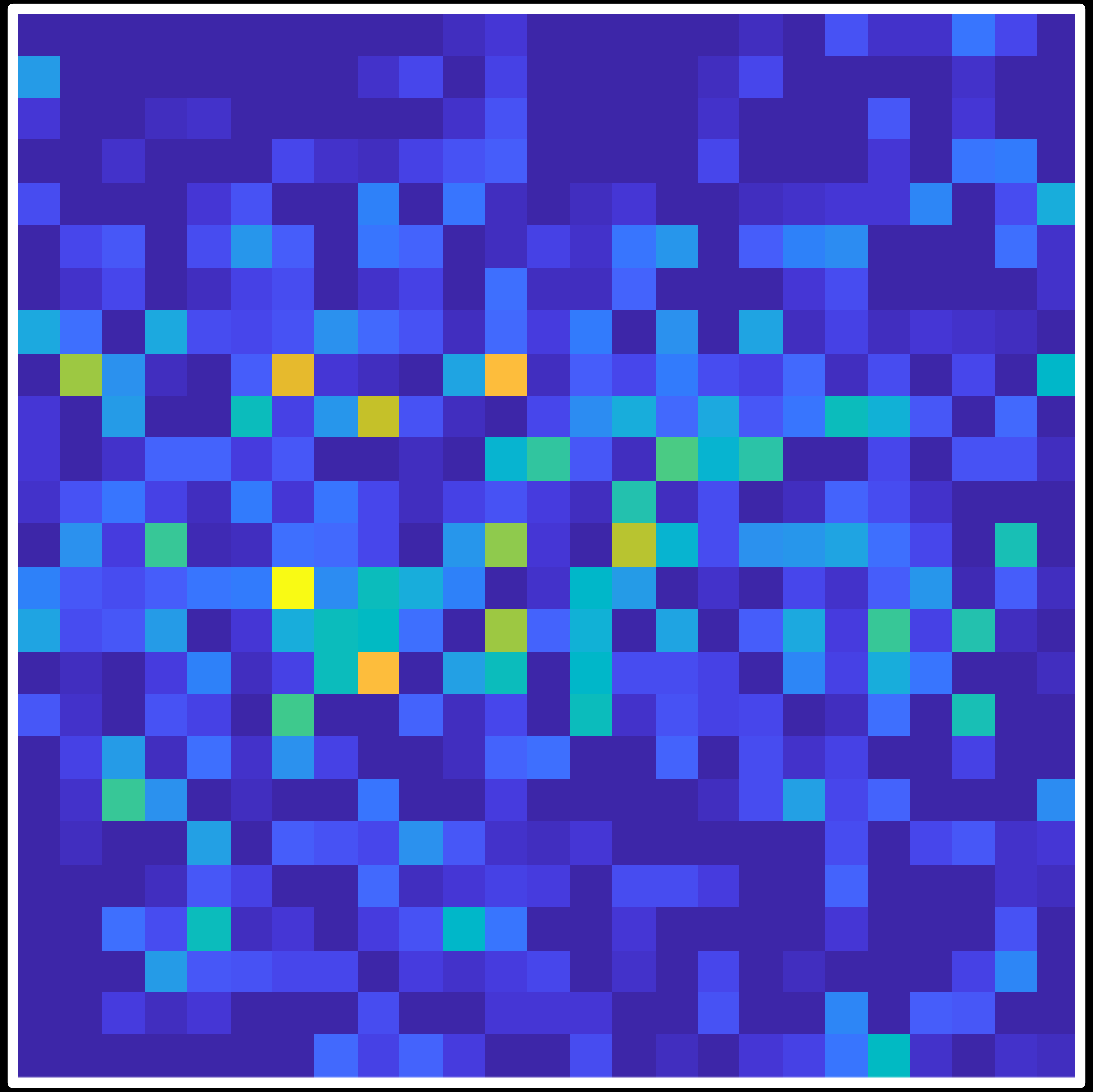

standard BDPT

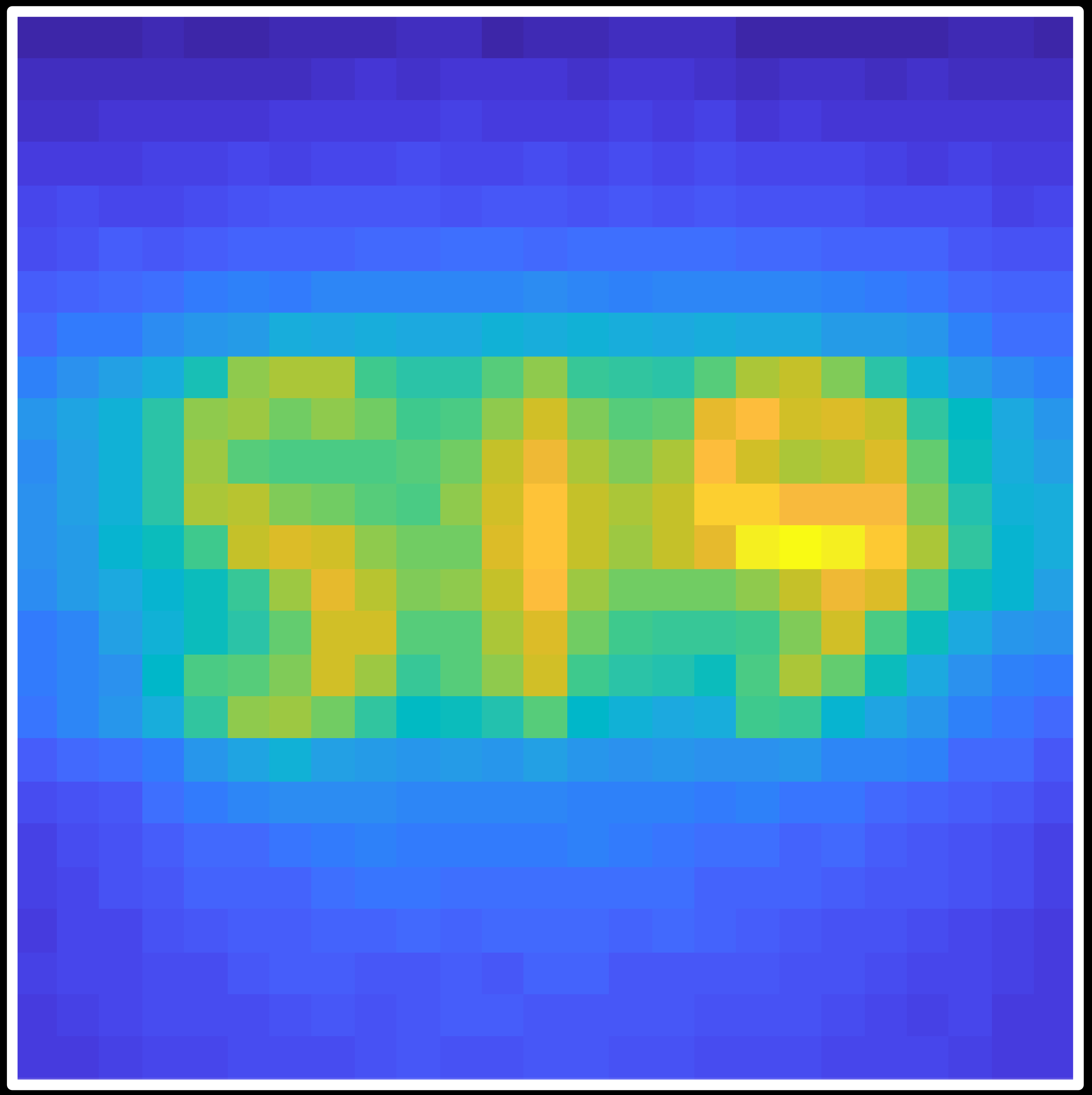

BDPT w/ ellipsoidal connections

Gate width: 4 ps (0.4% scene)
Rendering time: 3 hr

∗ simulation results

Design choices

ellipse size

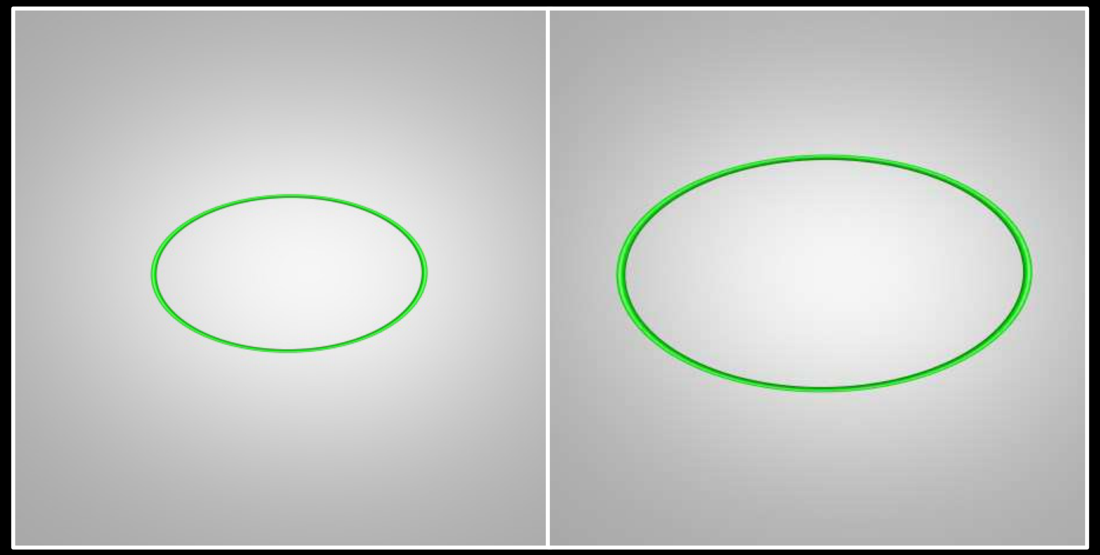

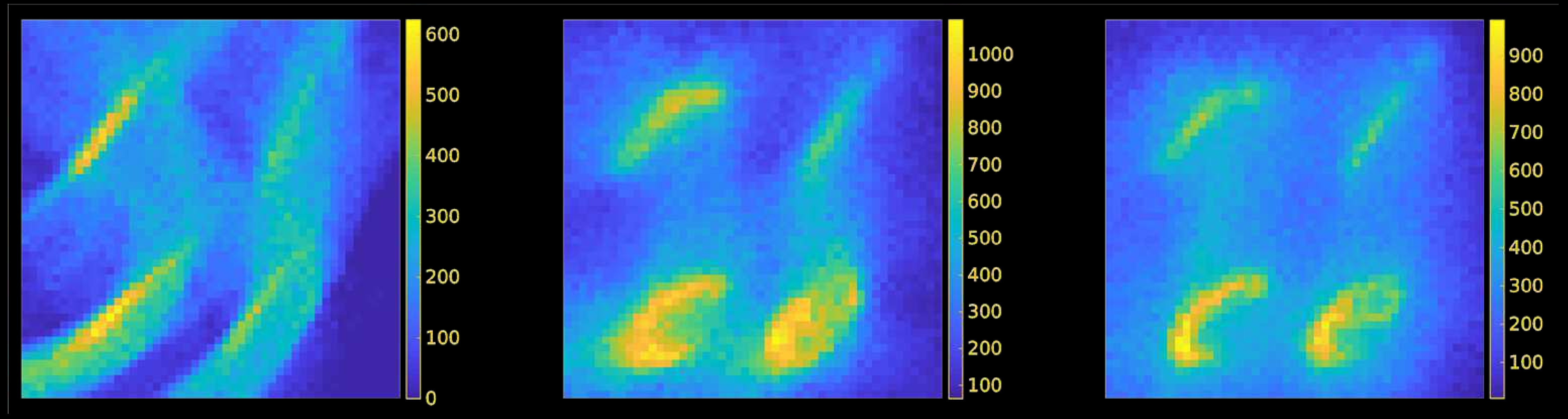

large ellipses result in better resolution

ellipse thickness

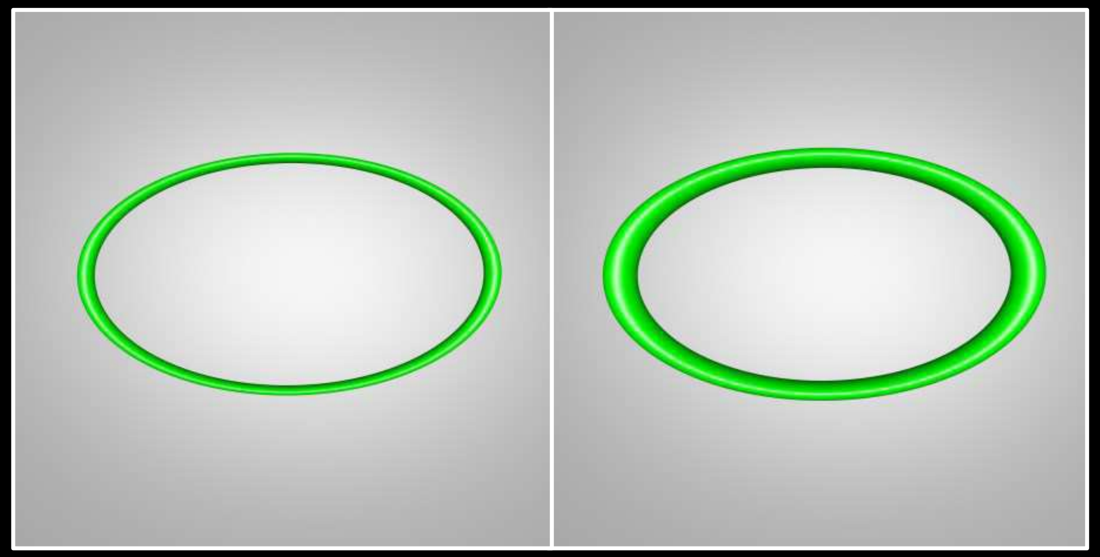

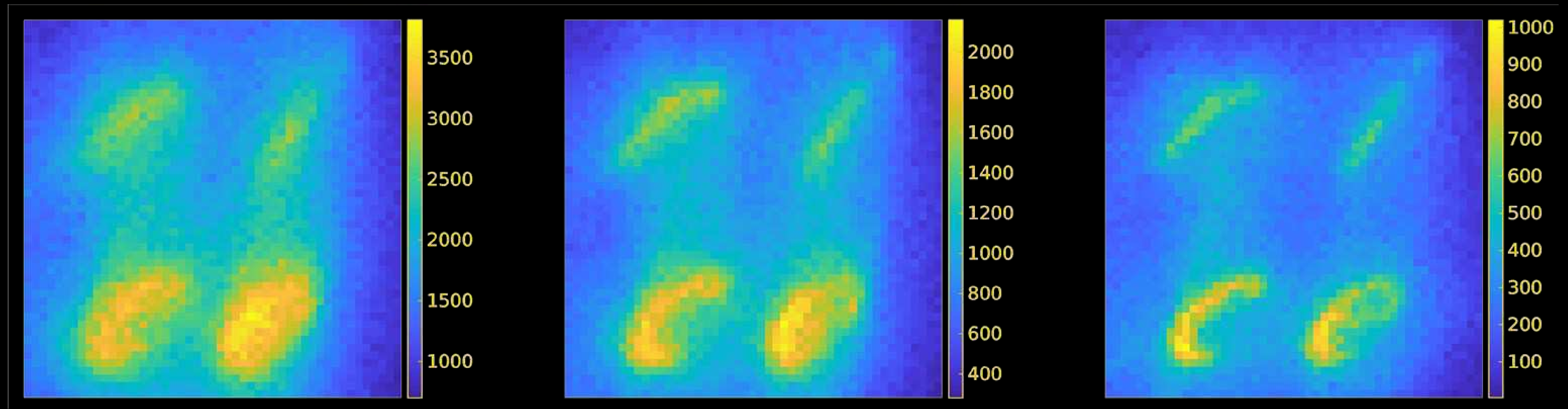

thinner ellipses result in better resolution, but looses light

temporal resolution

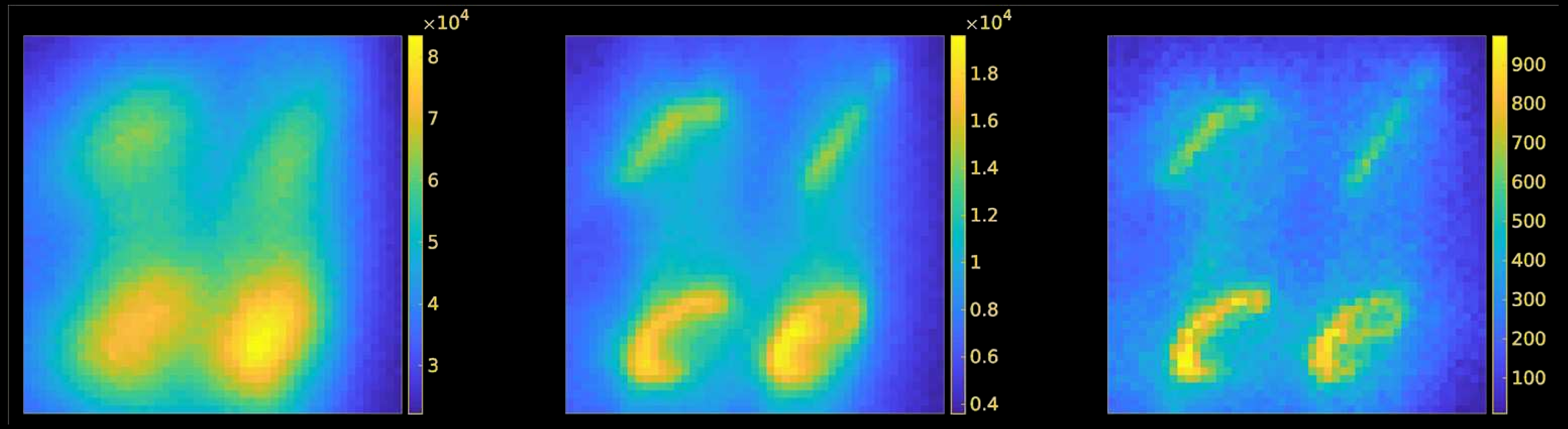

high resolution time-gate results in better resolution, but looses light

Hardware prototype

optical component

illumination galvo

imaging galvo

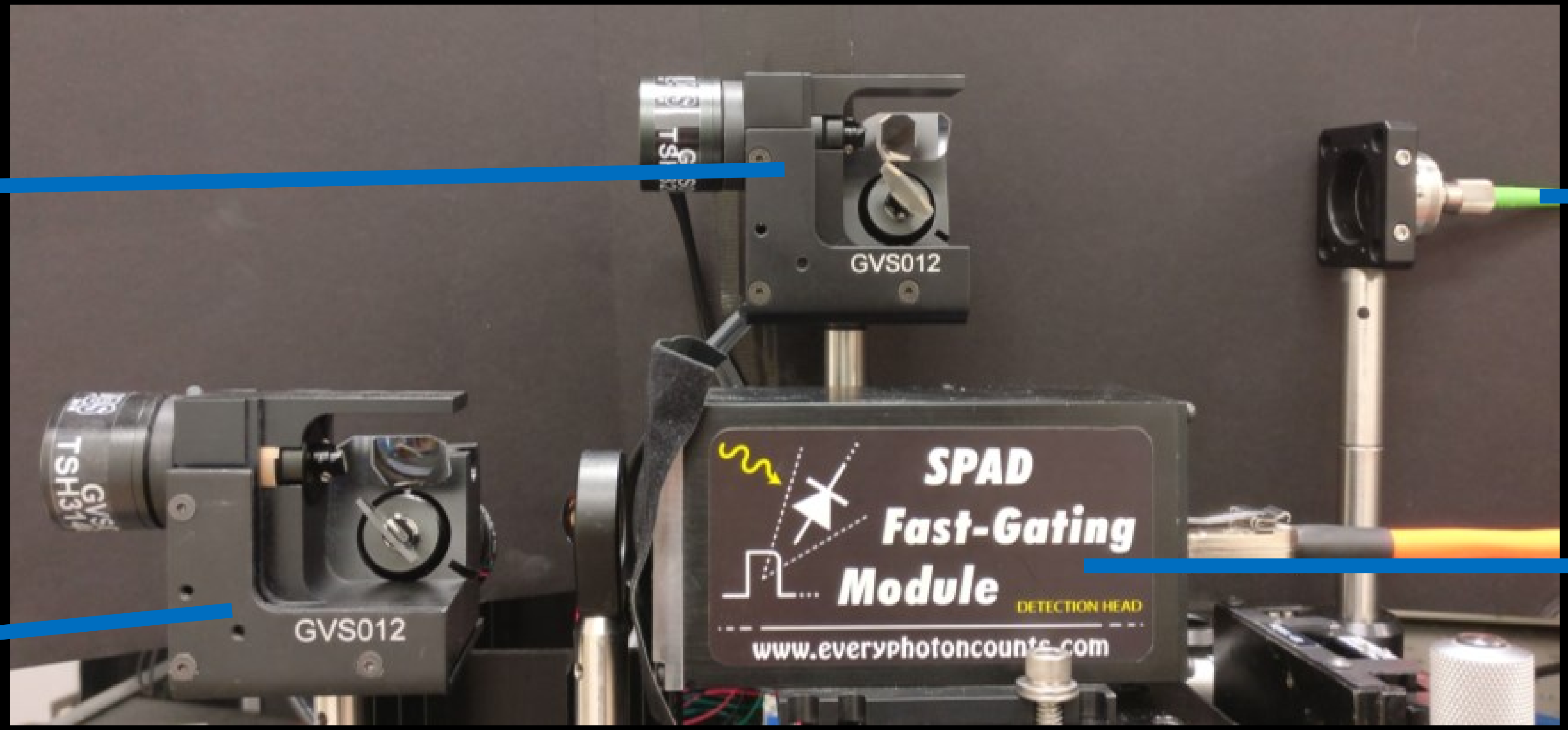

picosecond laser

SPAD

Size of ellipses

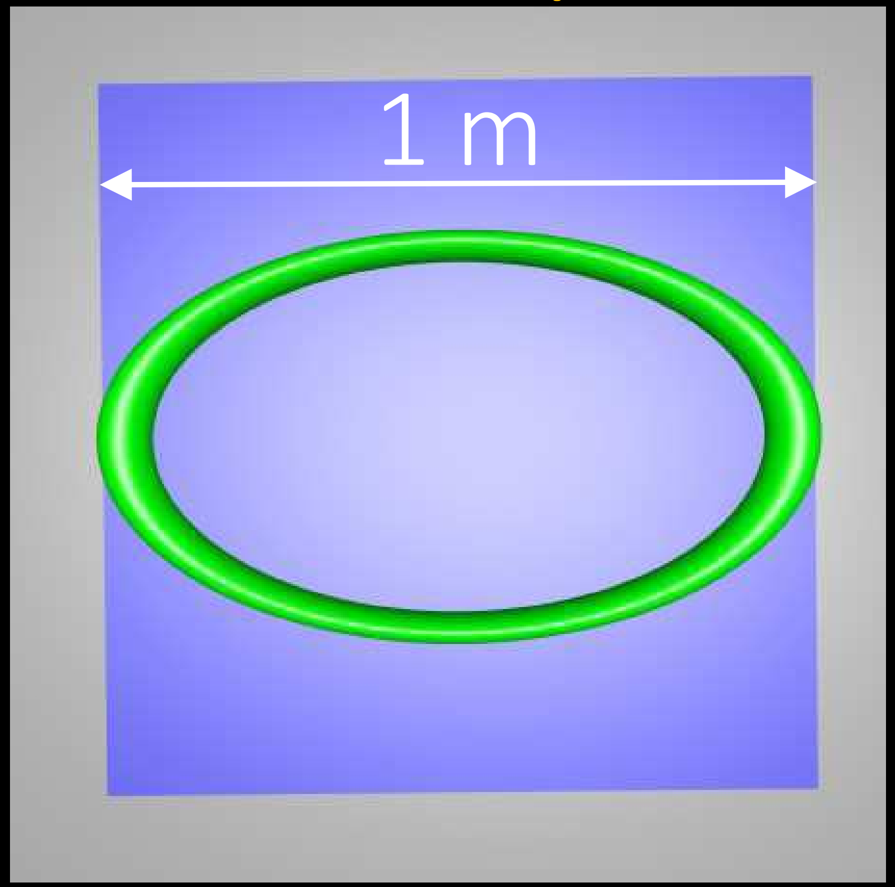

Thickness of ellipse (laser spot size)

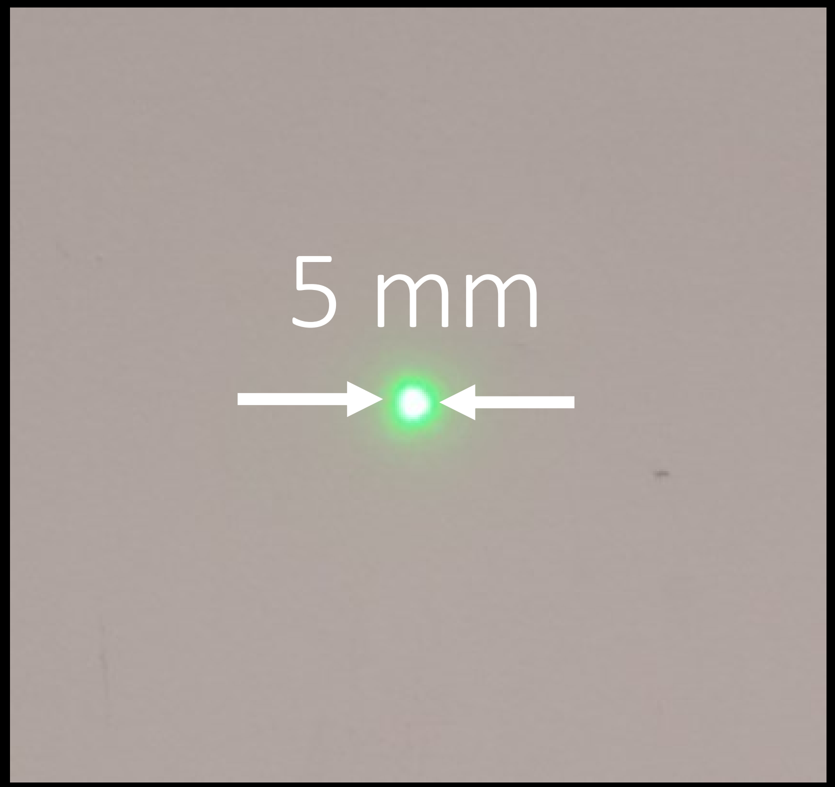

Measured Jitter

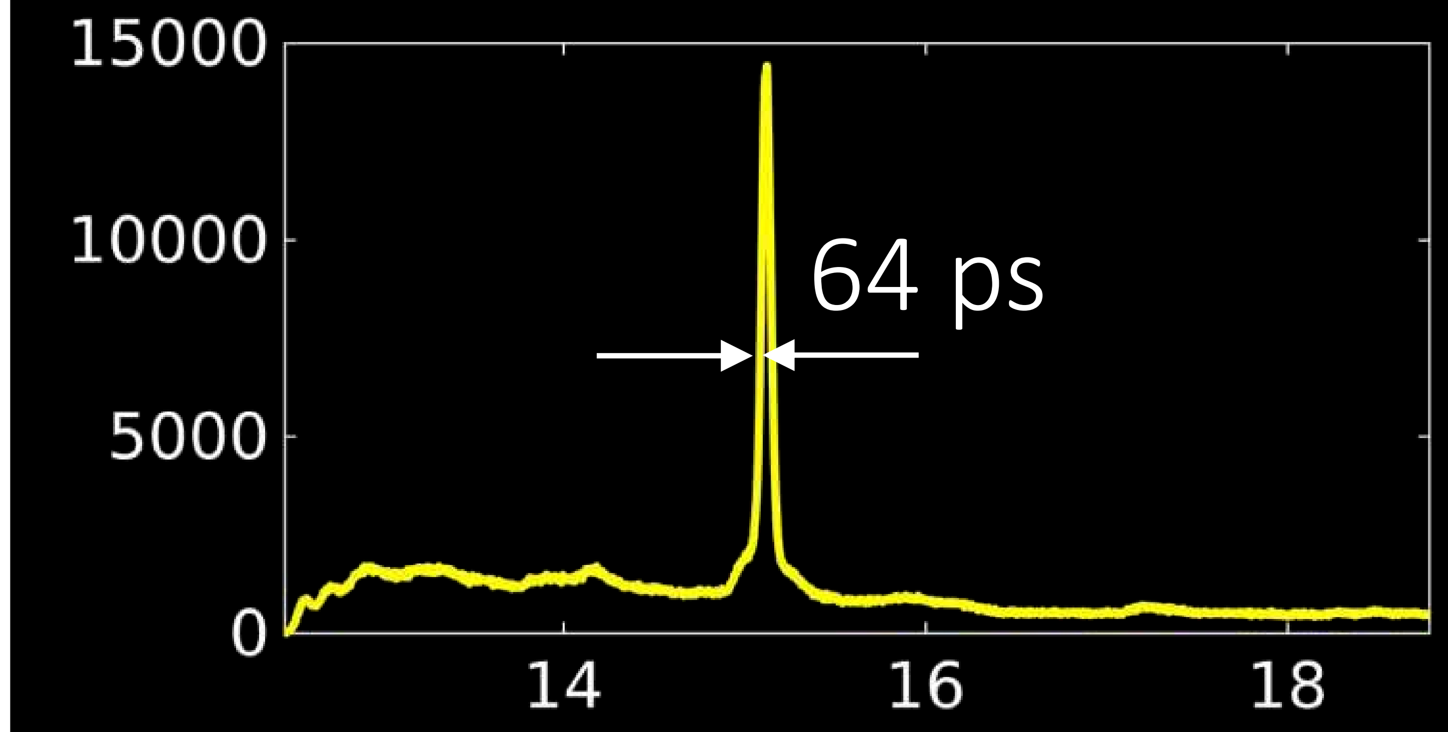

Pediredla et al. ICCP 2019.

Hardware prototype

optical component

illumination galvo

imaging galvo

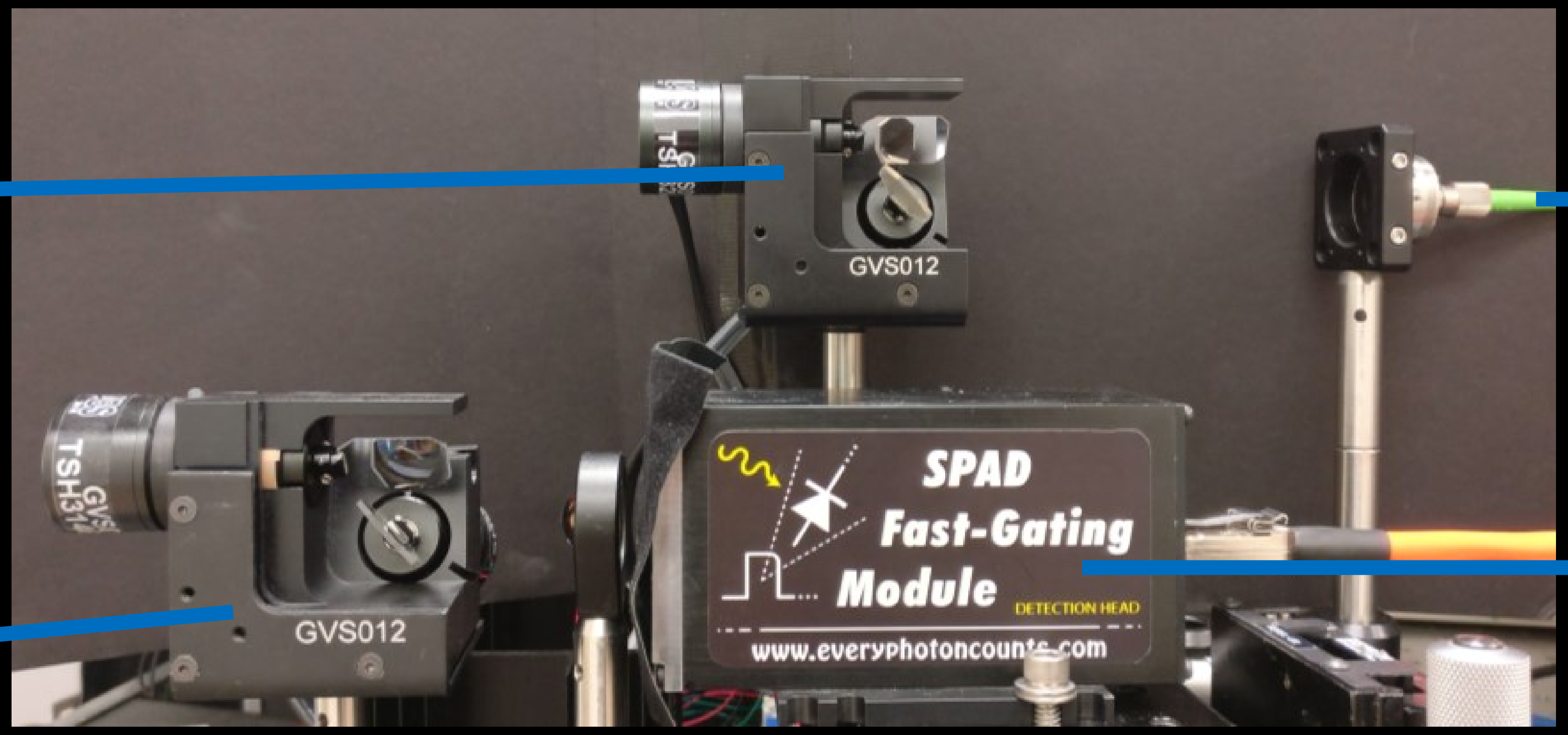

picosecond laser

SPAD

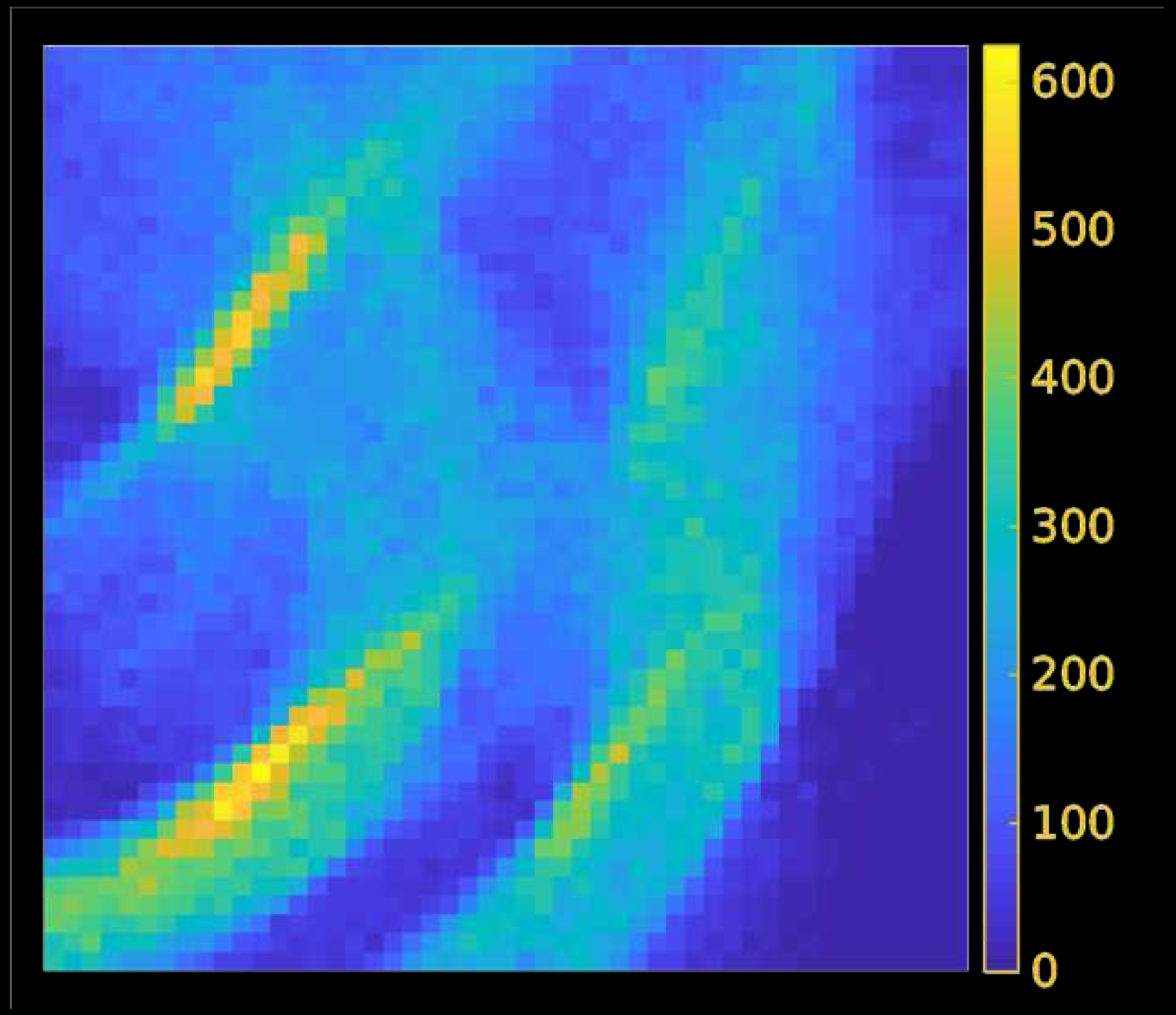

unoptimized

renderer driven optimization

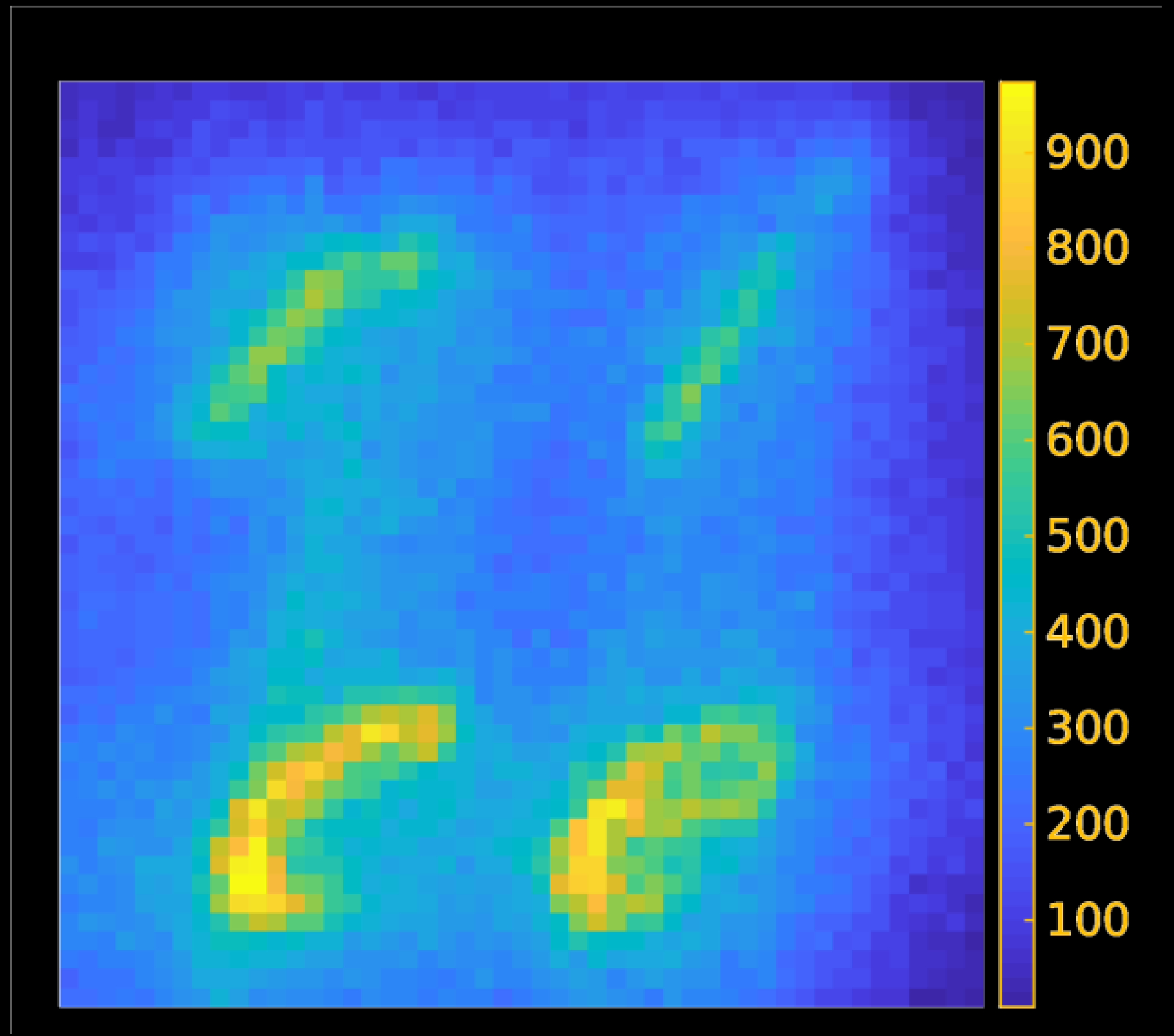

optimized

Pediredla et al. ICCP 2019.

Hardware prototype

optical component

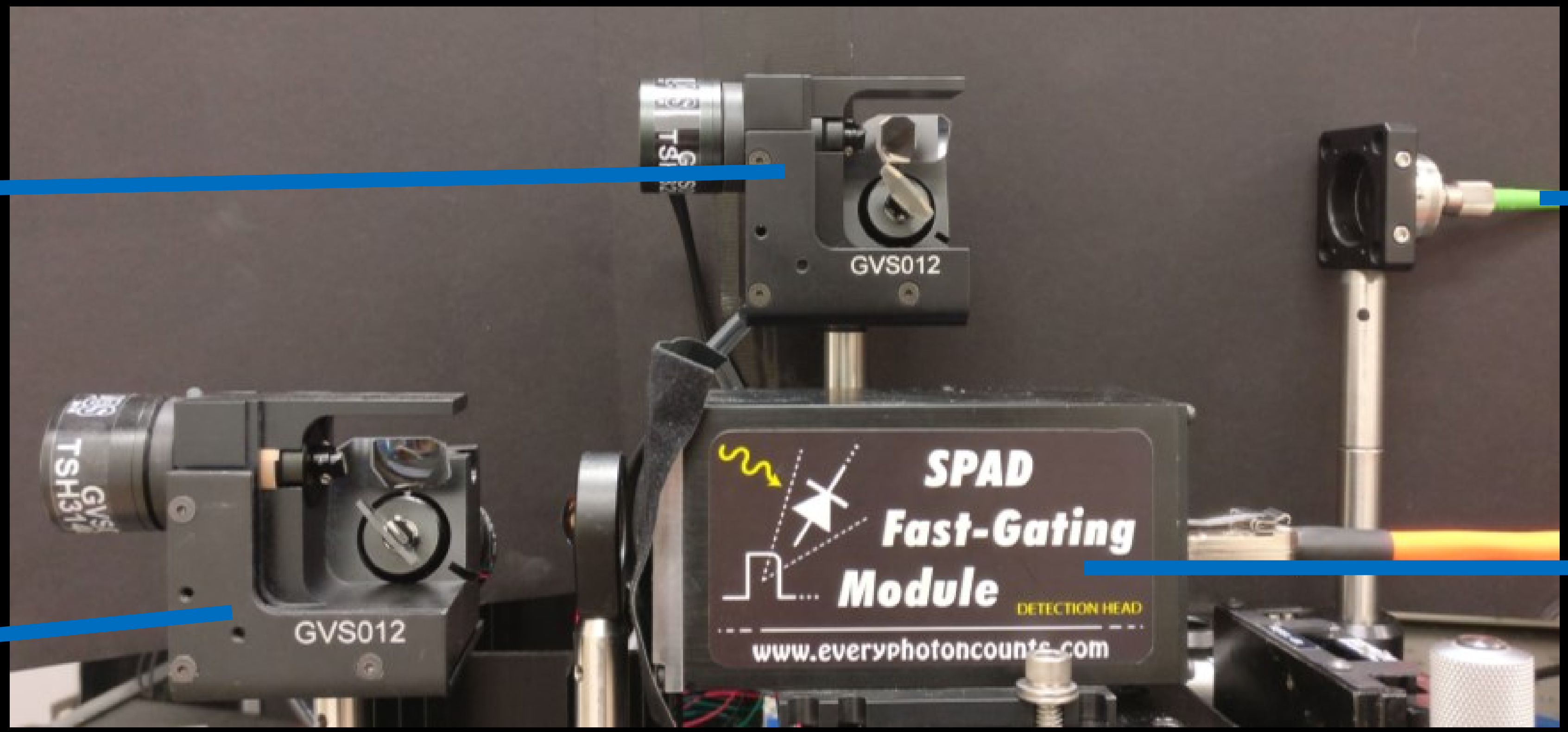

MEMS
Axicon
SLM
OPA

illumination galvo

imaging galvo

LED
SLED
supercontinuum
femtosecond laser

picosecond laser

streak
ICCD
kinect
PMD

SPAD

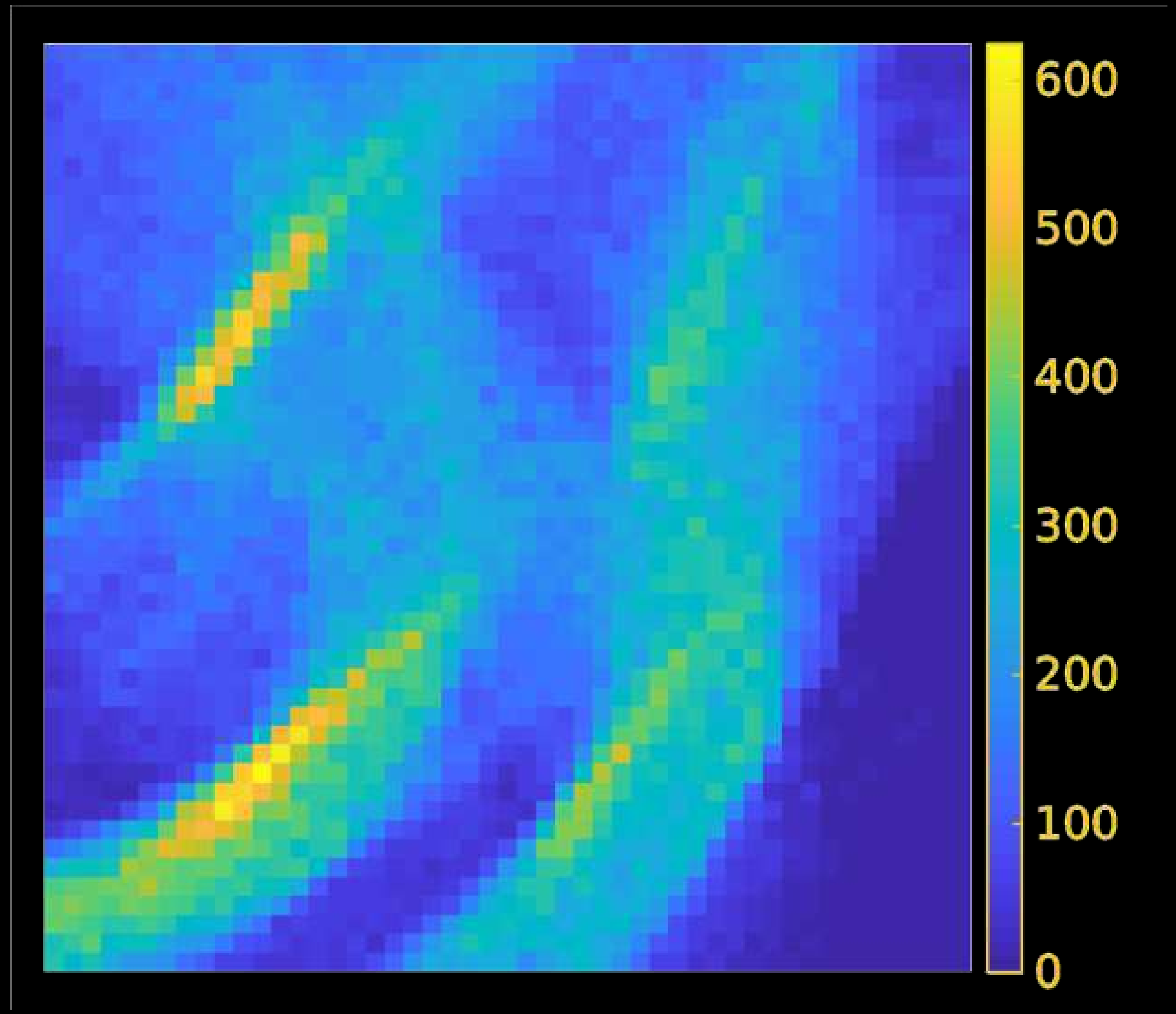

unoptimized

renderer driven optimization

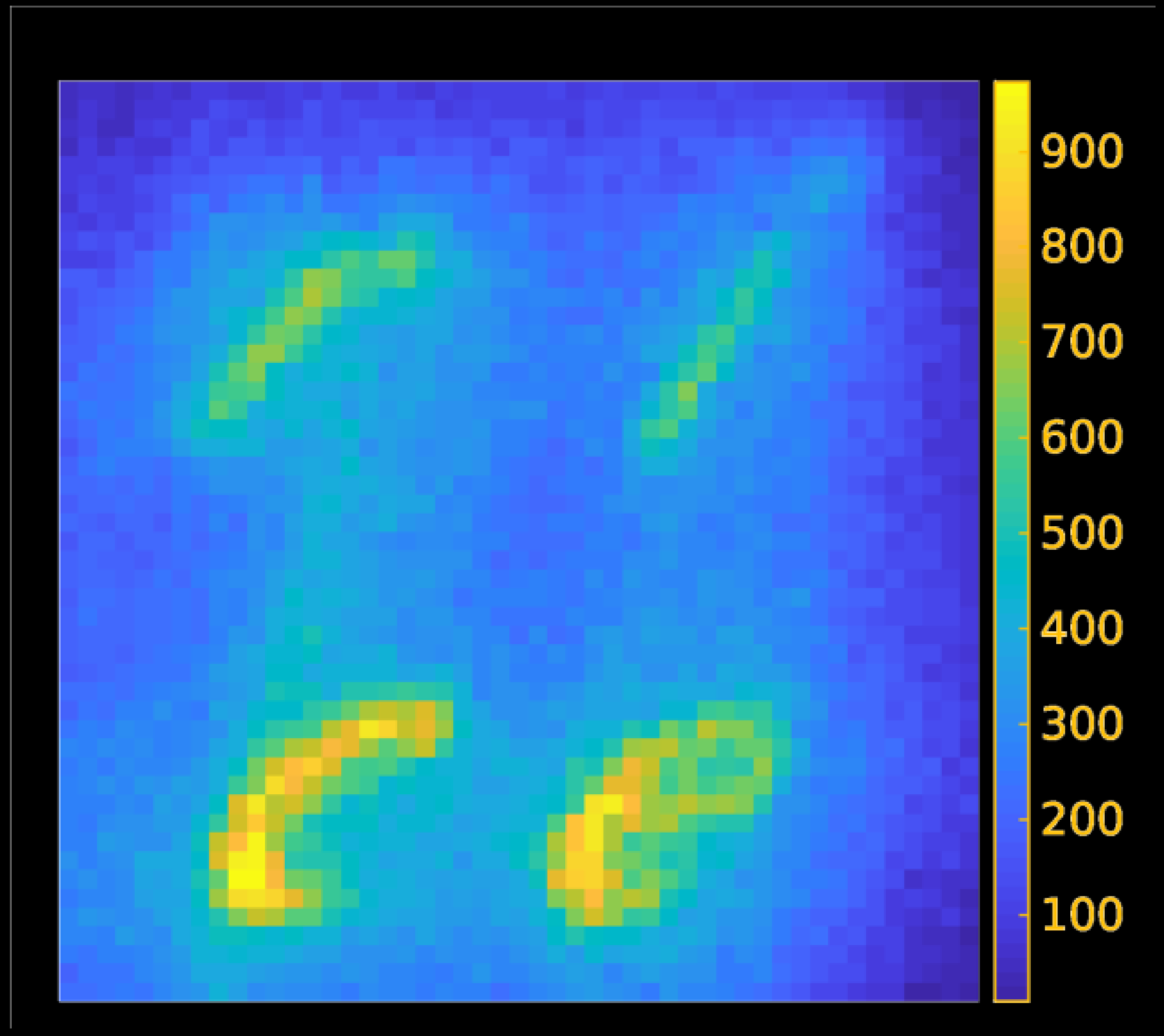

optimized

Pediredla et al. ICCP 2019.

Results: scanning limited ROI

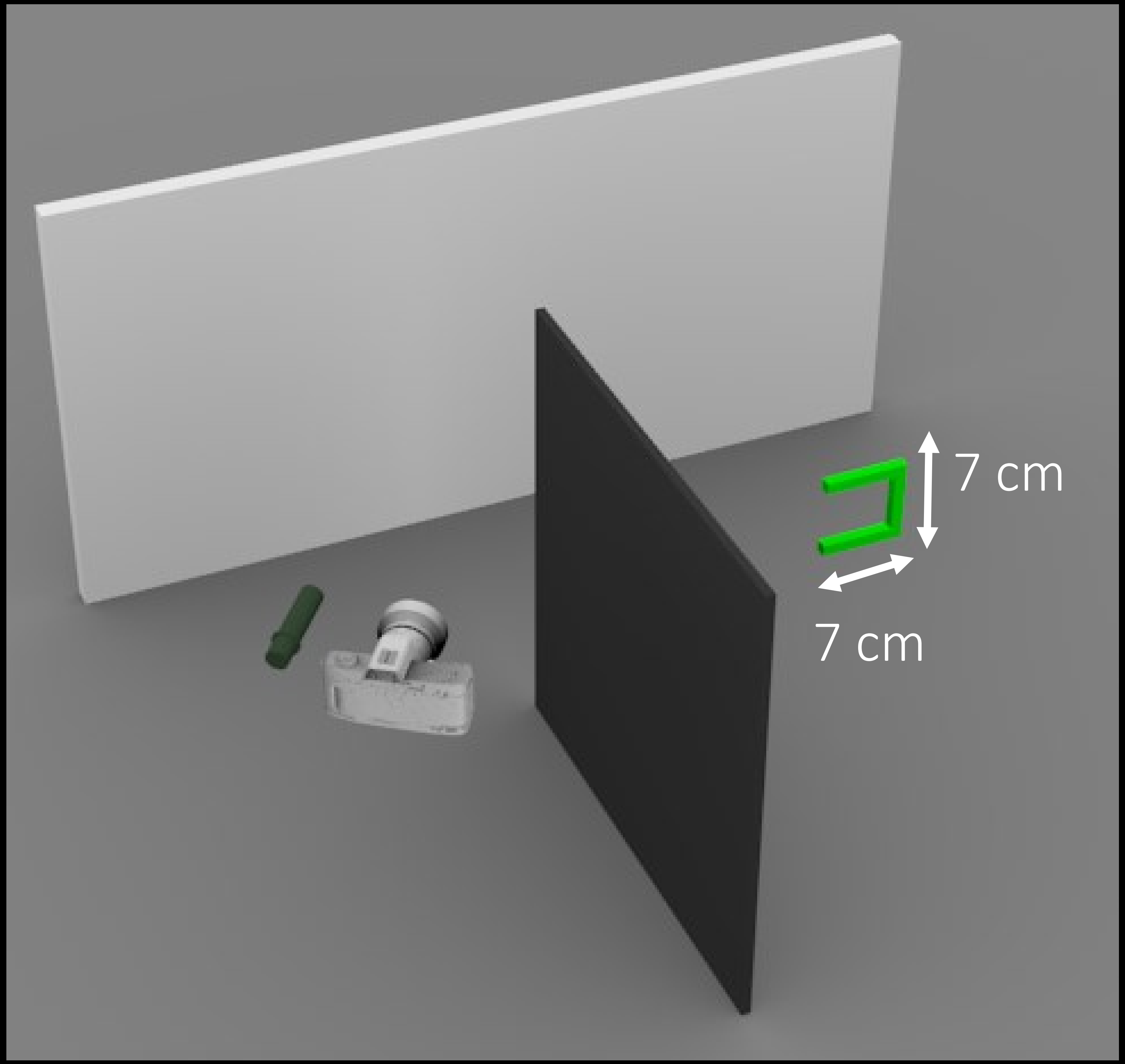

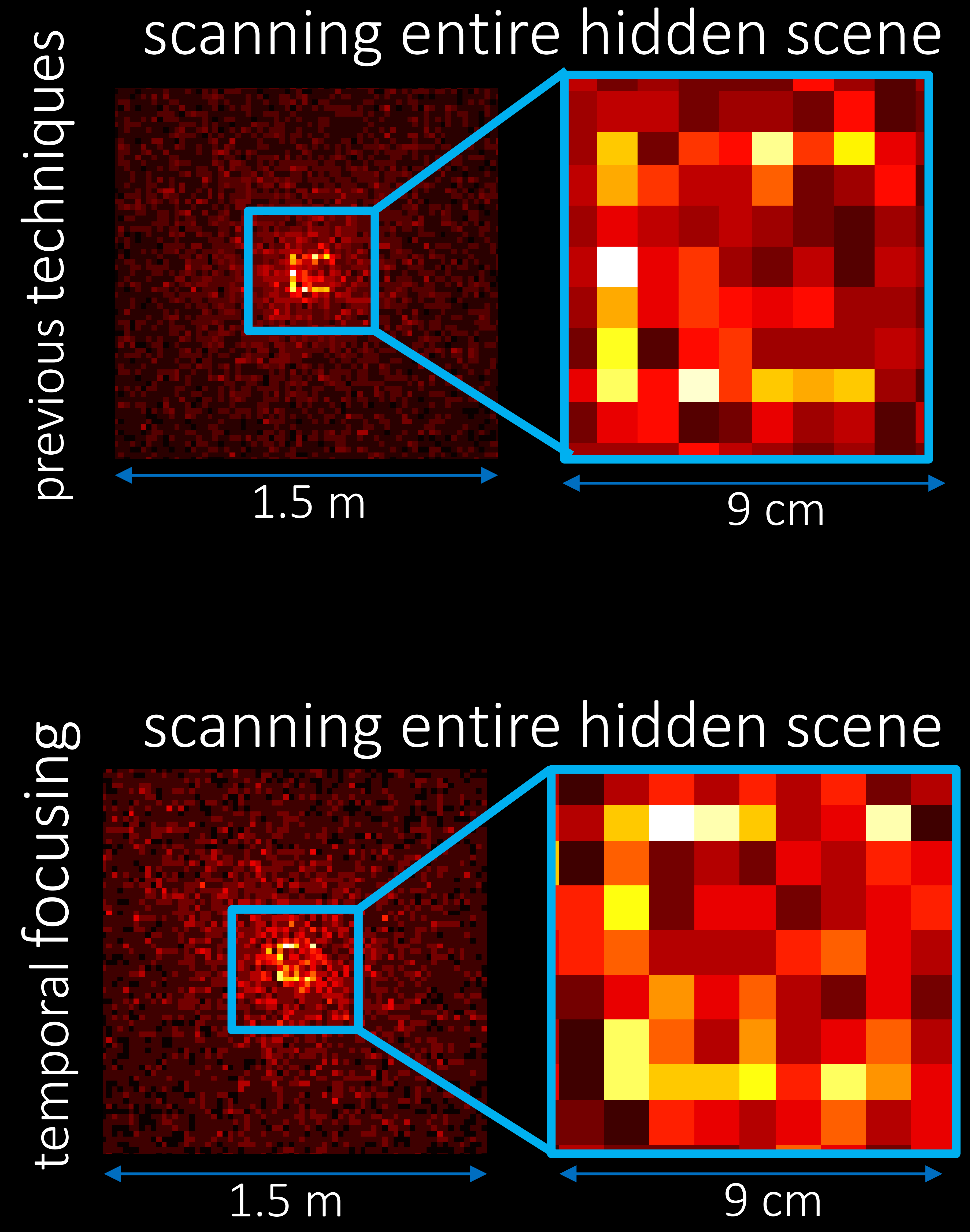

Results: scanning limited ROI

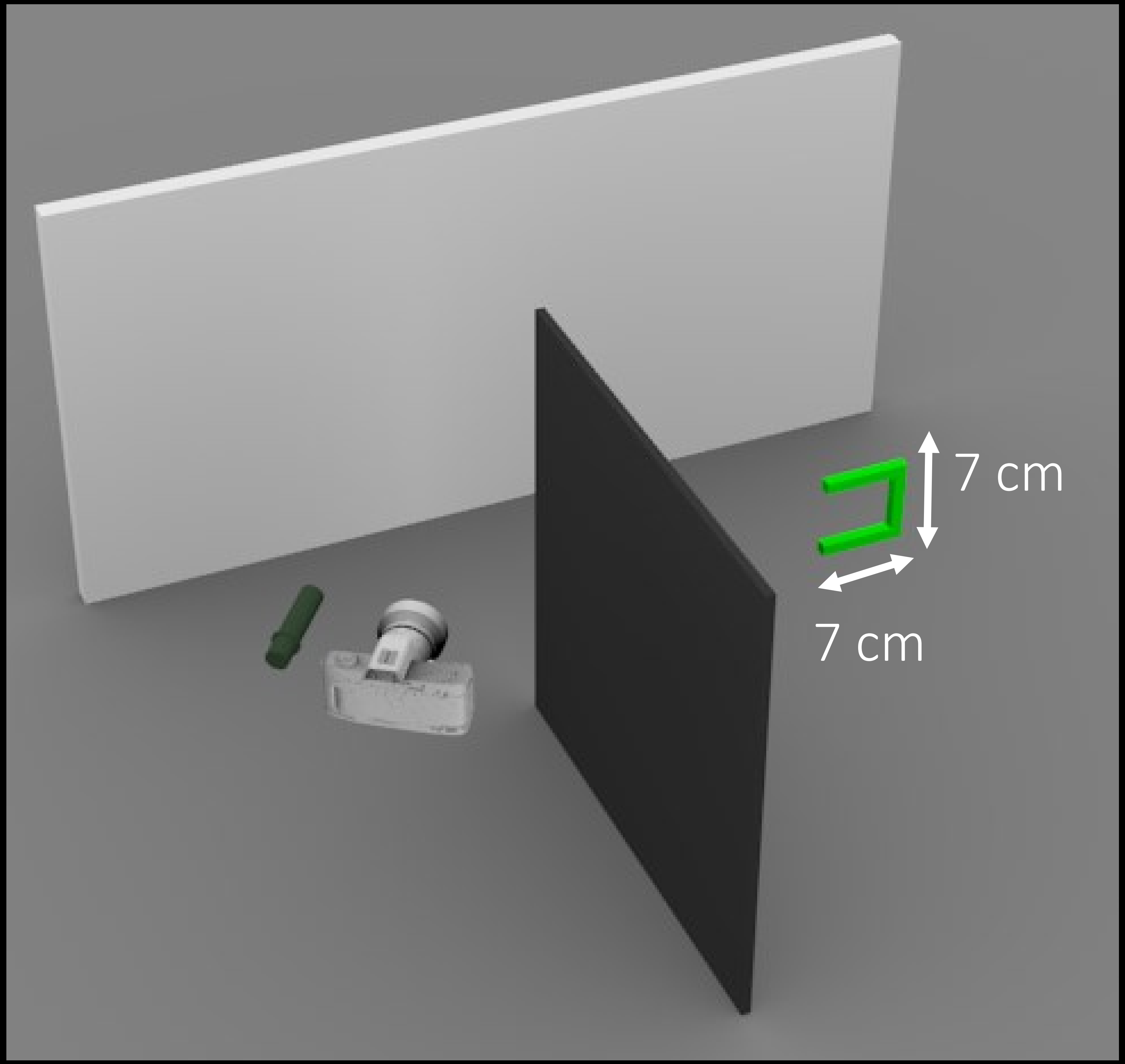

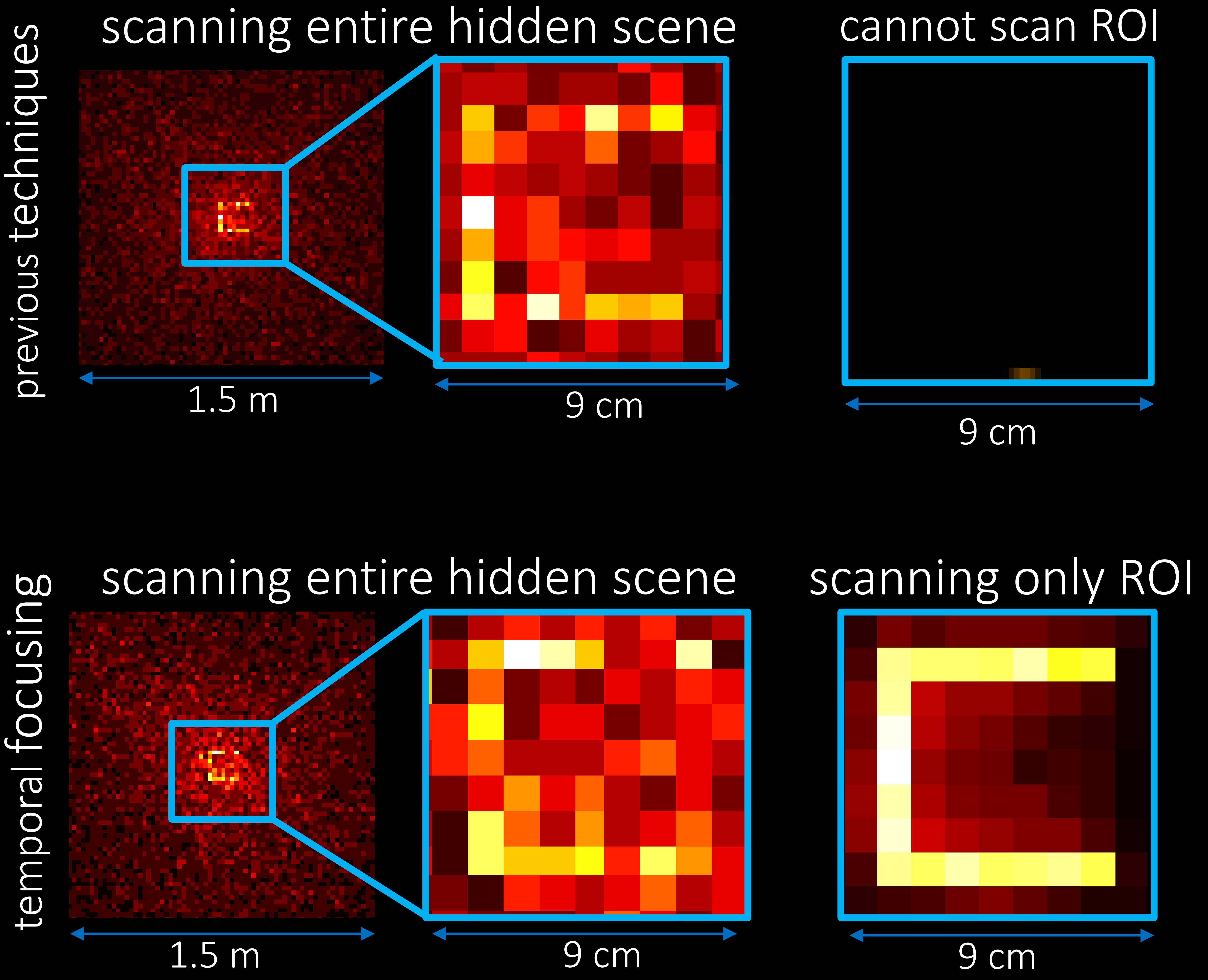

SNR of temporal focusing is > 10× higher for small ROI

Results: real-time occupancy detection

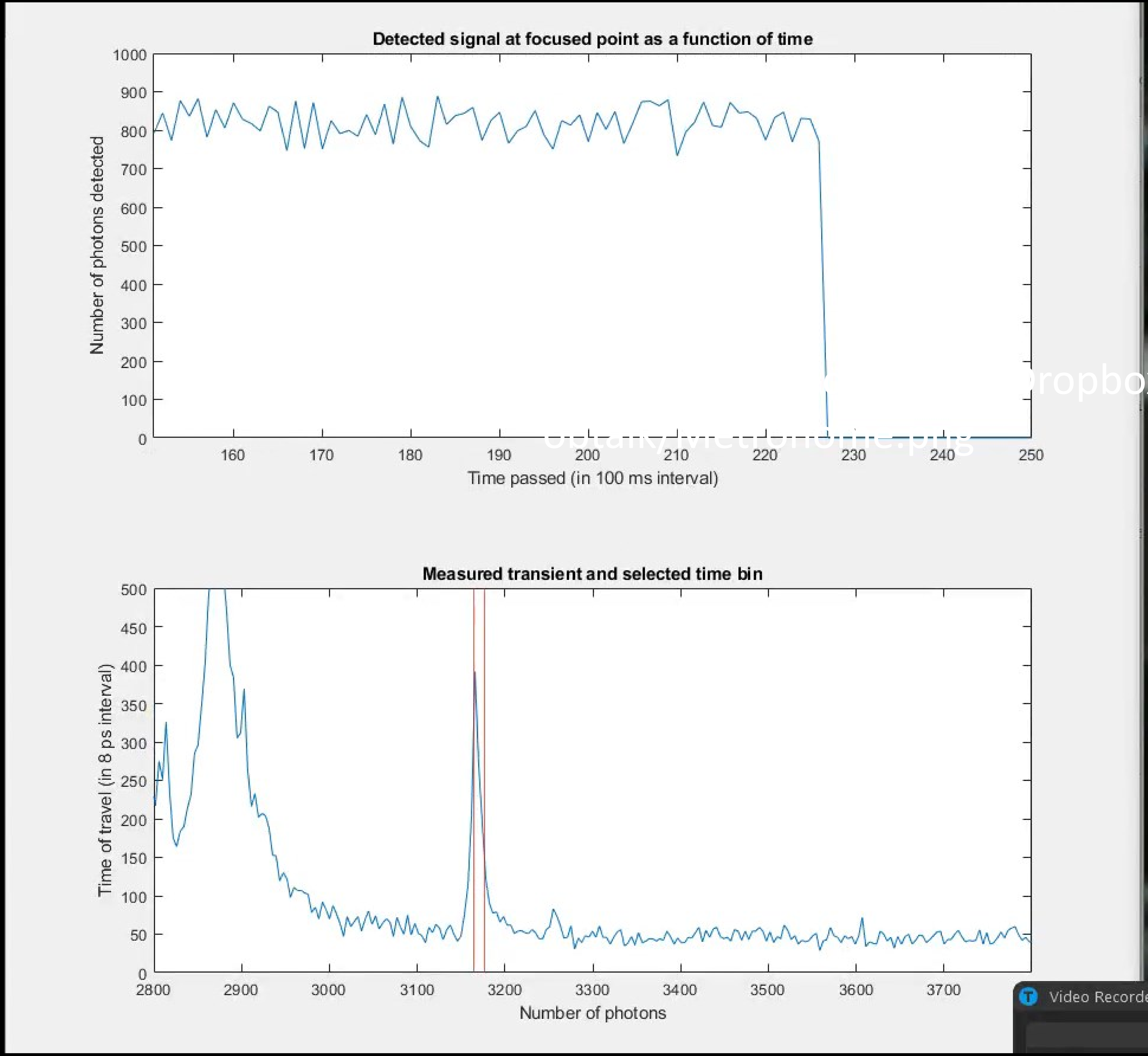

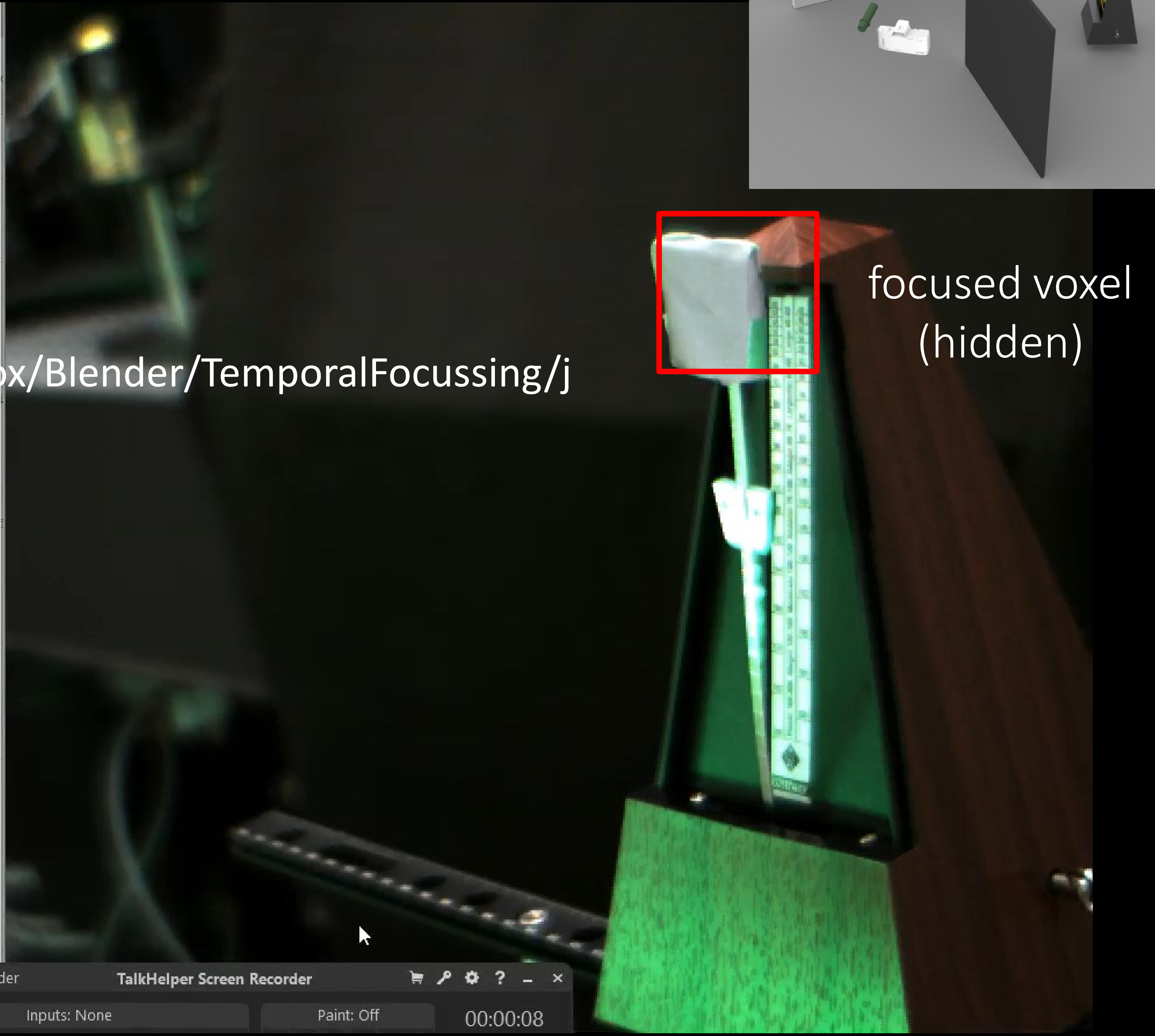

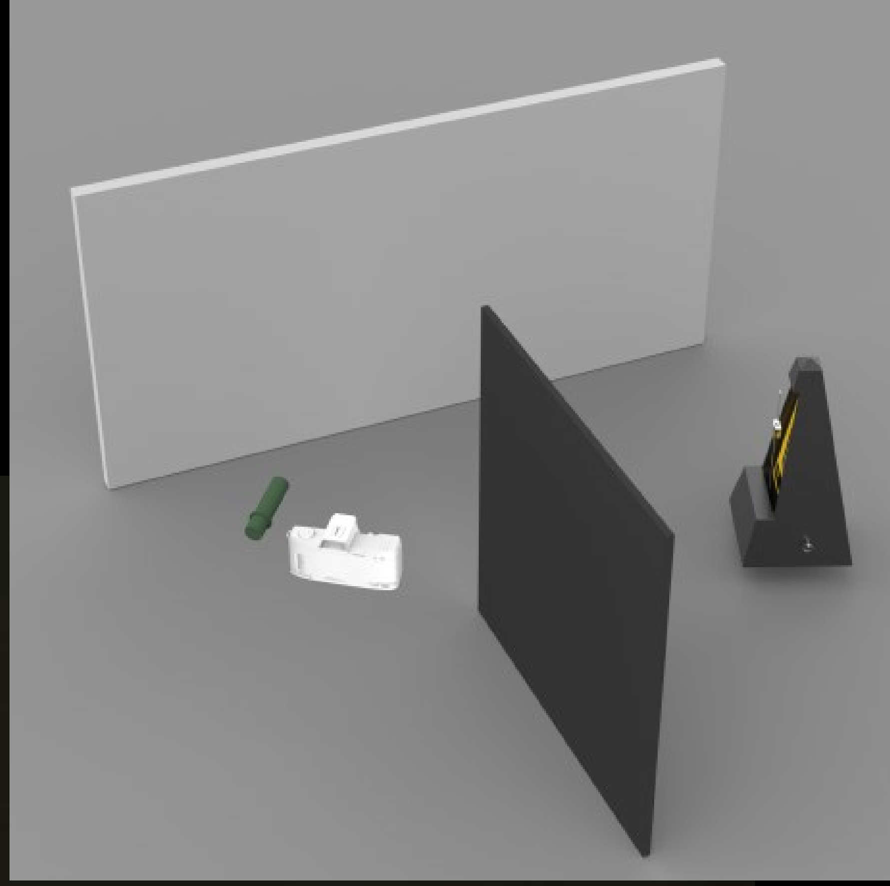

Physics-based rendering and its applications to computational imaging

forward rendering

- accurate and efficient simulation
- virtually design sensors, optics, and algorithms

inverse rendering

- accurate and efficient differentiable simulation
- tractably solve general inverse problems

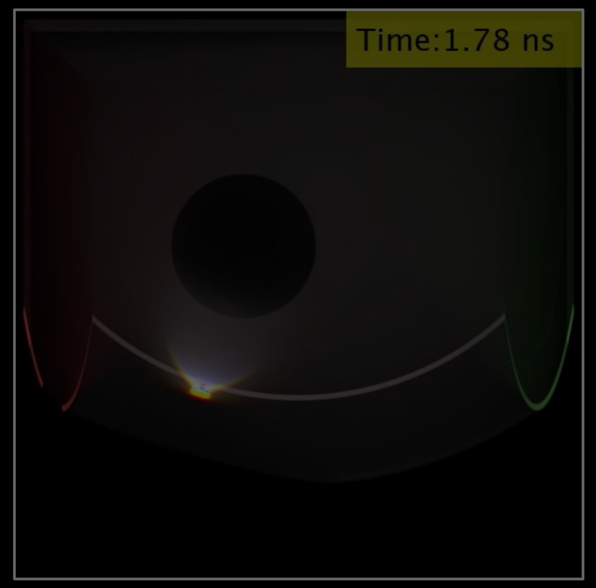

time-of-flight imaging

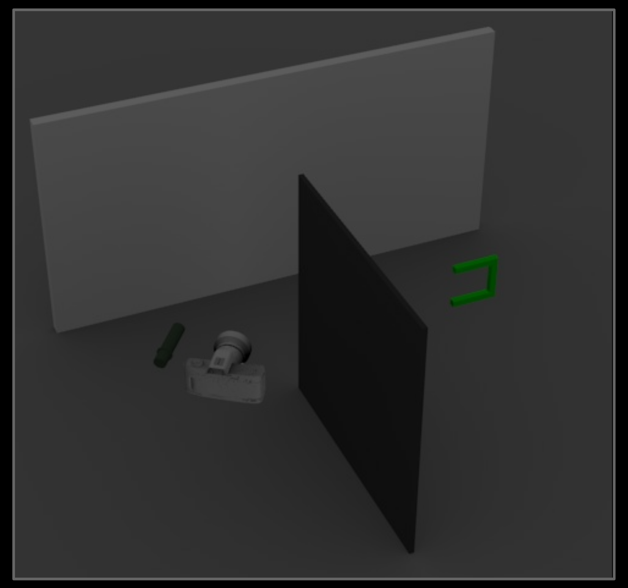

non-line-of-sight imaging

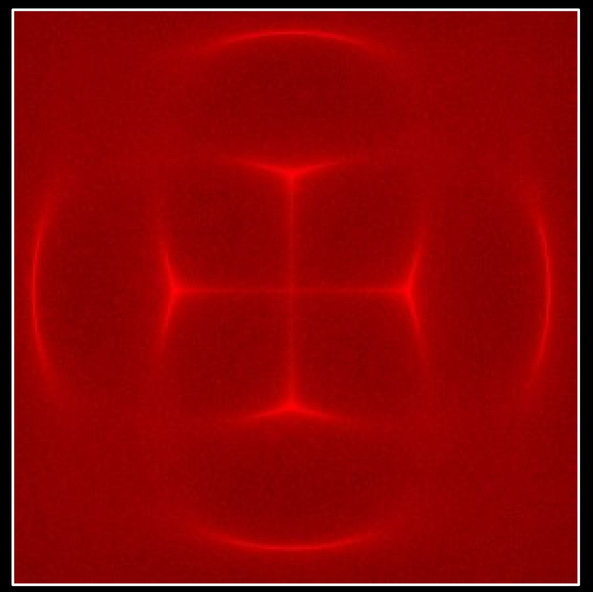

acousto-optic lensing

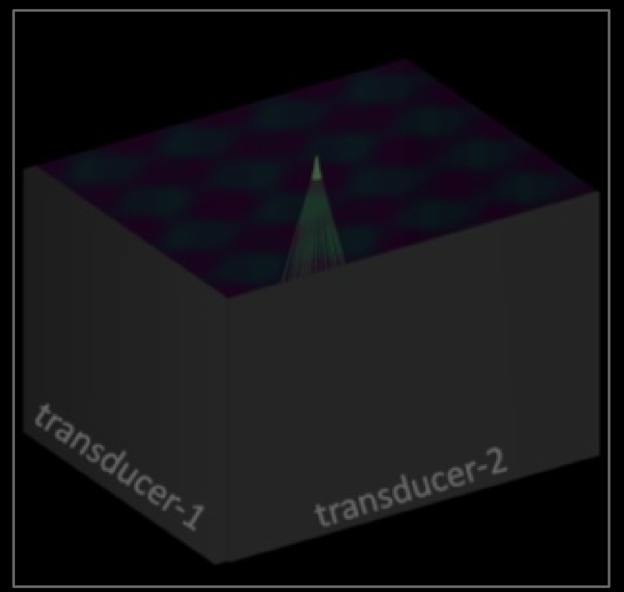

ultrafast light scanning

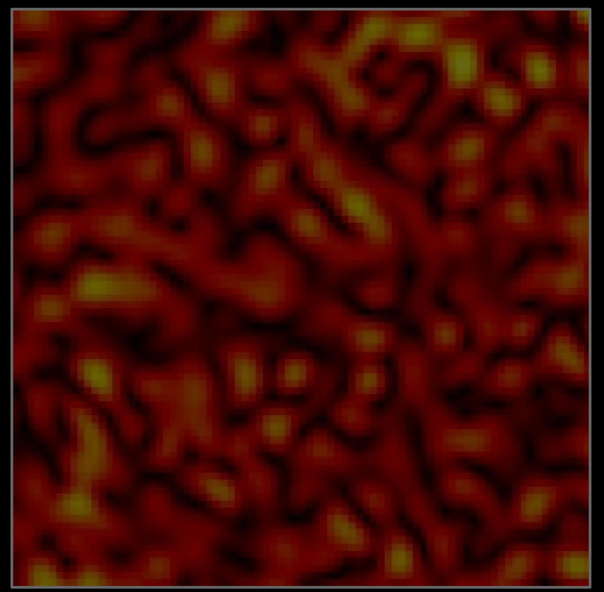

speckle imaging

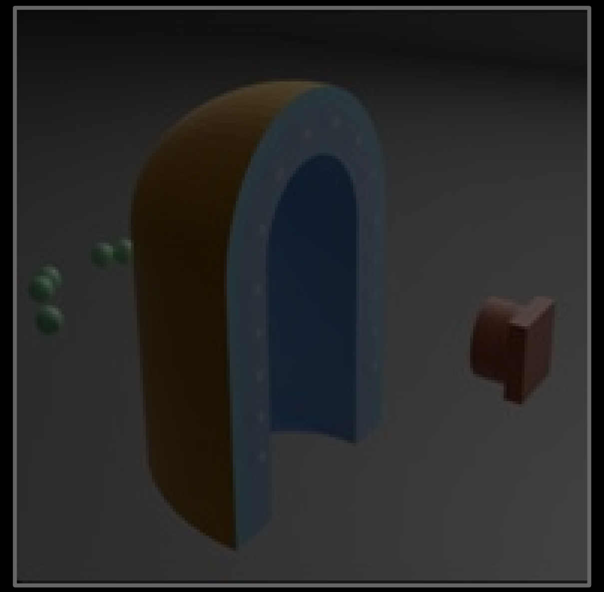

tactile sensor design

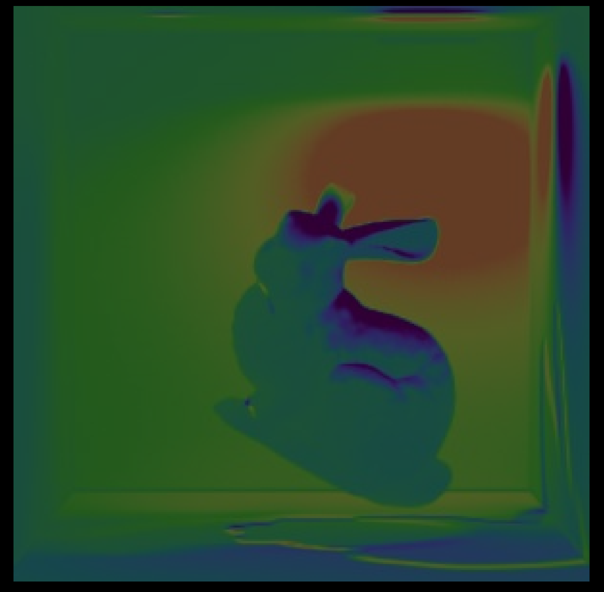

differentiable renderer

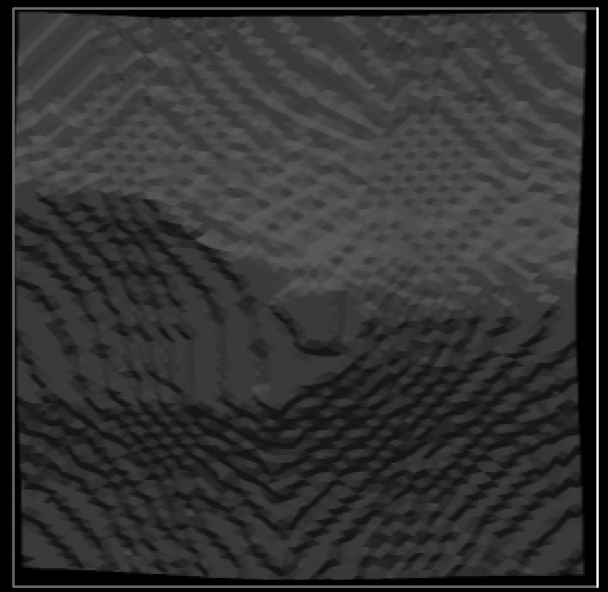

inverse problems

Focusing light inside tissue

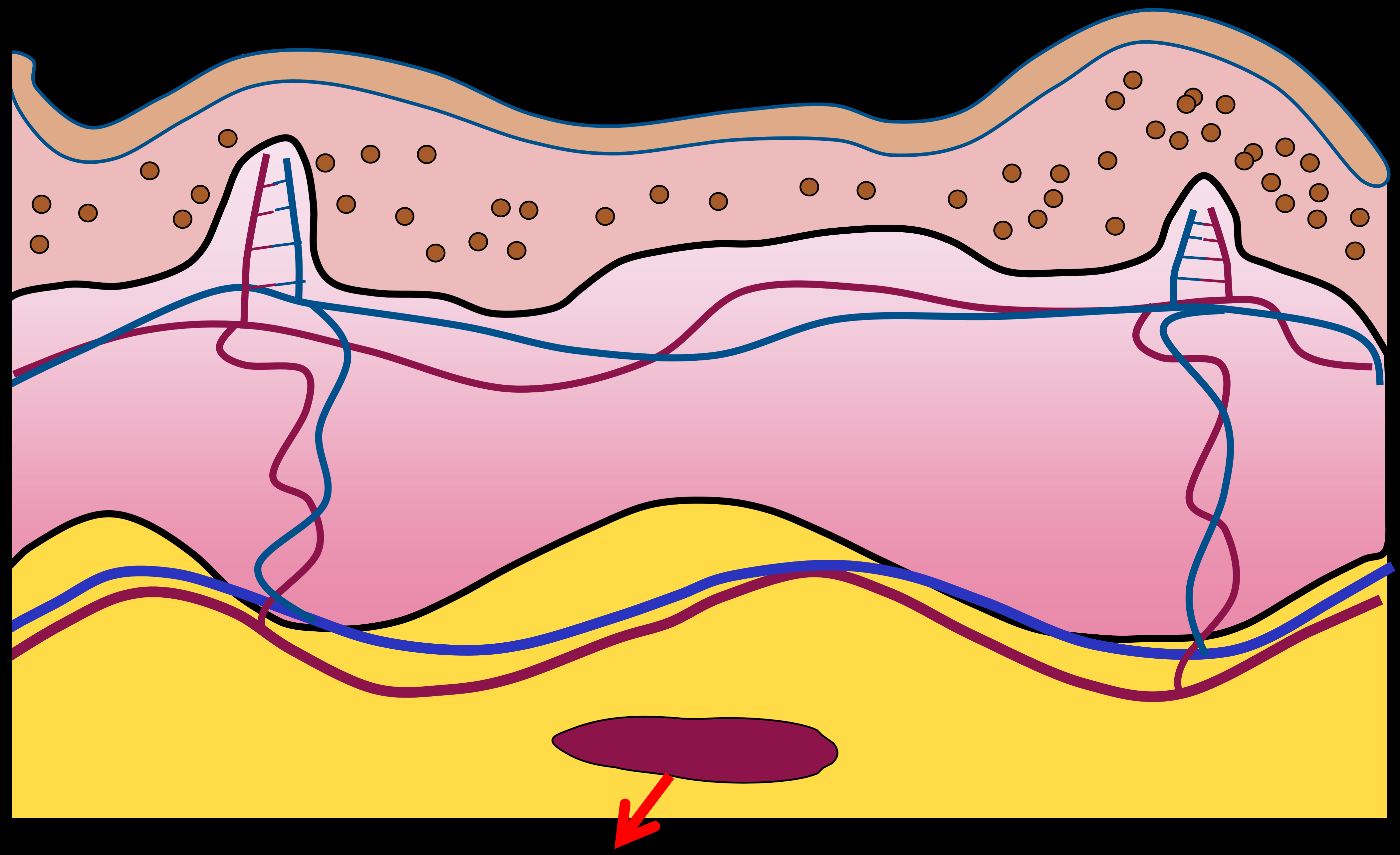

tumor

Focusing light inside tissue

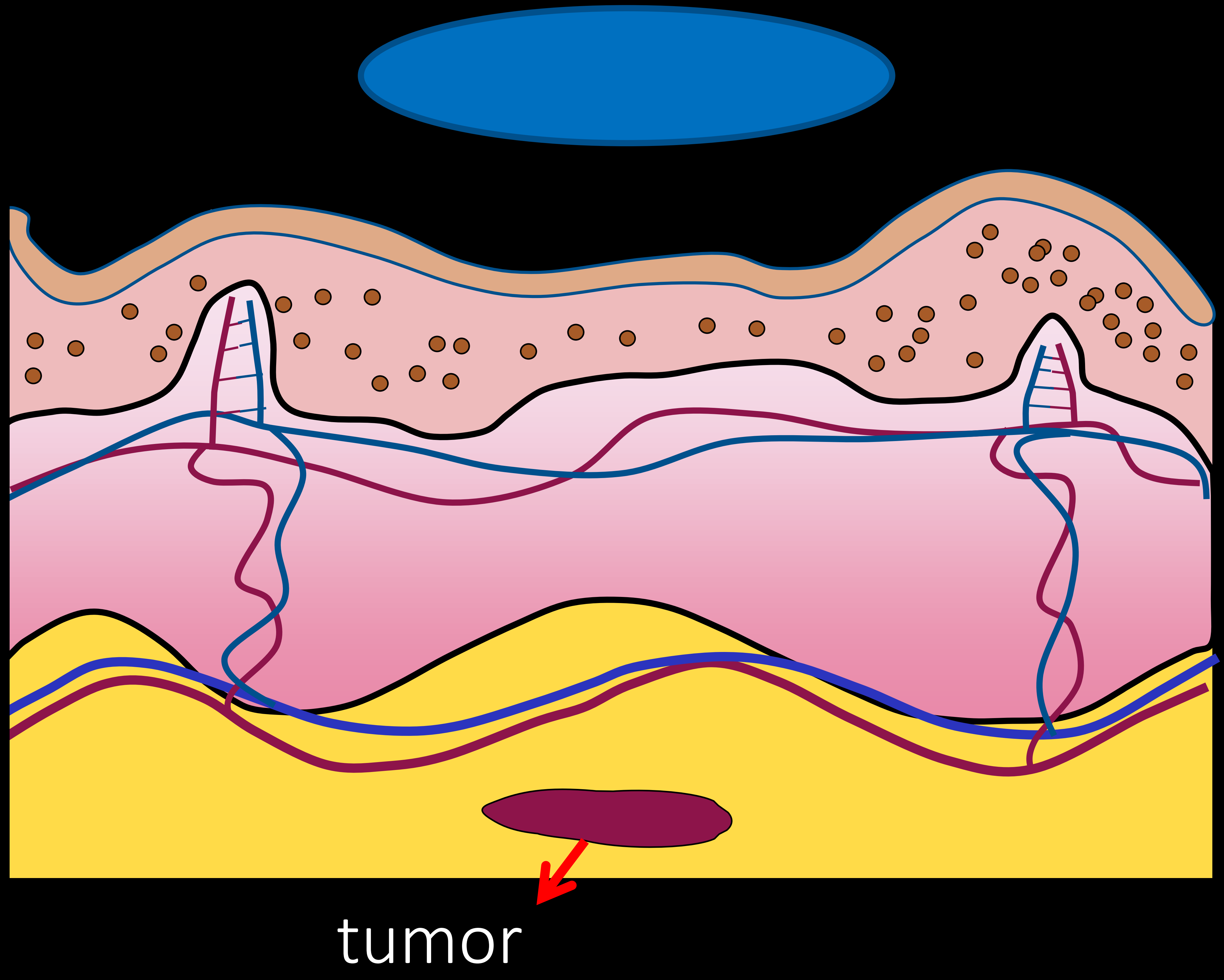

Focusing light inside tissue

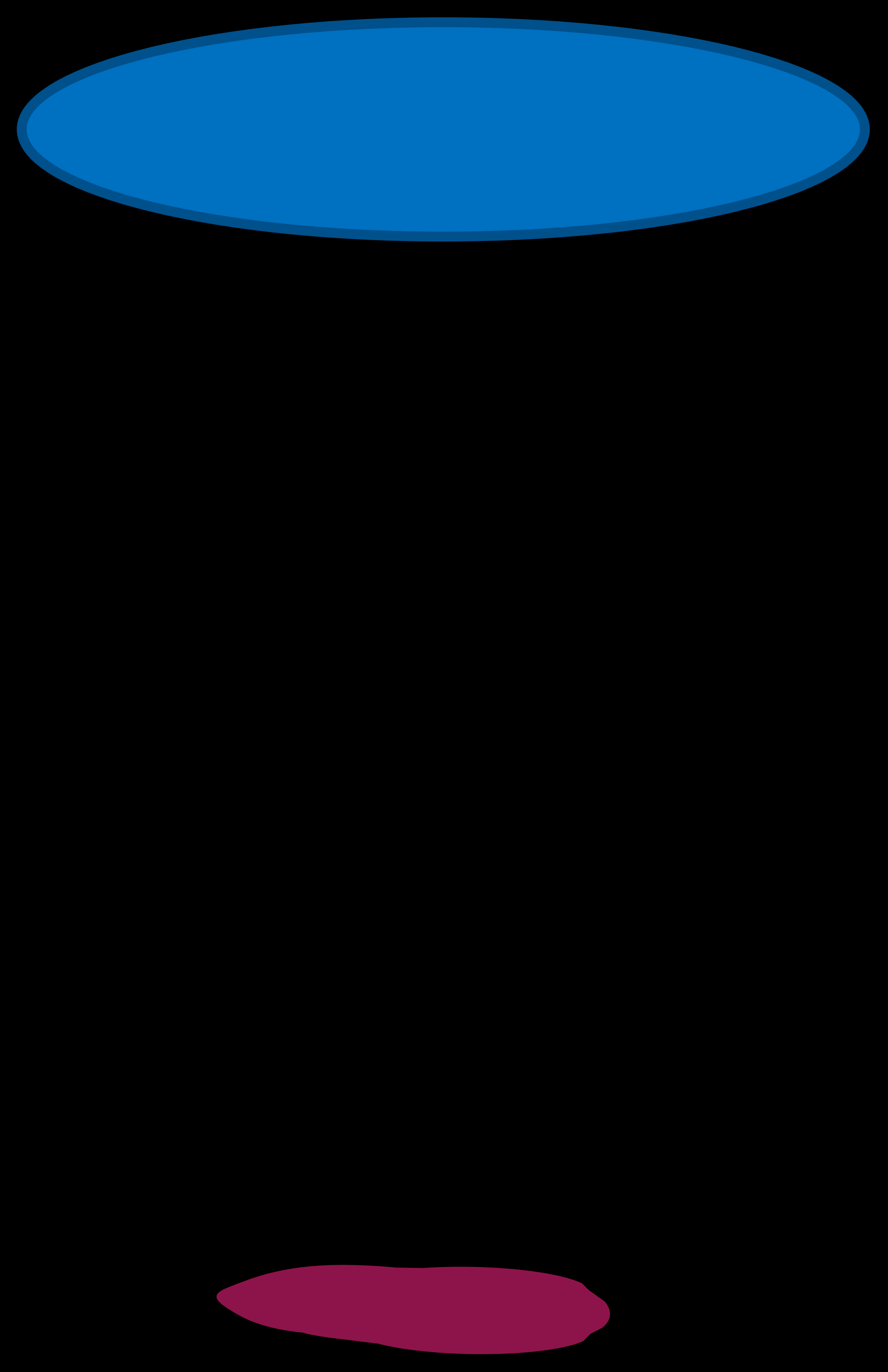

tumor

Focusing light inside tissue

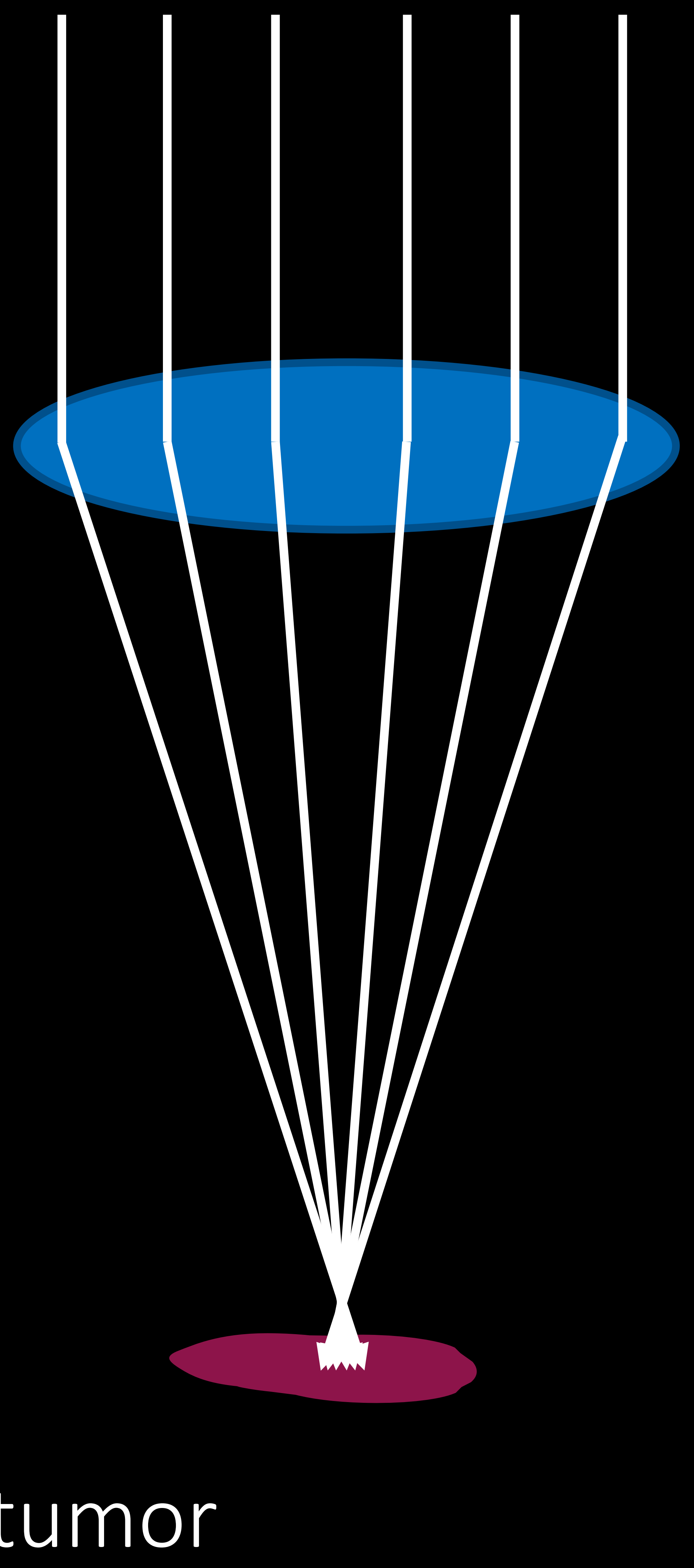

Focusing light inside tissue

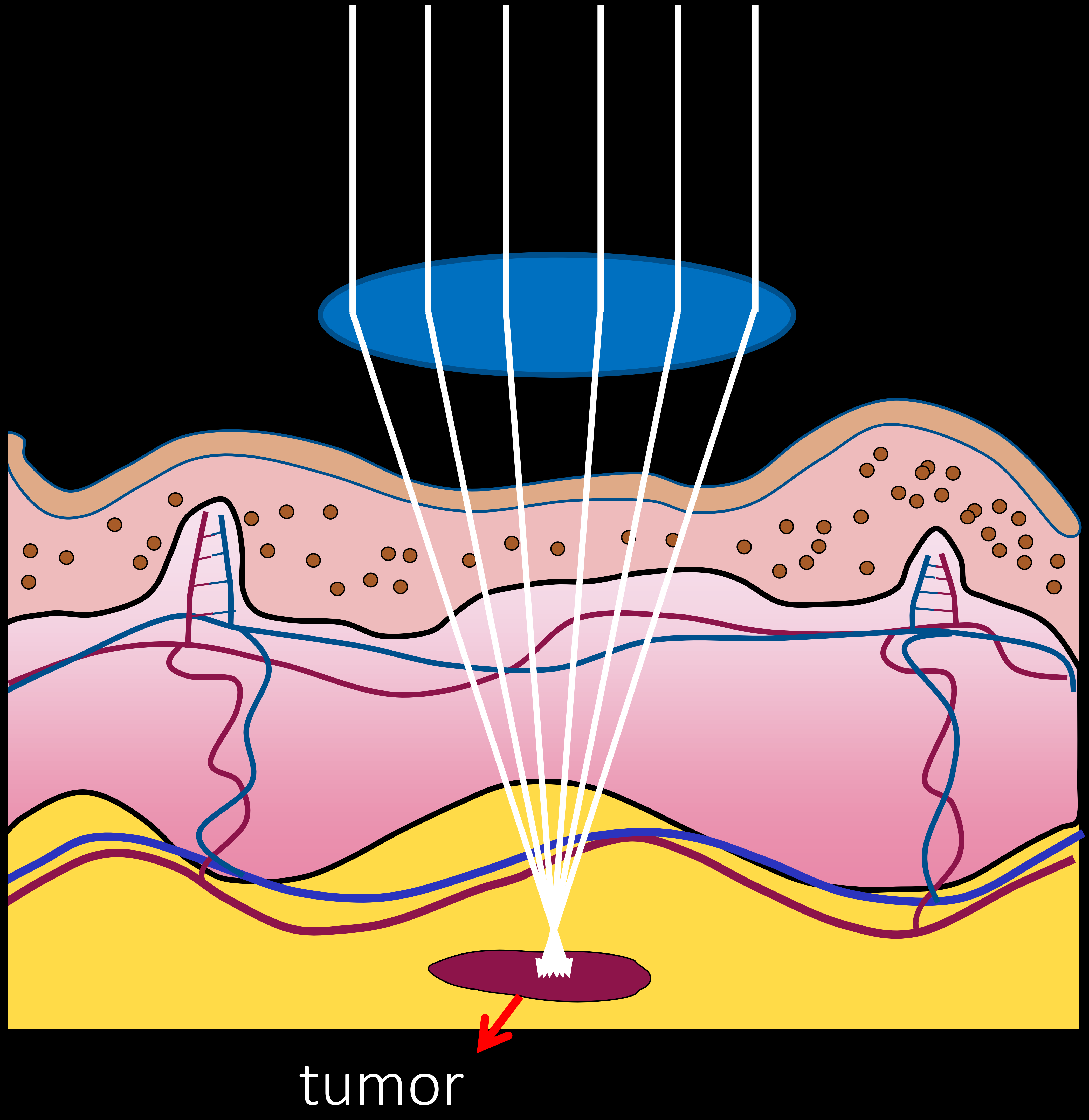

Focusing light inside tissue

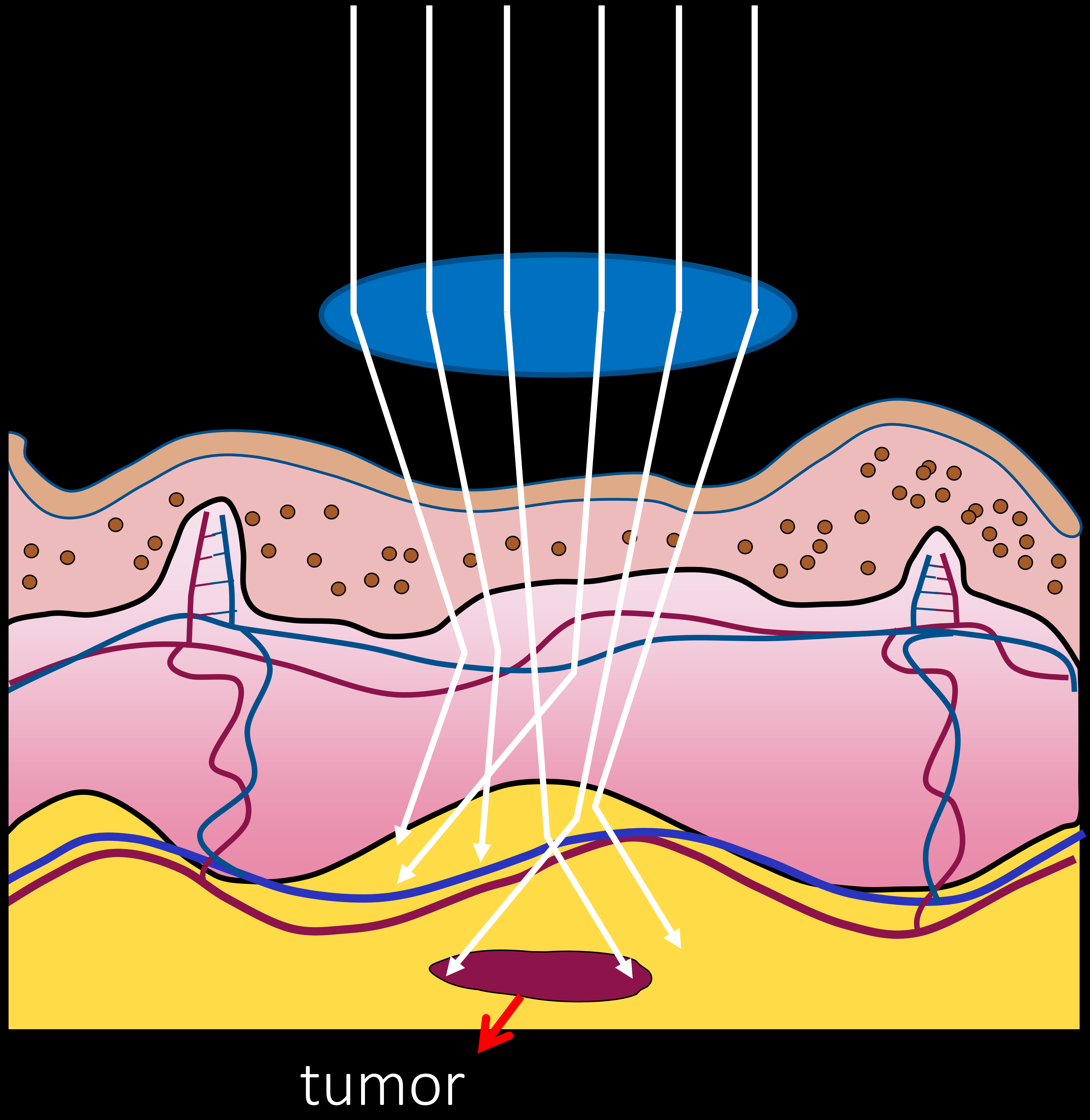

Focusing light inside tissue

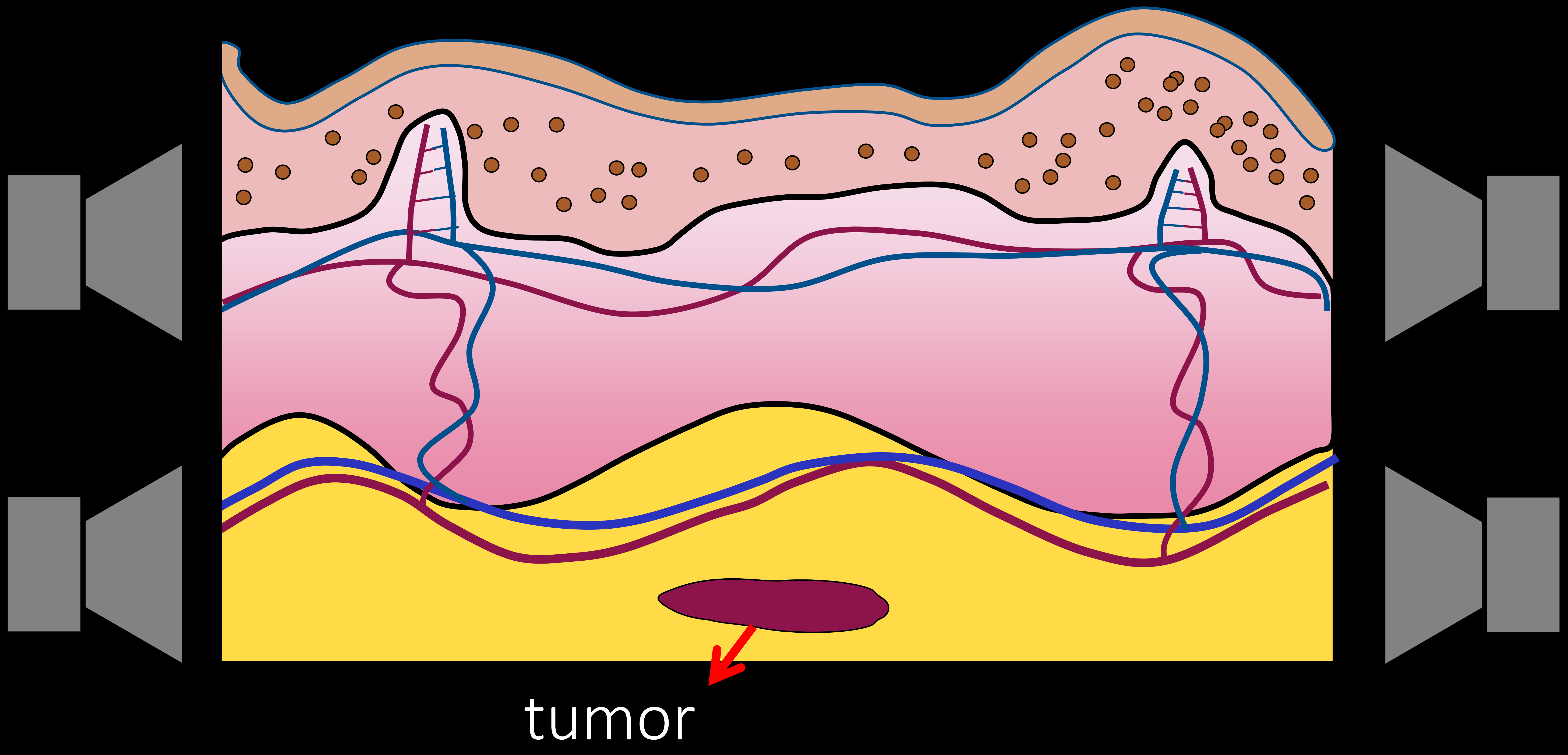

Focusing light inside tissue

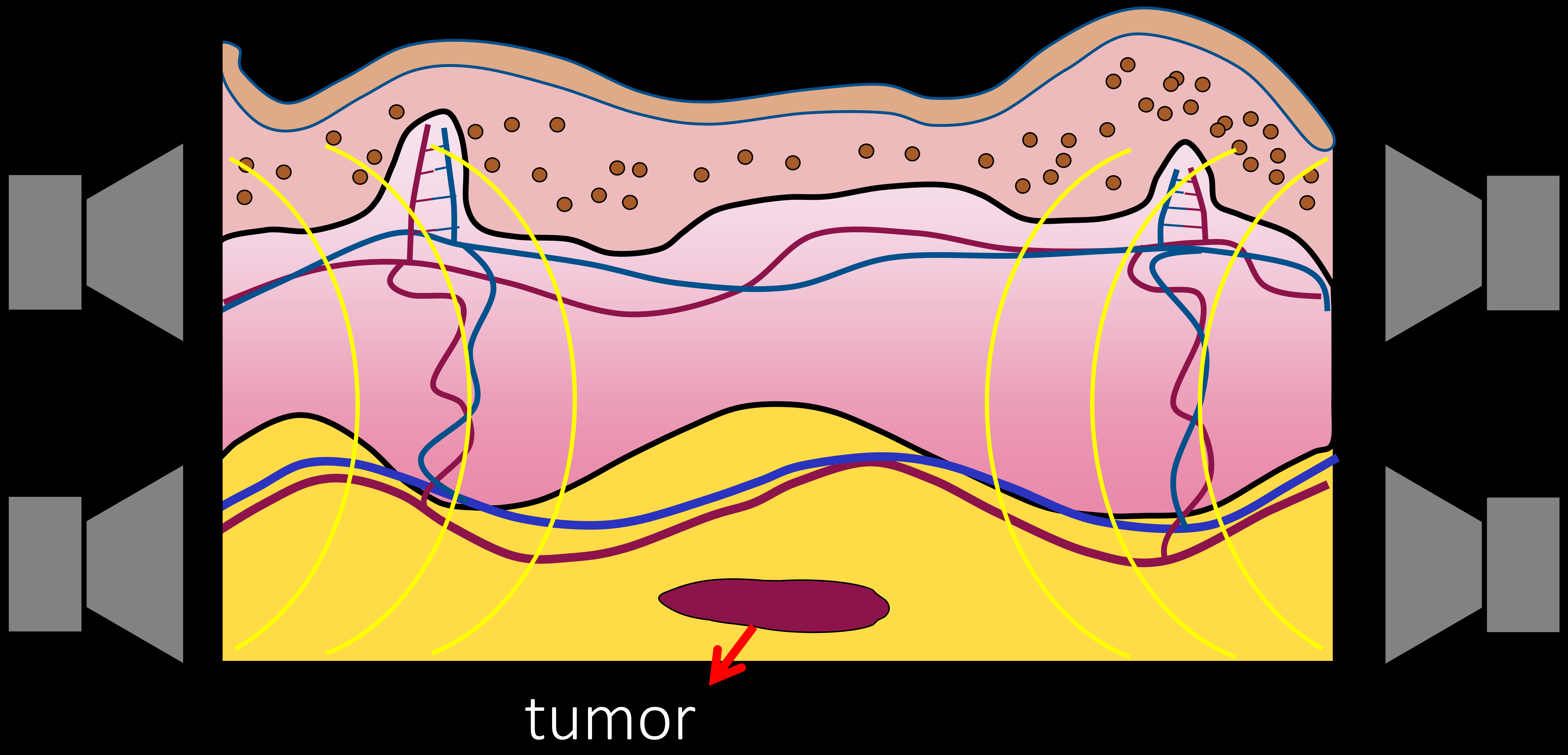

Focusing light inside tissue

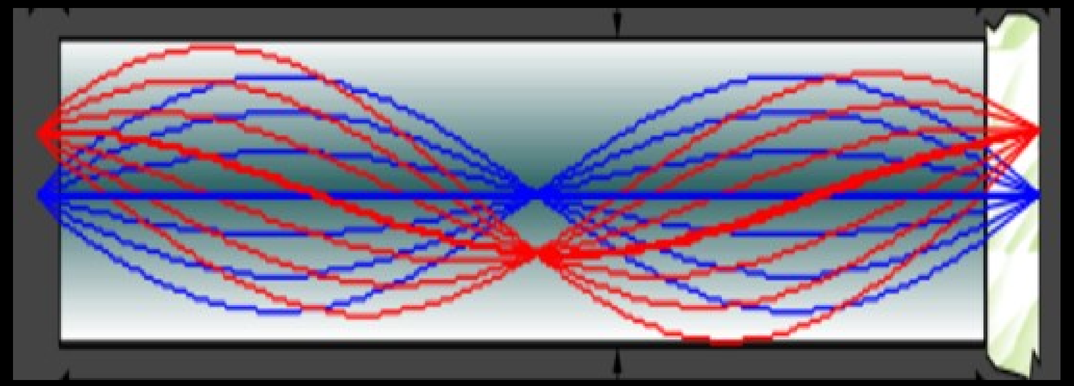
Gradient Refractive Index (GRIN) waveguide

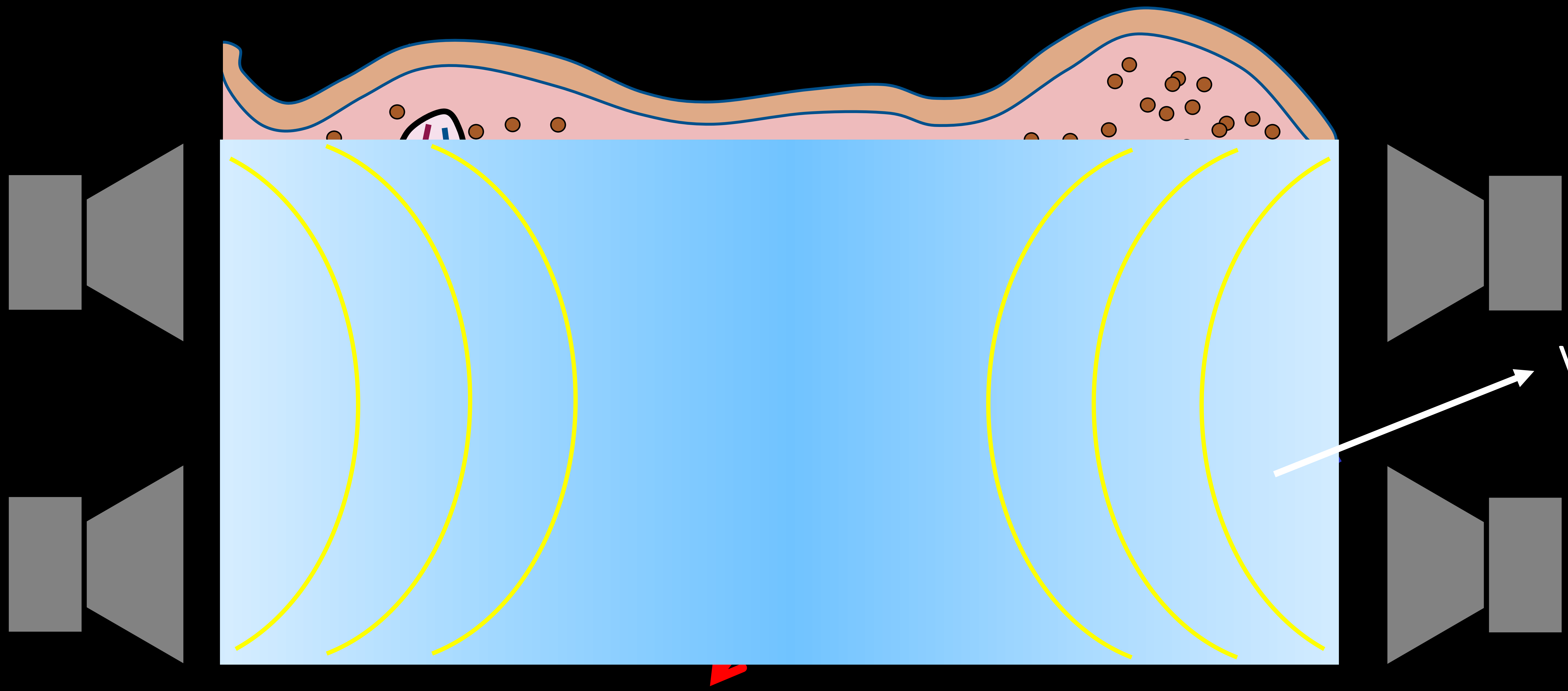

Focusing light inside tissue

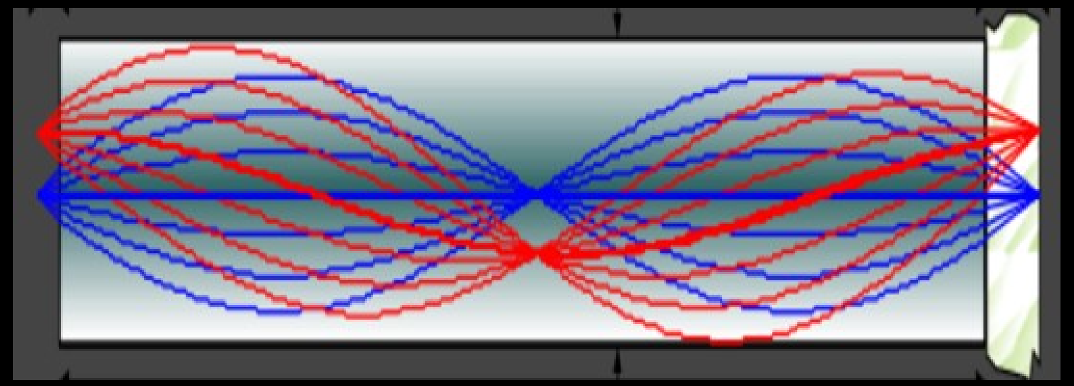

Gradient Refractive Index (GRIN) waveguide

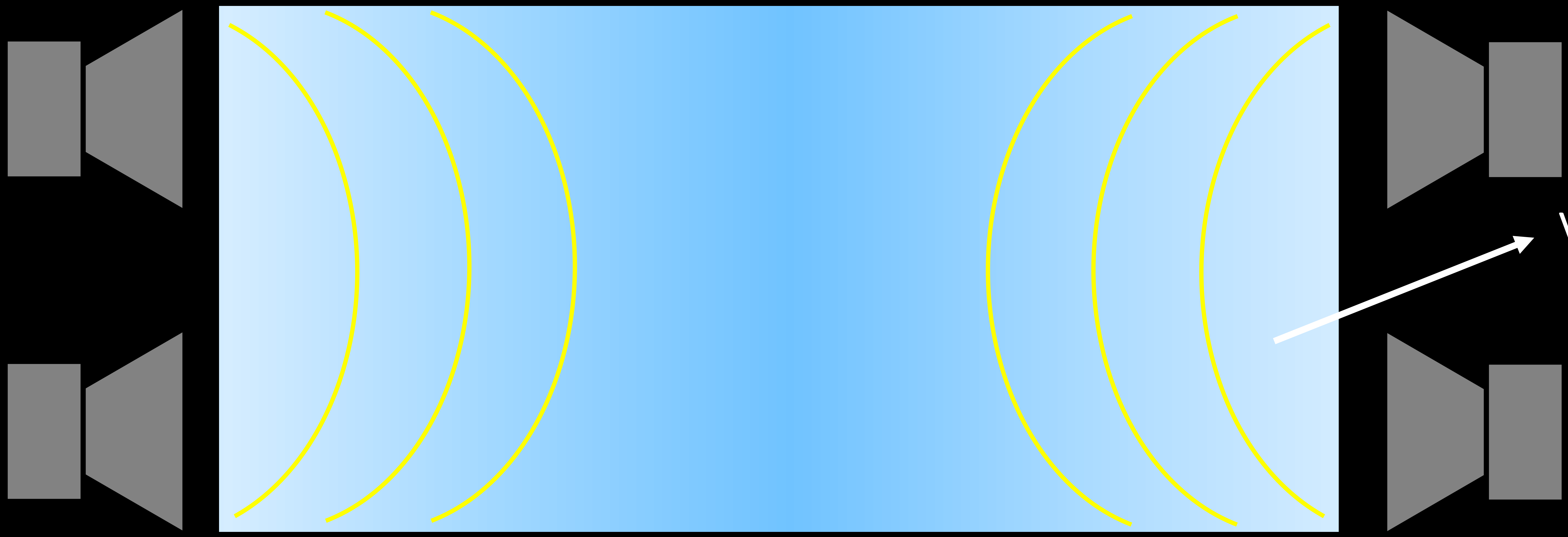

tumor

Focusing light inside tissue

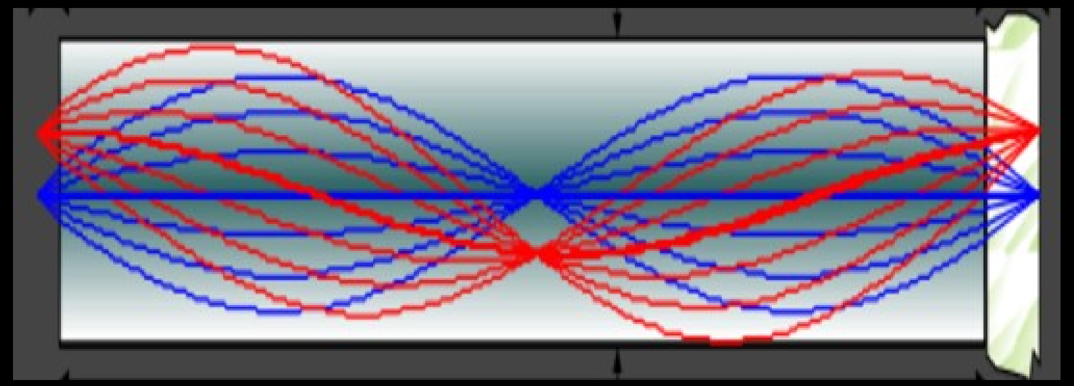

Gradient Refractive Index (GRIN) waveguide

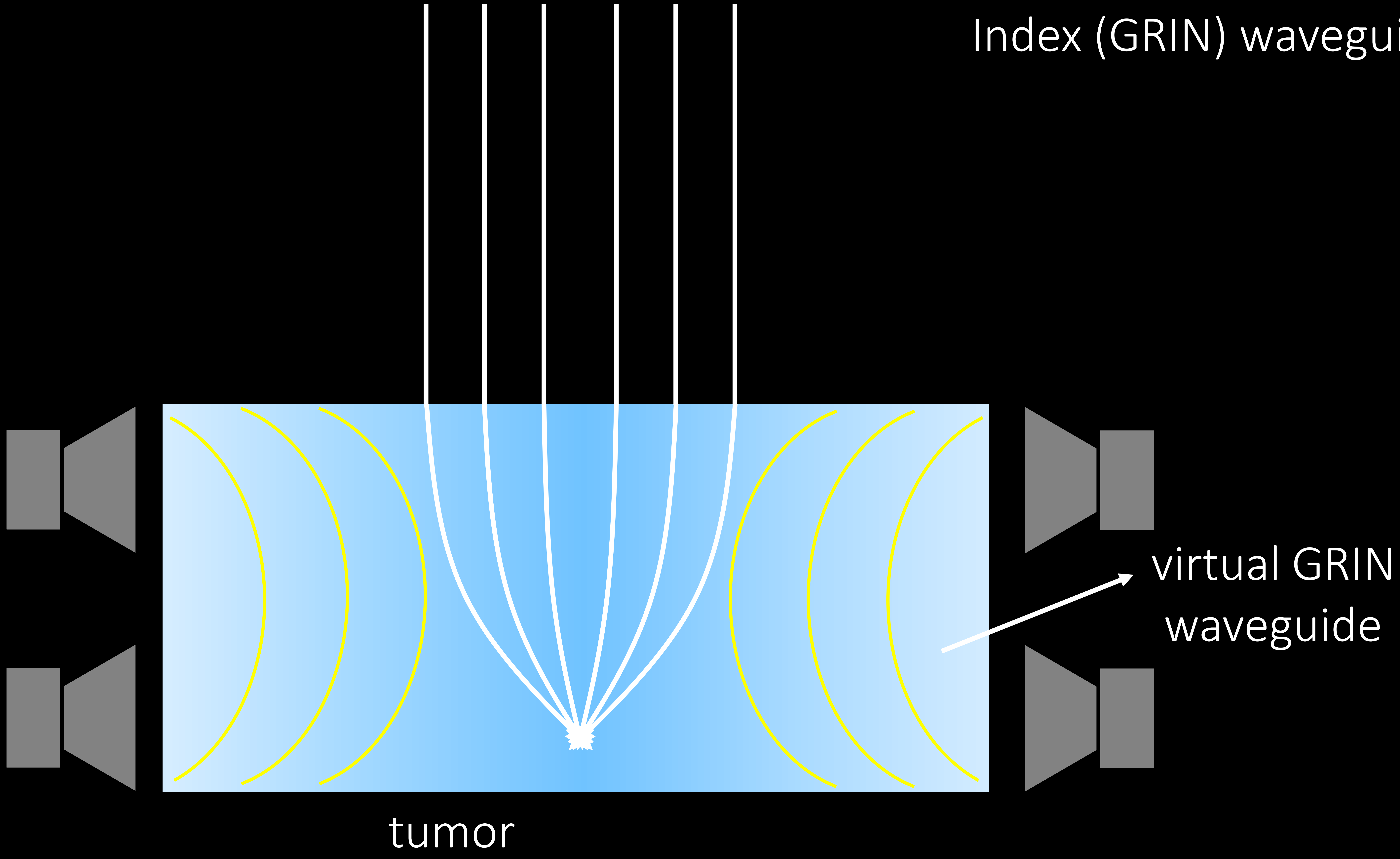

Focusing light inside tissue

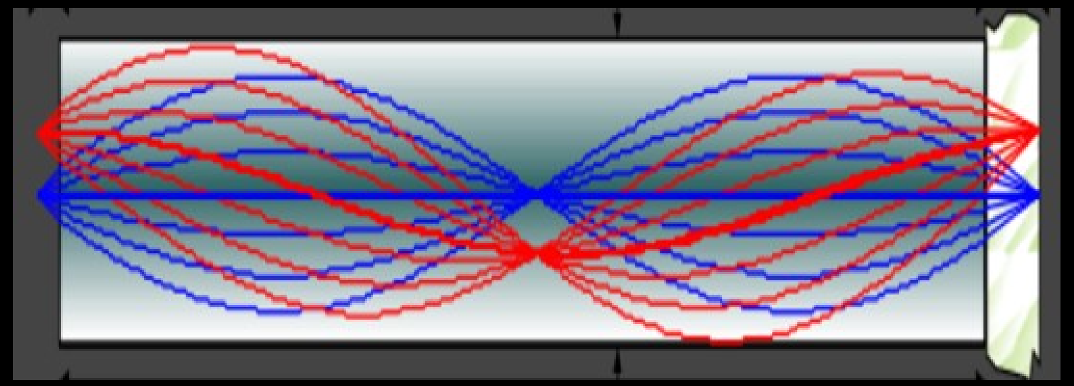

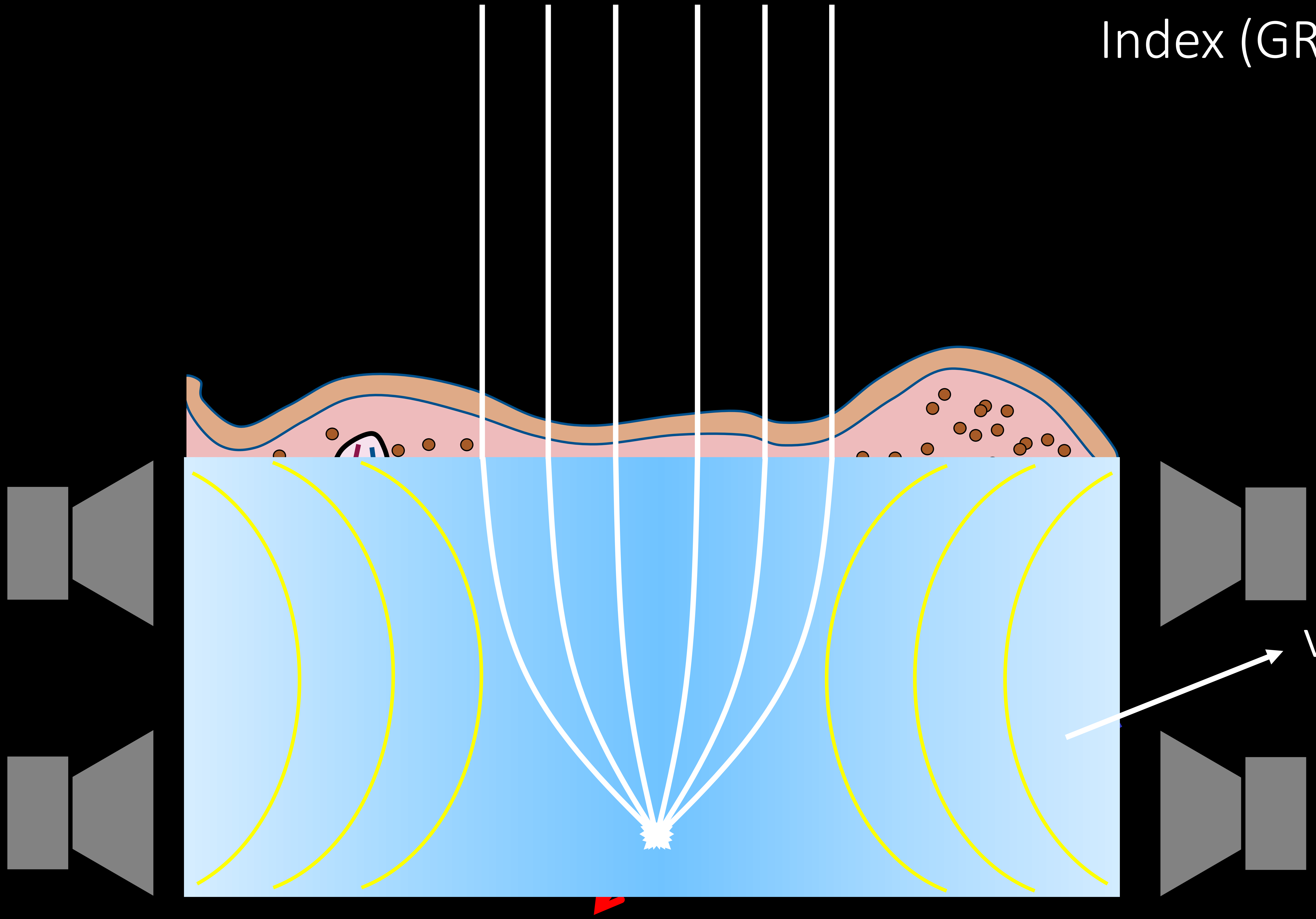

Focusing light inside tissue

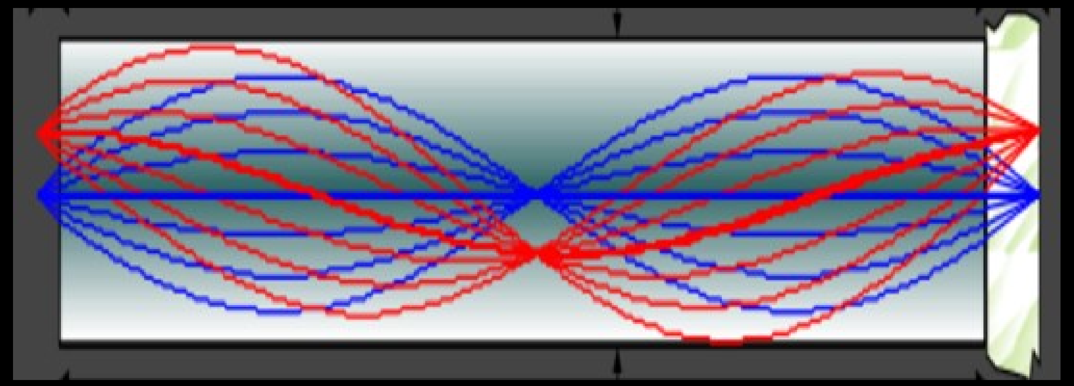

Gradient Refractive Index (GRIN) waveguide

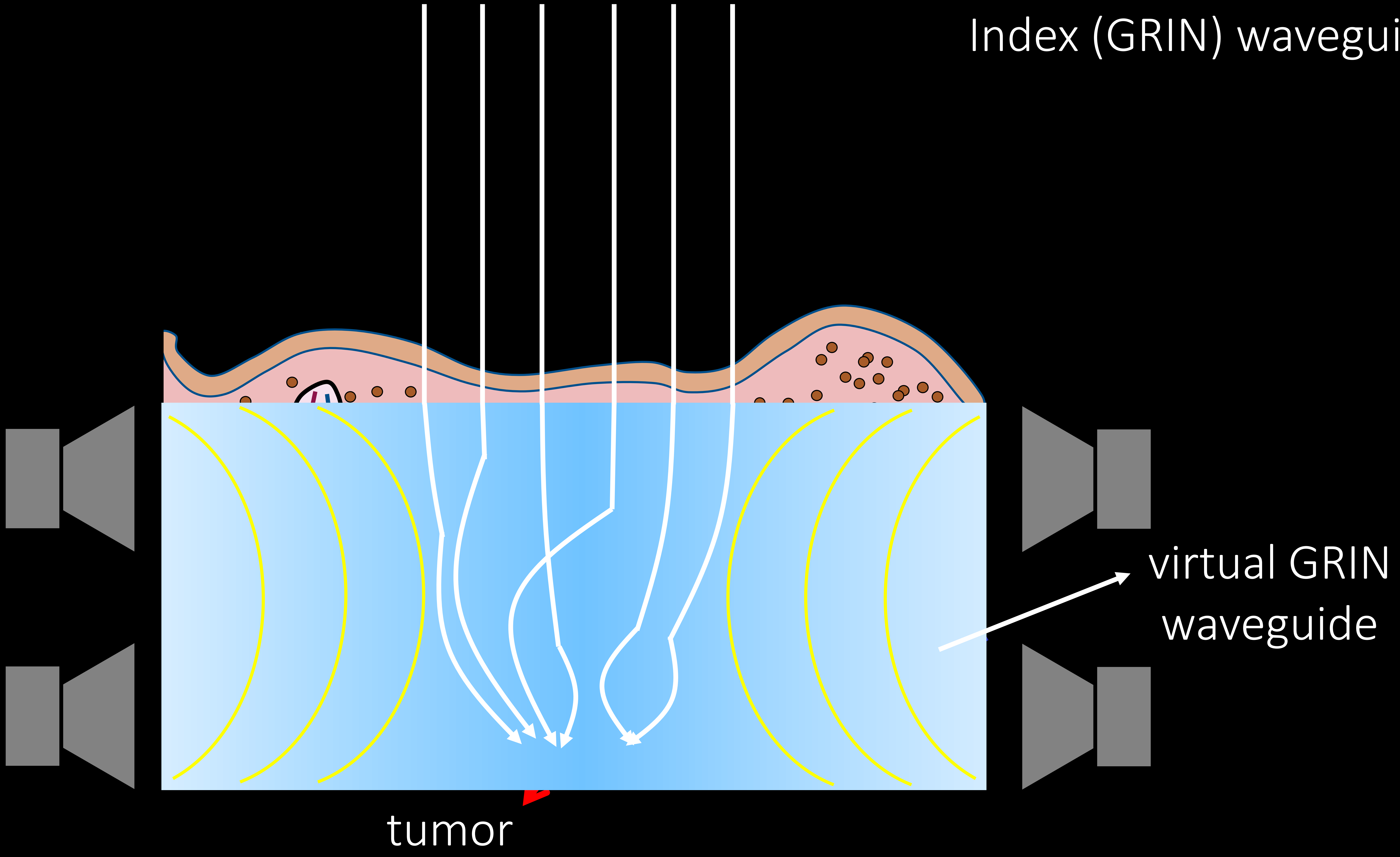

Ultrasonic light guiding inside tissue

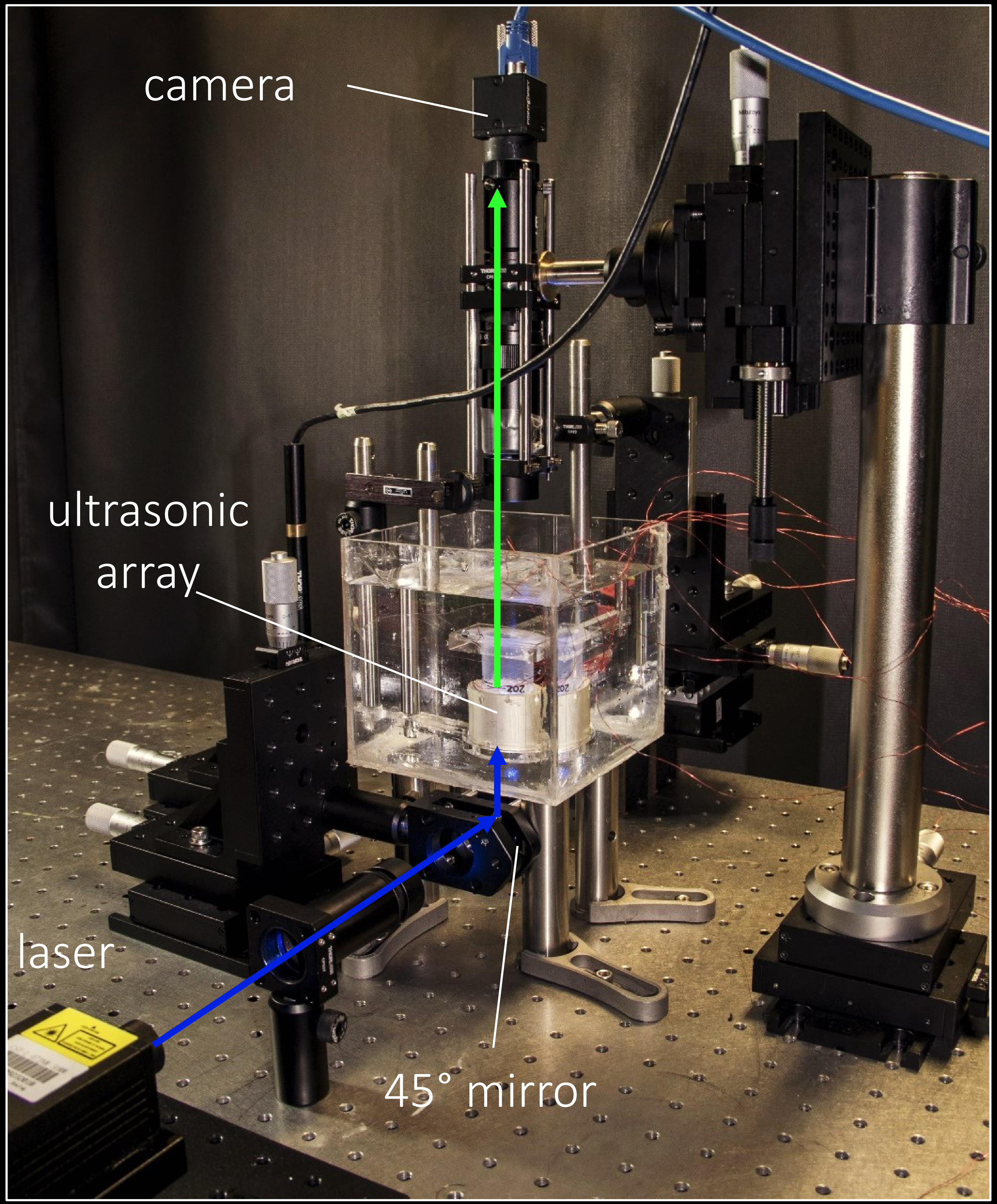

[Chamanzar et al., Nat. Comm. 2019]
[Karimi et al., Optics Express, 2019]
[Scopelliti et al., LSA, 2019]

Ultrasonic light guiding inside tissue

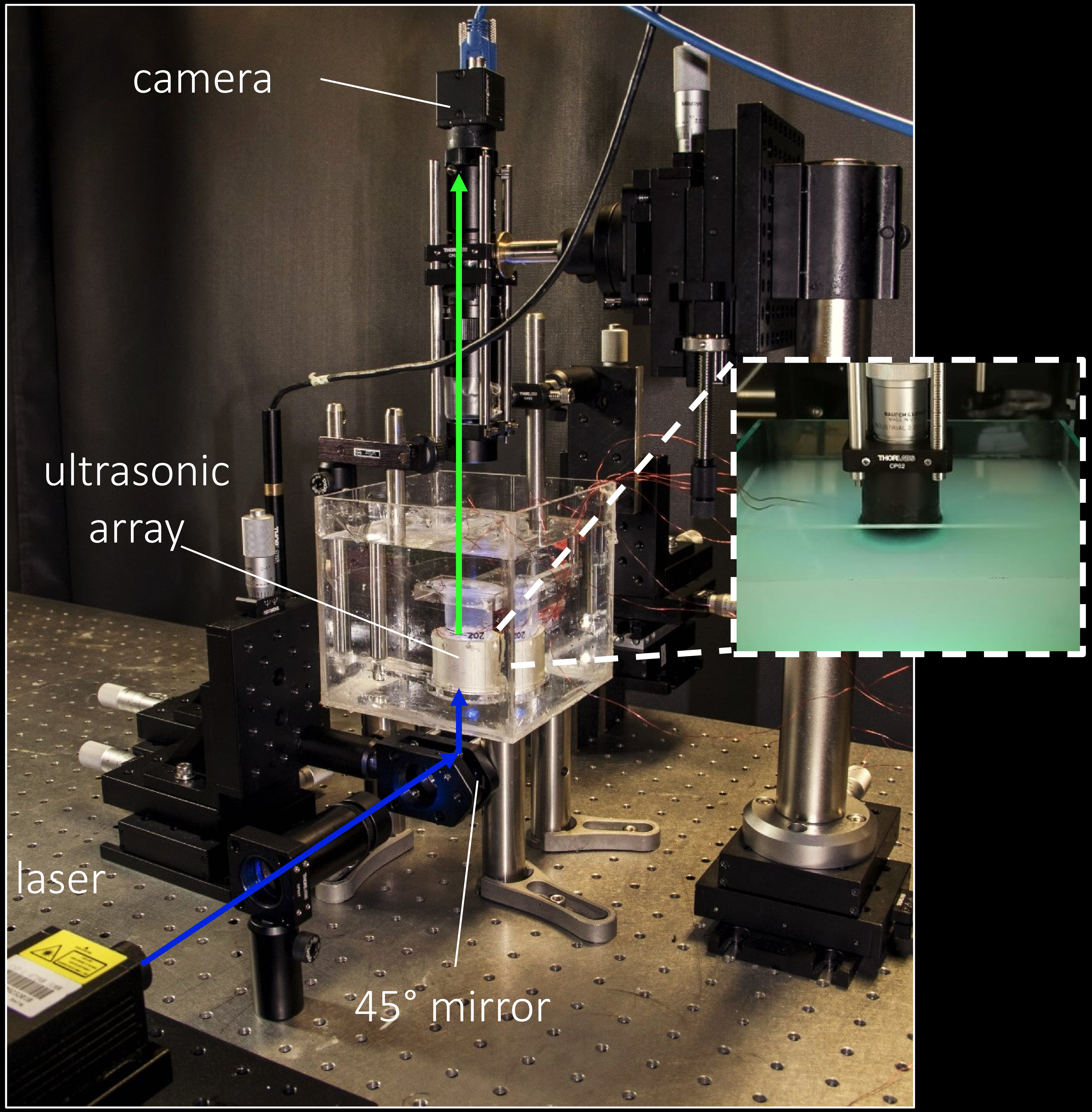

[Chamanzar et al., Nat. Comm. 2019]
[Karimi et al., Optics Express, 2019]
[Scopelliti et al., LSA, 2019]

Ultrasonic light guiding inside tissue

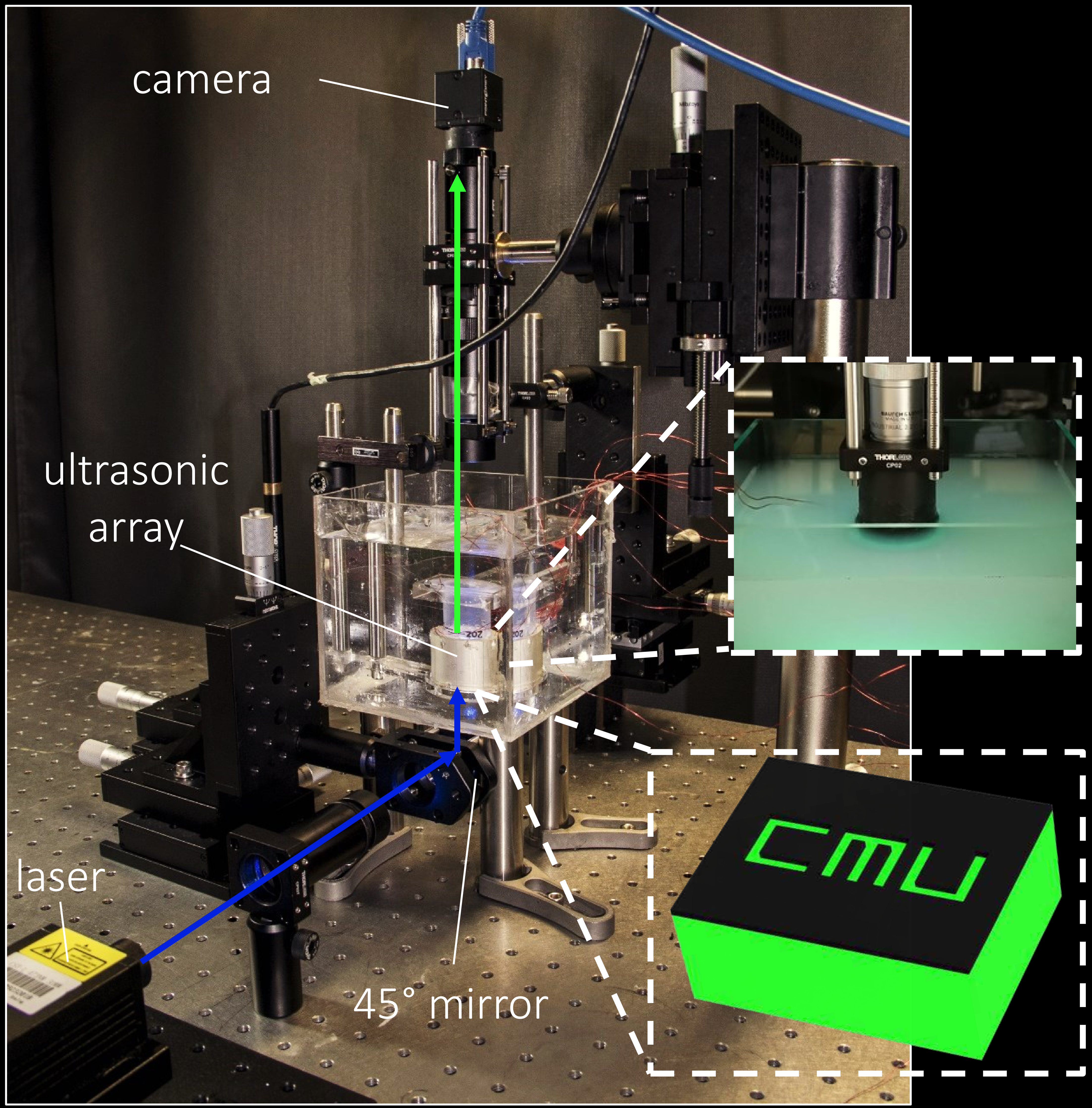

[Chamanzar et al., Nat. Comm. 2019]
[Karimi et al., Optics Express, 2019]
[Scopelliti et al., LSA, 2019]

Ultrasonic light guiding inside tissue

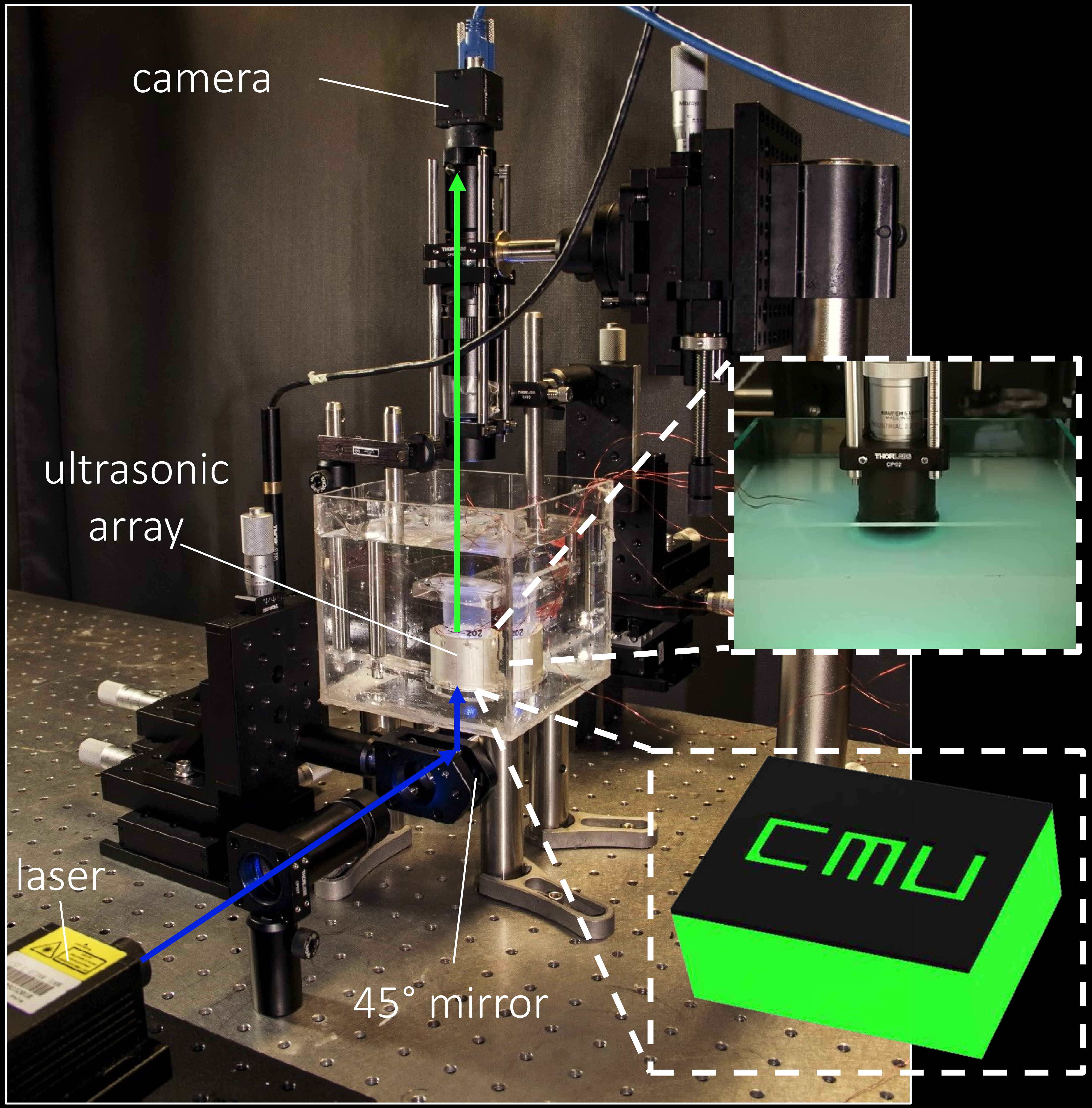

ultrasound off

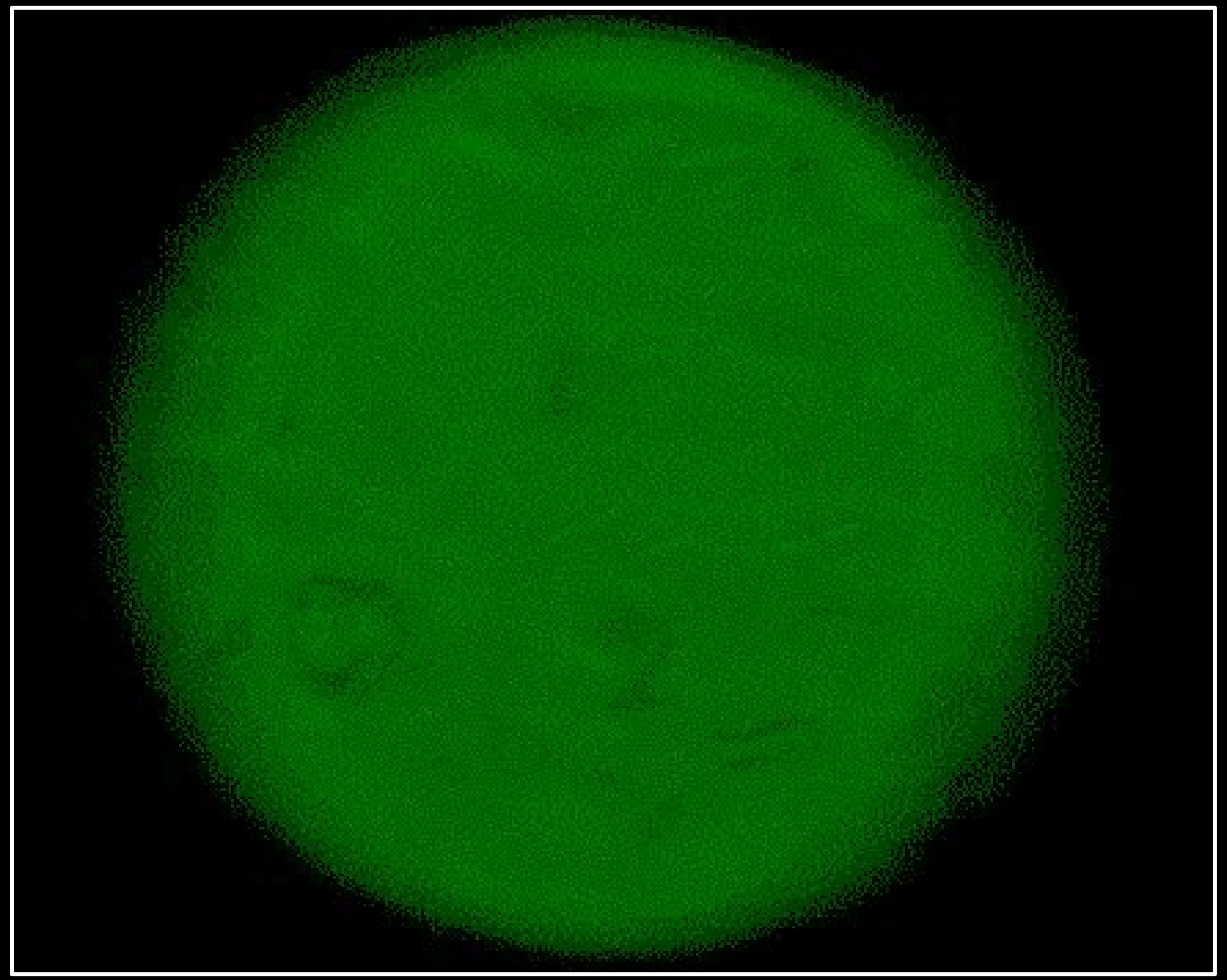

[Chamanzar et al., Nat. Comm. 2019]
[Karimi et al., Optics Express, 2019]
[Scopelliti et al., LSA, 2019]

Ultrasonic light guiding inside tissue

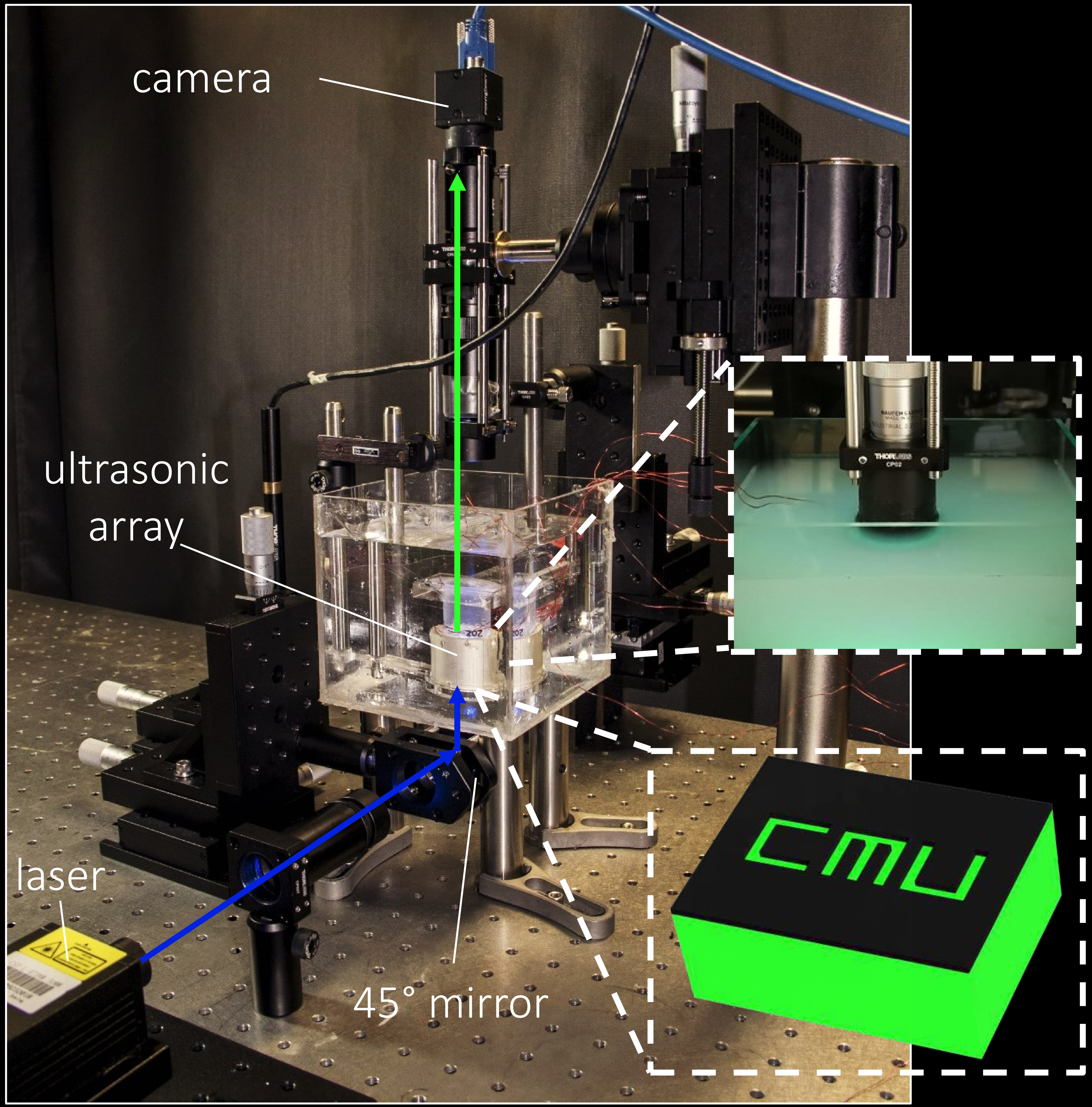

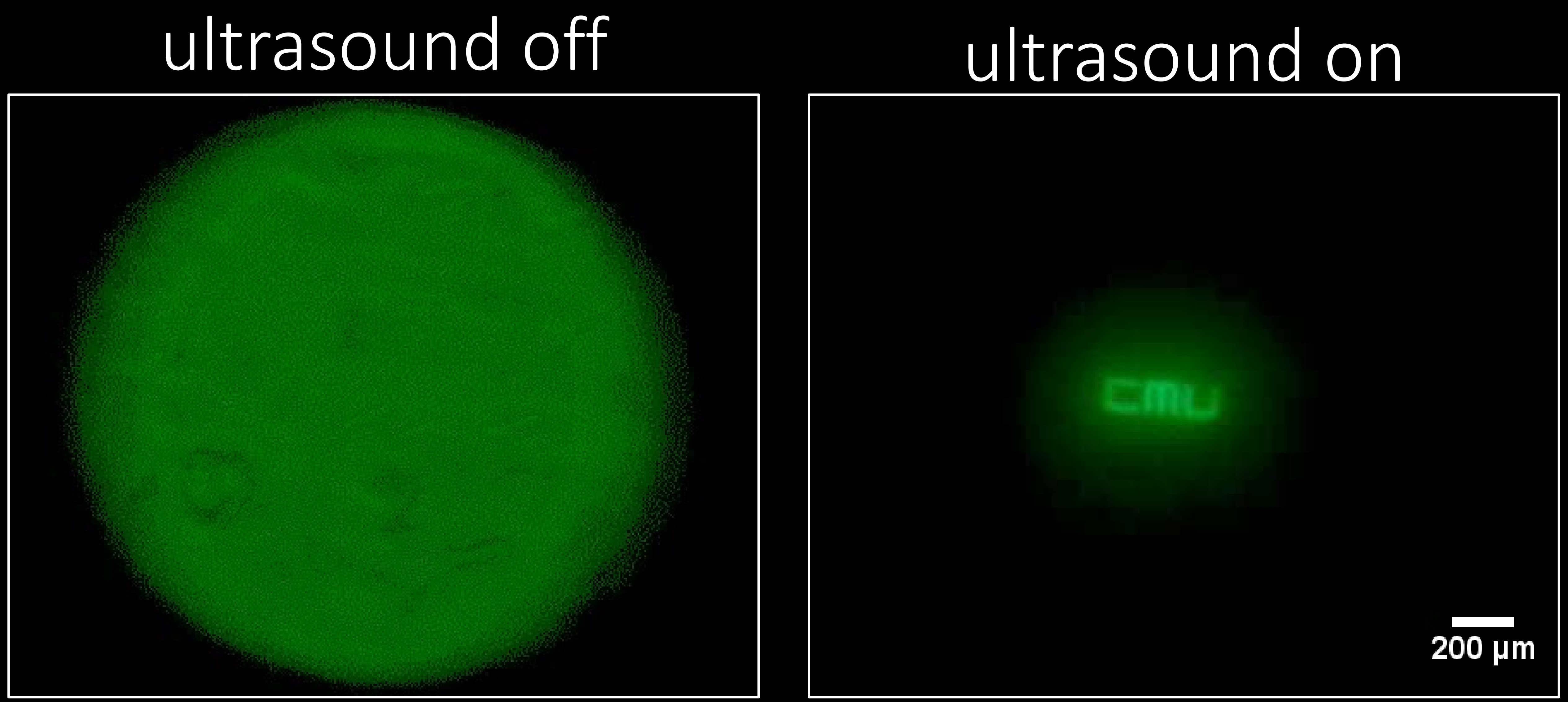

[Chamanzar et al., Nat. Comm. 2019]
[Karimi et al., Optics Express, 2019]
[Scopelliti et al., LSA, 2019]

Ultrasonic light guiding inside tissue

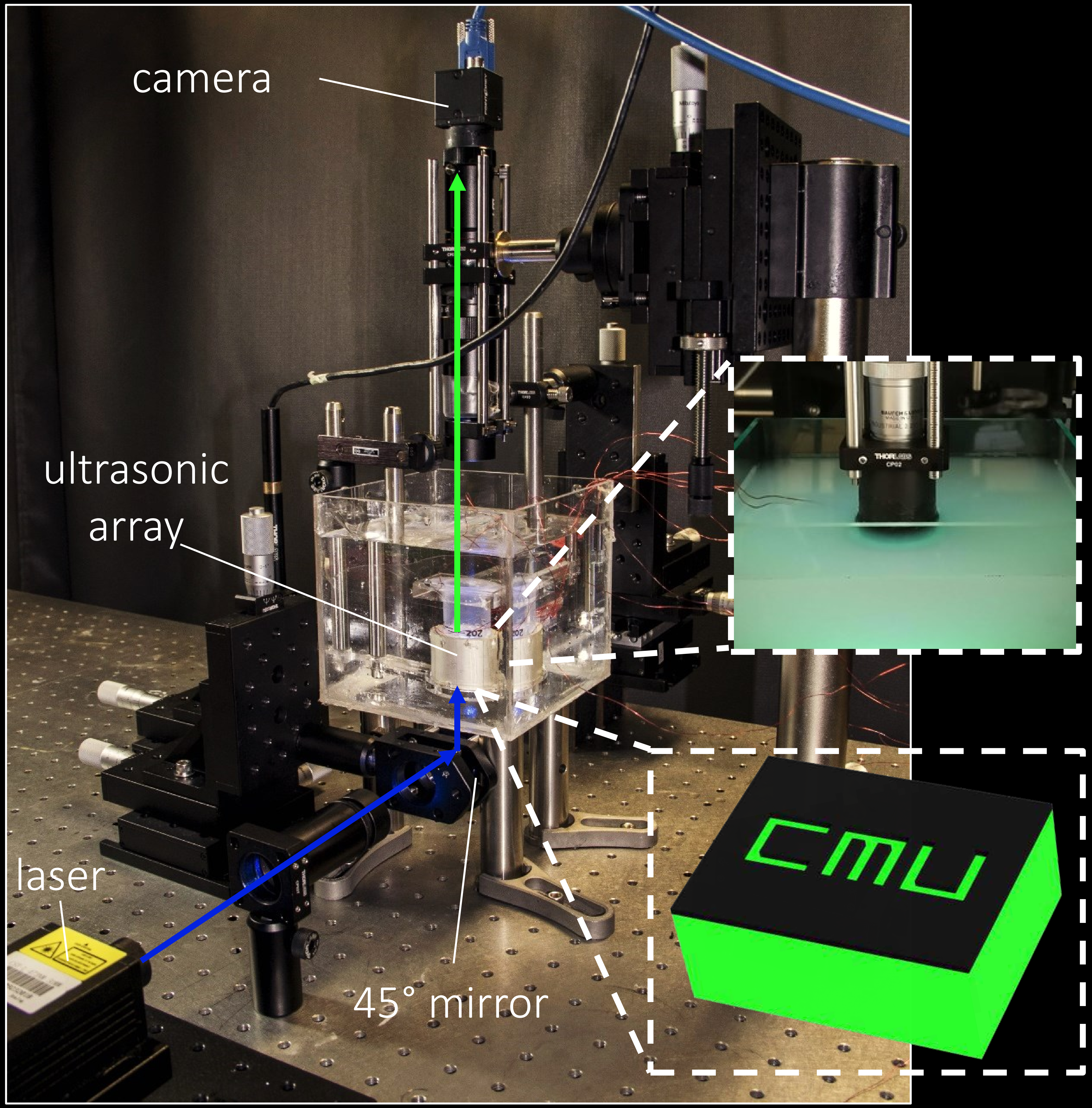

High-dimensional, highly-non-linear design problem:

- ultrasound frequency
- ultrasound voltage
- placement of transducers
- shape of waveguides
- waveform shape
- and more…

Ultrasonic light guiding inside tissue

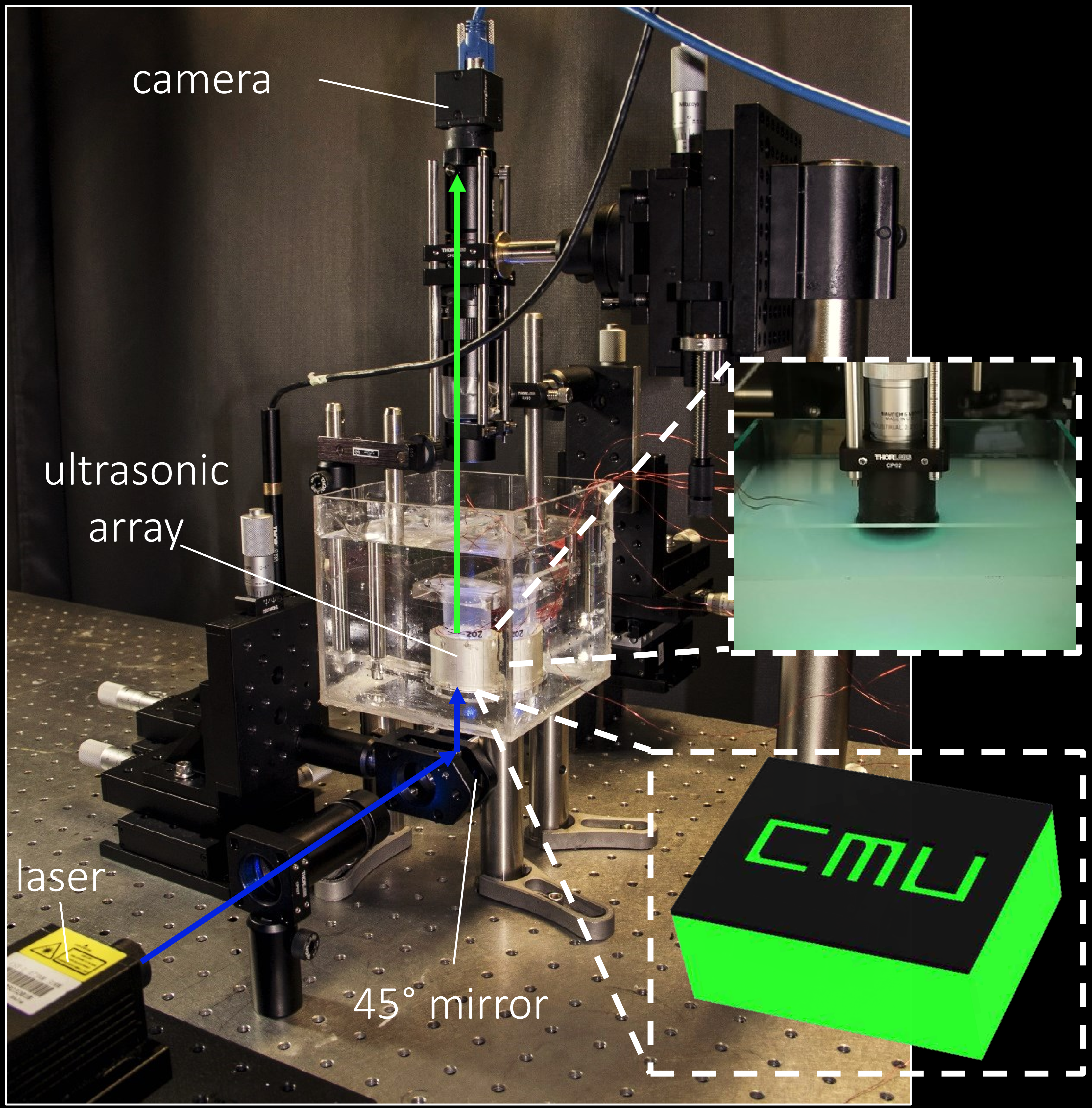

High-dimensional, highly-non-linear design problem:

- ultrasound frequency
- ultrasound voltage
- placement of transducers
- shape of waveguides
- waveform shape
- and more…

Efficiently explore using rendering

Ultrasonic light guiding inside tissue

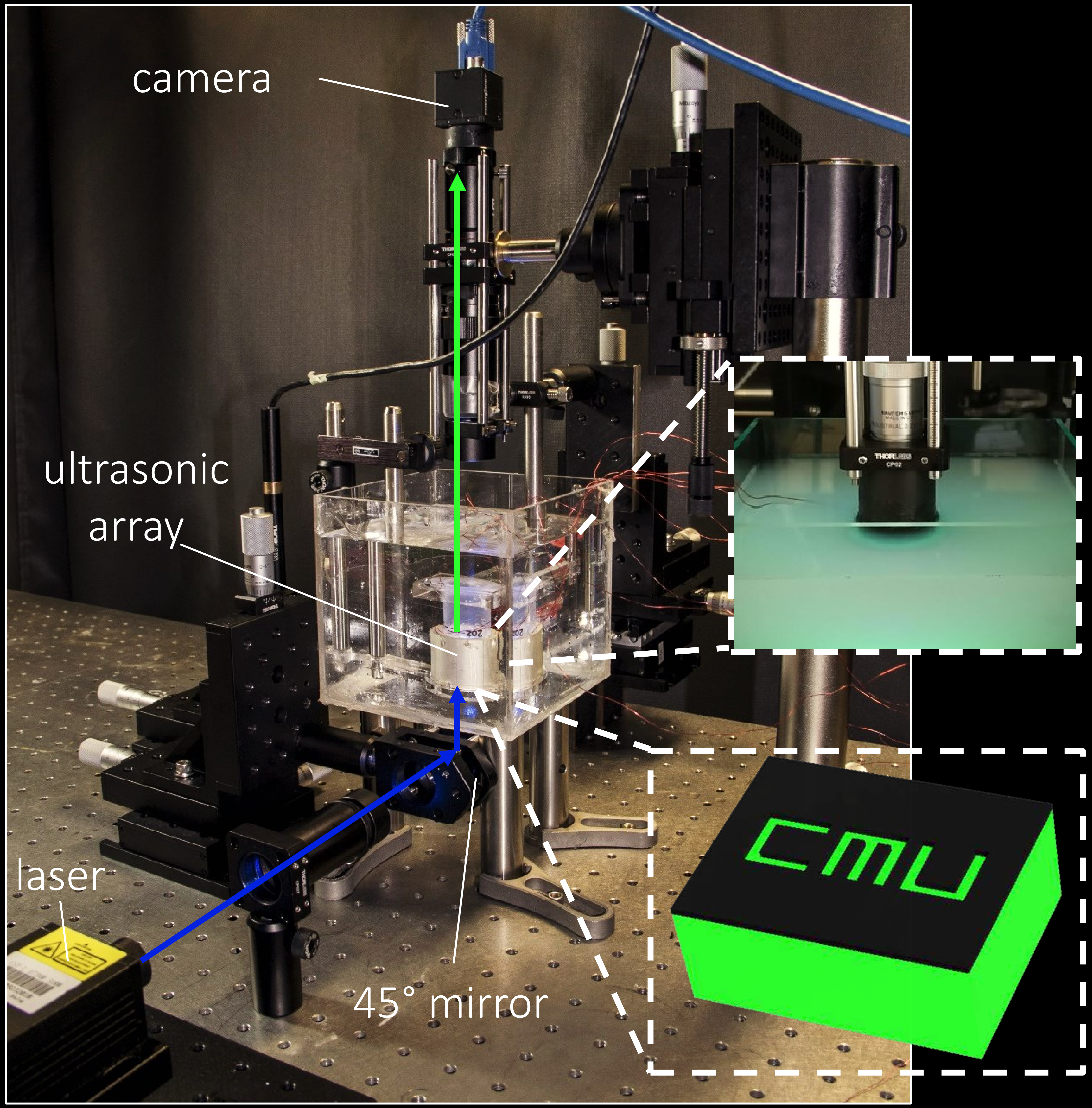

High-dimensional, highly-non-linear design problem:

- ultrasound frequency
- ultrasound voltage
- placement of transducers
- shape of waveguides
- waveform shape
- and more…

Efficiently explore using rendering

Build first rendering algorithm

Rendering continuous refraction and scattering

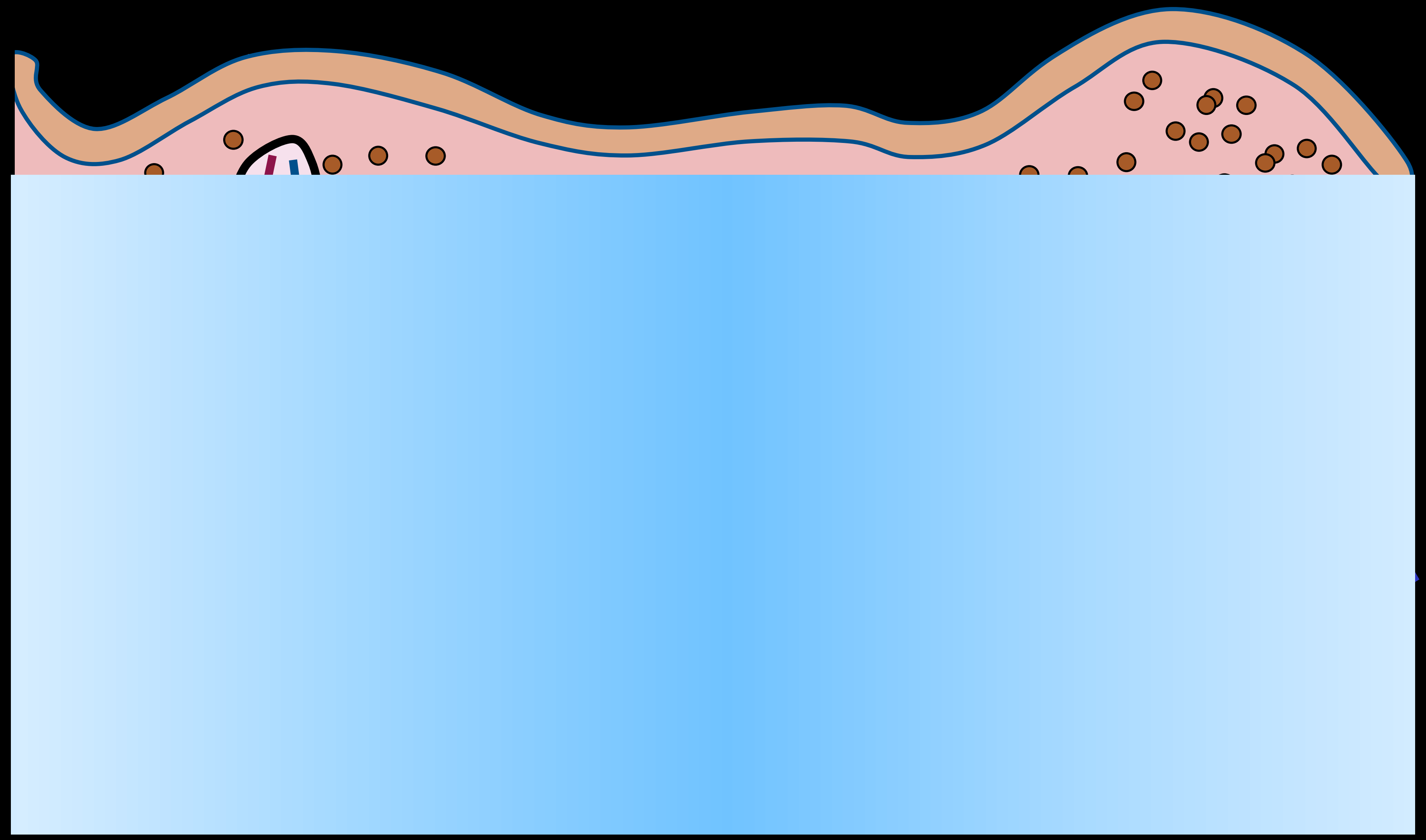

Rendering continuous refraction and scattering

continuous refraction

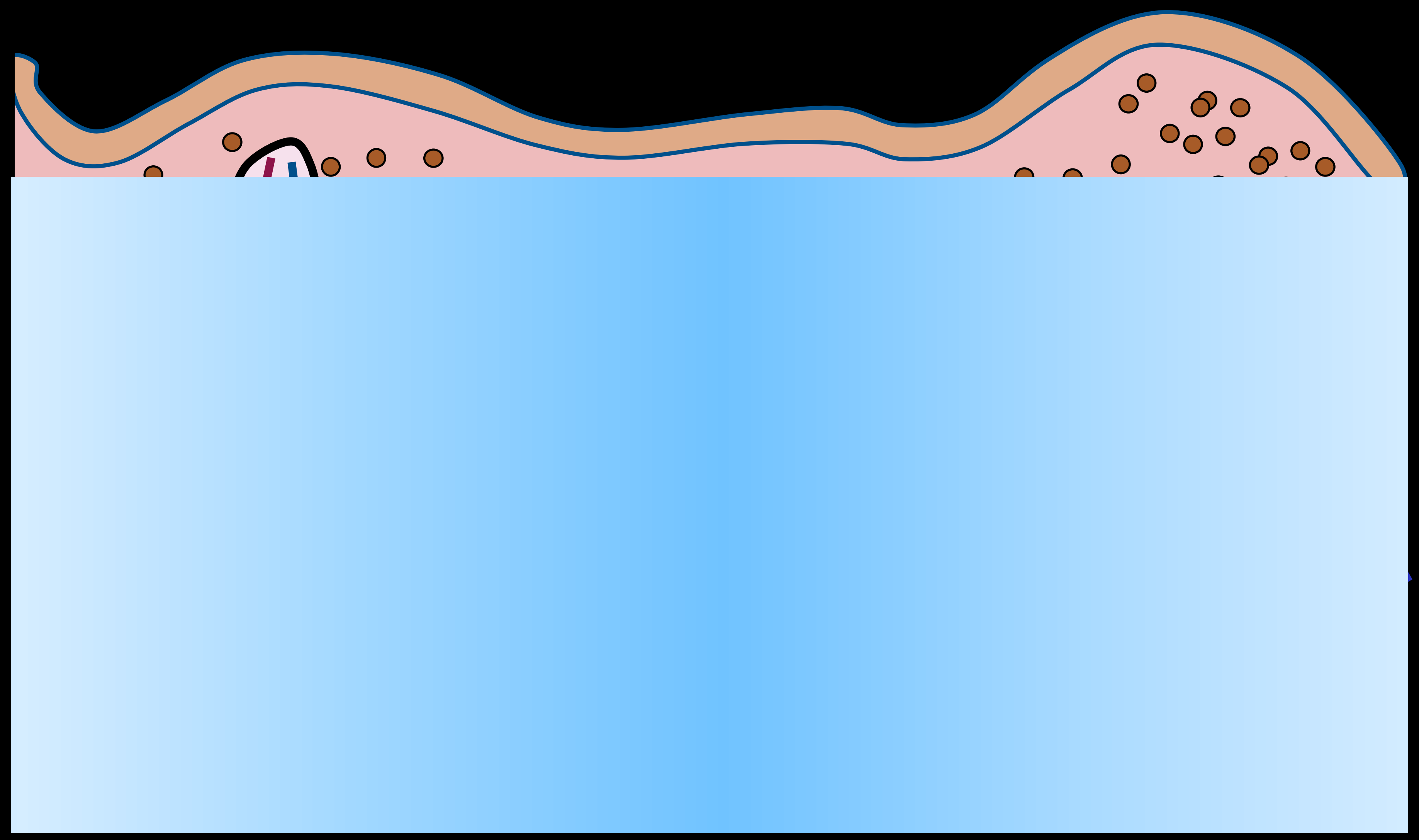

Rendering continuous refraction and scattering

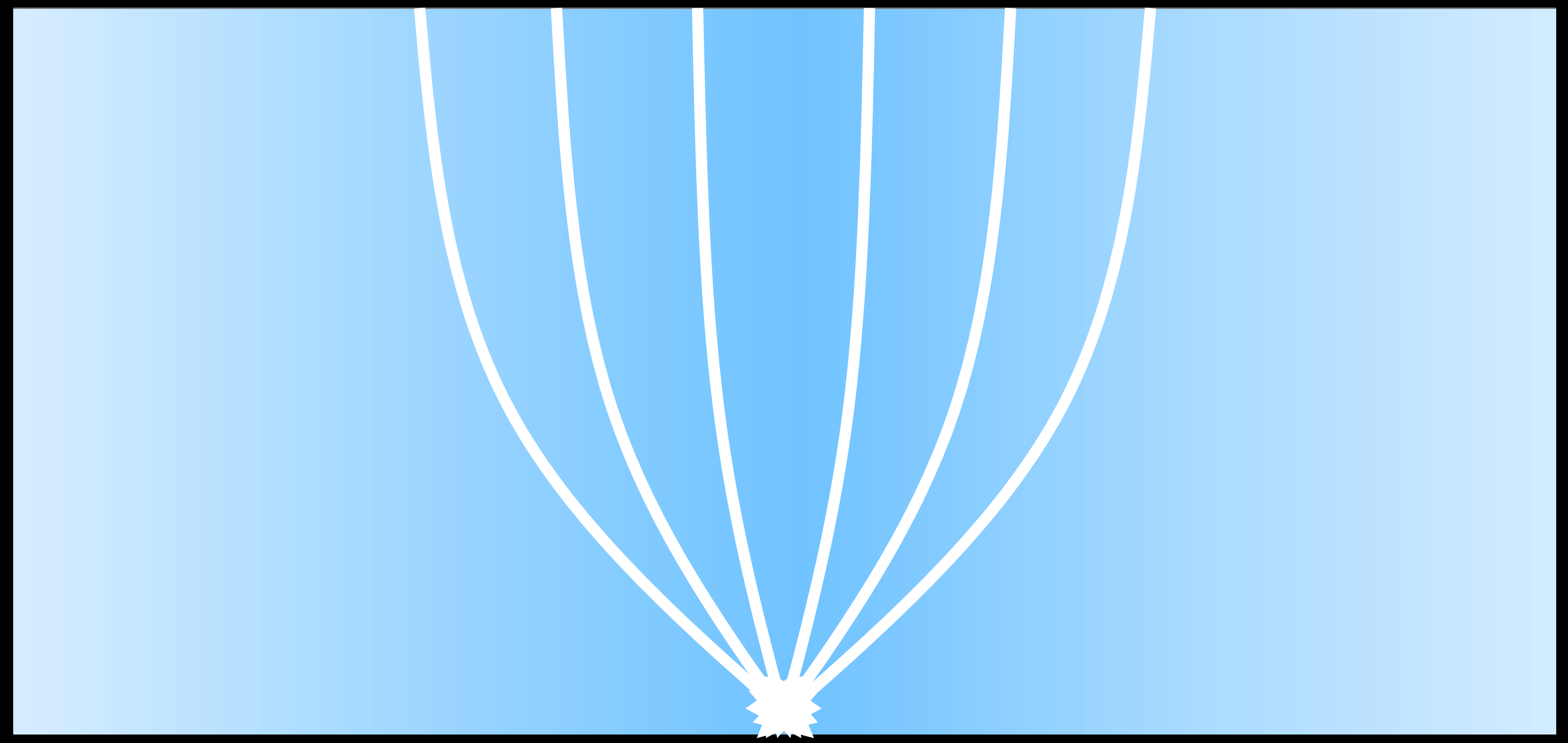

continuous refraction

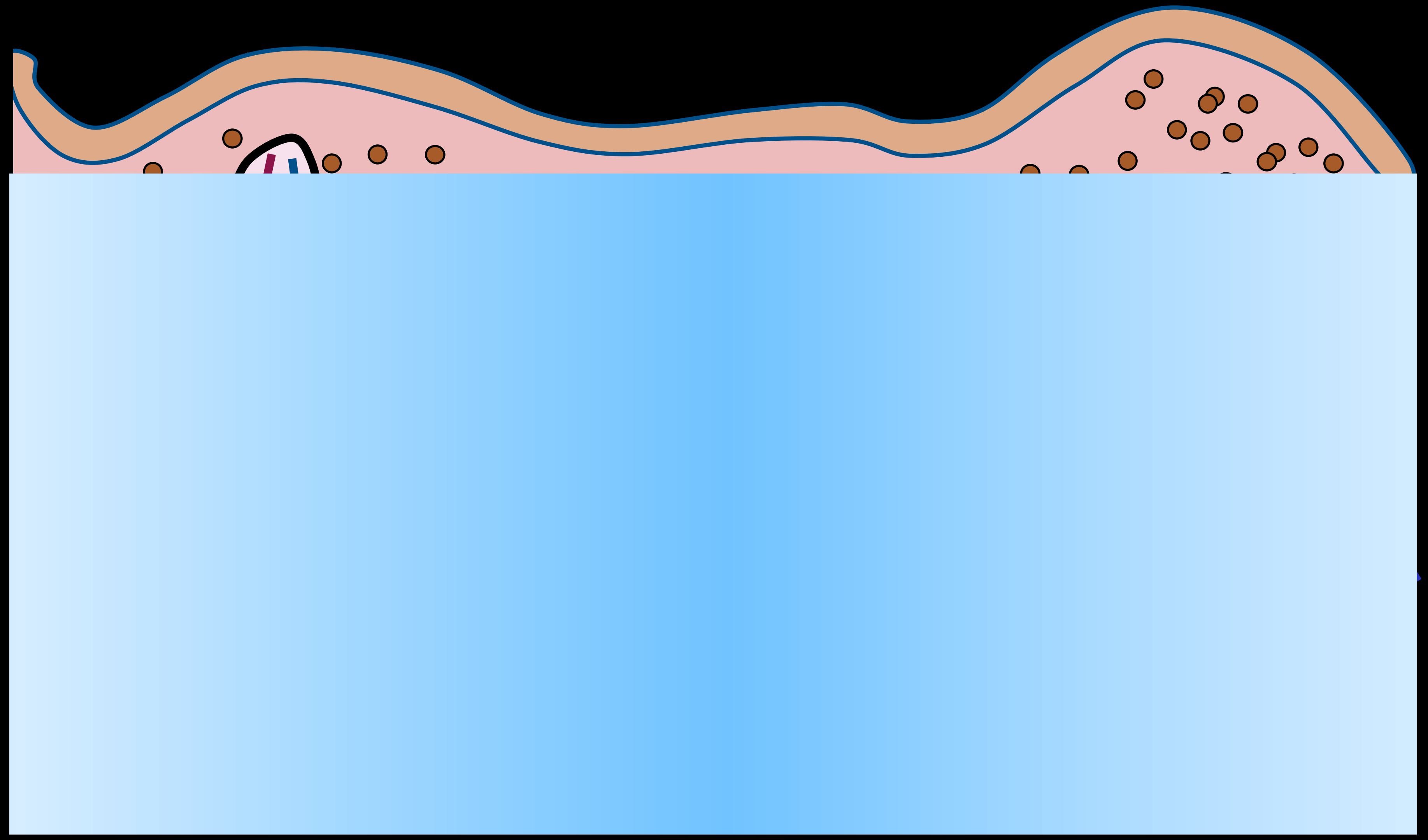

Rendering continuous refraction and scattering

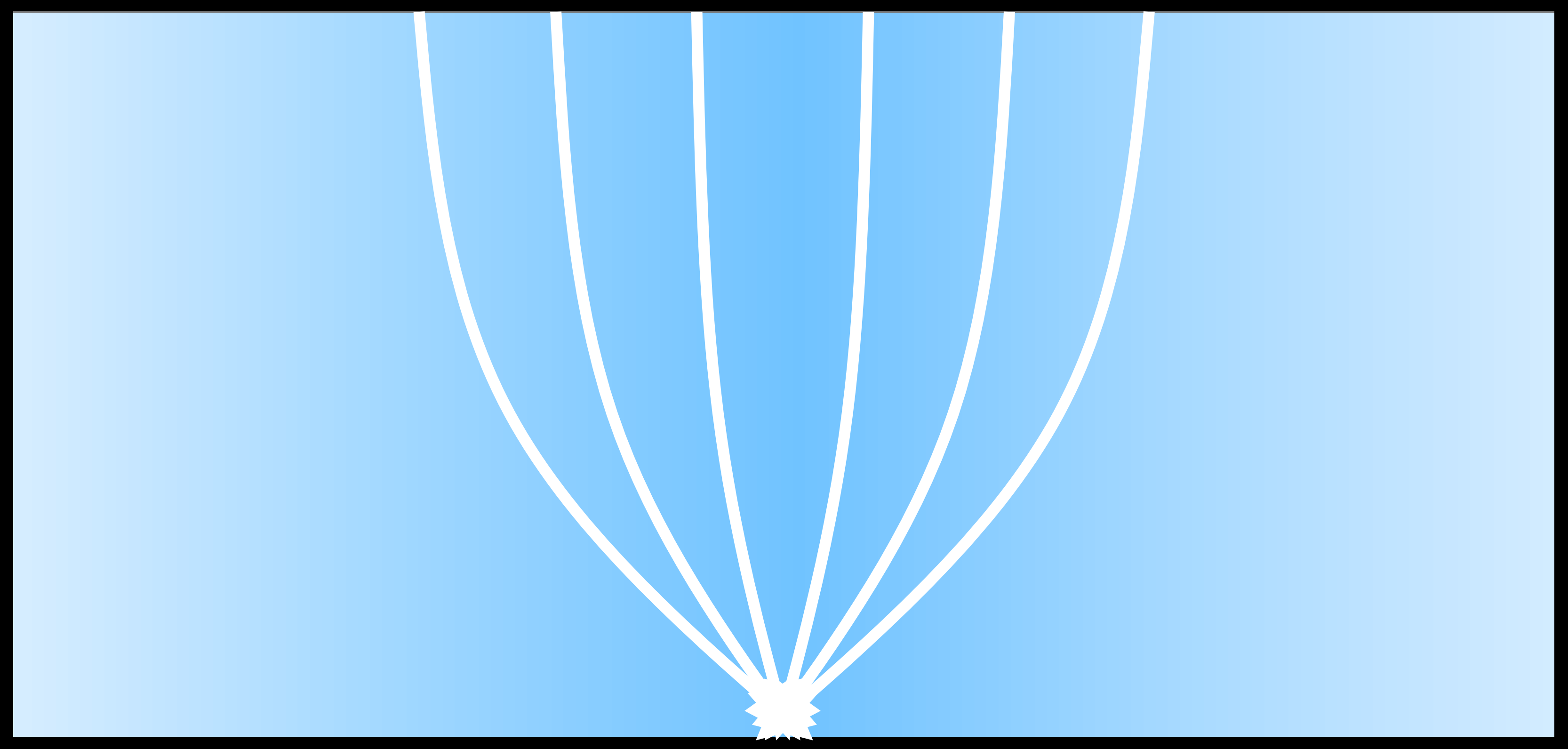

continuous refraction

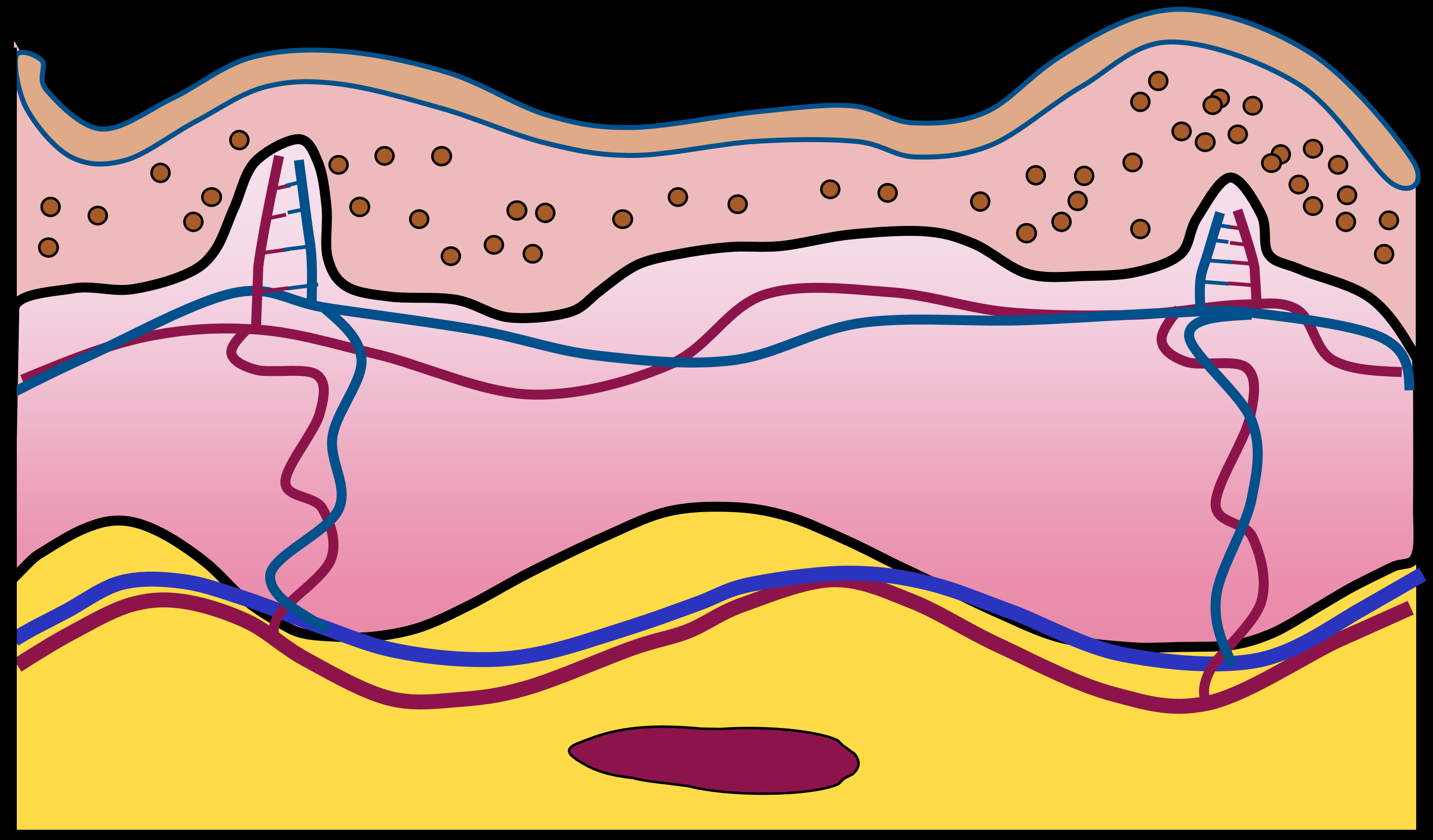

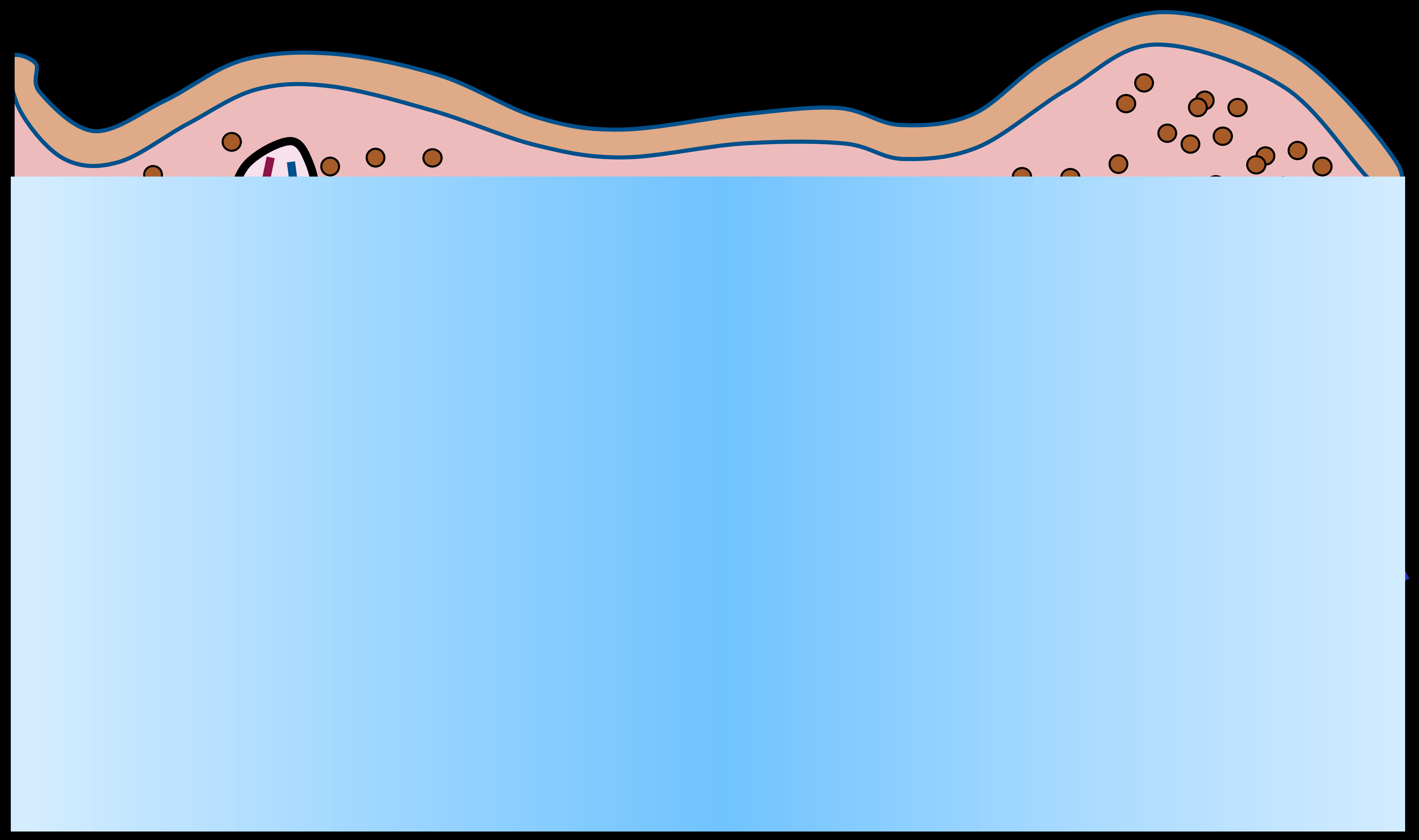

Rendering continuous refraction and scattering

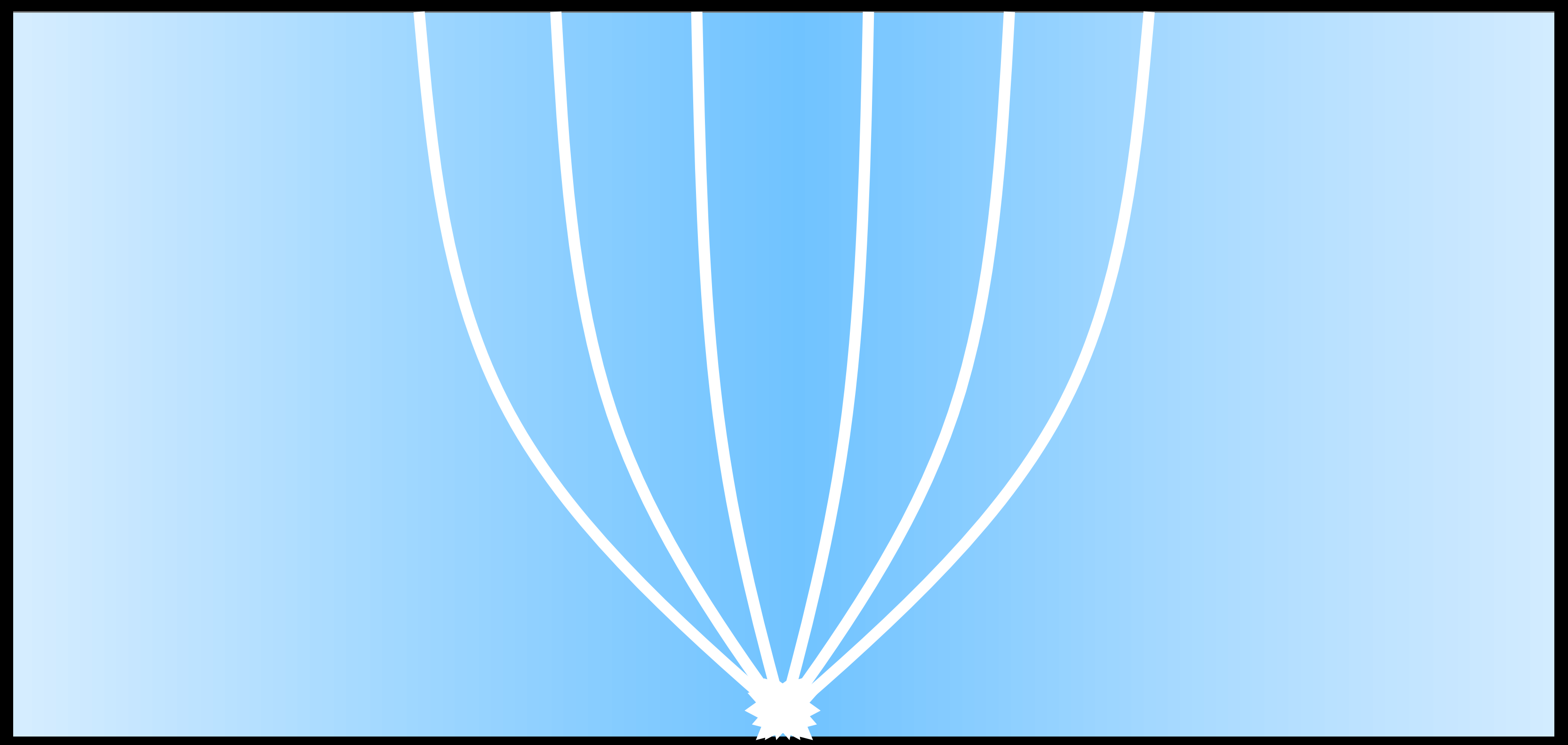

continuous refraction

+

scattering

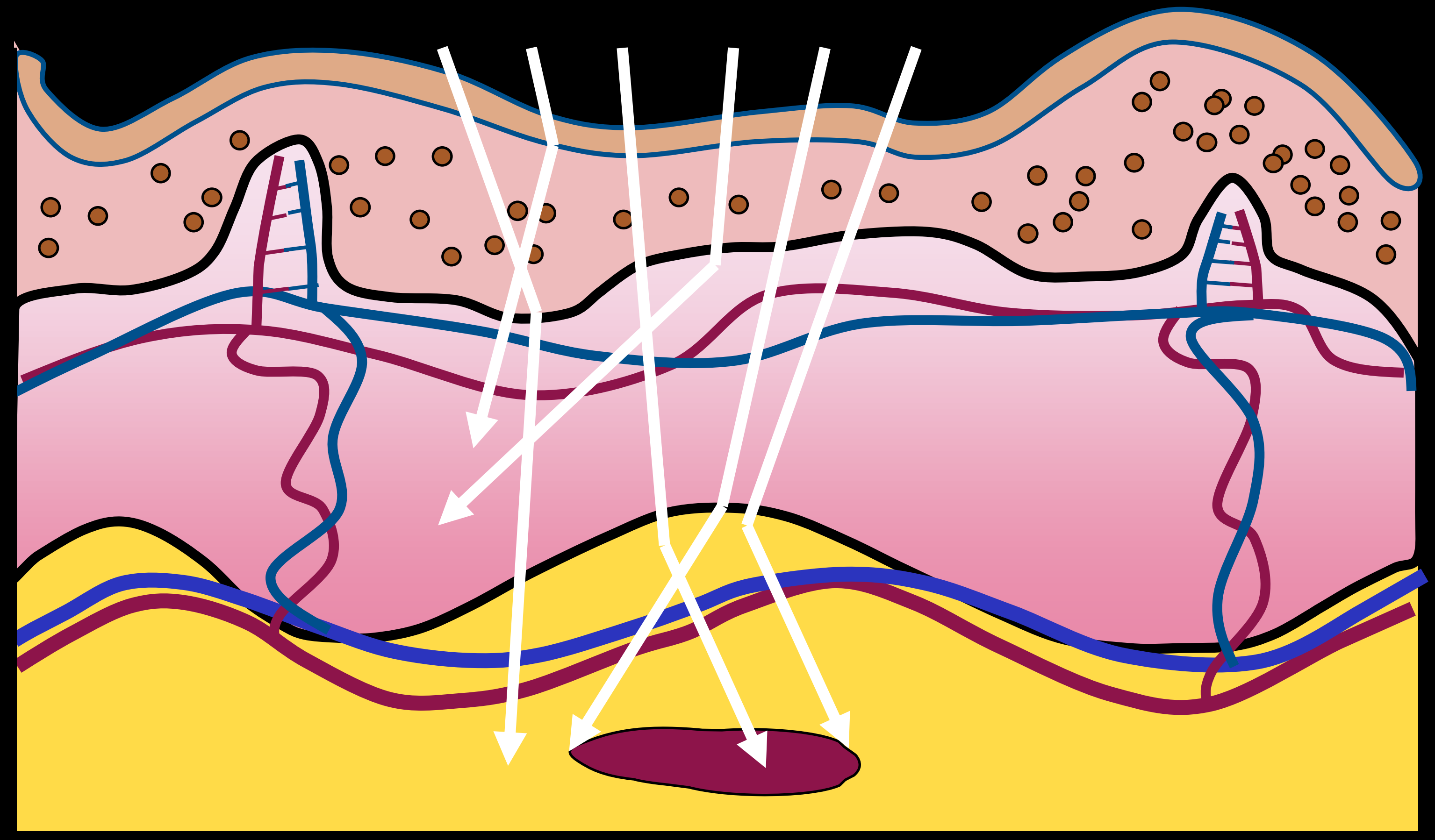

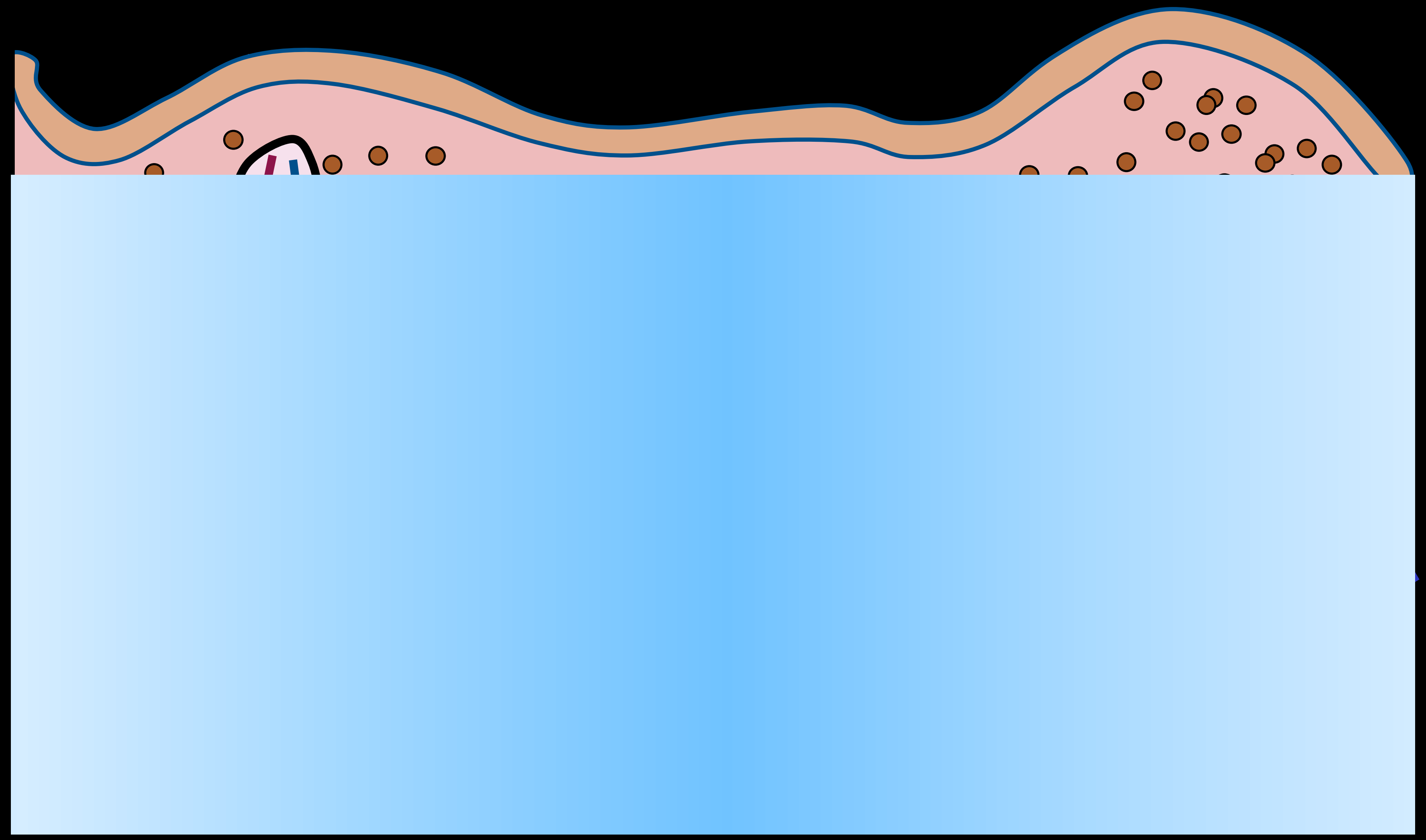

Rendering continuous refraction and scattering

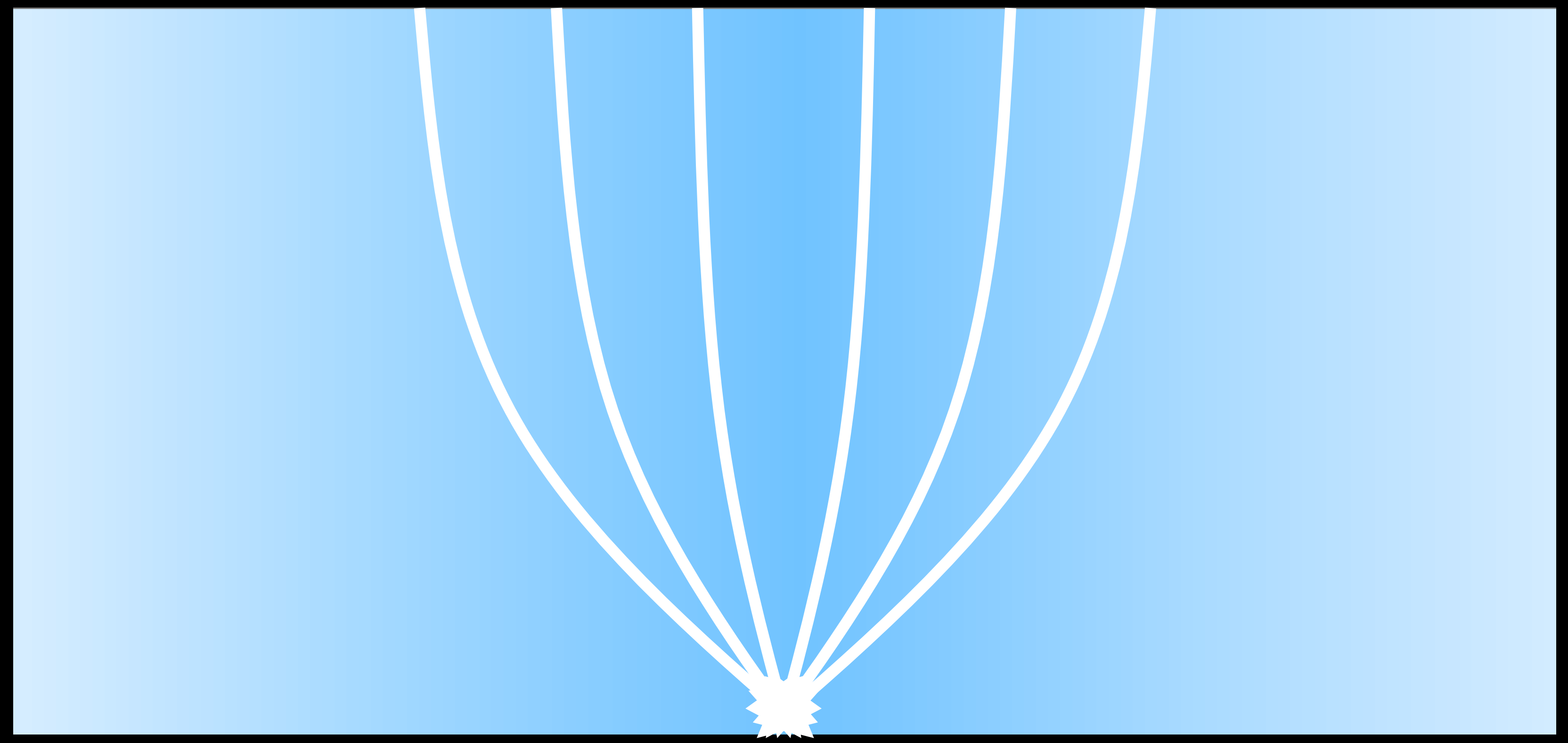

continuous refraction

+

scattering

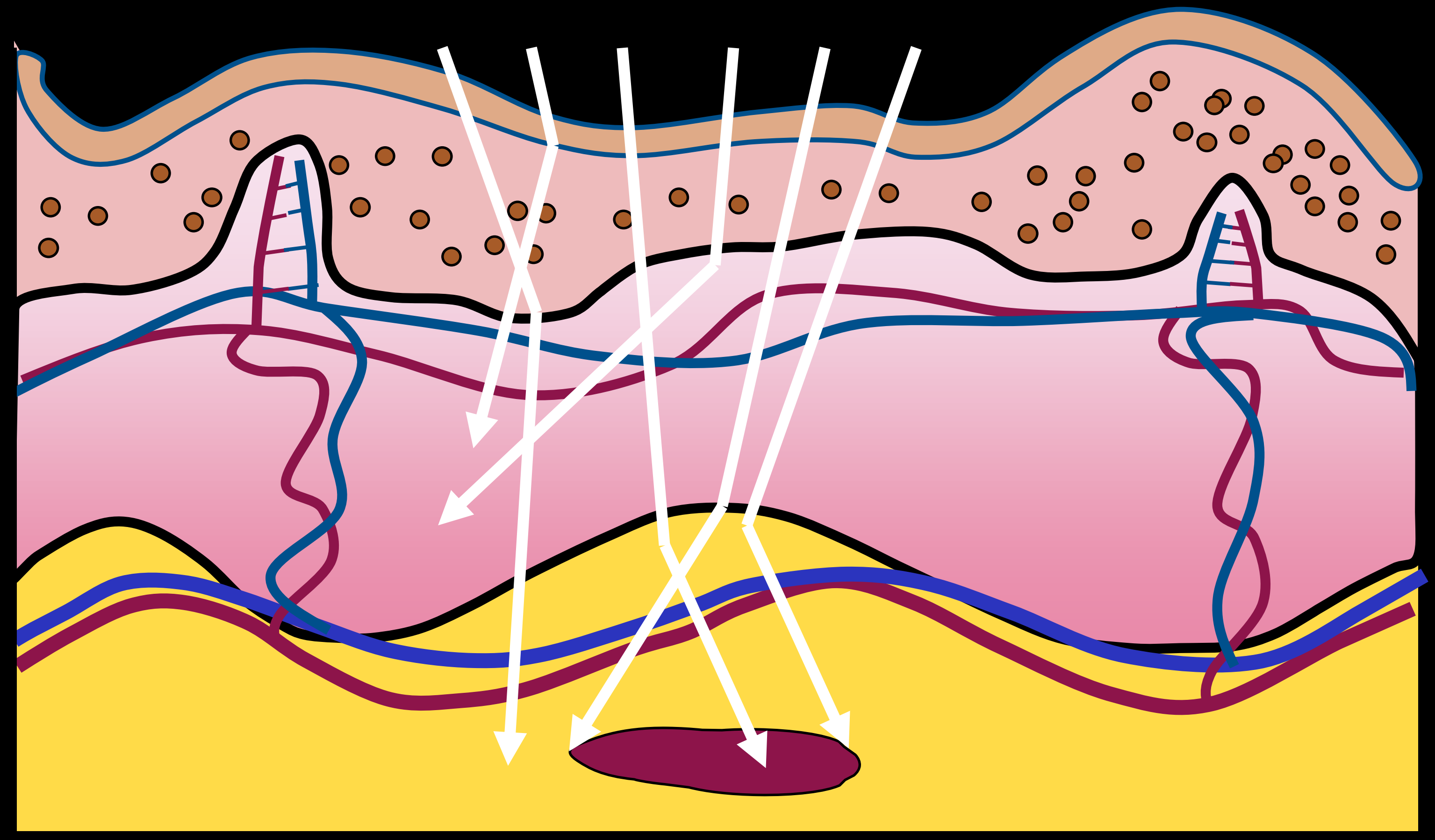

[Kravtsov and Orlov, Book, 1990]
[Gröller, Visual Comp., 1995]
[Stam and Languénou, Rend. Techn., 1996]
[Weiskopf et al., Com. Graph. forum, 2004]
[Guttirez et al., In Rend. Techn., 2005]
[Ihrke et al., ToG, 2007]
[Atcheson et al., ToG, 2008]
[Ji et al., CVPR, 2013]
[Pedrotti et al., Book, 2017]
[Scopelliti et al., Nature LSA, 2019]

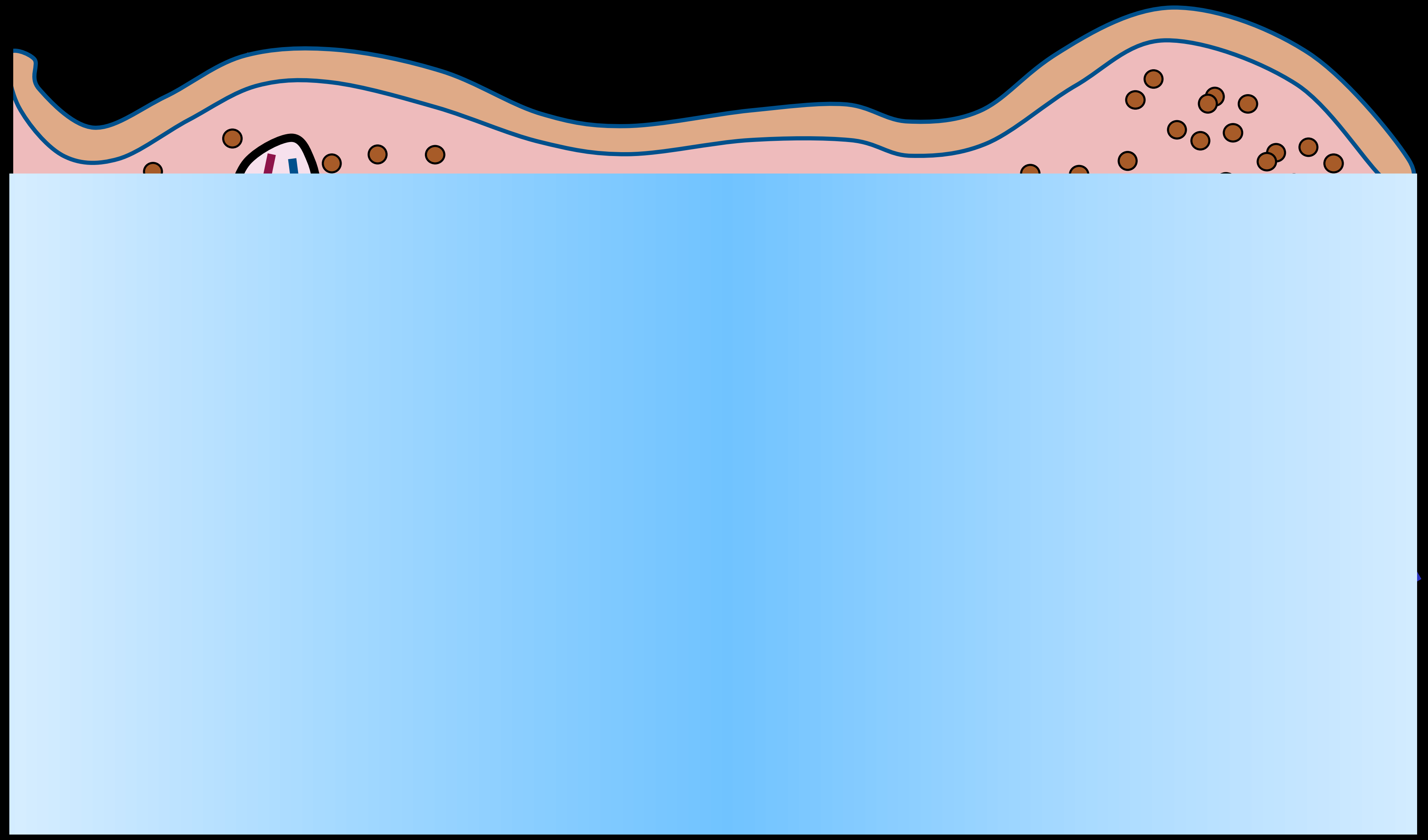

[Chandrasekhar, book, 1960]
[Lenoble, book, 1985]
[Lafortune and Willems, 1996]
[Cammarano and Jensen, 2002]
[Guttirez et al., Com. and Graph. 2006]
[Jarosz et al., Comp. Graph. forum, 2008]
[Jakob et al. ,ToG, 2010]
[Jarosz et al., ToG, 2011]
[Pediredla et al., JBO, 2016]
[Novak et al., Comp. Graph. forum, 2018]
[Bitterli et al., ToG, 2018]

Rendering continuous refraction ~~and scattering~~

[Kravtsov and Orlov, Book, 1990]
[Gröller, Visual Comp., 1995]
[Stam and Languénou, Rend. Techn., 1996]
[Weiskopf et al., Com. Graph. forum, 2004]
[Guttirez et al., In Rend. Techn., 2005]
[Ihrke et al., ToG, 2007]
[Atcheson et al., ToG, 2008]
[Ji et al., CVPR, 2013]
[Pedrotti et al., Book, 2017]
[Scopelliti et al., Nature LSA, 2019]

Rendering continuous refraction ~~and scattering~~

[Kravtsov and Orlov, Book, 1990]
[Gröller, Visual Comp., 1995]
[Stam and Languénou, Rend. Techn., 1996]
[Weiskopf et al., Com. Graph. forum, 2004]
[Guttirez et al., In Rend. Techn., 2005]
[Ihrke et al., ToG, 2007]
[Atcheson et al., ToG, 2008]
[Ji et al., CVPR, 2013]
[Pedrotti et al., Book, 2017]
[Scopelliti et al., Nature LSA, 2019]

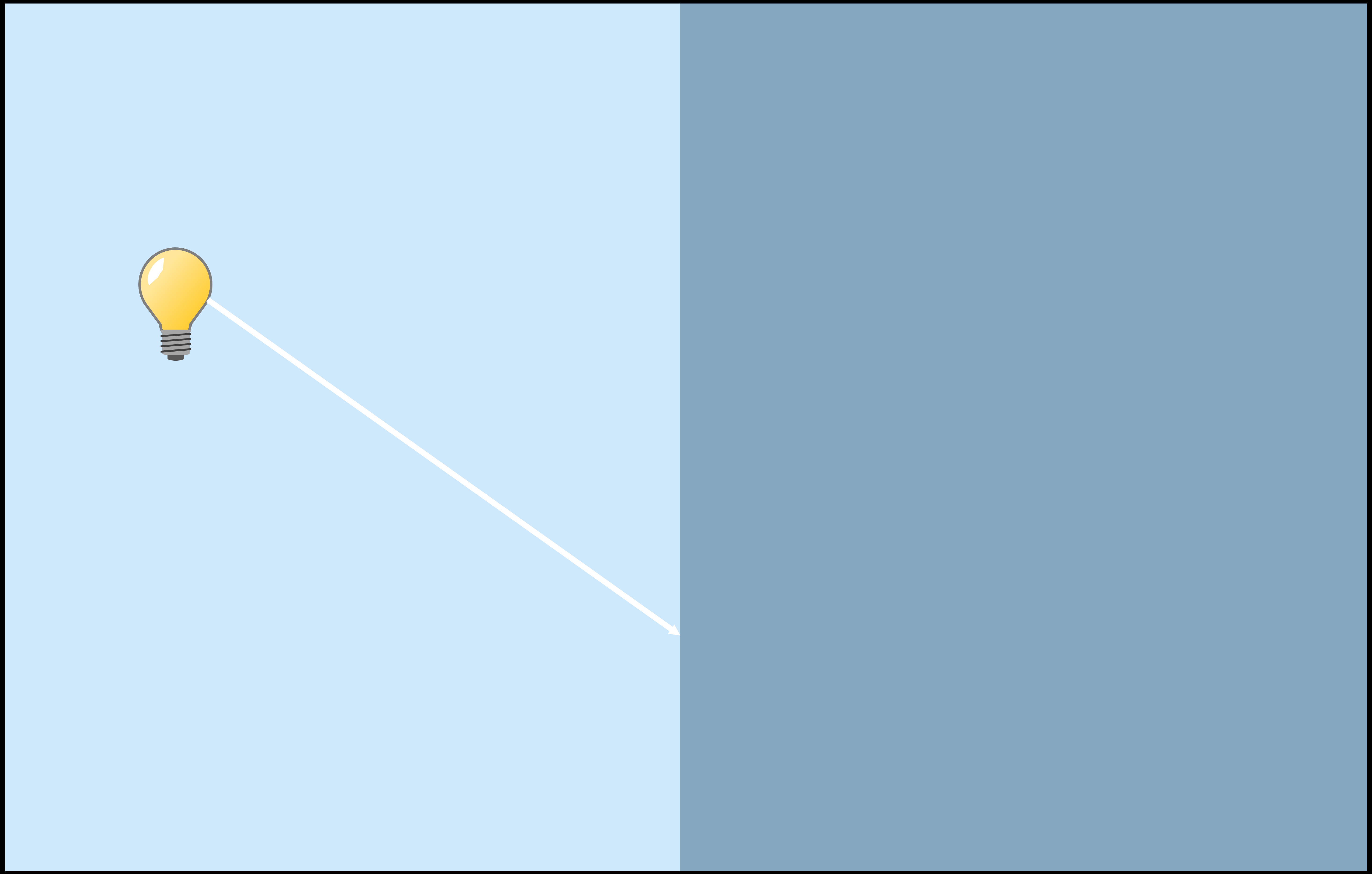

Rendering continuous refraction ~~and scattering~~

[Kravtsov and Orlov, Book, 1990]
[Gröller, Visual Comp., 1995]
[Stam and Languénou, Rend. Techn., 1996]
[Weiskopf et al., Com. Graph. forum, 2004]
[Guttirez et al., In Rend. Techn., 2005]
[Ihrke et al., ToG, 2007]
[Atcheson et al., ToG, 2008]
[Ji et al., CVPR, 2013]
[Pedrotti et al., Book, 2017]
[Scopelliti et al., Nature LSA, 2019]

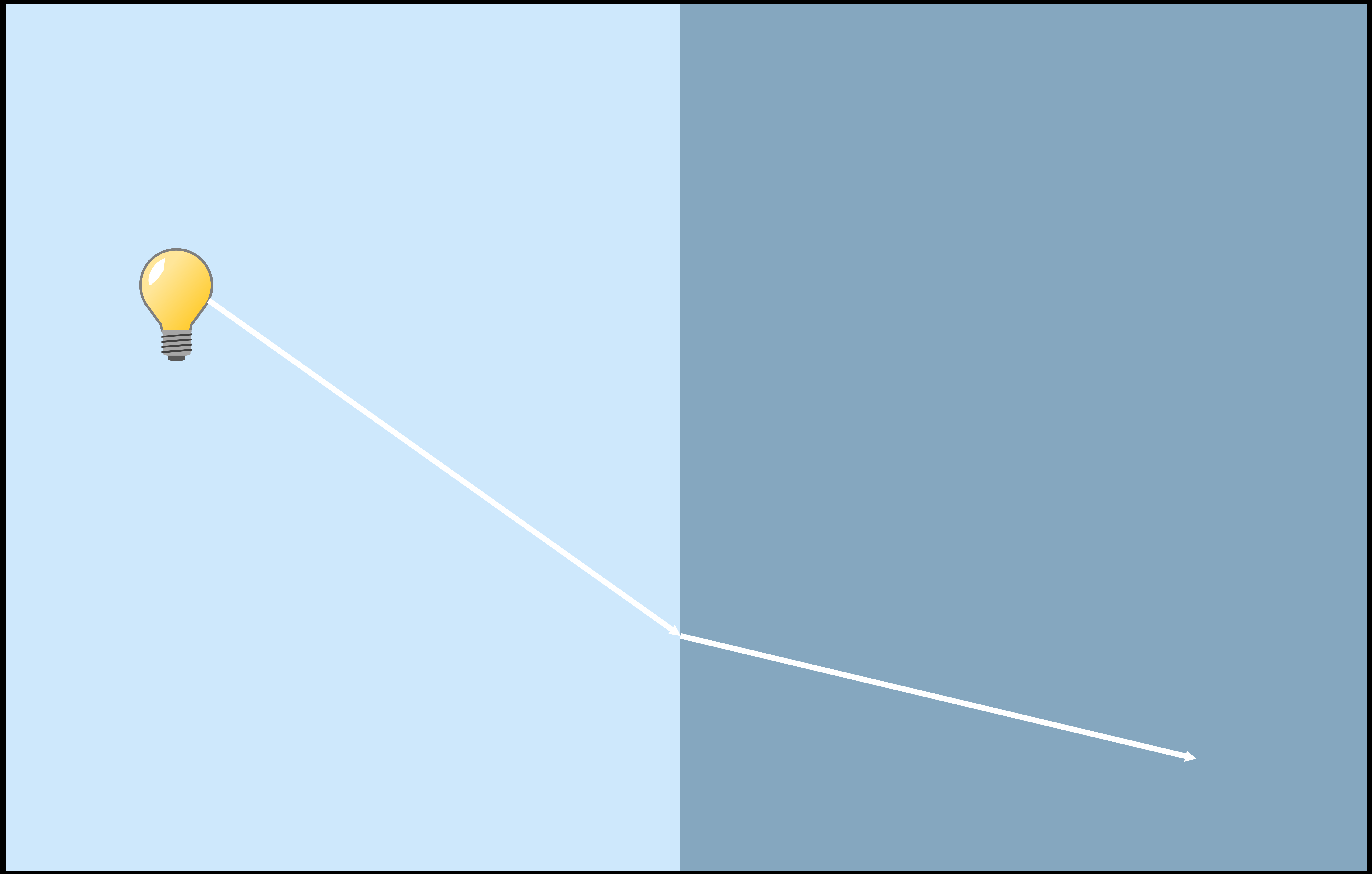

Rendering continuous refraction ~~and scattering~~

Snell's law

[Kravtsov and Orlov, Book, 1990]
[Gröller, Visual Comp., 1995]
[Stam and Languénou, Rend. Techn., 1996]
[Weiskopf et al., Com. Graph. forum, 2004]
[Guttirez et al., In Rend. Techn., 2005]
[Ihrke et al., ToG, 2007]
[Atcheson et al., ToG, 2008]
[Ji et al., CVPR, 2013]
[Pedrotti et al., Book, 2017]
[Scopelliti et al., Nature LSA, 2019]

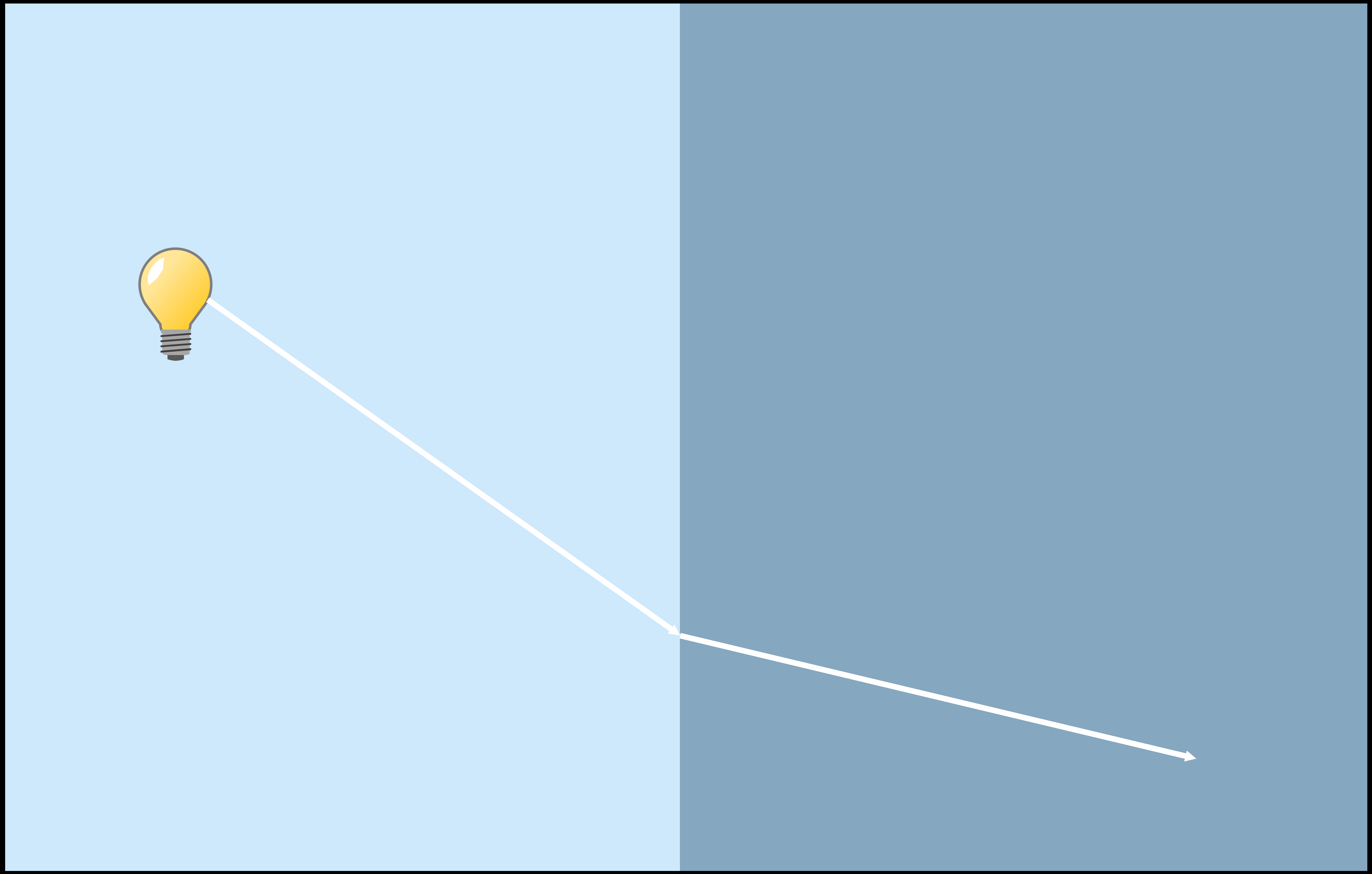

Rendering continuous refraction ~~and scattering~~

Snell's law

[Kravtsov and Orlov, Book, 1990]
[Gröller, Visual Comp., 1995]
[Stam and Languénou, Rend. Techn., 1996]
[Weiskopf et al., Com. Graph. forum, 2004]
[Guttirez et al., In Rend. Techn., 2005]
[Ihrke et al., ToG, 2007]
[Atcheson et al., ToG, 2008]
[Ji et al., CVPR, 2013]
[Pedrotti et al., Book, 2017]
[Scopelliti et al., Nature LSA, 2019]

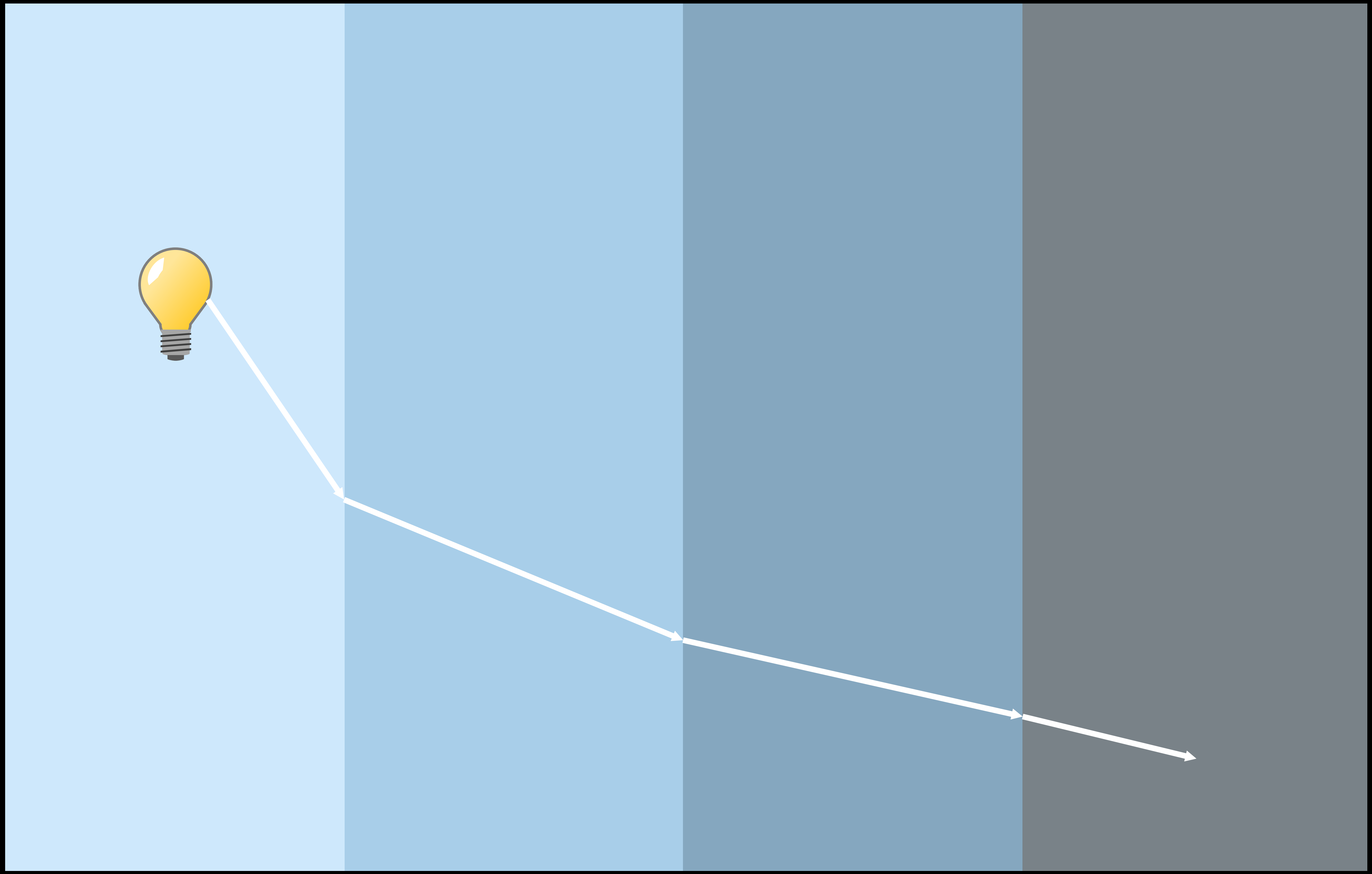

Rendering continuous refraction ~~and scattering~~

Snell's law

[Kravtsov and Orlov, Book, 1990]
[Gröller, Visual Comp., 1995]
[Stam and Languénou, Rend. Techn., 1996]
[Weiskopf et al., Com. Graph. forum, 2004]
[Guttirez et al., In Rend. Techn., 2005]
[Ihrke et al., ToG, 2007]
[Atcheson et al., ToG, 2008]
[Ji et al., CVPR, 2013]
[Pedrotti et al., Book, 2017]
[Scopelliti et al., Nature LSA, 2019]

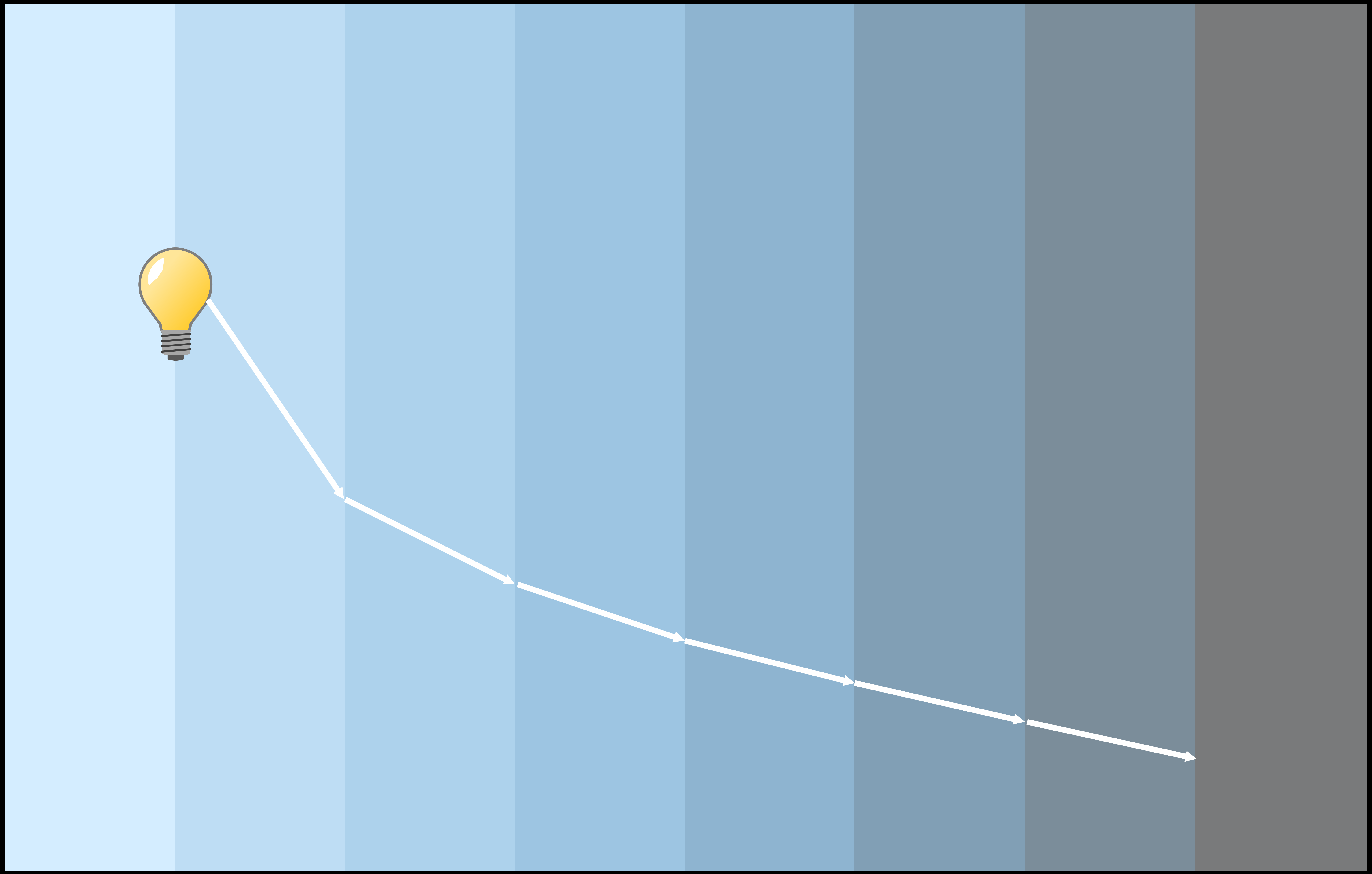

Rendering continuous refraction ~~and scattering~~

Snell's law

[Kravtsov and Orlov, Book, 1990]
[Gröller, Visual Comp., 1995]
[Stam and Languénou, Rend. Techn., 1996]
[Weiskopf et al., Com. Graph. forum, 2004]
[Guttirez et al., In Rend. Techn., 2005]
[Ihrke et al., ToG, 2007]
[Atcheson et al., ToG, 2008]
[Ji et al., CVPR, 2013]
[Pedrotti et al., Book, 2017]
[Scopelliti et al., Nature LSA, 2019]

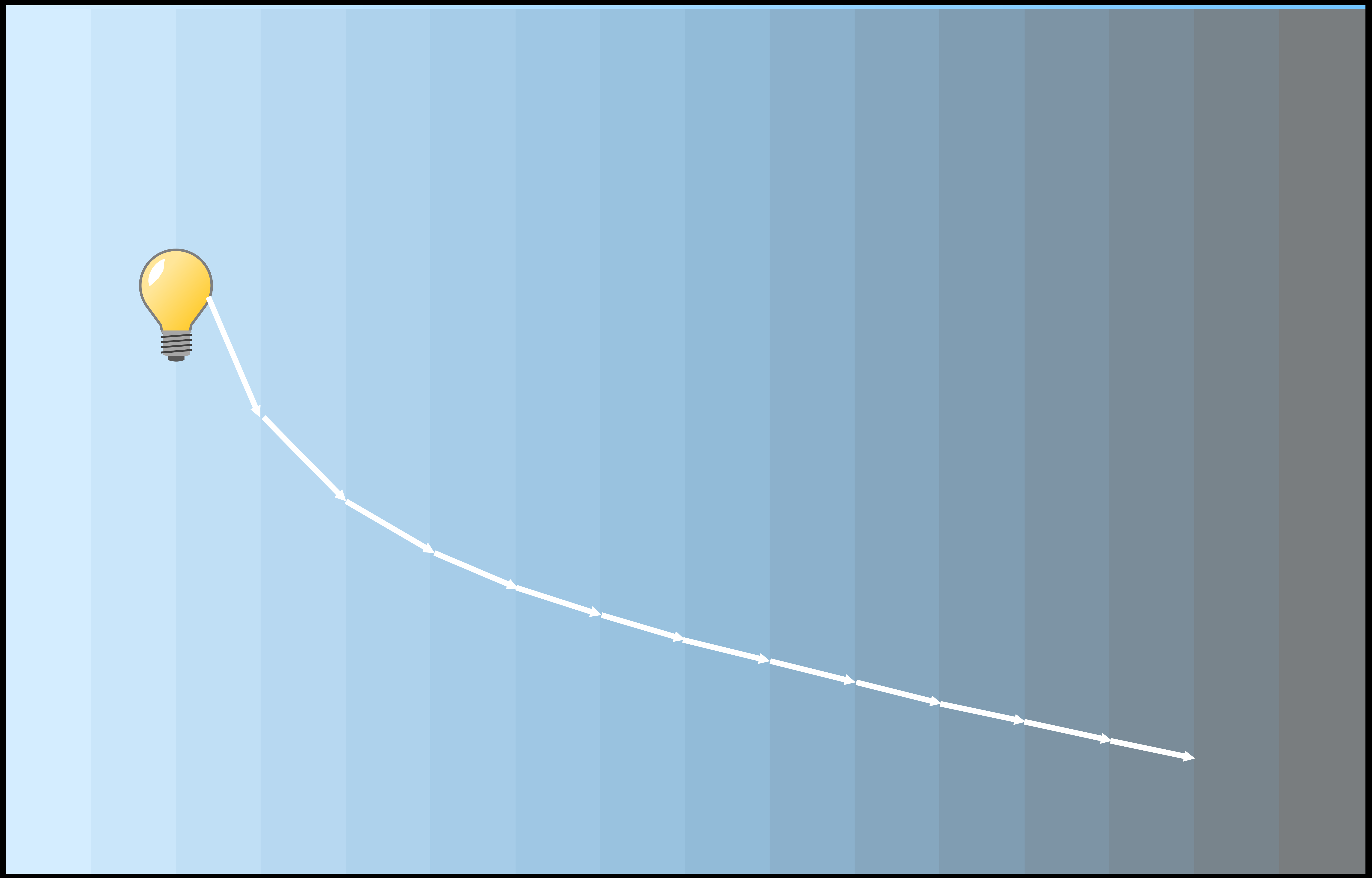

Rendering continuous refraction ~~and scattering~~

Snell’s law

[Kravtsov and Orlov, Book, 1990]
[Gröller, Visual Comp., 1995]
[Stam and Languénou, Rend. Techn., 1996]
[Weiskopf et al., Com. Graph. forum, 2004]
[Guttirez et al., In Rend. Techn., 2005]
[Ihrke et al., ToG, 2007]
[Atcheson et al., ToG, 2008]
[Ji et al., CVPR, 2013]
[Pedrotti et al., Book, 2017]
[Scopelliti et al., Nature LSA, 2019]

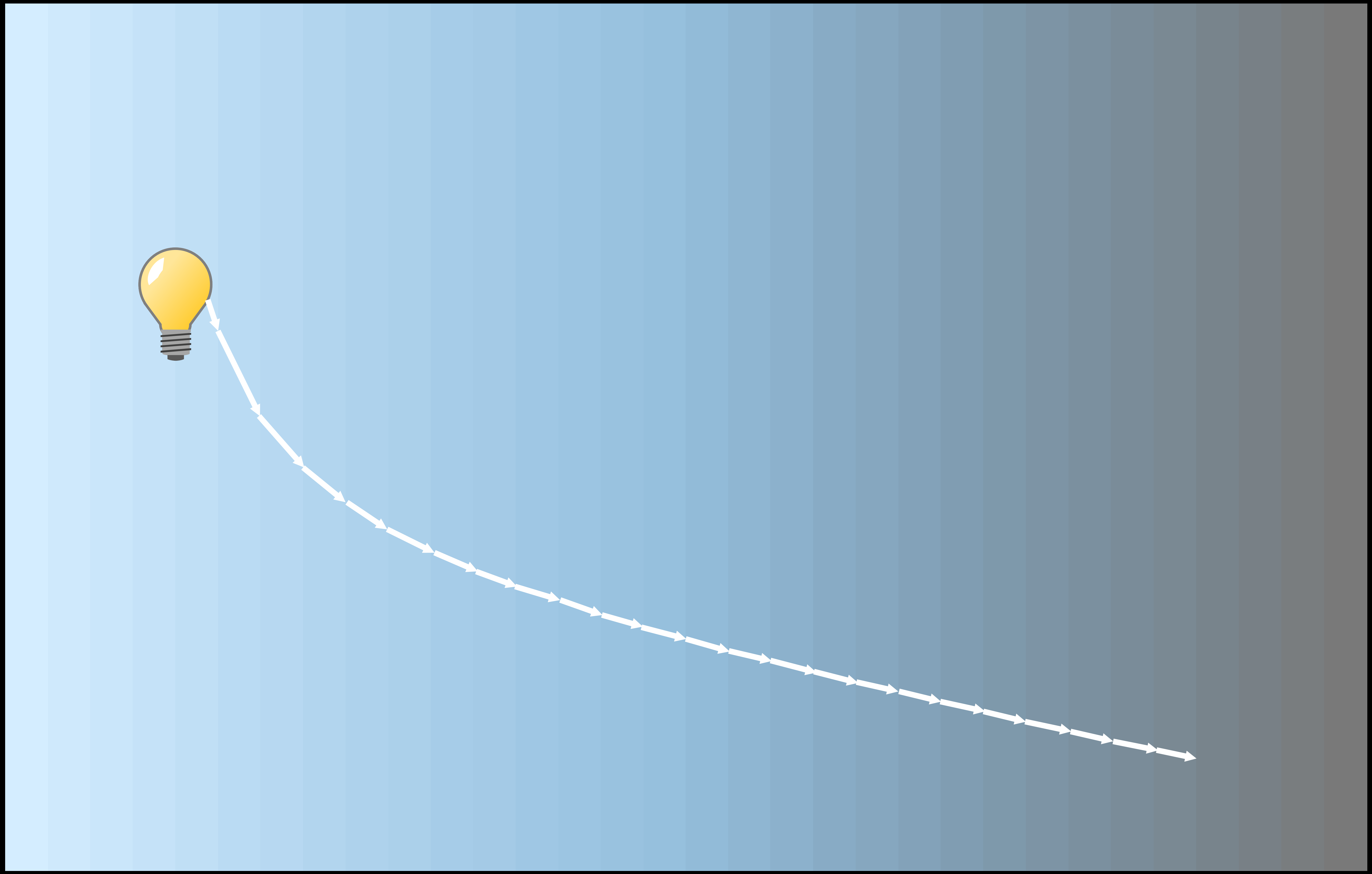

Rendering continuous refraction ~~and scattering~~

refractive ray tracing

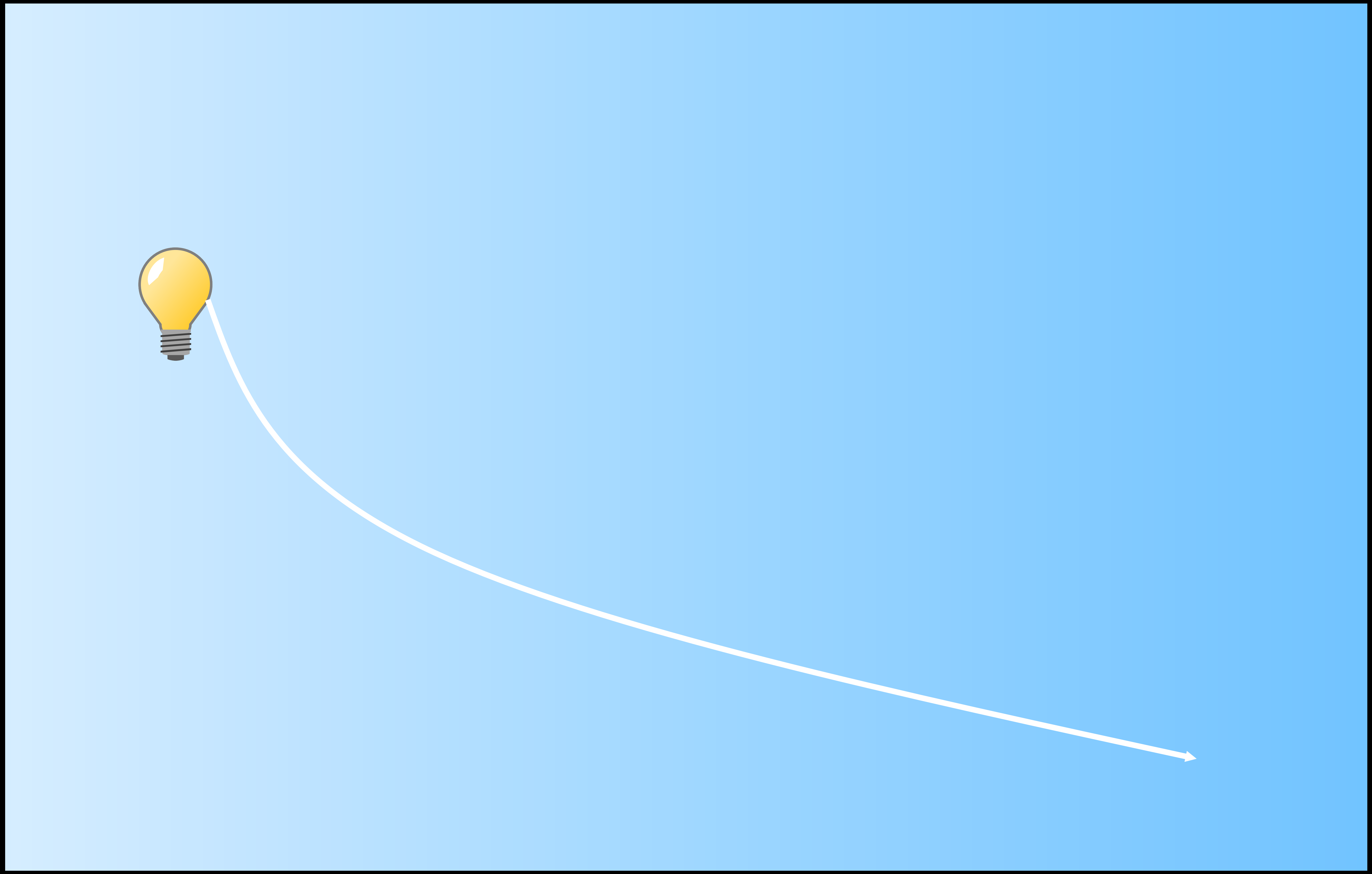

[Kravtsov and Orlov, Book, 1990]
[Gröller, Visual Comp., 1995]
[Stam and Languénou, Rend. Techn., 1996]
[Weiskopf et al., Com. Graph. forum, 2004]
[Guttirez et al., In Rend. Techn., 2005]
[Ihrke et al., ToG, 2007]
[Atcheson et al., ToG, 2008]
[Ji et al., CVPR, 2013]
[Pedrotti et al., Book, 2017]
[Scopelliti et al., Nature LSA, 2019]

Rendering continuous refraction and scattering

refractive ray tracing

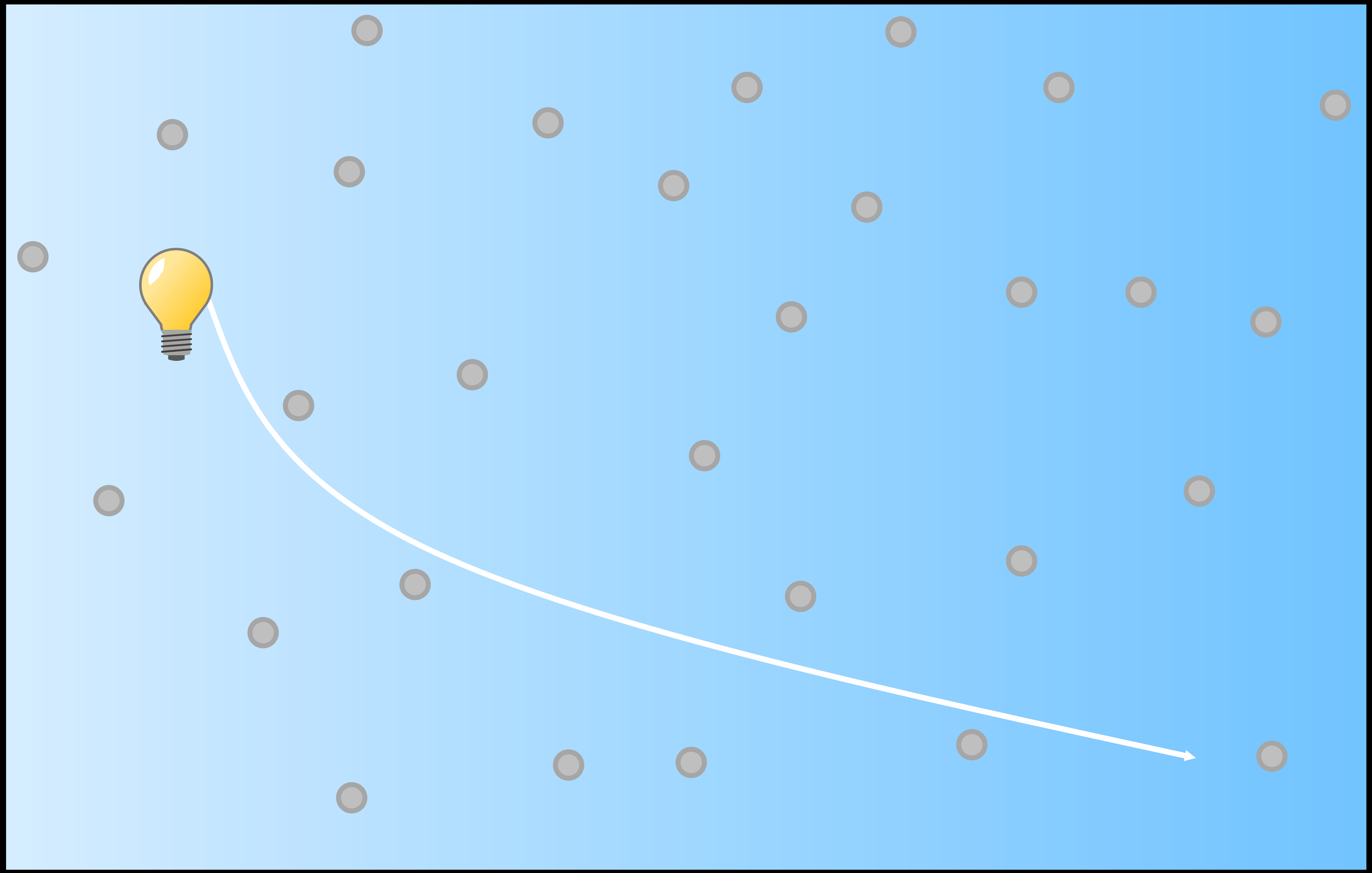

[Kravtsov and Orlov, Book, 1990]
[Gröller, Visual Comp., 1995]
[Stam and Languénou, Rend. Techn., 1996]
[Weiskopf et al., Com. Graph. forum, 2004]
[Guttirez et al., In Rend. Techn., 2005]
[Ihrke et al., ToG, 2007]
[Atcheson et al., ToG, 2008]
[Ji et al., CVPR, 2013]
[Pedrotti et al., Book, 2017]
[Scopelliti et al., Nature LSA, 2019]

Rendering continuous refraction and scattering

refractive ray tracing

[Kravtsov and Orlov, Book, 1990]
[Gröller, Visual Comp., 1995]
[Stam and Languénou, Rend. Techn., 1996]
[Weiskopf et al., Com. Graph. forum, 2004]
[Guttirez et al., In Rend. Techn., 2005]
[Ihrke et al., ToG, 2007]
[Atcheson et al., ToG, 2008]
[Ji et al., CVPR, 2013]
[Pedrotti et al., Book, 2017]
[Scopelliti et al., Nature LSA, 2019]

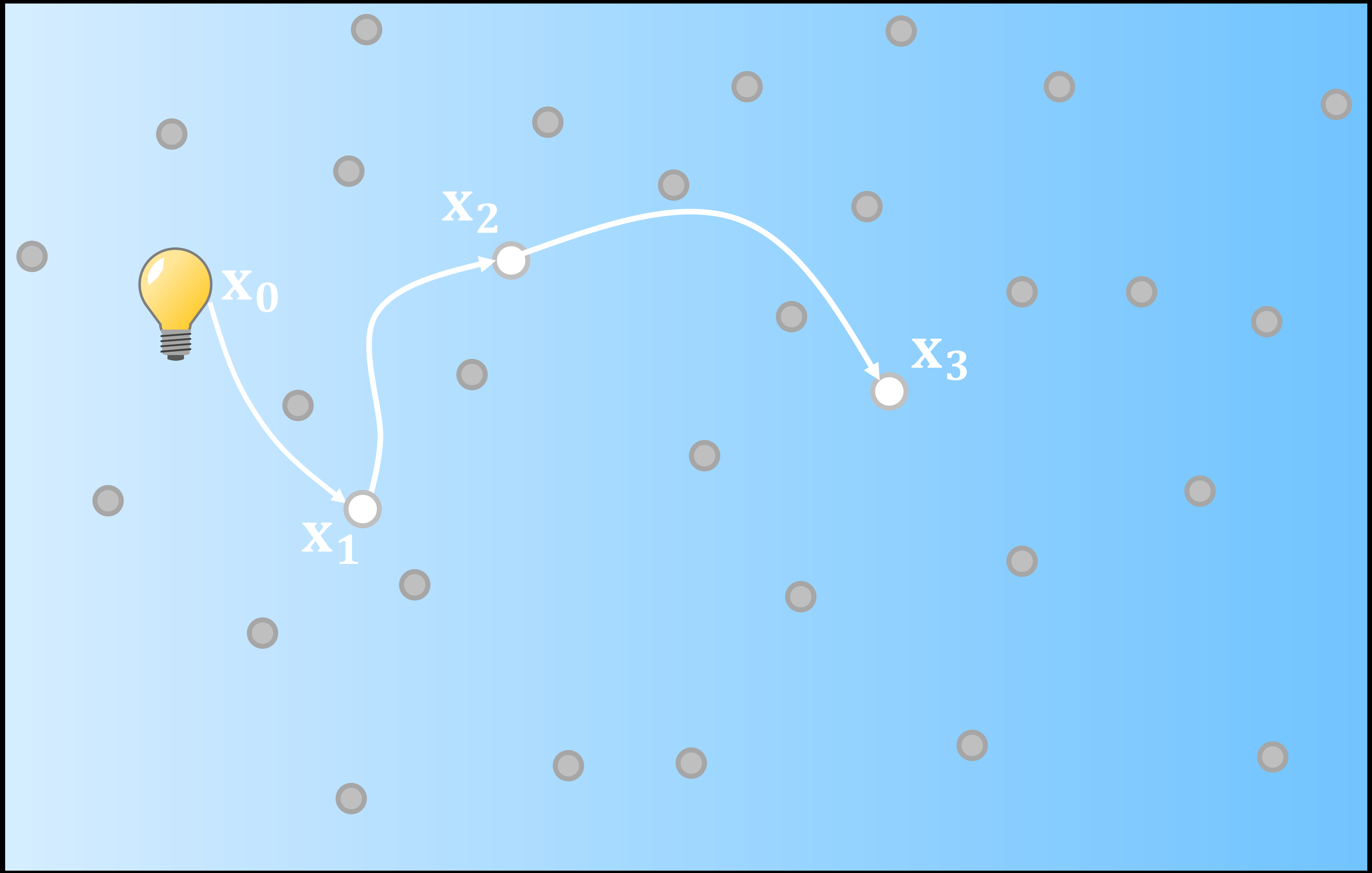

Rendering continuous refraction and scattering

refractive ray tracing

[Kravtsov and Orlov, Book, 1990]
[Gröller, Visual Comp., 1995]
[Stam and Languénou, Rend. Techn., 1996]
[Weiskopf et al., Com. Graph. forum, 2004]
[Guttirez et al., In Rend. Techn., 2005]
[Ihrke et al., ToG, 2007]
[Atcheson et al., ToG, 2008]
[Ji et al., CVPR, 2013]
[Pedrotti et al., Book, 2017]
[Scopelliti et al., Nature LSA, 2019]

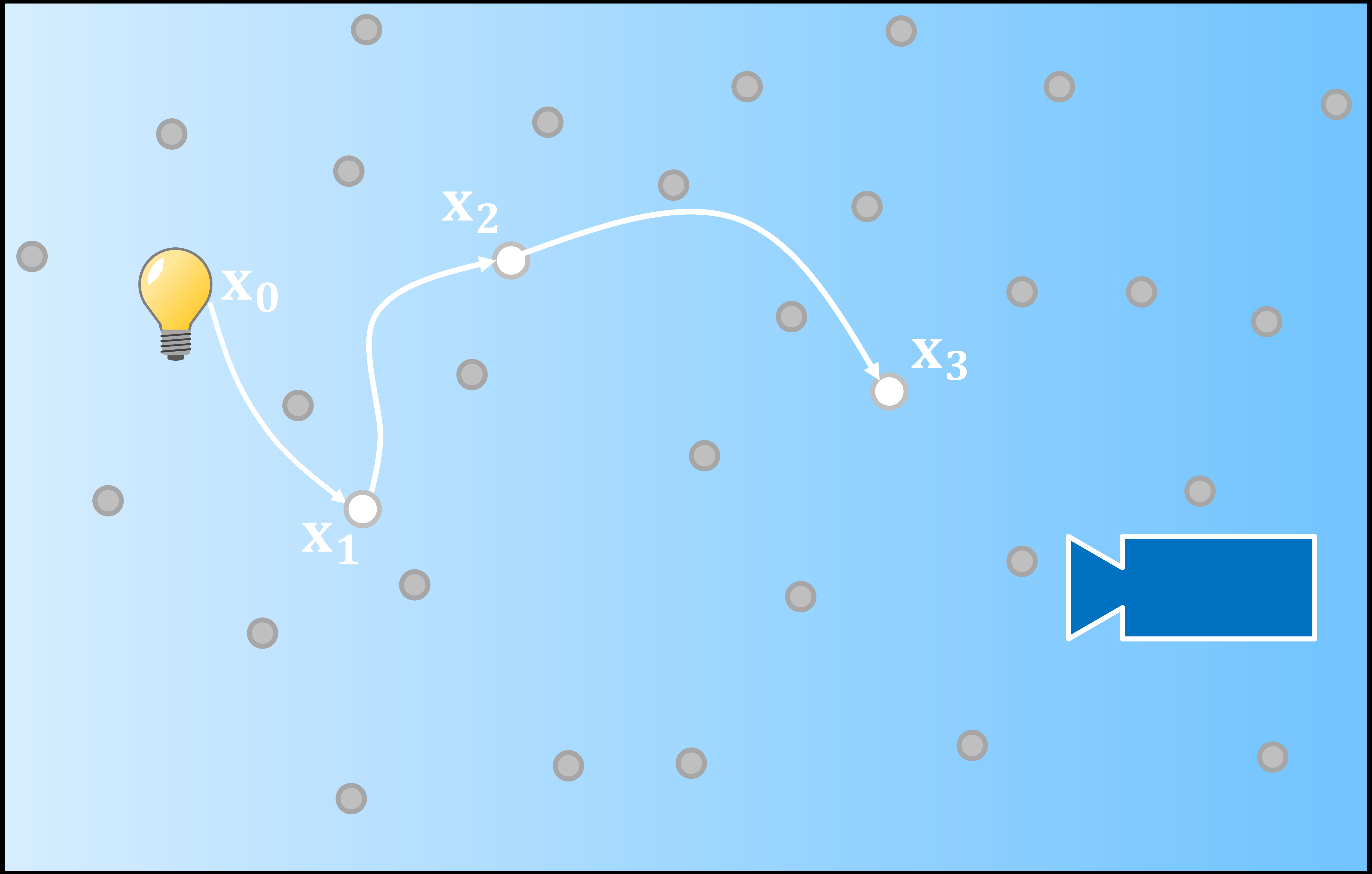

Rendering continuous refraction and scattering

radiative transfer equation

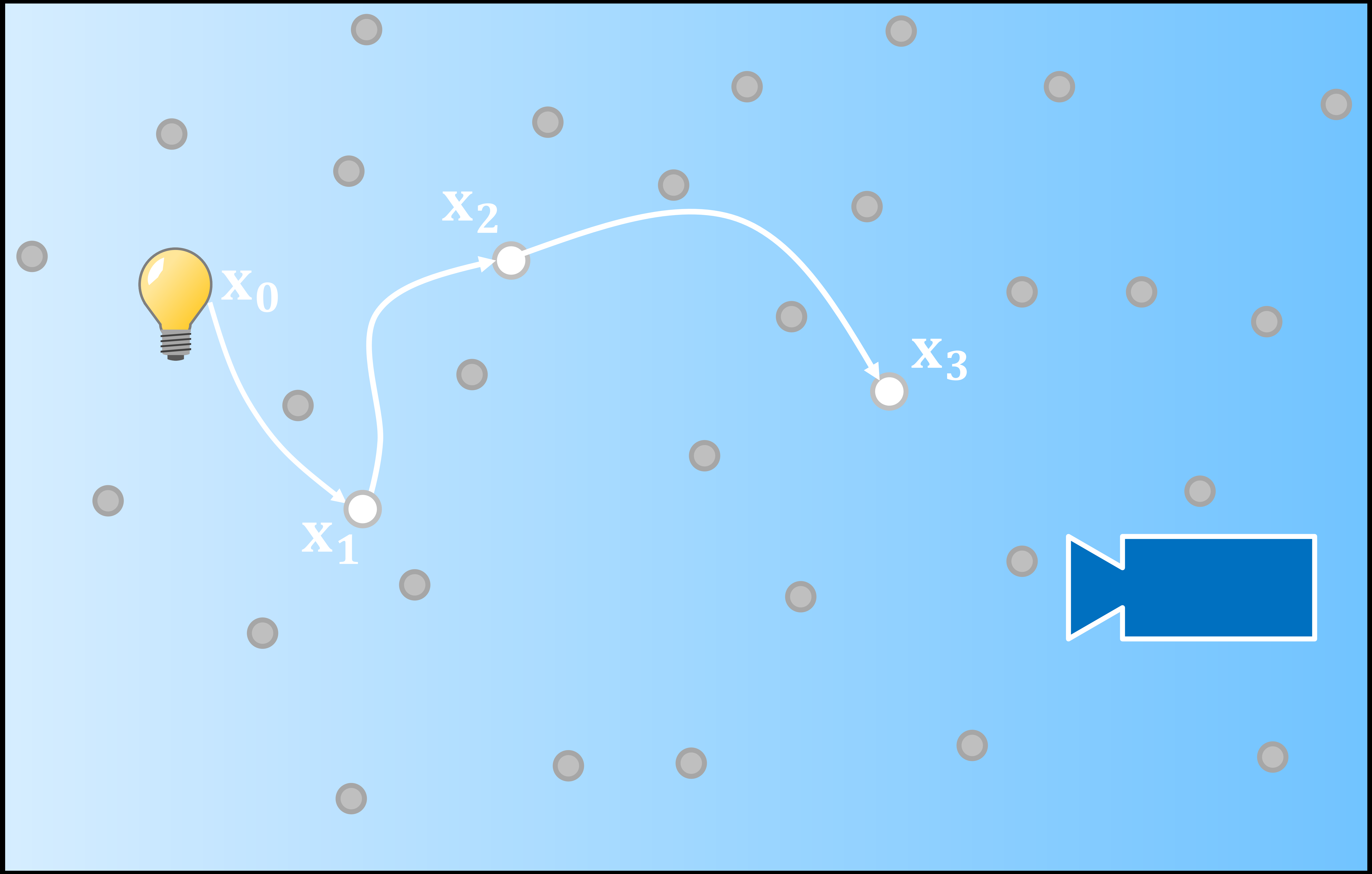

[Chandrasekhar, book, 1960]
[Lenoble, book, 1985]
[Lafortune and Willems, 1996]
[Cammarano and Jensen, 2002]
[Guttirez et al., Com. and Graph. 2006]
[Jarosz et al., Comp. Graph. forum, 2008]
[Jakob et al. ,ToG, 2010]
[Jarosz et al., ToG, 2011]
[Pediredla et al., JBO, 2016]
[Novak et al., Comp. Graph. forum, 2018]
[Bitterli et al., ToG, 2018]

Rendering continuous refraction and scattering

radiative transfer equation

bidirectional path tracing (BDPT):

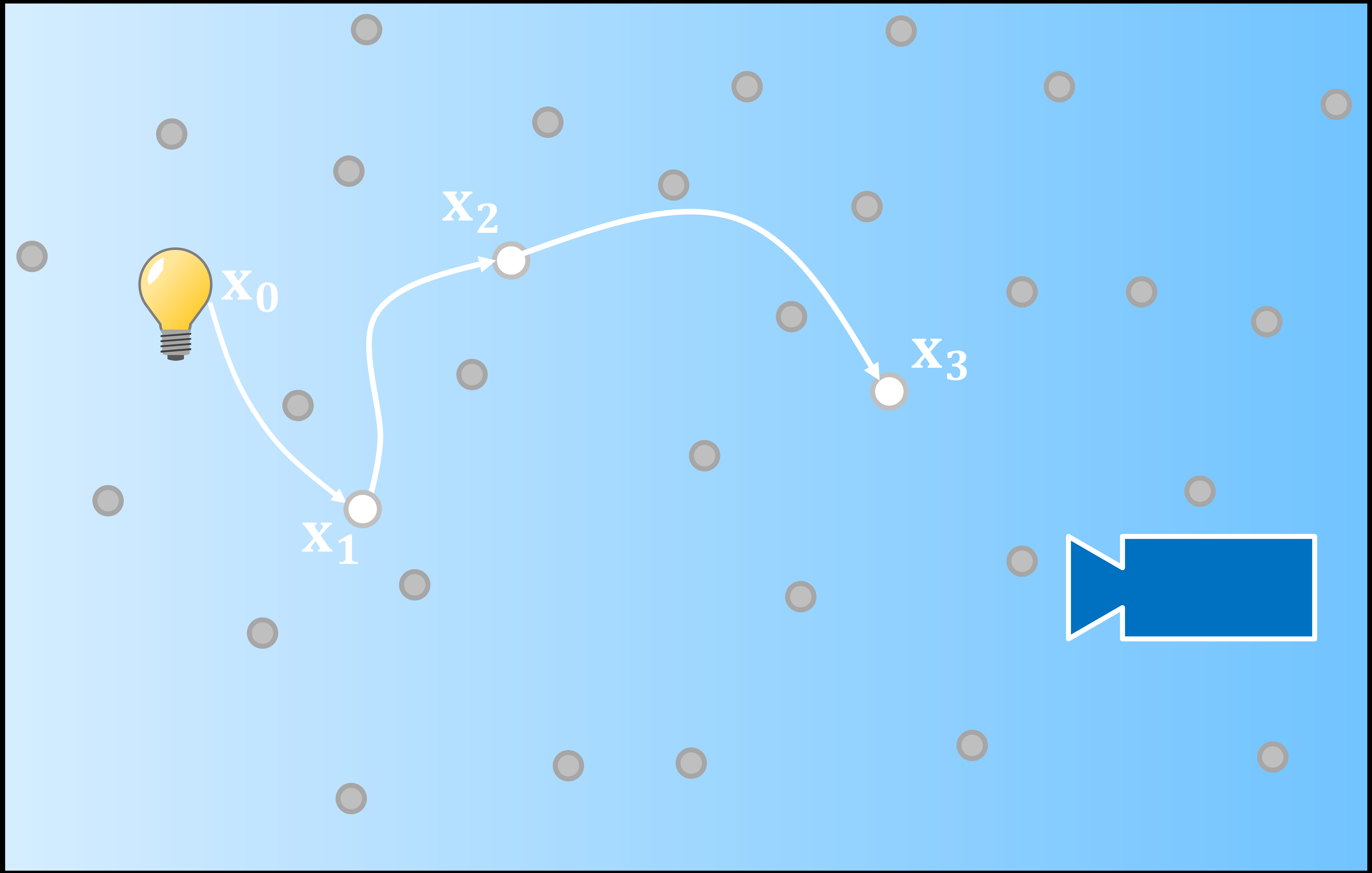

Rendering continuous refraction and scattering

radiative transfer equation

bidirectional path tracing (BDPT):

1. trace a random emitter subpath

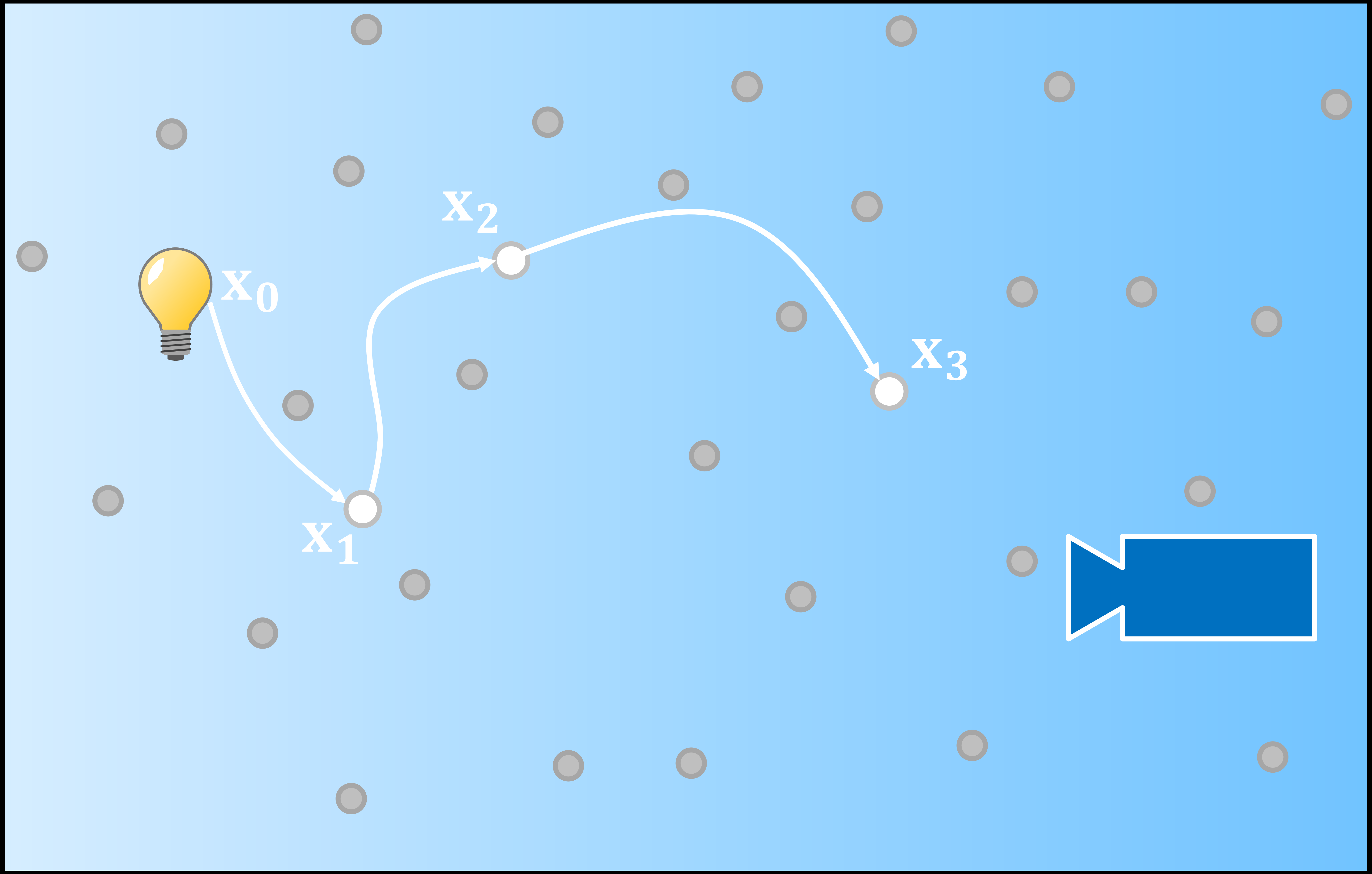

Rendering continuous refraction and scattering

radiative transfer equation

bidirectional path tracing (BDPT):

1. trace a random emitter subpath

2. trace a random sensor subpath

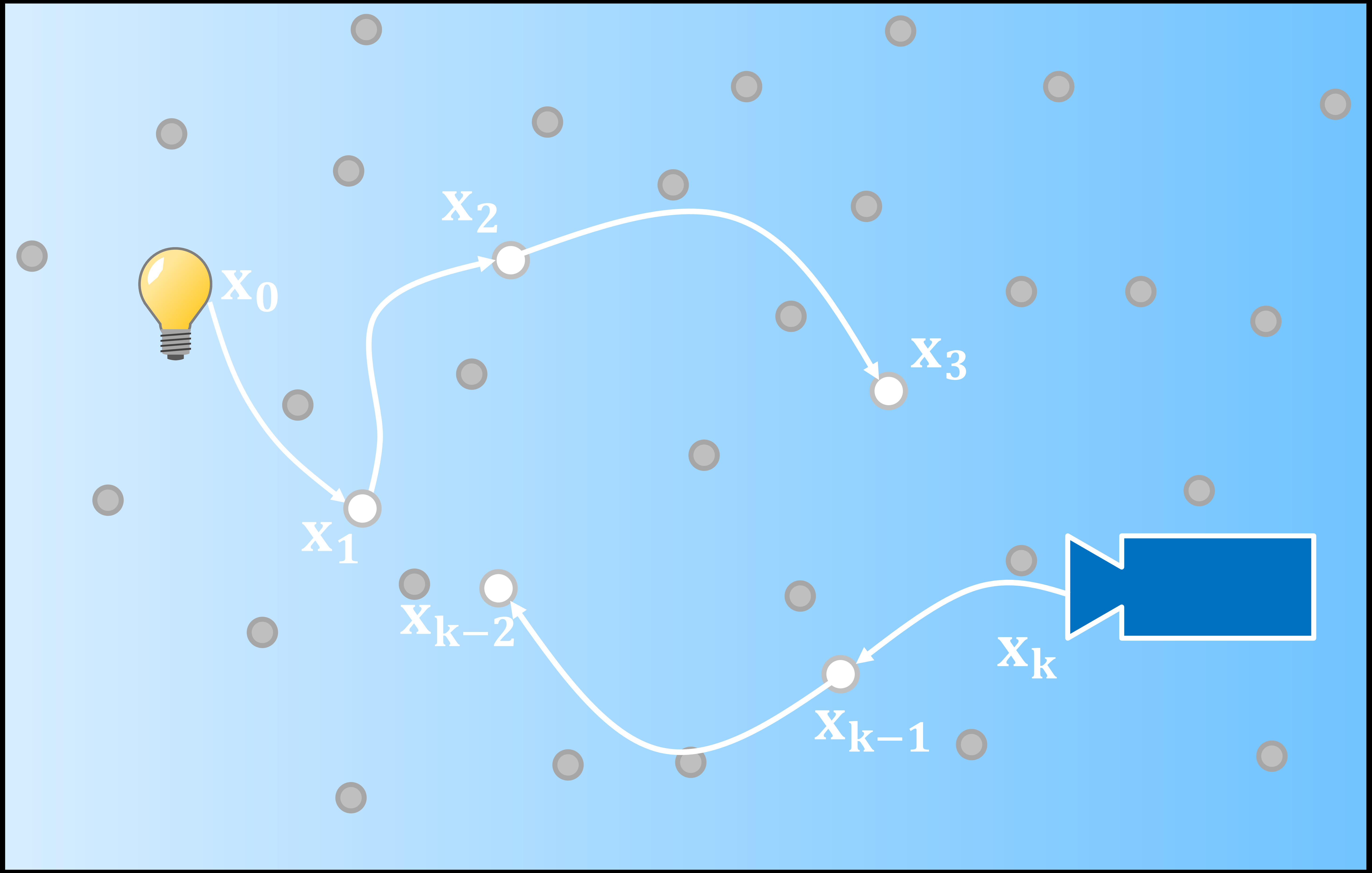

Rendering continuous refraction and scattering

radiative transfer equation

bidirectional path tracing (BDPT):

1. trace a random emitter subpath

2. trace a random sensor subpath

3. join vertices with a straight line

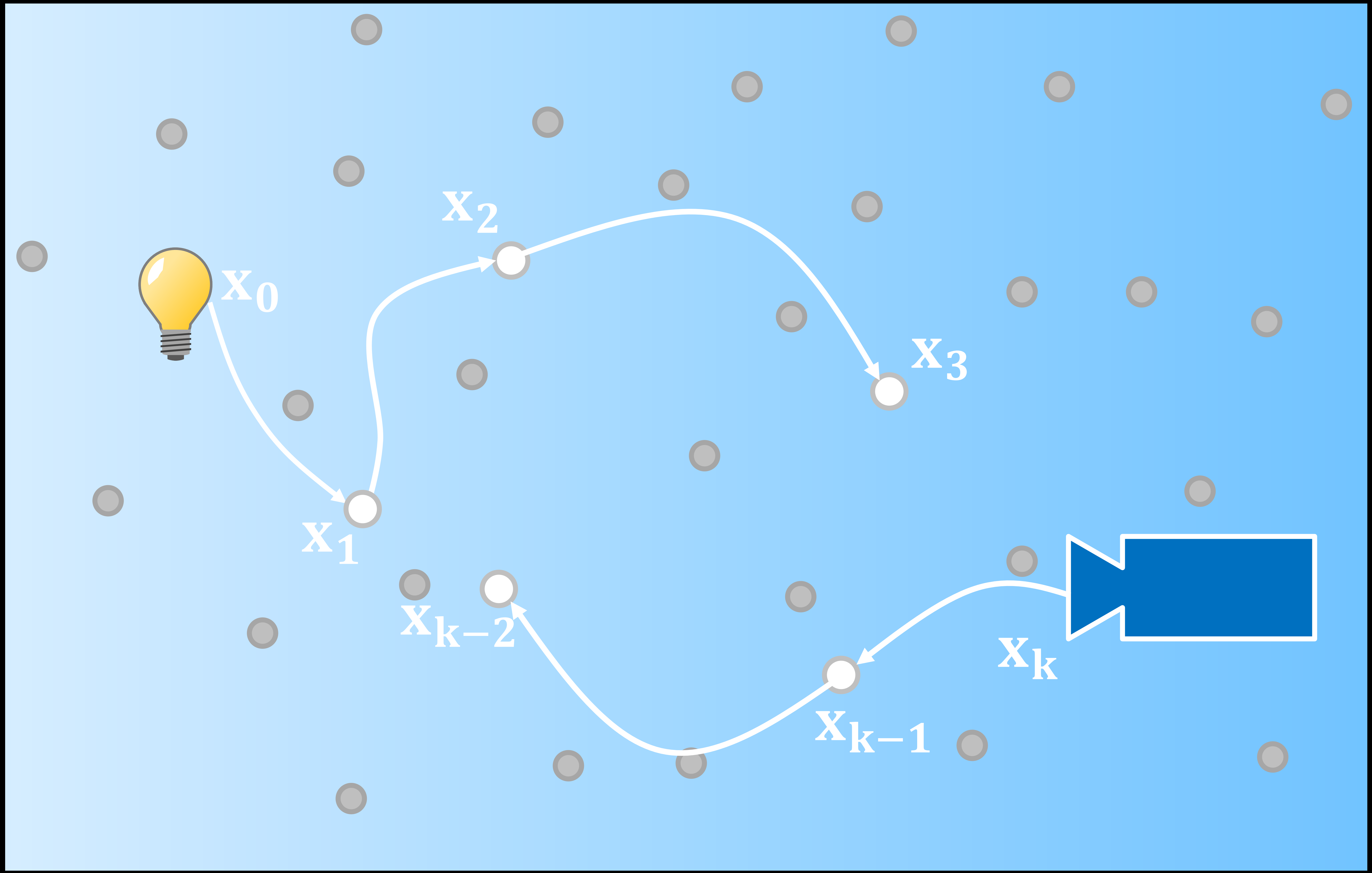

Rendering continuous refraction and scattering

radiative transfer equation

bidirectional path tracing (BDPT):

1. trace a random emitter subpath

2. trace a random sensor subpath

3. join vertices with a ~~straight line~~ curve

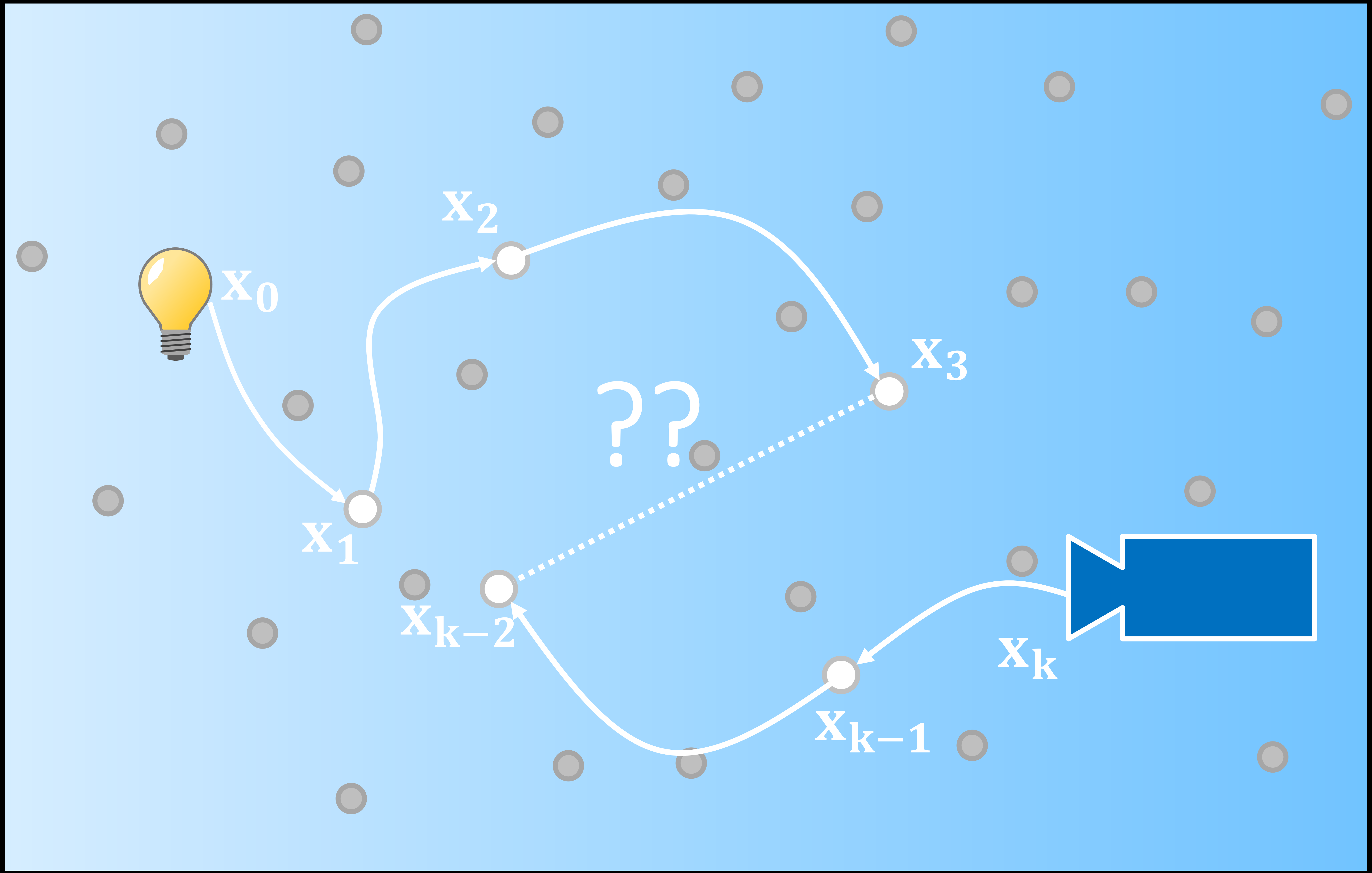

Rendering continuous refraction and scattering

radiative transfer equation

bidirectional path tracing (BDPT):

1. trace a random emitter subpath

2. trace a random sensor subpath

3. join vertices with a ~~straight line~~ curve

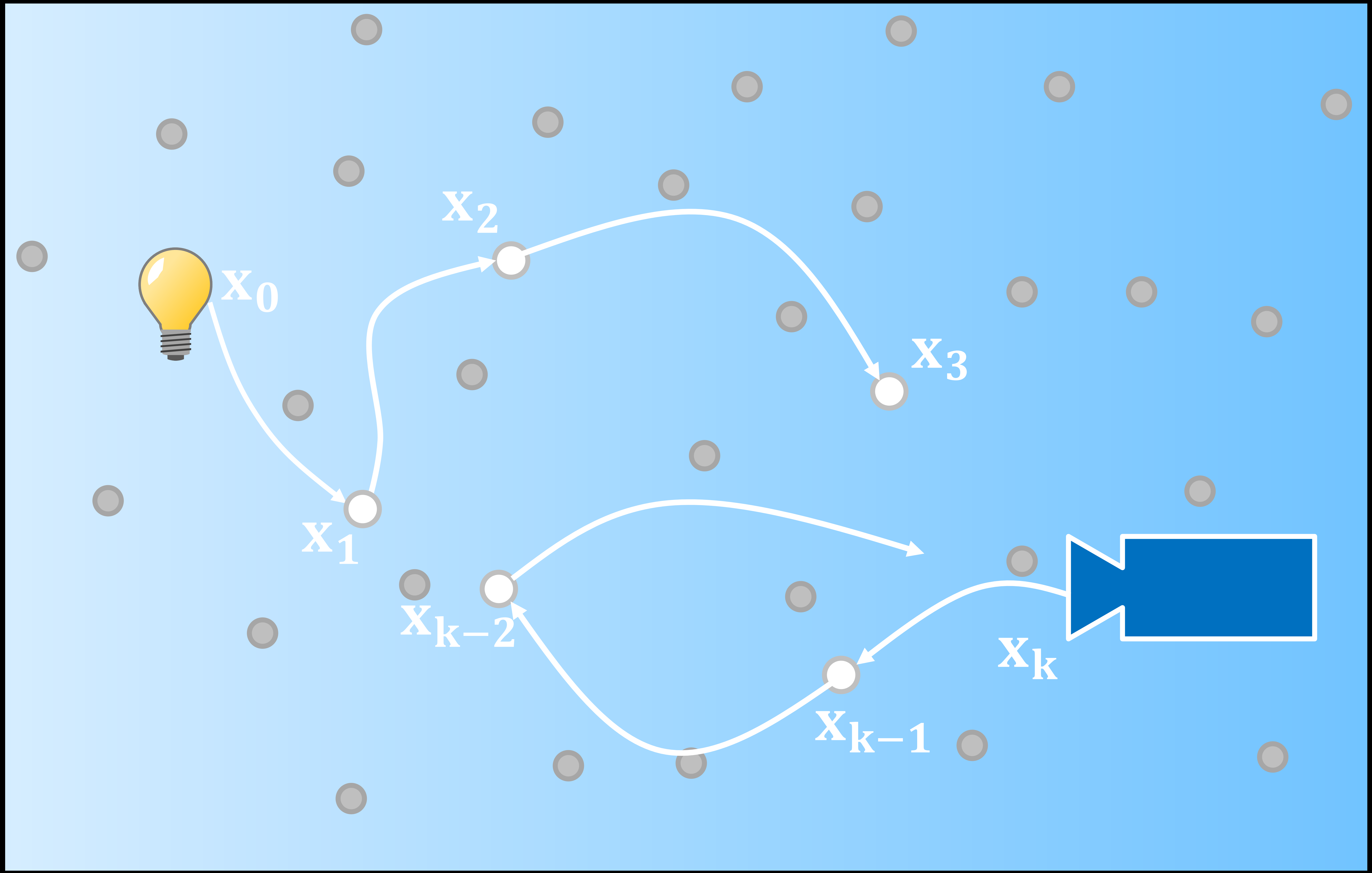

Rendering continuous refraction and scattering

radiative transfer equation

bidirectional path tracing (BDPT):

1. trace a random emitter subpath

2. trace a random sensor subpath

3. join vertices with a ~~straight line~~ curve

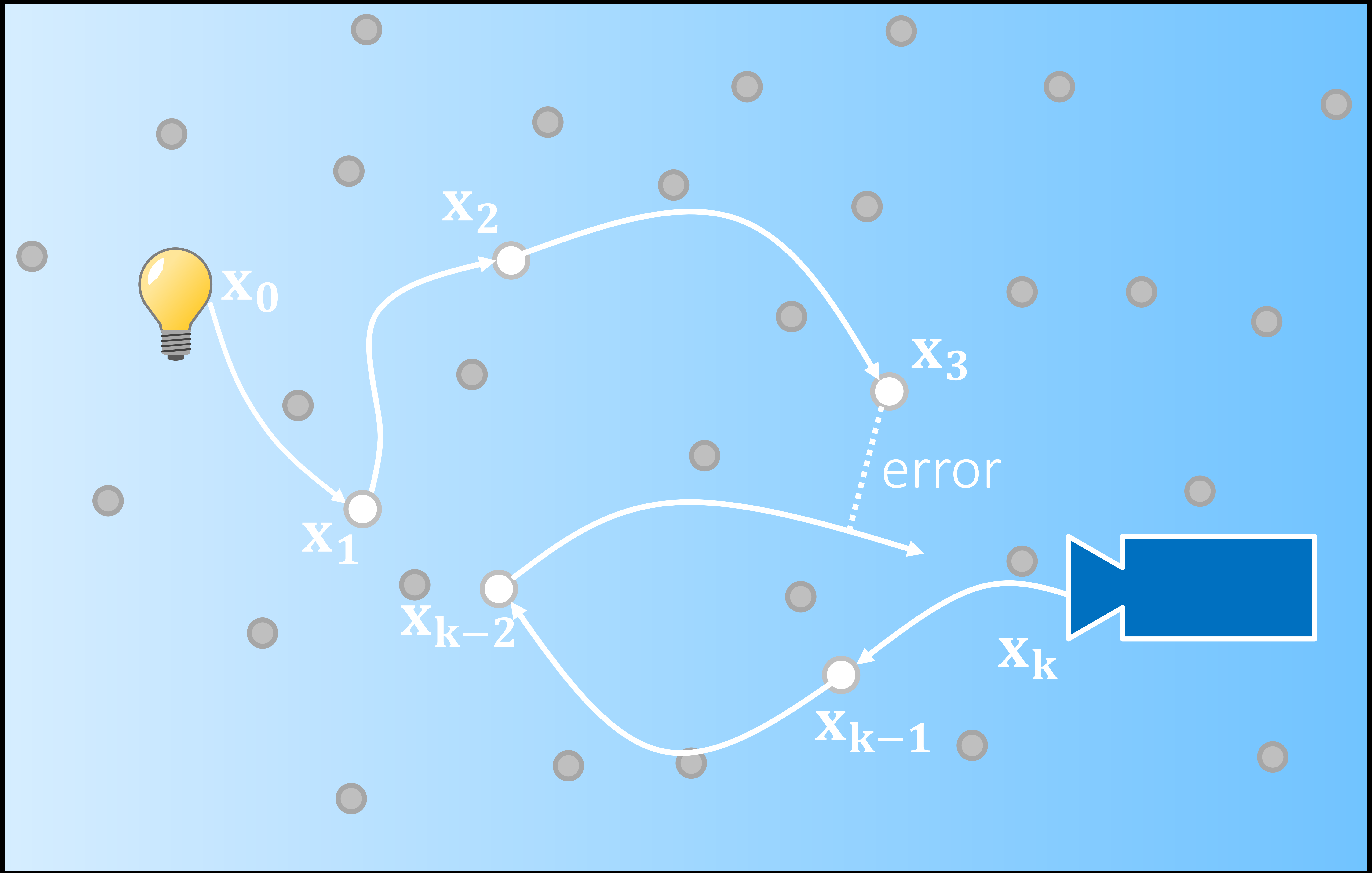

Rendering continuous refraction and scattering

radiative transfer equation

bidirectional path tracing (BDPT):

1. trace a random emitter subpath

2. trace a random sensor subpath

3. join vertices with a ~~straight line~~ curve

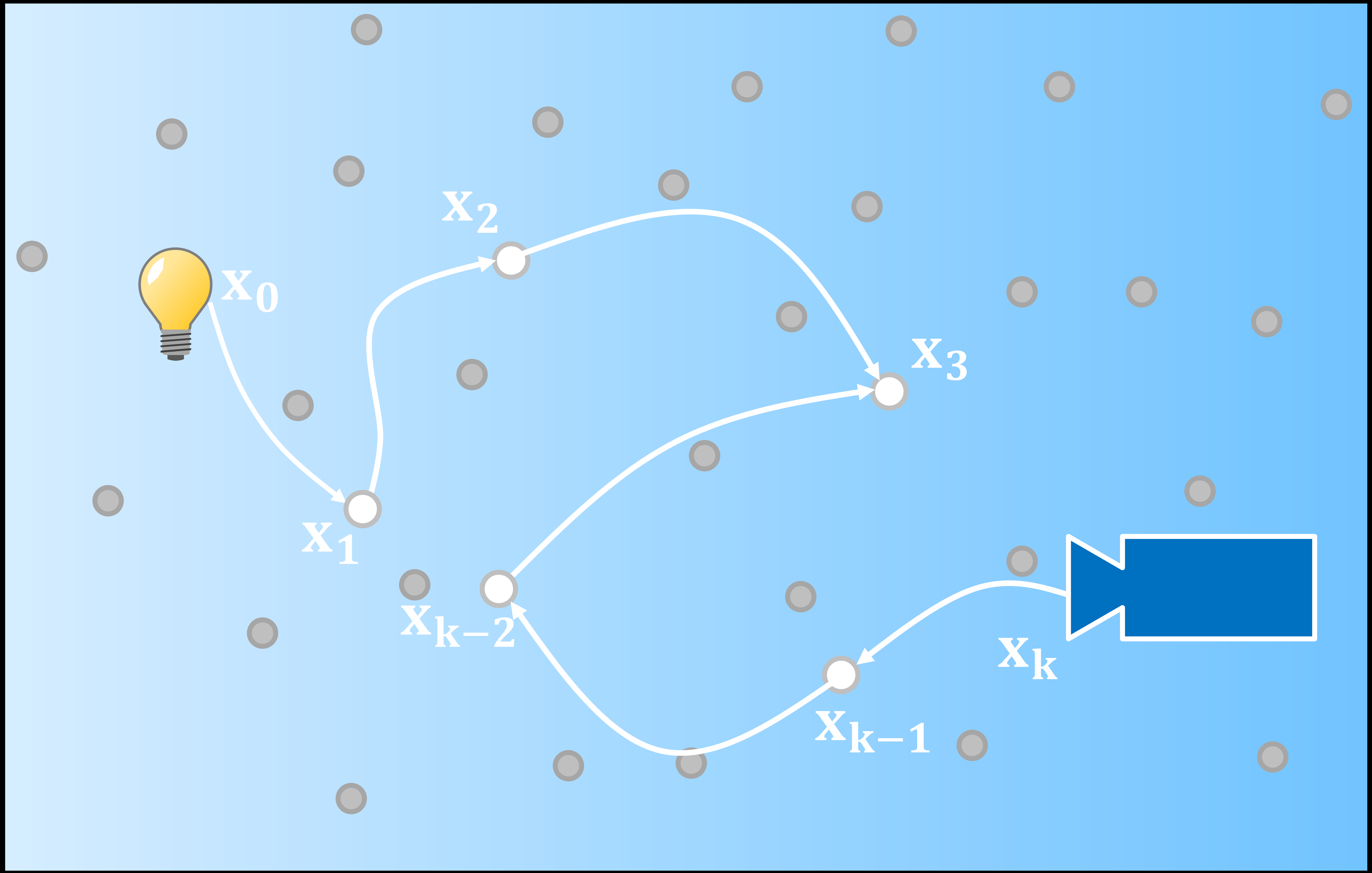

Rendering continuous refraction and scattering

$$\frac{\mathrm{d}\mathcal{L}}{\mathrm{d}\mathbf{v}_0} = (\mathbf{x}_{s^\star} - \mathbf{y})^T \frac{\mathrm{d}\mathbf{x}_{s^\star}}{\mathrm{d}\mathbf{v}_0},$$

$$\frac{\mathrm{d}\mathbf{x}_{s^\star}}{\mathrm{d}\mathbf{v}_0} = \frac{\partial \mathbf{x}_{s^\star}}{\partial \mathbf{v}_0} + \frac{\partial \mathbf{x}_{s^\star}}{\partial s^\star}\frac{\mathrm{d}s^\star}{\mathrm{d}\mathbf{v}_0}.$$

$$g(\mathbf{x}_{s^\star}) = 0 \Rightarrow \frac{\mathrm{d}g(\mathbf{x}_{s^\star})}{\mathrm{d}\mathbf{x}_{s^\star}}\frac{\mathrm{d}\mathbf{x}_{s^\star}}{\mathrm{d}\mathbf{v}_0} = 0$$

$$\Rightarrow \frac{\mathrm{d}s^\star}{\mathrm{d}\mathbf{v}_0} = -\frac{\frac{\mathrm{d}g(\mathbf{x}_{s^\star})}{\mathrm{d}\mathbf{x}_{s^\star}}\frac{\partial \mathbf{x}_{s^\star}}{\partial \mathbf{v}_0}}{\frac{\mathrm{d}g(\mathbf{x}_{s^\star})}{\mathrm{d}\mathbf{x}_{s^\star}}\frac{\partial \mathbf{x}_{s^\star}}{\partial s^\star}},$$

$$\frac{\mathrm{d}\mathbf{x}_{s^\star}}{\mathrm{d}\mathbf{v}_0} = \left(I_{3\times 3} - \frac{\frac{\partial \mathbf{x}_{s^\star}}{\partial s^\star}\frac{\mathrm{d}g(\mathbf{x}_{s^\star})}{\mathrm{d}\mathbf{x}_{s^\star}}}{\frac{\mathrm{d}g(\mathbf{x}_{s^\star})}{\mathrm{d}\mathbf{x}_{s^\star}}\frac{\partial \mathbf{x}_{s^\star}}{\partial s^\star}}\right)\frac{\partial \mathbf{x}_{s^\star}}{\partial \mathbf{v}_0}.$$

Algorithm 2: Symplectic integration for derivative tracing

Input: $n(\mathbf{x}), \nabla n(\mathbf{x}), H_n(\mathbf{x}), \mathrm{ray}(\mathbf{x}, \mathbf{v}), \frac{\partial \mathbf{x}_{s^\star}}{\partial \mathbf{v}_0} = O_3, \frac{\partial \mathbf{v}_{s^\star}}{\partial \mathbf{v}_0} = I_3,$
nSteps, s = step size

Output: $\frac{\partial \mathbf{x}_{s^\star}}{\partial \mathbf{v}_0}, \frac{\partial \mathbf{v}_{s^\star}}{\partial \mathbf{v}_0}$

for $i = 1 : nSteps$ **do**

$\quad \mathrm{ray}.\mathbf{v}{+} = 0.5s\nabla n(\mathrm{ray}.\mathbf{x});$

$\quad \frac{\partial \mathbf{v}_{s^\star}}{\partial \mathbf{v}_0}{+} = 0.5sH_n(\mathrm{ray}.\mathbf{x})\frac{\partial \mathbf{x}_{s^\star}}{\partial \mathbf{v}_0};$

$\quad \mathrm{ray}.\mathbf{x}{+} = s\frac{\mathrm{ray}.\mathbf{v}}{n(\mathrm{ray}.\mathbf{x})};$

$\quad \frac{\partial \mathbf{x}_{s^\star}}{\partial \mathbf{v}_0}{+} = s\left(-\frac{\mathbf{v}_s \nabla n(\mathrm{ray}.\mathbf{x})}{n(\mathrm{ray}.\mathbf{x})^2}\frac{\partial \mathbf{x}_s}{\partial \mathbf{v}_0} + \frac{1}{n(\mathrm{ray}.\mathbf{x})}\frac{\partial \mathbf{v}_s}{\partial \mathbf{v}_0}\right);$

$\quad \mathrm{ray}.\mathbf{v}{+} = 0.5s\nabla n(\mathrm{ray}.\mathbf{x});$

$\quad \frac{\partial \mathbf{v}_{s^\star}}{\partial \mathbf{v}_0}{+} = 0.5sH_n(\mathrm{ray}.\mathbf{x})\frac{\partial \mathbf{x}_{s^\star}}{\partial \mathbf{v}_0};$

end

Pediredla et al. *Path Tracing Estimators for Refractive Radiative Transfer,* TOG 2020

Application: simulate Luneburg lenses

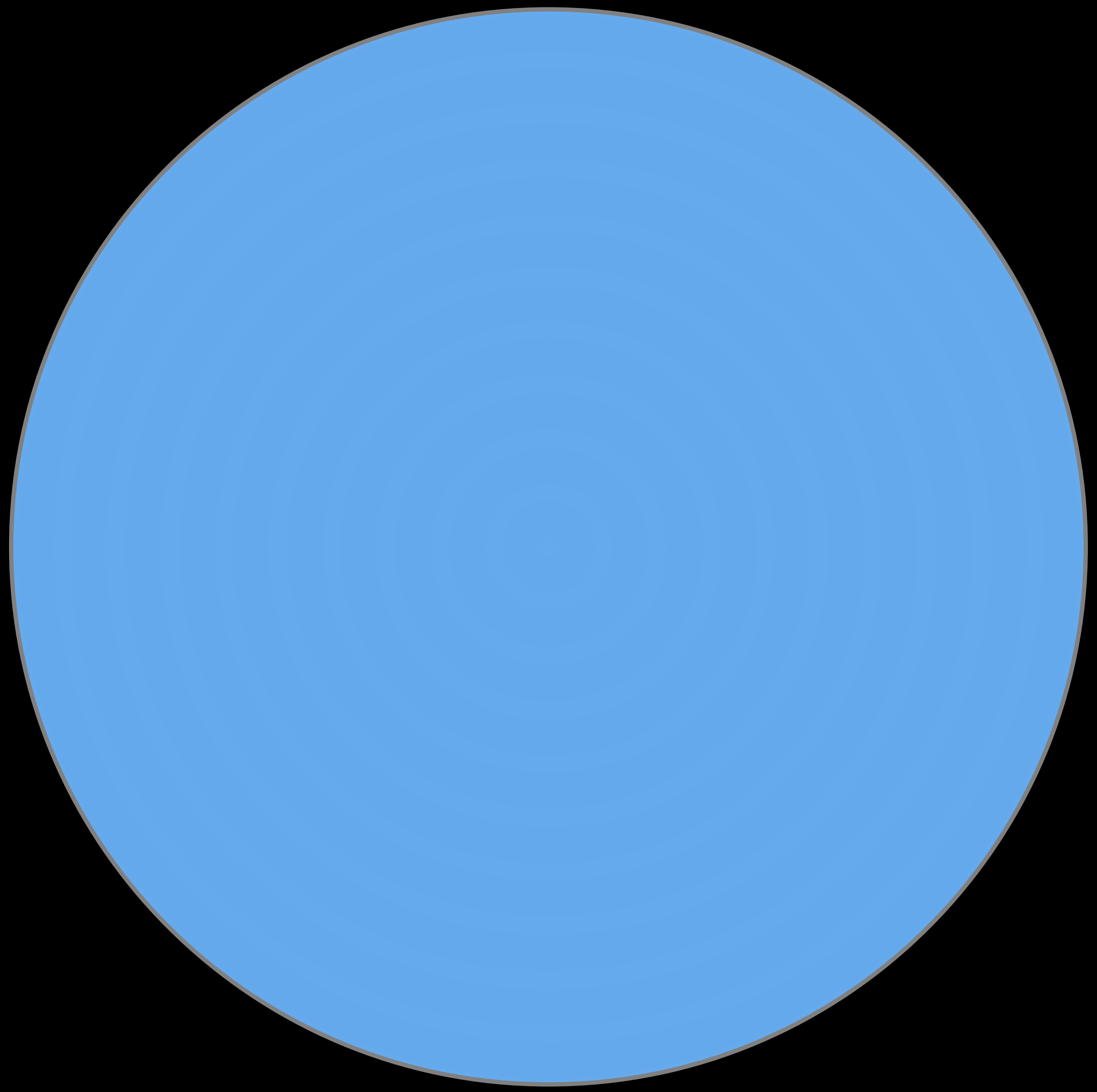

https://en.wikipedia.org/wiki/Luneburg_lens

Application: simulate Luneburg lenses

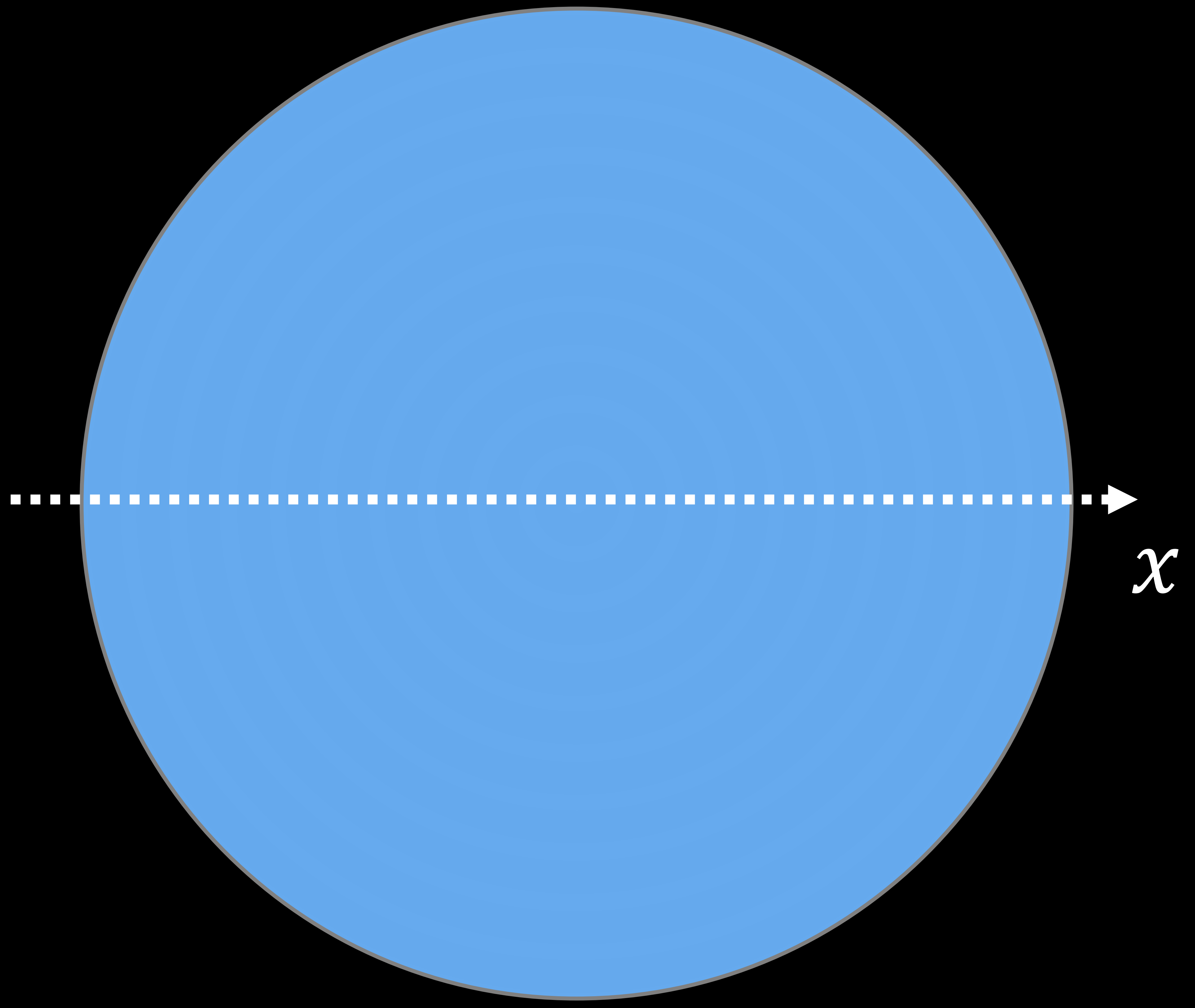

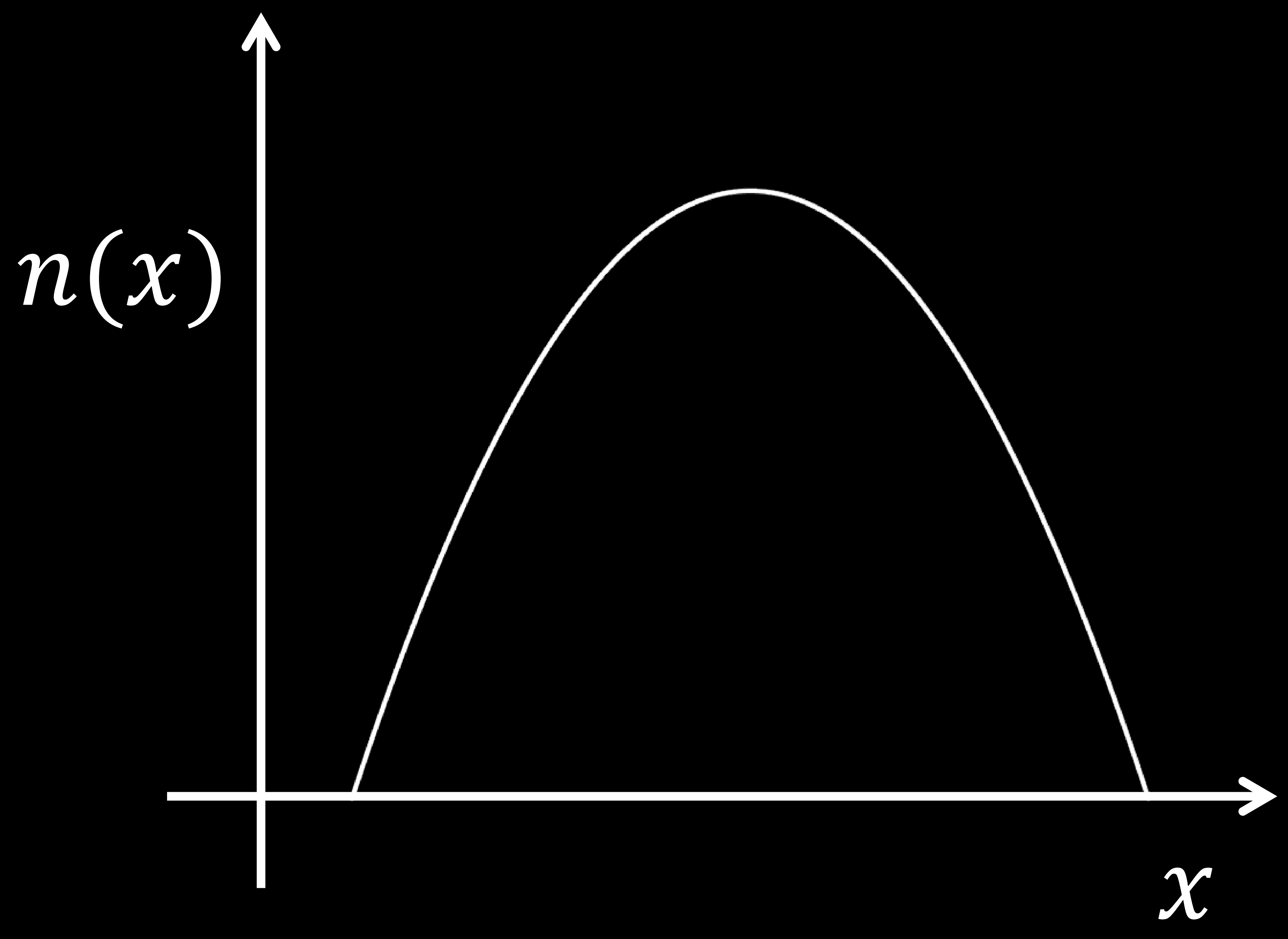

https://en.wikipedia.org/wiki/Luneburg_lens

Application: simulate Luneburg lenses

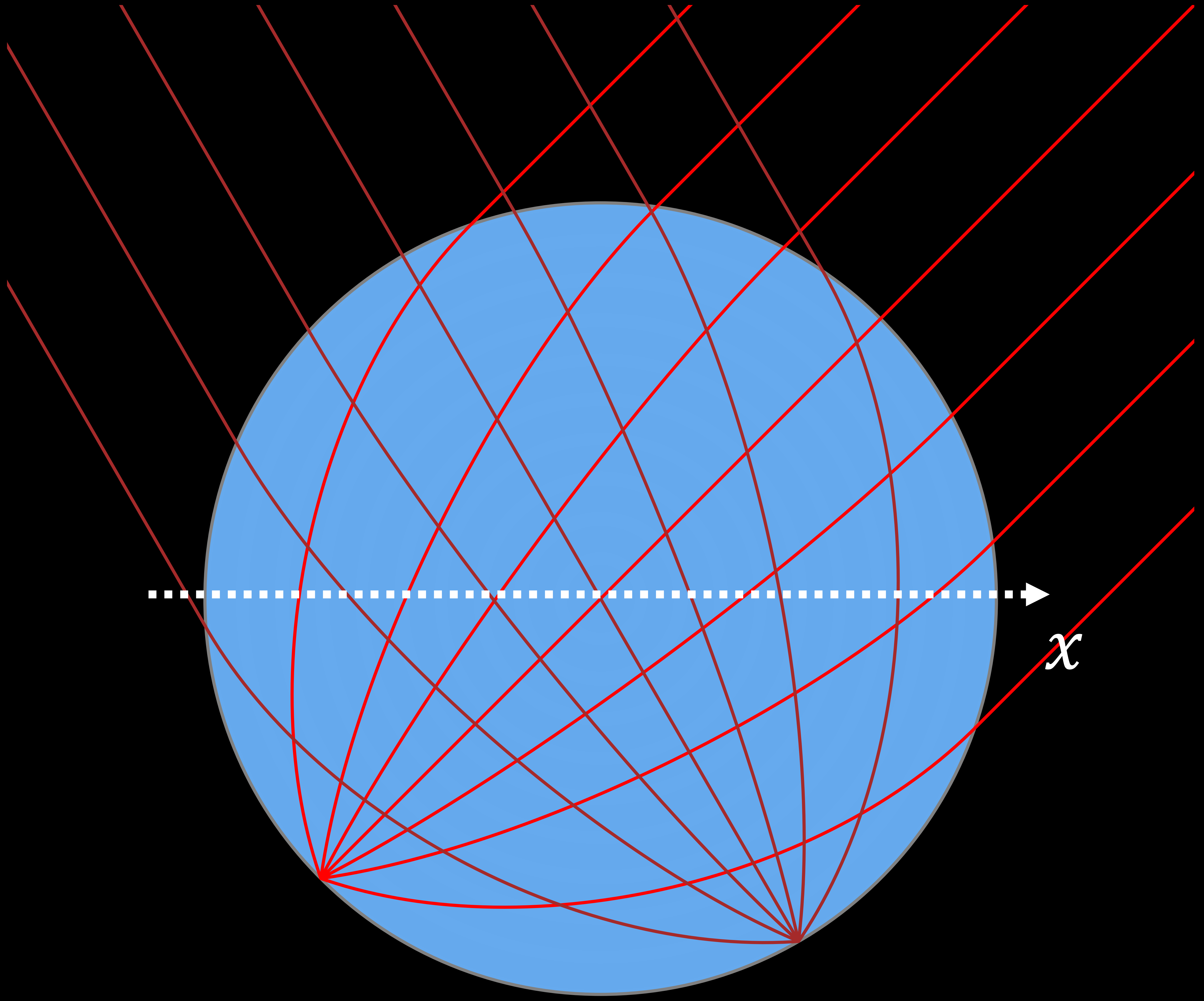

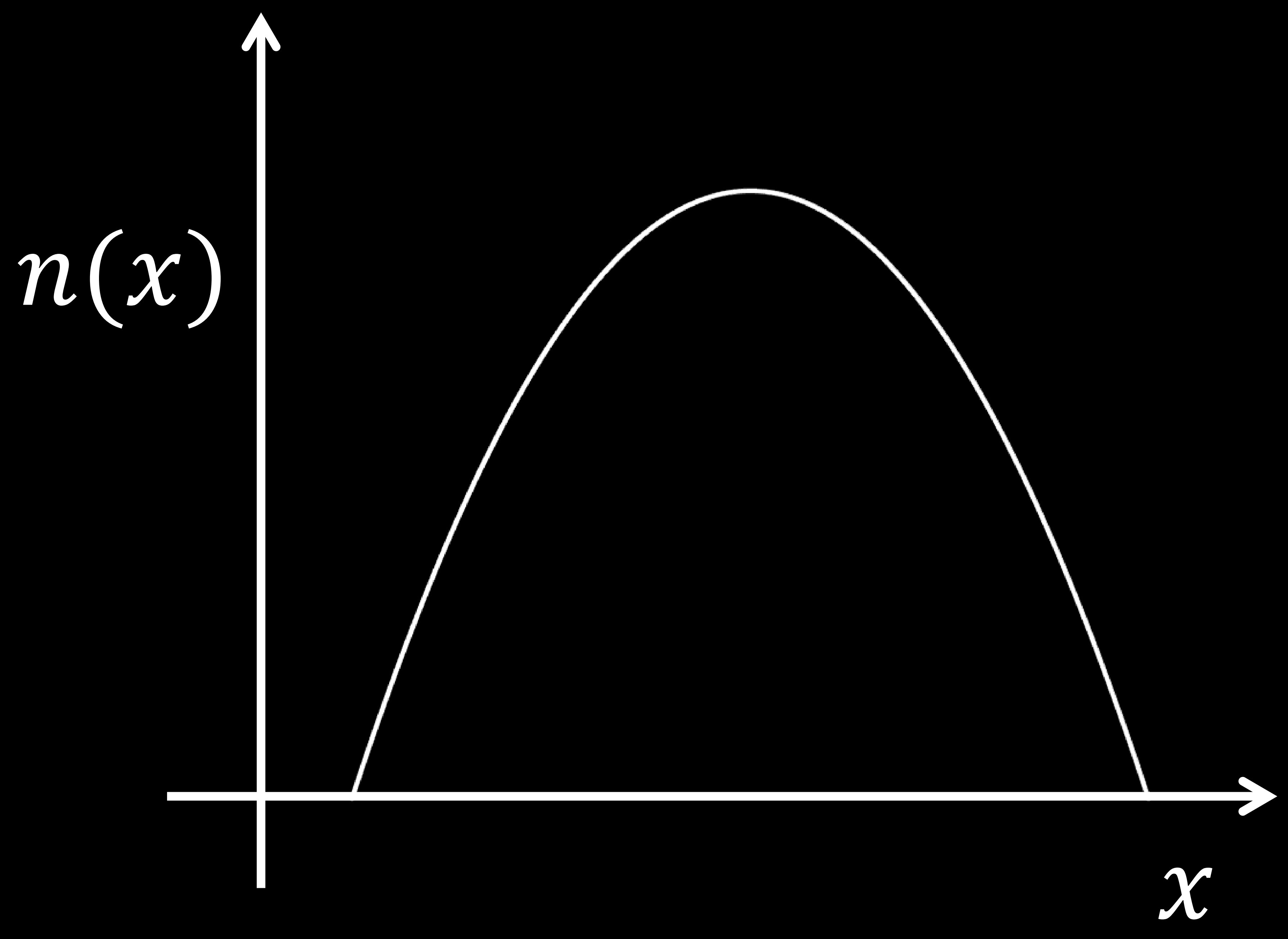

https://en.wikipedia.org/wiki/Luneburg_lens

Application: simulate Luneburg lenses

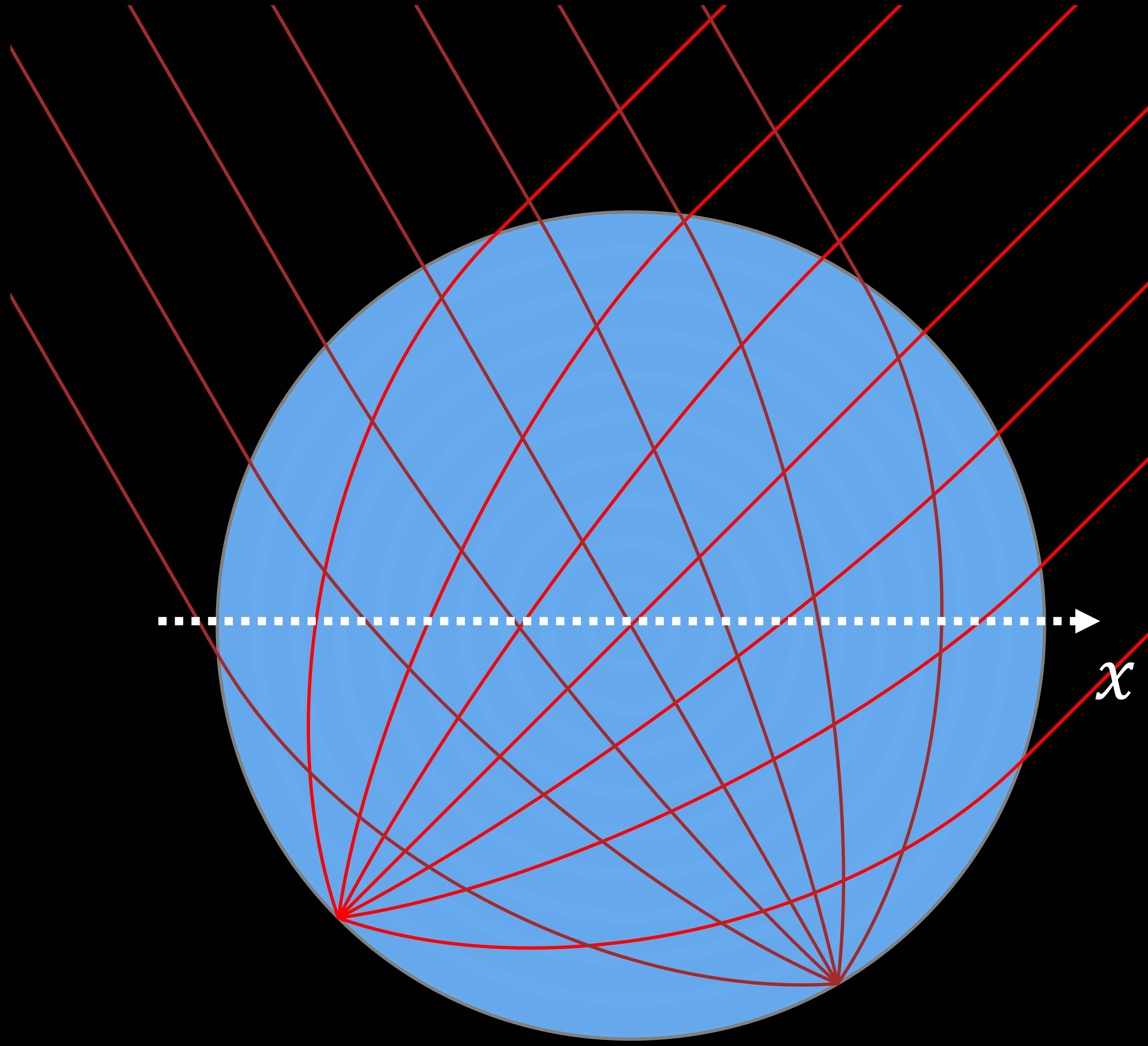

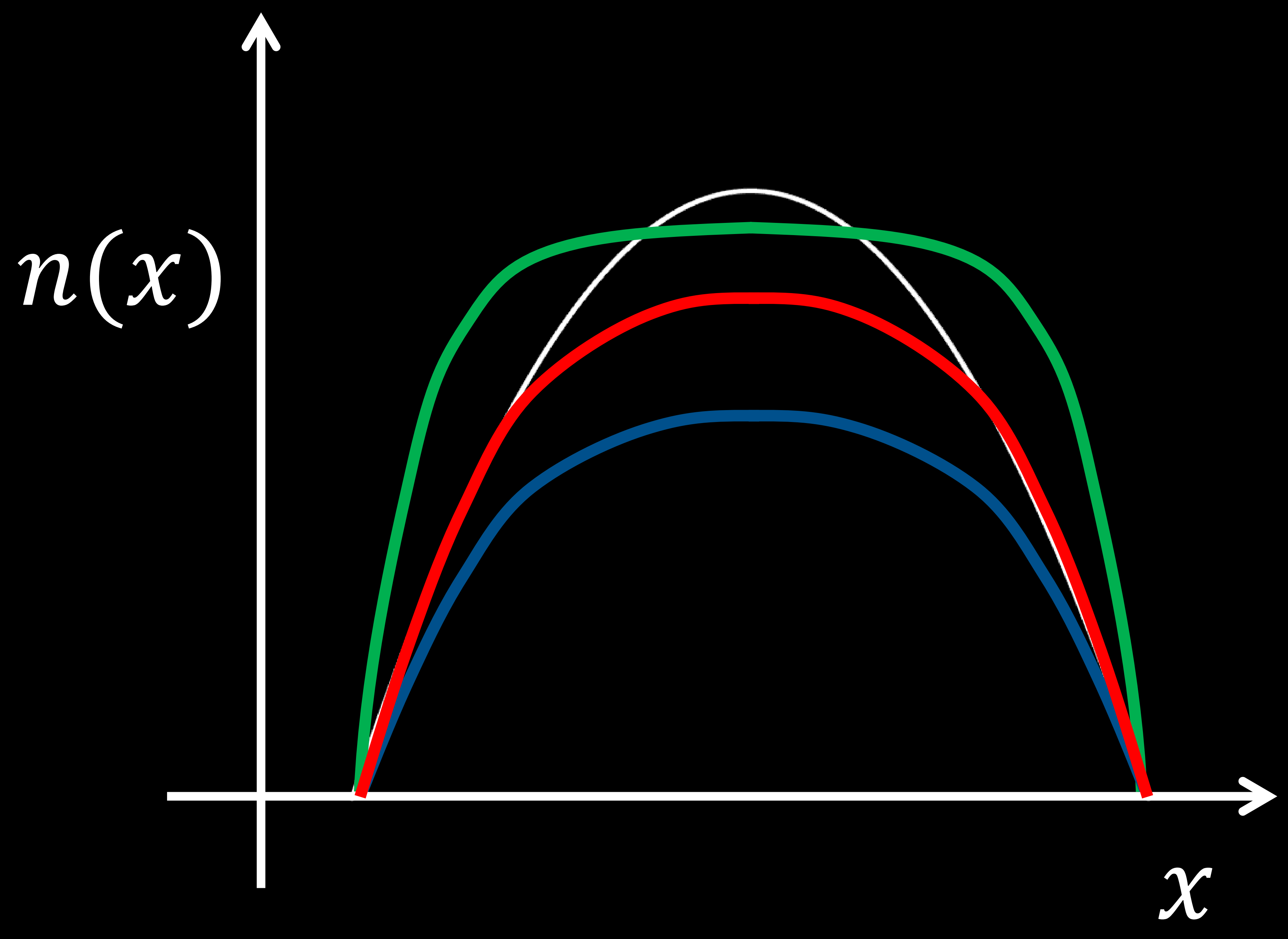

https://en.wikipedia.org/wiki/Luneburg_lens

Luneburg lenses

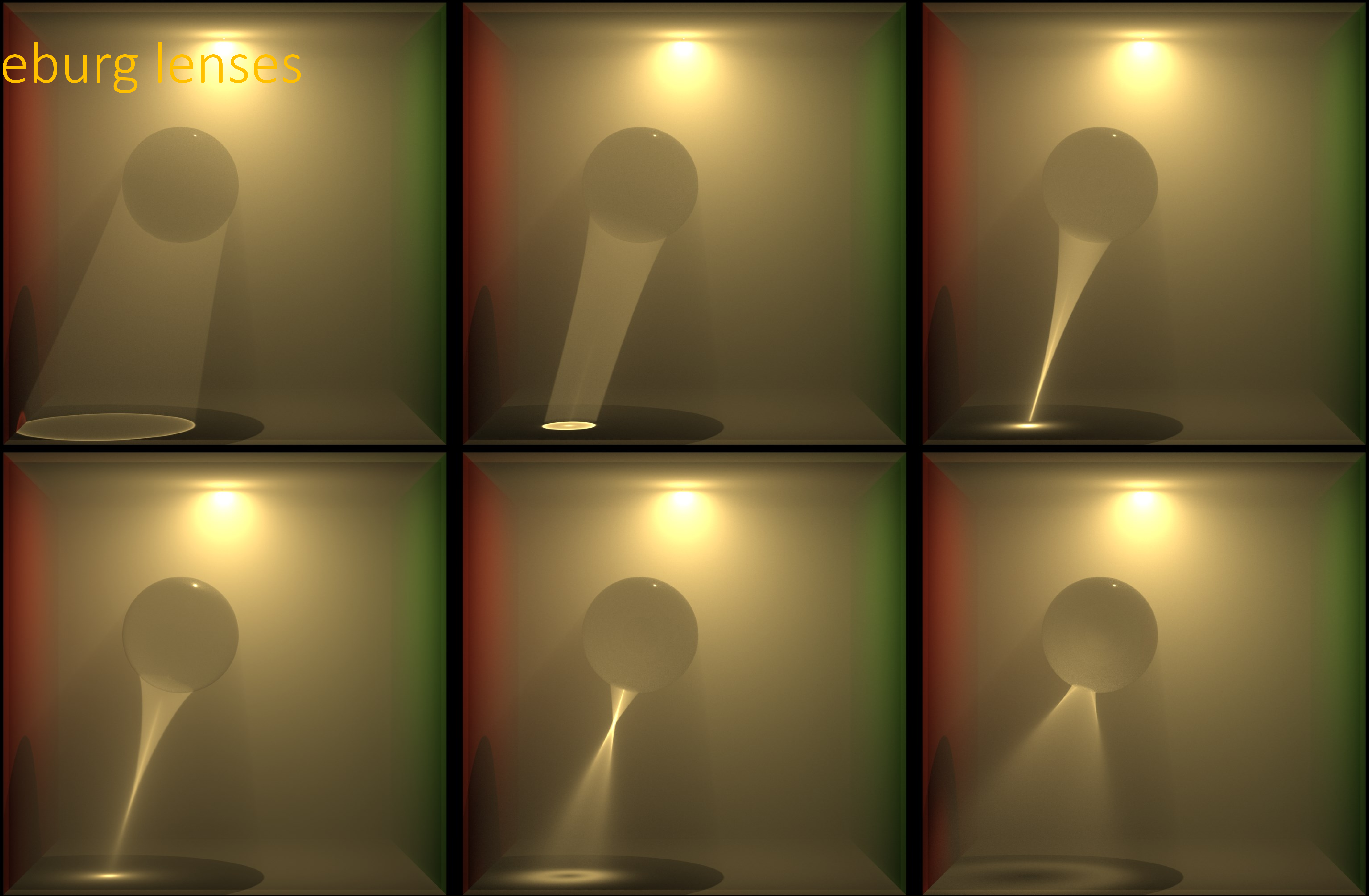

Application: transient rendering

constant refractive index

continuous refractive index

Application: transient rendering

constant refractive index

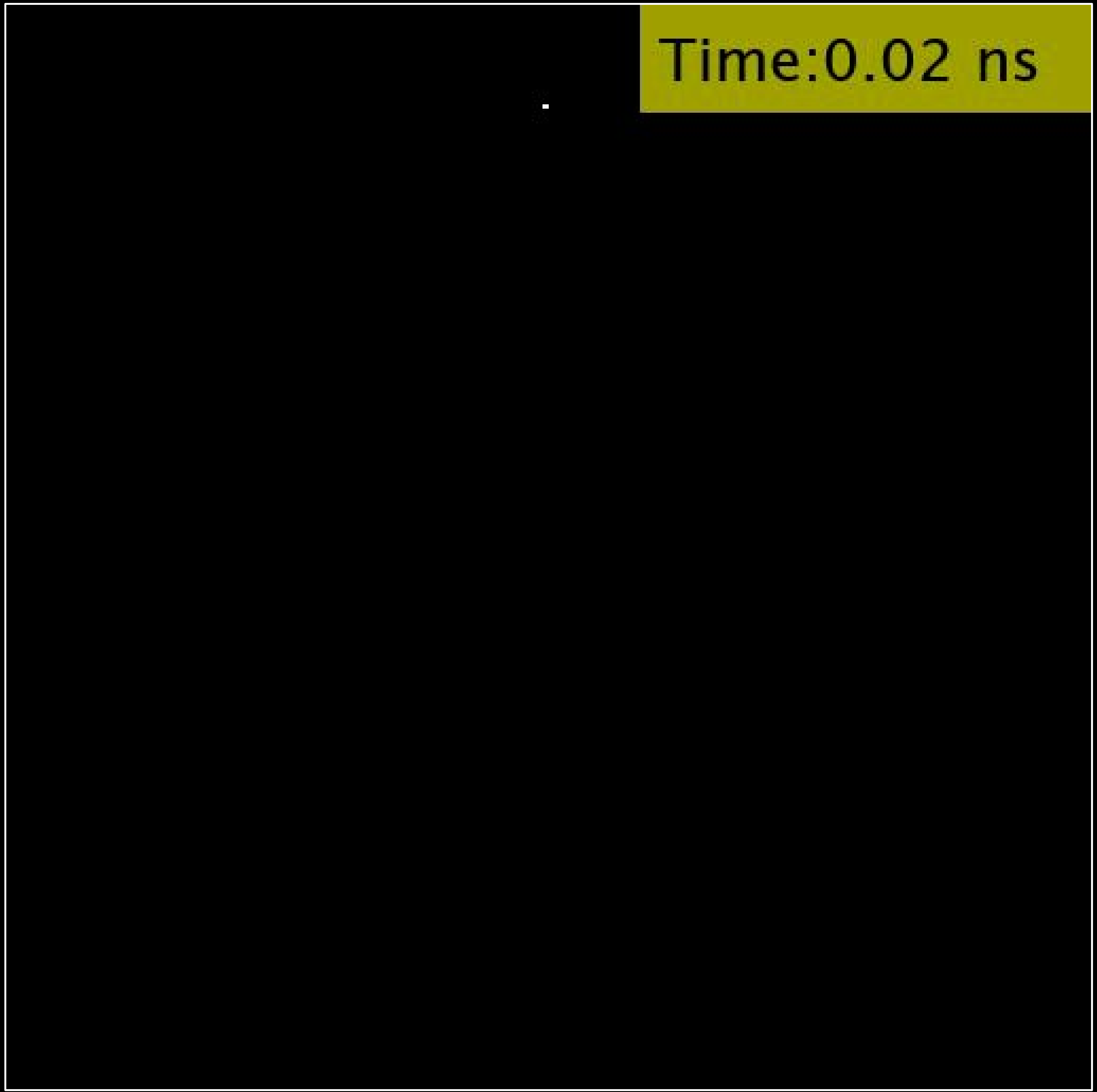

continuous refractive index

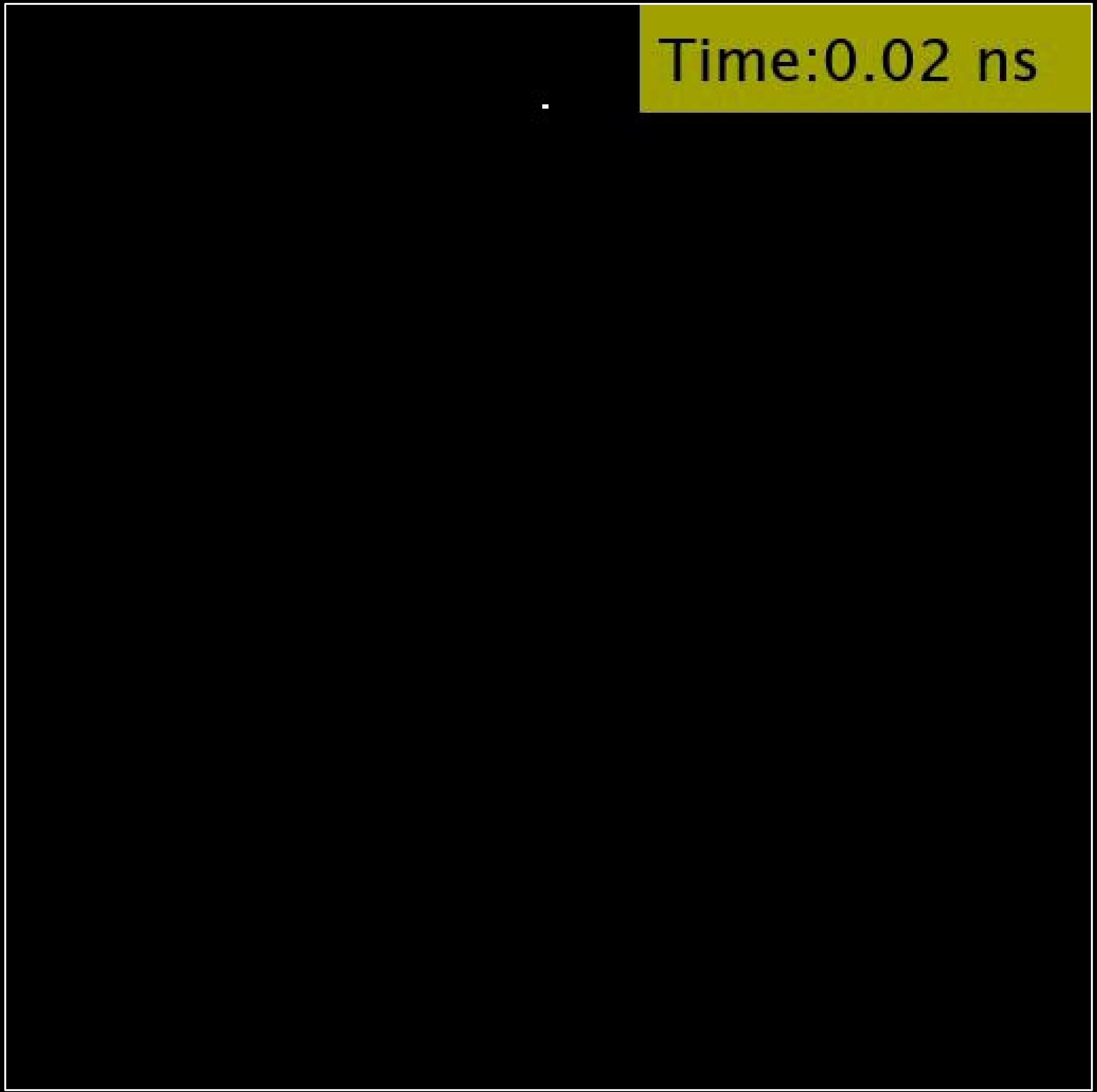

Application: transient rendering

constant refractive index

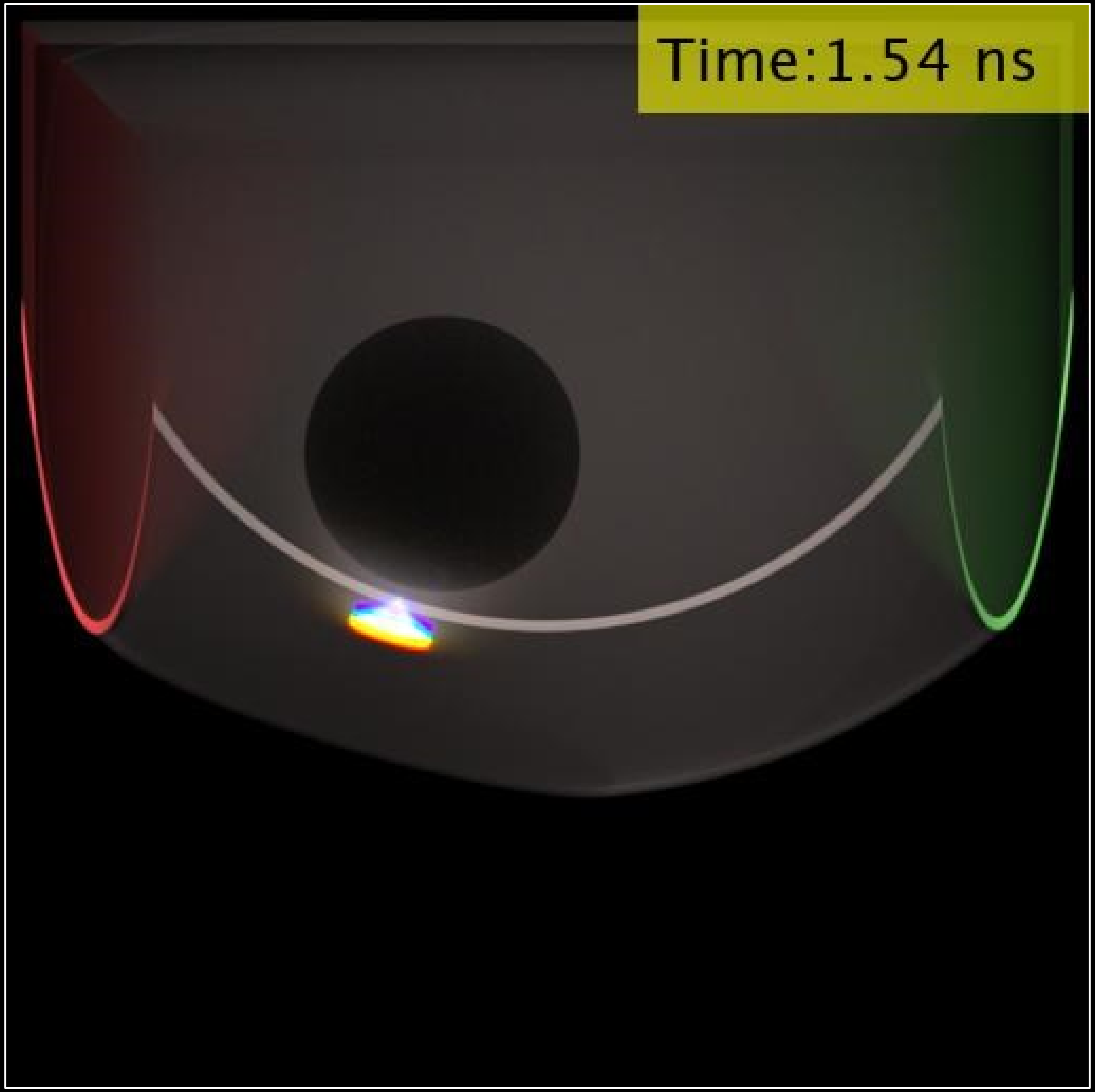

continuous refractive index

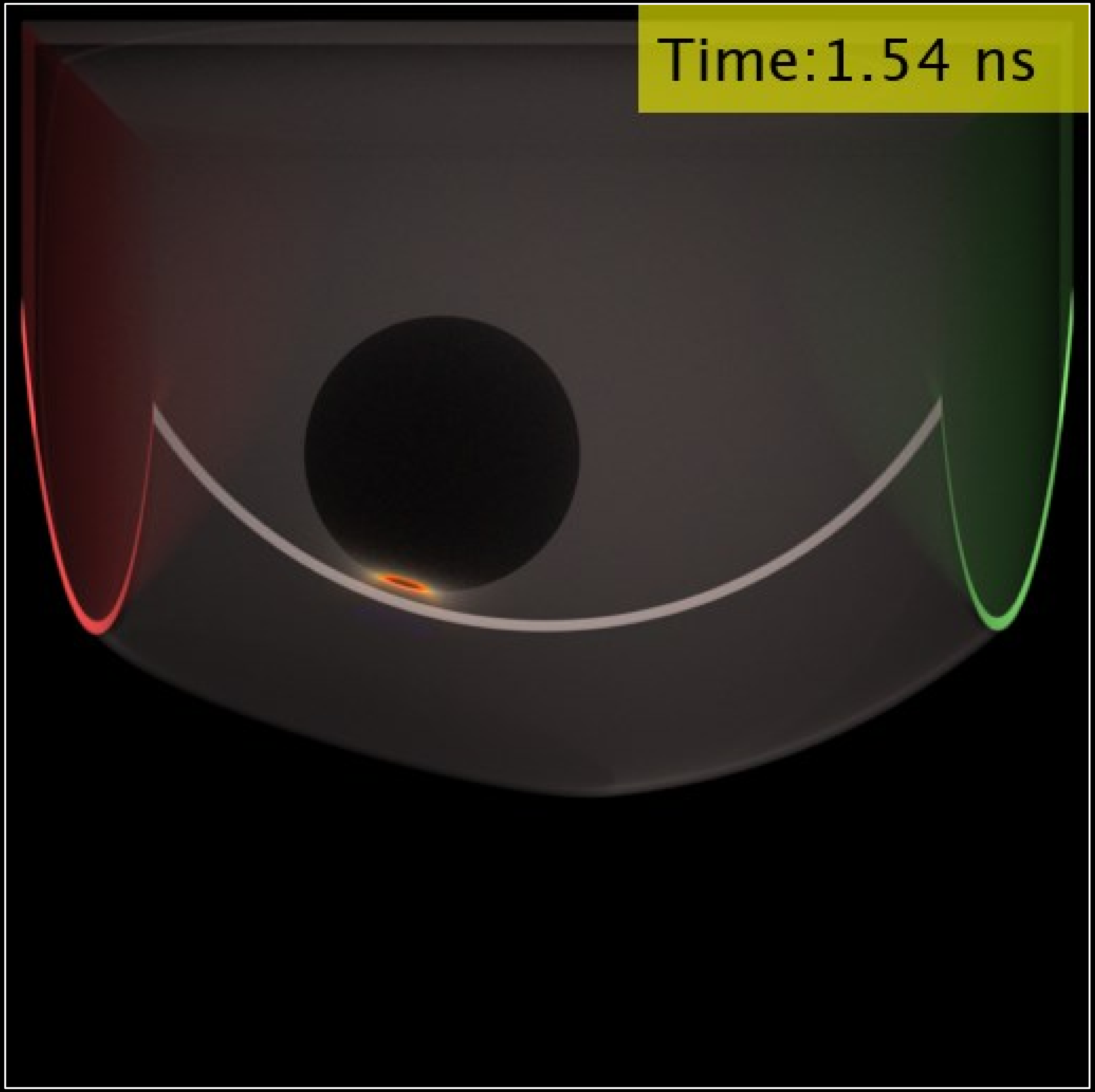

Application: transient rendering

constant refractive index

continuous refractive index

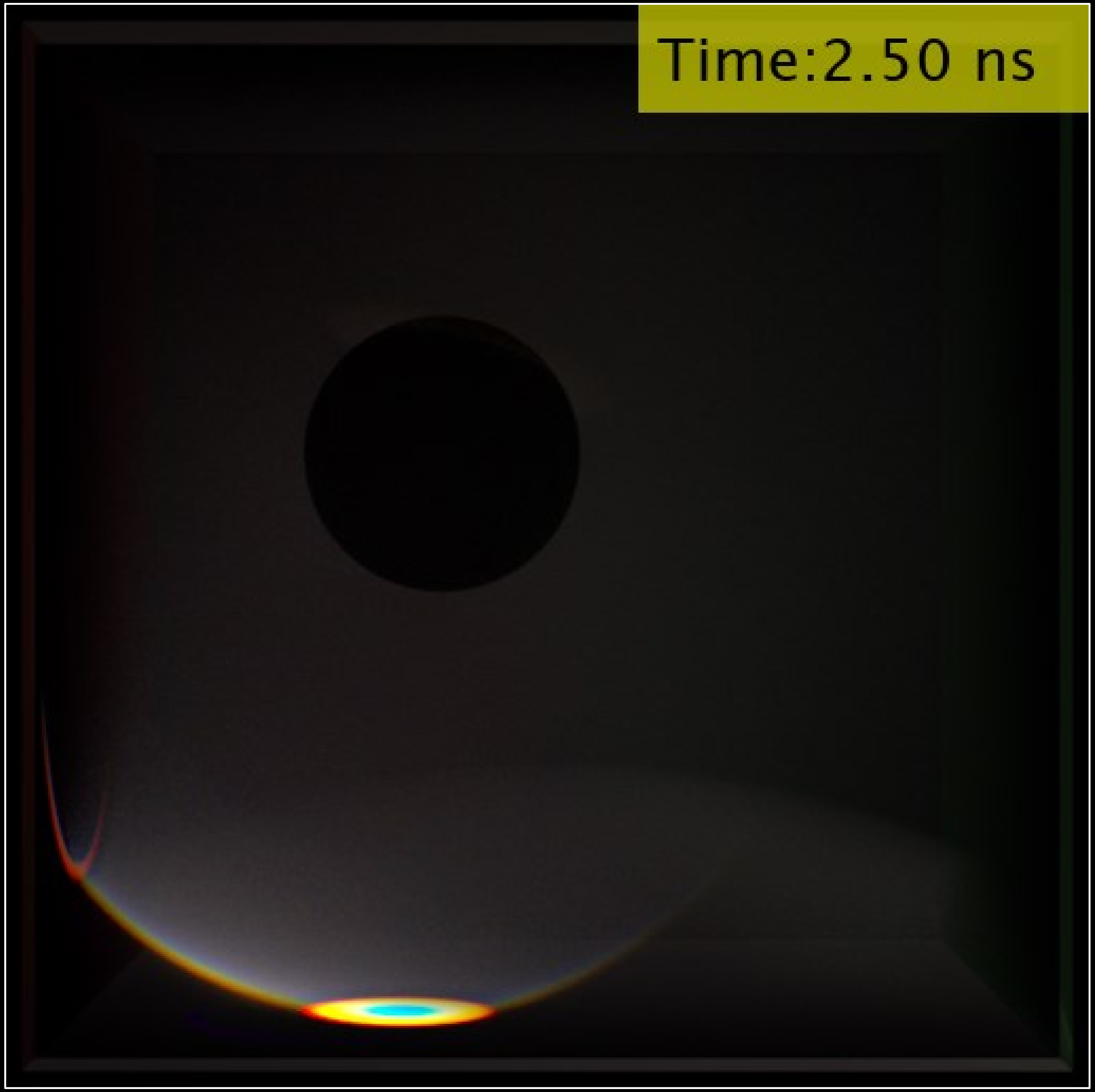

Application: focusing light inside tissue

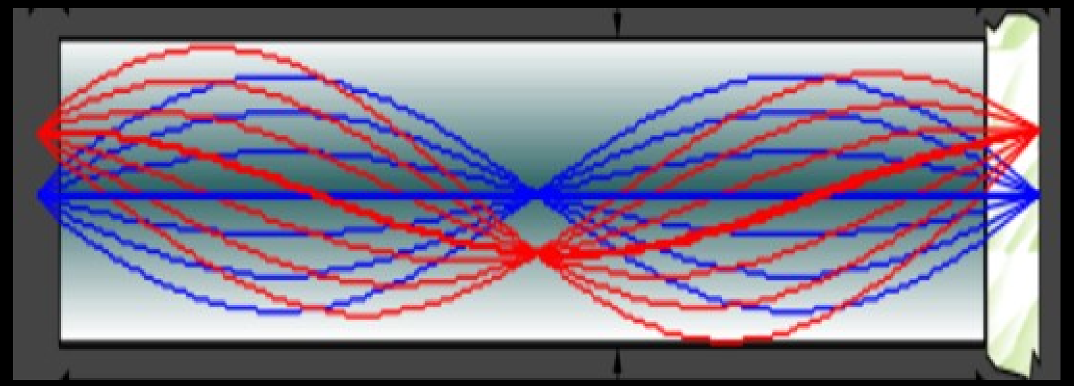

Gradient Refractive Index (GRIN) waveguide

High-dimensional, highly-non-linear design problem:

- ultrasound frequency
- ultrasound voltage
- placement of transducers
- waveform shape
- and more…

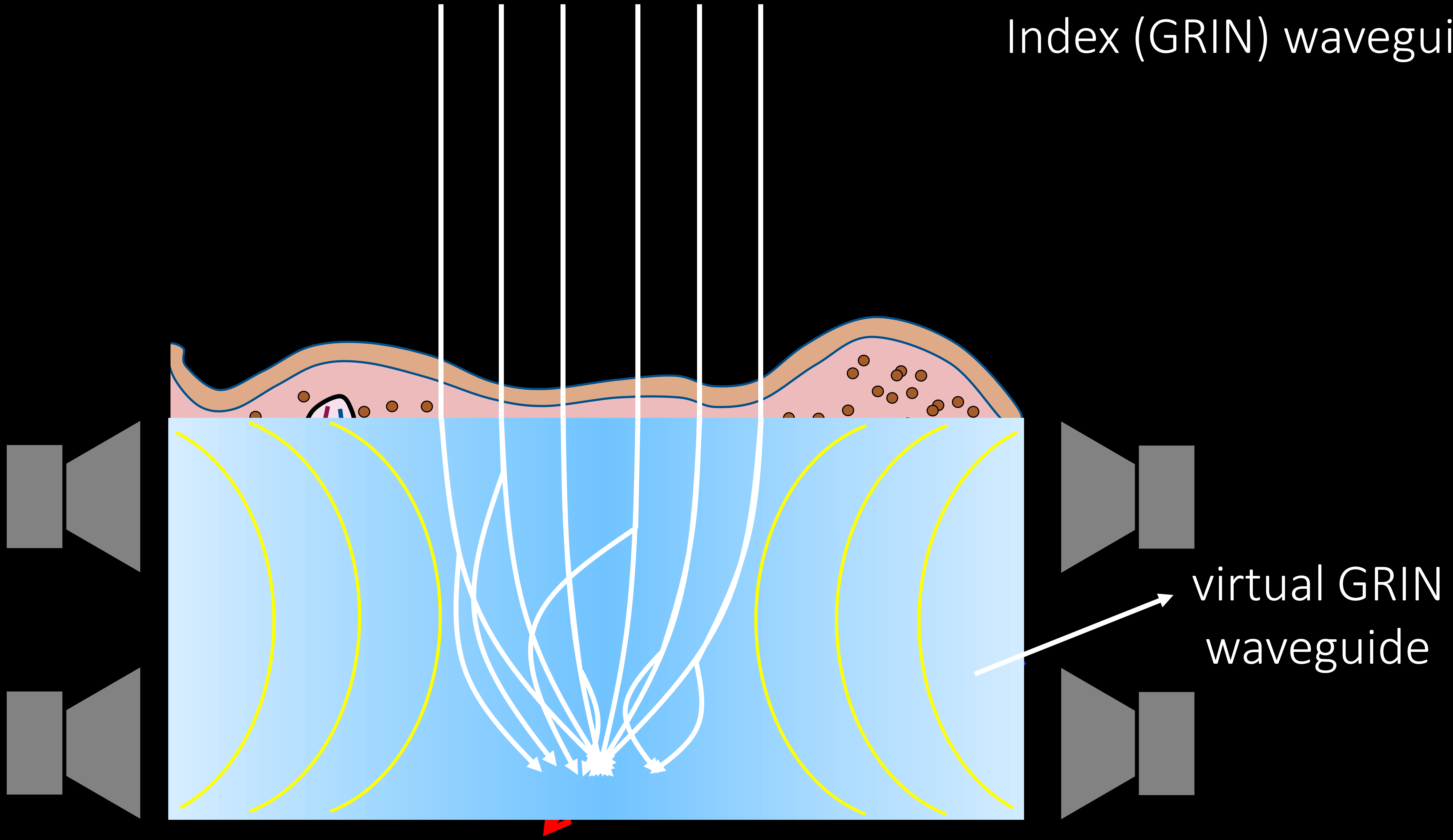

Efficiently explore using rendering

Rendering virtual ultrasonic waveguides

real measurement

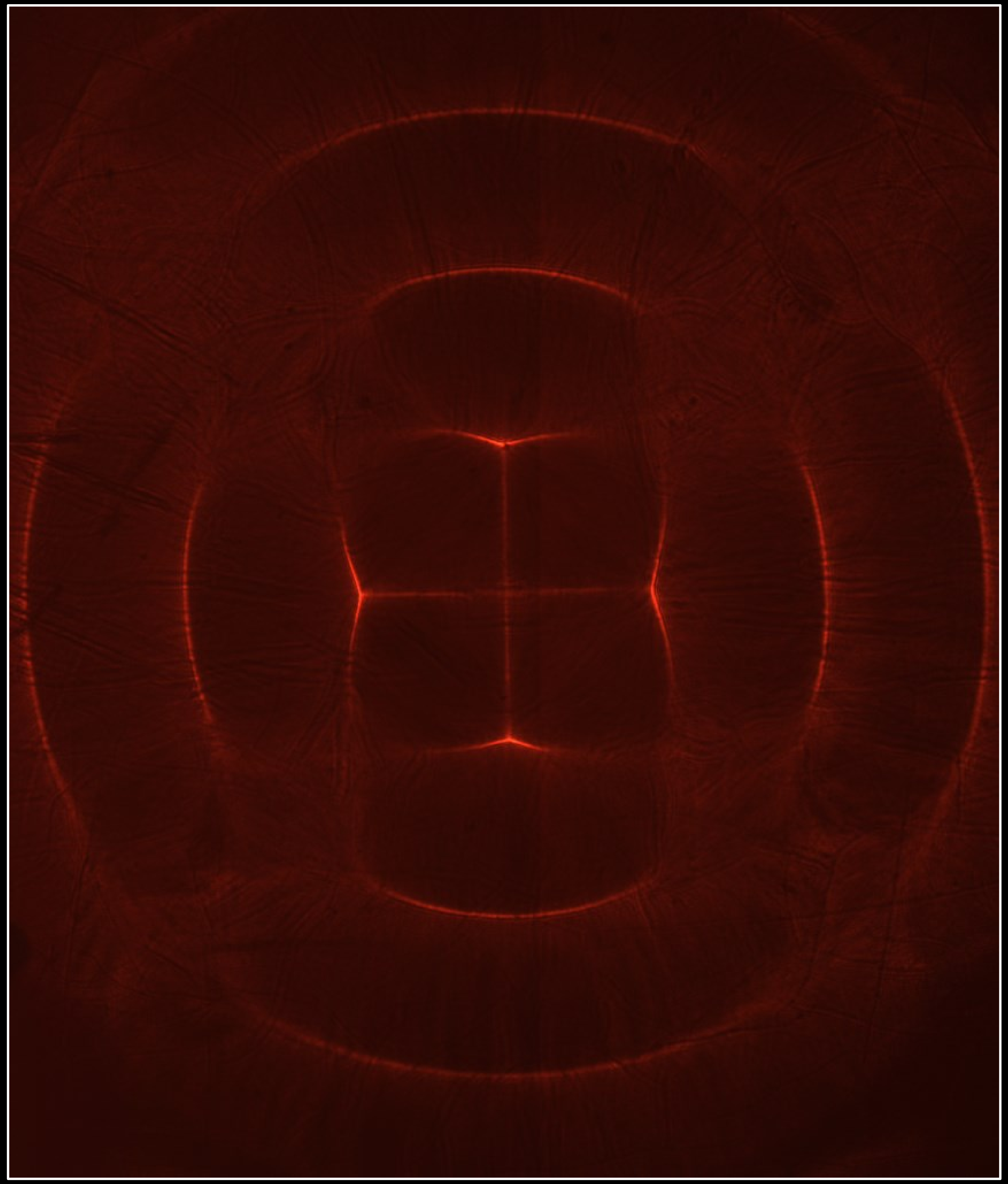

BDPT
(our technique)

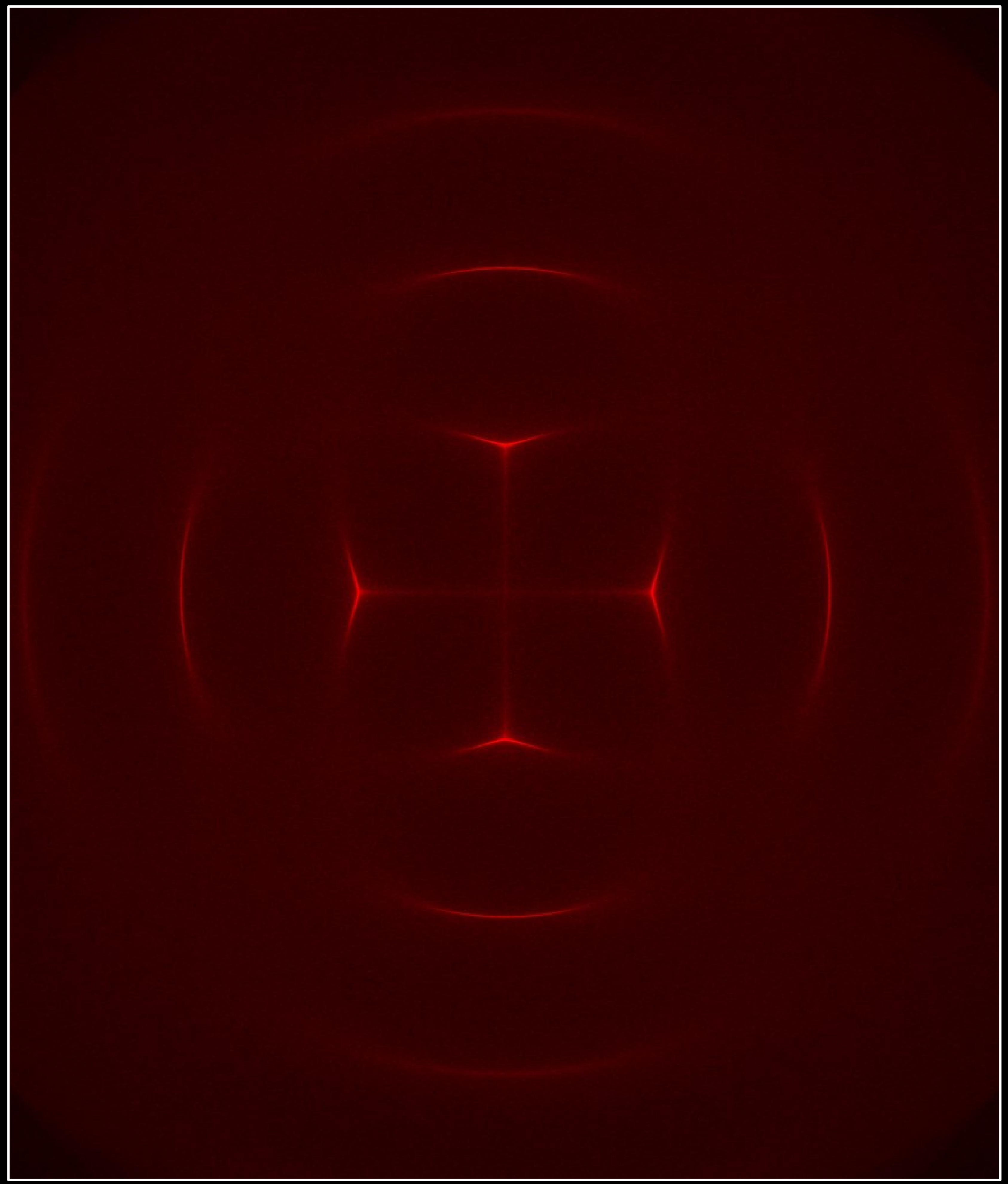

photon mapping
(previous technique)

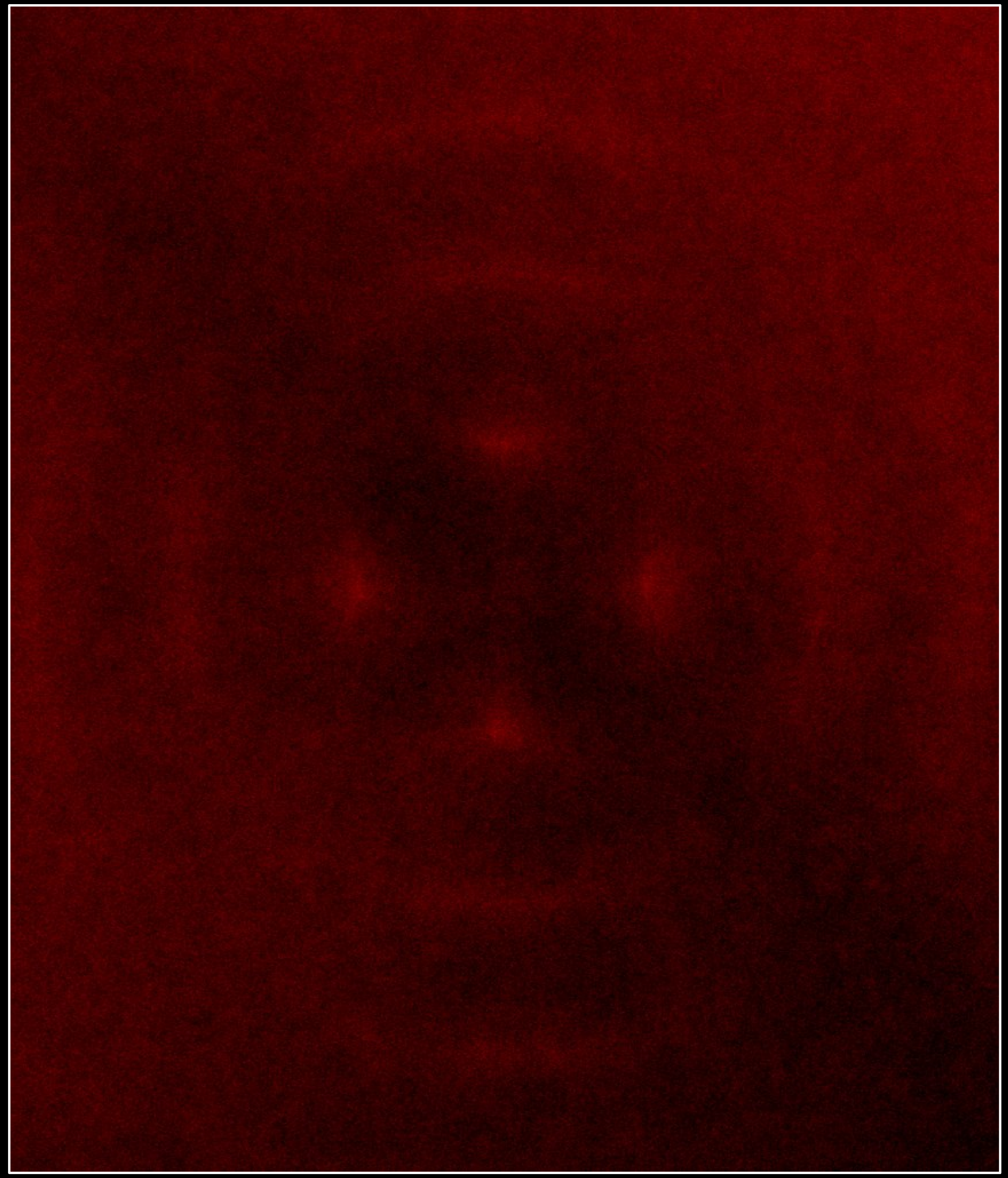

Validation of simulated data

experimental data

first focus

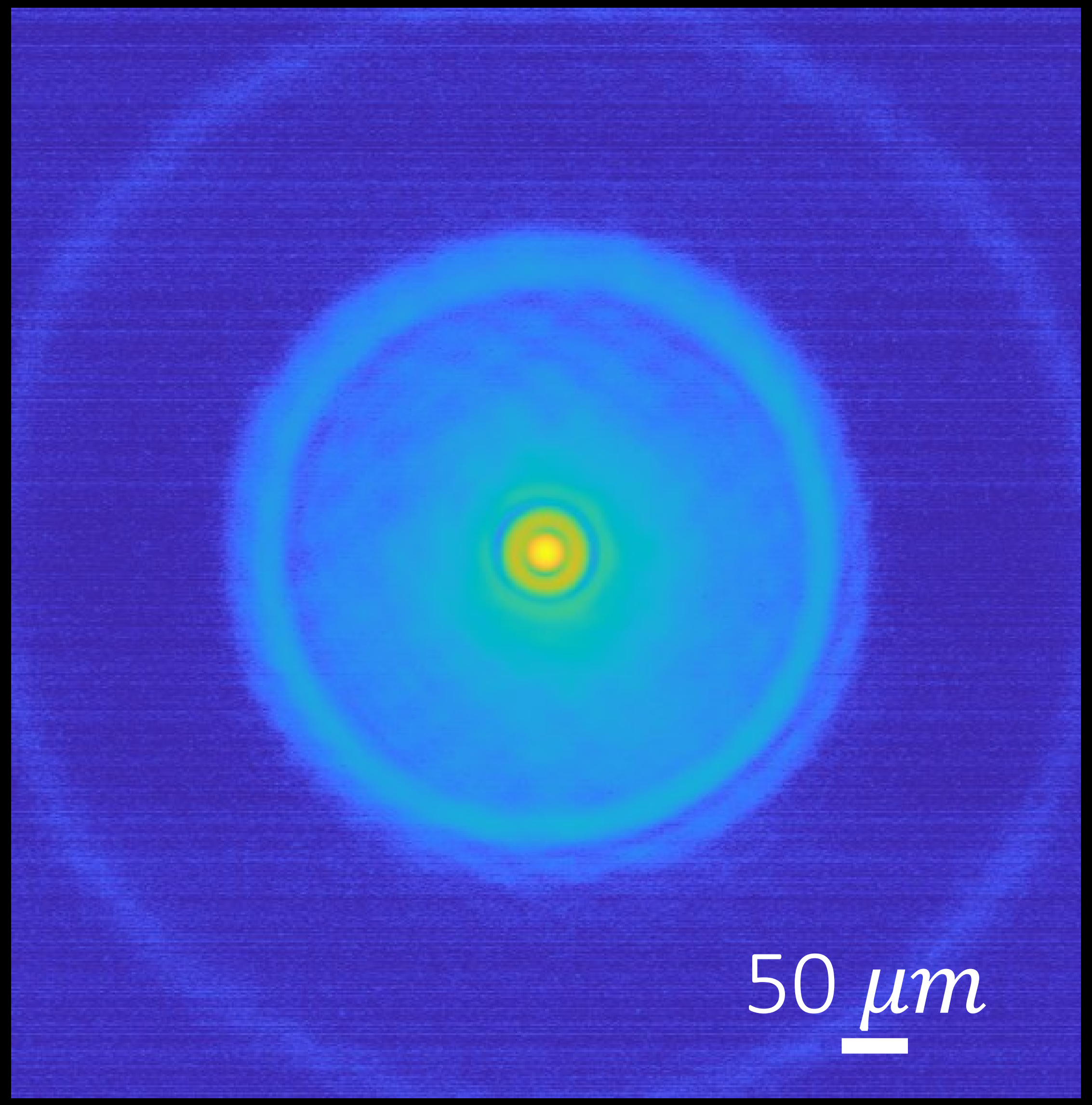

second focus

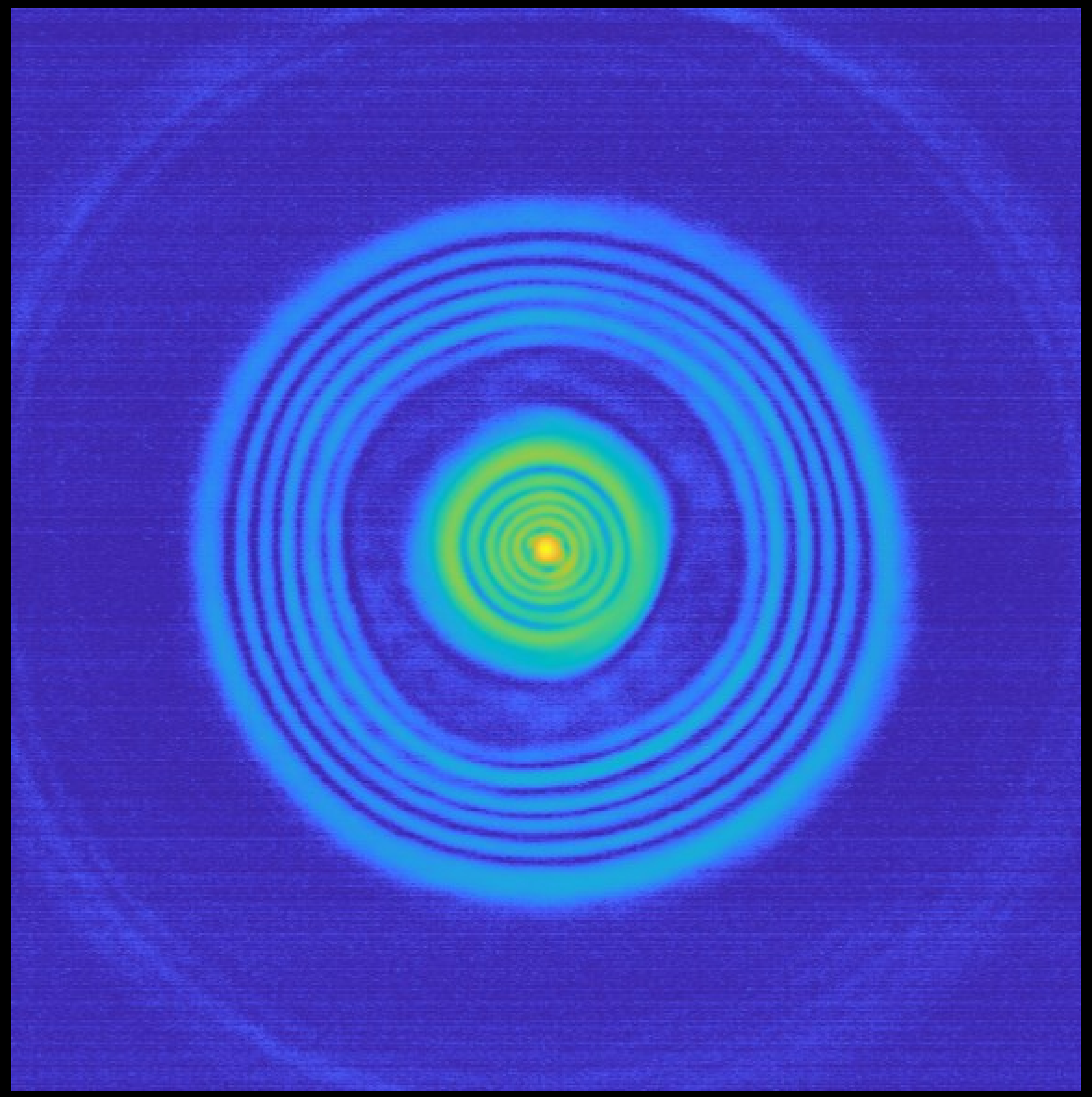

Validation of simulated data

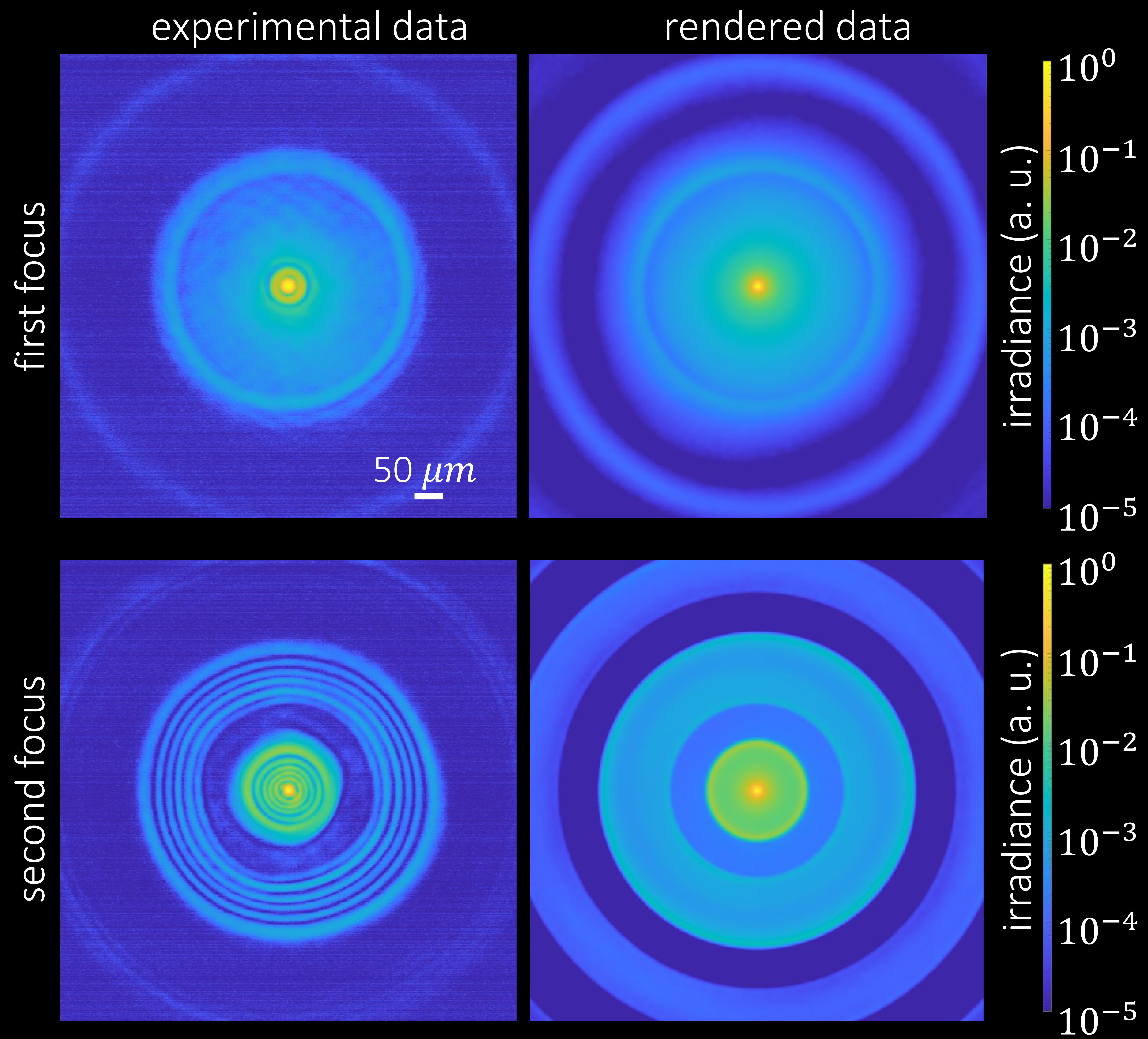

Validation of simulated data

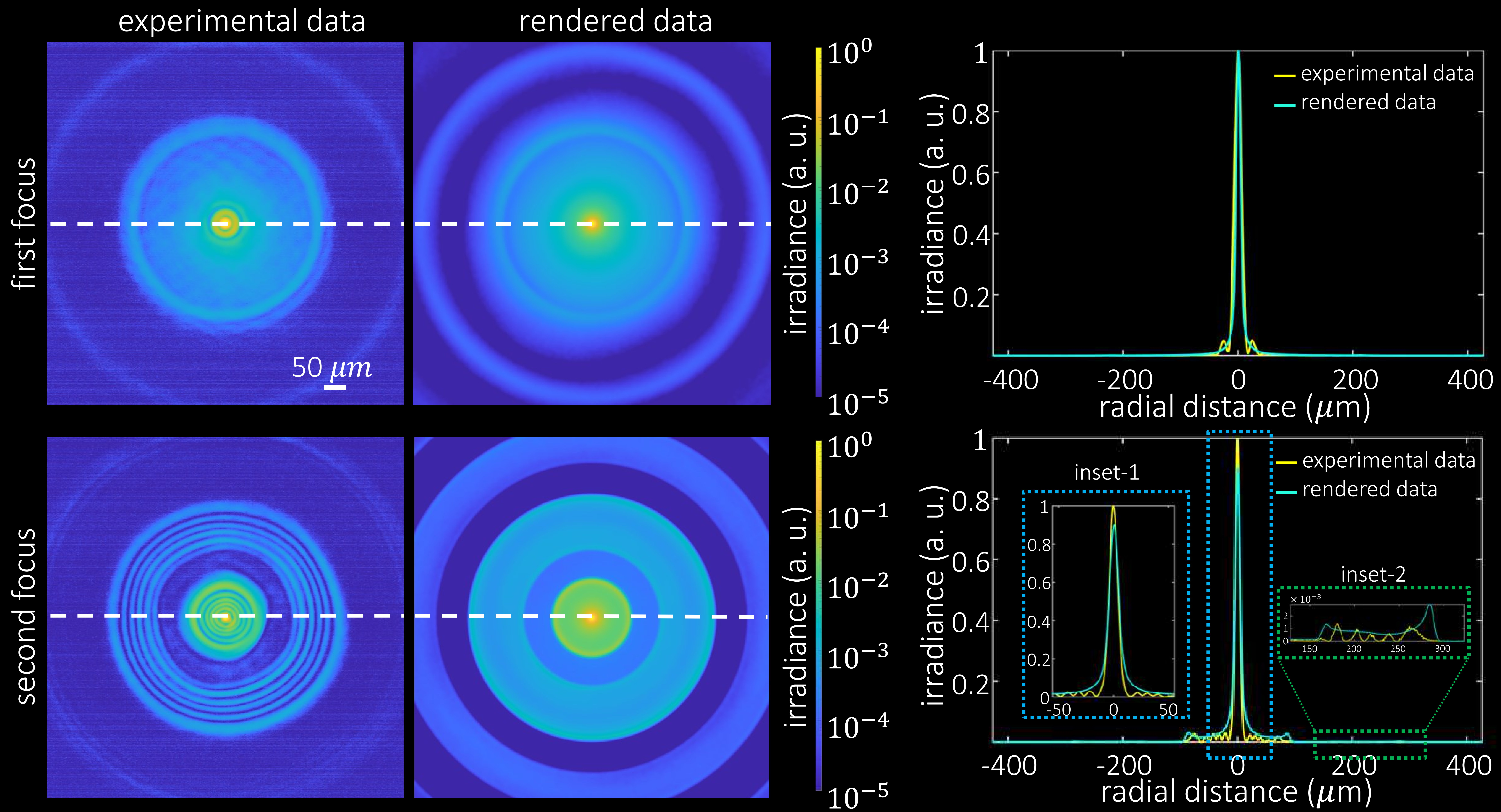

Optimized configurations are better than ideal external lens

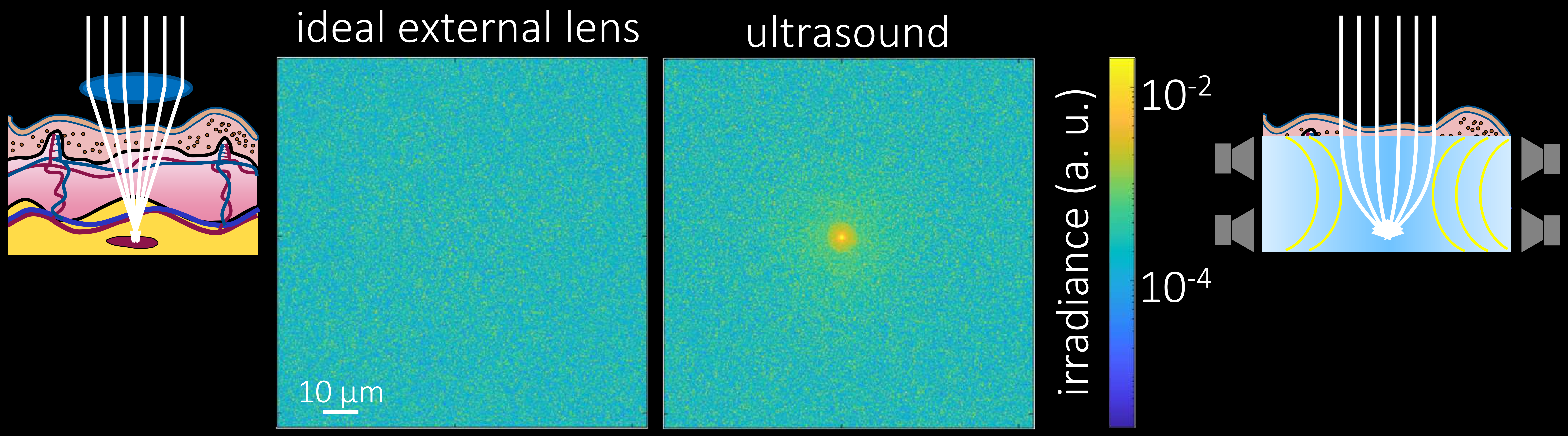

On human bladder (10 scattering lengths, 2.67 mm thick)

- 50% higher focusing performance than external lens.
- 300% higher focusing performance than previous designs.

On brain tissue (50 scattering lengths, 7.5 mm thick)

- 15% higher focusing performance than external lens.
- Experimentally validated on tissue phantoms.

[Pediredla et al., to appear in Nature Communications]

Optimized configurations are better than ideal external lens

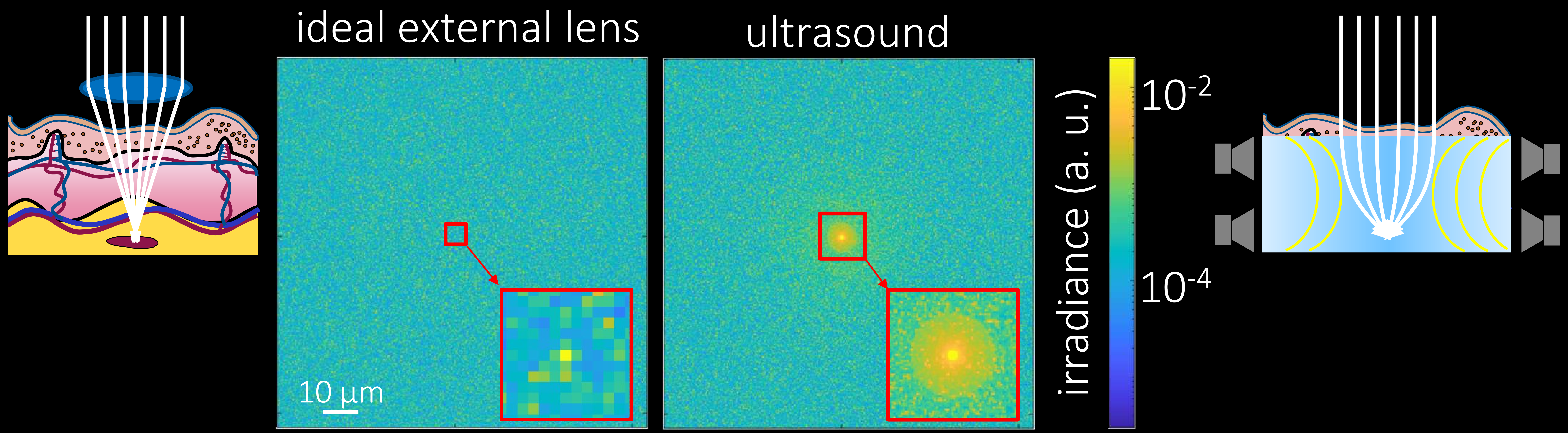

On human bladder (10 scattering lengths, 2.67 mm thick)

- 50% higher focusing performance than external lens.
- 300% higher focusing performance than previous designs.

On brain tissue (50 scattering lengths, 7.5 mm thick)

- 15% higher focusing performance than external lens.
- Experimentally validated on tissue phantoms.

[Pediredla et al., to appear in Nature Communications]

Physics-based rendering and its applications to computational imaging

forward rendering

- accurate and efficient simulation
- virtually design sensors, optics, and algorithms

inverse rendering

- accurate and efficient differentiable simulation
- tractably solve general inverse problems

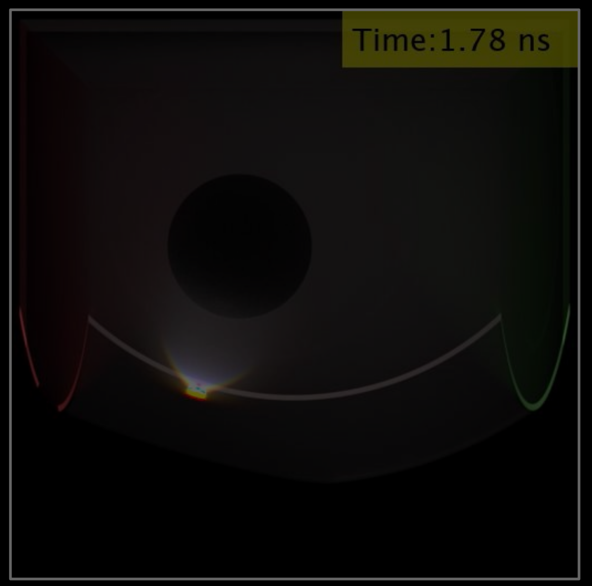

time-of-flight imaging

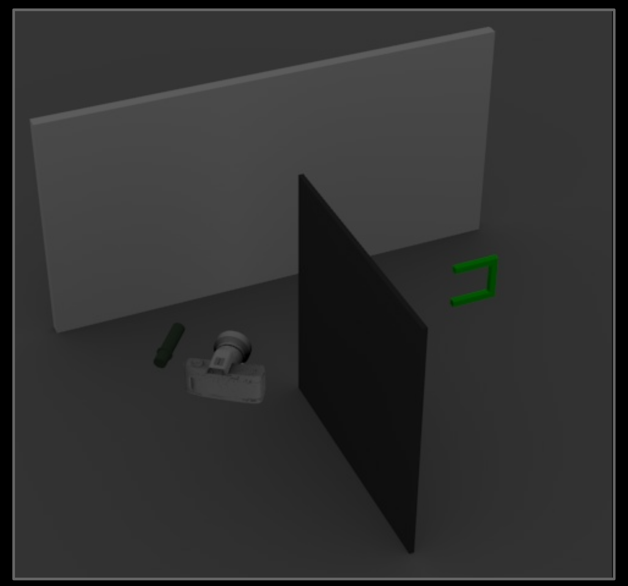

non-line-of-sight imaging

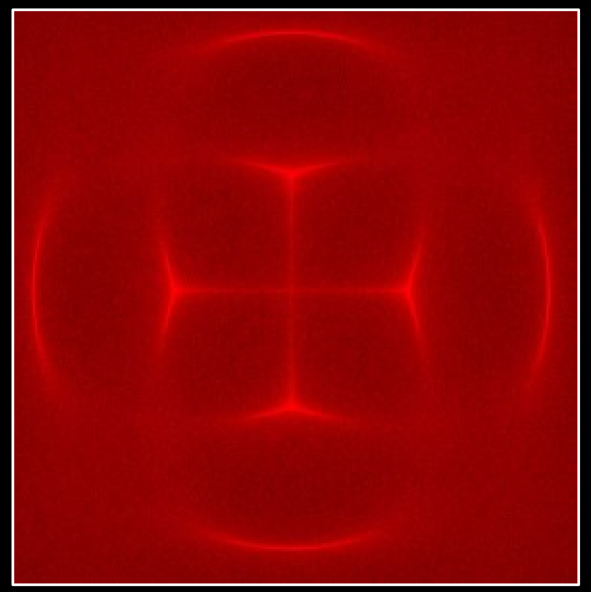

acousto-optic lensing

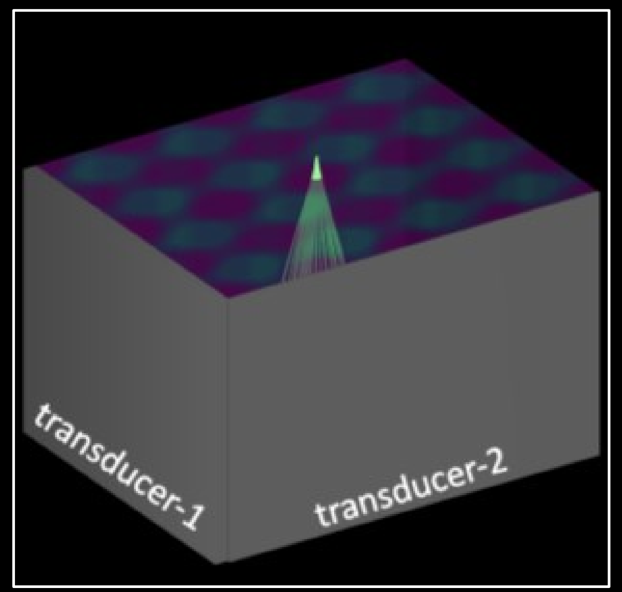

ultrafast light scanning

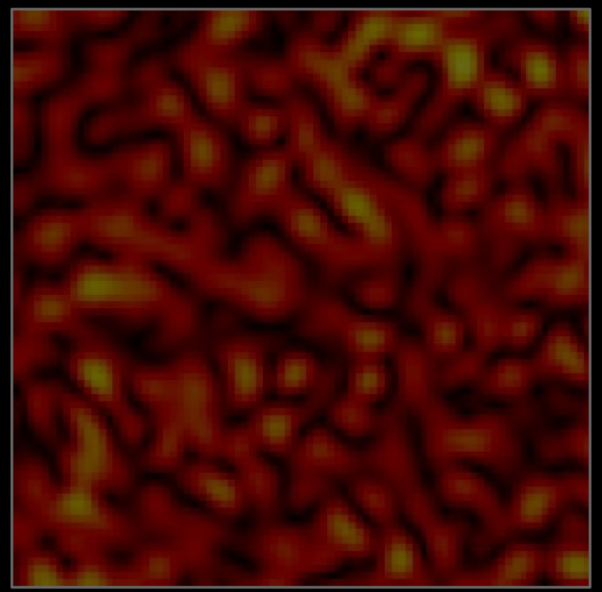

speckle imaging

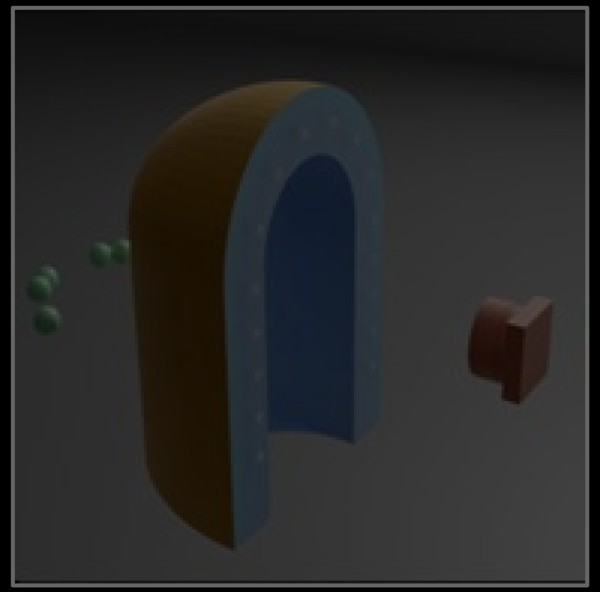

tactile sensor design

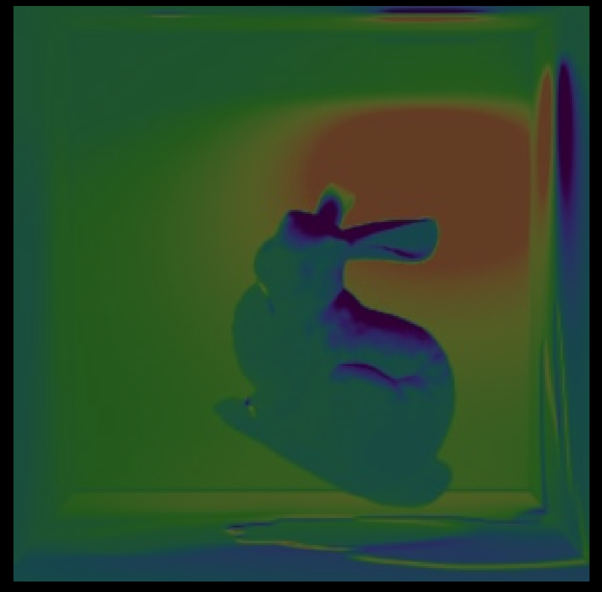

differentiable renderer

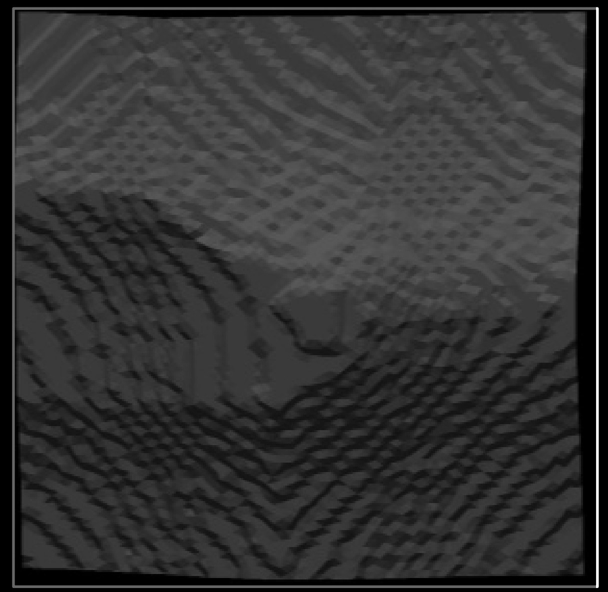

inverse problems

scanning with galvos (1 kHz) is slow due to moving parts

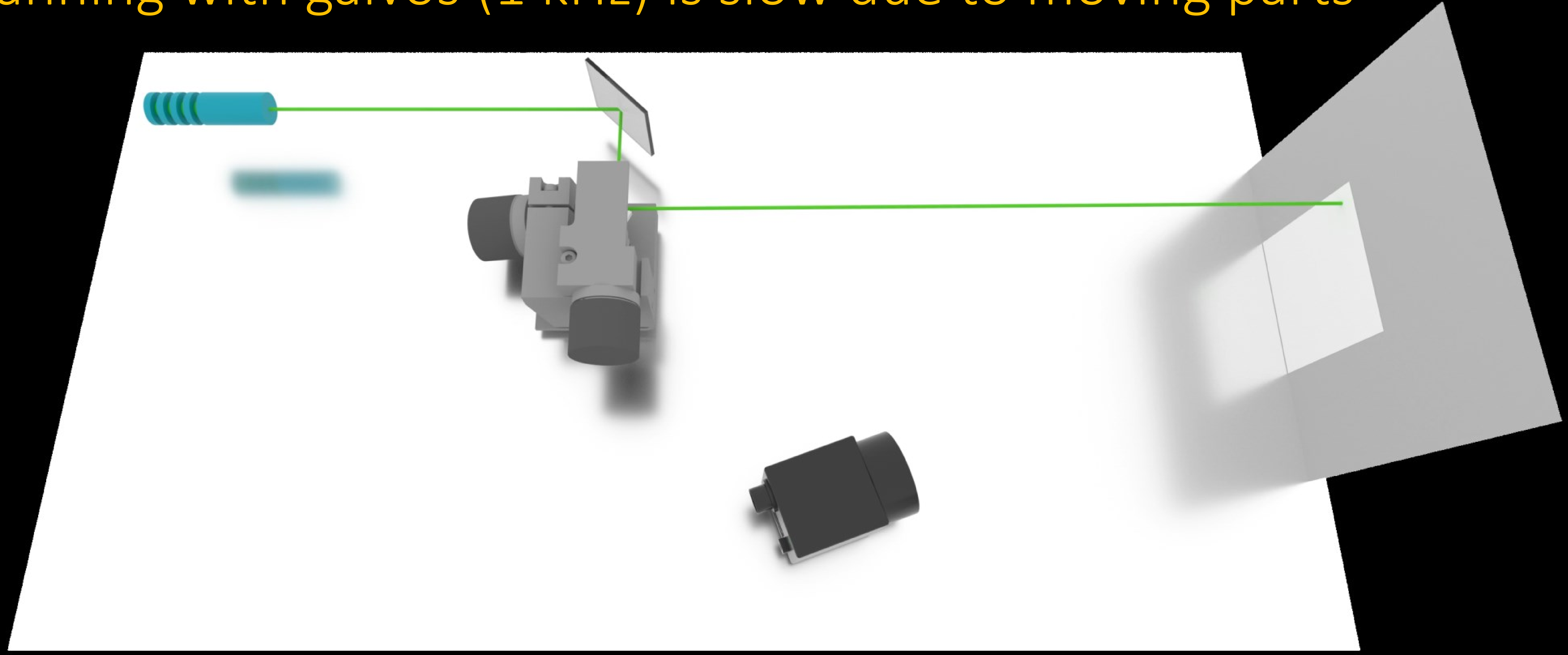

projector

microscopy

lidar

our scanning technique (1MHZ) is fast without moving parts

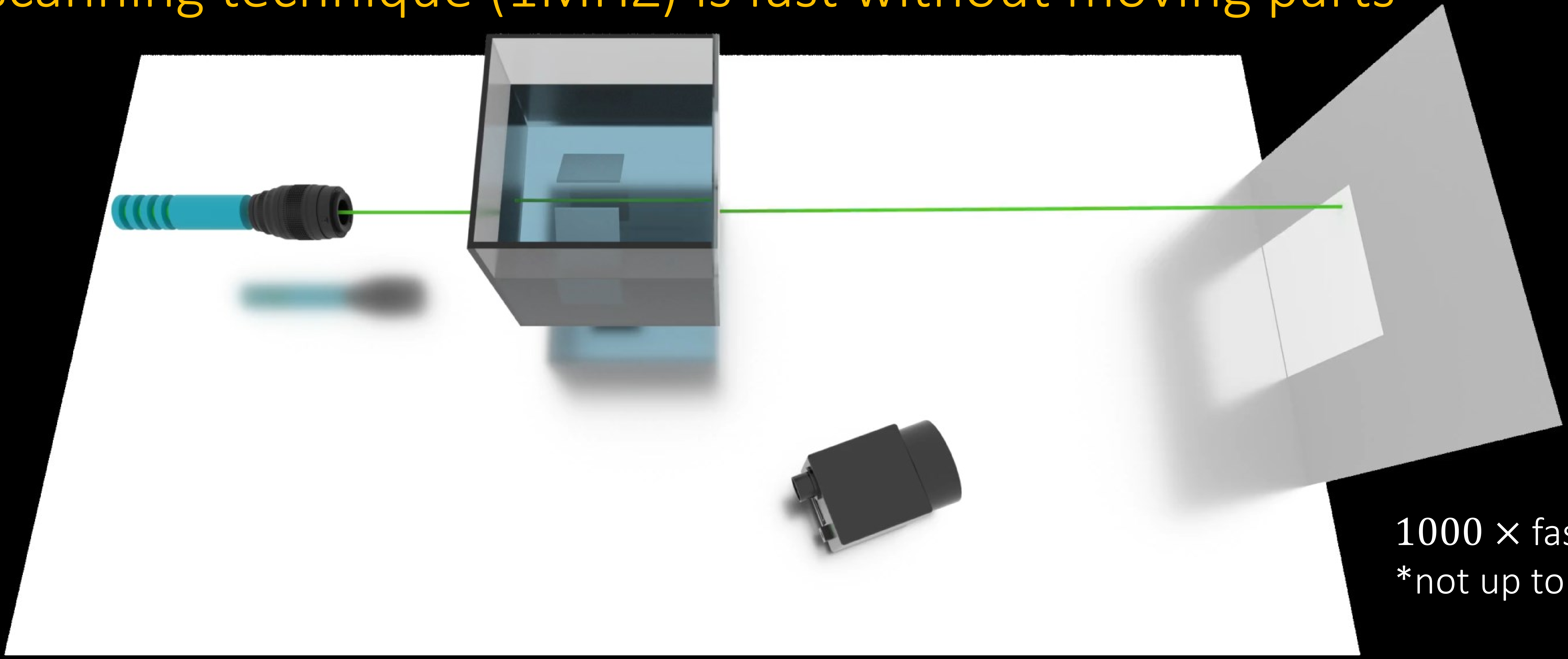

1000 × faster
*not up to scale

projector

microscopy

lidar

our scanning technique (1MHZ) is fast without moving parts

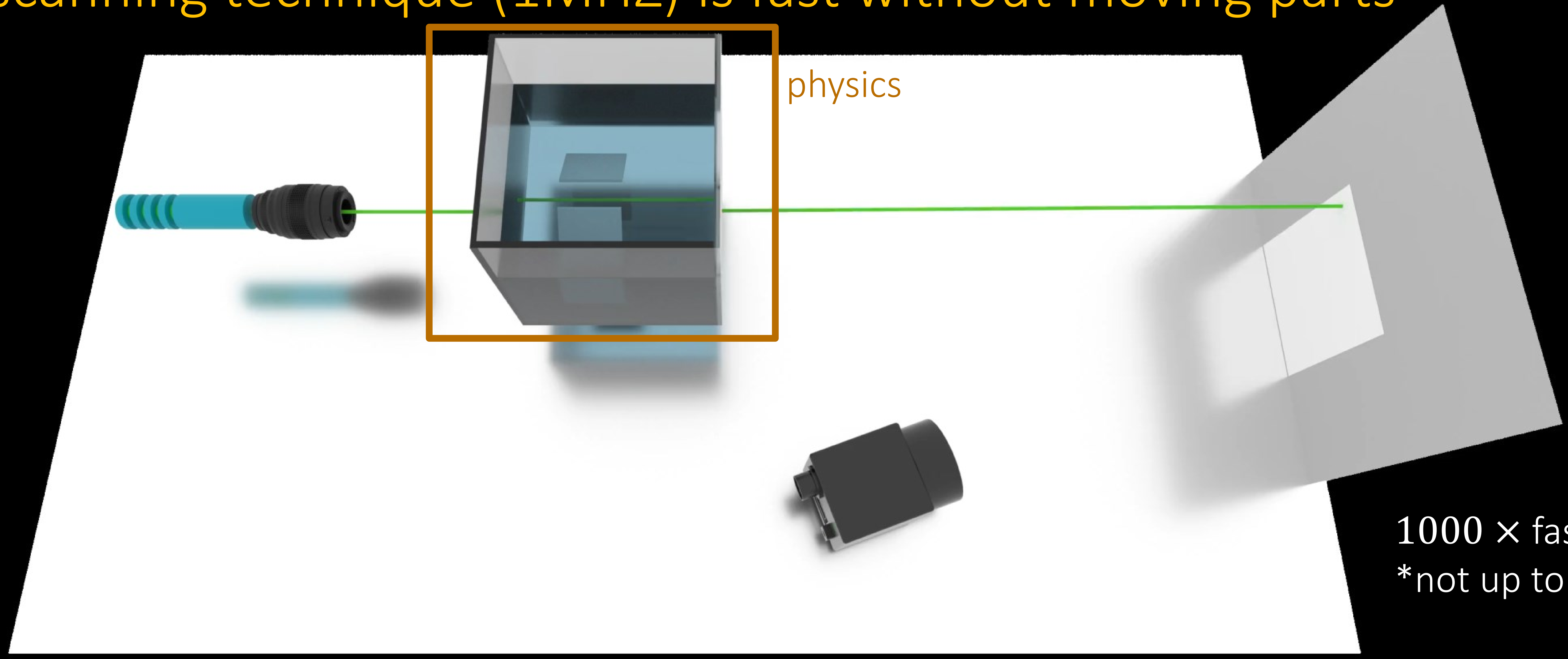

1000 × faster
*not up to scale

projector

microscopy

lidar

our scanning technique (1MHZ) is fast without moving parts

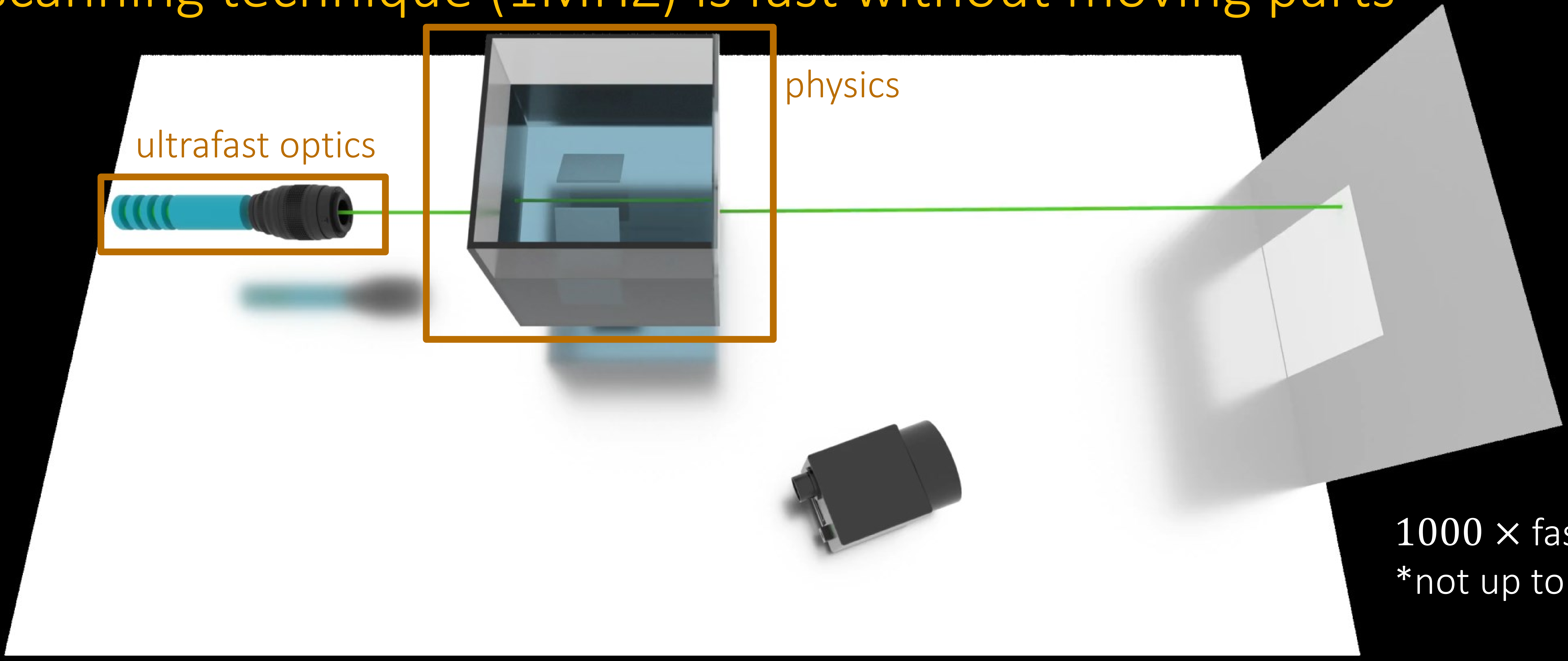

1000 × faster
*not up to scale

projector

microscopy

lidar

our scanning technique (1MHZ) is fast without moving parts

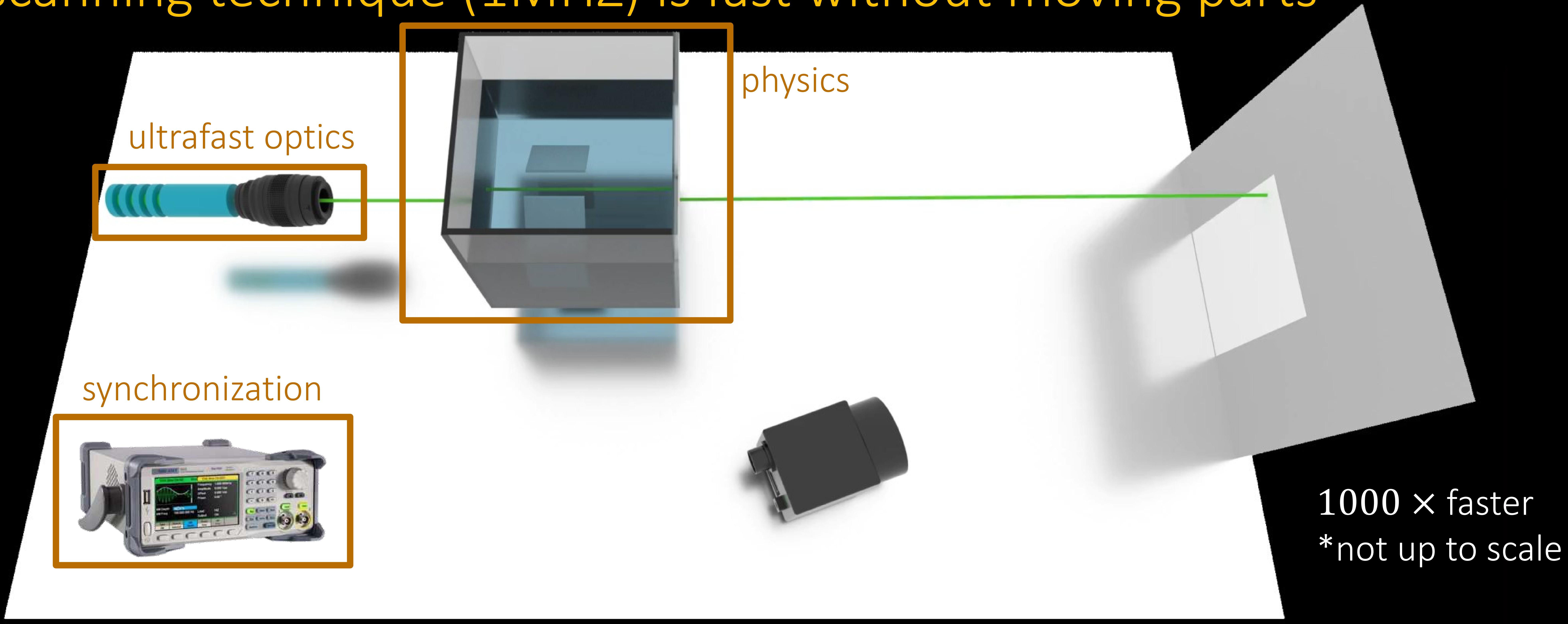

projector

microscopy

lidar

our scanning technique (1MHZ) is fast without moving parts

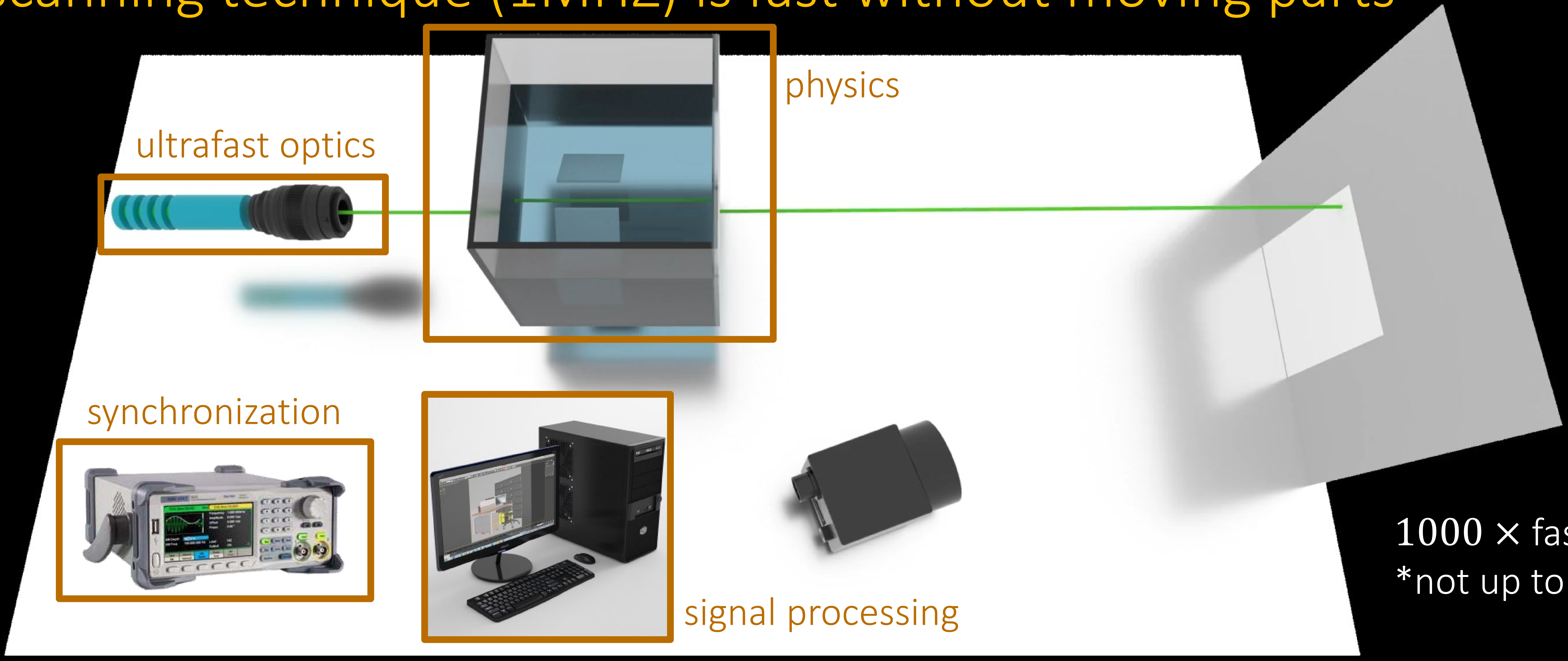

1000 × faster
*not up to scale

projector

microscopy

lidar

Physics sound, light, and matter interaction

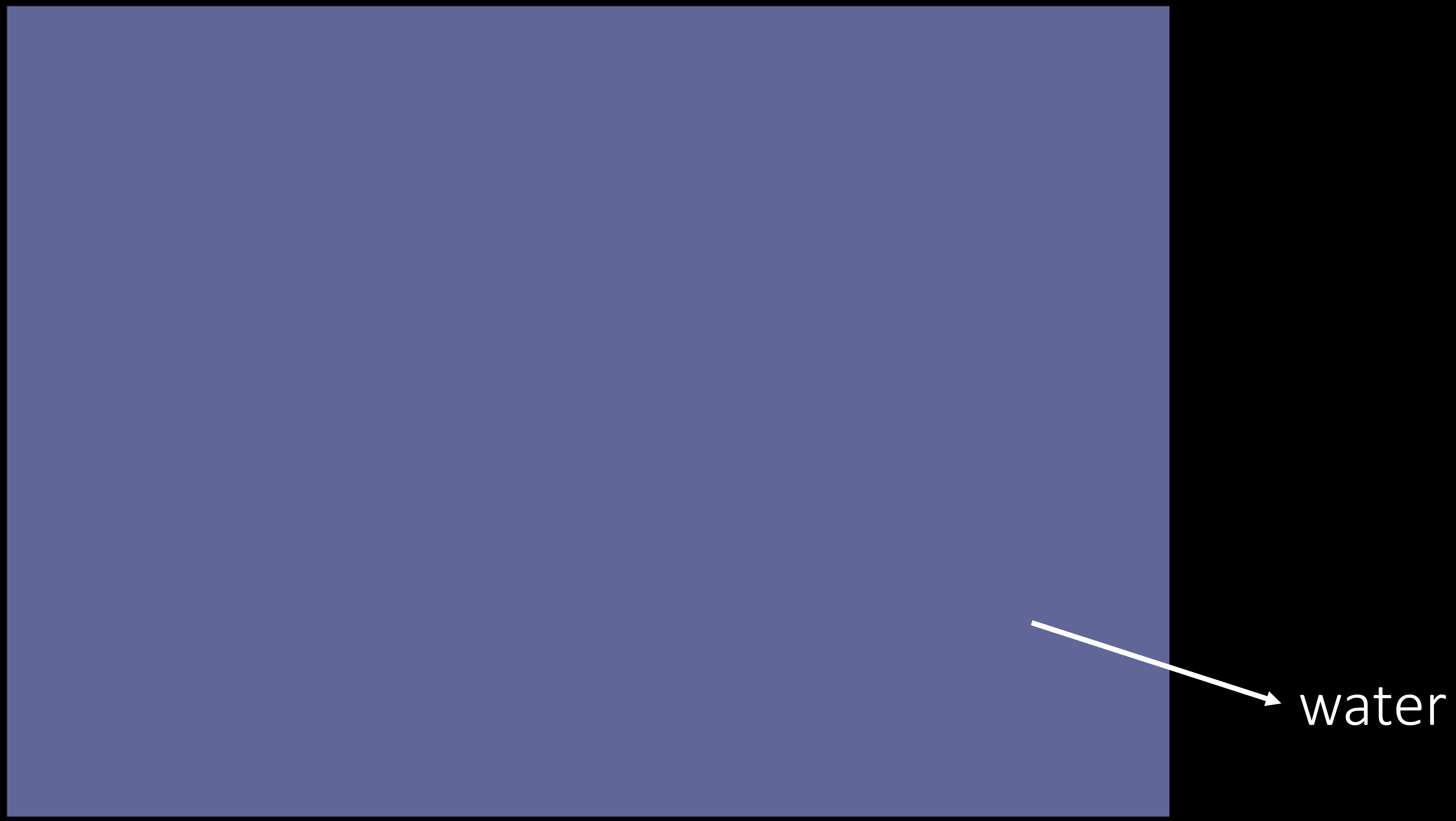

2D visualization

Physics sound, light, and matter interaction

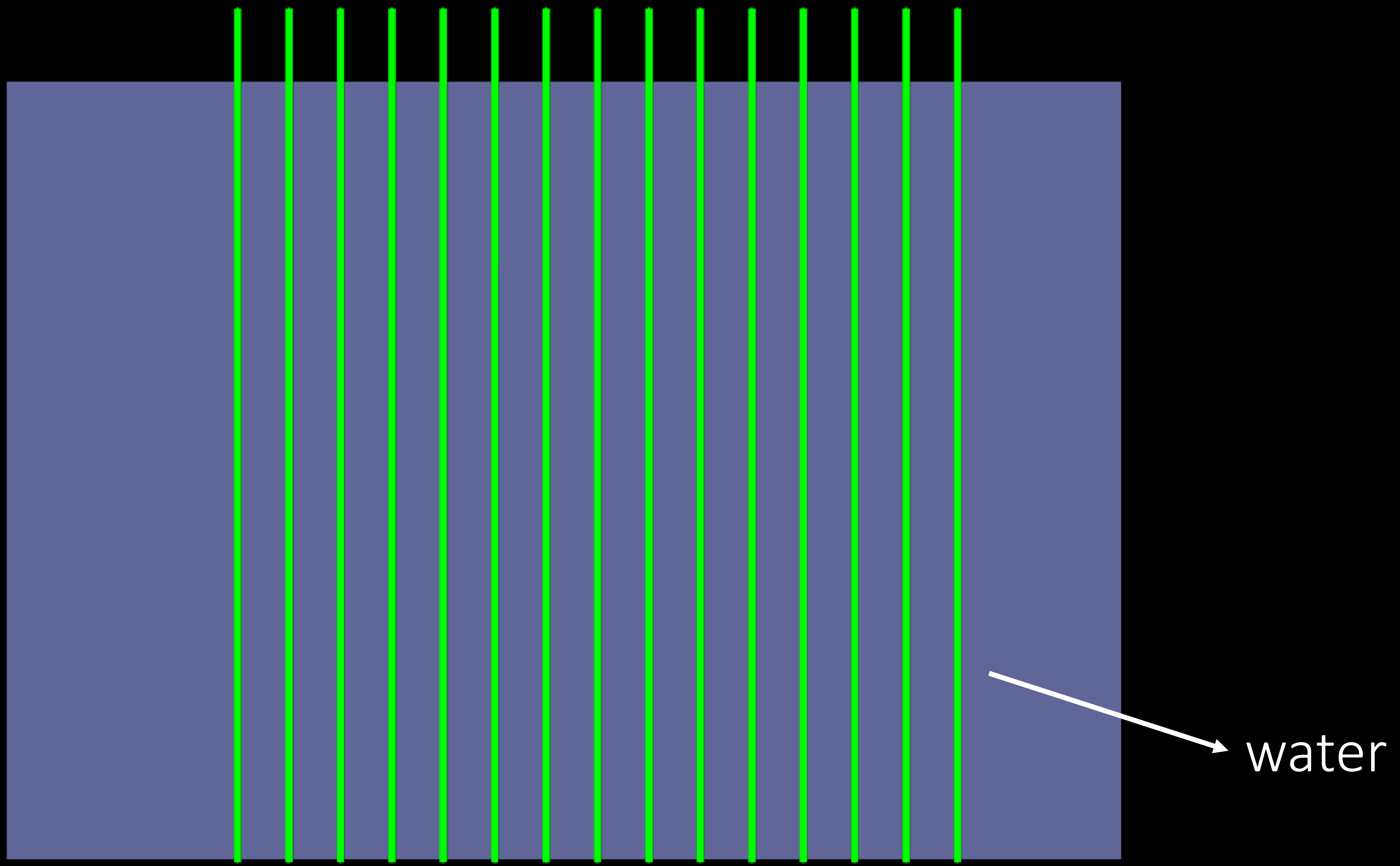

2D visualization

Physics sound, light, and matter interaction

2D visualization

Physics sound, light, and matter interaction

nm scale

(exaggerated)

2D visualization

Physics sound, light, and matter interaction

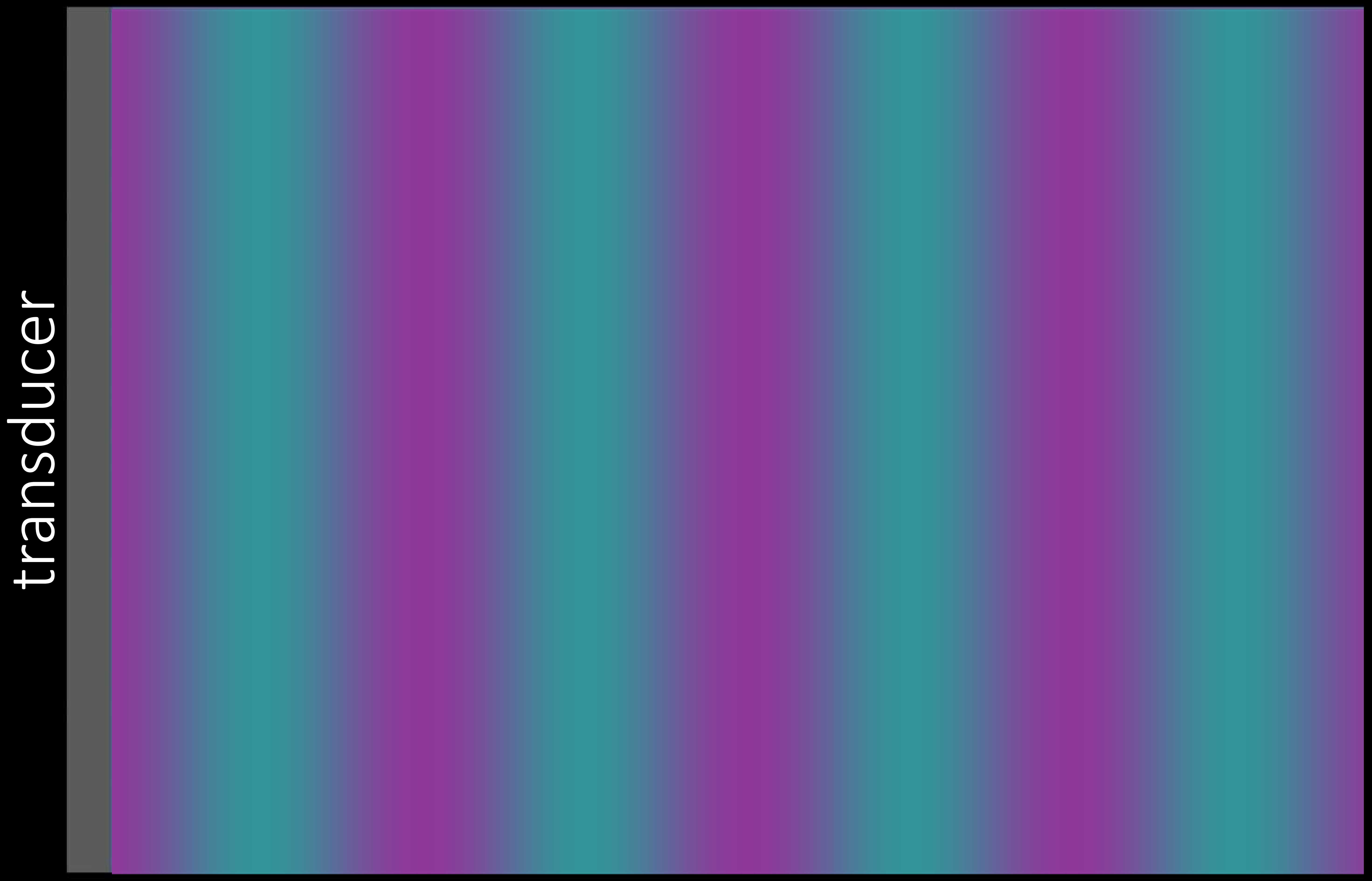

2D visualization

Physics sound, light, and matter interaction

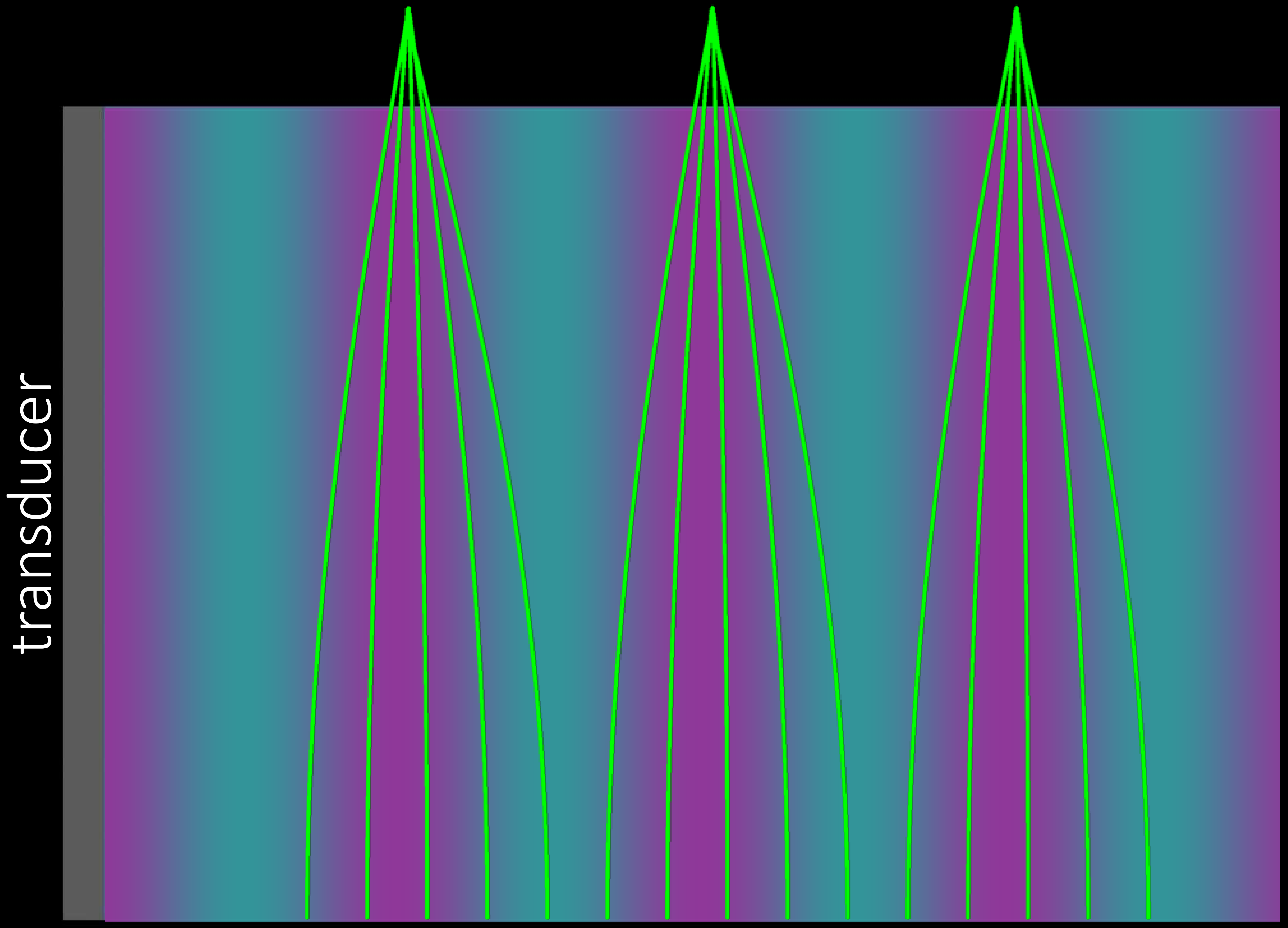

2D visualization

Physics sound, light, and matter interaction

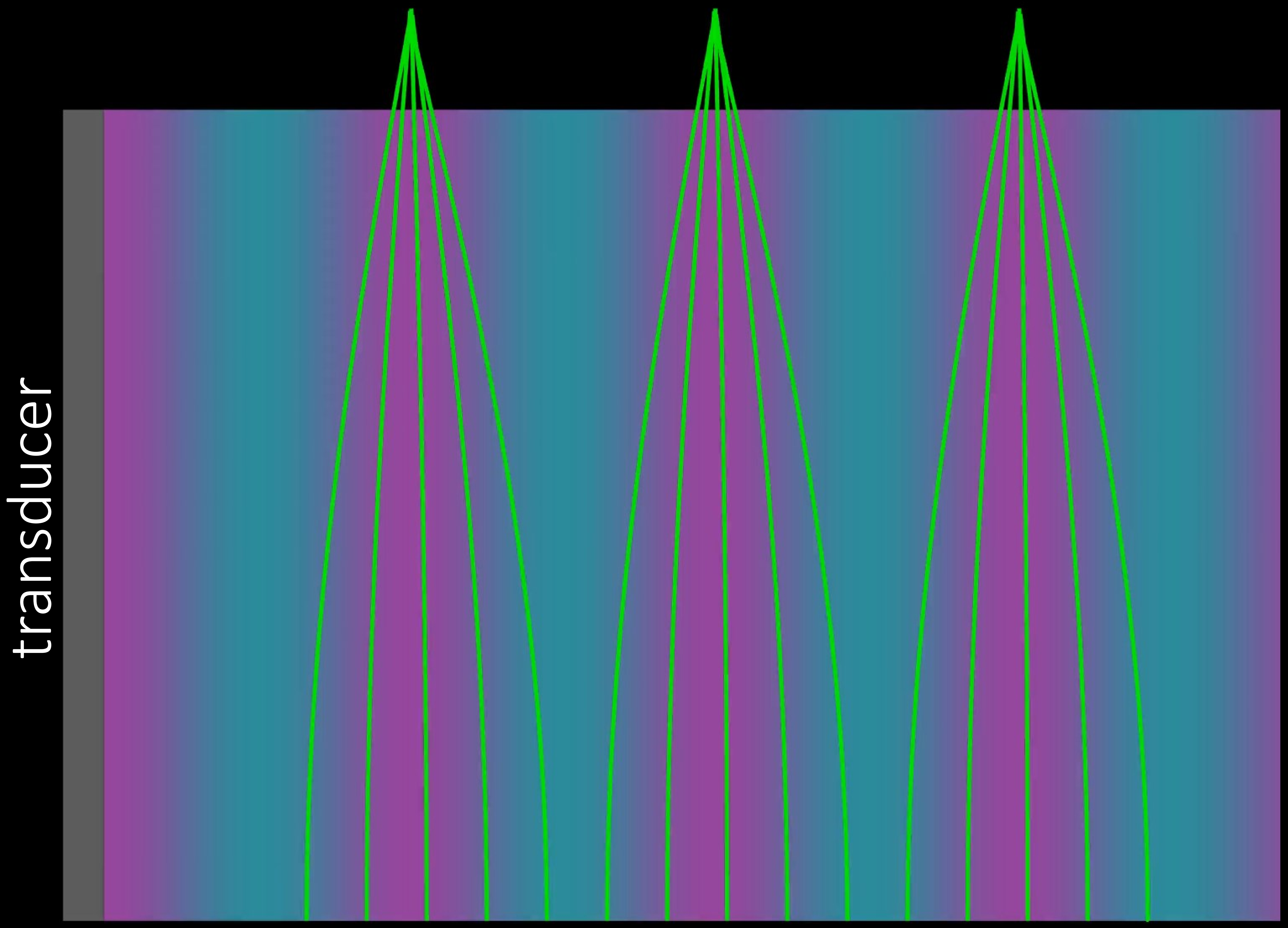

focus travels at the speed of 1.5 kmps

2D visualization

Ultrafast optics and synchronization

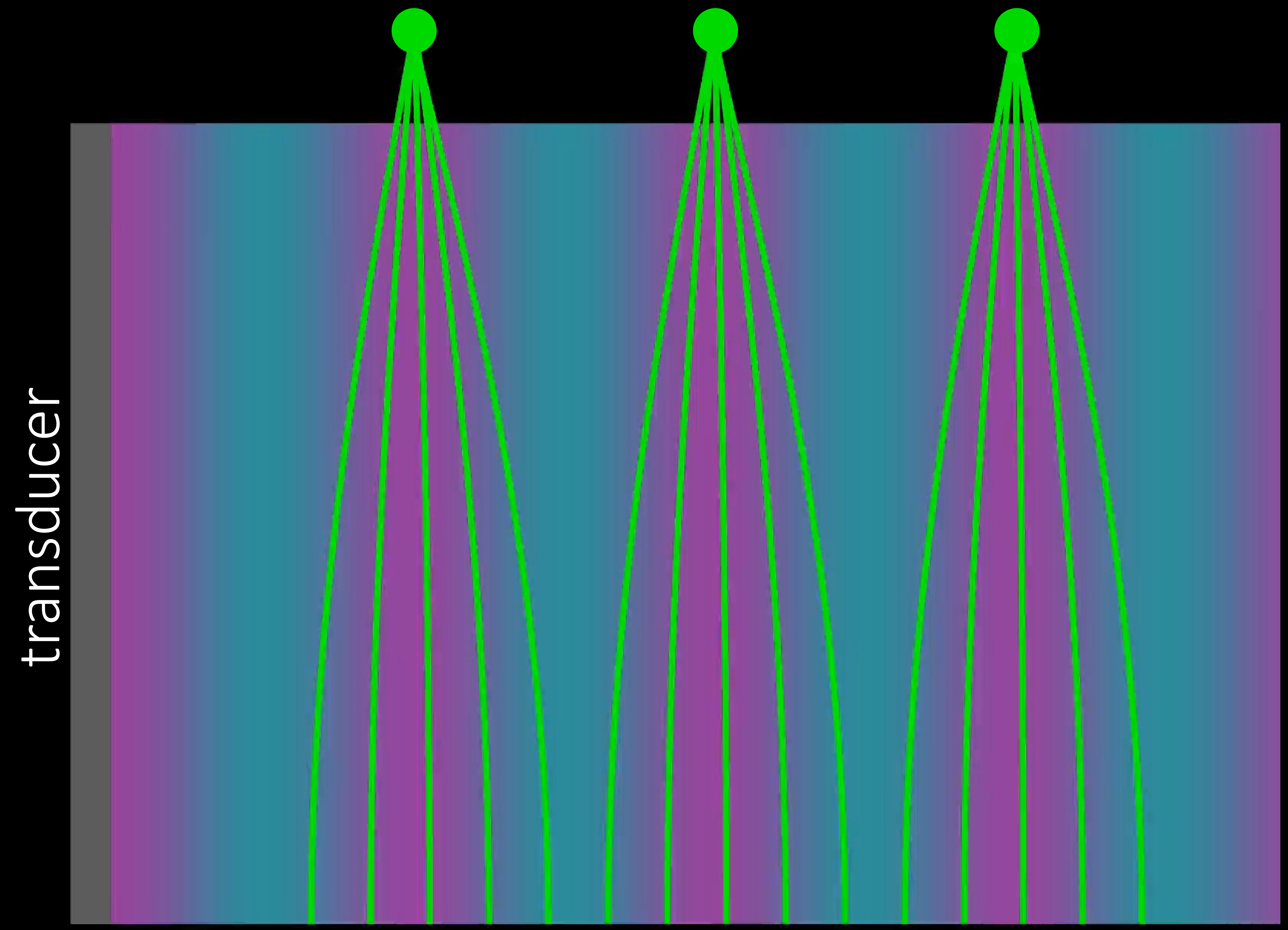

ultrafast synchronized optics that illuminates same spot

2D visualization

Ultrafast optics and synchronization

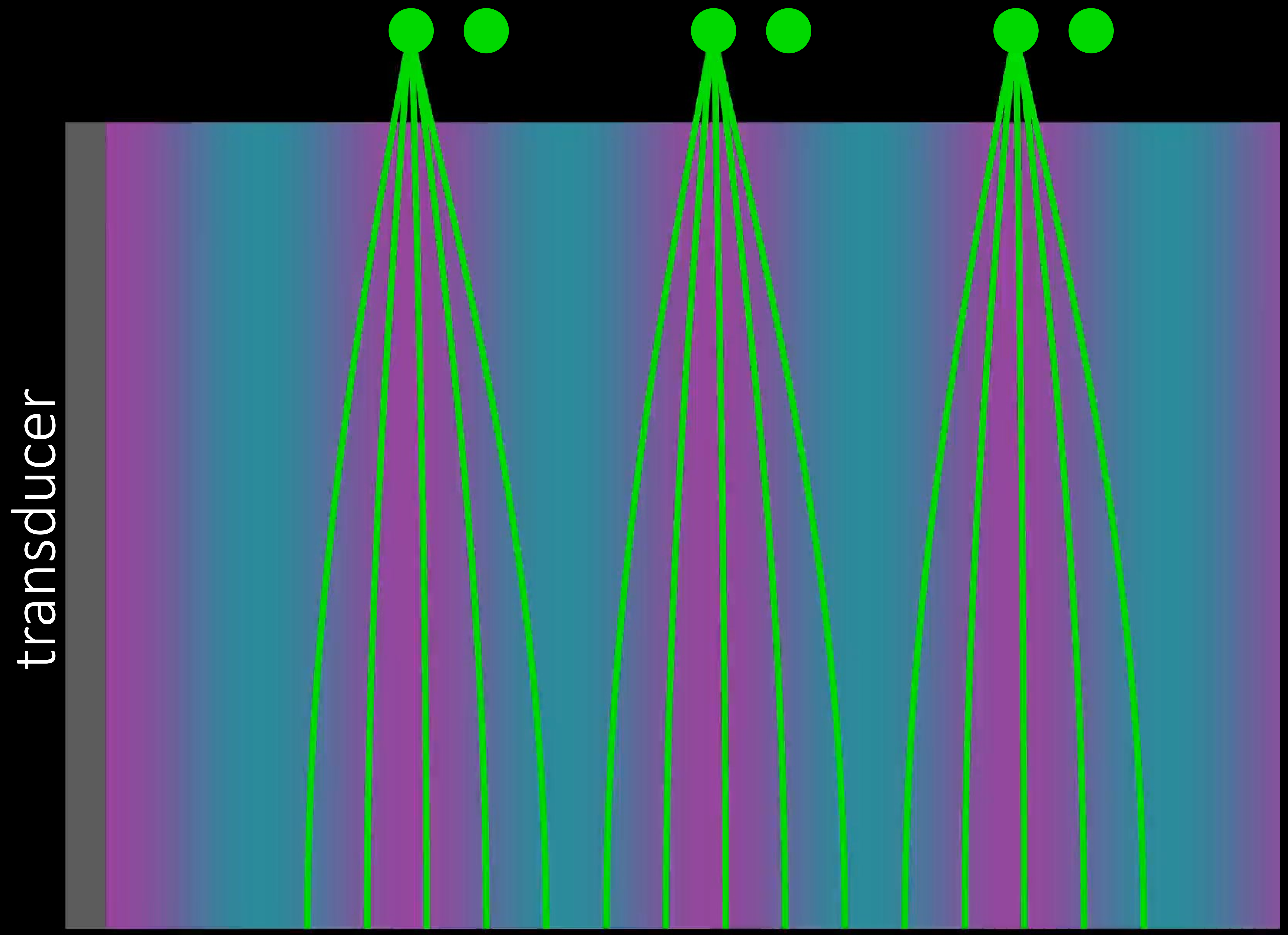

illuminating two spots per cycle

2D visualization

Dot projector

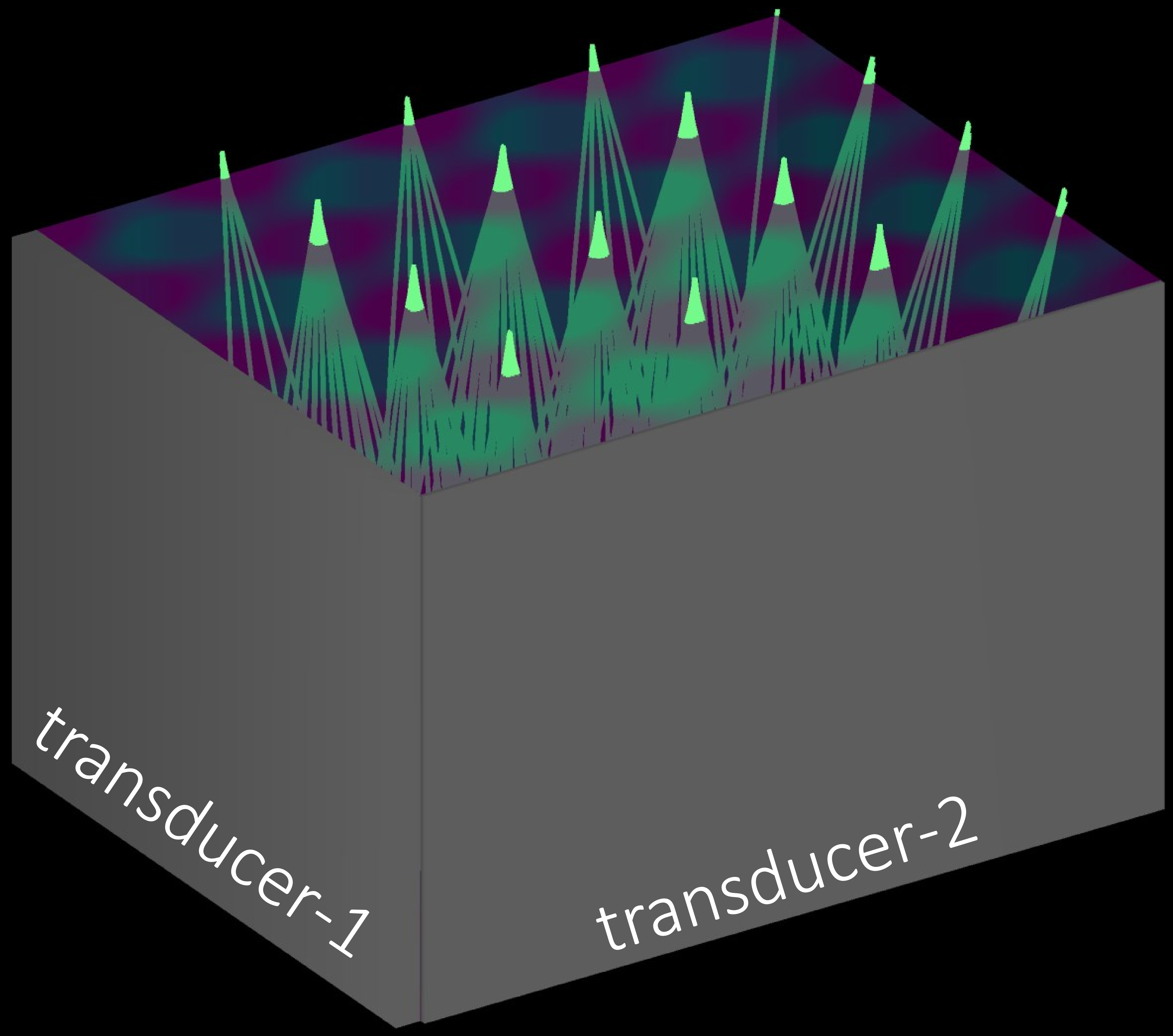

2D visualization

Dot projector

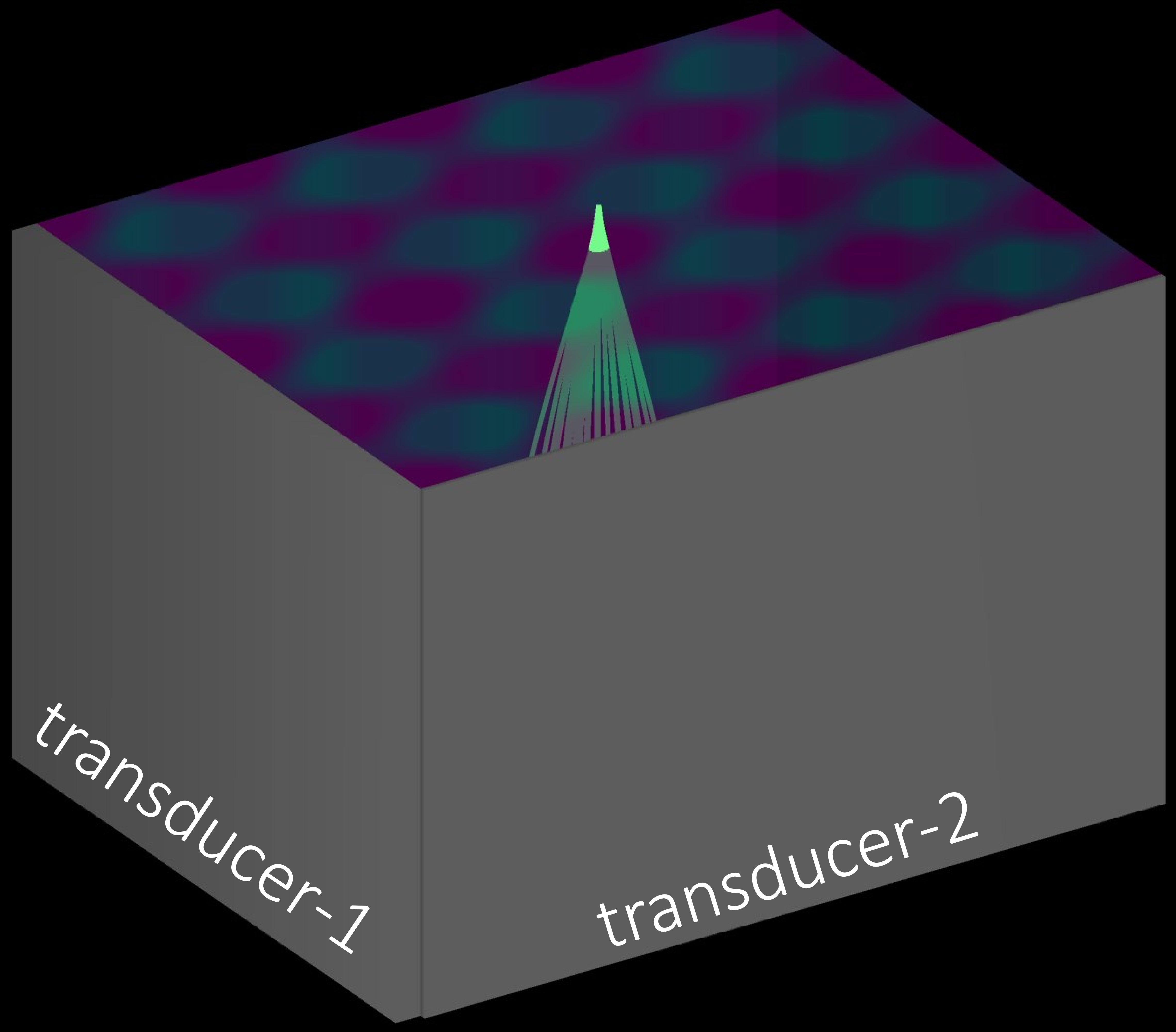

2D visualization

Dot projector

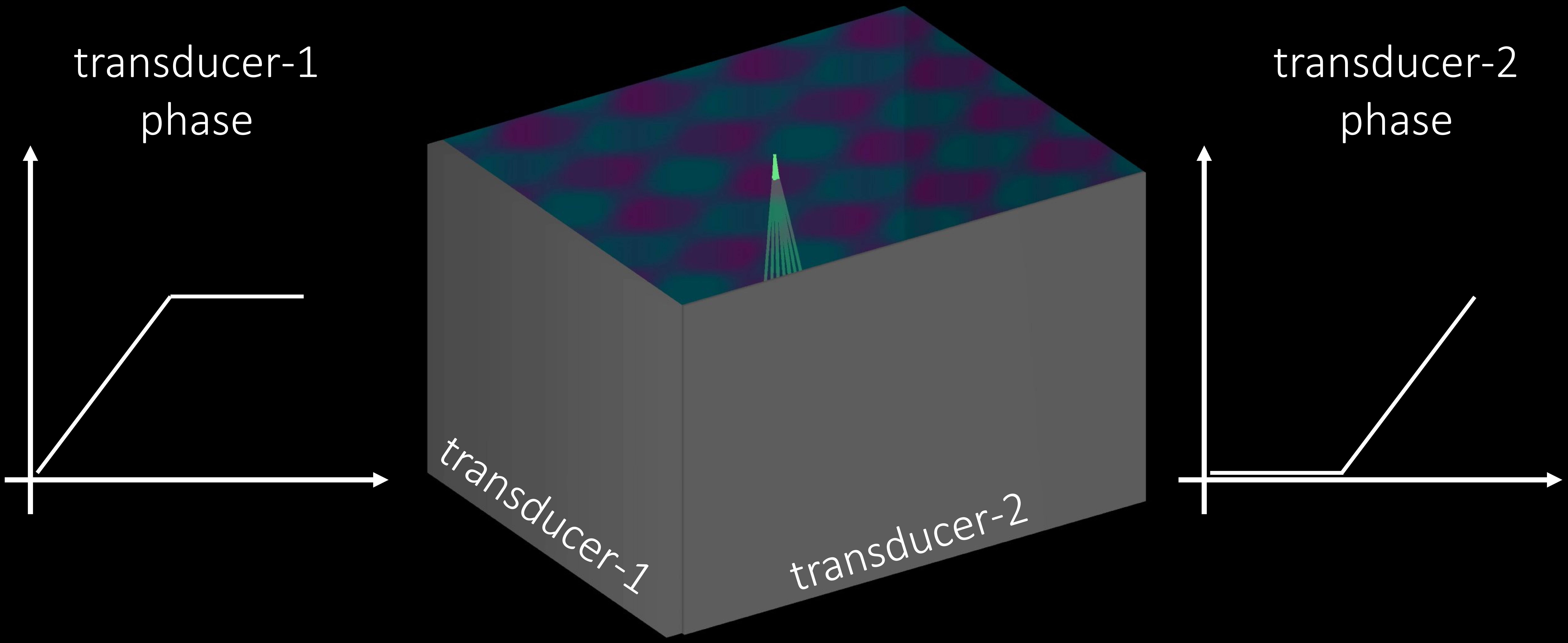

Hardware experiments

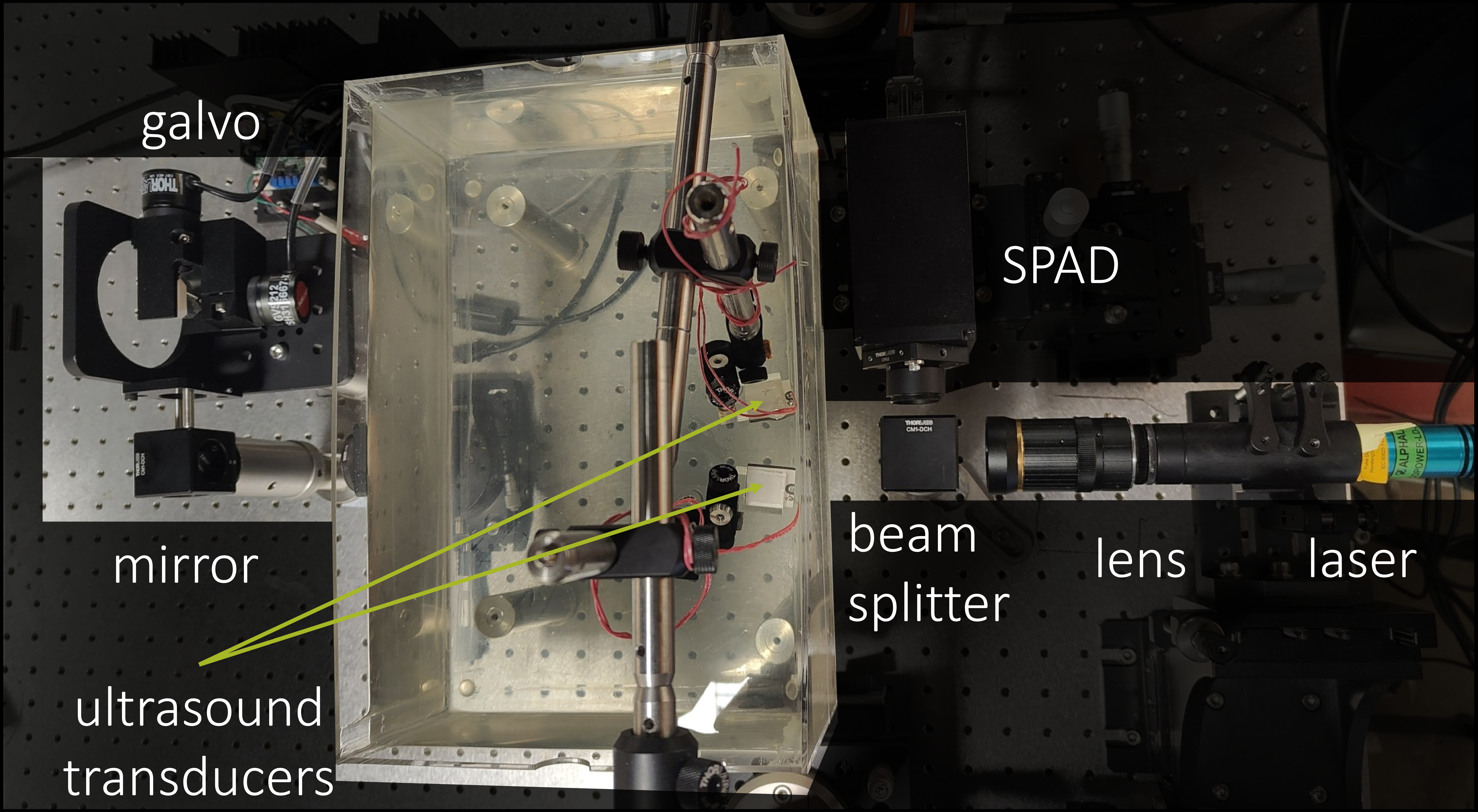

Renderer vs. Hardware

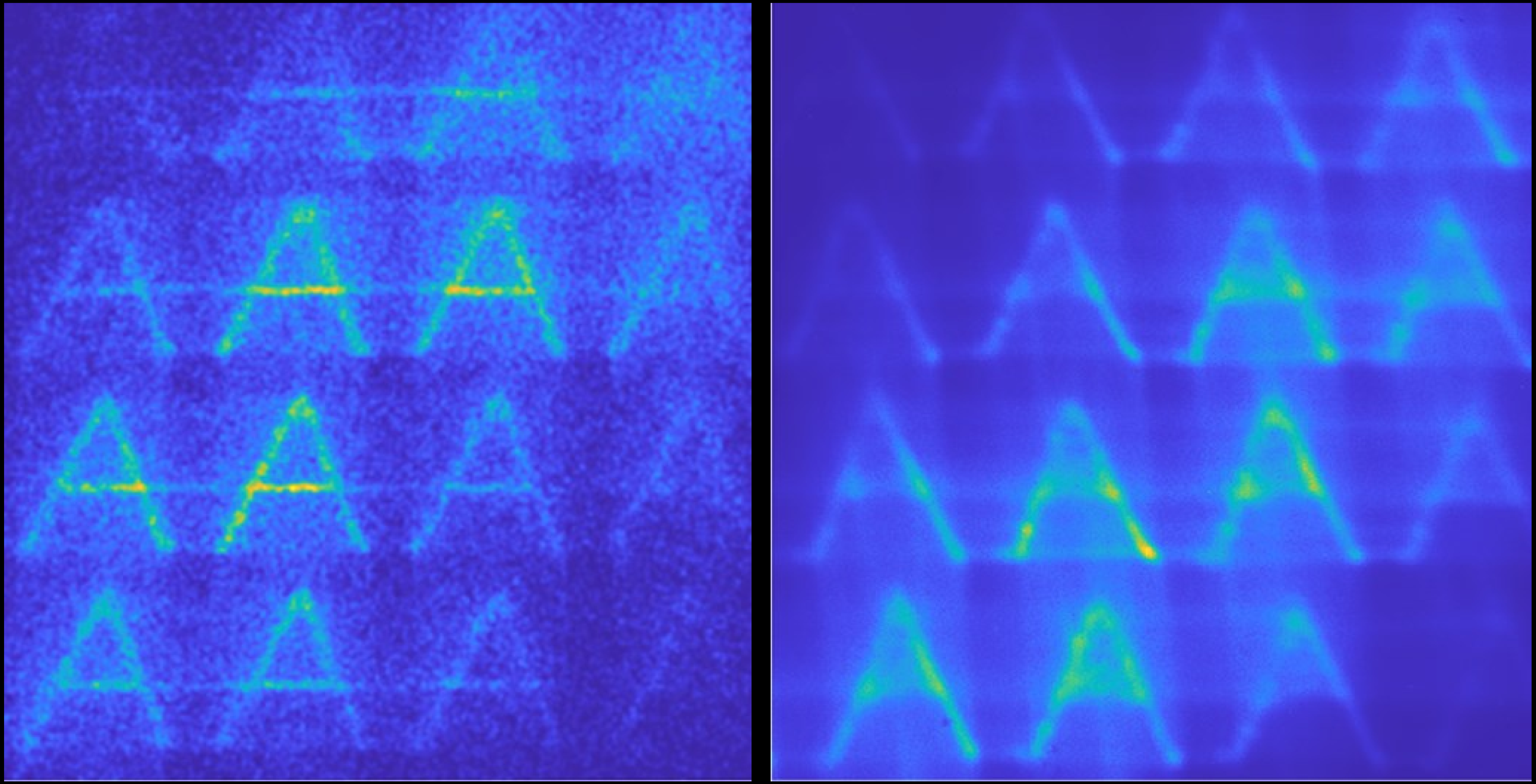

Hardware results: dot projector

Hardware results: dot projector

Hardware results: Lidar

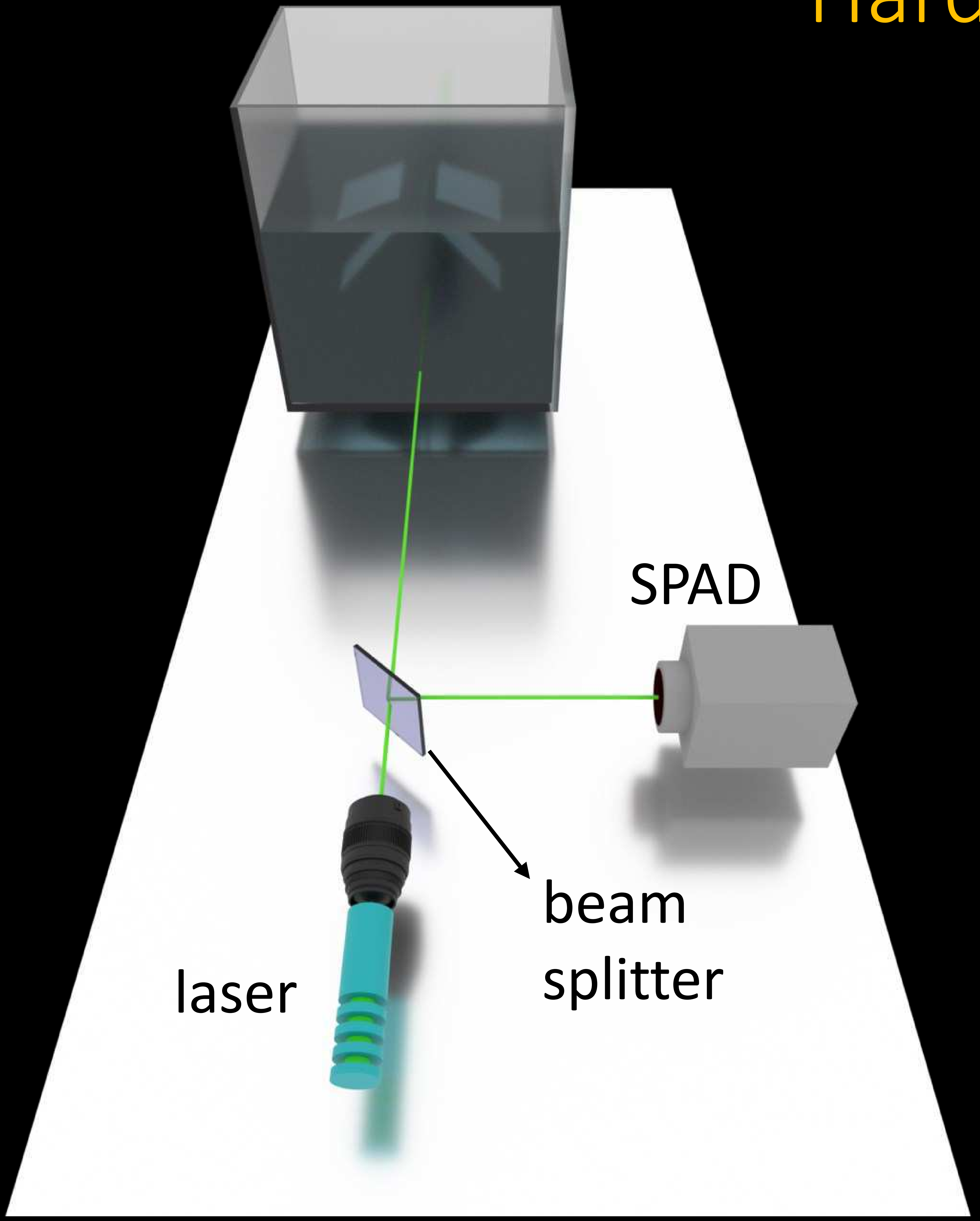

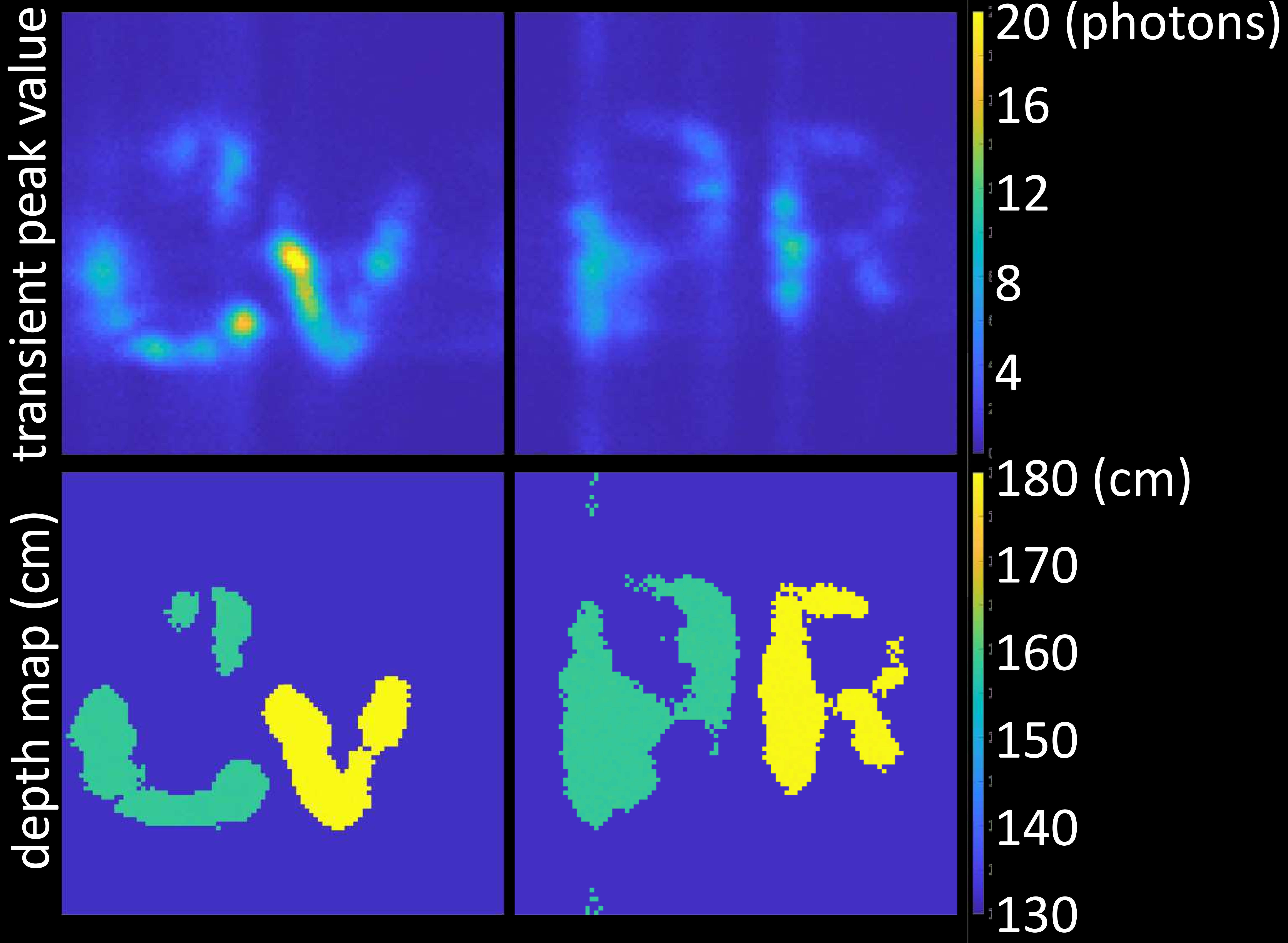

100 × faster than standard lidar

Hardware results: adaptive depth measurement

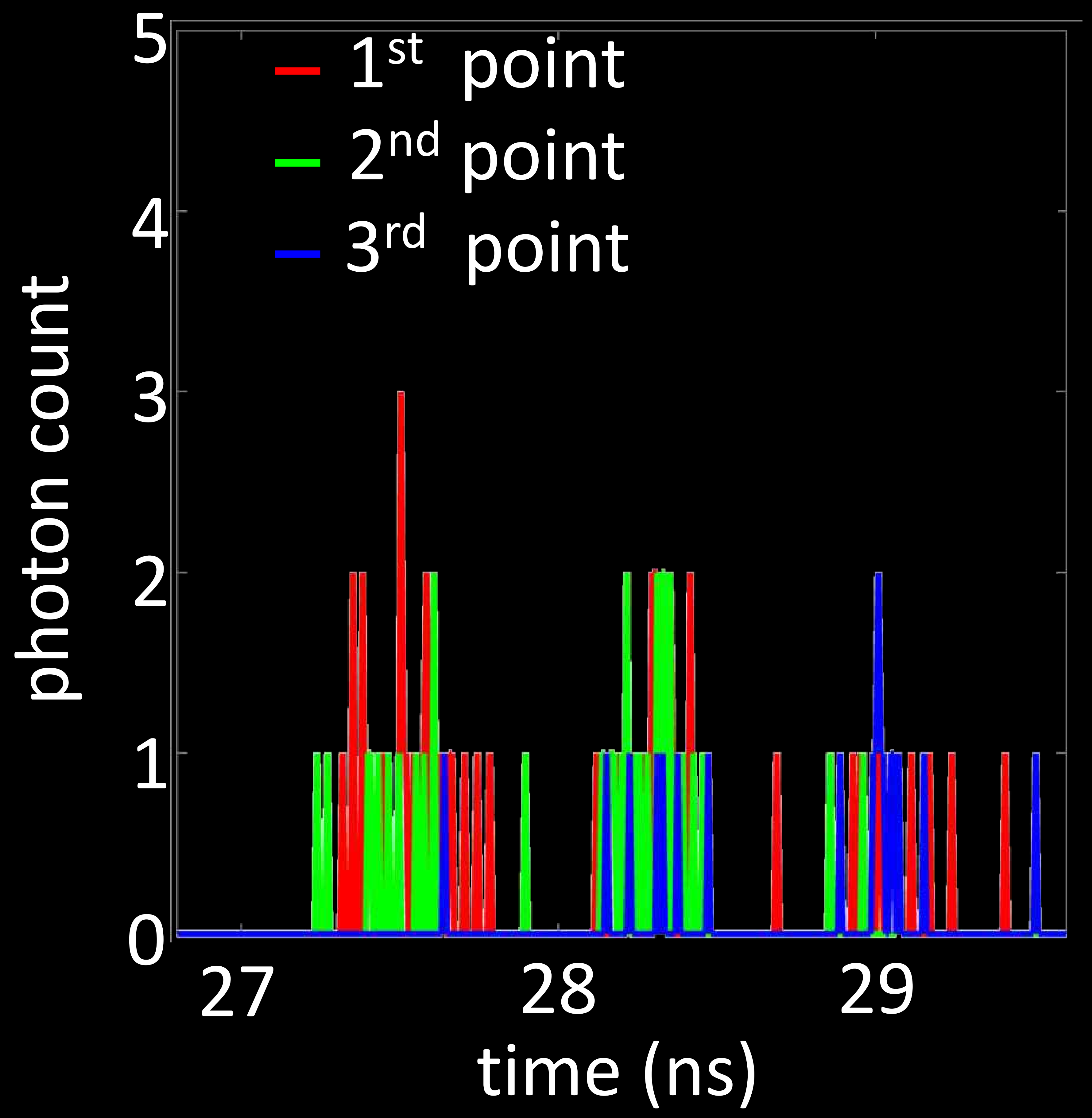

standard galvo (depth error = 51.3 cm)

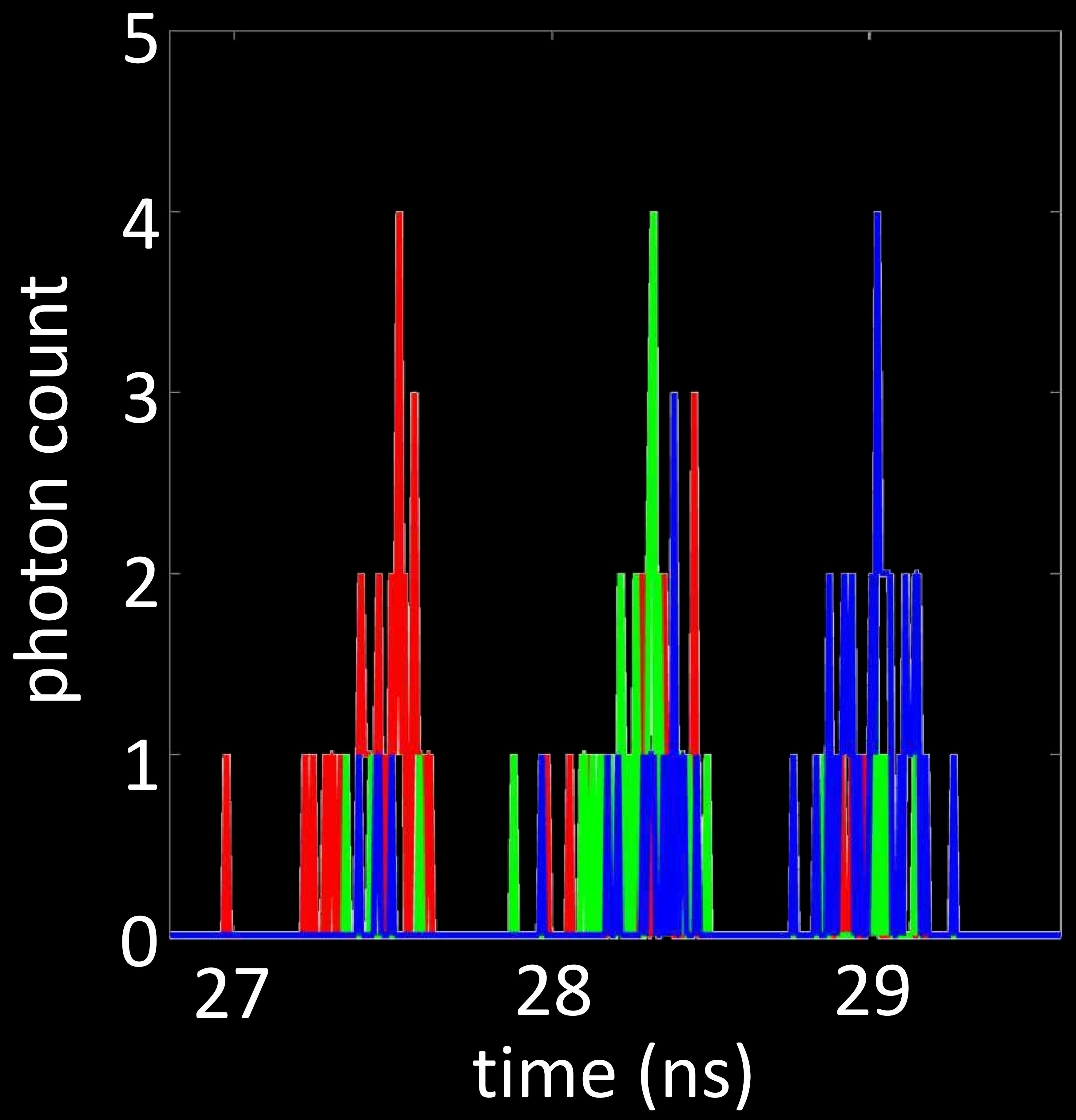

our technique (depth error = 3.28 cm)

15 × depth accuracy

Limitation

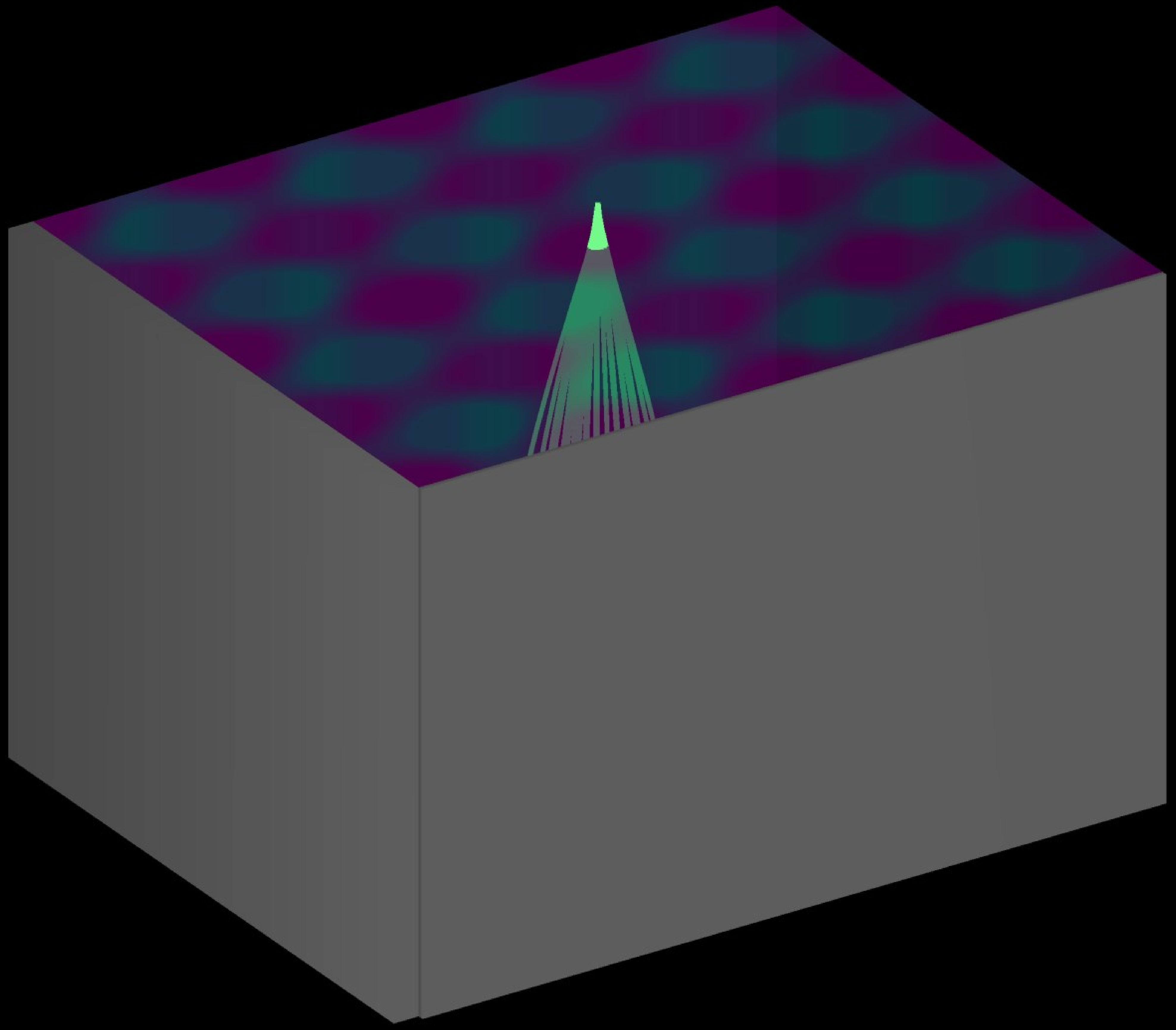

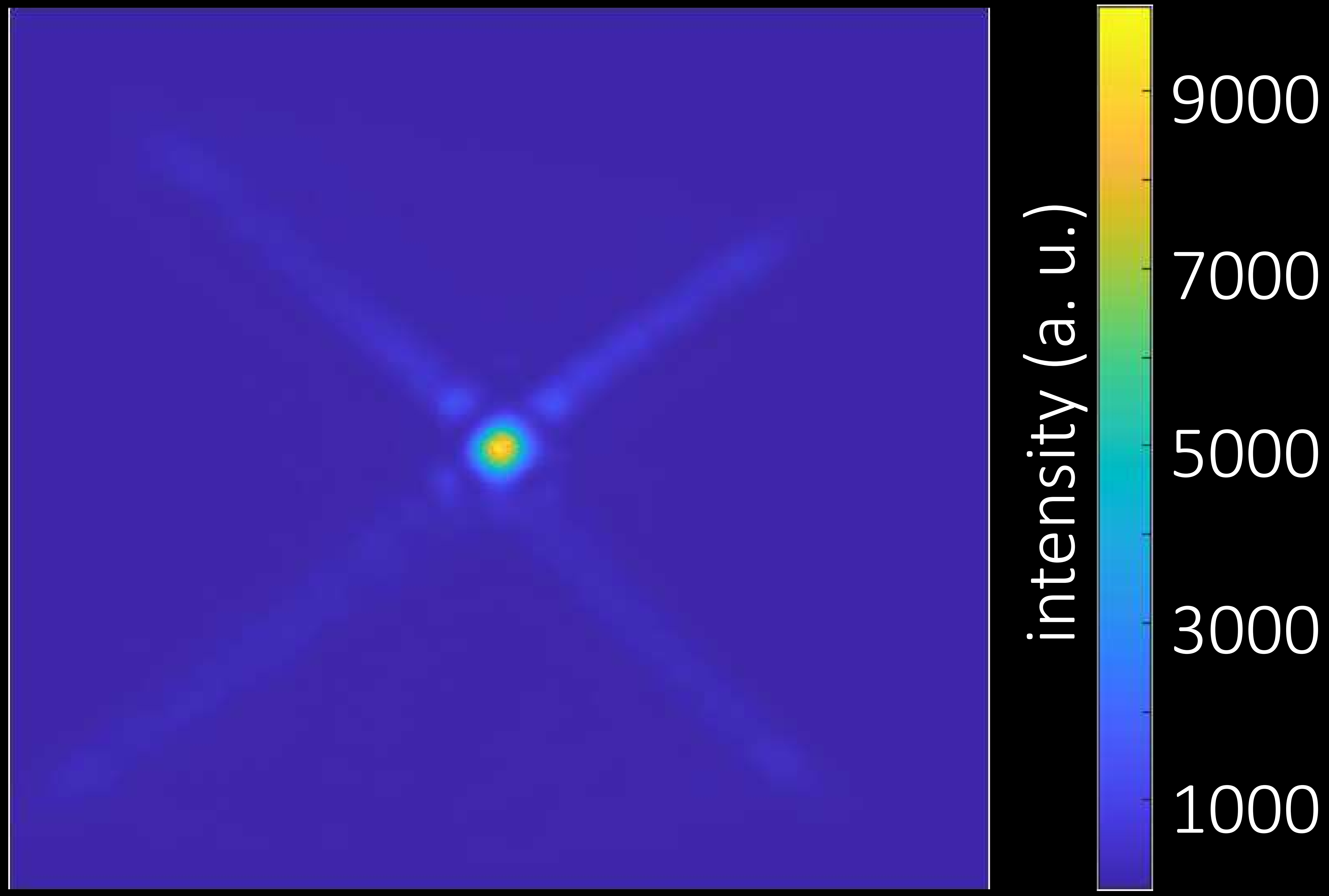

Pediredla et al. CVPR 2023.

Physics-based rendering and its applications to computational imaging

forward rendering

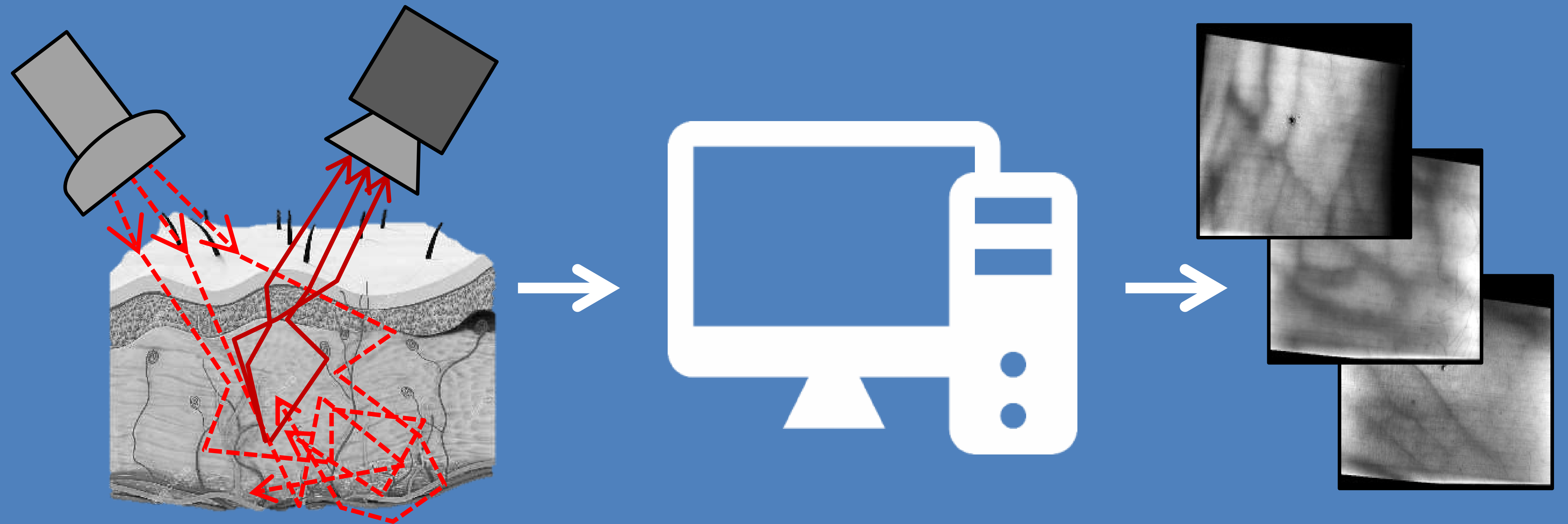

- accurate and efficient simulation
- virtually design sensors, optics, and algorithms

inverse rendering

- accurate and efficient differentiable simulation
- tractably solve general inverse problems

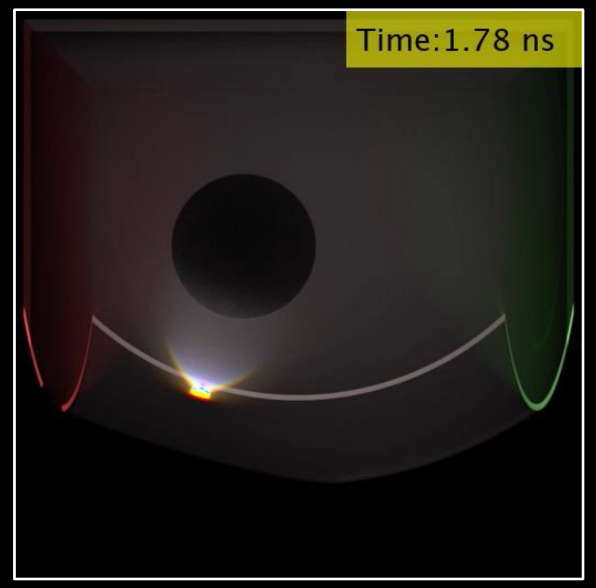

time-of-flight imaging

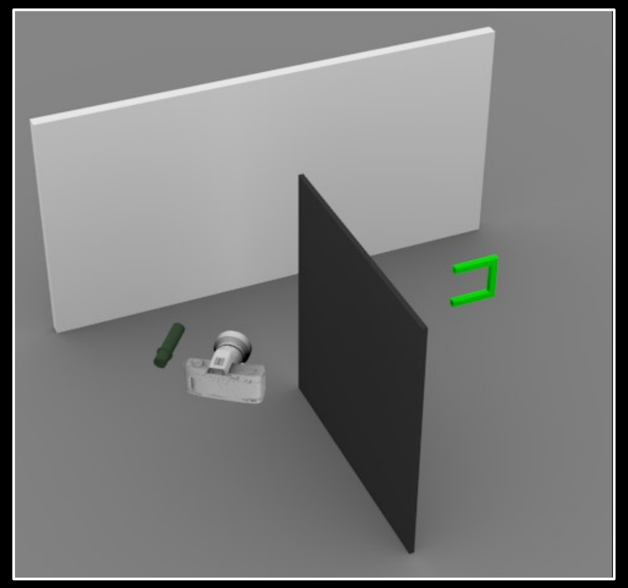

non-line-of-sight imaging

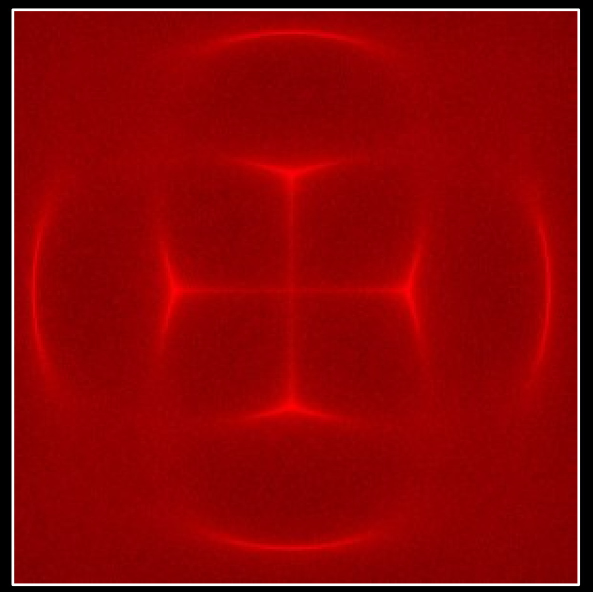

acousto-optic lensing

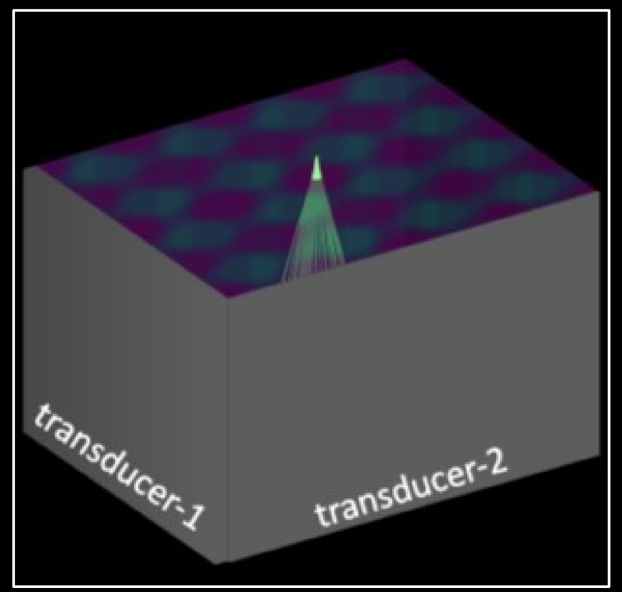

ultrafast light scanning

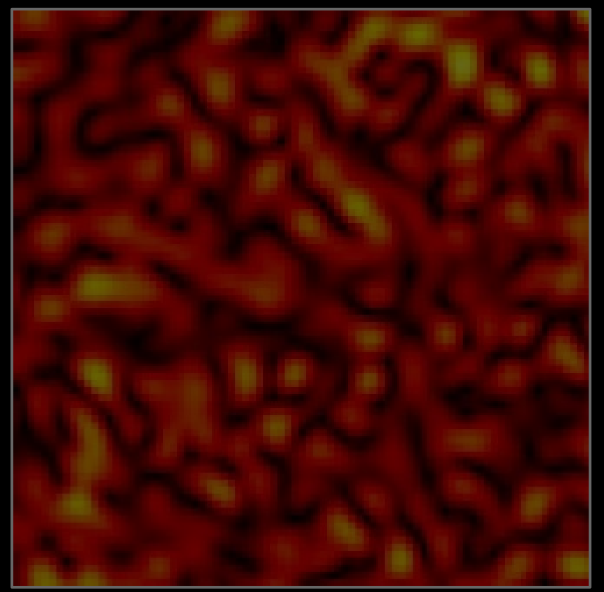

speckle imaging

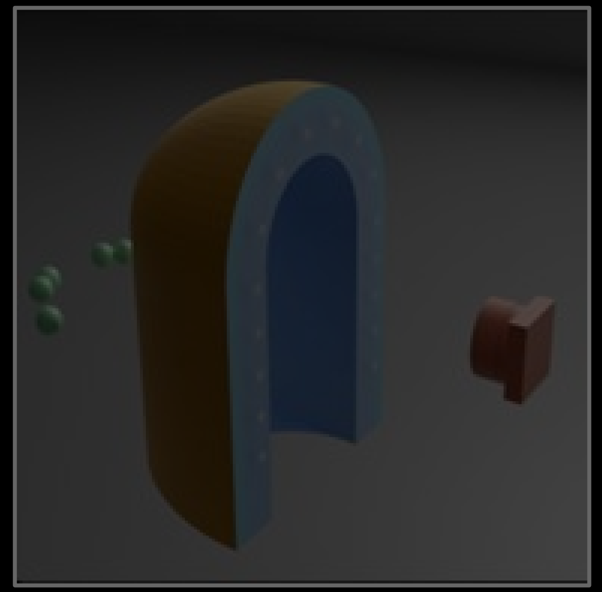

tactile sensor design

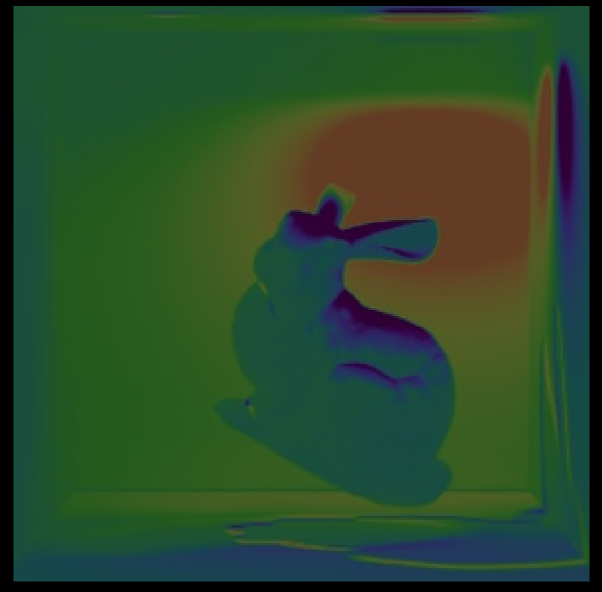

differentiable renderer

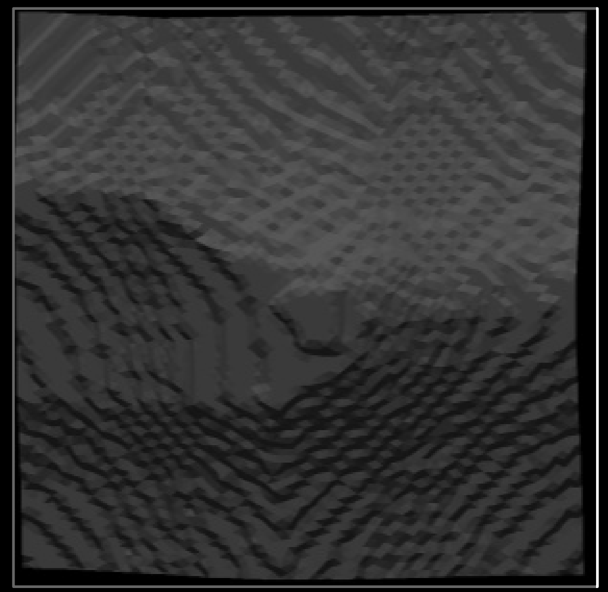

inverse problems

Physics-based rendering and its applications to computational imaging

forward rendering

- accurate and efficient simulation
- virtually design sensors, optics, and algorithms

inverse rendering

- accurate and efficient differentiable simulation
- tractably solve general inverse problems

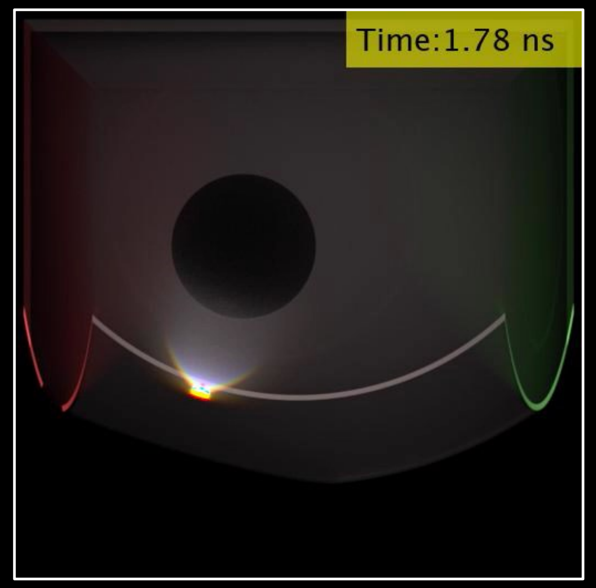

time-of-flight imaging

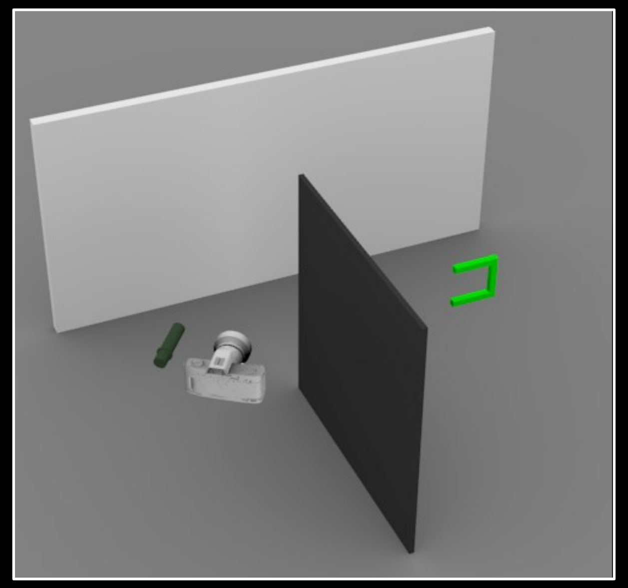

non-line-of-sight imaging

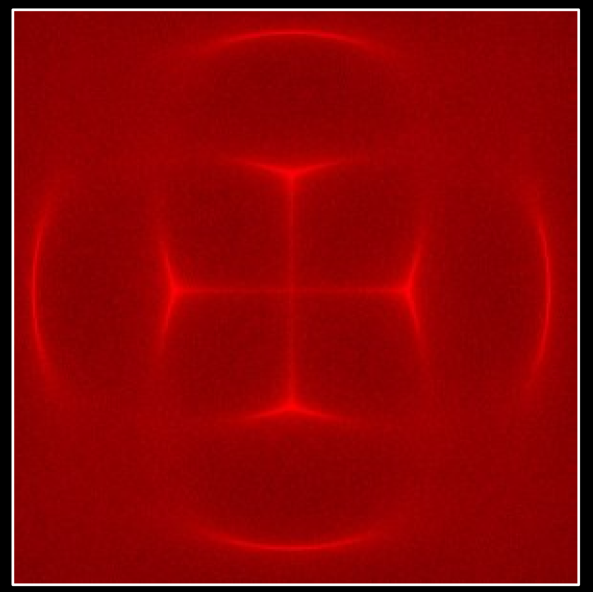

acousto-optic lensing

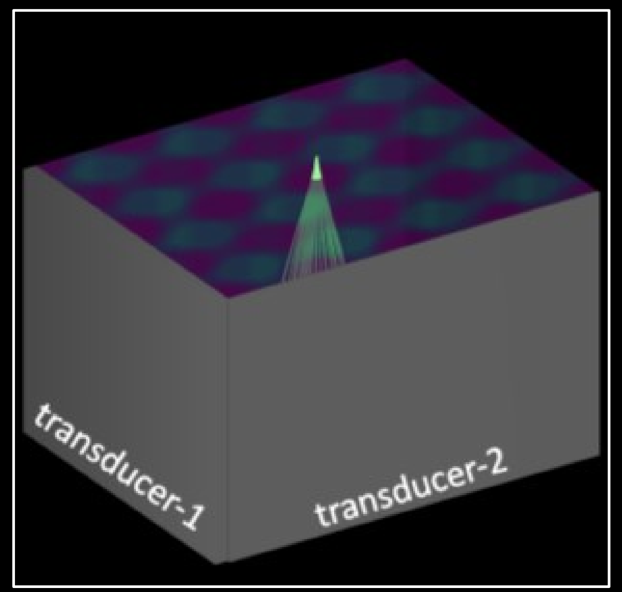

ultrafast light scanning

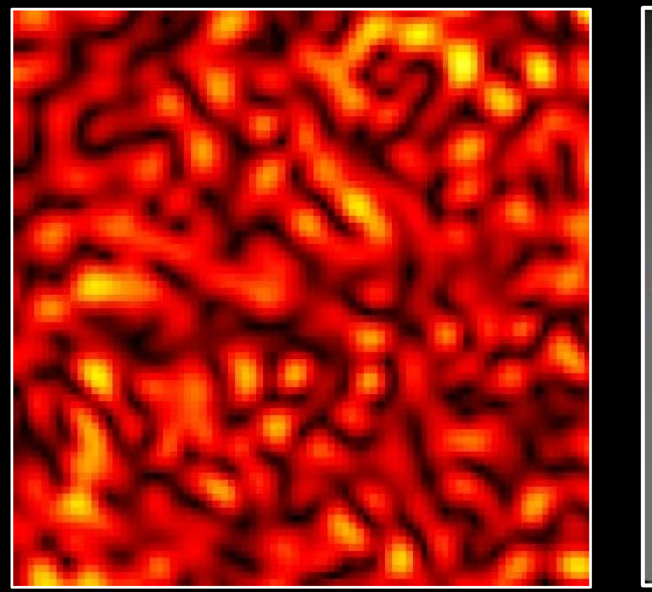

speckle imaging

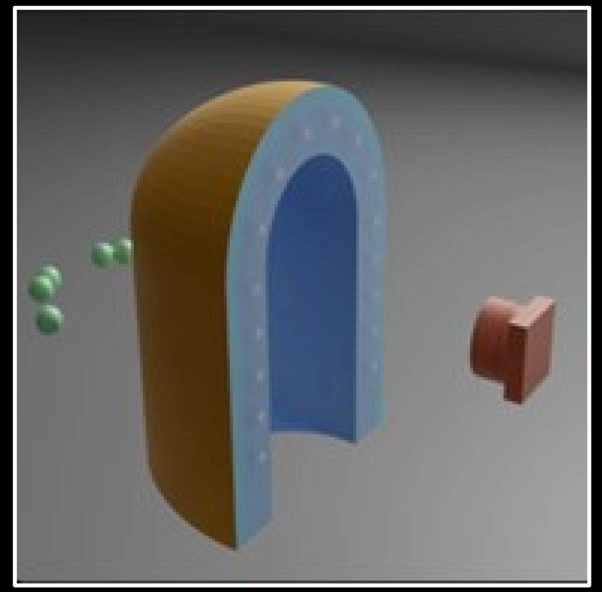

tactile sensor design

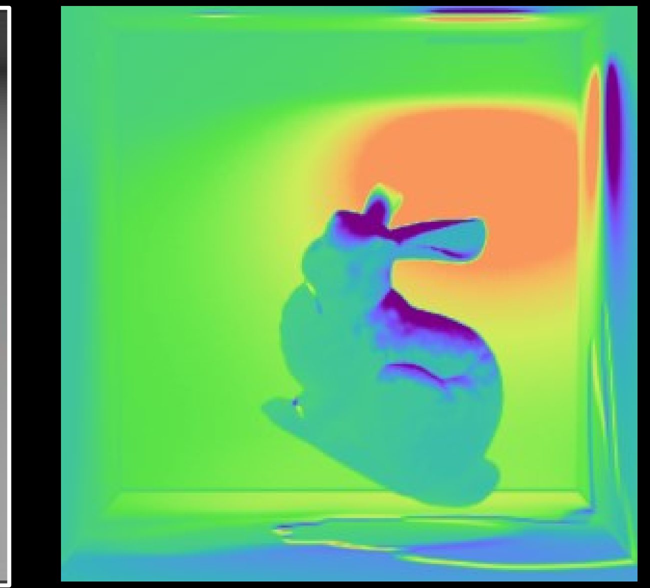

differentiable renderer

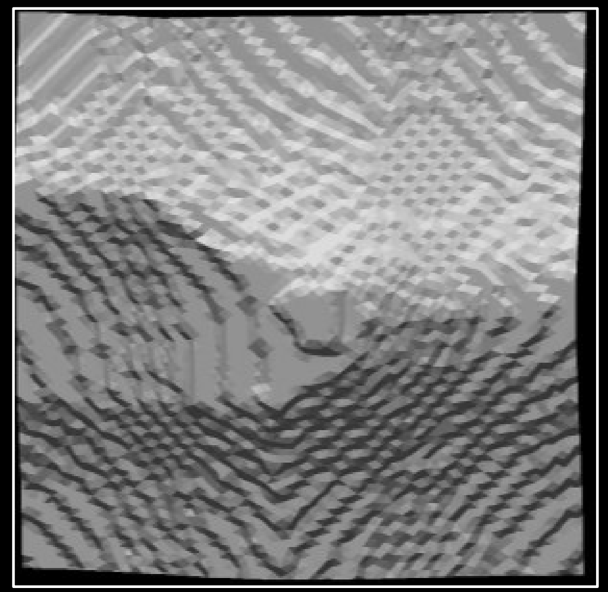

inverse problems

Coffee break

See you at 3.30 PM

Physics-based rendering and its applications to computational imaging

forward rendering

- accurate and efficient simulation
- virtually design sensors, optics, and algorithms

inverse rendering

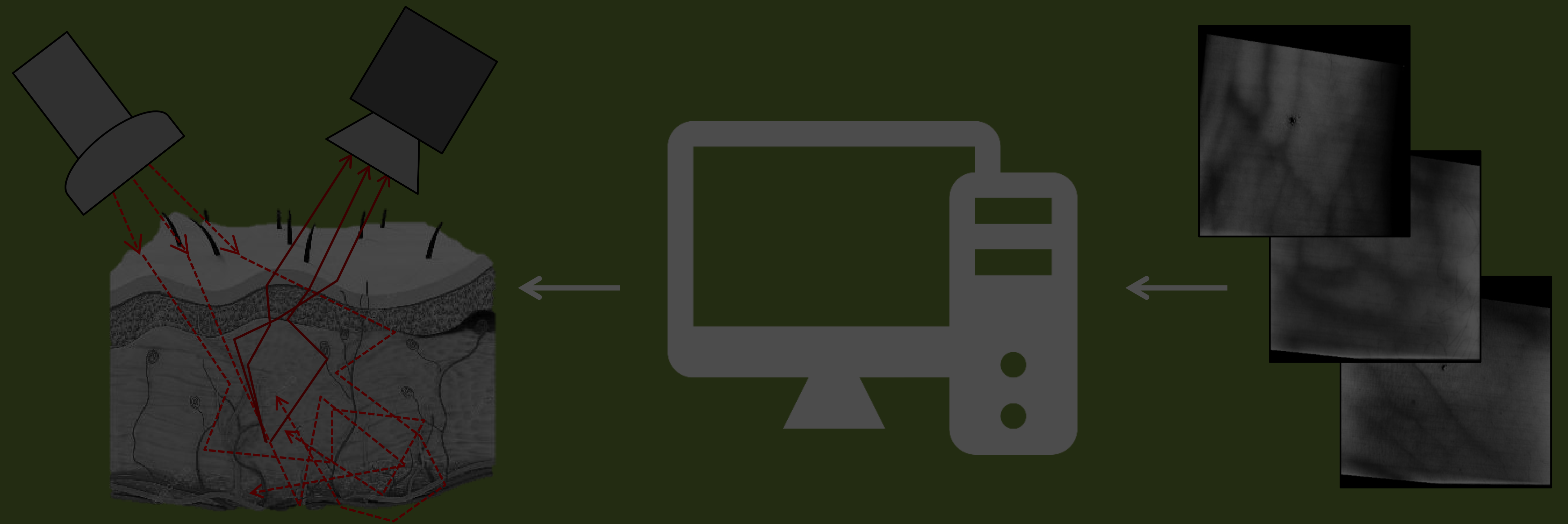

- accurate and efficient differentiable simulation
- tractably solve general inverse problems

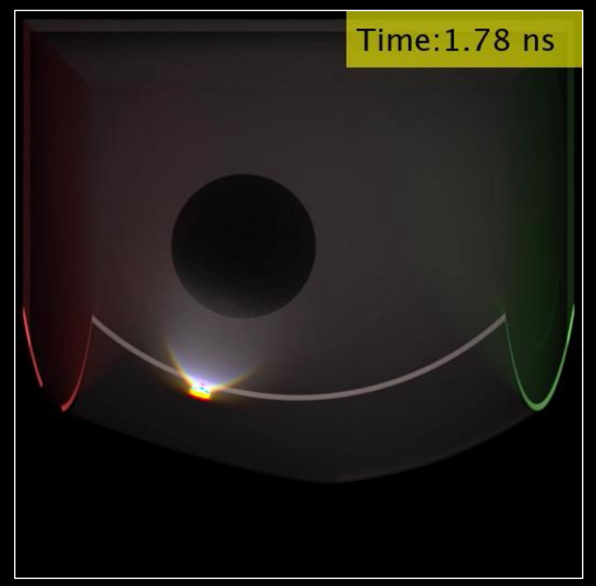

time-of-flight imaging

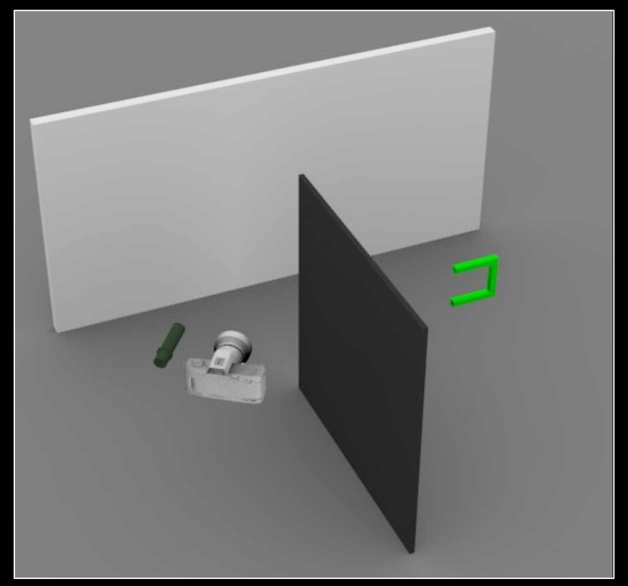

non-line-of-sight imaging

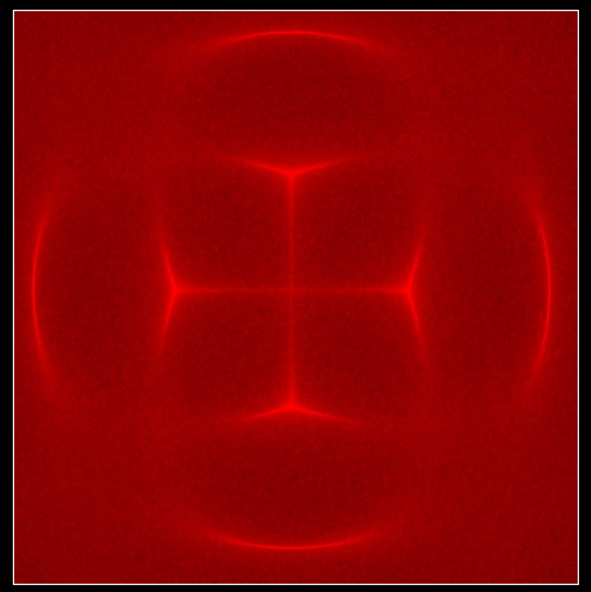

acousto-optic lensing

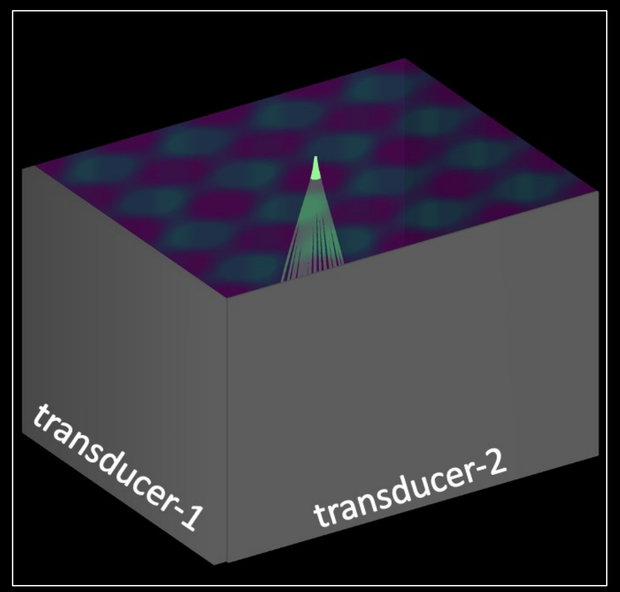

ultrafast light scanning

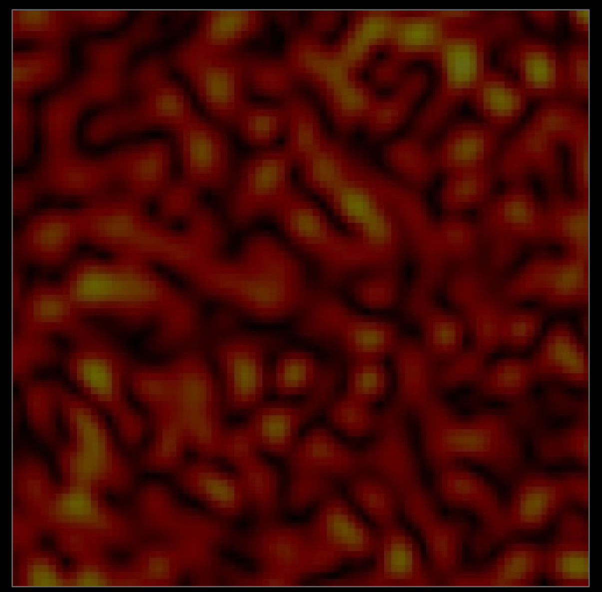

speckle imaging

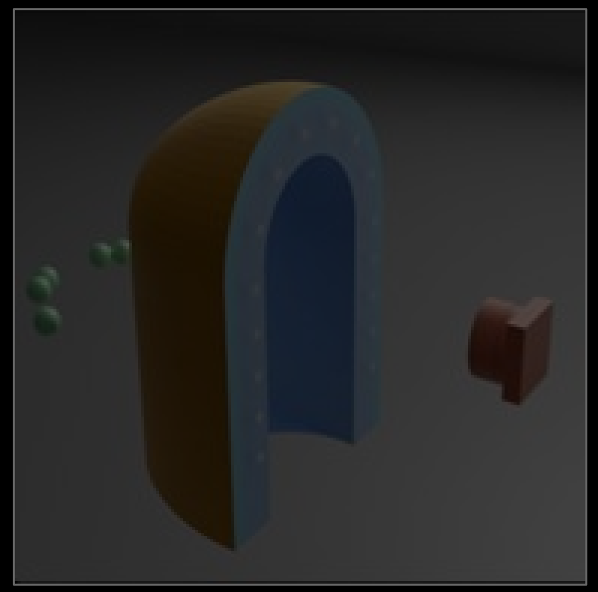

tactile sensor design

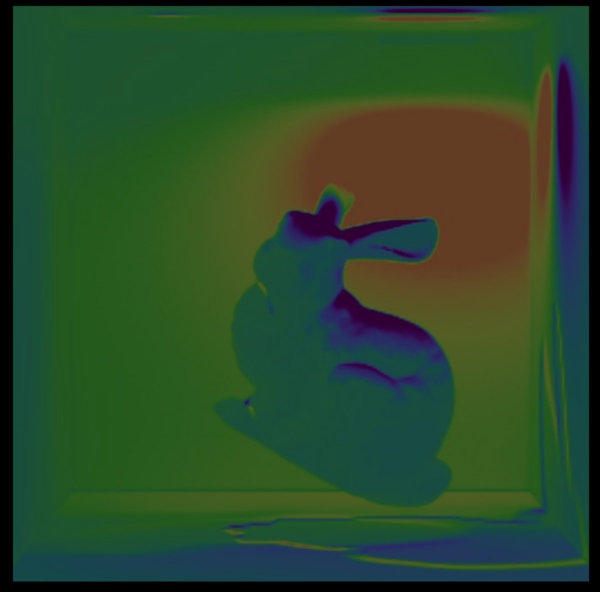

differentiable renderer

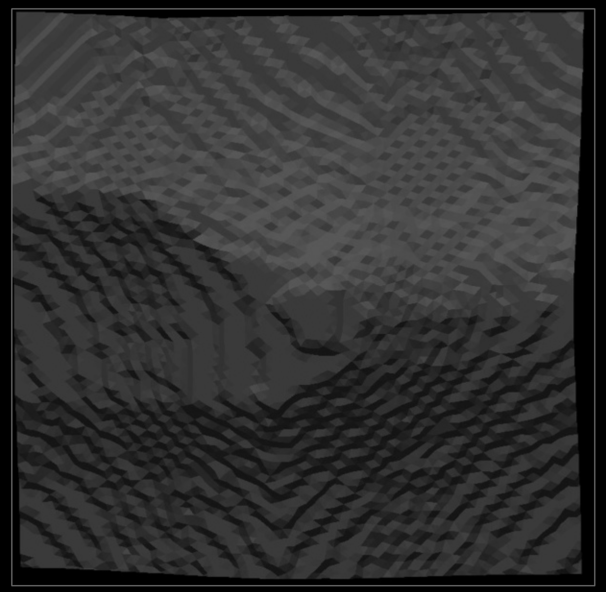

inverse problems

Physics-based rendering and its applications to computational imaging

forward rendering

- accurate and efficient simulation
- virtually design sensors, optics, and algorithms

inverse rendering

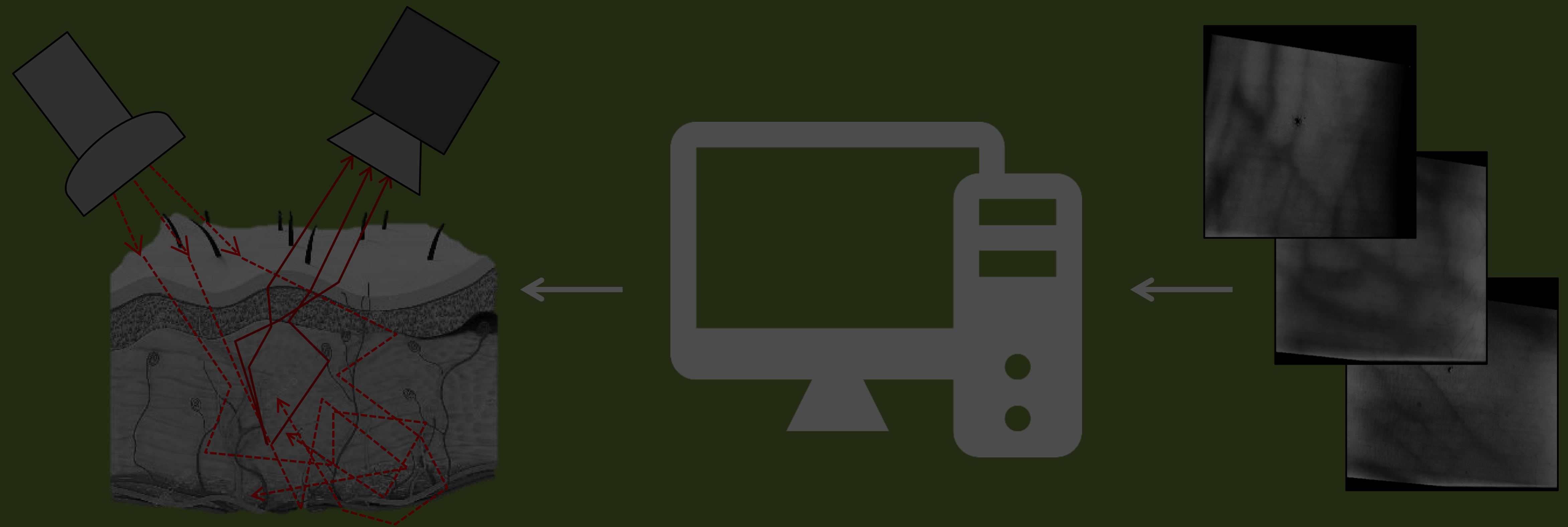

- accurate and efficient differentiable simulation
- tractably solve general inverse problems

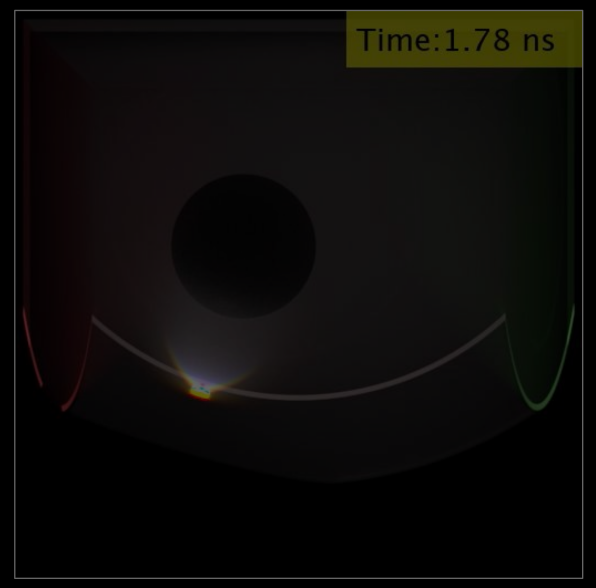

time-of-flight imaging

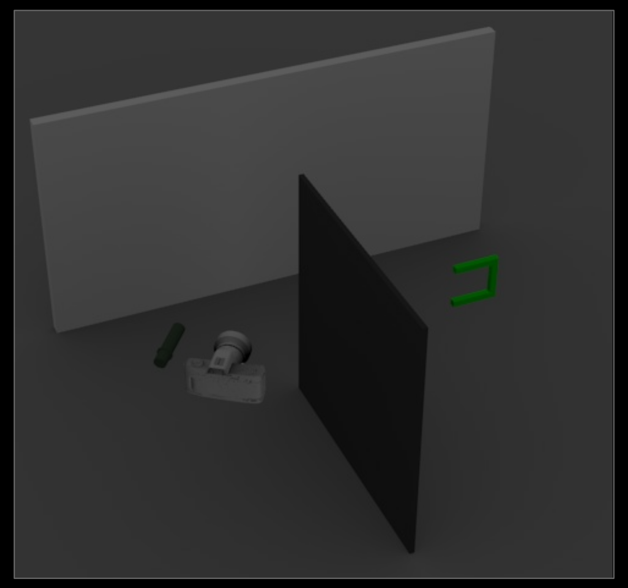

non-line-of-sight imaging

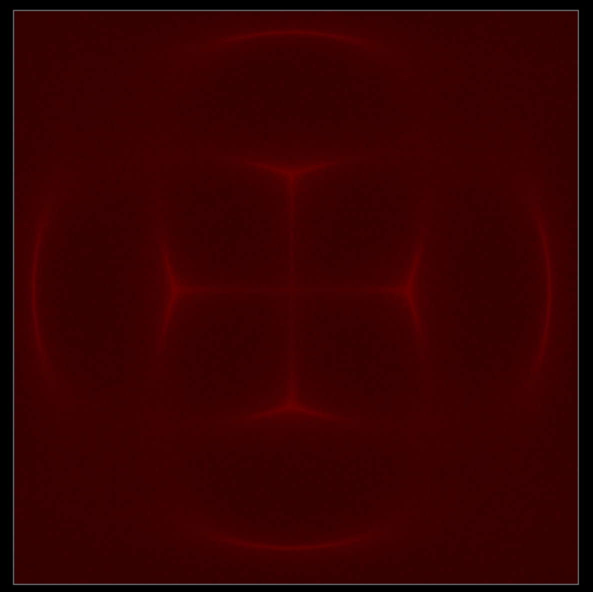

acousto-optic lensing

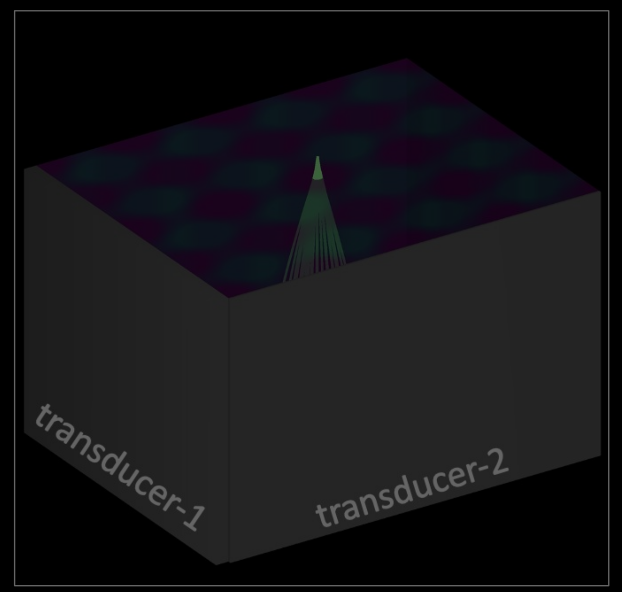

ultrafast light scanning

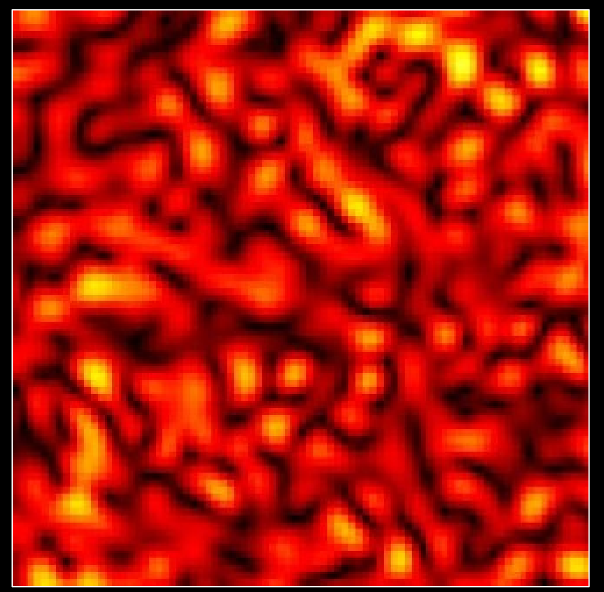

speckle imaging

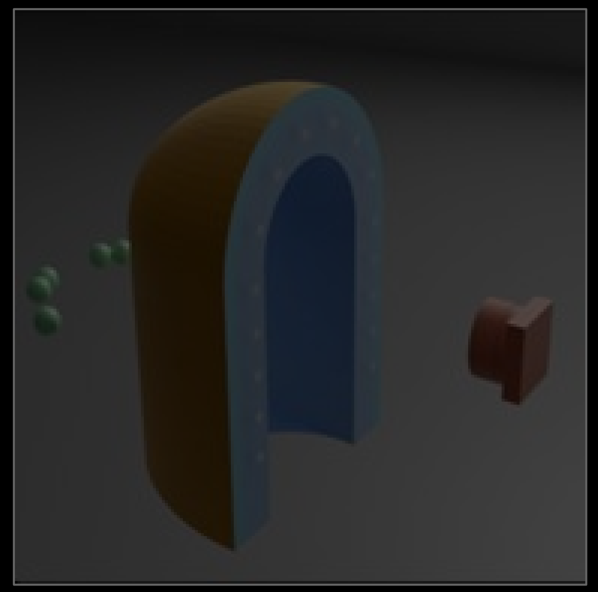

tactile sensor design

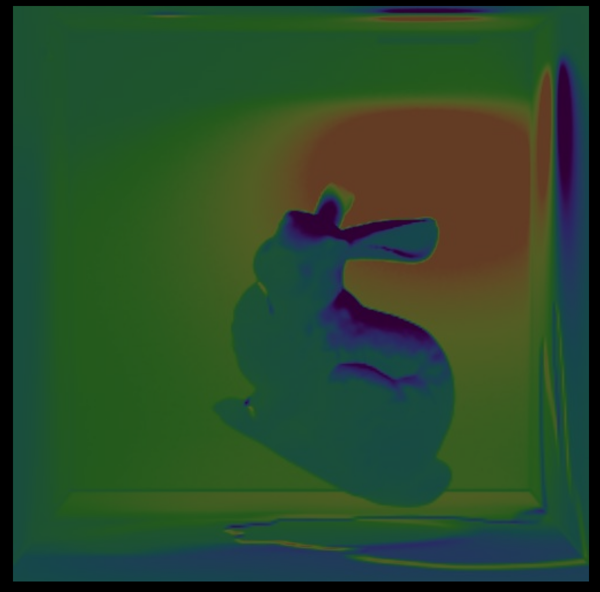

differentiable renderer

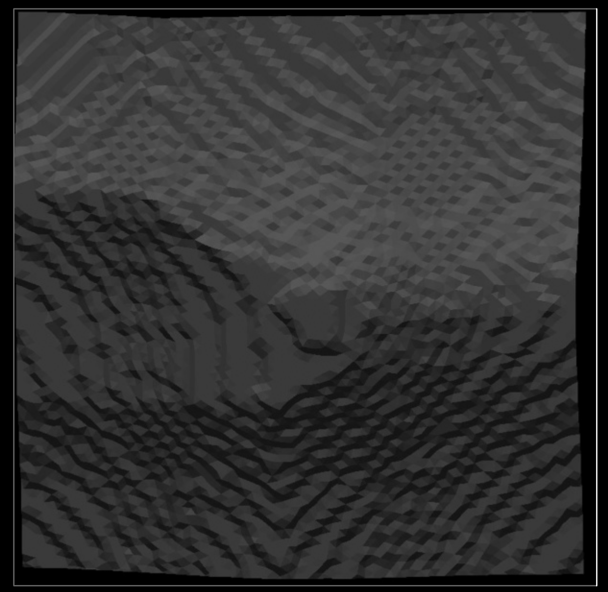

inverse problems

Rendering wave-optics effects

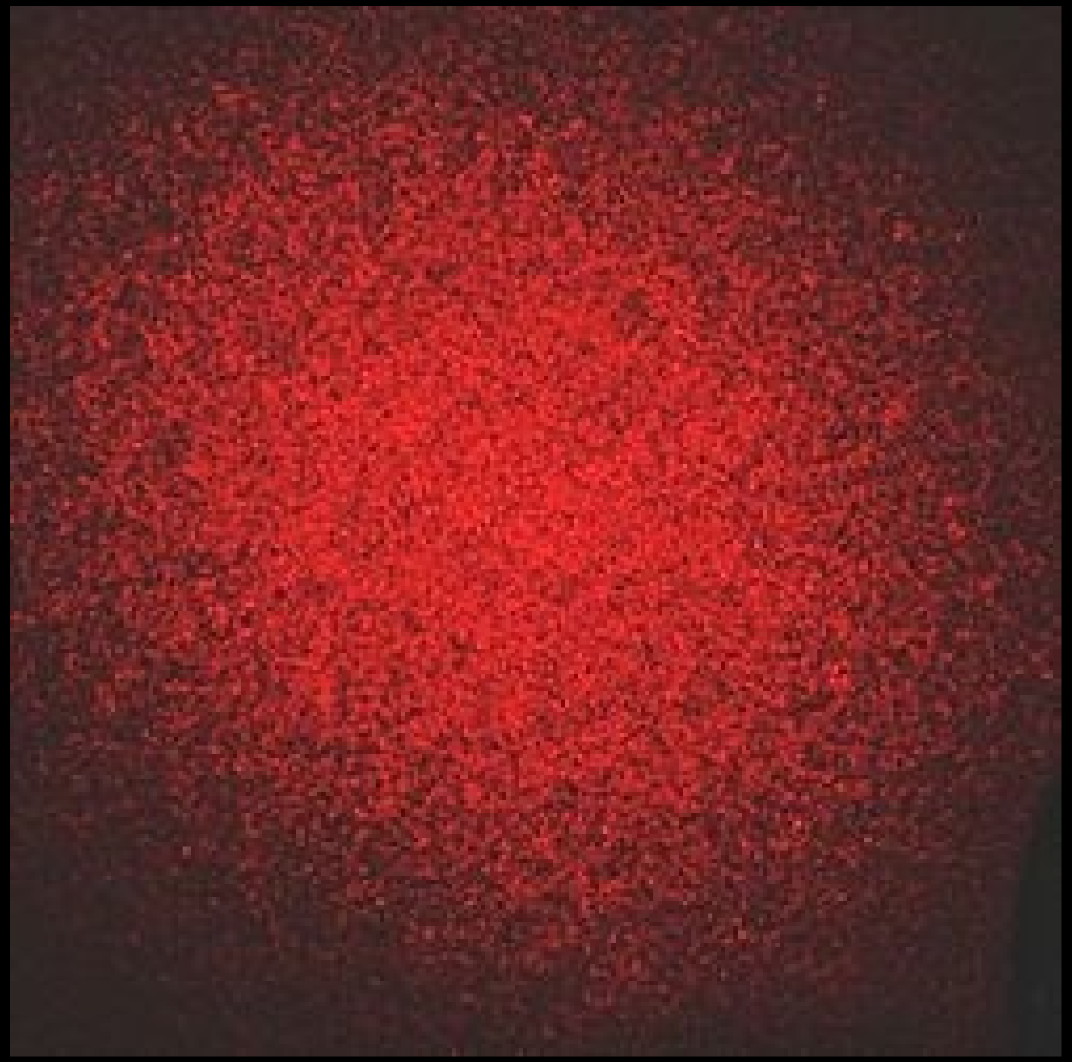

what real laser
images look like

Rendering wave-optics effects

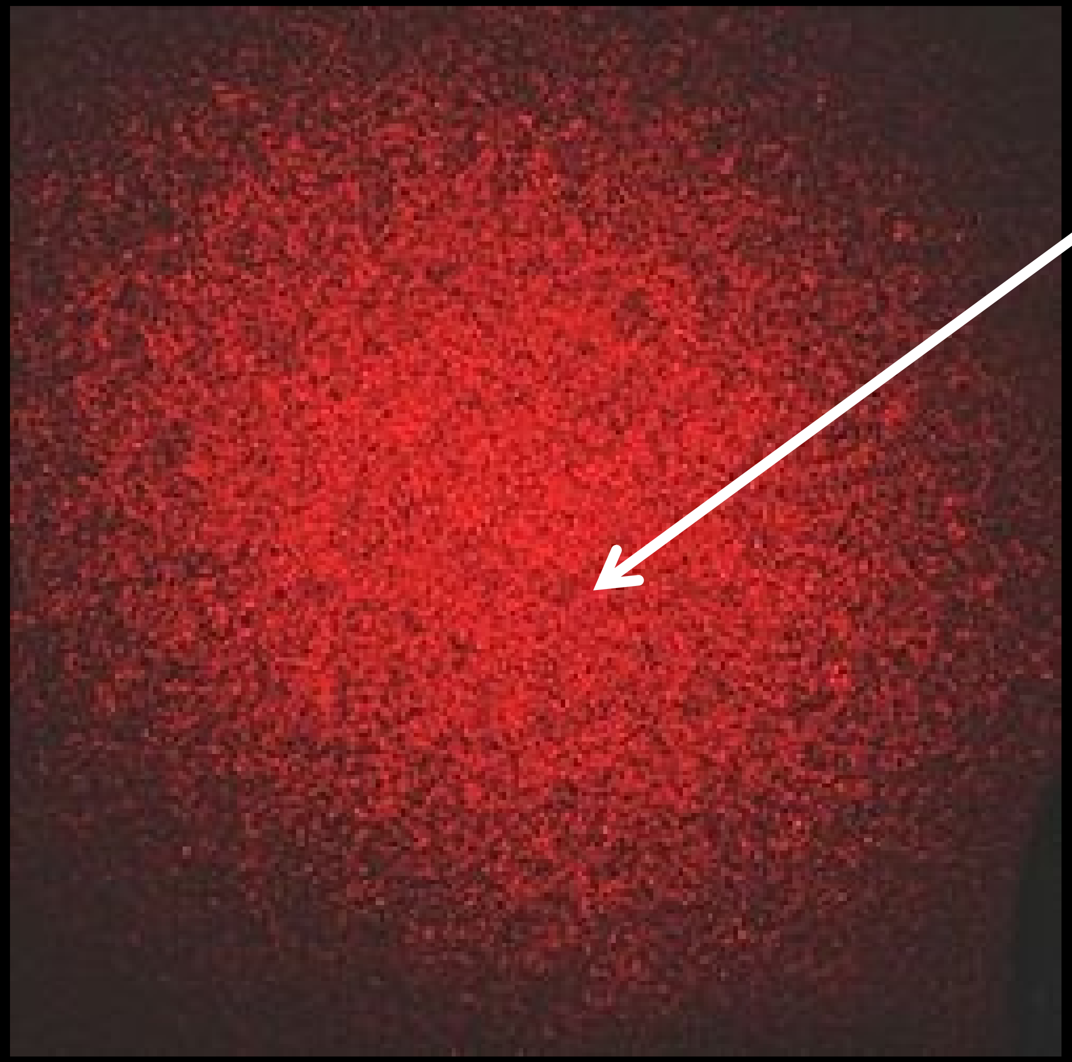

speckle: noise-like pattern

what real laser images look like

Rendering wave-optics effects

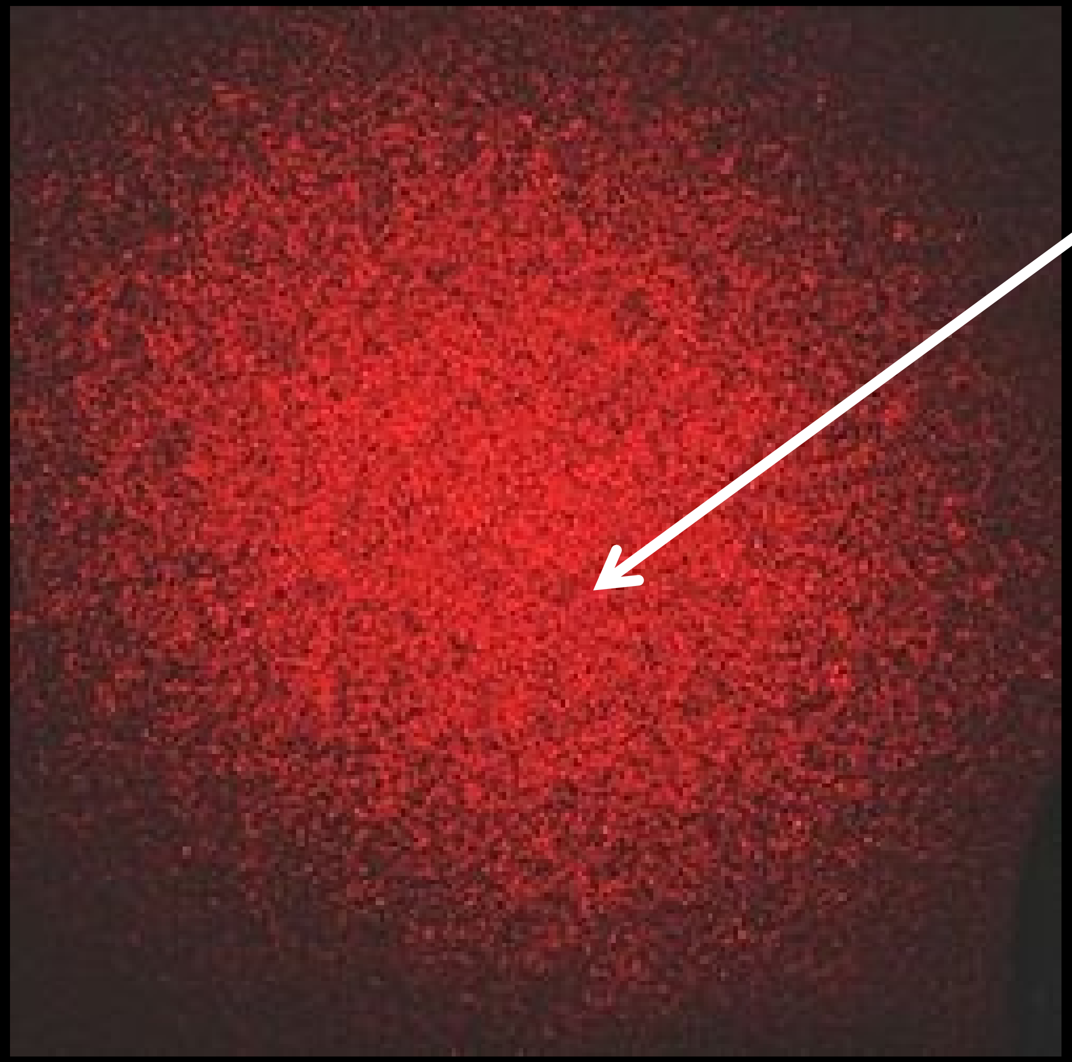

speckle: noise-like pattern

what real laser images look like

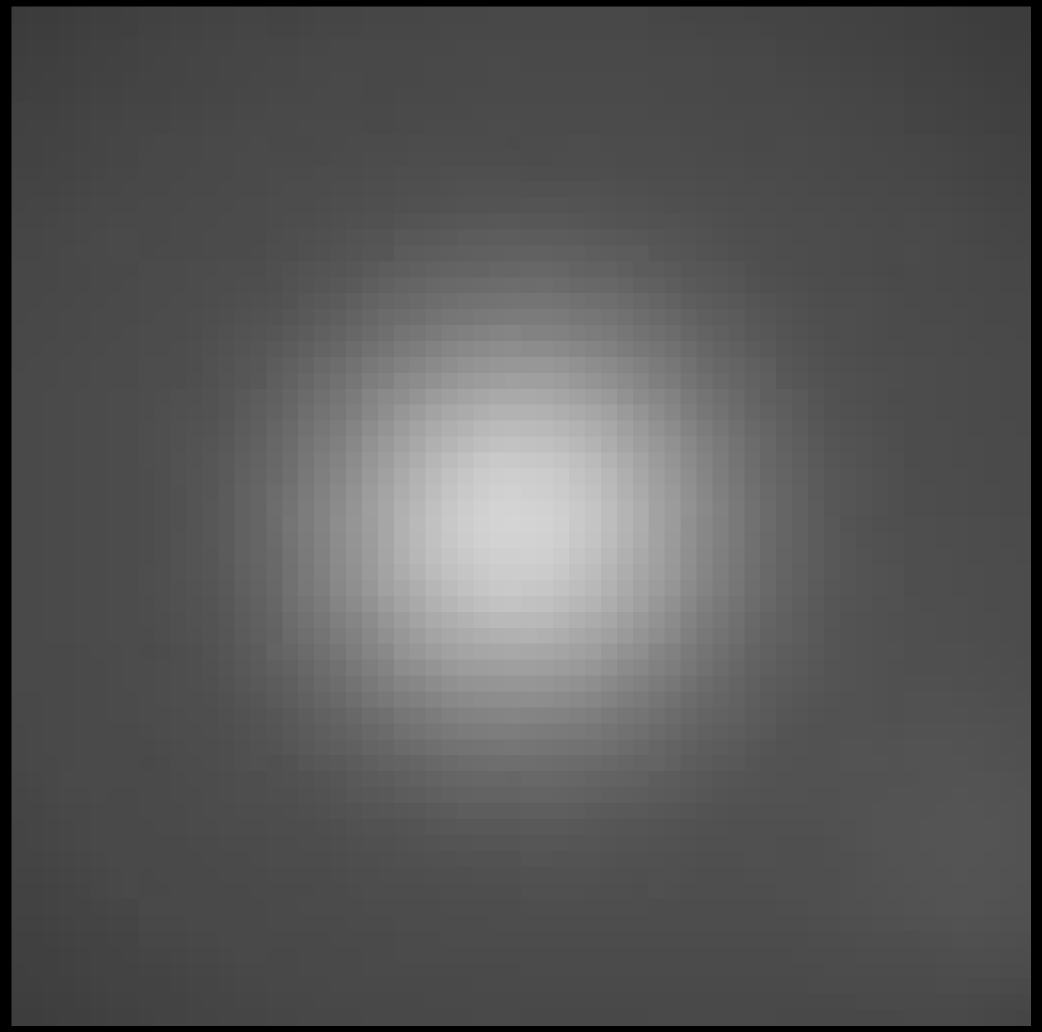

what standard Monte Carlo renderings look like

Rendering wave-optics effects

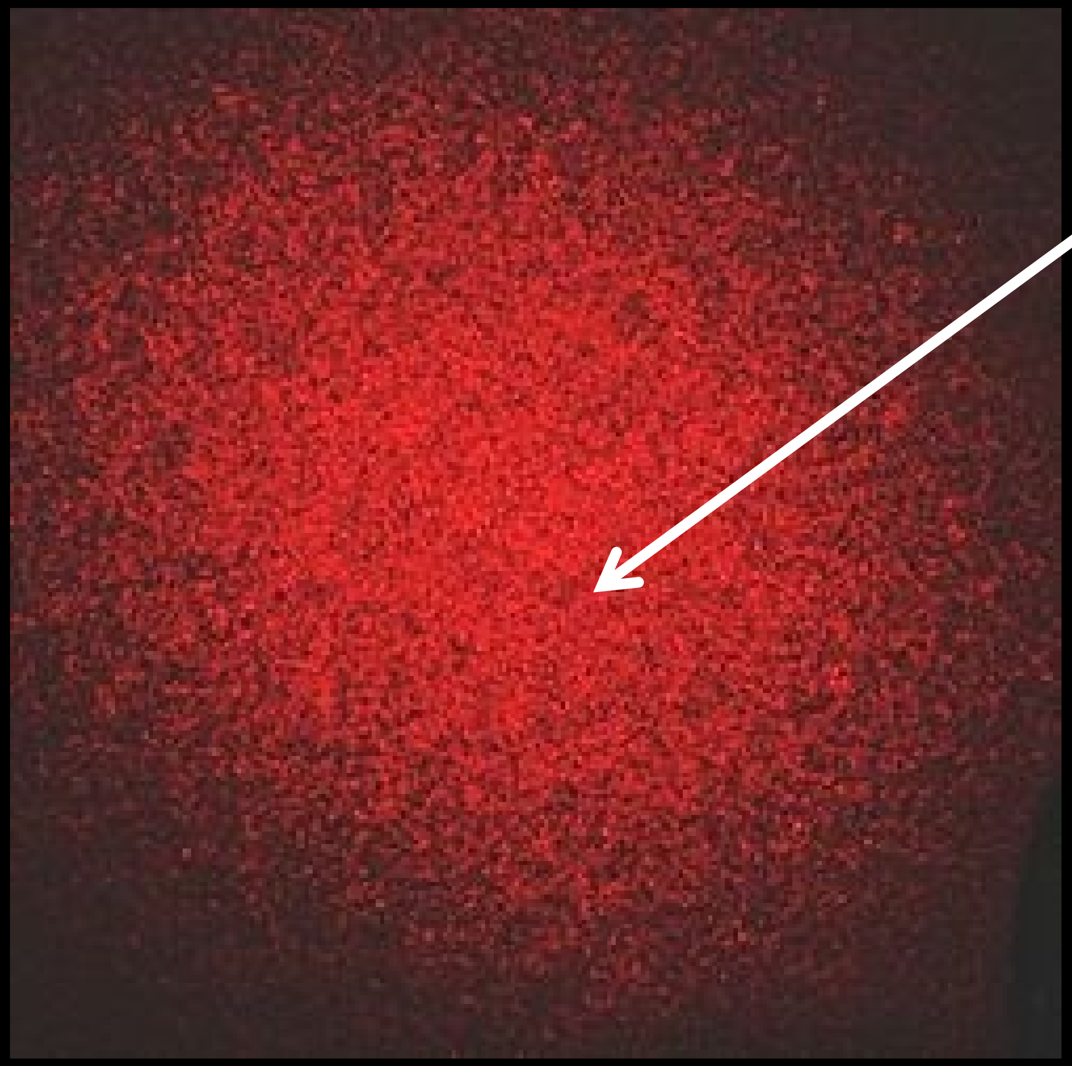

speckle: noise-like pattern

what real laser images look like

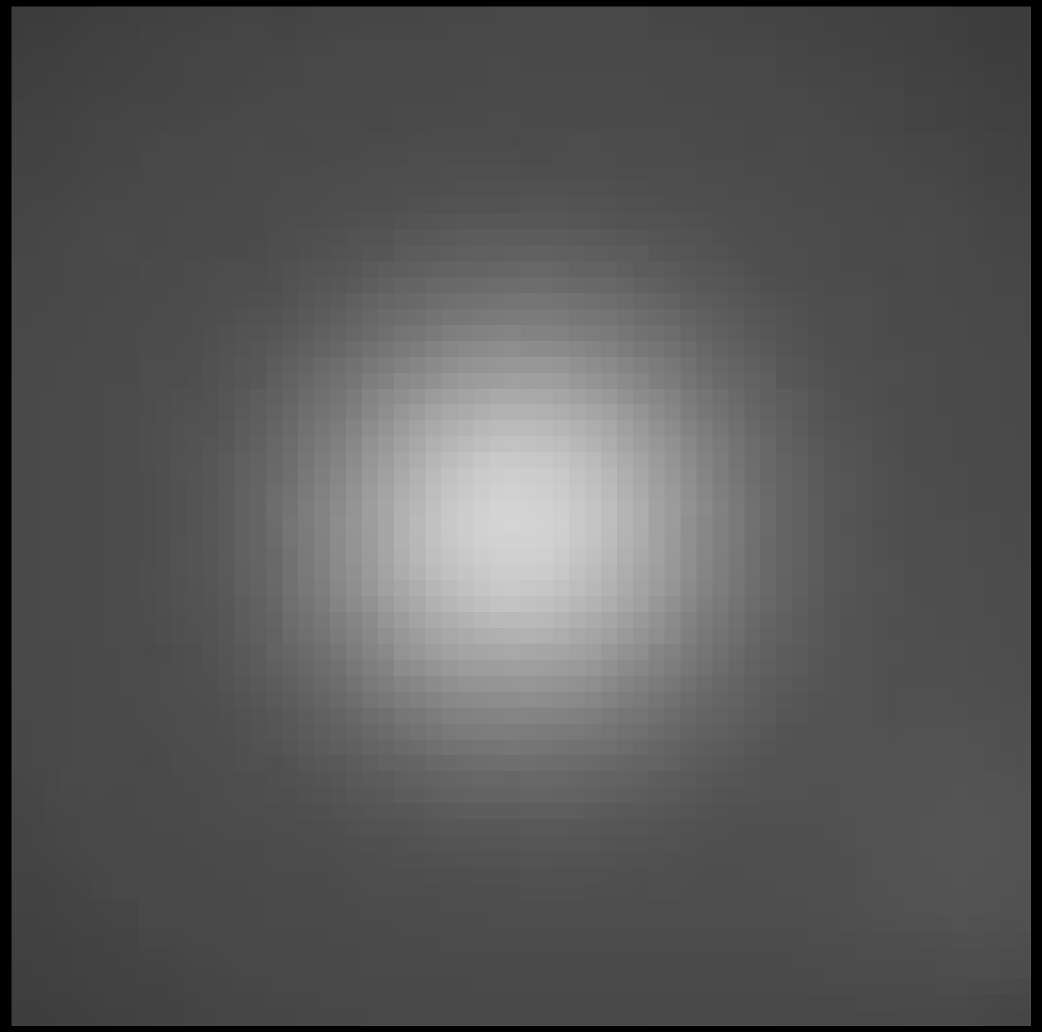

what standard Monte Carlo renderings look like

projected speckle image

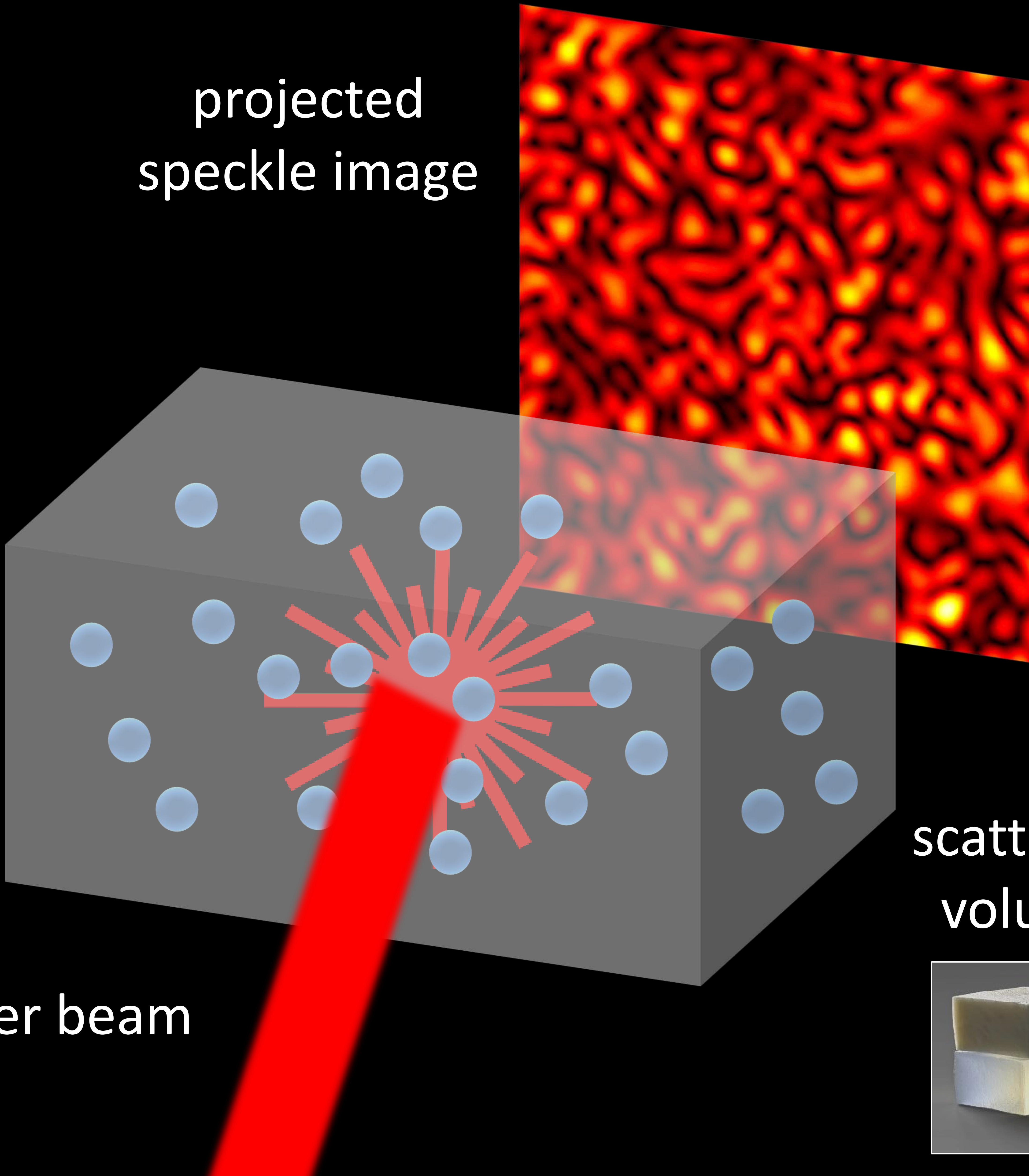

laser beam

scattering volume

Rendering wave-optics effects

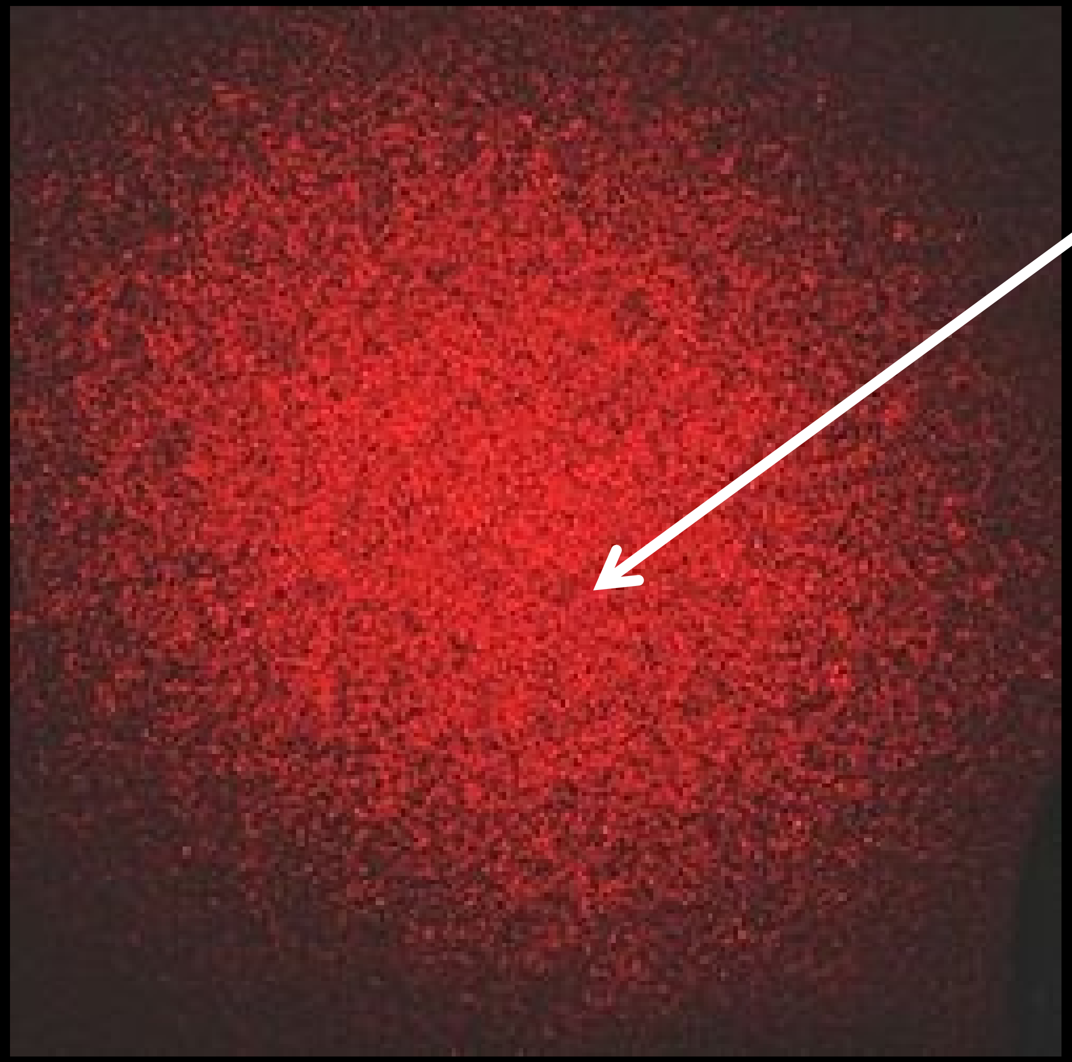

speckle: noise-like pattern

what real laser images look like

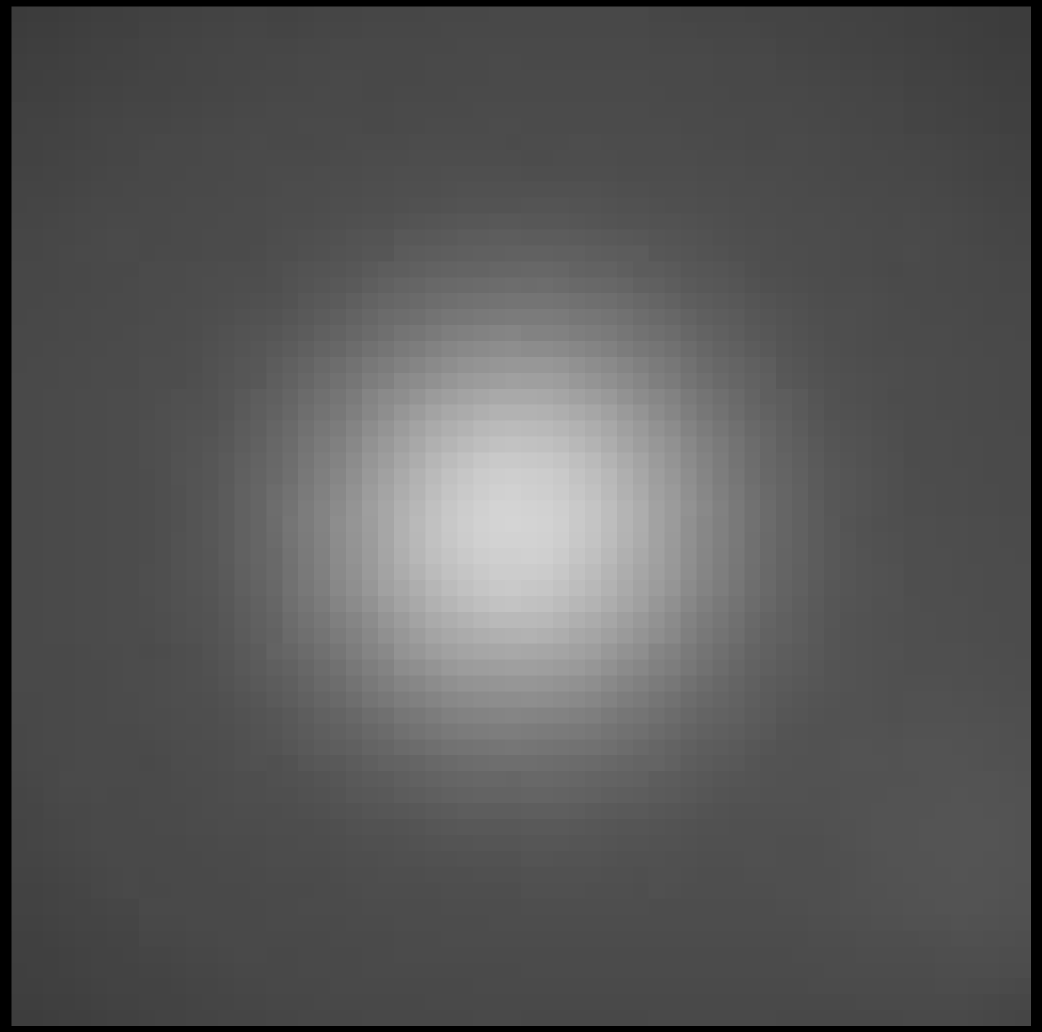

what standard Monte Carlo renderings look like

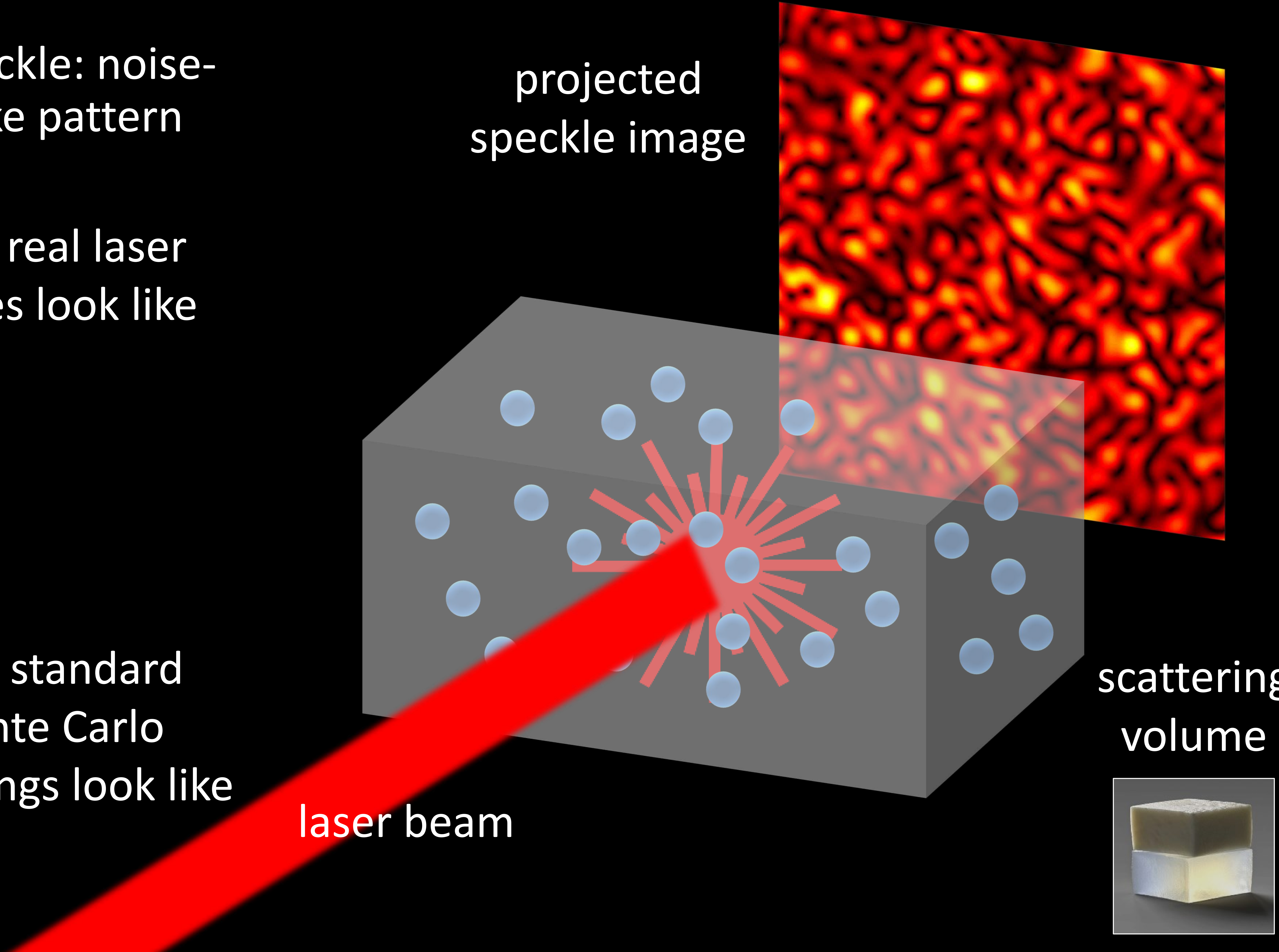

Applications of memory effect

SCIENTIFIC REPORTS

OPEN **Memory-effect based deconvolution microscopy for super-resolution imaging through scattering media**

Eitan Edrei & Giuliano Scarcelli

Received: 26 April 2016
Accepted: 30 August 2016
Published: 16 September 2016

High-resolution imaging through turbid media is a fundamental challenge of optical sciences that has attracted a lot of attention in recent years for its wide range of potential applications. Here, we demonstrate that the resolution of imaging systems looking behind a highly scattering medium can be improved below the diffraction-limit. To achieve this, we demonstrate a novel microscopy technique enabled by the optical memory effect that uses a deconvolution image processing and thus it does not require iterative focusing, scanning or phase retrieval procedures. We show that this newly established ability of direct imaging through turbid media provides fundamental and practical advantages such as three-dimensional refocusing and unambiguous object reconstruction.

OPEN **Single-sh**

Xiaohan Li, Andrew Steve

Physica A 168 (1990) 49–65
North-Holland

LOOKING THROUGH WALLS AND AROUND CORNERS

Isaac FREUND
Department of Physics, Bar-Ilan University, Ramat-Gan, Israel

ARTICLES
PUBLISHED ONLINE: 29 JUNE 2015 | DOI: 10.1038/NPHYS3373

Translation correlations in anisotropica[lly] scattering media

Benjamin Judkewitz[1,2*], Roarke Horstmeyer[2†], Ivo M. Vellekoop[3], Ioannis N. Pap[adopoulos] and Changhuei Yang[2]

nature photonics
ARTICLES
PUBLISHED ONLINE: 31 AUGUST 2014 | DOI: 10.1038/NPHOTON.2014.189

Non-invasive single-shot imaging through scattering layers and around corners via speckle correlations

Ori Katz[1,2*], Pierre Heidmann[1], Mathias Fink[1] and Sylvain Gigan[1,2]

Optical imaging through and inside complex samples is a difficult challenge with important applications in many fields. The fundamental problem is that inhomogeneous samples such as biological tissue randomly scatter and diffuse light, preventing the formation of diffraction-limited images. Despite many recent advances, no current method can perform non-invasive imaging in real-time using diffused light. Here, we show that, owing to the 'memory-effect' for speckle correlations, a single high-resolution image of the scattered light, captured with a standard camera, encodes sufficient information to image through visually opaque layers and around corners with diffraction-limited resolution. We experimentally demonstrate single-shot imaging through scattering media and around corners using spatially incoherent light and various samples, from white paint to dynamic biological samples. Our single-shot lensless technique is simple, does not require wavefront-shaping nor time-gated or interferometric detection, and is realized here using a camera-phone. It has the potential to enable imaging in currently inaccessible scenarios.

LETTER
doi:10.1038/nature11578

[Non]-invasive imaging through opaque scattering [layer]s

[Bert]olotti[1,2]*, Elbert G. van Putten[1]†*, Christian Blum[3], Ad Lagendijk[1,4], Willem L. Vos[1] & Allard P. Mosk[1]

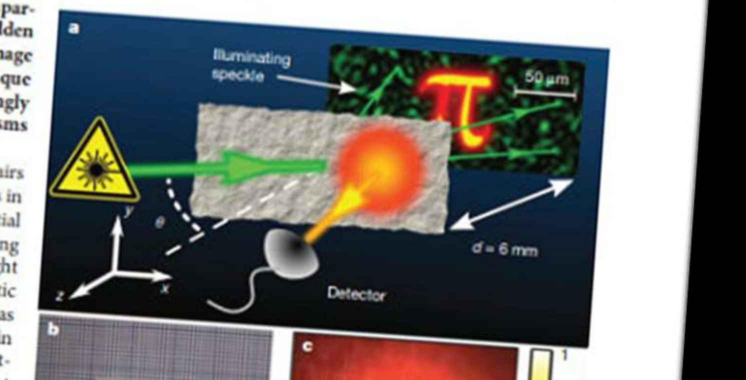

Vol. 2, No. 5 / May 2015 / Optica 424

[Opt]ica

[Speckle] correlation resolution enhancement of [wide-fiel]d fluorescence imaging

[H]ELBERT G. VAN PUTTEN,[1,2] JACOPO BERTOLOTTI,[1,3] AD LAGENDIJK,[1] [A]ND ALLARD P. MOSK[1]

[Received] 21 March 2015 (Doc. ID 226377); published 27 April 2015
doi 10.1364/OPTICA.2.000424

Speckle-based fluorescence microscopy

fluorescent particles

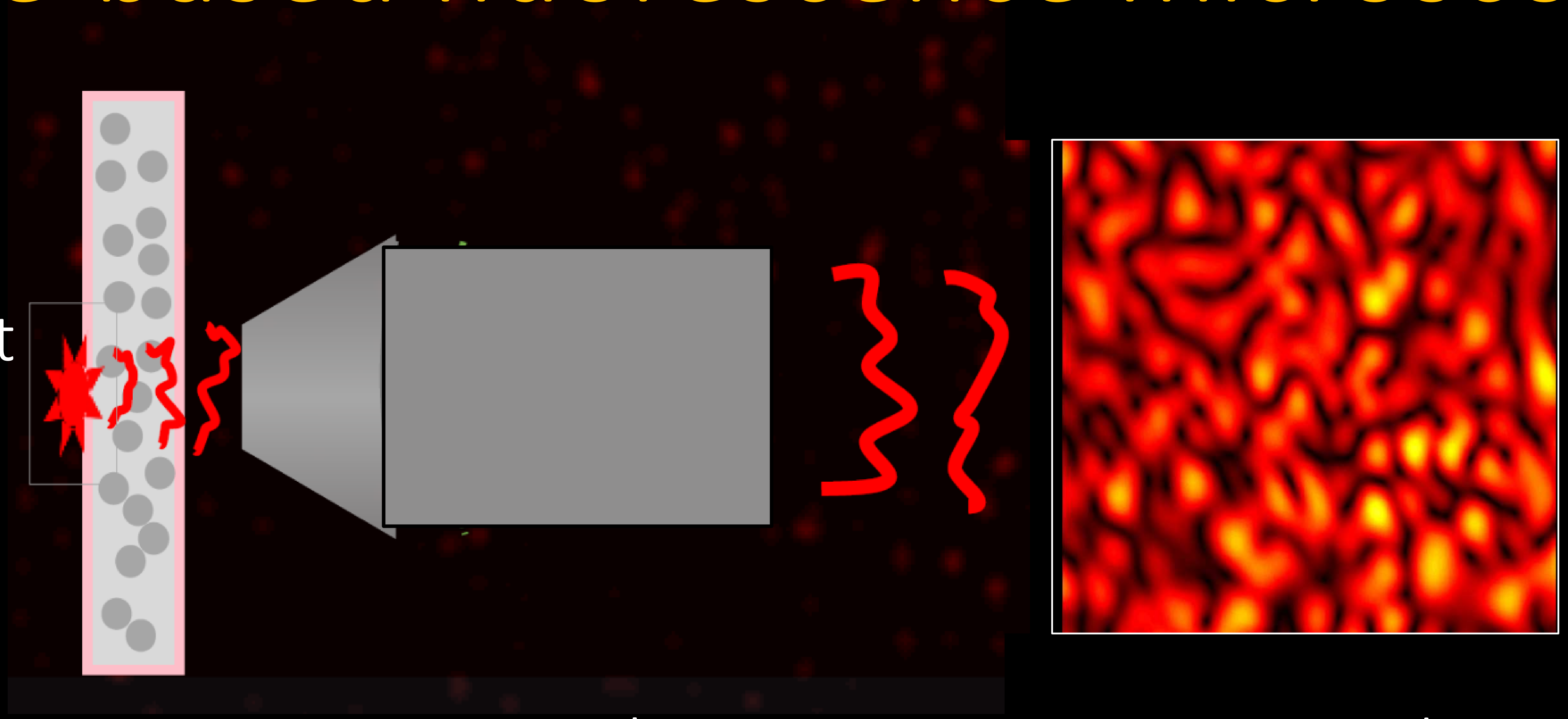

scattering sample

microscope objective

captured image

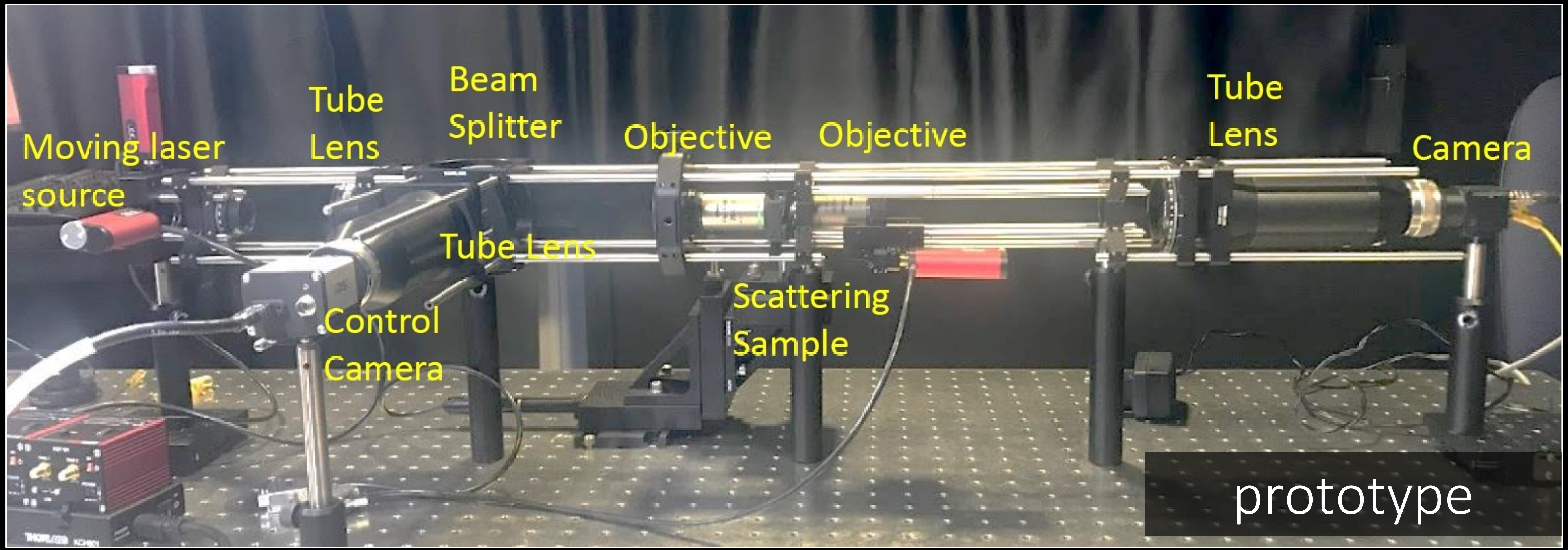

Speckle-based fluorescence microscopy

fluorescent particles

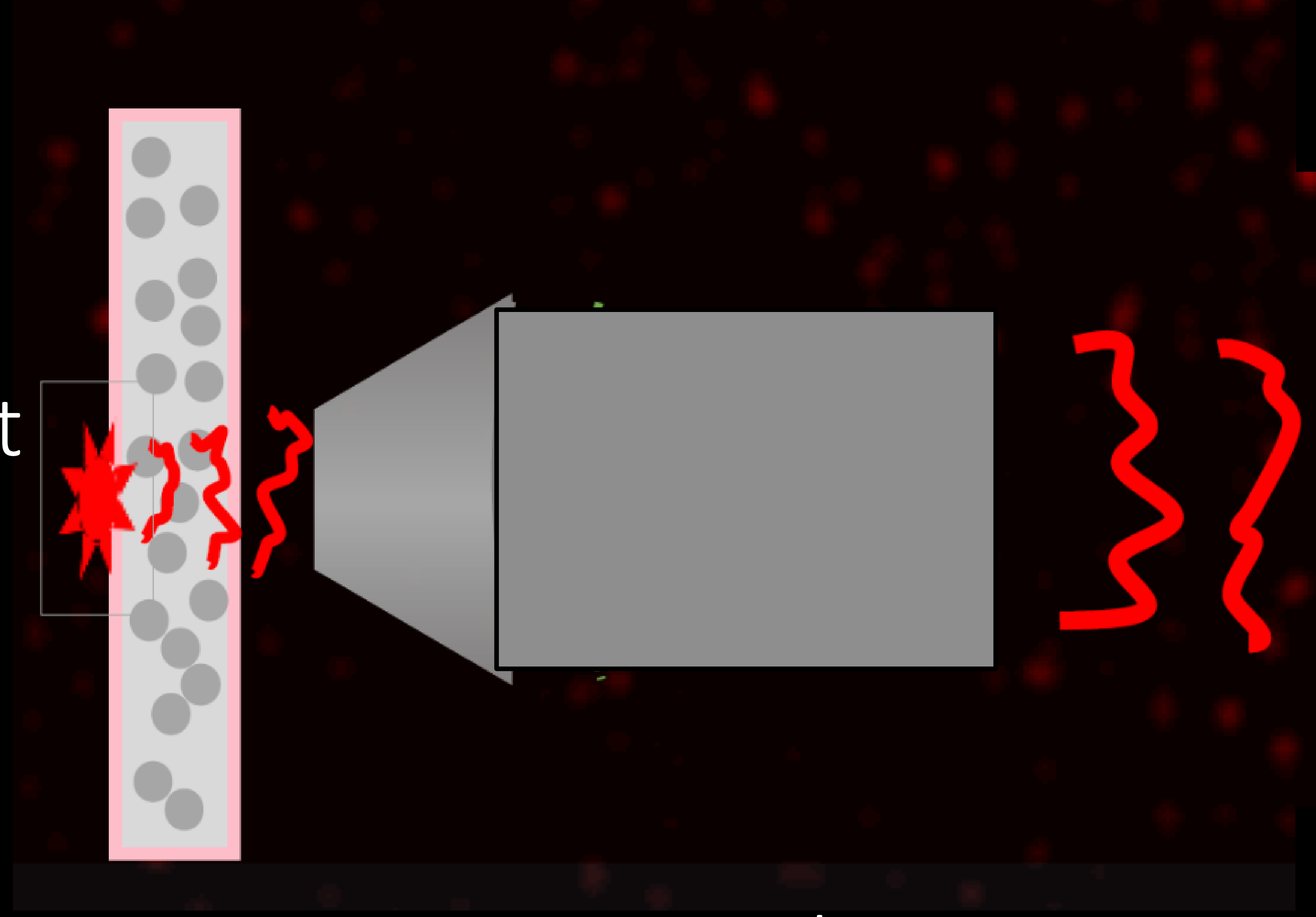

scattering sample

microscope objective

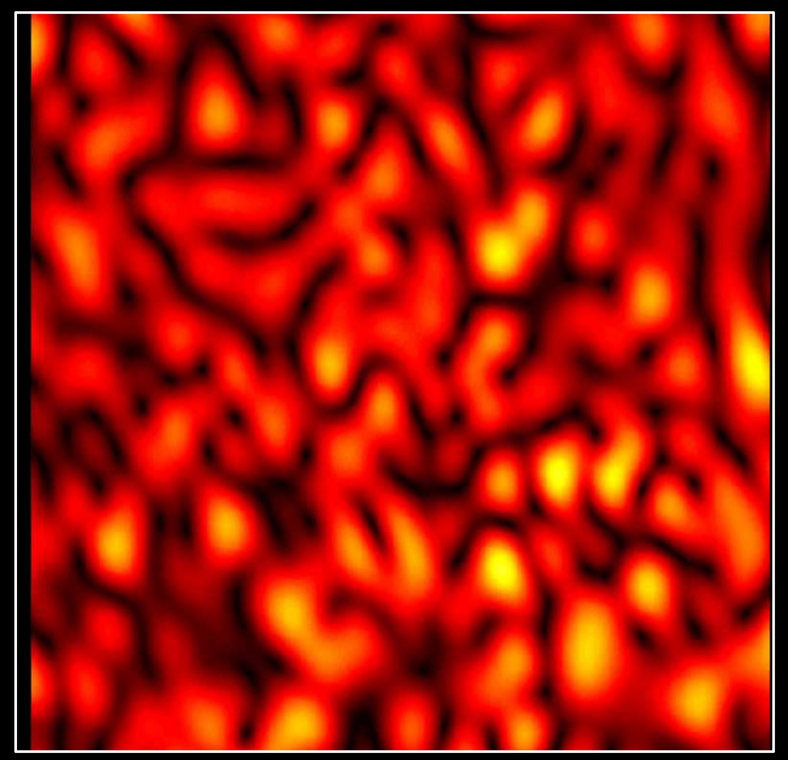

captured image

→ ? →

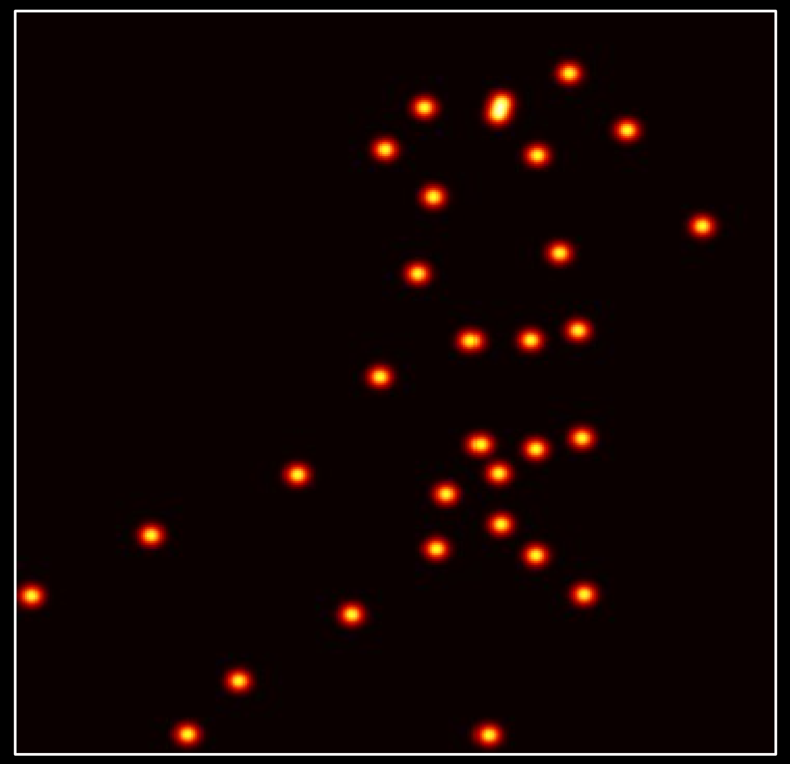

scattering-free image

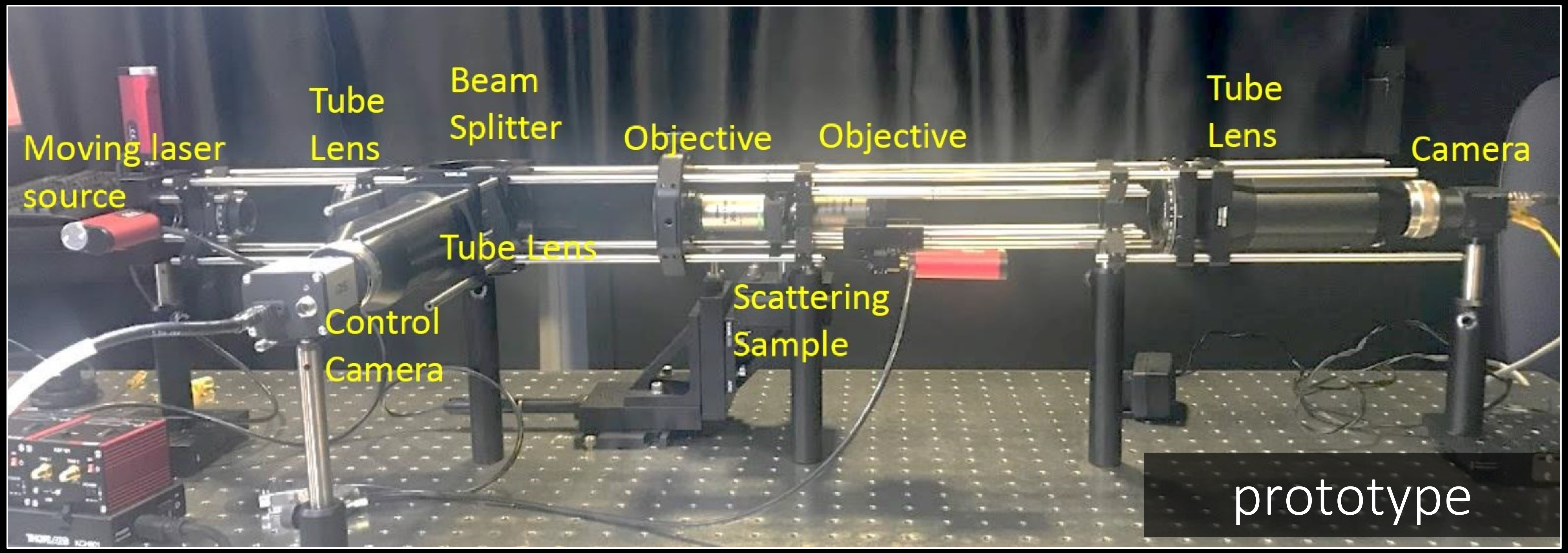

Use the memory effect to image through scattering

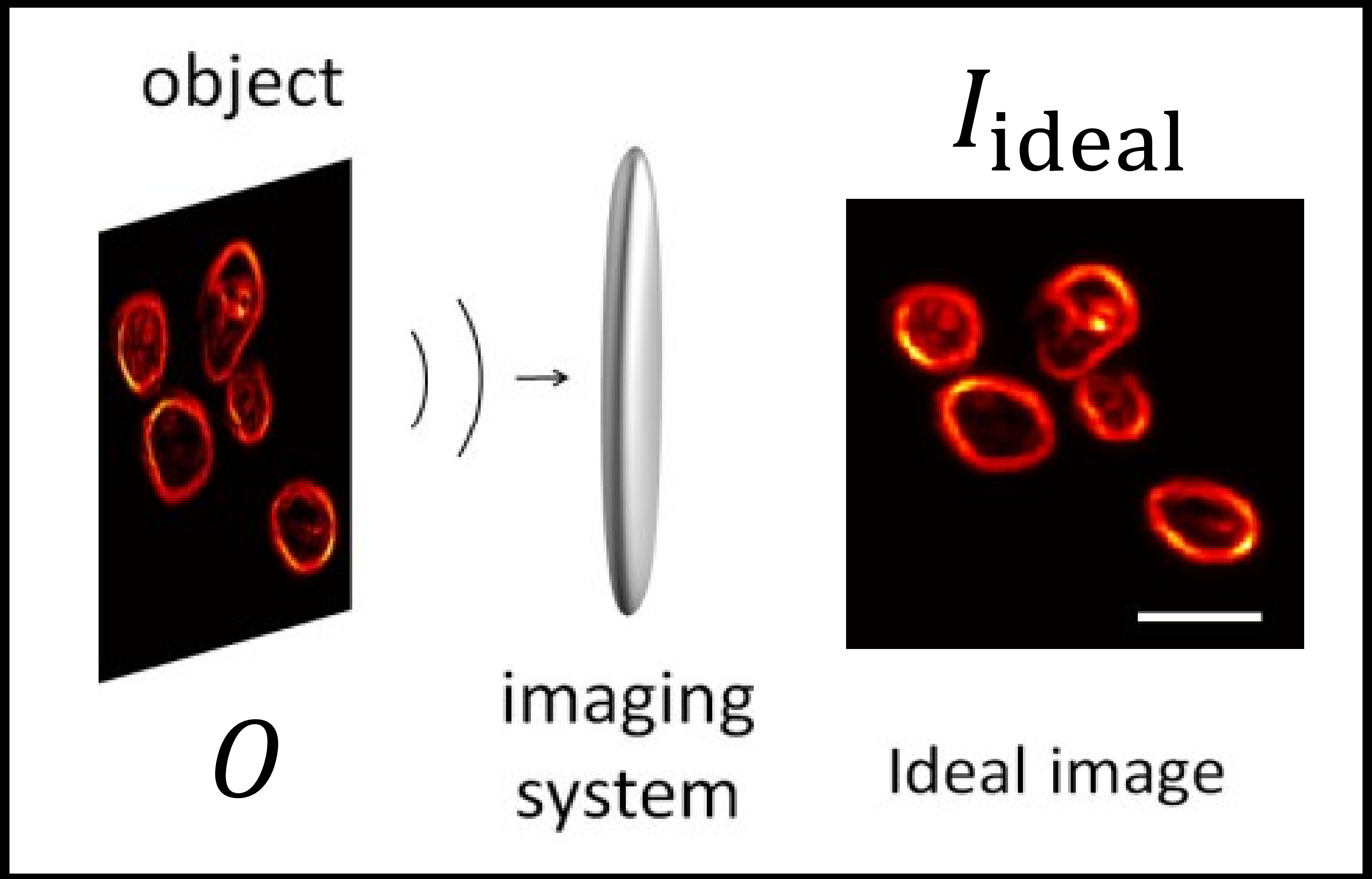

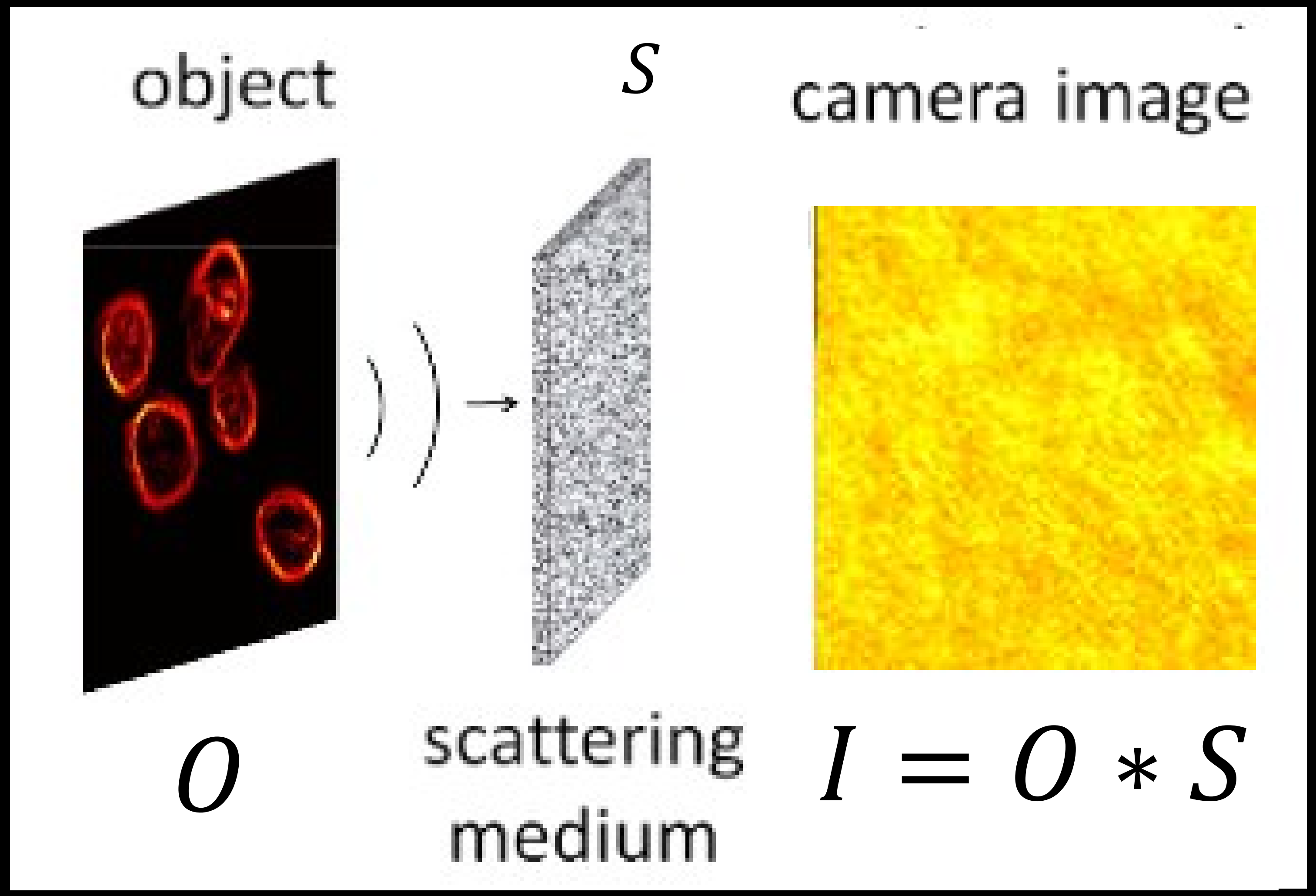

[Katz et al., 2014]

Use the memory effect to image through scattering

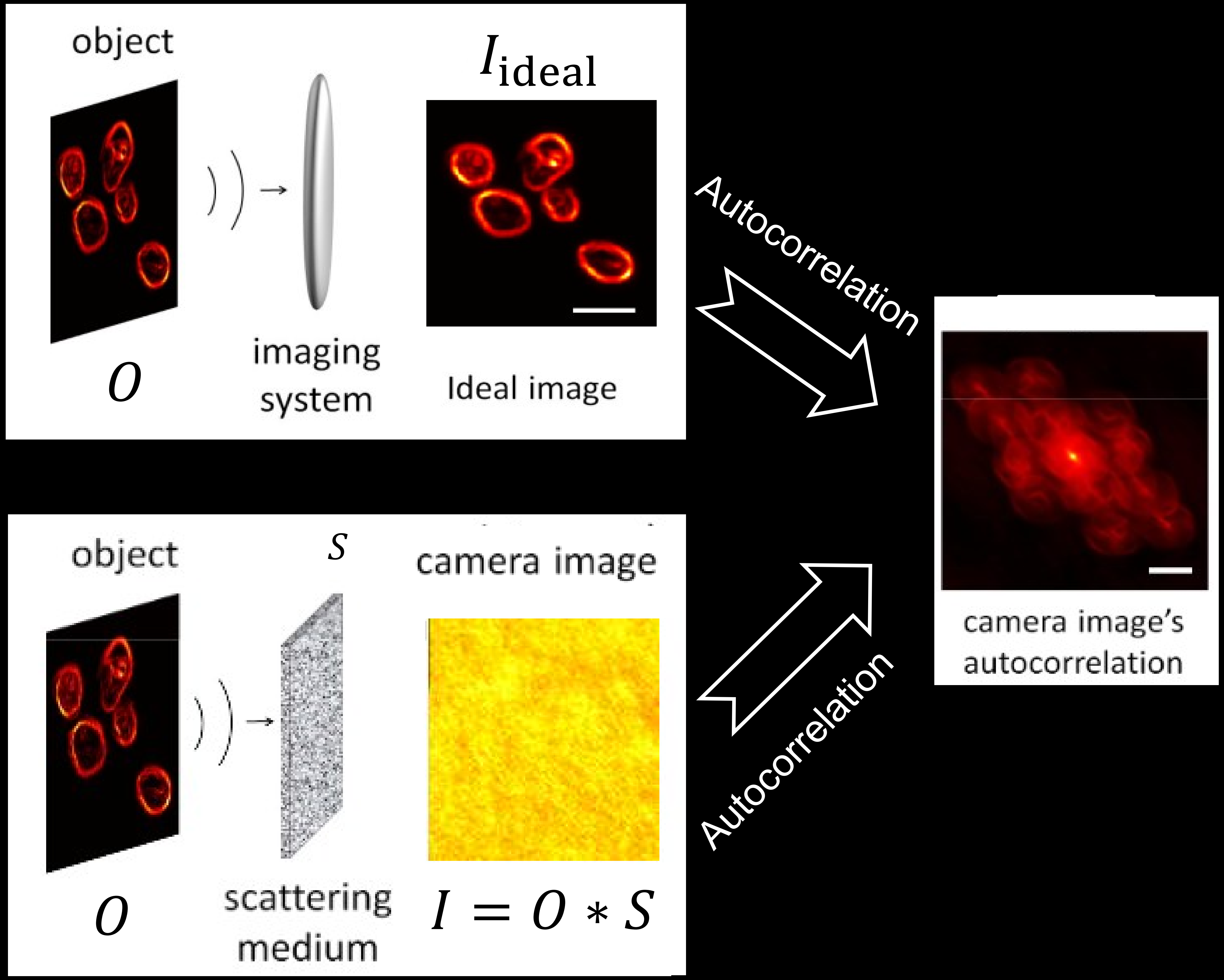

[Katz et al., 2014]

Use the memory effect to image through scattering

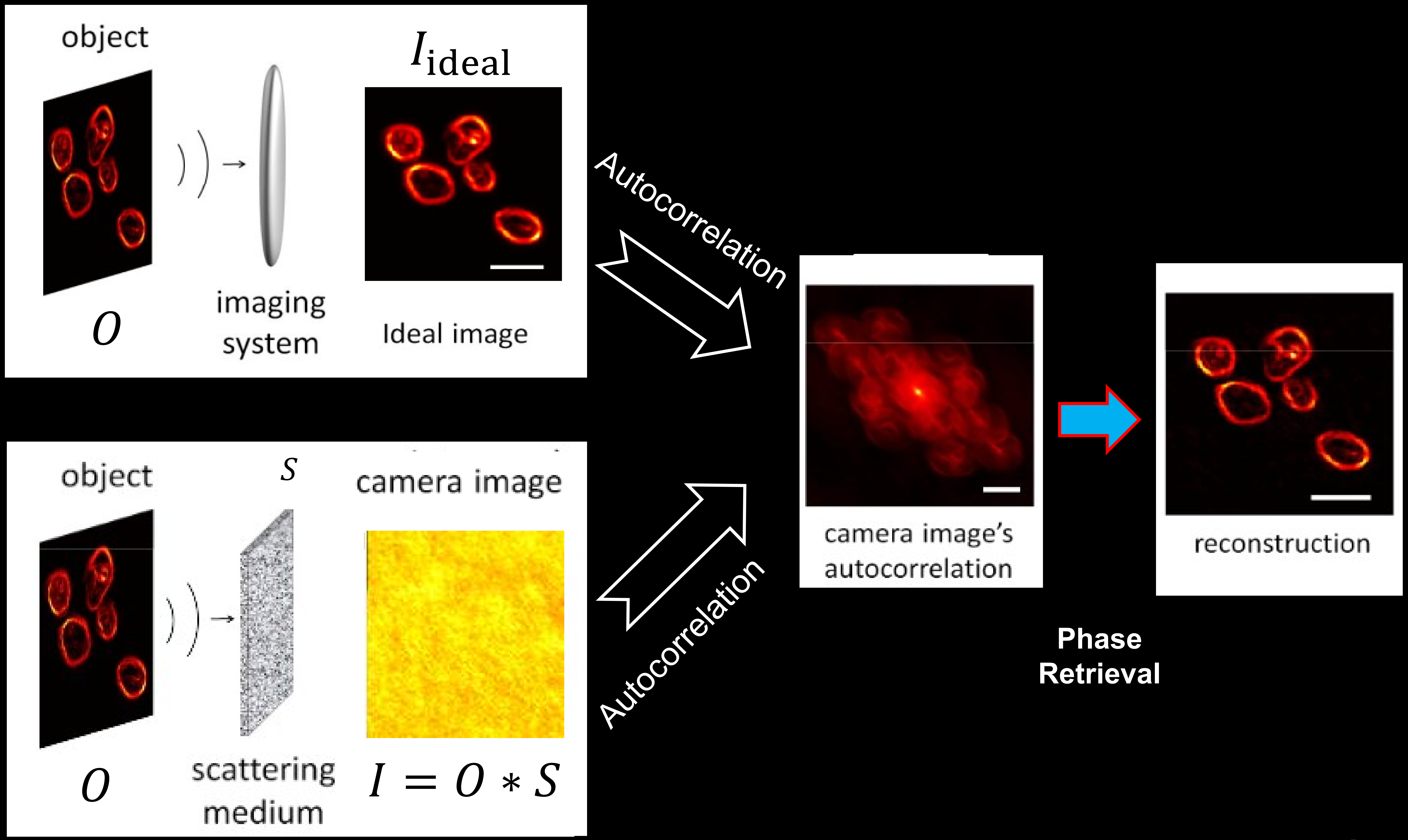

[Katz et al., 2014]

Use the memory effect to image through scattering

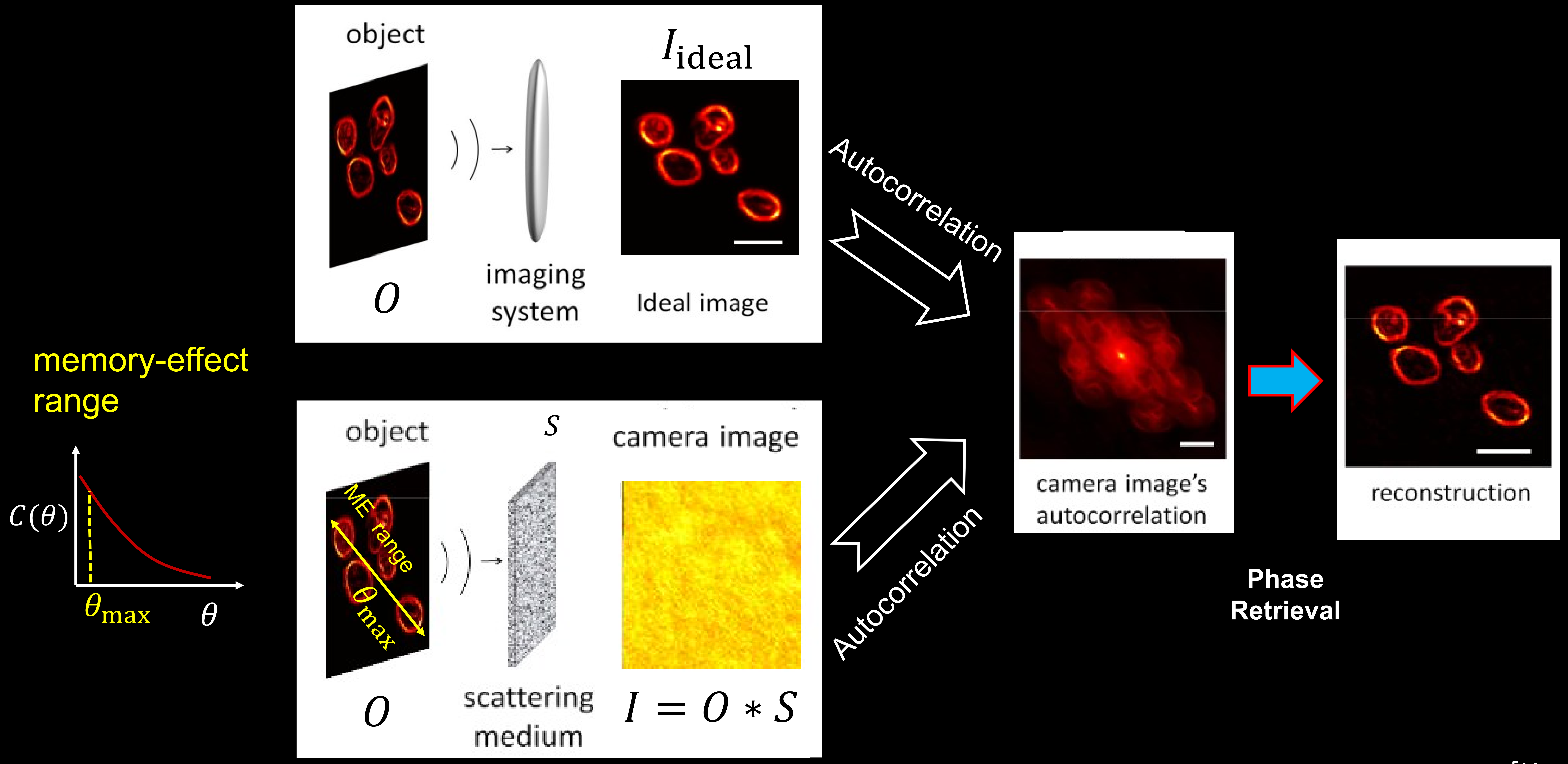

[Katz et al., 2014]

Speckle-based fluorescence microscopy

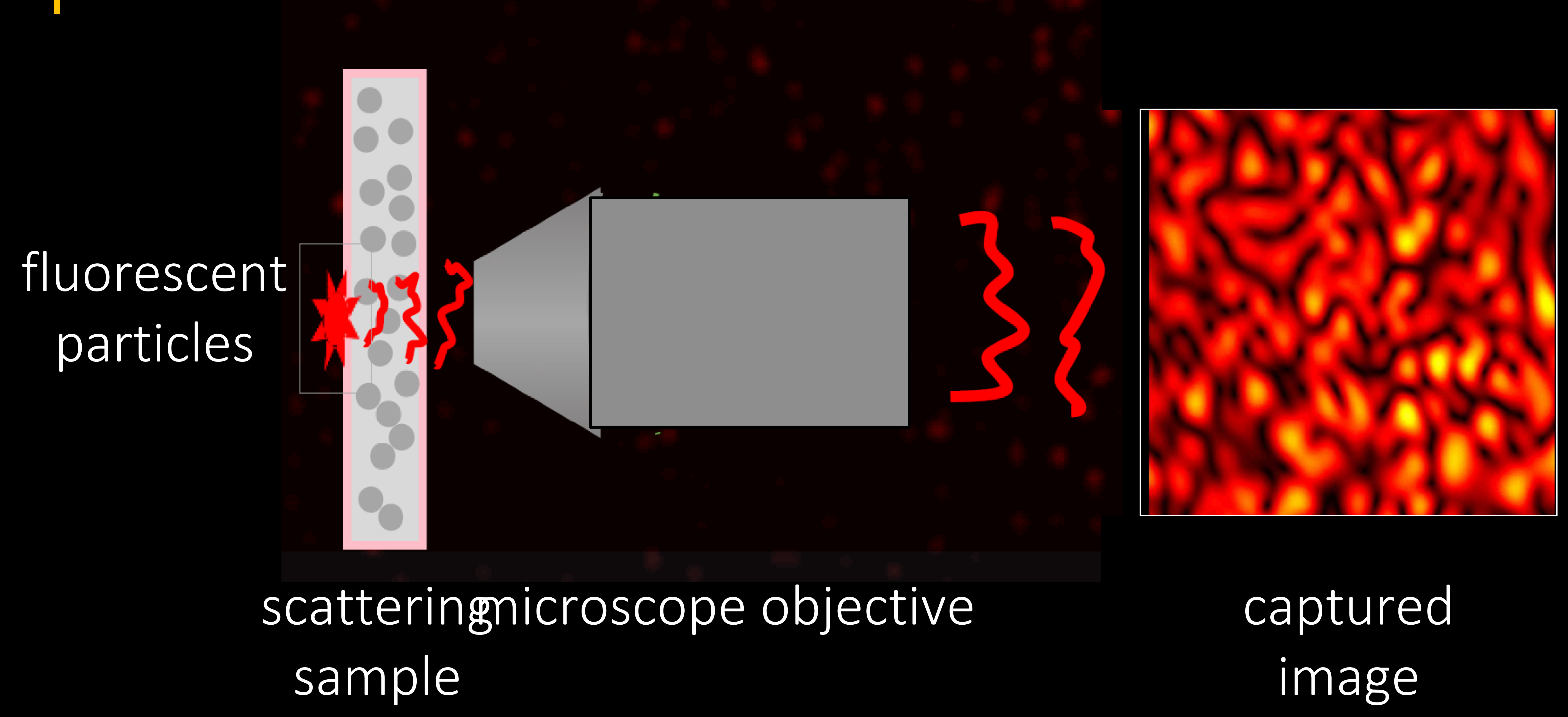

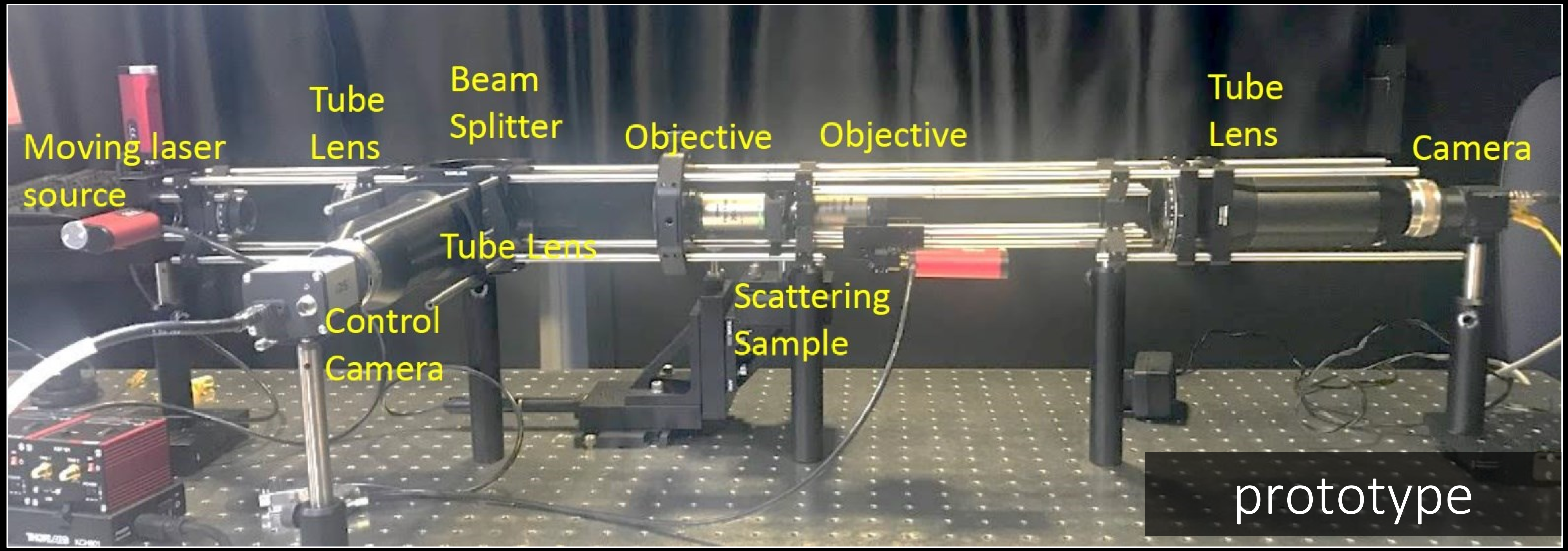

[PIs: Gkioulekas, Levin]

Speckle-based fluorescence microscopy

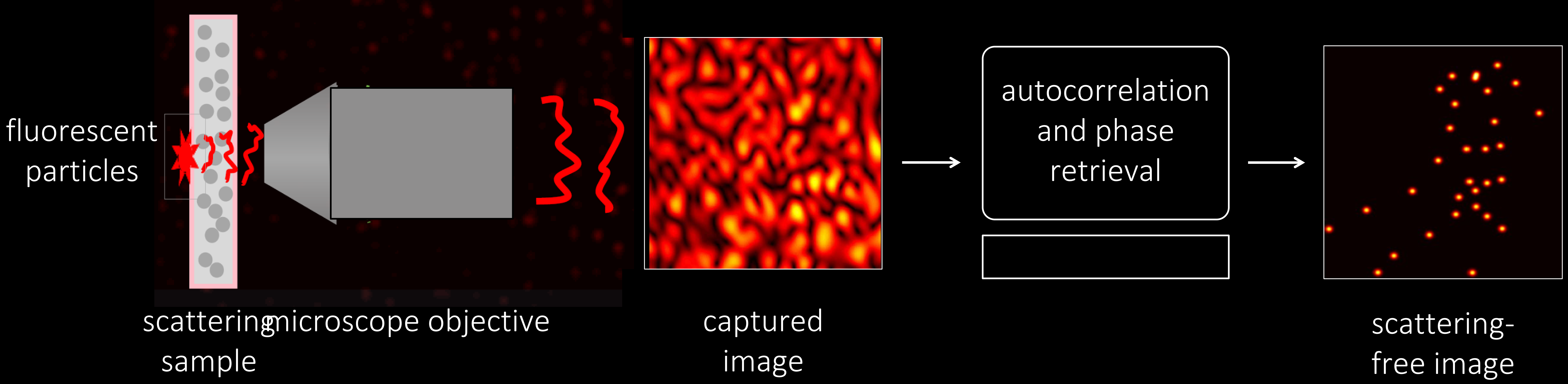

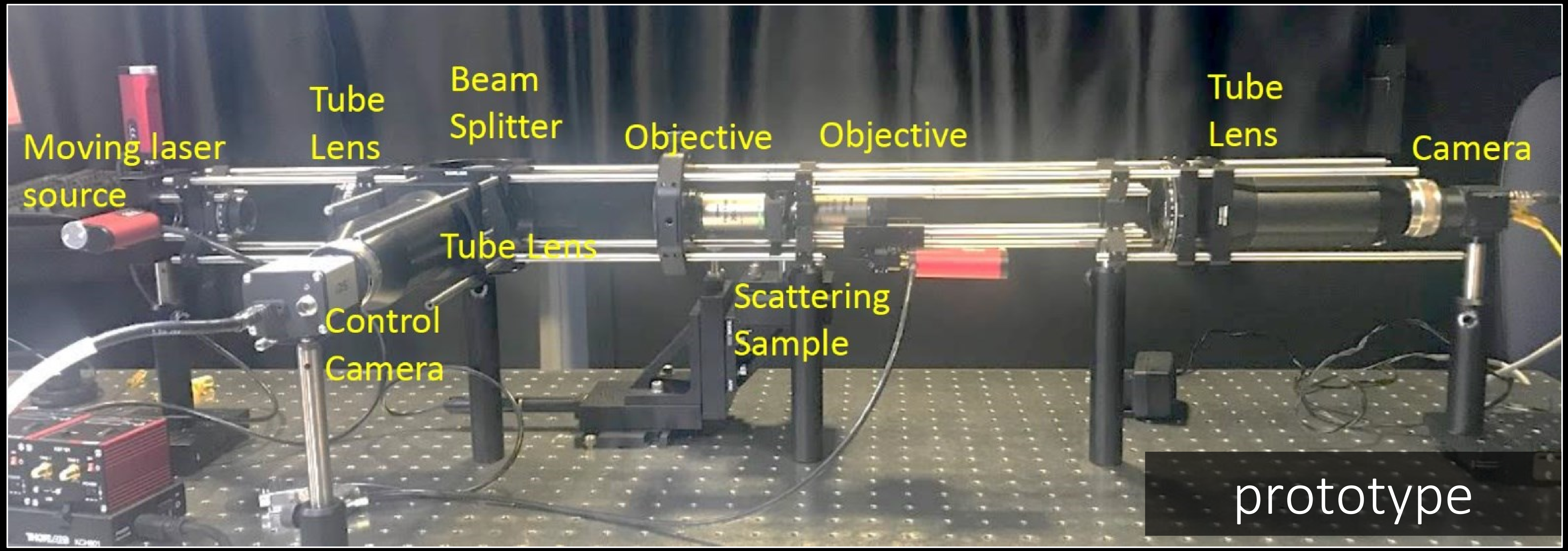

[PIs: Gkioulekas, Levin]

Speckle-based fluorescence microscopy

Performance strongly depends on:

- speckle statistics
- image priors
- tissue parameters

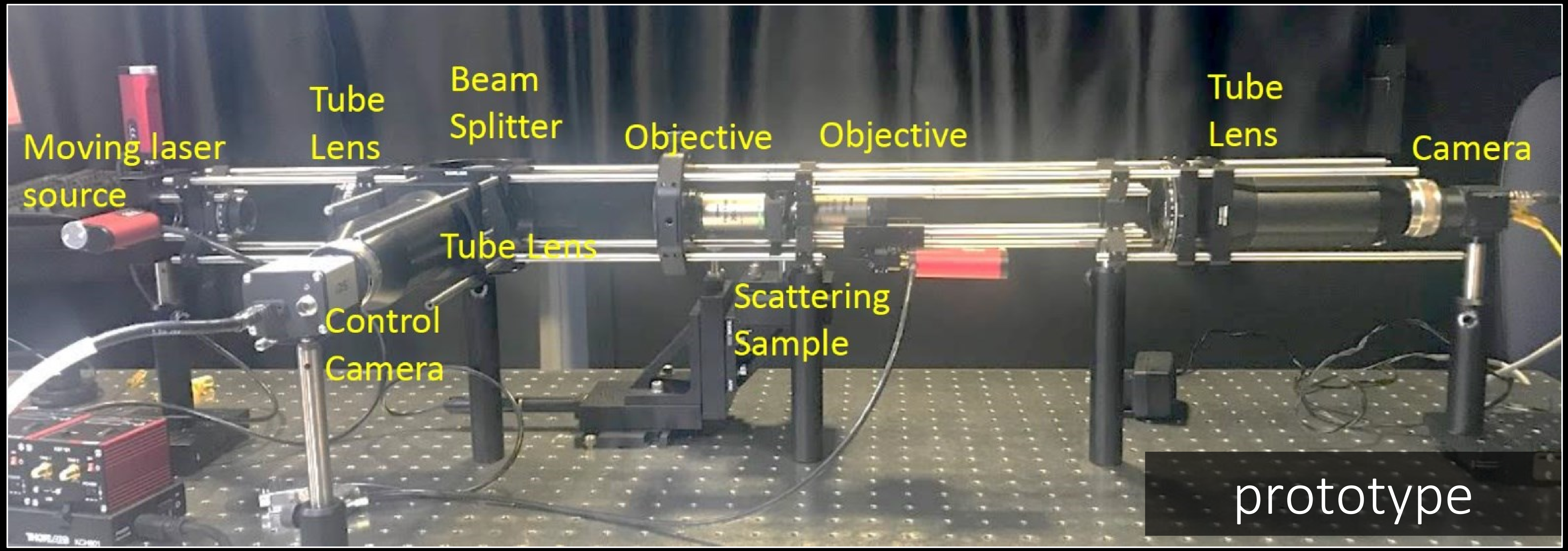

[PIs: Gkioulekas, Levin]

Recap: Monte Carlo (volumetric) rendering

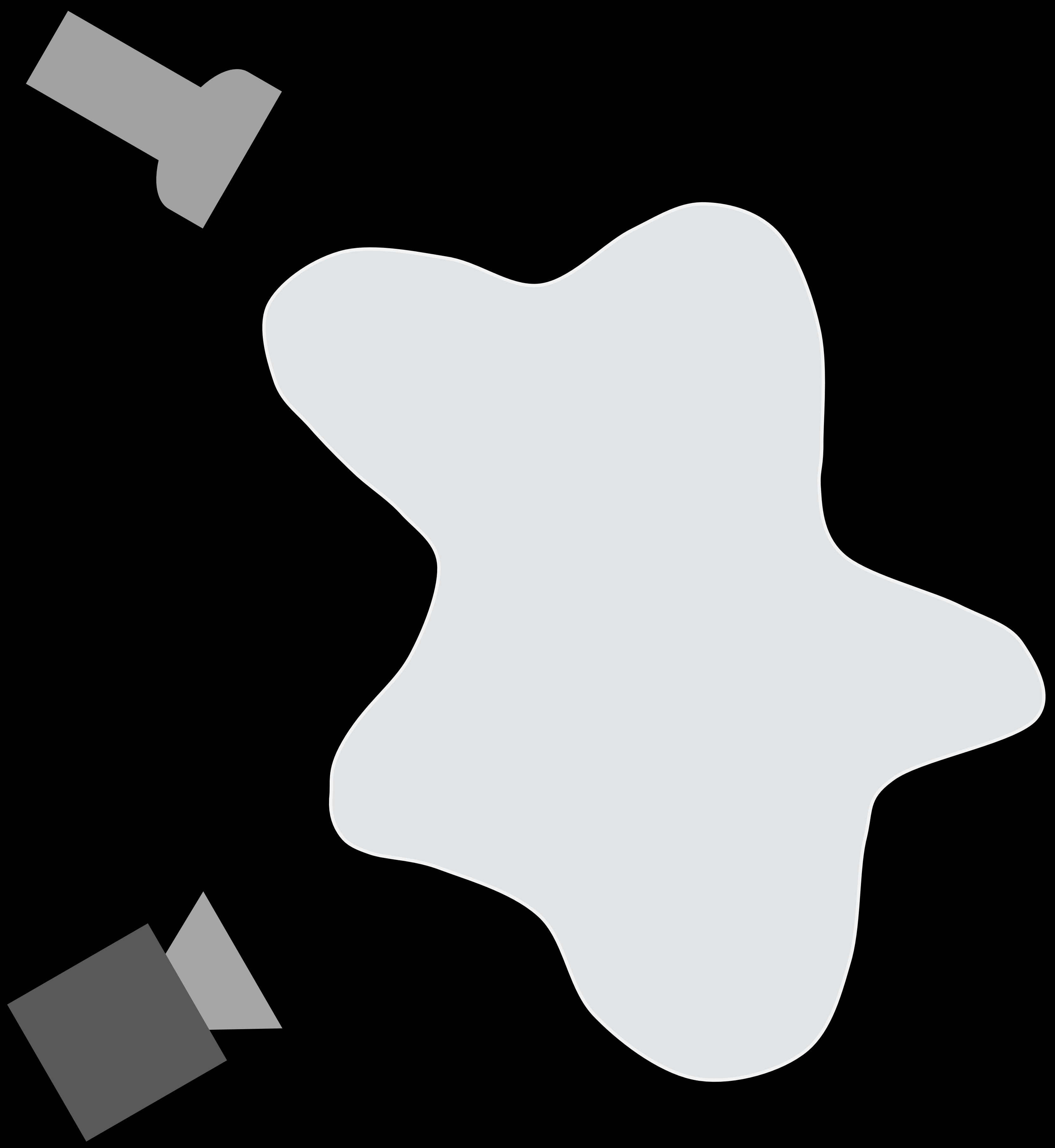

$$\text{Image} = \int_{\text{paths}} f(\text{path})$$

[Bar et al., 2019]

Recap: Monte Carlo (volumetric) rendering

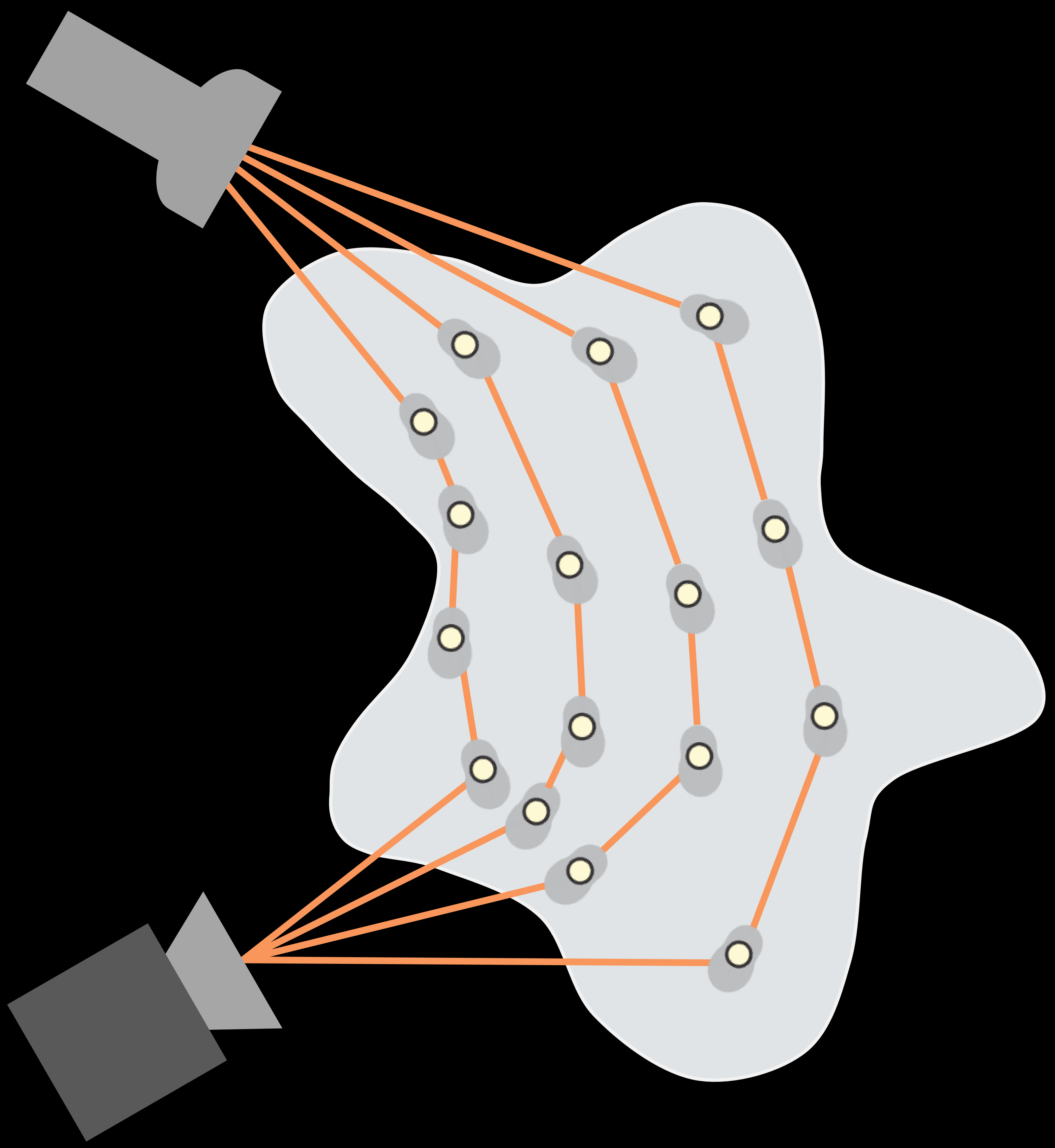

$$\text{Image} = \int_{\text{paths}} f(\text{path})$$

[Bar et al., 2019]

Recap: Monte Carlo (volumetric) rendering

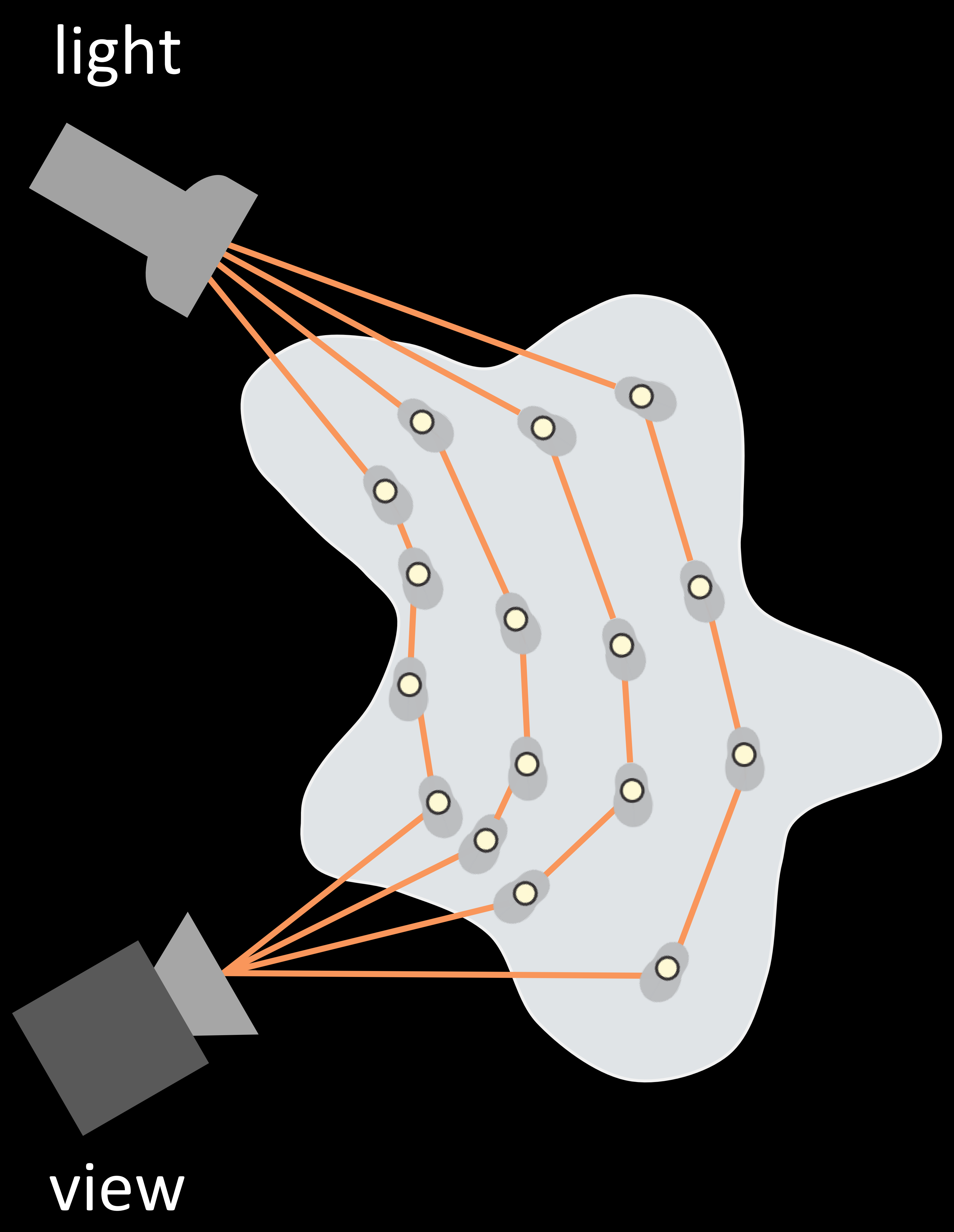

$$\text{Image} = \int_{\text{paths}} f(\text{path})$$

Path contribution, depends on the scattering material

[Bar et al., 2019]

Recap: Monte Carlo (volumetric) rendering

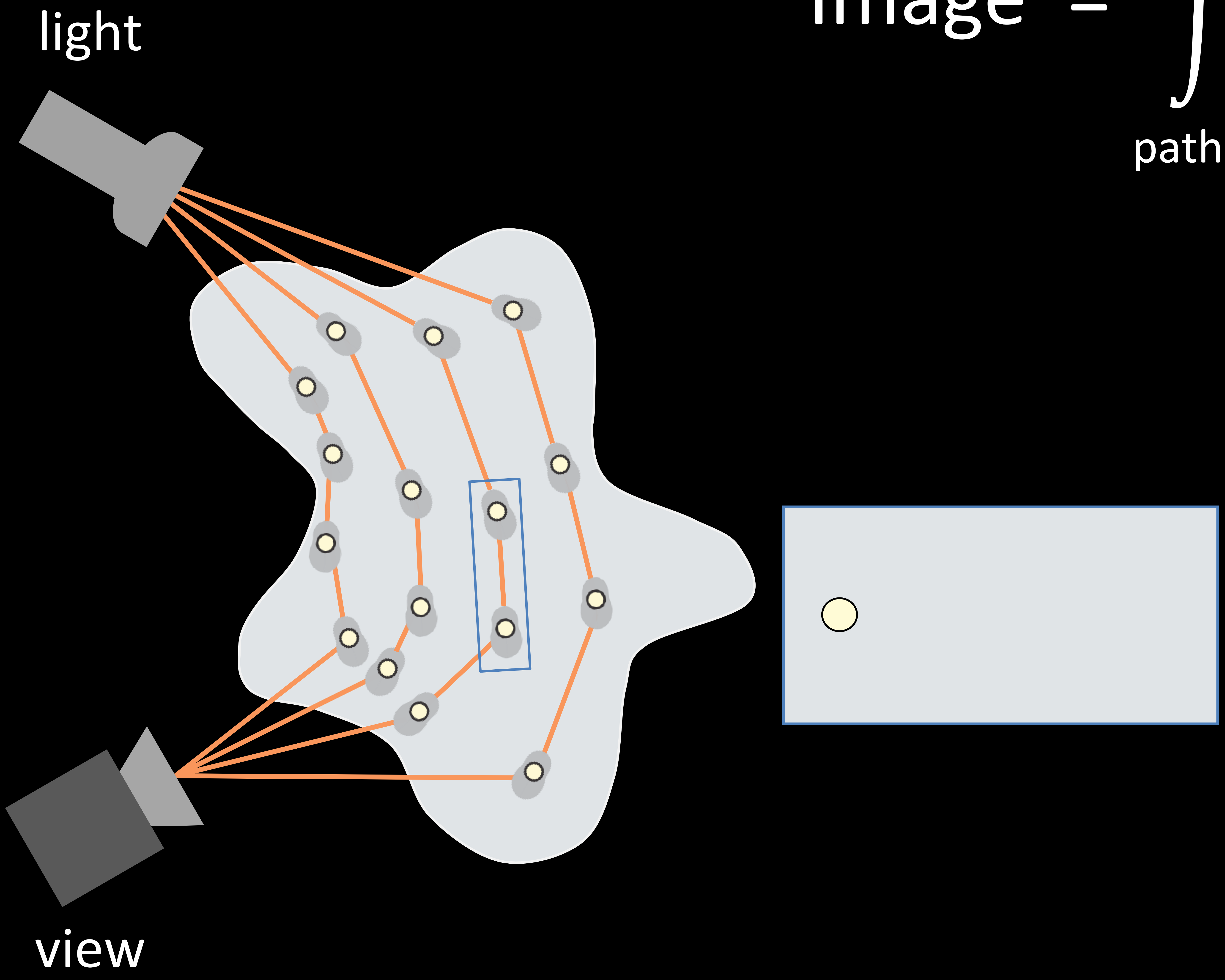

$$\text{Image} = \int_{\text{paths}} f(\text{path})$$

Path contribution, depends on the scattering material

[Bar et al., 2019]

Recap: Monte Carlo (volumetric) rendering

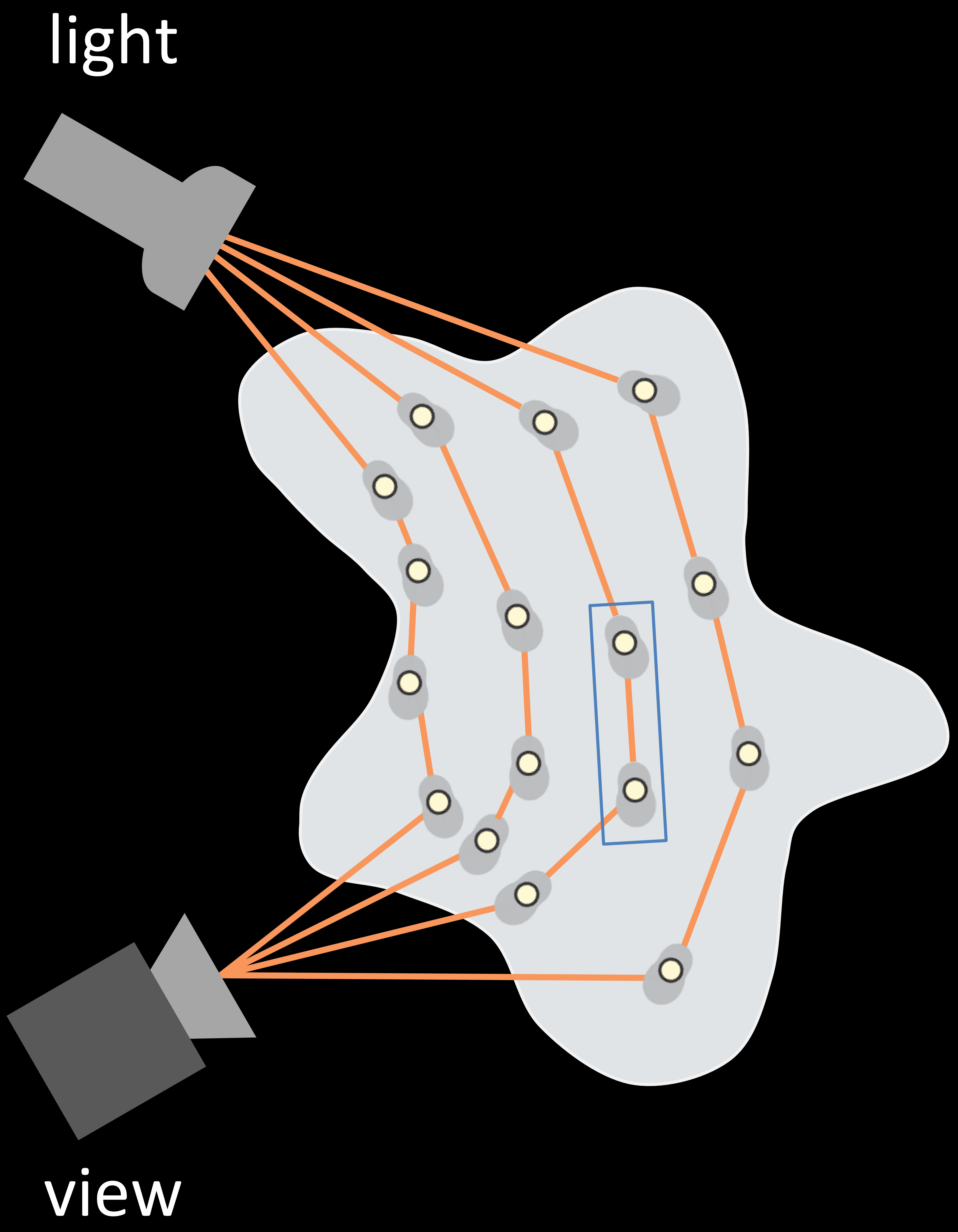

$$\text{Image} = \int_{\text{paths}} f(\text{path})$$

Path contribution, depends on the scattering material

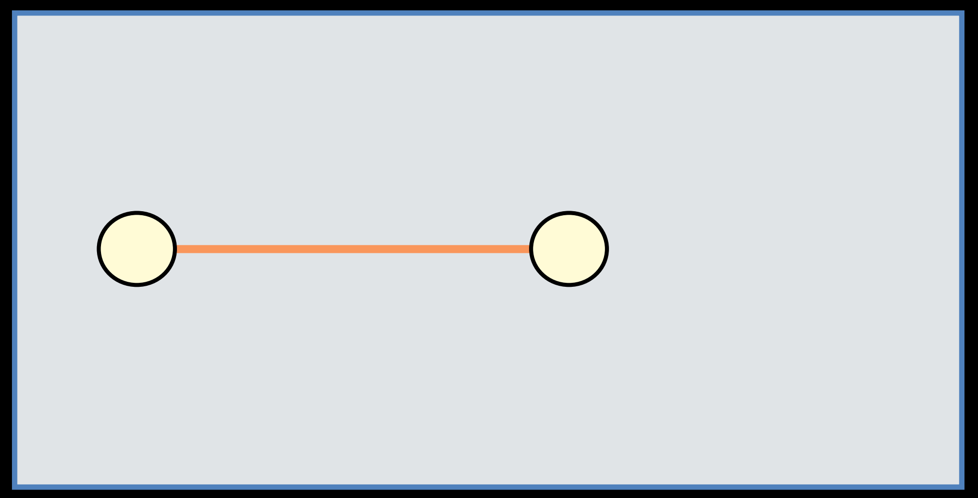

volumetric density

(extinction coefficient) σ

[Bar et al., 2019]

Recap: Monte Carlo (volumetric) rendering

$$\text{Image} = \int_{\text{paths}} f(\text{path})$$

Path contribution, depends on the scattering material

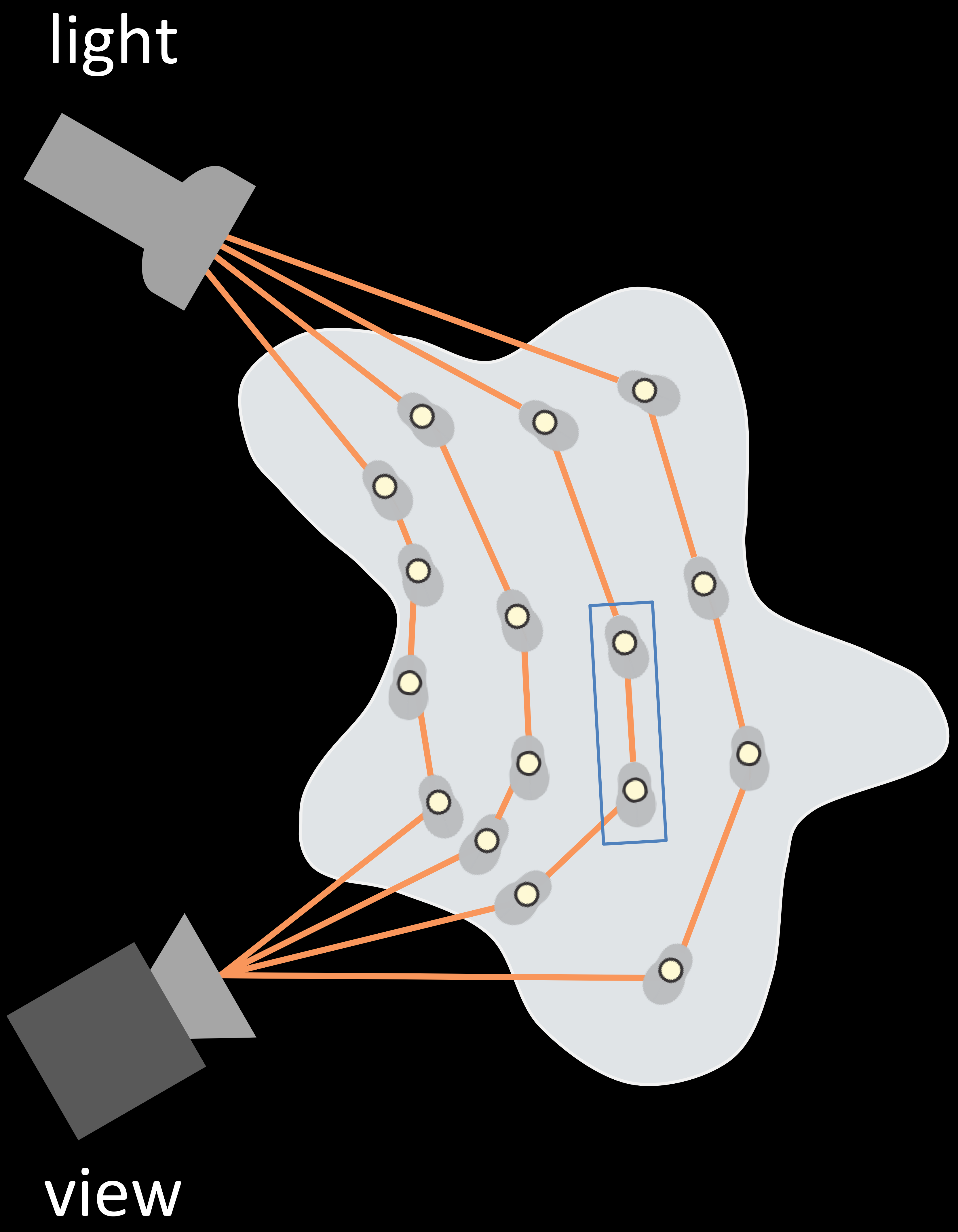

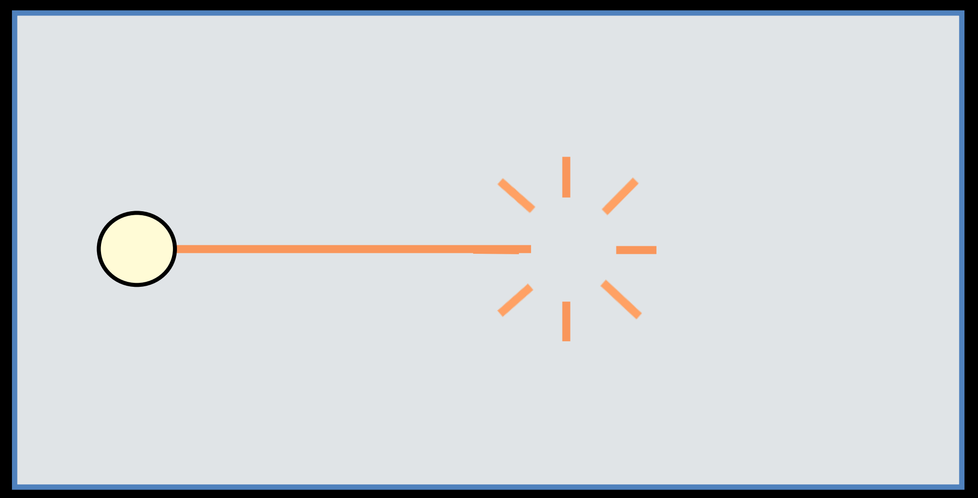

volumetric density (extinction coefficient) σ

scattering albedo a

[Bar et al., 2019]

Recap: Monte Carlo (volumetric) rendering

$$\text{Image} = \int_{\text{paths}} f(\text{path})$$

Path contribution, depends on the scattering material

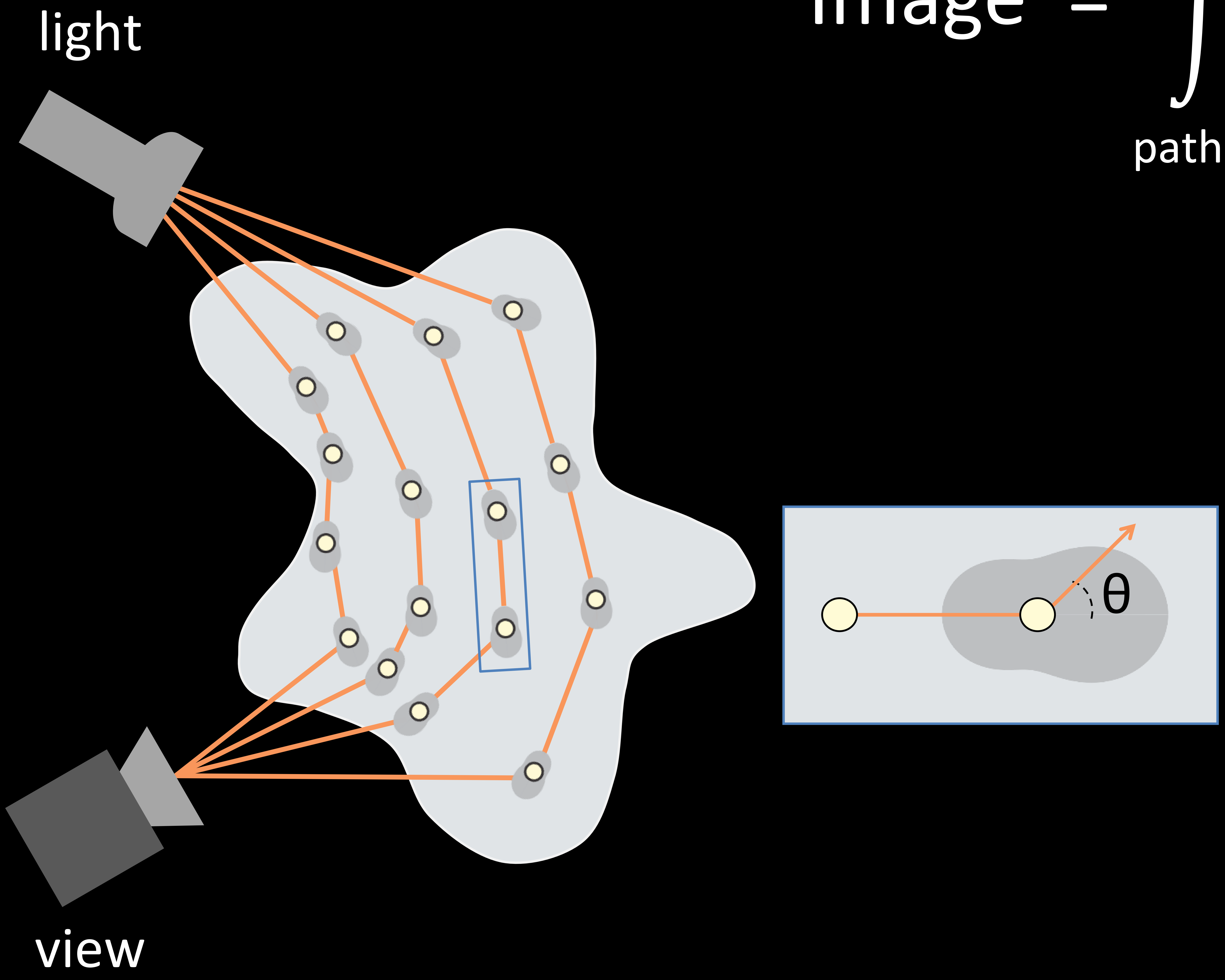

volumetric density (extinction coefficient) σ

scattering albedo a

phase function p_θ

[Bar et al., 2019]

Recap: Monte Carlo (volumetric) rendering

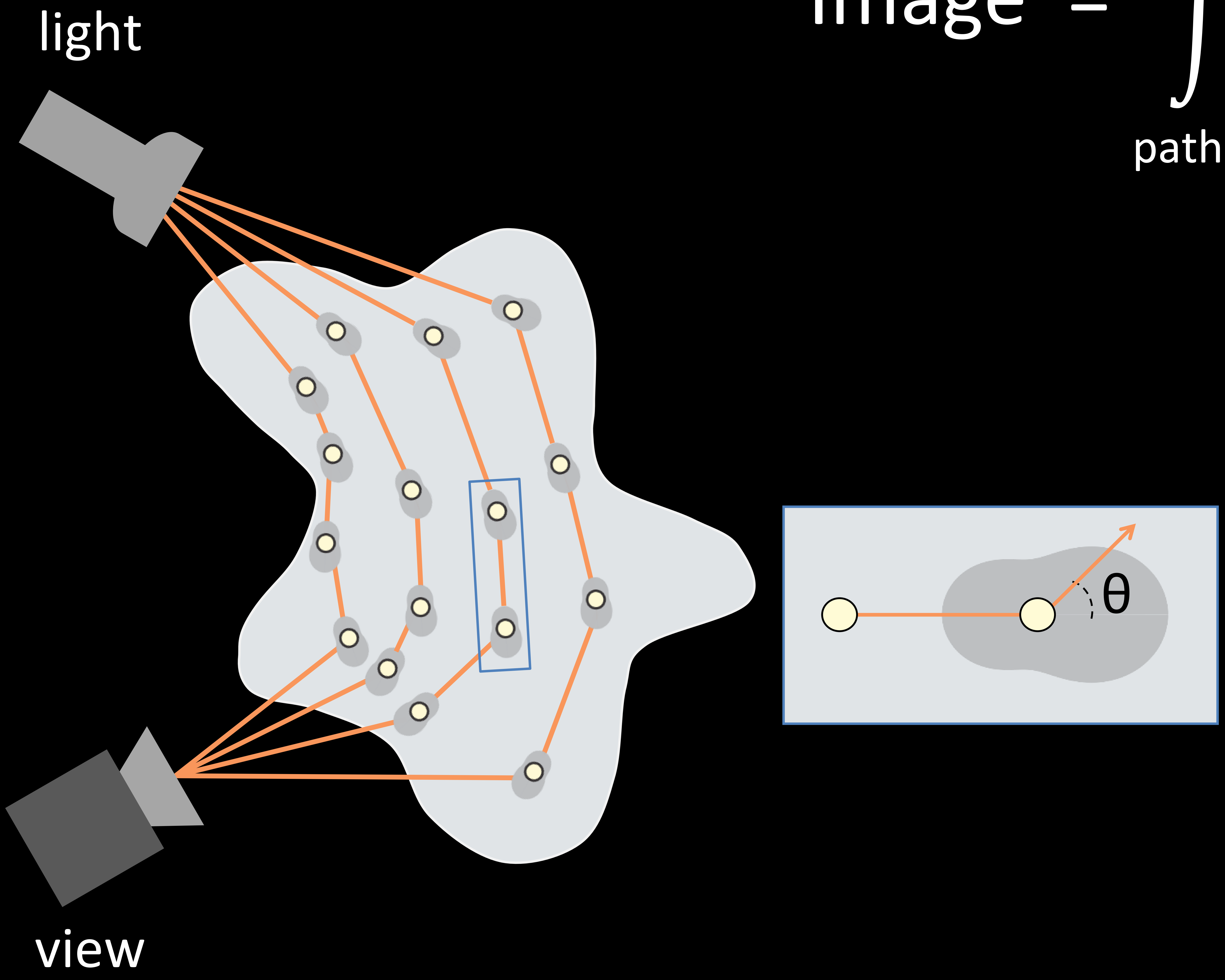

$$\text{Image} = \int_{\text{paths}} f(\text{path})$$

Path contribution, depends on the scattering material

$$\text{material} = \begin{bmatrix} \sigma \\ a \\ p_\theta \end{bmatrix}$$

[Bar et al., 2019]

Recap: Monte Carlo (volumetric) rendering

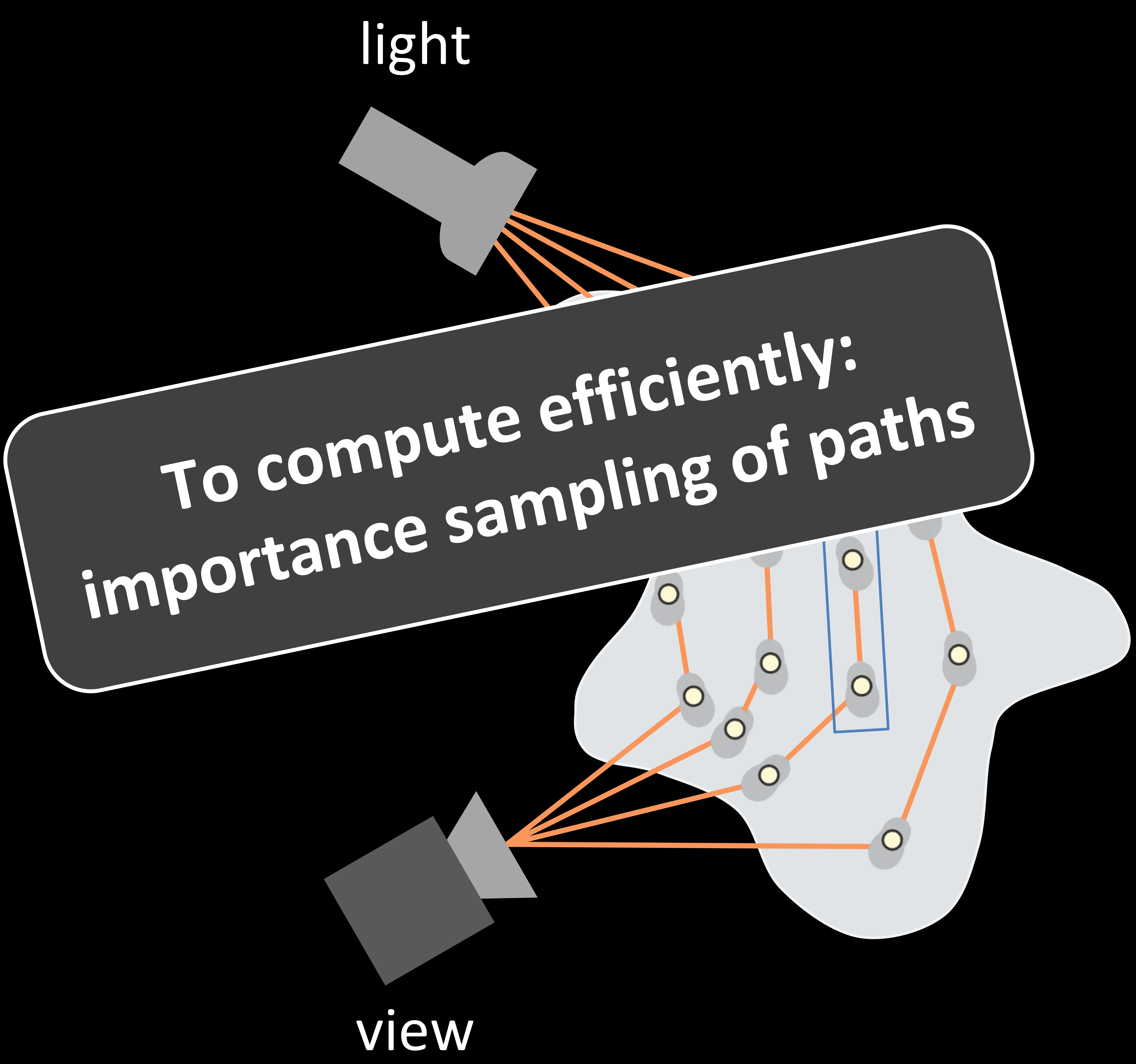

$$\text{Image} = \int_{\text{paths}} f(\text{path})$$

Path contribution, depends on the scattering material

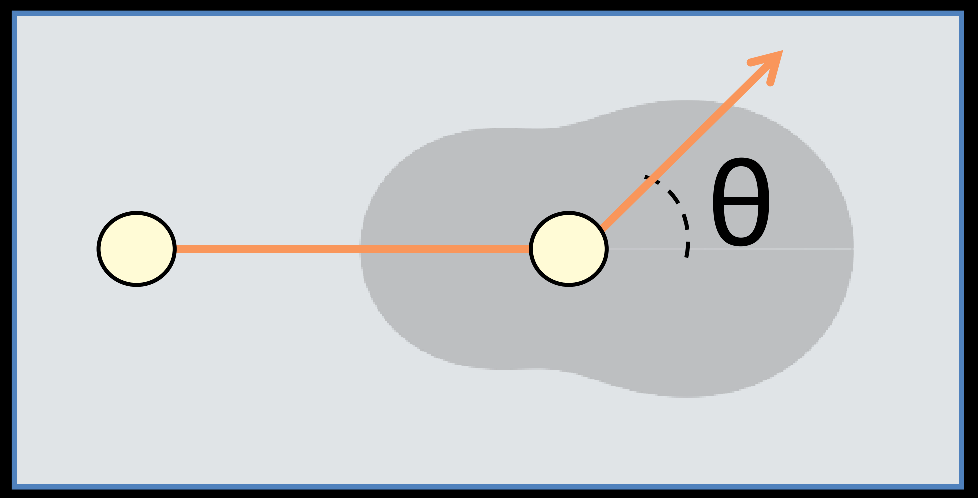

$$\text{material} = \begin{bmatrix} \sigma \\ a \\ p_\theta \end{bmatrix}$$

[Bar et al., 2019]

Memory effect: simulate *covariance* of speckle images

$$\text{Covariance} = \int_{\text{path}_1,\text{path}_2} u(\text{path}_1) \cdot u^*(\text{path}_2)$$

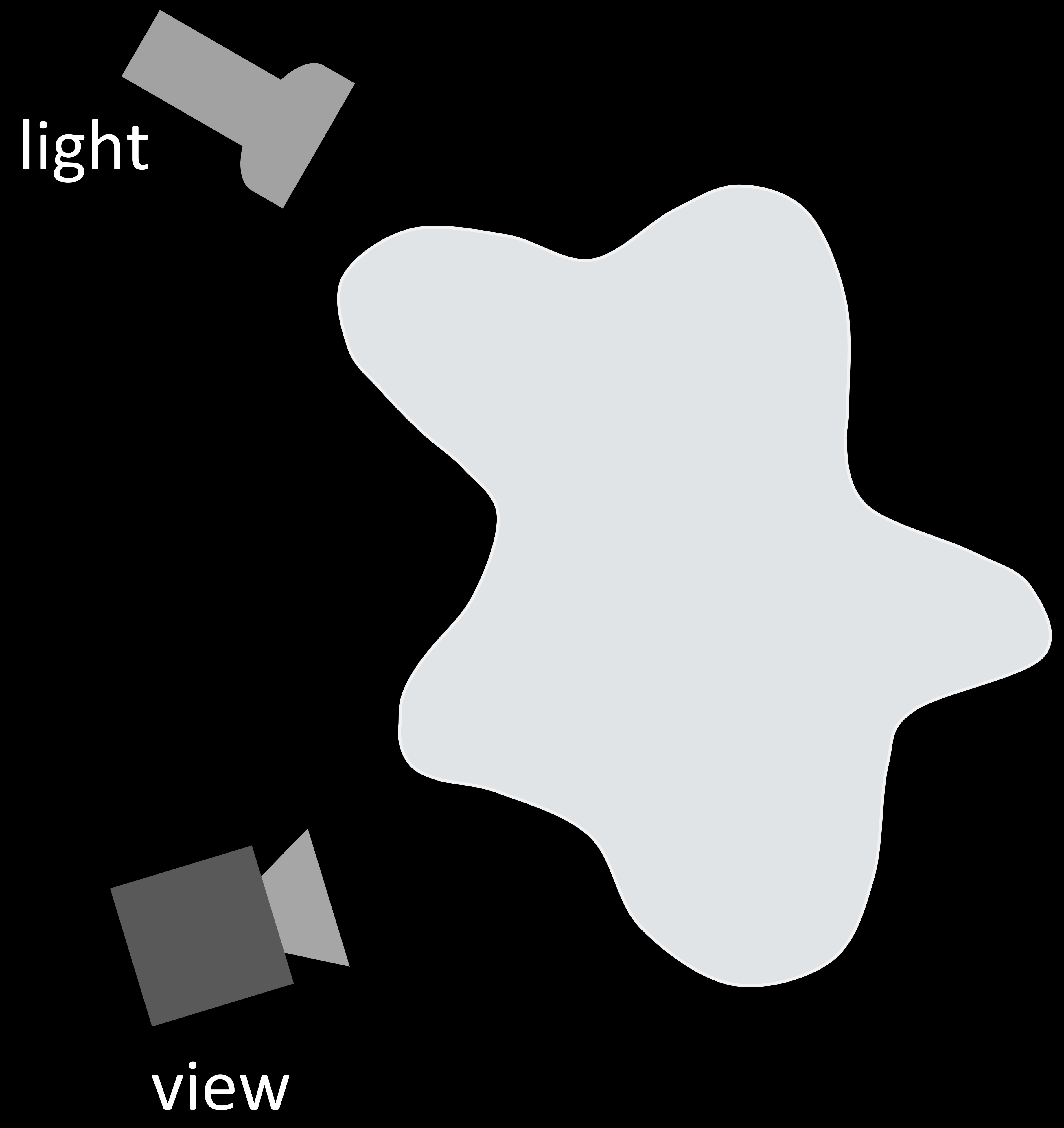

[Bar et al., 2019]

Memory effect: simulate *covariance* of speckle images

$$\text{Covariance} = \int_{\text{path}_1,\text{path}_2} u(\text{path}_1) \cdot u^*(\text{path}_2)$$

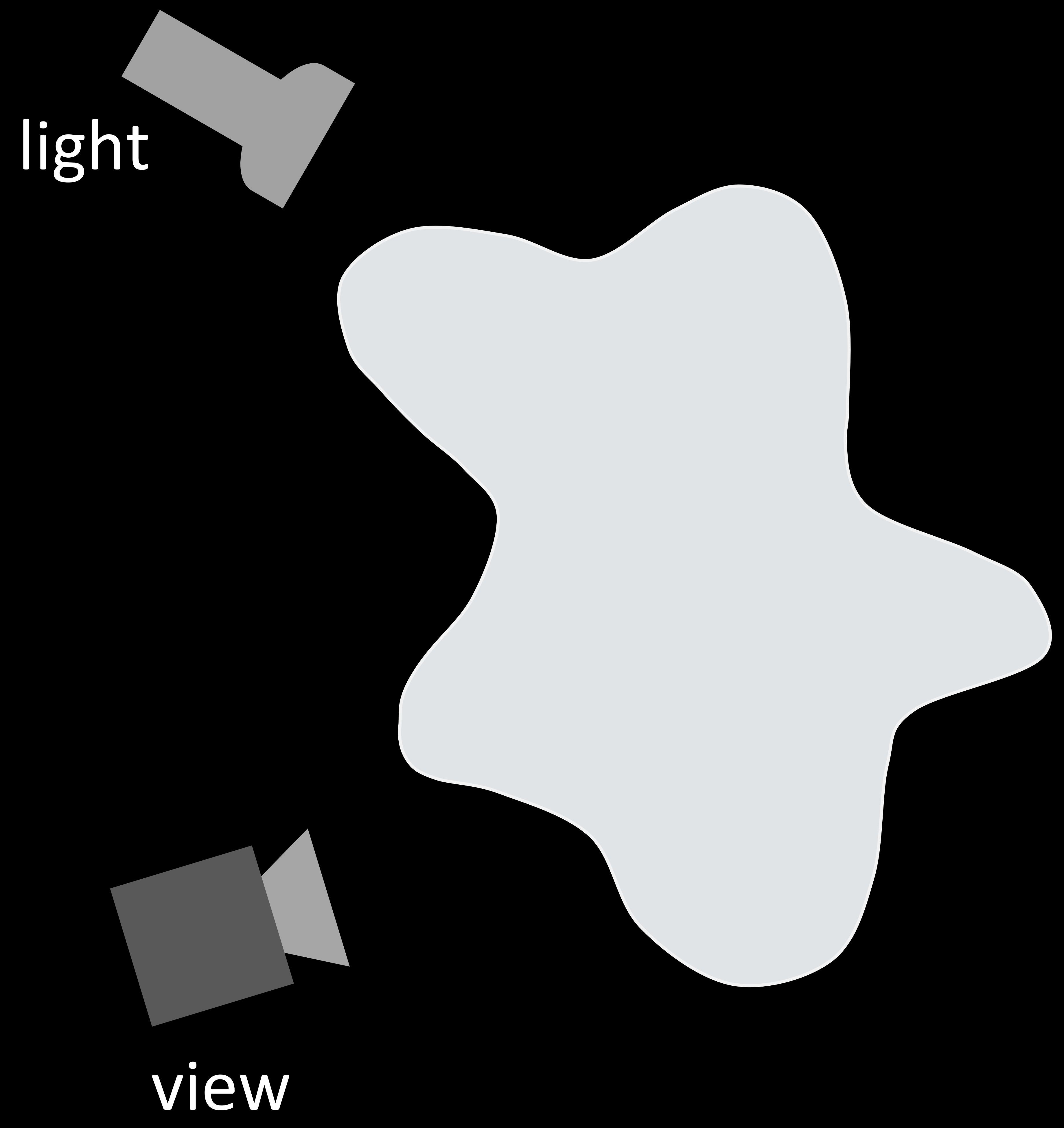

Need to consider products of ***pairs*** of paths

[Bar et al., 2019]

Memory effect: simulate *covariance* of speckle images

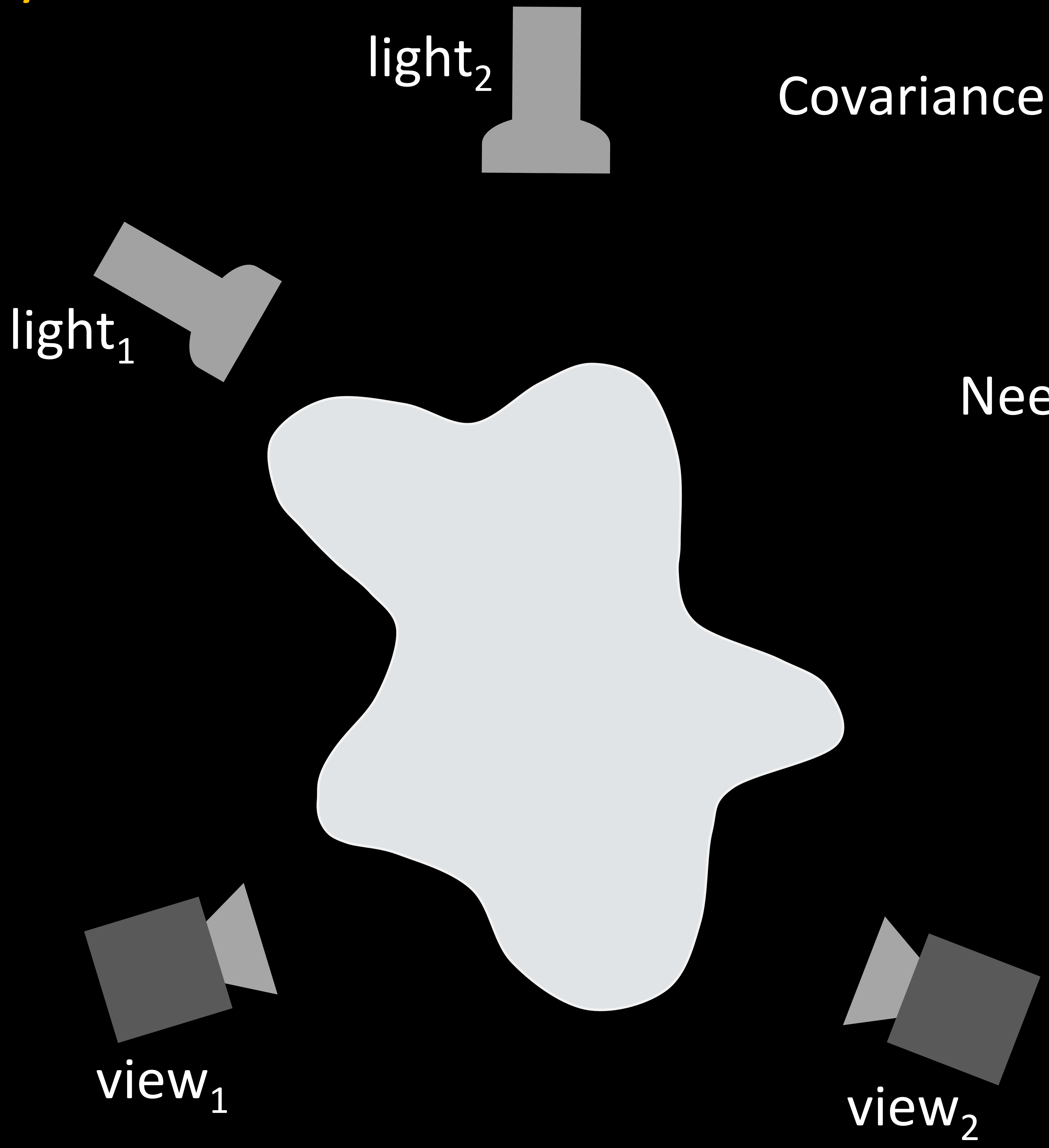

$$\text{Covariance} = \int_{\text{path}_1,\text{path}_2} u(\text{path}_1) \cdot u^*(\text{path}_2)$$

Need to consider products of ***pairs*** of paths

[Bar et al., 2019]

Memory effect: simulate *covariance* of speckle images

$$\text{Covariance} = \int_{\text{path}_1,\text{path}_2} u(\text{path}_1) \cdot u^*(\text{path}_2)$$

Need to consider products of ***pairs*** of paths

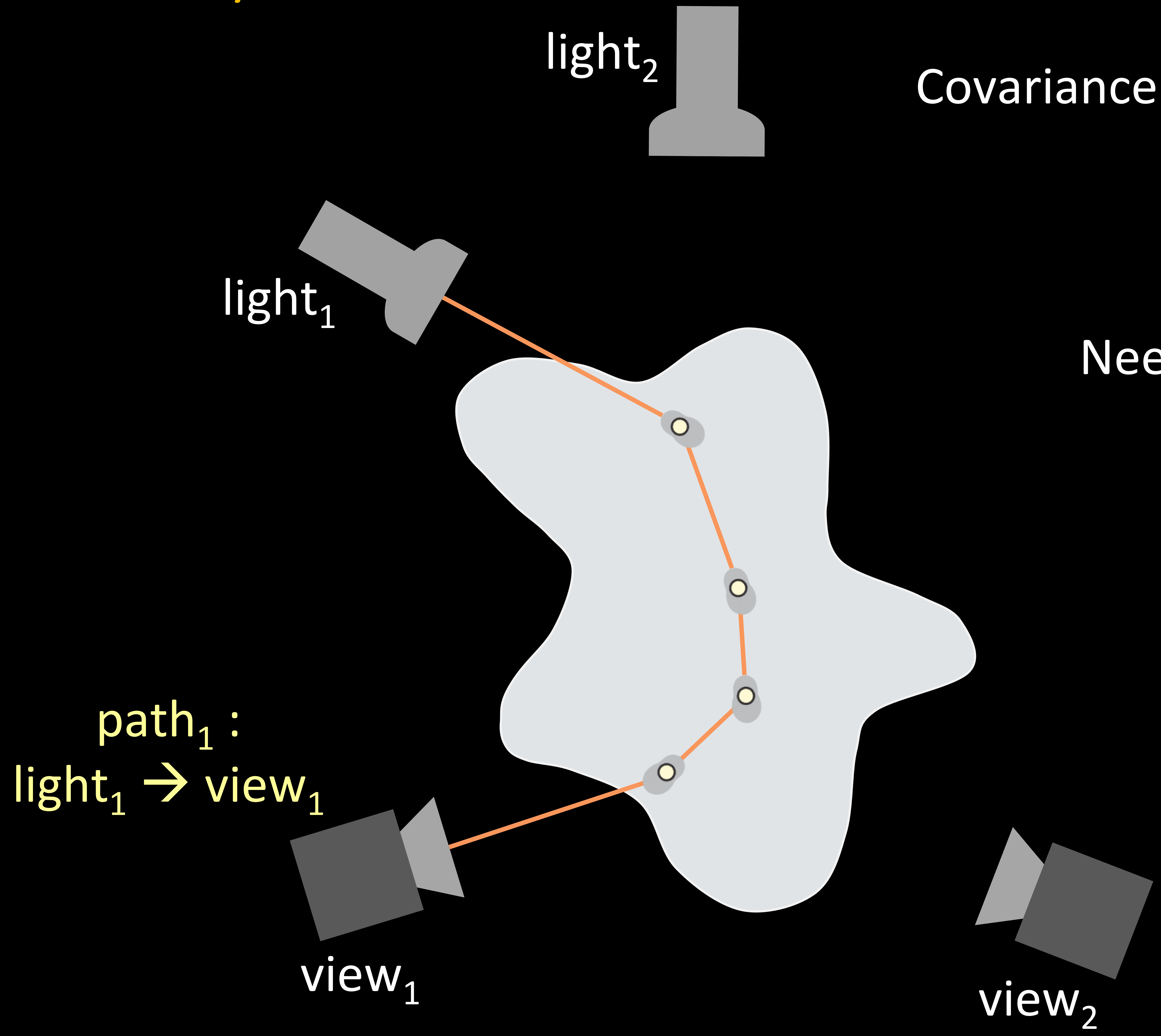

[Bar et al., 2019]

Memory effect: simulate *covariance* of speckle images

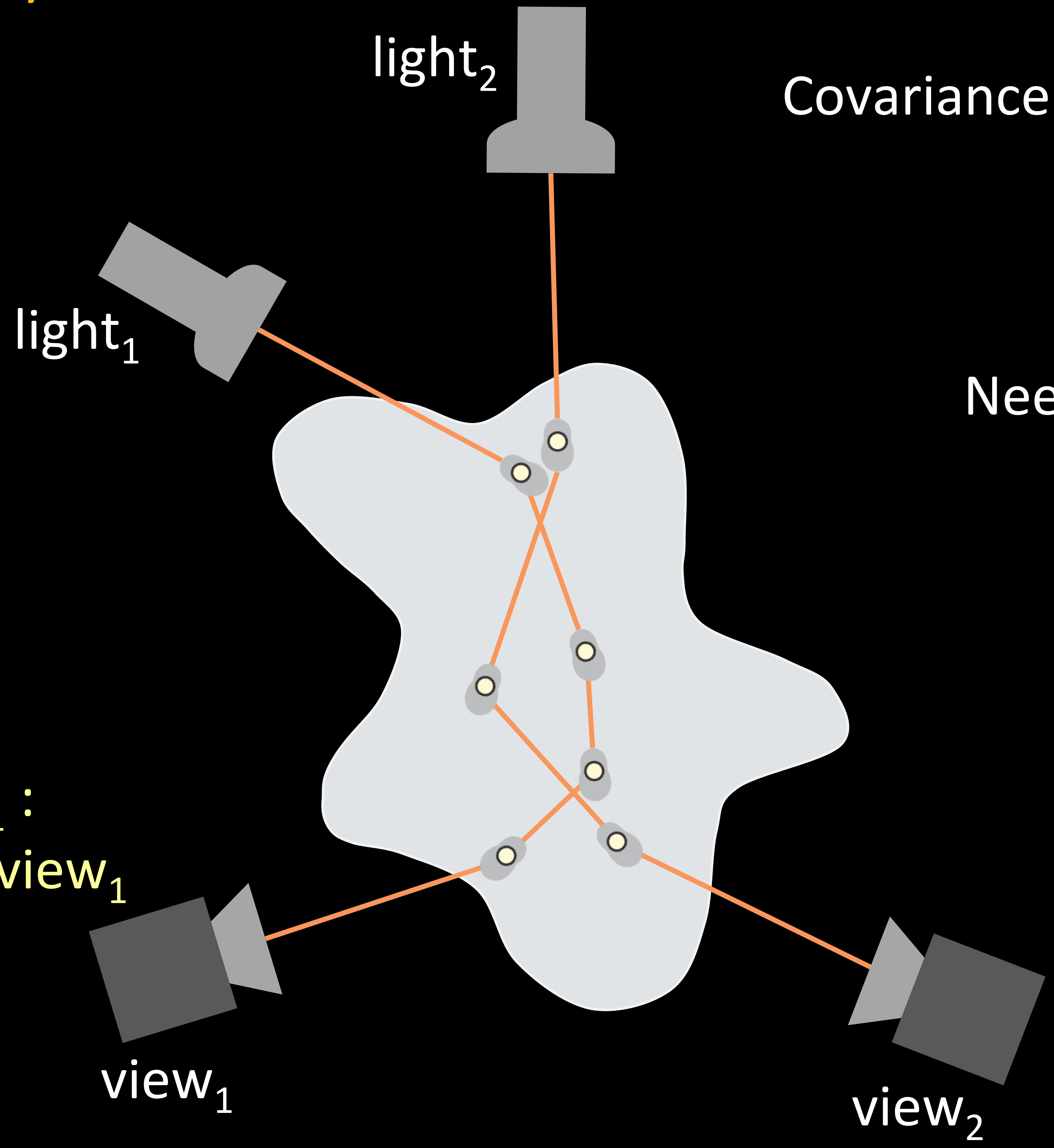

$$\text{Covariance} = \int_{\text{path}_1,\text{path}_2} u(\text{path}_1) \cdot u^*(\text{path}_2)$$

Need to consider products of ***pairs*** of paths

path$_1$:
light$_1$ → view$_1$

path$_2$:
light$_2$ → view$_2$

[Bar et al., 2019]

Memory effect: simulate *covariance* of speckle images

$$\text{Covariance} = \int_{\text{path}_1,\text{path}_2} u(\text{path}_1) \cdot u^*(\text{path}_2)$$

$u = |u| \, e^{i \cdot \text{phase}}$

Need to consider products of ***pairs*** of paths

Each path contributes a complex number u

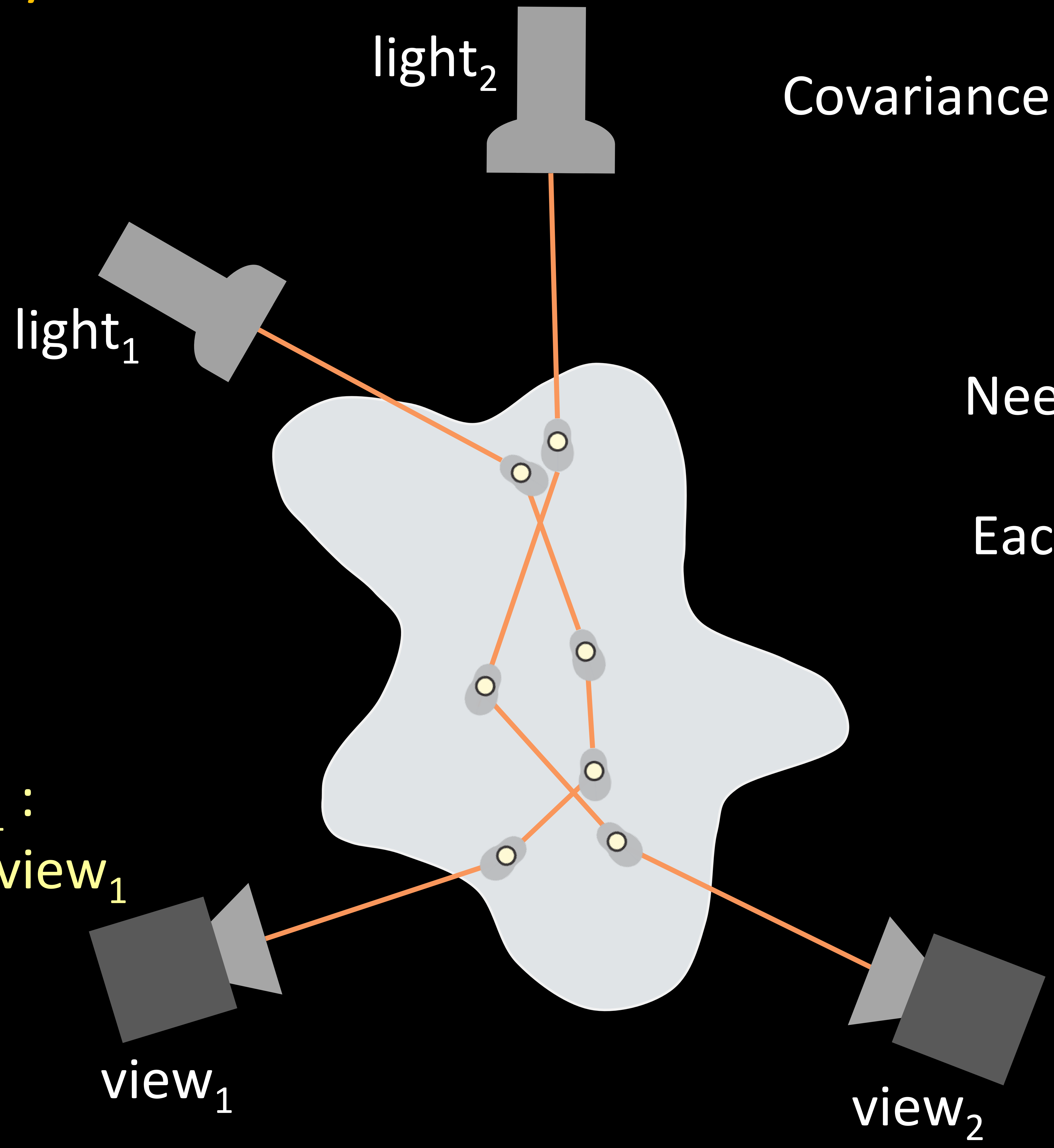

path$_1$:
light$_1$ → view$_1$

path$_2$:
light$_2$ → view$_2$

[Bar et al., 2019]

Memory effect: simulate *covariance* of speckle images

$$\text{Covariance} = \int_{\text{path}_1,\text{path}_2} u(\text{path}_1) \cdot u^*(\text{path}_2)$$

$$u = |u| \, e^{i \cdot \text{phase}}$$

Need to consider products of ***pairs*** of paths

Each path contributes a complex number u

phase ∝ Length (path)

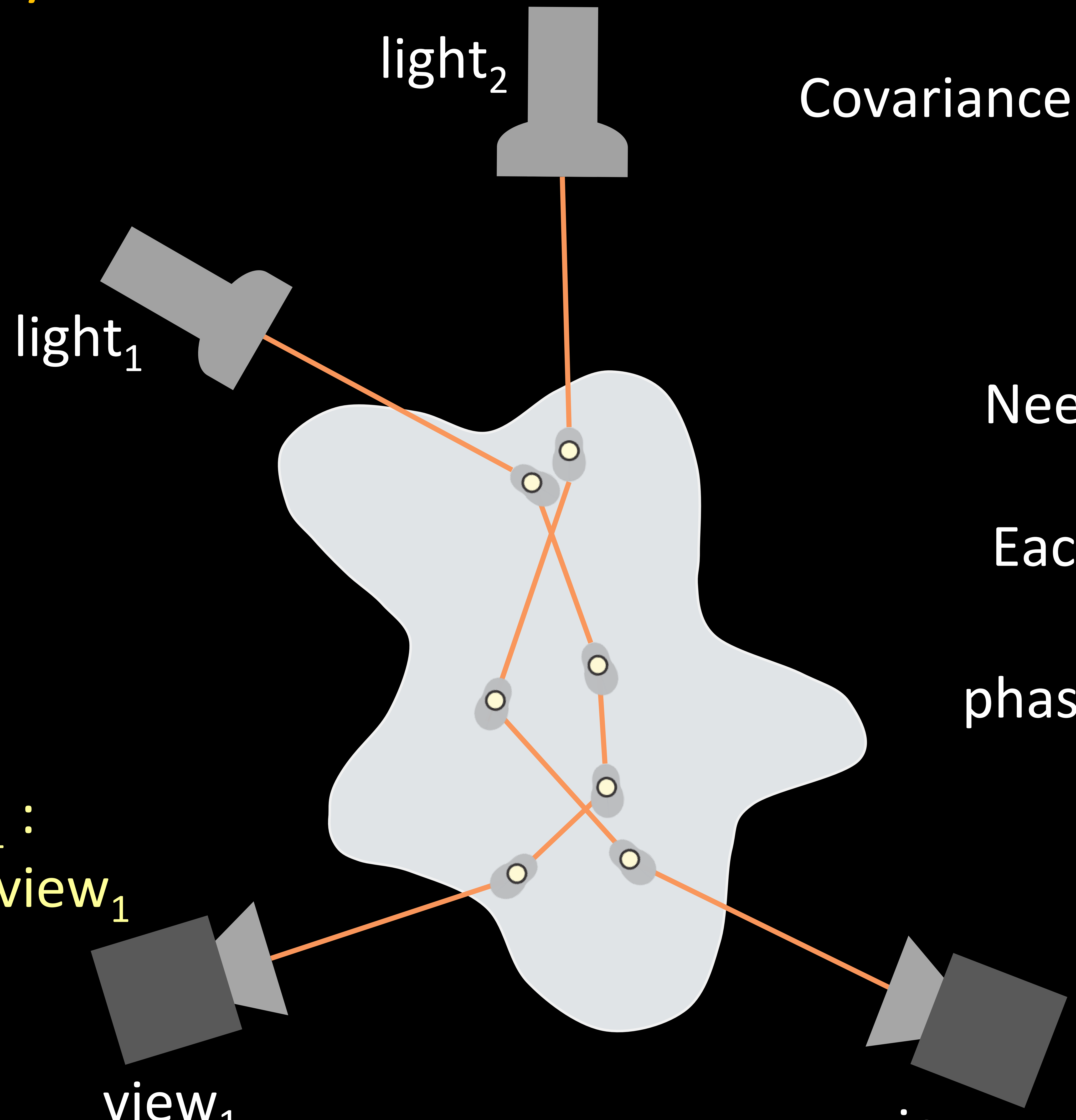

[Bar et al., 2019]

Memory effect: simulate *covariance* of speckle images

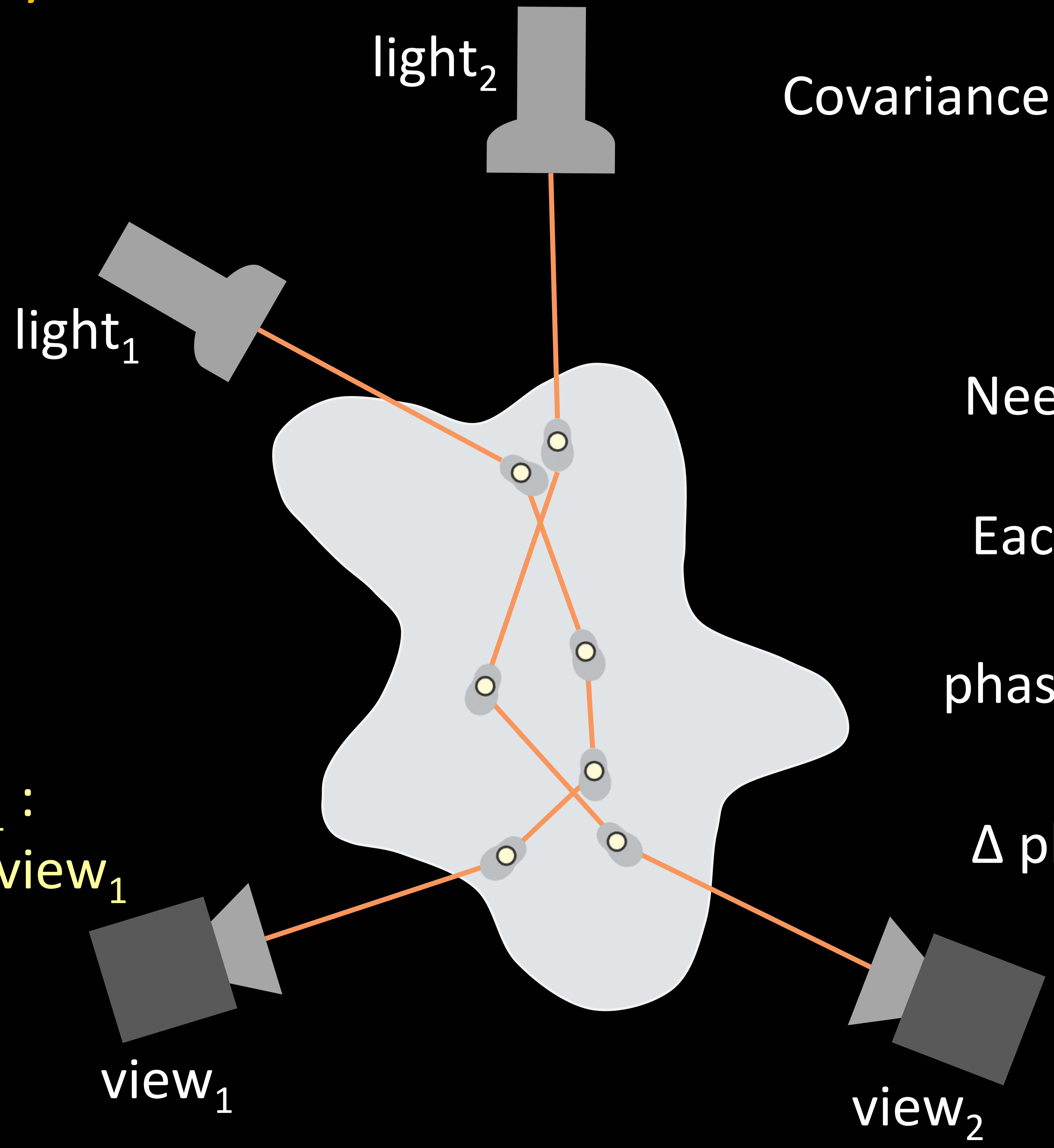

path$_1$:
light$_1$ → view$_1$

path$_2$:
light$_2$ → view$_2$

$$\text{Covariance} = \int_{\text{path}_1,\text{path}_2} u(\text{path}_1) \cdot u^*(\text{path}_2)$$

$$u = |u|\, e^{i \cdot \text{phase}}$$

Need to consider products of ***pairs*** of paths

Each path contributes a complex number u

phase ∝ Length (path)

Δ phase ∝ Length (path$_1$) - Length (path$_2$)

[Bar et al., 2019]

Memory effect: simulate *covariance* of speckle images

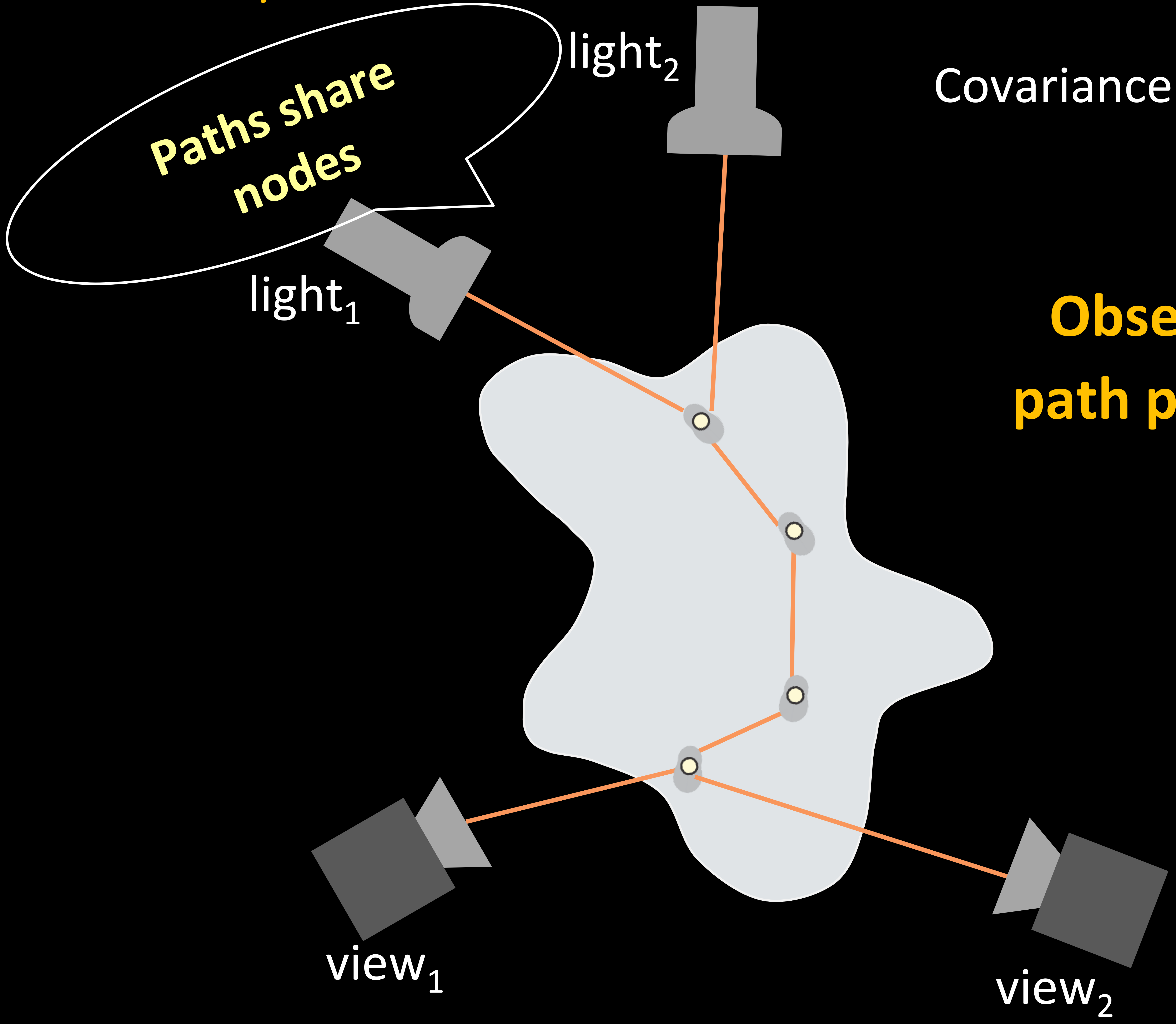

$$\text{Covariance} = \int_{\text{path}_1,\text{path}_2} u(\text{path}_1) \cdot u^*(\text{path}_2)$$

Observation: need to consider only path pairs that share the *same* nodes

(except start and end)

⇩

All other path pairs are averaged out in the integration

[Bar et al., 2019]

Memory effect: simulate *covariance* of speckle images

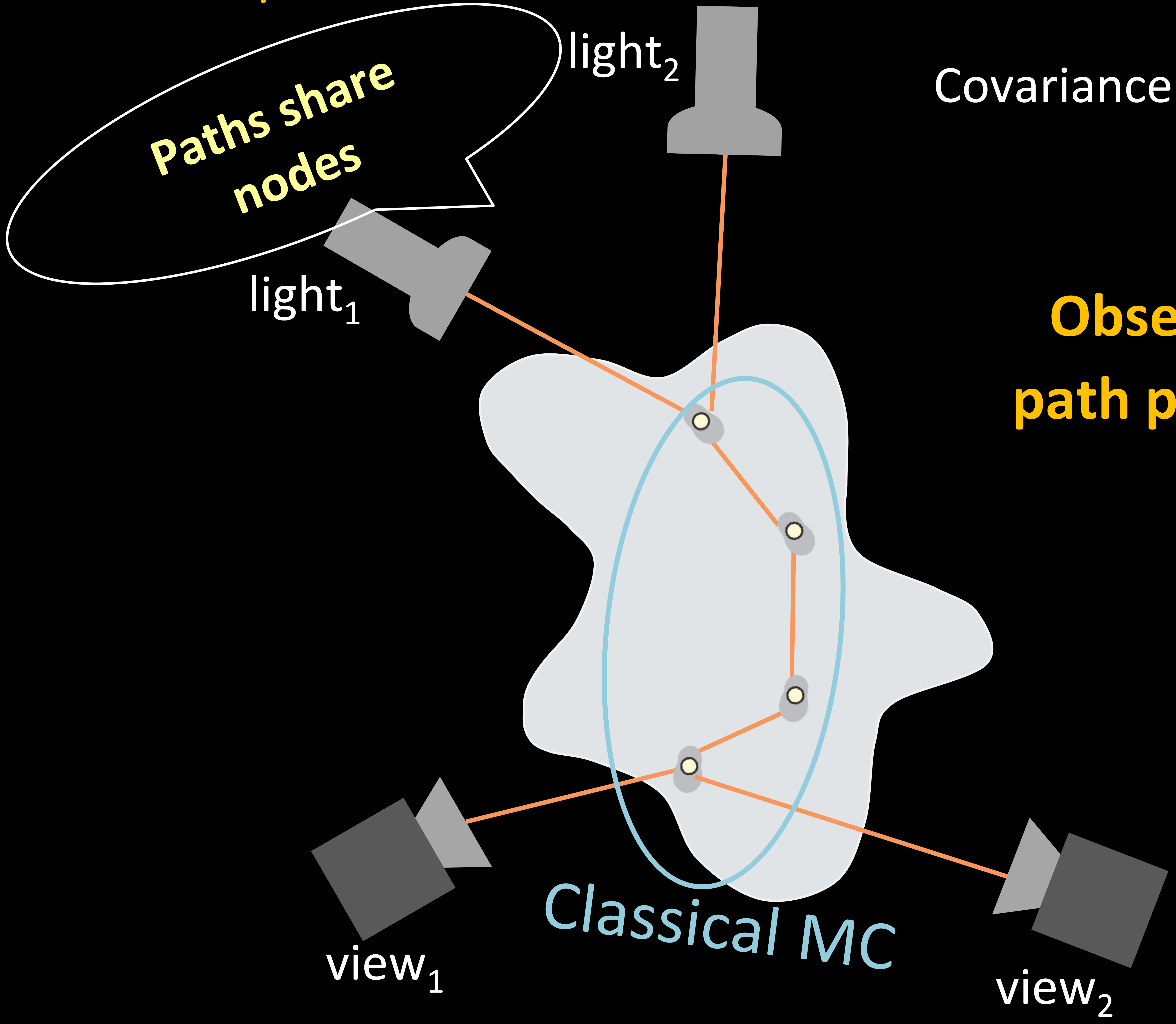

$$\text{Covariance} = \int_{\text{path}_1,\text{path}_2} u(\text{path}_1) \cdot u^*(\text{path}_2)$$

Observation: need to consider only path pairs that share the *same* nodes

(except start and end)

⇩

All other path pairs are averaged out in the integration

[Bar et al., 2019]

Memory effect: simulate *covariance* of speckle images

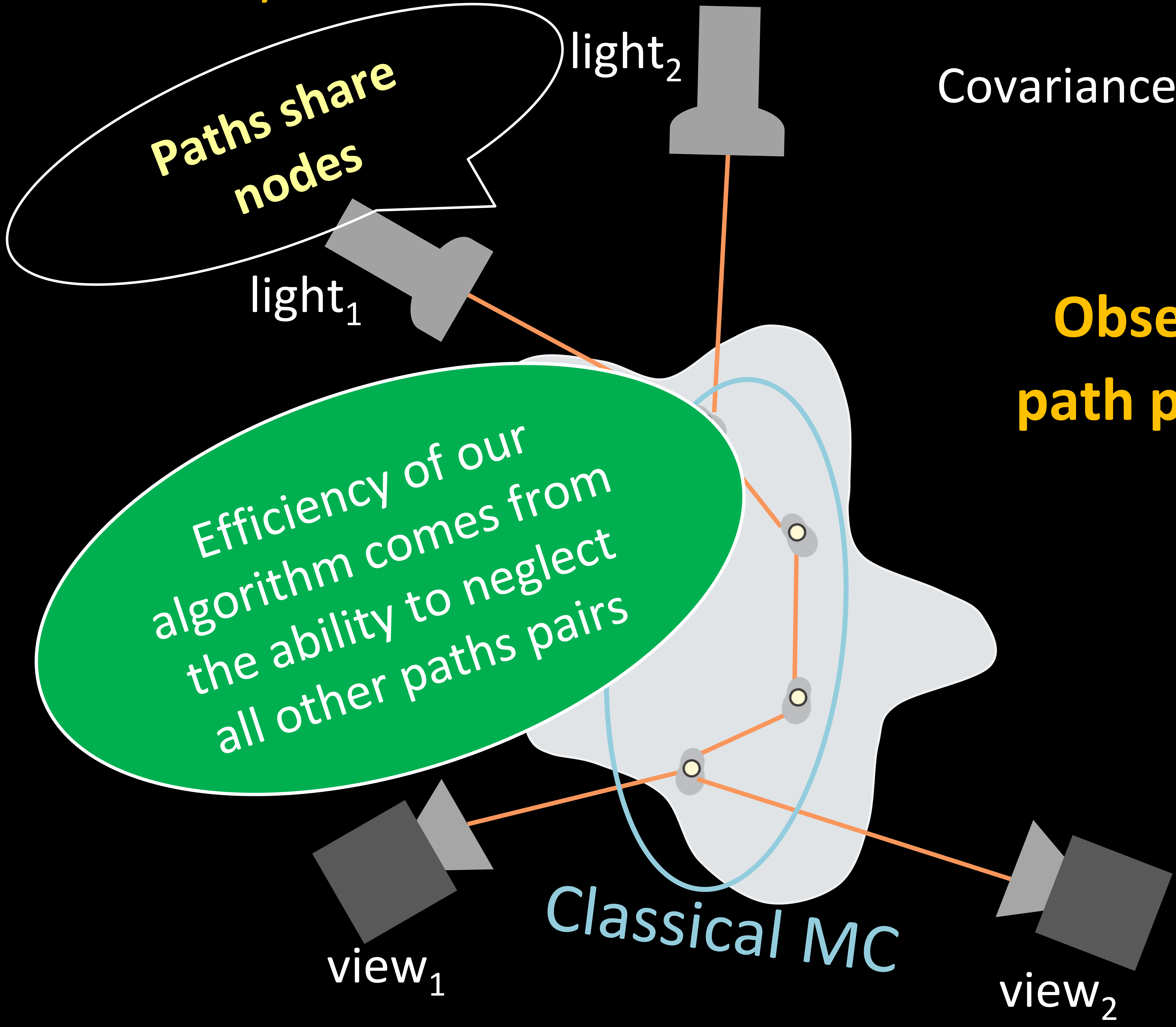

$$\text{Covariance} = \int_{path_1, path_2} u(path_1) \cdot u^*(path_2)$$

Observation: need to consider only path pairs that share the *same* nodes

(except start and end)

⇩

All other path pairs are averaged out in the integration

[Bar et al., 2019]

Memory effect: simulate *covariance* of speckle images

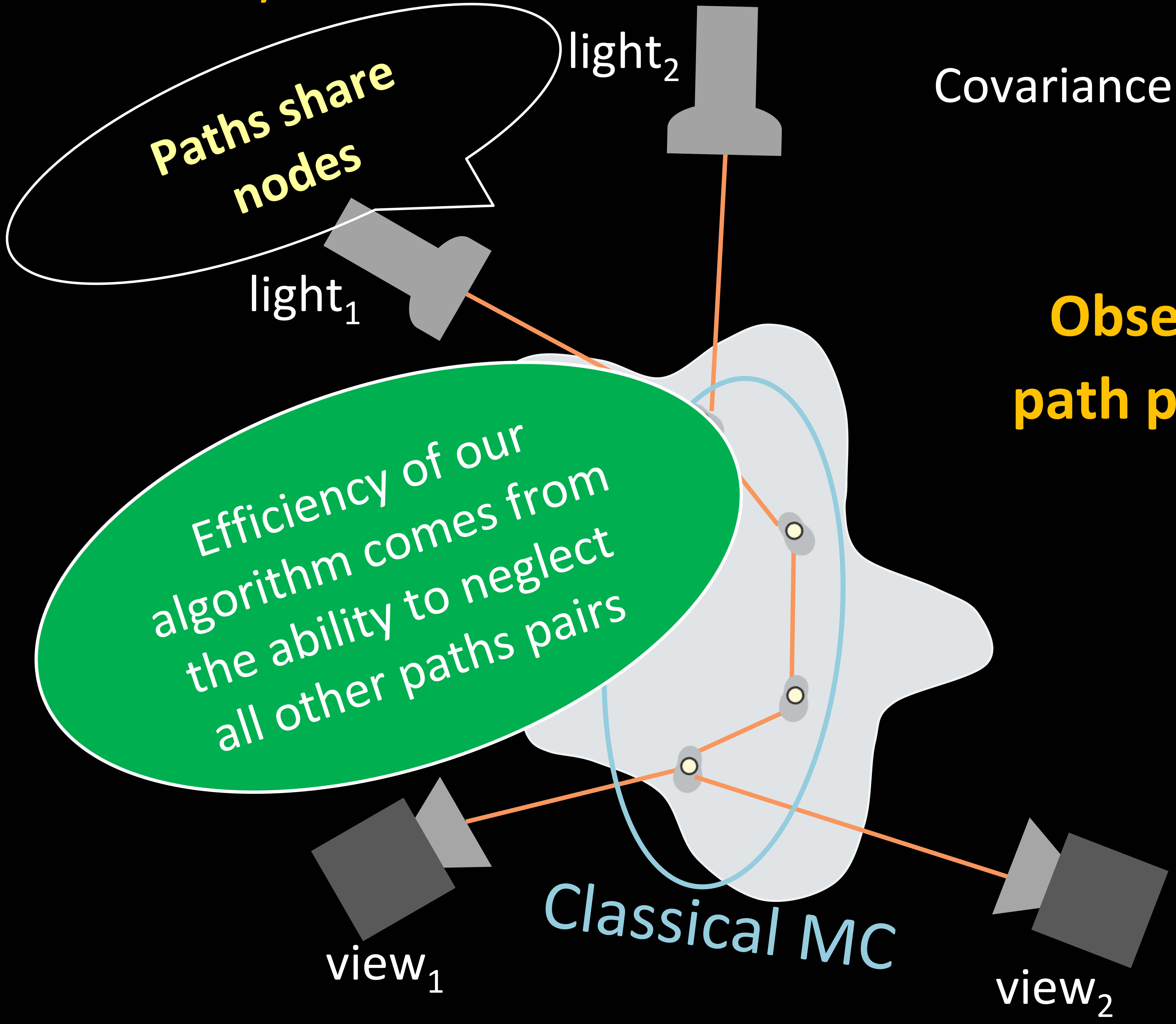

$$\text{Covariance} = \int_{\text{path}_1,\text{path}_2} u(\text{path}_1) \cdot u^*(\text{path}_2)$$

Observation: need to consider only path pairs that share the *same* nodes

(except start and end)

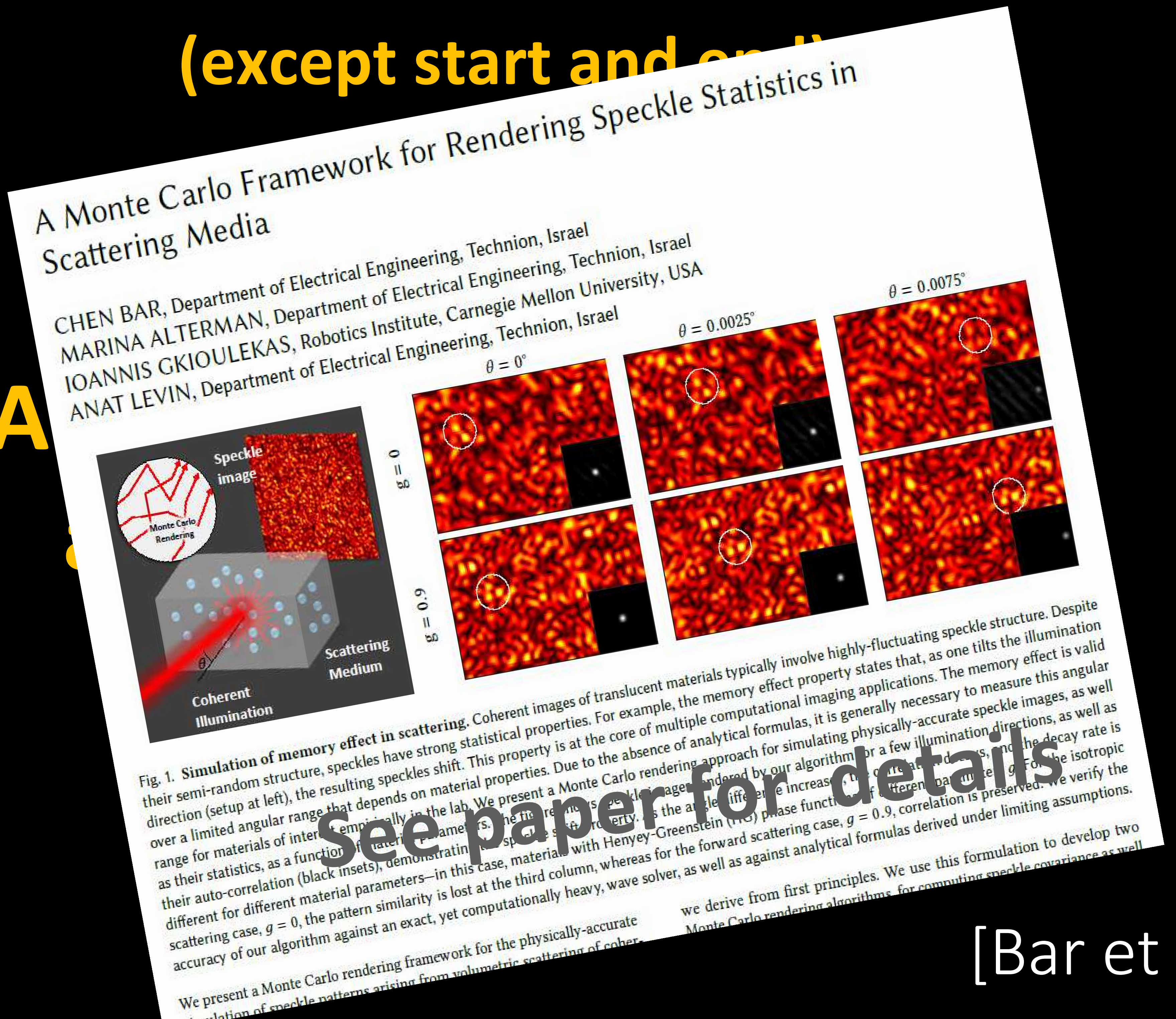

A Monte Carlo Framework for Rendering Speckle Statistics in Scattering Media

CHEN BAR, Department of Electrical Engineering, Technion, Israel
MARINA ALTERMAN, Department of Electrical Engineering, Technion, Israel
IOANNIS GKIOULEKAS, Robotics Institute, Carnegie Mellon University, USA
ANAT LEVIN, Department of Electrical Engineering, Technion, Israel

Fig. 1. **Simulation of memory effect in scattering.** Coherent images of translucent materials typically involve highly-fluctuating speckle structure. Despite their semi-random structure, speckles have strong statistical properties. For example, the memory effect property states that, as one tilts the illumination direction (setup at left), the resulting speckles shift. This property is at the core of multiple computational imaging applications. The memory effect is valid over a limited angular range that depends on material properties. Due to the absence of analytical formulas, it is generally necessary to measure this angular range for materials of inter[illegible] empirically in the lab. We present a Monte Carlo rendering approach for simulating physically-accurate speckle images, as well as their statistics, as a function [illegible] [illegible] parameters. [illegible] speckle images rendered by our algorithm for a few illumination directions, as well as their auto-correlation (black insets), demonstrating [illegible] [illegible] property. As the angle difference increases, the [illegible] decays, and the decay rate is different for different material parameters—in this case, material with Henyey-Greenstein (HG) phase function [illegible] parameter g. For the isotropic scattering case, $g = 0$, the pattern similarity is lost at the third column, whereas for the forward scattering case, $g = 0.9$, correlation is preserved. We verify the accuracy of our algorithm against an exact, yet computationally heavy, wave solver, as well as against analytical formulas derived under limiting assumptions.

We present a Monte Carlo rendering framework for the physically-accurate [illegible]

we derive from first principles. We use this formulation to develop two Monte Carlo rendering algorithms [illegible]

See paper for details

[Bar et al., 2019]

Comparison with wave-equation solver and real measurements

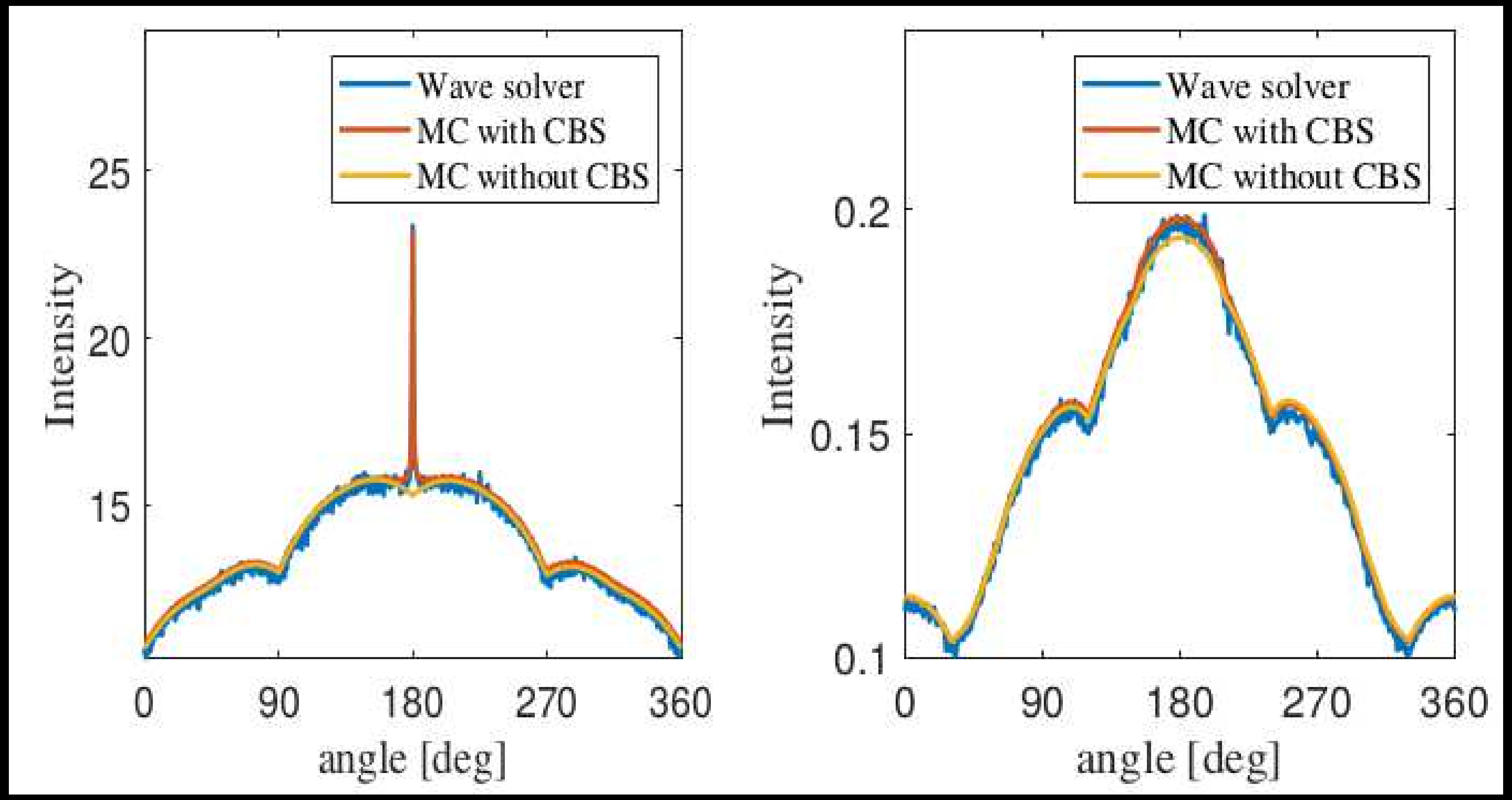

match wave equation solvers, **<u>10^5x faster</u>**

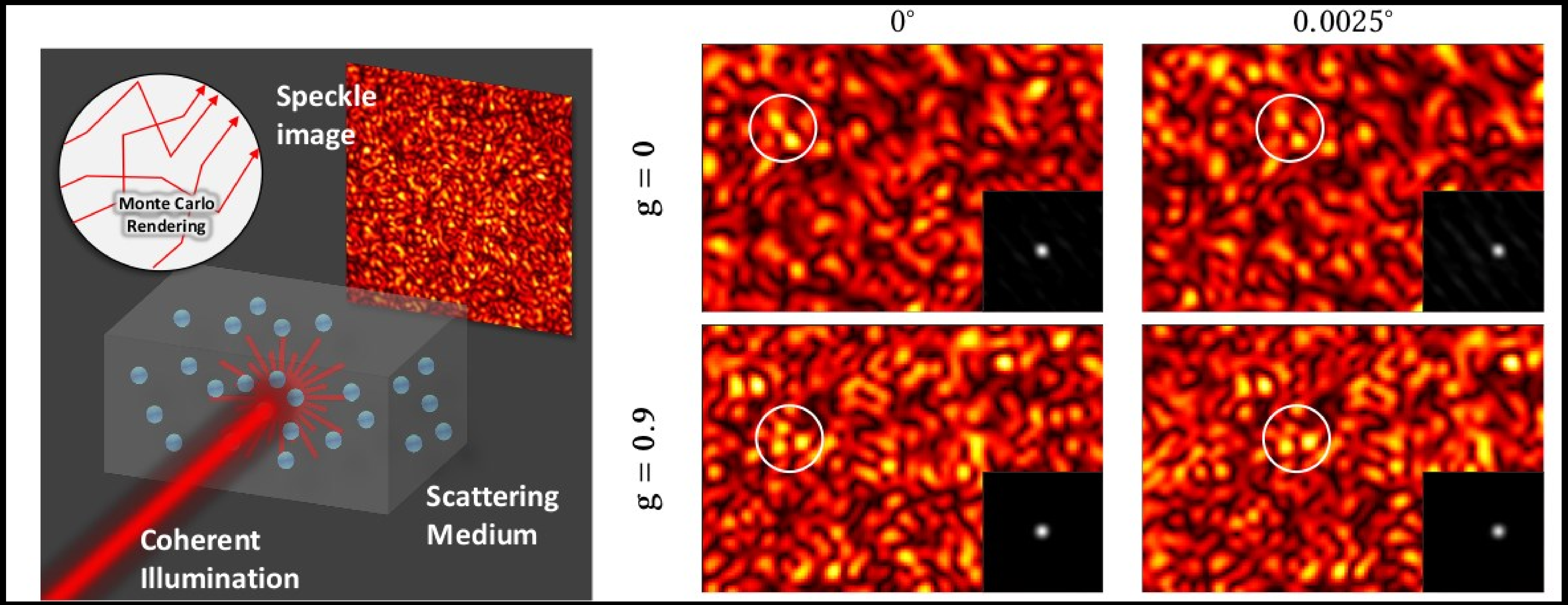

match real measurements of memory effect

[Bar et al., 2019]

Speckle-based fluorescence microscopy

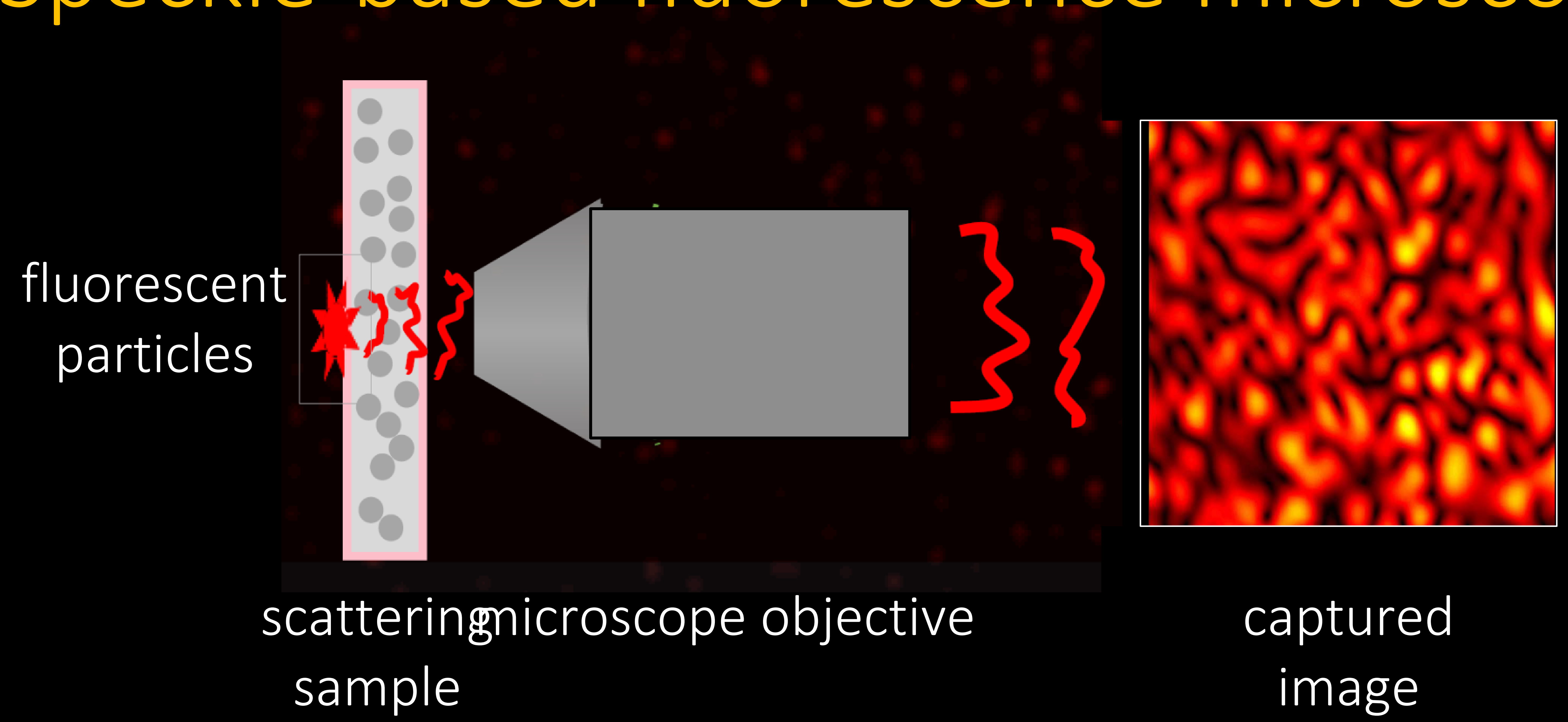

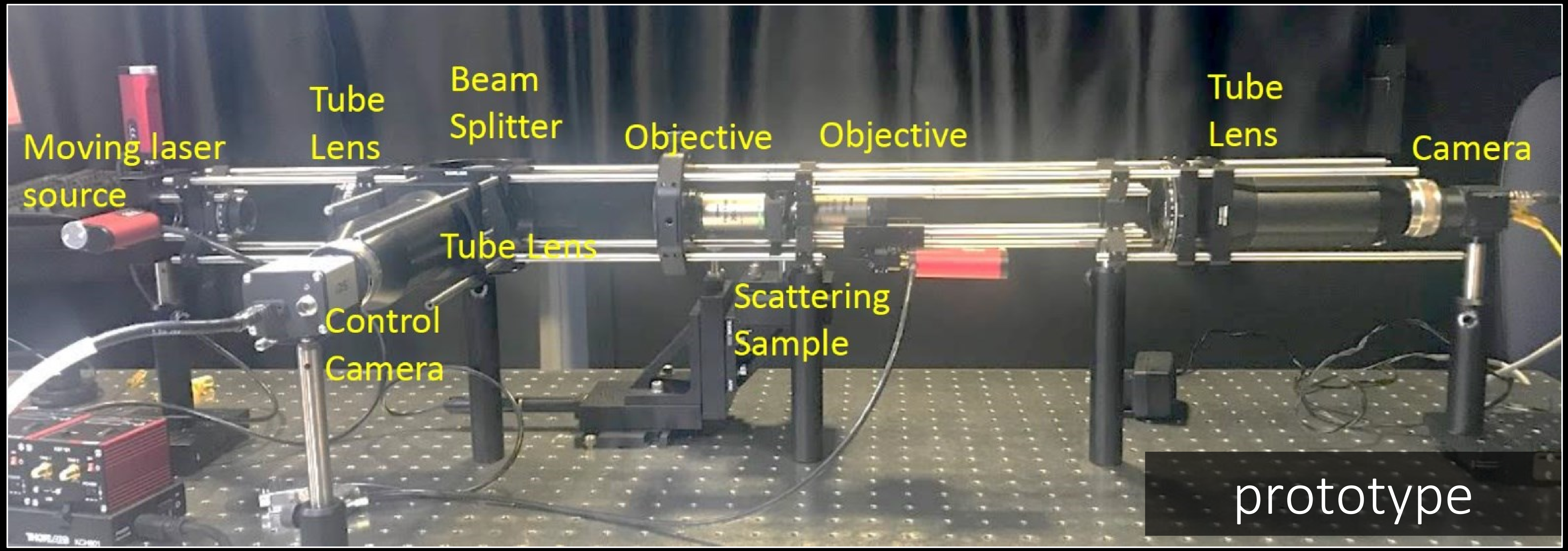

[Alterman et al., 2021]

Speckle-based fluorescence microscopy

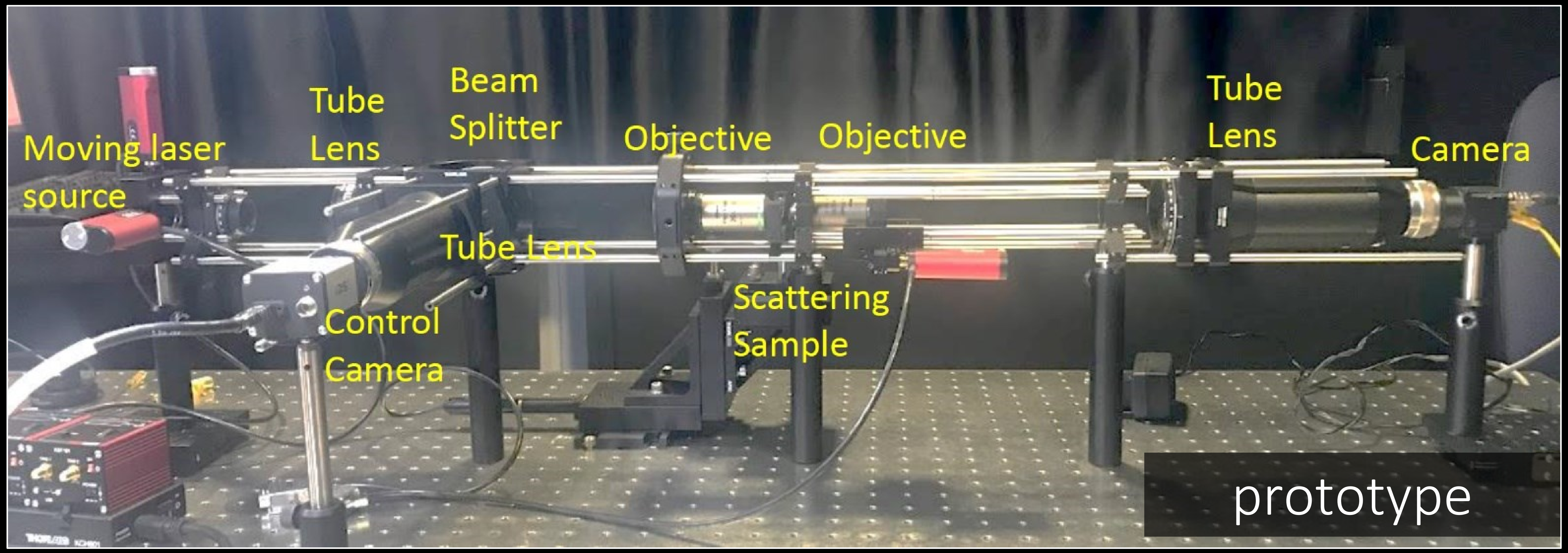

[Alterman et al., 2021]

Speckle-based fluorescence microscopy

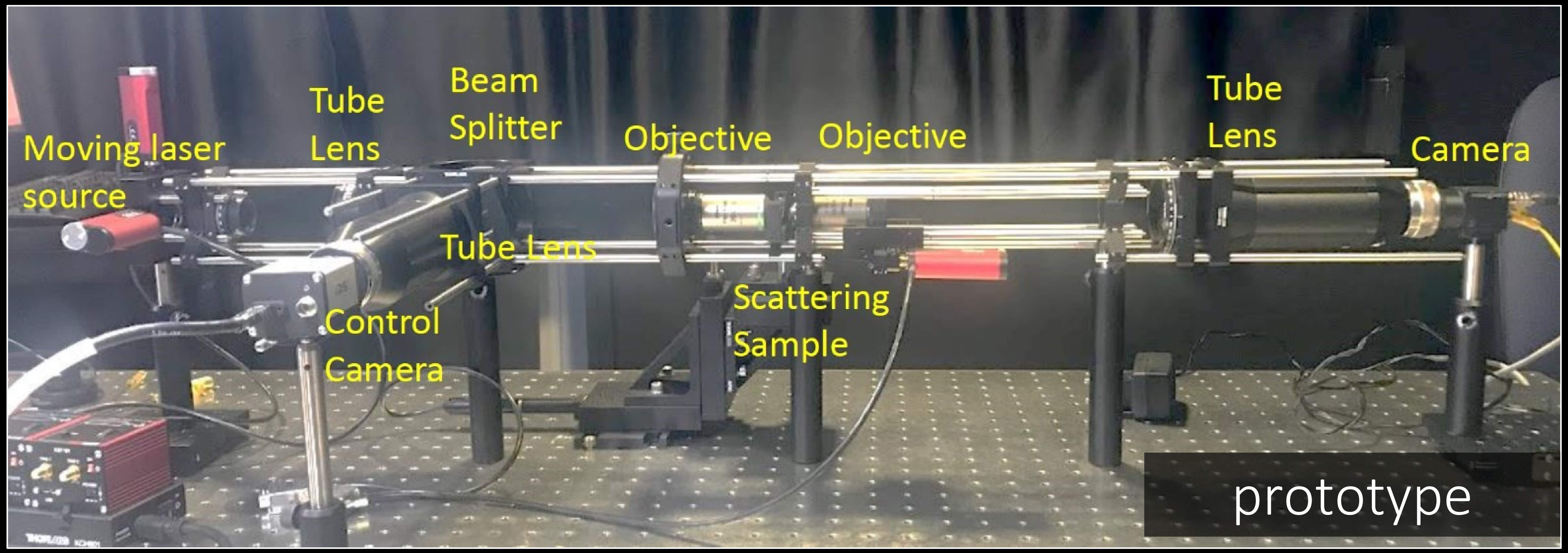

Performance strongly depends on:

- speckle statistics
- image priors
- tissue parameters

[Alterman et al., 2021]

Evaluate the memory effect

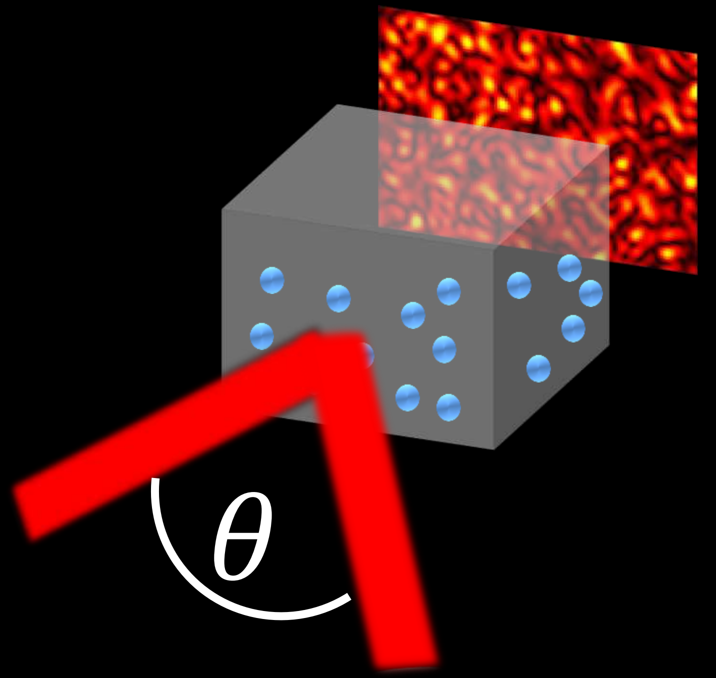

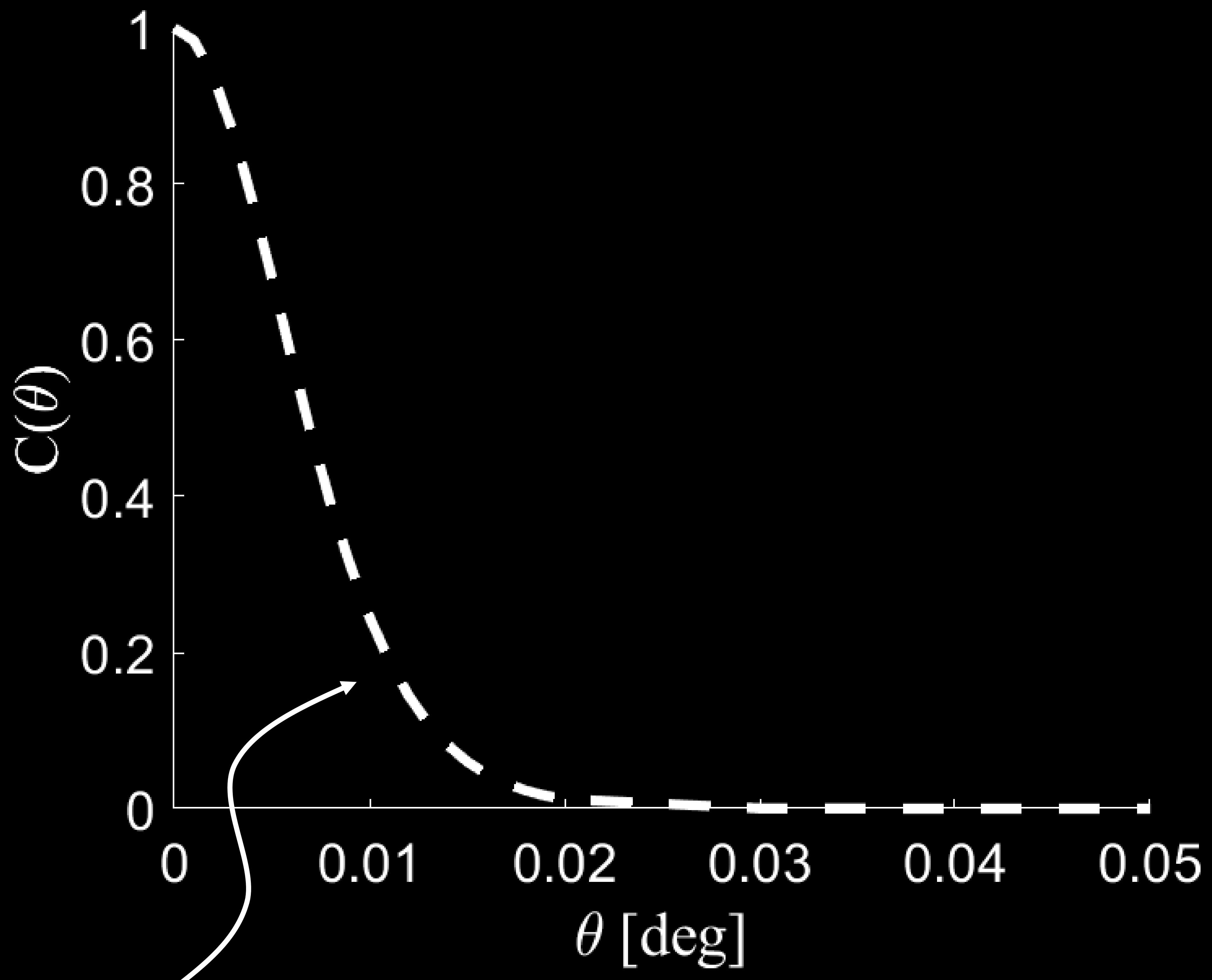

Analytical solution based on diffusion approximation

[Alterman et al., 2021]

Evaluate the memory effect

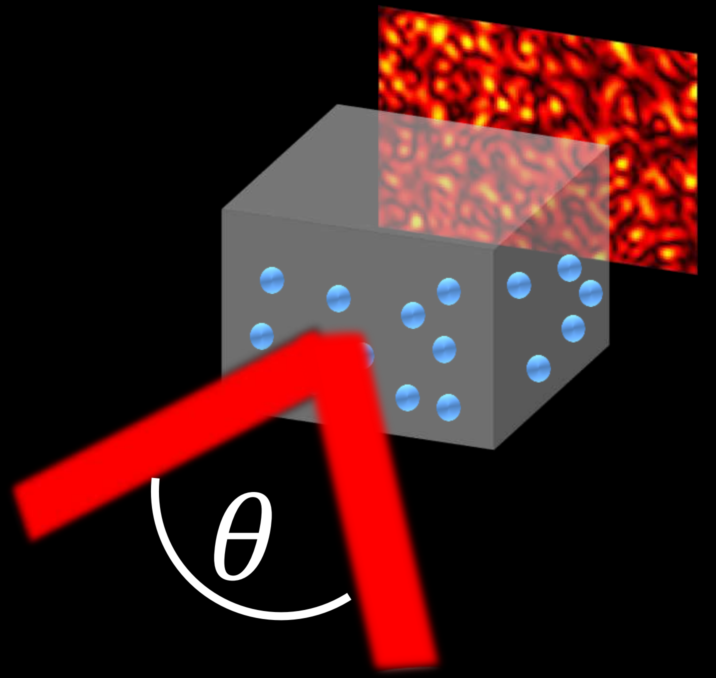

This approximation is correct for some materials and configurations

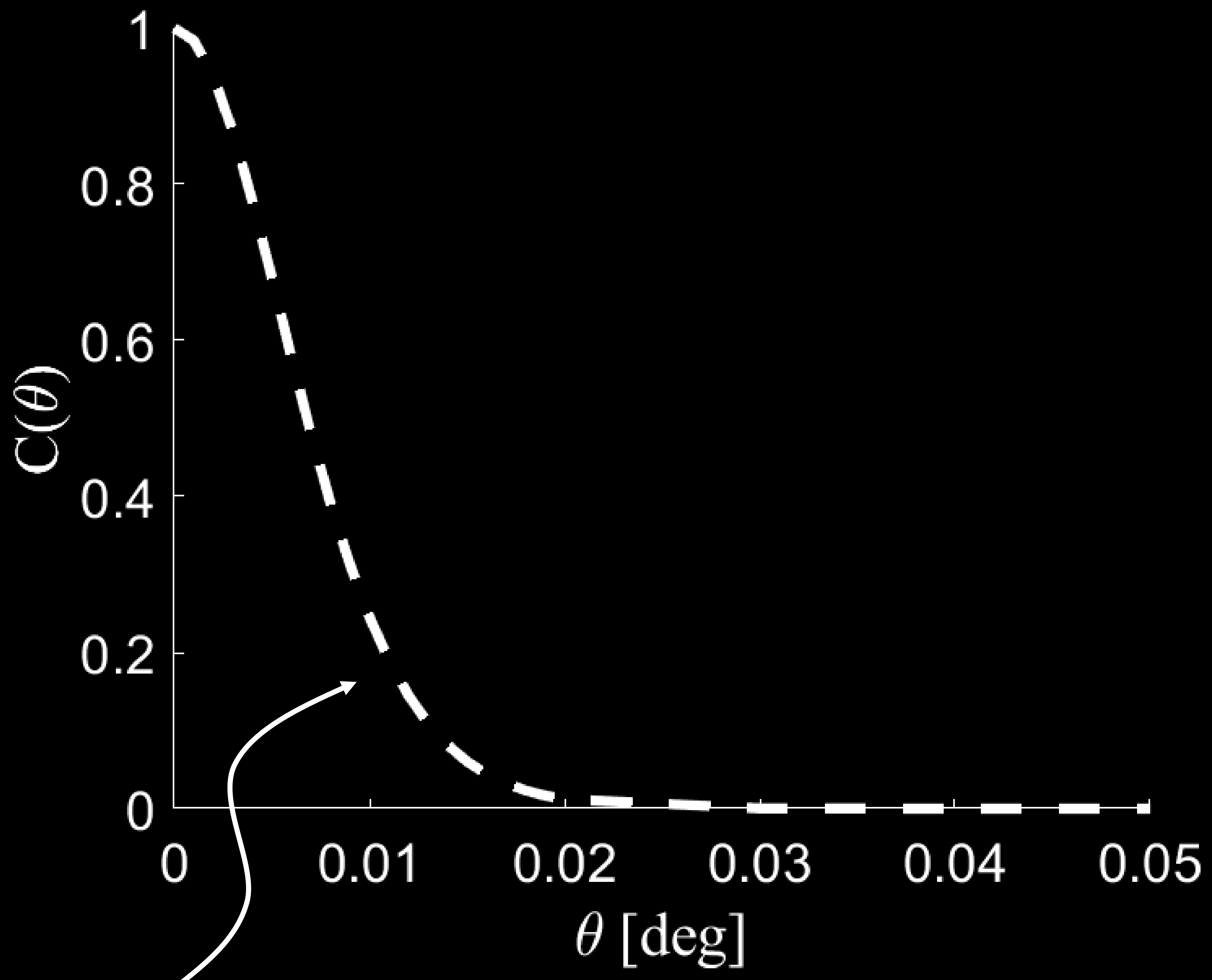

Analytical solution based on diffusion approximation

[Alterman et al., 2021]

Evaluate the memory effect

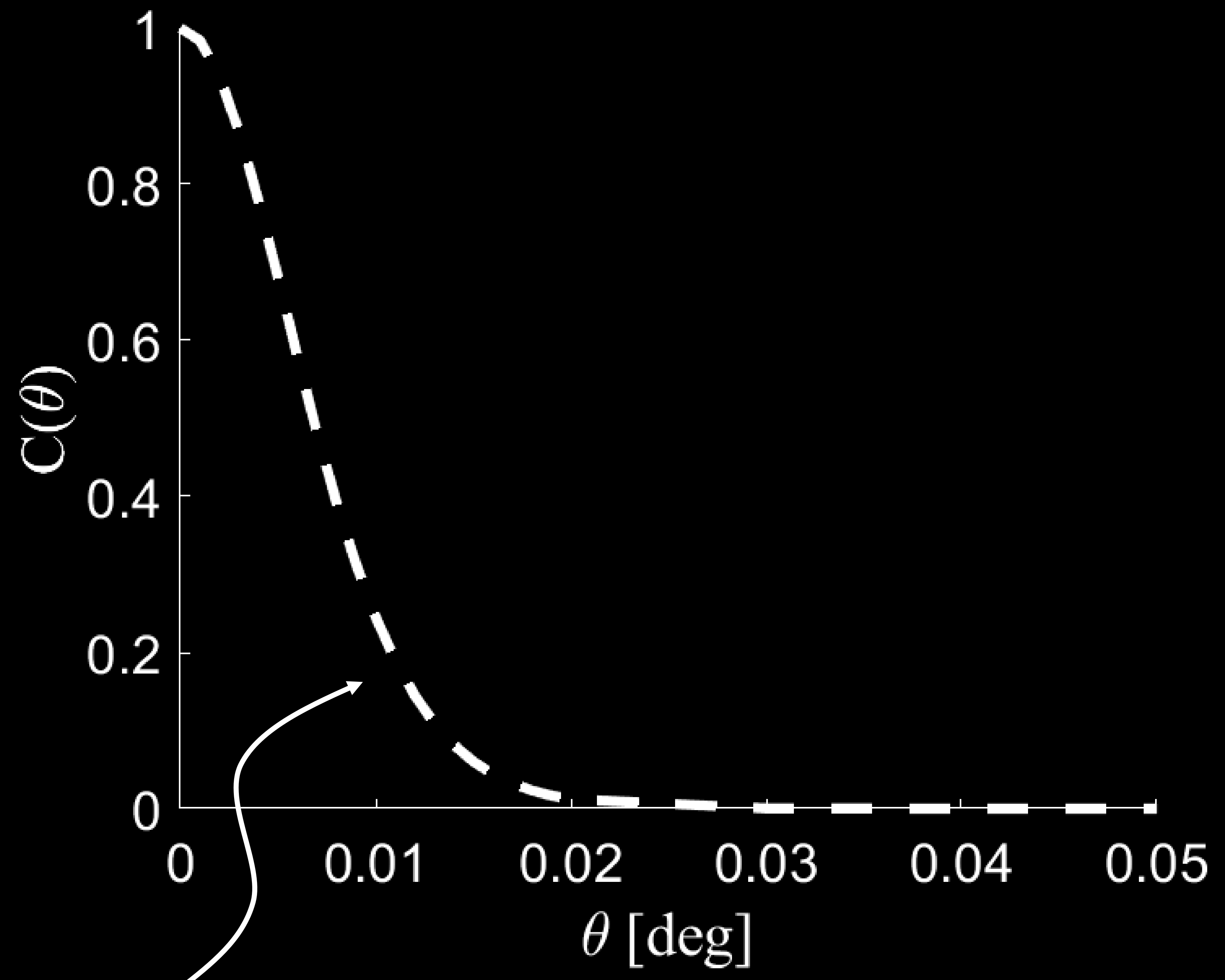

Analytical solution based on diffusion approximation

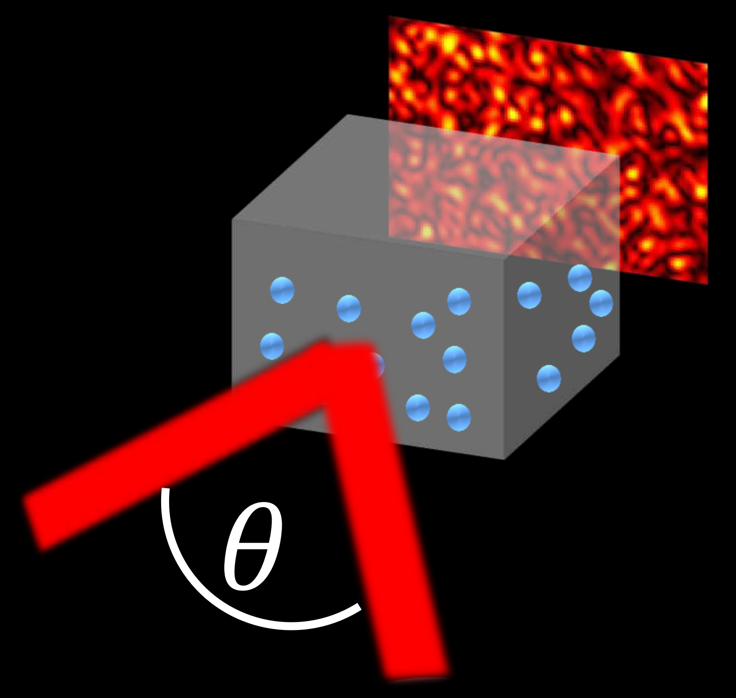

This approximation is correct for some materials and configurations

In practice ME extent is often wider

[Alterman et al., 2021]

Evaluate the memory effect

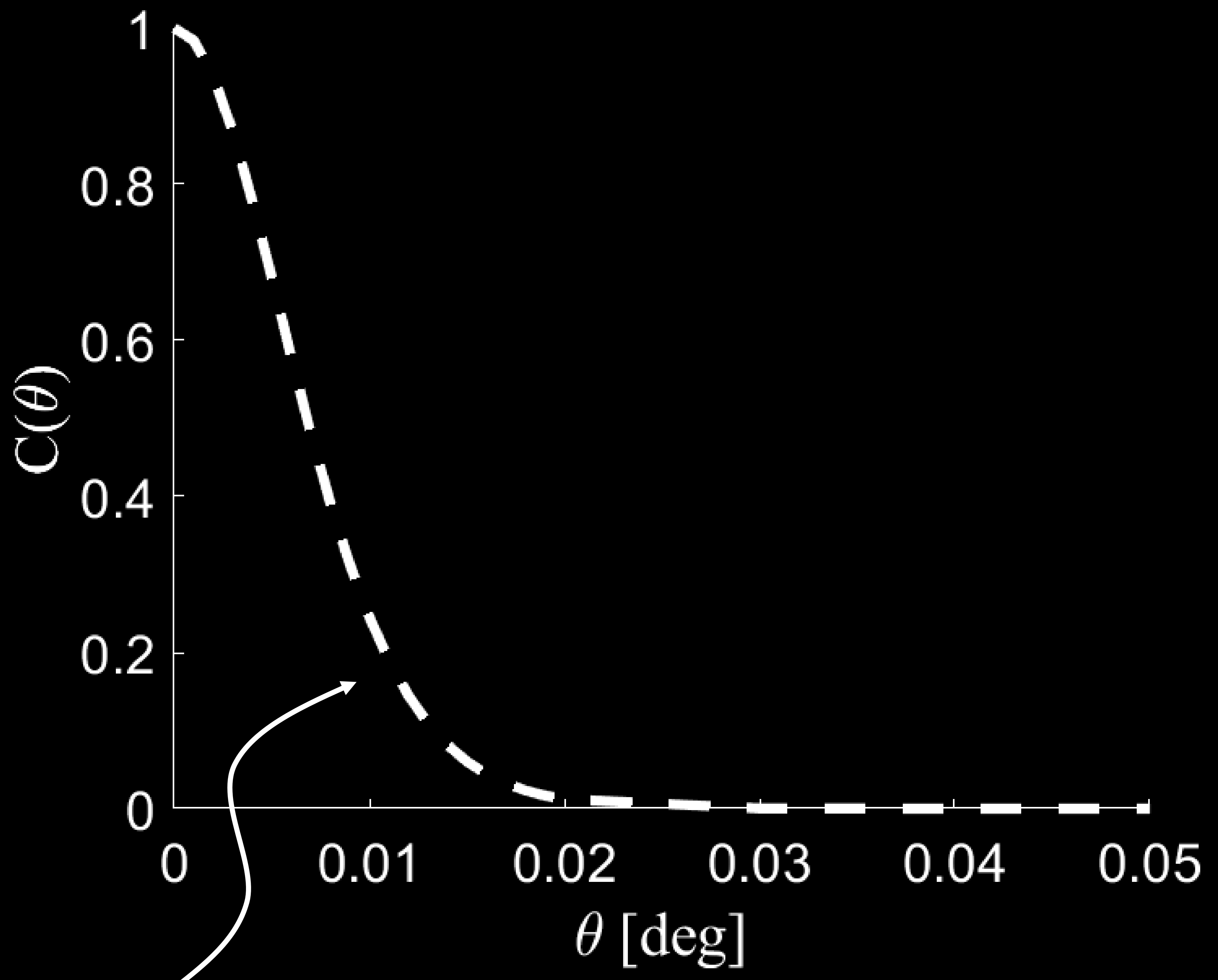

Analytical solution based on diffusion approximation

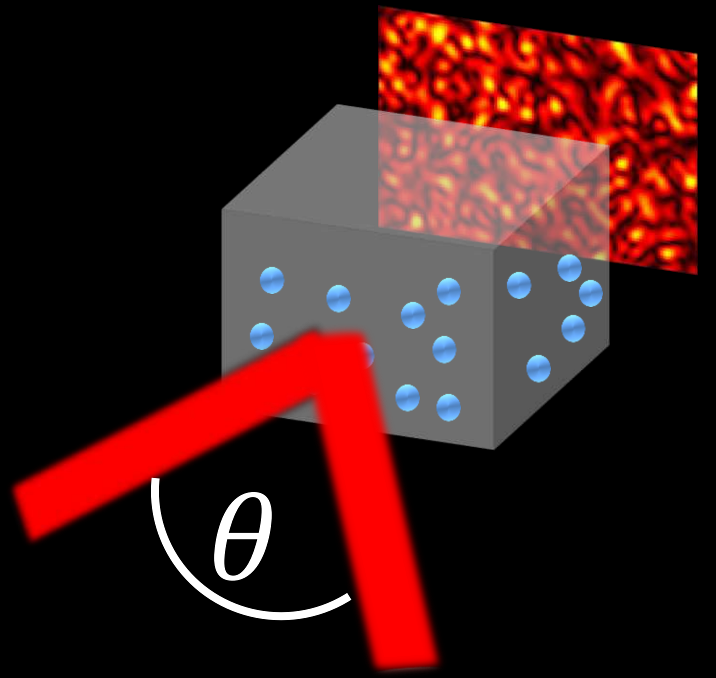

This approximation is correct for some materials and configurations

In practice ME extent is often wider

Currently: measured *empirically* in the lab

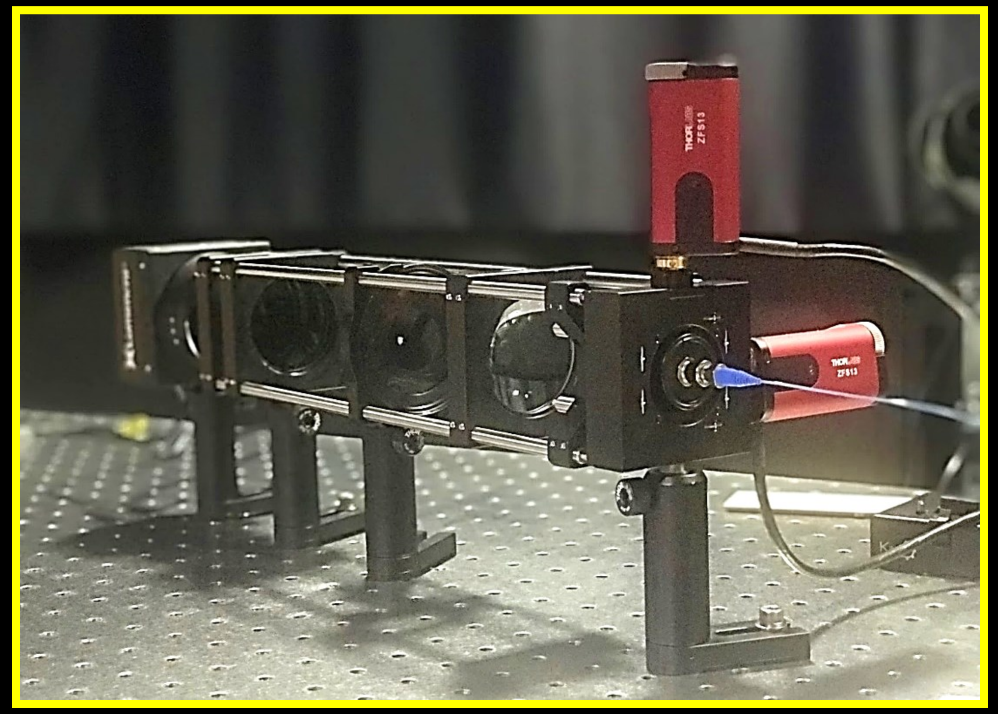

[Alterman et al., 2021]

Evaluate the memory effect

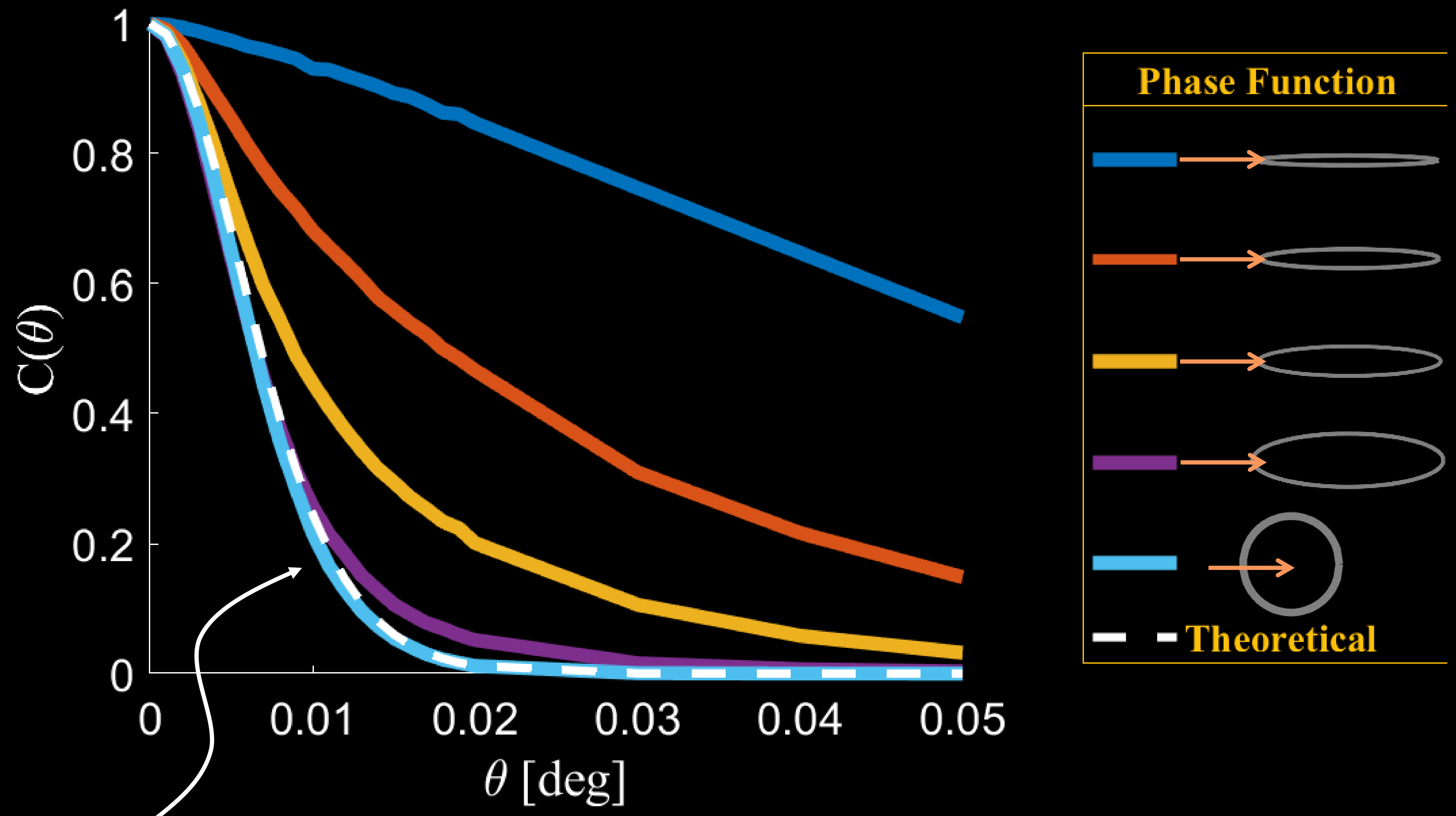

Analytical solution based on diffusion approximation

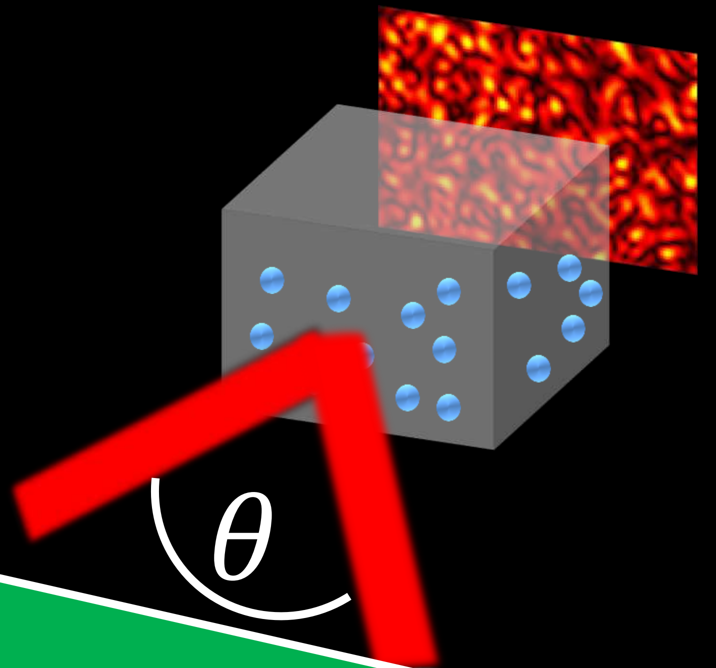

Now we can efficiently compute ME curves for all scattering parameters

This a[...]e

r[...]

In practice ME exte[...]r

Currently: measured *empirically* in the lab

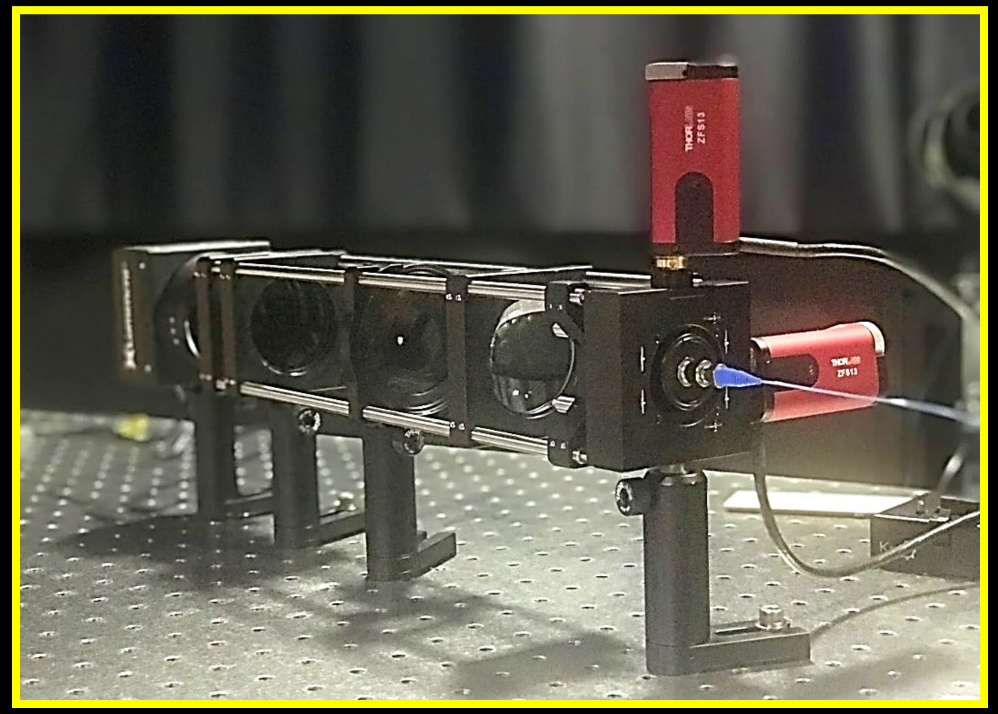

[Alterman et al., 2021]

Evaluate the memory effect

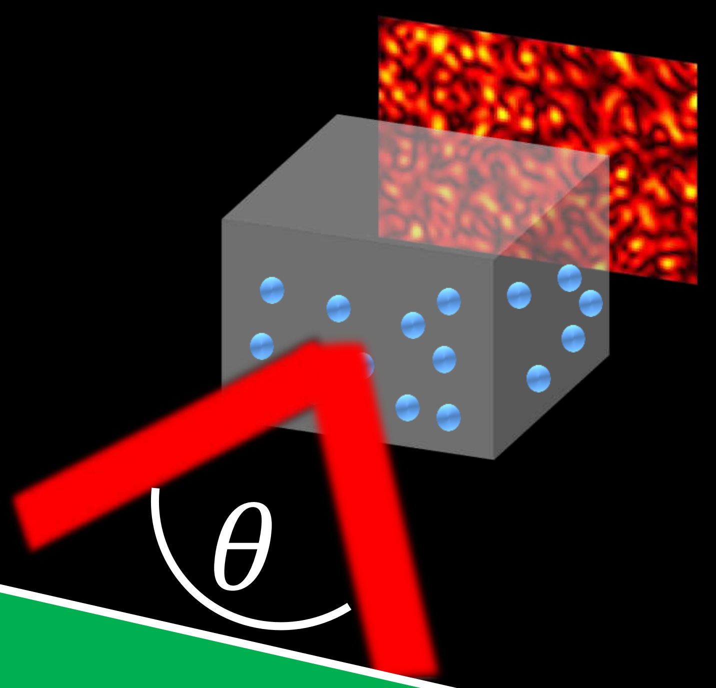

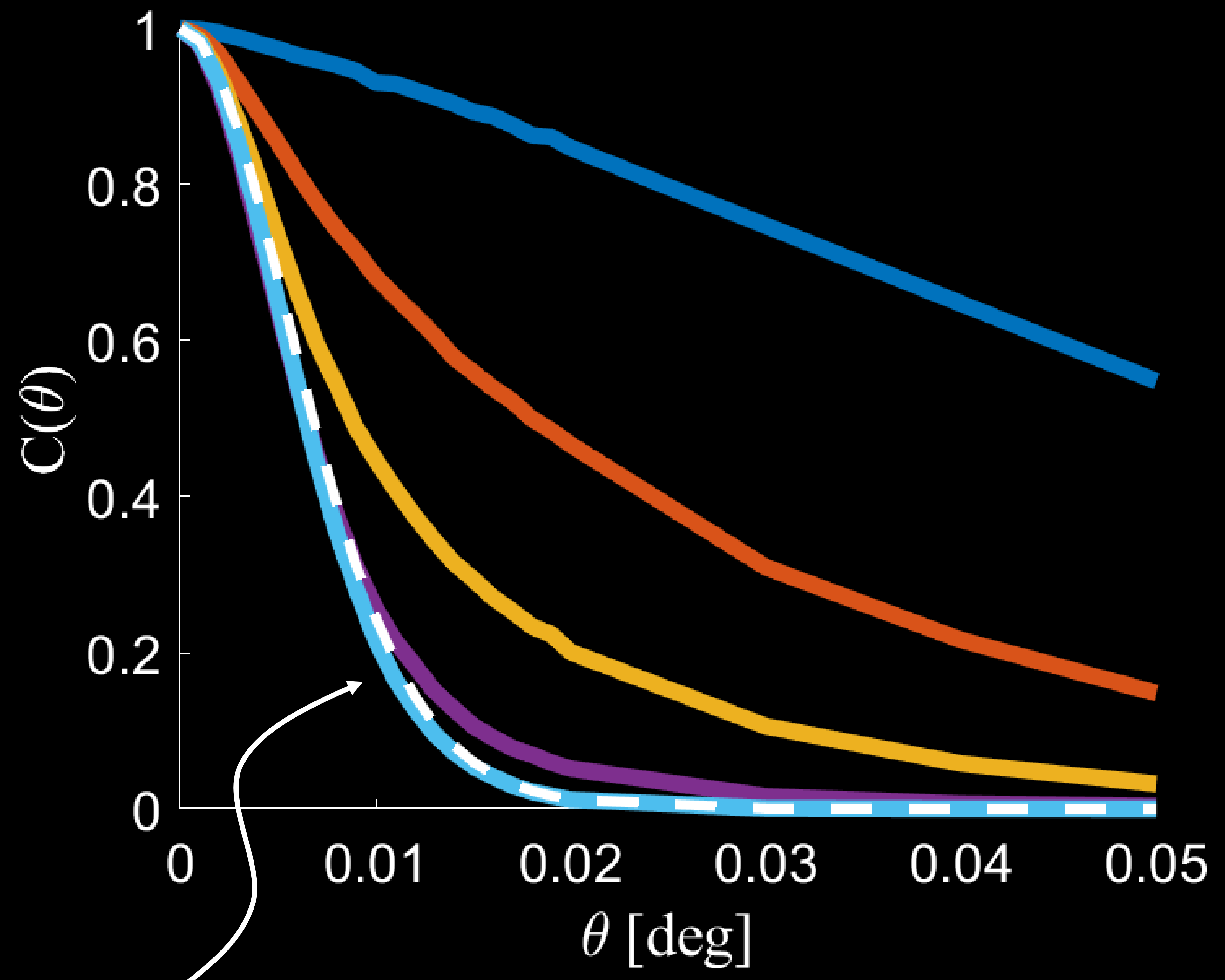

Analytical solution based on diffusion approximation

This a... e

r...

...E exten... r

...*piricaly* in the

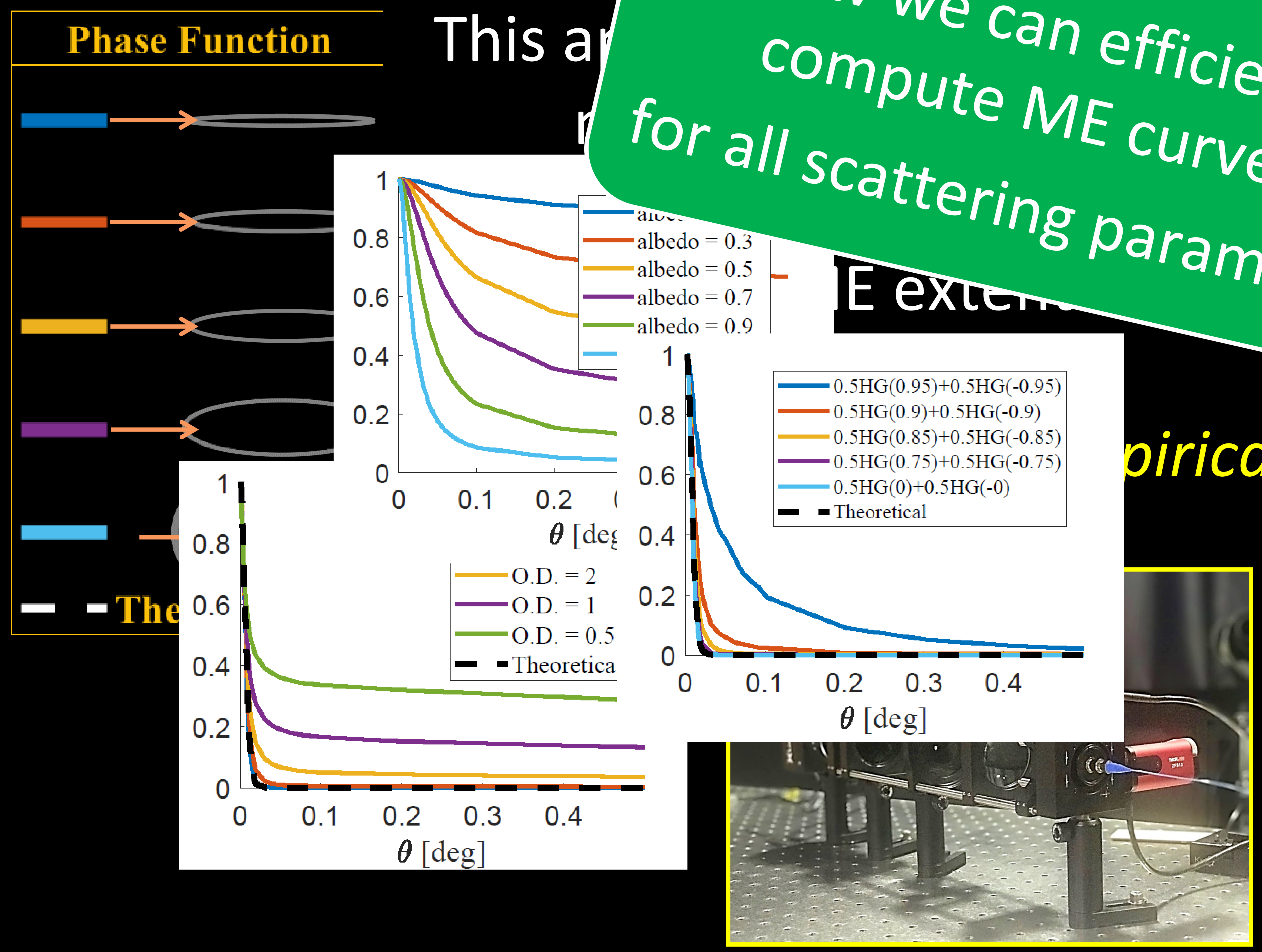

Now we can efficiently compute ME curves for all scattering parameters

[Alterman et al., 2021]

Better algorithms for fluorescence microscopy

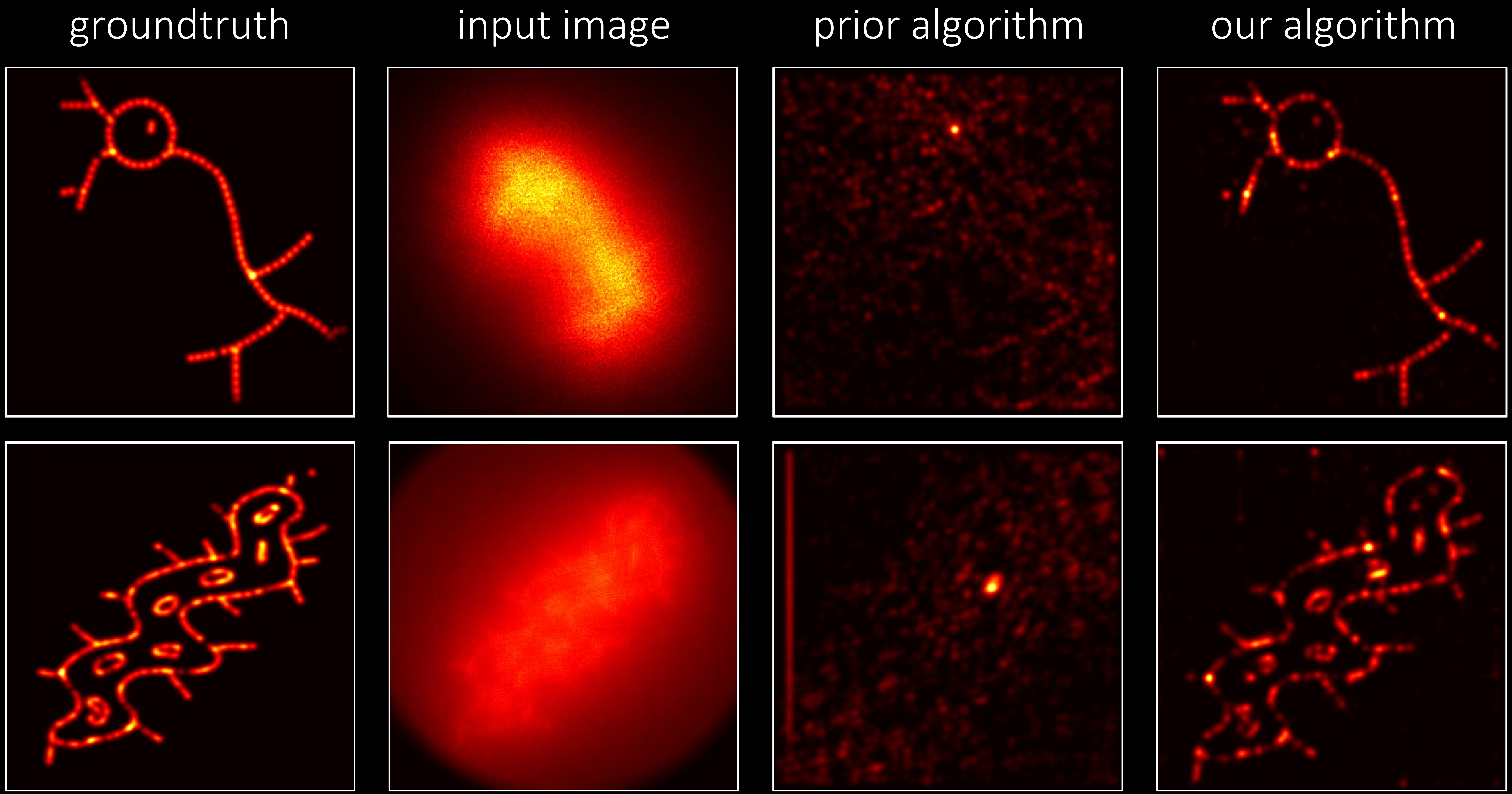

[Alterman et al., 2021]

Acquisition of scattering materials

Use differentiable speckle rendering to recover material parameters from speckle images

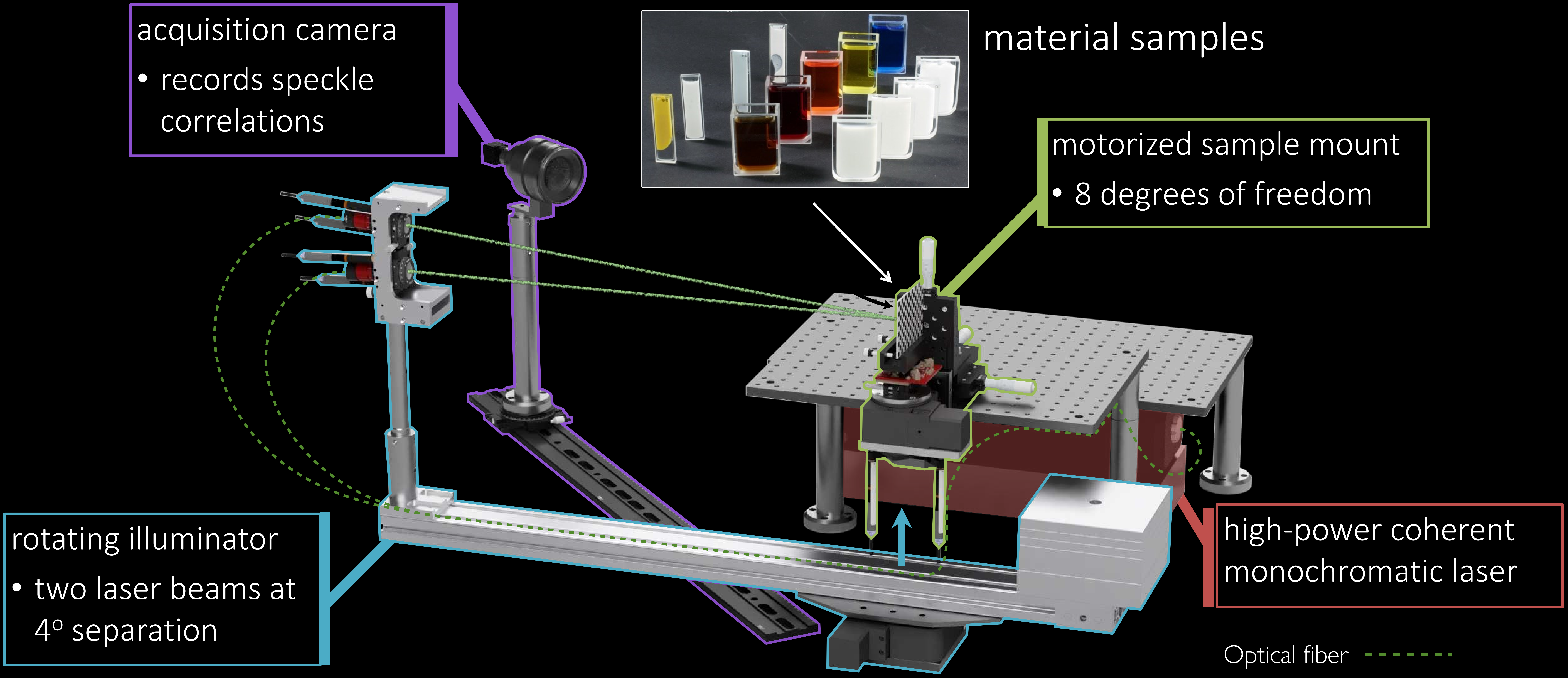


Acquisition
Speckle Video
(Camera Feed)
Scattering Soap Sample

Rendering wave optics is a very active area

A Generic Framework for Physical Light Transport

SHLOMI STEINBERG, University of California, Santa Barbara, USA
LING-QI YAN, University of California, Santa Barbara, USA

Physics-based rendering and its applications to computational imaging

forward rendering

- accurate and efficient simulation
- virtually design sensors, optics, and algorithms

inverse rendering

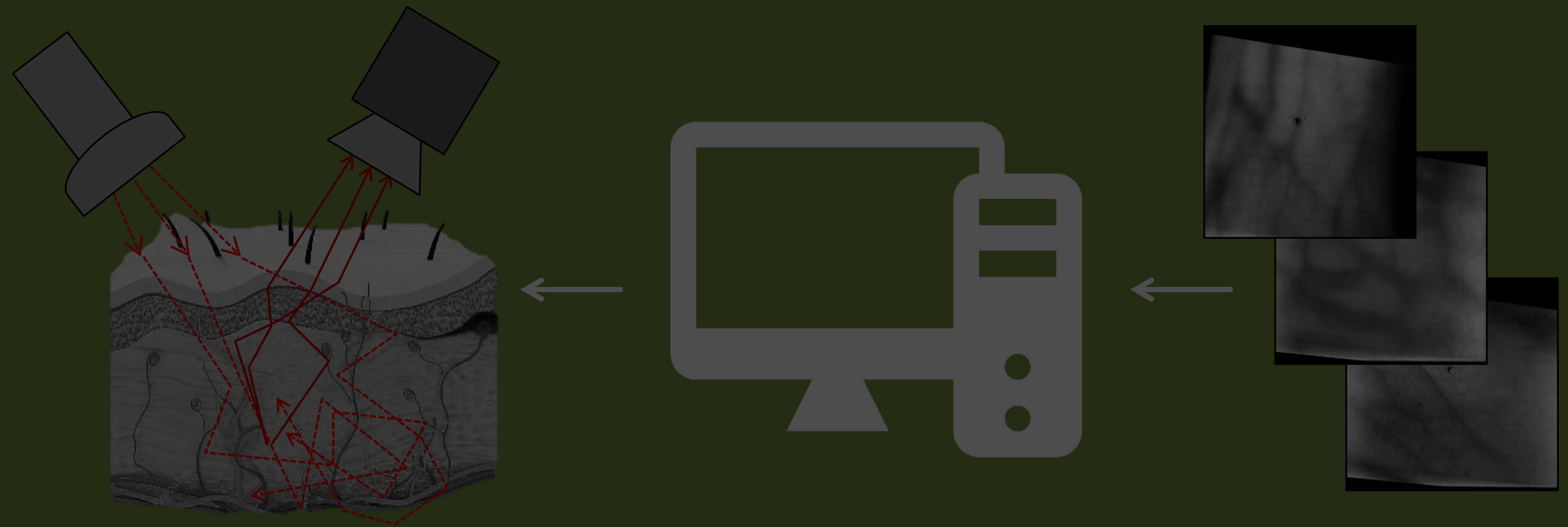

- accurate and efficient differentiable simulation
- tractably solve general inverse problems

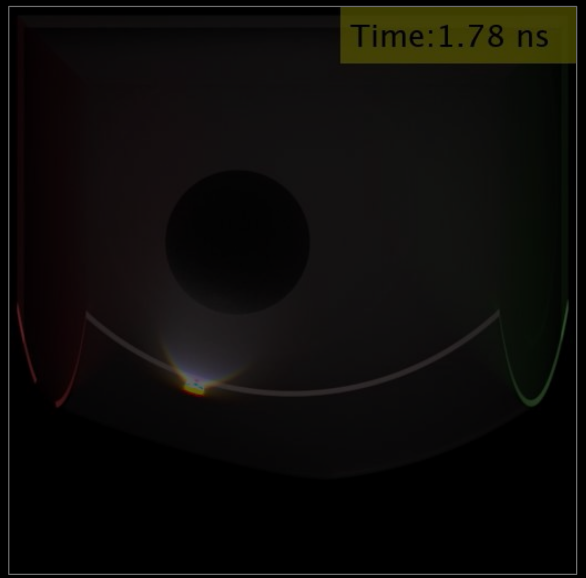

time-of-flight imaging

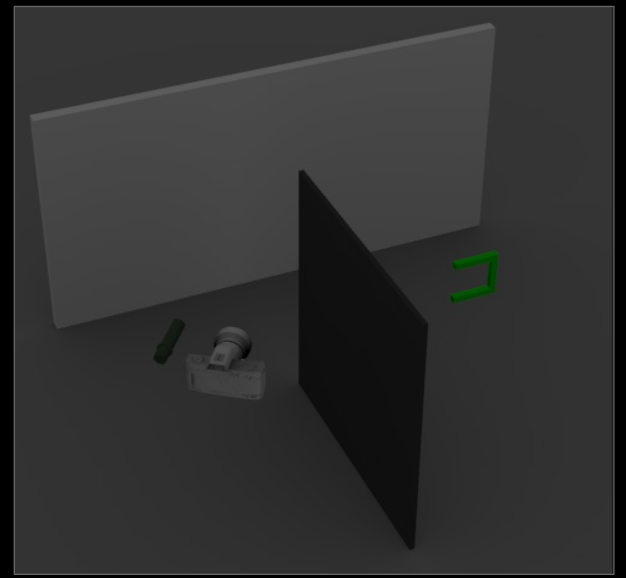

non-line-of-sight imaging

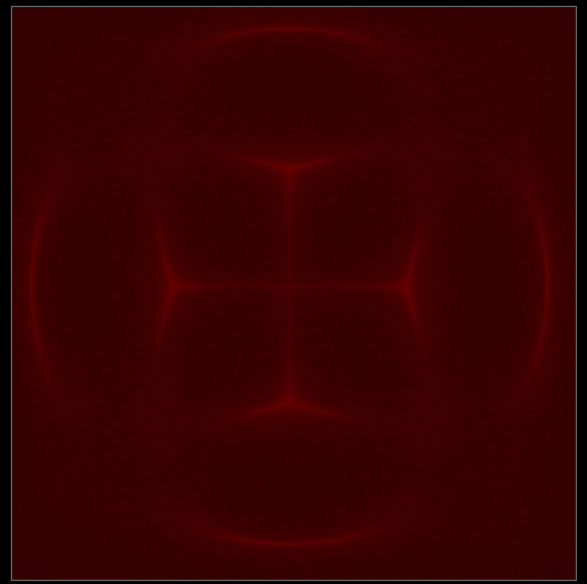

acousto-optic lensing

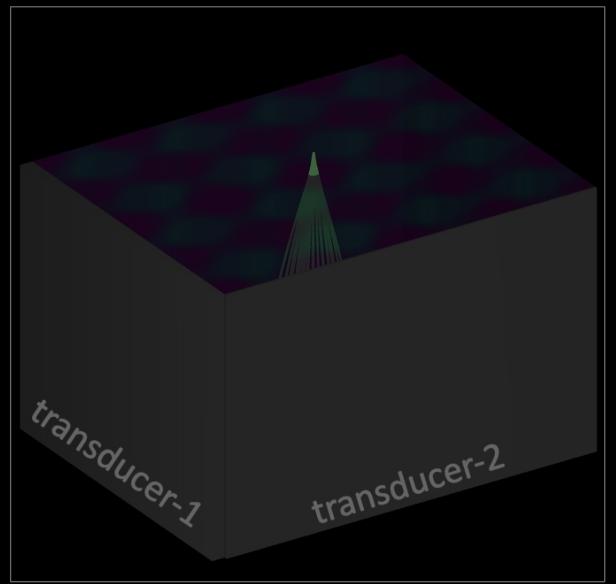

ultrafast light scanning

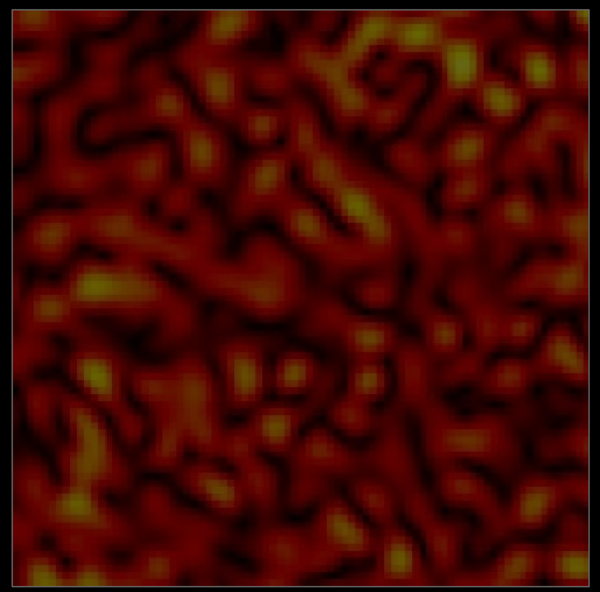

speckle imaging

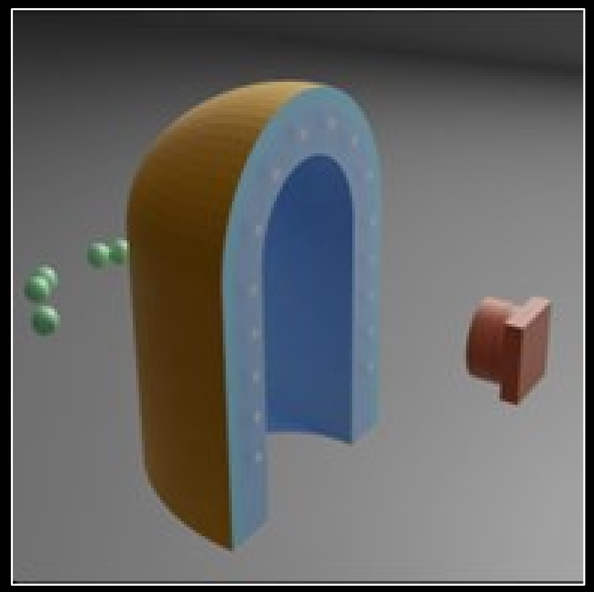

tactile sensor design

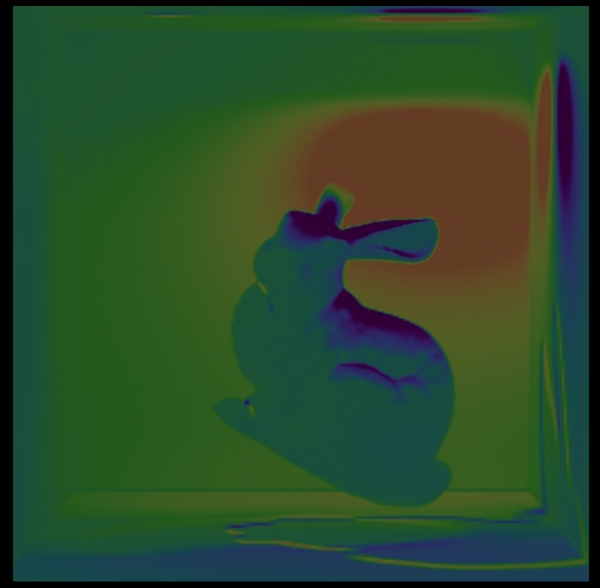

differentiable renderer

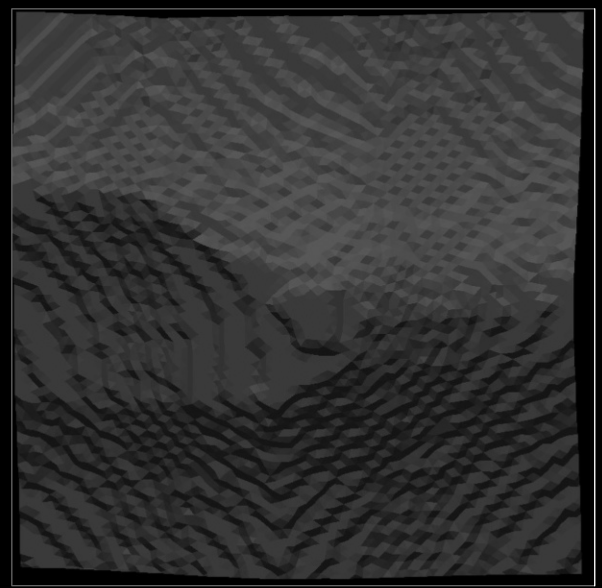

inverse problems

Why tactile sensing?

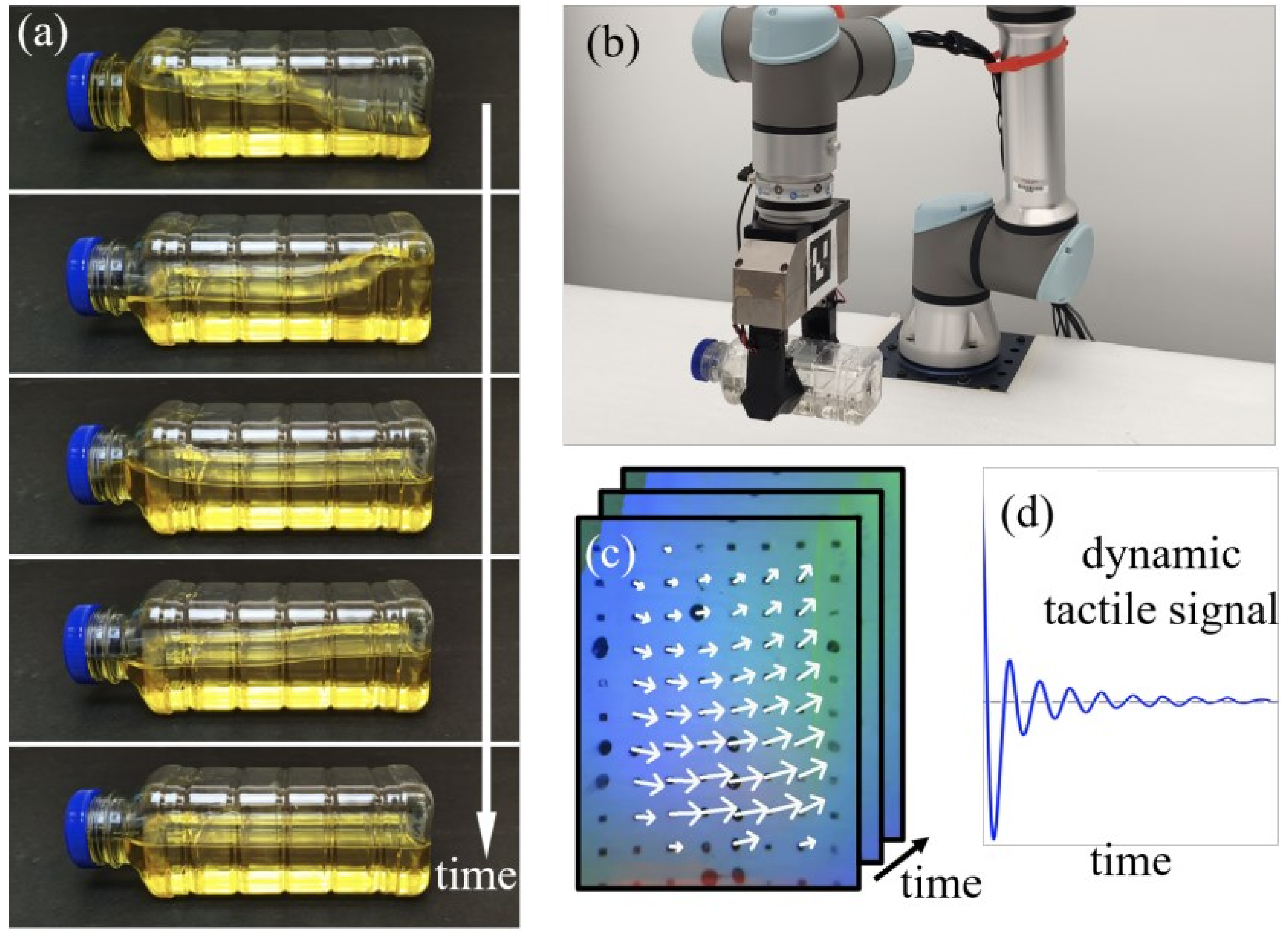

Object perception
[Huang et.al. 2022]

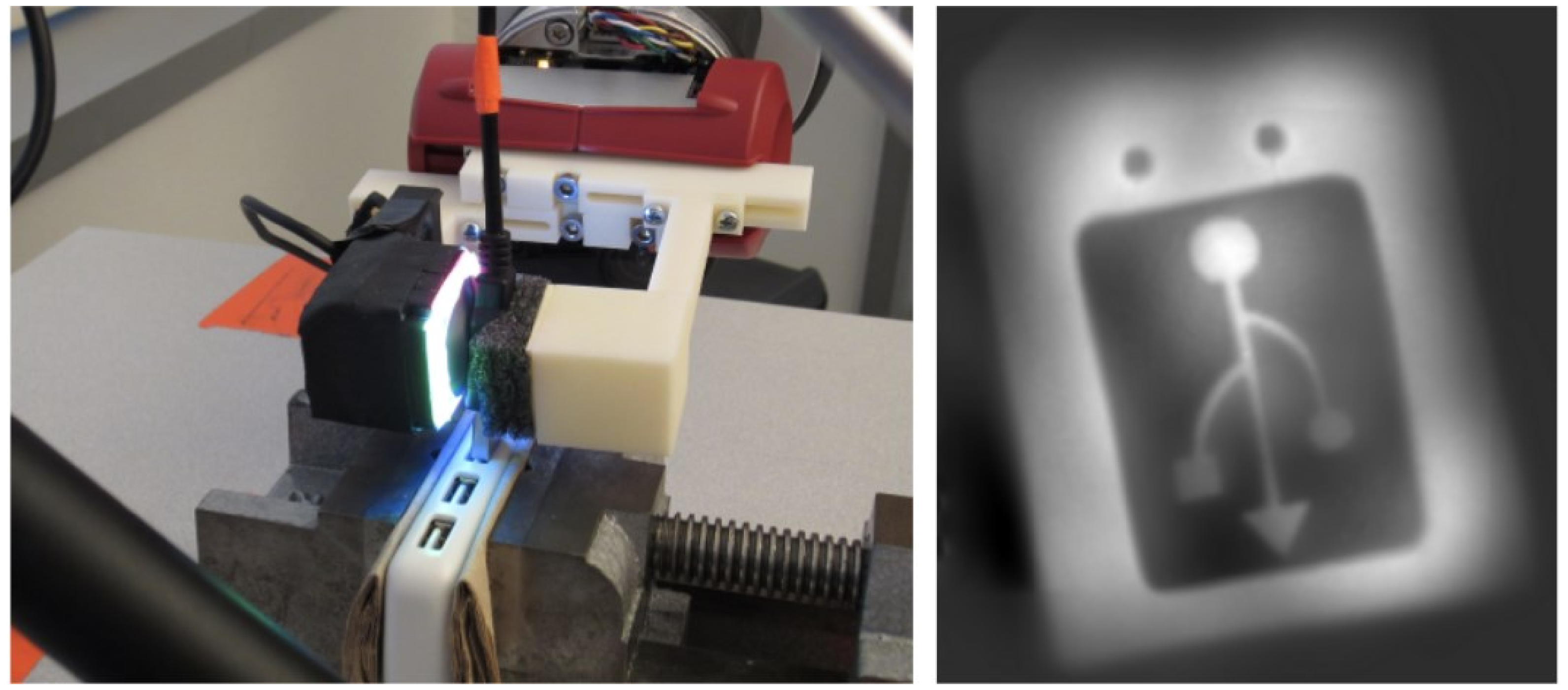

Advanced manufacturing
[Li et.al. 2014]

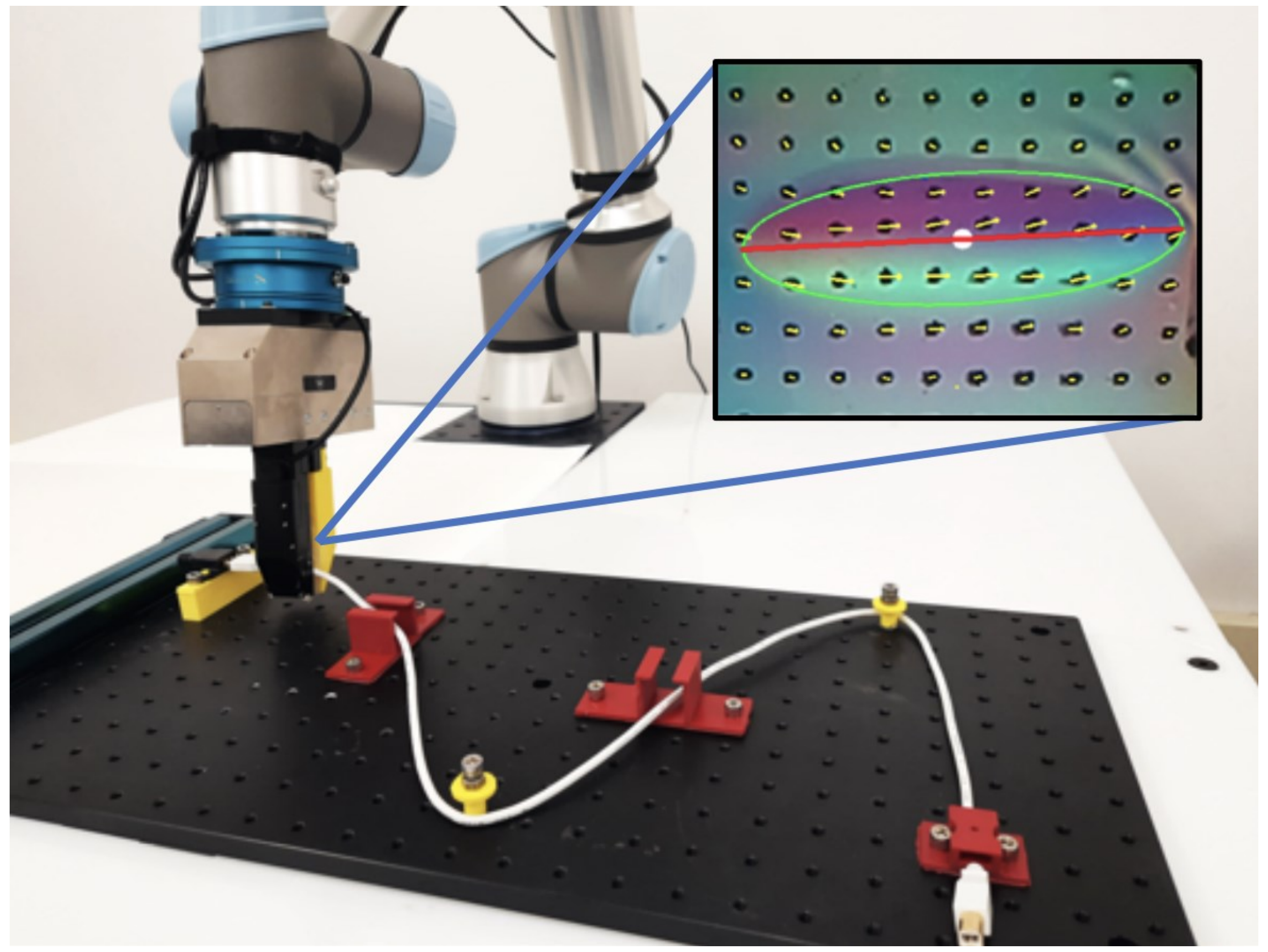

Robotic manipulation
[Yuan et.al. 2018]
[Wilson et.al. 2023]

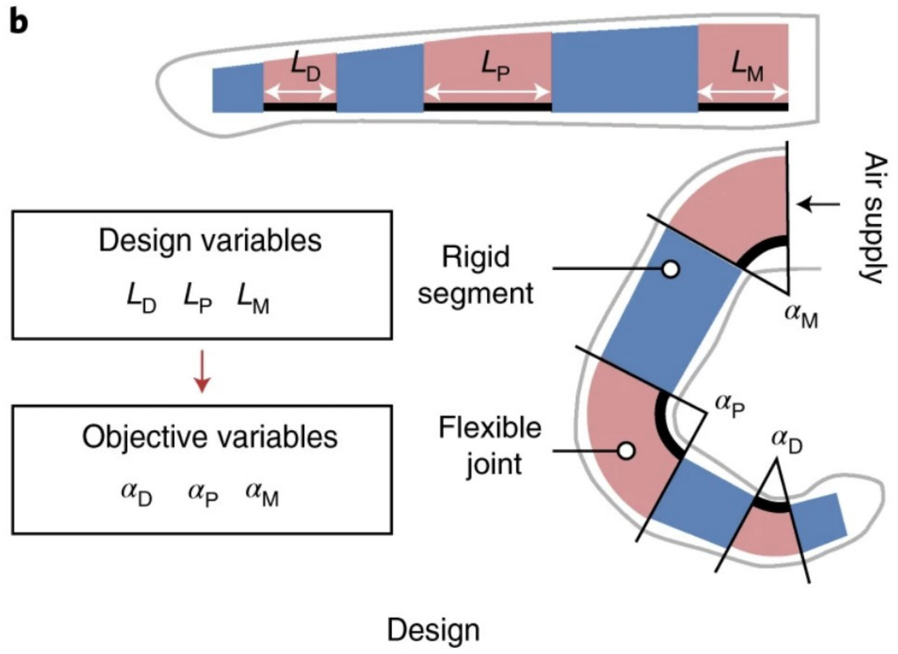

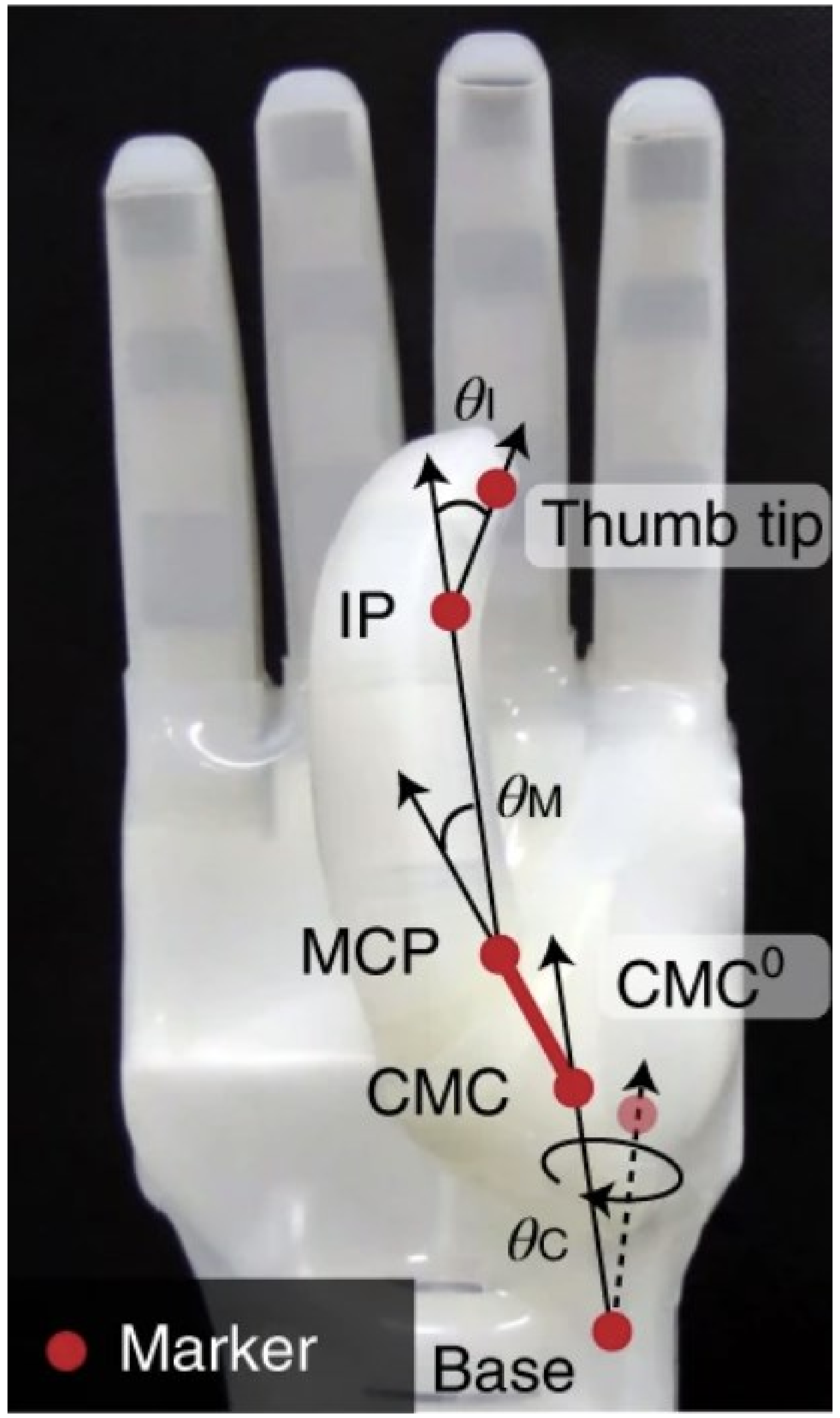

Neuroprosthetics
[Gu et.al. 2023]

Tactile sensors

BioTac
ionically-conductive fluid based

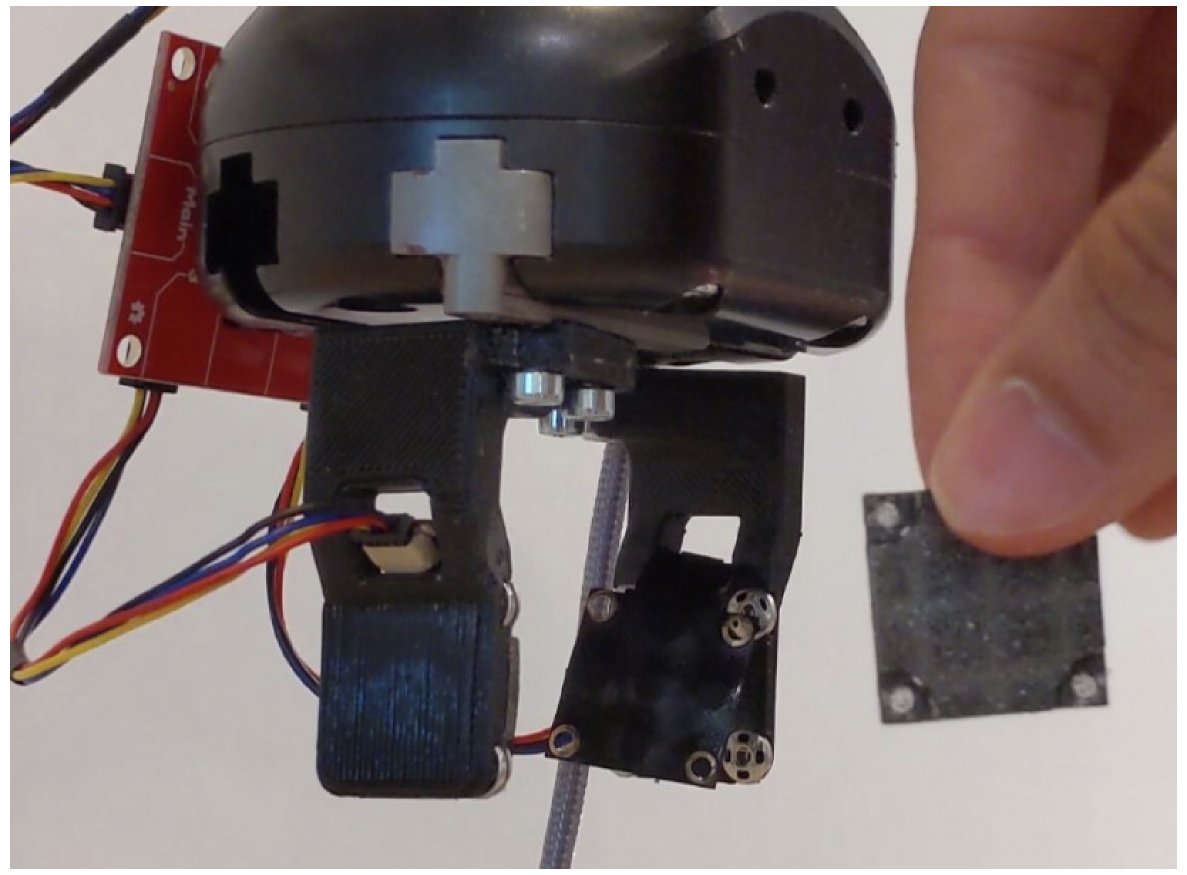

ReSkin
Magnetic field based

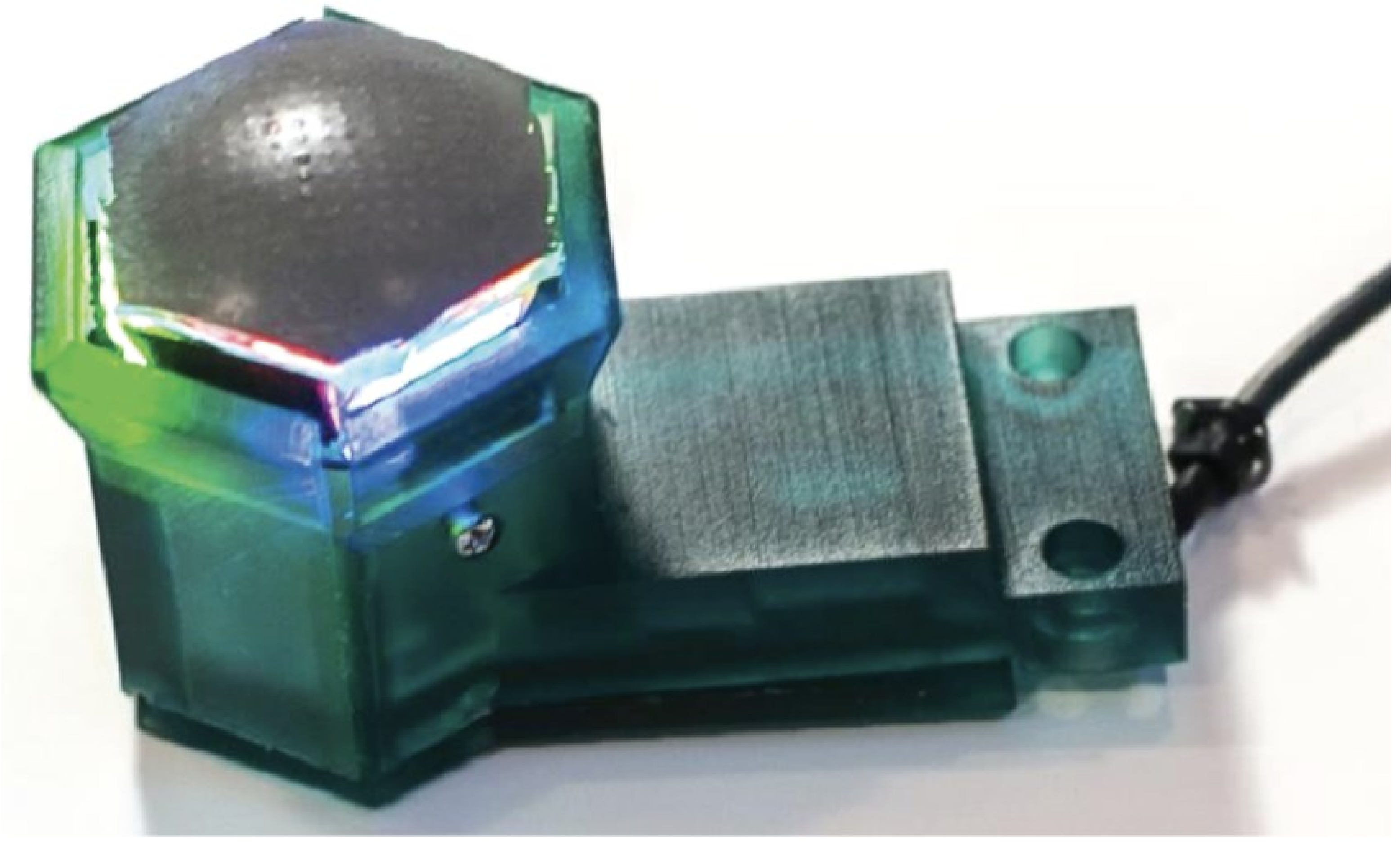

GelSight
Vision-based

Tactile sensors

BioTac
ionically-conductive fluid based

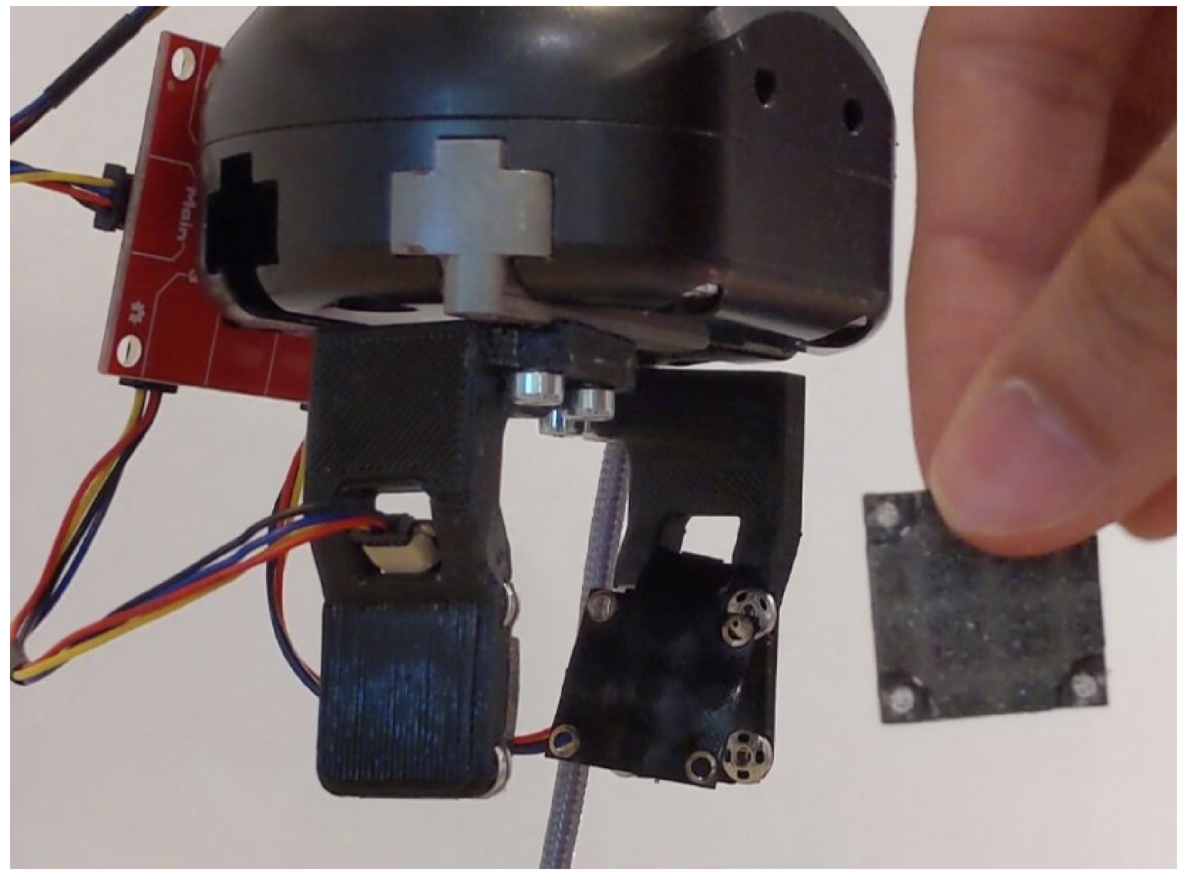

ReSkin
Magnetic field based

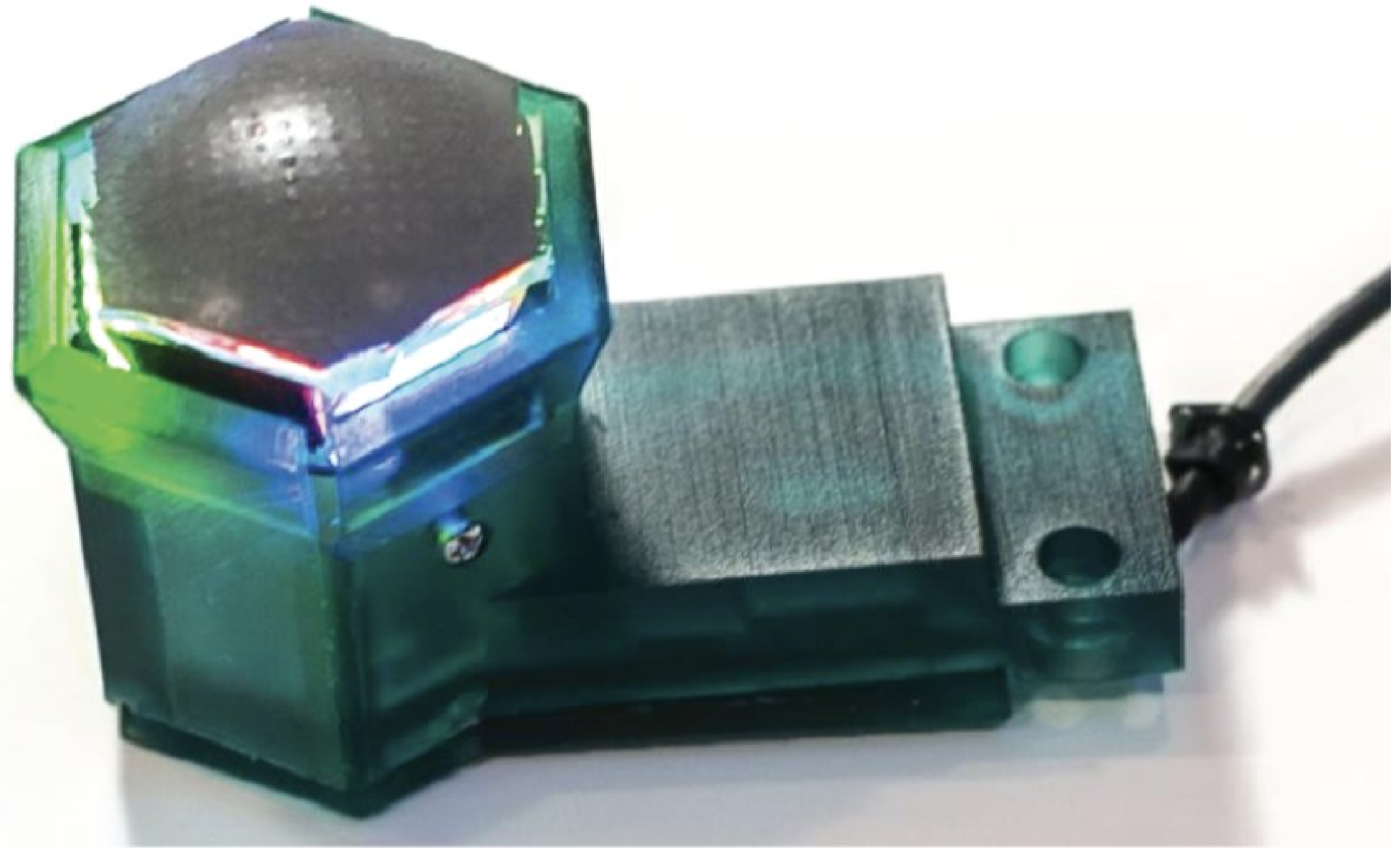

GelSight
Vision-based

Vision-based tactile sensors: working principle

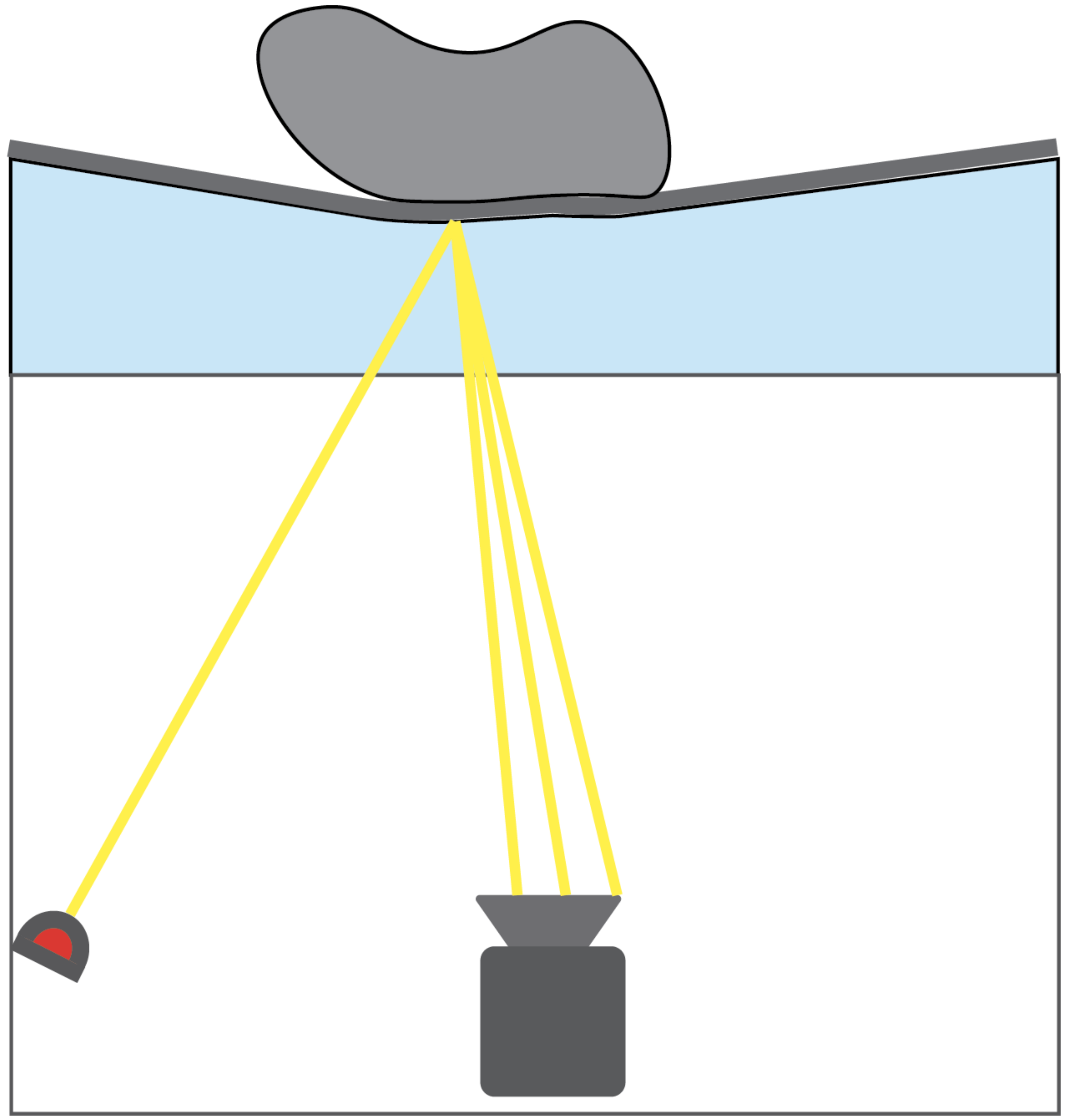

Sensor schematic

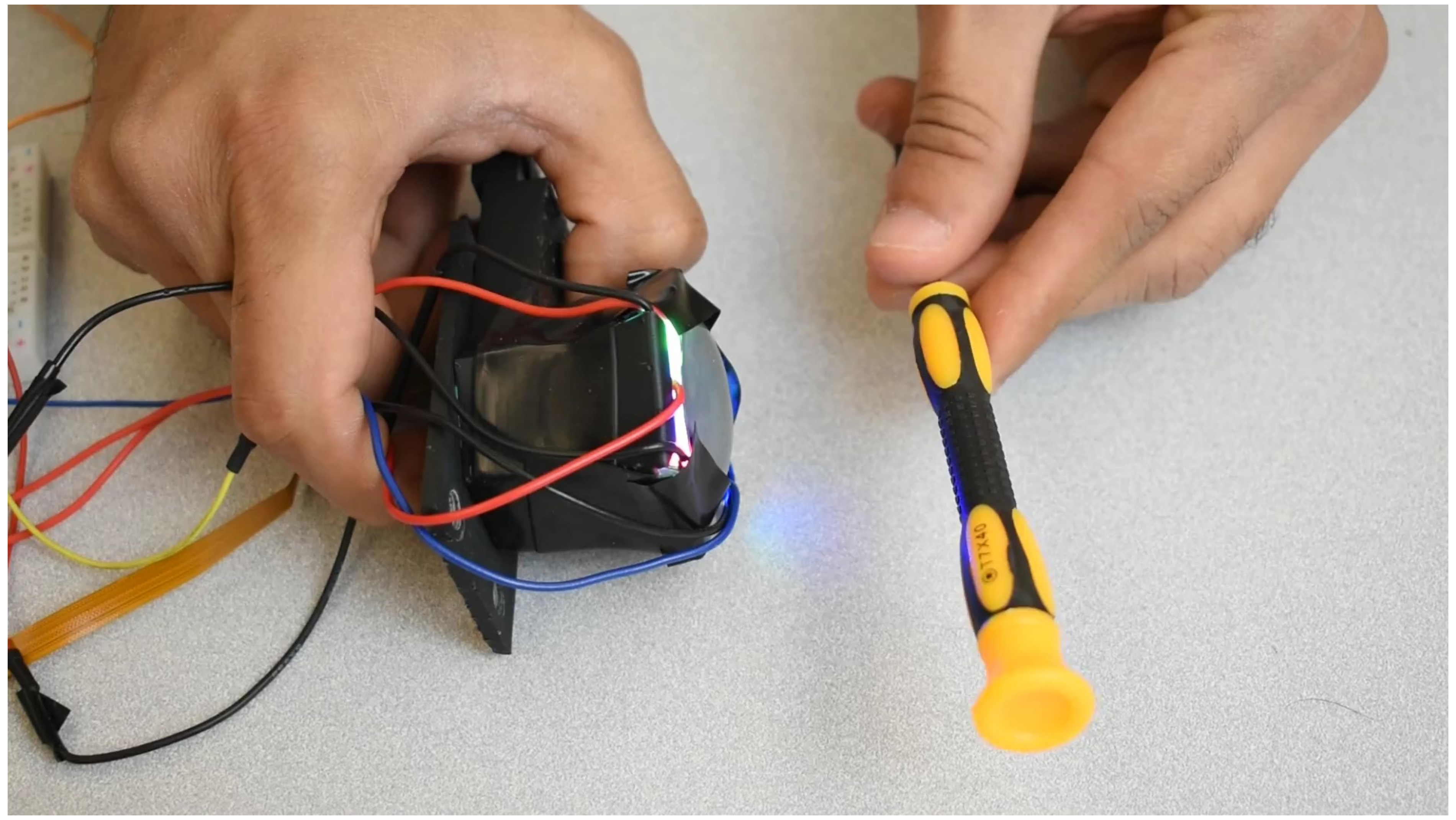

Live view

Sensor view

[Johnson and Adelson, 2021]

Vision-based tactile sensors: photometric stereo

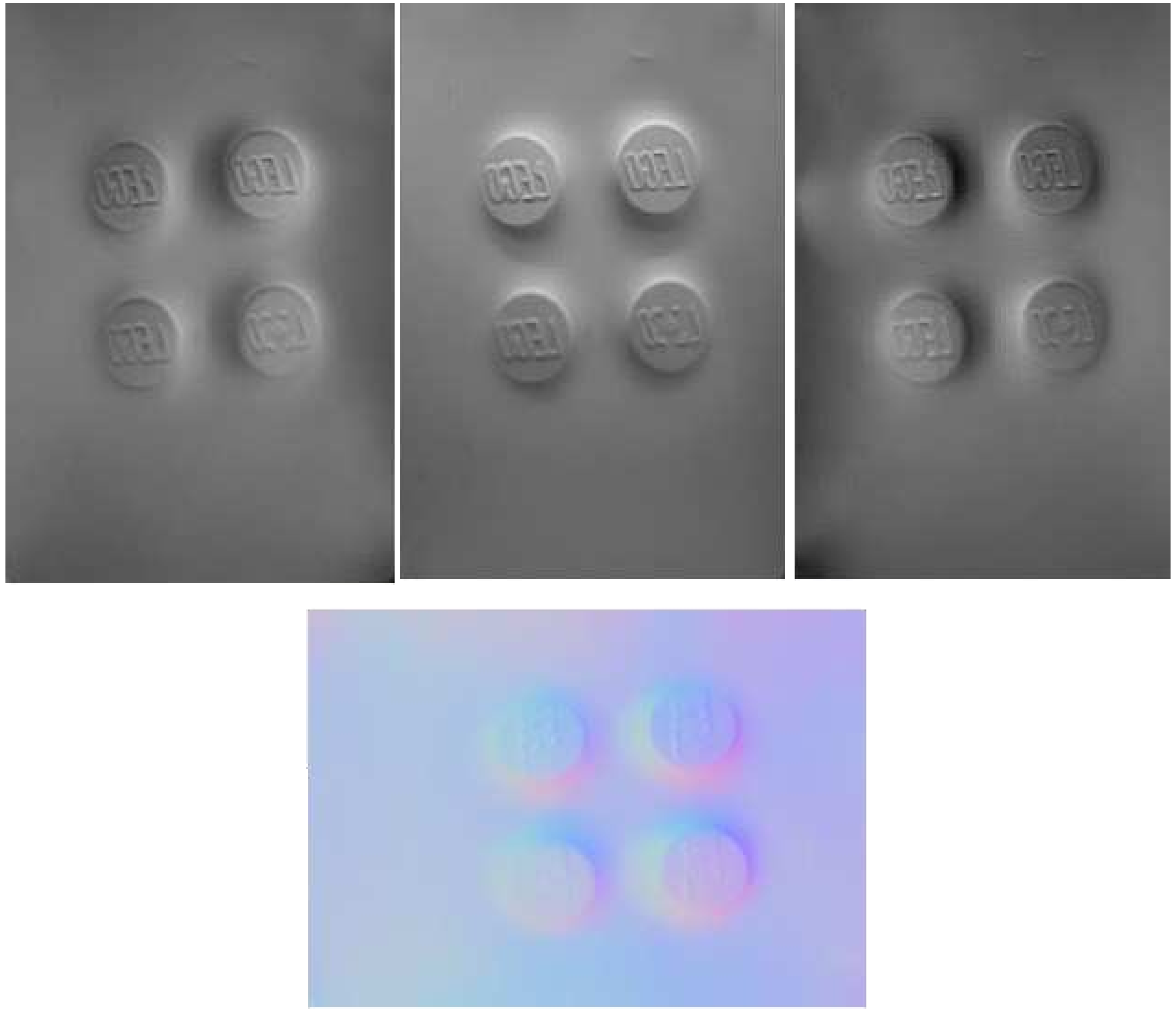

Camera Images

Normals

With photometric stereo, GelSight can encode surface normals as an RGB image.

[Johnson and Adelson, 2021]

Vision-based tactile sensors: design variants

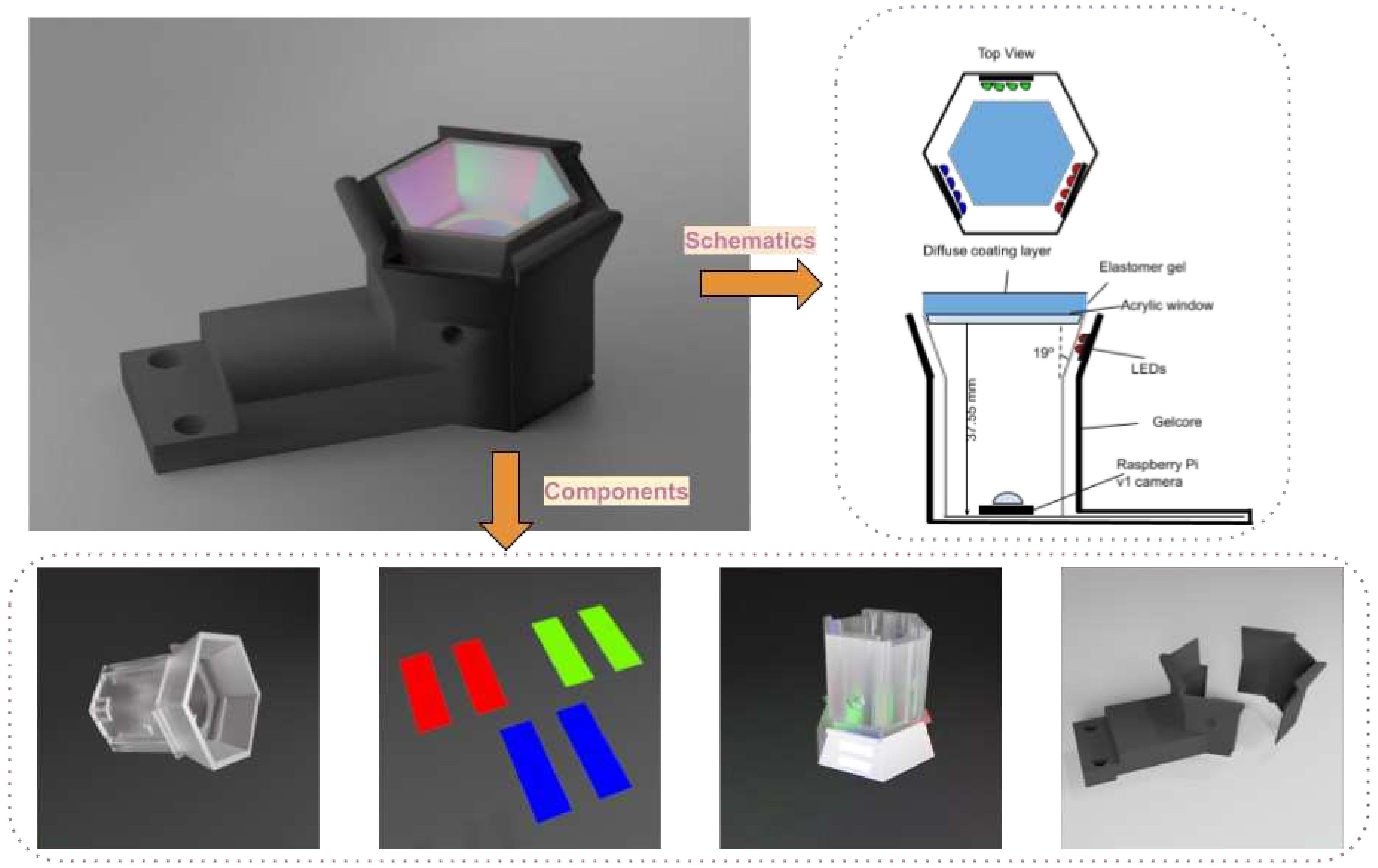

FlatGel GelSight
Dong et. al. 2017
Agarwal et. al. 2021

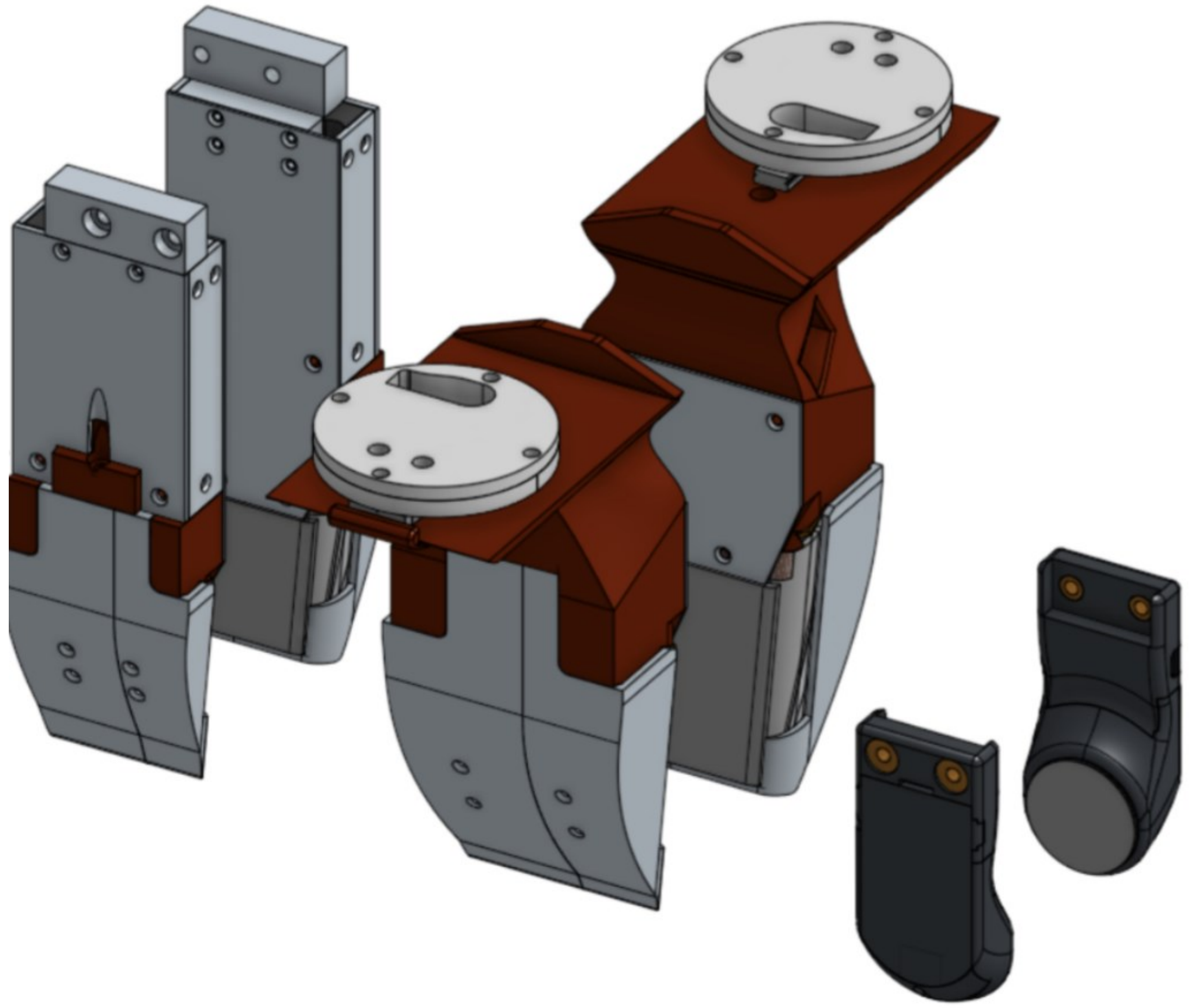

GelSlim Family
Donlon et. al. 2018
Ma et. al. 2019
Hogan et. al. 2020
Taylor et. al. 2021

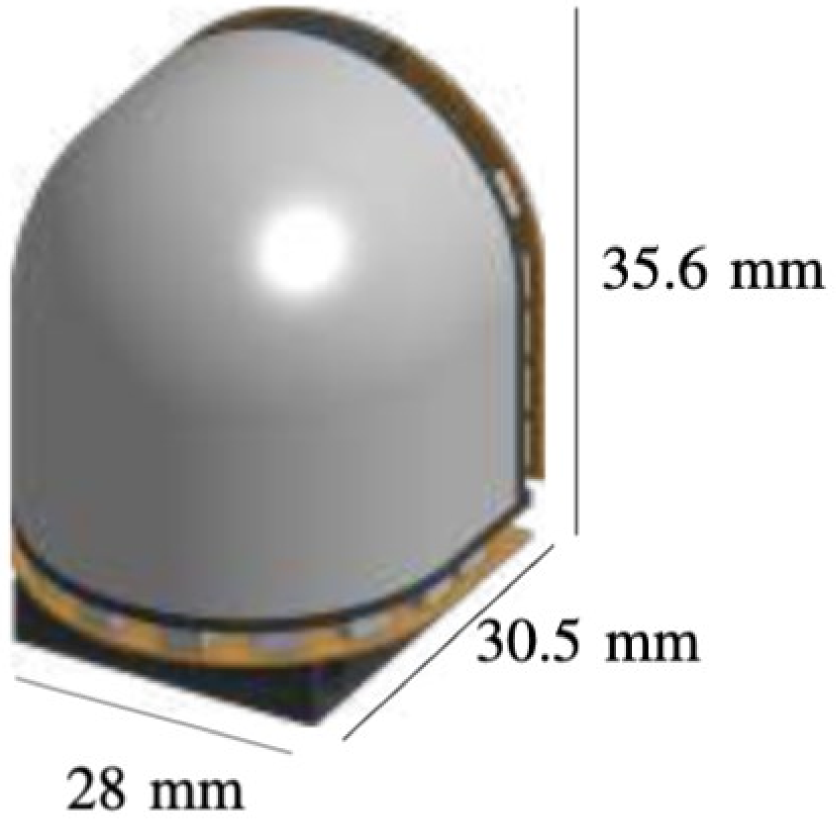

RoundTip GelSight
Romero et. al. 2020

Designing VBTS is hard

[Agarwal et al., 2023]

Designing VBTS is hard

- Diversity of sensor shape and required form-factor

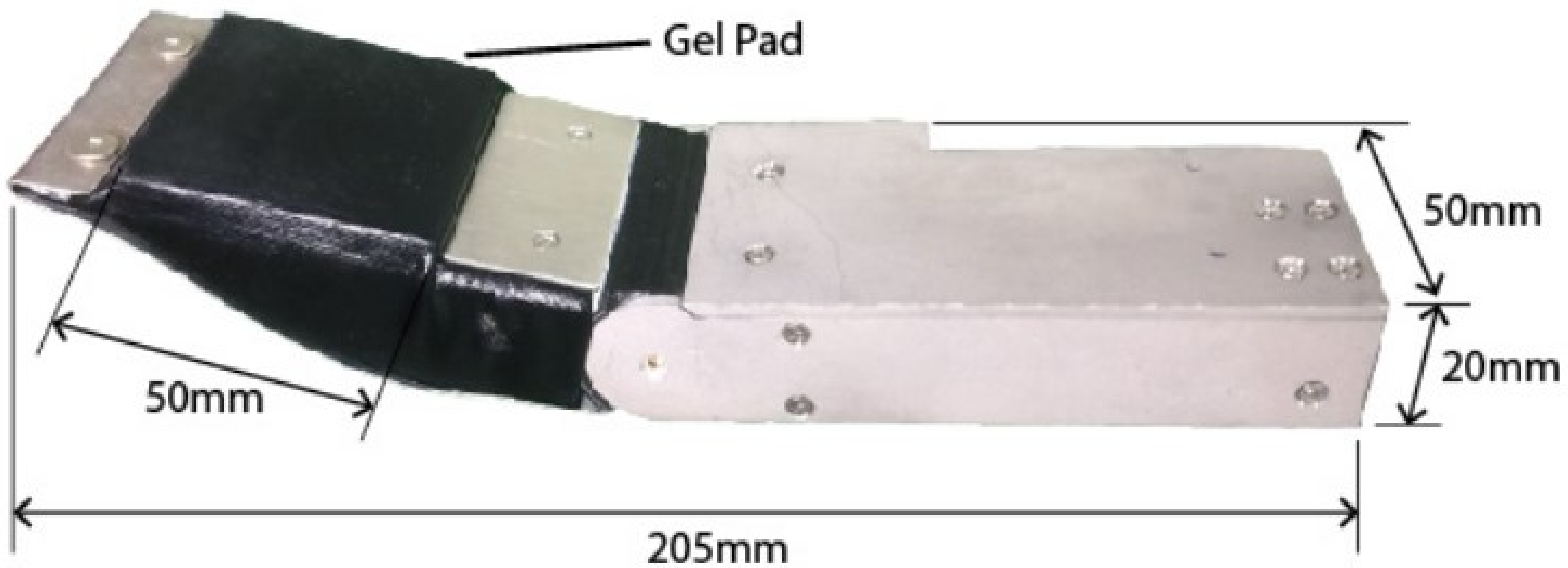

Flat sensing surface

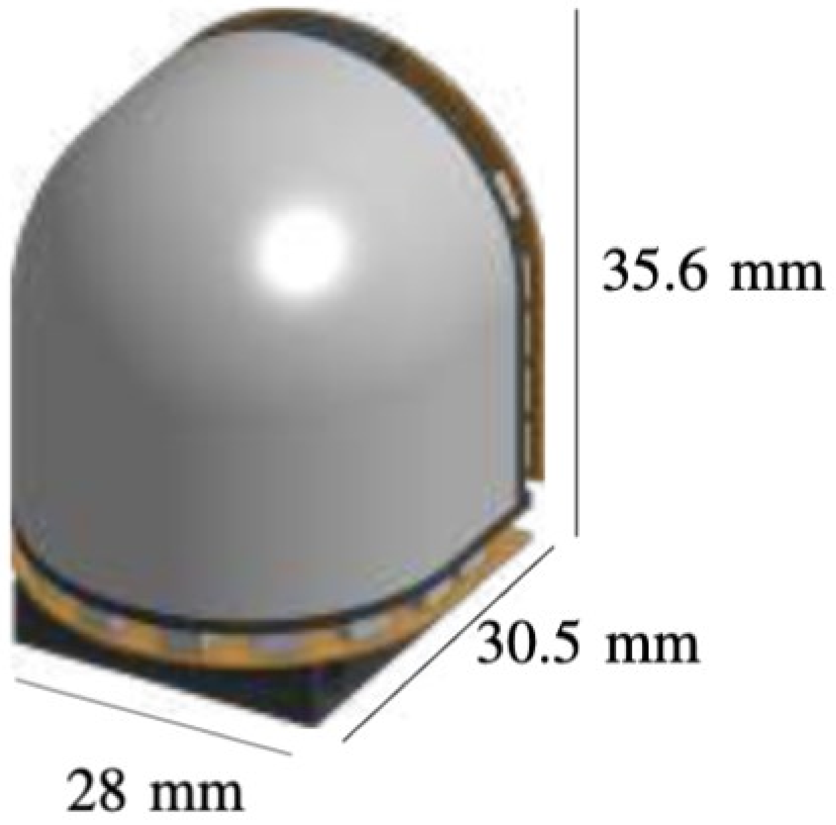

Curved sensing surface

[Agarwal et al., 2023]

Designing VBTS is hard

- Diversity of sensor shape and required form-factor
- Complex light interaction

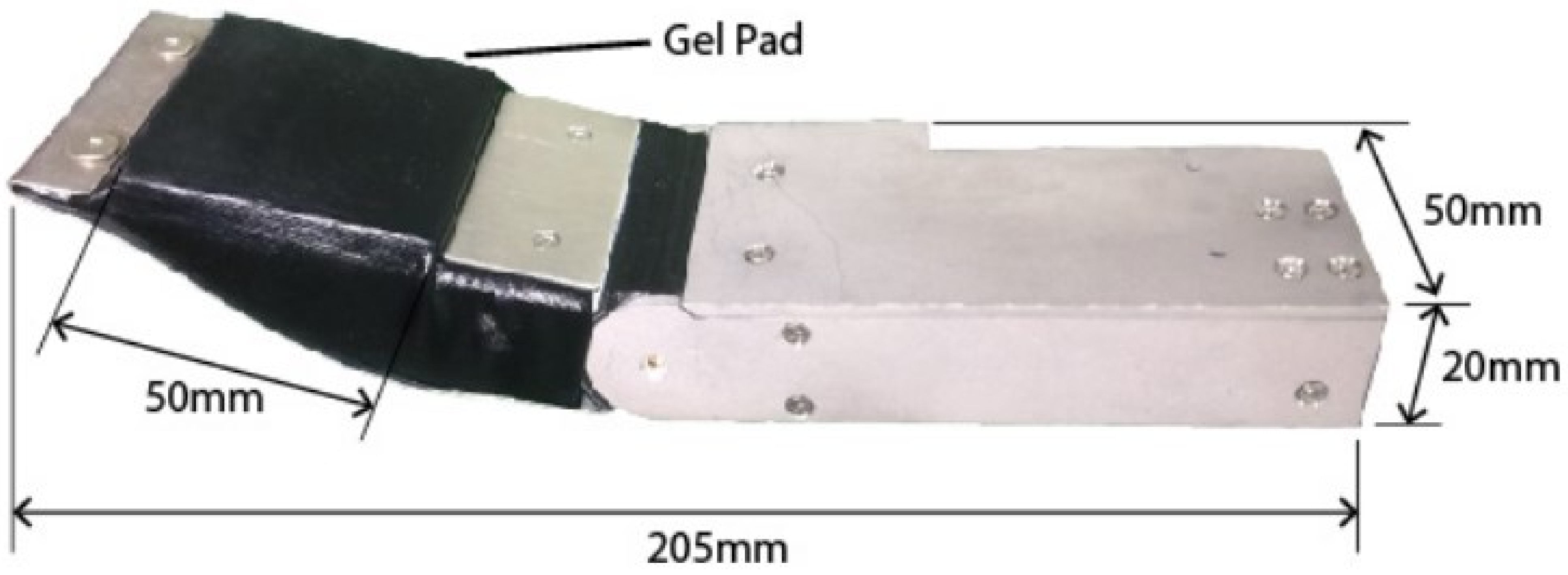

Flat sensing surface

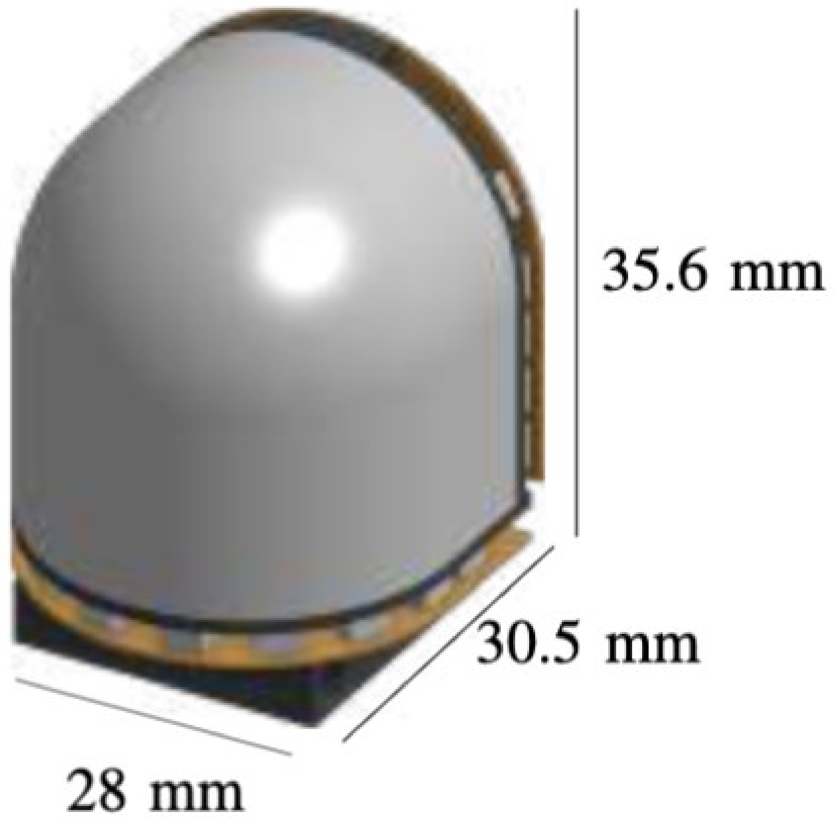

Curved sensing surface

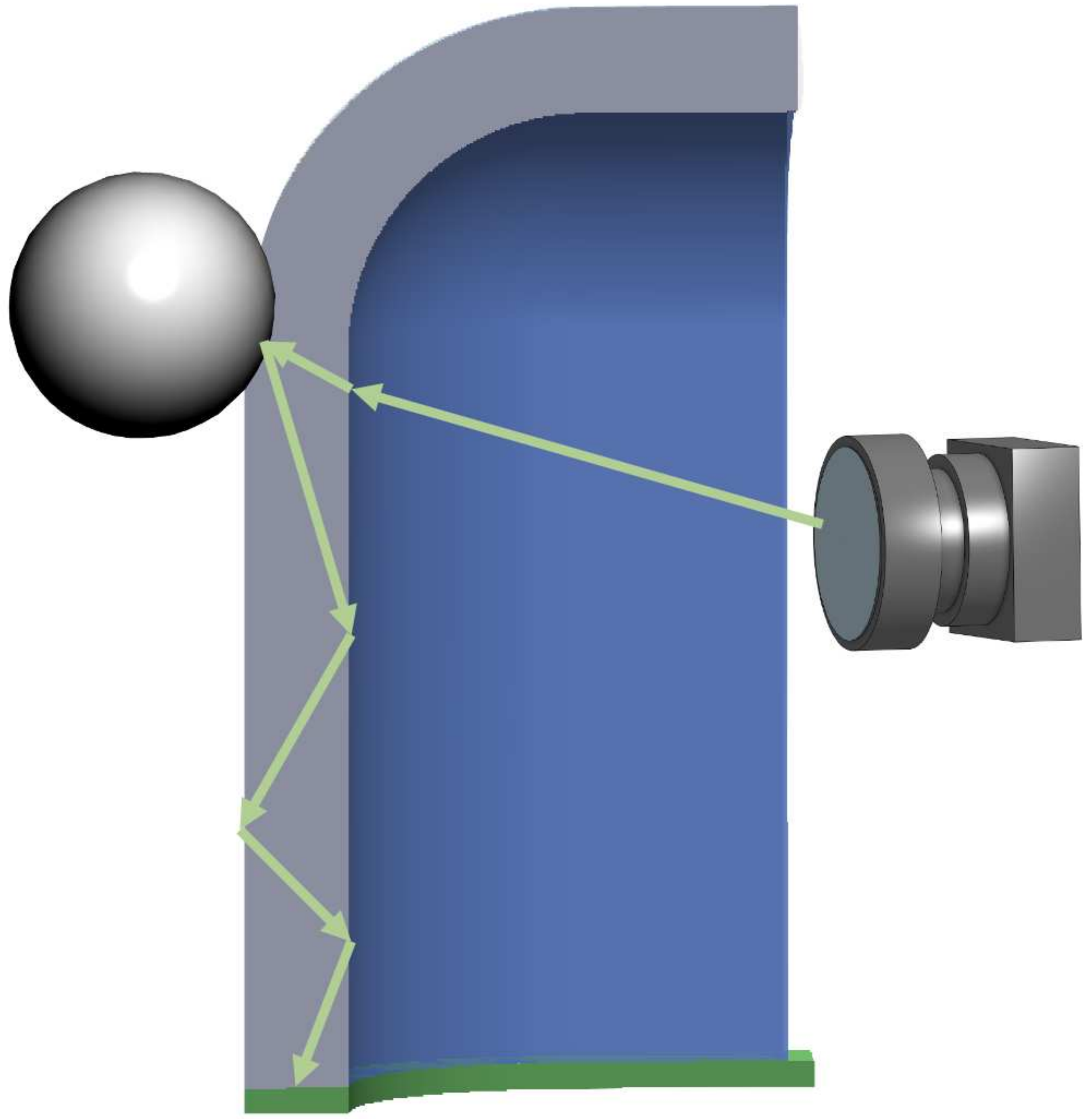

[Agarwal et al., 2023]

Curved tactile sensor

[Agarwal et al., 2023]

Curved tactile sensor

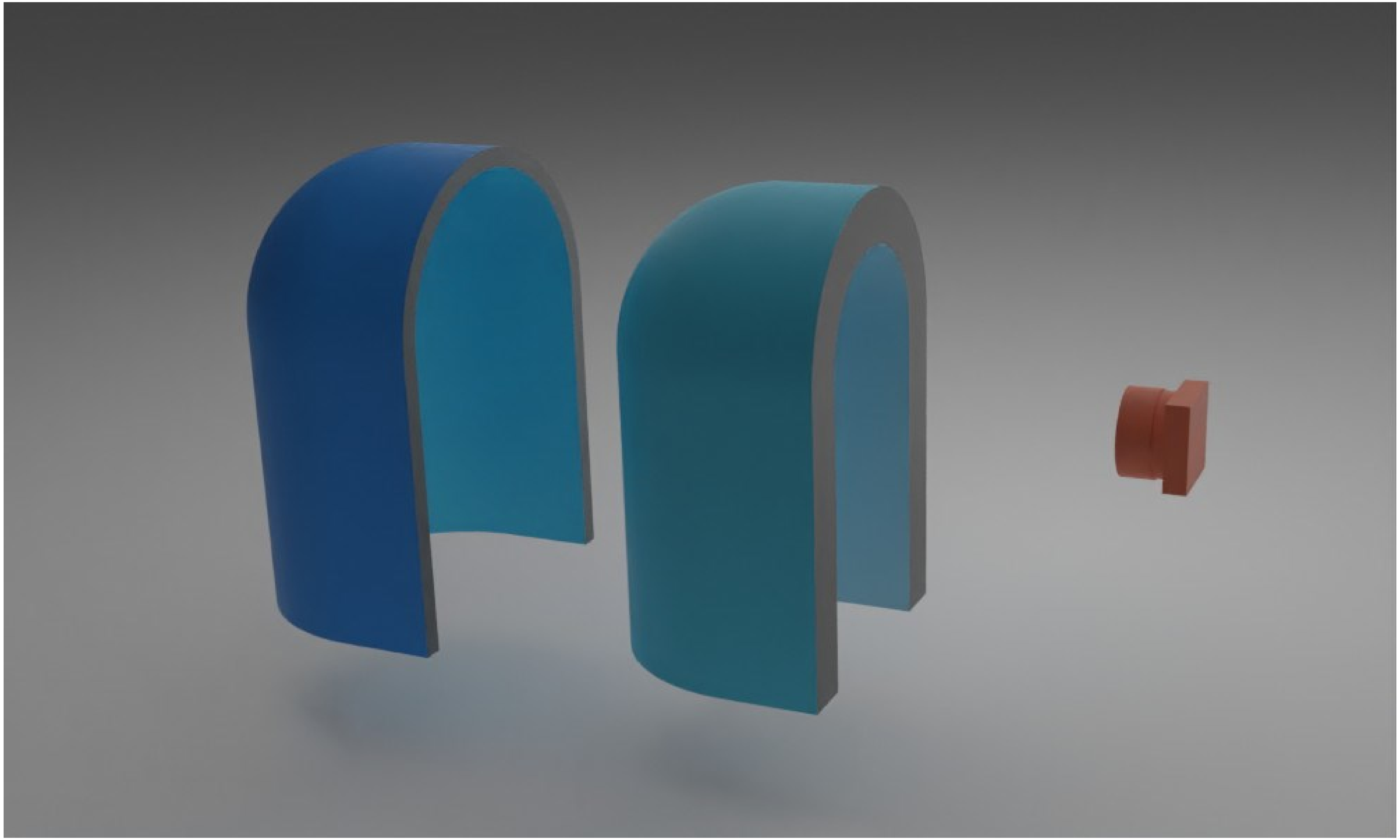

[Agarwal et al., 2023]

Curved tactile sensor: *working principle*

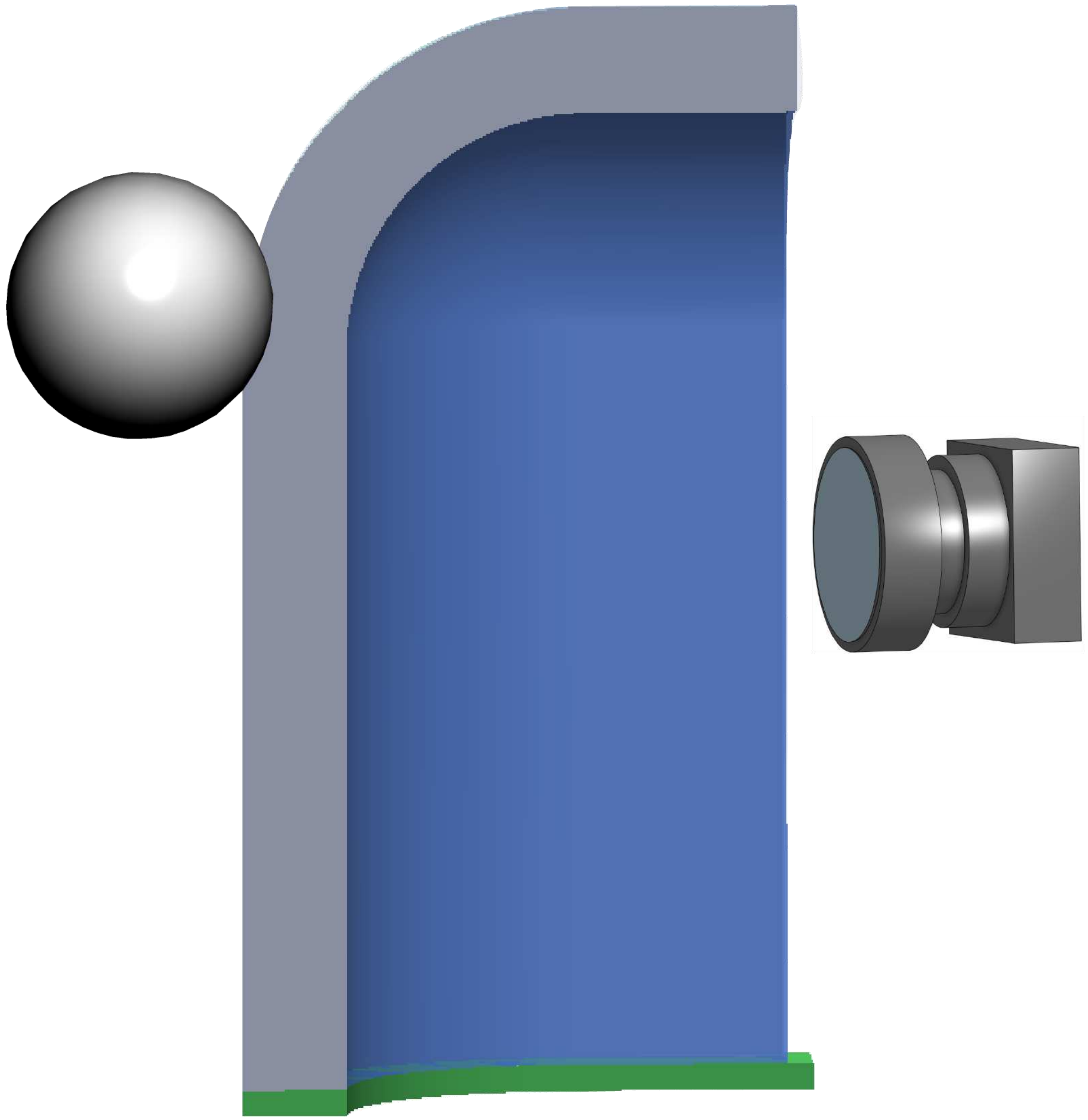

Section View

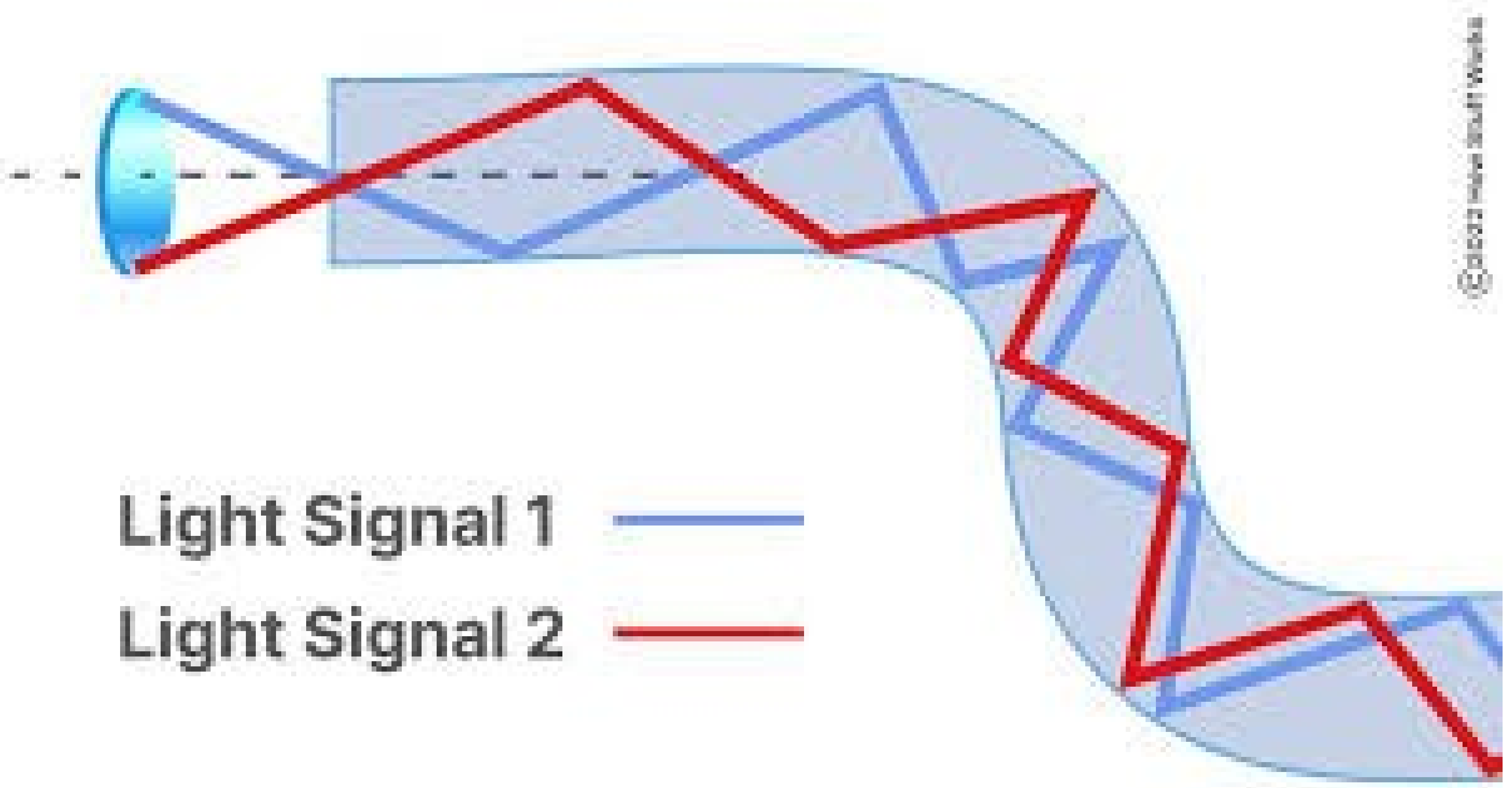

Light Piping

[Agarwal et al., 2023]

Curved tactile sensor: *working principle*

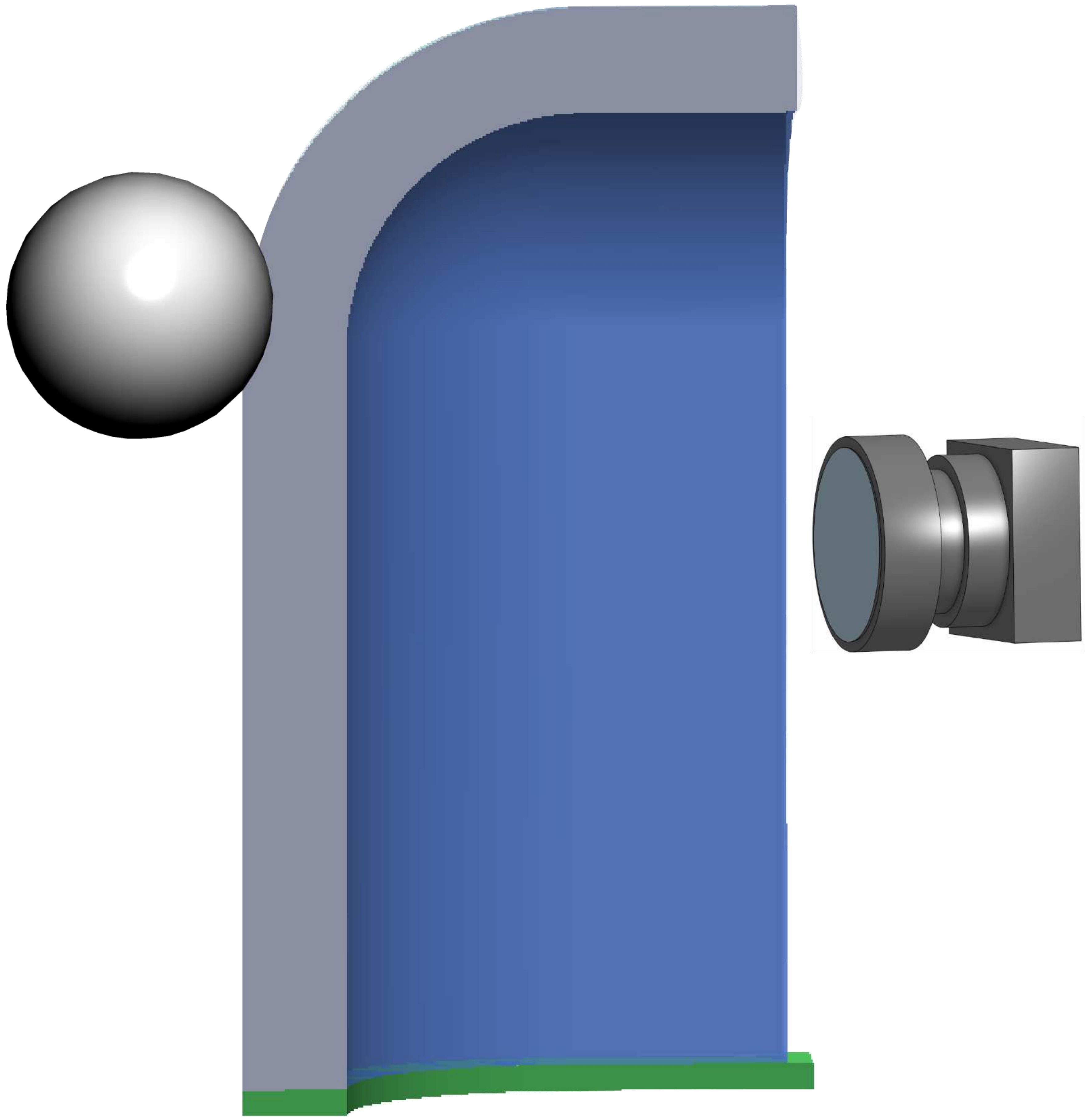

Section View

[Agarwal et al., 2023]

Curved tactile sensor: *working principle*

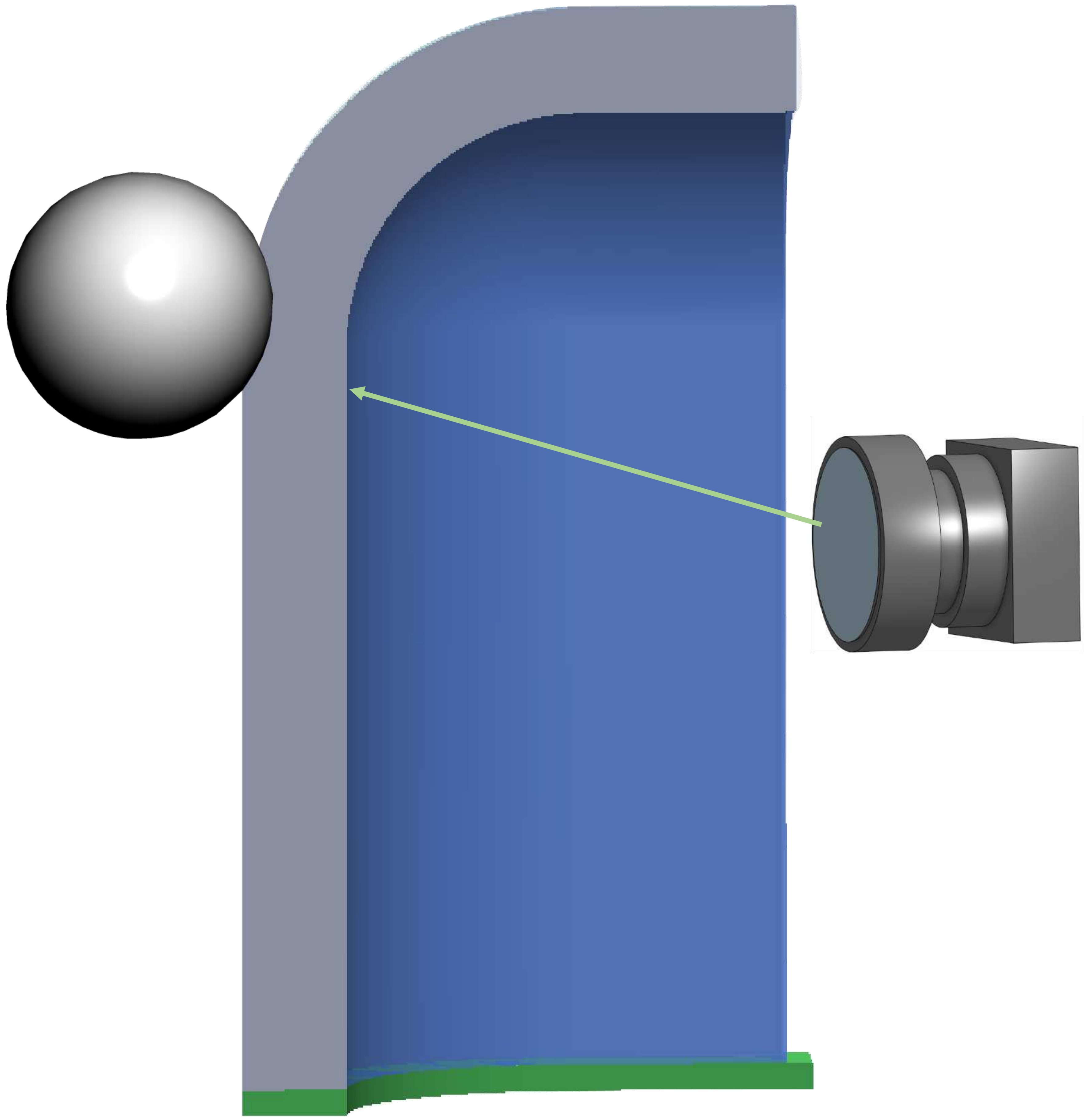

Section View

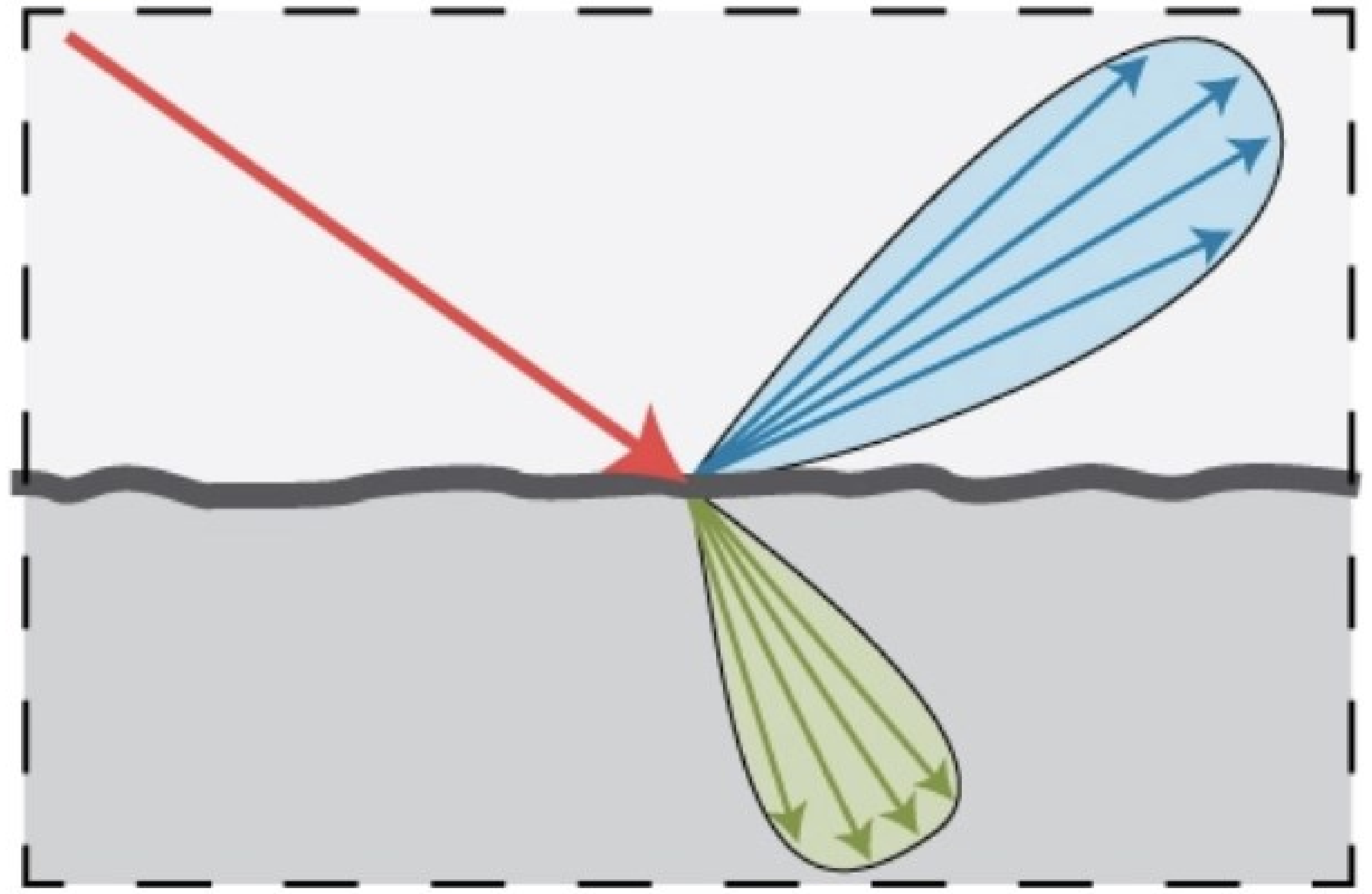

Refraction at rough interface

[Agarwal et al., 2023]

Curved tactile sensor: *working principle*

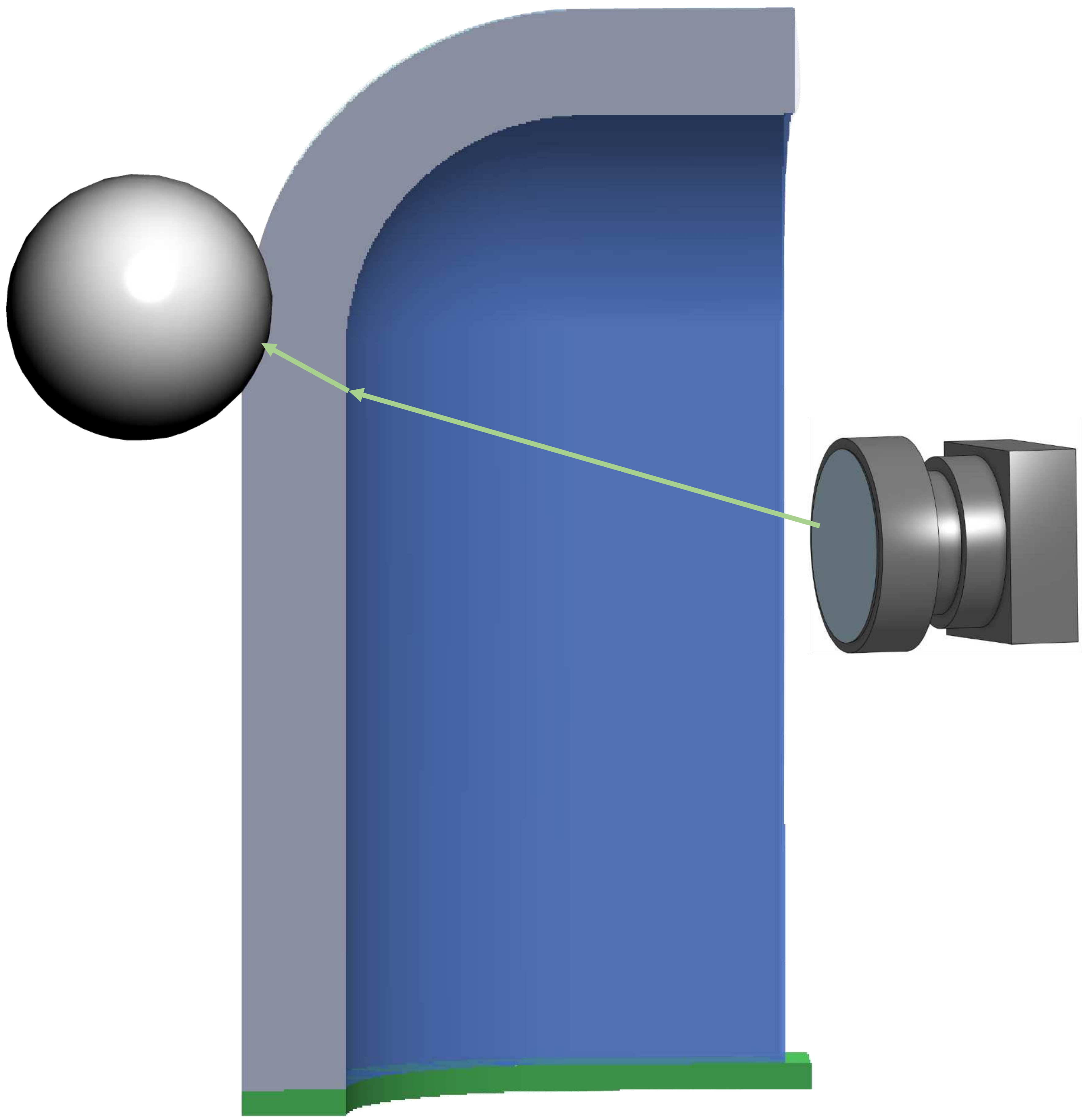

Section View

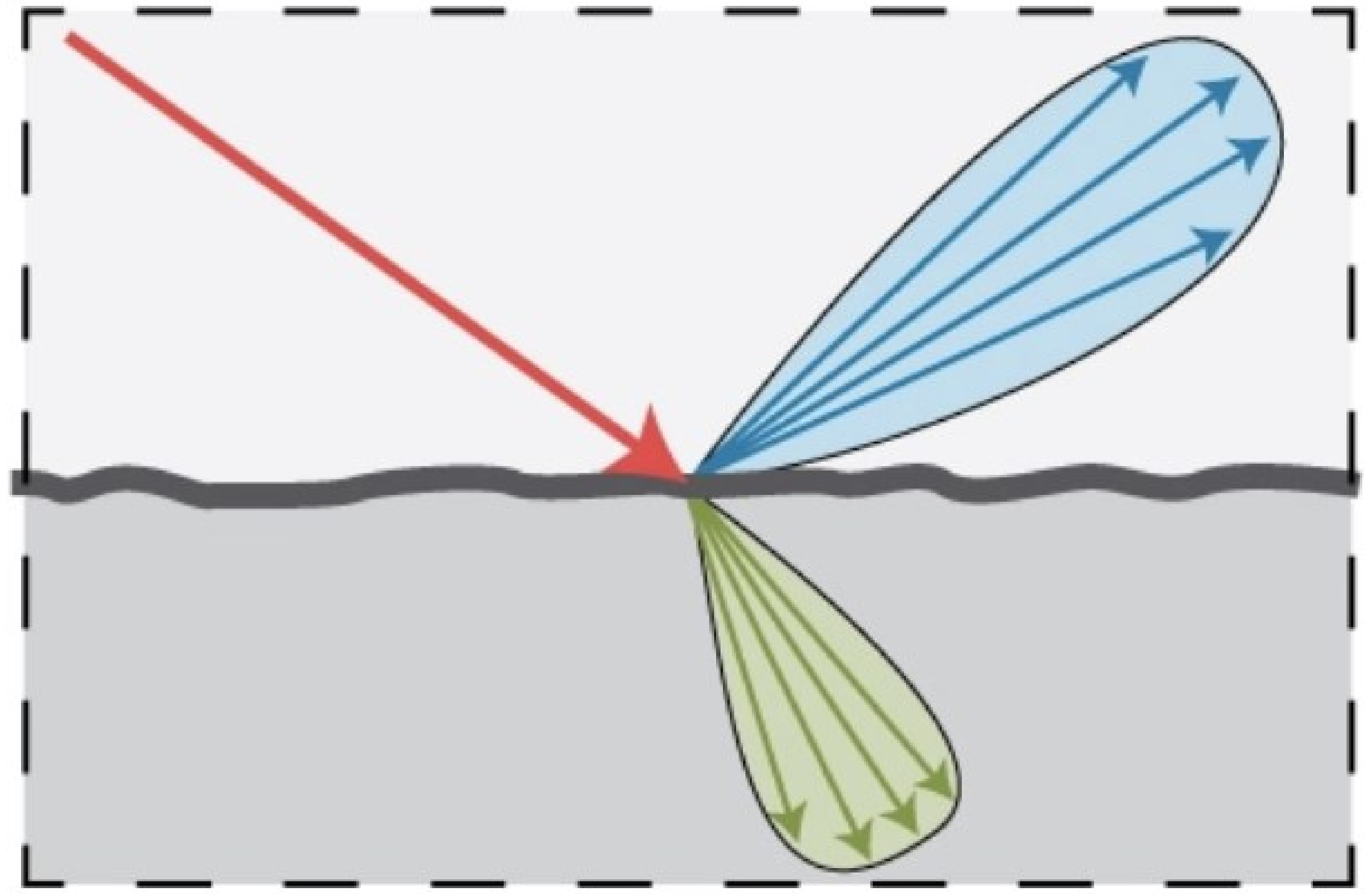

Refraction at rough interface

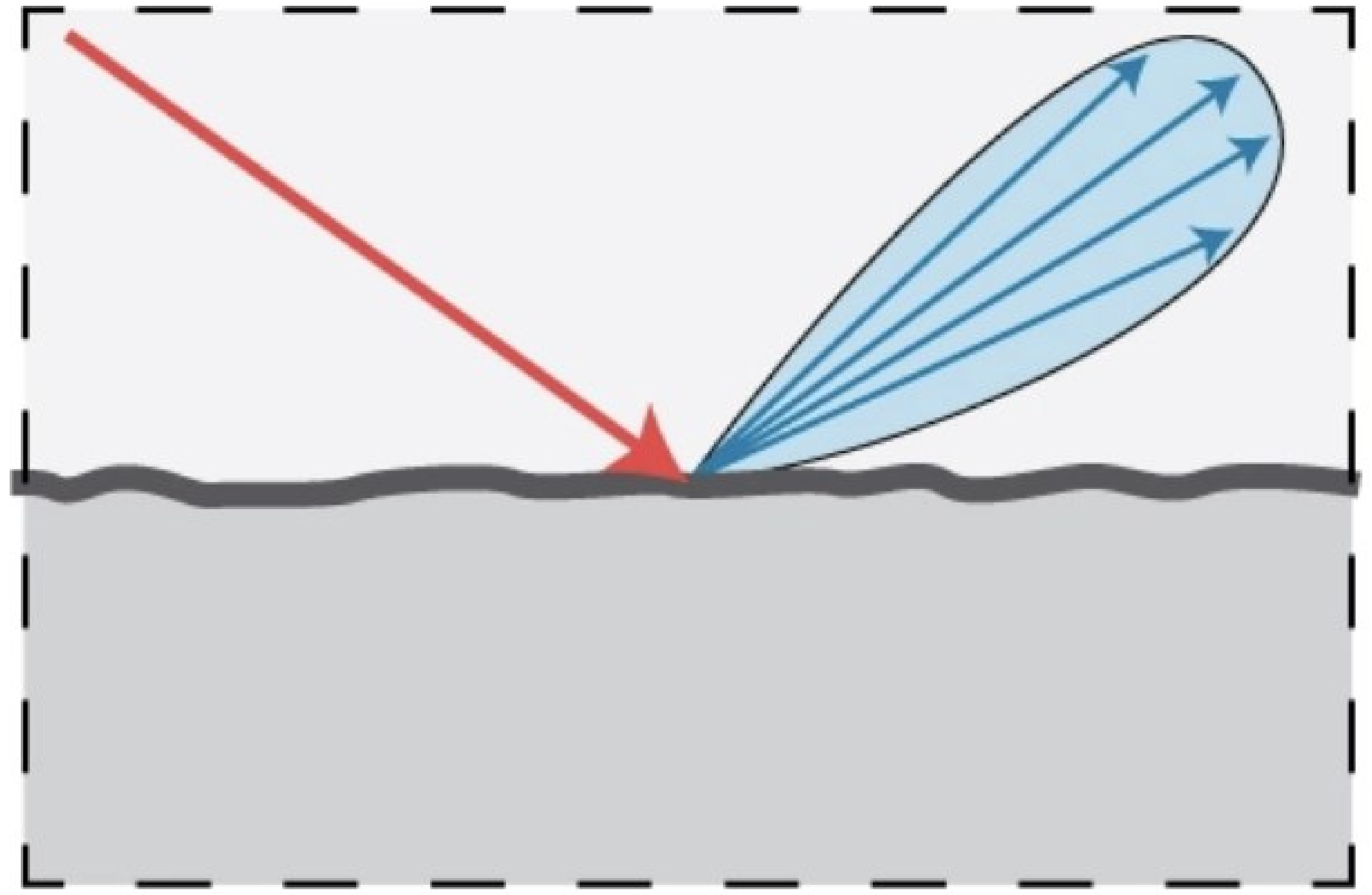

Reflection at glossy surfaces

[Agarwal et al., 2023]

Curved tactile sensor: *working principle*

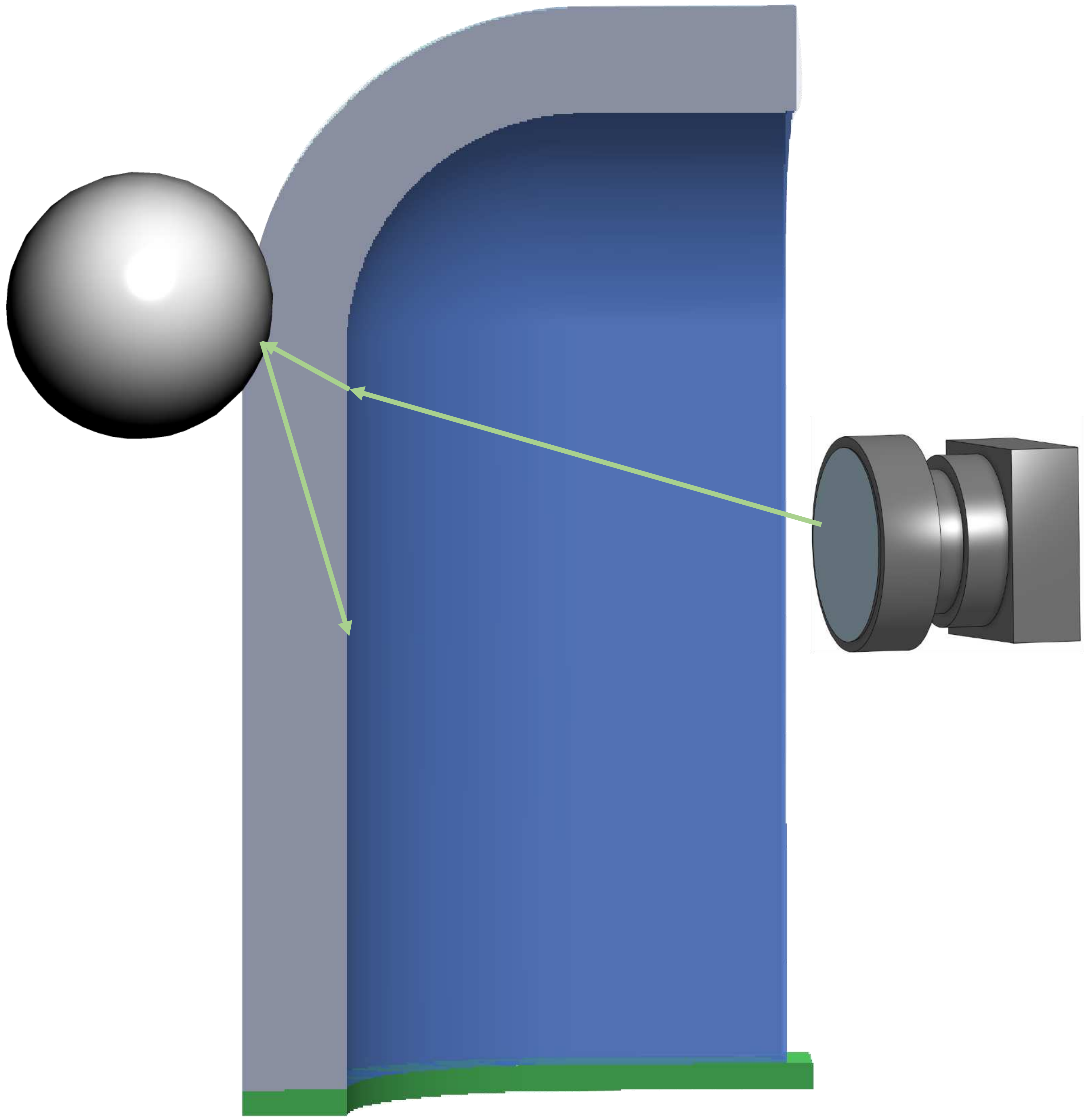
Section View

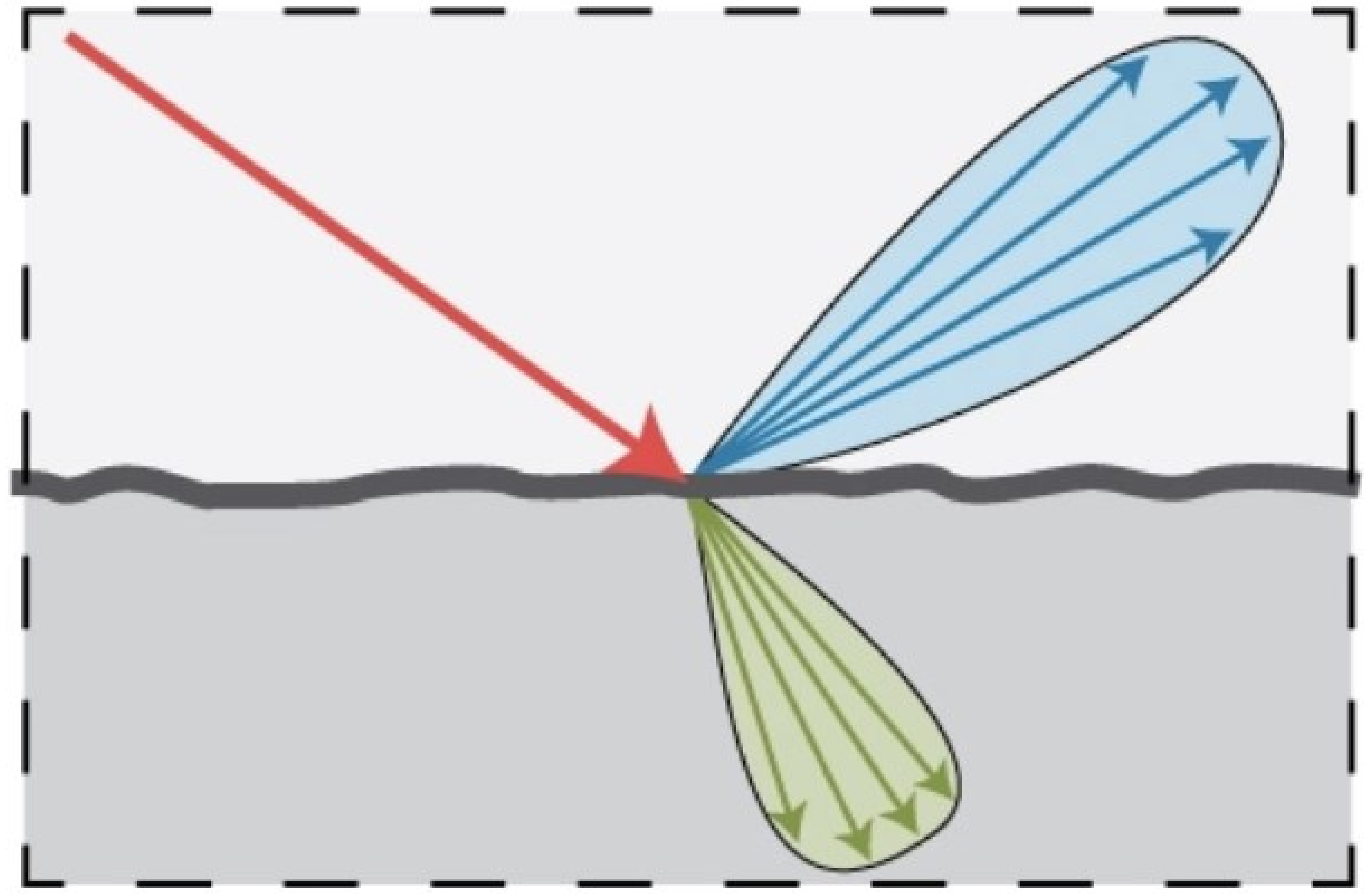
Refraction at rough interface

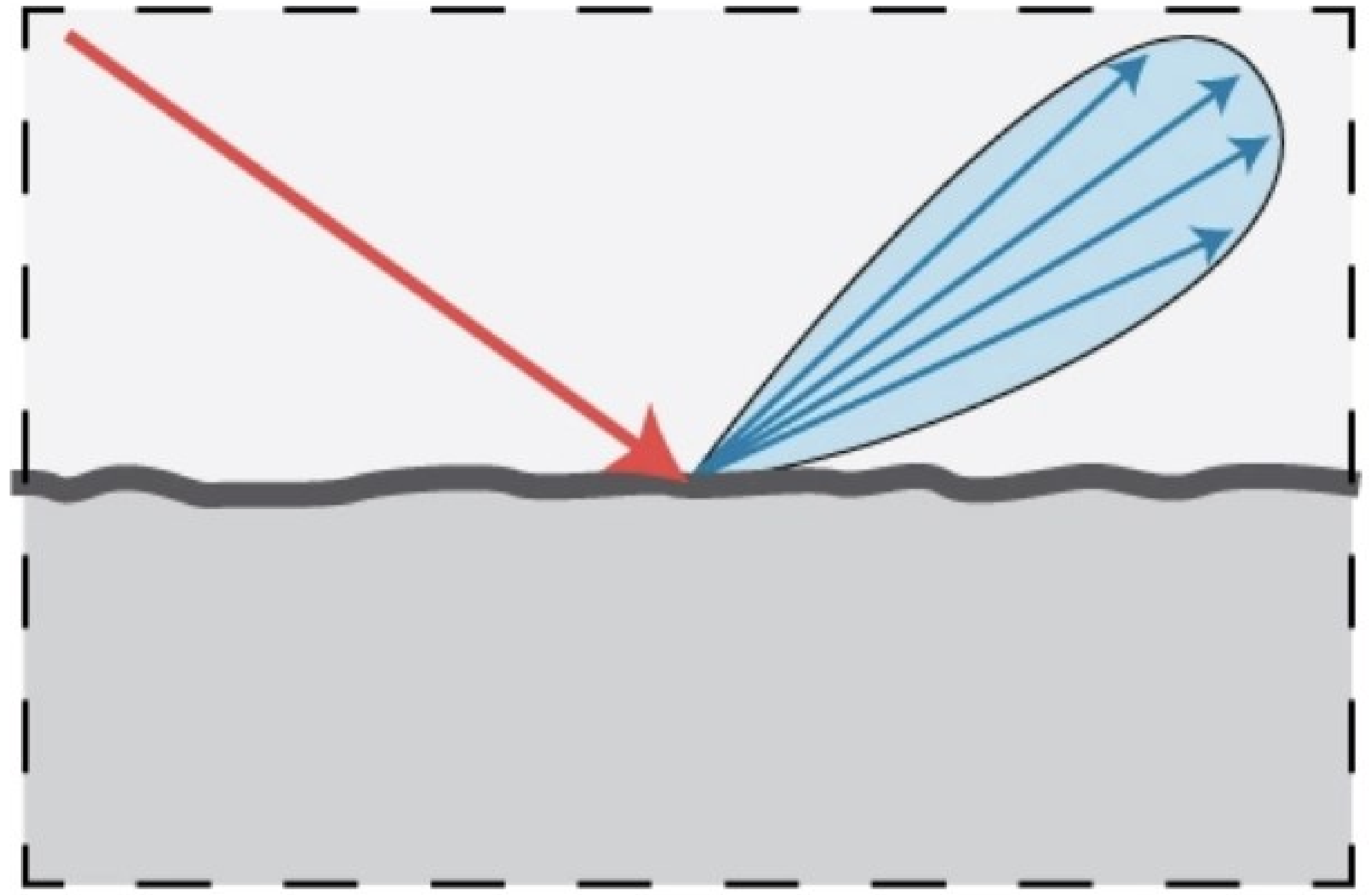
Reflection at glossy surfaces

[Agarwal et al., 2023]

Curved tactile sensor: *working principle*

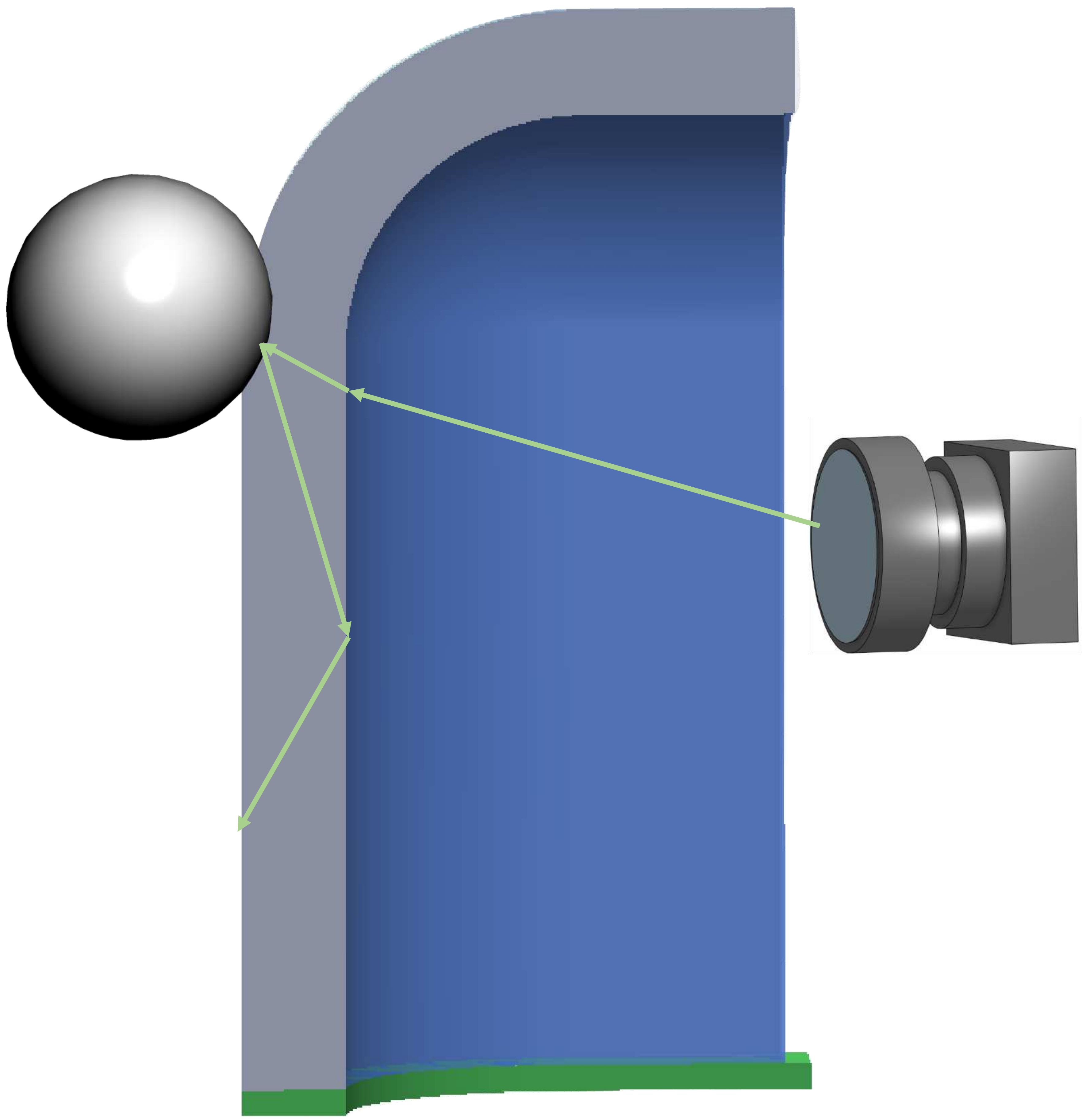

Section View

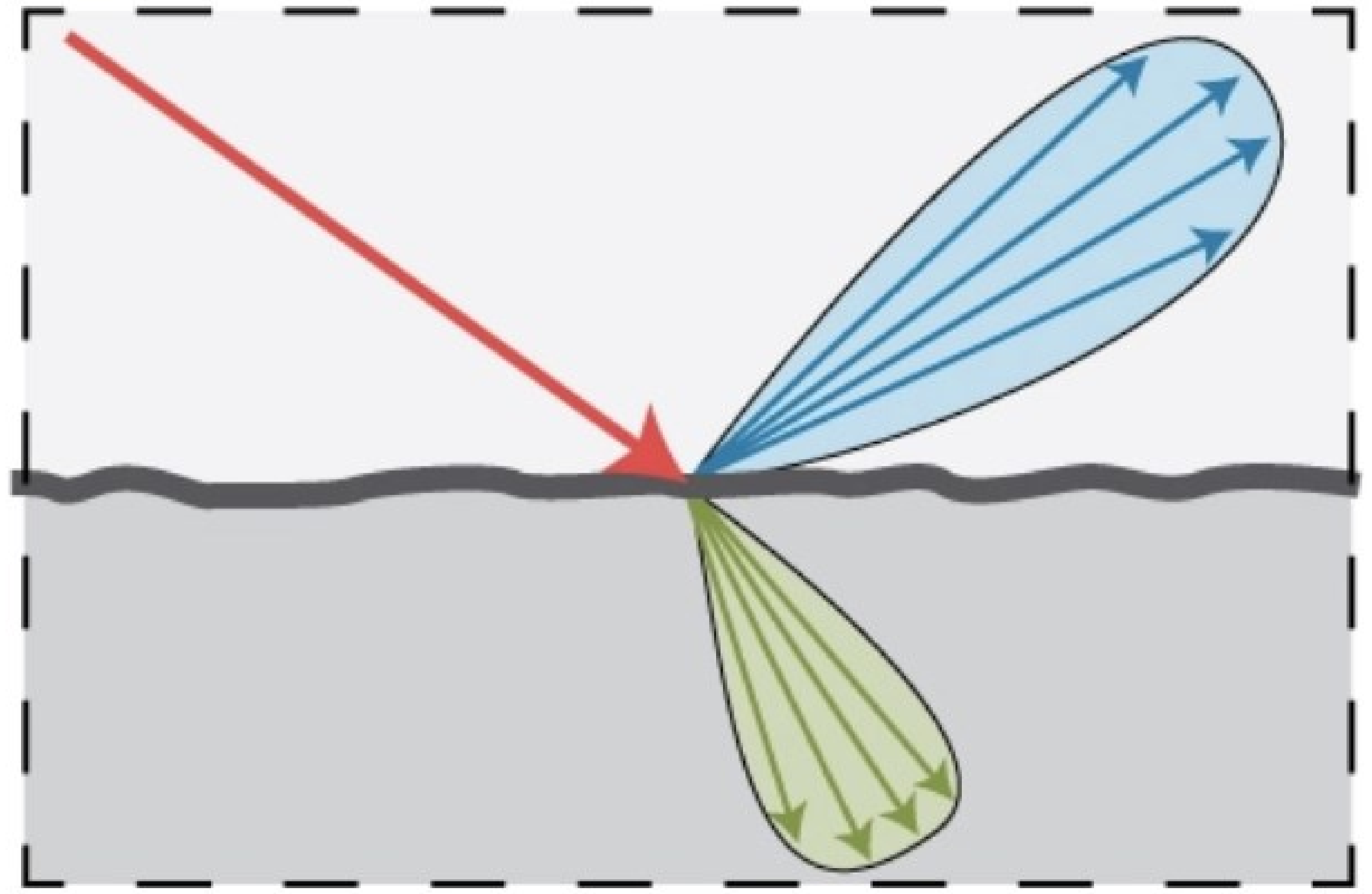

Refraction at rough interface

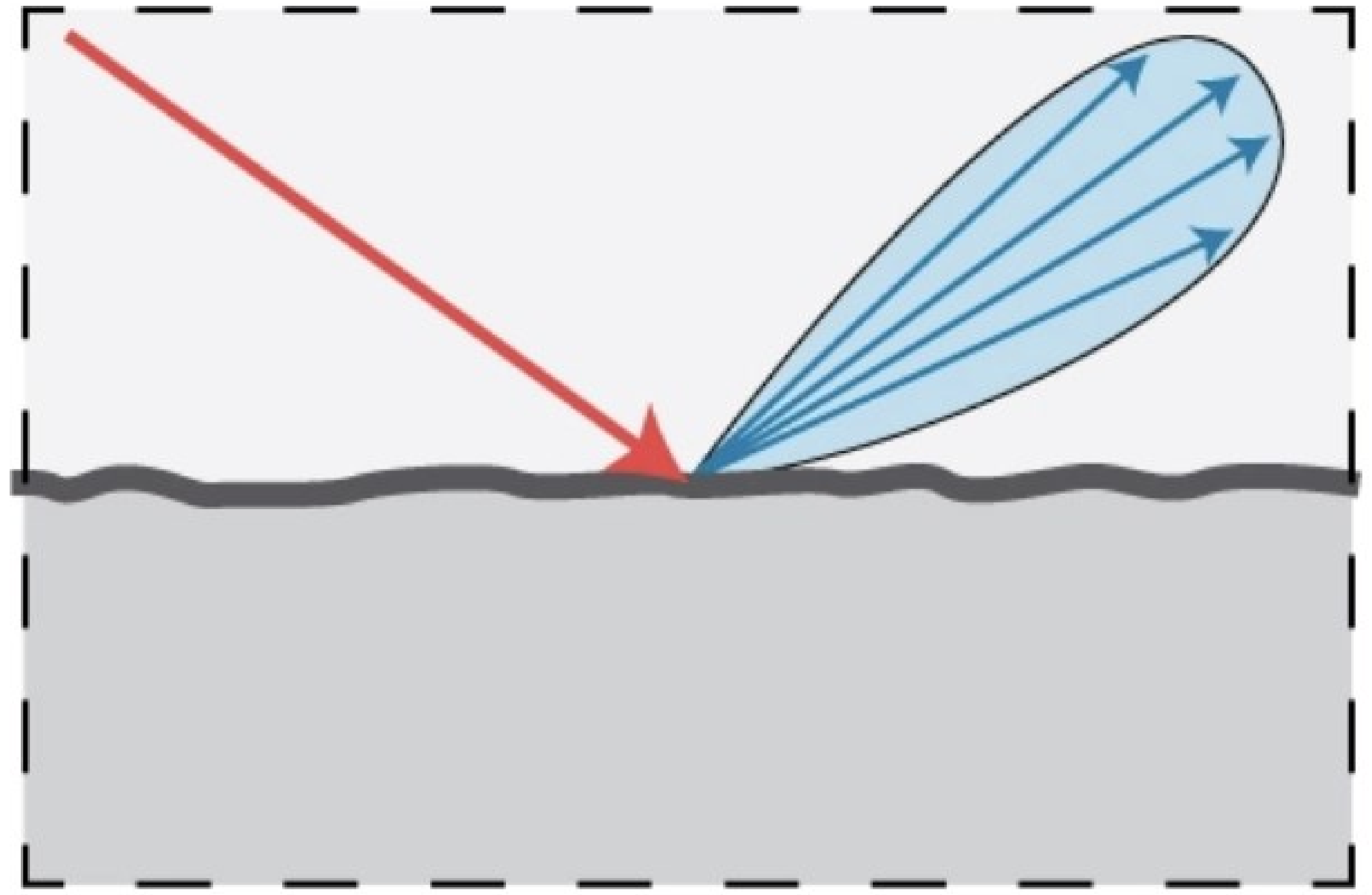

Reflection at glossy surfaces

[Agarwal et al., 2023]

Curved tactile sensor: *working principle*

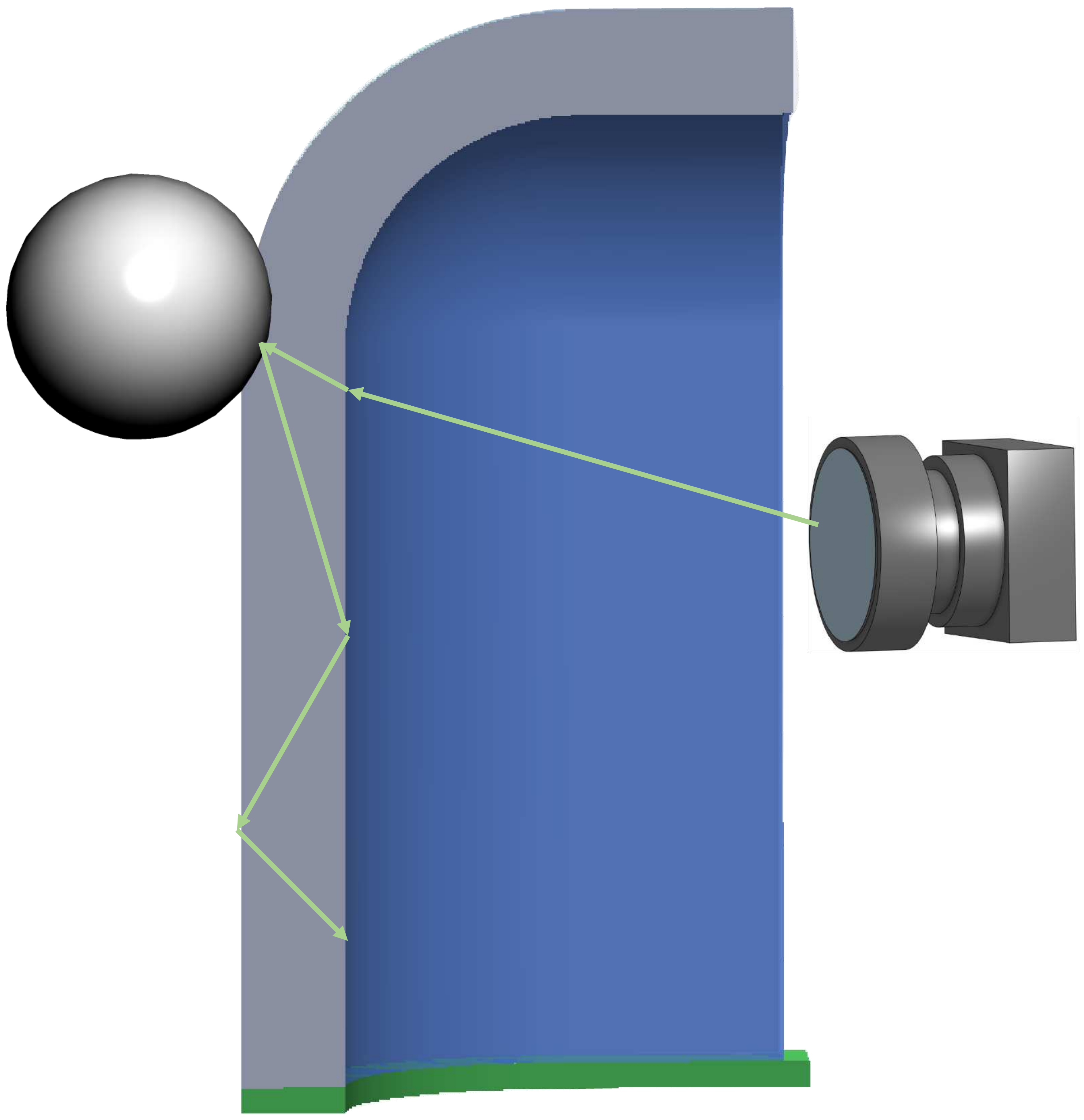

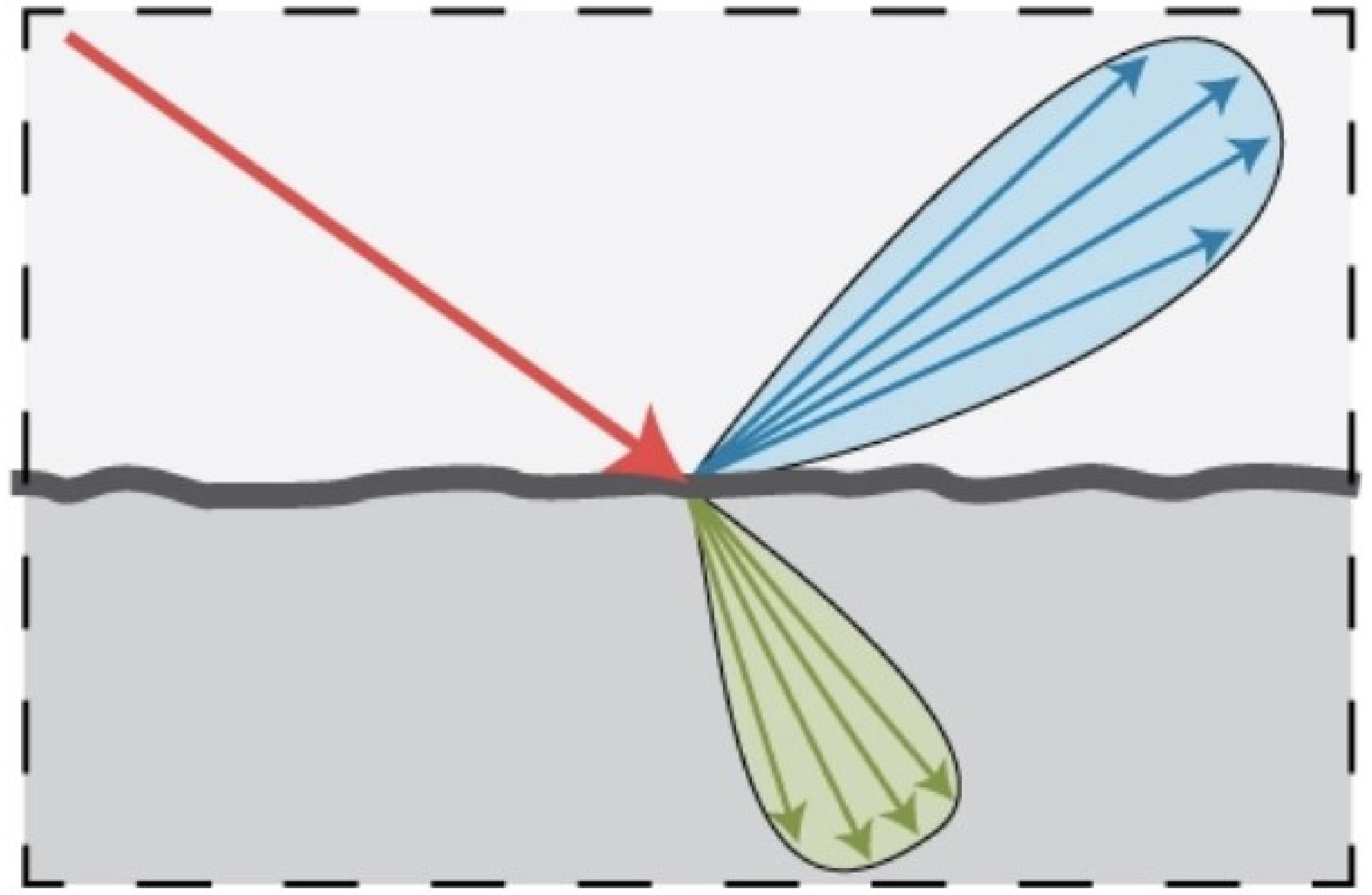
Refraction at rough interface

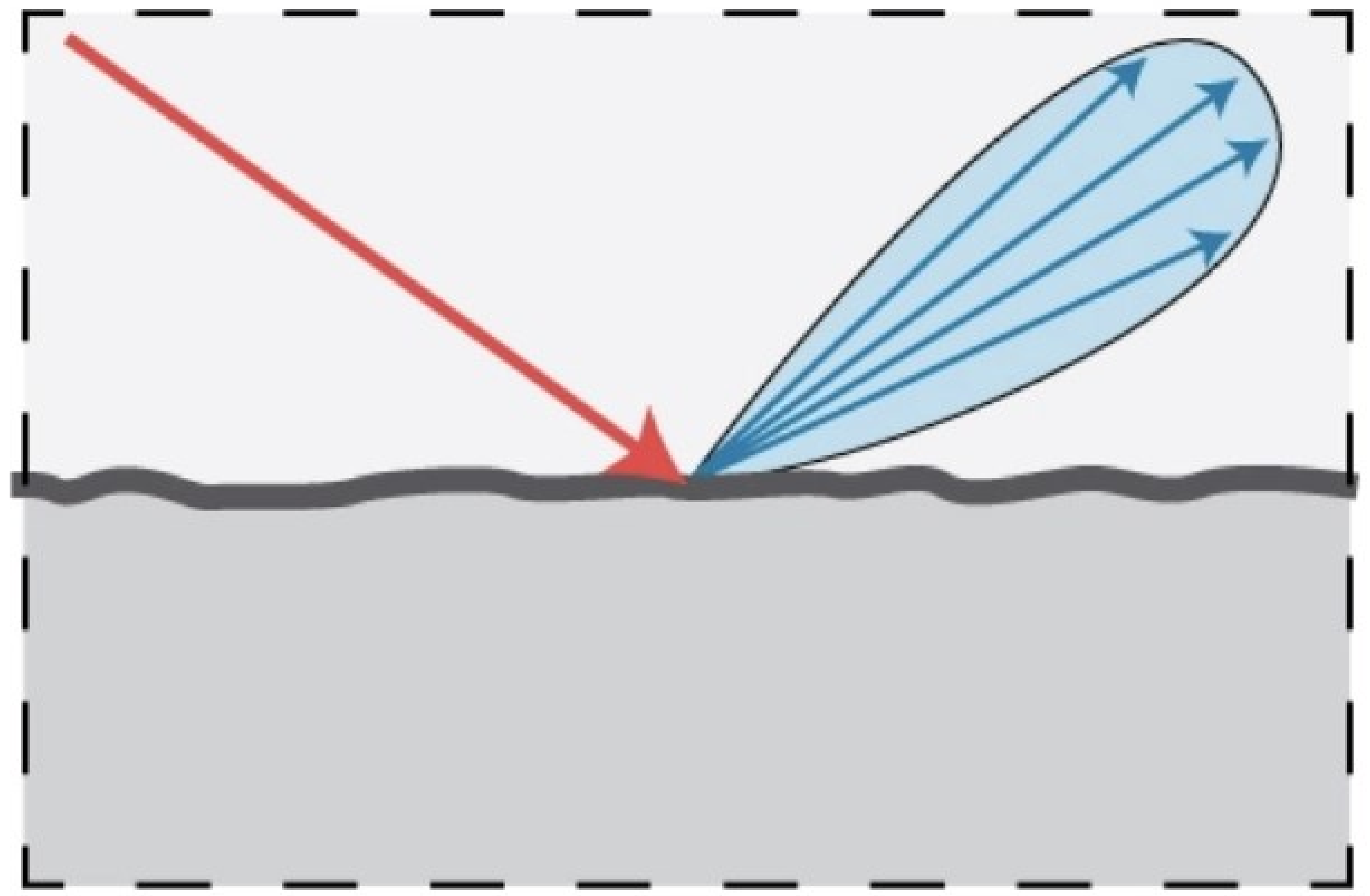
Reflection at glossy surfaces

[Agarwal et al., 2023]

Curved tactile sensor: *working principle*

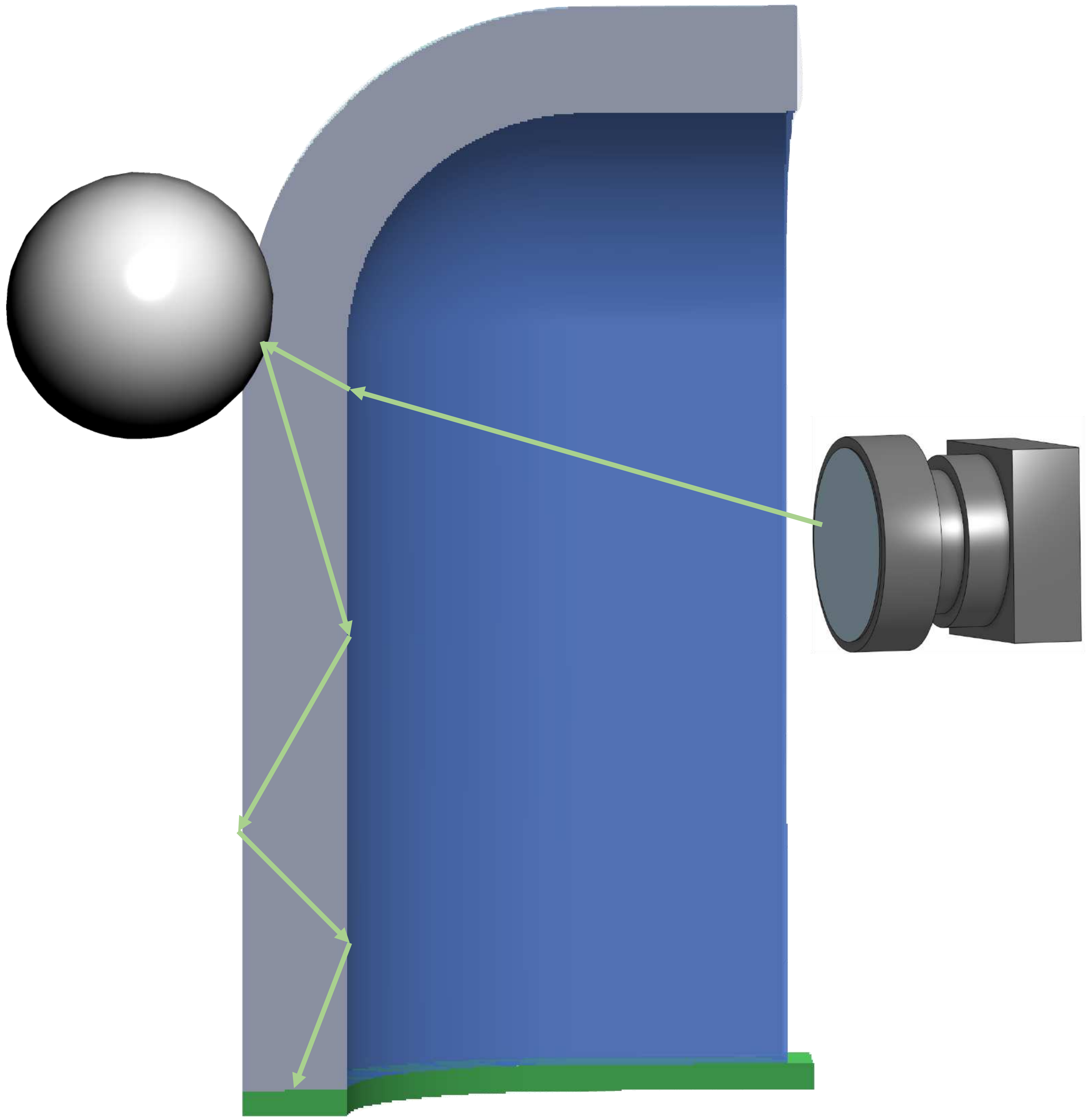

Section View

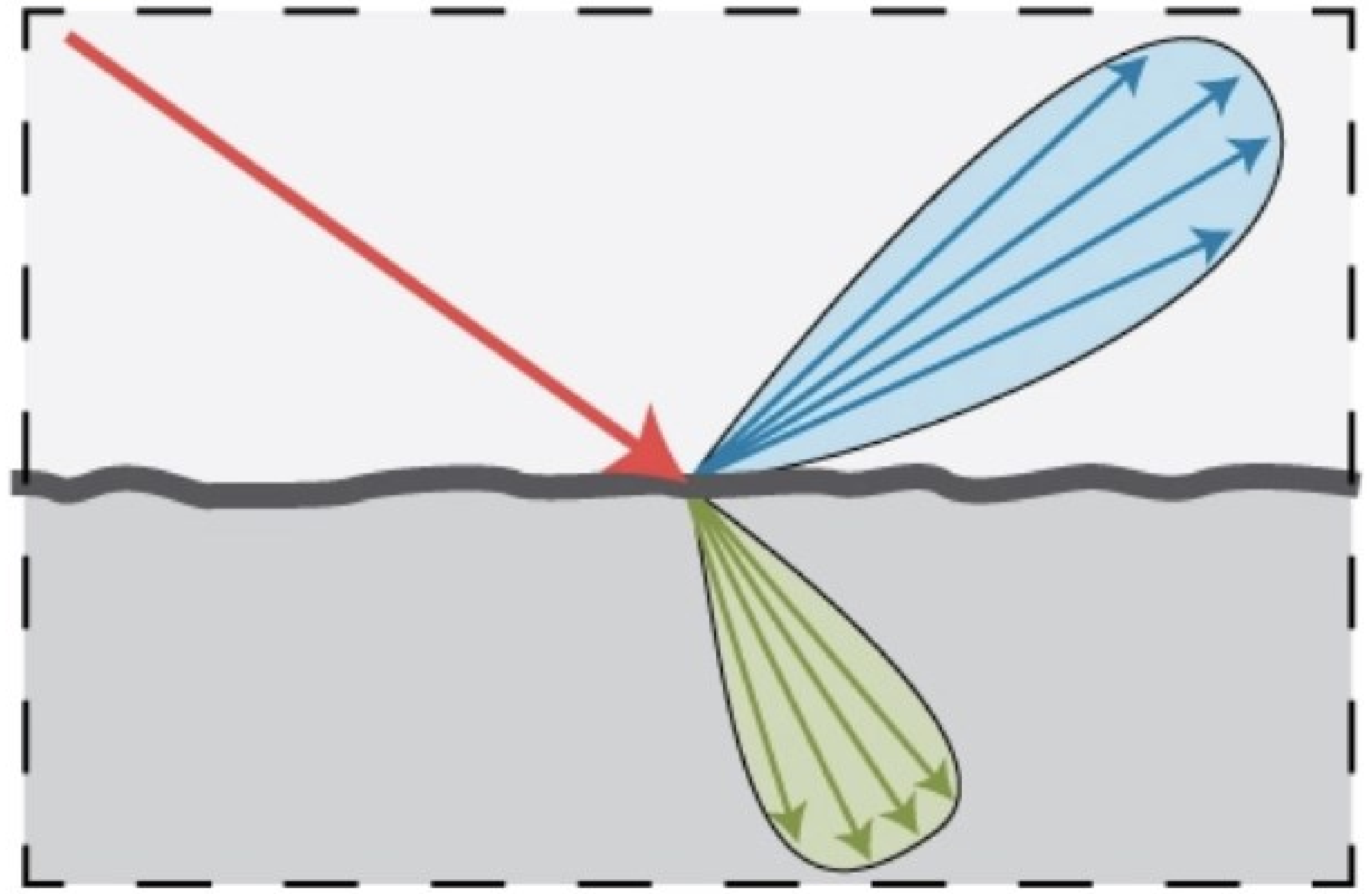

Refraction at rough interface

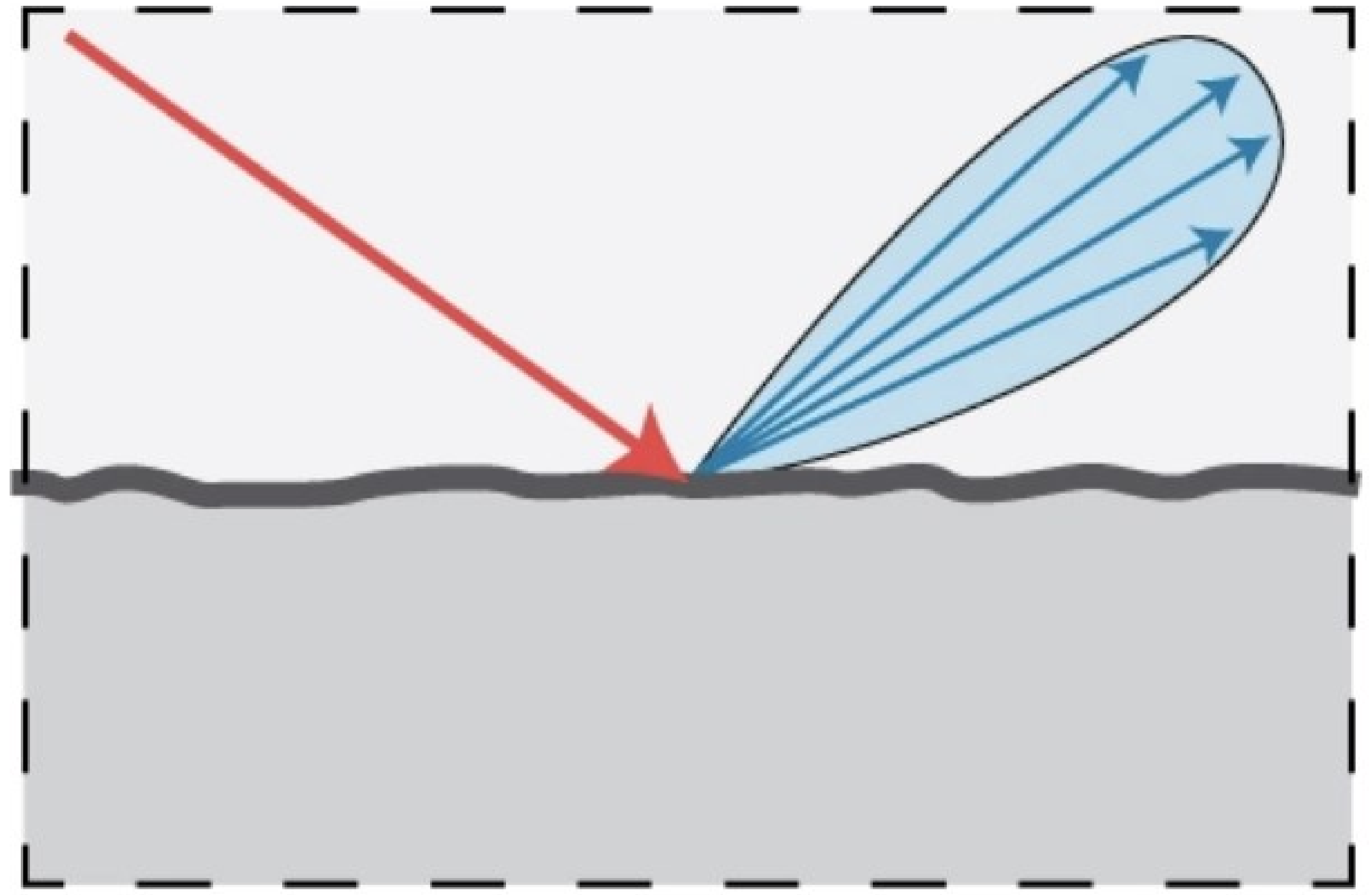

Reflection at glossy surfaces

[Agarwal et al., 2023]

Sensor design framework: *optical simulation*

- Sensor geometry
- Material specifications
- Placement of camera and lights

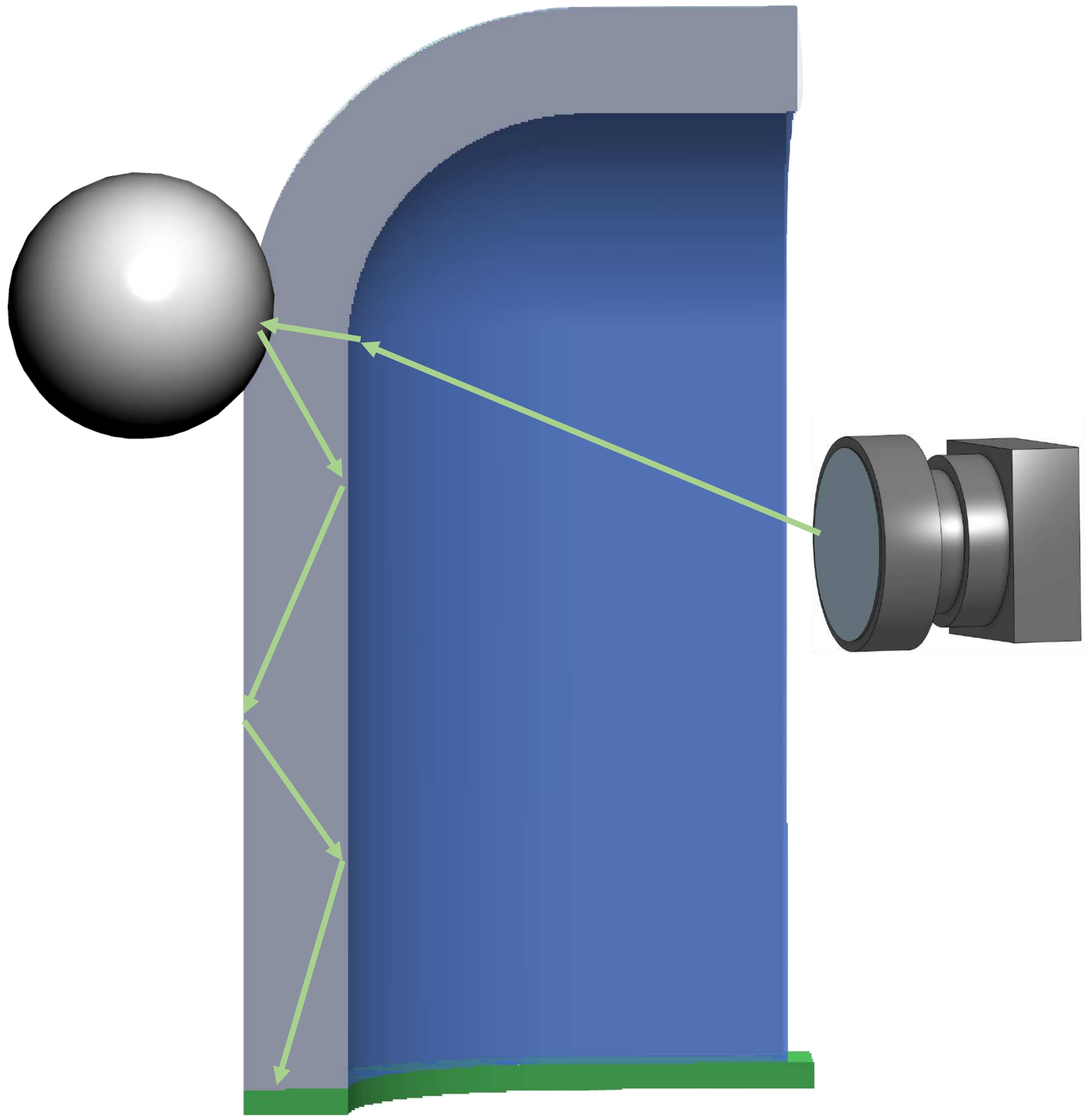

Section view

Tactile image [Agarwal et al., 2023]

Sensor design framework: *optical simulation*

- Sensor geometry
- Material specifications
- Placement of camera and lights

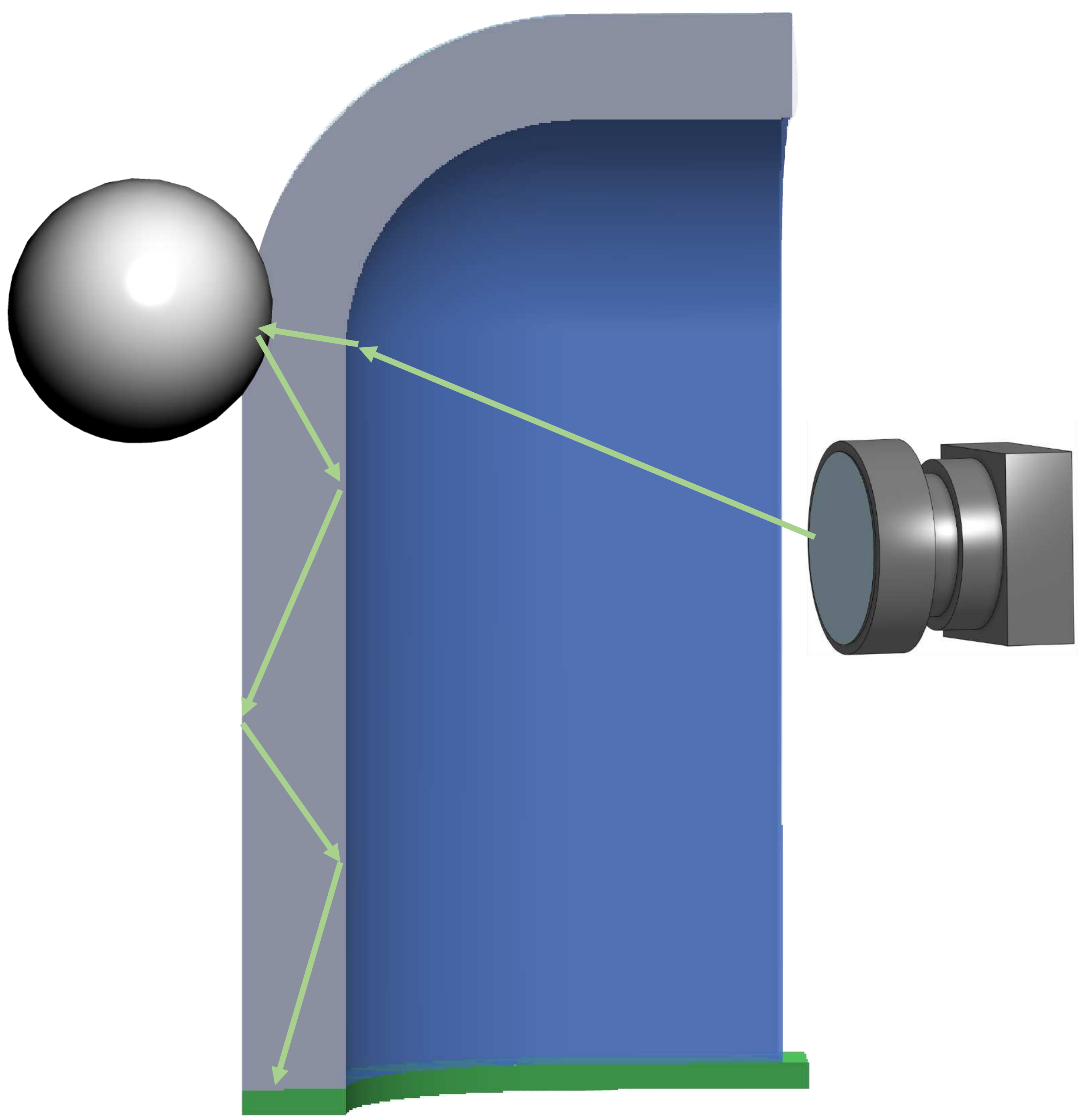

Section view

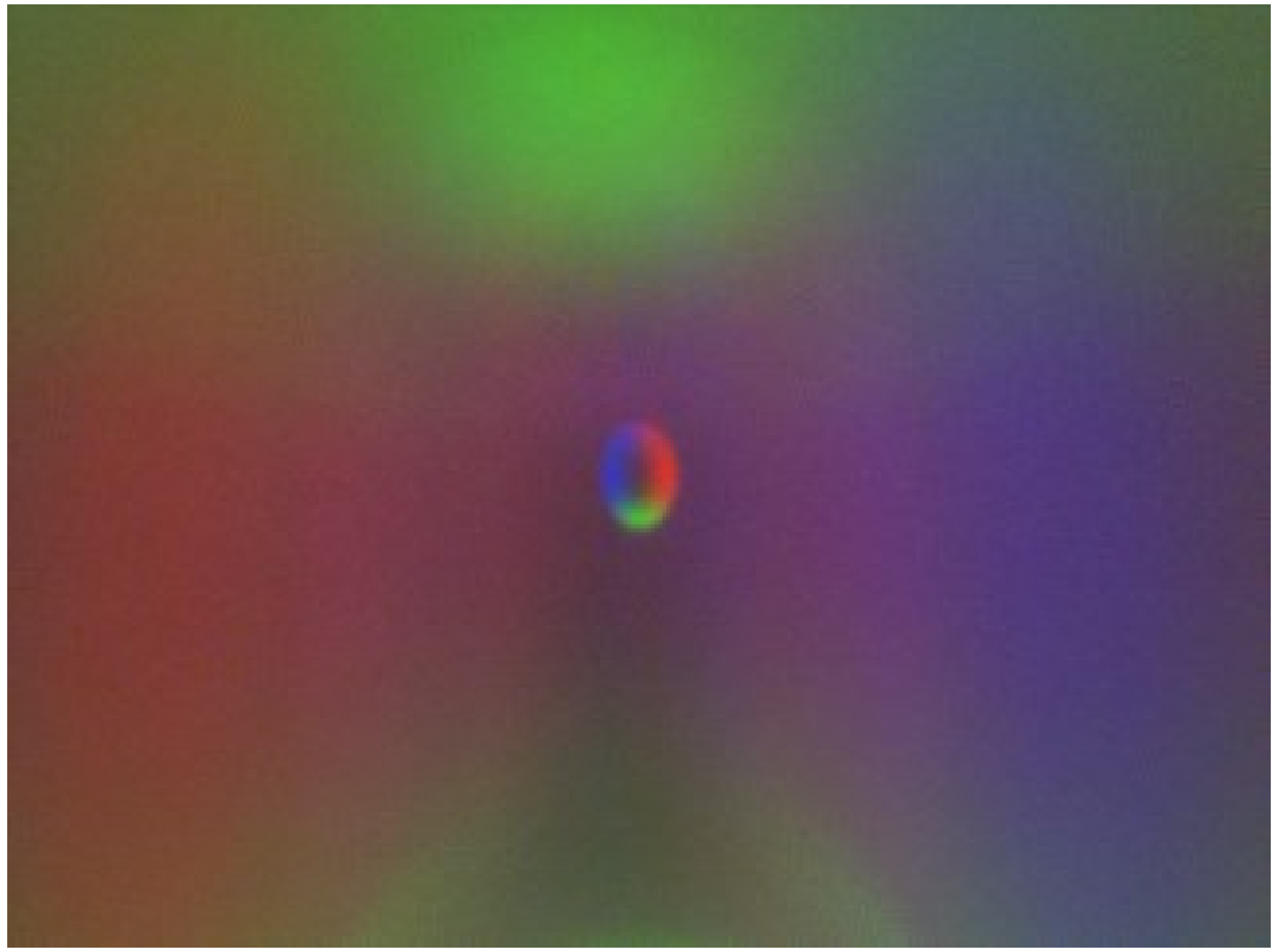

Tactile image [Agarwal et al., 2023]

Sensor design framework: <u>*optical simulation*</u>

- What makes simulation challenging

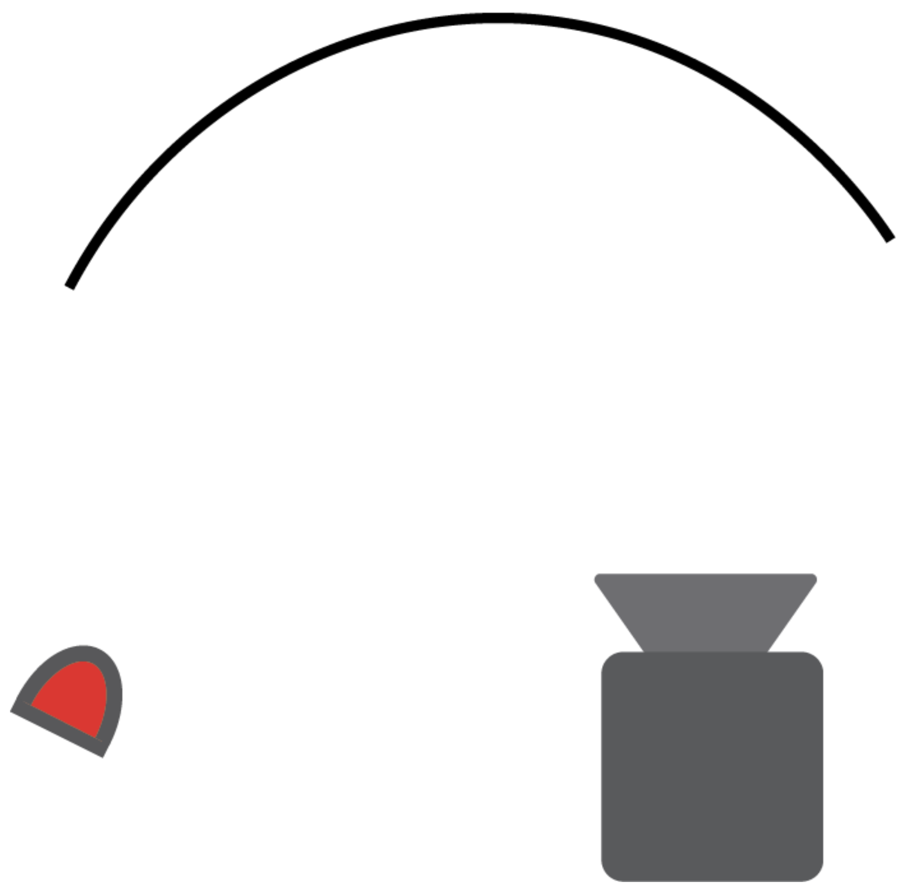

(Relatively) easy cases

Hard case

[Agarwal et al., 2023]

Sensor design framework: *optical simulation*

- What makes simulation challenging

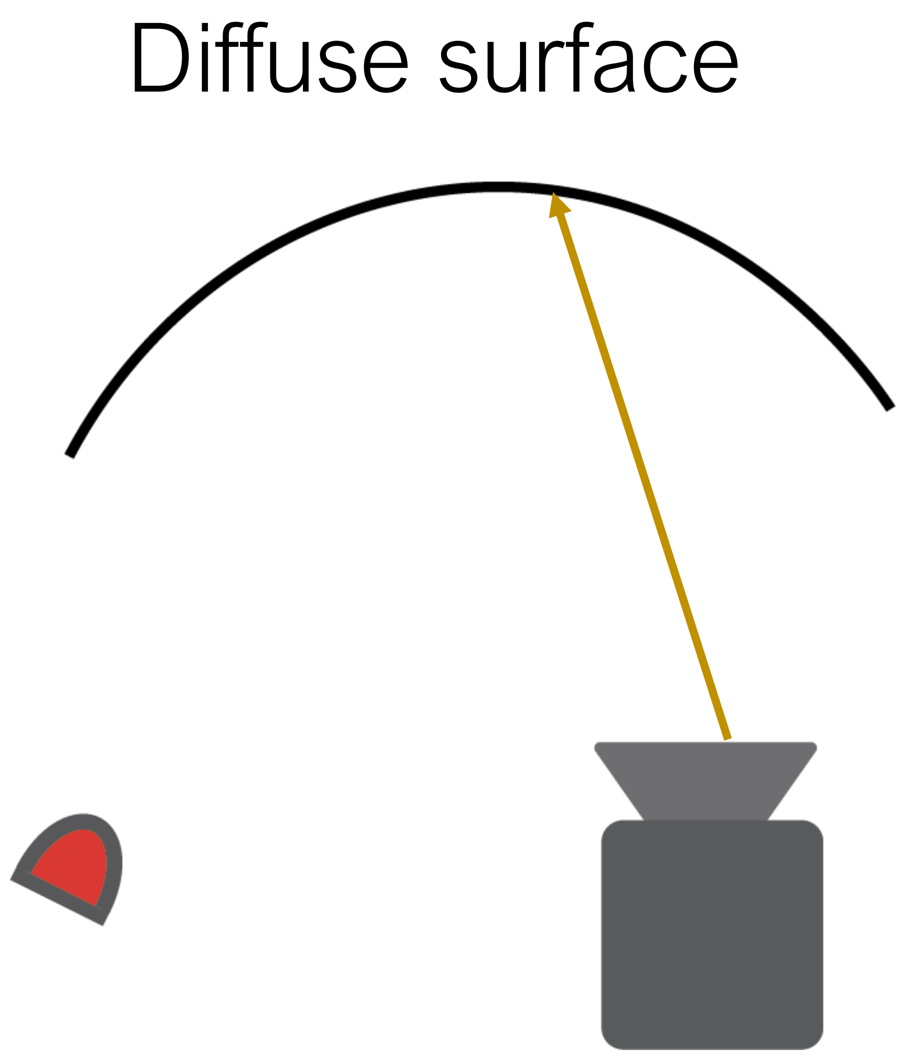

(Relatively) easy cases

Hard case

[Agarwal et al., 2023]

Sensor design framework: *optical simulation*

- What makes simulation challenging

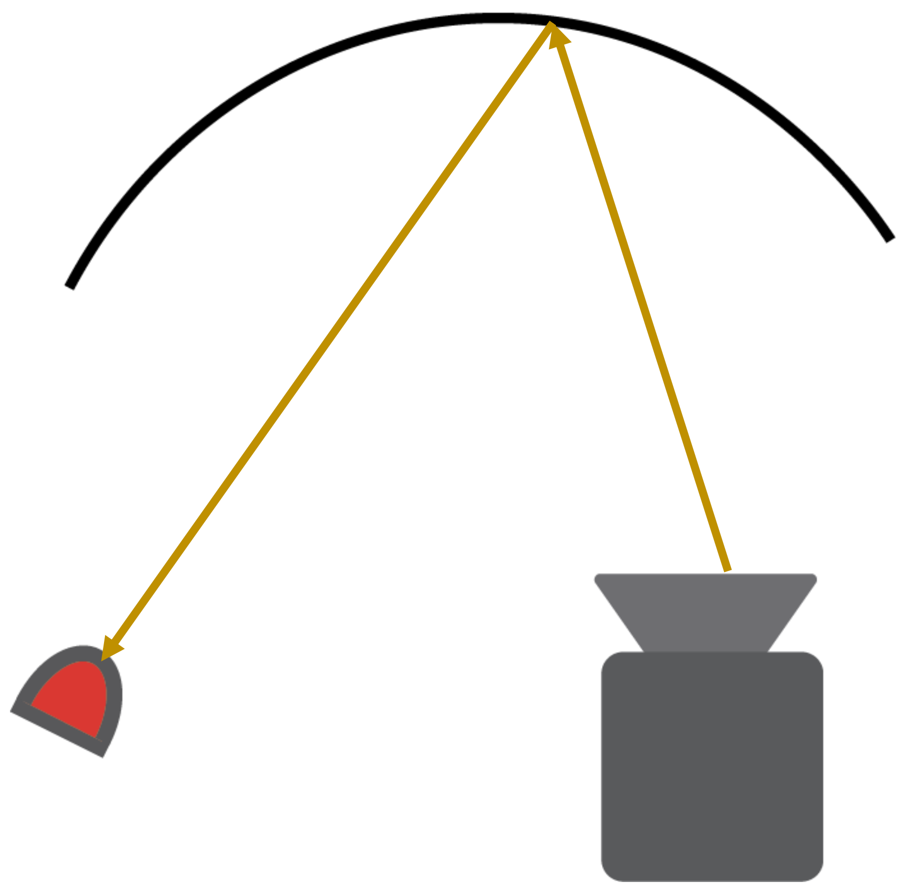

(Relatively) easy cases

Hard case

[Agarwal et al., 2023]

Sensor design framework: *optical simulation*

- What makes simulation challenging

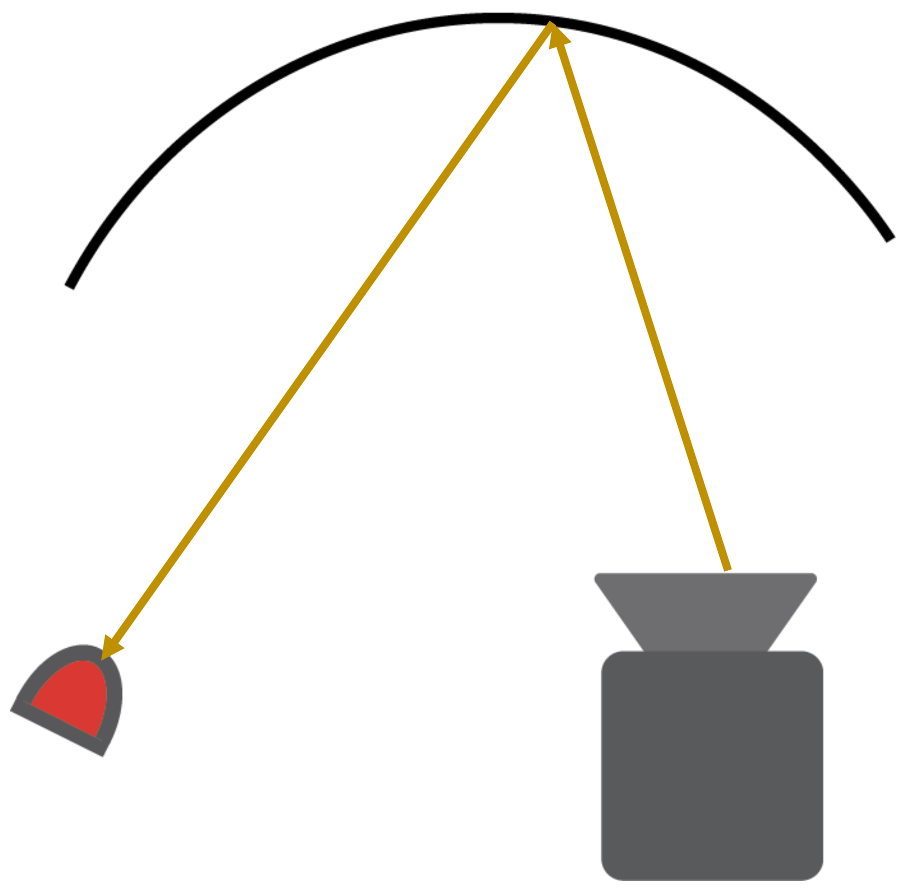

(Relatively) easy cases

Hard case

[Agarwal et al., 2023]

Sensor design framework: *optical simulation*

- What makes simulation challenging

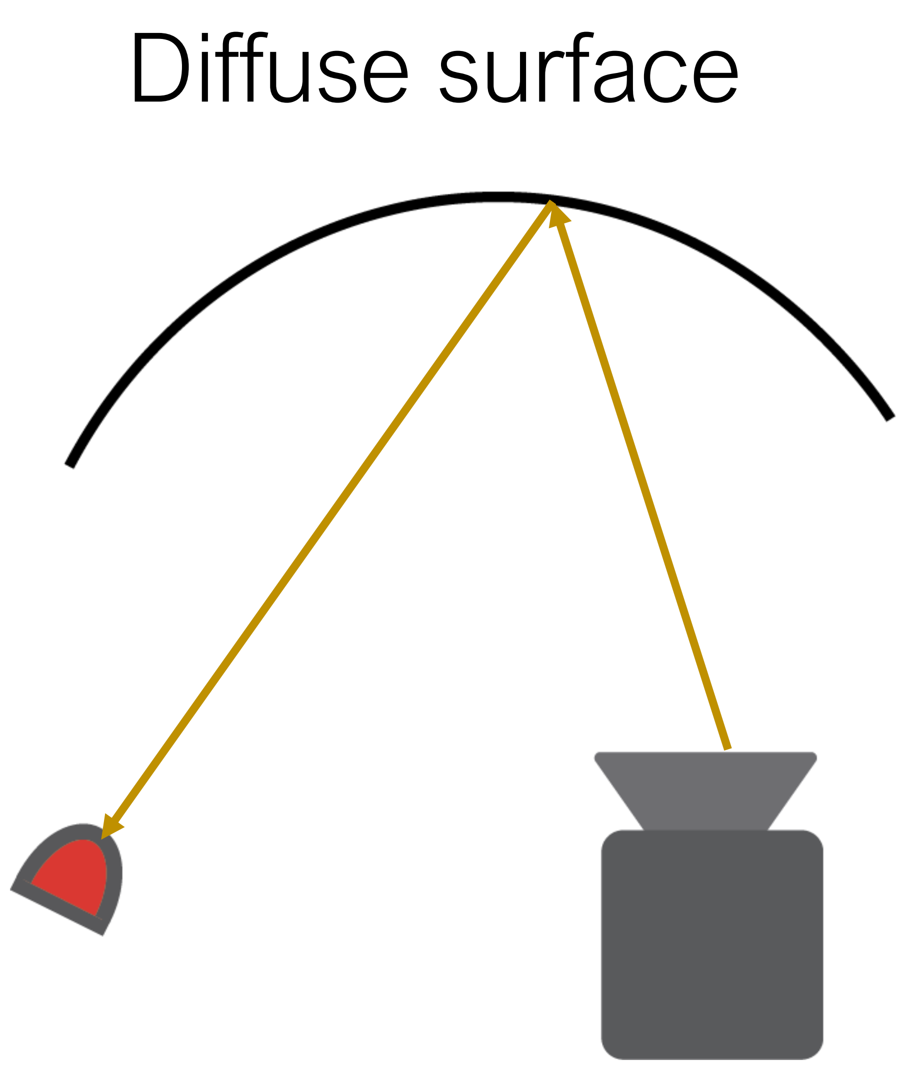

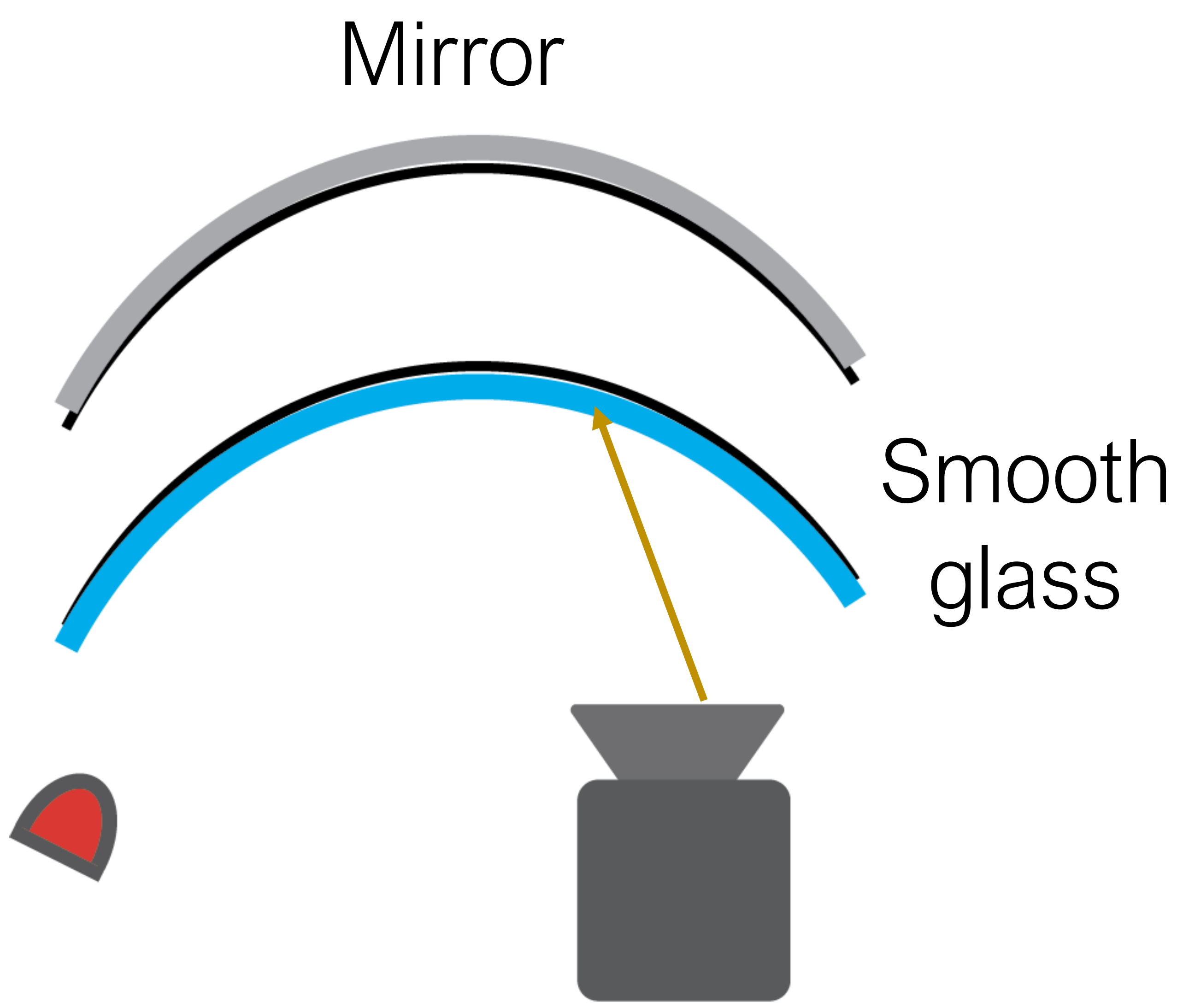

(Relatively) easy cases

Hard case

[Agarwal et al., 2023]

Sensor design framework: <u>*optical simulation*</u>

- What makes simulation challenging

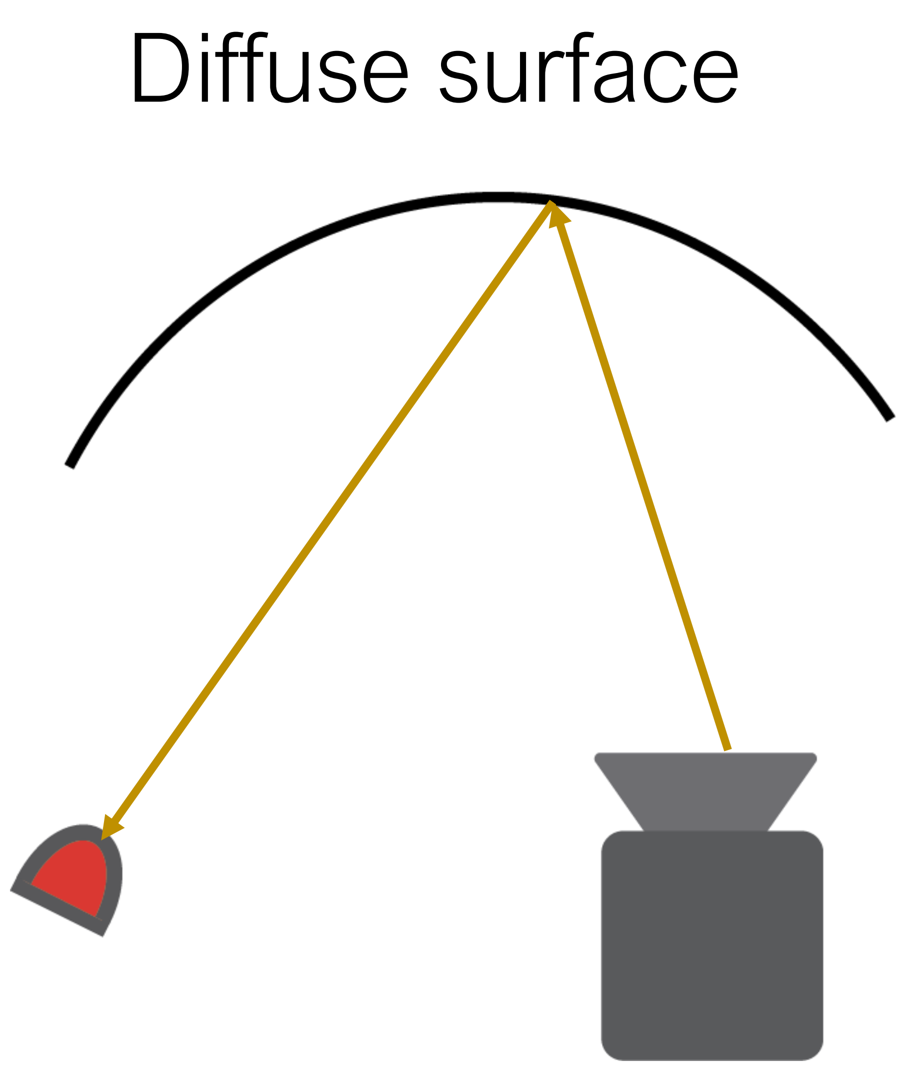

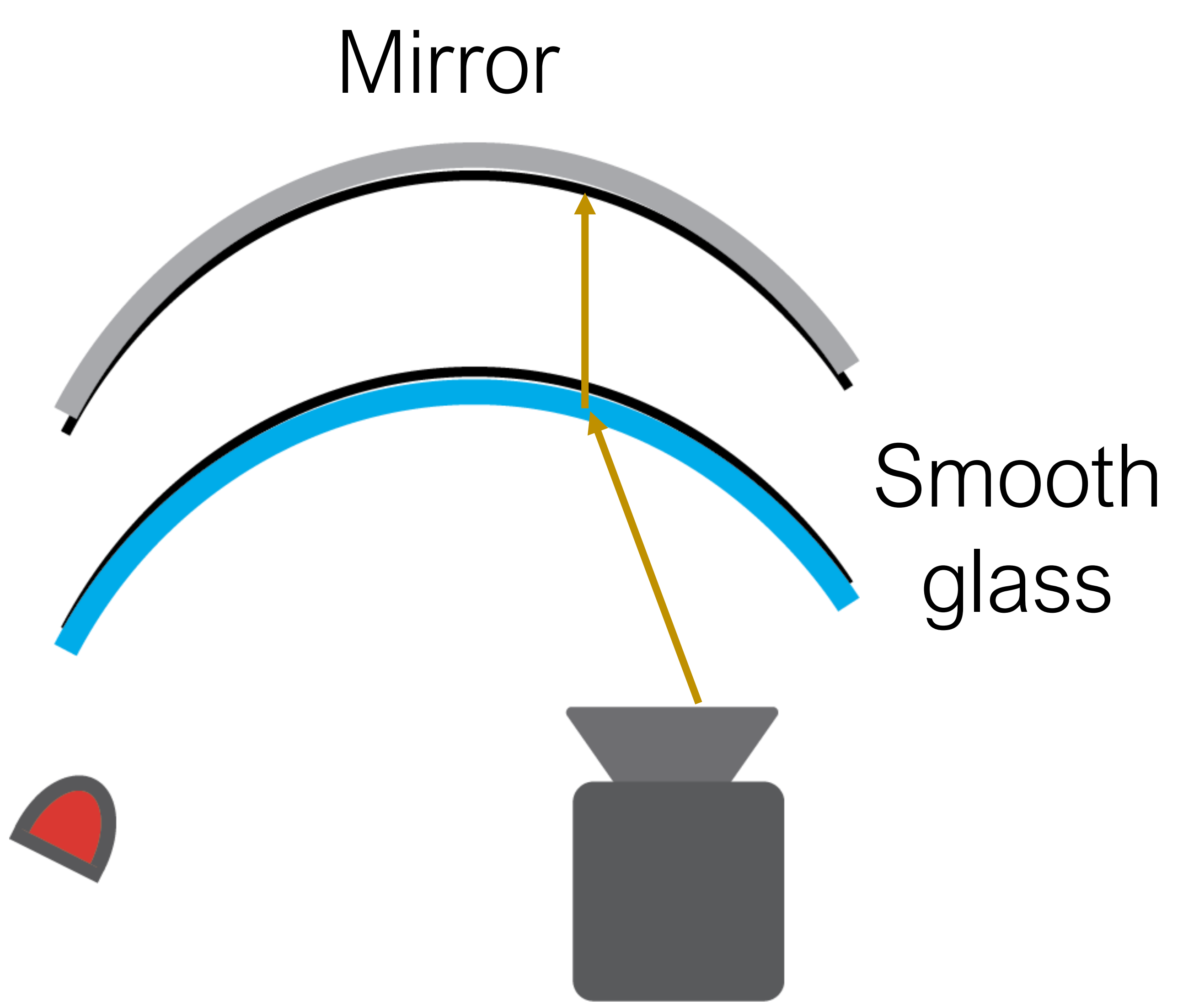

(Relatively) easy cases

Hard case

[Agarwal et al., 2023]

Sensor design framework: *optical simulation*

- What makes simulation challenging

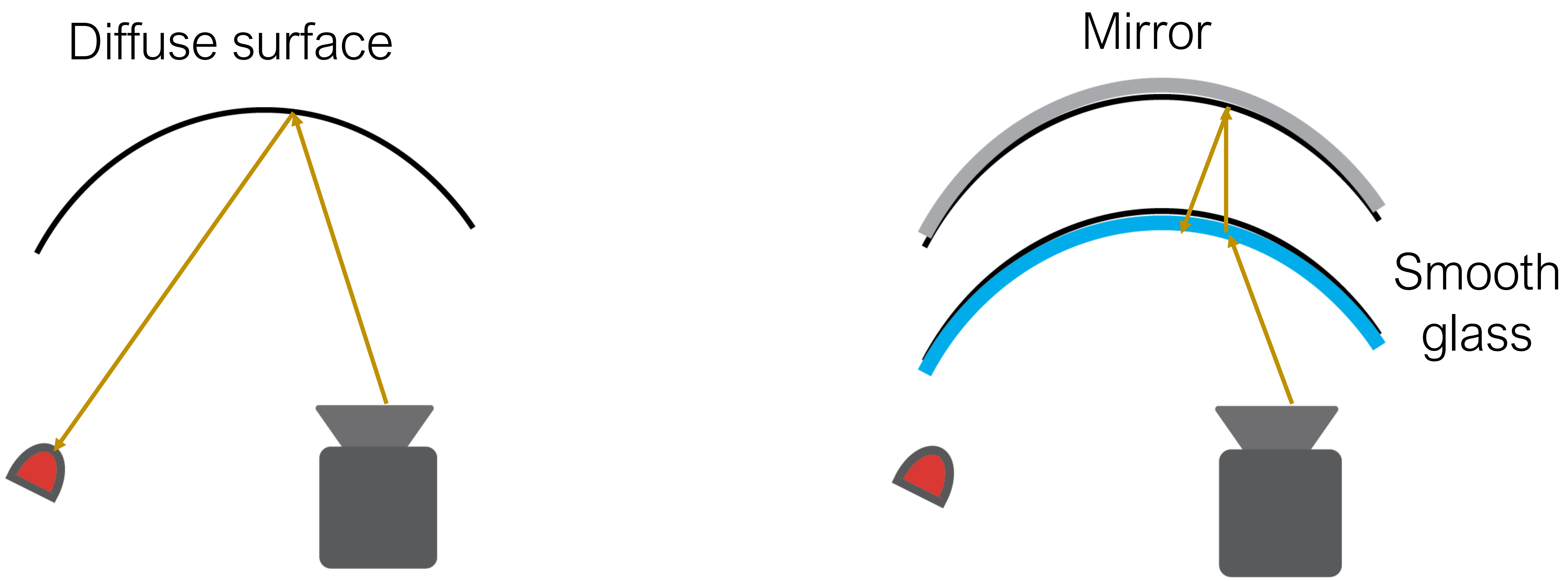

(Relatively) easy cases

Hard case

[Agarwal et al., 2023]

Sensor design framework: ***optical simulation***

- What makes simulation challenging

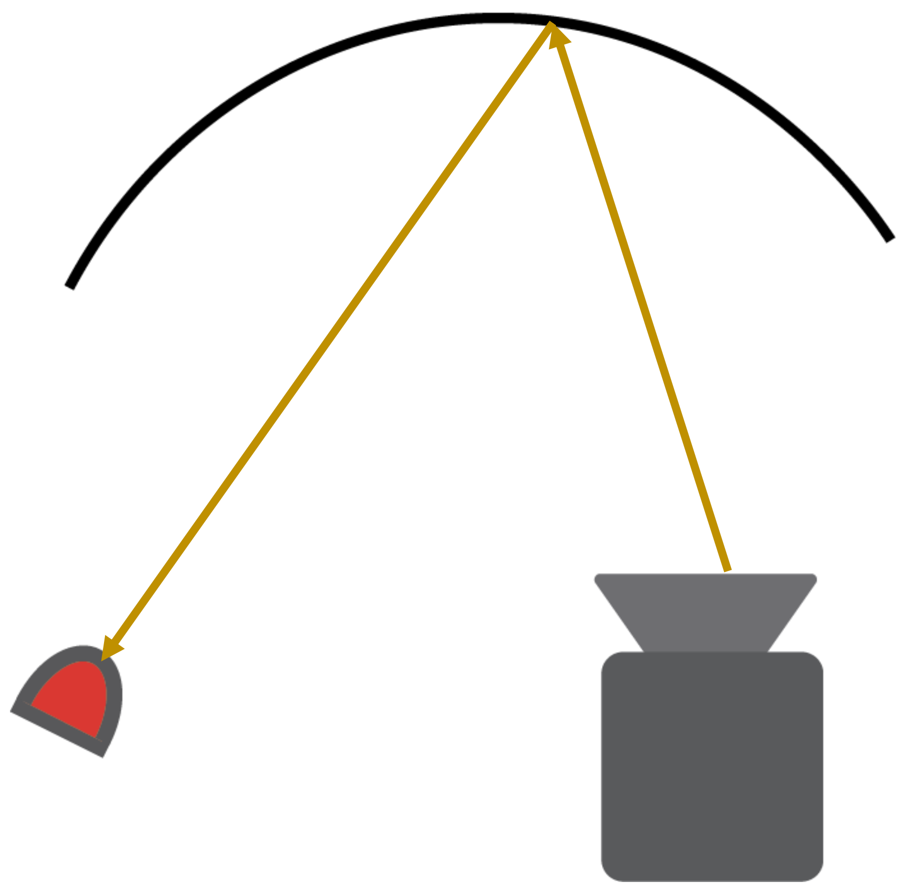

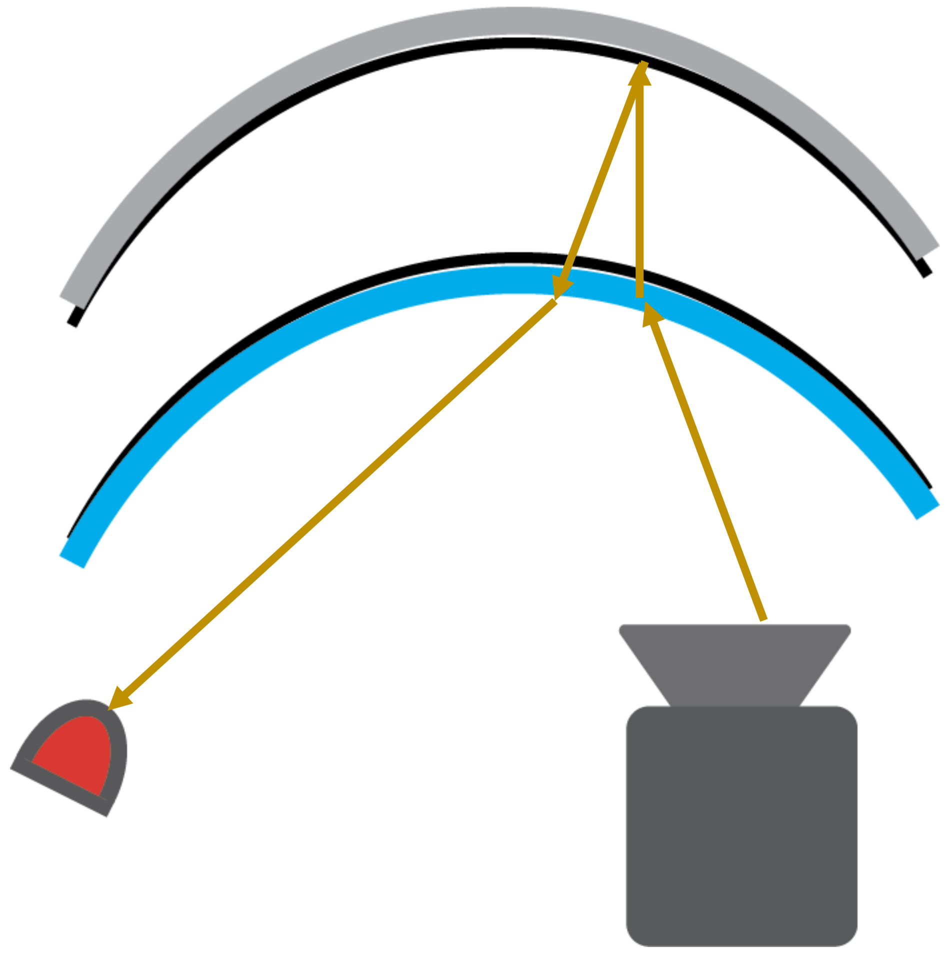

(Relatively) easy cases

Hard case

[Agarwal et al., 2023]

Sensor design framework: *optical simulation*

- What makes simulation challenging

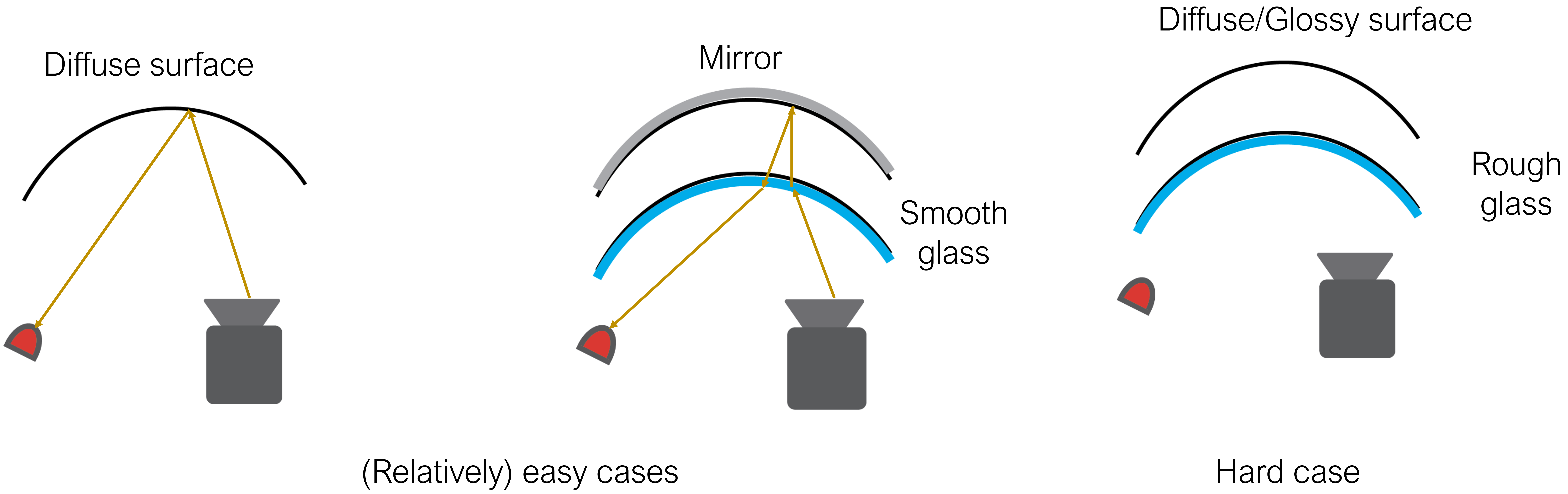

[Agarwal et al., 2023]

Sensor design framework: *optical simulation*

- What makes simulation challenging

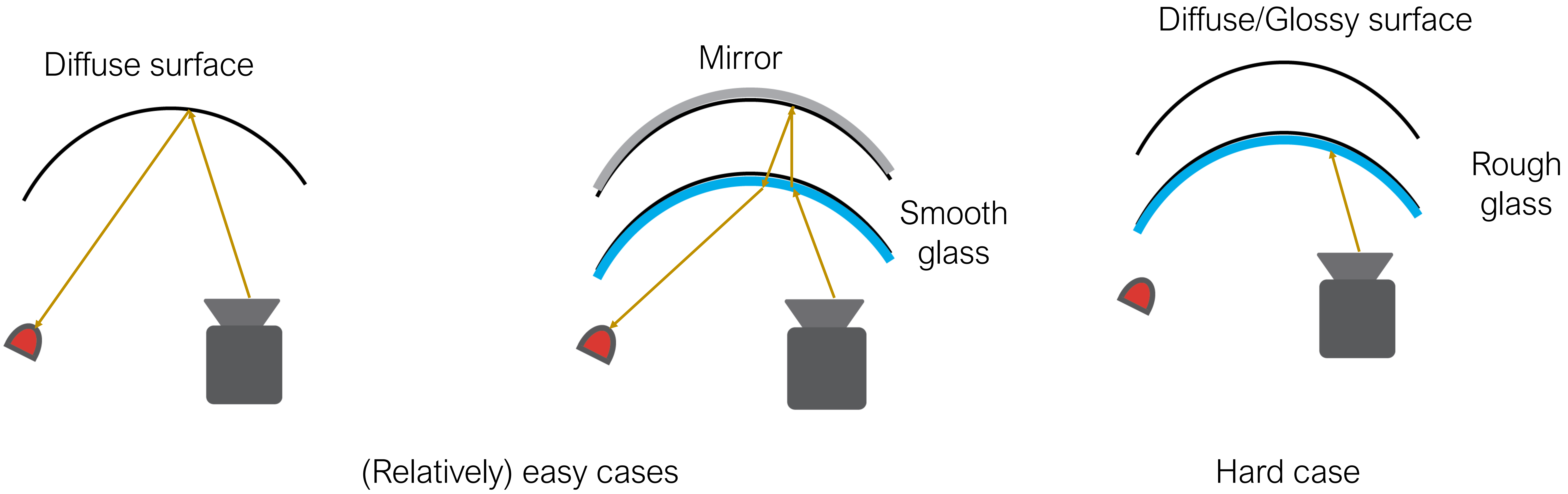

[Agarwal et al., 2023]

Sensor design framework: *optical simulation*

- What makes simulation challenging

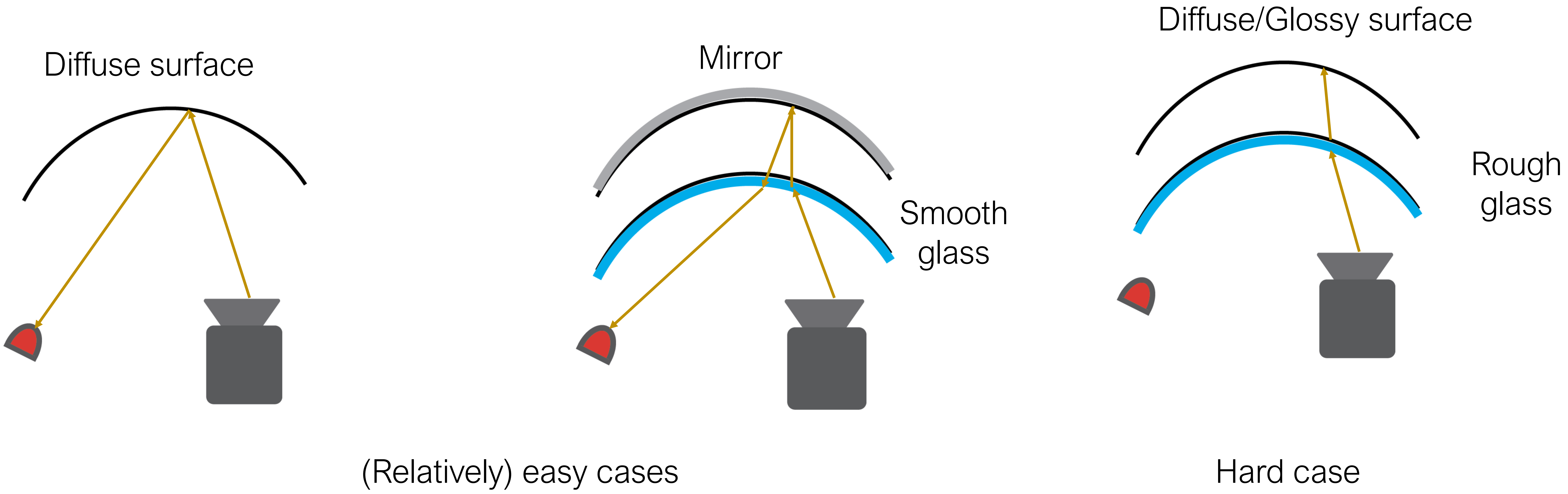

[Agarwal et al., 2023]

Sensor design framework: *optical simulation*

- What makes simulation challenging

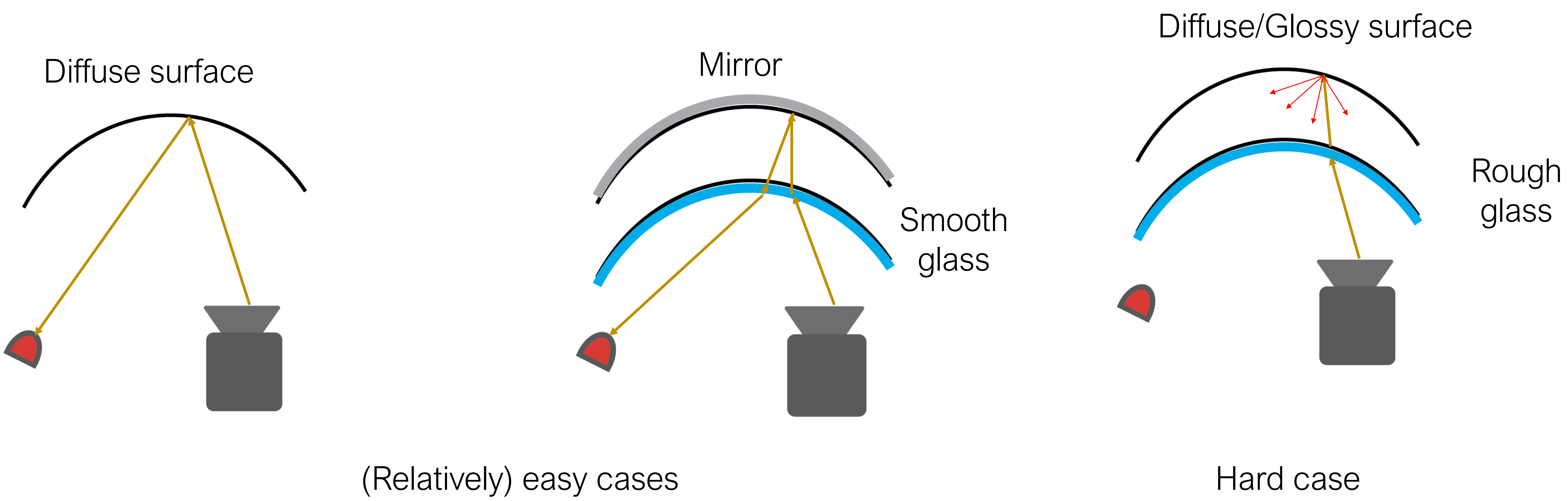

[Agarwal et al., 2023]

Sensor design framework: *optical simulation*

- What makes simulation challenging

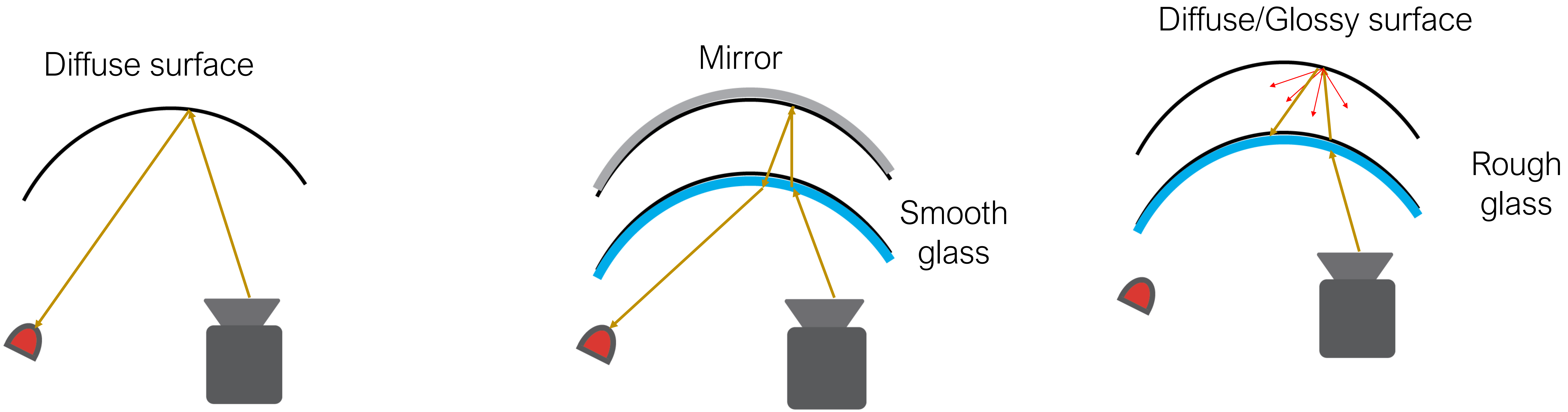

(Relatively) easy cases

Hard case

[Agarwal et al., 2023]

Sensor design framework: *optical simulation*

- What makes simulation challenging

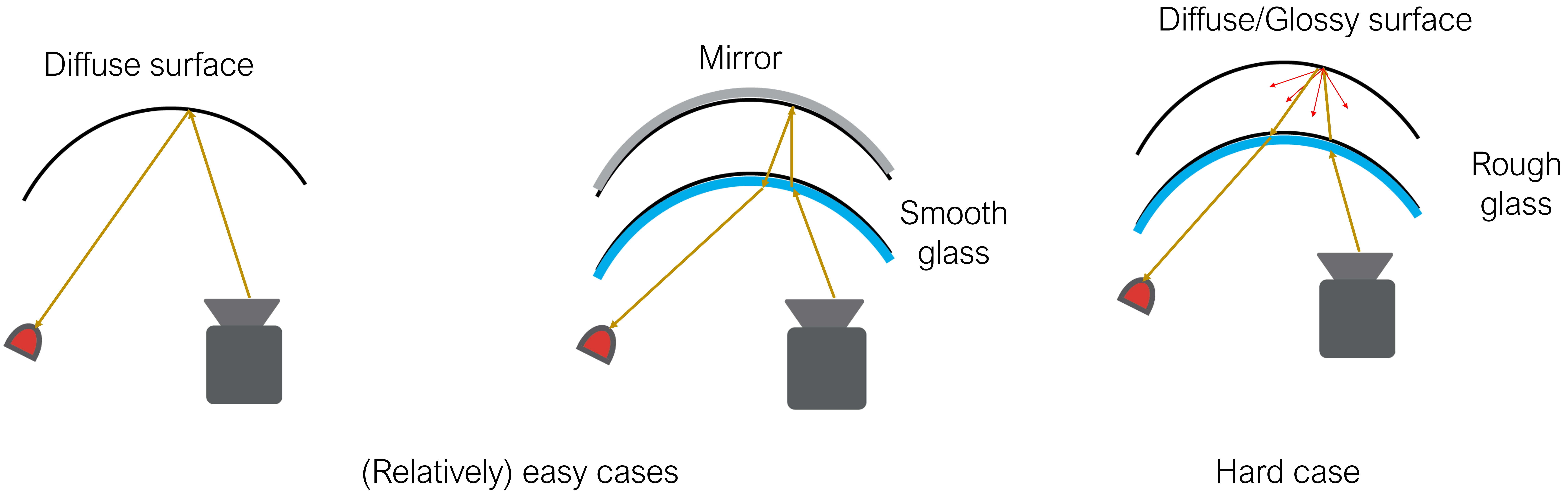

[Agarwal et al., 2023]

Sensor design framework: *optical simulation*

- What makes simulation challenging
  - SDS light paths
  - Indirect illumination

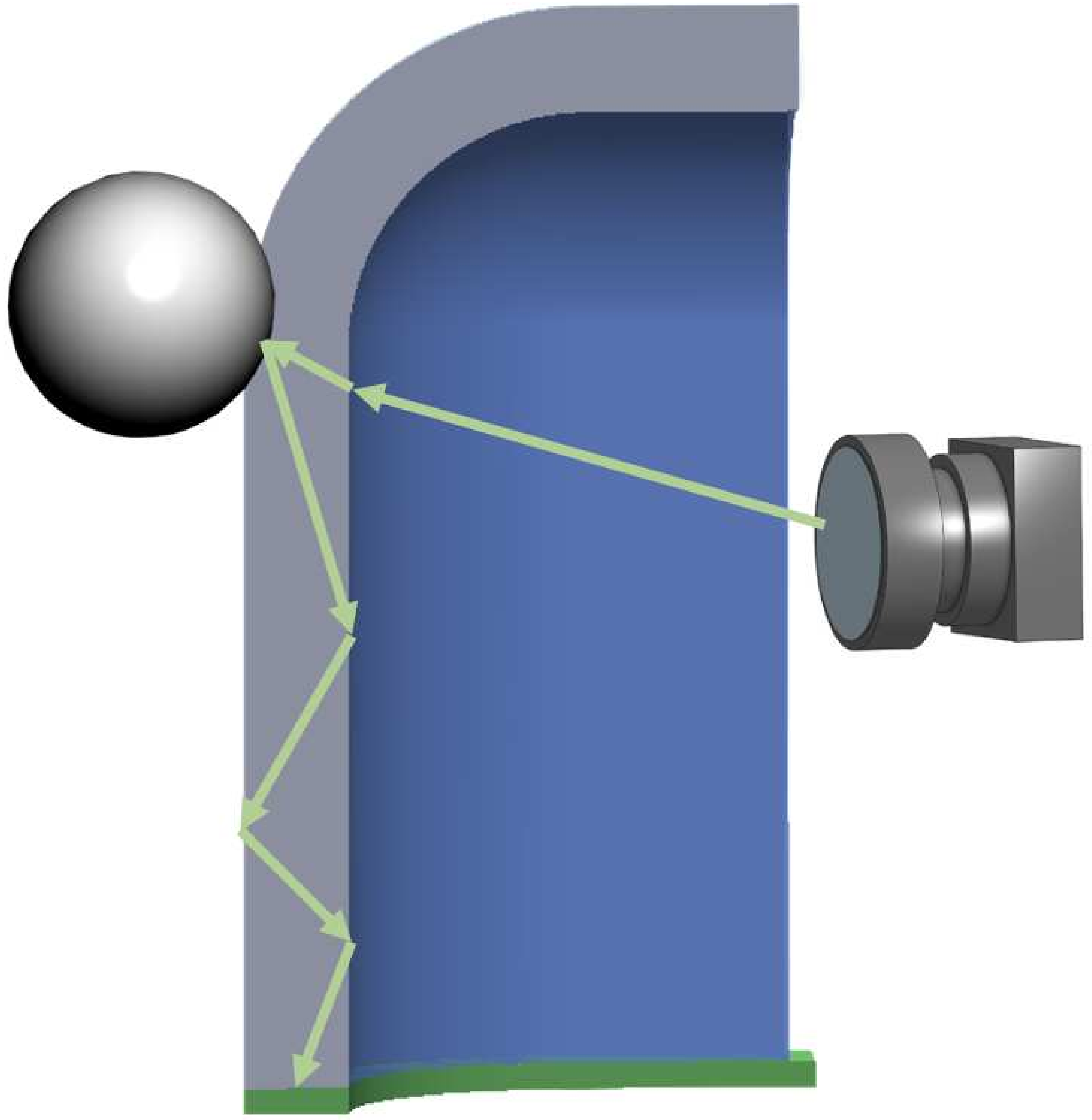
Section View

[Agarwal et al., 2023]

Sensor design framework: *optical simulation*

- What makes simulation challenging
  - SDS light paths
  - Indirect illumination
- Require Markov Chain Monte Carlo rendering techniques
  - Key idea → Slowly mutate paths to generate useful paths

[Agarwal et al., 2023]

Sensor design framework: *optical simulation*

- What makes simulation challenging
  - SDS light paths
  - Indirect illumination
- Require Markov Chain Monte Carlo rendering techniques
  - Key idea → Slowly mutate paths to generate useful paths

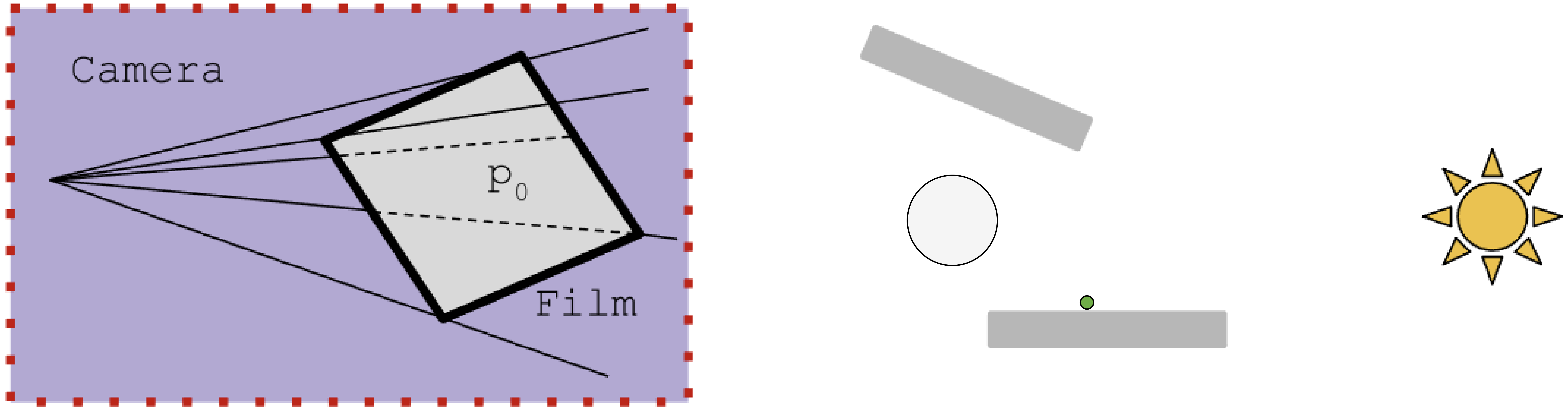

[Agarwal et al., 2023]

Sensor design framework: *optical simulation*

- What makes simulation challenging
  - SDS light paths
  - Indirect illumination
- Require Markov Chain Monte Carlo rendering techniques
  - Key idea → Slowly mutate paths to generate useful paths

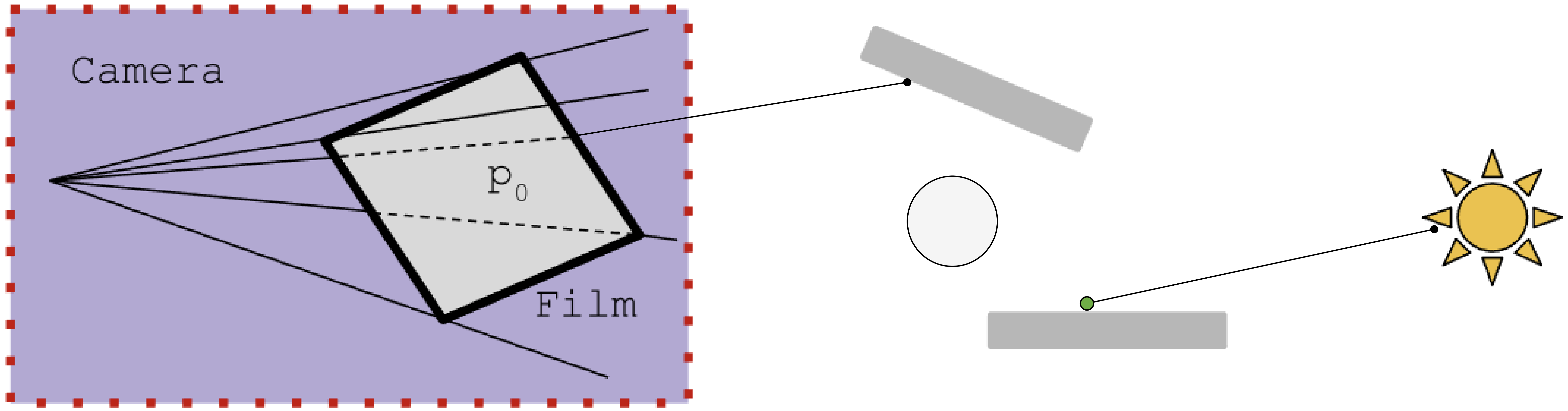

[Agarwal et al., 2023]

Sensor design framework: *optical simulation*

- What makes simulation challenging
  - SDS light paths
  - Indirect illumination
- Require Markov Chain Monte Carlo rendering techniques
  - Key idea → Slowly mutate paths to generate useful paths

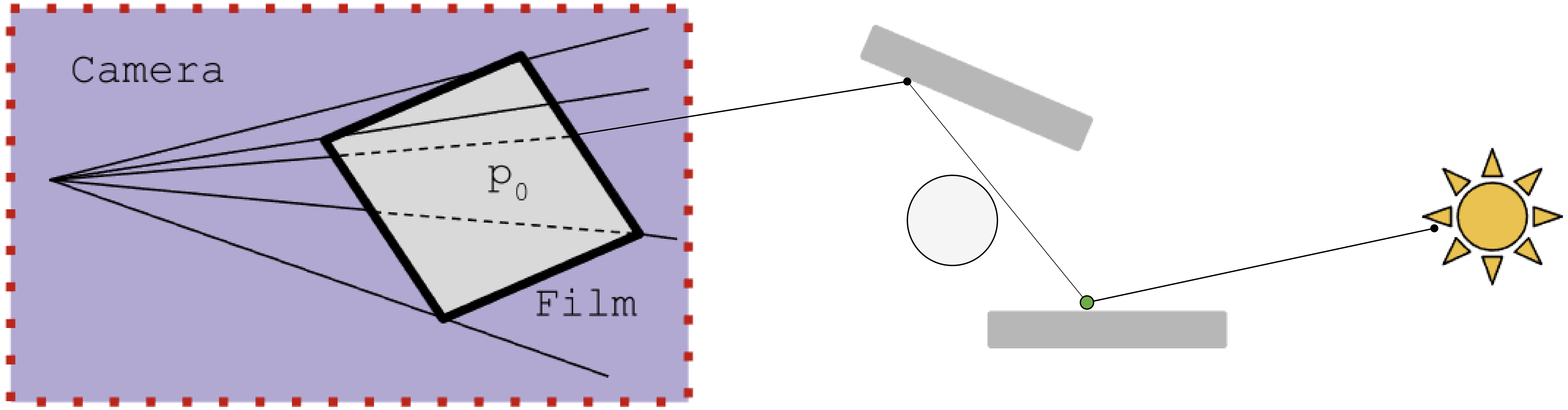

[Agarwal et al., 2023]

Sensor design framework: *optical simulation*

- What makes simulation challenging
  - SDS light paths
  - Indirect illumination
- Require Markov Chain Monte Carlo rendering techniques
  - Key idea → Slowly mutate paths to generate useful paths

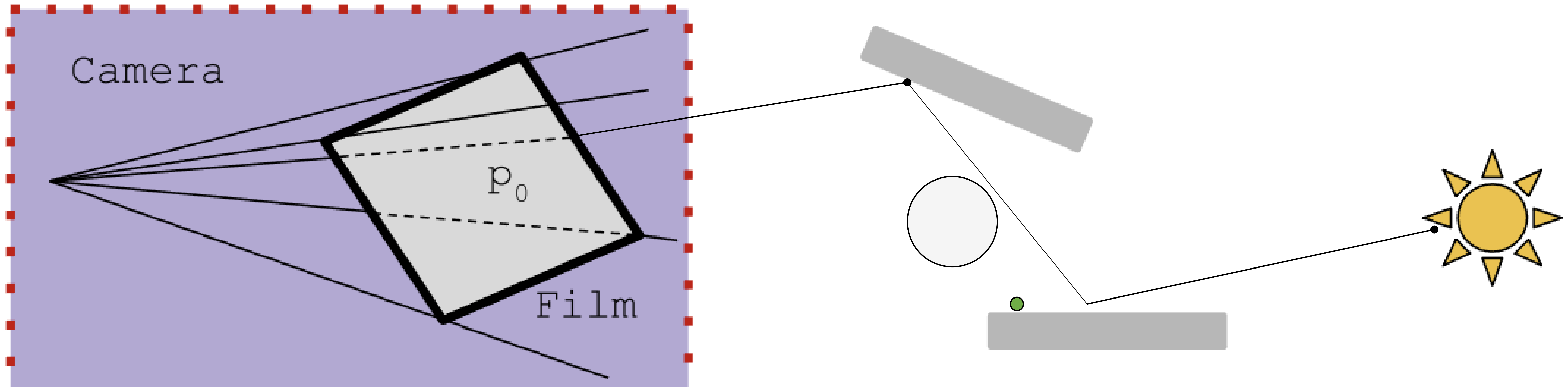

[Agarwal et al., 2023]

Sensor design framework: *optical simulation*

- What makes simulation challenging
  - SDS light paths
  - Indirect illumination
- Require Markov Chain Monte Carlo rendering techniques
  - Key idea → Slowly mutate paths to generate useful paths

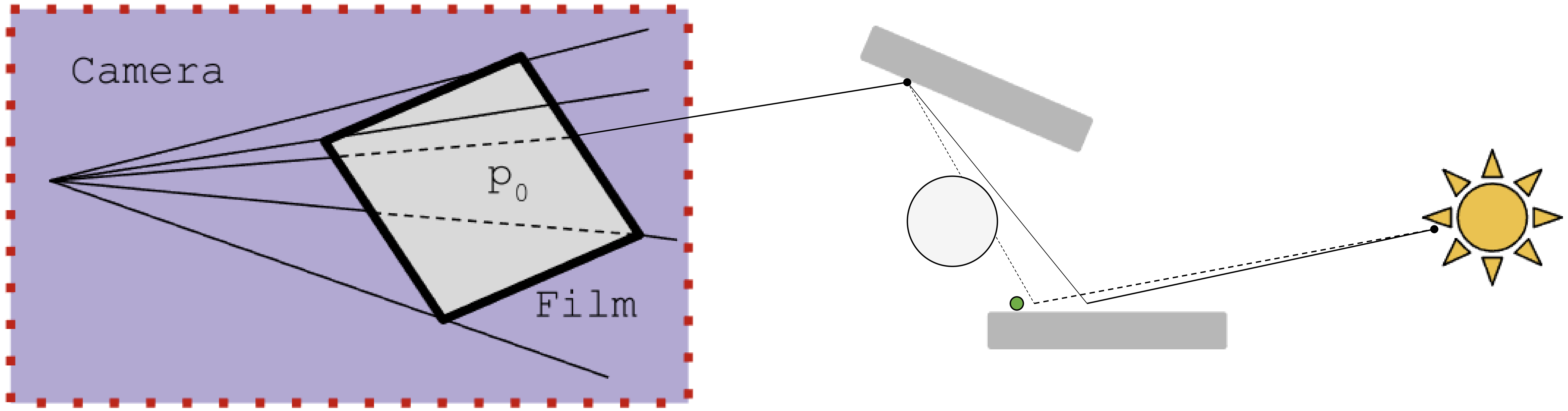

[Agarwal et al., 2023]

Sensor design framework: *optical simulation*

- What makes simulation challenging
  - SDS light paths
  - Indirect illumination
- Require Markov Chain Monte Carlo rendering techniques
  - Key idea → Slowly mutate paths to generate useful paths

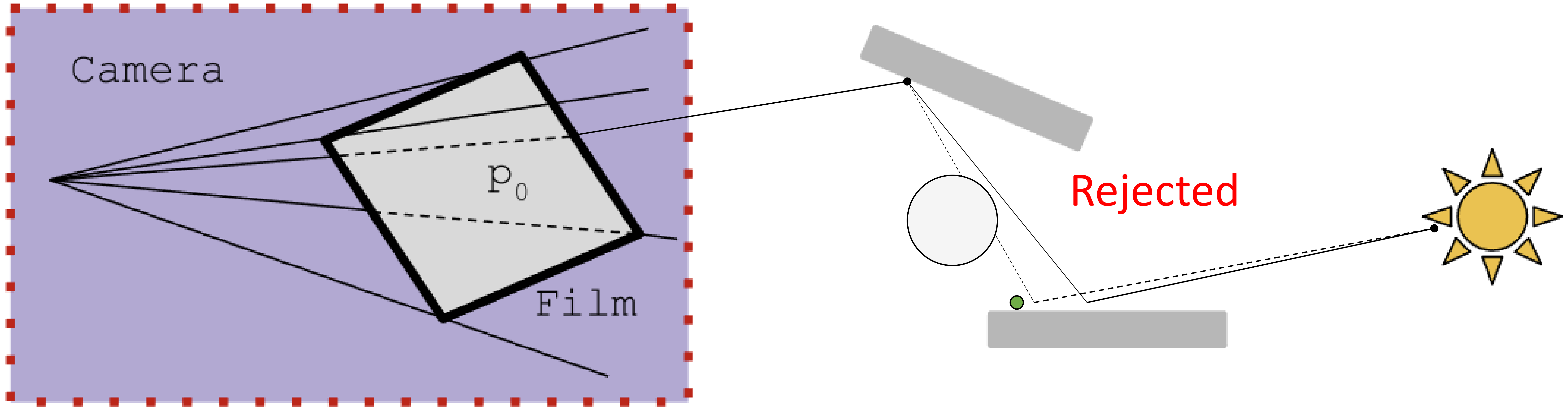

[Agarwal et al., 2023]

Sensor design framework: *optical simulation*

- What makes simulation challenging
  - SDS light paths
  - Indirect illumination
- Require Markov Chain Monte Carlo rendering techniques
  - Key idea → Slowly mutate paths to generate useful paths

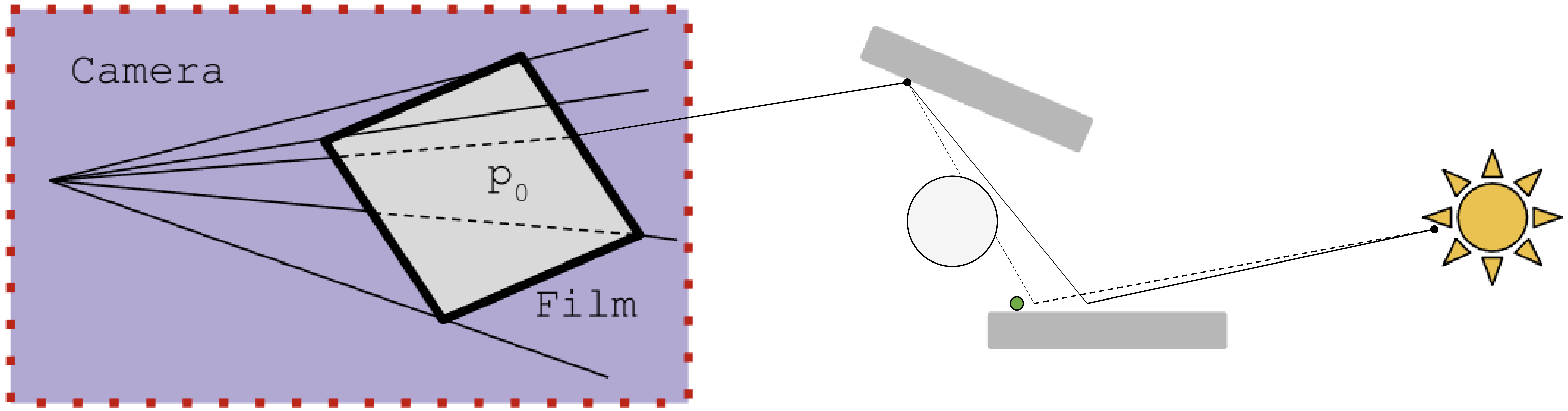

[Agarwal et al., 2023]

Sensor design framework: *optical simulation*

- What makes simulation challenging
  - SDS light paths
  - Indirect illumination
- Require Markov Chain Monte Carlo rendering techniques
  - Key idea ➡ Slowly mutate paths to generate useful paths

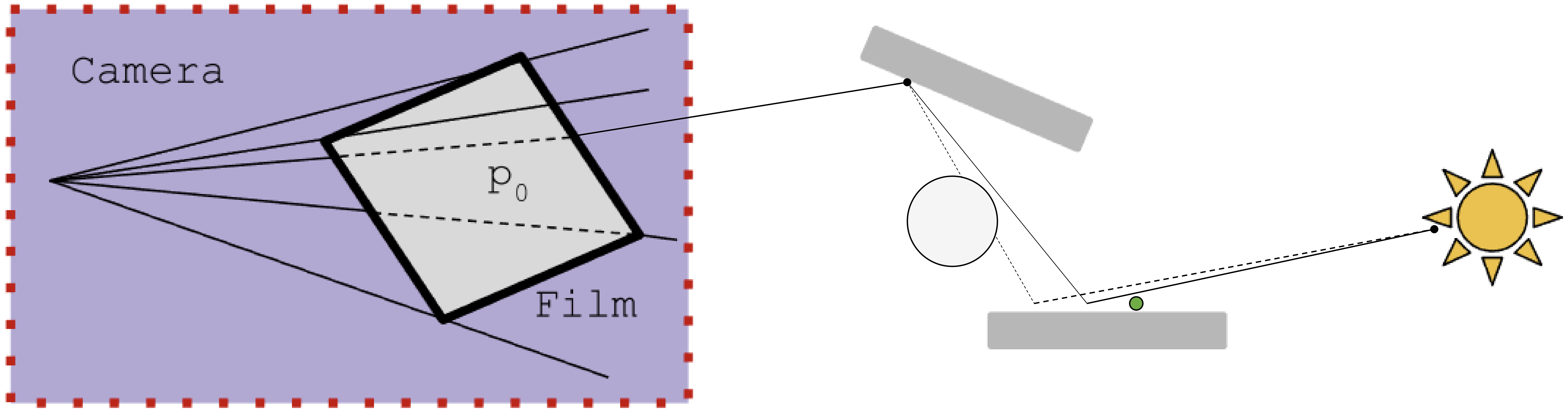

[Agarwal et al., 2023]

Sensor design framework: *optical simulation*

- What makes simulation challenging
  - SDS light paths
  - Indirect illumination
- Require Markov Chain Monte Carlo rendering techniques
  - Key idea → Slowly mutate paths to generate useful paths

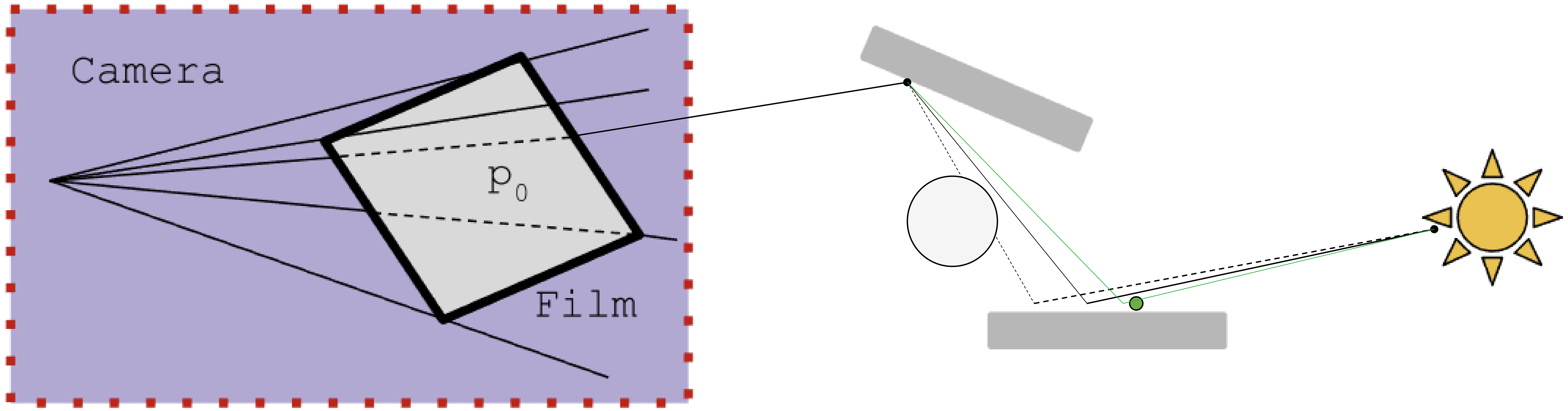

[Agarwal et al., 2023]

Sensor design framework: *optical simulation*

- What makes simulation challenging
  - SDS light paths
  - Indirect illumination
- Require Markov Chain Monte Carlo rendering techniques
  - Key idea ➡ Slowly mutate paths to generate useful paths

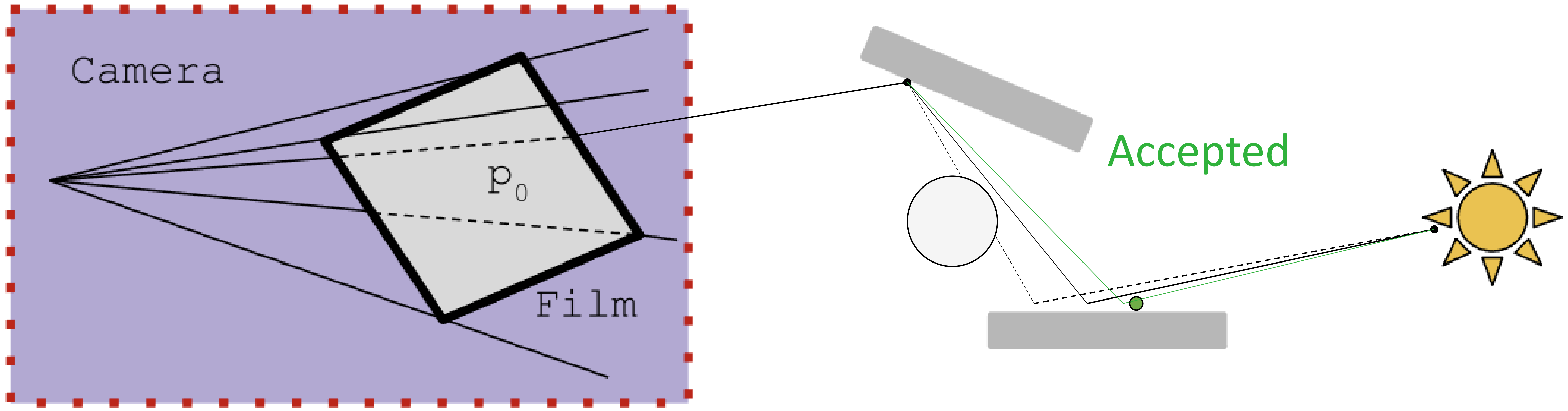

[Agarwal et al., 2023]

Optimization:
- Stochastic Gradient Descent (SGD)

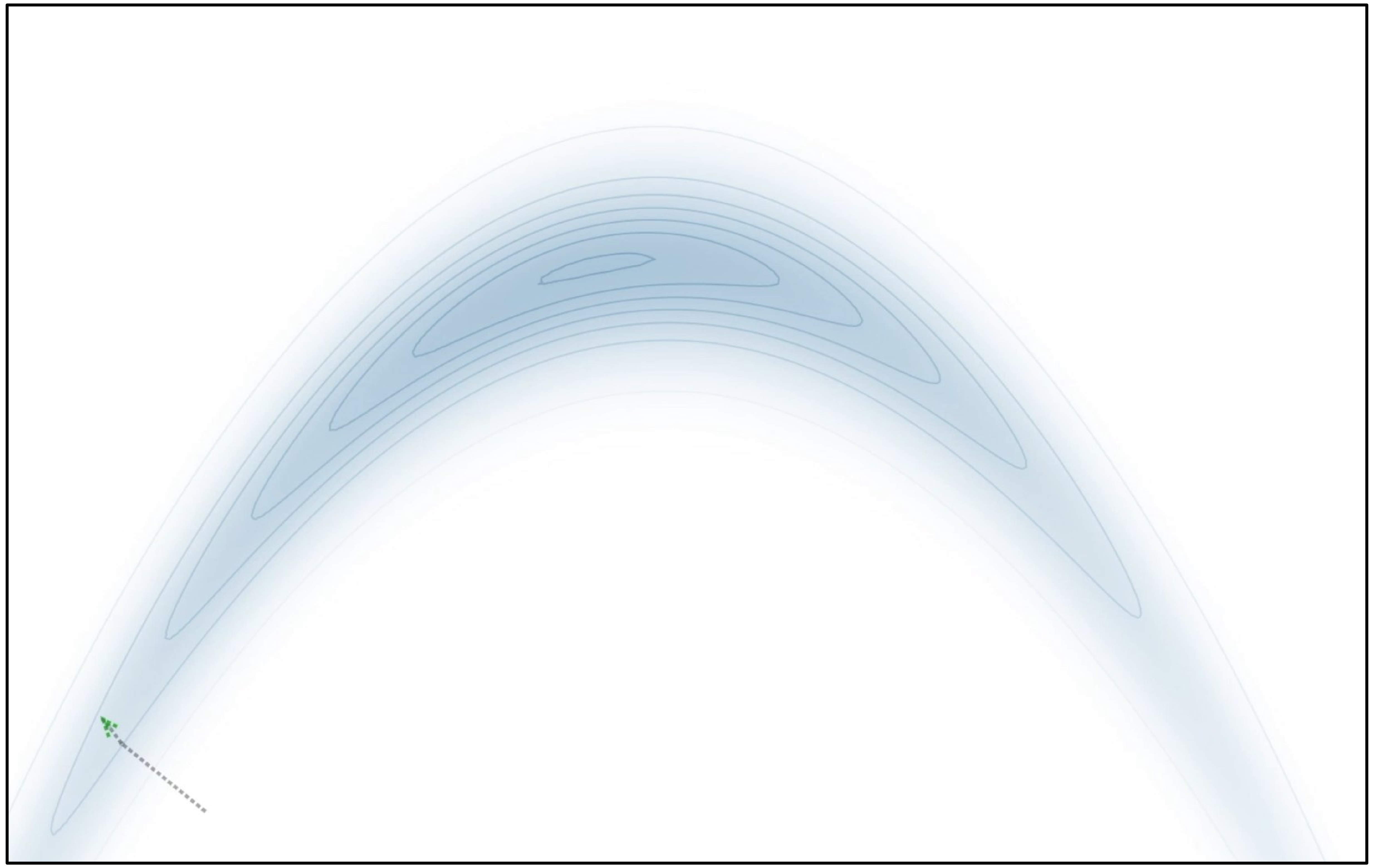

MCMC sampling:
- Langevin Monte Carlo (LMC)

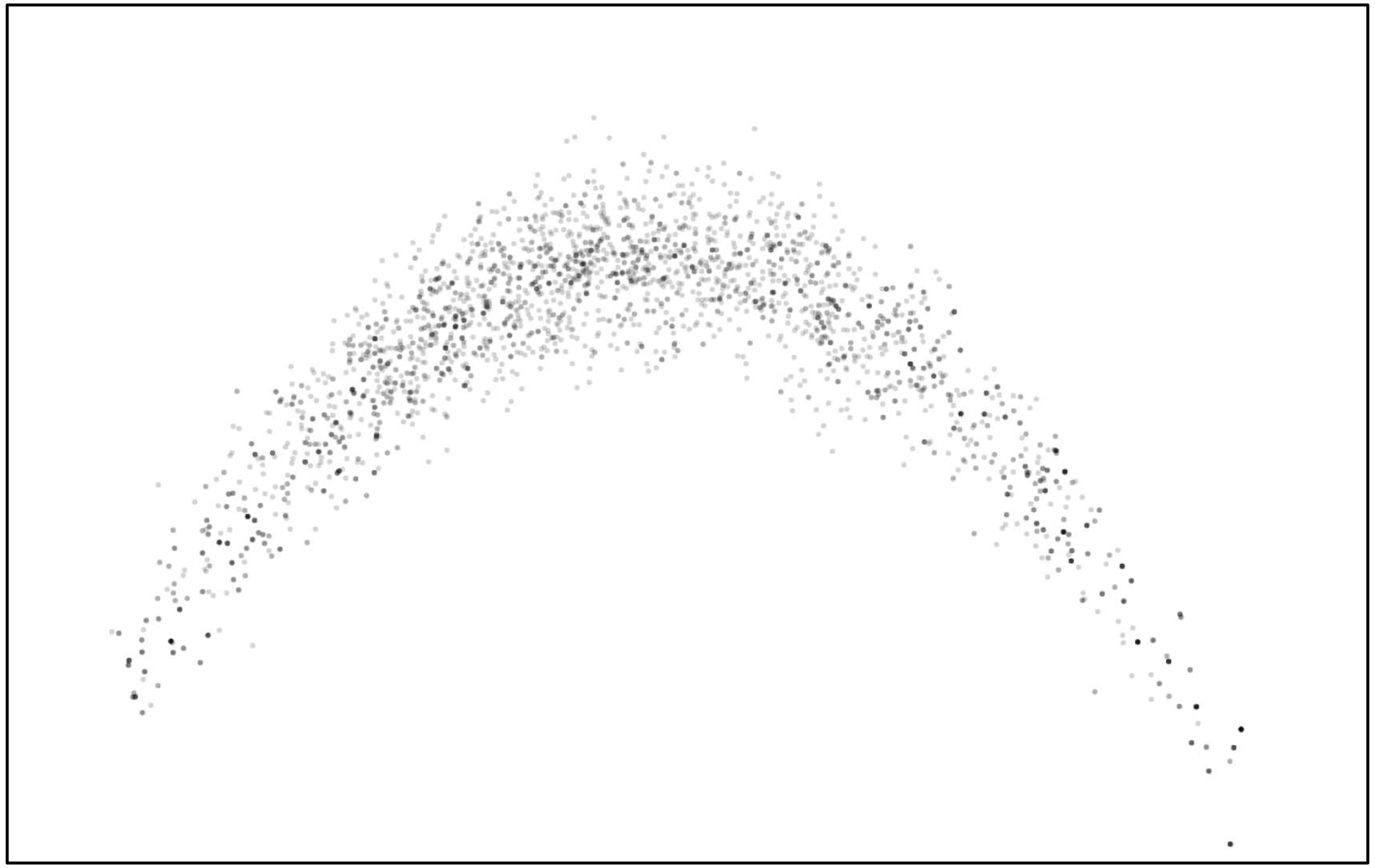

[Luan et al., 2020]

GD OVERVIEW

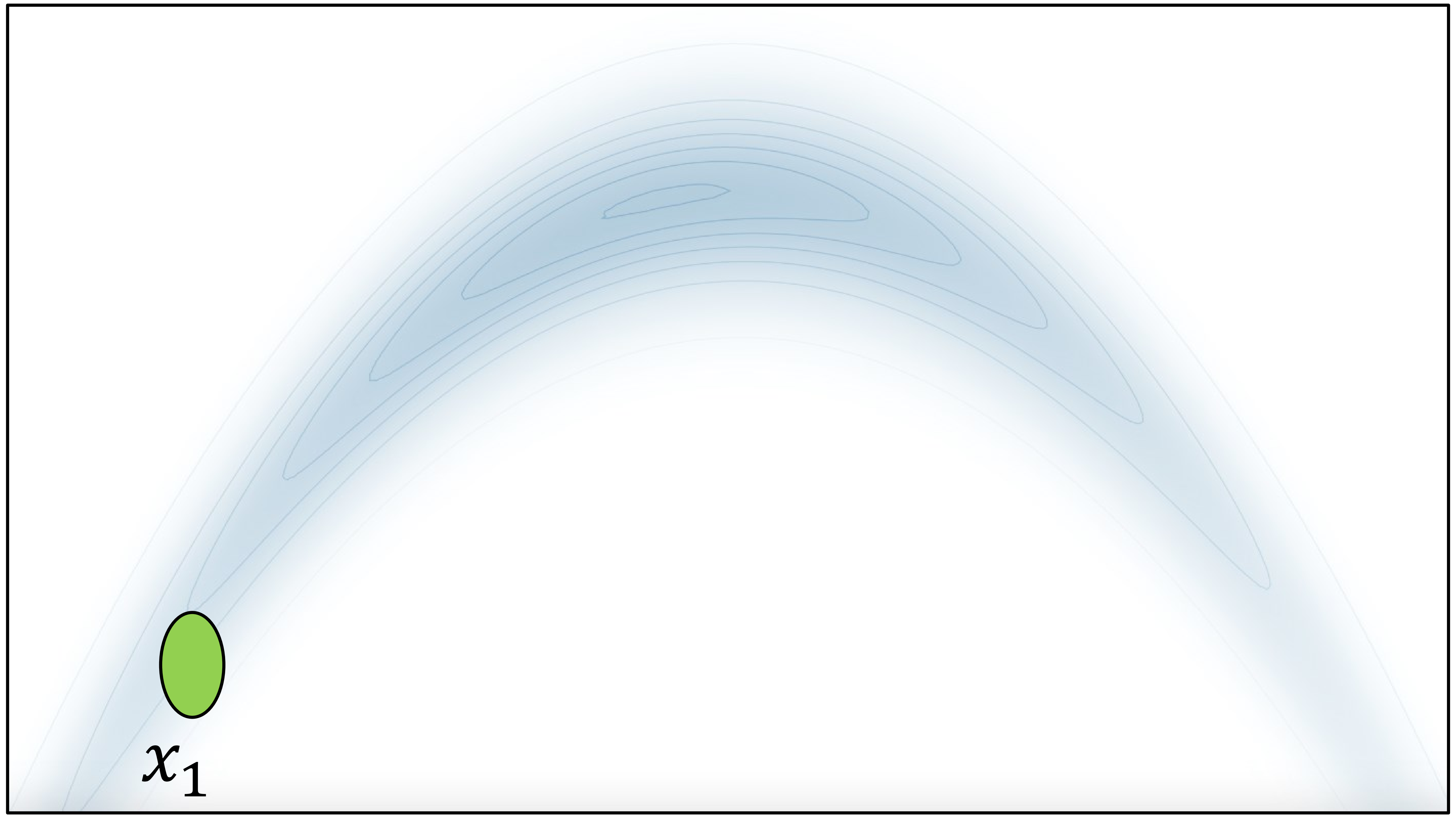

Optimization problem:

$$\max_{\boldsymbol{x}} f(\boldsymbol{x})$$

Gradient descent/ascent:

$$\boldsymbol{x}_t = \boldsymbol{x}_{t-1} + s_{t-1}\nabla f(\boldsymbol{x}_{t-1})$$

[Luan et al., 2020]

GD OVERVIEW

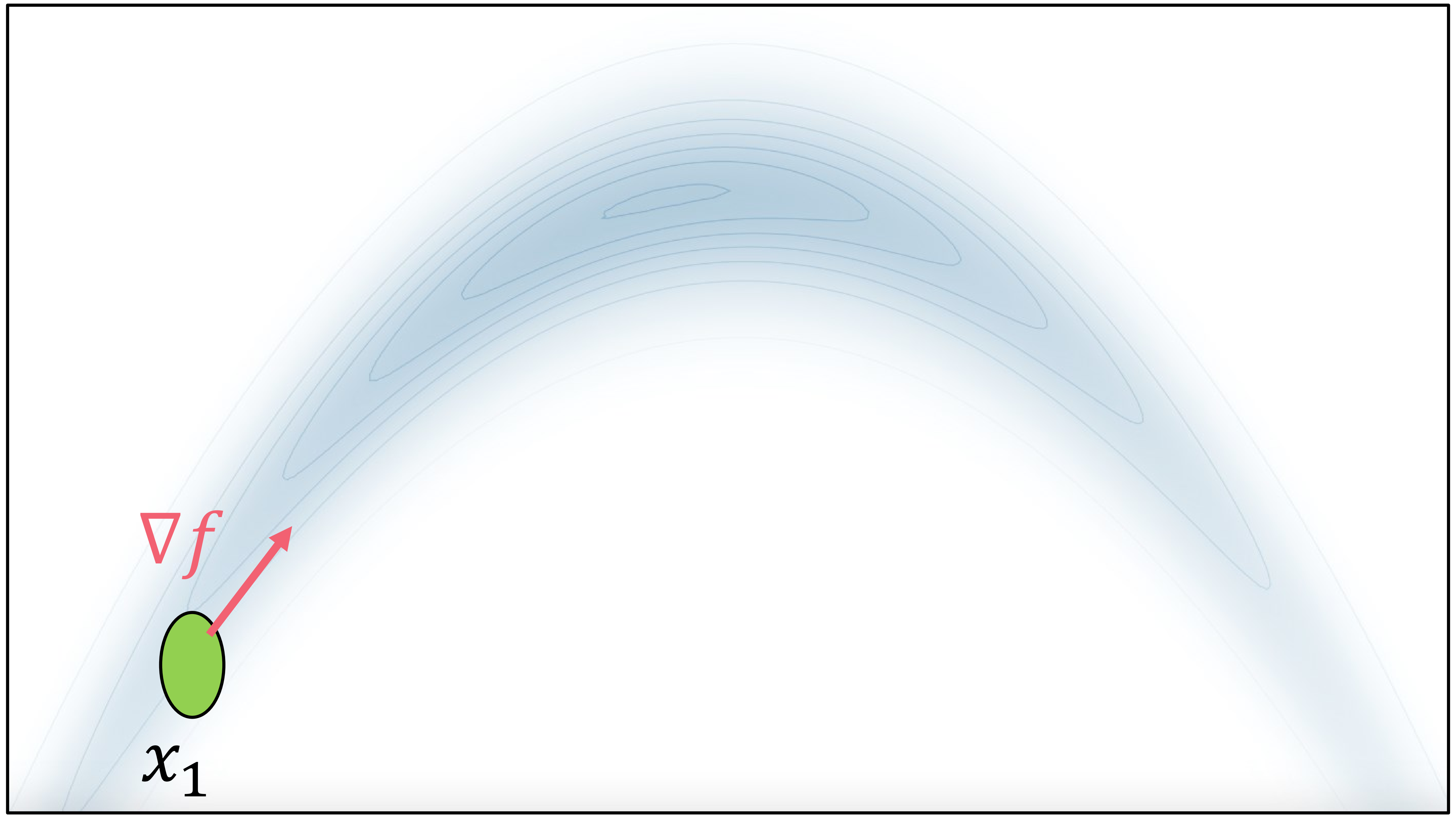

Optimization problem:

$$\max_{\boldsymbol{x}} f(\boldsymbol{x})$$

Gradient descent/ascent:

$$\boldsymbol{x}_t = \boldsymbol{x}_{t-1} + s_{t-1} \nabla f(\boldsymbol{x}_{t-1})$$

[Luan et al., 2020]

GD OVERVIEW

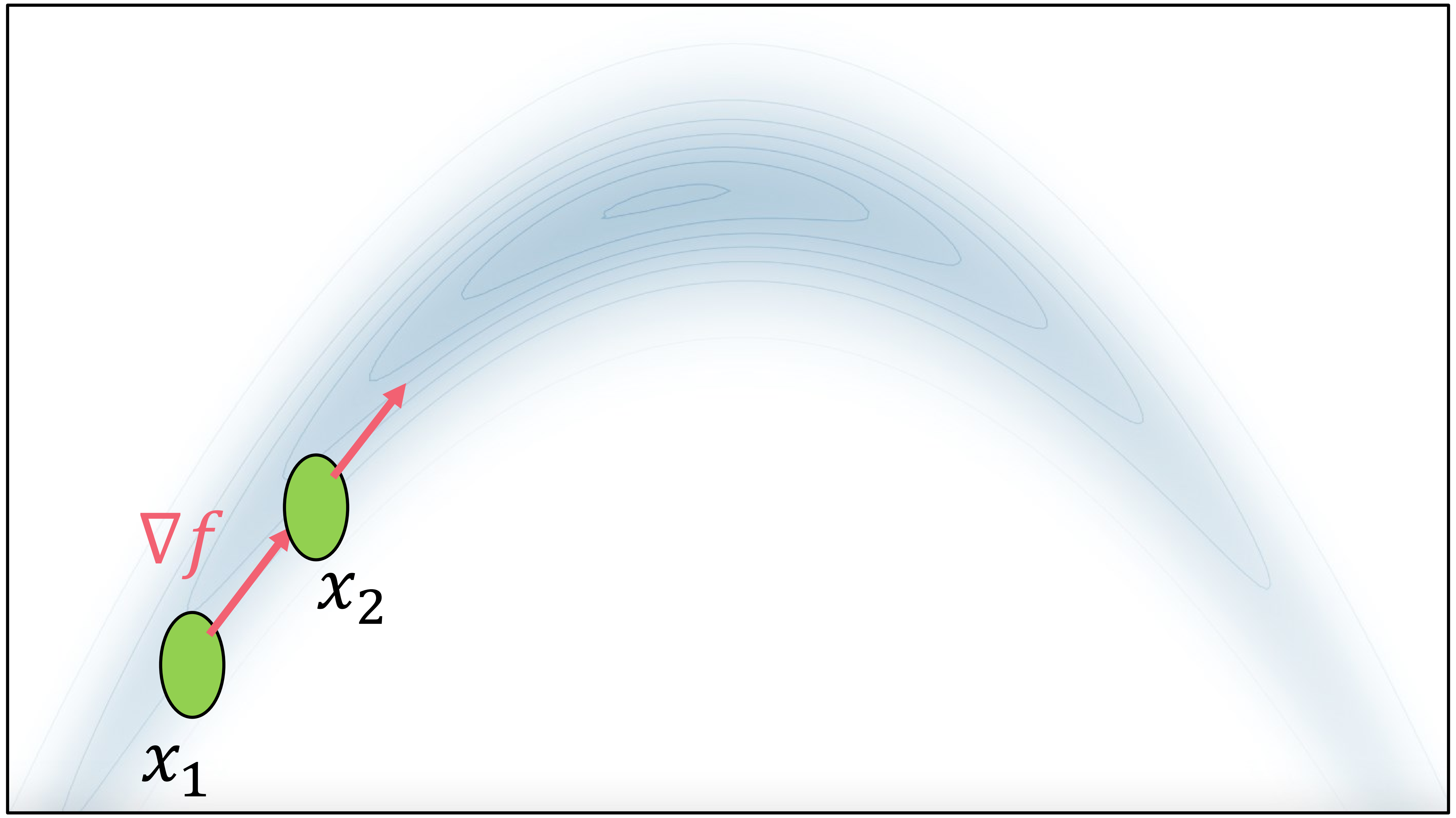

Optimization problem:

$$\max_{\boldsymbol{x}} f(\boldsymbol{x})$$

Gradient descent/ascent:

$$\boldsymbol{x}_t = \boldsymbol{x}_{t-1} + s_{t-1} \nabla f(\boldsymbol{x}_{t-1})$$

[Luan et al., 2020]

GD OVERVIEW

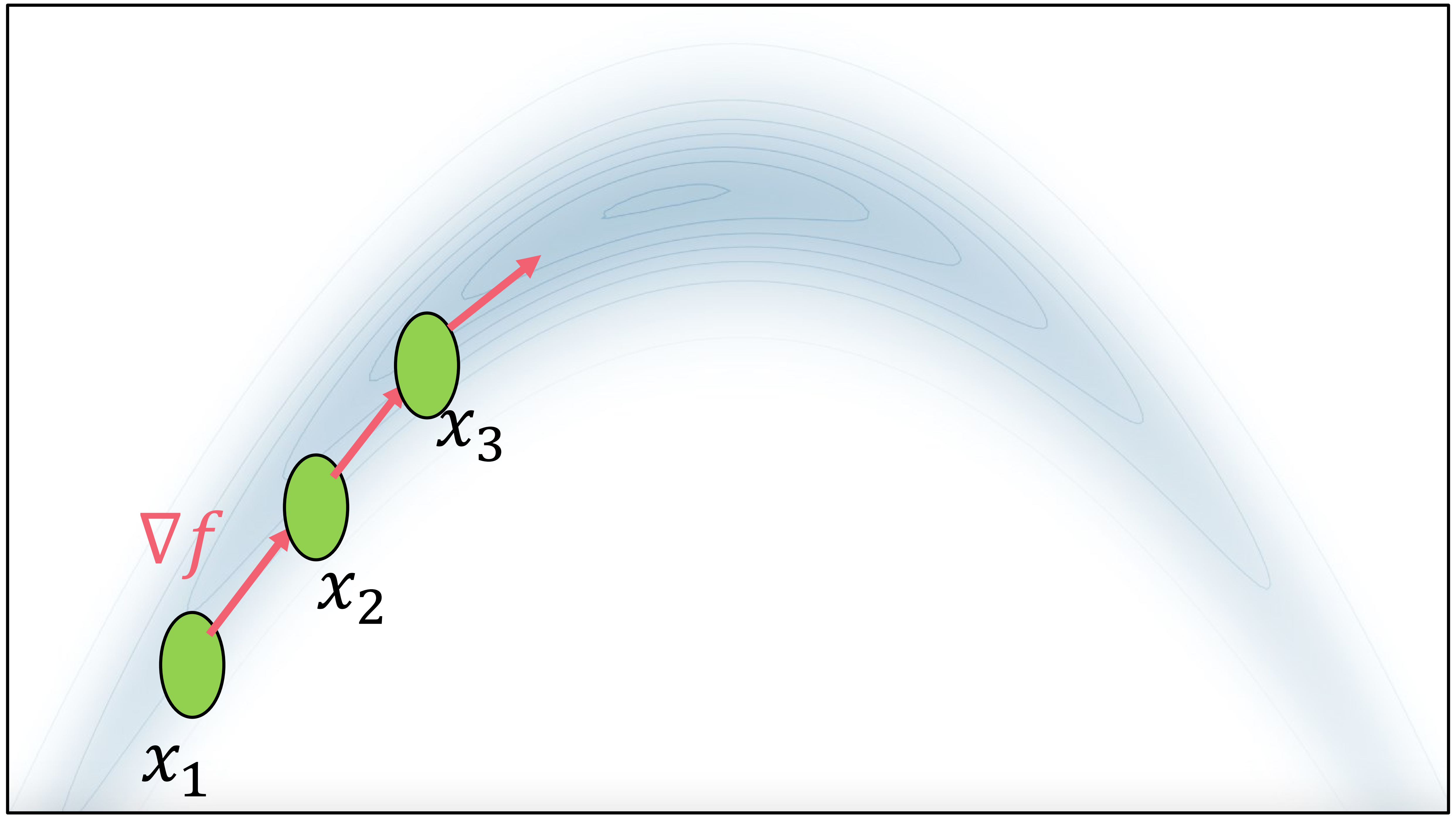

Optimization problem:

$$\max_{\boldsymbol{x}} f(\boldsymbol{x})$$

Gradient descent/ascent:

$$\boldsymbol{x}_t = \boldsymbol{x}_{t-1} + s_{t-1} \nabla f(\boldsymbol{x}_{t-1})$$

[Luan et al., 2020]

GD OVERVIEW

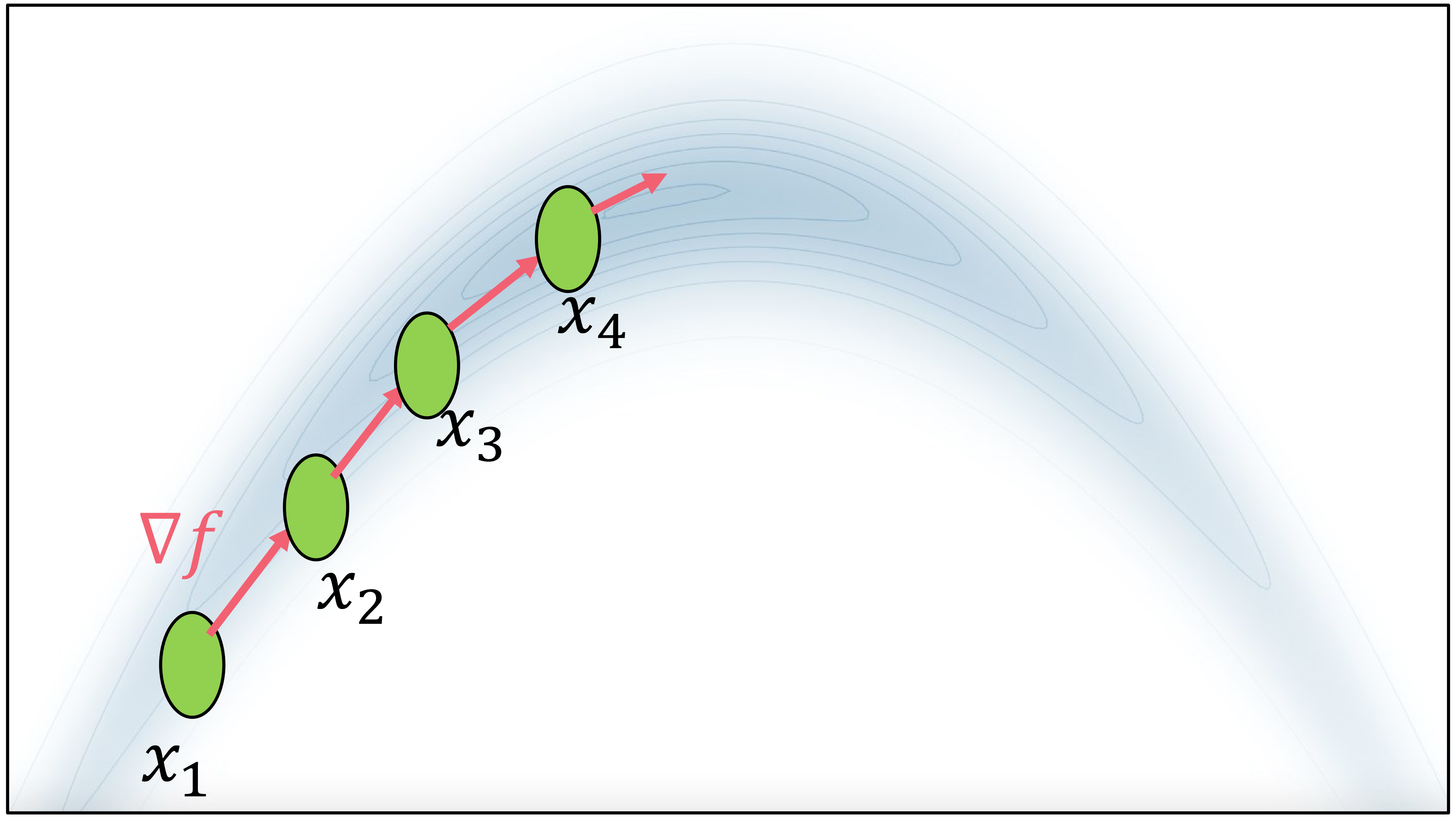

Optimization problem:

$$\max_{\boldsymbol{x}} f(\boldsymbol{x})$$

Gradient descent/ascent:

$$\boldsymbol{x}_t = \boldsymbol{x}_{t-1} + s_{t-1}\nabla f(\boldsymbol{x}_{t-1})$$

[Luan et al., 2020]

GD OVERVIEW

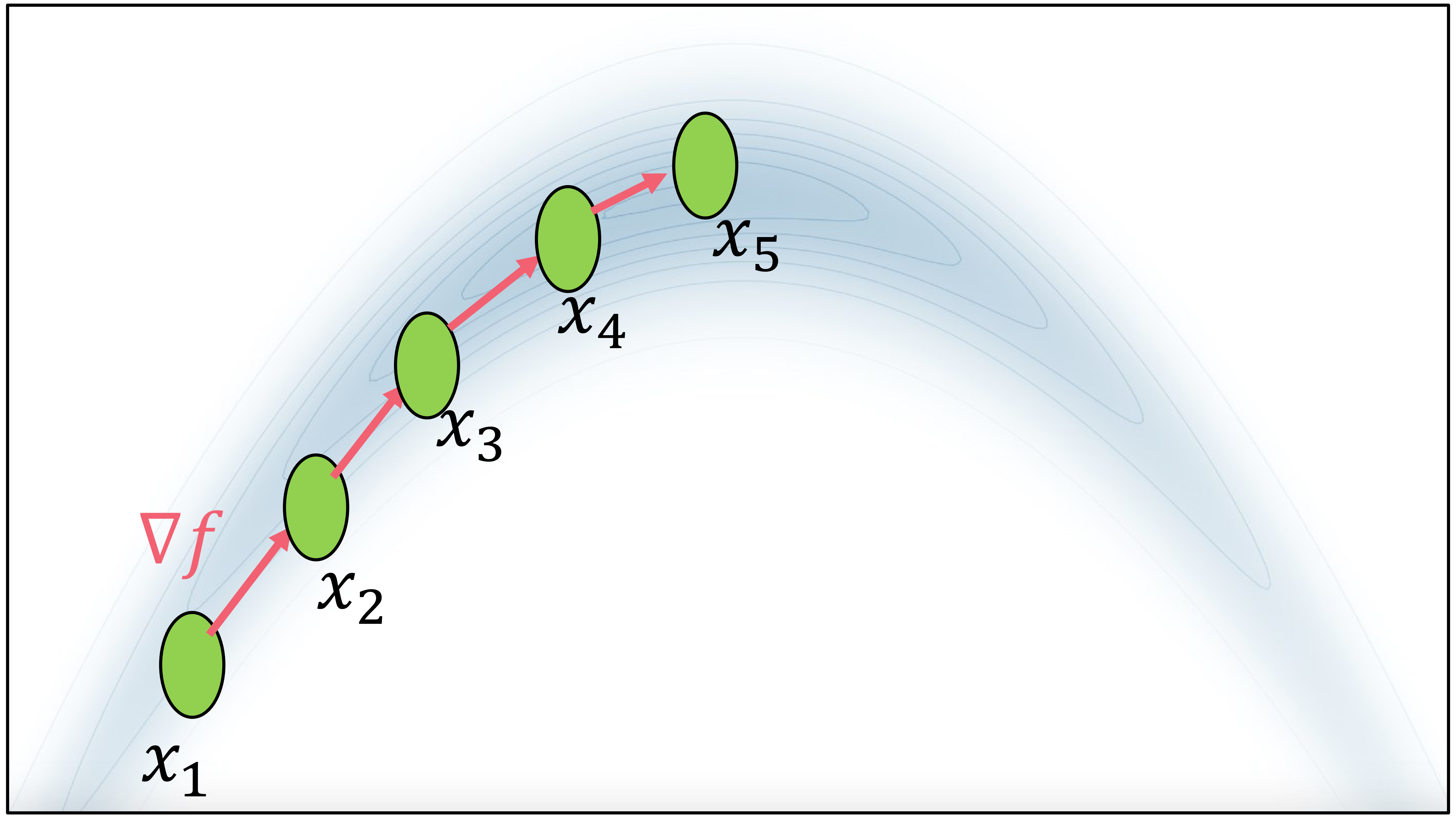

Optimization problem:

$$\max_{\boldsymbol{x}} f(\boldsymbol{x})$$

Gradient descent/ascent:

$$\boldsymbol{x}_t = \boldsymbol{x}_{t-1} + s_{t-1}\nabla f(\boldsymbol{x}_{t-1})$$

[Luan et al., 2020]

GD OVERVIEW

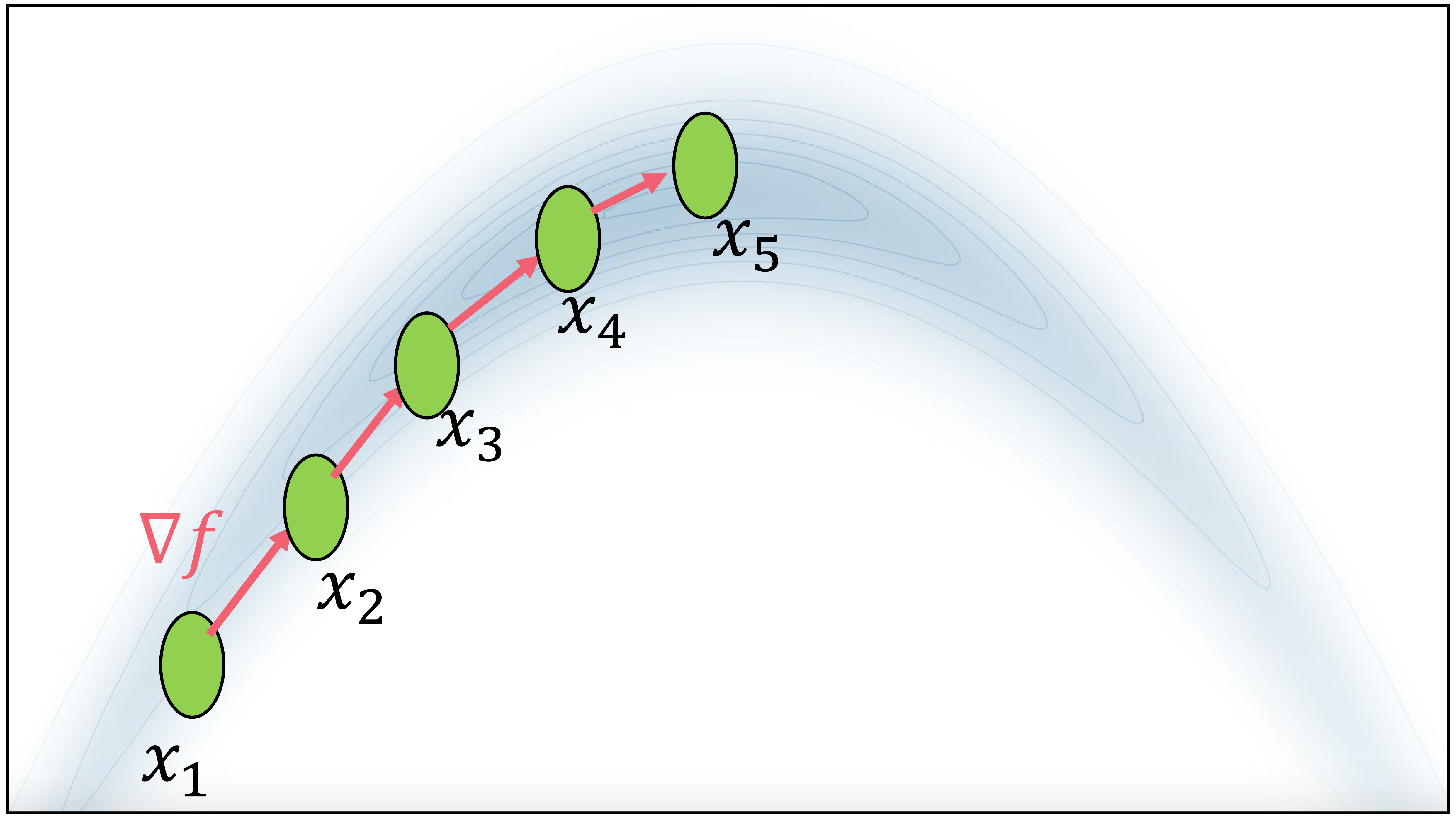

Optimization problem:

$$\max_{\boldsymbol{x}} f(\boldsymbol{x})$$

Gradient descent/ascent:

$$\boldsymbol{x}_t = \boldsymbol{x}_{t-1} + s_{t-1} \nabla f(\boldsymbol{x}_{t-1})$$

scalar step size

[Luan et al., 2020]

LMC OVERVIEW

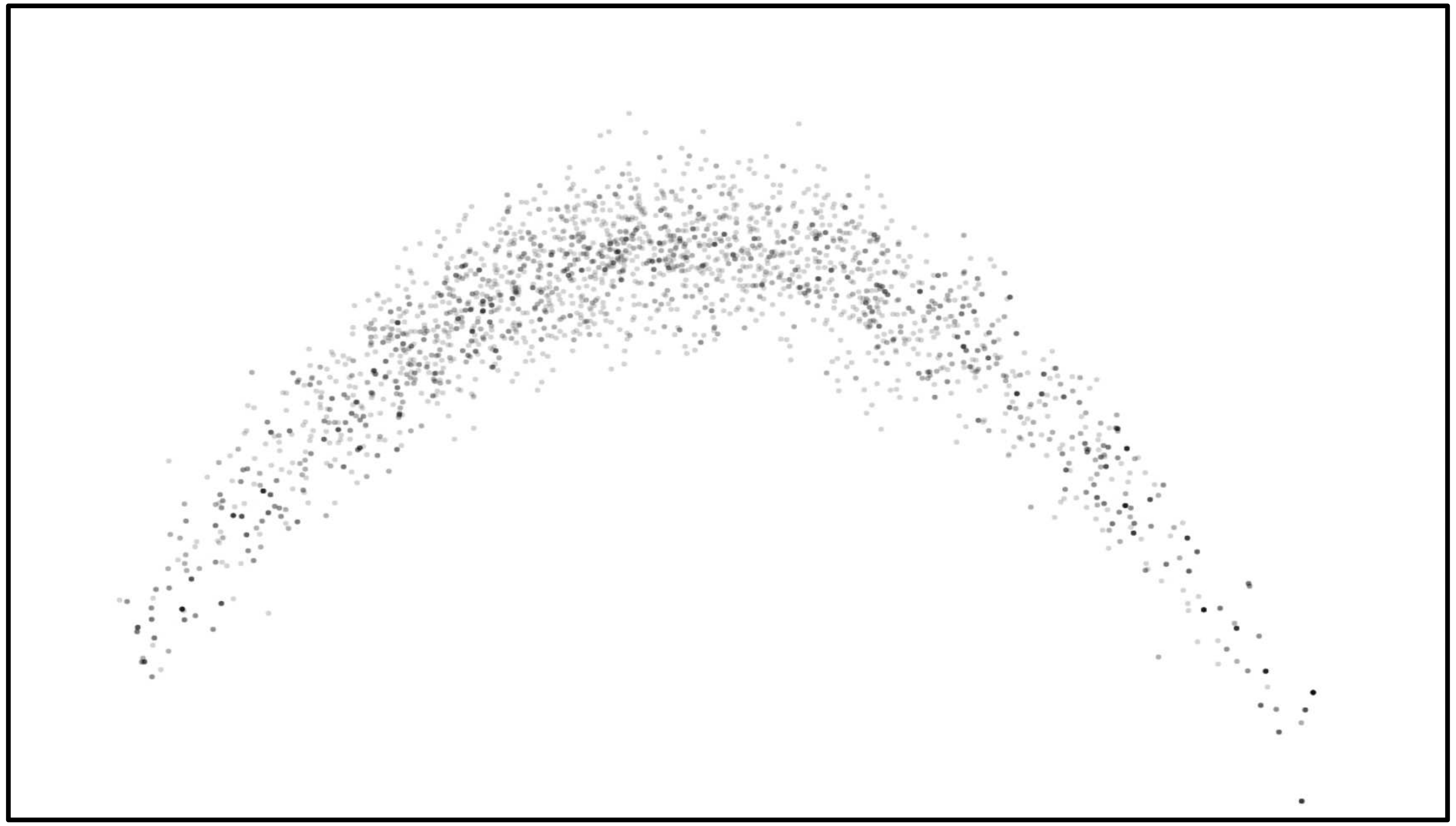

Sampling problem:

$$\boldsymbol{x}_t \sim f$$

Langevin MC:

$$\boldsymbol{x}_t = \boldsymbol{x}_{t-1} + s_{t-1} \nabla f(\boldsymbol{x}_{t-1}) + \frac{1}{s_{t-1}} N(0, \sigma^2 \boldsymbol{I})$$

Apply Metropolis Hastings to accept/reject

Paul Langevin

[Luan et al., 2020]

LMC OVERVIEW

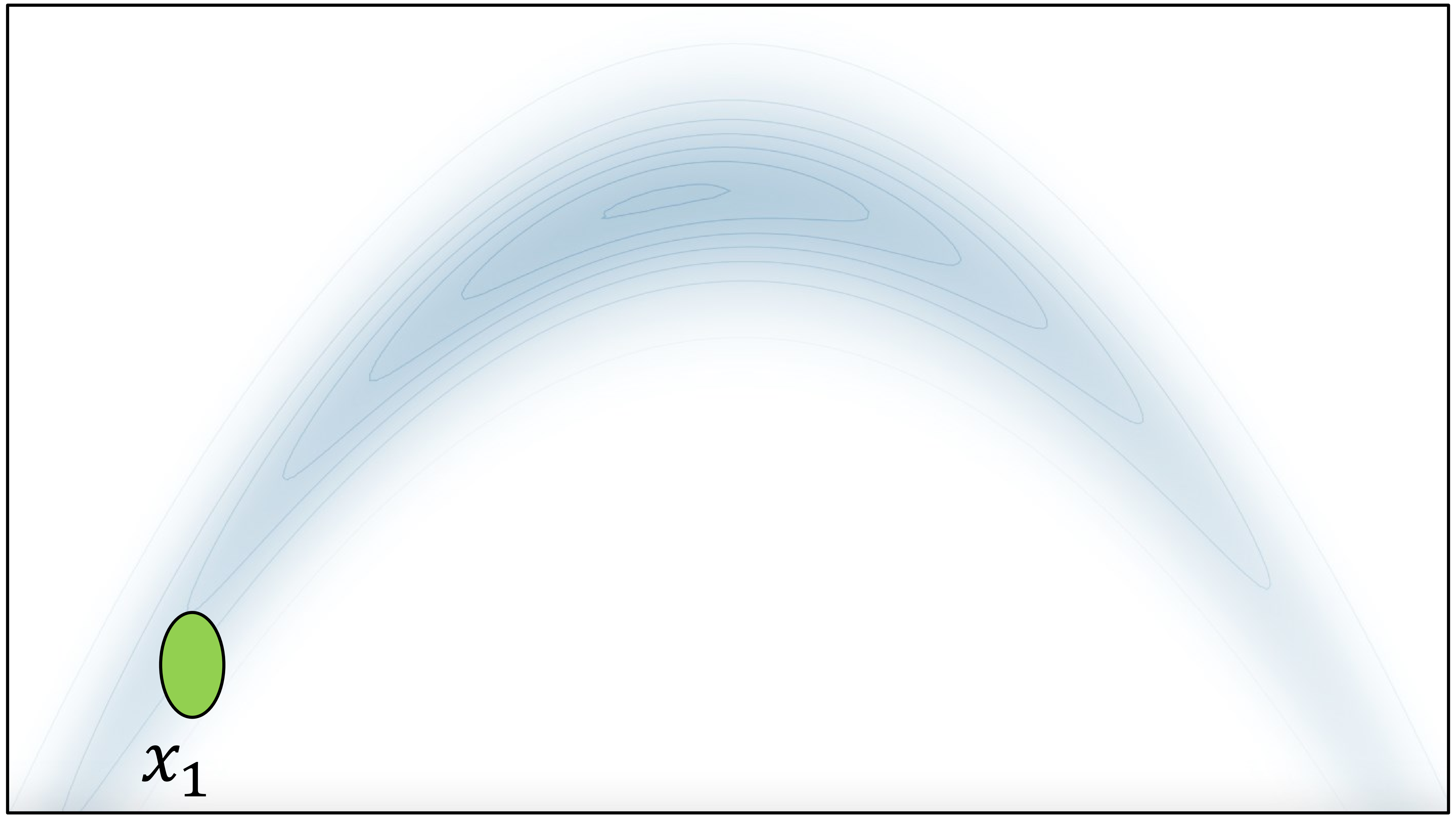

Sampling problem:

$$\boldsymbol{x}_t \sim f$$

Langevin MC:

$$\boldsymbol{x}_t = \boldsymbol{x}_{t-1} + s_{t-1}\nabla f(\boldsymbol{x}_{t-1}) + \frac{1}{s_{t-1}} N(0, \sigma^2 \boldsymbol{I})$$

Apply Metropolis Hastings to accept/reject

[Luan et al., 2020]

LMC OVERVIEW

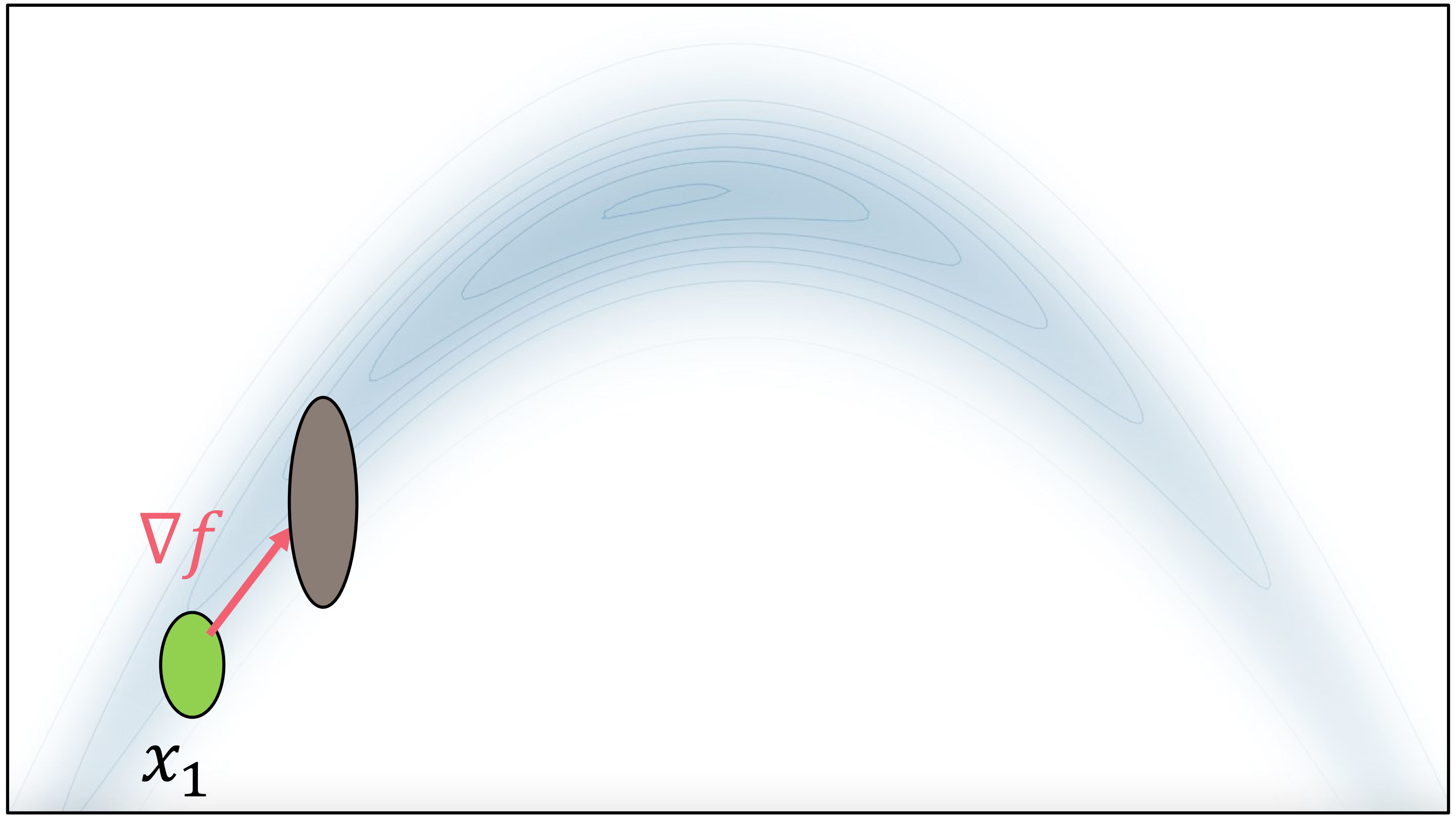

Sampling problem:

$$\boldsymbol{x}_t \sim f$$

Langevin MC:

$$\boldsymbol{x}_t = \boldsymbol{x}_{t-1} + s_{t-1} \nabla f(\boldsymbol{x}_{t-1}) + \frac{1}{s_{t-1}} N(0, \sigma^2 \boldsymbol{I})$$

Apply Metropolis Hastings to accept/reject

[Luan et al., 2020]

LMC OVERVIEW

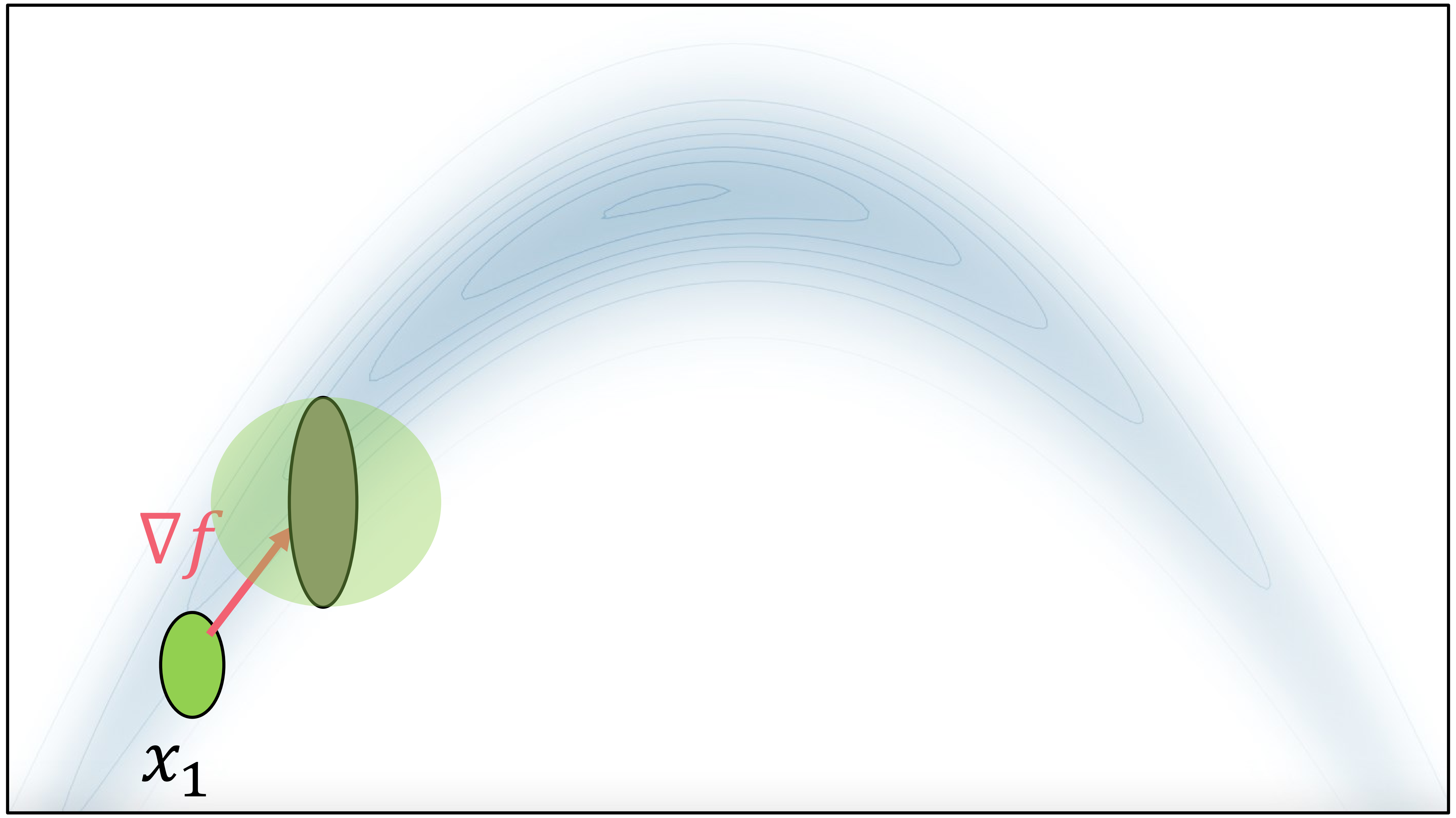

Sampling problem:

$$\boldsymbol{x}_t \sim f$$

Langevin MC:

$$\boldsymbol{x}_t = \boldsymbol{x}_{t-1} + s_{t-1}\nabla f(\boldsymbol{x}_{t-1}) + \frac{1}{s_{t-1}} N(0, \sigma^2 \boldsymbol{I})$$

Apply Metropolis Hastings to accept/reject

[Luan et al., 2020]

LMC OVERVIEW

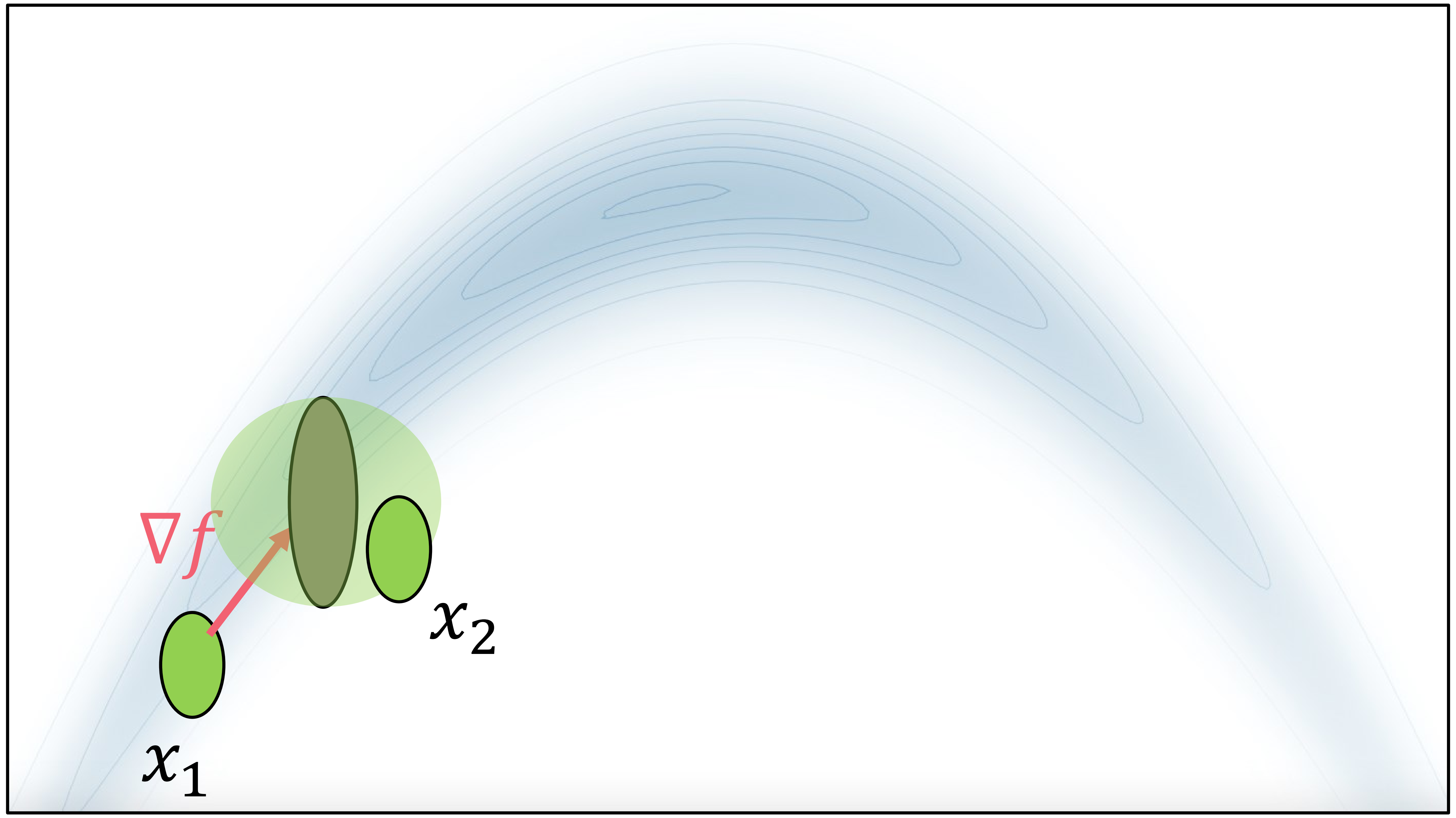

Sampling problem:

$$\boldsymbol{x}_t \sim f$$

Langevin MC:

$$\boldsymbol{x}_t = \boldsymbol{x}_{t-1} + s_{t-1}\nabla f(\boldsymbol{x}_{t-1}) + \frac{1}{s_{t-1}} N(0, \sigma^2 \boldsymbol{I})$$

Apply Metropolis Hastings to accept/reject

[Luan et al., 2020]

LMC OVERVIEW

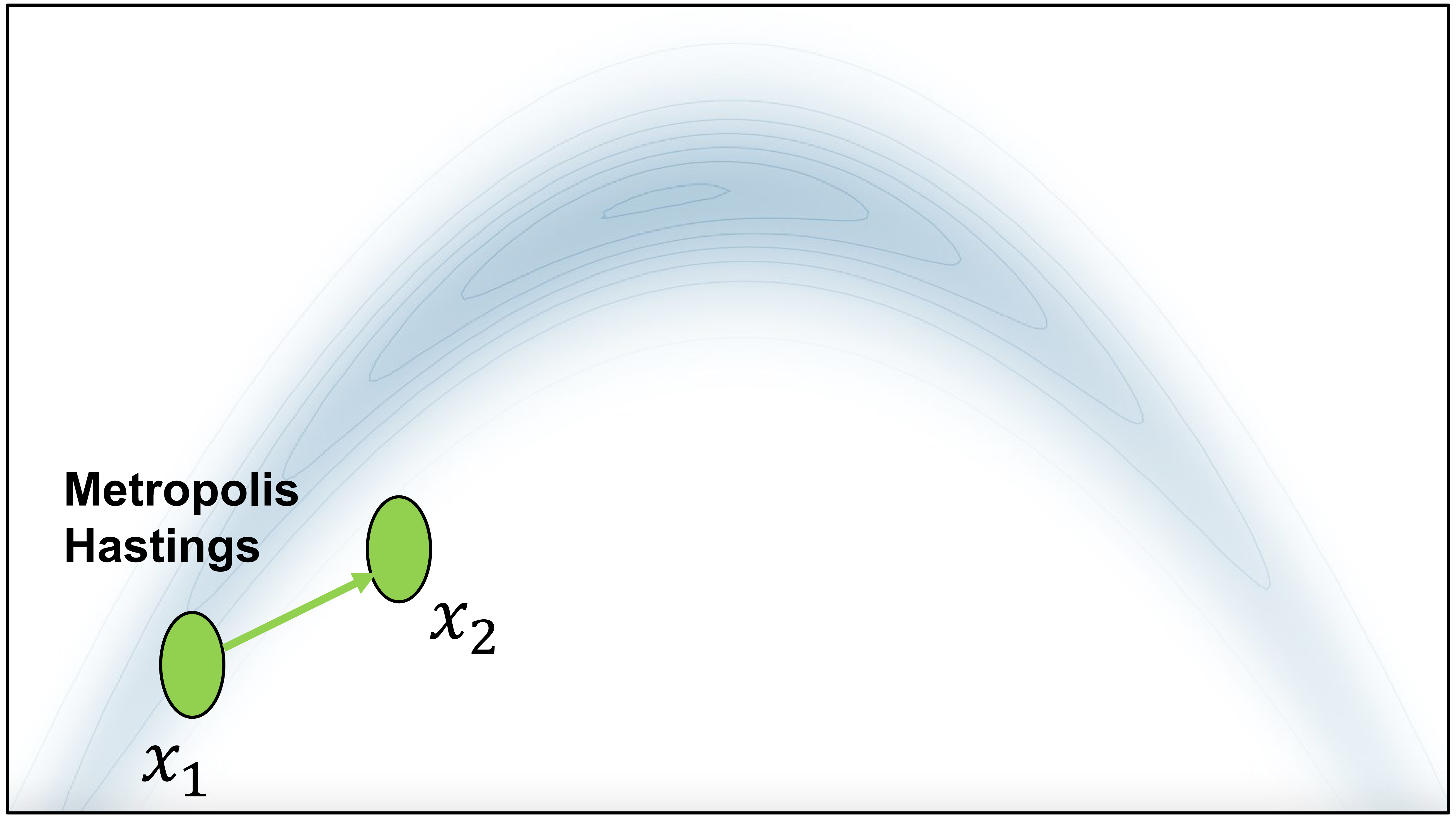

Sampling problem:

$$\boldsymbol{x}_t \sim f$$

Langevin MC:

$$\boldsymbol{x}_t = \boldsymbol{x}_{t-1} + s_{t-1} \nabla f(\boldsymbol{x}_{t-1}) + \frac{1}{s_{t-1}} N(0, \sigma^2 \boldsymbol{I})$$

Apply Metropolis Hastings to accept/reject

[Luan et al., 2020]

LMC OVERVIEW

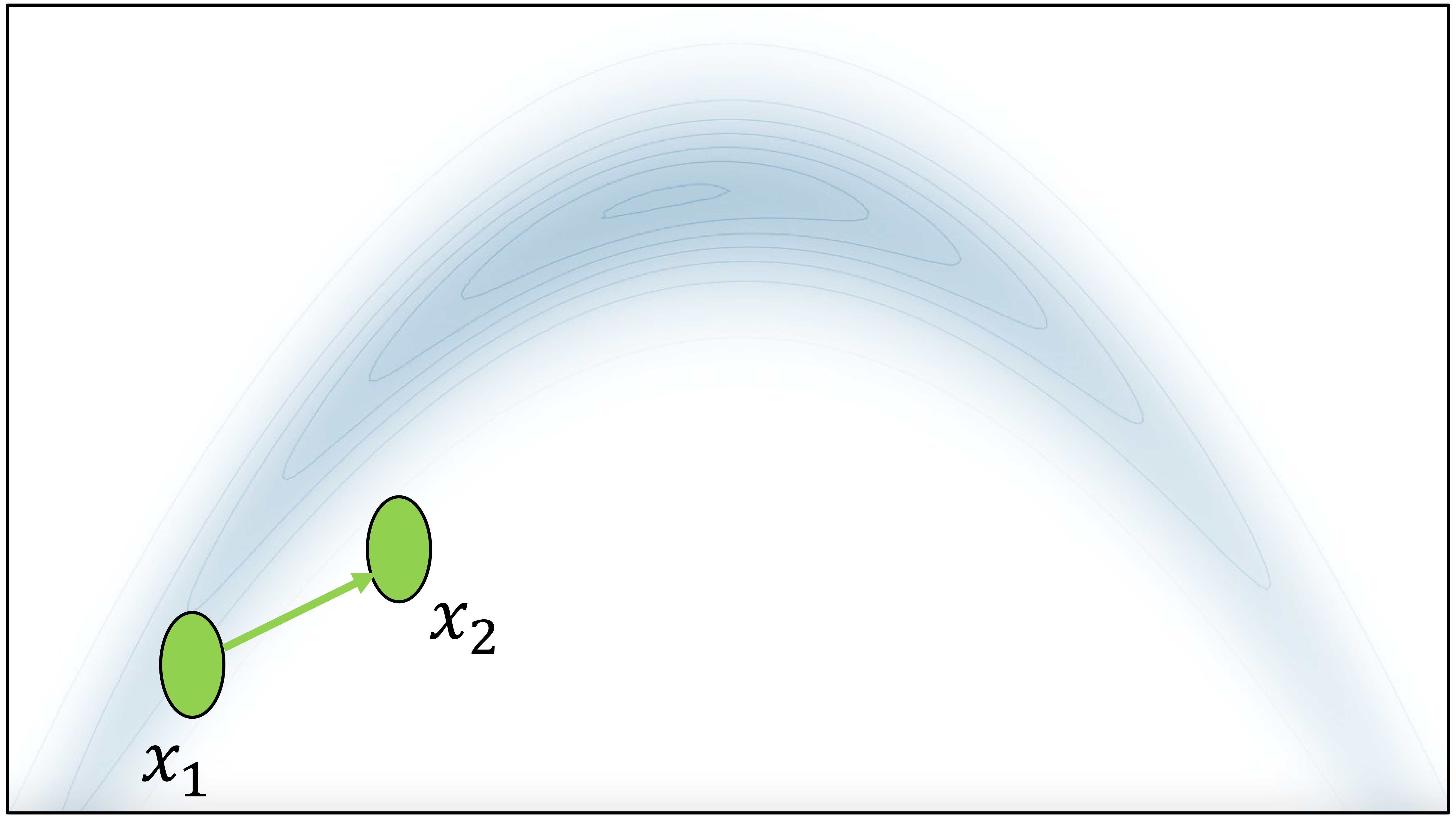

Sampling problem:

$$\boldsymbol{x}_t \sim f$$

Langevin MC:

$$\boldsymbol{x}_t = \boldsymbol{x}_{t-1} + s_{t-1}\nabla f(\boldsymbol{x}_{t-1}) + \frac{1}{s_{t-1}} N(0, \sigma^2 \boldsymbol{I})$$

Apply Metropolis Hastings to accept/reject

[Luan et al., 2020]

LMC OVERVIEW

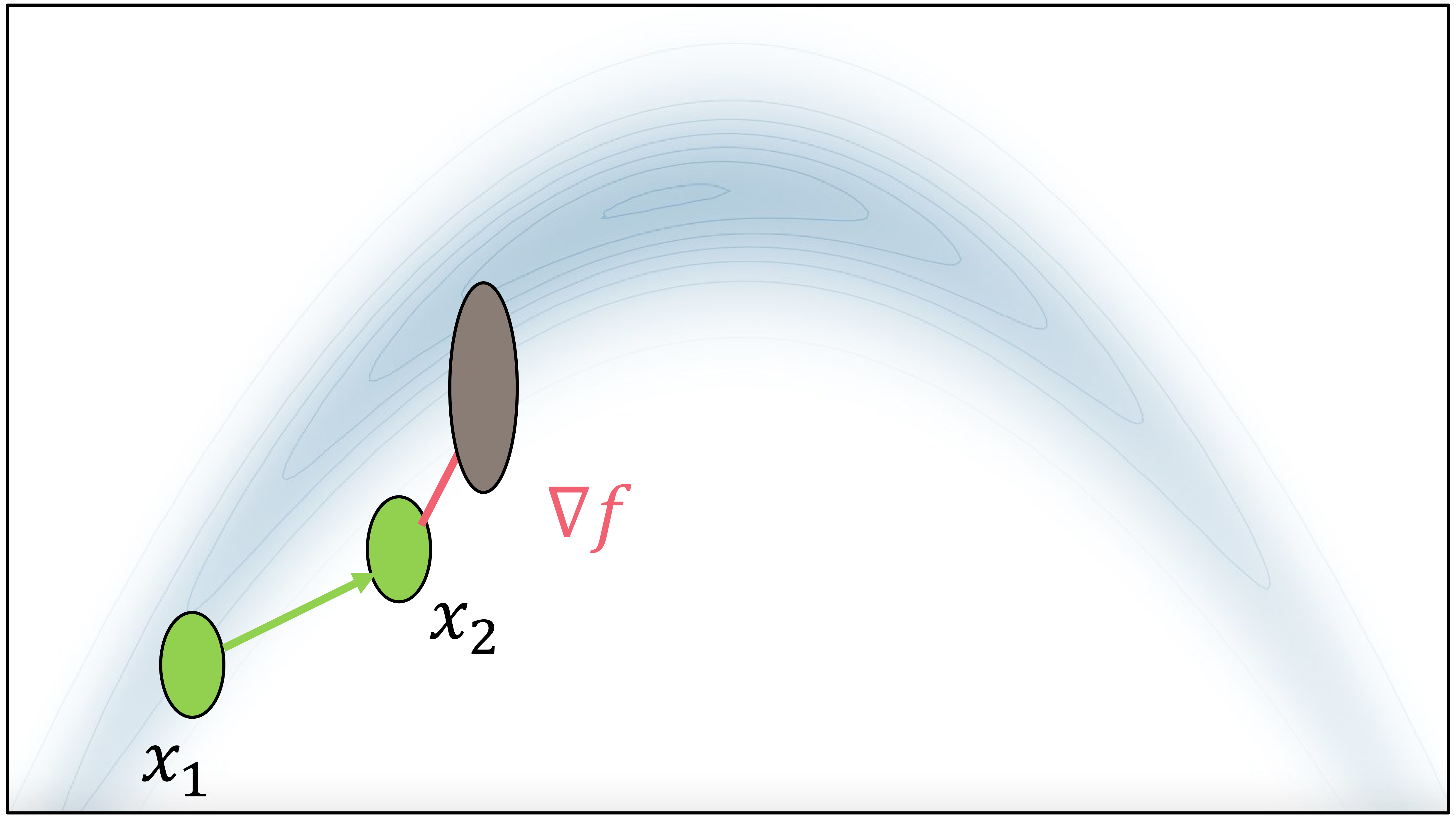

Sampling problem:

$$\boldsymbol{x}_t \sim f$$

Langevin MC:

$$\boldsymbol{x}_t = \boldsymbol{x}_{t-1} + s_{t-1}\nabla f(\boldsymbol{x}_{t-1}) + \frac{1}{s_{t-1}} N(0, \sigma^2 \boldsymbol{I})$$

Apply Metropolis Hastings to accept/reject

[Luan et al., 2020]

LMC OVERVIEW

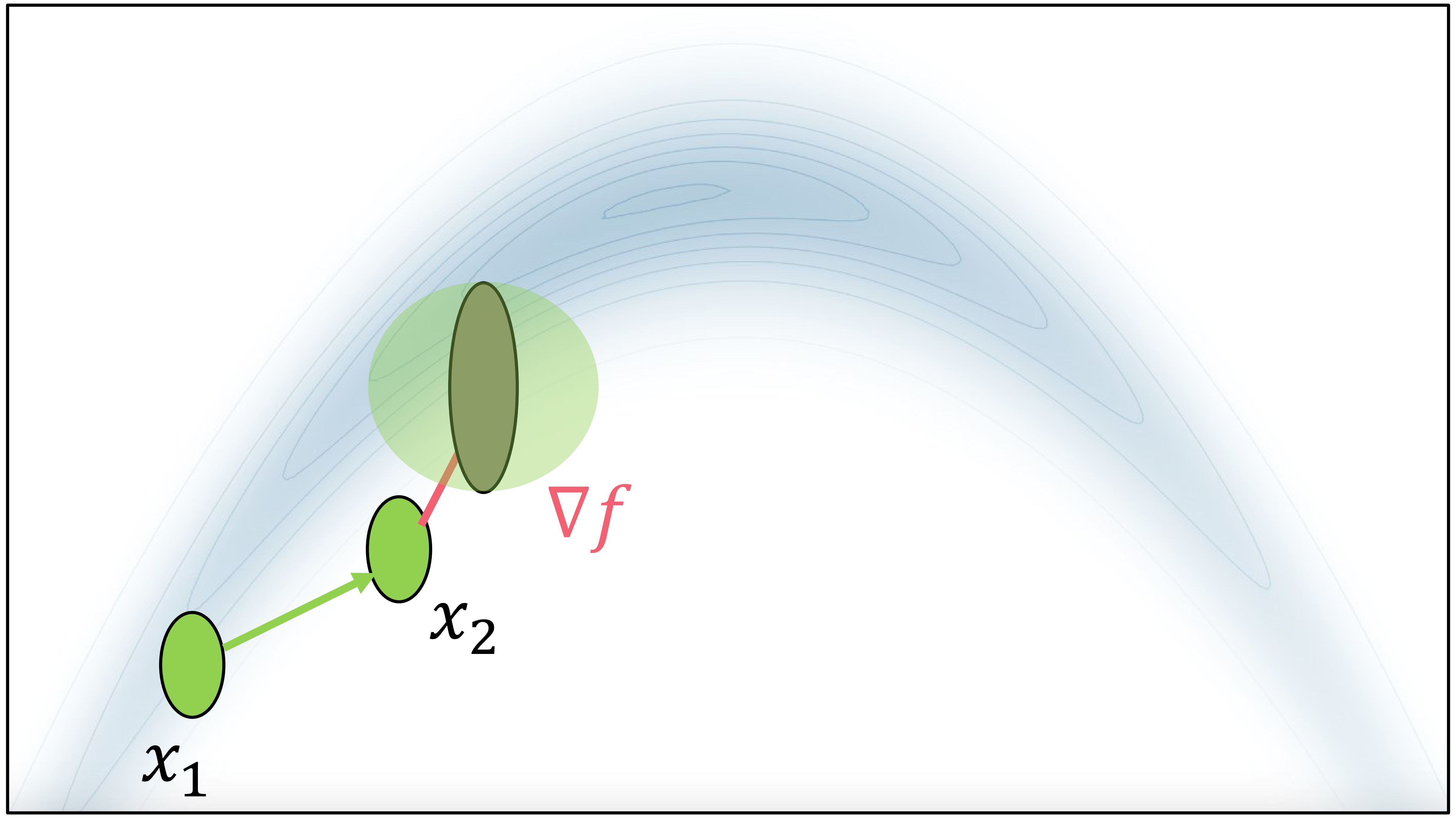

Sampling problem:

$$\boldsymbol{x}_t \sim f$$

Langevin MC:

$$\boldsymbol{x}_t = \boldsymbol{x}_{t-1} + s_{t-1}\nabla f(\boldsymbol{x}_{t-1}) + \frac{1}{s_{t-1}} N(0, \sigma^2 \boldsymbol{I})$$

Apply Metropolis Hastings to accept/reject

[Luan et al., 2020]

LMC OVERVIEW

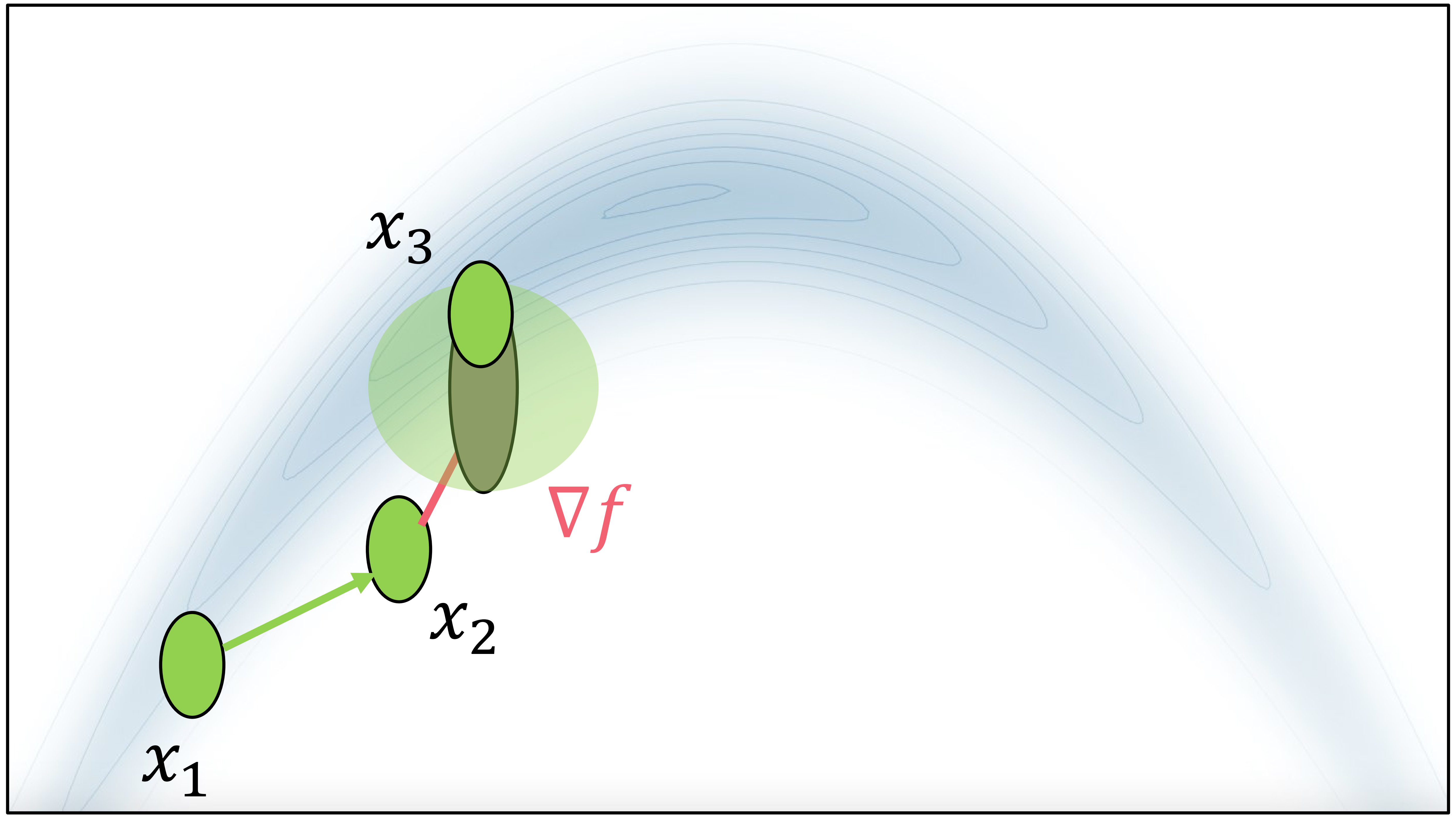

Sampling problem:

$$\boldsymbol{x}_t \sim f$$

Langevin MC:

$$\boldsymbol{x}_t = \boldsymbol{x}_{t-1} + s_{t-1} \nabla f(\boldsymbol{x}_{t-1}) + \frac{1}{s_{t-1}} N(0, \sigma^2 \boldsymbol{I})$$

Apply Metropolis Hastings to accept/reject

[Luan et al., 2020]

LMC OVERVIEW

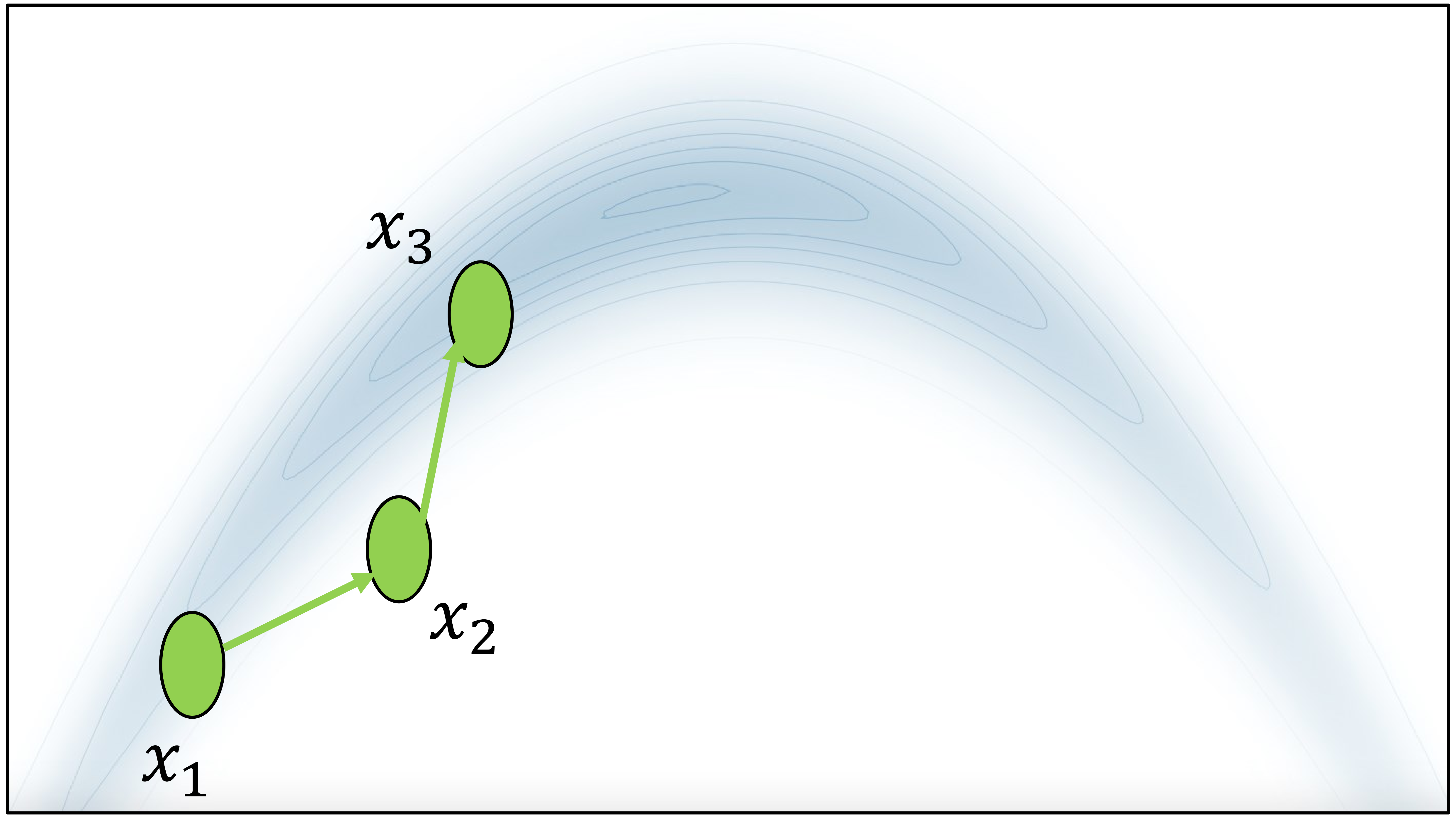

Sampling problem:

$$\boldsymbol{x}_t \sim f$$

Langevin MC:

$$\boldsymbol{x}_t = \boldsymbol{x}_{t-1} + s_{t-1} \nabla f(\boldsymbol{x}_{t-1}) + \frac{1}{s_{t-1}} N(0, \sigma^2 \boldsymbol{I})$$

Apply Metropolis Hastings to accept/reject

[Luan et al., 2020]

GD VS. LMC

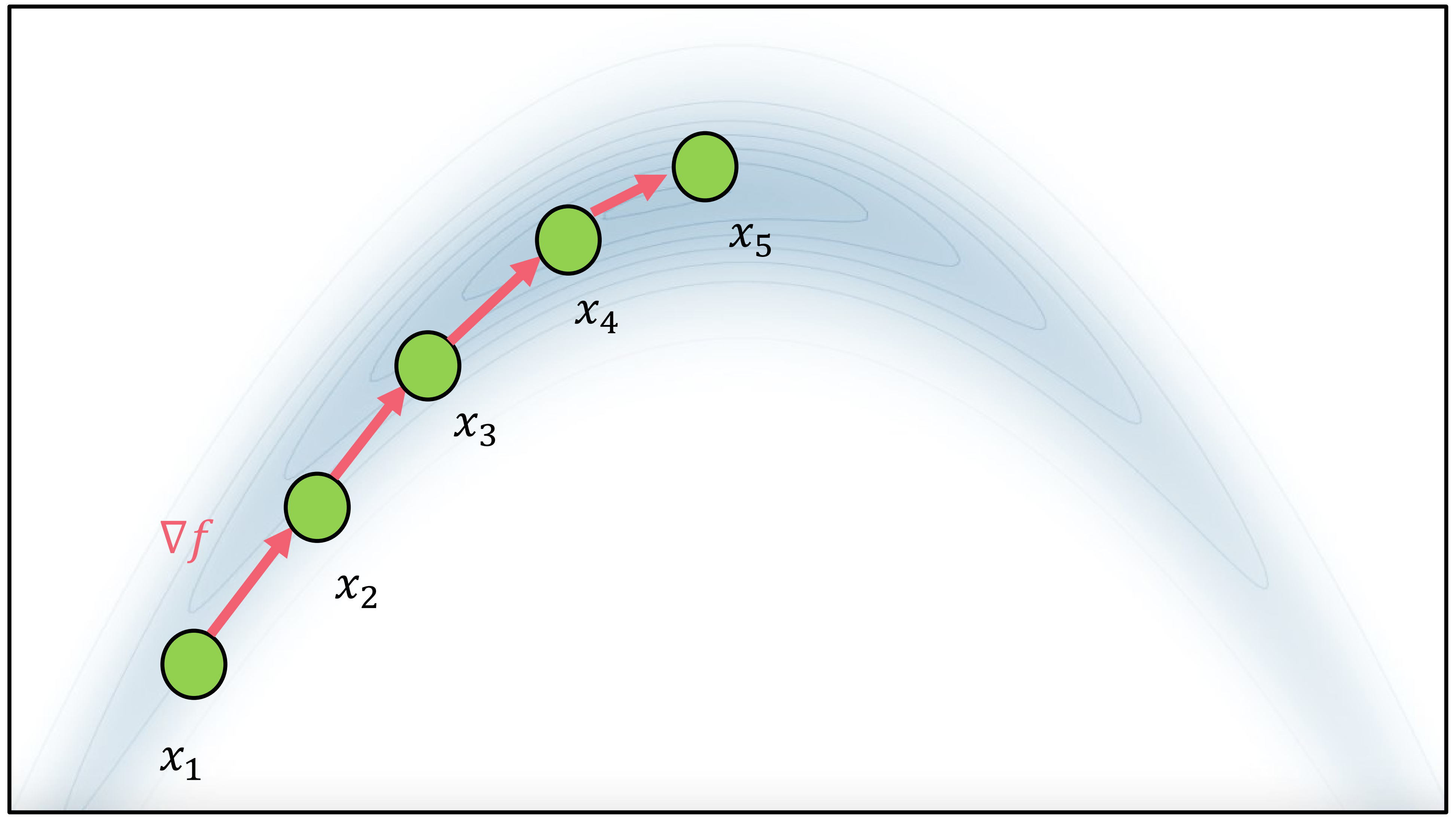

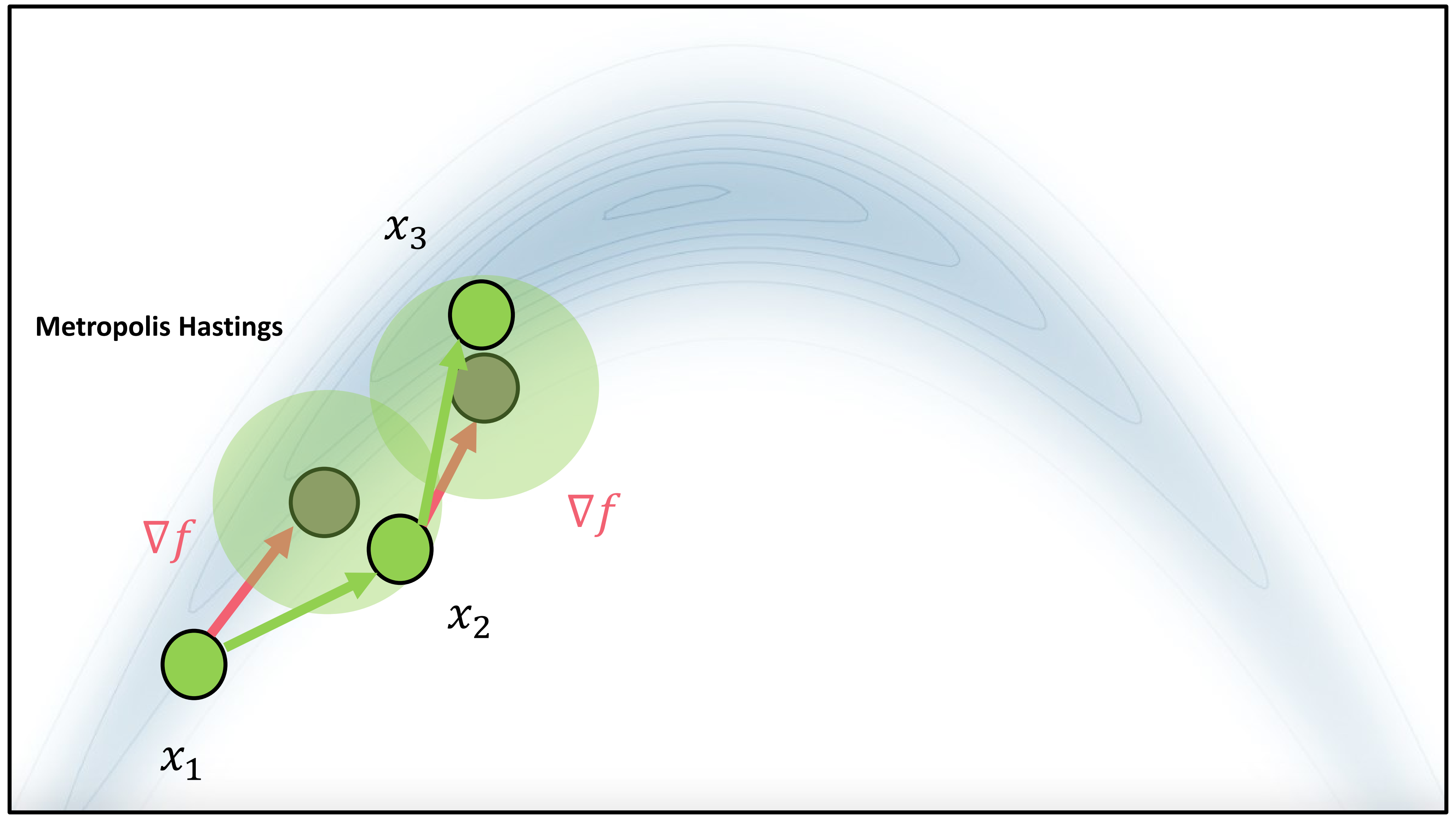

Optimization:

$$\max_{\boldsymbol{x}} f(\boldsymbol{x})$$

GD:

$$\boldsymbol{x}_t = \boldsymbol{x}_{t-1} + s_{t-1} \nabla f(\boldsymbol{x}_{t-1})$$

Sampling:

$$\boldsymbol{x}_t \sim f$$

LMC:

$$\boldsymbol{x}_t = \boldsymbol{x}_{t-1} + s_{t-1} \nabla f(\boldsymbol{x}_{t-1}) + \frac{1}{s_{t-1}} N(0, \sigma^2 \boldsymbol{I})$$

[Luan et al., 2020]

GD VS. LMC

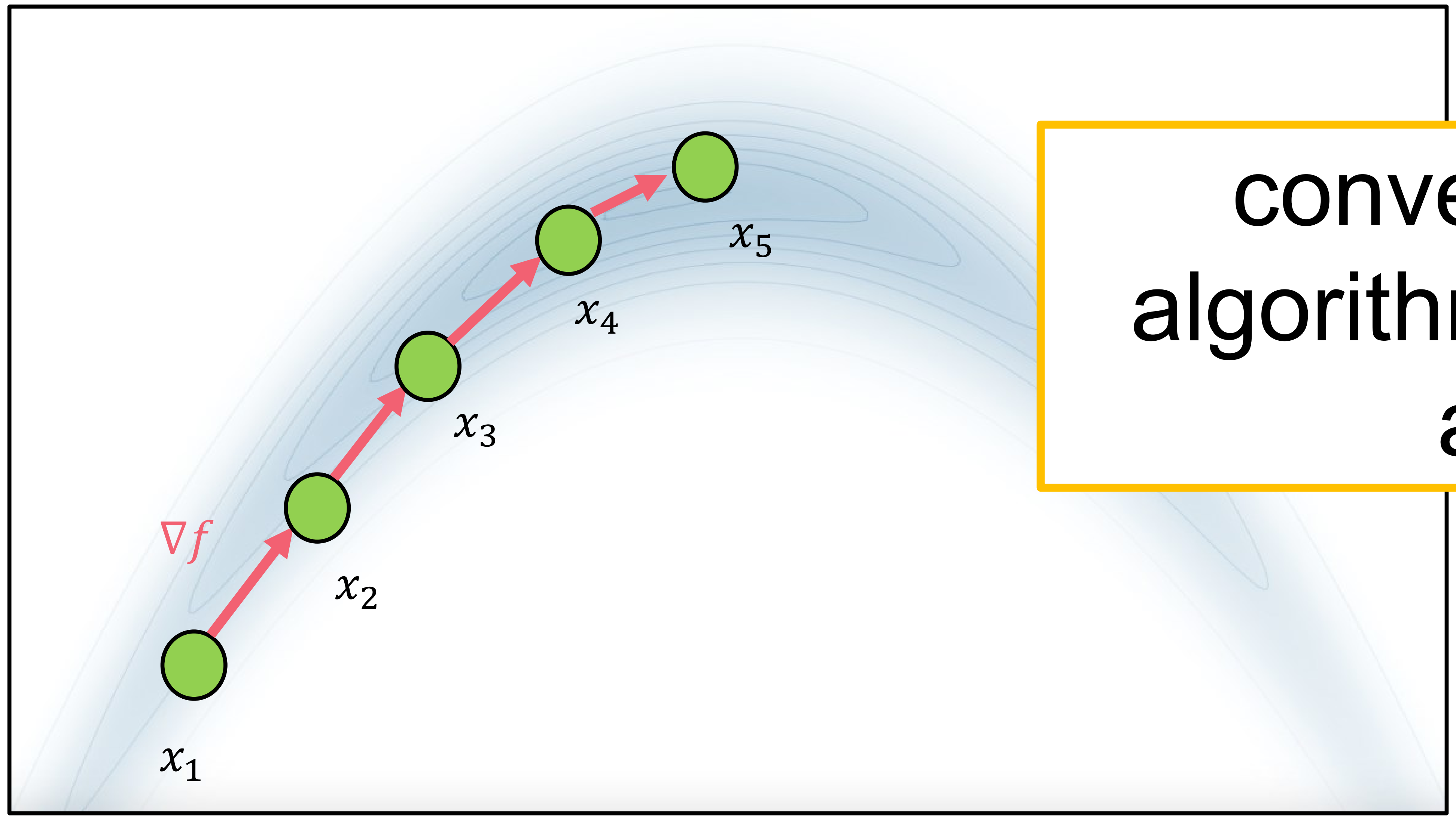

convert optimization algorithms into rendering algorithms

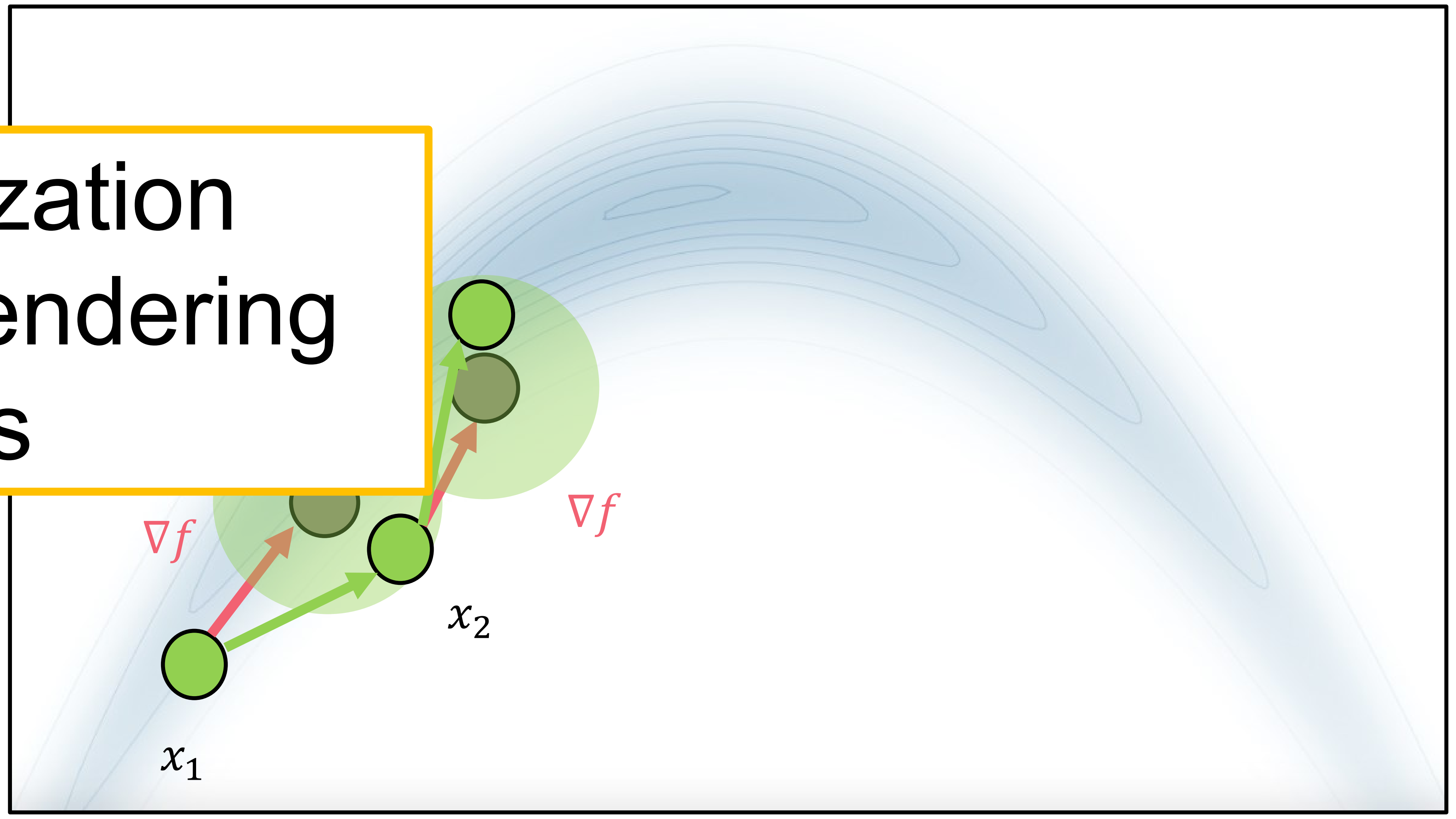

Optimization:

$$\max_{\boldsymbol{x}} f(\boldsymbol{x})$$

GD:

$$\boldsymbol{x}_t = \boldsymbol{x}_{t-1} + s_{t-1} \nabla f(\boldsymbol{x}_{t-1})$$

Sampling:

$$\boldsymbol{x}_t \sim f$$

LMC:

$$\boldsymbol{x}_t = \boldsymbol{x}_{t-1} + s_{t-1} \nabla f(\boldsymbol{x}_{t-1}) + \frac{1}{s_{t-1}} N(0, \sigma^2 \boldsymbol{I})$$

[Luan et al., 2020]


SIGGRAPH
MCMC
LANGEVIN
2020
SIGGRAPH
Prior
10x acceleration
Ours


Prior
20x acceleration
Ours

Evaluating optical simulation framework

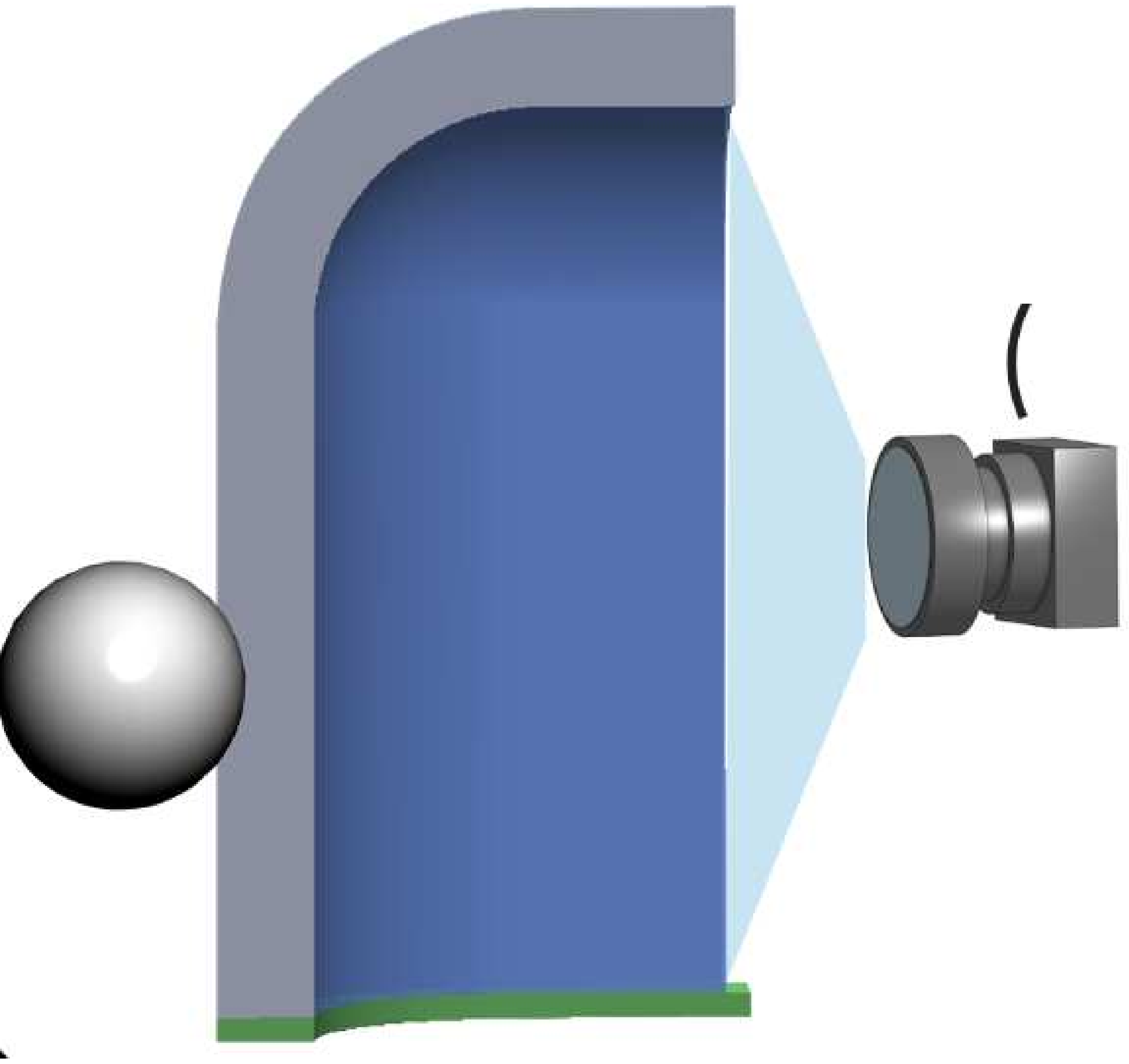

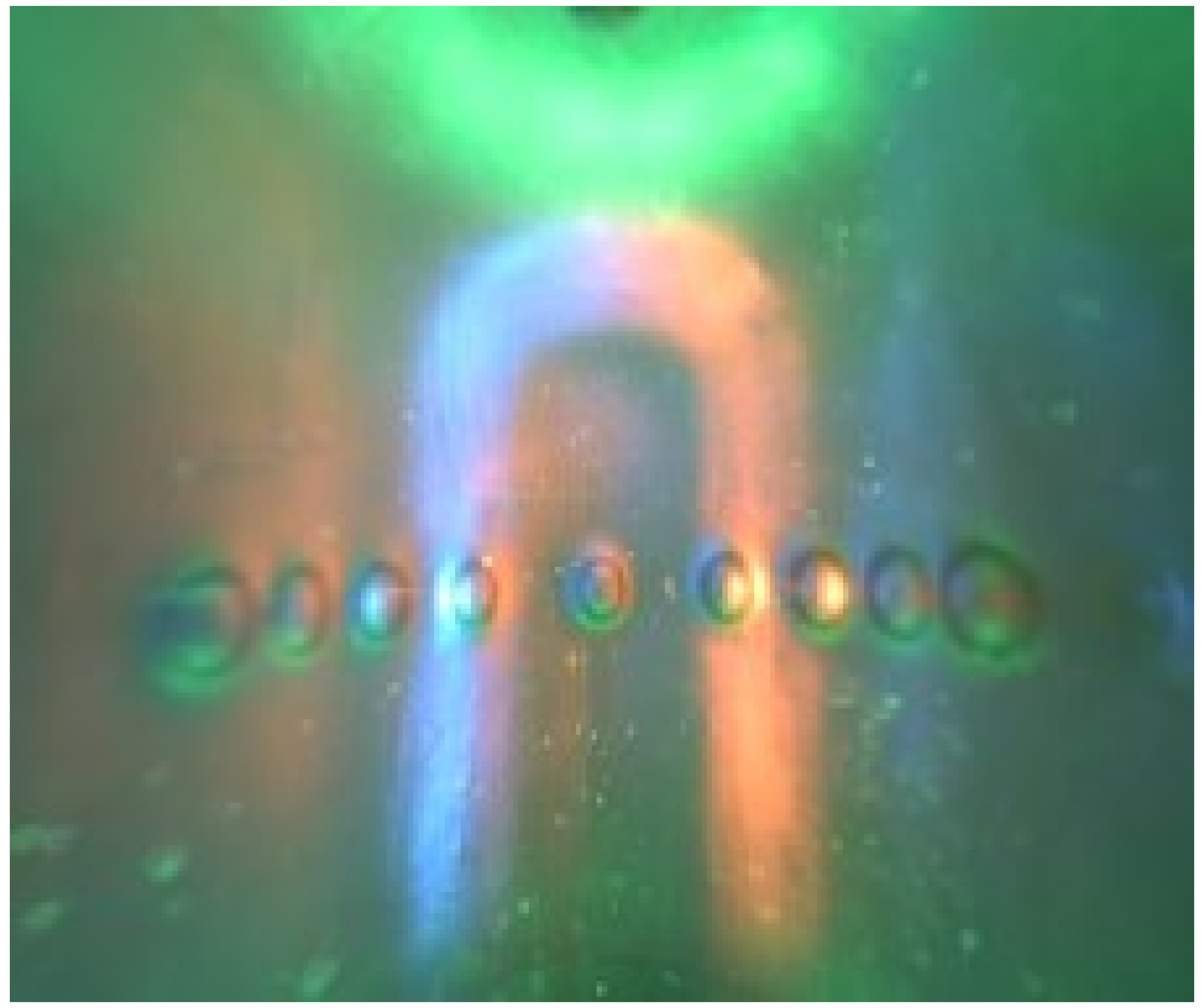

Real-world prototype

[Agarwal et al., 2023]

Evaluating optical simulation framework

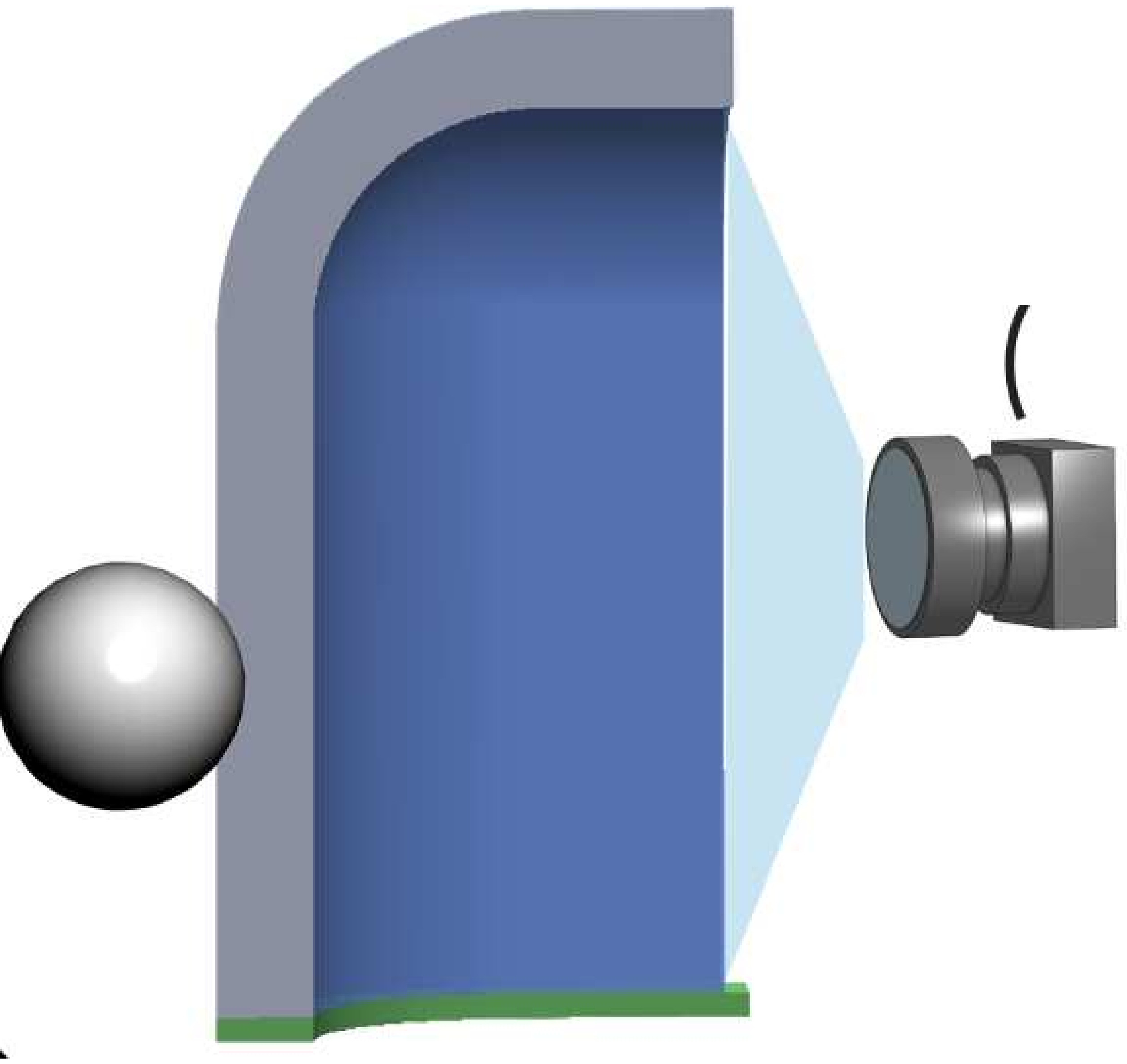

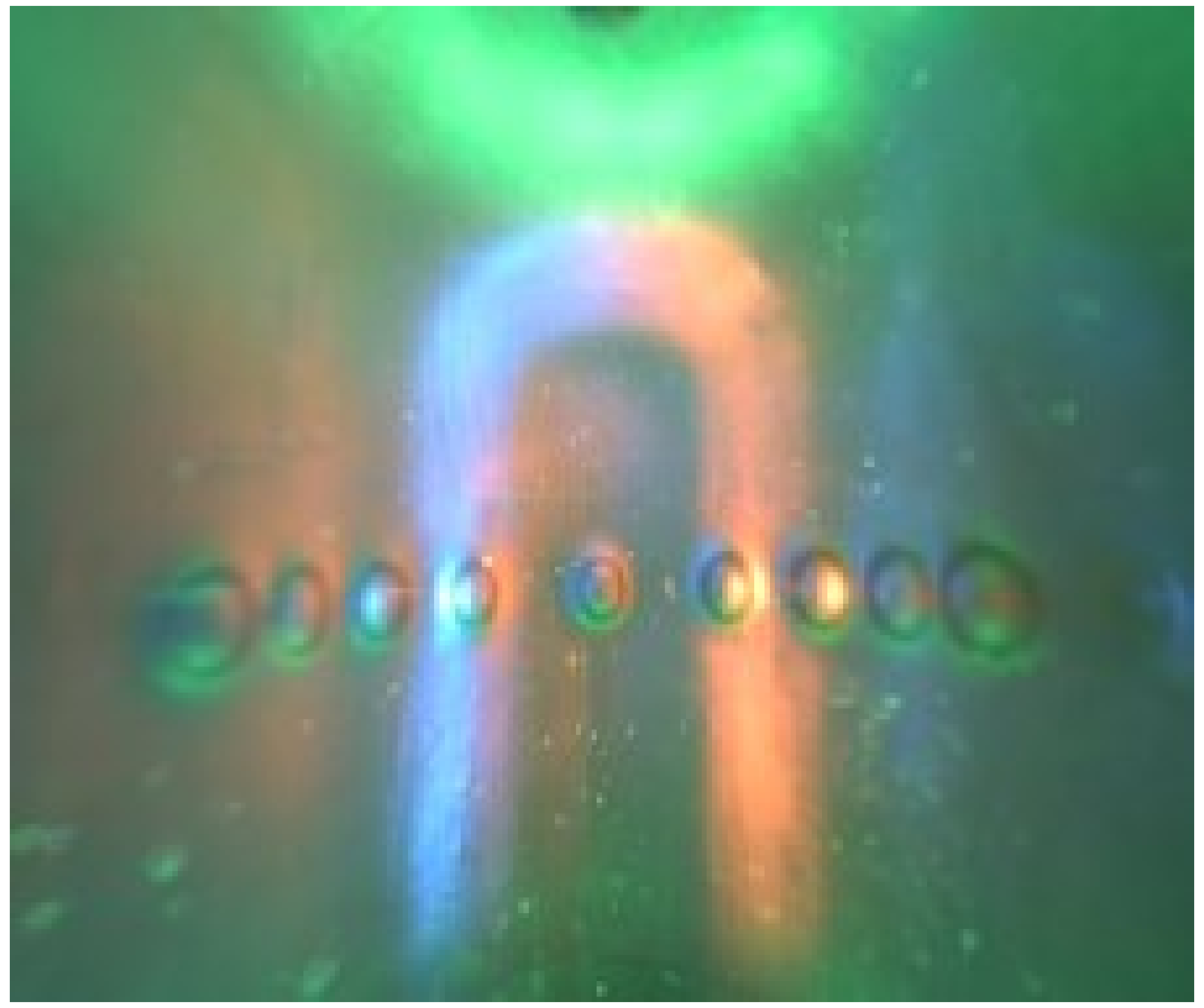

Real-world prototype

Rasterization

[Agarwal et al., 2023]

Evaluating optical simulation framework

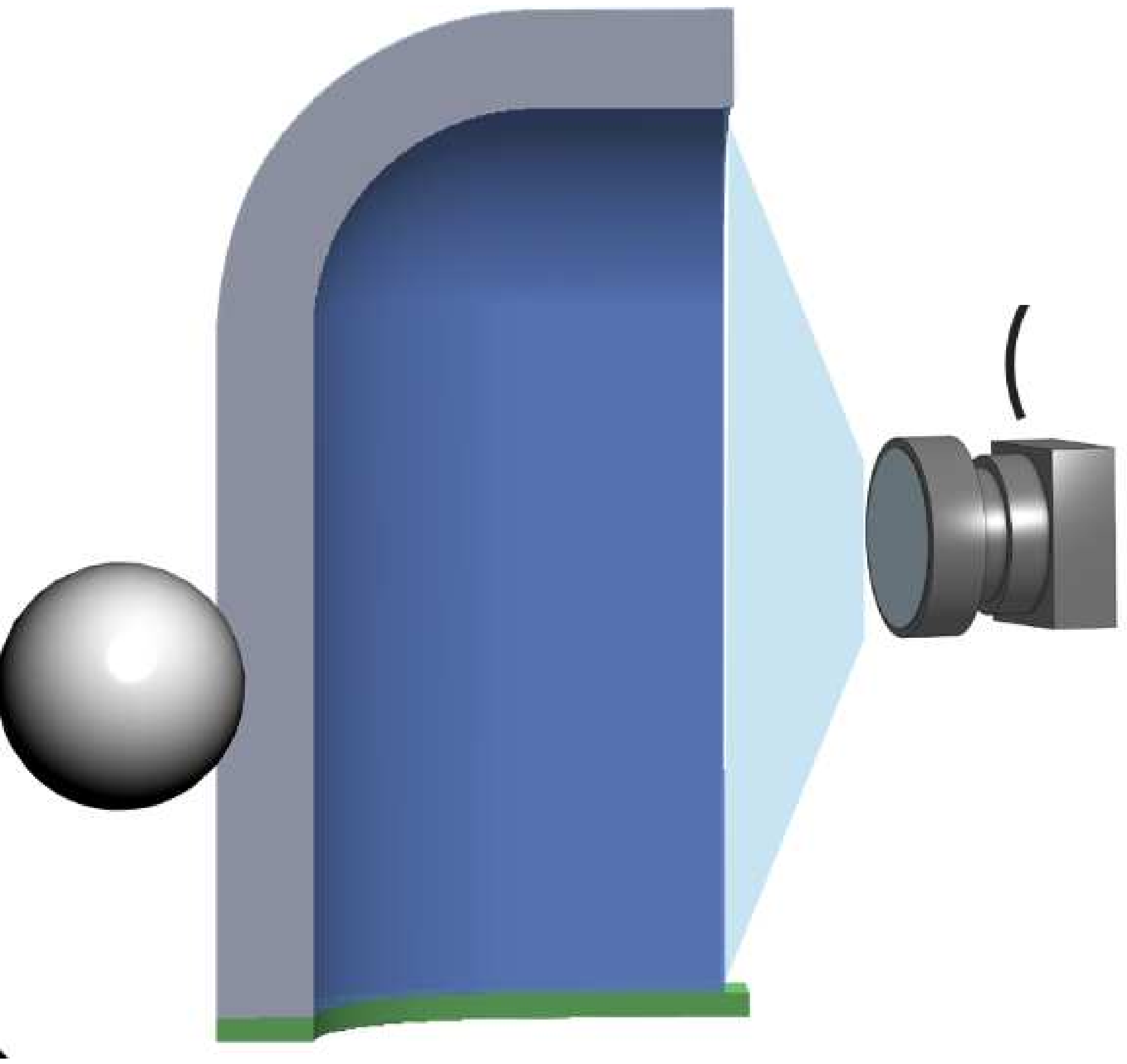

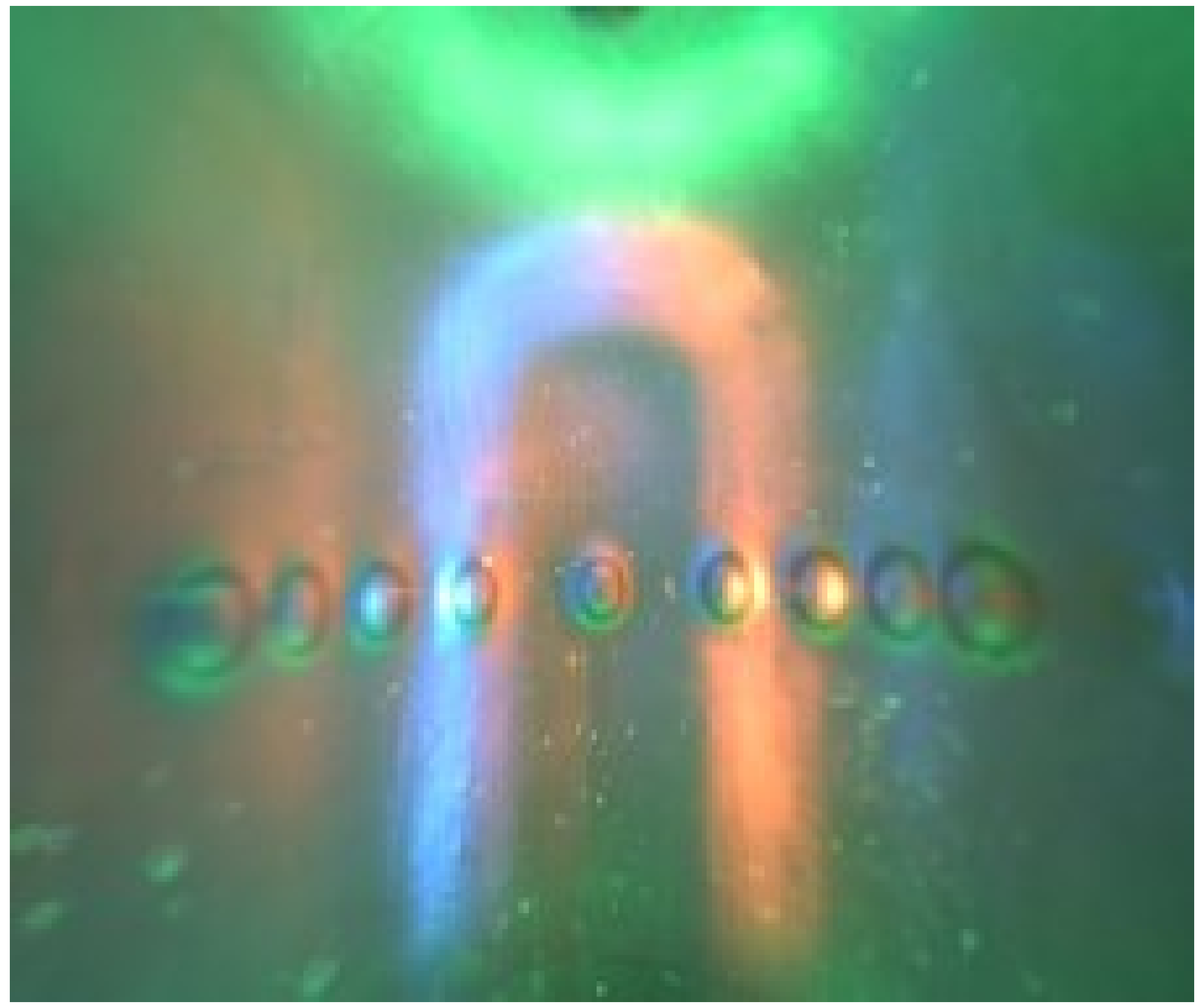

Real-world prototype

Rasterization

Path tracing

[Agarwal et al., 2023]

Evaluating optical simulation framework

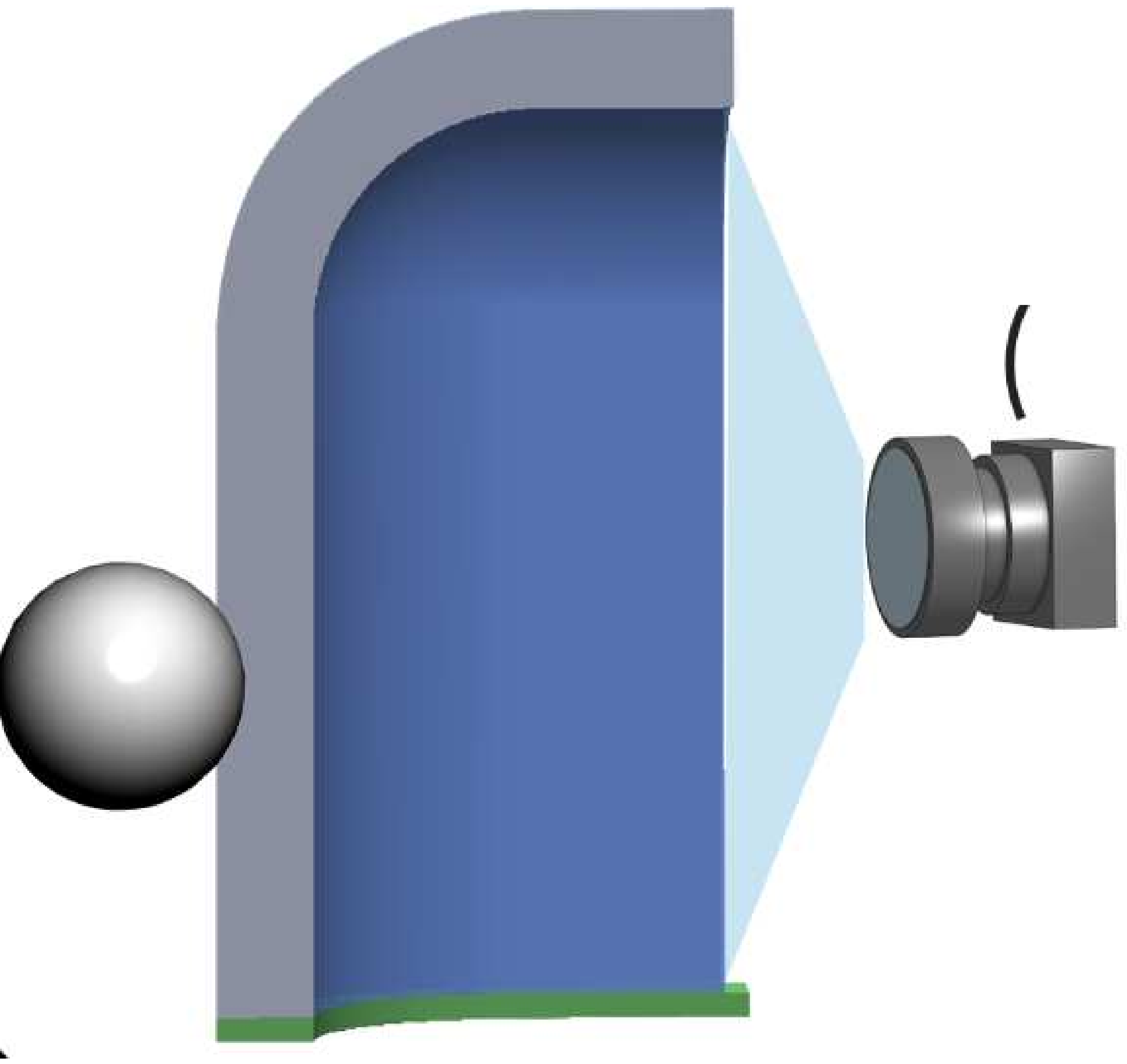

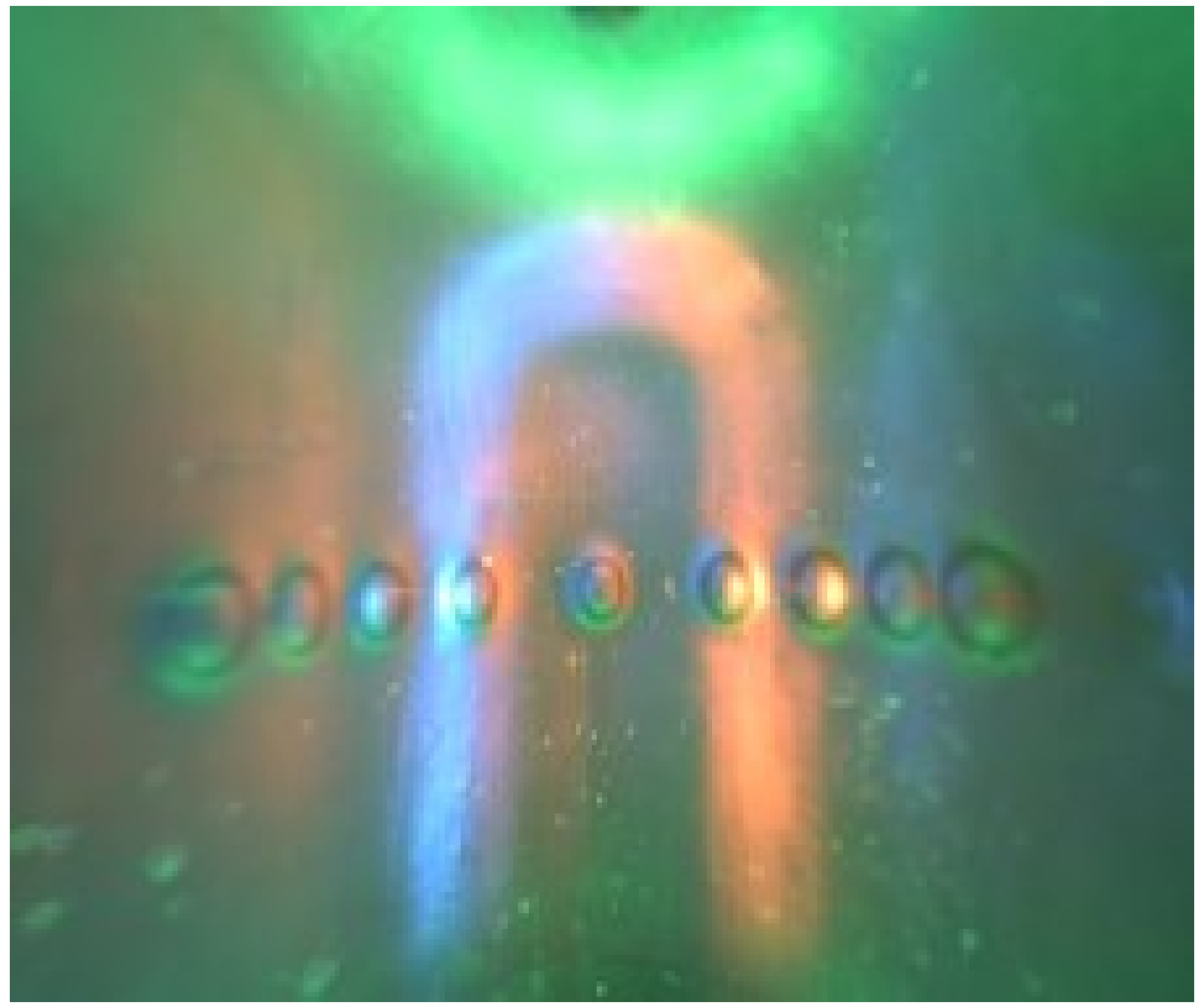

Real-world prototype

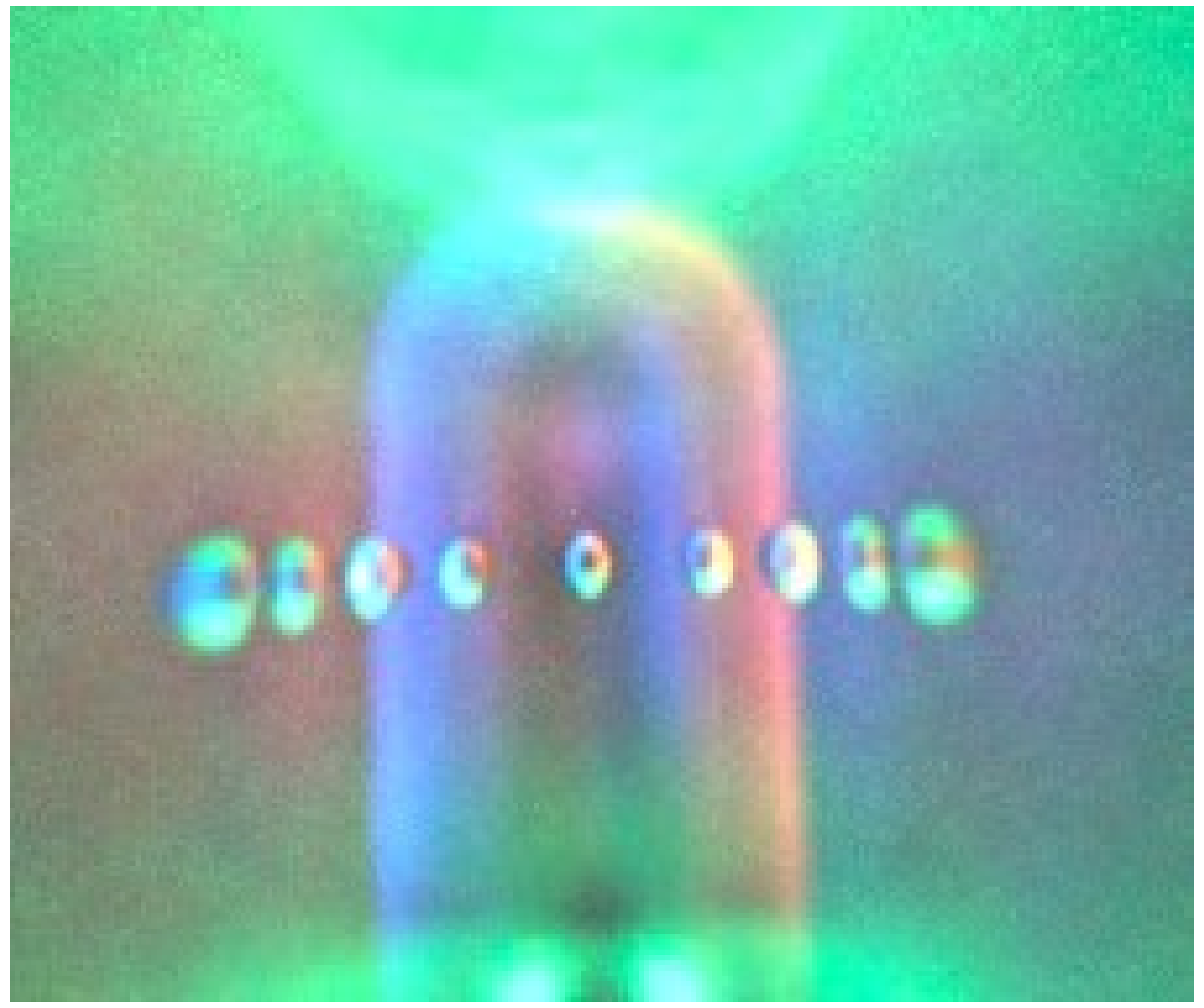

Our simulation result

Rasterization

Path tracing

[Agarwal et al., 2023]

Evaluating optical simulation framework

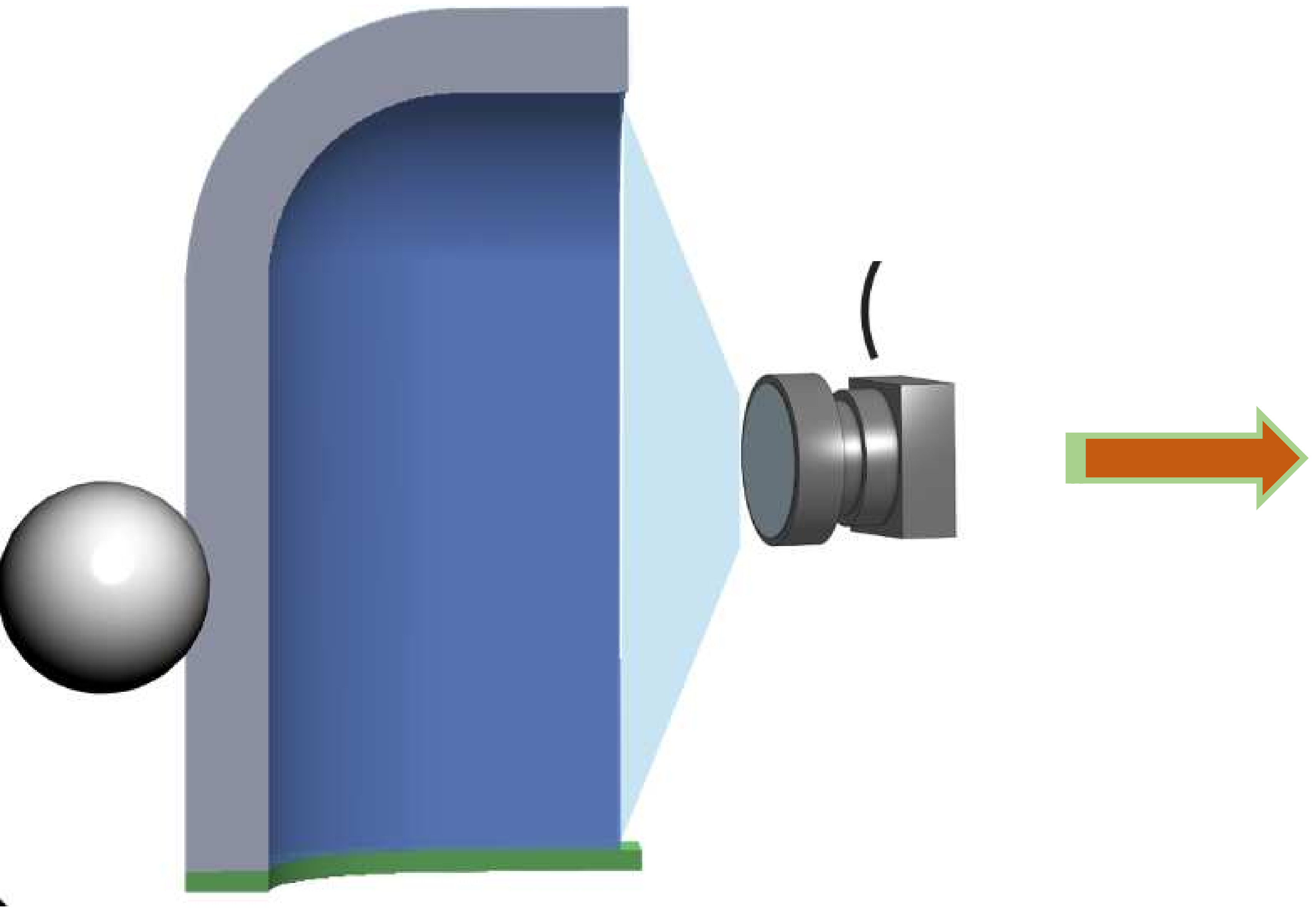

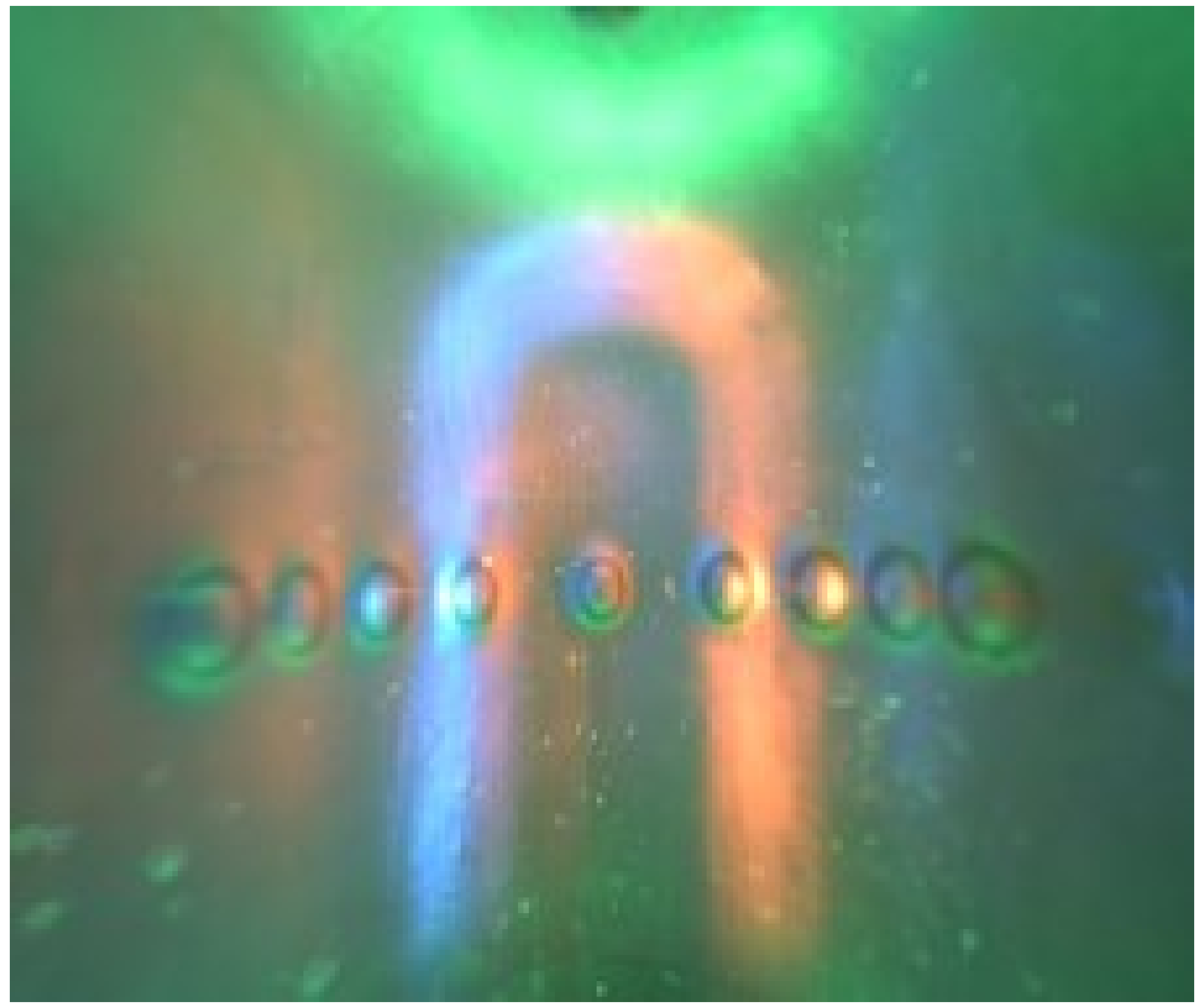

Real-world prototype

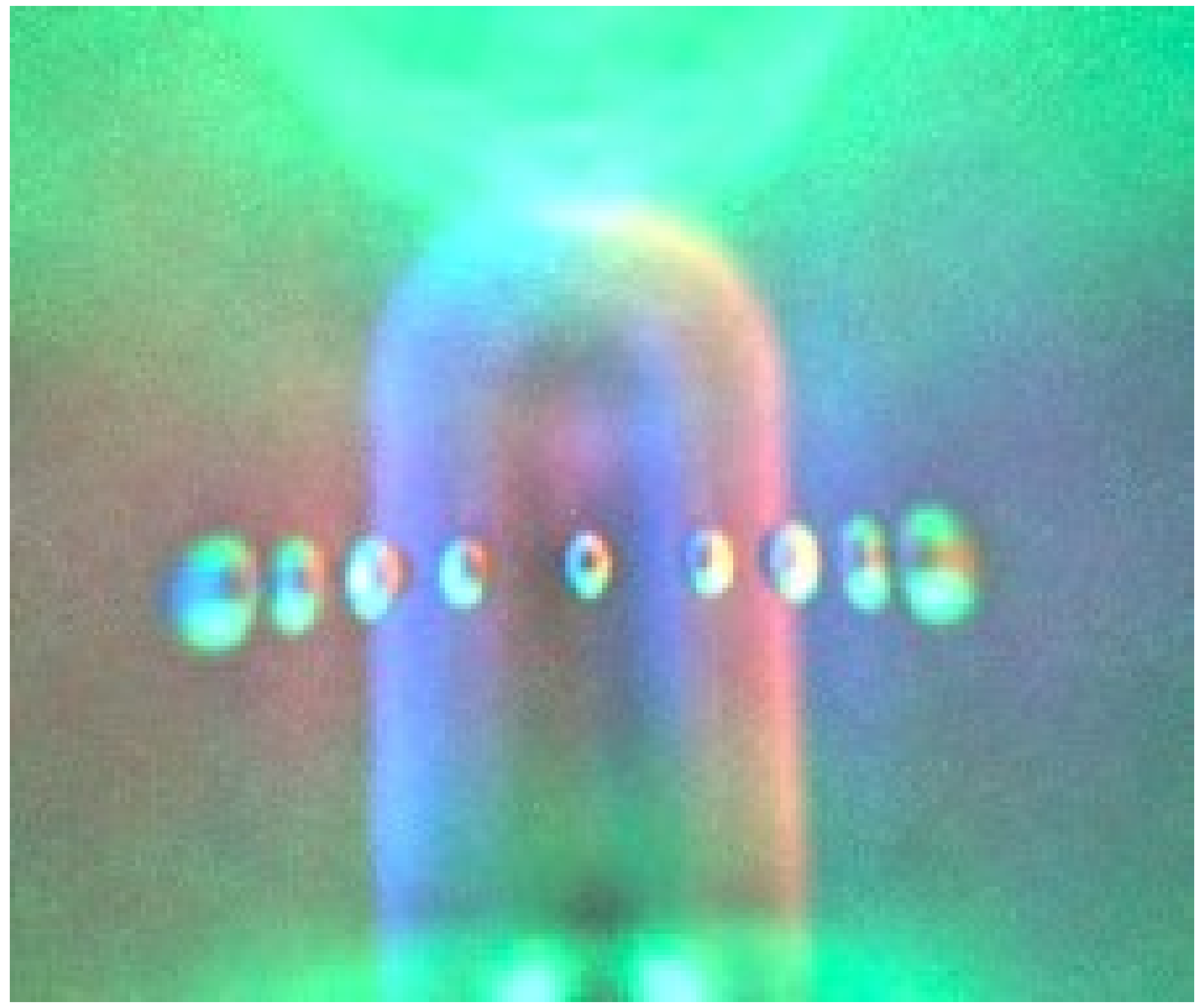

Our simulation result

Rasterization

Path tracing

[Agarwal et al., 2023]

Curved sensor material design

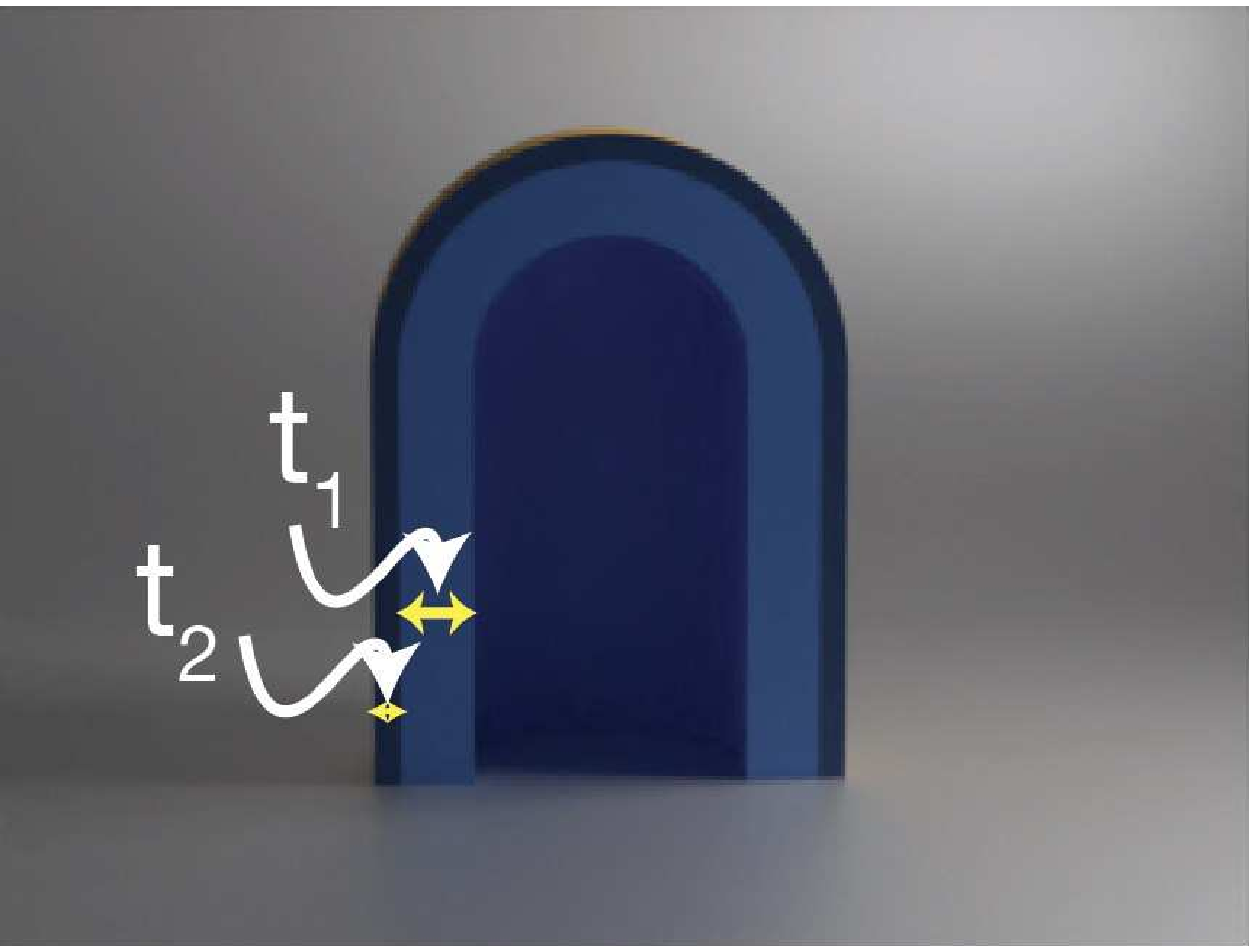

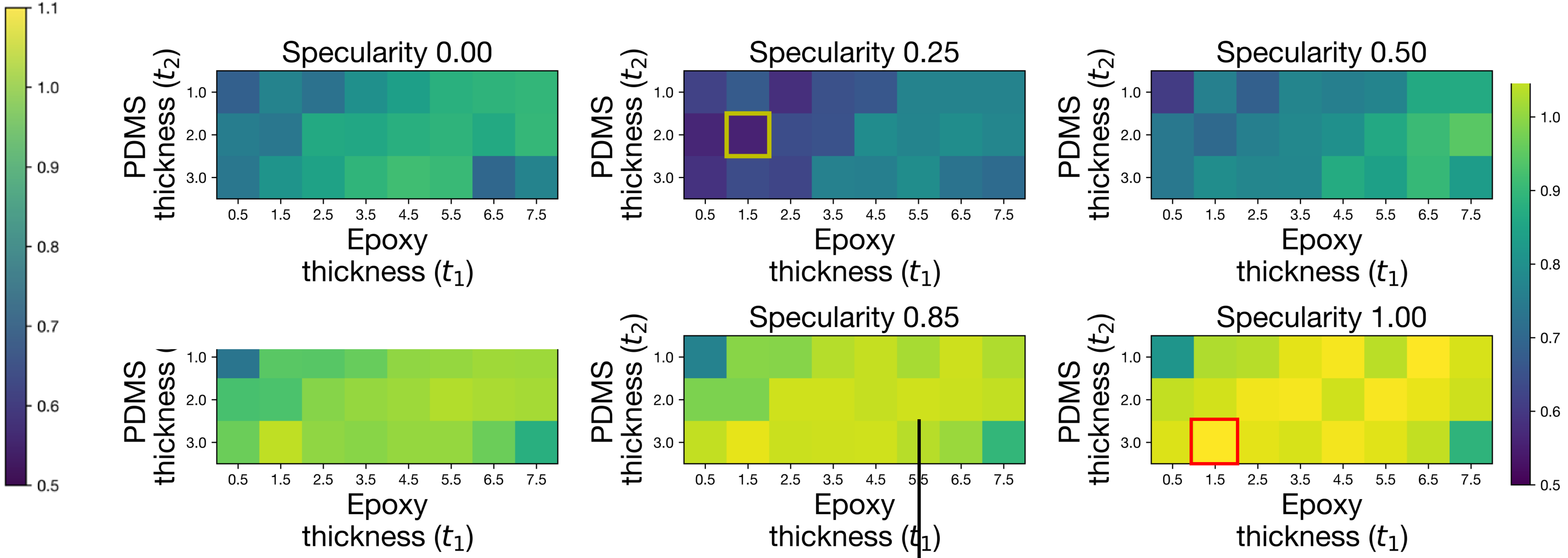

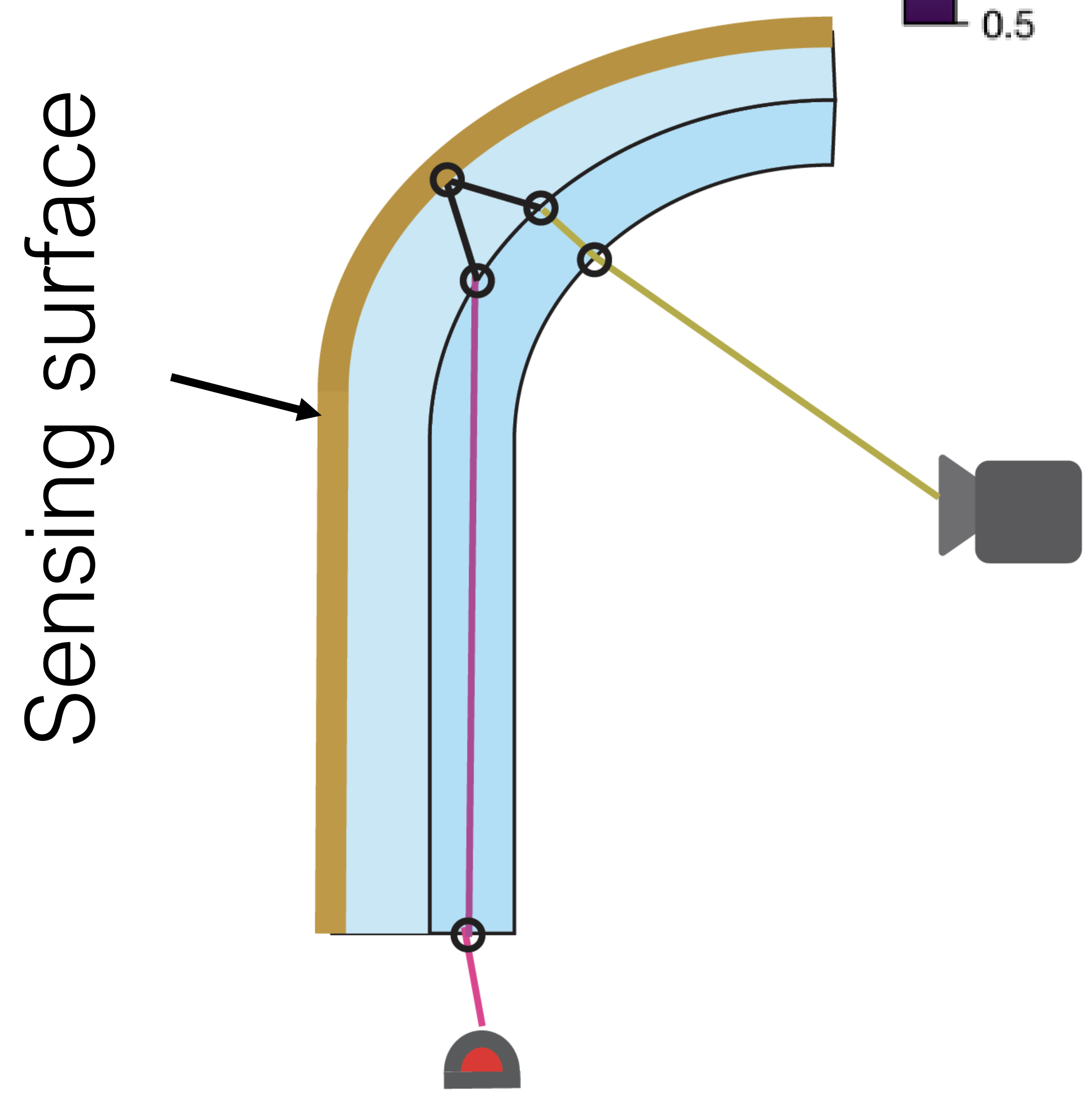

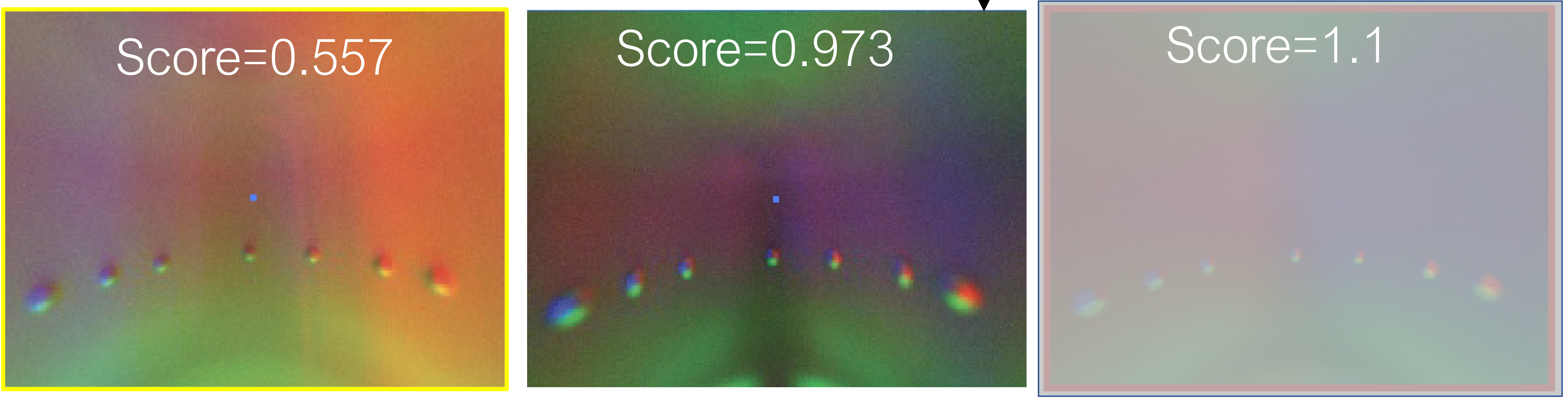

[Agarwal et al., 2023]

Curved sensor illumination design

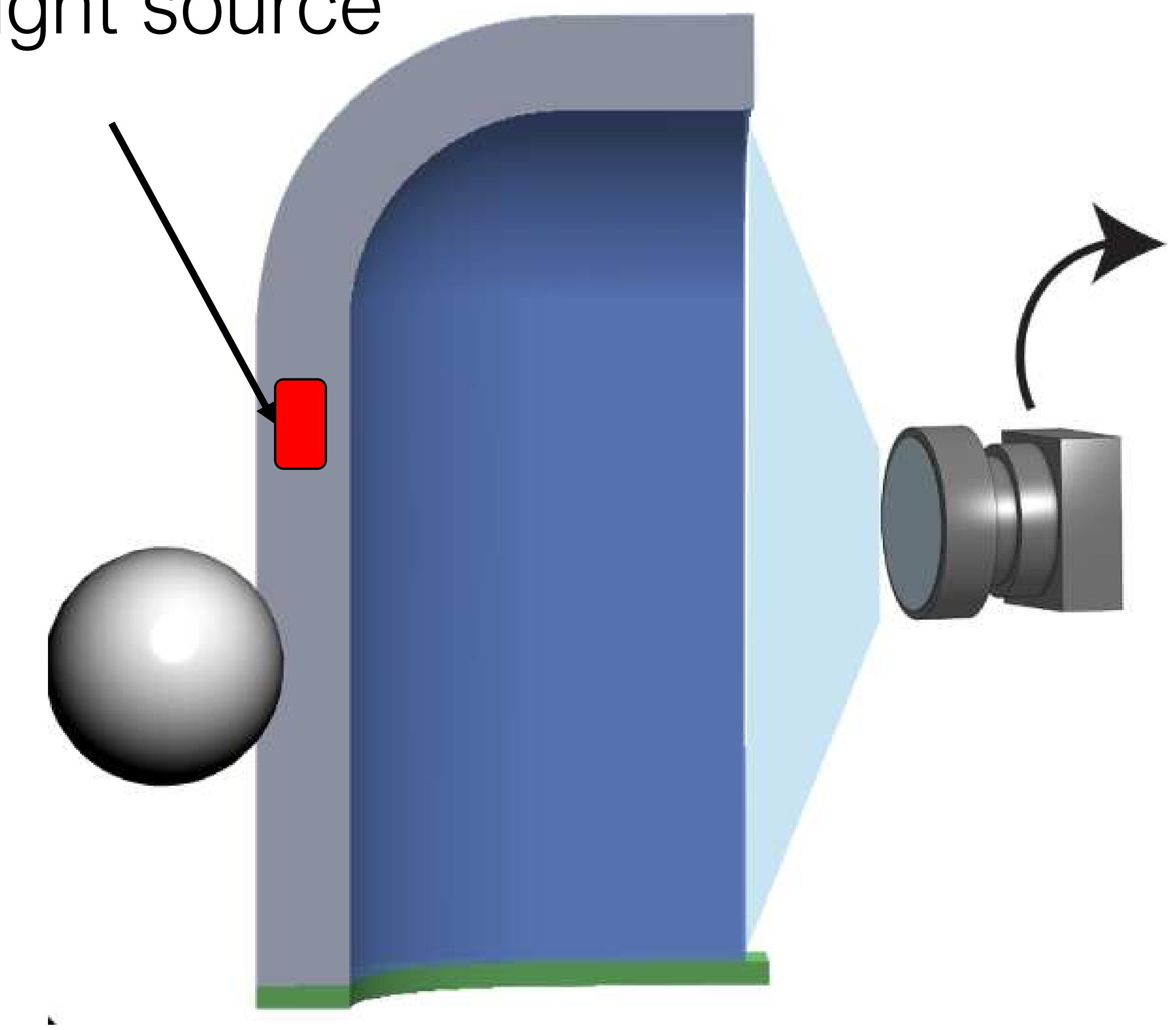

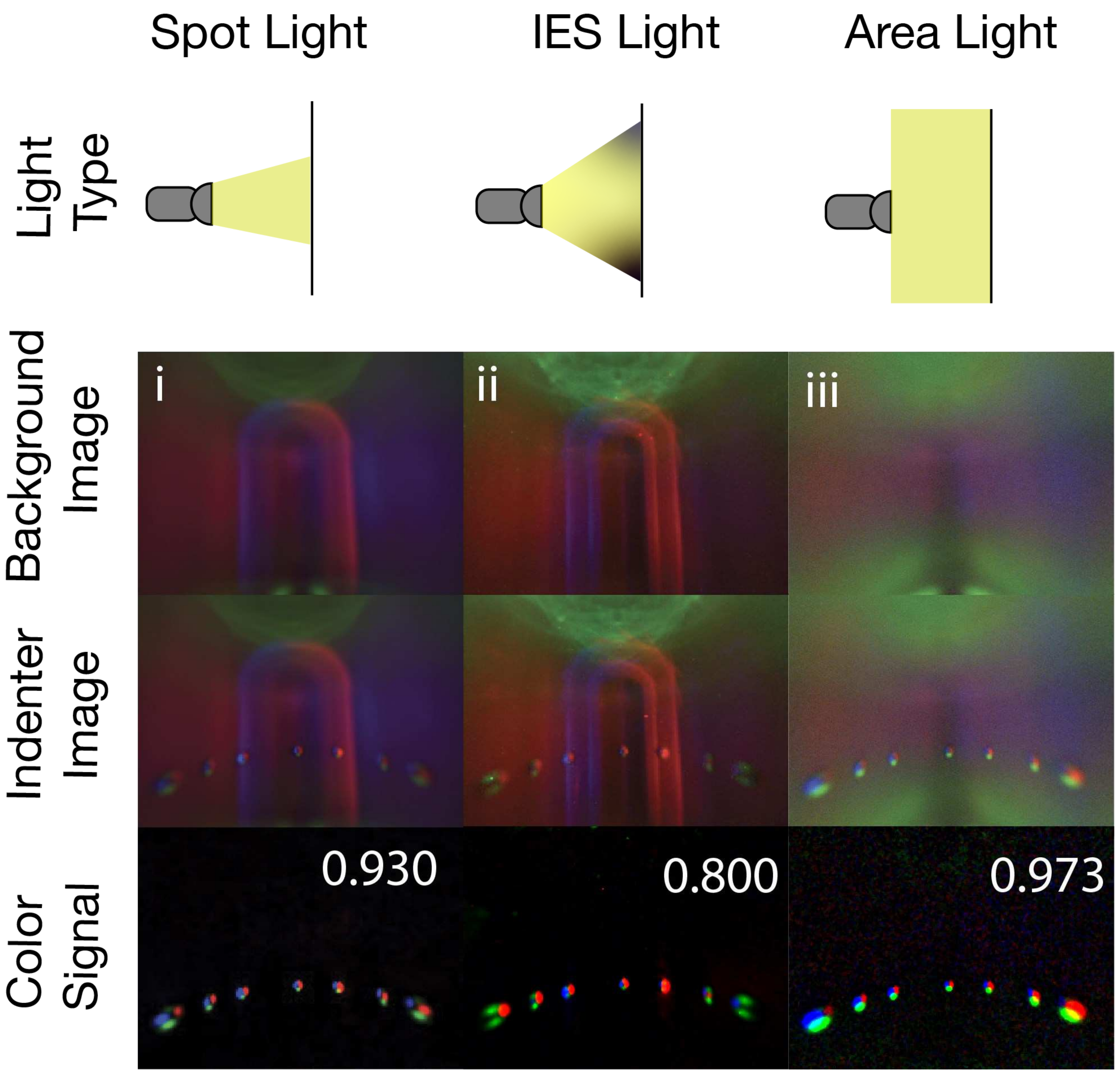

Curved sensor shape design

- Used gradient-free optimization, CMA-ES, for optimizing the sensor shape
- Optimized sensor design is 35% better than initial design
- Optimized sensor design outperforms human-expert design in 3D shape reconstruction

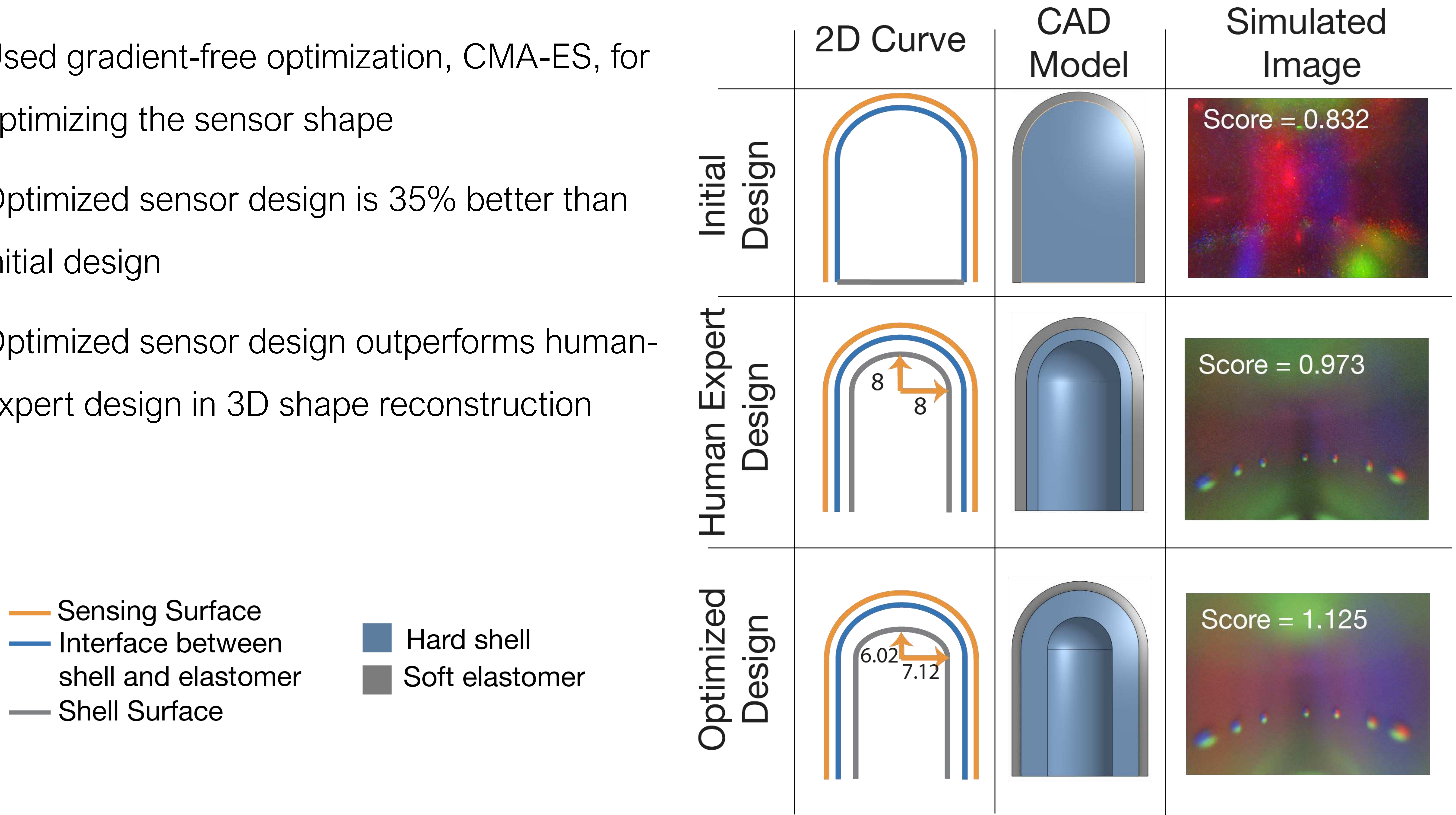

Results: Robotic grasping

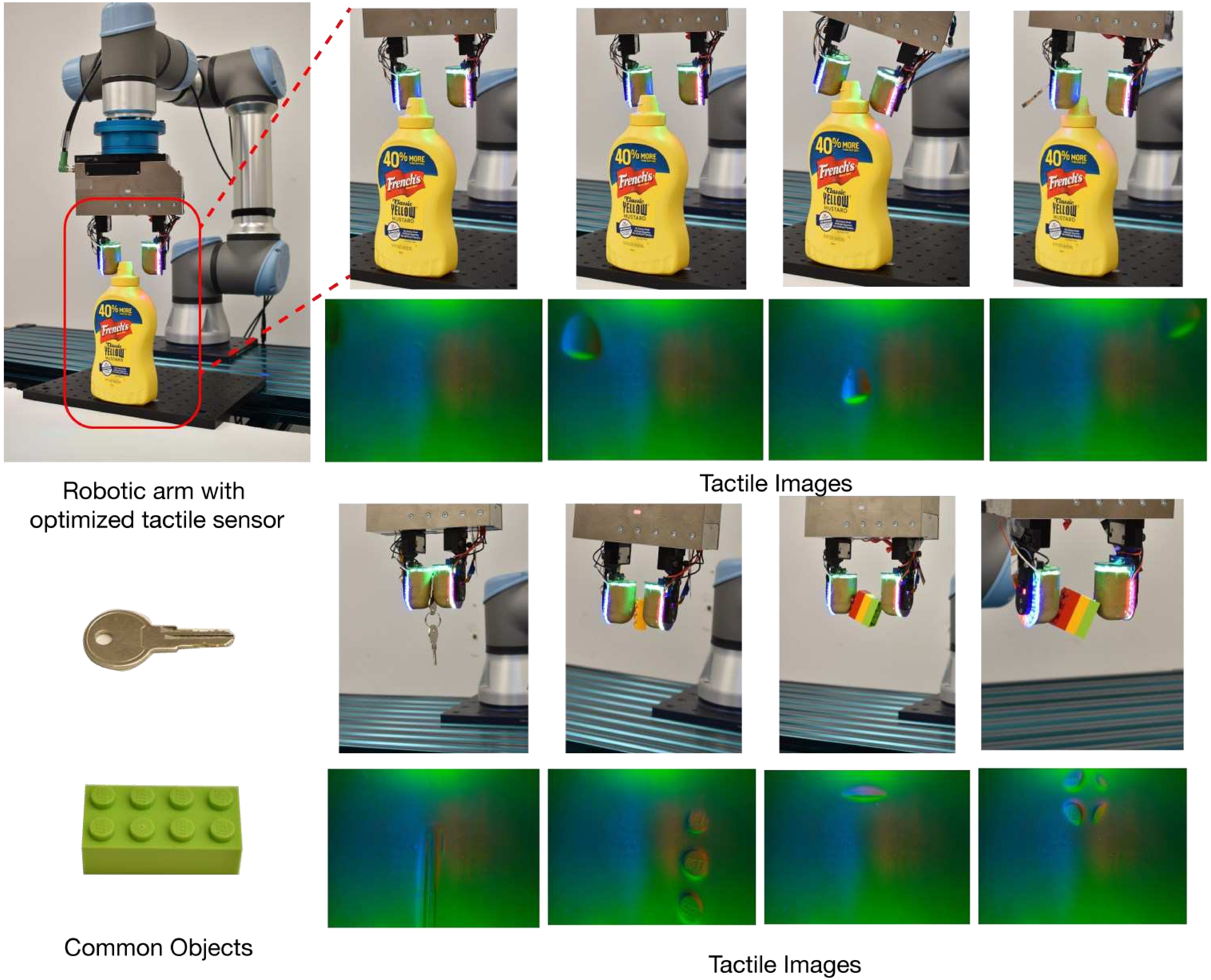

[Agarwal et al., 2023]

Results: surface inspection

Experiment 1: Detection accuracy vs text size

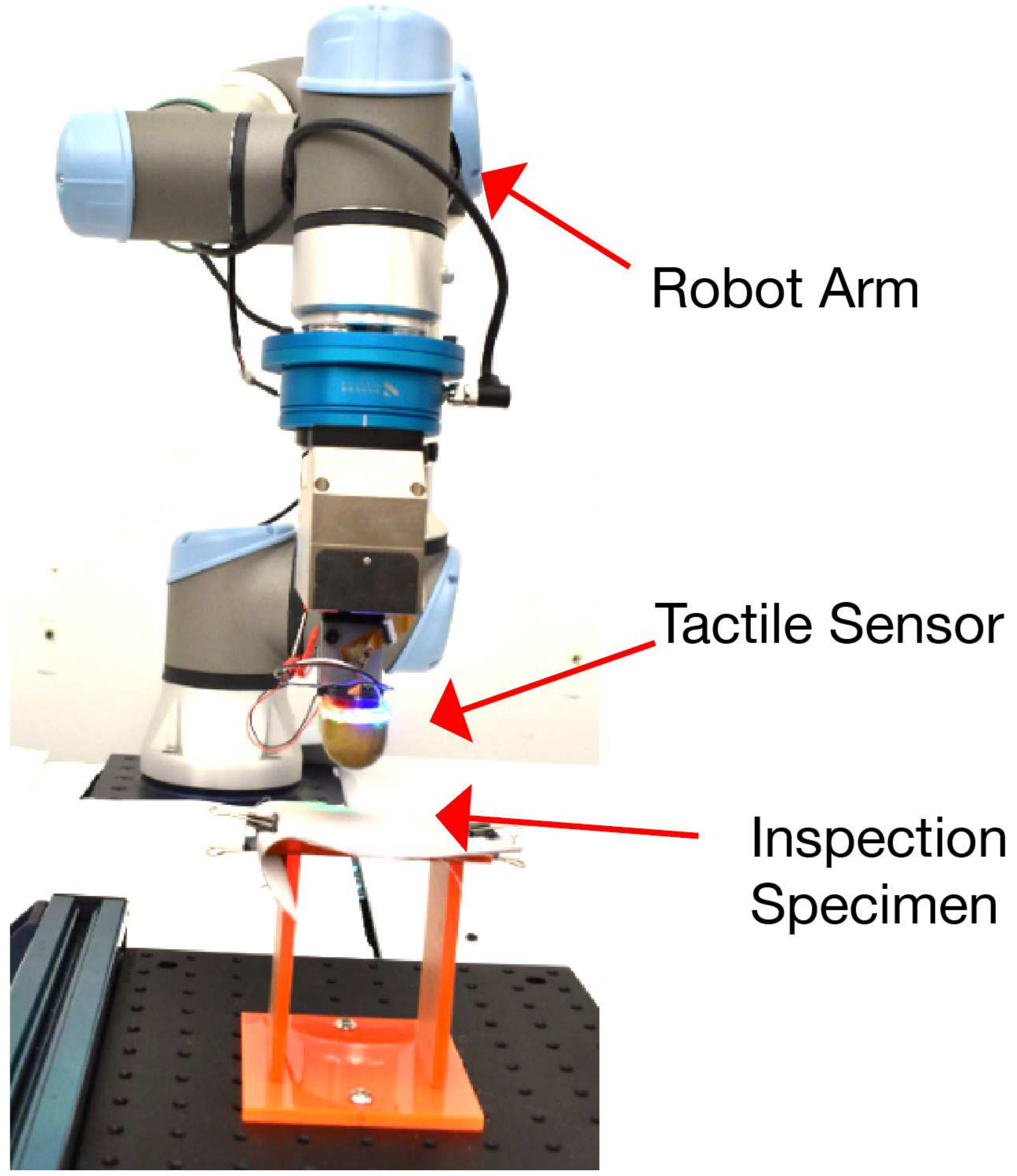

Experiment setup

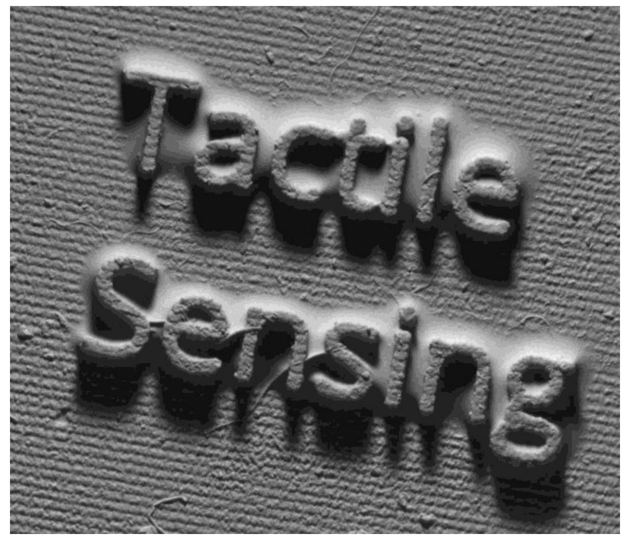

Text size = 1.5 mm

Text size = 1.0 mm

Text description:
Tactile
Sensing

Human expert design

Optimized design

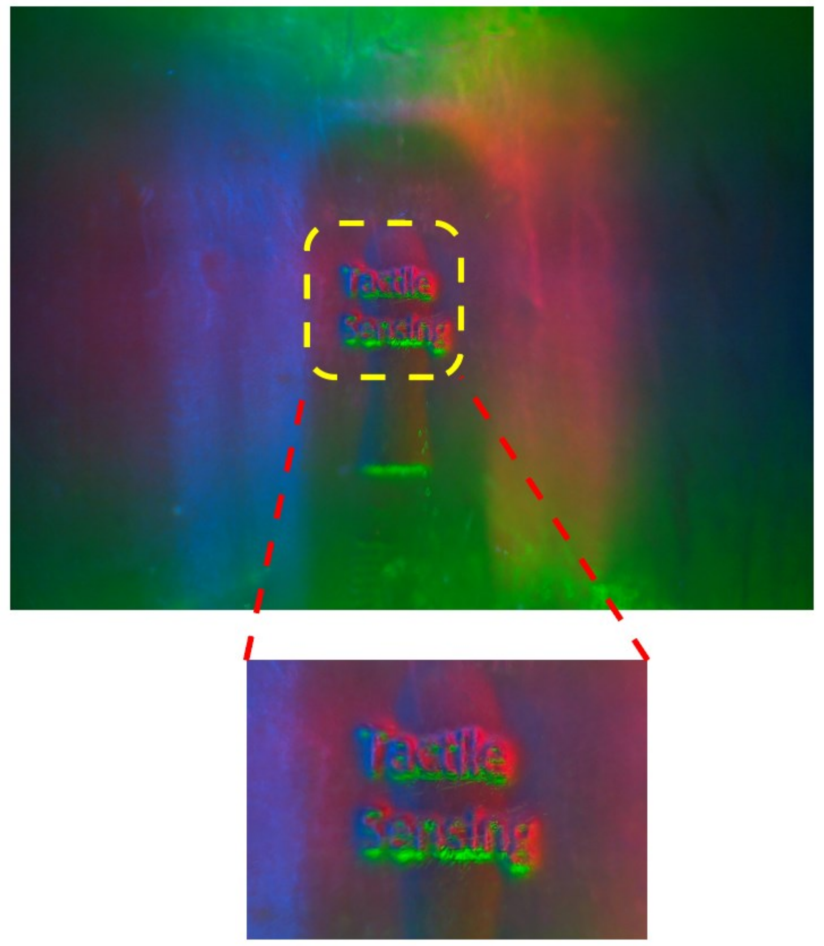

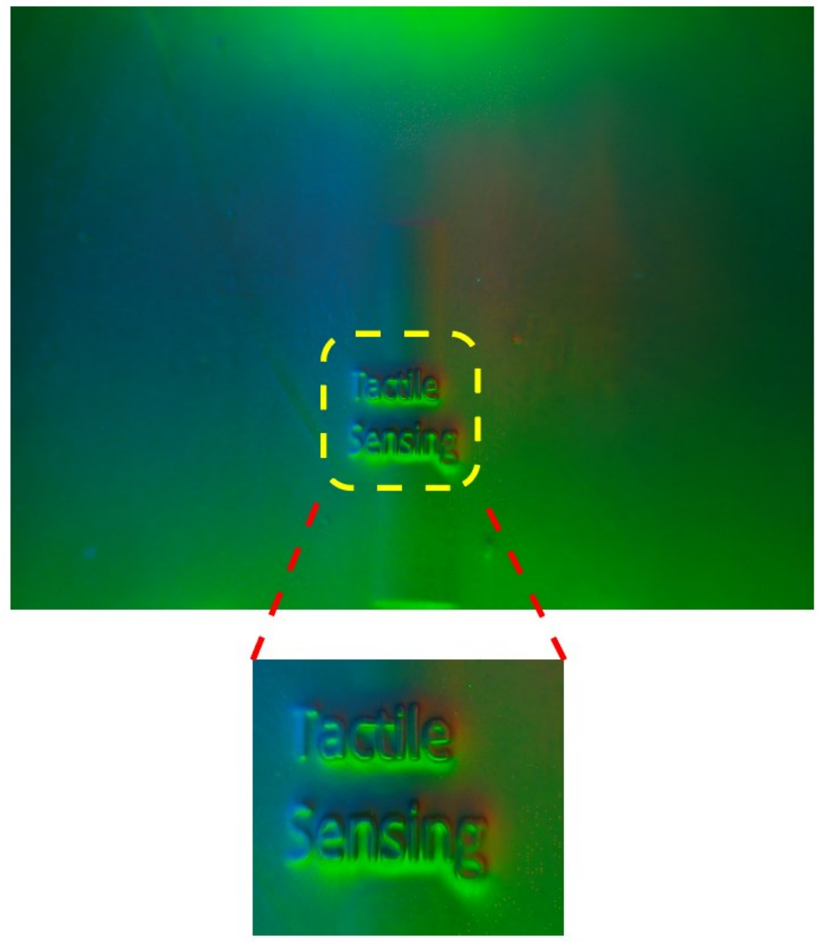

“Tatle Sending”

“Tacolle Sending”

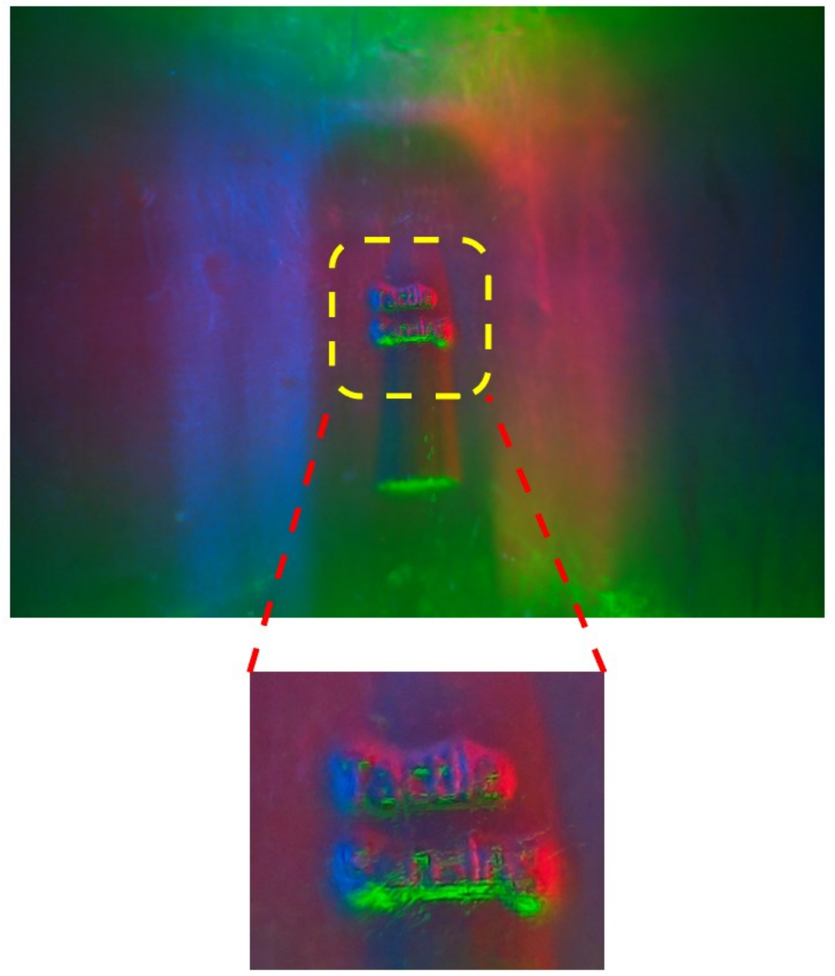

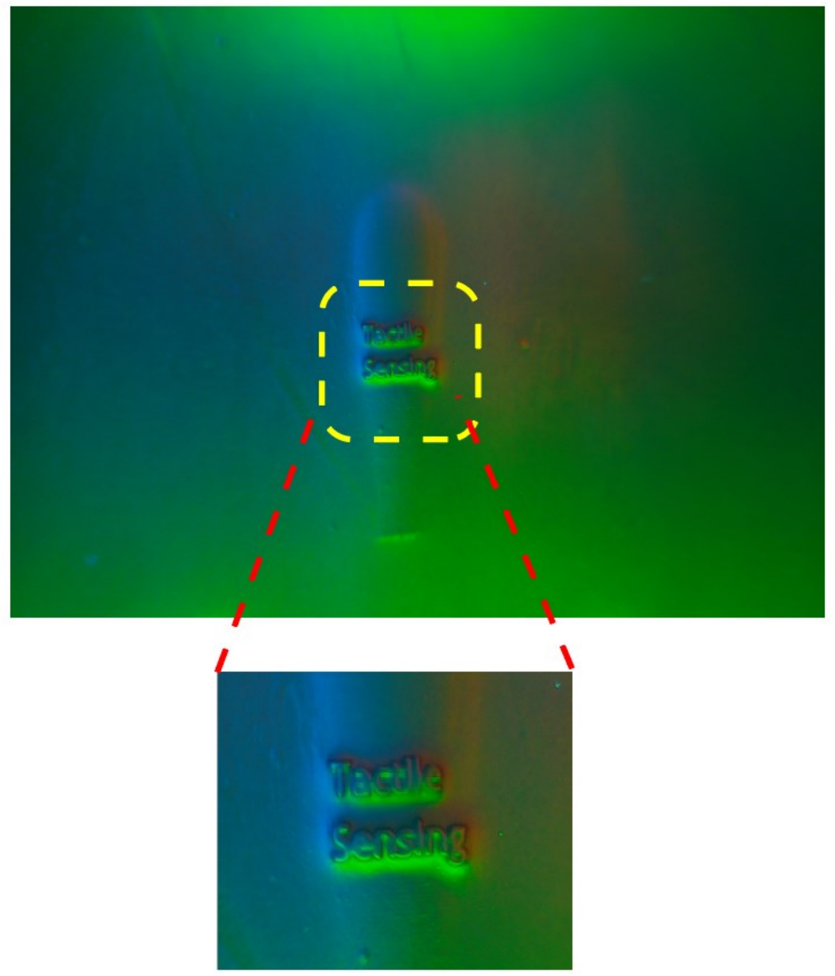

“_”

“Tacolle Sensing”

[Agarwal et al., 2023]

Results: surface inspection

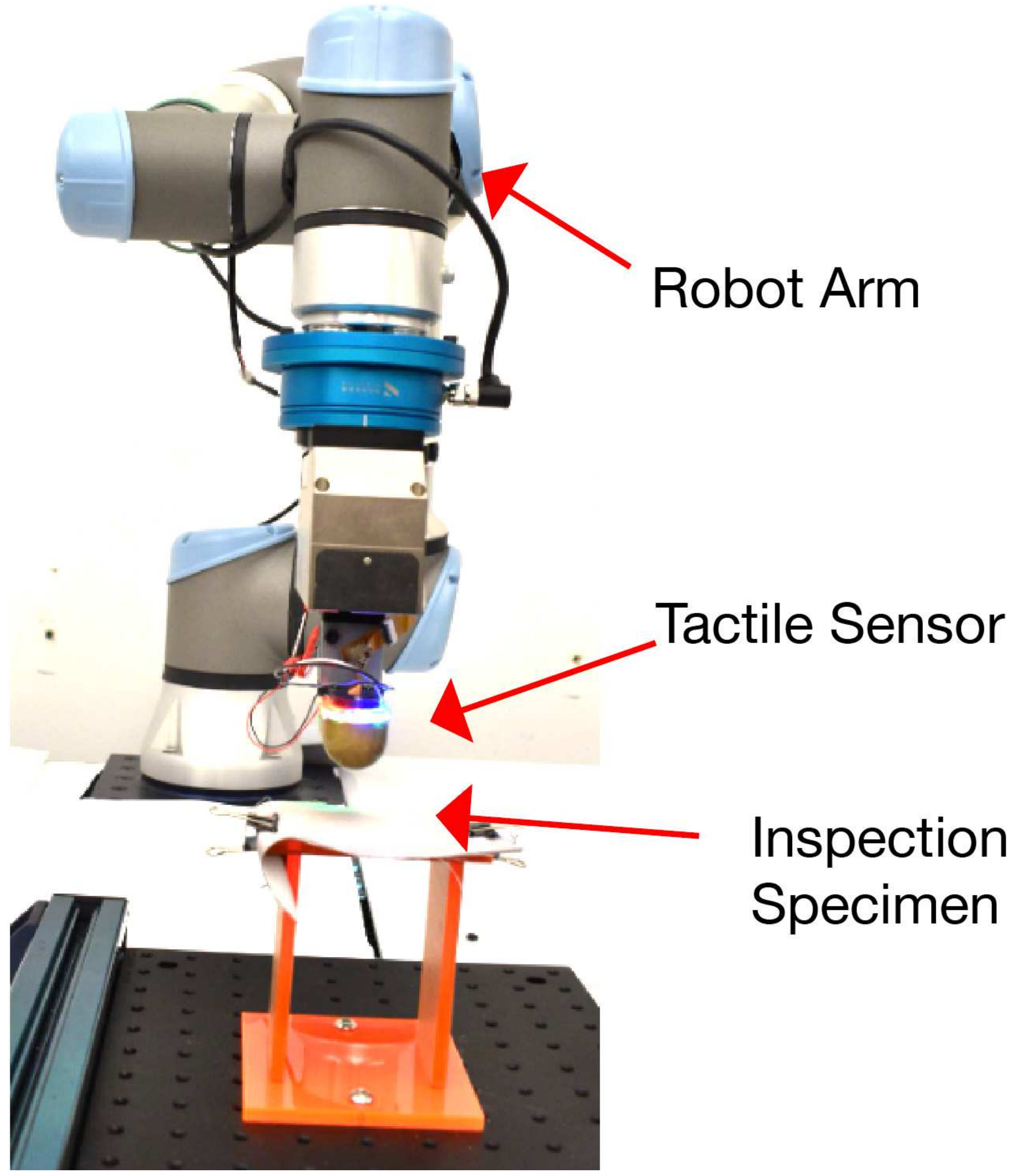

Experiment setup

Text description: Feeling of Touch

Experiment 2: Detection accuracy vs contact location

Human expert design

Optimized design

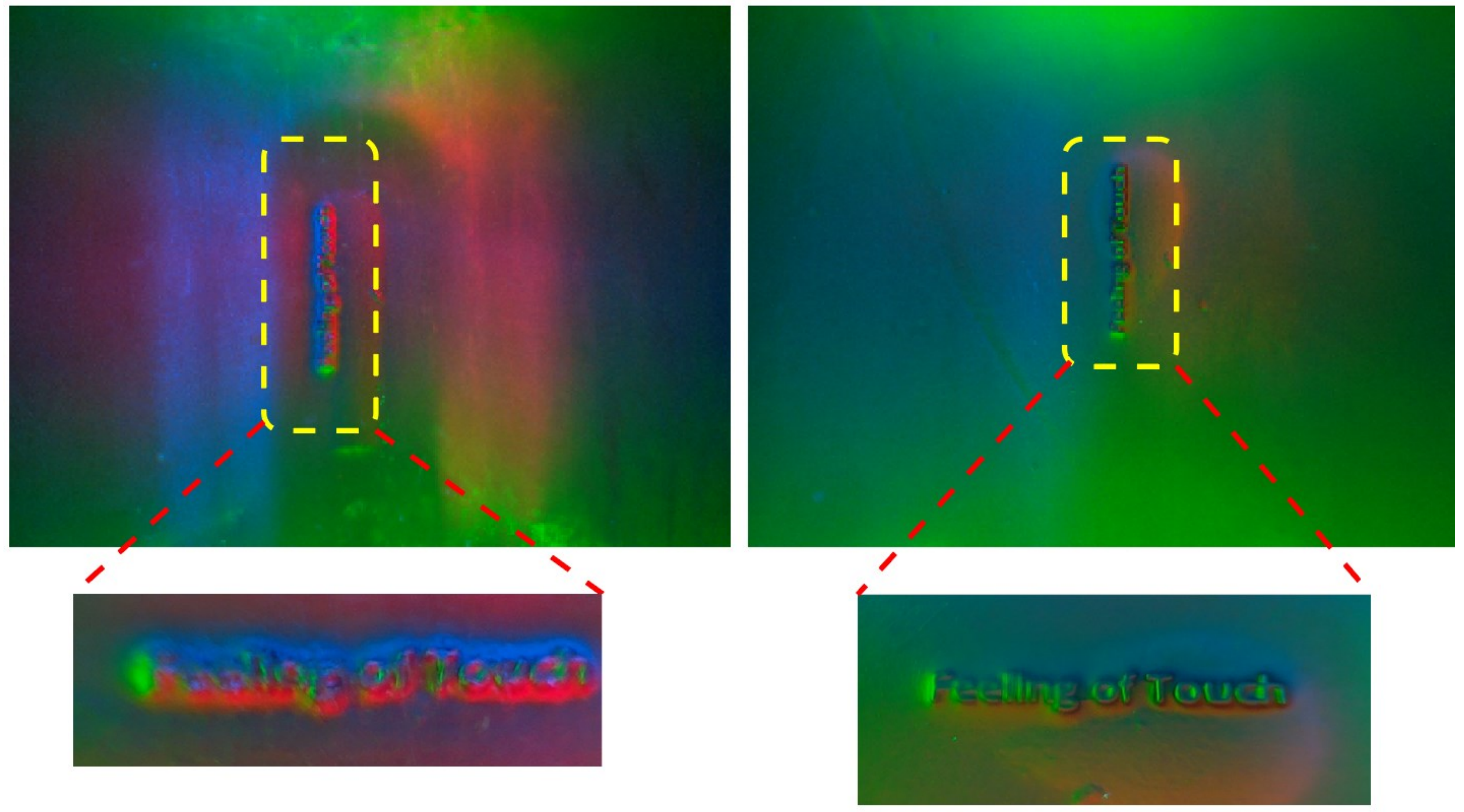

“-”

“Feeling of Touch”

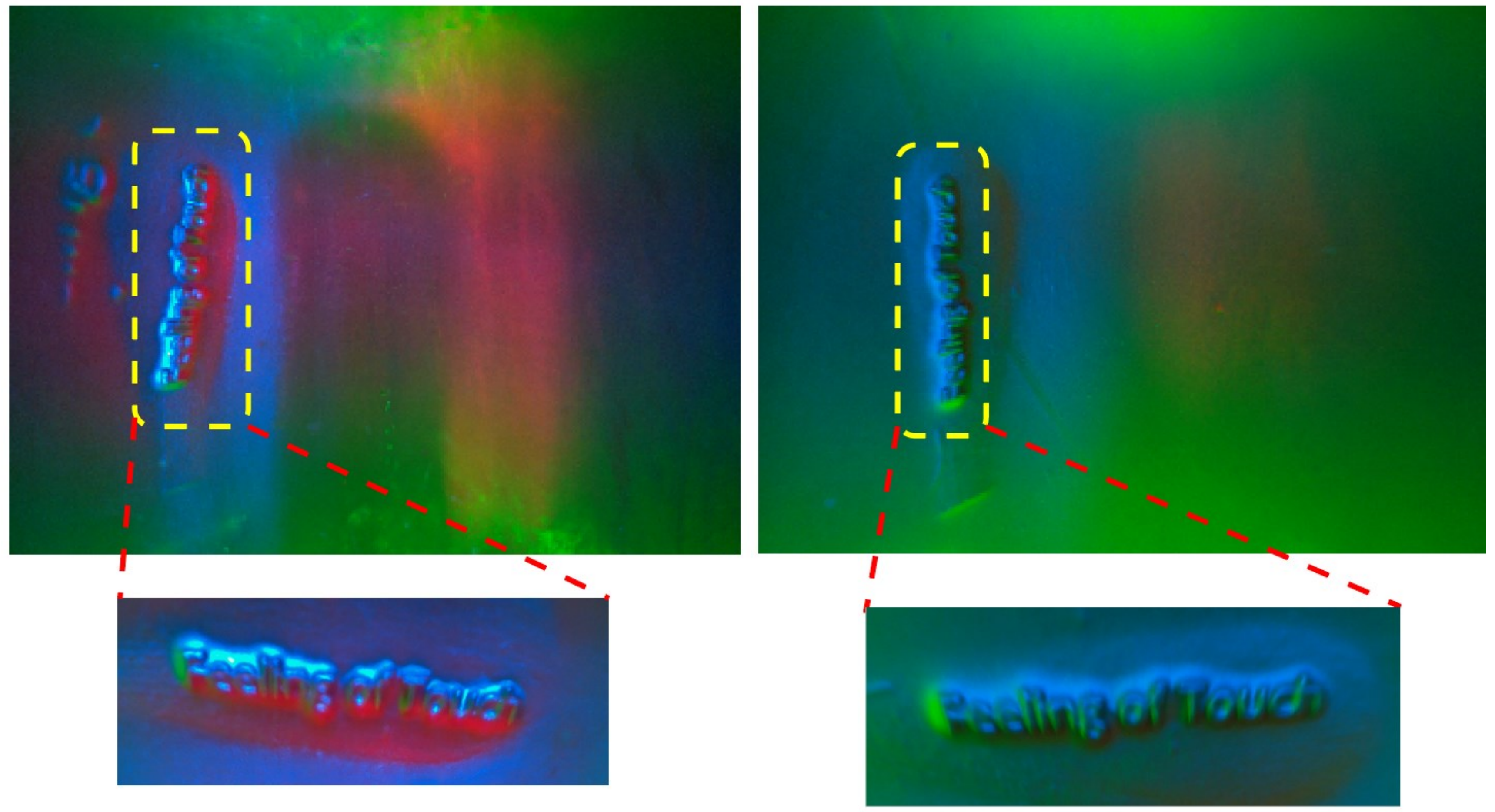

“-”

“Peeling of Touch”

[Agarwal et al., 2023]

Results: surface inspection

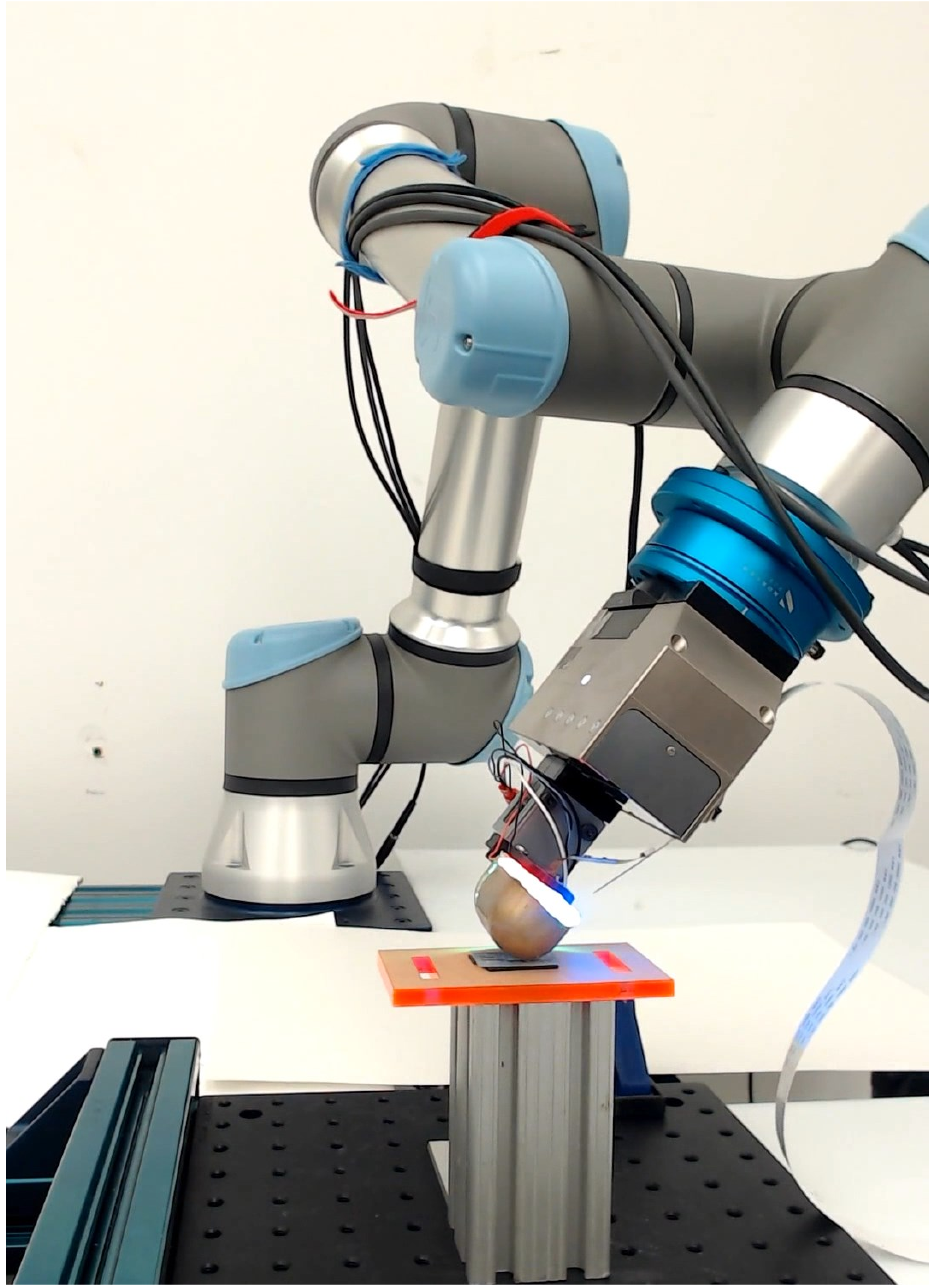

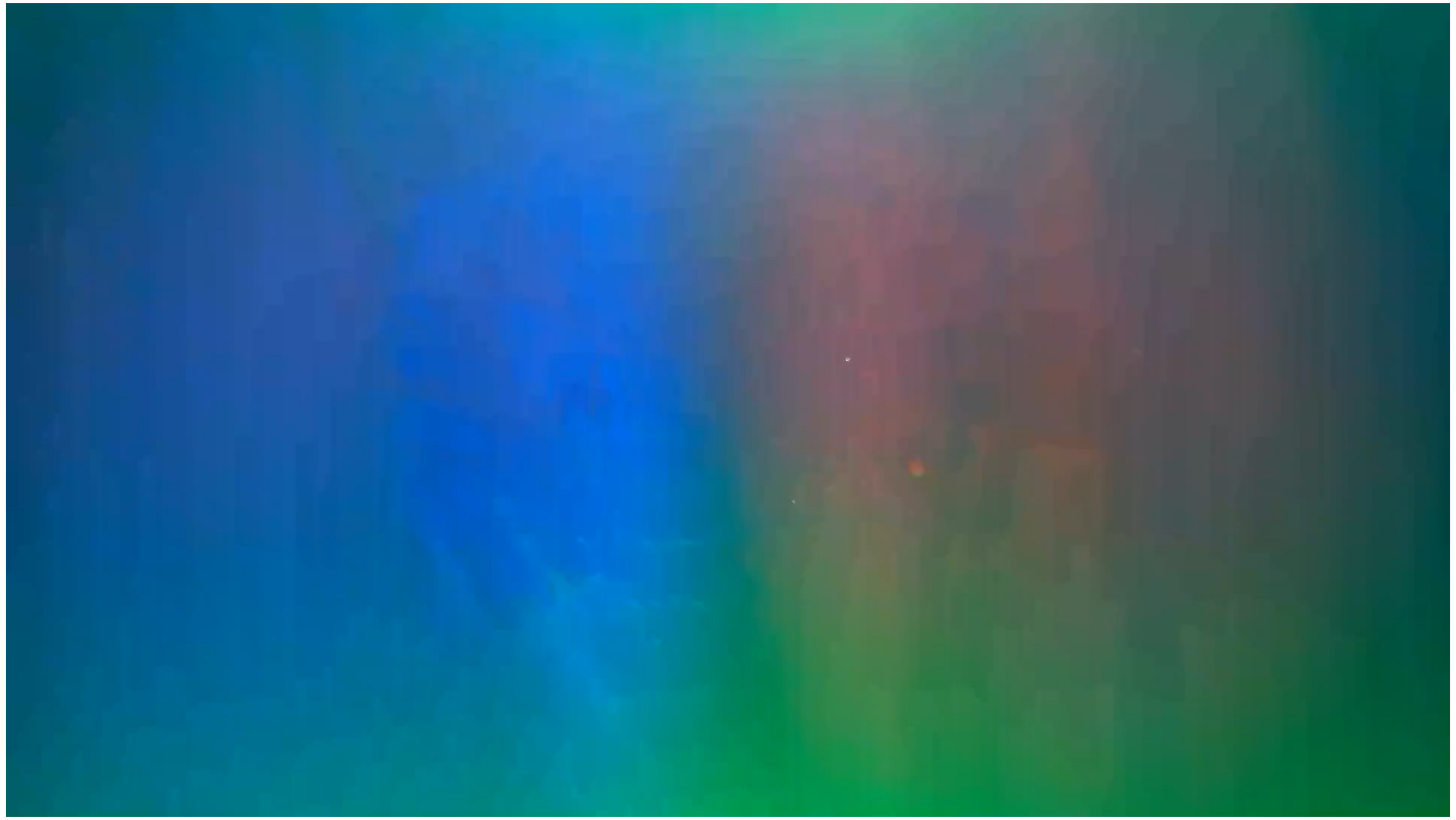

[Agarwal et al., 2023]

Physics-based rendering and its applications to computational imaging

forward rendering

- accurate and efficient simulation
- virtually design sensors, optics, and algorithms

inverse rendering

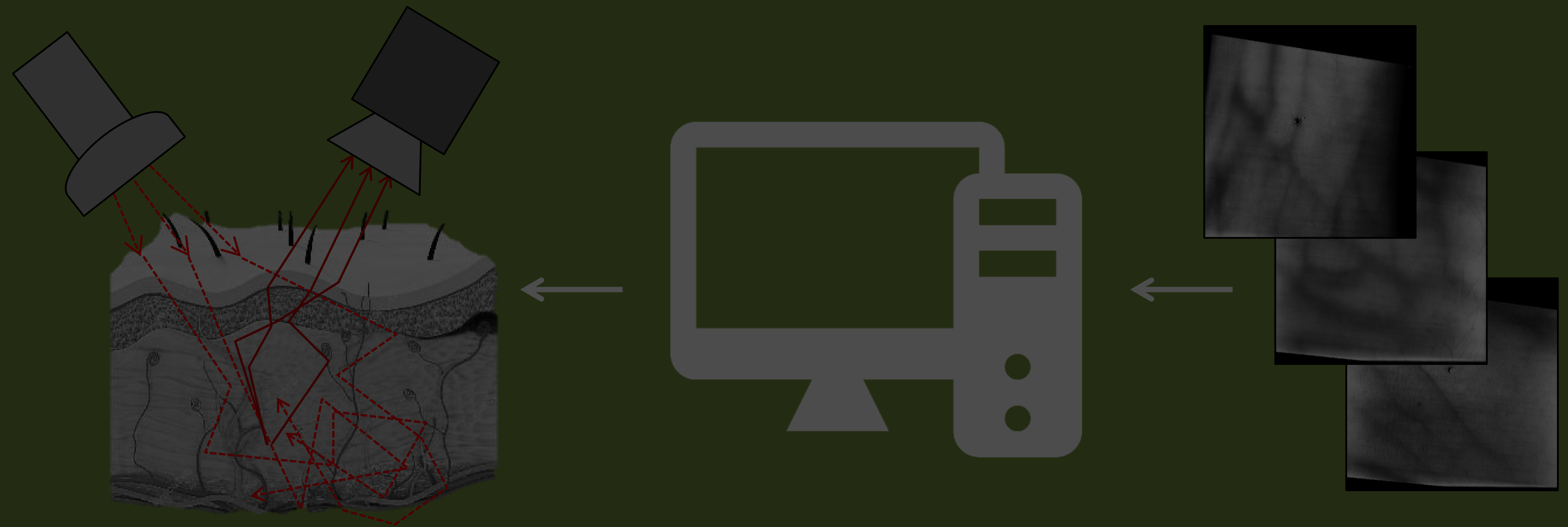

- accurate and efficient differentiable simulation
- tractably solve general inverse problems

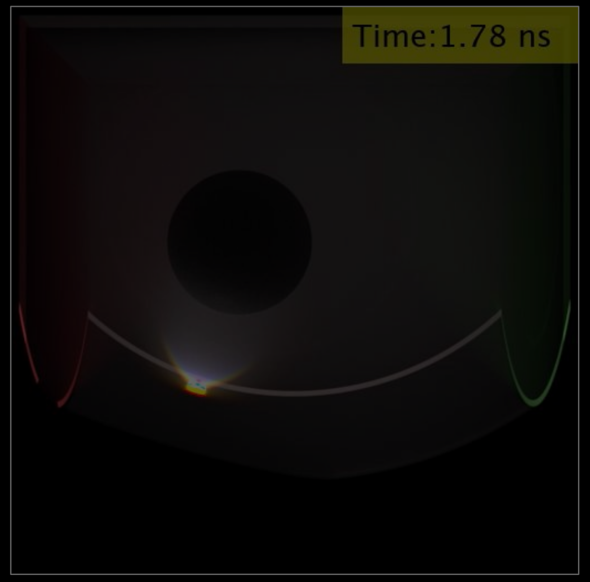

time-of-flight imaging

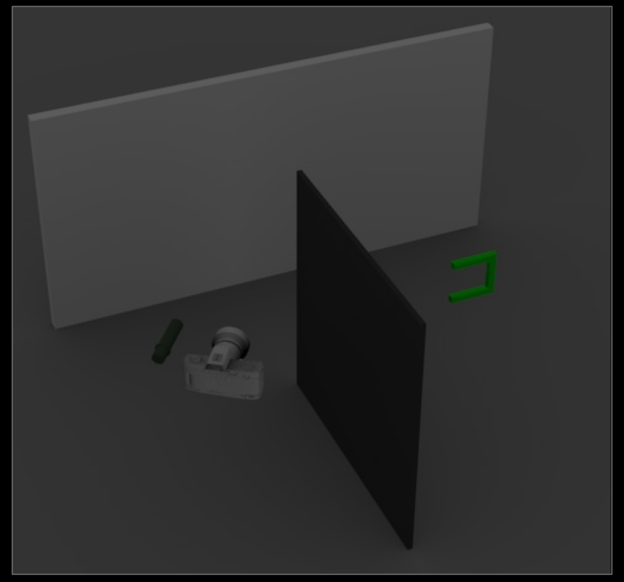

non-line-of-sight imaging

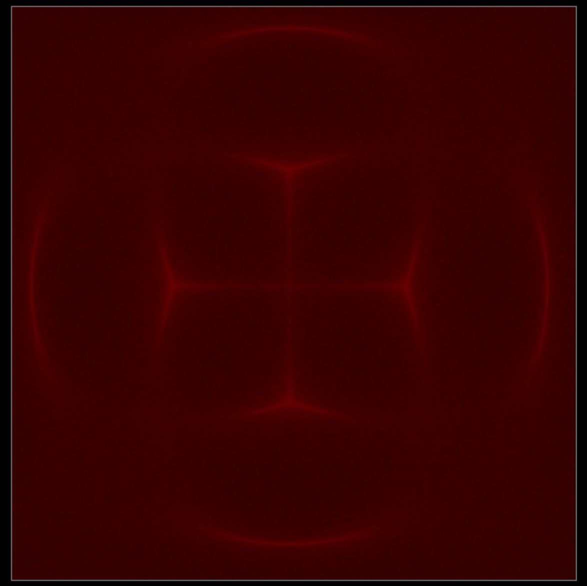

acousto-optic lensing

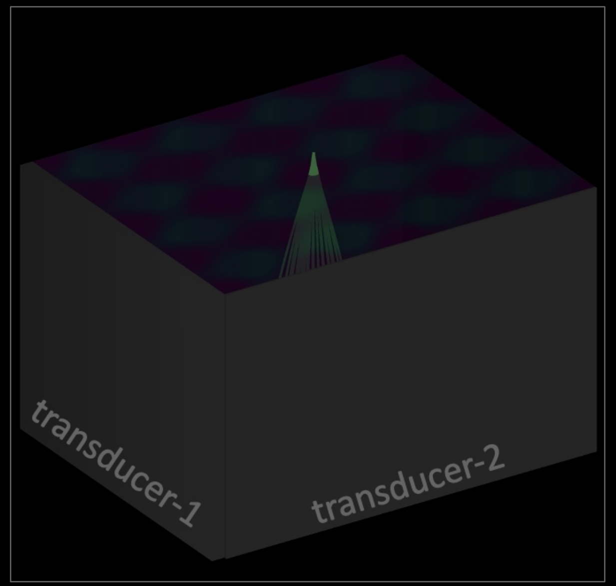

ultrafast light scanning

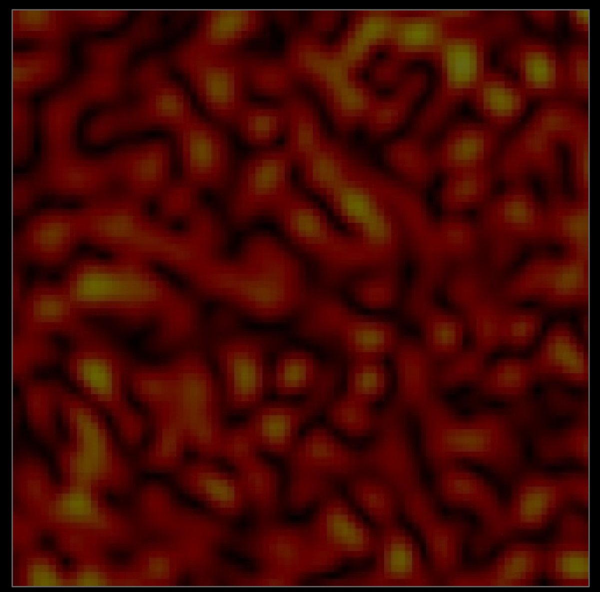

speckle imaging

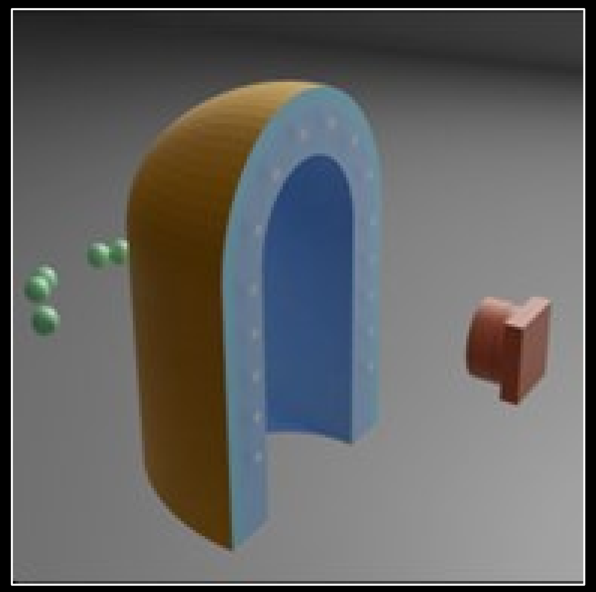

tactile sensor design

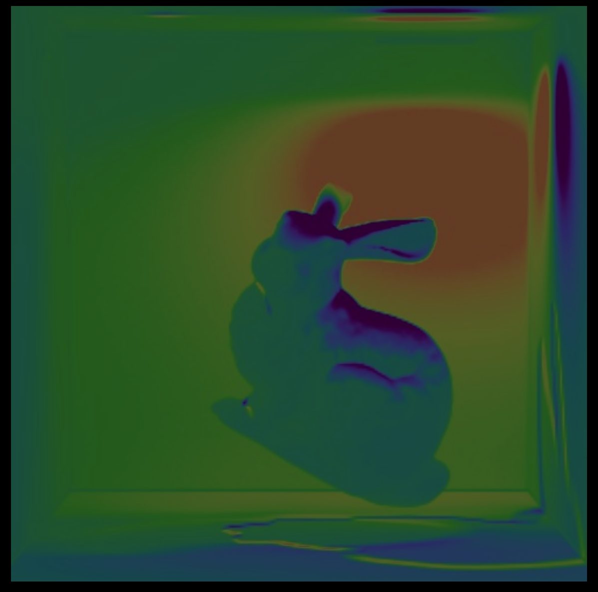

differentiable renderer

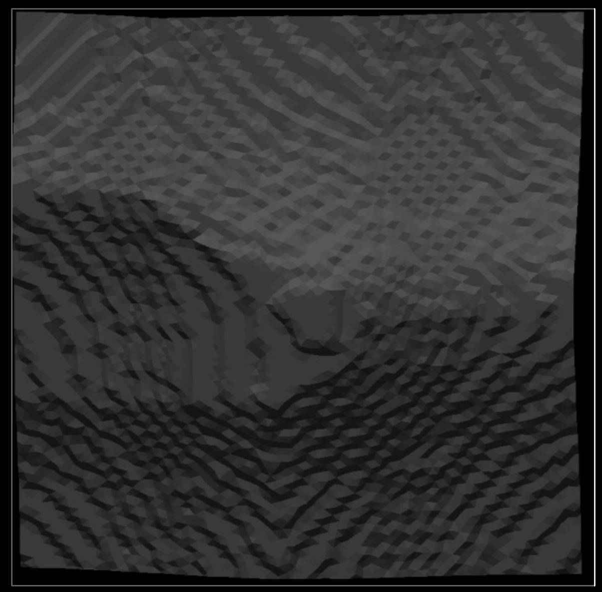

inverse problems

Physics-based rendering and its applications to computational imaging

forward rendering

- accurate and efficient simulation
- virtually design sensors, optics, and algorithms

inverse rendering

- accurate and efficient differentiable simulation
- tractably solve general inverse problems

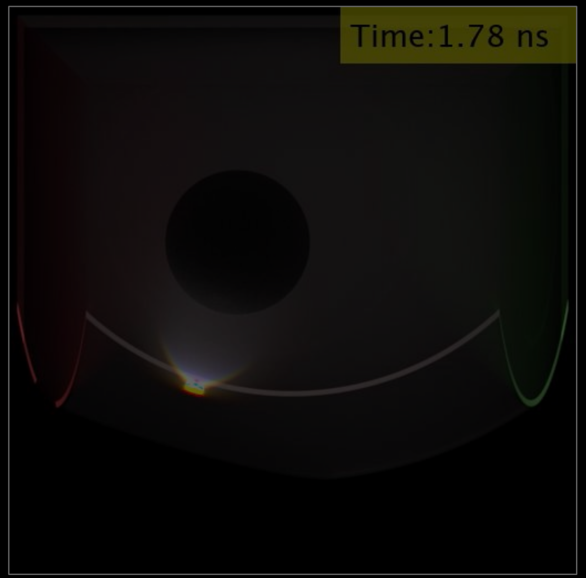

time-of-flight imaging

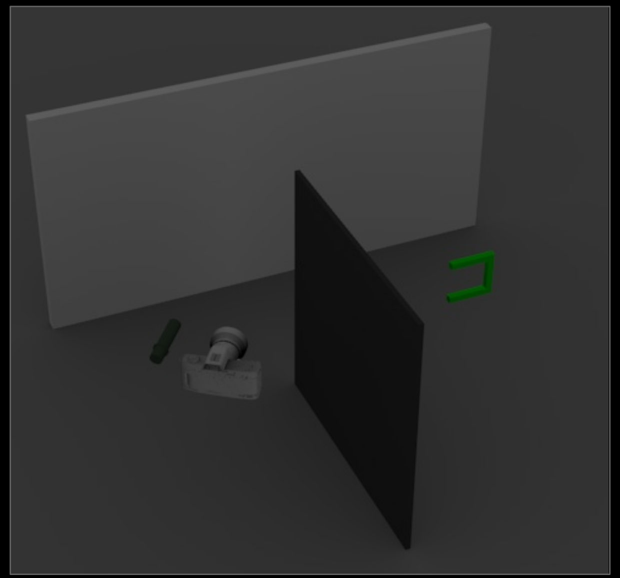

non-line-of-sight imaging

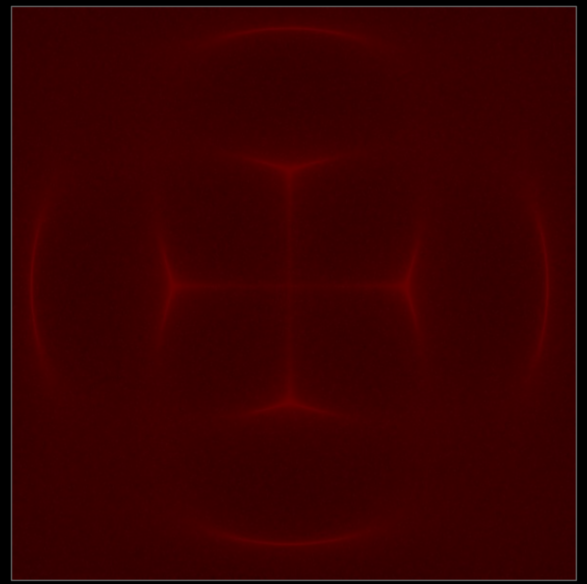

acousto-optic lensing

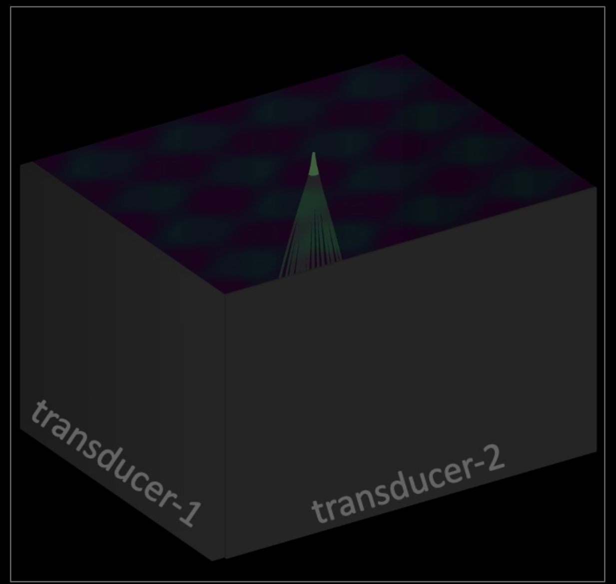

ultrafast light scanning

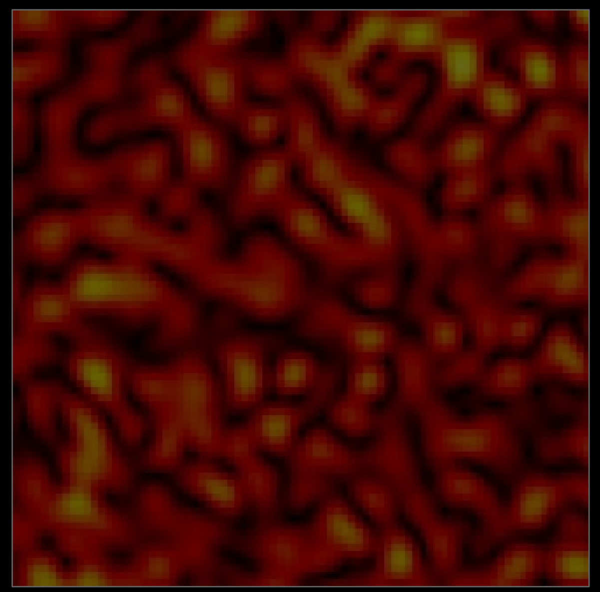

speckle imaging

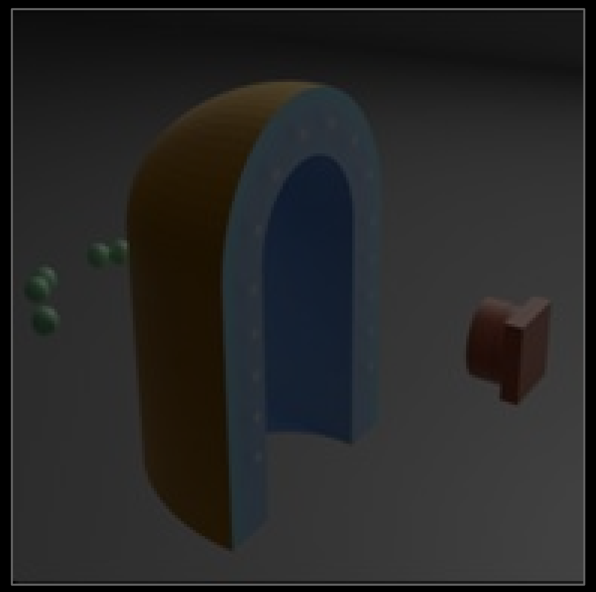

tactile sensor design

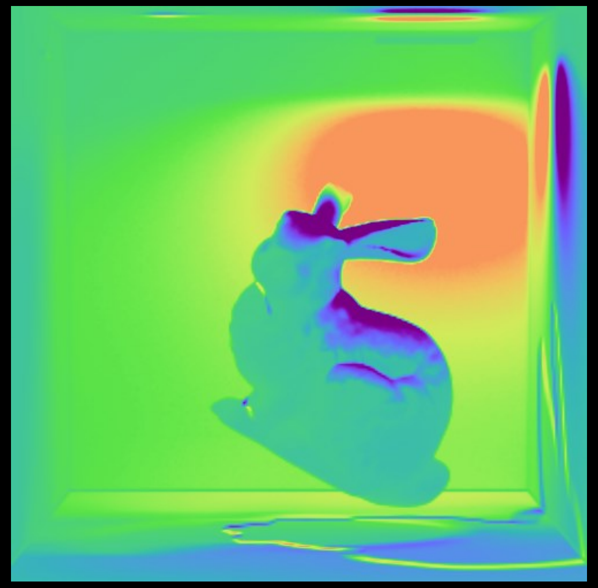

differentiable renderer

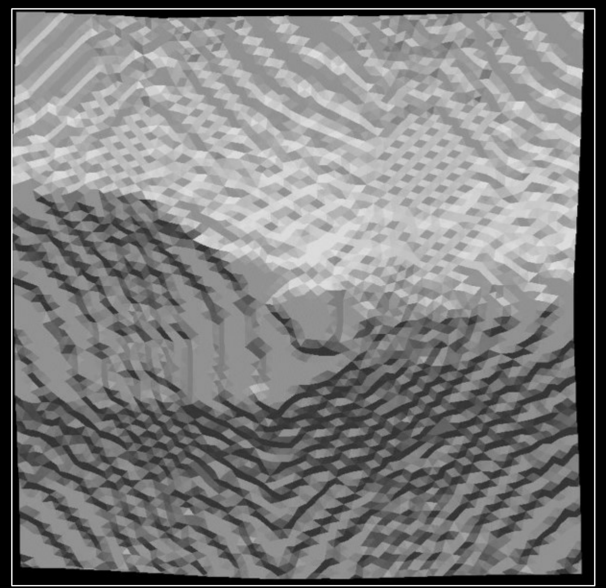

inverse problems

Forward rendering

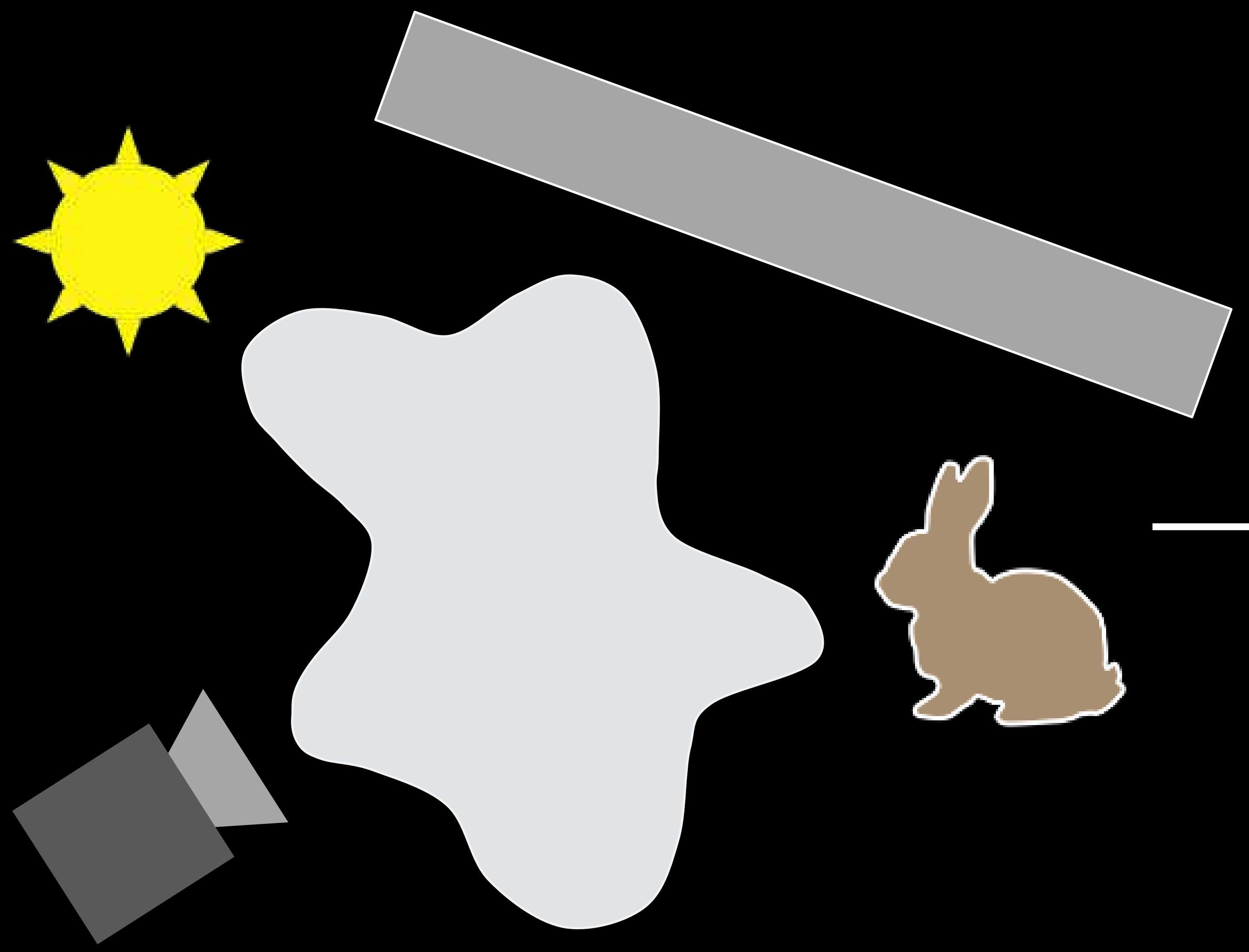

digital scene specification
(geometry, materials,
optics, light sources)

physically-accurate
rendering

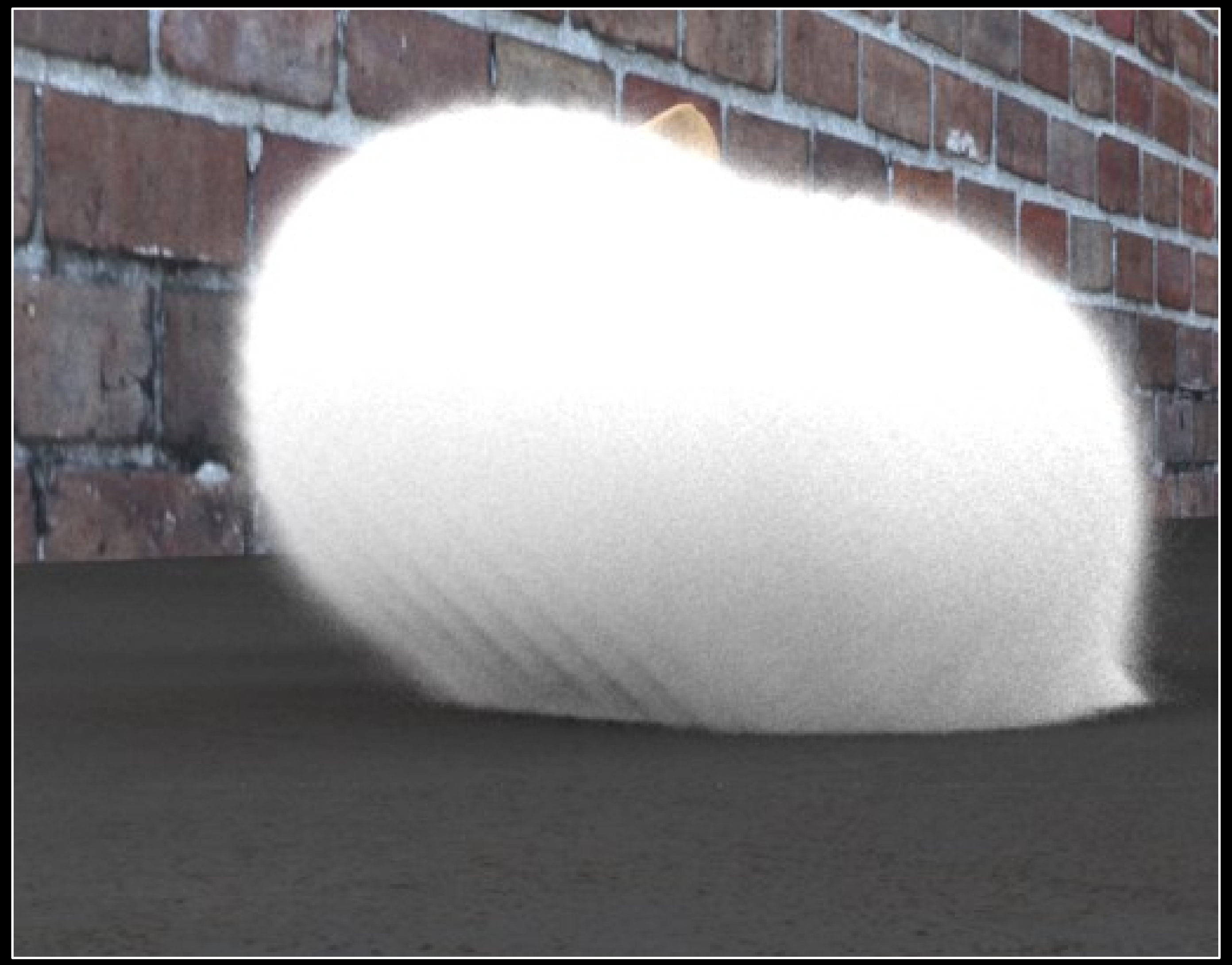

photorealistic
simulated image

Inverse rendering

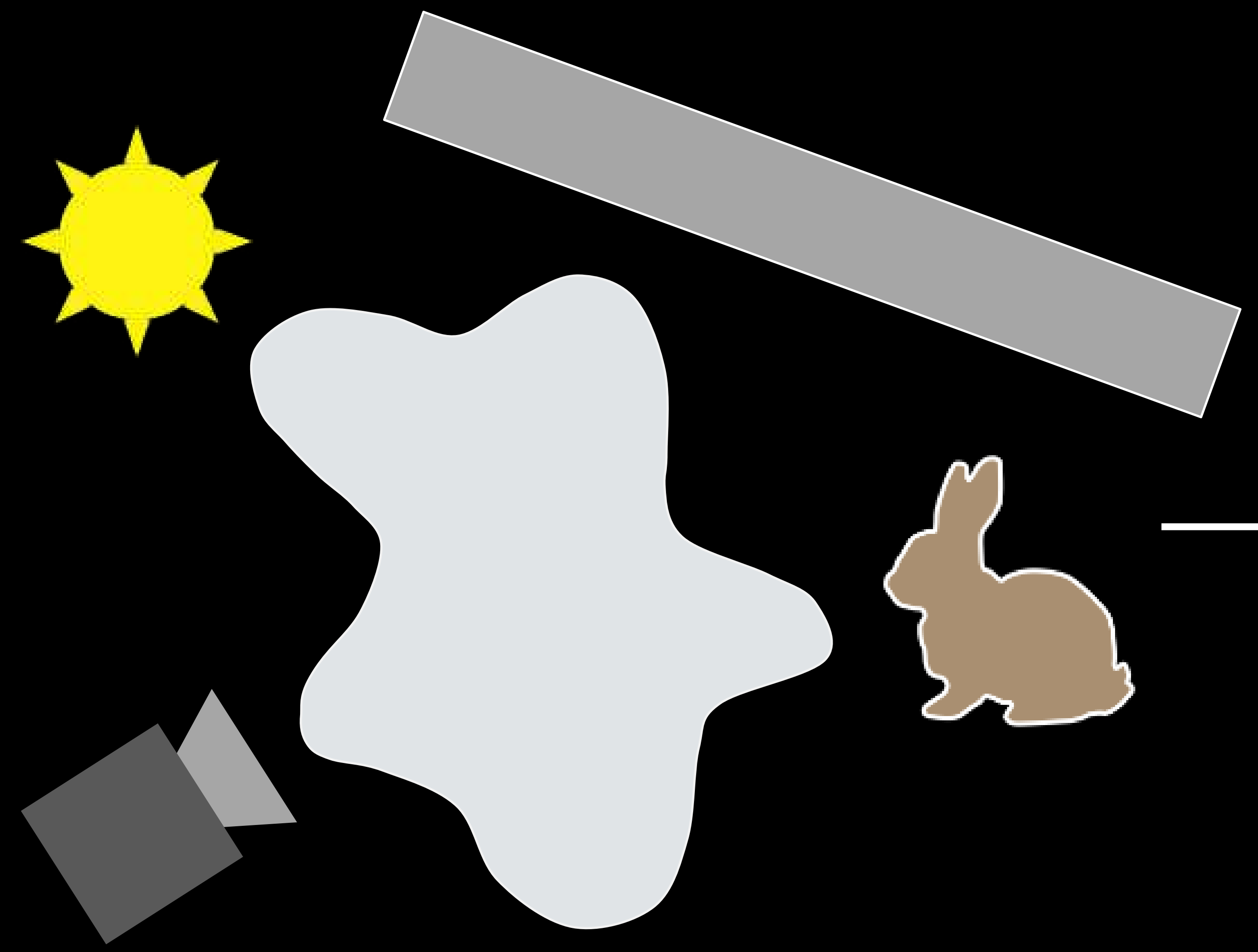

digital scene specification
(geometry, materials,
camera, light sources)

physically-accurate
inverse rendering

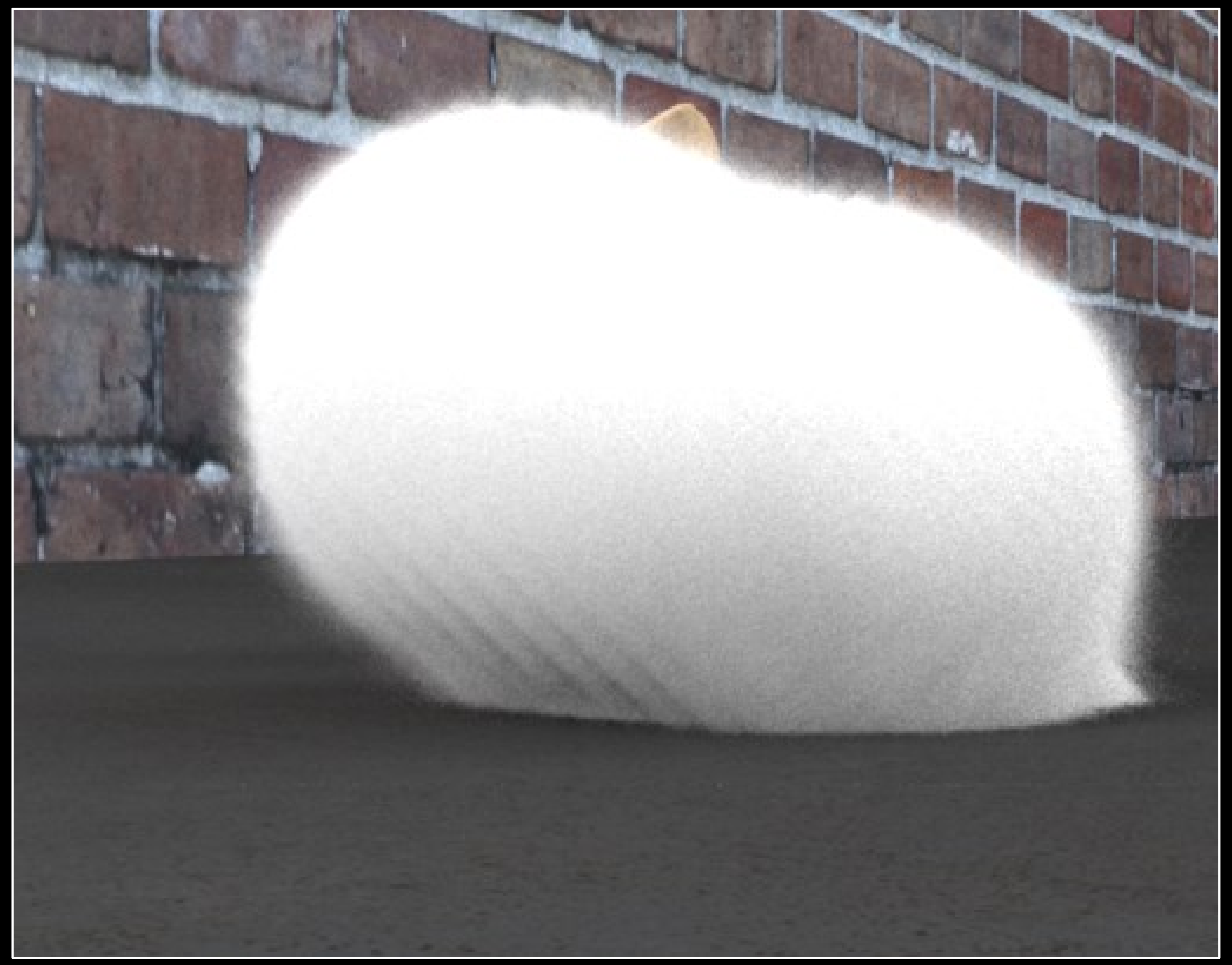

photorealistic
synthetic image

Inverse rendering

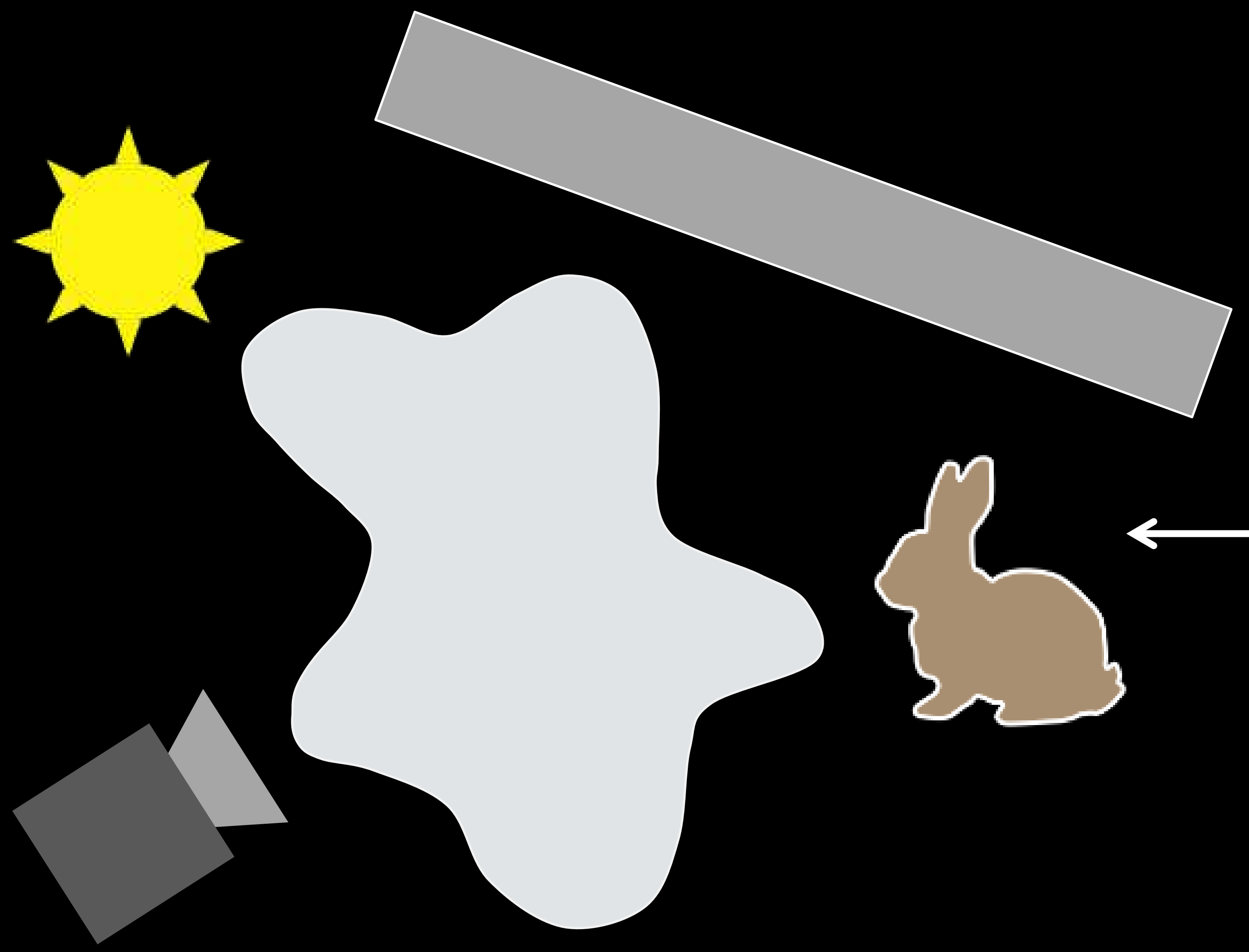

digital scene specification
(geometry, materials,
camera, light sources)

←

physically-accurate
inverse rendering

←

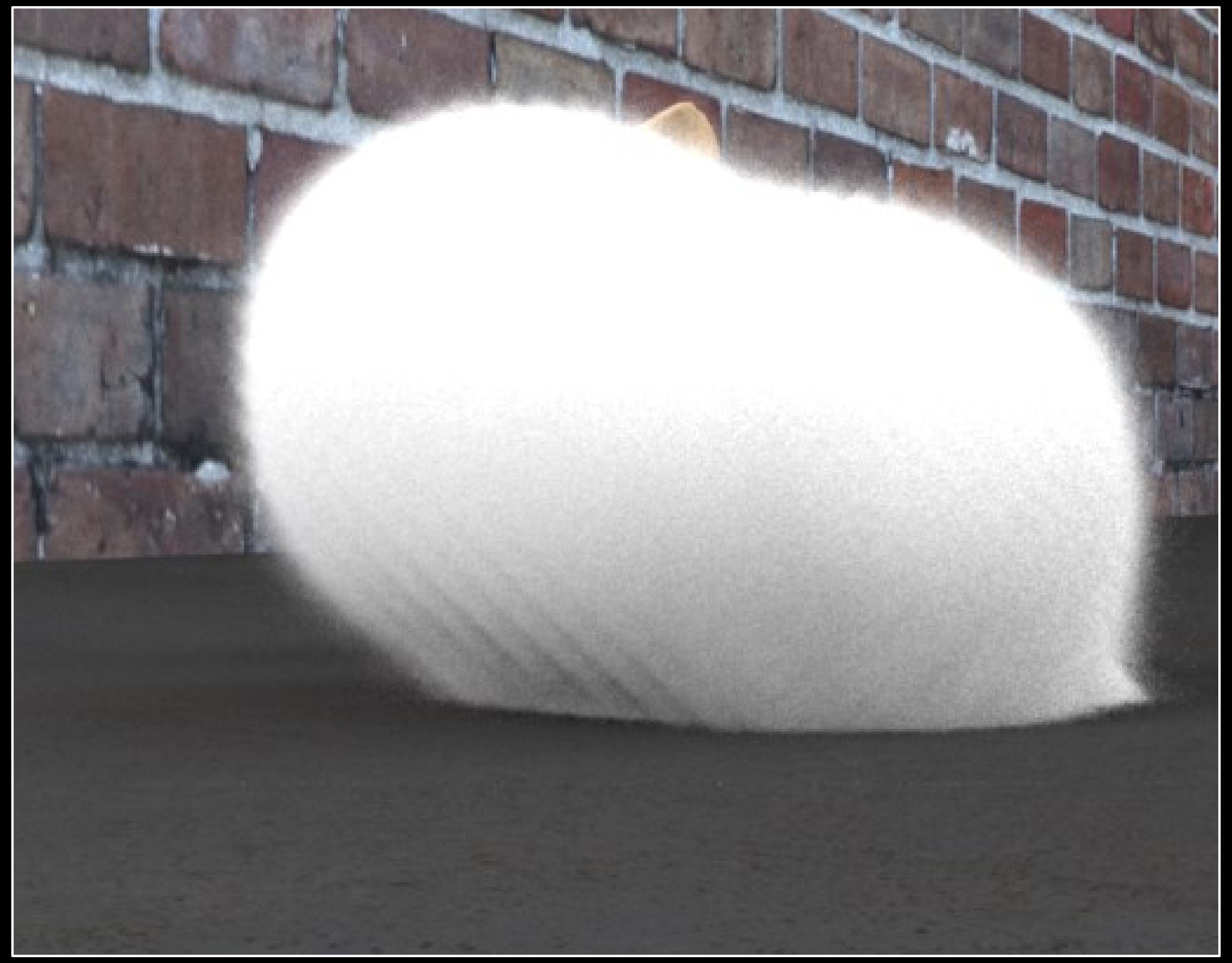

image measurements

Analysis by synthesis (a.k.a. inverse rendering)

$\min$ $\|$ 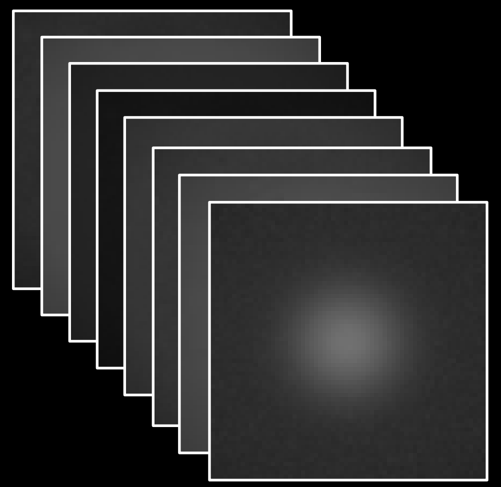 $-$ image(m) $\|^2$

unknowns m
(tissue properties)

Analysis by synthesis (a.k.a. inverse rendering)

captured measurements

min ‖ 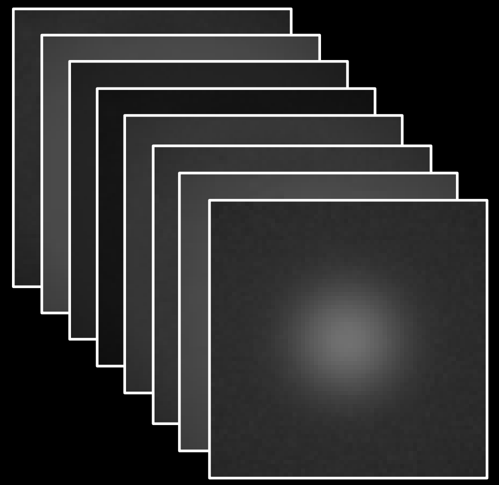 - image(m) ‖^2

unknowns m (tissue properties)

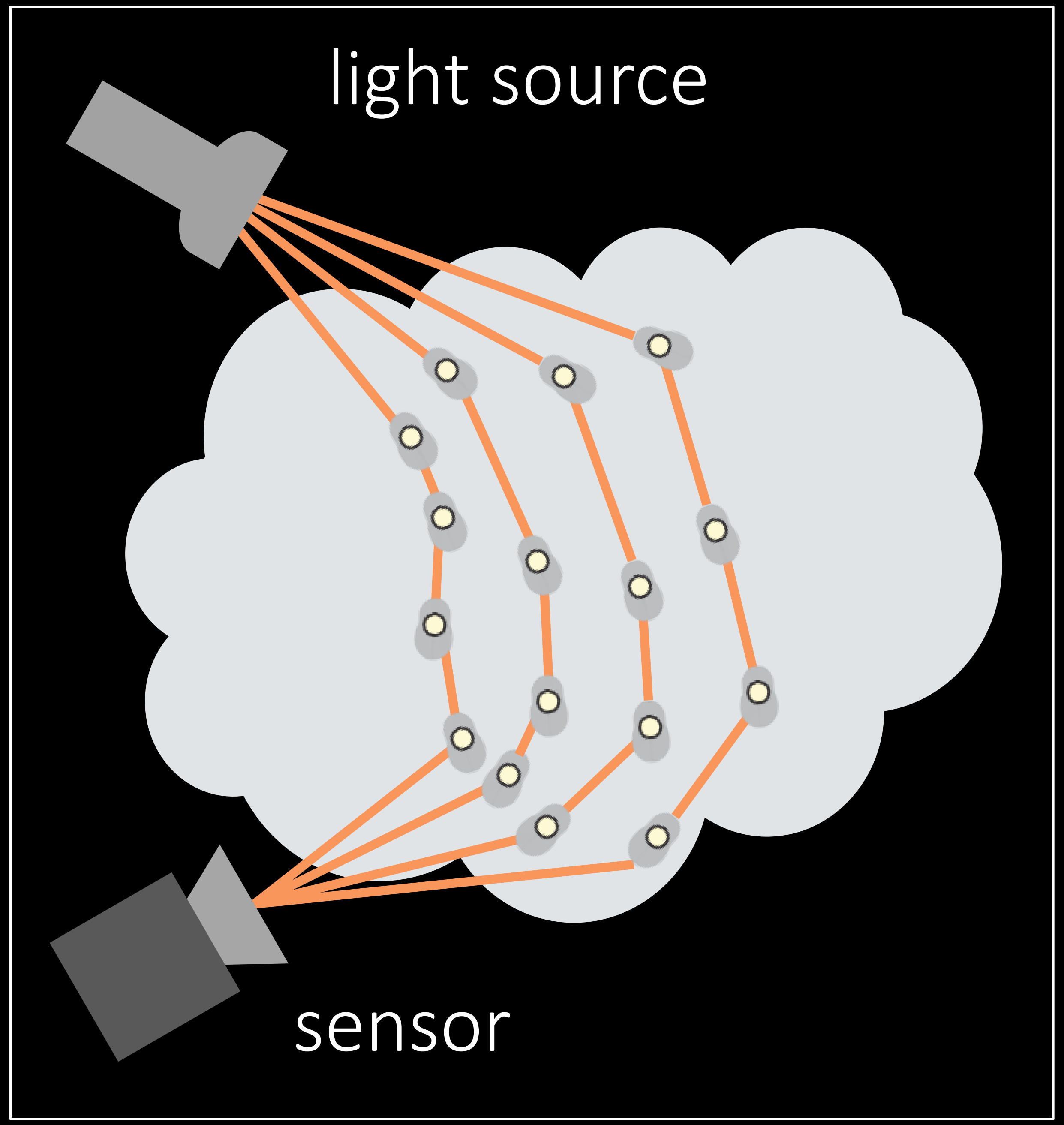

Analysis by synthesis (a.k.a. inverse rendering)

min ‖ 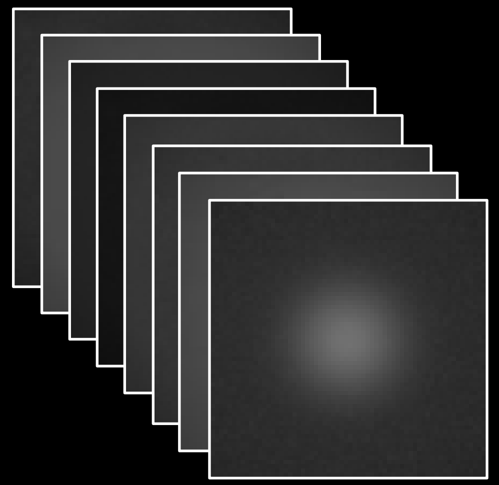 - image(m) $\|^2$

unknowns m
(tissue properties)

solve with exhaustive search

for all parameters m

evaluate loss(m) ← computed with rendering

image(m)

↑

physically-accurate rendering

↑ unknown parameters m (tissue properties)

↑ known parameters (camera, shape)

Analysis by synthesis (a.k.a. inverse rendering)

min ‖ 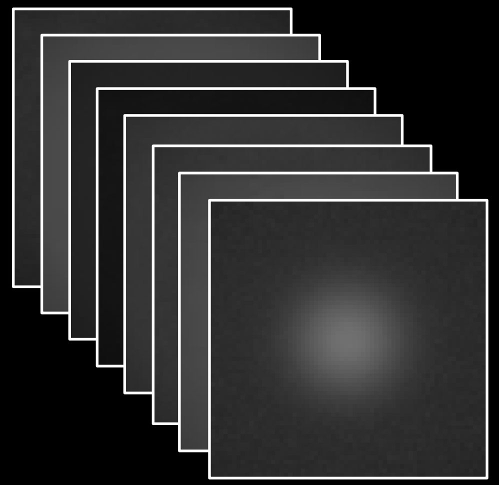 - image(m) $\|^2$

unknowns m

(tissue properties)

solve with gradient descent

while (not converged)

update m with $\boxed{\frac{\partial \text{loss}(m)}{\partial m}}$ ← computed with differentiable rendering

$$\frac{\partial \text{image}(m)}{\partial m}$$

↑

differentiable rendering

↑ unknown parameters m (tissue properties)

↑ known parameters (camera, shape)

Analysis by synthesis (a.k.a. inverse rendering)

Analysis-by-synthesis optimization:

$\min_{\substack{\text{scene}\\ \text{unknowns } \pi}} \text{loss}\Big[$  $, \text{render}\left(\substack{\text{scene}\\ \text{unknowns } \pi}\right)\Big]$

Analysis by synthesis (a.k.a. inverse rendering)

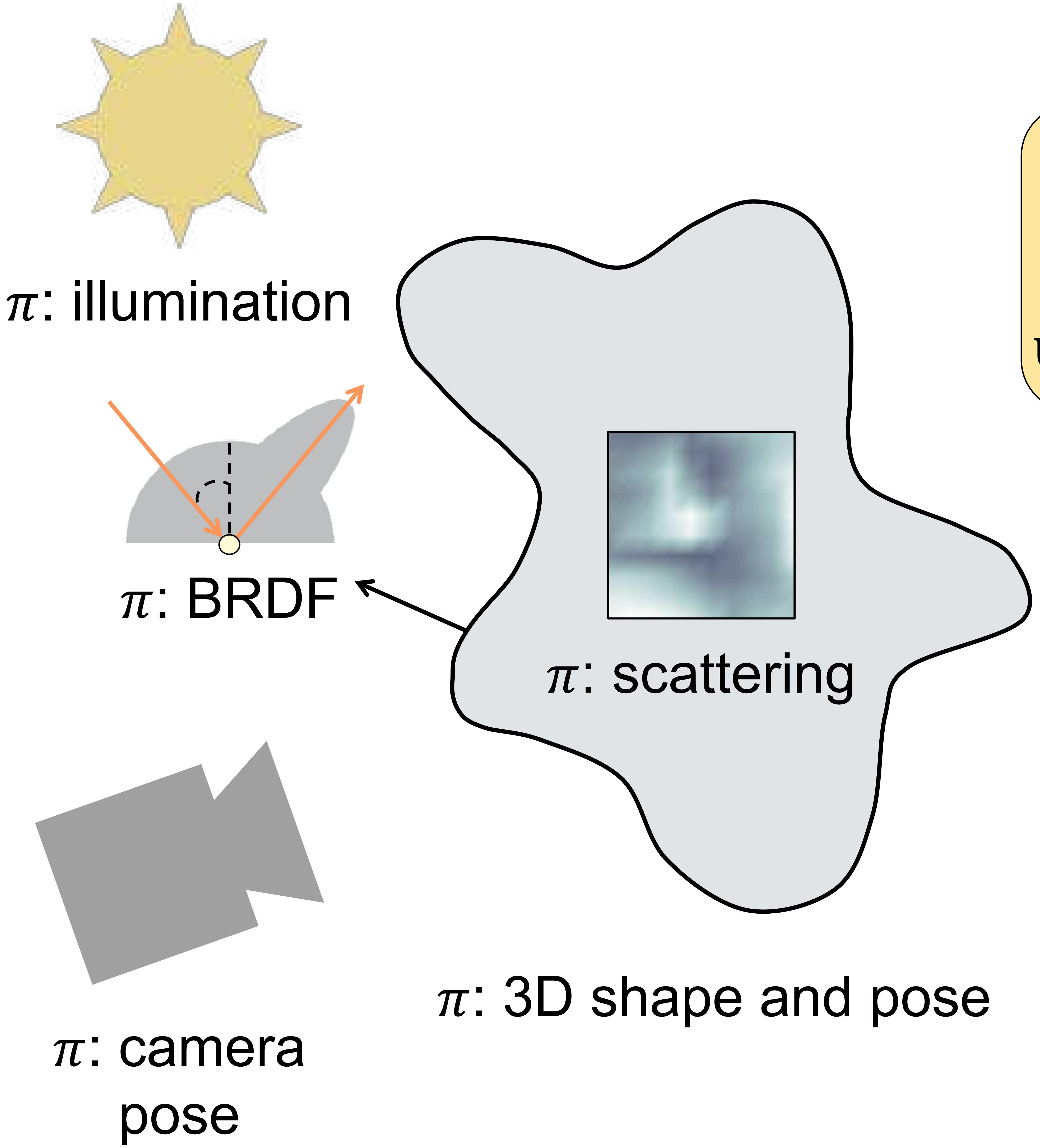

Analysis-by-synthesis optimization:

$\min\limits_{\substack{\text{scene}\\ \text{unknowns }\pi}} \text{loss}\Big[$  $, \text{render}\Big(\substack{\text{scene}\\ \text{unknowns }\pi}\Big)\Big]$

Analysis by synthesis (a.k.a. inverse rendering)

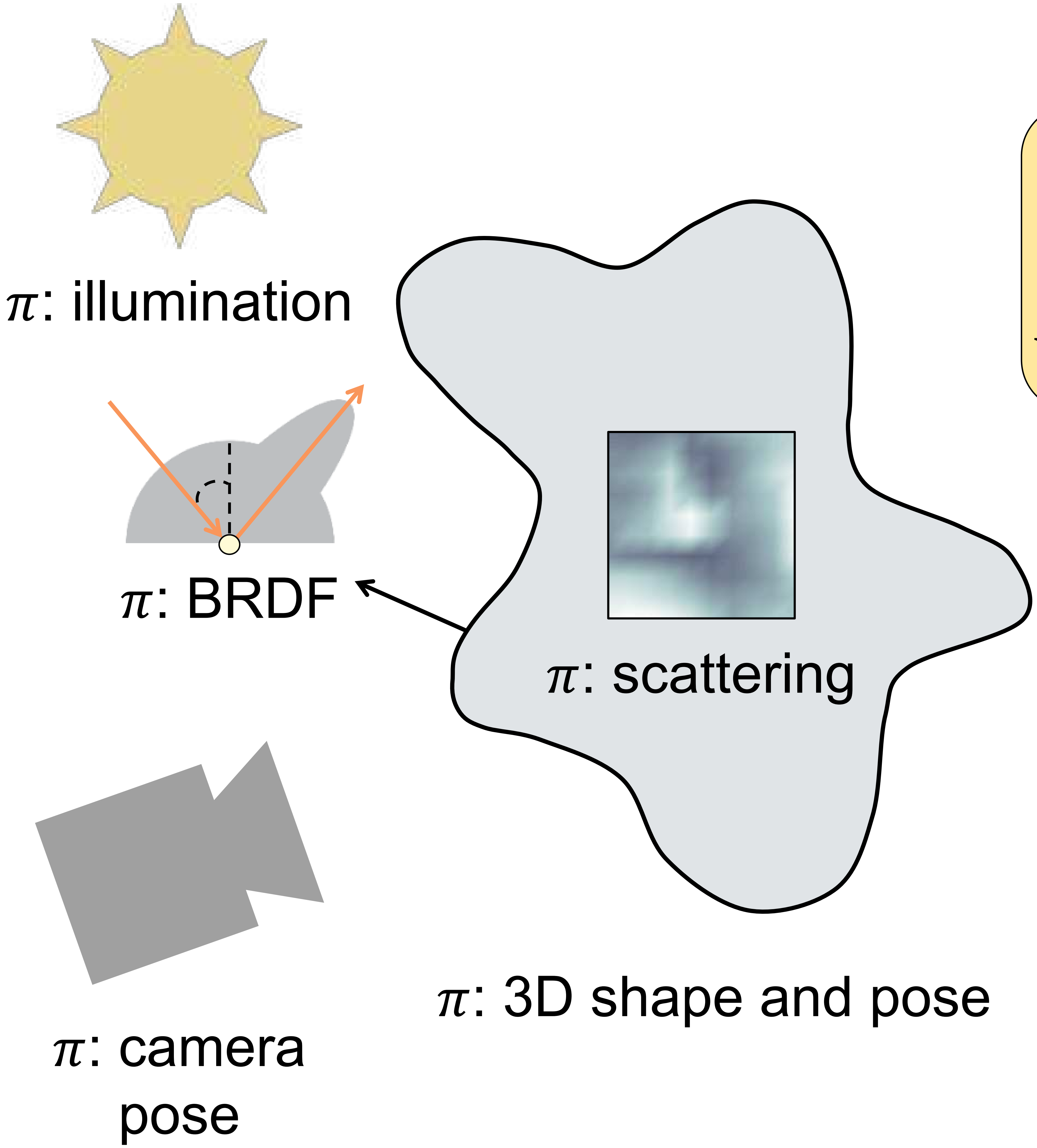

Analysis-by-synthesis optimization:

$$\min_{\substack{\text{scene} \\ \text{unknowns } \pi}} \ \text{loss}\left[\right.$$  $$\left., \text{render}\left(\substack{\text{scene} \\ \text{unknowns } \pi}\right)\right]$$

Stochastic gradient descent (e.g., Adam):

initialize $\pi \leftarrow \pi_0$

while (not converged)

update $\pi \leftarrow \pi + \eta \cdot \dfrac{\mathrm{dloss}(\pi)}{\mathrm{d}\pi}$

Analysis by synthesis (a.k.a. inverse rendering)

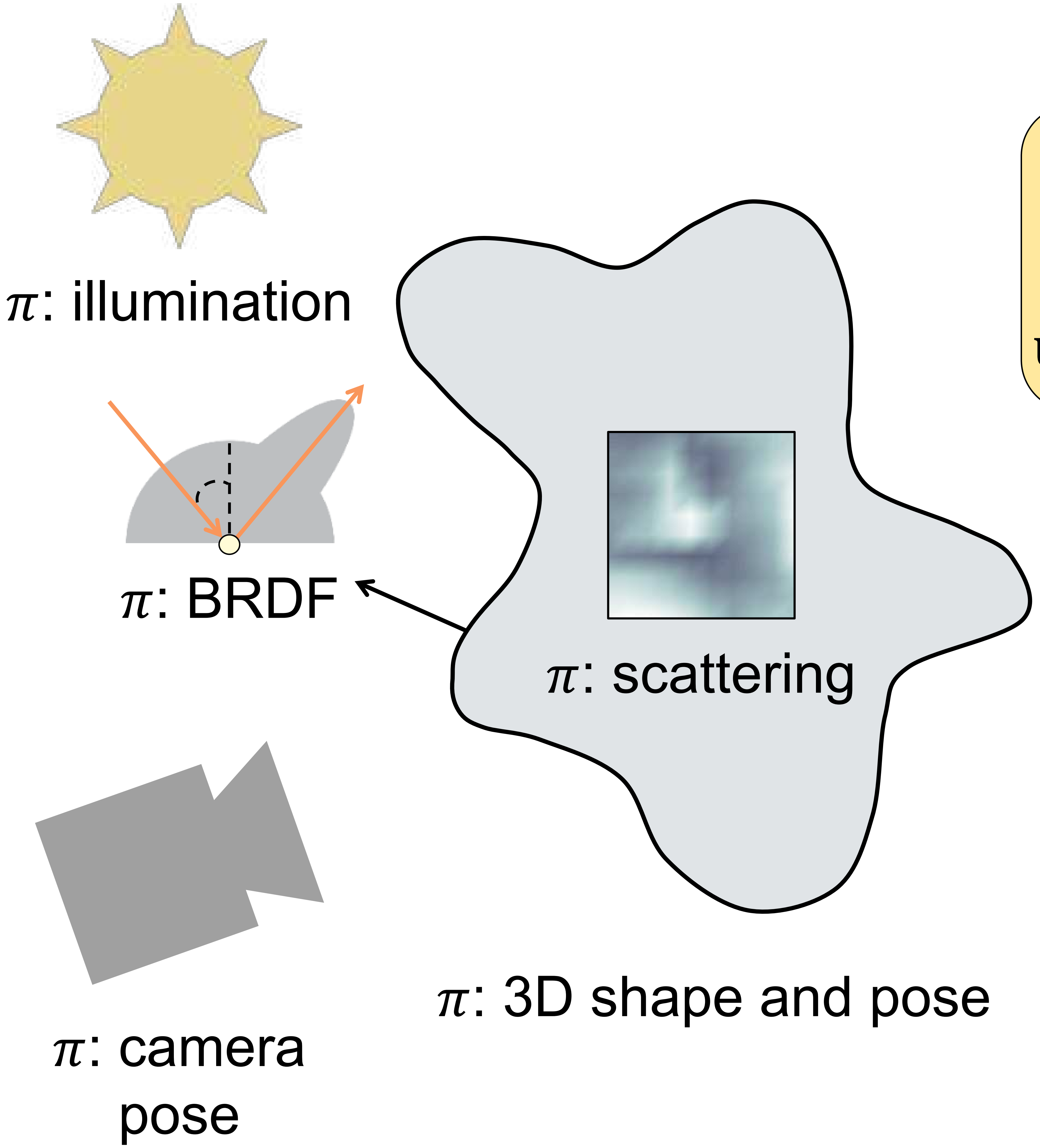

Analysis-by-synthesis optimization:

$$\min_{\substack{\text{scene}\\ \text{unknowns }\pi}} \ \text{loss}\Bigg[$$

$$, \text{render}\left(\text{scene unknowns }\pi\right)\Bigg]$$

Stochastic gradient descent (e.g., Adam):

initialize $\pi \leftarrow \pi_0$

while (not converged)

update $\pi \leftarrow \pi + \eta \cdot \boxed{\dfrac{\mathrm{dloss}(\pi)}{\mathrm{d}\pi}}$

Differentiable rendering

How do we differentiate light transport?

sensor weight

source weight

image $$I = \int_{\mathcal{P}} W_e(\mathbf{x}_0, \mathbf{x}_1) L_e(\mathbf{x}_k, \mathbf{x}_{k-1}) T(\bar{\mathbf{x}})\, d\bar{\mathbf{x}}$$ light path

path throughput

space of all light paths

$$T(\bar{\mathbf{x}}) = G(\mathbf{x}_0, \mathbf{x}_1) \prod_{j=1}^{k-1} f(\mathbf{x}_j, \mathbf{x}_{j+1}, \mathbf{x}_{j-1}) G(\mathbf{x}_j, \mathbf{x}_{j+1})$$

BSDF

geometry

REMINDER (?) FROM CALCULUS

Reminder from calculus

$$\frac{\mathrm{d}}{\mathrm{d}\pi}\int_{a(\pi)}^{b(\pi)} f(x,\pi)\,\mathrm{d}x \stackrel{?}{=}$$

Reminder from calculus

$$\frac{\mathrm{d}}{\mathrm{d}\pi}\int_{a(\pi)}^{b(\pi)} f(x,\pi)\mathrm{d}x \overset{?}{=}$$

Reminder from calculus

Differentiation under the integral sign

Also known as the Leibniz integral rule

$$\frac{\mathrm{d}}{\mathrm{d}\pi}\int_{a(\pi)} f(x,\pi)\,\mathrm{d}x \overset{?}{=}$$

Reminder from calculus

Differentiation under the integral sign
Also known as the Leibniz integral rule

$$\frac{\mathrm{d}}{\mathrm{d}\pi}\int_{a(\pi)} f(x,\pi)\mathrm{d}x = \int_{a(\pi)}^{b(\pi)} \frac{\mathrm{d}}{\mathrm{d}\pi} f(x,\pi)\mathrm{d}x$$

$$+ \; f(b(\pi),\pi)\frac{\mathrm{d}b(\pi)}{\mathrm{d}\pi} - f(\alpha(\pi);\pi)\frac{\mathrm{d}a(\pi)}{\mathrm{d}\pi}$$

$$+ \; \sum_i \left(f(c_i(\pi)^-,\pi) - f(c_i(\pi)^+,\pi)\right)\frac{\mathrm{d}c_i(\pi)}{\mathrm{d}\pi}$$

Reminder from calculus

Differentiation under the integral sign
Also known as the Leibniz integral rule

$$\frac{\mathrm{d}}{\mathrm{d}\pi}\int_{a(\pi)} f(x,\pi)\mathrm{d}x = \int_{a(\pi)}^{b(\pi)} \frac{\mathrm{d}}{\mathrm{d}\pi} f(x,\pi)\mathrm{d}x$$

Move derivative inside integral

$$+ f(b(\pi),\pi)\frac{\mathrm{d}b(\pi)}{\mathrm{d}\pi} - f(\alpha(\pi);\pi)\frac{\mathrm{d}a(\pi)}{\mathrm{d}\pi}$$

$$+ \sum_i \left(f(c_i(\pi)^-,\pi) - f(c_i(\pi)^+,\pi)\right)\frac{\mathrm{d}c_i(\pi)}{\mathrm{d}\pi}$$

Reminder from calculus

Differentiation under the integral sign
Also known as the Leibniz integral rule

$$\frac{\mathrm{d}}{\mathrm{d}\pi}\int_{a(\pi)} f(x,\pi)\mathrm{d}x = \int_{a(\pi)}^{b(\pi)} \frac{\mathrm{d}}{\mathrm{d}\pi} f(x,\pi)\mathrm{d}x$$

Move derivative inside integral

Account for changes in integration limits

$$+\ f(b(\pi),\pi)\frac{\mathrm{d}b(\pi)}{\mathrm{d}\pi} - f(\alpha(\pi);\pi)\frac{\mathrm{d}a(\pi)}{\mathrm{d}\pi}$$

$$+\ \sum_i \Big(f(c_i(\pi)^-,\pi) - f(c_i(\pi)^+,\pi)\Big)\frac{\mathrm{d}c_i(\pi)}{\mathrm{d}\pi}$$

Reminder from calculus

Differentiation under the integral sign
Also known as the Leibniz integral rule

$$\frac{\mathrm{d}}{\mathrm{d}\pi}\int_{a(\pi)} f(x,\pi)\mathrm{d}x \;=\; \int_{a(\pi)}^{b(\pi)} \frac{\mathrm{d}}{\mathrm{d}\pi} f(x,\pi)\mathrm{d}x$$

Move derivative inside integral

Account for changes in integration limits

$$+\; f(b(\pi),\pi)\frac{\mathrm{d}b(\pi)}{\mathrm{d}\pi} - f(\alpha(\pi);\pi)\frac{\mathrm{d}a(\pi)}{\mathrm{d}\pi}$$

Account for discontinuities of integrand that depend on π

$$+\; \sum_i \Big(f(c_i(\pi)^-,\pi) - f(c_i(\pi)^+,\pi)\Big)\frac{\mathrm{d}c_i(\pi)}{\mathrm{d}\pi}$$

A simple example

$$f(x,\pi) = \begin{cases} 0 & \text{if } x < 2\pi \\ 1 & \text{if } x \geq 2\pi \end{cases}$$

$$\frac{\mathrm{d}}{\mathrm{d}\pi}\int_0^{4\pi} f(x,\pi)\mathrm{d}x \qquad =$$

A simple example

$$f(x, \pi) = \begin{cases} 0 & \text{if } x < 2\pi \\ 1 & \text{if } x \geq 2\pi \end{cases}$$

$$\frac{\mathrm{d}}{\mathrm{d}\pi} \int_0^{4\pi} f(x, \pi) \mathrm{d}x \qquad =$$

A simple example

$$f(x, \pi) = \begin{cases} 0 & \text{if } x < 2\pi \\ 1 & \text{if } x \geq 2\pi \end{cases}$$

$$\frac{\mathrm{d}}{\mathrm{d}\pi} \int_0^{4\pi} f(x, \pi) \mathrm{d}x \quad = \int_0^{2\pi} \frac{\mathrm{d}}{\mathrm{d}\pi} 0 \mathrm{d}x + \int_{2\pi}^{4\pi} \frac{\mathrm{d}}{\mathrm{d}\pi} 1 \mathrm{d}x$$

Move derivative inside integral

A simple example

$$f(x,\pi) = \begin{cases} 0 & \text{if } x < 2\pi \\ 1 & \text{if } x \geq 2\pi \end{cases}$$

$$\frac{\mathrm{d}}{\mathrm{d}\pi}\int_{0}^{4\pi} f(x,\pi)\mathrm{d}x = \int_0^{2\pi}\frac{\mathrm{d}}{\mathrm{d}\pi}0\mathrm{d}x + \int_{2\pi}^{4\pi}\frac{\mathrm{d}}{\mathrm{d}\pi}1\mathrm{d}x$$

Move derivative inside integral

Account for changes in integration limits

$$+\ 1\frac{\mathrm{d}(4\pi)}{\mathrm{d}\pi} - 0\frac{\mathrm{d}0}{\mathrm{d}\pi}$$

A simple example

$$f(x,\pi) = \begin{cases} 0 & \text{if } x < 2\pi \\ 1 & \text{if } x \geq 2\pi \end{cases}$$

$$\frac{\mathrm{d}}{\mathrm{d}\pi}\int_0^{4\pi} f(x,\pi)\mathrm{d}x \quad = \int_0^{2\pi} \frac{\mathrm{d}}{\mathrm{d}\pi} 0 \mathrm{d}x + \int_{2\pi}^{4\pi} \frac{\mathrm{d}}{\mathrm{d}\pi} 1 \mathrm{d}x$$

Move derivative inside integral

Account for changes in integration limits

$$+ \; 1\frac{\mathrm{d}(4\pi)}{\mathrm{d}\pi} - 0\frac{\mathrm{d}0}{\mathrm{d}\pi}$$

Account for discontinuities of integrand that depend on π

$$+ \; (0-1)\frac{\mathrm{d}(2\pi)}{\mathrm{d}\pi}$$

Leibniz integral rule

Differentiation under the integral sign
Also known as the Leibniz integral rule

$$\frac{\mathrm{d}}{\mathrm{d}\pi}\int_{a(\pi)} f(x,\pi)\mathrm{d}x = \int_{a(\pi)}^{b(\pi)} \frac{\mathrm{d}}{\mathrm{d}\pi} f(x,\pi)\mathrm{d}x$$

Move derivative inside integral

Account for changes in integration limits

$$+ \; f(b(\pi),\pi)\frac{\mathrm{d}b(\pi)}{\mathrm{d}\pi} - f(\alpha(\pi);\pi)\frac{\mathrm{d}a(\pi)}{\mathrm{d}\pi}$$

Account for discontinuities of integrand that depend on π

$$+ \; \sum_i \left(f(c_i(\pi)^-,\pi) - f(c_i(\pi)^+,\pi)\right)\frac{\mathrm{d}c_i(\pi)}{\mathrm{d}\pi}$$

Leibniz integral rule

Differentiation under the integral sign
Also known as the Leibniz integral rule

$$\frac{\mathrm{d}}{\mathrm{d}\pi}\int_{a(\pi)} f(x,\pi)\mathrm{d}x = \int_{a(\pi)}^{b(\pi)} \frac{\mathrm{d}}{\mathrm{d}\pi} f(x,\pi)\mathrm{d}x$$

Move derivative inside integral

Account for changes in integration limits

$$+ \; f(b(\pi),\pi)\frac{\mathrm{d}b(\pi)}{\mathrm{d}\pi} - f(\alpha(\pi);\pi)\frac{\mathrm{d}a(\pi)}{\mathrm{d}\pi}$$

Account for discontinuities of integrand that depend on π

$$+ \; \sum_i \Big(f(c_i(\pi)^-,\pi) - f(c_i(\pi)^+,\pi)\Big)\frac{\mathrm{d}c_i(\pi)}{\mathrm{d}\pi}$$

Leibniz integral rule

Differentiation under the integral sign
Also known as the Leibniz integral rule

Interior integral

$$\frac{\mathrm{d}}{\mathrm{d}\pi}\int_{a(\pi)} f(x,\pi)\mathrm{d}x = \int_{a(\pi)}^{b(\pi)} \frac{\mathrm{d}}{\mathrm{d}\pi} f(x,\pi)\mathrm{d}x$$

Move derivative inside integral

Boundary terms

Account for changes in integration limits

$$+ \; f(b(\pi),\pi)\frac{\mathrm{d}b(\pi)}{\mathrm{d}\pi} - f(\alpha(\pi);\pi)\frac{\mathrm{d}a(\pi)}{\mathrm{d}\pi}$$

Account for discontinuities of integrand that depend on π

$$+ \; \sum_i \Big(f(c_i(\pi)^-,\pi) - f(c_i(\pi)^+,\pi)\Big)\frac{\mathrm{d}c_i(\pi)}{\mathrm{d}\pi}$$

Reynolds transport theorem

$$\frac{\mathrm{d}}{\mathrm{d}\pi}\int_{\Omega(\pi)} f(x,\pi)\mathrm{d}A(x) \stackrel{?}{=}$$

Reynolds transport theorem

$$\frac{\mathrm{d}}{\mathrm{d}\pi}\int_{\Omega(\pi)} f(x,\pi)\,\mathrm{d}A(x) \overset{?}{=}$$

Reynolds transport theorem

$$\frac{\mathrm{d}}{\mathrm{d}\pi}\int_{\Omega(\pi)} f(x,\pi)\,\mathrm{d}A(x) \stackrel{?}{=}$$

Reynolds transport theorem [1903]
Generalization of the Leibniz rule

Reynolds transport theorem

$$\frac{\mathrm{d}}{\mathrm{d}\pi}\int_{\Omega(\pi)} f(x,\pi)\mathrm{d}A(x) = \int_{\Omega(\pi)} \frac{\mathrm{d}f(x,\pi)}{\mathrm{d}\pi}\mathrm{d}A(x) + \int_{\partial\Omega(\pi)} g(x,\pi)\mathrm{d}l(x)$$

Reynolds transport theorem [1903]
Generalization of the Leibniz rule

Reynolds transport theorem

$$\frac{\mathrm{d}}{\mathrm{d}\pi}\int_{\Omega(\pi)} f(x,\pi)\mathrm{d}A(x) = \int_{\Omega(\pi)} \frac{\mathrm{d}f(x,\pi)}{\mathrm{d}\pi}\mathrm{d}A(x) + \int_{\partial\Omega(\pi)} g(x,\pi)\mathrm{d}l(x)$$

Boundary domain

||

discontinuity points ∪ boundary of domain Ω
(if they depend on π)

Reynolds transport theorem [1903]
Generalization of the Leibniz rule

Reynolds transport theorem

$$\frac{\mathrm{d}}{\mathrm{d}\pi}\int_{\Omega(\pi)} f(x,\pi)\mathrm{d}A(x) = \int_{\Omega(\pi)} \frac{\mathrm{d}f(x,\pi)}{\mathrm{d}\pi}\mathrm{d}A(x) + \int_{\partial\Omega(\pi)} g(x,\pi)\mathrm{d}l(x)$$

Boundary domain

||

discontinuity points ∪ boundary of domain Ω
(if they depend on π)

Reynolds transport theorem [1903]
Generalization of the Leibniz rule

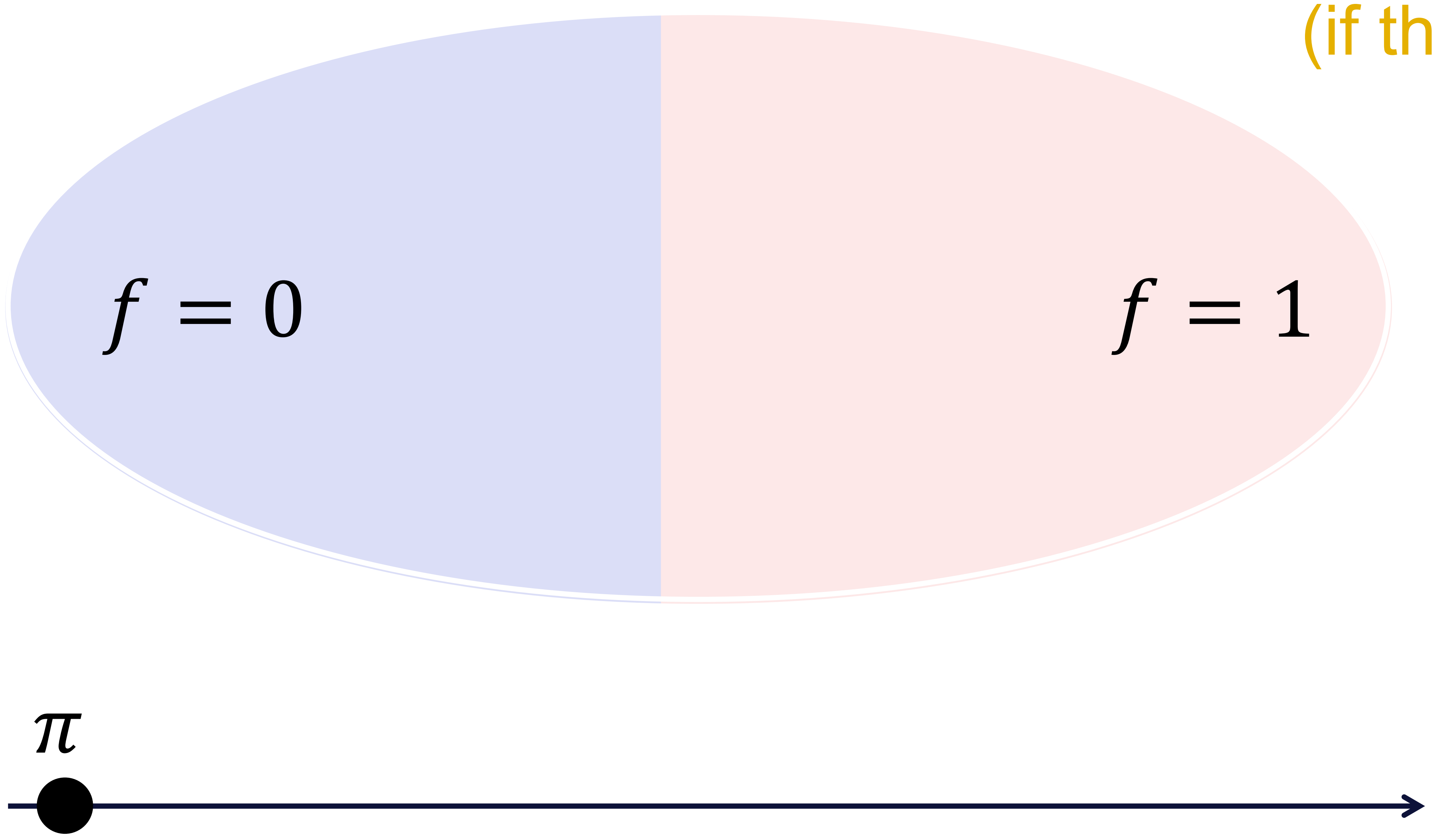

Reynolds transport theorem

$$\frac{\mathrm{d}}{\mathrm{d}\pi}\int_{\Omega(\pi)} f(x,\pi)\mathrm{d}A(x) = \int_{\Omega(\pi)} \frac{\mathrm{d}f(x,\pi)}{\mathrm{d}\pi}\mathrm{d}A(x) + \underbrace{\int_{\partial\Omega(\pi)} g(x,\pi)\mathrm{d}l(x)}_{\text{Boundary domain}}$$

Boundary domain

||

discontinuity points ∪ boundary of domain Ω
(if they depend on π)

Reynolds transport theorem [1903]
Generalization of the Leibniz rule

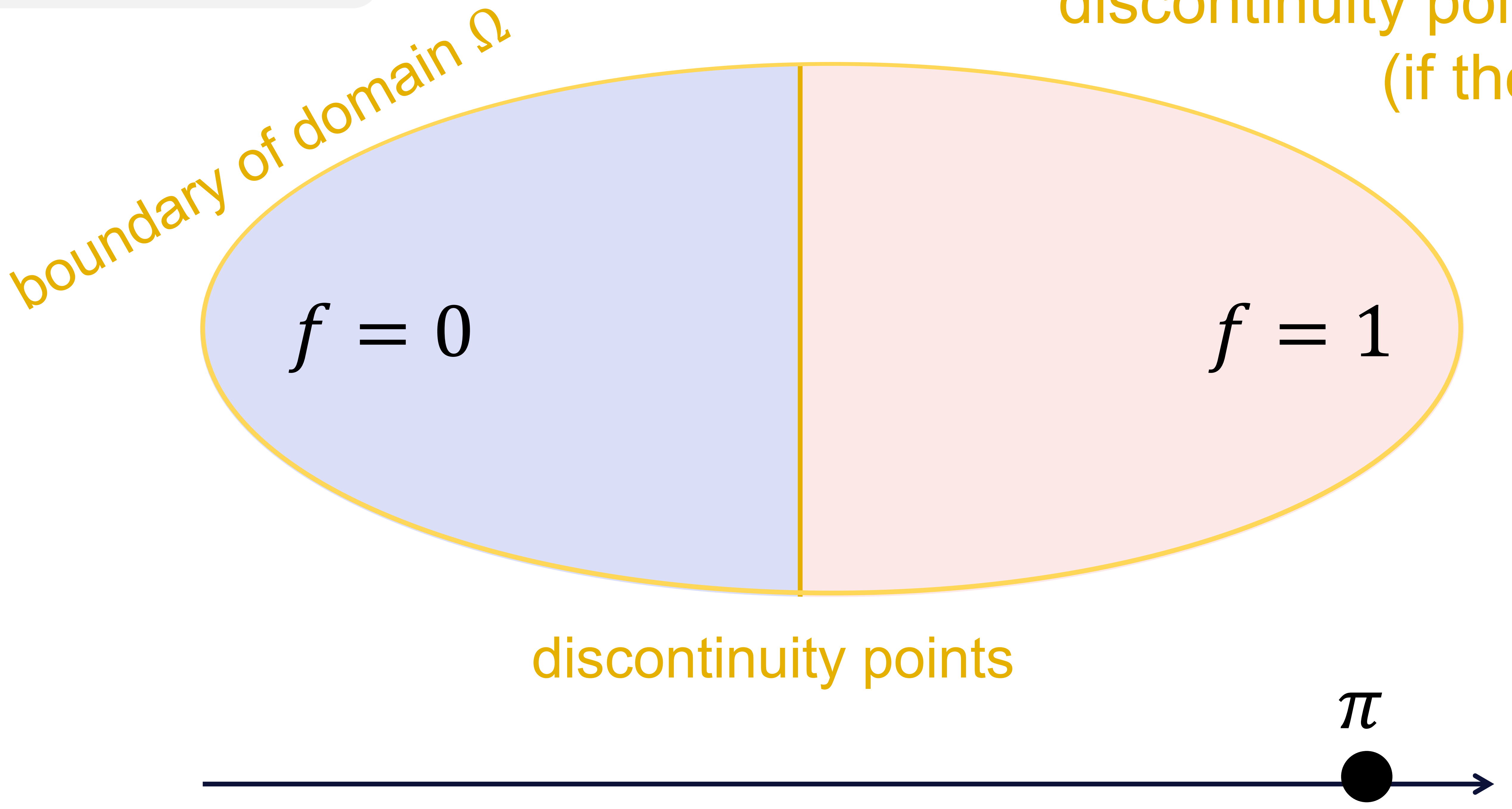

Reynolds transport theorem

$$\frac{\mathrm{d}}{\mathrm{d}\pi}\int_{\Omega(\pi)} f(x,\pi)\mathrm{d}A(x) = \int_{\Omega(\pi)} \frac{\mathrm{d}f(x,\pi)}{\mathrm{d}\pi}\mathrm{d}A(x) + \int_{\partial\Omega(\pi)} g(x,\pi)\mathrm{d}l(x)$$

Interior integral

Boundary integral

Reynolds transport theorem [1903]
Generalization of the Leibniz rule

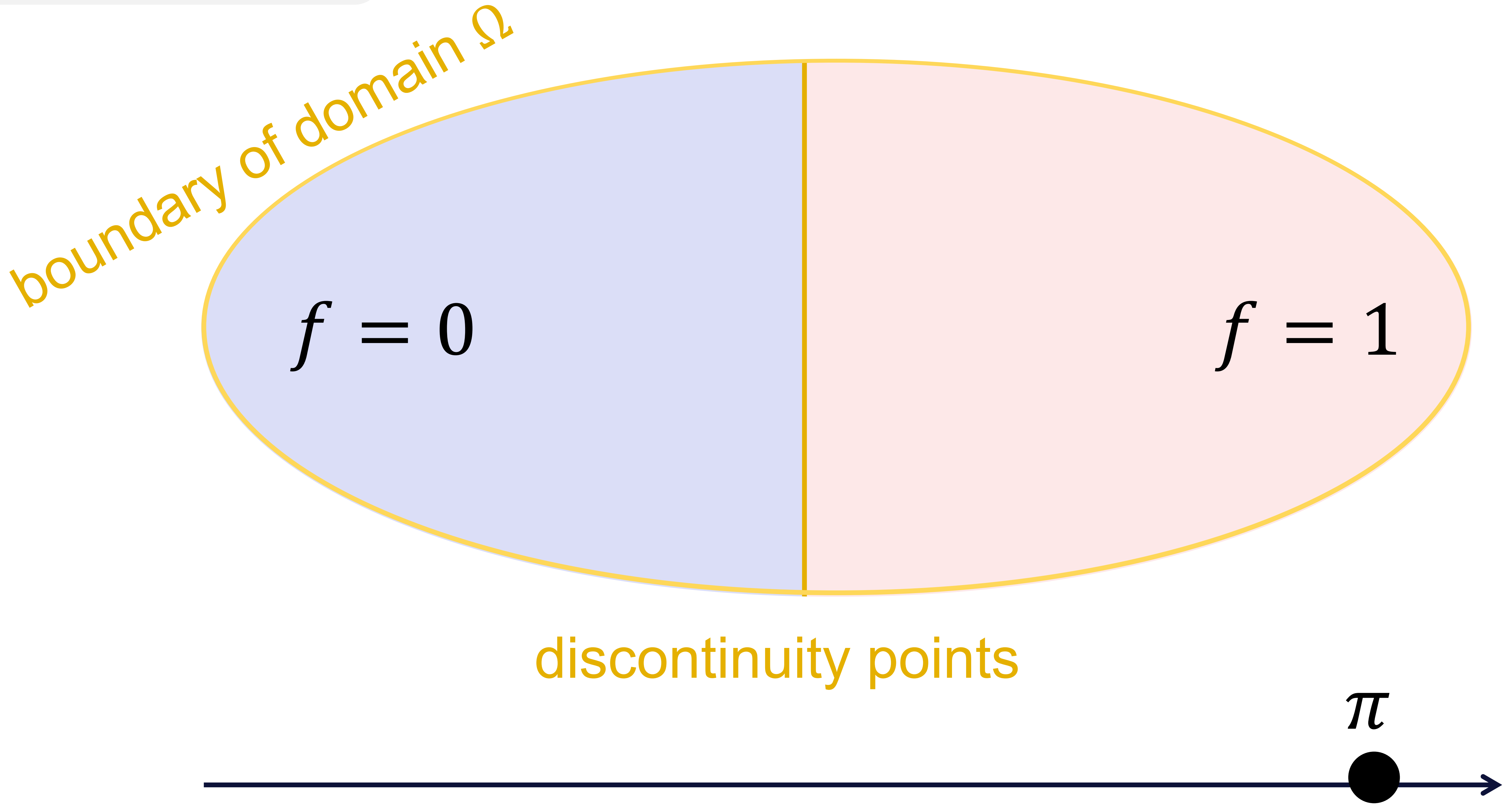

DIFFERENTIATING DIRECT ILLUMINATION

Direct illumination integral

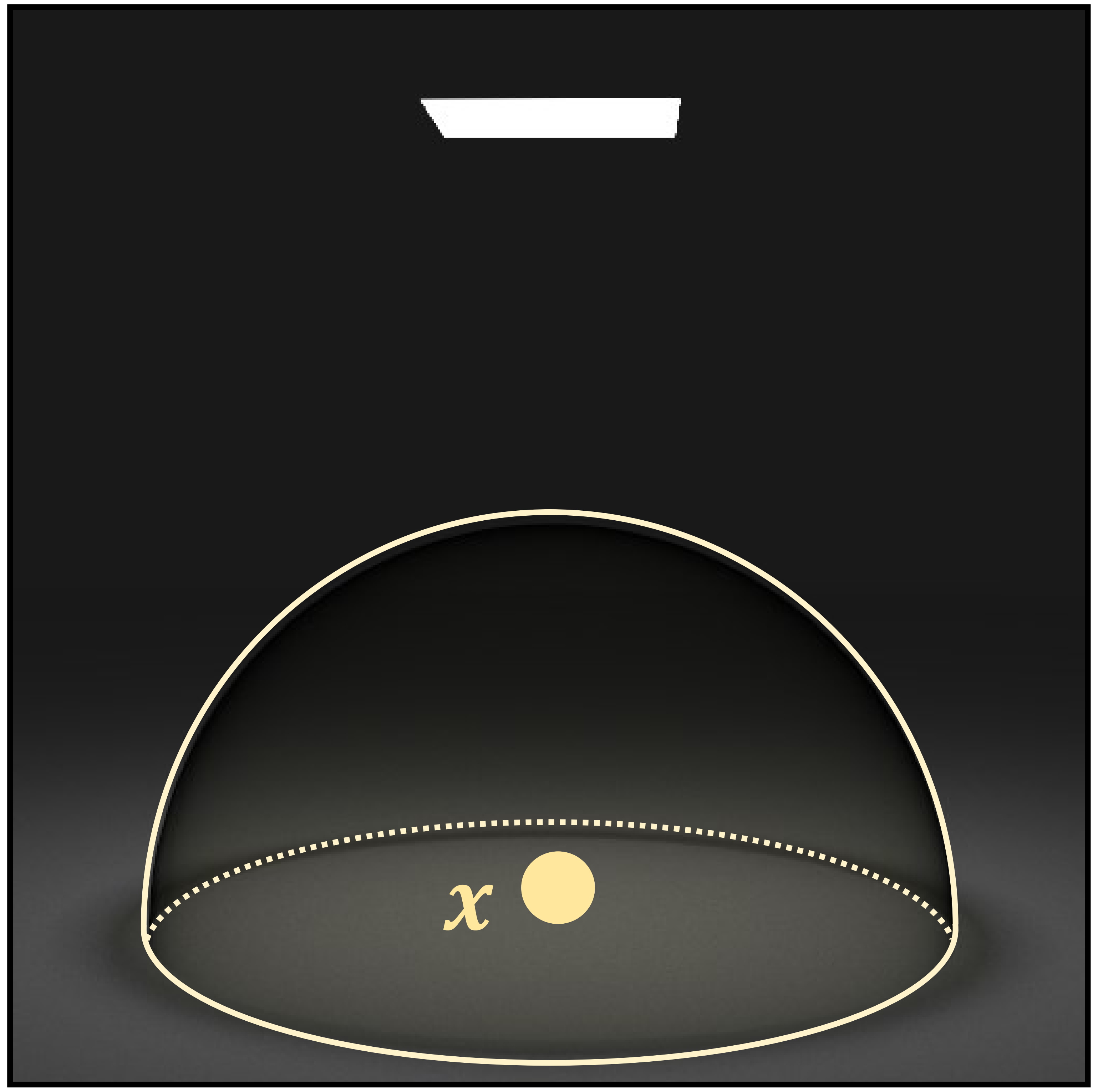

Radiance from x:

$$I = \int_{\mathbb{H}^2} f_r(\omega_i, \omega_o)\, L_i(\omega_i)\, (n \cdot \omega_i)\, \mathrm{d}\sigma(\omega_i)$$

Direct illumination integral

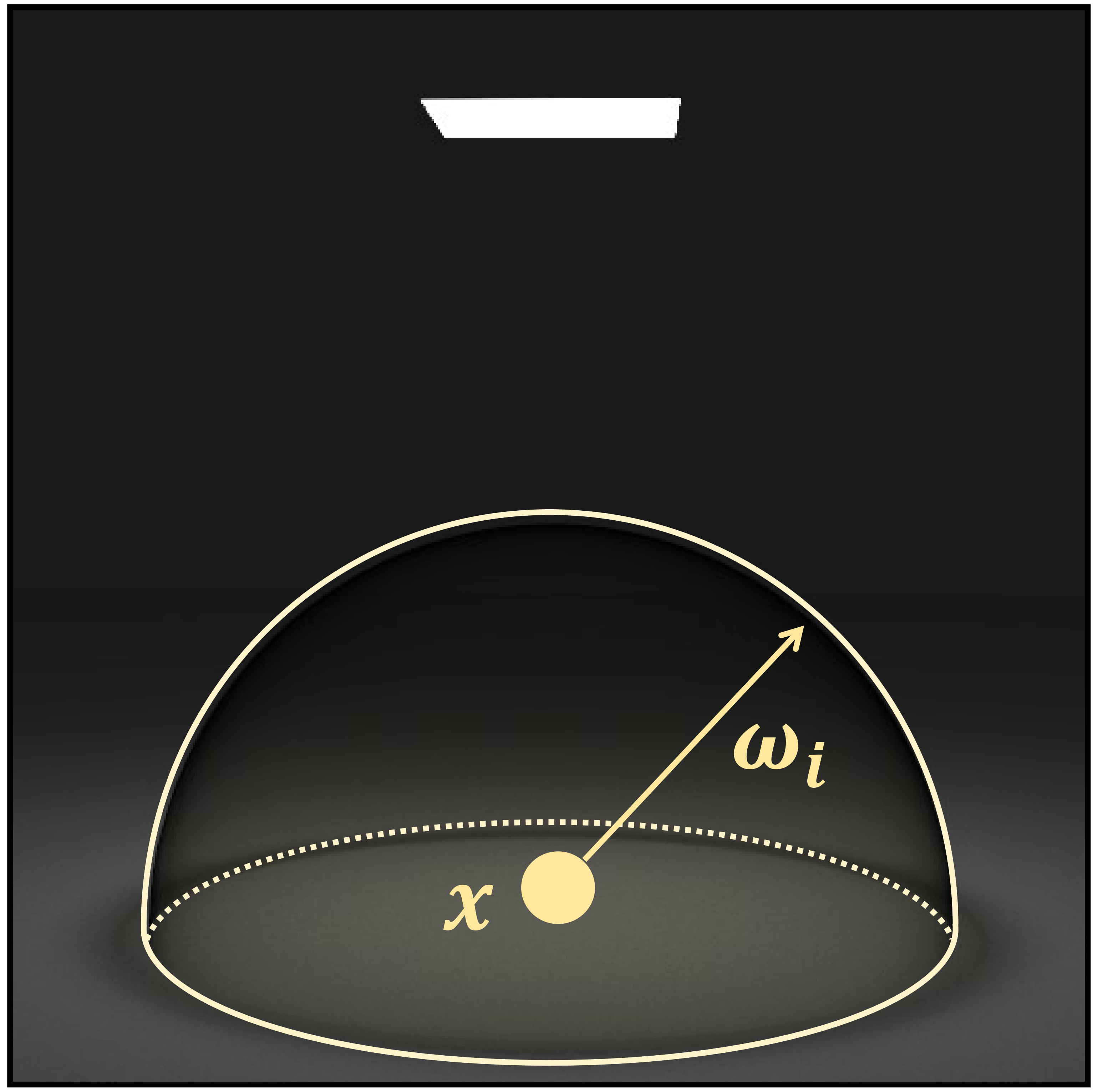

Radiance from x:

$$I = \int_{\mathbb{H}^2} f_r(\omega_i, \omega_o)\, L_i(\omega_i)\, (n \cdot \omega_i)\, \mathrm{d}\sigma(\omega_i)$$

Unit hemisphere

Direct illumination integral

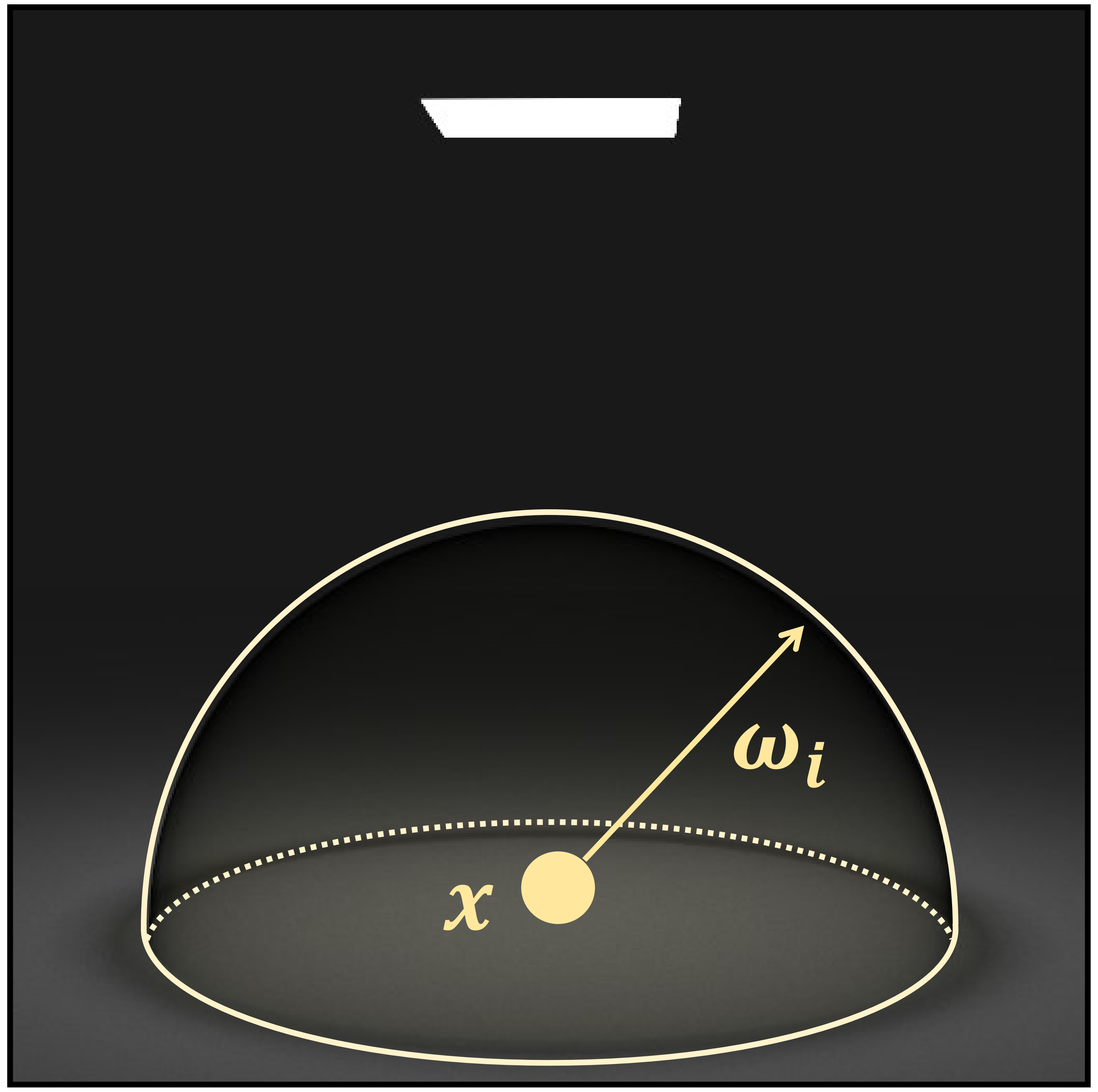

Radiance from x:

Incident radiance

$$I = \int_{\mathbb{H}^2} f_r(\omega_i, \omega_o)\, L_i(\omega_i)\, (n \cdot \omega_i)\, \mathrm{d}\sigma(\omega_i)$$

Unit hemisphere

Direct illumination integral

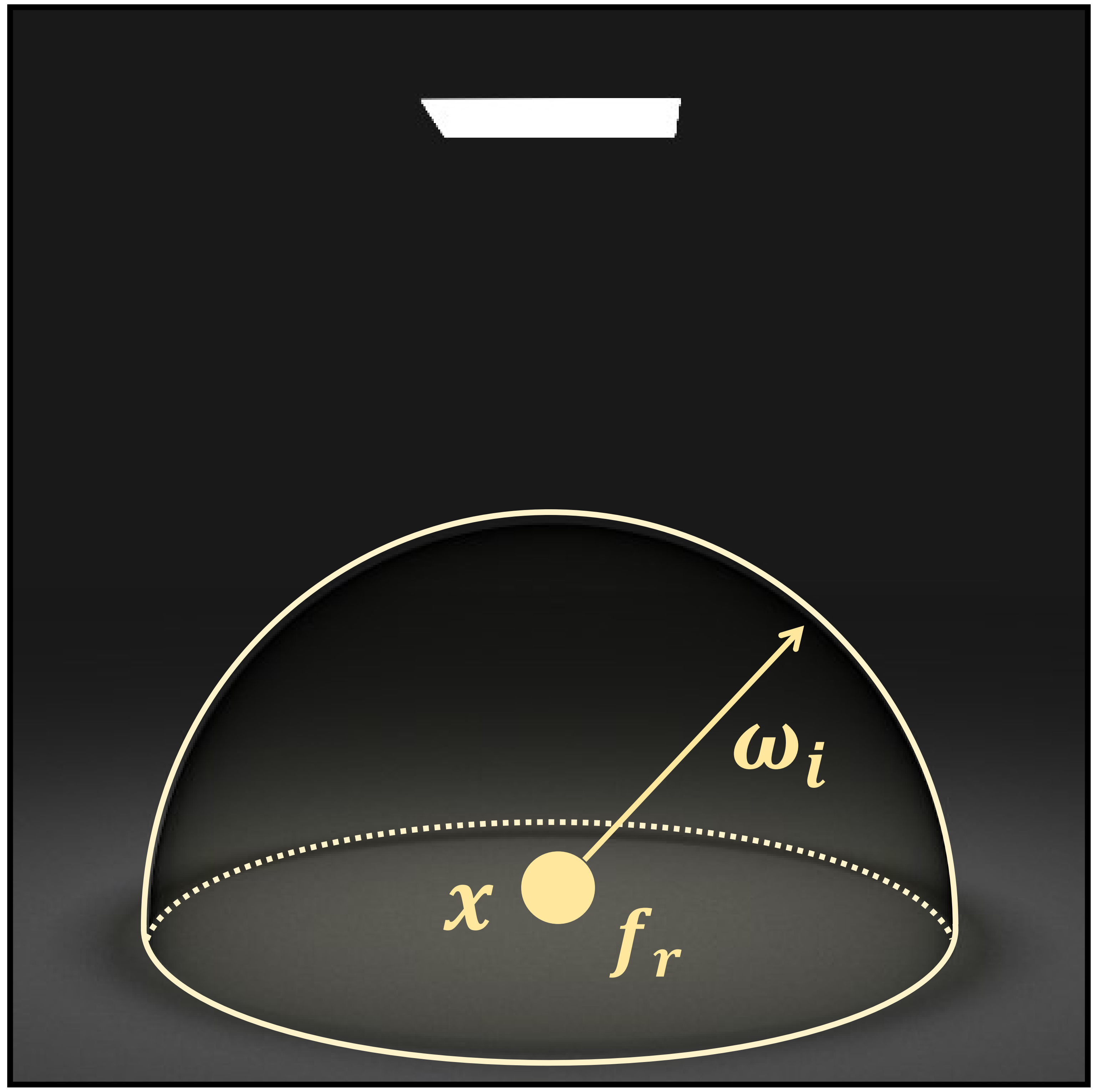

Radiance from x:

Reflectance (BRDF)

Incident radiance

$$I = \int_{\mathbb{H}^2} f_r(\omega_i, \omega_o)\, L_i(\omega_i)\, (n \cdot \omega_i)\, \mathrm{d}\sigma(\omega_i)$$

Unit hemisphere

Direct illumination integral

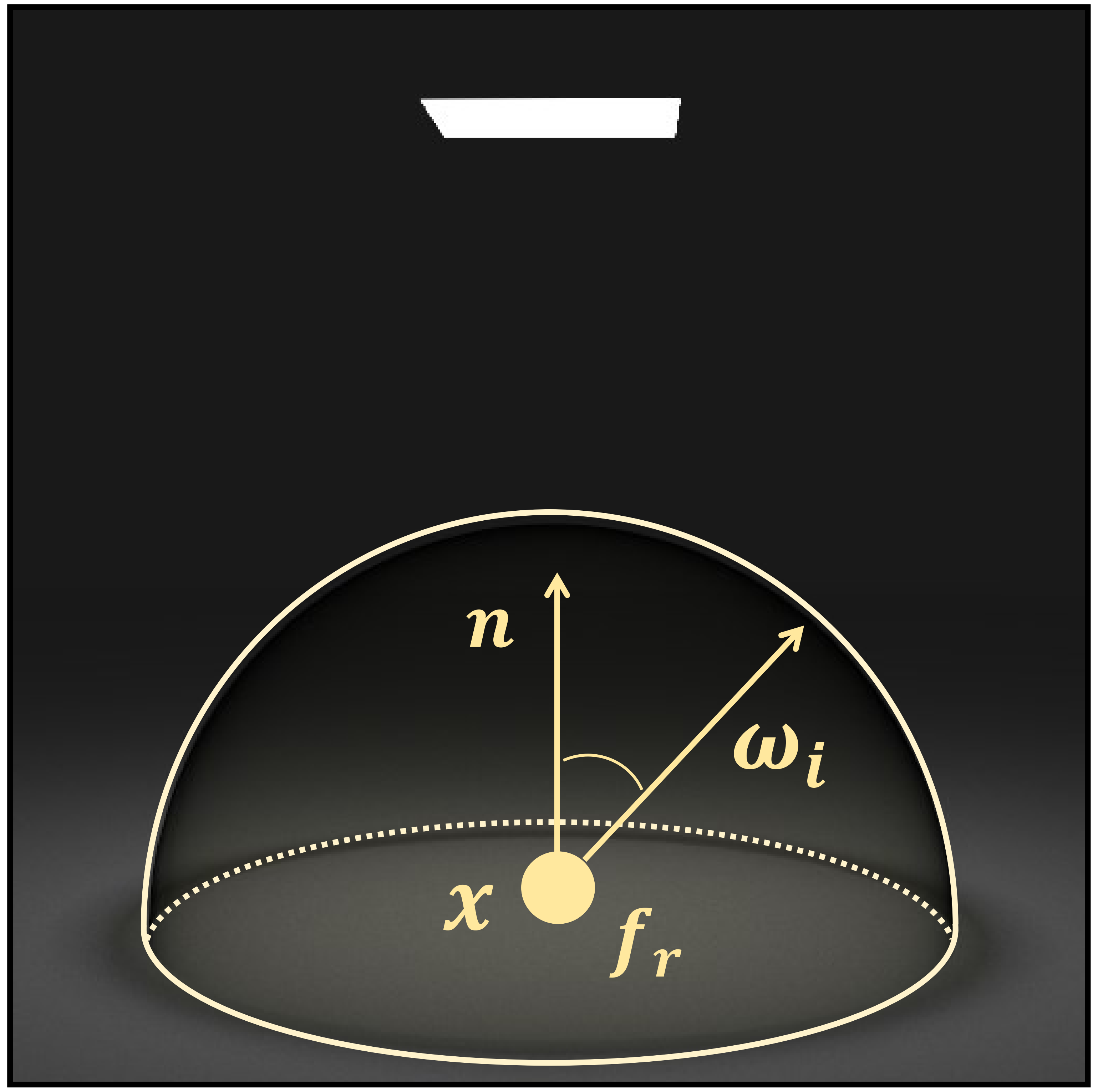

Radiance from x:

Reflectance (BRDF) · Incident radiance · Shading wrt normal $\boldsymbol{n}$

$$I = \underbrace{\int_{\mathbb{H}^2}}_{\text{Unit hemisphere}} \underbrace{f_r(\omega_i, \omega_o)}_{\text{Reflectance (BRDF)}} \underbrace{L_i(\omega_i)}_{\text{Incident radiance}} \underbrace{(n \cdot \omega_i)}_{\text{Shading wrt normal } \boldsymbol{n}} \, \mathrm{d}\sigma(\omega_i)$$

Unit hemisphere

Direct illumination integral

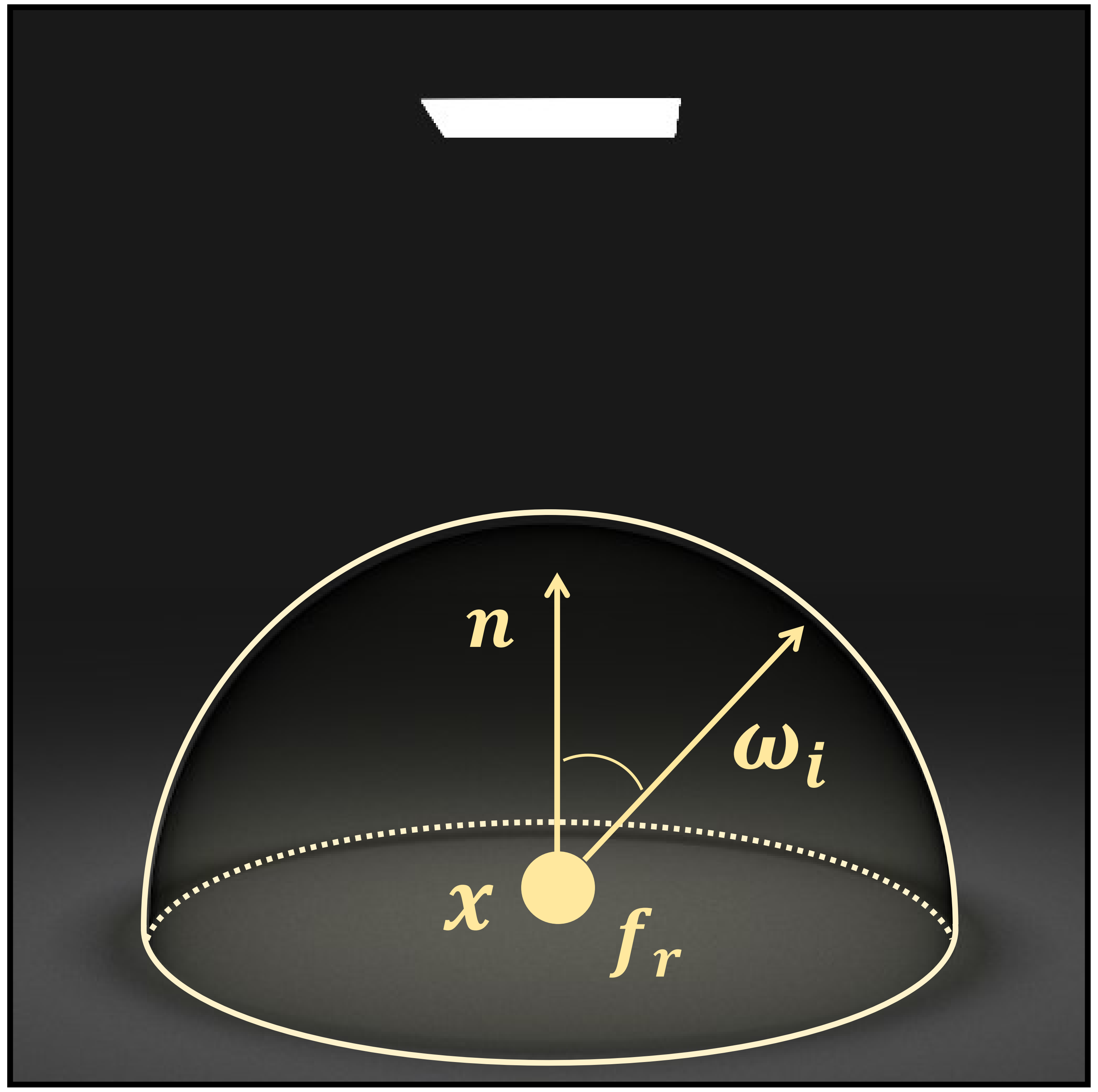

Radiance from x:

Reflectance (BRDF) — Incident radiance — Shading wrt normal $\boldsymbol{n}$

$$I = \int_{\mathbb{H}^2} f_r(\omega_i, \omega_o)\, L_i(\omega_i)\, (n \cdot \omega_i)\, \mathrm{d}\sigma(\omega_i)$$

Unit hemisphere

Monte Carlo rendering:

Direct illumination integral

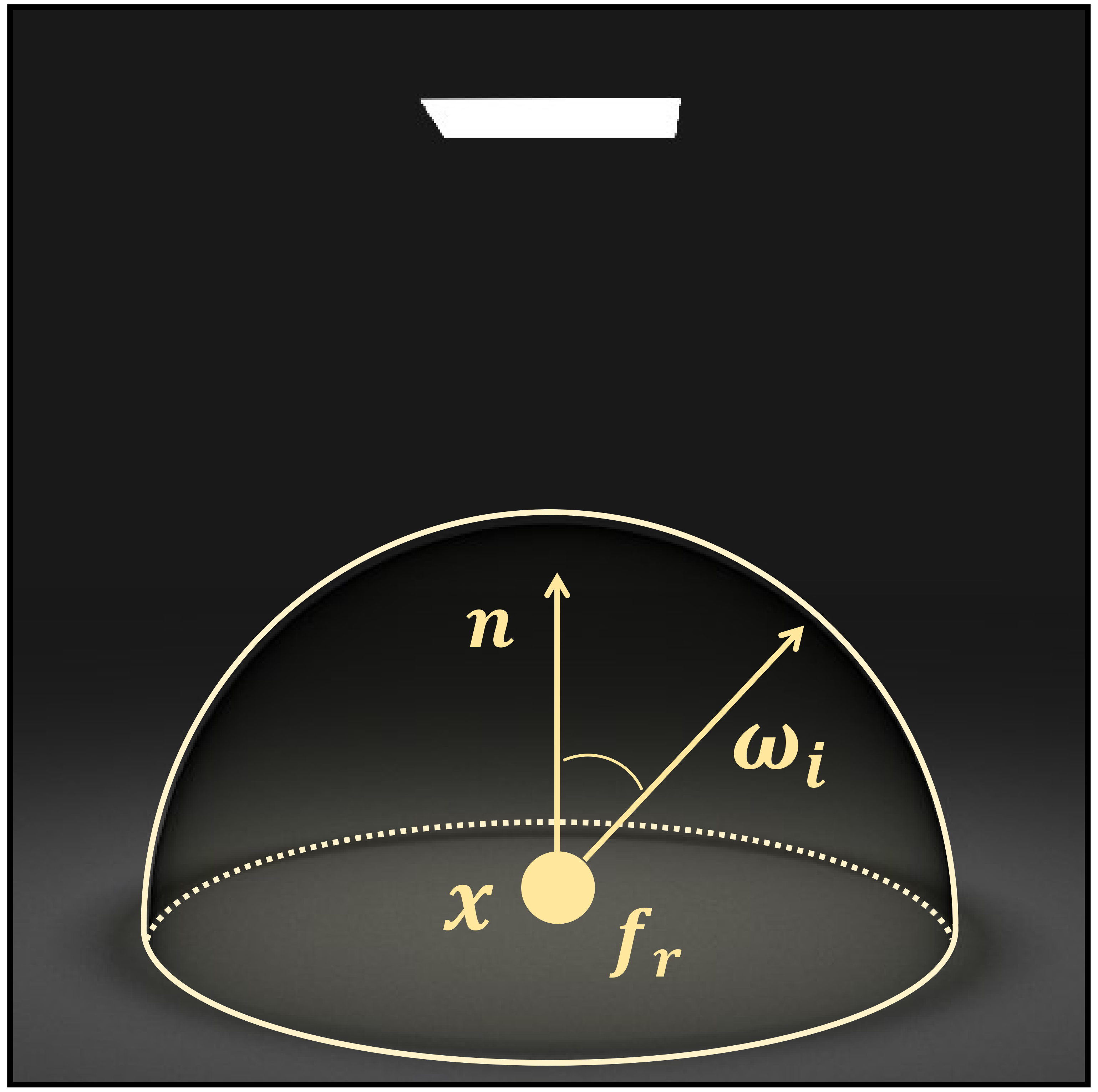

Radiance from x:

$$I = \underbrace{\int_{\mathbb{H}^2}}_{\text{Unit hemisphere}} \underbrace{f_r(\omega_i, \omega_o)}^{\text{Reflectance (BRDF)}} \underbrace{L_i(\omega_i)}^{\text{Incident radiance}} \underbrace{(n \cdot \omega_i)}^{\text{Shading wrt normal } \boldsymbol{n}} \, \mathrm{d}\sigma(\omega_i)$$

Monte Carlo rendering:

- Sample random directions ω_i^s from PDF $p(\omega_i)$

Direct illumination integral

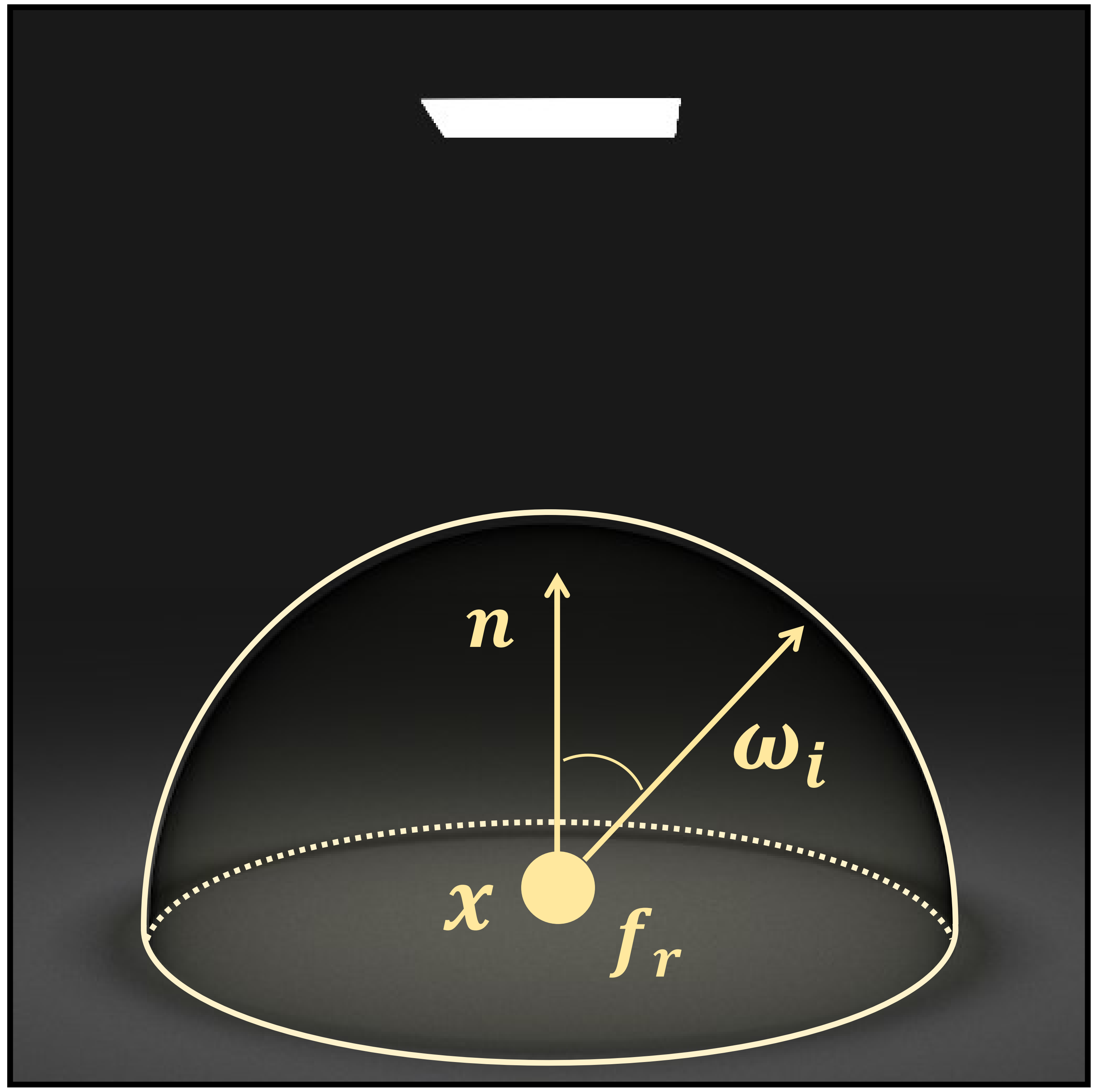

Radiance from x:

Reflectance (BRDF) | Incident radiance | Shading wrt normal $\boldsymbol{n}$

$$I = \int_{\mathbb{H}^2} f_r(\omega_i, \omega_o)\, L_i(\omega_i)\, (n \cdot \omega_i)\, \mathrm{d}\sigma(\omega_i)$$

Unit hemisphere

Monte Carlo rendering:

- Sample random directions ω_i^s from PDF $p(\omega_i)$
- Form estimator

$$I \approx \sum_s \frac{f_r(\omega_i^s, \omega_o)\, L_i(\omega_i^s)\, (n \cdot \omega_i^s)}{p(\omega_i^s)}$$

Differential direct illumination

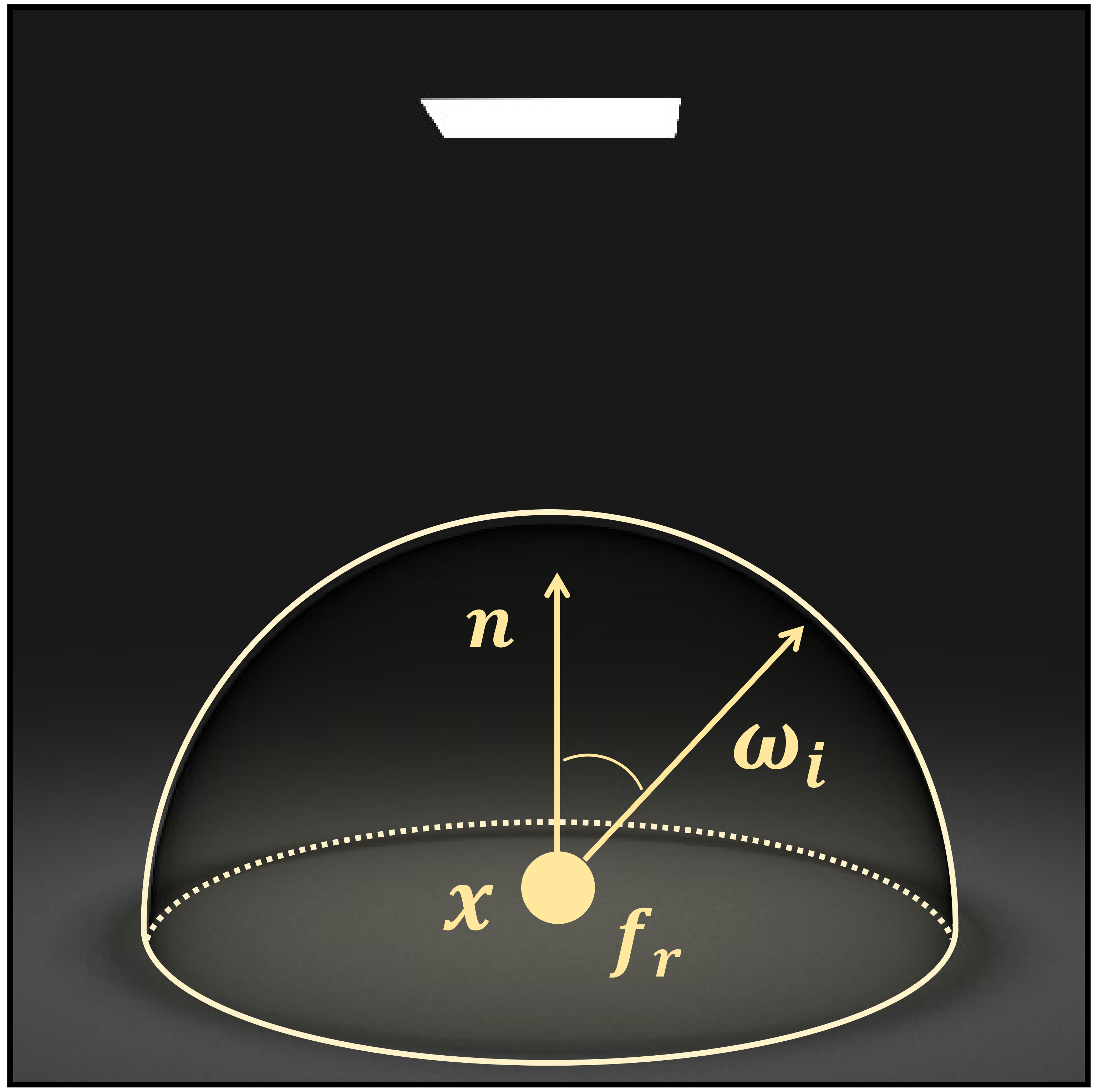

Differential radiance from x:

$$\frac{\mathrm{d}I}{\mathrm{d}\pi} = \frac{\mathrm{d}}{\mathrm{d}\pi} \int_{\mathbb{H}^2} f_r(\omega_i, \omega_o)\, L_i(\omega_i)\, (n \cdot \omega_i)\, \mathrm{d}\sigma(\omega_i)$$

Differential direct illumination: local parameters

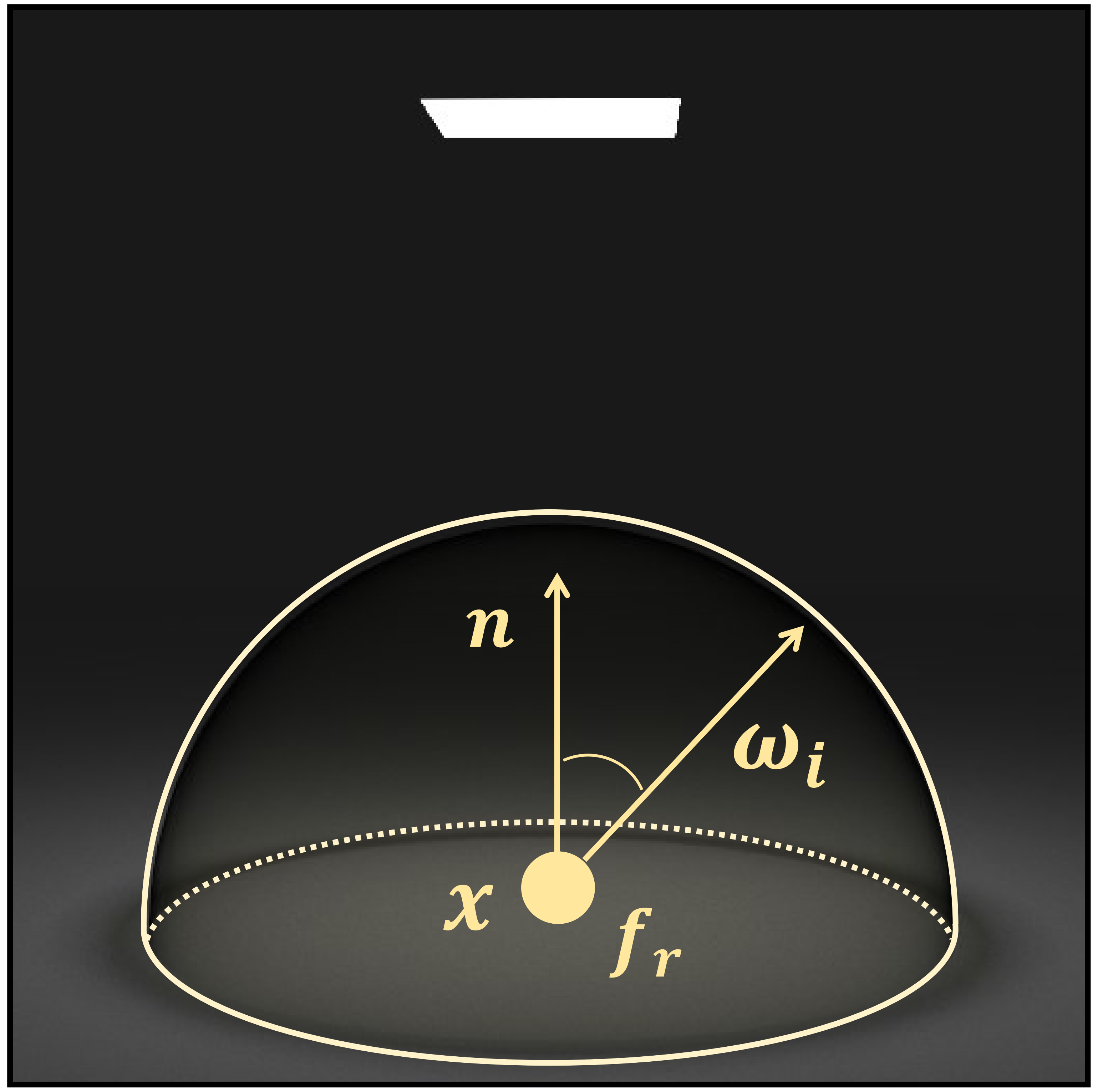

Differential radiance from x:

$$\frac{\mathrm{d}I}{\mathrm{d}\pi} = \frac{\mathrm{d}}{\mathrm{d}\pi}\int_{\mathbb{H}^2} f_r(\omega_i, \omega_o)\, L_i(\omega_i)\, (n \cdot \omega_i)\, \mathrm{d}\sigma(\omega_i)$$

Differential direct illumination: local parameters

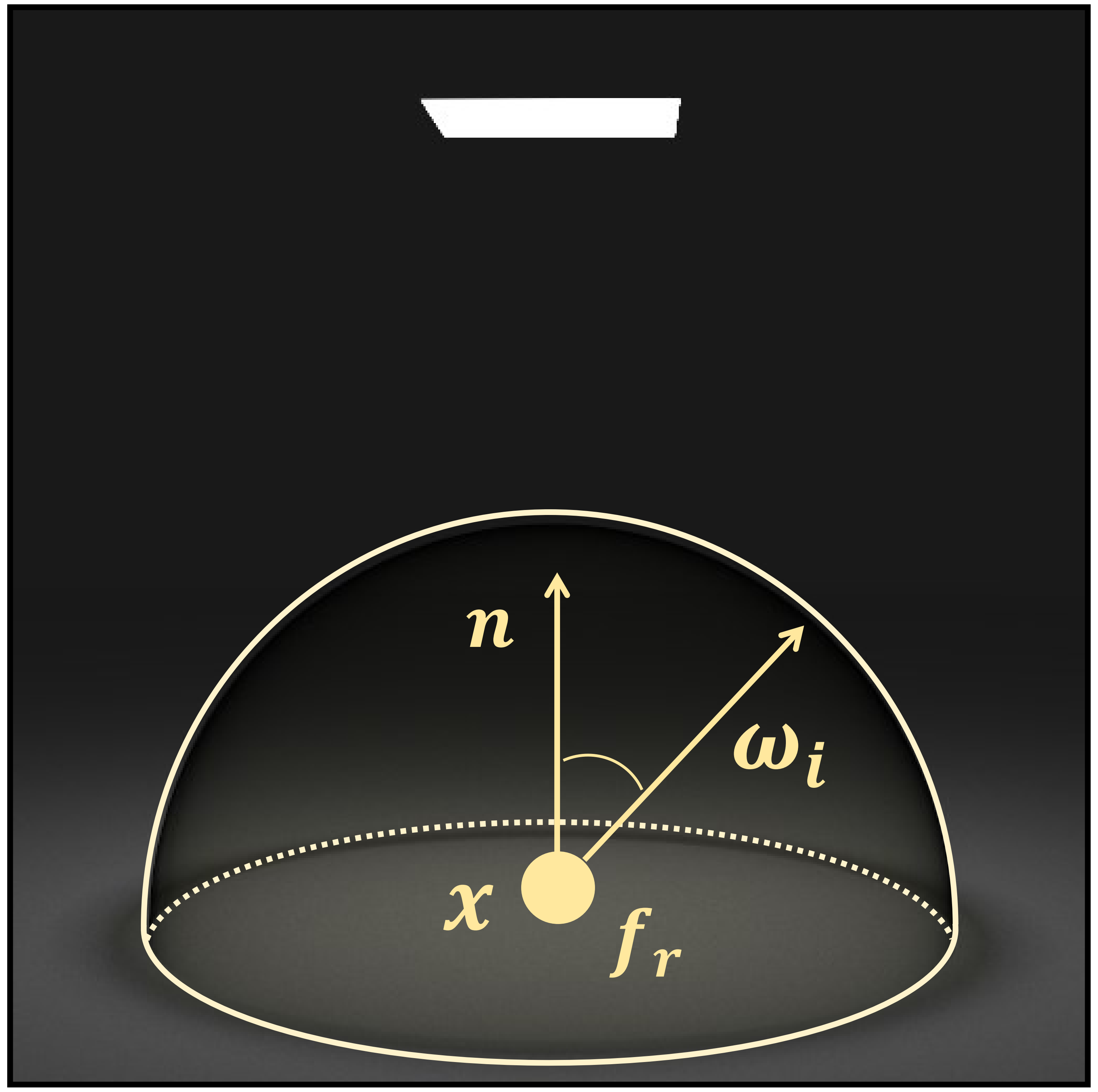

Differential radiance from x:

$$\frac{\mathrm{d}I}{\mathrm{d}\pi} = \frac{\mathrm{d}}{\mathrm{d}\pi} \int_{\mathbb{H}^2} f_r(\omega_i, \omega_o)\, L_i(\omega_i)\, (n \cdot \omega_i)\, \mathrm{d}\sigma(\omega_i)$$

$\boldsymbol{\pi}$: *local* parameters

- BRDF parameters
- *shading* normal
- illumination brightness

Differential direct illumination: local parameters

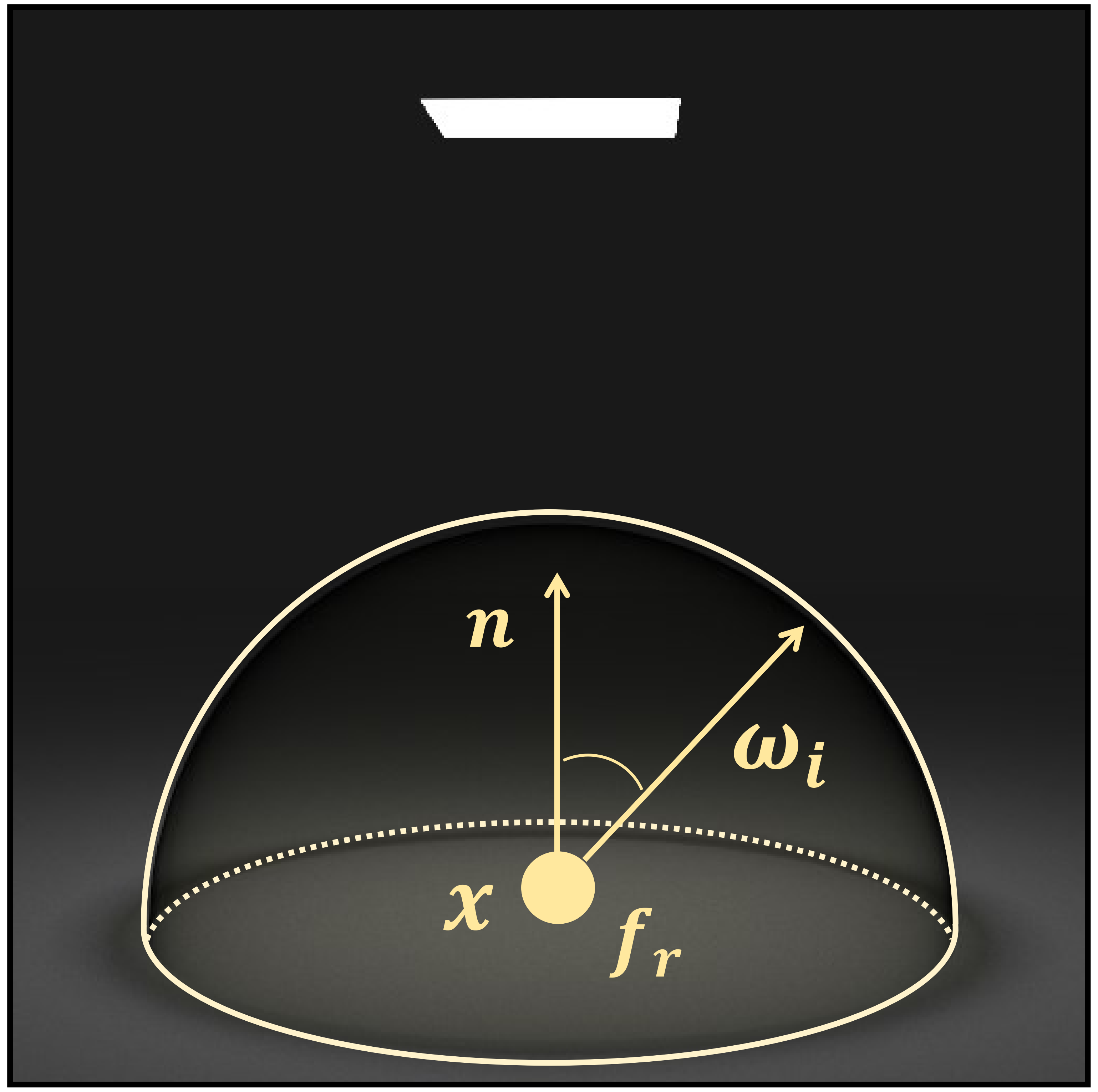

Differential radiance from x:

$$\frac{\mathrm{d}I}{\mathrm{d}\pi} = \int_{\mathbb{H}^2} \frac{\mathrm{d}}{\mathrm{d}\pi}\{f_r(\omega_i, \omega_o)\, L_i(\omega_i)\, (n \cdot \omega_i)\}\, \mathrm{d}\sigma(\omega_i)$$

Just move derivative inside integral

π: *local* parameters

- BRDF parameters
- *shading* normal
- illumination brightness

Differential direct illumination: local parameters

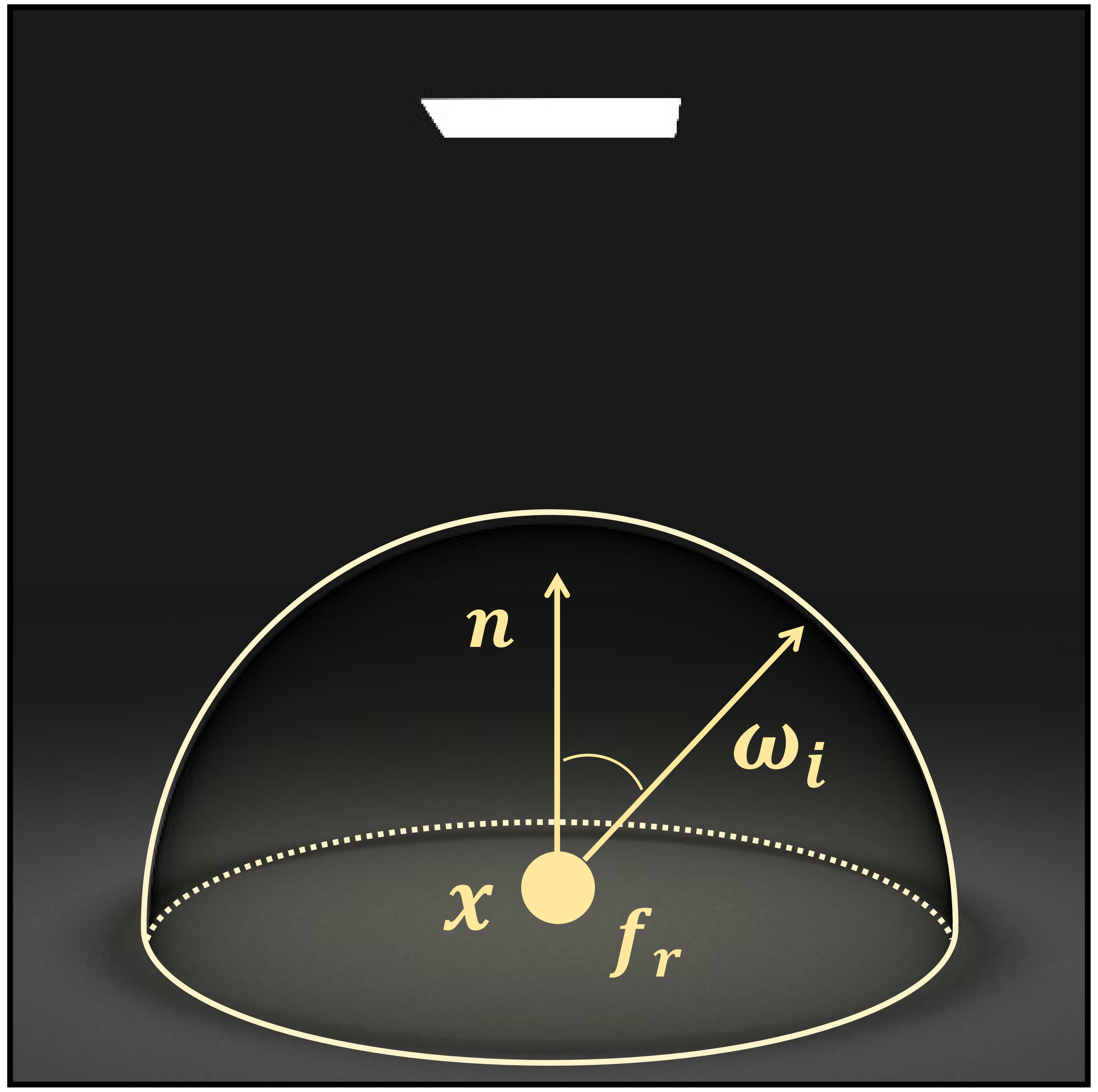

$\boldsymbol{\pi}$: *local* parameters
- BRDF parameters
- *shading* normal
- illumination brightness

Differential radiance from x:

$$\frac{\mathrm{d}I}{\mathrm{d}\pi} = \int_{\mathbb{H}^2} \frac{\mathrm{d}}{\mathrm{d}\pi}\{f_r(\omega_i,\omega_o)\, L_i(\omega_i)\, (n\cdot\omega_i)\}\, \mathrm{d}\sigma(\omega_i)$$

Just move derivative inside integral

Monte Carlo differentiable rendering:
- Sample random directions ω_i^s from PDF $p(\omega_i)$
- Form estimator

Just differentiate numerator
[Khungurn et al. 2015, Gkioulekas et al. 2015]

$$\frac{\mathrm{d}I}{\mathrm{d}\pi} \approx \sum_s \frac{\frac{\mathrm{d}}{\mathrm{d}\pi}\{f_r(\omega_i^s,\omega_o)\, L_i(\omega_i^s)\, (n\cdot\omega_i^s)\}}{p(\omega_i^s)}$$

Alternative estimator

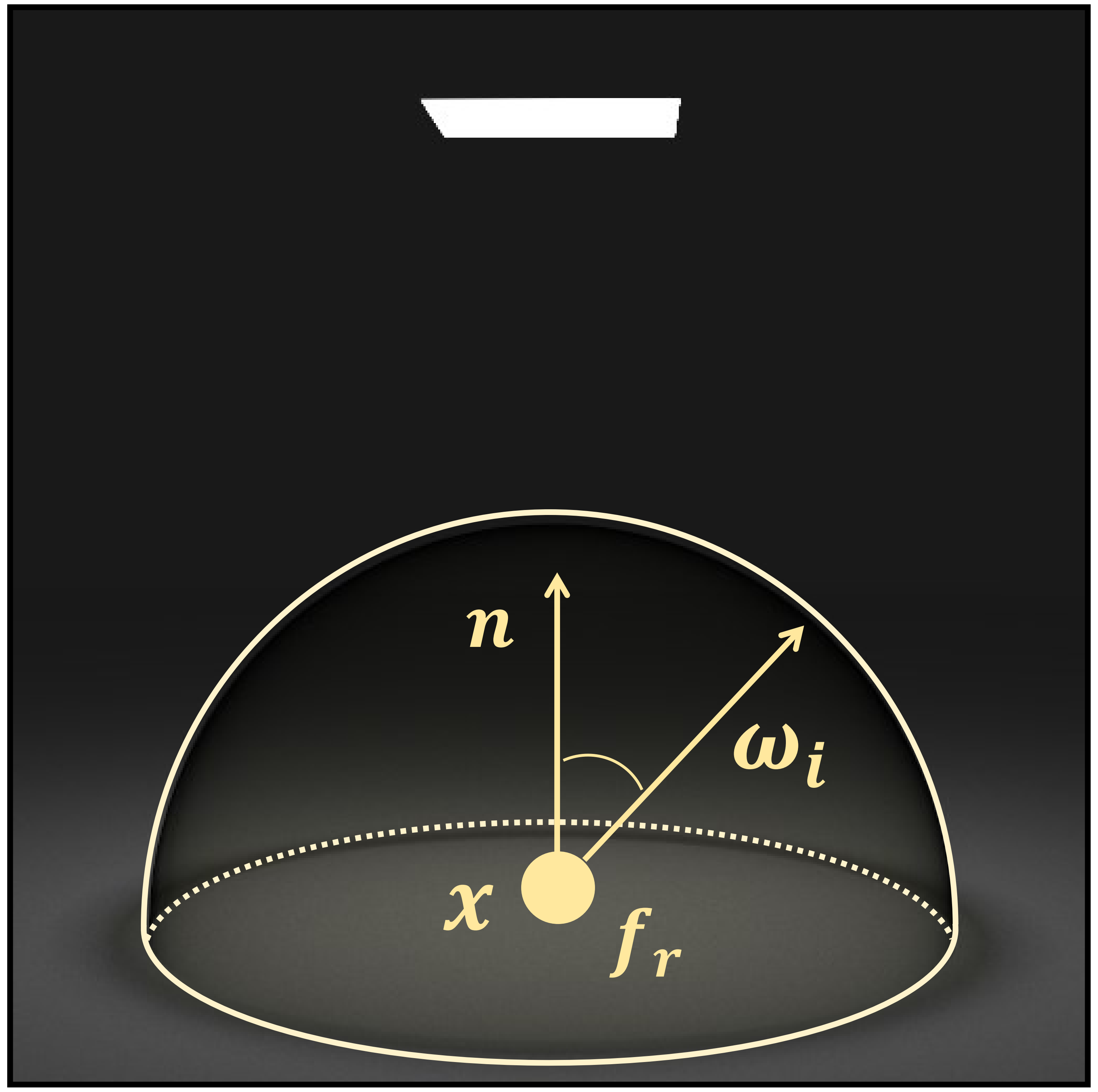

π: *local* parameters

- BRDF parameters

Differential radiance from x:

$$\frac{\mathrm{d}I}{\mathrm{d}\pi} = \int_{\mathbb{H}^2} \frac{\mathrm{d}}{\mathrm{d}\pi}\{f_r(\omega_i, \omega_o, \pi) L_i(\omega_i)(n \cdot \omega_i)\} \mathrm{d}\sigma(\omega_i)$$

Just move derivative inside integral

Monte Carlo estimation:

- Sample random directions ω_i^s from PDF $p(\omega_i, \pi)$
- Form estimator

$$\frac{\mathrm{d}I}{\mathrm{d}\pi} \approx \sum_s \frac{\frac{\mathrm{d}}{\mathrm{d}\pi}\{f_r(\omega_i^s, \omega_o, \pi)\, L_i(\omega_i^s)\, (n \cdot \omega_i^s)\}}{p(\omega_i^s, \pi)}$$

Alternative estimator

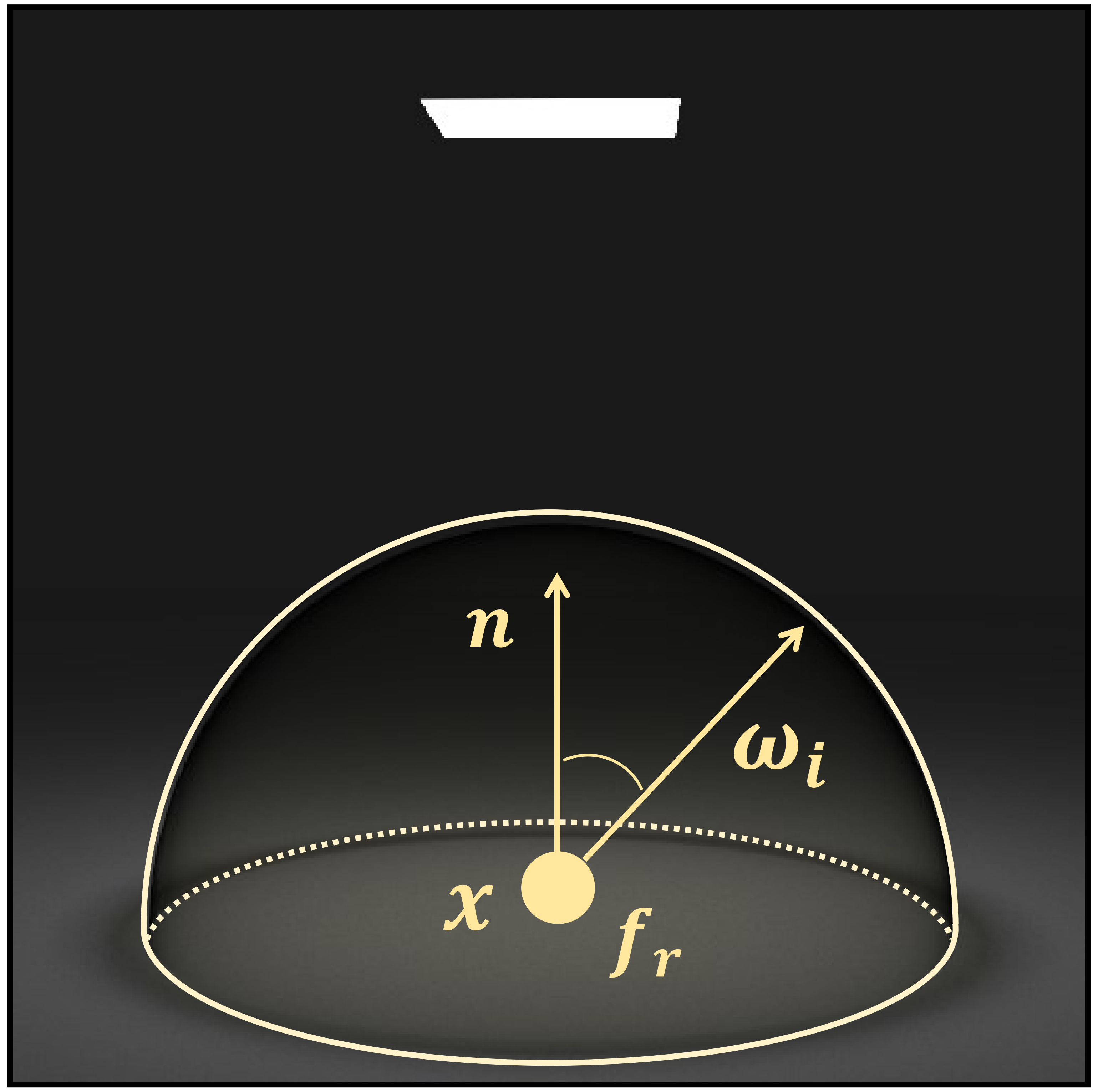

π: *local* parameters

- BRDF parameters

Differential radiance from x:

$$\frac{\mathrm{d}I}{\mathrm{d}\pi} = \int_{\mathbb{H}^2} \frac{\mathrm{d}}{\mathrm{d}\pi} \{f_r(\omega_i, \omega_o, \pi) L_i(\omega_i)(n \cdot \omega_i)\} \mathrm{d}\sigma(\omega_i)$$

Just move derivative inside integral

Monte Carlo estimation:

- Sample random directions ω_i^s from PDF $p(\omega_i, \pi)$
- Form estimator

Differentiate entire contribution [Zeltner et al. 2021]

$$\frac{\mathrm{d}I}{\mathrm{d}\pi} \approx \sum_s \frac{\mathrm{d}}{\mathrm{d}\pi} \left\{ \frac{f_r(\omega_i^s, \omega_o, \pi)\, L_i(\omega_i^s)\, (n \cdot \omega_i^s)}{p(\omega_i^s, \pi)} \right\}$$

Differential direct illumination: global parameters

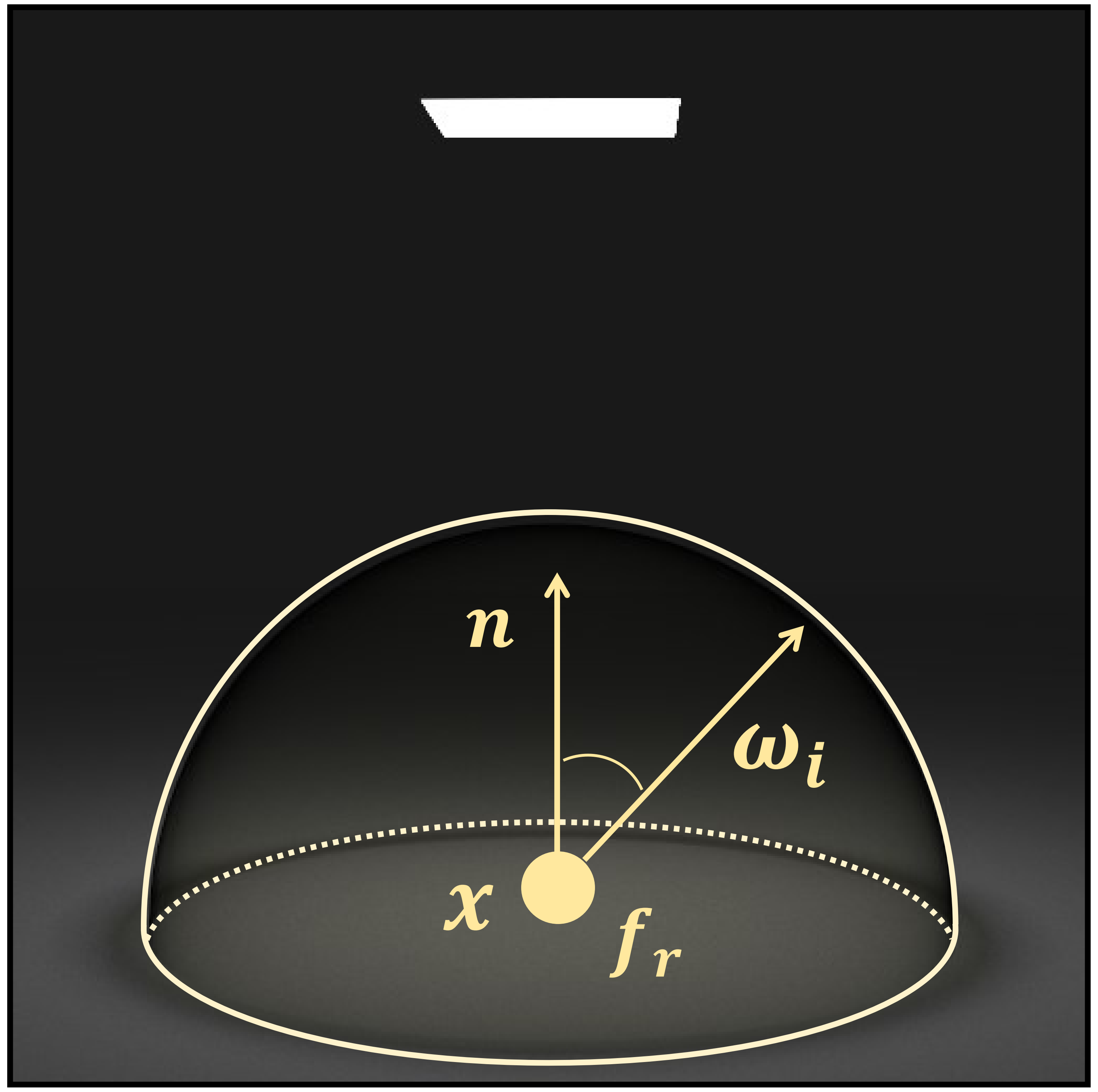

π: *global* parameters

- shape and pose of different scene elements (camera, sources, objects)

Differential radiance from x:

$$\frac{\mathrm{d}I}{\mathrm{d}\pi} = \frac{\mathrm{d}}{\mathrm{d}\pi} \int_{\mathbb{H}^2} f_r(\omega_i, \omega_o)\, L_i(\omega_i)\, (n \cdot \omega_i)\, \mathrm{d}\sigma(\omega_i)$$

Differential direct illumination: global parameters

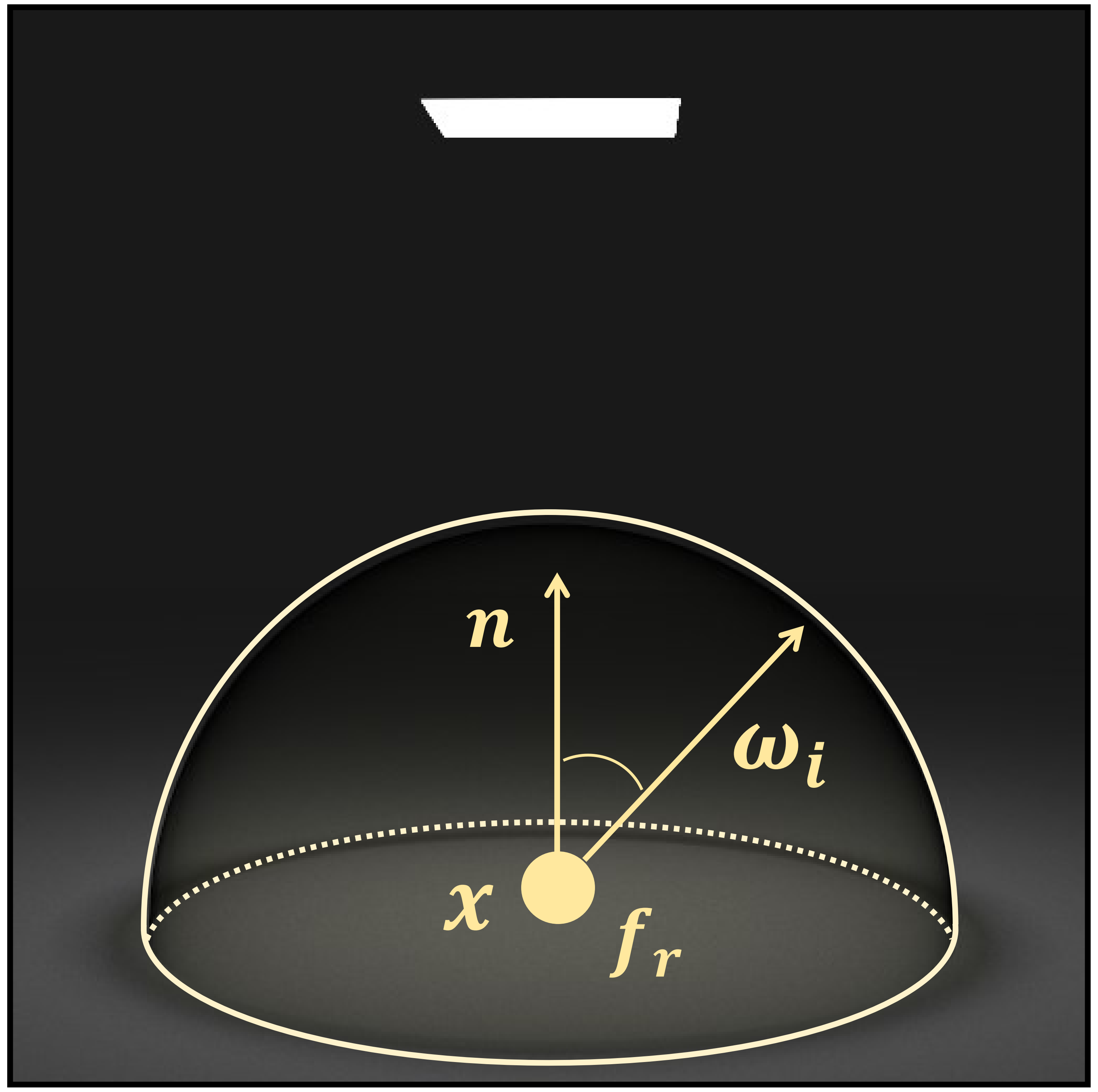

Differential radiance from x:

$$\frac{\mathrm{d}I}{\mathrm{d}\pi} = \frac{\mathrm{d}}{\mathrm{d}\pi} \int_{\mathbb{H}^2} f_r(\omega_i, \omega_o)\, L_i(\omega_i)\, (n \cdot \omega_i)\, \mathrm{d}\sigma(\omega_i)$$

$$\cancel{= \int_{\mathbb{H}^2} \frac{\mathrm{d}}{\mathrm{d}\pi} \{f_r(\omega_i, \omega_o)\, L_i(\omega_i)\, (n \cdot \omega_i)\}\, \mathrm{d}\sigma(\omega_i)}$$

Need to use full Reynolds transport theorem

π: *global* parameters

- shape and pose of different scene elements (camera, sources, objects)

Discontinuities in the integrand

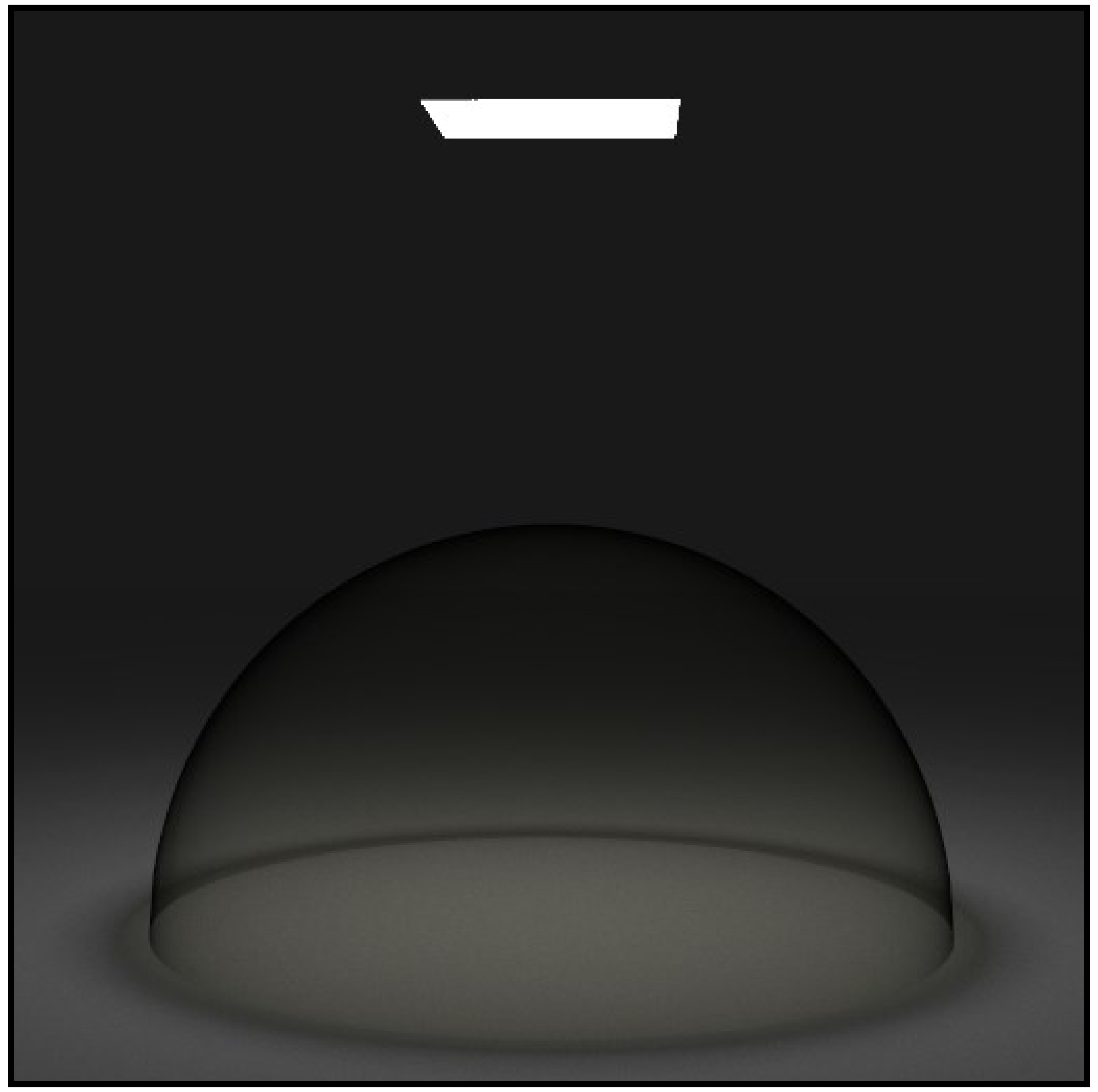

π: size of the emitter

$$I = \int_{\mathbb{H}^2} \underbrace{f_r(\omega_i, \omega_o) L_i(\omega_i)(n \cdot \omega_i)}_{f(\omega_i)} \mathrm{d}\sigma(\omega_i)$$

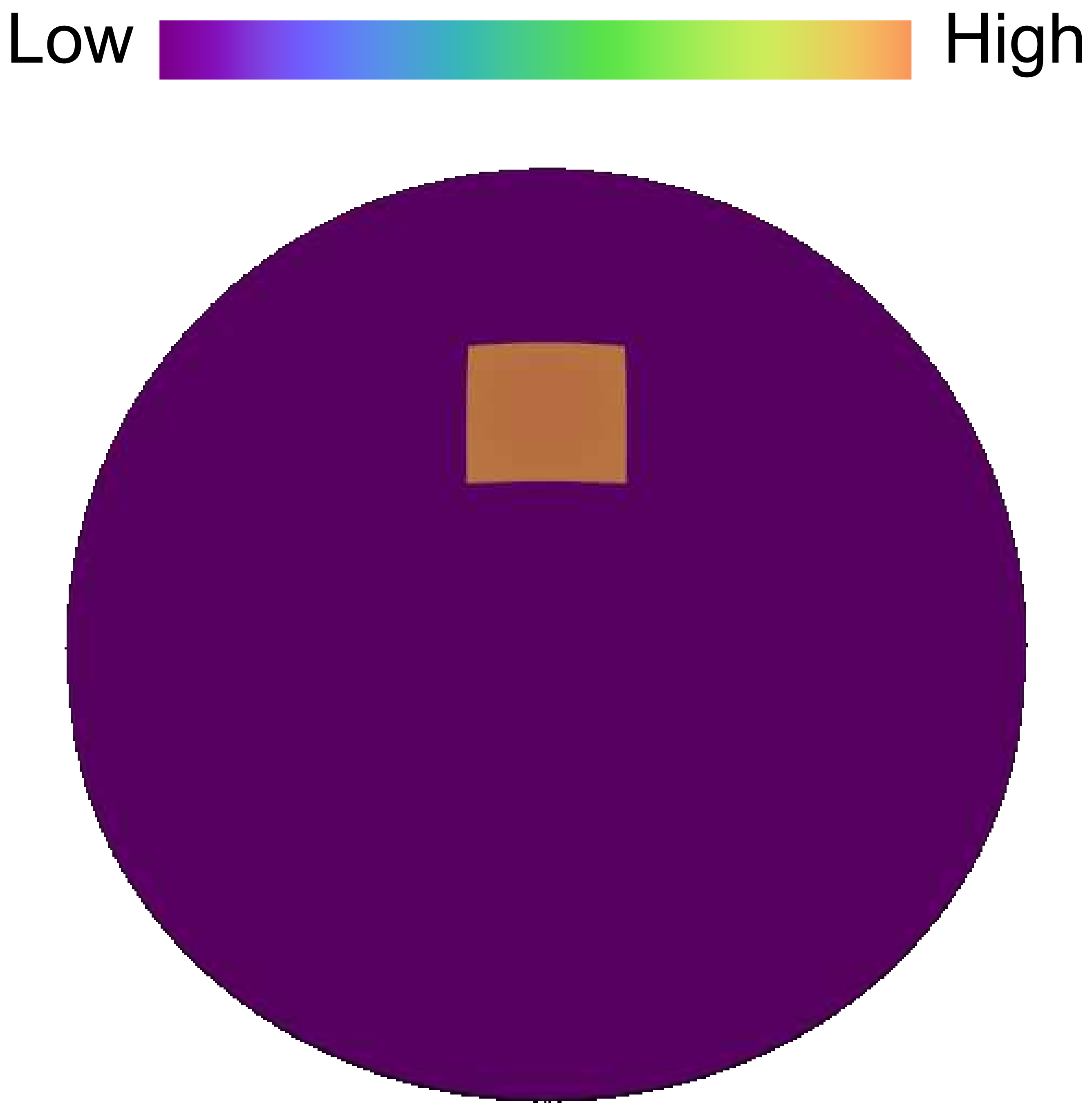

Integrand
$f(\omega_i)$

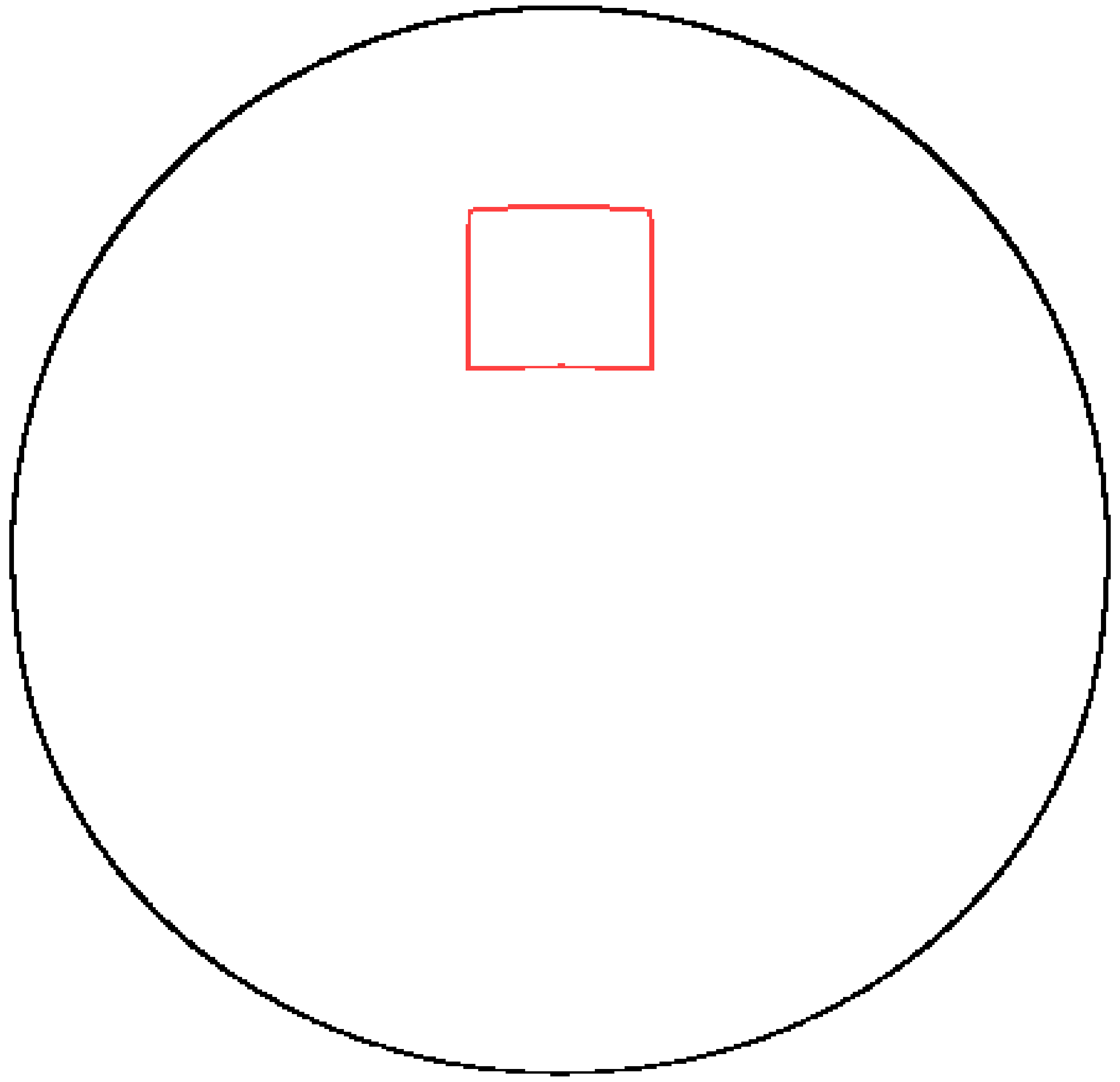

Discontinuous points
(π-dependent)

Applying the Reynolds transport theorem

$$I = \int_{\mathbb{H}^2} f(\omega_i, \omega_o) \mathrm{d}\sigma(\omega_i)$$

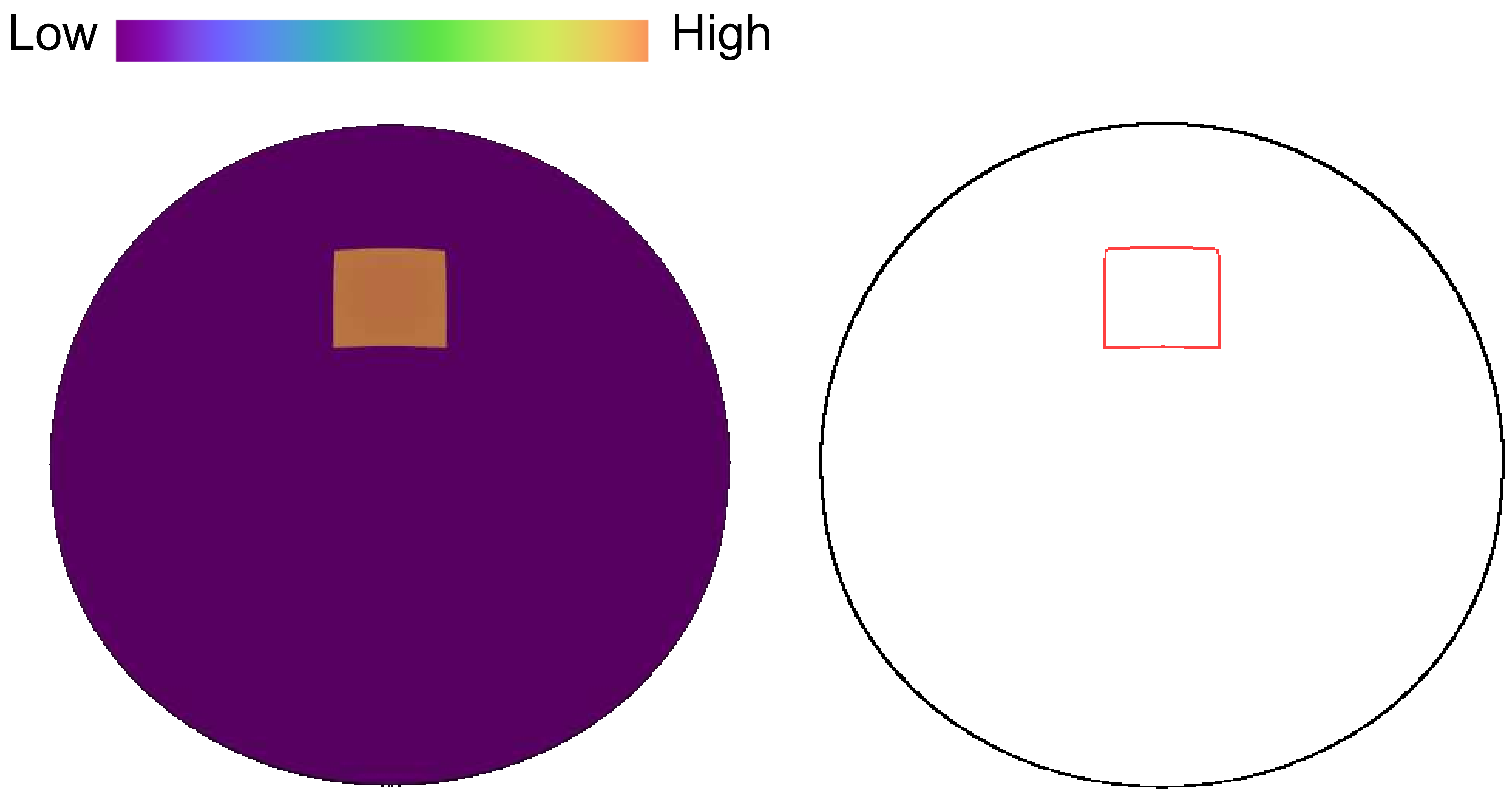

Integrand
$f(\omega_i)$

Discontinuous points
(π-dependent)

Applying the Reynolds transport theorem

$$I = \int_{\mathbb{H}^2} f(\omega_i, \omega_o)\mathrm{d}\sigma(\omega_i)$$

$$\frac{\mathrm{d}I}{\mathrm{d}\pi} = \int_{\mathbb{H}^2} \frac{\mathrm{d}f}{\mathrm{d}\pi}\,\mathrm{d}\sigma + \int_{\partial\mathbb{H}^2} g\,\mathrm{d}l$$

Interior integral (same as for local parameters)

Boundary integral

[Ramamoorthi et al. 2007, Li et al. 2019]

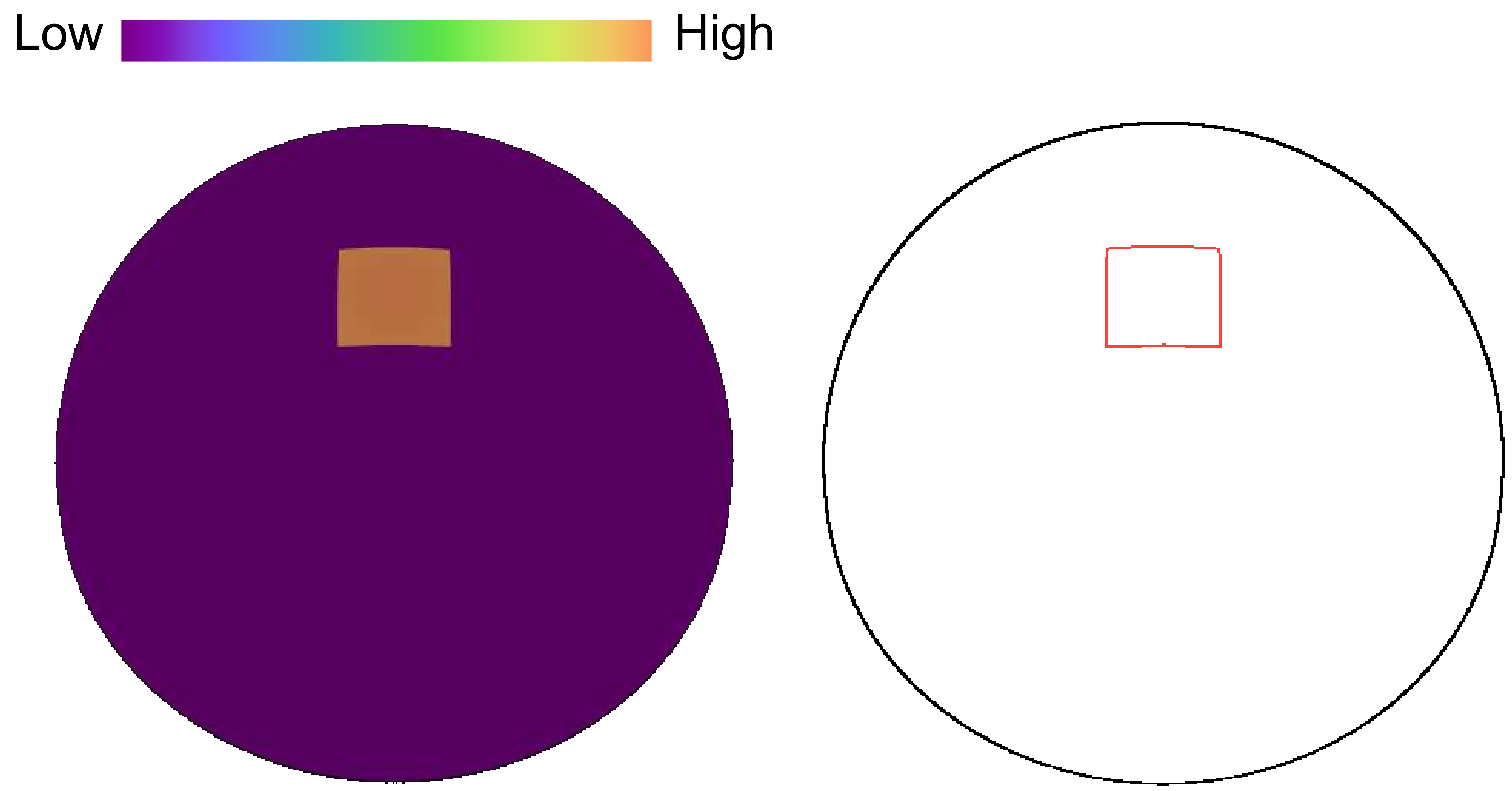

Integrand $f(\omega_i)$

Discontinuous points (π-dependent)

Reparameterizing the direct illumination integral

Hemispherical integral

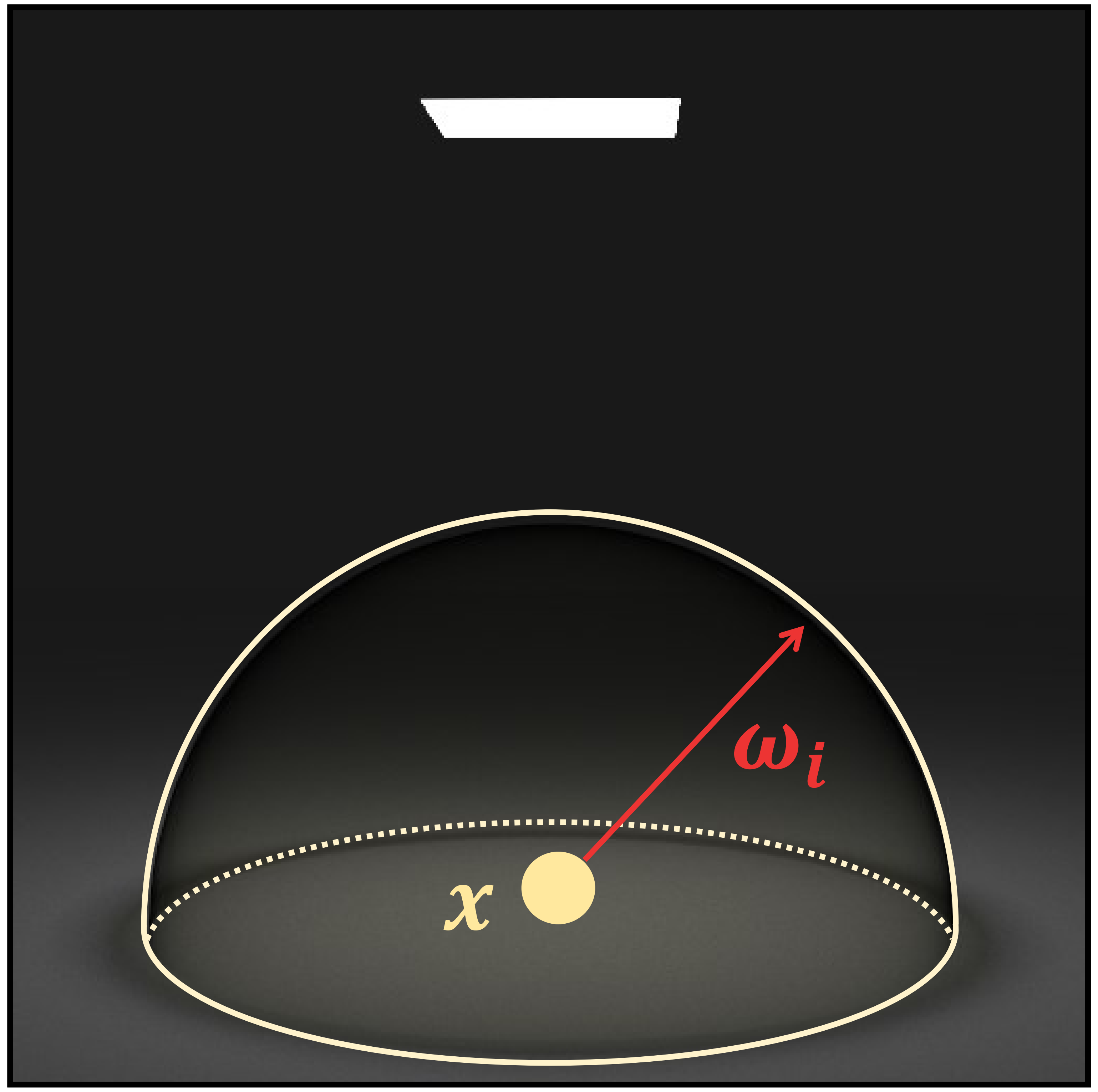

$$I = \int_{\mathbb{H}^2} f(\omega_i)\, \mathrm{d}\sigma(\omega_i)$$

Reparameterizing the direct illumination integral

Hemispherical integral

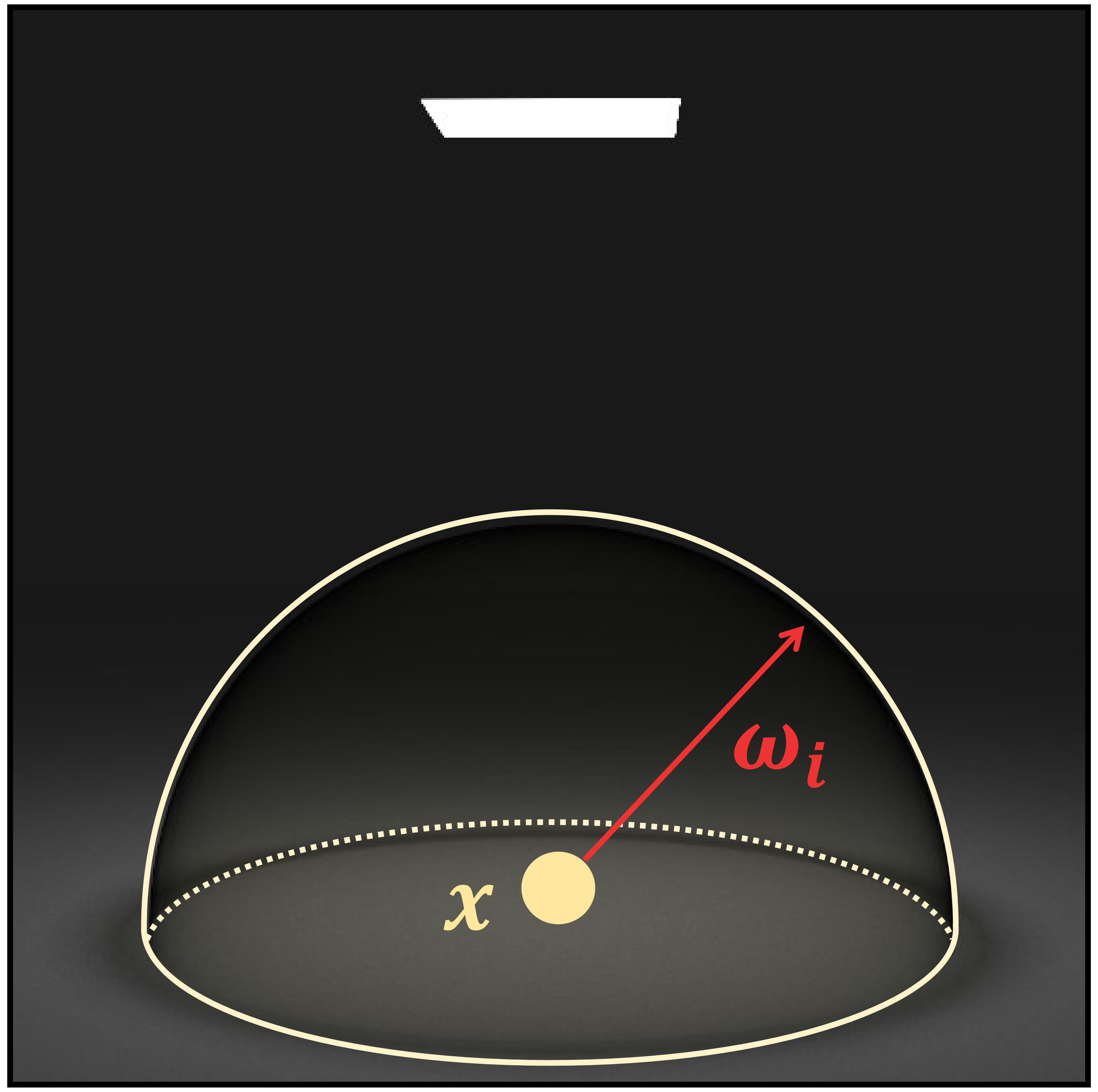

Change of variables

Surface integral

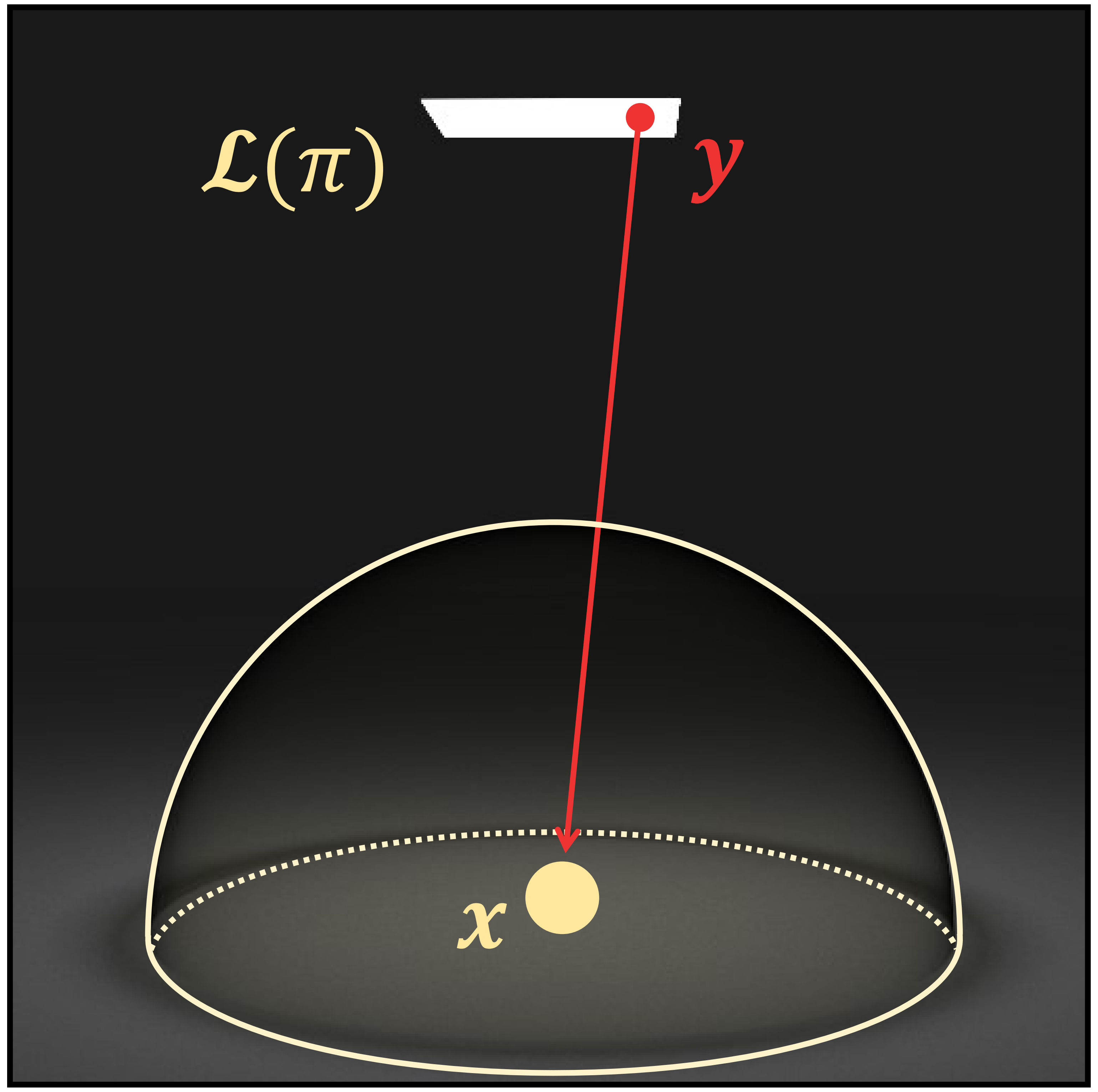

$$I = \int_{\mathbb{H}^2} f(\boldsymbol{\omega_i})\, \mathrm{d}\sigma(\boldsymbol{\omega_i})$$

$$I = \int_{\mathcal{L}(\pi)} f(\boldsymbol{y} \to \boldsymbol{x})\, G(\boldsymbol{x}, \boldsymbol{y})\, \mathrm{d}A(\boldsymbol{y})$$

Reparameterizing the direct illumination integral

Hemispherical integral

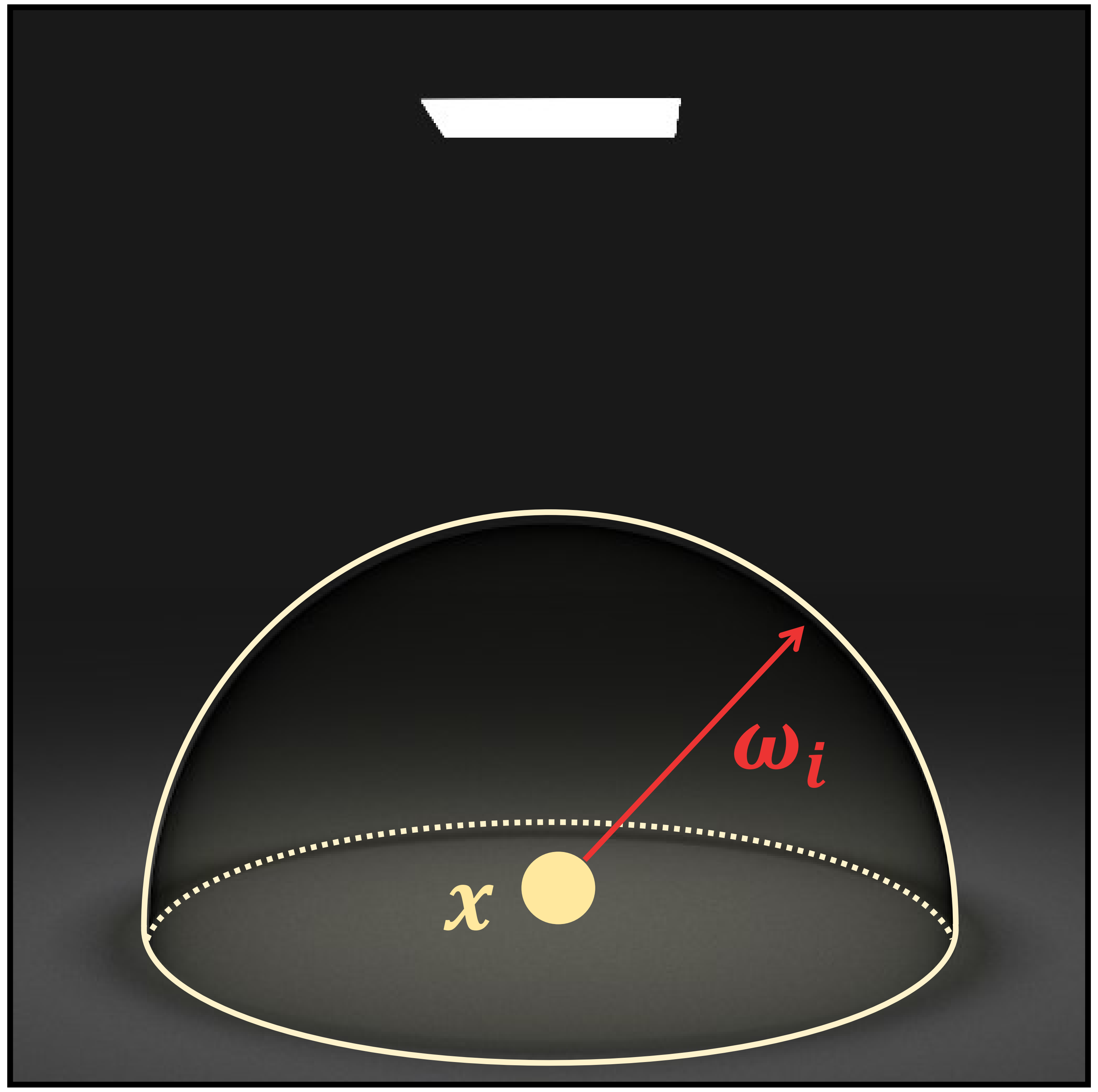

$$I = \int_{\mathbb{H}^2} f(\boldsymbol{\omega_i})\, \mathrm{d}\sigma(\boldsymbol{\omega_i})$$

Change of variables

Surface integral

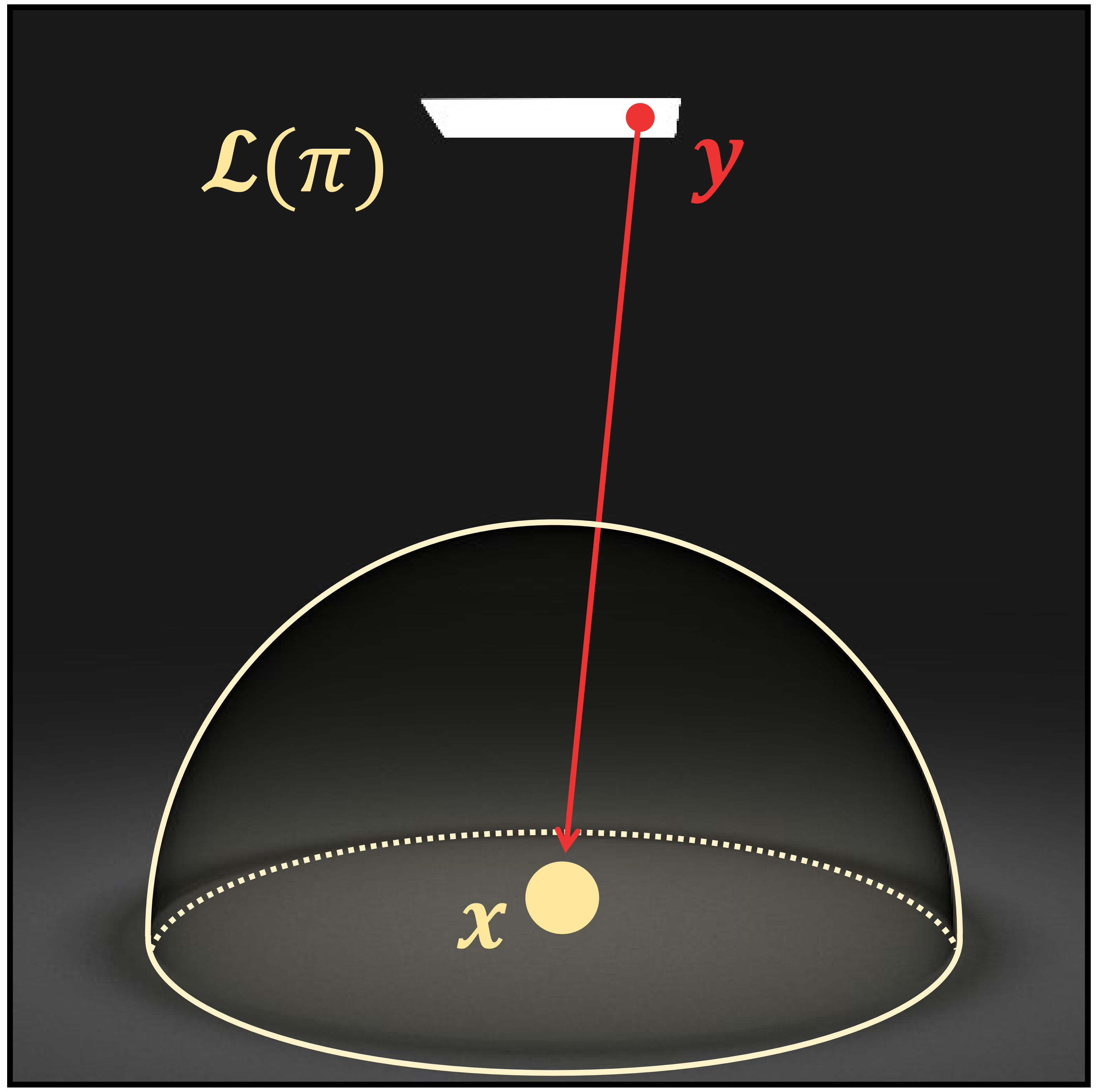

$$I = \int_{\mathcal{L}(\pi)} f(\boldsymbol{y} \to \boldsymbol{x})\, \boxed{G(\boldsymbol{x}, \boldsymbol{y})}\, \mathrm{d}A(\boldsymbol{y})$$

Includes visibility, fall-off, and foreshortening terms

Reparameterizing the direct illumination integral

Hemispherical integral

Surface integral

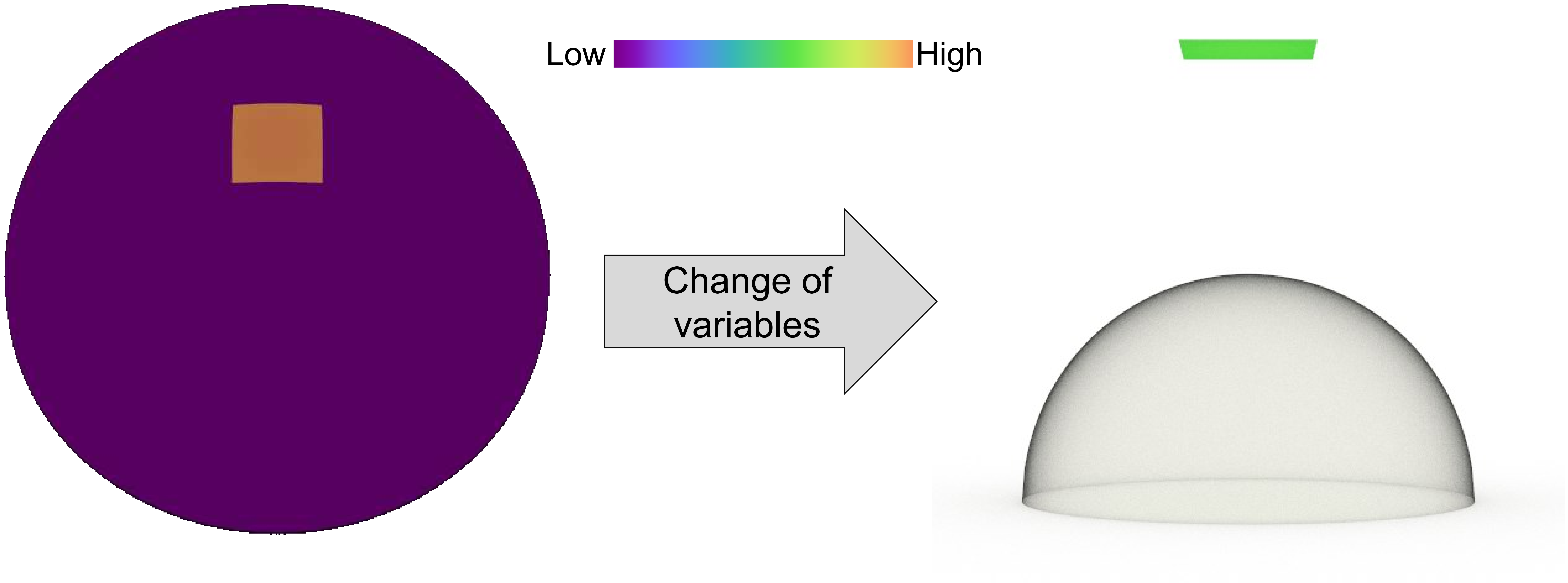

$$I = \int_{\mathbb{H}^2} f(\omega_i)\, \mathrm{d}\sigma(\omega_i)$$

$$I = \int_{\mathcal{L}(\pi)} f(y \to x)\, G(x, y)\, \mathrm{d}A(y)$$

Reparameterizing the direct illumination integral

Hemispherical integral

Surface integral

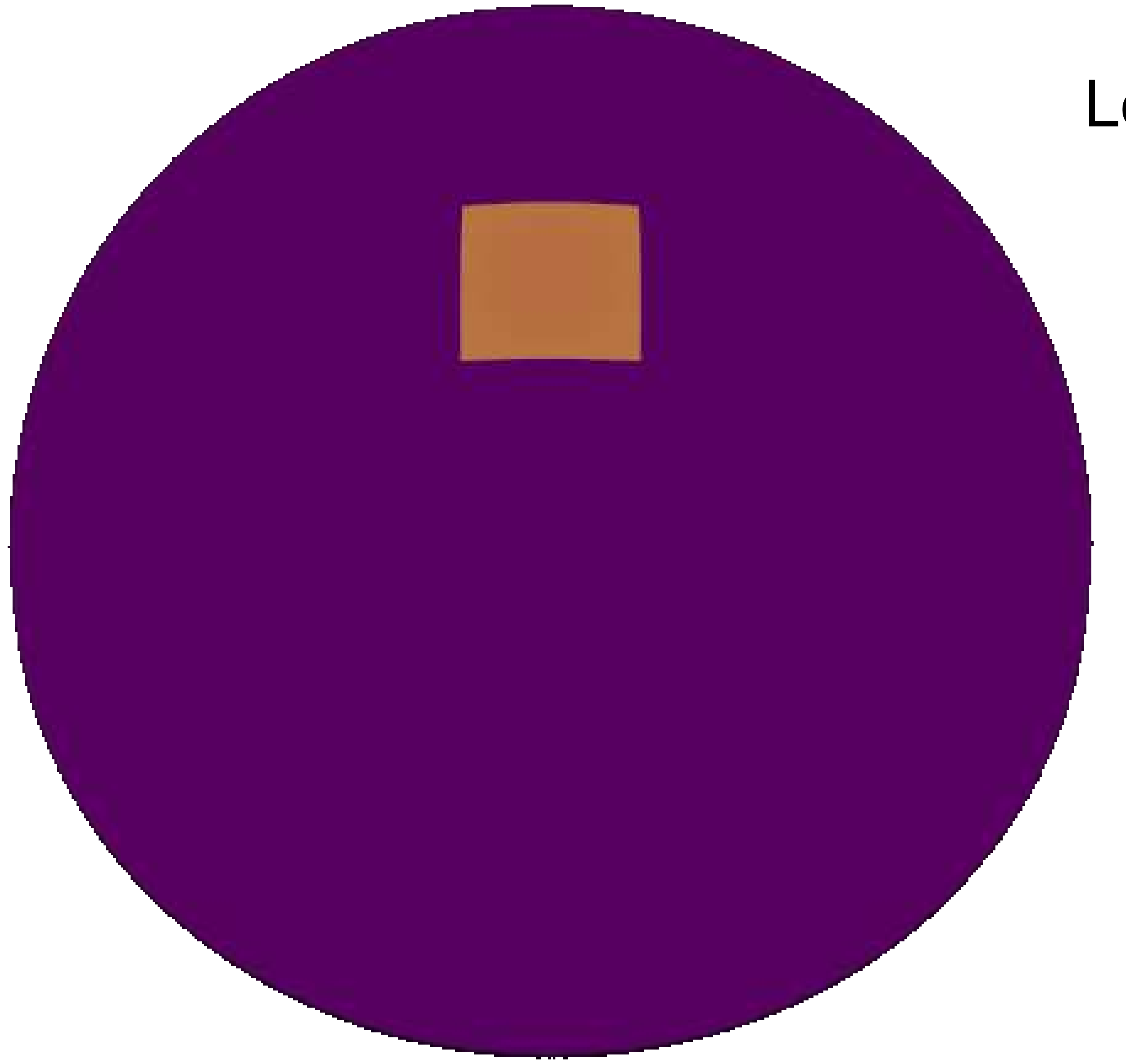

Change of variables

discontinuous

$$I = \int_{\mathbb{H}^2} f(\omega_i)\, \mathrm{d}\sigma(\omega_i)$$

continuous

$$I = \int_{\mathcal{L}(\pi)} f(y \to x)\, G(x, y)\, \mathrm{d}A(y)$$

Reparameterizing the direct illumination integral

Hemispherical integral

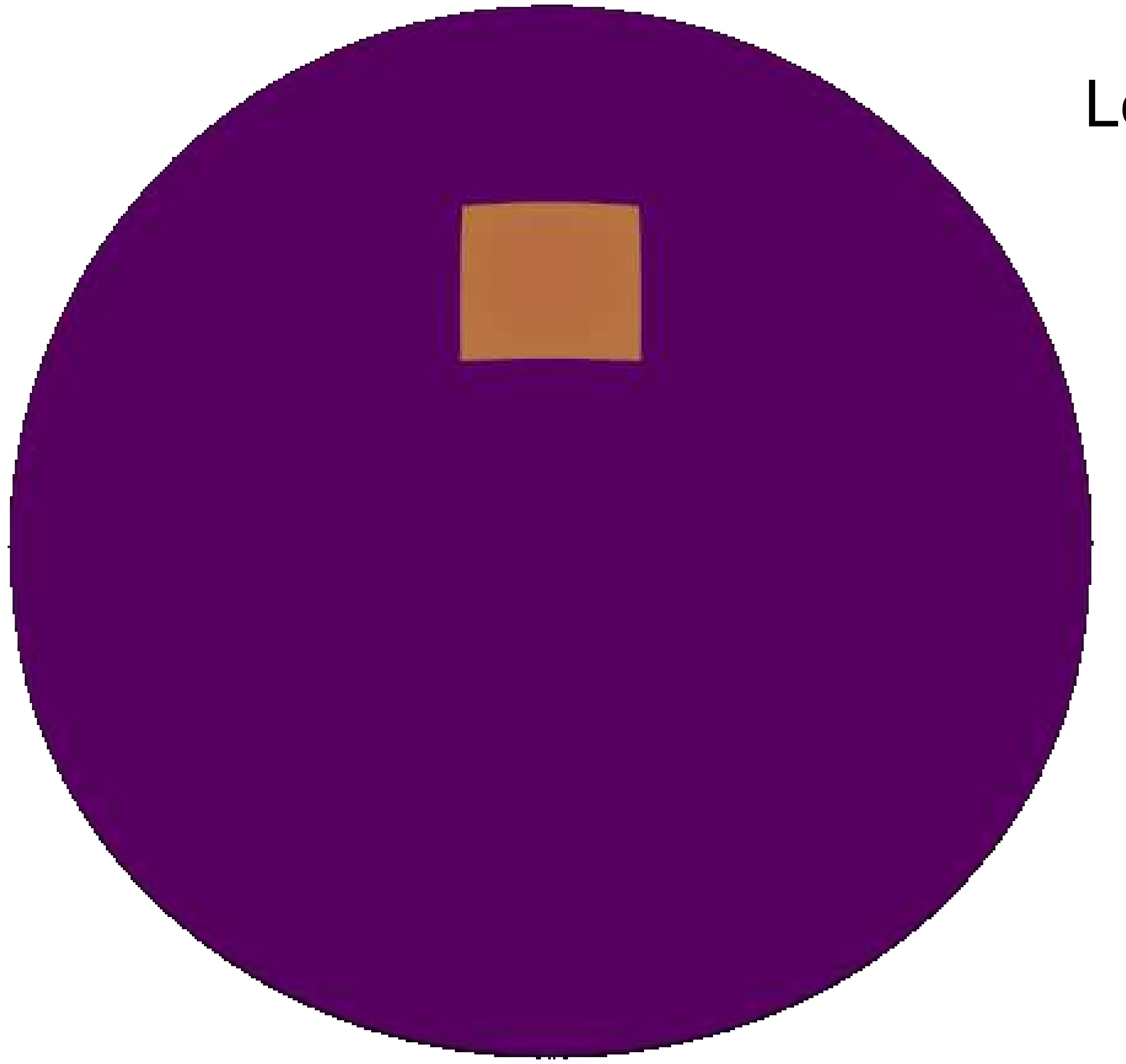

Low High

Change of variables

Surface integral

discontinuous

$$I = \int_{\mathbb{H}^2} f(\omega_i)\, \mathrm{d}\sigma(\omega_i)$$

constant domain

continuous

$$I = \int_{\mathcal{L}(\pi)} f(y \to x)\, G(x, y)\, \mathrm{d}A(y)$$

evolving domain

Differentiating the hemispherical integral

π: size of the emitter

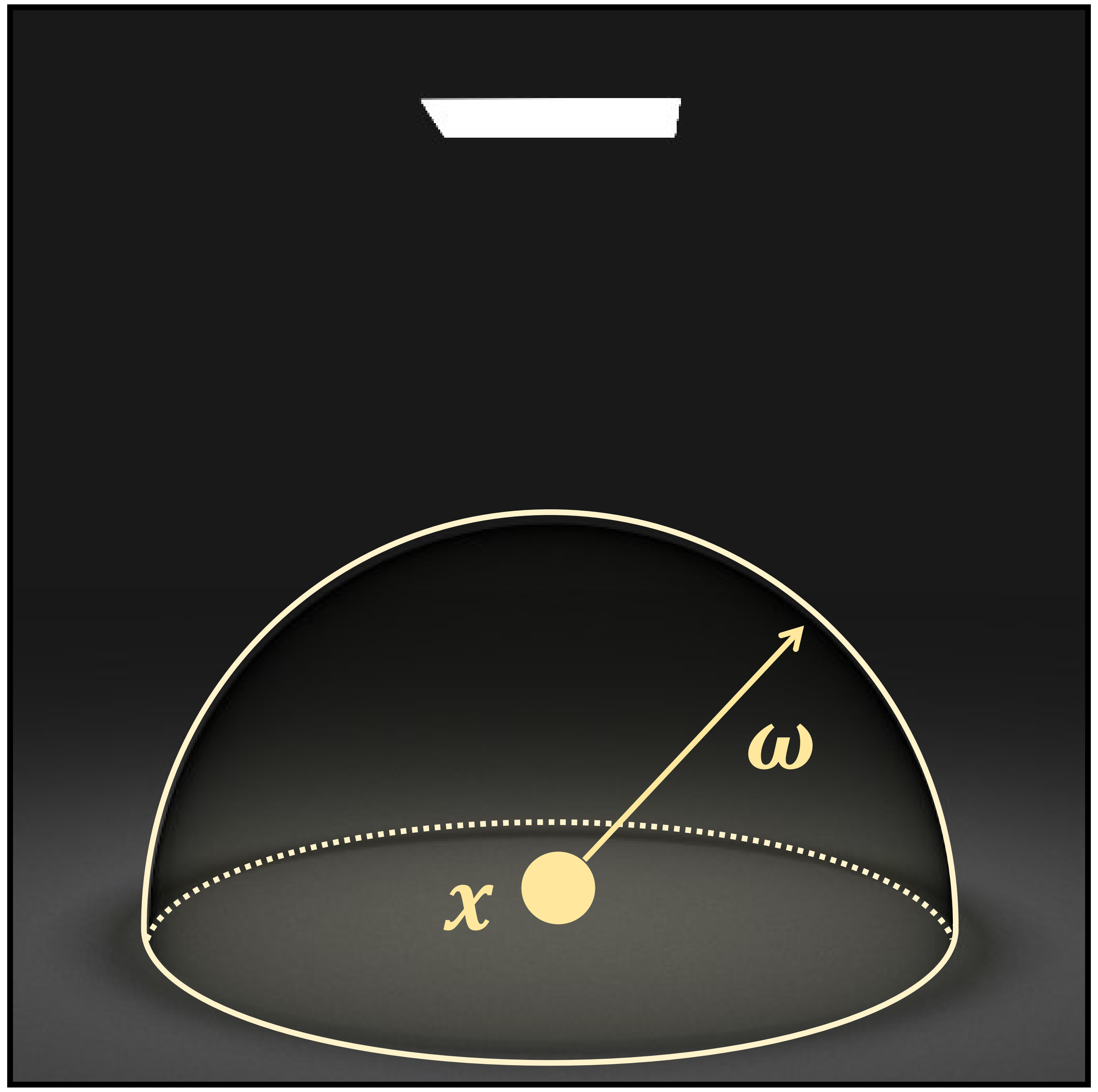

$$I = \int_{\mathbb{H}^2} f(\omega_i)\,\mathrm{d}\sigma(\omega_i)$$

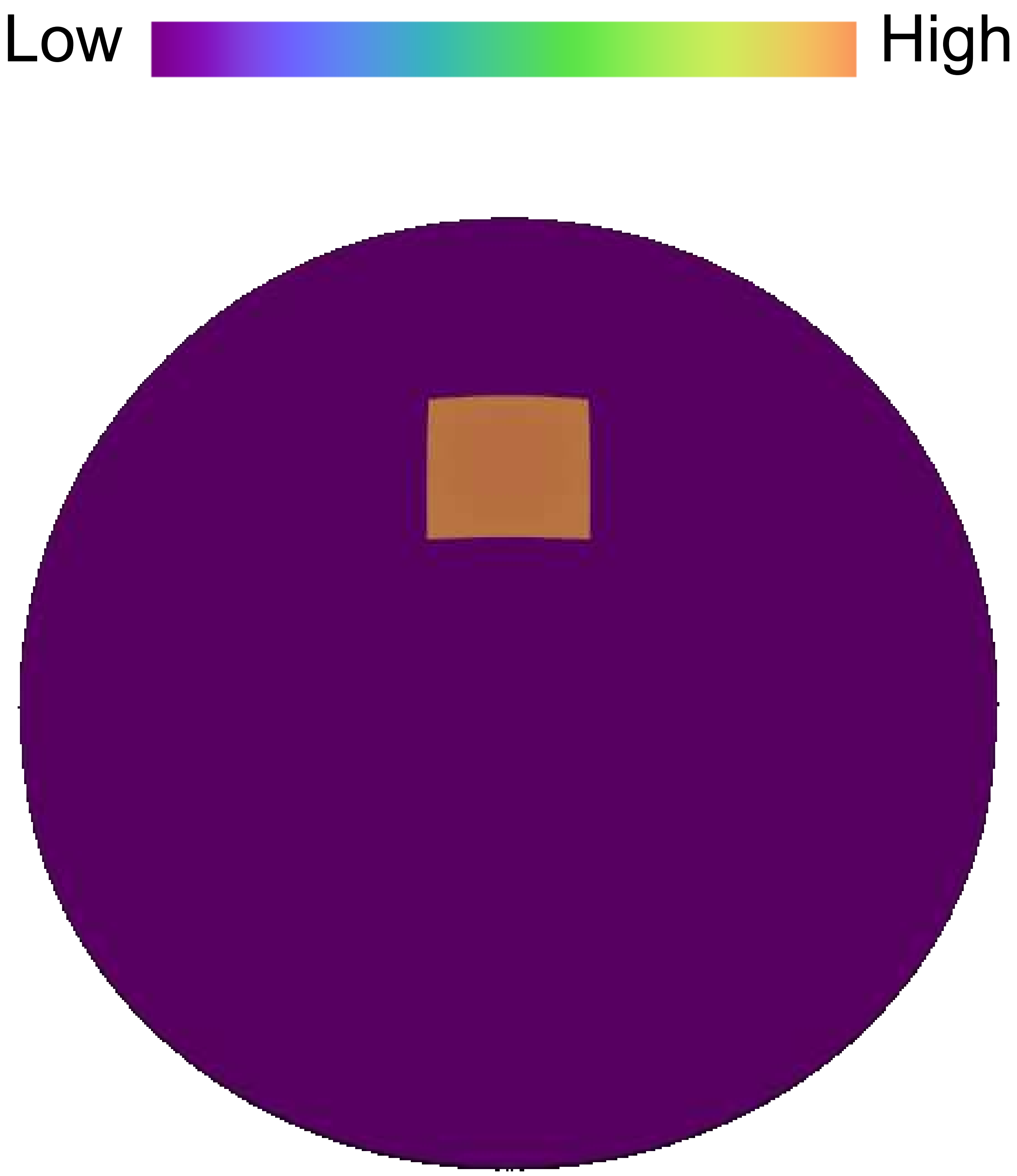

Discontinuities of f

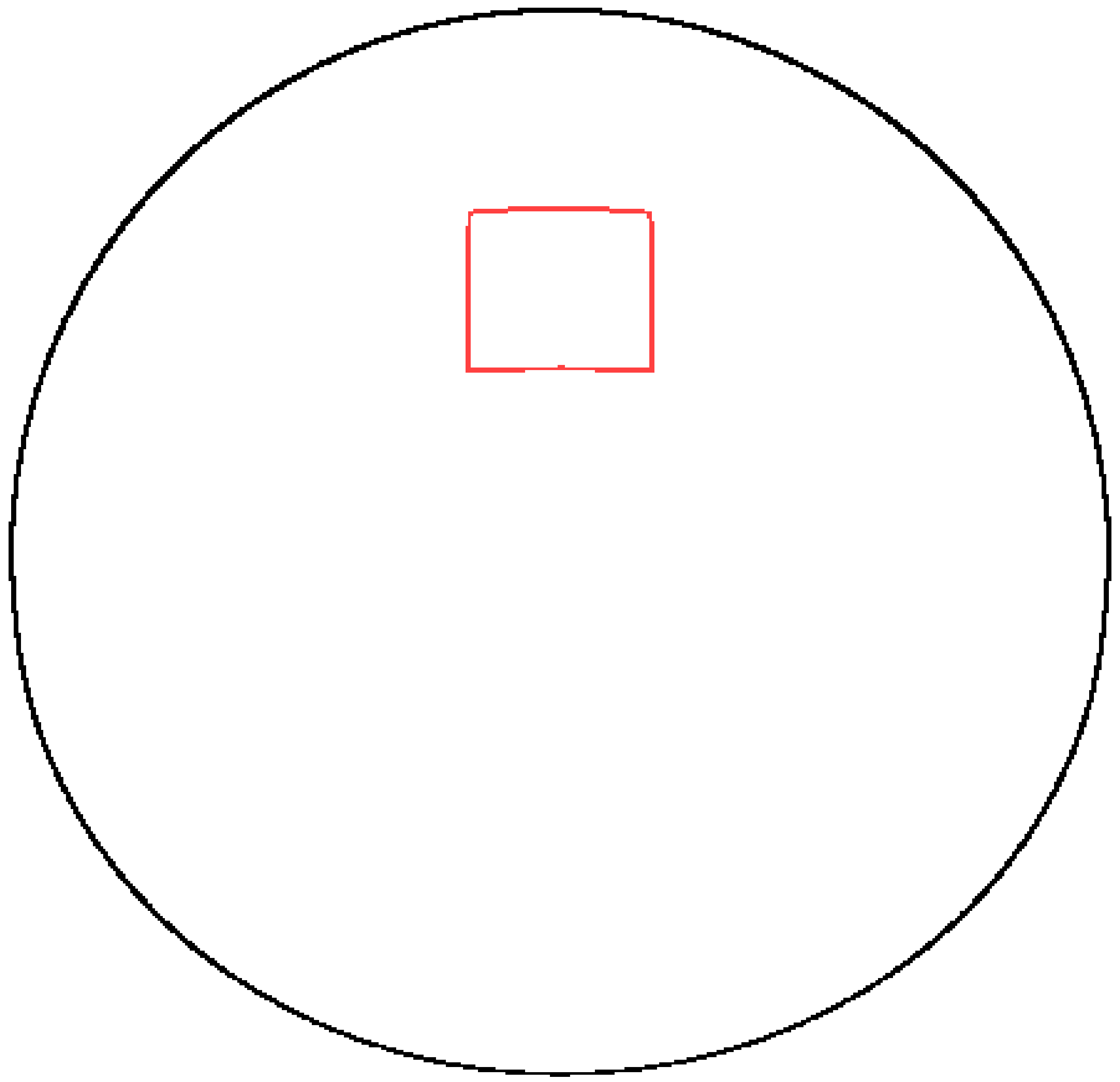

Differentiation

Reynolds transport theorem

$$\frac{\mathrm{d}I}{\mathrm{d}\pi} = \int_{\mathbb{H}^2} \frac{\mathrm{d}(f)}{\mathrm{d}\pi}\,\mathrm{d}\sigma + \int_{\partial\mathbb{H}^2} g\,\mathrm{d}l$$

Interior

Boundary

Differentiating the area integral

π: size of the emitter

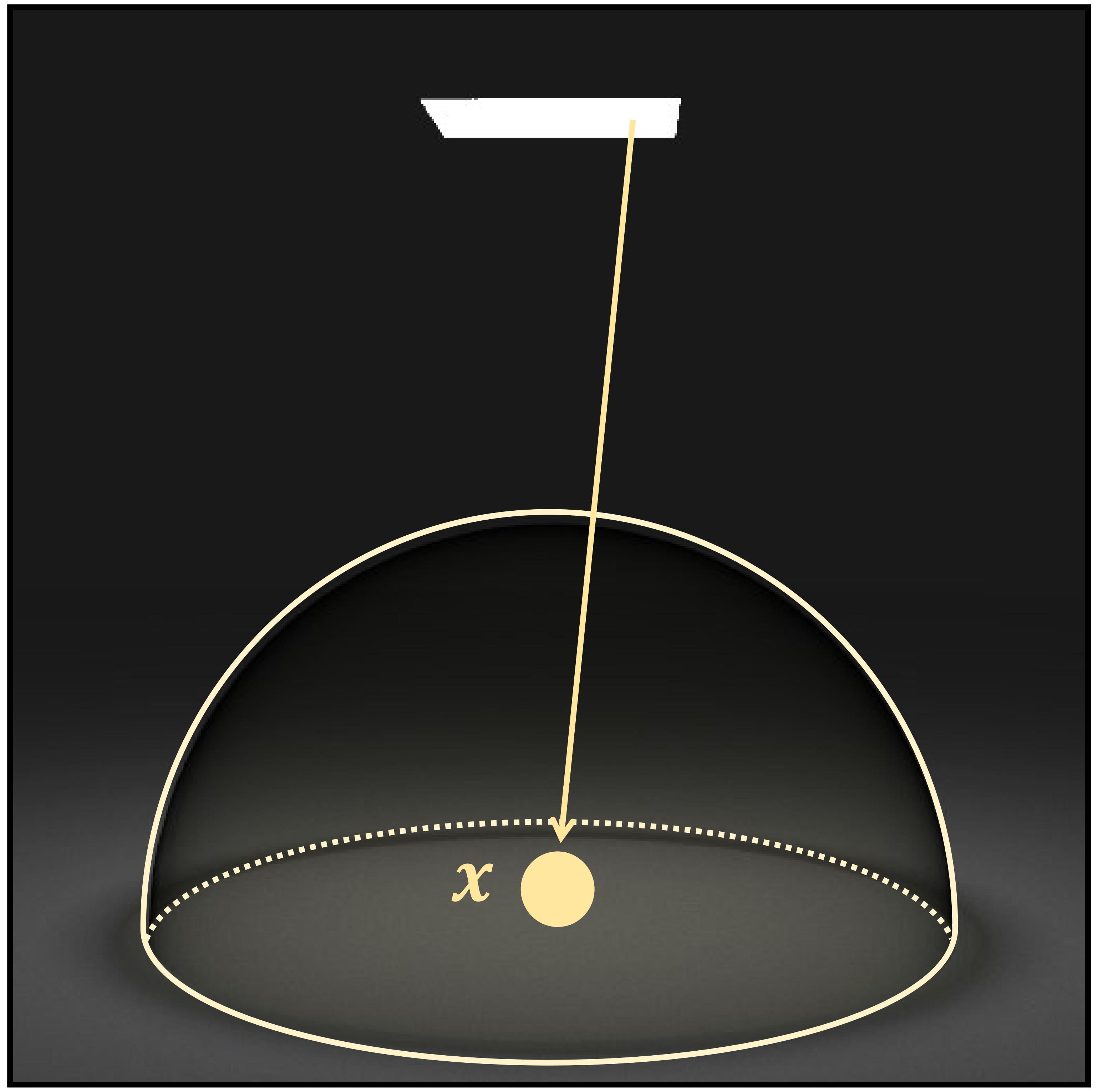

$$I = \int_{\mathcal{L}(\pi)} f(y \to x) G(x, y) \mathrm{d}A(y)$$

Low High

Differentiation

Reynolds transport theorem

Boundary of $\boldsymbol{\mathcal{L}}(\pi)$

$$\frac{\mathrm{d}I}{\mathrm{d}\pi} = \int_{\boldsymbol{\mathcal{L}}(\pi)} \frac{\mathrm{d}(fG)}{\mathrm{d}\pi} \mathrm{d}A + \int_{\partial\boldsymbol{\mathcal{L}}(\pi)} g \ \mathrm{d}l$$

Interior Boundary

Sources of discontinuities

Boundary edge 

Sharp edge 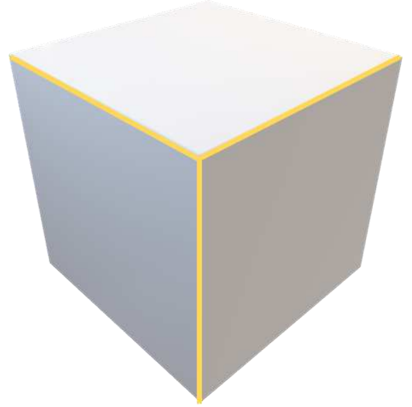

Silhouette edge 

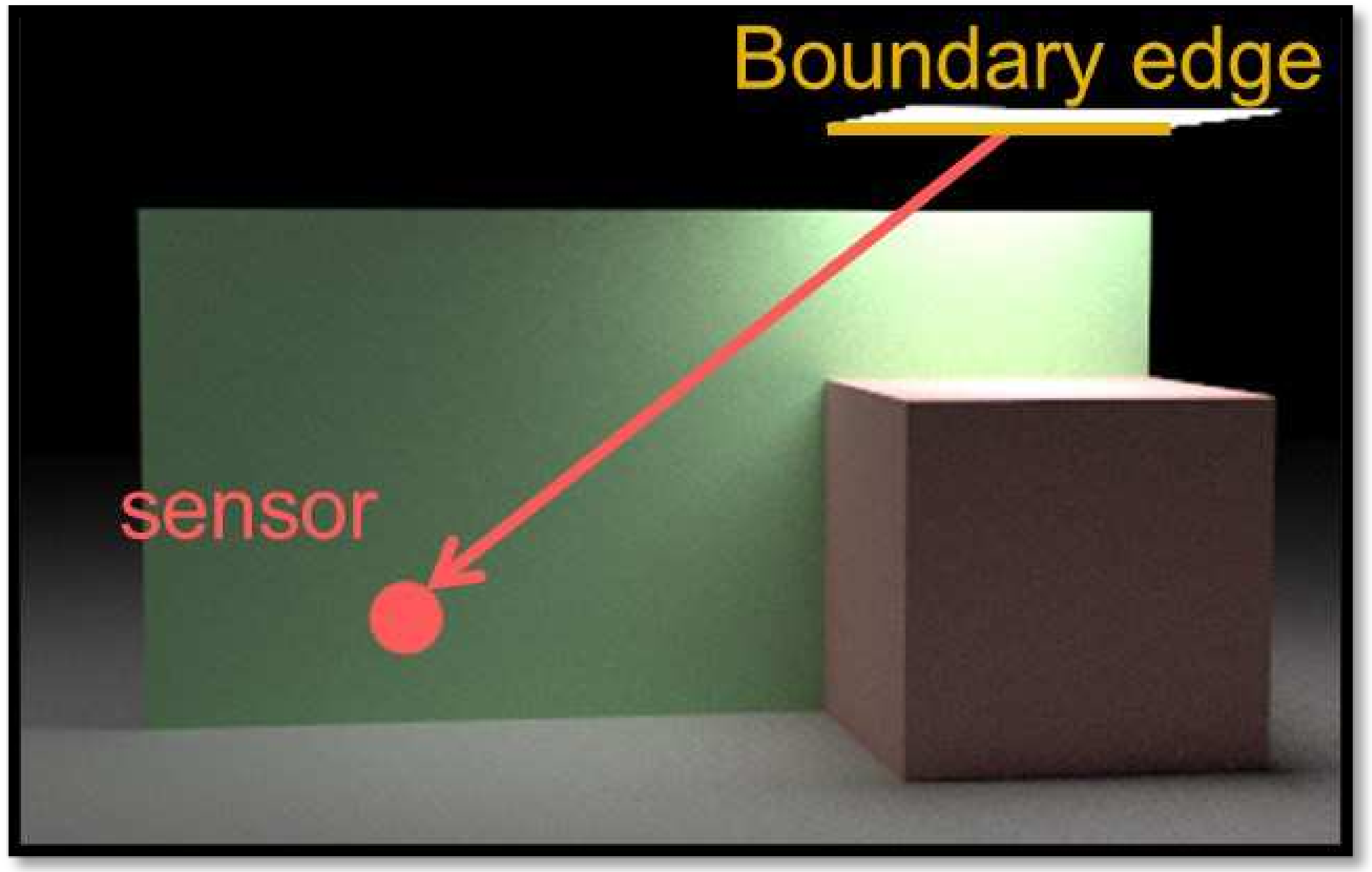

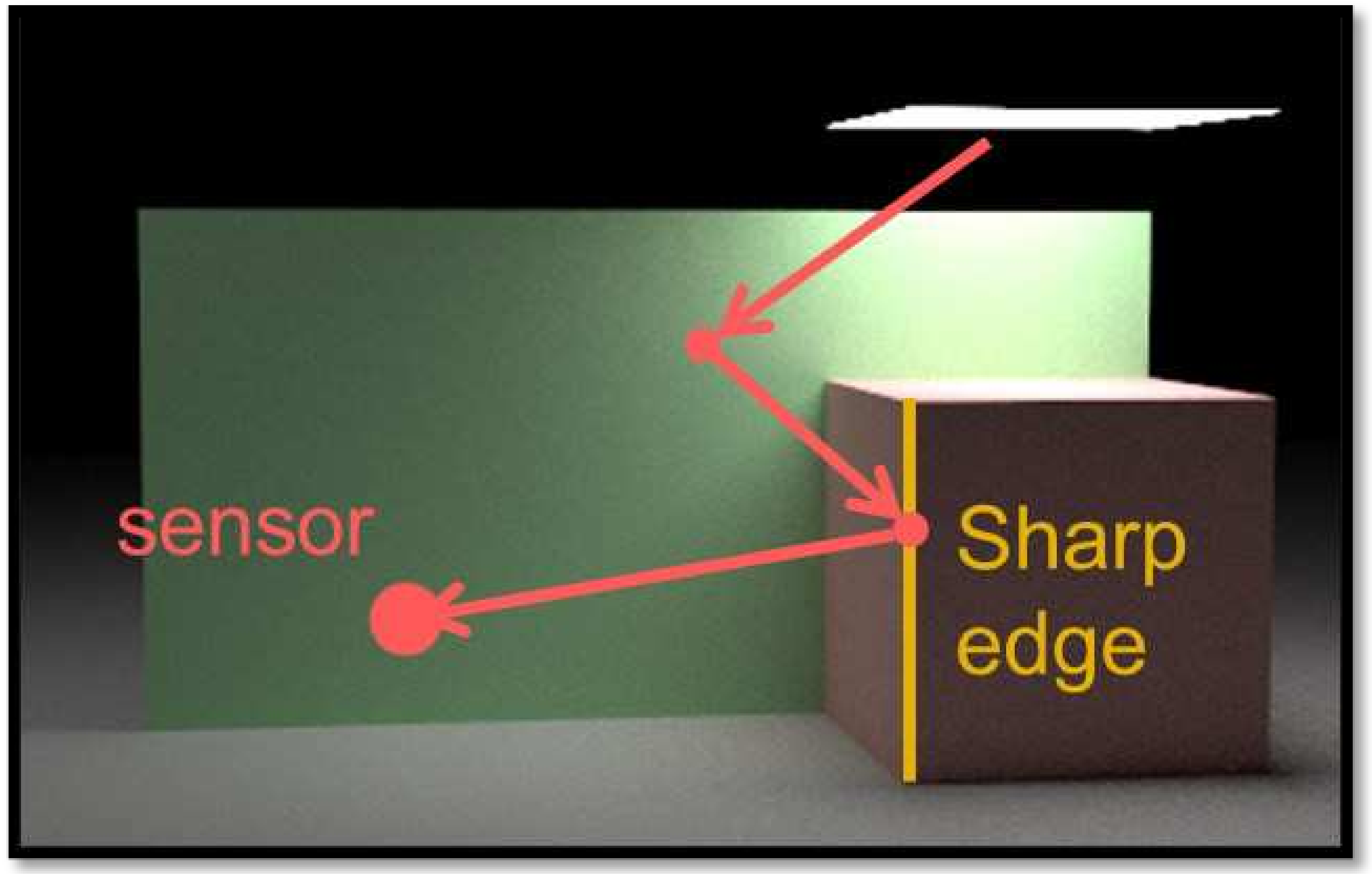

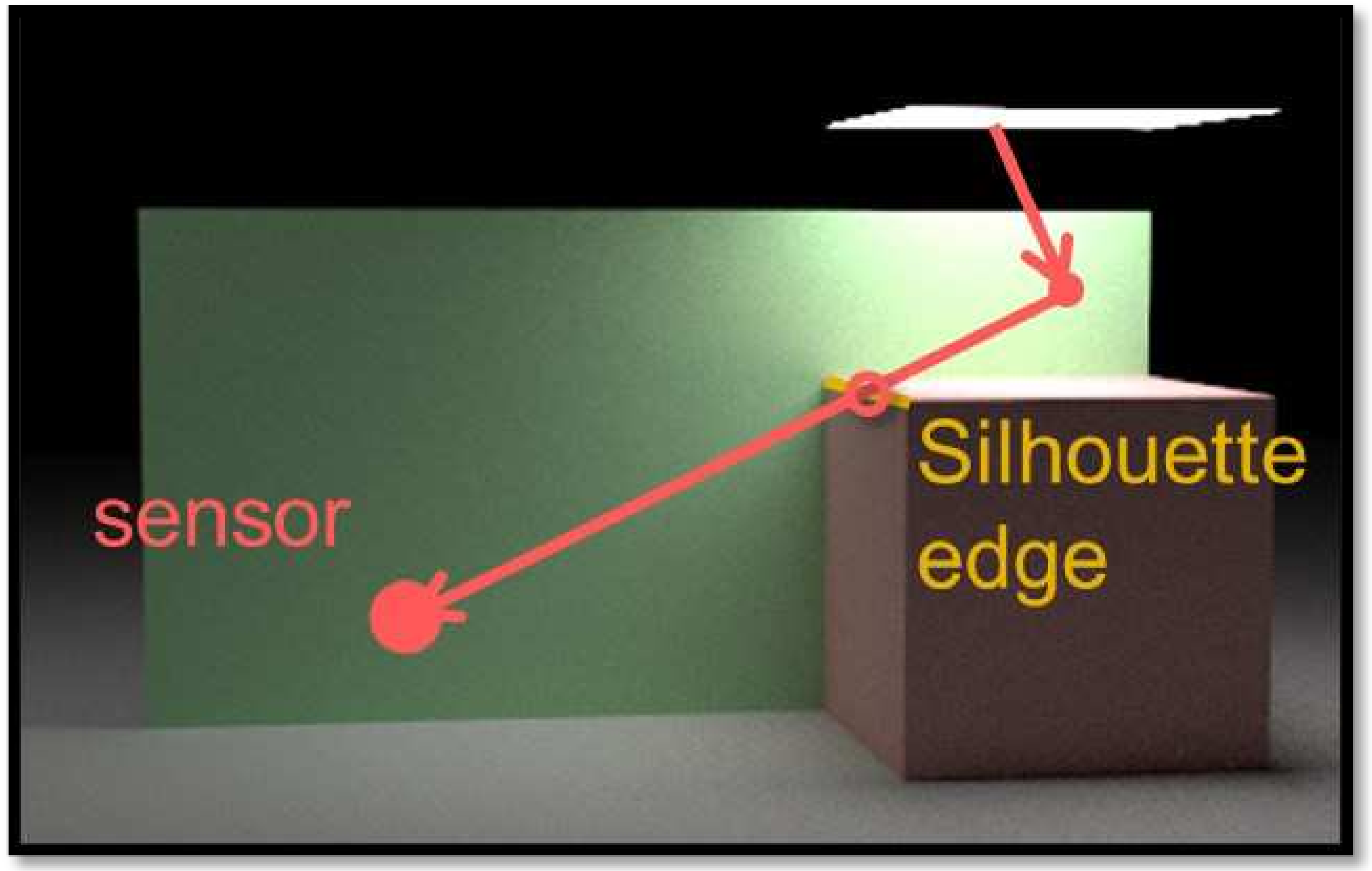

Sources of discontinuities

Boundary edge 

Sharp edge 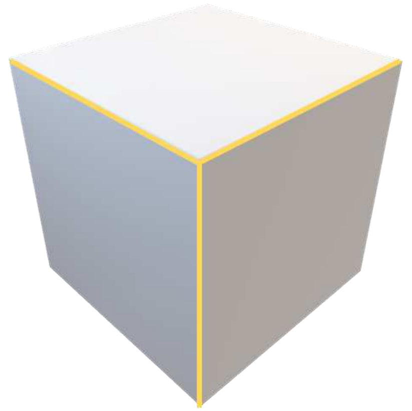

Silhouette edge 

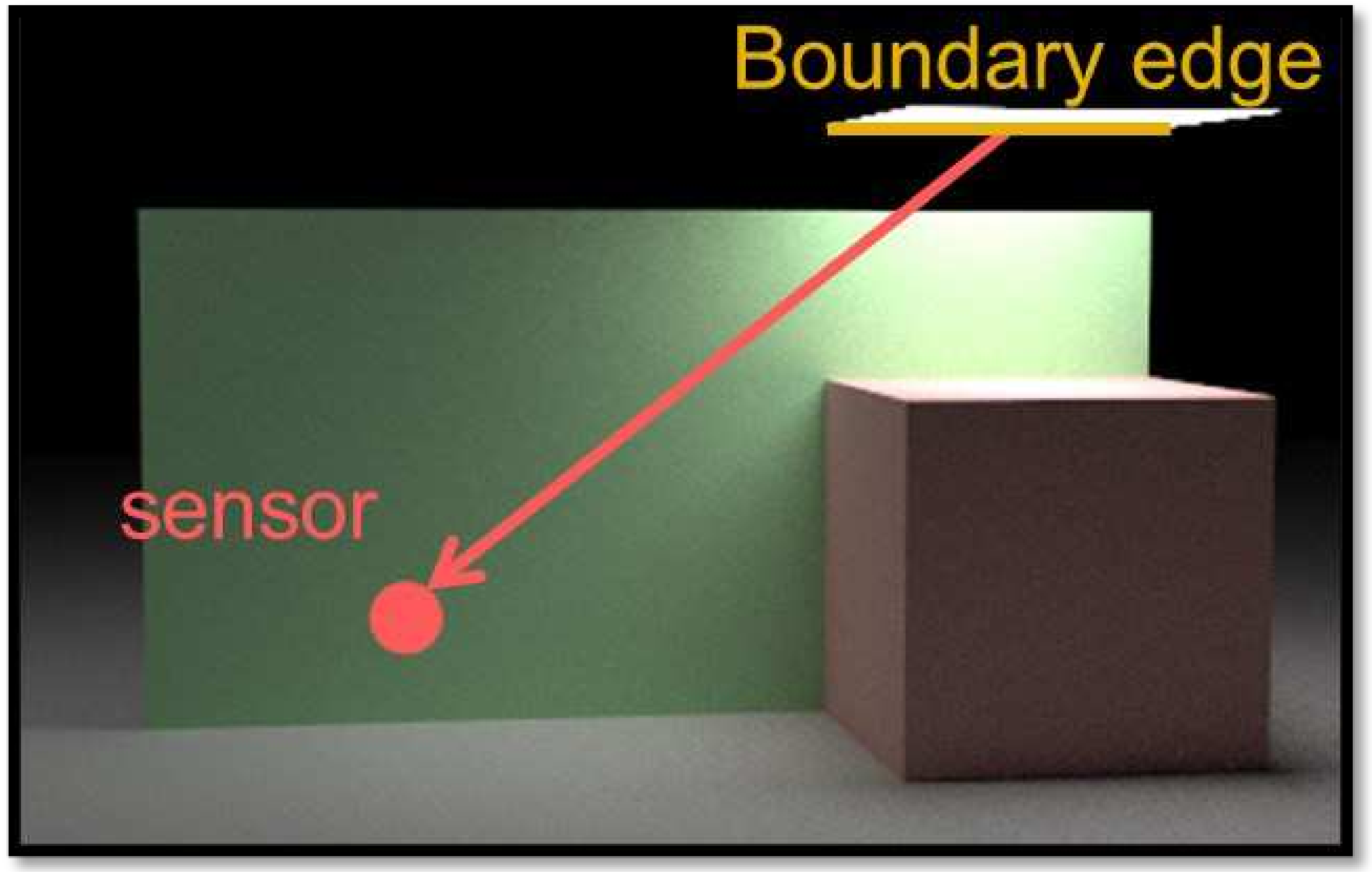

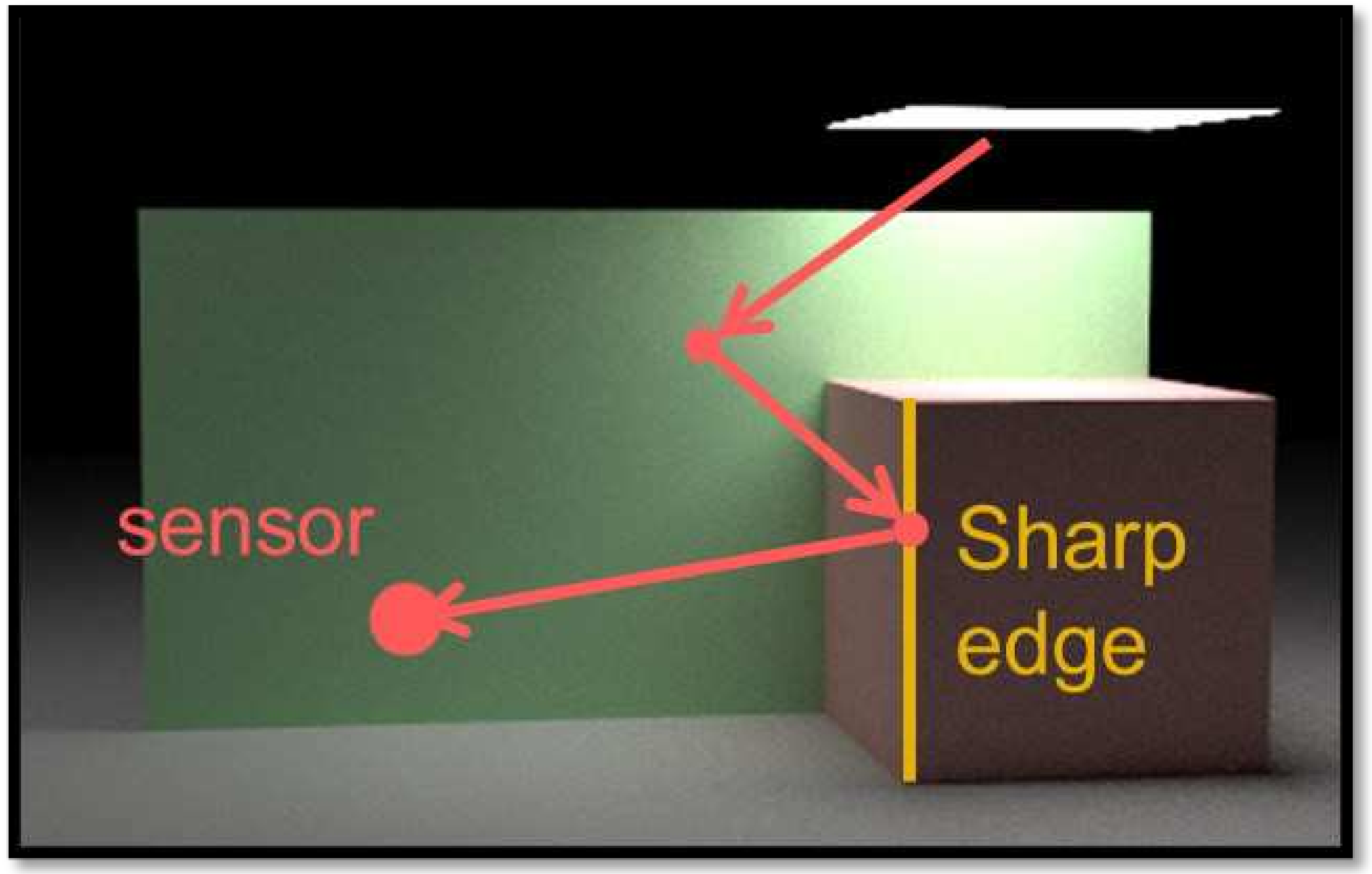

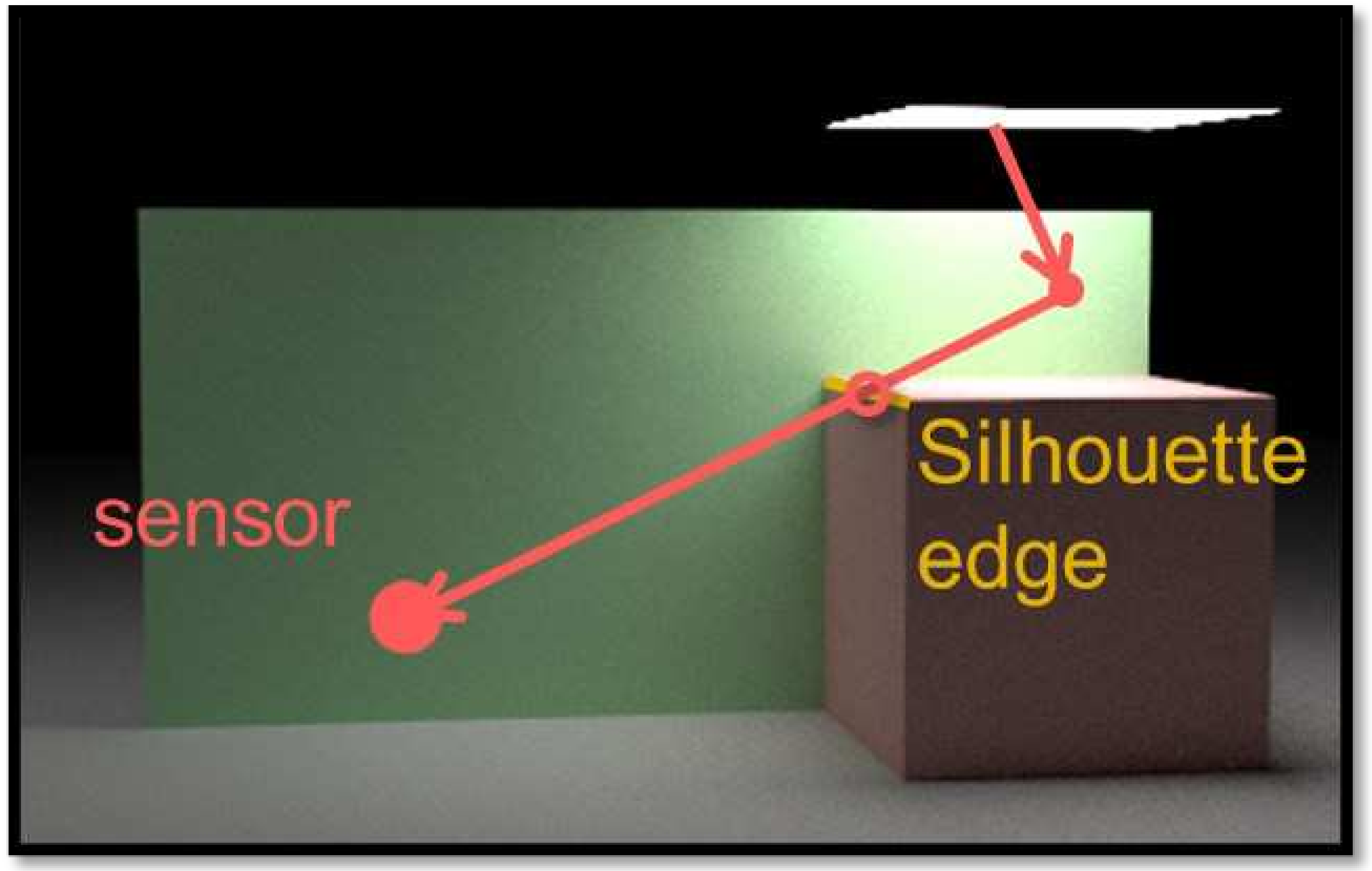

Sources of discontinuities

Boundary edge 

Sharp edge 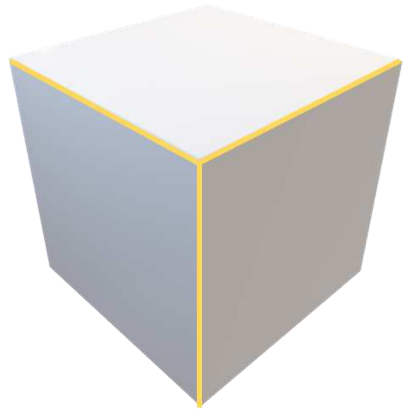

Silhouette edge 

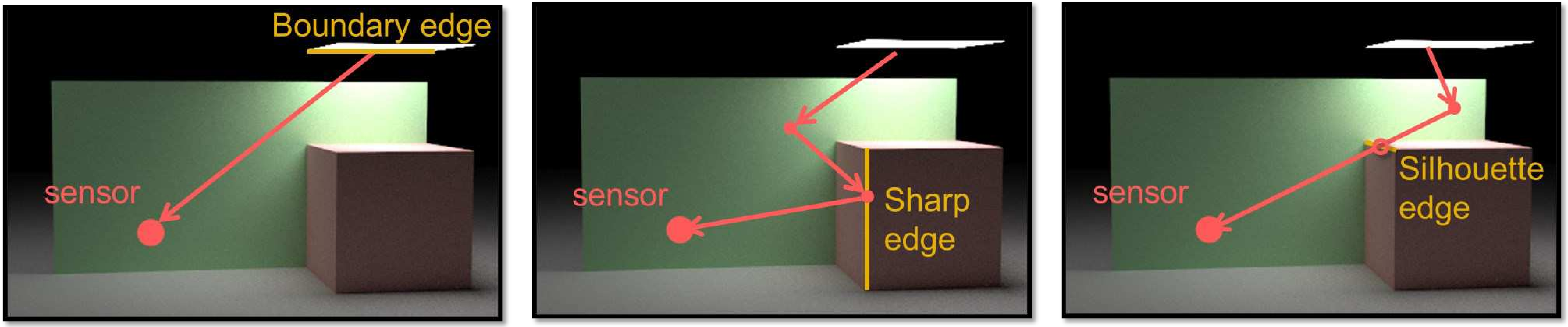

Sources of discontinuities

Boundary edge 

Sharp edge 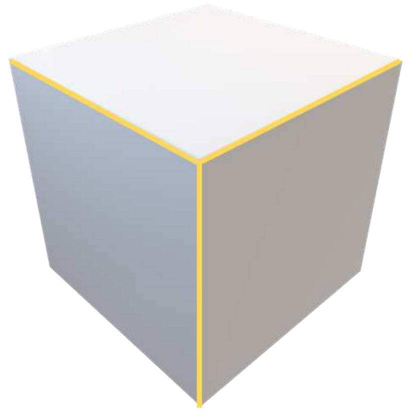

Silhouette edge 

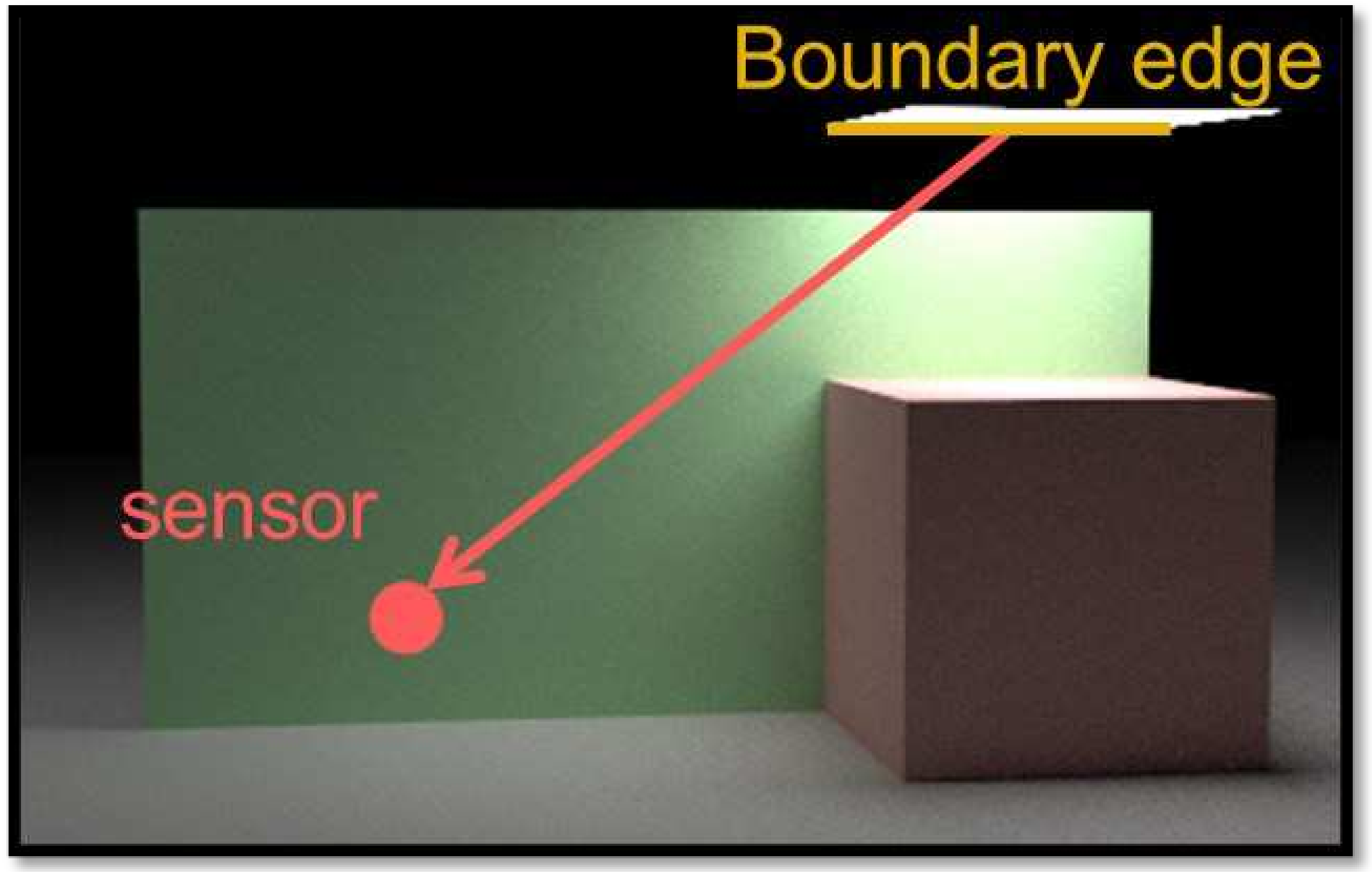

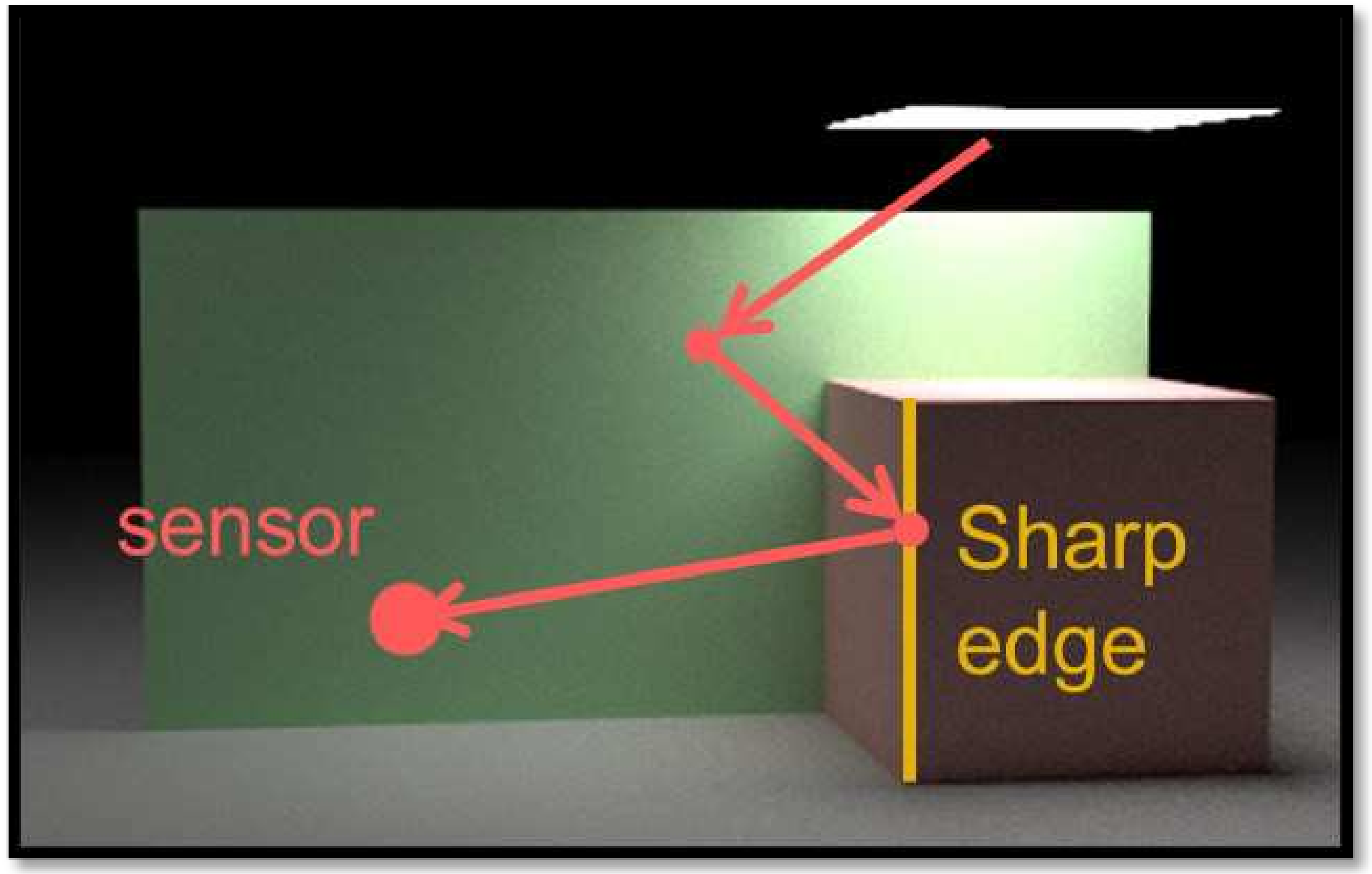

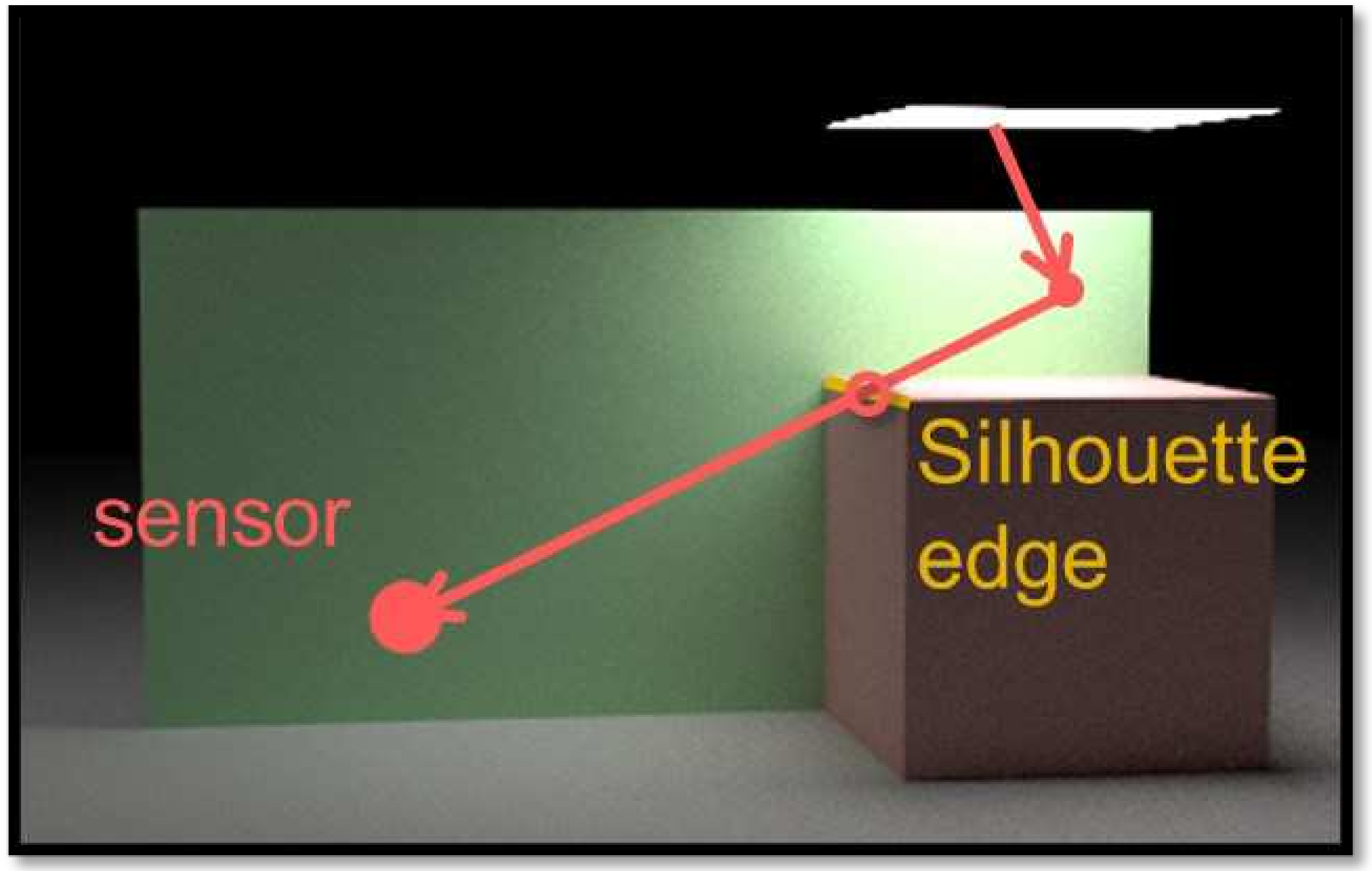

Sources of discontinuities

Boundary edge  Sharp edge 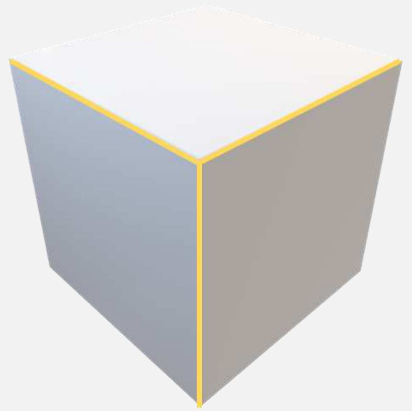 Silhouette edge 

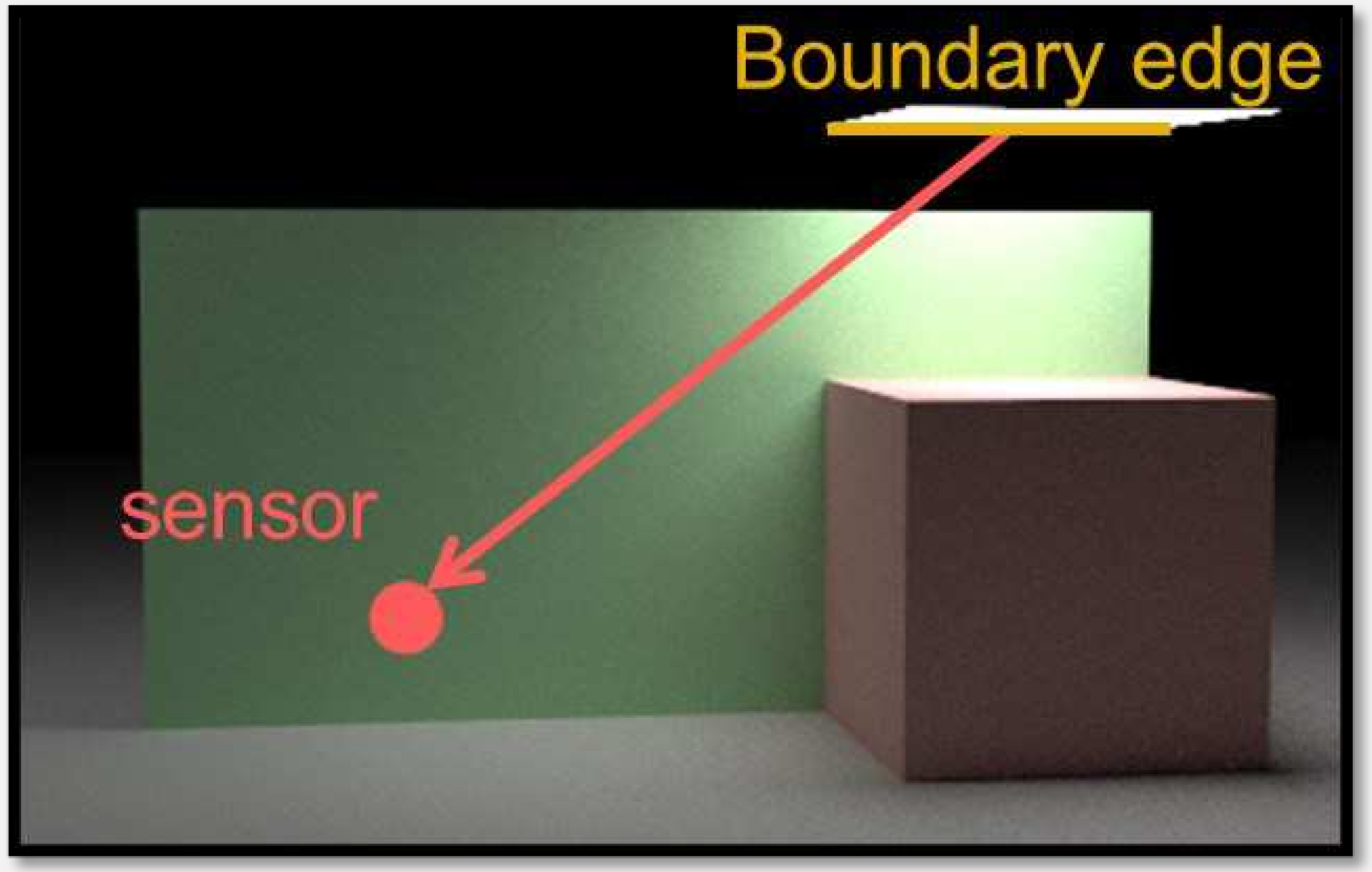

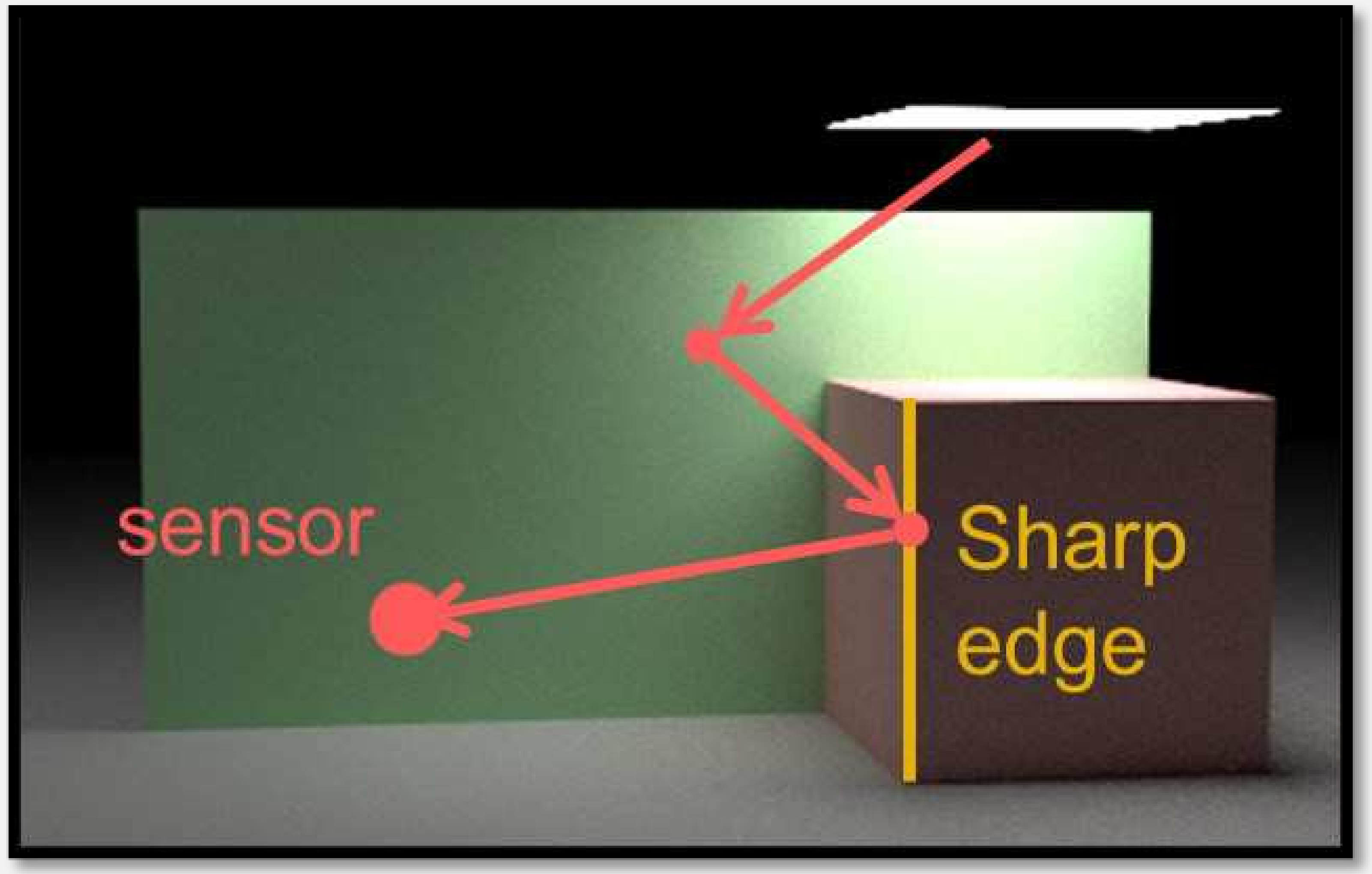

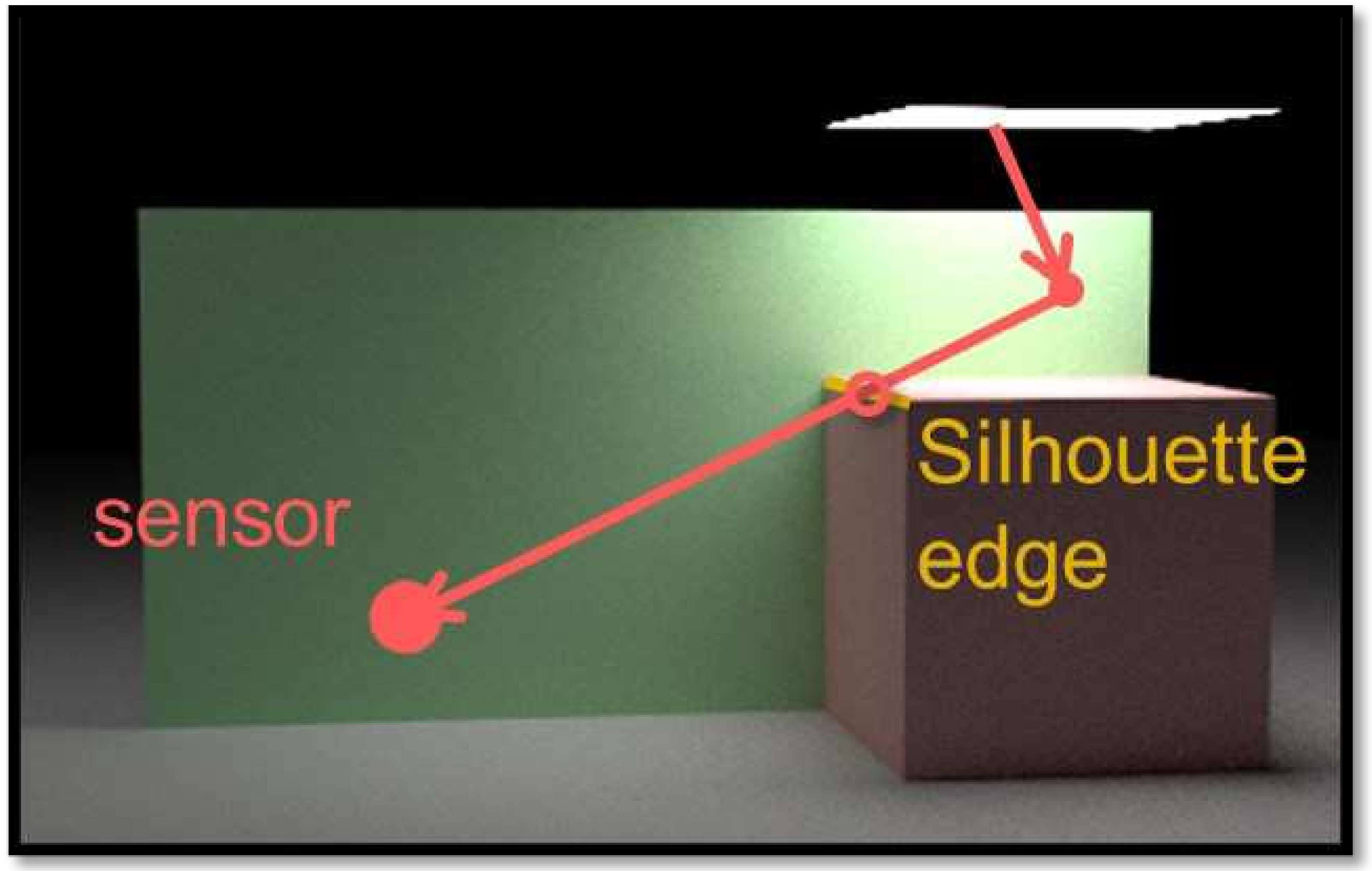

Topology-driven

Visibility-driven

Sources of discontinuities

Boundary edge 

Sharp edge 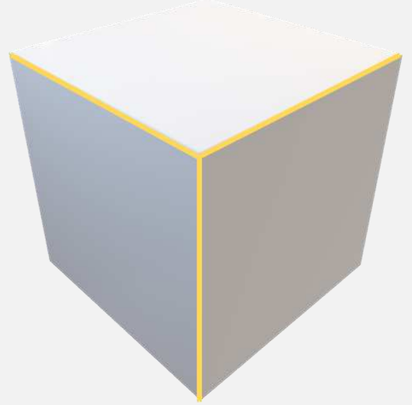

Silhouette edge 

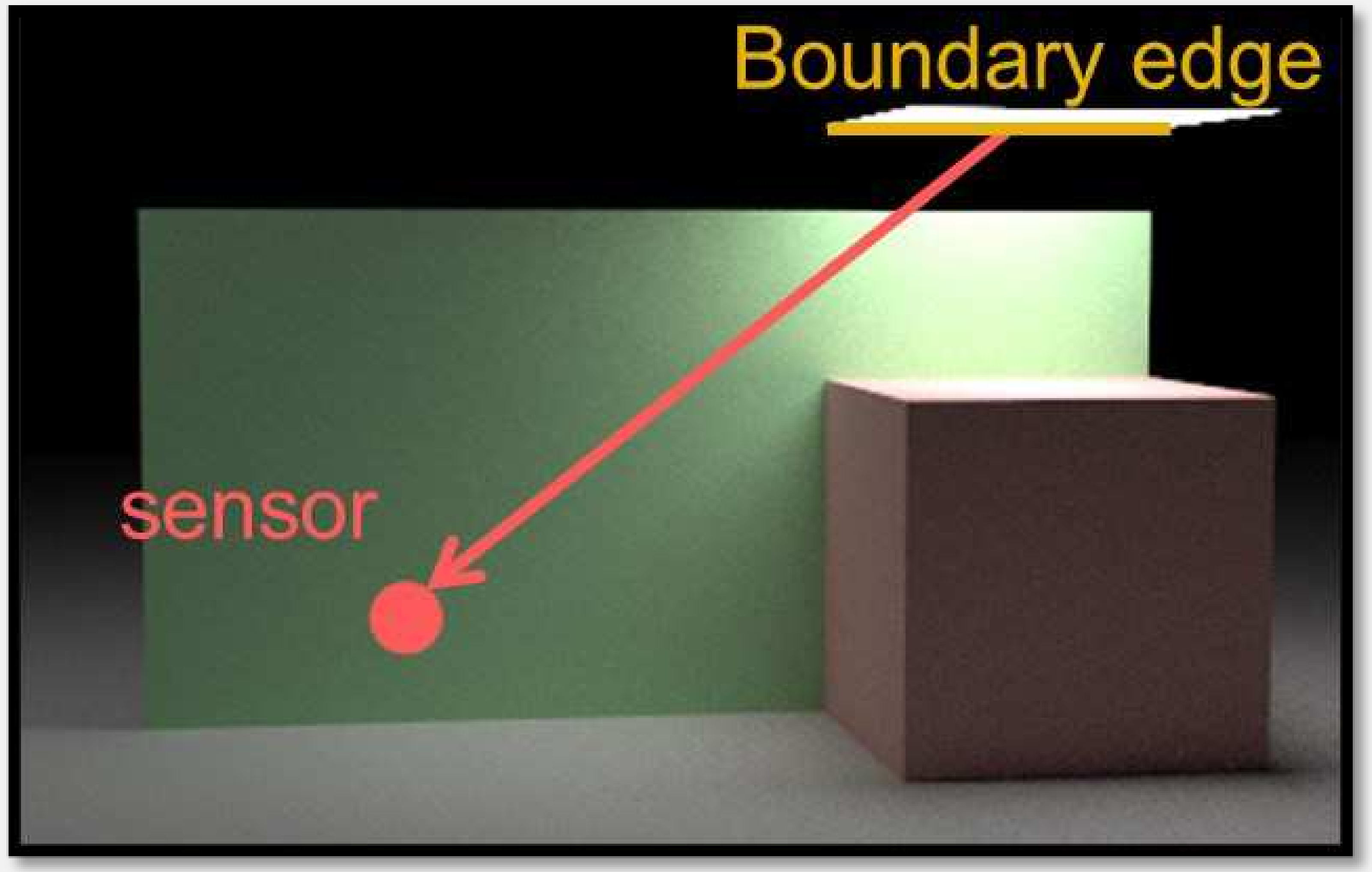

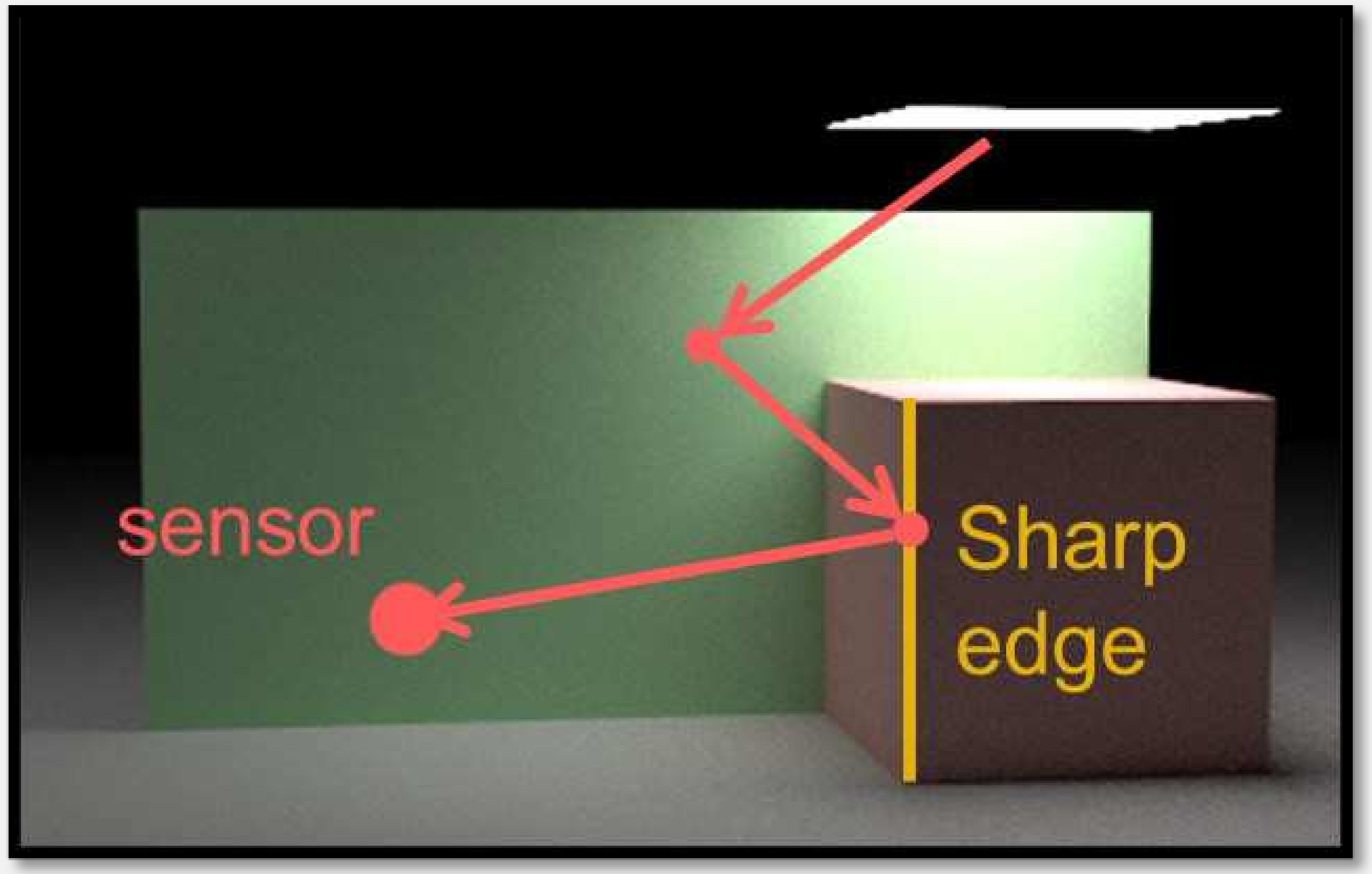

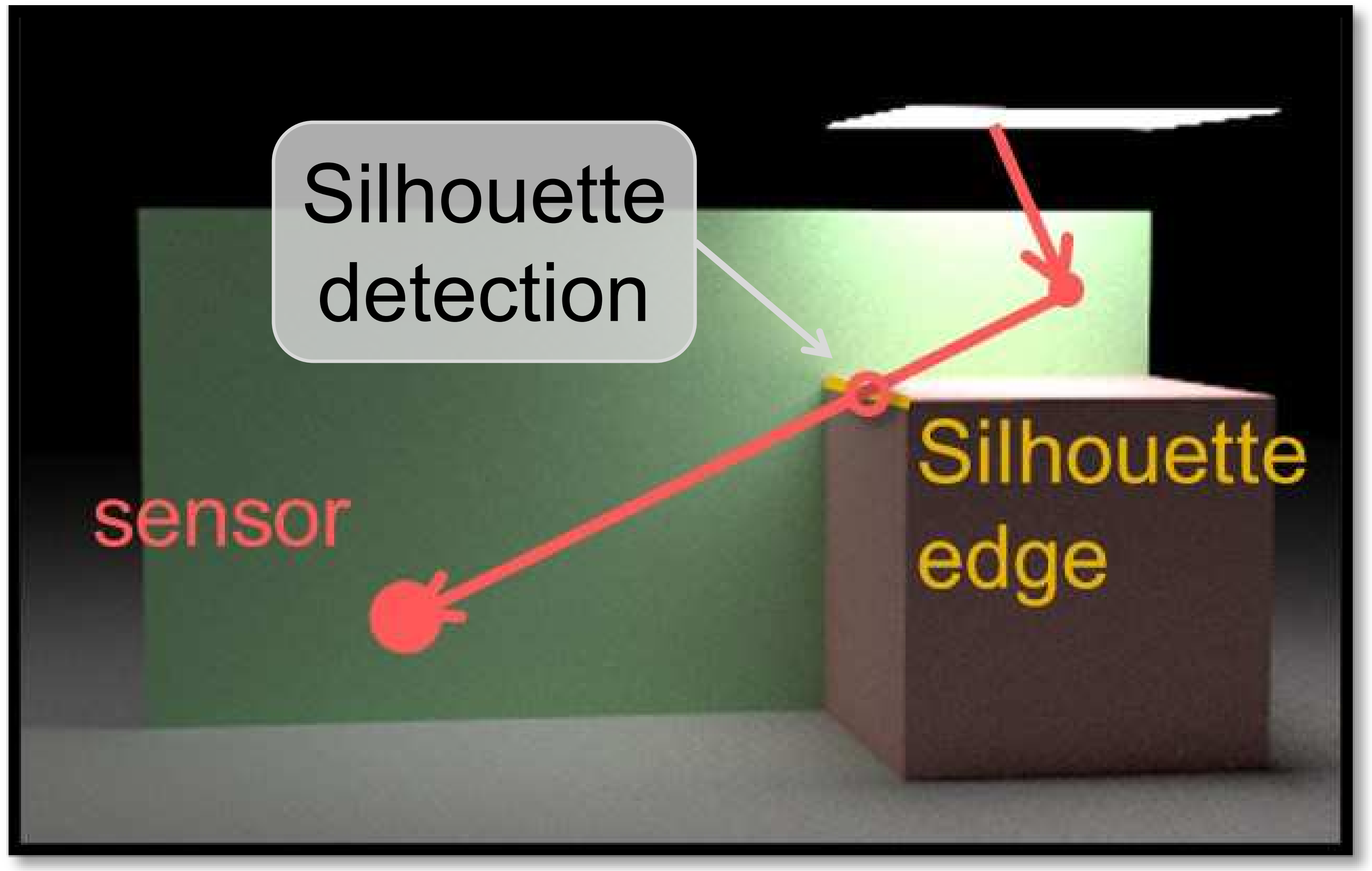

Topology-driven

Visibility-driven

Sources of discontinuities

- We still need to account for discontinuities when using smooth closed surfaces (e.g., neural SDFs)

Boundary edge 

Sharp edge 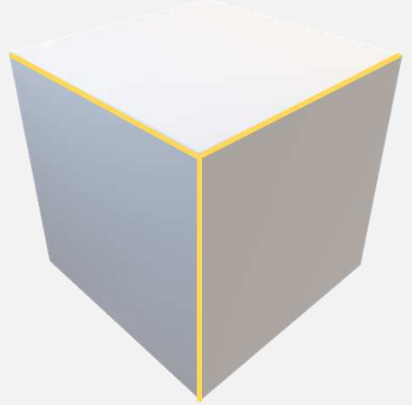

Silhouette edge 

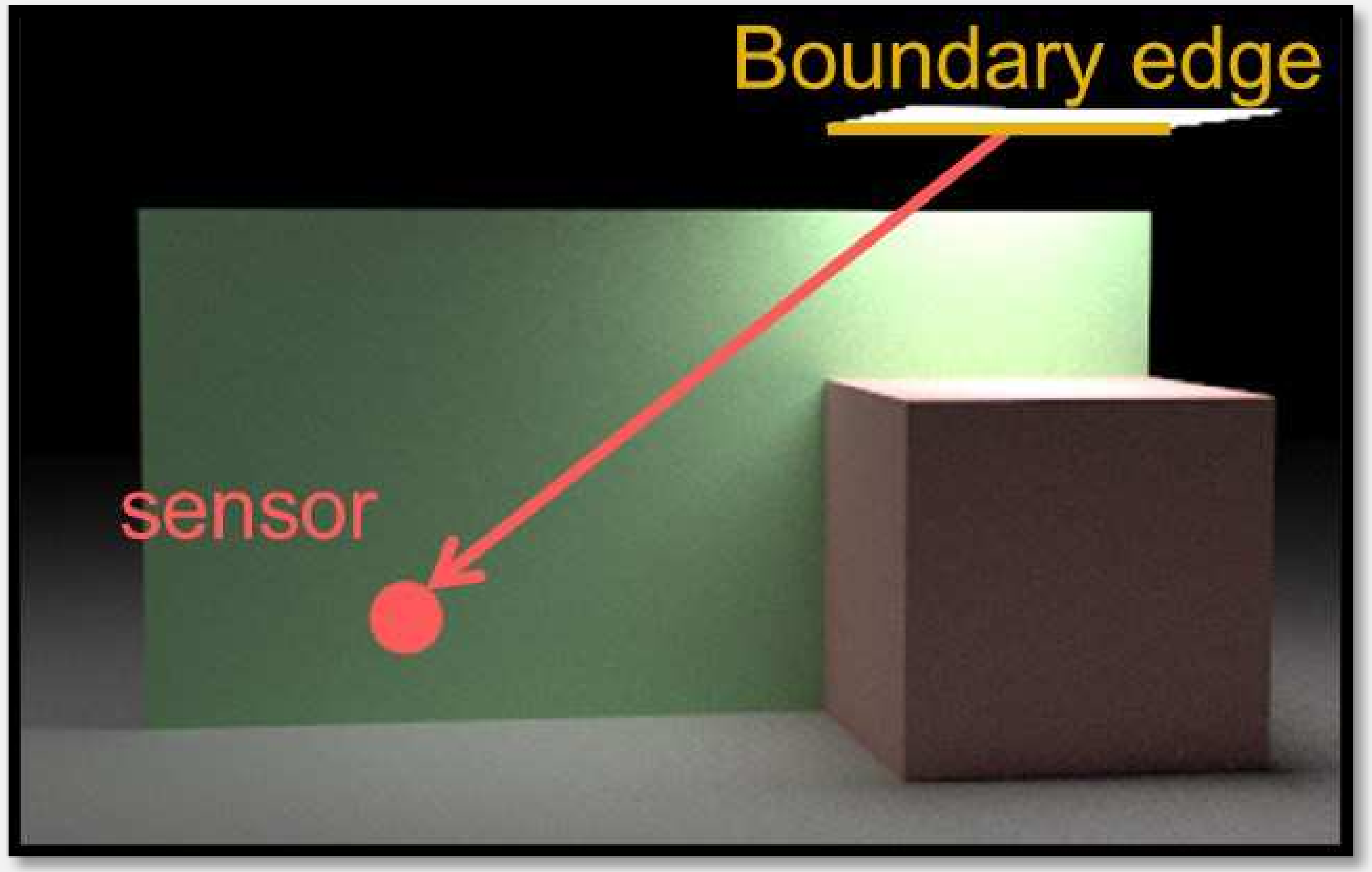

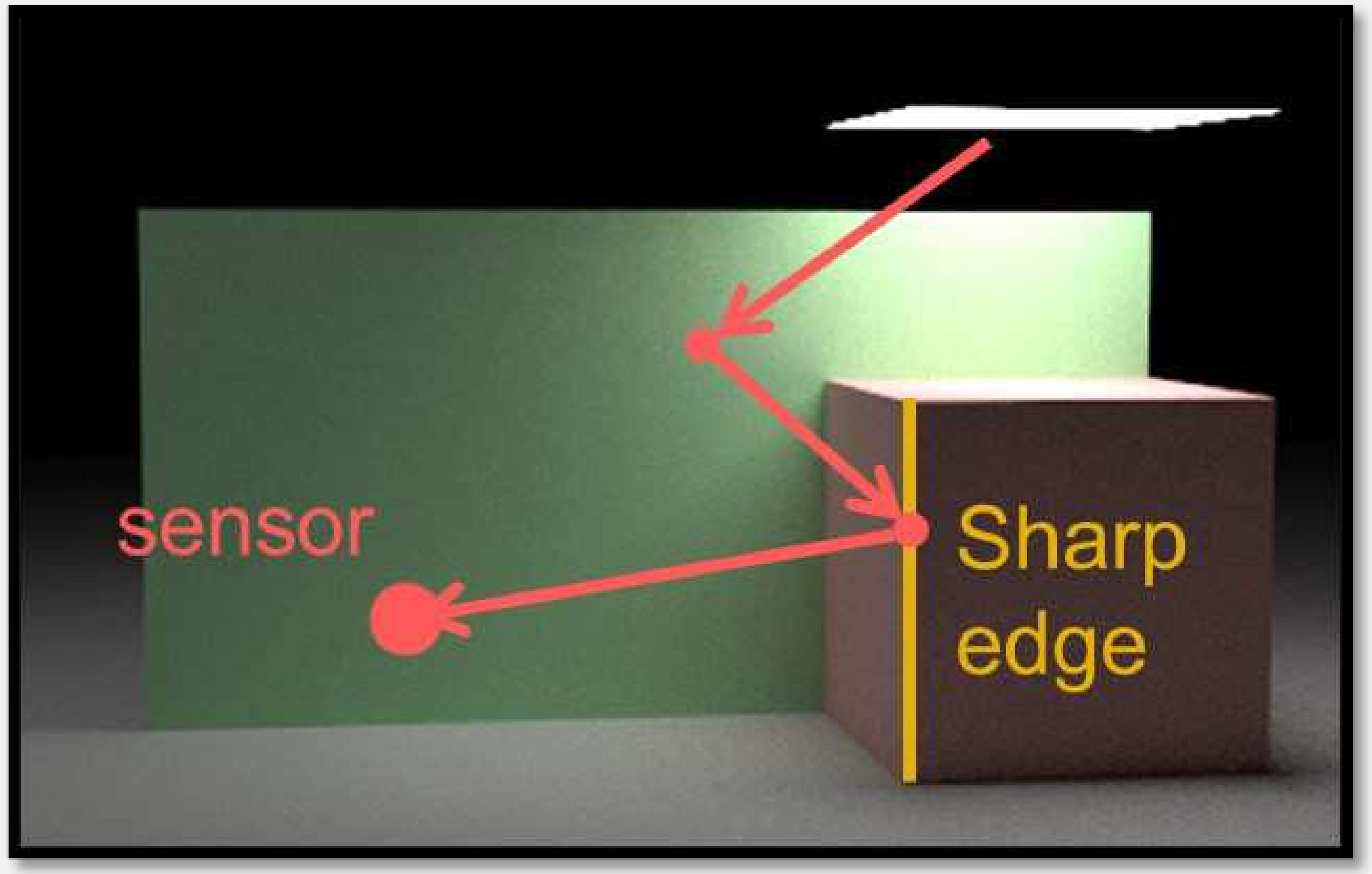

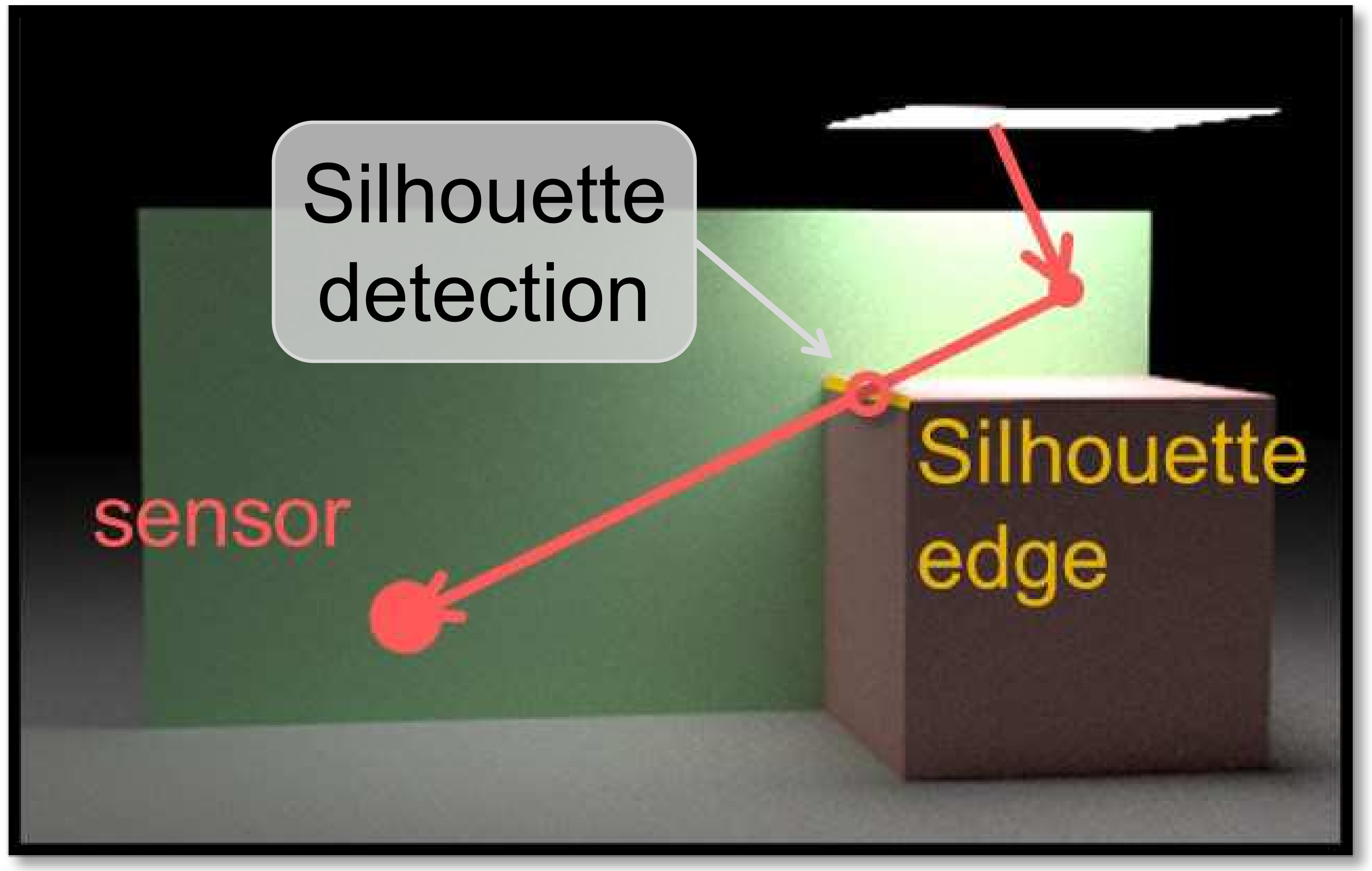

Topology-driven

Visibility-driven

Sources of discontinuities

- We still need to account for discontinuities when using smooth closed surfaces (e.g., neural SDFs)

Boundary edge

Sharp edge

Silhouette edge 

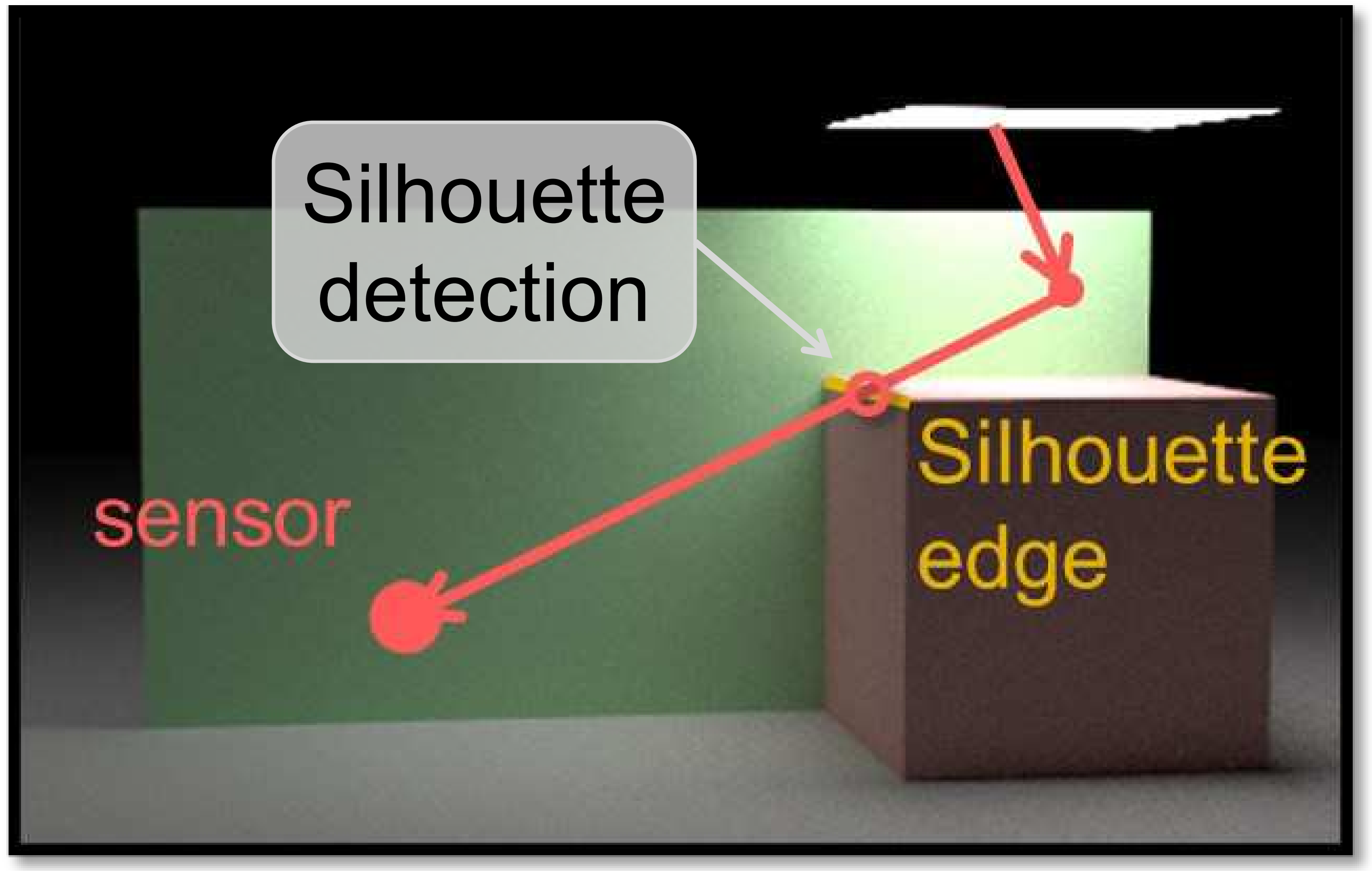

Topology-driven

Visibility-driven

Sources of discontinuities

- We still need to account for discontinuities when using smooth closed surfaces (e.g., neural SDFs)

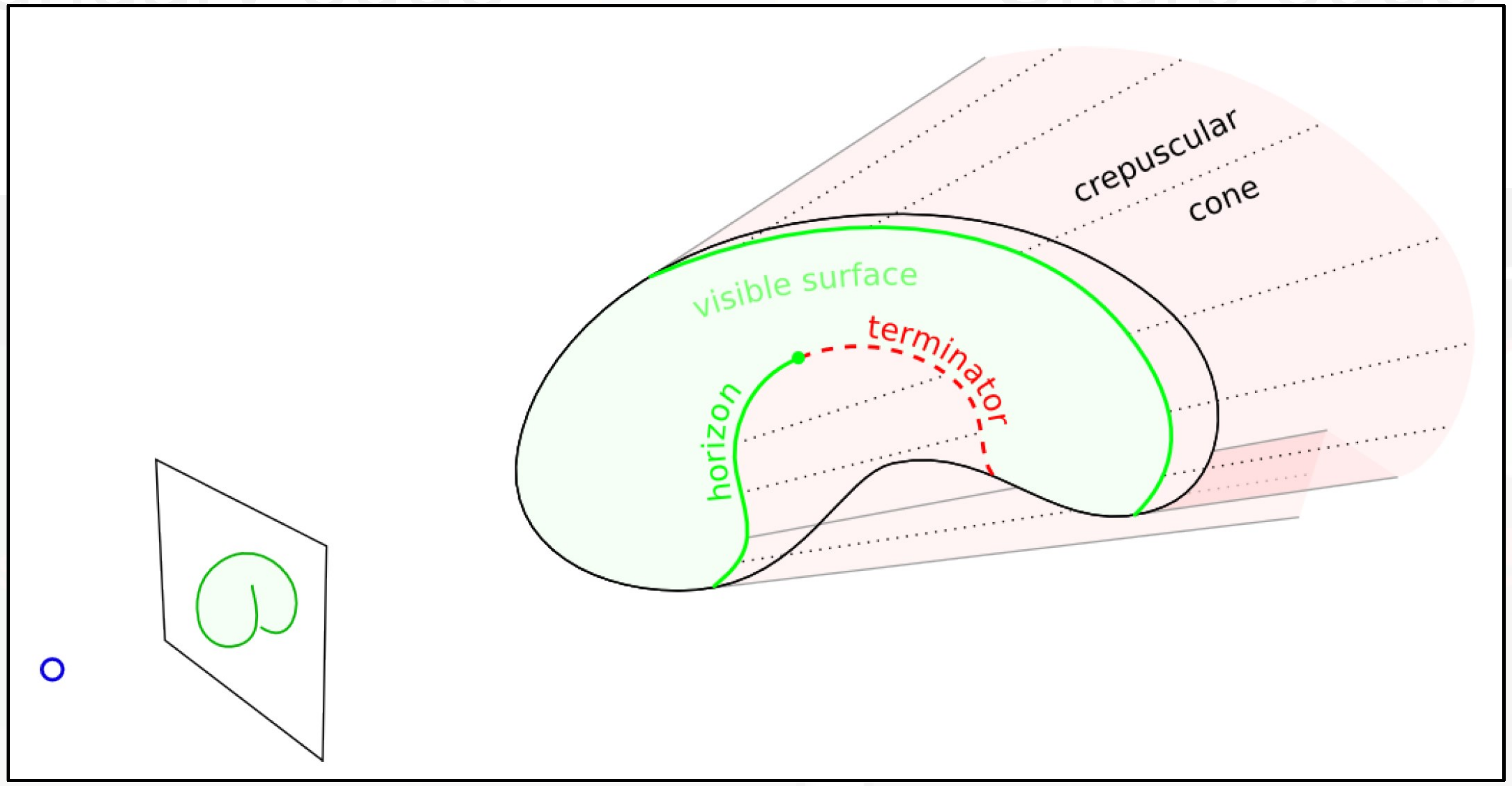

[Gargallo et al., ICCV 2007]

Silhouette edge

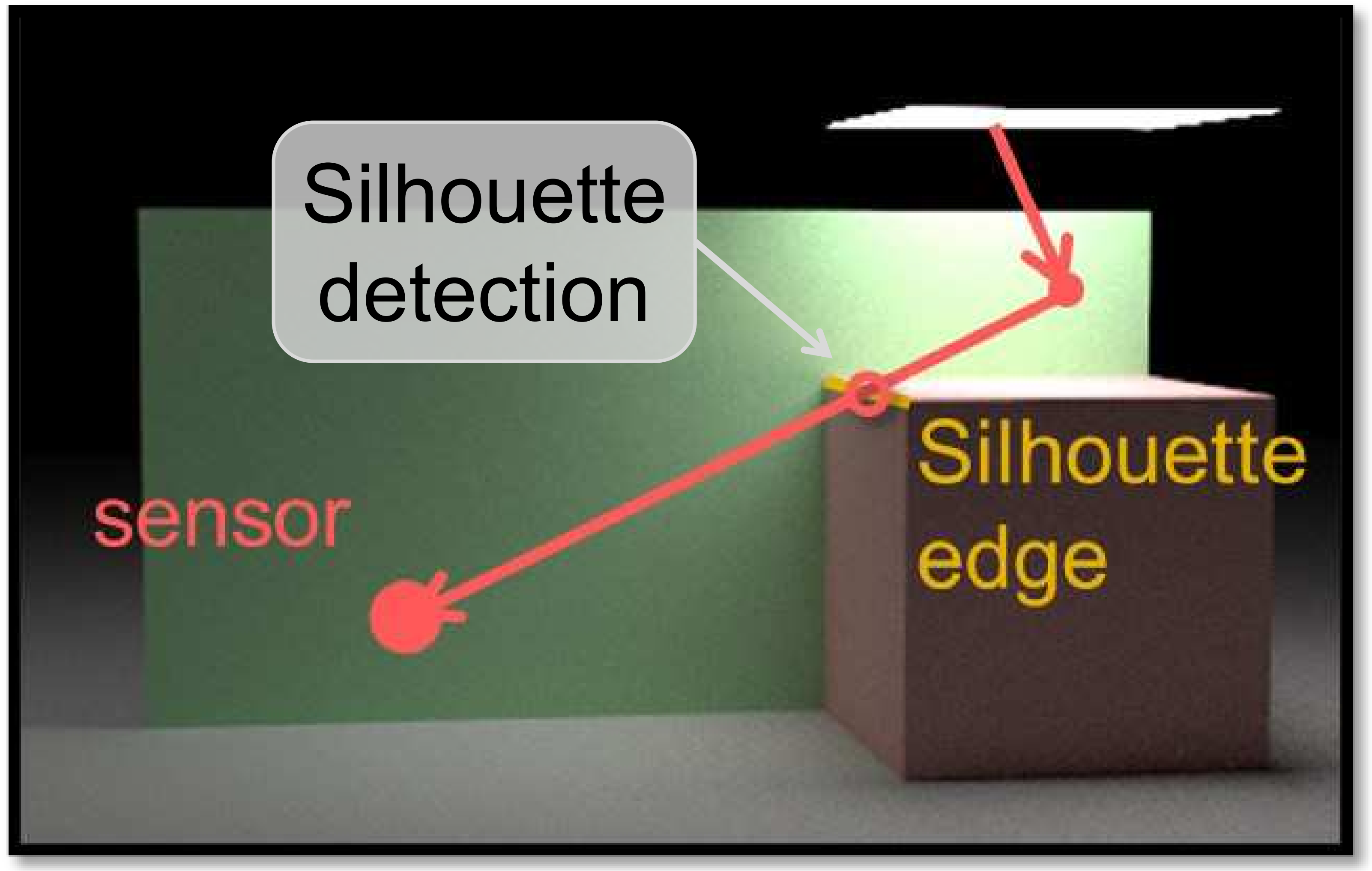

Visibility-driven

Significance of the boundary integral

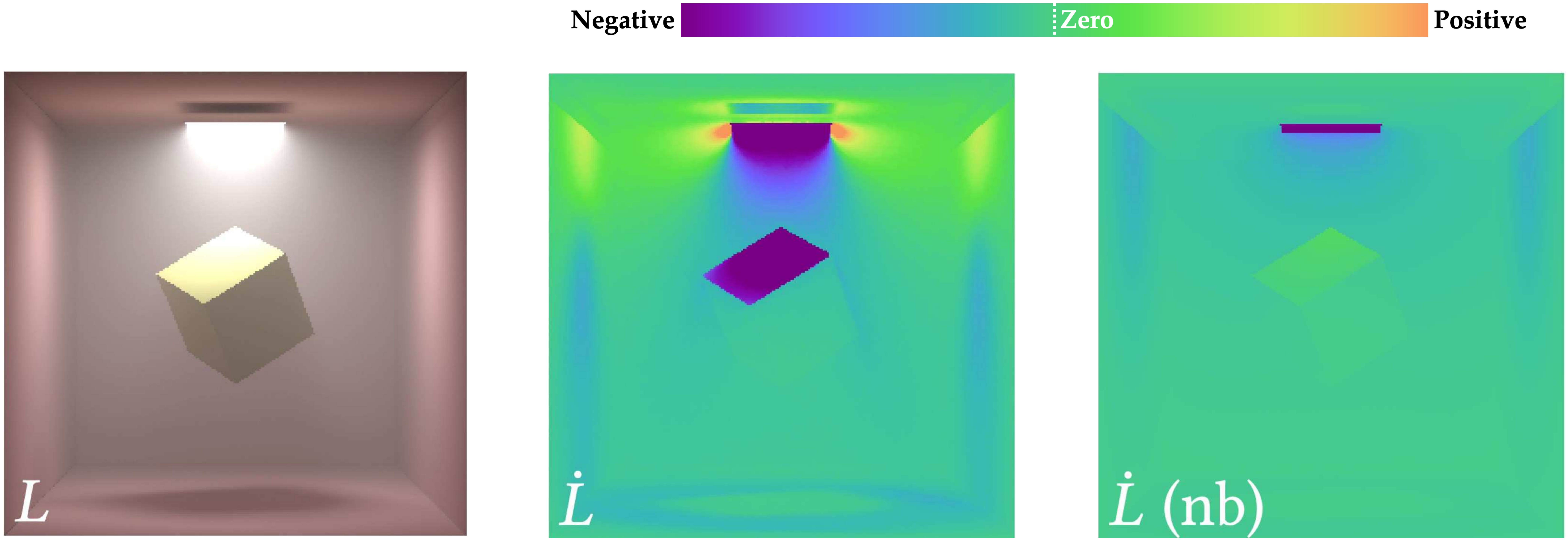

Original image

Derivative image
w.r.t. vertical offset of
the area light and the cube

Derivative image
w/o boundary integral

Significance of the boundary integral

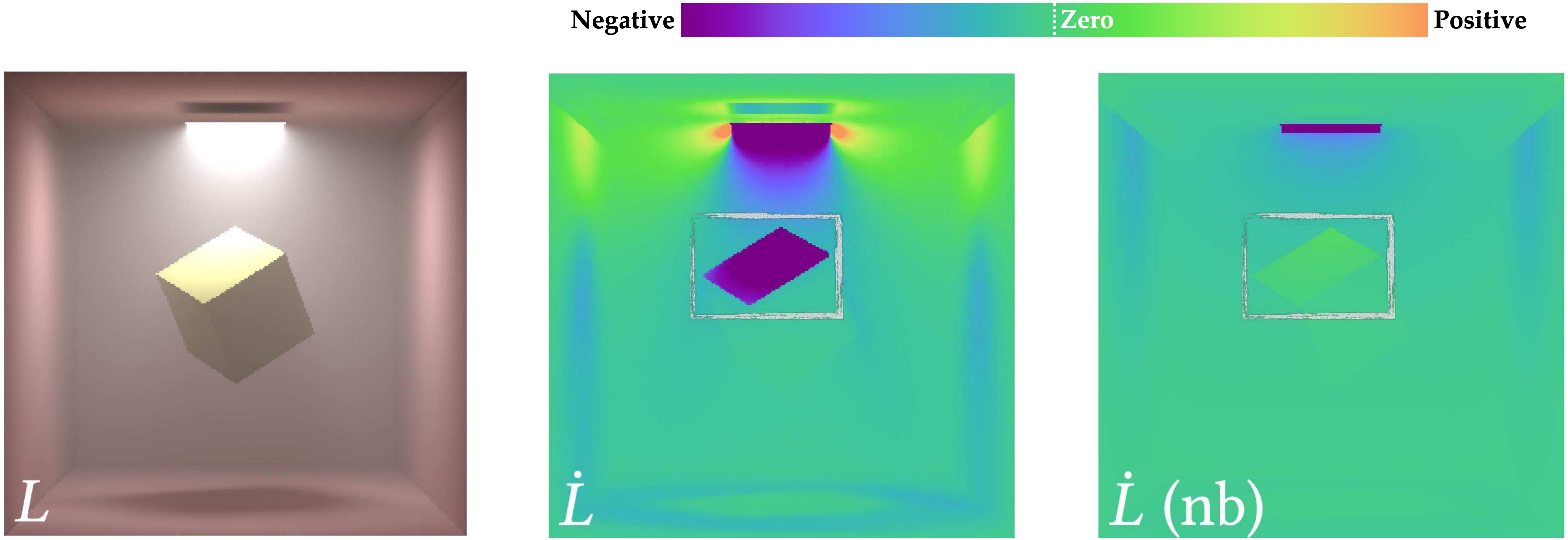

Original image

Derivative image
w.r.t. vertical offset of
the area light and the cube

Derivative image
w/o boundary integral

Gradient Accuracy Matters

Inverse-rendering results with *identical* optimization settings

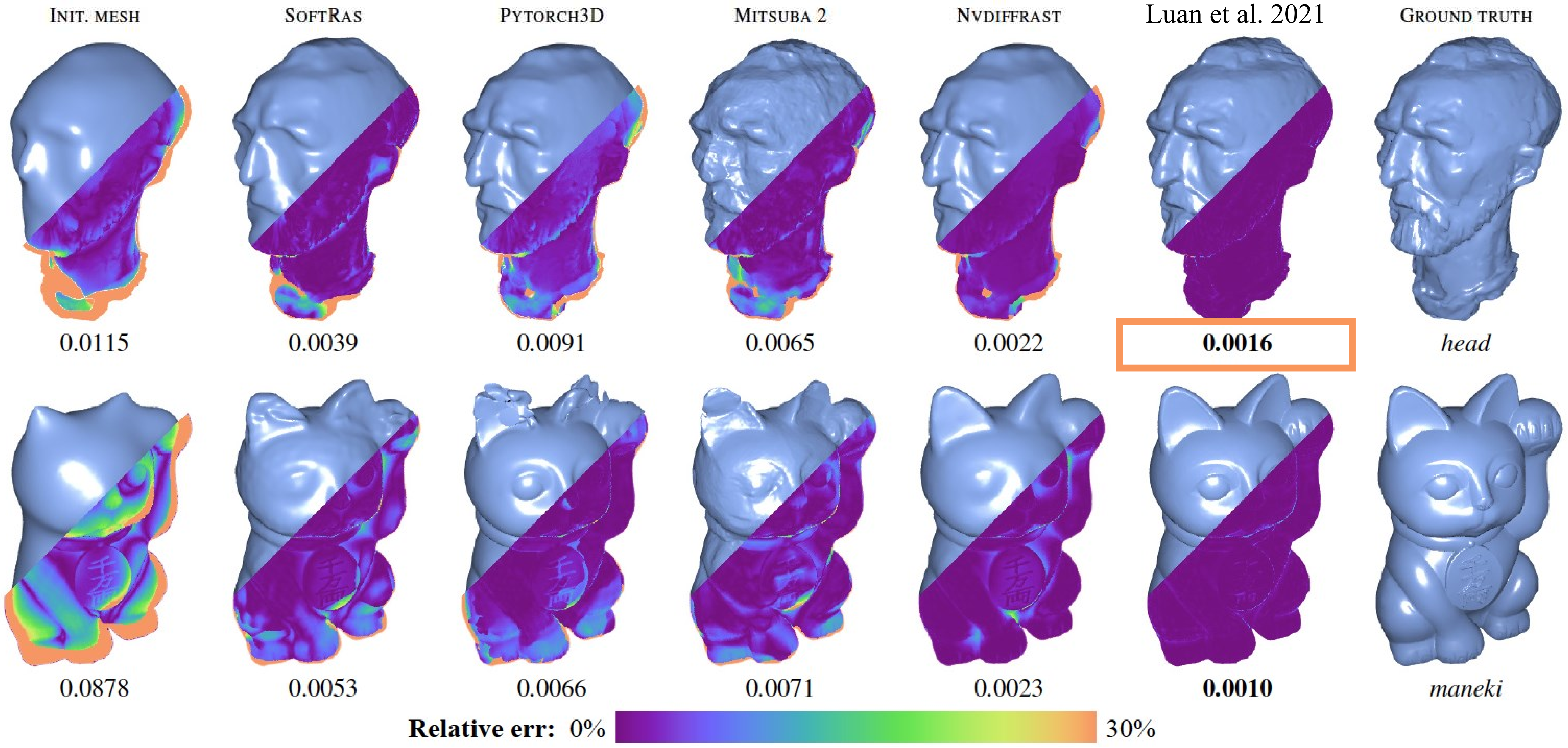

Differential Global Illumination

Very active area of research

Path-Space Differentiable Rendering

CHENG ZHANG, University of California, Irvine
BAILEY MILLER, Carnegie Mellon University
KALYAN, University of California, Irvine

Mitsuba 2: A Retargetable Forward and Inverse Renderer

MERLIN NIMIER-DAVID*, École Polytechnique Fédérale de Lausanne
DELIO VICINI*, École Polytechnique Fédérale de Lausanne
TIZIAN ZELTNER, École Polytechnique Fédérale de Lausanne
WENZEL JAKOB, École Polytechnique Fédérale de Lausanne

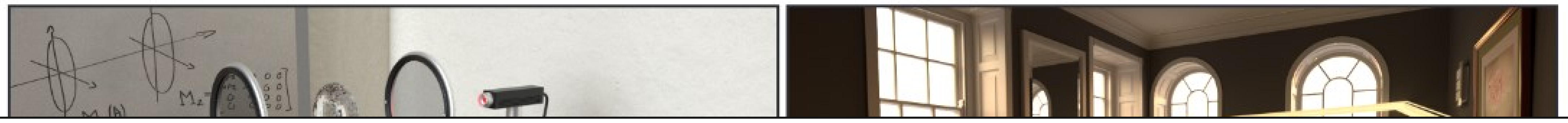

Reparameterizing Discontinuous Integrands for Differentiable Rendering

GUILLAUME LOUBET, École Polytechnique Fédérale de Lausanne (EPFL)
NICOLAS HOLZSCHUCH, Inria, Univ. Grenoble-Alpes, CNRS, LJK
WENZEL JAKOB, École Polytechnique Fédérale de Lausanne (EPFL)

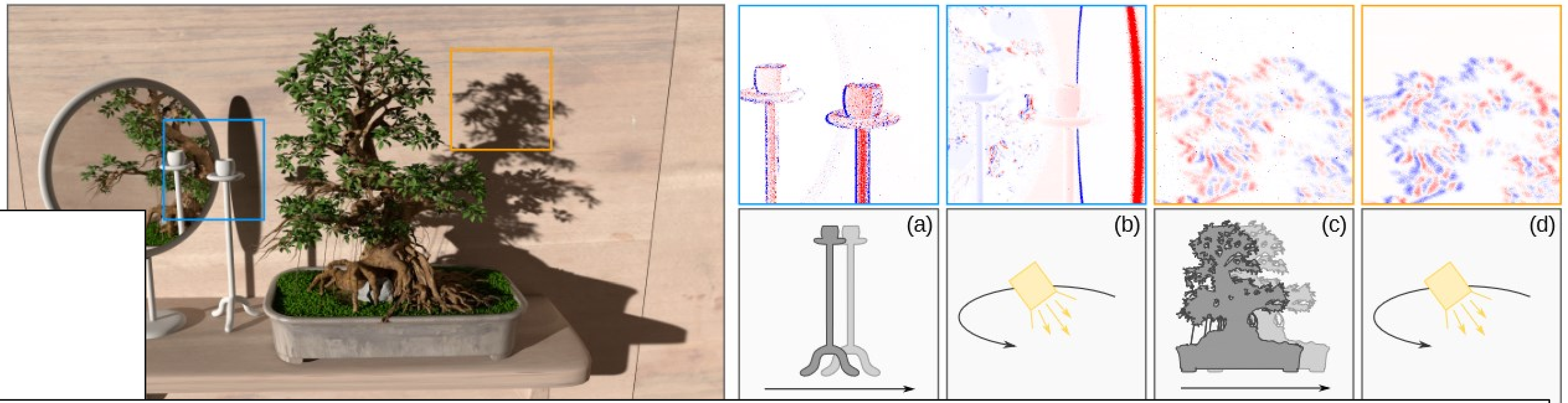

Path Replay Backpropagation: Differentiating Light Paths using Constant Memory and Linear Time

DELIO VICINI, École Polytechnique Fédérale de Lausanne (EPFL), Switzerland
SÉBASTIEN SPEIERER, École Polytechnique Fédérale de Lausanne (EPFL), Switzerland
WENZEL JAKOB, École Polytechnique Fédérale de Lausanne (EPFL), Switzerland

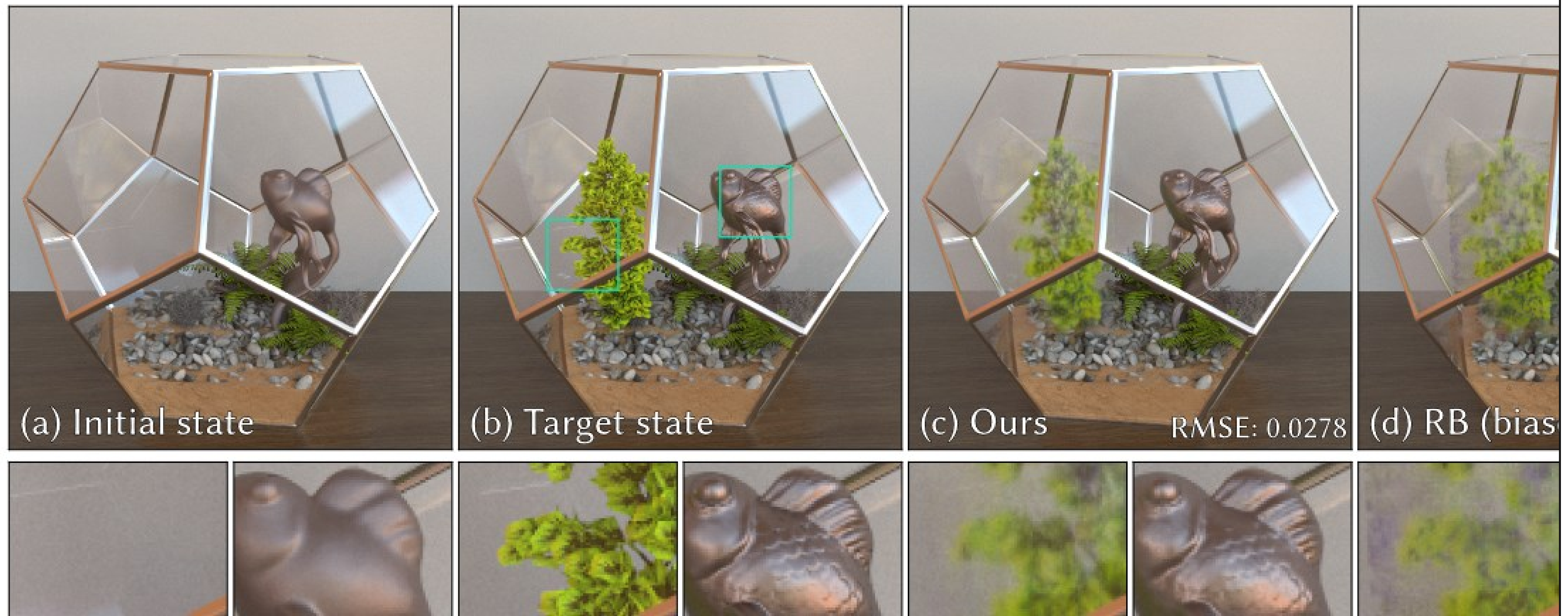

Differentiable Monte Carlo Ray Tracing through Edge Sampling

TZU-MAO LI, MIT CSAIL
MIIKA AITTALA, MIT CSAIL
FRÉDO DURAND, MIT CSAIL
JAAKKO LEHTINEN, Aalto University & NVIDIA

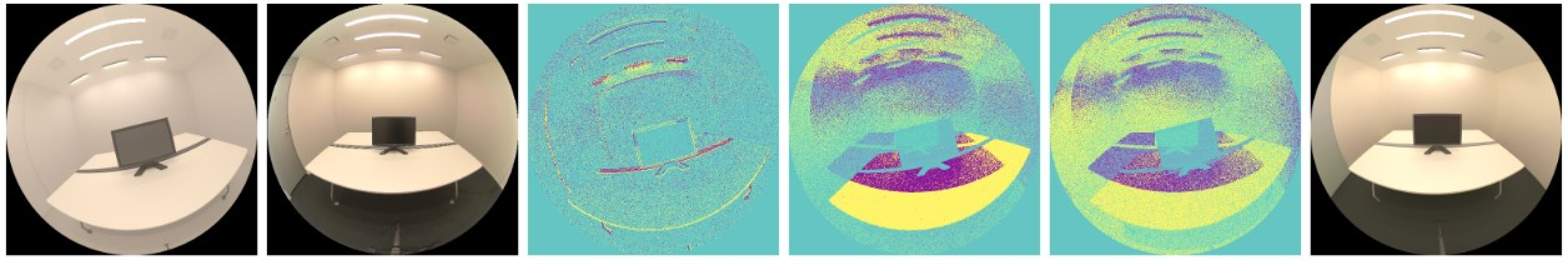

(a) initial guess (b) real photograph (c) camera gradient (per-pixel contribution) (d) table albedo gradient (per-pixel contribution) (e) light gradient (per-pixel contribution) (f) our fitted result

Remember: Path Integral for Global Illumination

Measurement contribution

Pixel value

$$I = \int_{\Omega} f(\bar{\boldsymbol{x}}) \, \mathrm{d}\mu(\bar{\boldsymbol{x}})$$

Path space

Area-product measure

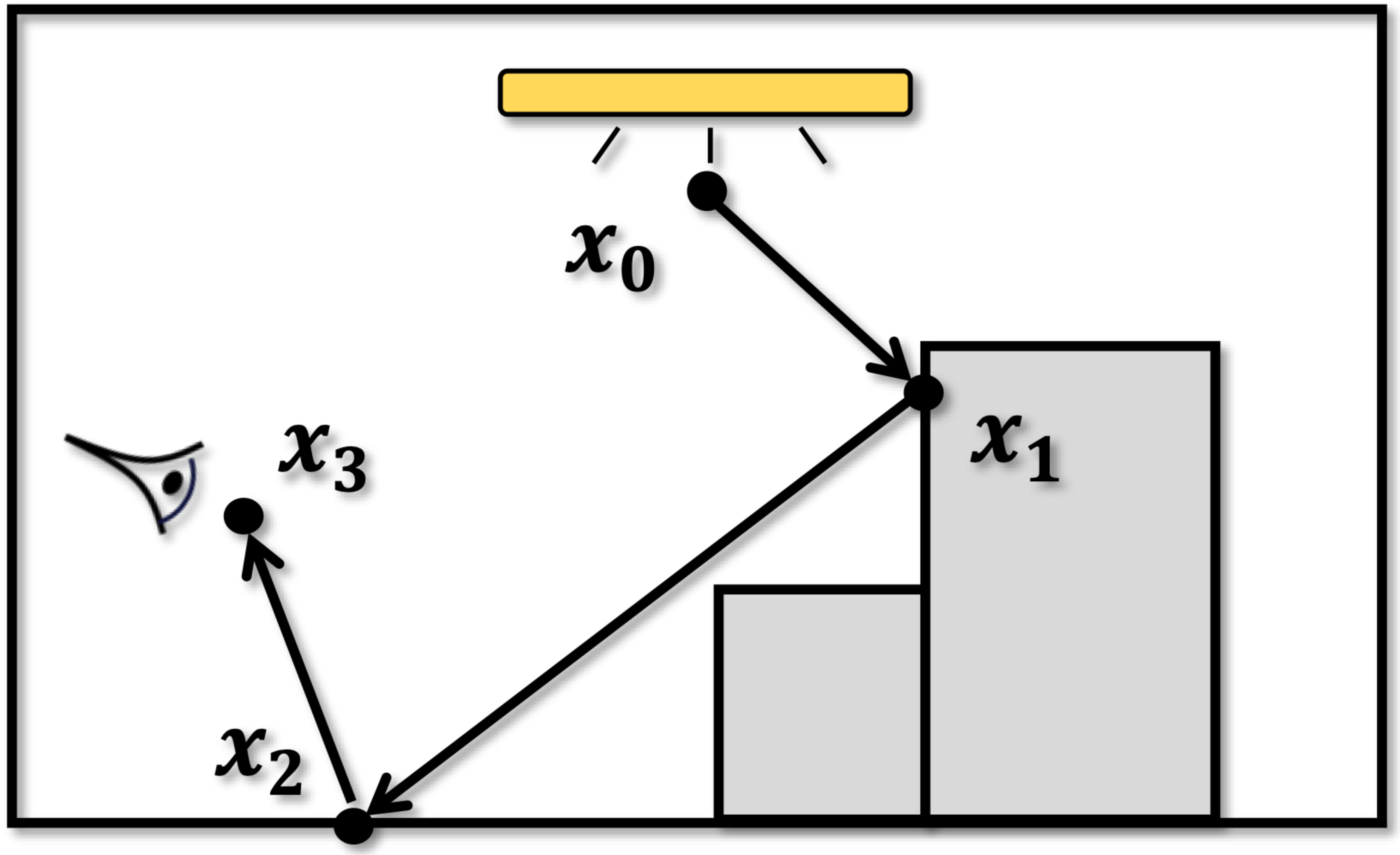

Light path $\bar{\boldsymbol{x}} = (x_0, x_1, x_2, x_3)$

[Zhang et al., 2020]

Differential Path Integral

Path-space differentiable rendering

$$\frac{\mathrm{d}}{\mathrm{d}\theta}\left(\int_{\Omega} f(\bar{\boldsymbol{x}})\,\mathrm{d}\mu(\bar{\boldsymbol{x}})\right) = \int_{\Omega} \dot{f}(\bar{\boldsymbol{x}})\,\mathrm{d}\mu(\bar{\boldsymbol{x}}) + \int_{\partial\Omega} g(\bar{\boldsymbol{x}})\,\mathrm{d}\mu'(\bar{\boldsymbol{x}})$$

Interior integral

Boundary integral

[Zhang et al., 2020]

Differential Path Integral

Path-space differentiable rendering

$$\frac{\mathrm{d}}{\mathrm{d}\theta}\left(\int_{\Omega} f(\bar{\boldsymbol{x}})\,\mathrm{d}\mu(\bar{\boldsymbol{x}})\right) = \int_{\Omega} \dot{f}(\bar{\boldsymbol{x}})\,\mathrm{d}\mu(\bar{\boldsymbol{x}}) + \int_{\partial\Omega} g(\bar{\boldsymbol{x}})\,\mathrm{d}\mu'(\bar{\boldsymbol{x}})$$

Interior integral

Boundary integral

We now derive $\partial I_N/\partial\pi$ in Eq. (25) using the recursive relations provided by Eqs. (21) and (24). Let

$$h_n^{(0)} := \left[\prod_{n'=n+1}^{N} g(\boldsymbol{x}_{n'};\, \boldsymbol{x}_{n'-2}, \boldsymbol{x}_{n'-1})\right] W_e(\boldsymbol{x}_N \to \boldsymbol{x}_{N-1}), \quad (52)$$

$$h_n^{(1)} := \sum_{n'=n+1}^{N} \kappa(\boldsymbol{x}_{n'})\, V(\boldsymbol{x}_{n'}), \quad (53)$$

$$\Delta h_{n,n'}^{(0)} := h_n^{(0)}\, \Delta g(\boldsymbol{x}_{n'};\boldsymbol{x}_{n'-2},\boldsymbol{x}_{n'-1})/g(\boldsymbol{x}_{n'};\boldsymbol{x}_{n'-2},\boldsymbol{x}_{n'-1}), \quad (54)$$

for $0 \le n < n' \le N$. We omit the dependencies of $h_n^{(0)}$, $h_n^{(1)}$, and $\Delta h_{n,n'}^{(0)}$ on $\boldsymbol{x}_{n+1}, \ldots, \boldsymbol{x}_N$ for notational convenience.

We now show that, for all $0 \le n < N$, it holds that

$$h_n(\boldsymbol{x}_n;\, \boldsymbol{x}_{n-1}) = \int_{\mathcal{M}^{N-n}} h_n^{(0)} \prod_{n'=n+1}^{N} \mathrm{d}A(\boldsymbol{x}_{n'}), \quad (55)$$

and

$$\dot{h}_n(\boldsymbol{x}_n;\, \boldsymbol{x}_{n-1}) = \int_{\mathcal{M}^{N-n}} \left[\left(h_n^{(0)}\right)^{\cdot} - h_n^{(0)} h_n^{(1)}\right] \prod_{n'=n+1}^{N} \mathrm{d}A(\boldsymbol{x}_{n'}) + \sum_{n'=n+1}^{N} \int \Delta h_{n,n'}^{(0)}\, V_{\overline{\partial\mathcal{M}}_{n'}}(\boldsymbol{x}_{n'})\, \mathrm{d}\ell(\boldsymbol{x}_{n'}) \prod_{\substack{n<i\le N \\ i\ne n'}} \mathrm{d}A(\boldsymbol{x}_i), \quad (56)$$

where the integral domain of the second term on the right-hand side, which is omitted for notational clarity, is $\mathcal{M}(\pi)$ for each $\boldsymbol{x}_i$ with $i \ne n'$ and $\overline{\partial\mathcal{M}}_{n'}(\pi)$, which depends on $\boldsymbol{x}_{n'-1}$, for $\boldsymbol{x}_{n'}$.

It is easy to verify that Eqs. (55) and (56) hold for $n = N - 1$. We now show that, if they hold for some $0 < n < N$, then it is also the case for $n - 1$. Let $g_{n-1} := g(\boldsymbol{x}_n;\, \boldsymbol{x}_{n-2}, \boldsymbol{x}_{n-1})$ for all $0 < n \le N$. Then,

$$\begin{aligned} h_{n-1}(\boldsymbol{x}_{n-1};\, \boldsymbol{x}_{n-2}) &= \int_{\mathcal{M}} g_{n-1} \int_{\mathcal{M}^{N-n}} h_n^{(0)} \prod_{n'=n+1}^{N} \mathrm{d}A(\boldsymbol{x}_{n'})\, \mathrm{d}A(\boldsymbol{x}_n) \\ &= \int_{\mathcal{M}^{N-n+1}} h_{n-1}^{(0)} \prod_{n'=n}^{N} \mathrm{d}A(\boldsymbol{x}_{n'}), \end{aligned} \quad (57)$$

and

$$\begin{aligned} &\dot{h}_{n-1}(\boldsymbol{x}_{n-1};\, \boldsymbol{x}_{n-2}) \\ &= \int_{\mathcal{M}} \left[\dot{g}_{n-1}\, h_n + g_{n-1}(\dot{h}_n - h_n\, \kappa(\boldsymbol{x}_n)\, V(\boldsymbol{x}_n))\right] \mathrm{d}A(\boldsymbol{x}_n) \\ &\quad + \int_{\overline{\partial\mathcal{M}}_n} \Delta g_{n-1}\, h_n\, V_{\overline{\partial\mathcal{M}}_n}\, \mathrm{d}\ell(\boldsymbol{x}_n) \\ &= \int_{\mathcal{M}^{N-n+1}} \left\{\dot{g}_{n-1}\, h_n^{(0)} + g_{n-1}\left[\left(h_n^{(0)}\right)^{\cdot} - h_n^{(0)} h_{n-1}^{(1)}\right]\right\} \prod_{n'=k}^{N} \mathrm{d}A(\boldsymbol{x}_{n'}) \\ &\quad + \sum_{n'=n+1}^{N} \int g_{n-1}\, \Delta h_{n,n'}^{(0)}\, V_{\overline{\partial\mathcal{M}}_{n'}}(\boldsymbol{x}_{n'})\, \mathrm{d}\ell(\boldsymbol{x}_{n'}) \prod_{\substack{n\le i\le N \\ i\ne n'}} \mathrm{d}A(\boldsymbol{x}_i) \\ &\quad + \int \Delta g_{n-1}\, h_n^{(0)}\, V_{\overline{\partial\mathcal{M}}_n}\, \mathrm{d}\ell(\boldsymbol{x}_n) \prod_{n'=n+1}^{N} \mathrm{d}A(\boldsymbol{x}_{n'}) \\ &= \int_{\mathcal{M}^{N-n+1}} \left[\left(h_{n-1}^{(0)}\right)^{\cdot} - h_{n-1}^{(0)} h_{n-1}^{(1)}\right] \prod_{n'=n}^{N} \mathrm{d}A(\boldsymbol{x}_{n'}) \\ &\quad + \sum_{n'=n}^{N} \int \Delta h_{n-1,n'}^{(0)}\, V_{\overline{\partial\mathcal{M}}_{n'}}(\boldsymbol{x}_{n'})\, \mathrm{d}\ell(\boldsymbol{x}_{n'}) \prod_{\substack{n\le i\le N \\ i\ne n'}} \mathrm{d}A(\boldsymbol{x}_i). \end{aligned} \quad (58)$$

Thus, using mathematical induction, we know that Eqs. (55) and (56) hold for all $0 \le n < N$.

Notice that $h_0^{(0)} = f$ and $\Delta h_{0,n'}^{(0)} = \Delta f_{n'}$, where $\Delta f_{n'}$ follows the definition in Eq. (28). Letting $n = 0$ in Eq. (56) yields

$$\dot{h}_0(\boldsymbol{x}_0) = \int_{\mathcal{M}^N} \left[\dot{f}(\bar{\boldsymbol{x}}) - f(\bar{\boldsymbol{x}}) \sum_{n'=1}^{N} \kappa(\boldsymbol{x}_{n'})\, V(\boldsymbol{x}_{n'})\right] \prod_{n'=1}^{N} \mathrm{d}A(\boldsymbol{x}_{n'}) + \sum_{n'=1}^{N} \int \Delta f_{n'}(\bar{\boldsymbol{x}})\, V_{\overline{\partial\mathcal{M}}_{n'}}\, \mathrm{d}\ell(\boldsymbol{x}_{n'}) \prod_{\substack{0<i\le N \\ i\ne n'}} \mathrm{d}A(\boldsymbol{x}_i). \quad (59)$$

Lastly, based on the assumption that h_0 is continuous in $\boldsymbol{x}_0$, Eq. (25) can be obtained by differentiating Eq. (23):

$$\begin{aligned} \frac{\partial I_N}{\partial\pi} &= \frac{\partial}{\partial\pi} \int_{\mathcal{M}} h_0(\boldsymbol{x}_0)\, \mathrm{d}A(\boldsymbol{x}_0) \\ &= \int_{\mathcal{M}} \left[\dot{h}_0(\boldsymbol{x}_0) - h_0(\boldsymbol{x}_0)\, \kappa(\boldsymbol{x}_0)\, V(\boldsymbol{x}_0)\right] \mathrm{d}A(\boldsymbol{x}_0) \\ &\quad + \int_{\overline{\partial\mathcal{M}}_0} h_0(\boldsymbol{x}_0)\, V_{\overline{\partial\mathcal{M}}_0}(\boldsymbol{x}_0)\, \mathrm{d}\ell(\boldsymbol{x}_0) \\ &= \int_{\Omega_N} \left[\dot{f}(\bar{\boldsymbol{x}}) - f(\bar{\boldsymbol{x}}) \sum_{K=0}^{N} \kappa(\boldsymbol{x}_K)\, V(\boldsymbol{x}_K)\right] \mathrm{d}\mu(\bar{\boldsymbol{x}}) \\ &\quad + \sum_{K=0}^{N} \int_{\Omega_{N,K}} \Delta f_K(\bar{\boldsymbol{x}})\, V_{\overline{\partial\mathcal{M}}_K}\, \mathrm{d}\mu'_{N,K}(\bar{\boldsymbol{x}}). \end{aligned} \quad (60)$$

(The full derivation is quite involved…)

[Zhang et al., 2020]

Differential Path Integral

Path-space differentiable rendering

$$\frac{\mathrm{d}}{\mathrm{d}\theta}\left(\int_{\Omega} f(\bar{\boldsymbol{x}})\mathrm{d}\mu(\bar{\boldsymbol{x}})\right) = \int_{\Omega} \dot{f}(\bar{\boldsymbol{x}})\mathrm{d}\mu(\bar{\boldsymbol{x}}) + \int_{\partial\Omega} g(\bar{\boldsymbol{x}})\mathrm{d}\mu'(\bar{\boldsymbol{x}})$$

Interior integral

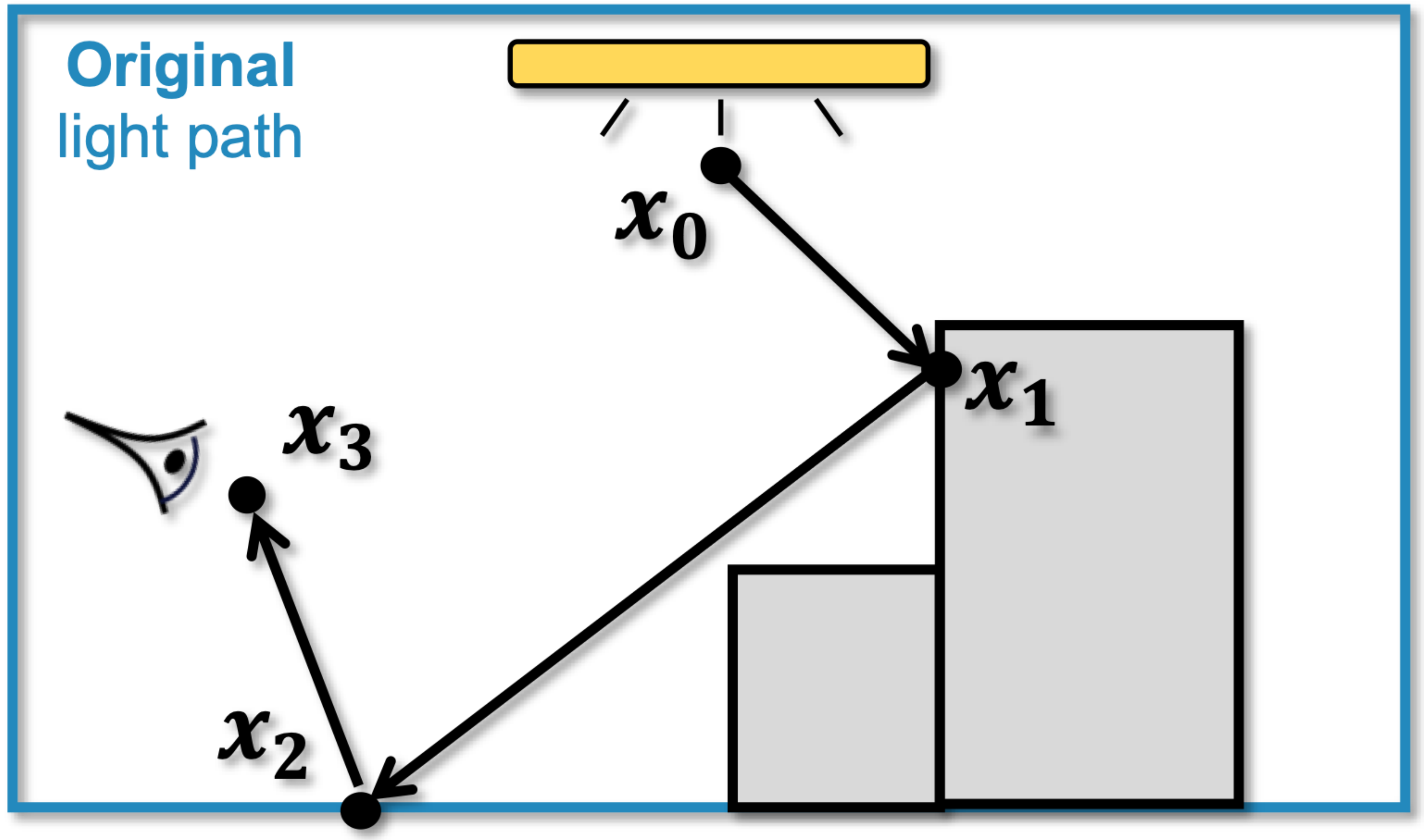

Interior integral

- Defined on the ordinary path space Ω
- The integrand $\dot{f}$ can be obtained by differentiating the ordinary *measurement contribution function* f

[Zhang et al., 2020]

Differential Path Integral

Path-space differentiable rendering

$$\frac{\mathrm{d}}{\mathrm{d}\theta}\left(\int_\Omega f(\bar{\boldsymbol{x}})\mathrm{d}\mu(\bar{\boldsymbol{x}})\right) = \int_\Omega \dot{f}(\bar{\boldsymbol{x}})\mathrm{d}\mu(\bar{\boldsymbol{x}}) + \boxed{\int_{\partial\Omega} g(\bar{\boldsymbol{x}})\mathrm{d}\mu'(\bar{\boldsymbol{x}})}$$

Boundary integral

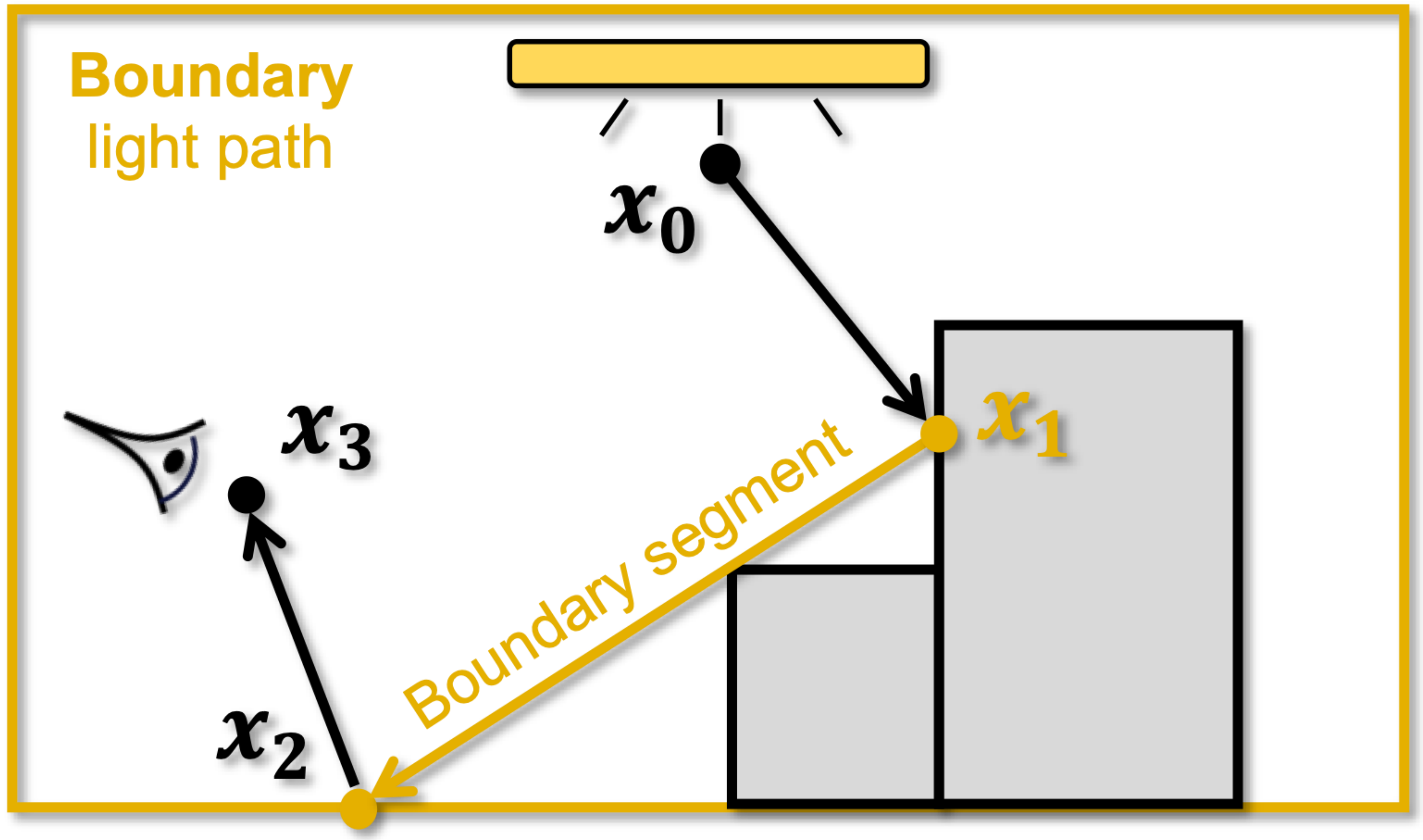

Boundary integral

- Defined on the boundary path space $\partial\Omega$
- A **boundary** light path is the same as an original one except having exactly one boundary segment

Path-Space Differentiable Path Tracing

Unidirectional estimator

- **Interior**: *unidirectional* path tracing
- **Boundary**: *unidirectional* sampling of subpaths

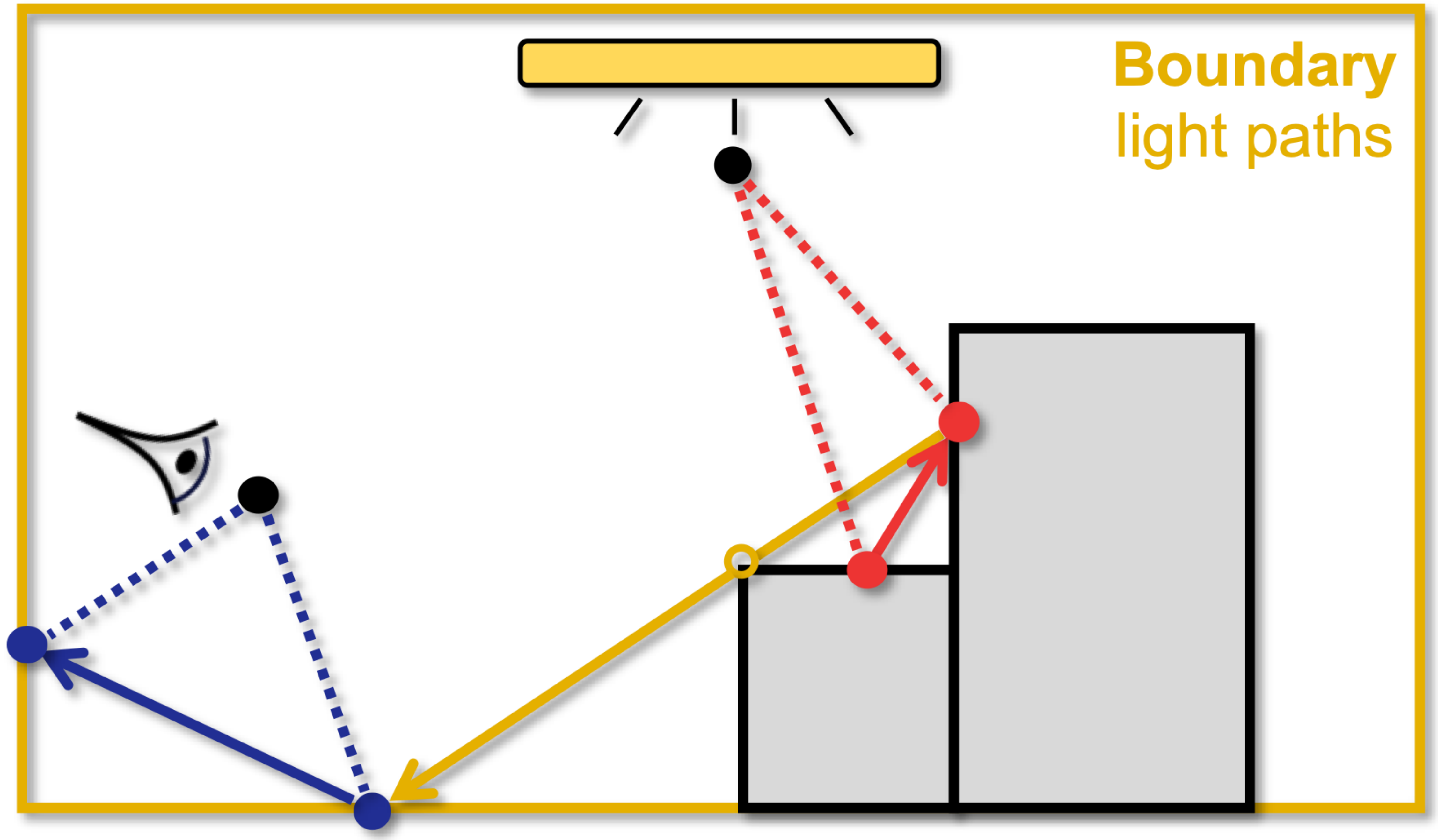

Unidirectional path tracing + NEE

[Zhang et al., 2020]

Path-Space Differentiable Path Tracing

Unidirectional **estimator**

- **Interior**: *unidirectional* path tracing
- **Boundary**: *unidirectional* sampling of subpaths

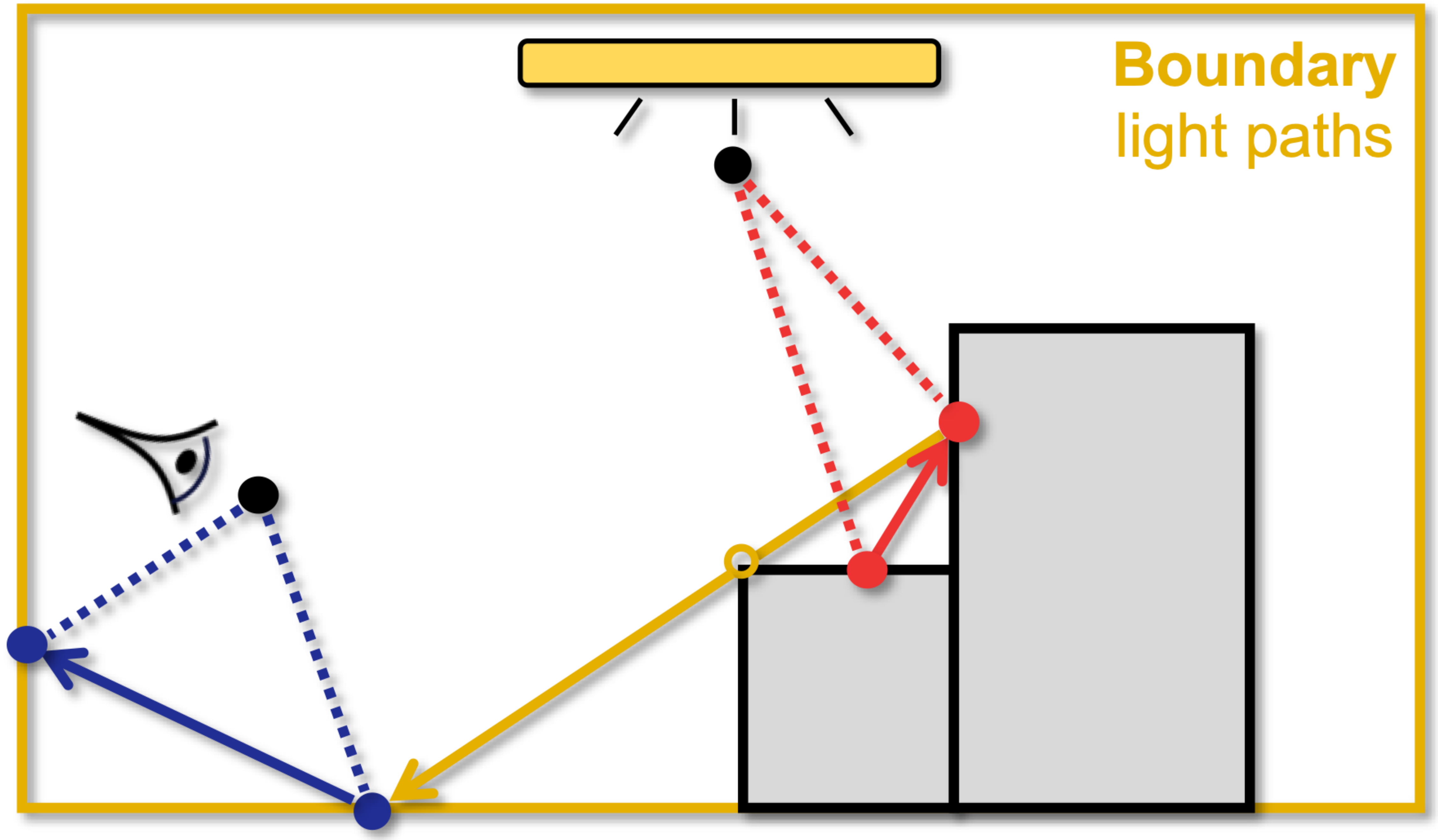

Unidirectional path tracing + NEE

Bidirectional **estimator**

- **Interior**: *bidirectional* path tracing
- **Boundary**: *bidirectional* sampling of subpaths

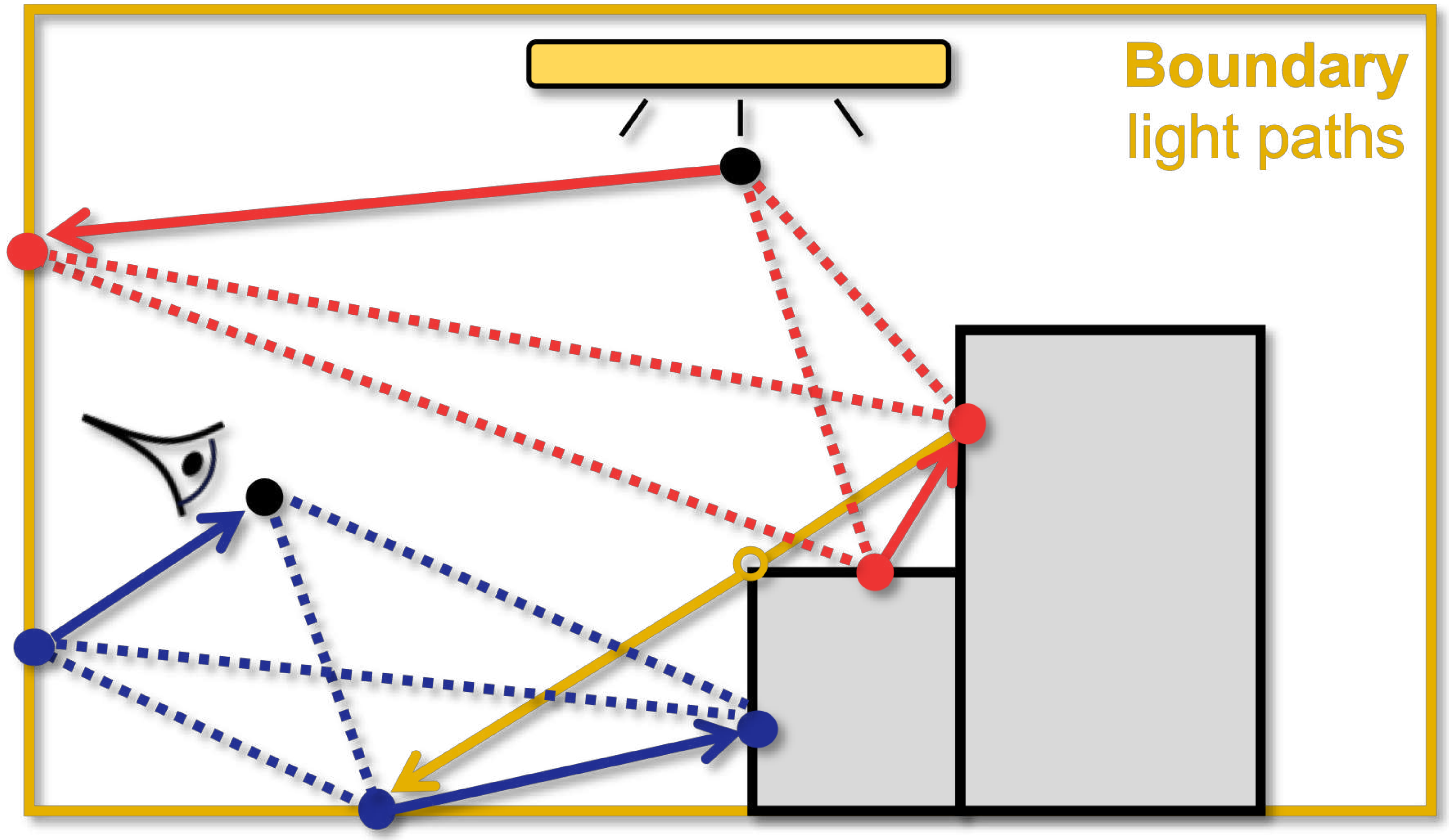

Bidirectional path tracing

[Zhang et al., 2020]

Application: neural rendering

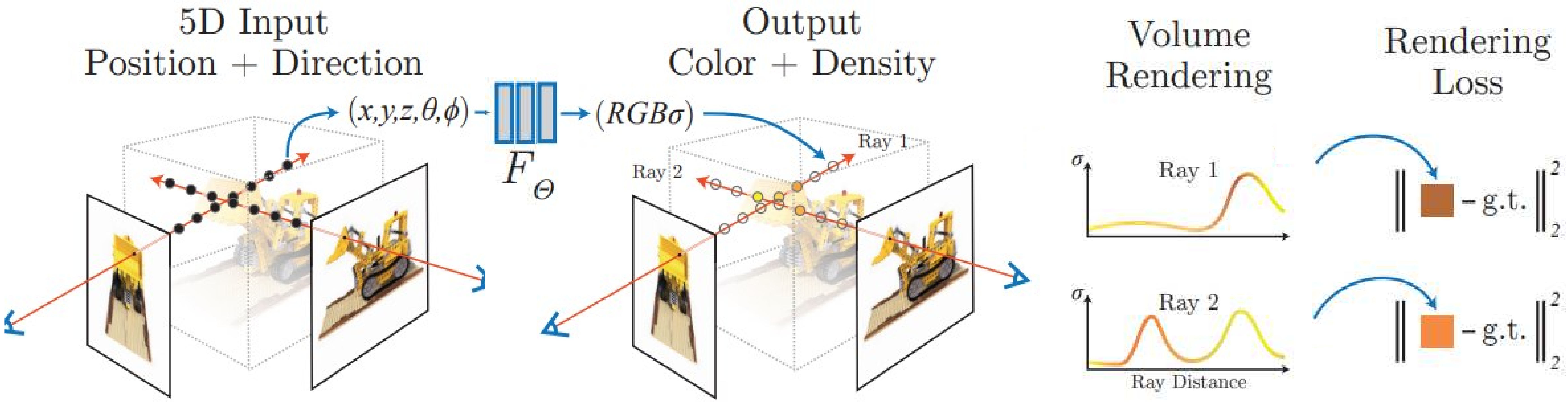

NeRF: Representing Scenes as Neural Radiance Fields for View Synthesis [MildenHall et al. ECCV 2020]

Acquisition of scattering materials

[Gkioulekas et al., 2013]

Acquisition setup

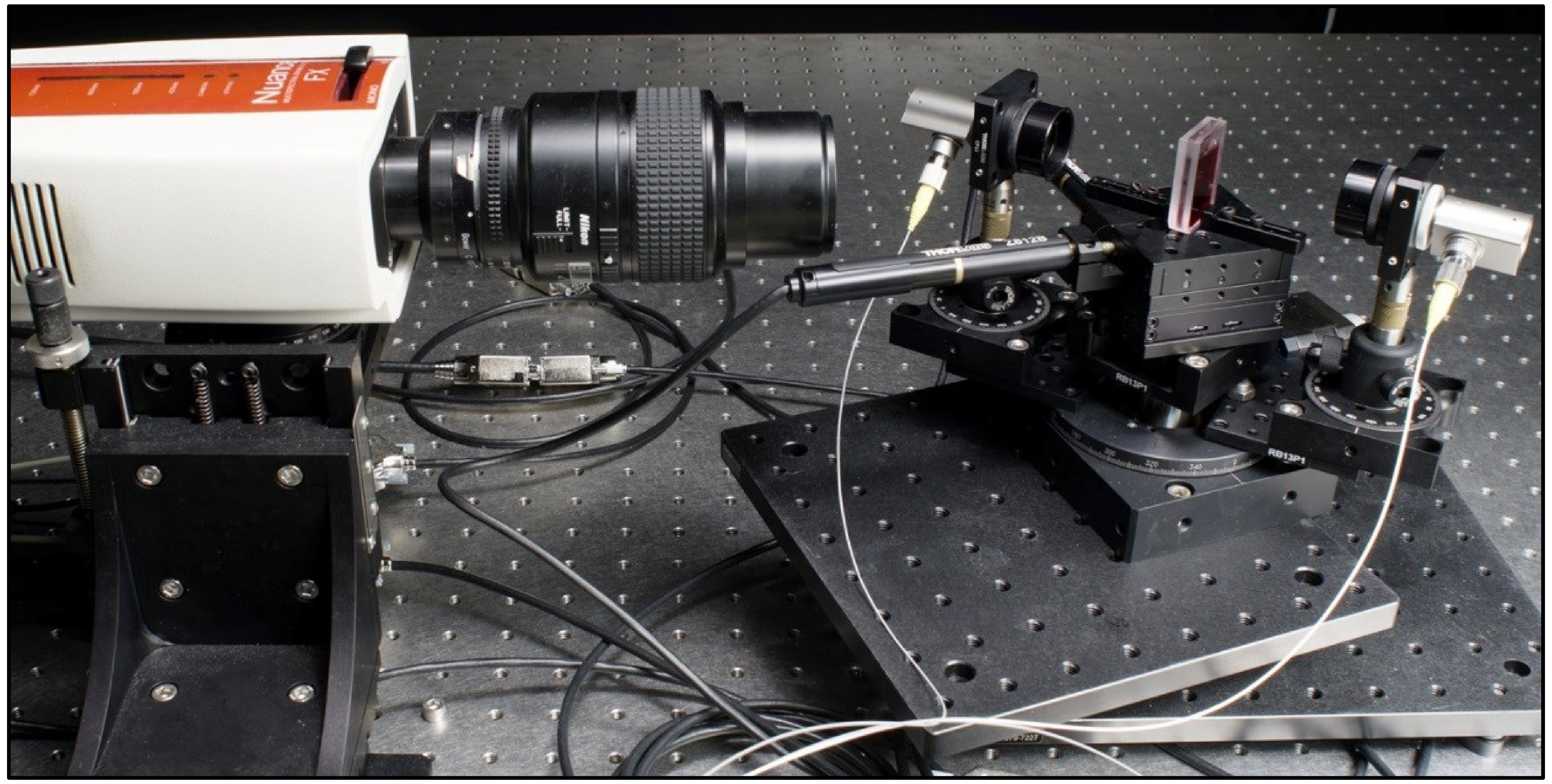

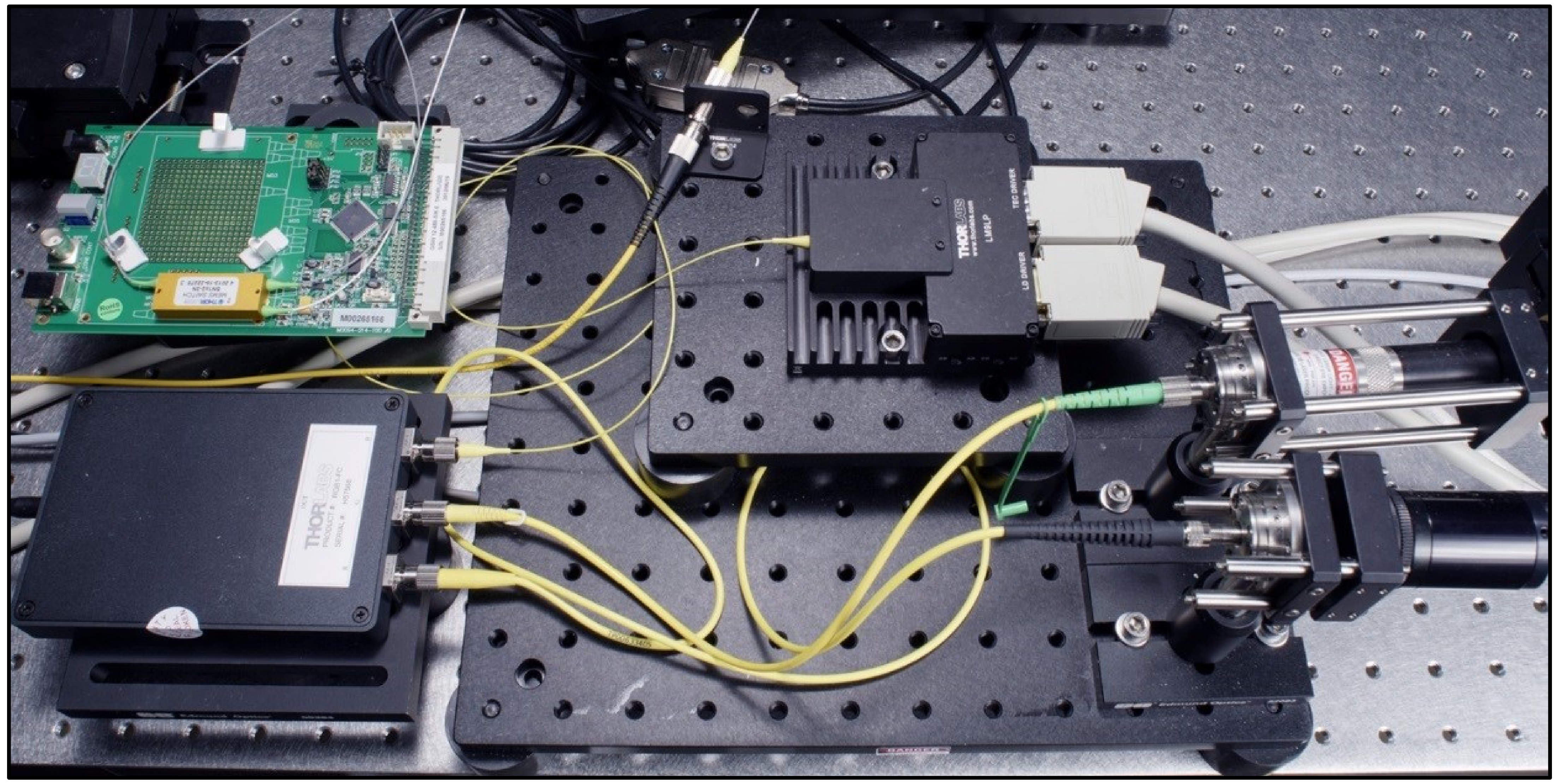

[Gkioulekas et al., 2013]

Acquisition setup

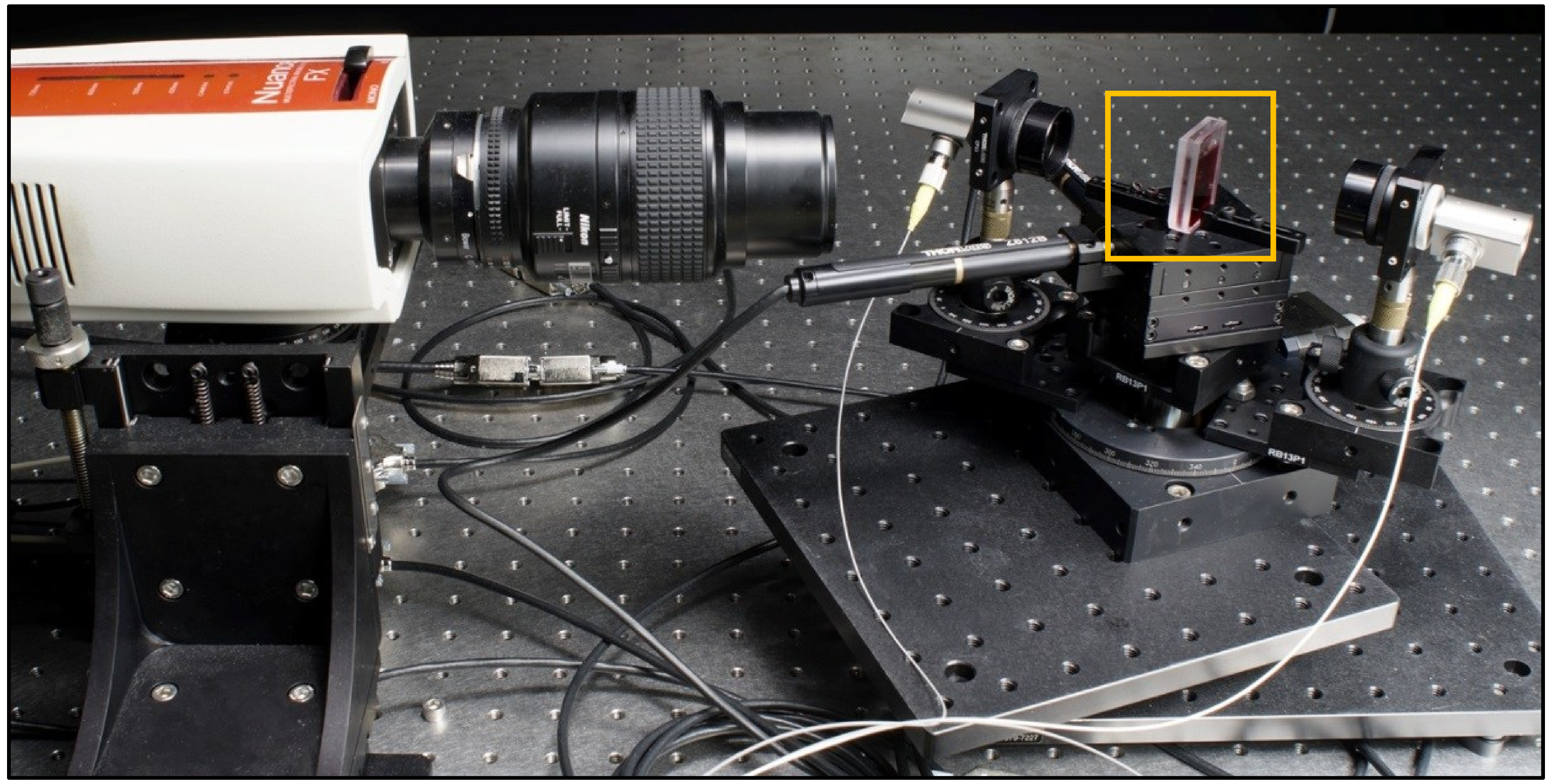

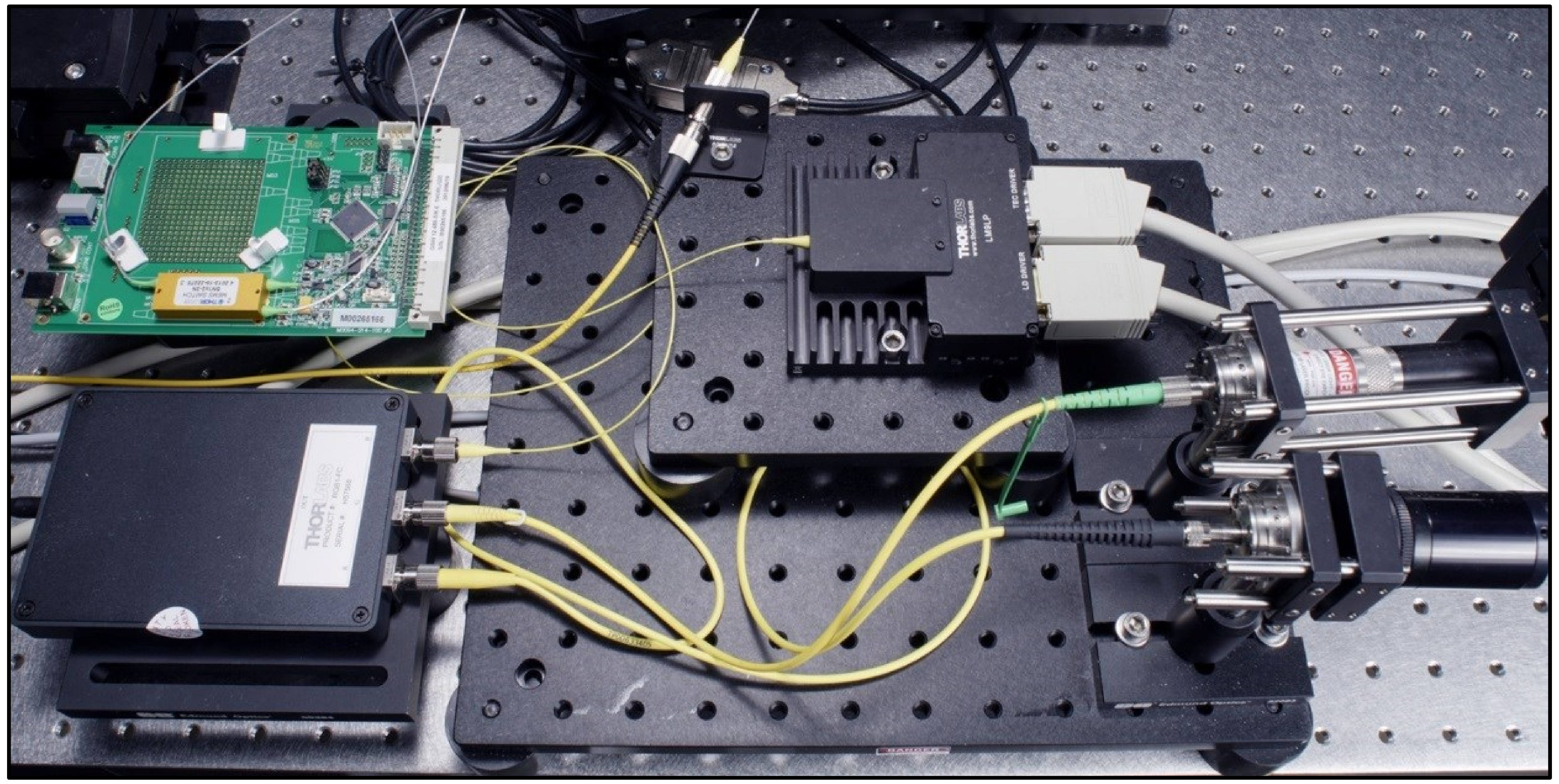

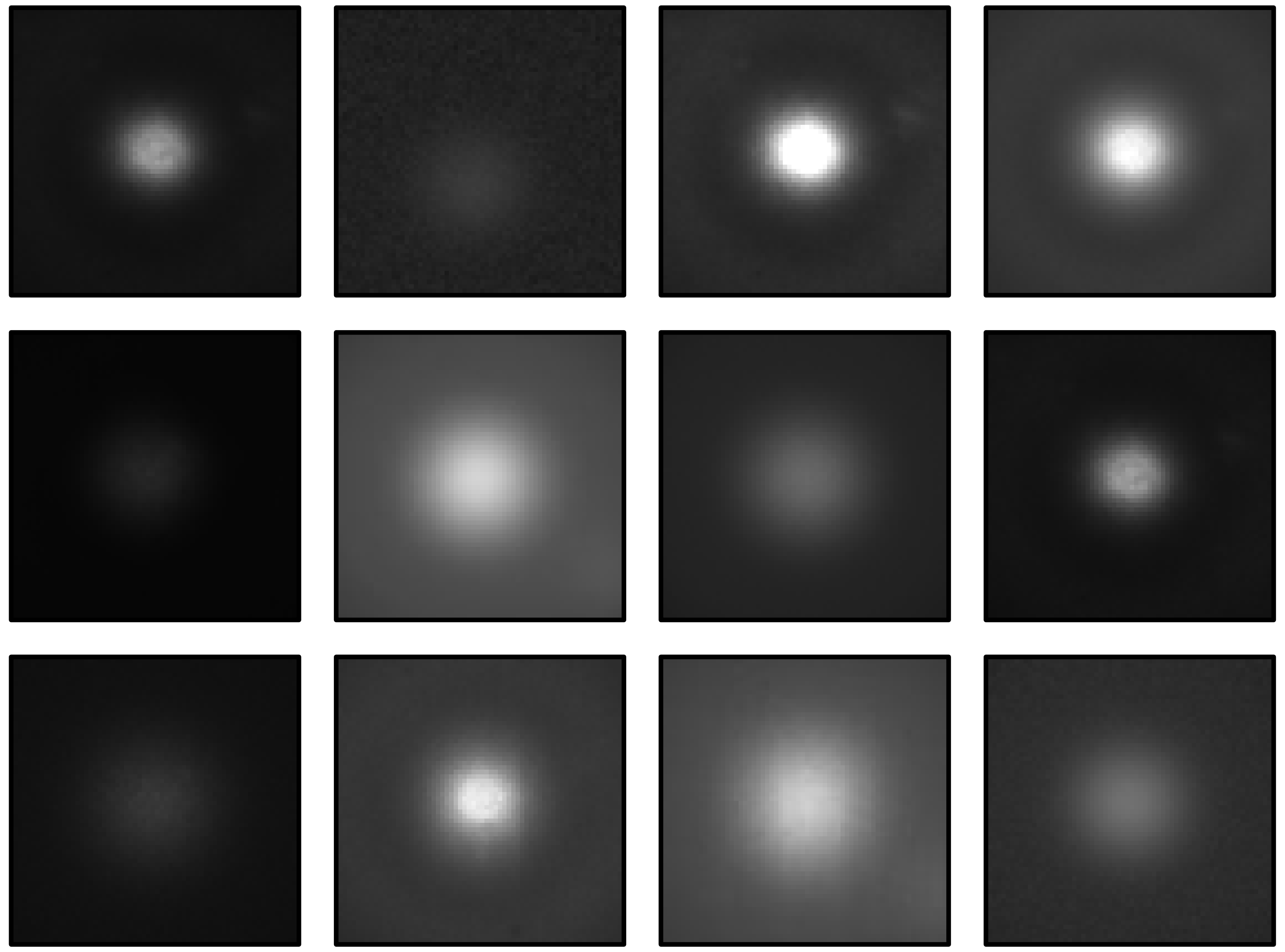

[Gkioulekas et al., 2013]

Acquisition setup

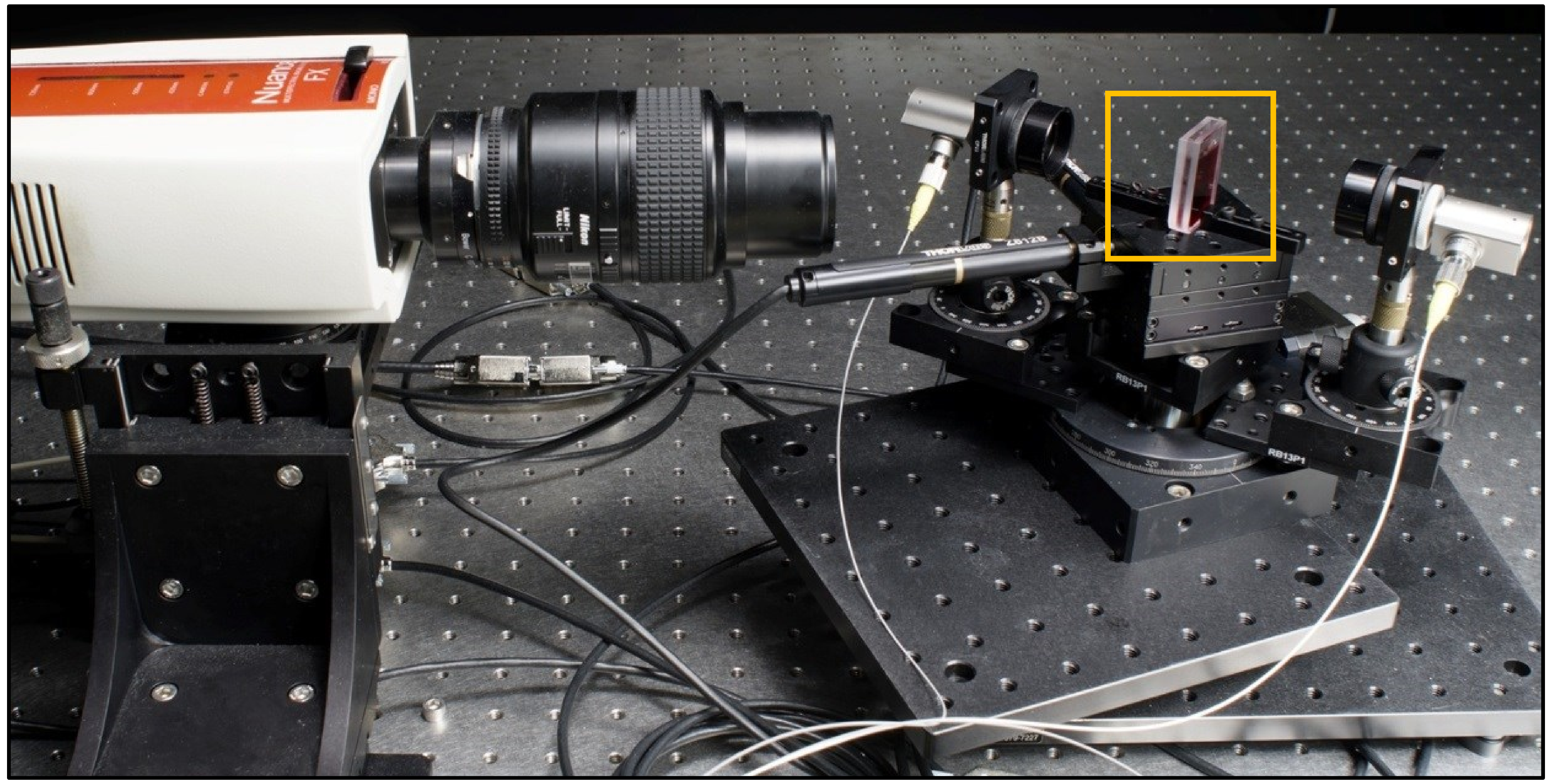

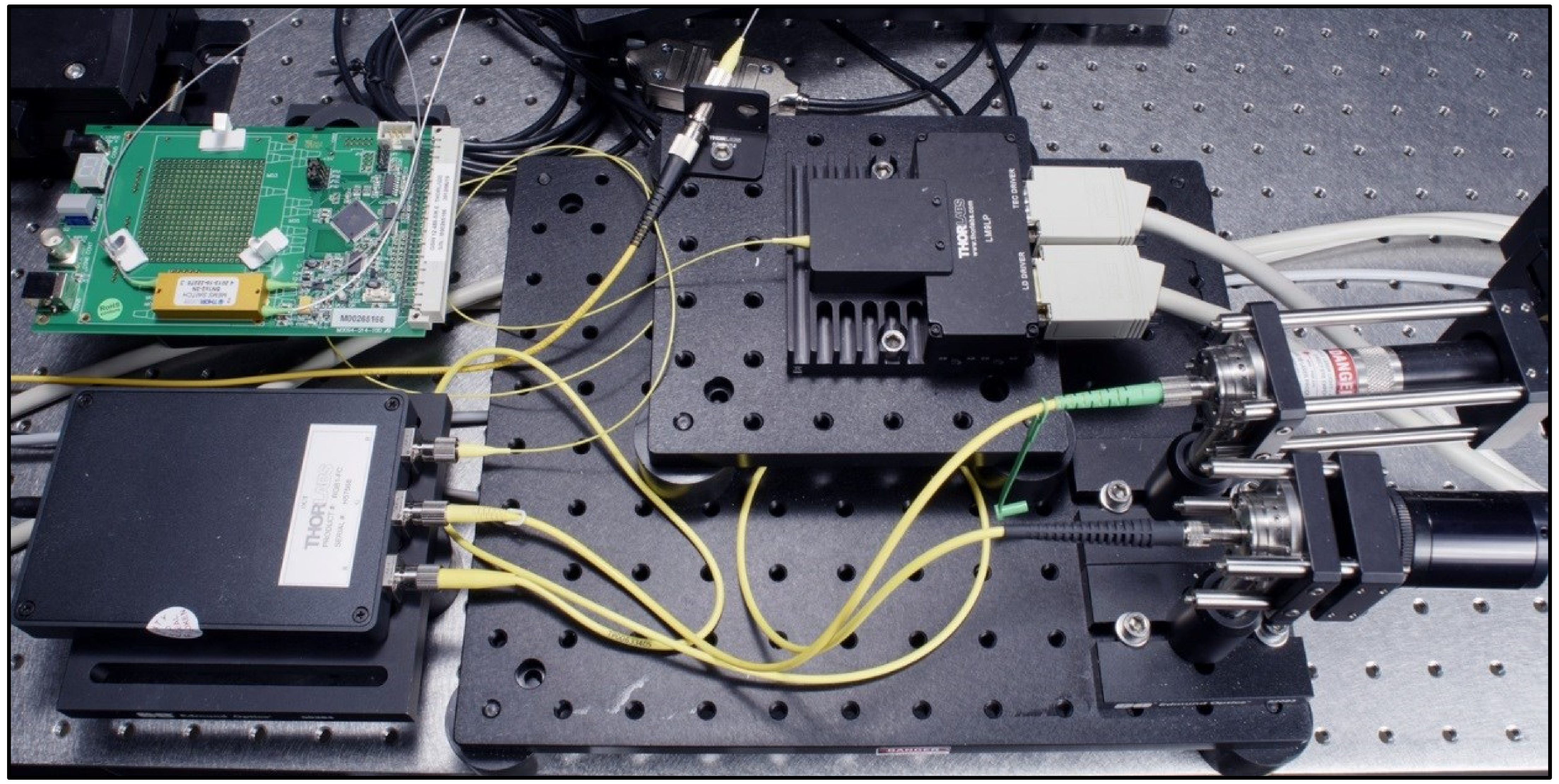

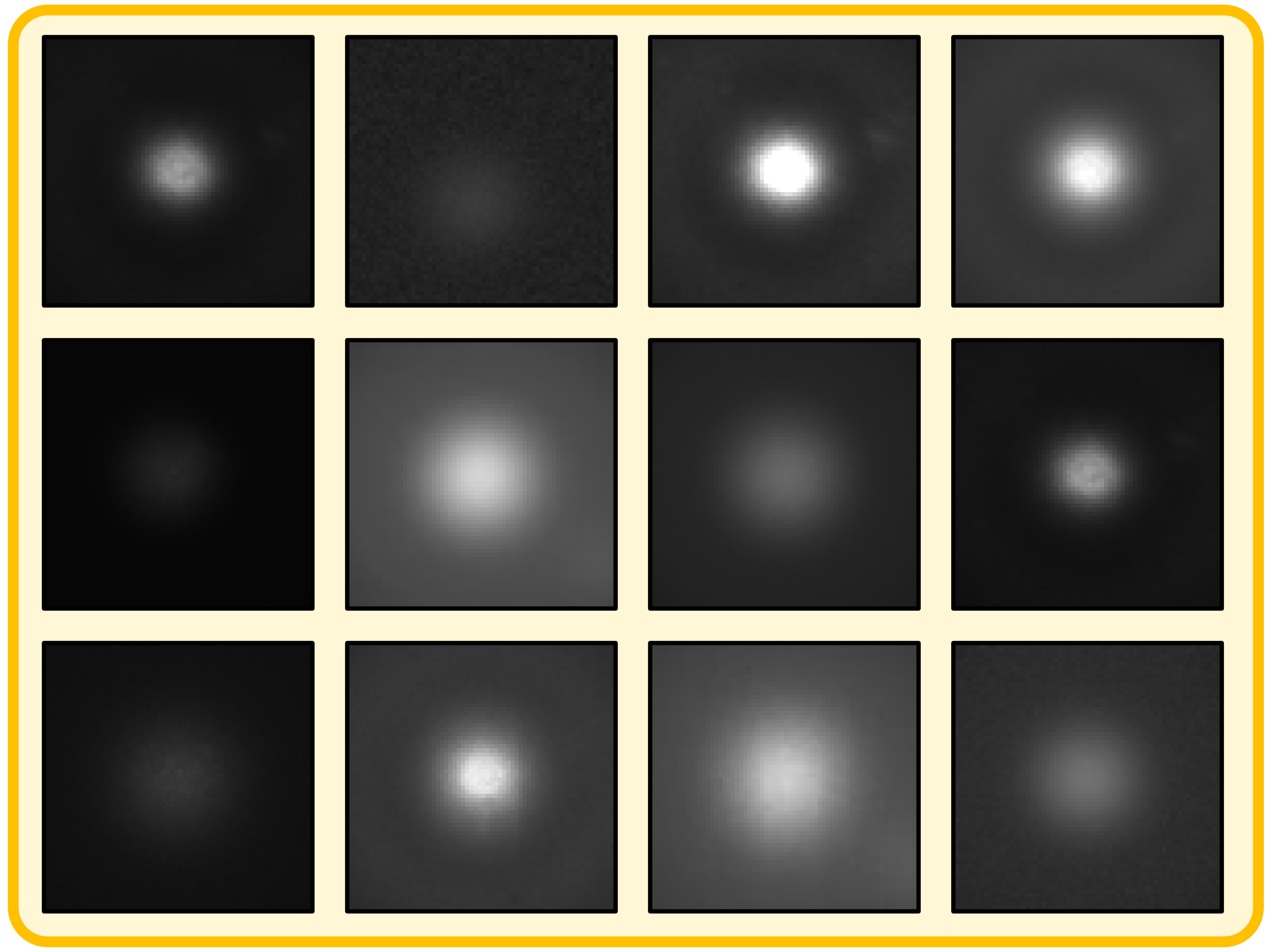

Invert using differentiable rendering

[Gkioulekas et al., 2013]

Synthetic renderings

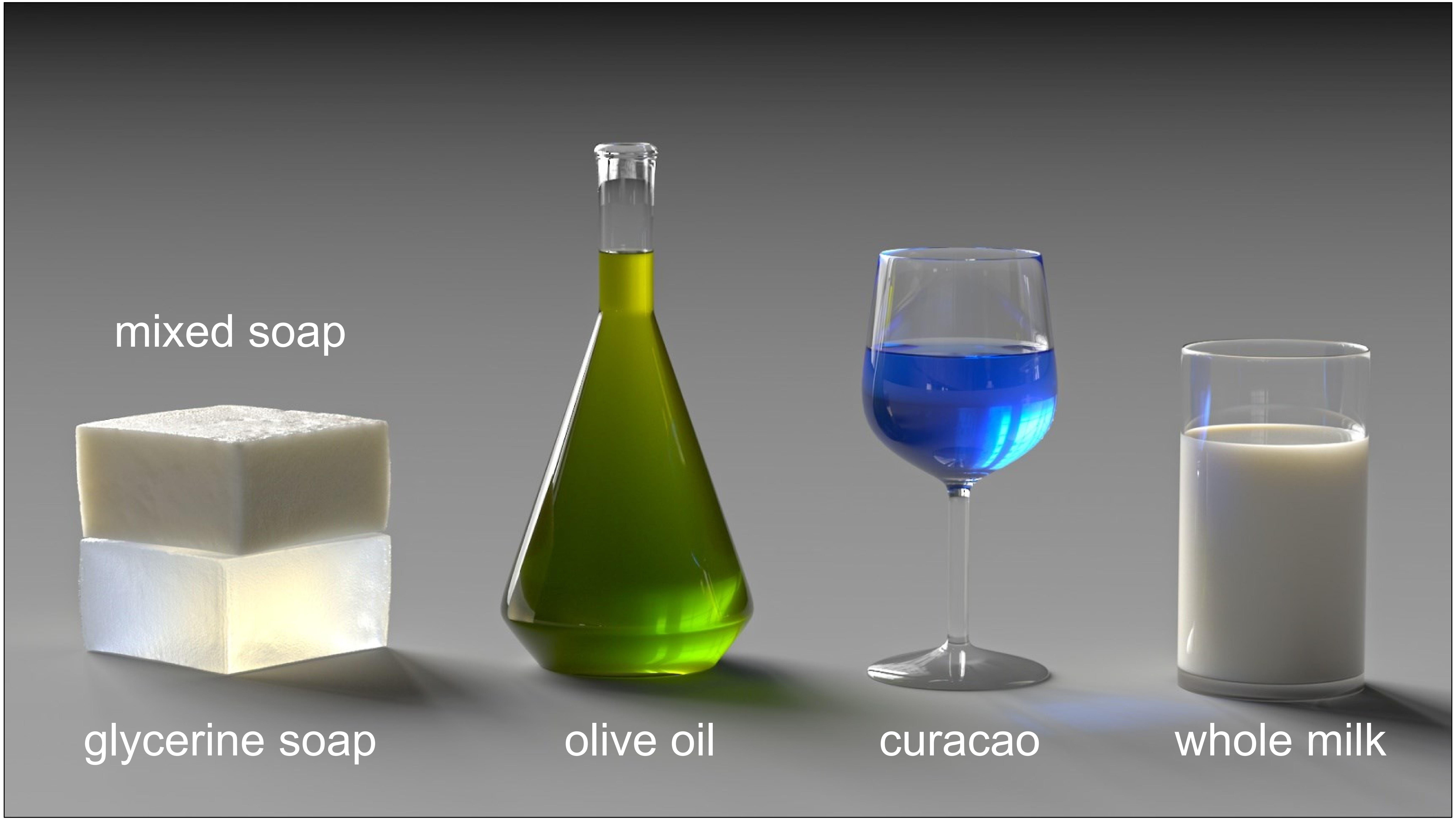

[Gkioulekas et al., 2013]

Particle sizing of industrial nanodispersions

[Gkioulekas et al., 2013]

Particle sizing of industrial nanodispersions

unknown nanodispersion

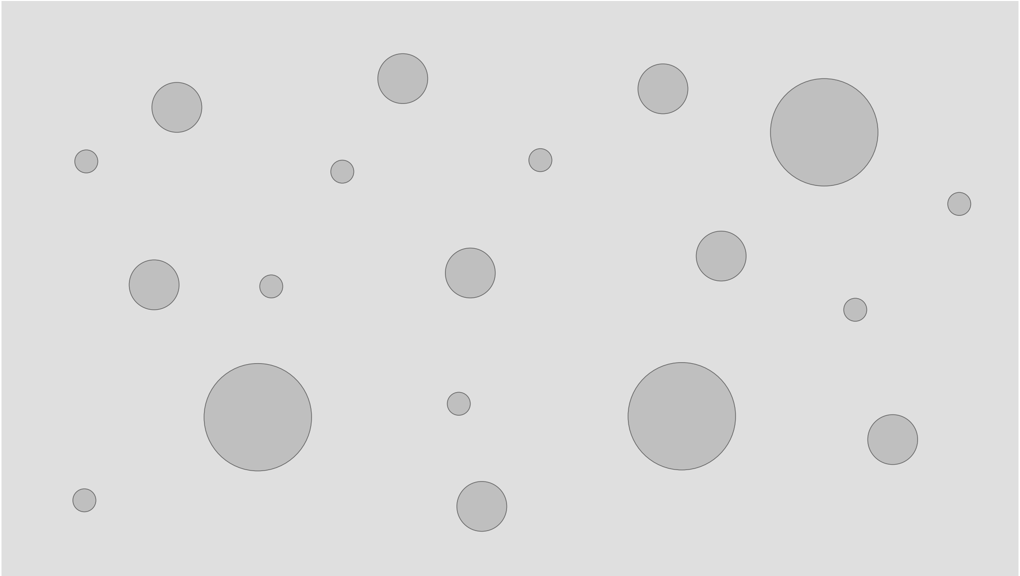

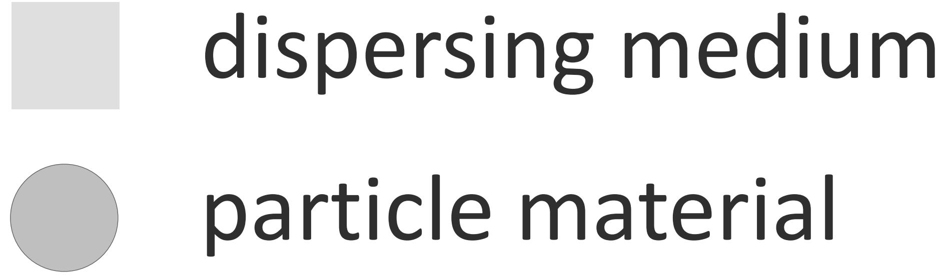

[Gkioulekas et al., 2013]

Particle sizing of industrial nanodispersions

unknown nanodispersion

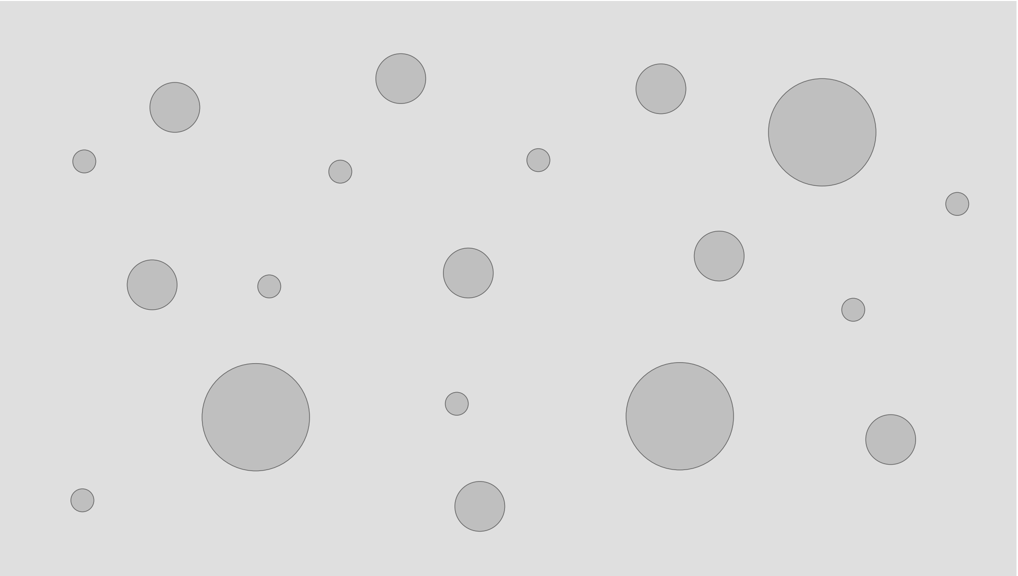

dispersing medium

particle material

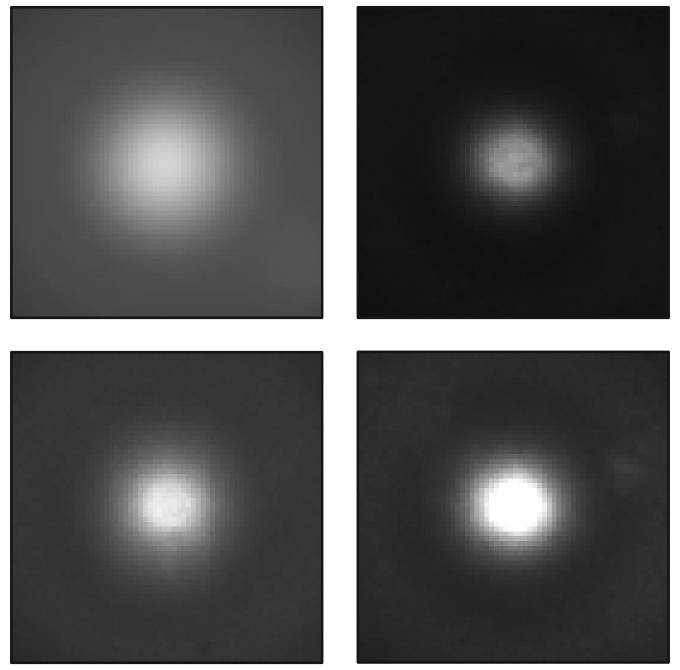

measurements

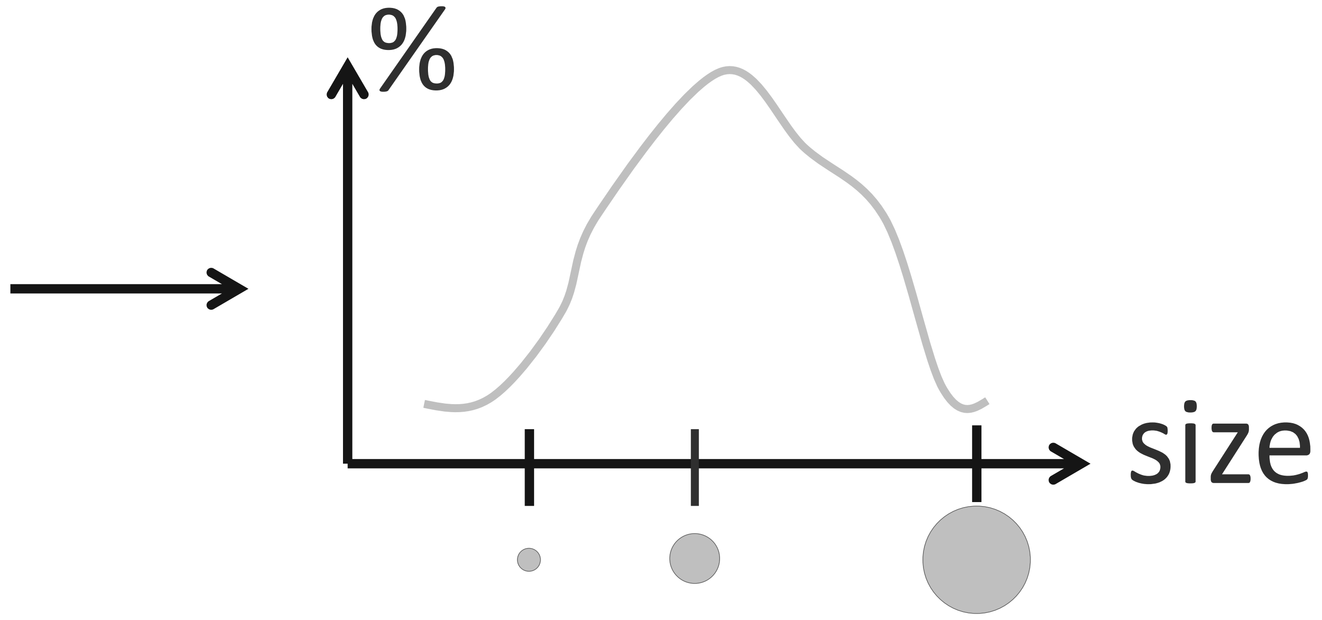

[Gkioulekas et al., 2013]

Particle sizing of industrial nanodispersions

unknown nanodispersion

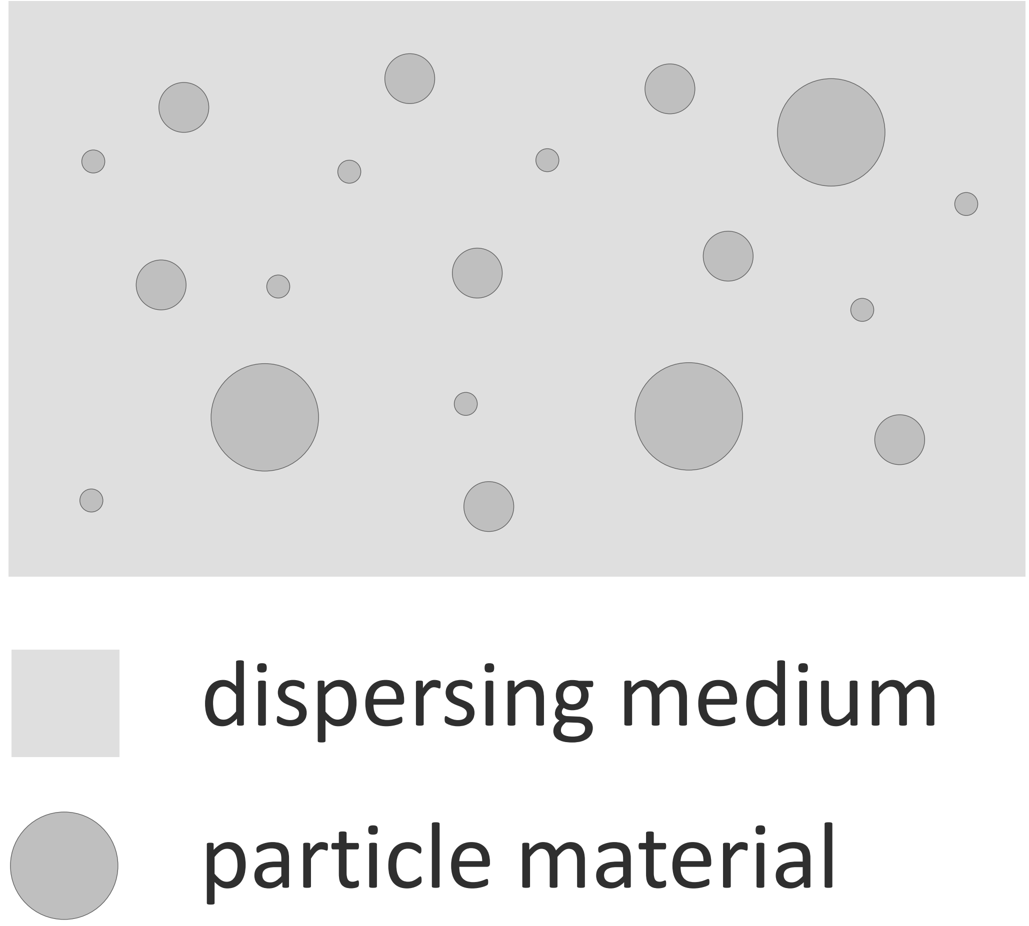

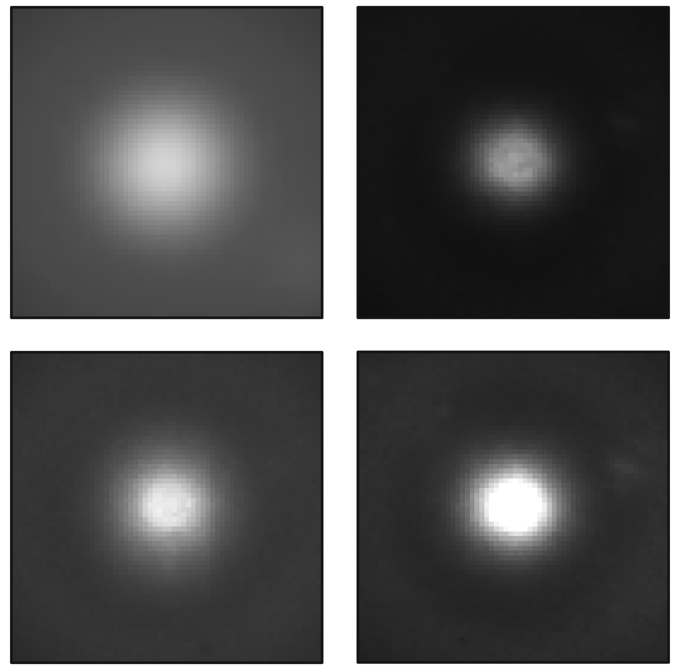

measurements

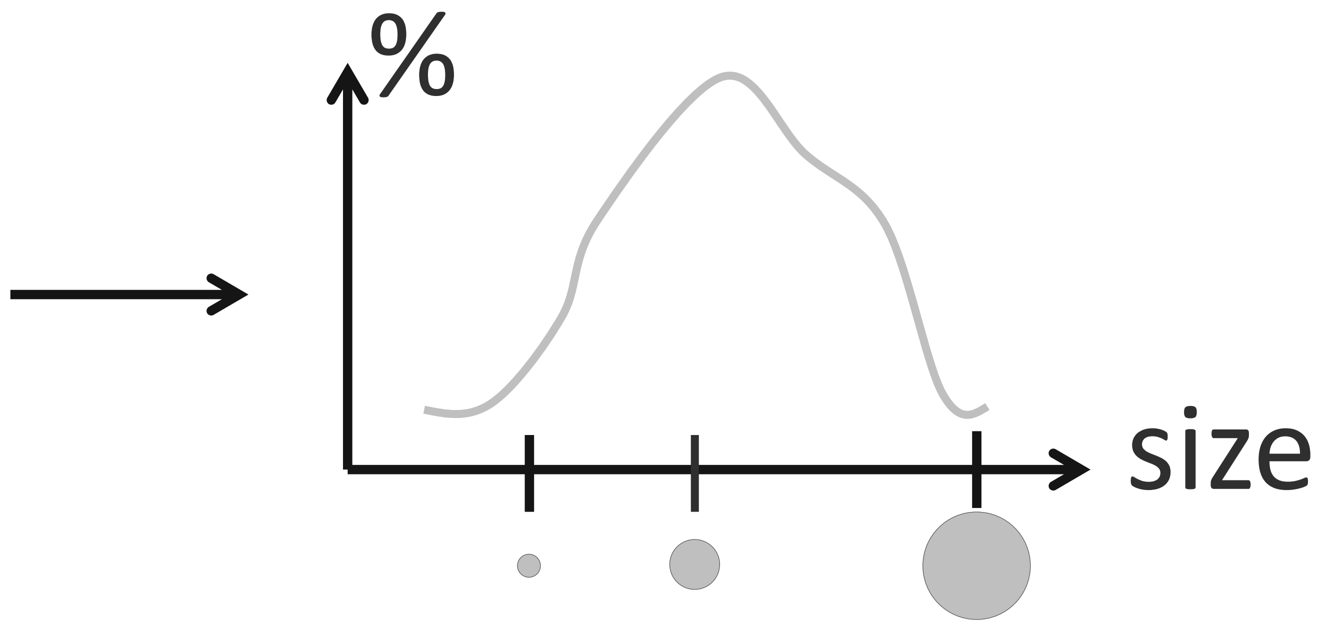

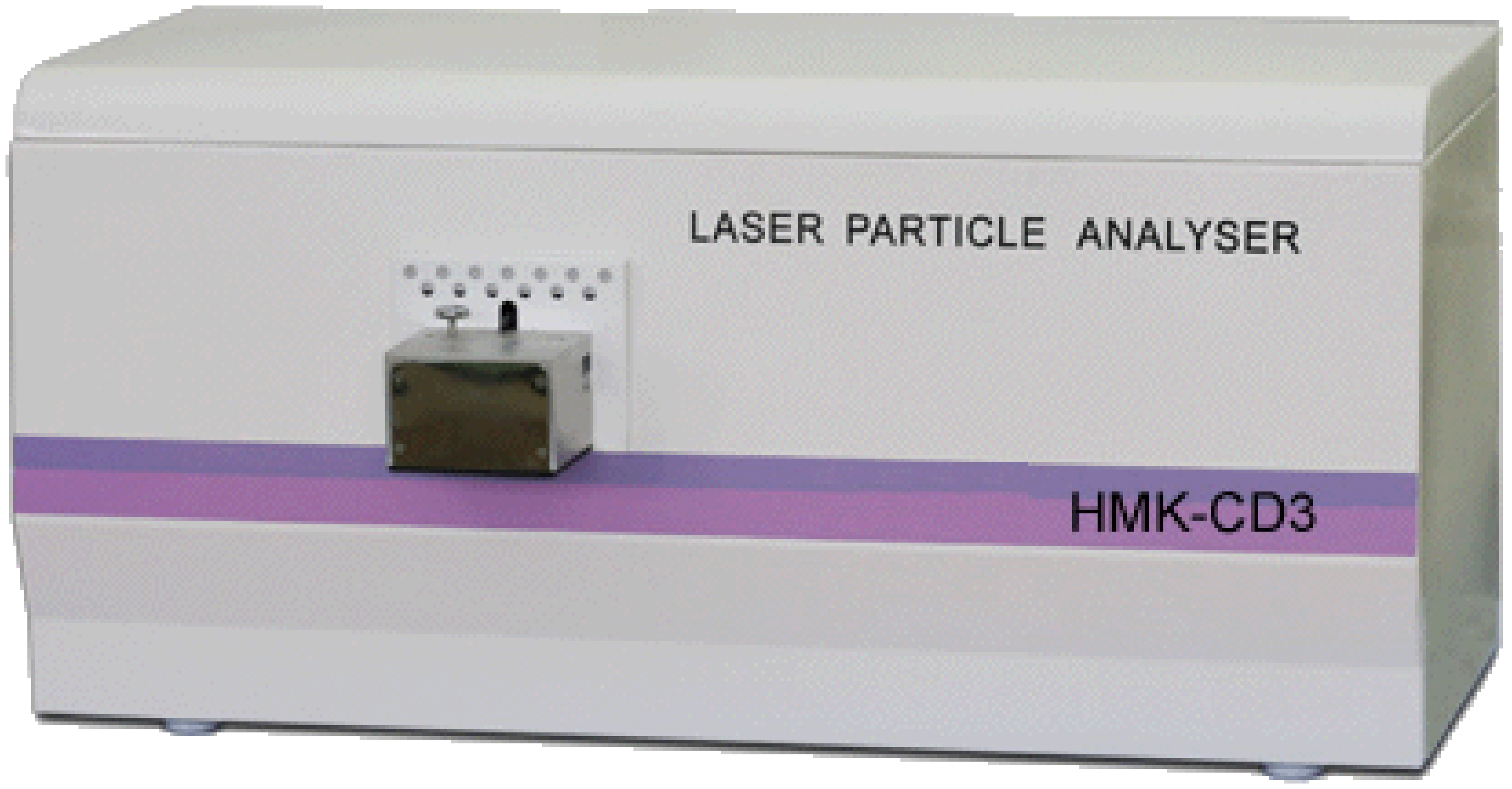

[Gkioulekas et al., 2013]

Particle sizing of industrial nanodispersions

polystyrene

aluminum oxide

very precise dispersions (NIST Traceable Standards)

[Gkioulekas et al., 2013]

Particle sizing of industrial nanodispersions

polystyrene

aluminum oxide

very precise dispersions (NIST Traceable Standards)

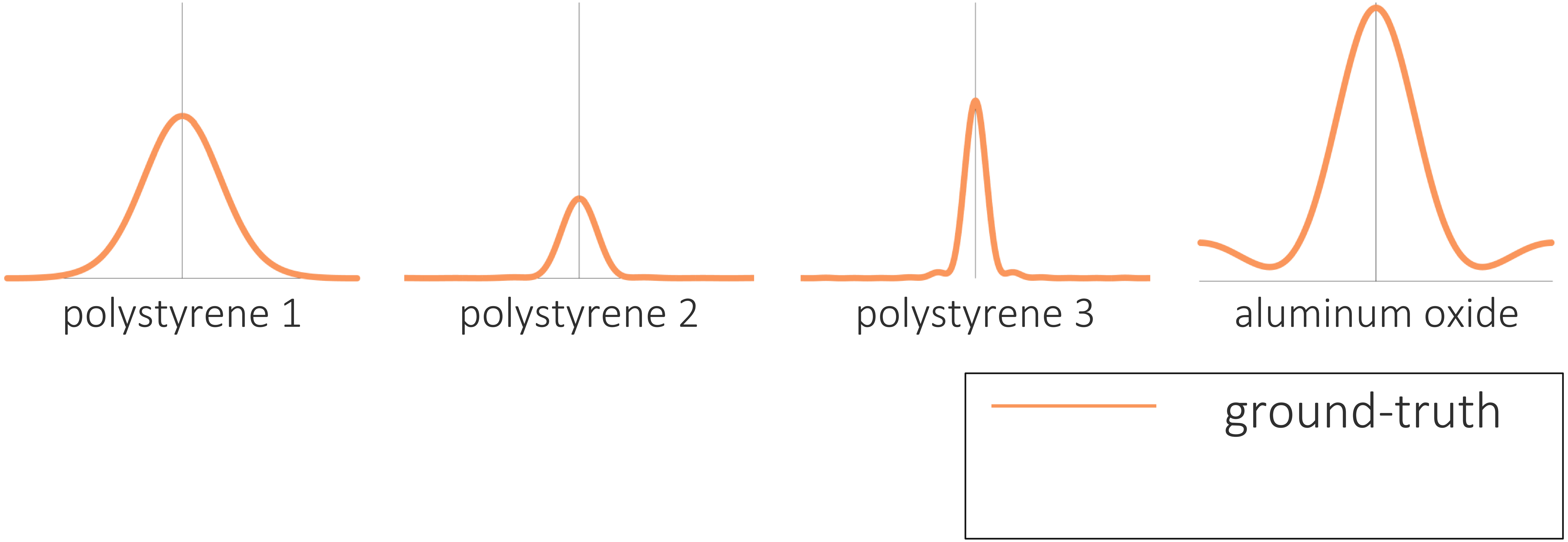

[Gkioulekas et al., 2013]

Particle sizing of industrial nanodispersions

polystyrene

aluminum oxide

very precise dispersions (NIST Traceable Standards)

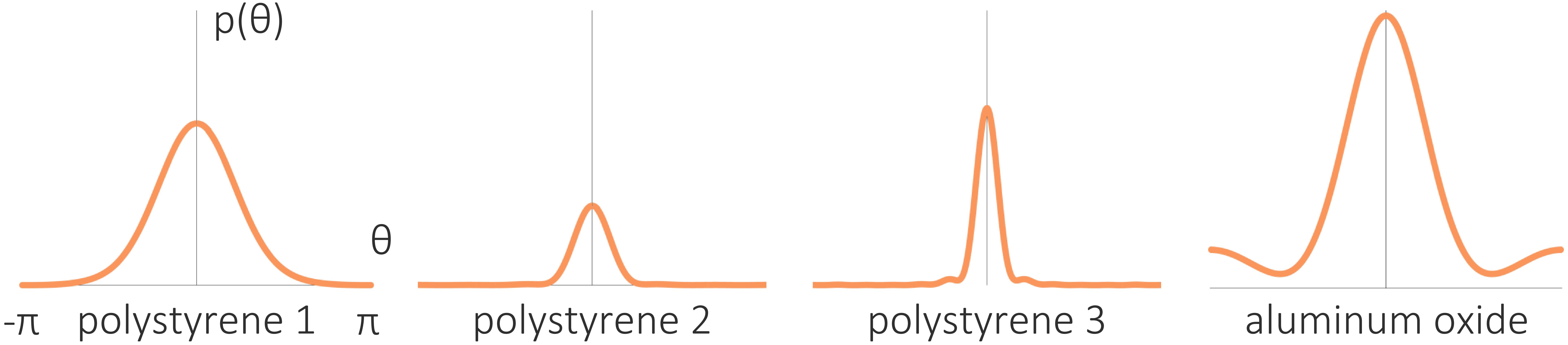

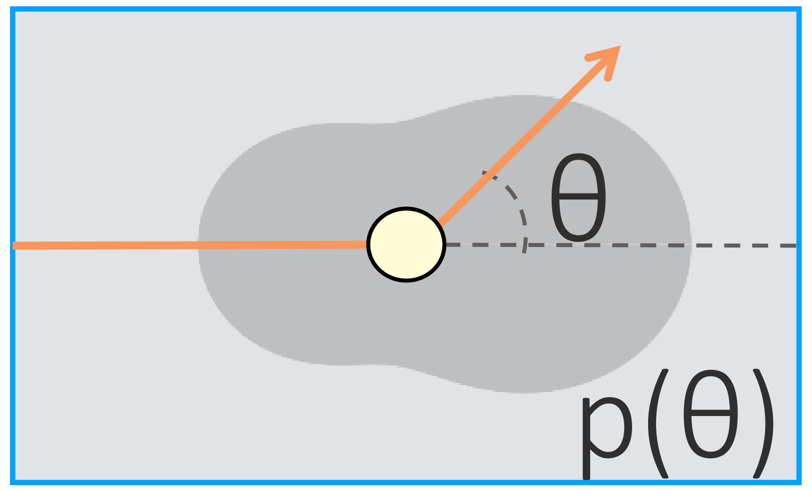

[Gkioulekas et al., 2013]

Particle sizing of industrial nanodispersions

polystyrene

aluminum oxide

very precise dispersions (NIST Traceable Standards)

polystyrene 1 | polystyrene 2 | polystyrene 3 | aluminum oxide

ground-truth

[Gkioulekas et al., 2013]

Particle sizing of industrial nanodispersions

polystyrene

aluminum oxide

very precise dispersions (NIST Traceable Standards)

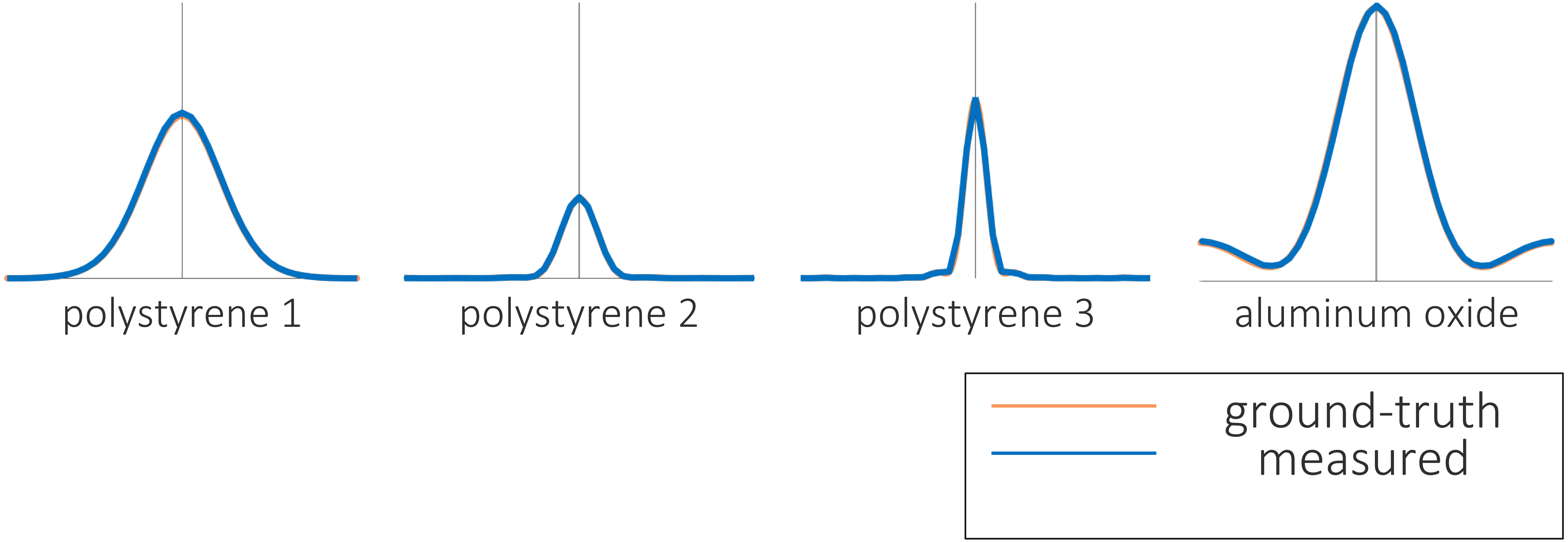

[Gkioulekas et al., 2013]

Particle sizing of industrial nanodispersions

polystyrene

aluminum oxide

very precise dispersions (NIST Traceable Standards)

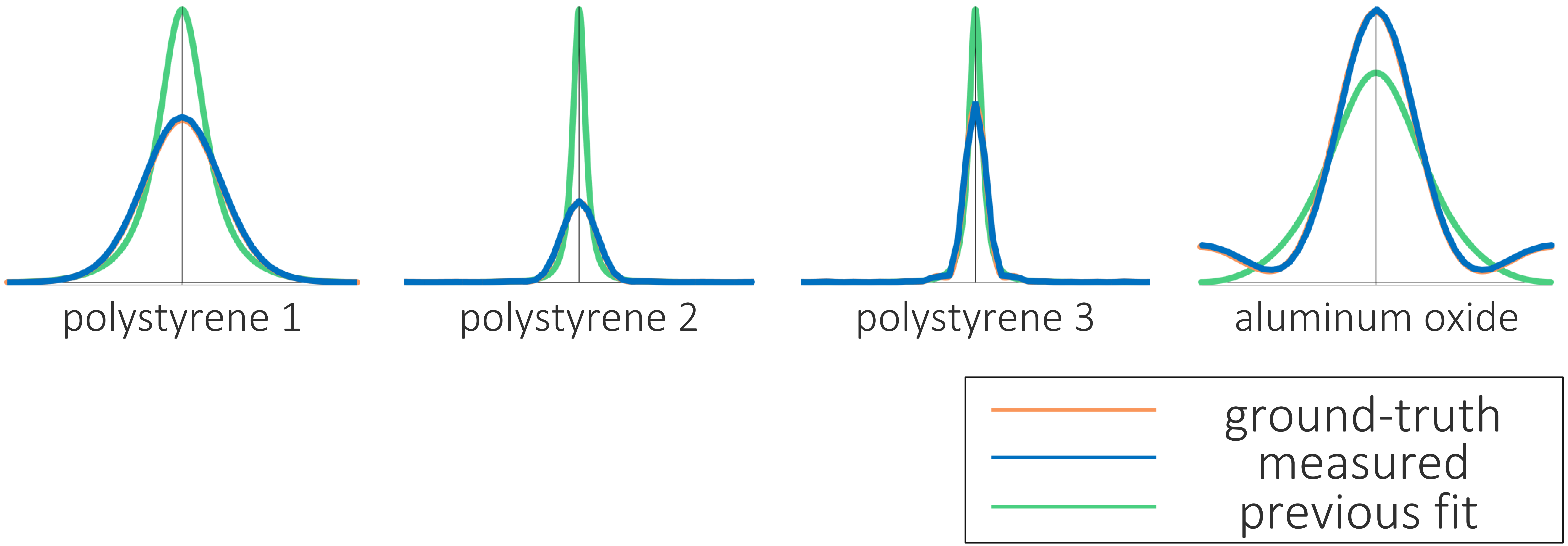

[Gkioulekas et al., 2013]

Optical tomography

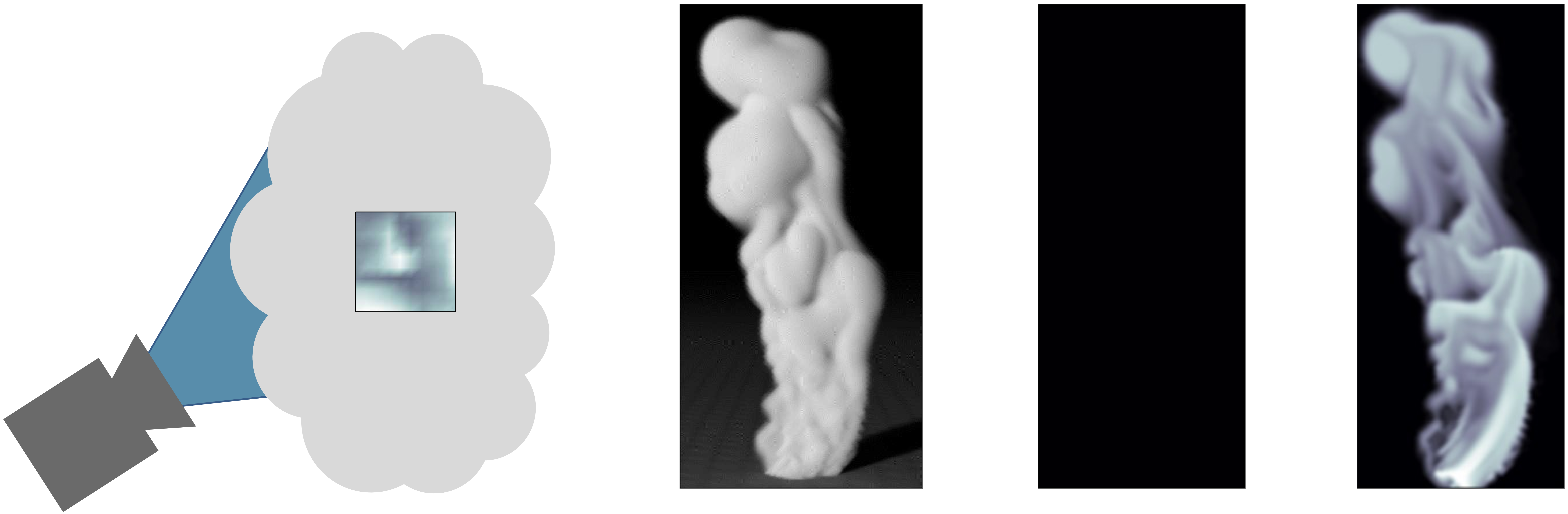

camera | thick smoke cloud | simulated camera measurements | reconstructed cloud volume | slice through the cloud

[Gkioulekas et al., 2015]

Computational Fabrication

Determining the material configuration for individual voxels in full-color inkjet 3D printing

[Nindel et al. 2021]

Active area of research

industrial dispersions
[Gkioulekas et al. 2013]

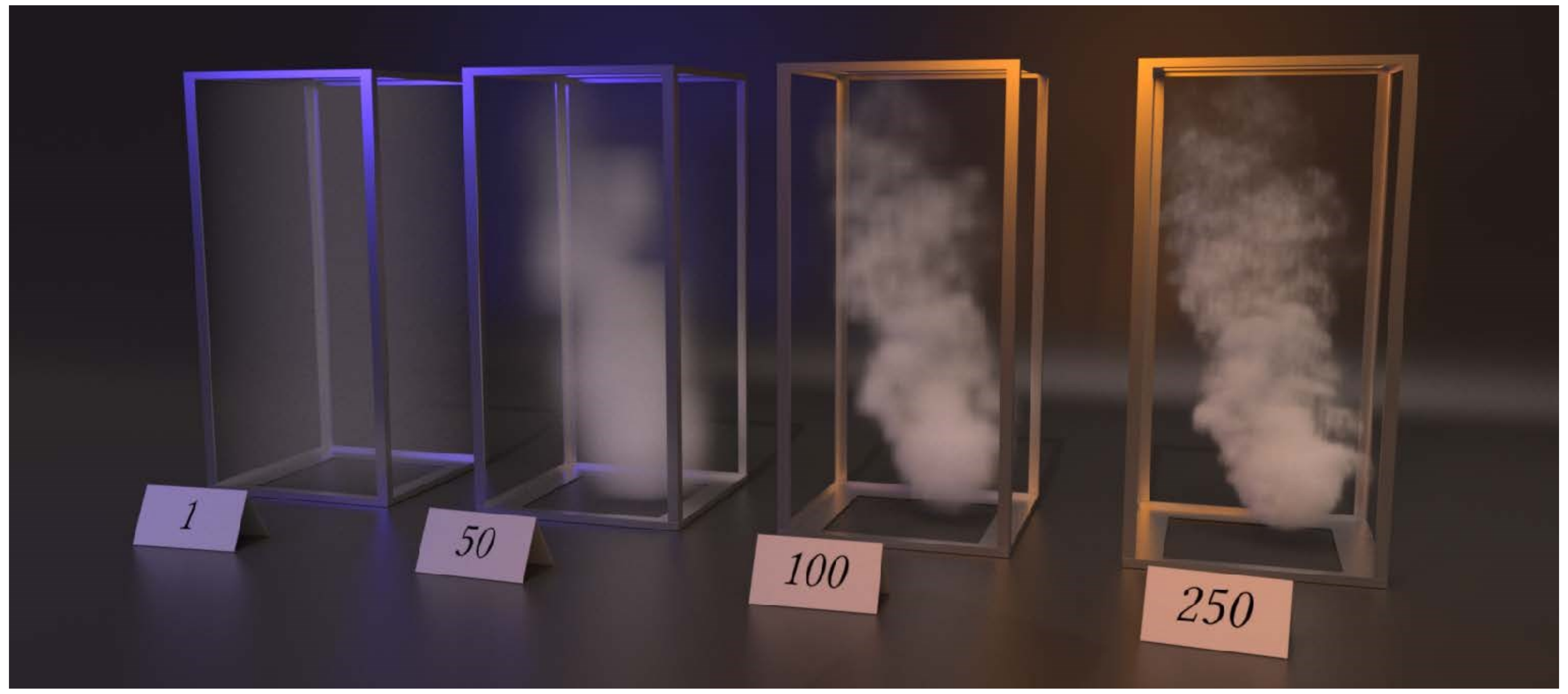

efficient algorithms
[Nimier-David et al. 2019, 2020]

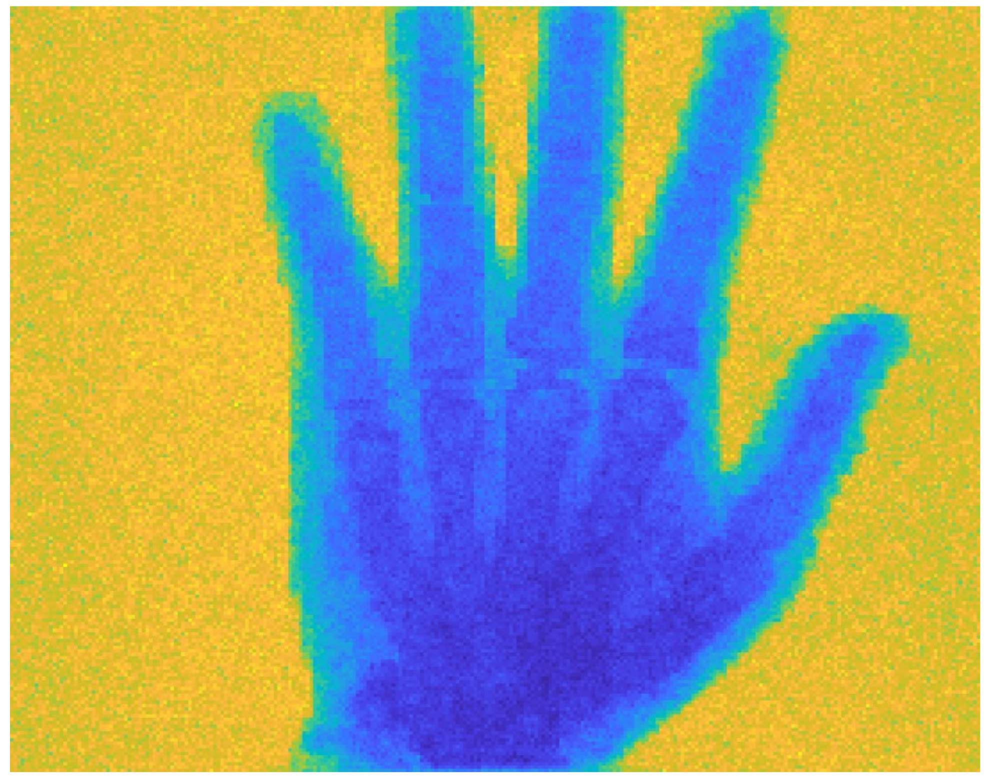

computed tomography
[Geva et al. 2018]

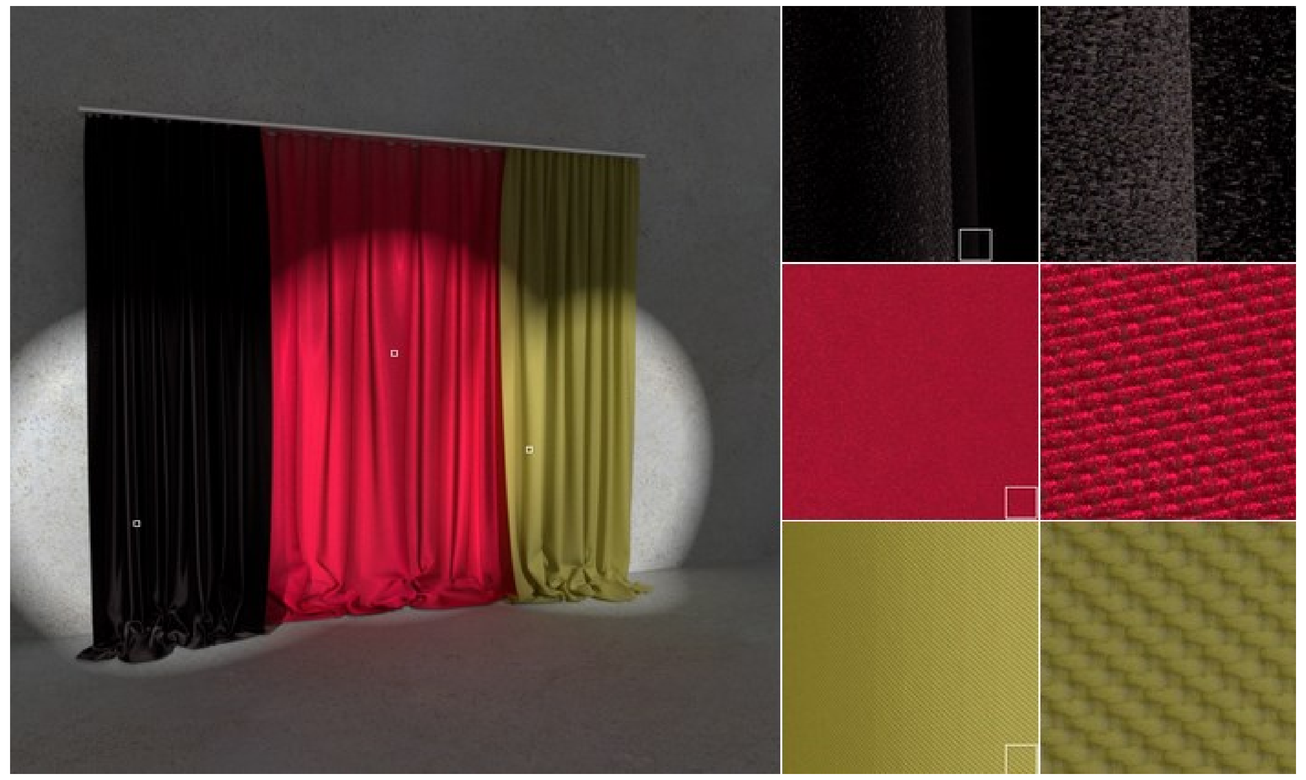

woven fabrics
[Khungurn et al. 2015,
Zhao et al. 2016]

3D printing
[Elek et al. 2019,
Nindel et al. 2021]

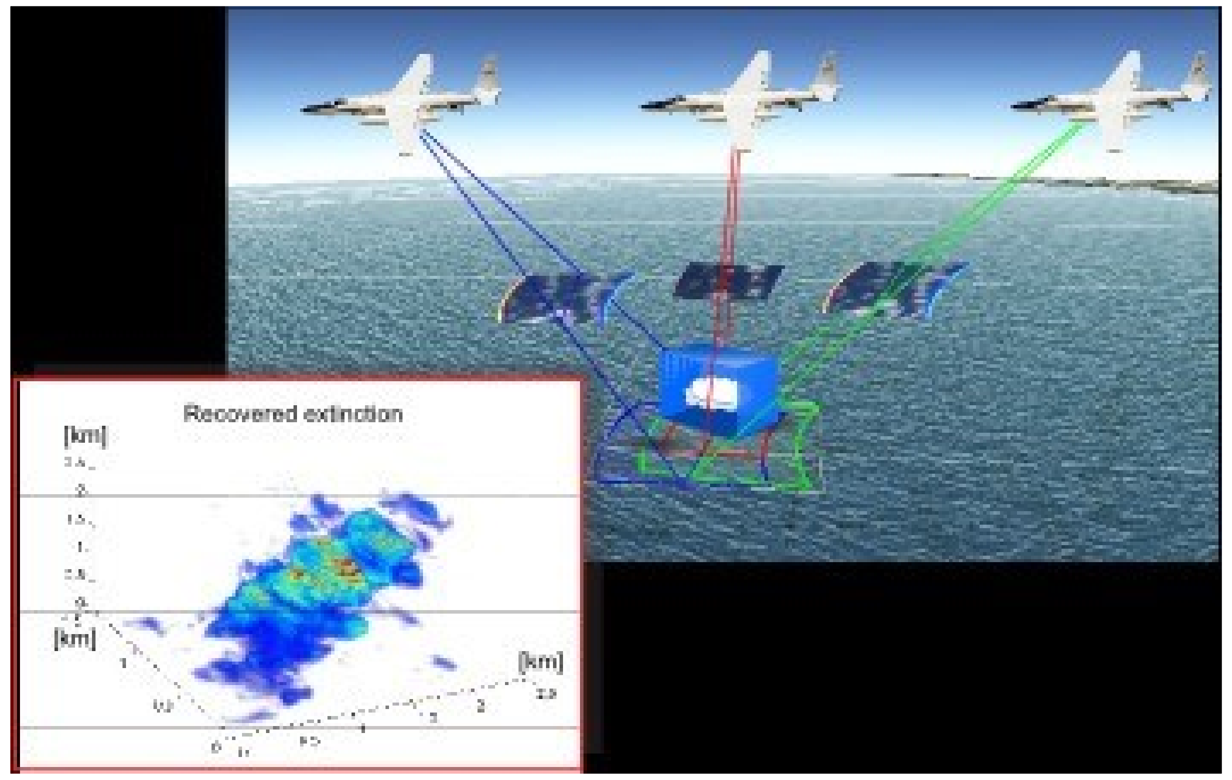

cloud tomography
[Levis et al. 2015,
2017, 2020]

Non-line-of-sight (NLOS) imaging

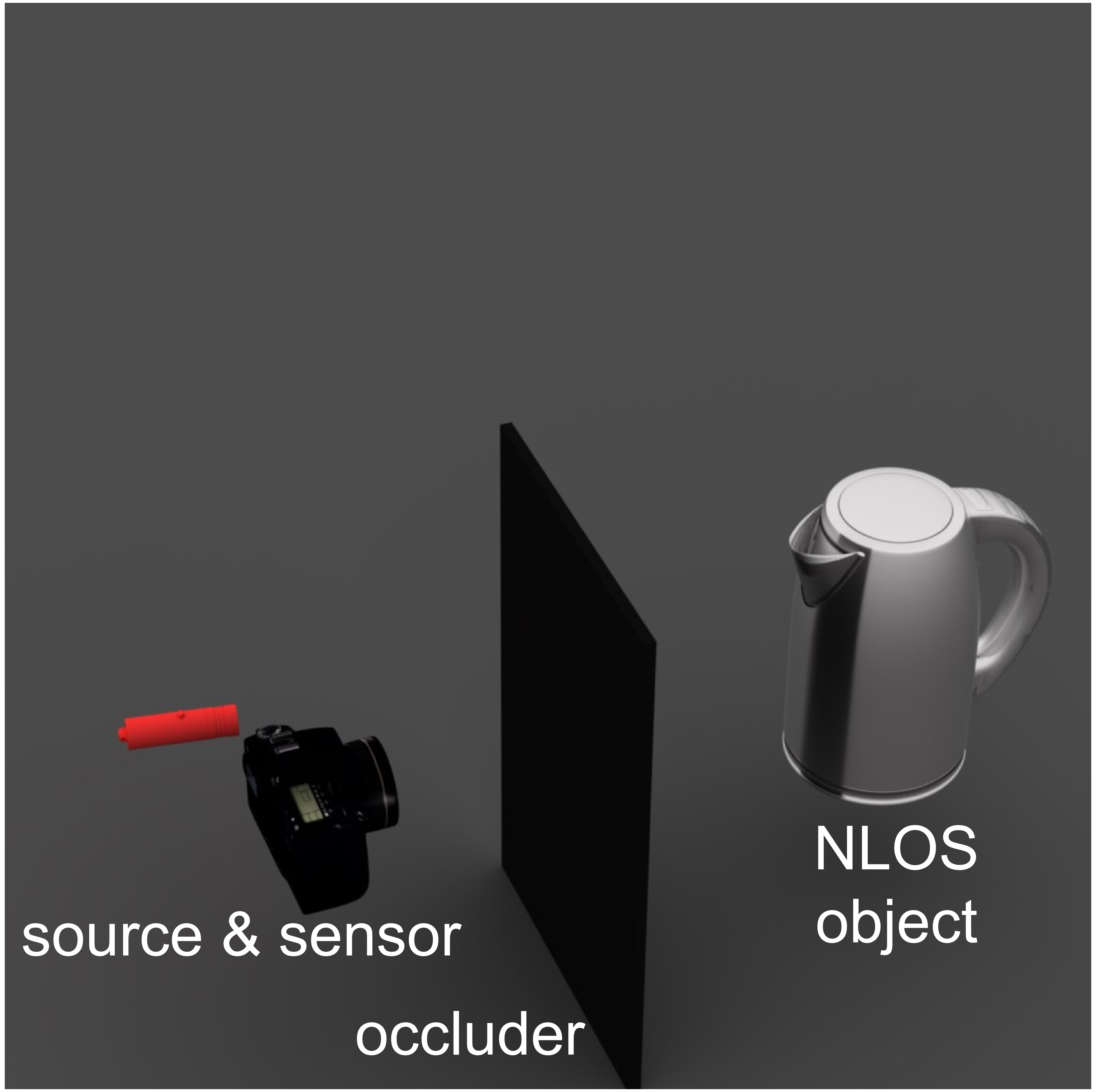

Non-line-of-sight (NLOS) imaging

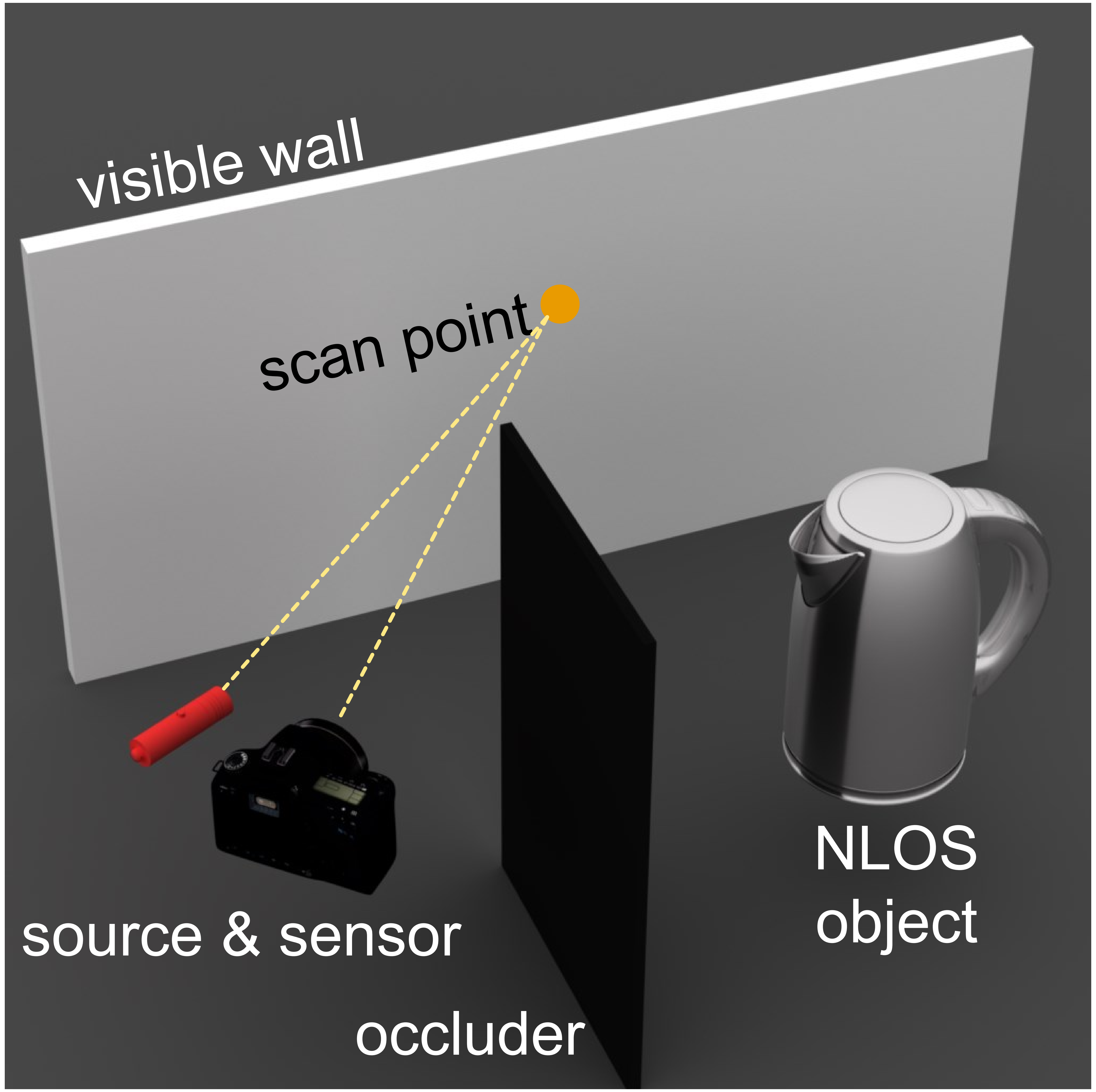

Non-line-of-sight (NLOS) imaging

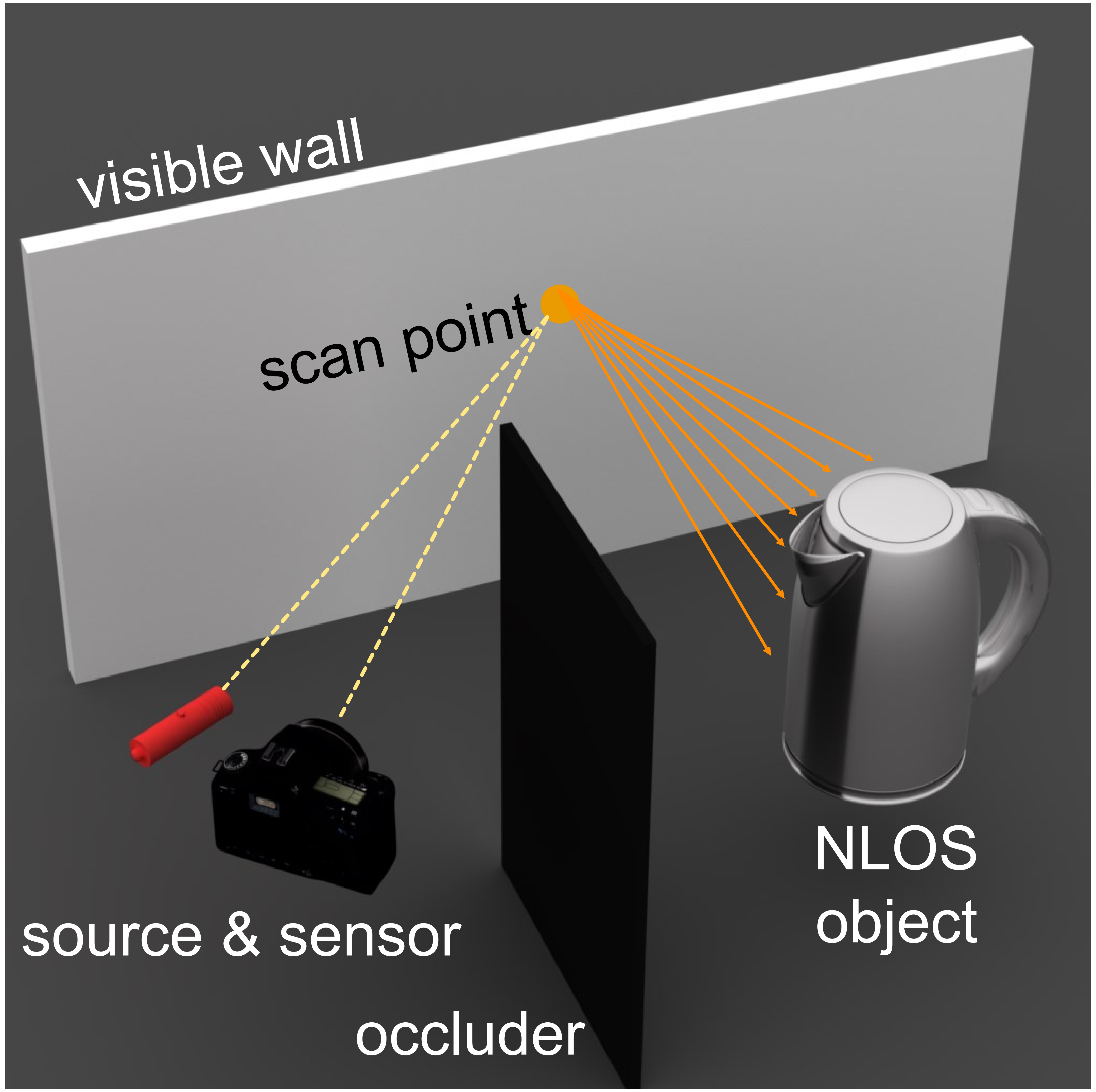

Non-line-of-sight (NLOS) imaging

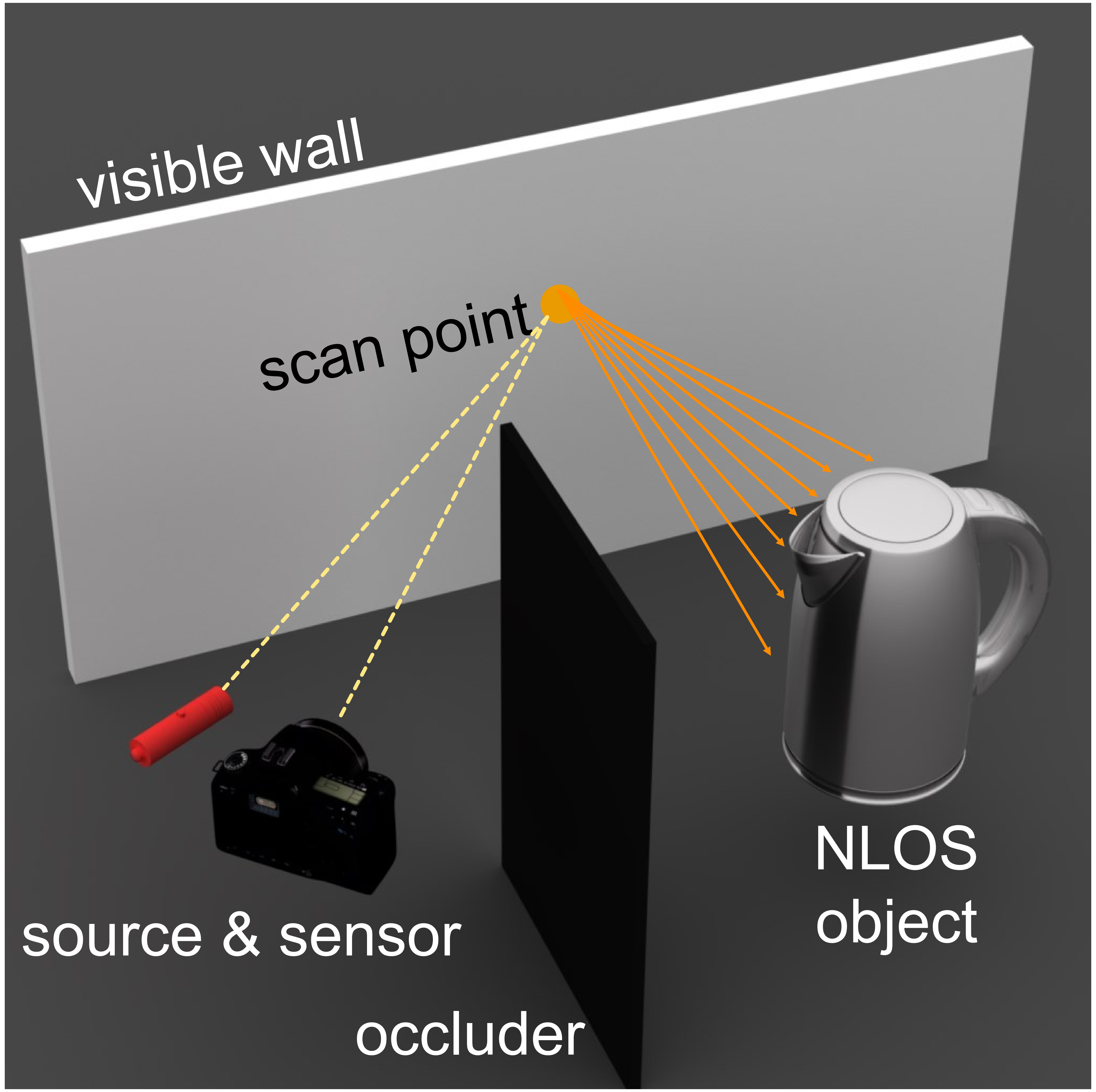

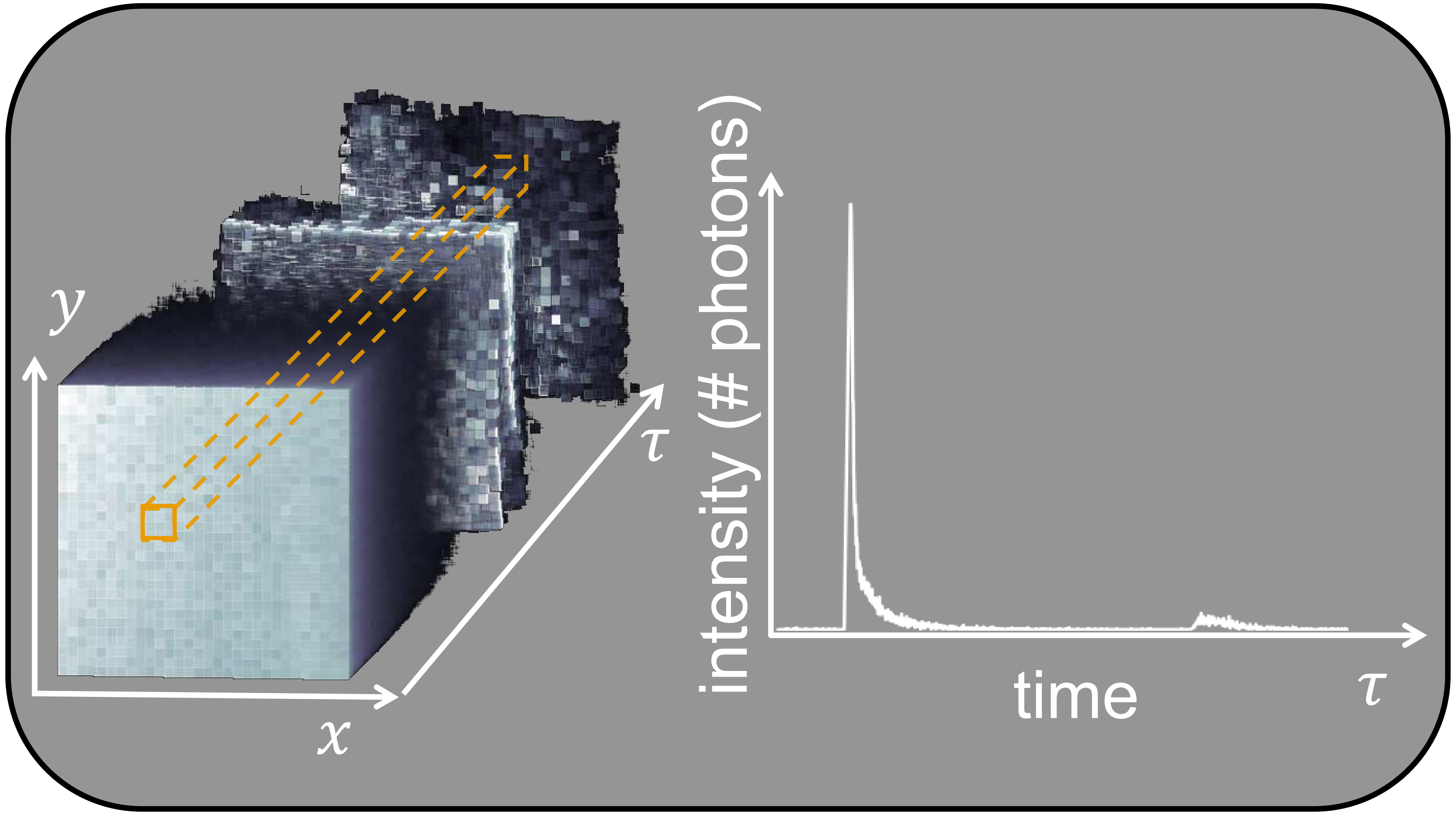

Time-of-flight measurements

Non-line-of-sight (NLOS) imaging

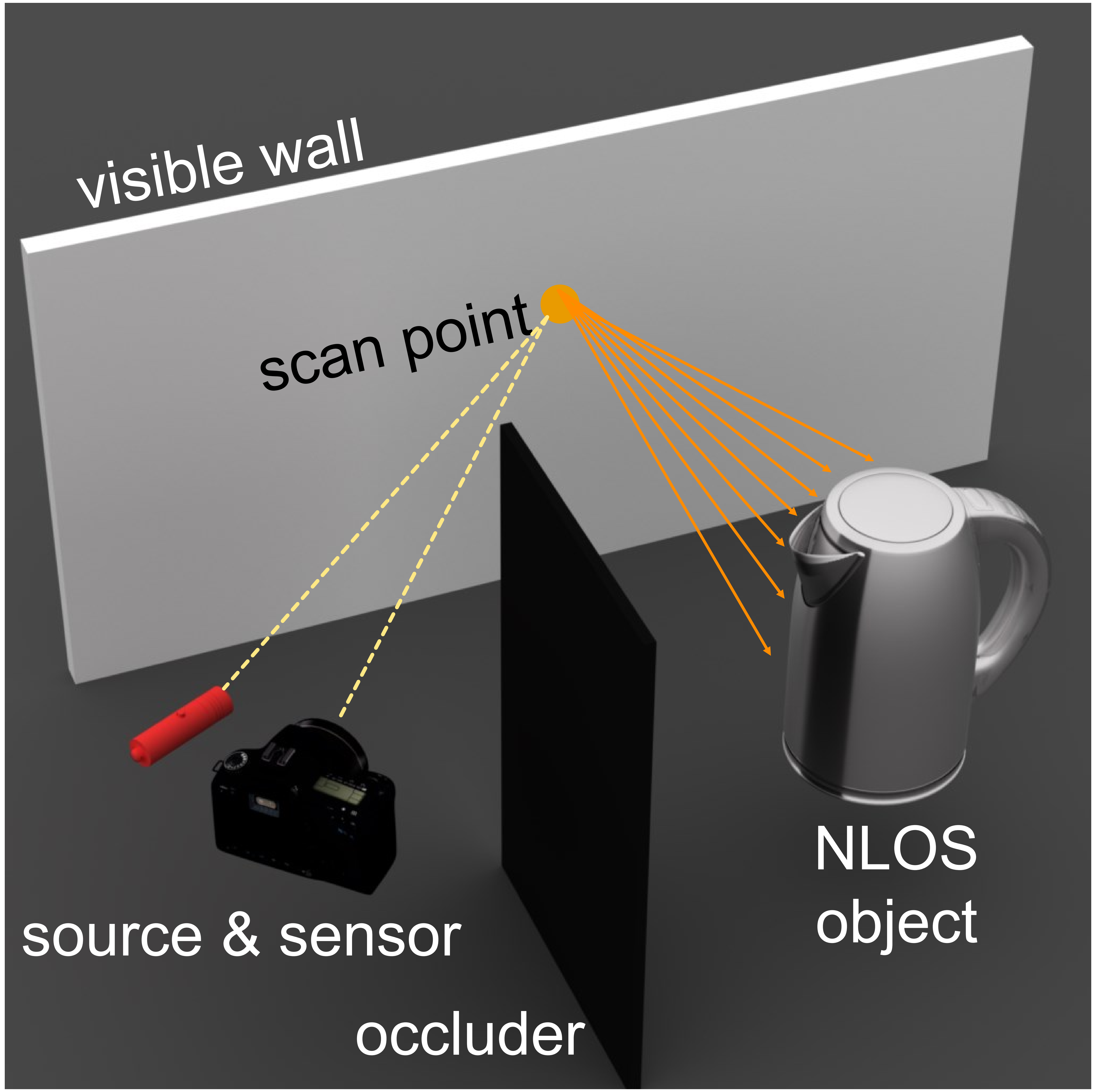

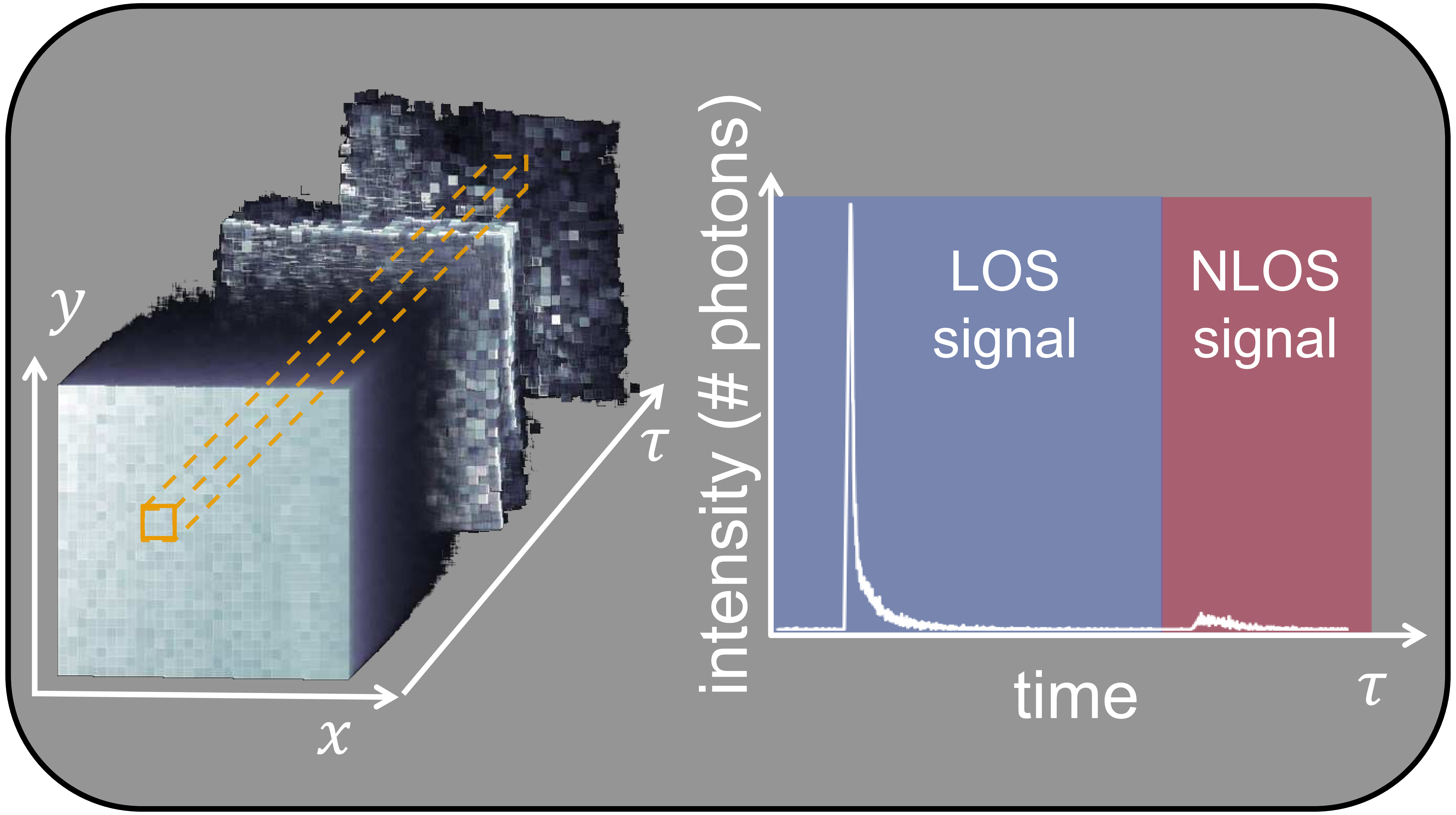

Time-of-flight measurements

SPAD-based lidar

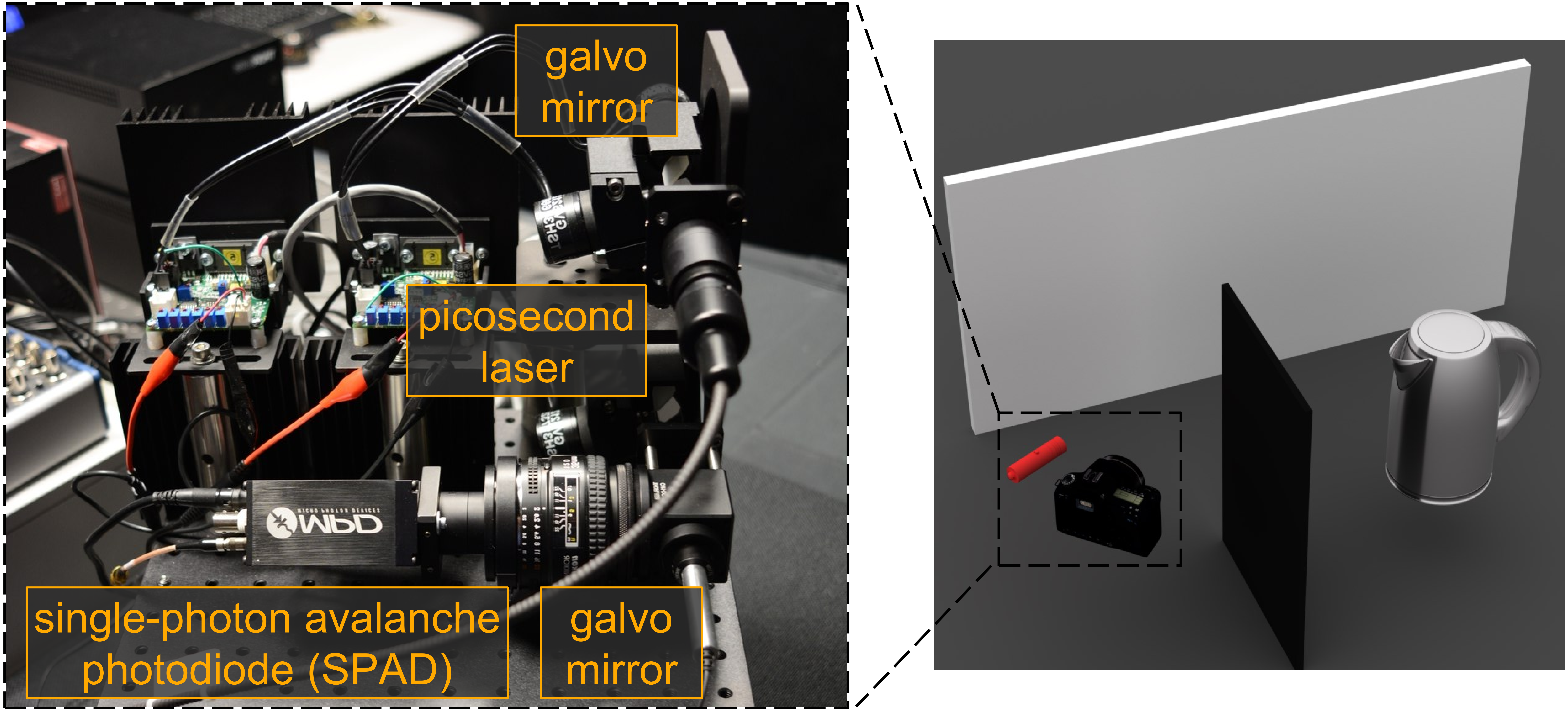

NLOS shape optimization

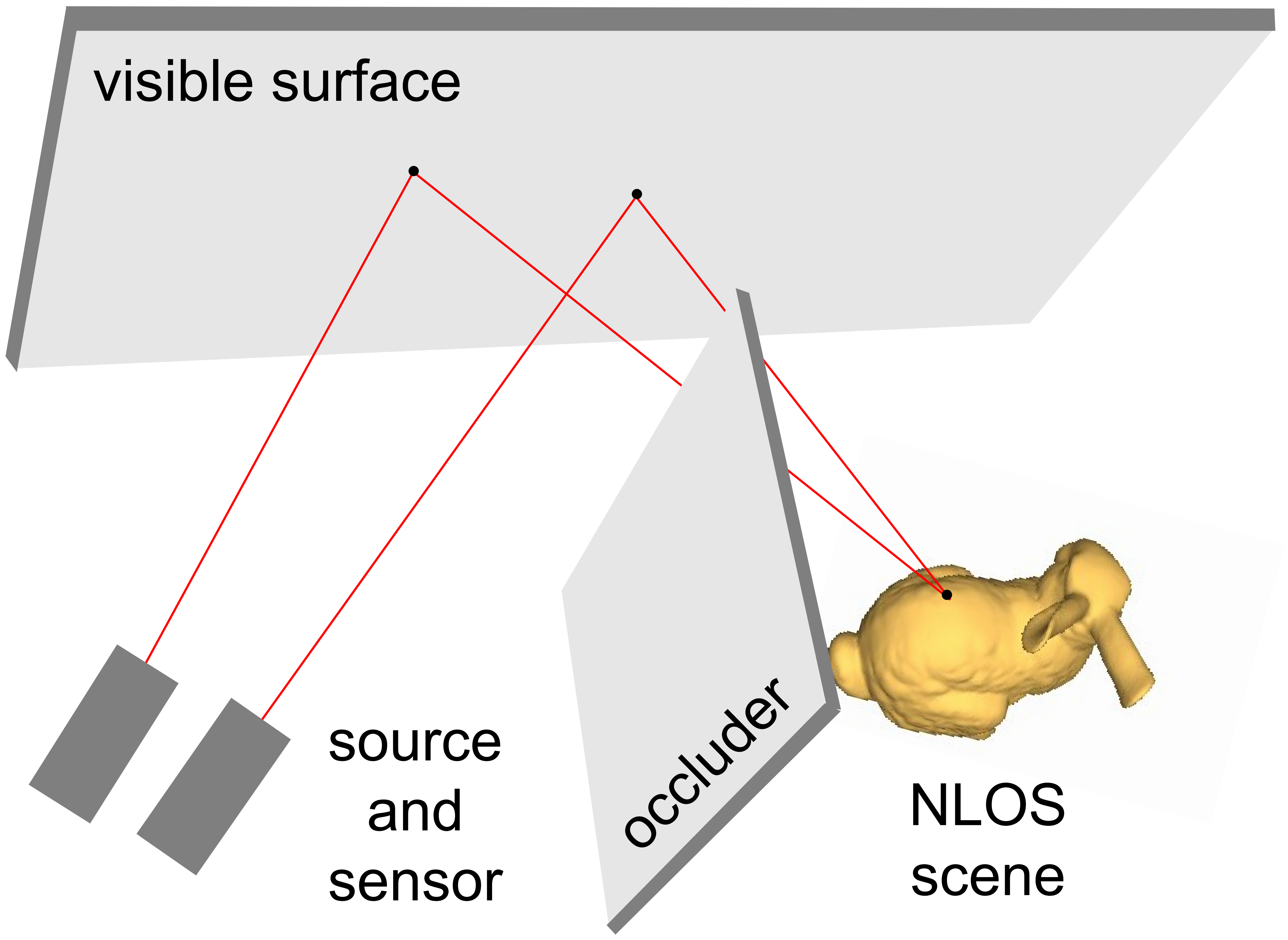

Simulated time-of-flight data

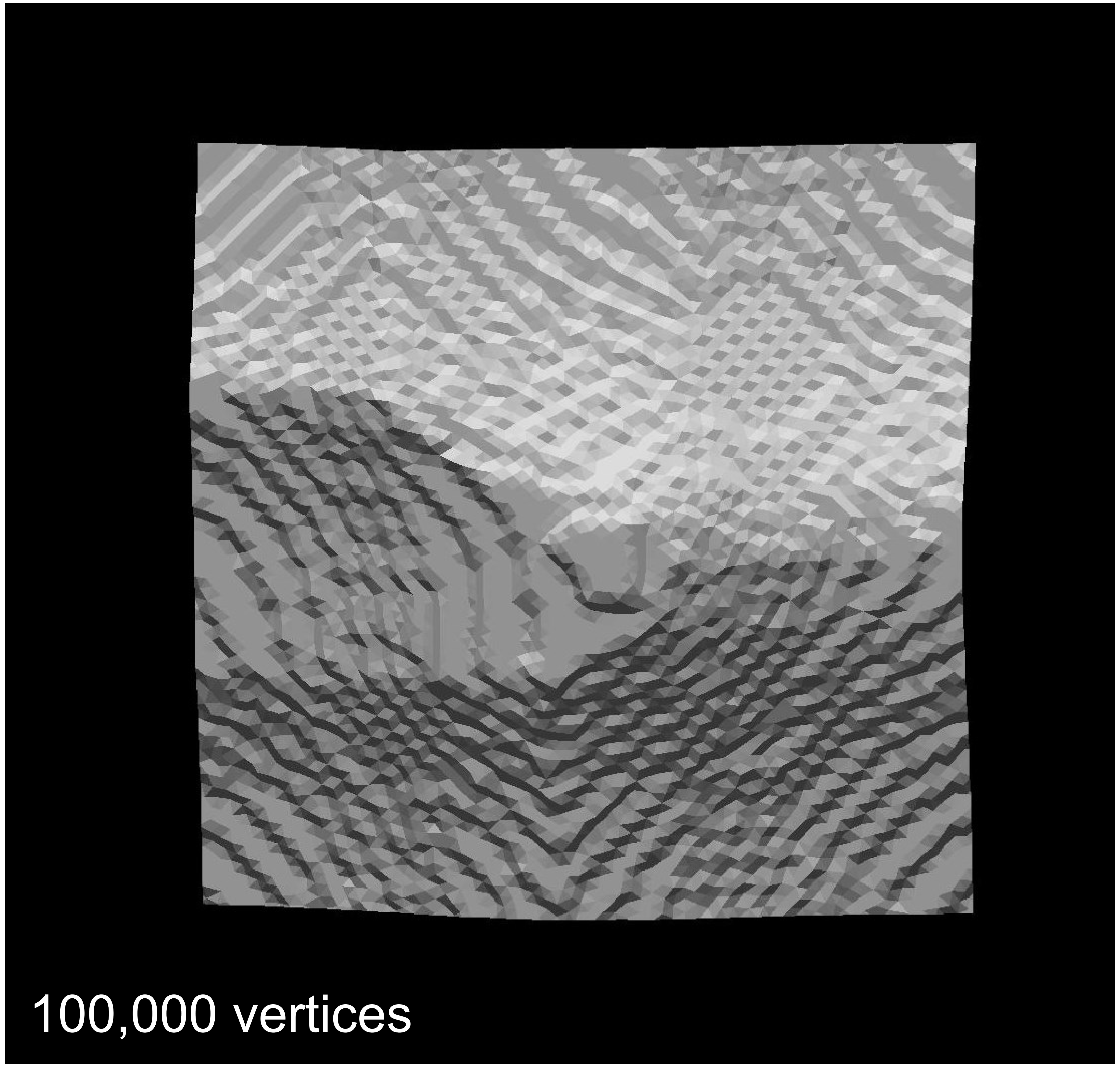

[Tsai et al., 2019]

Underwater 3D using imaging SONAR

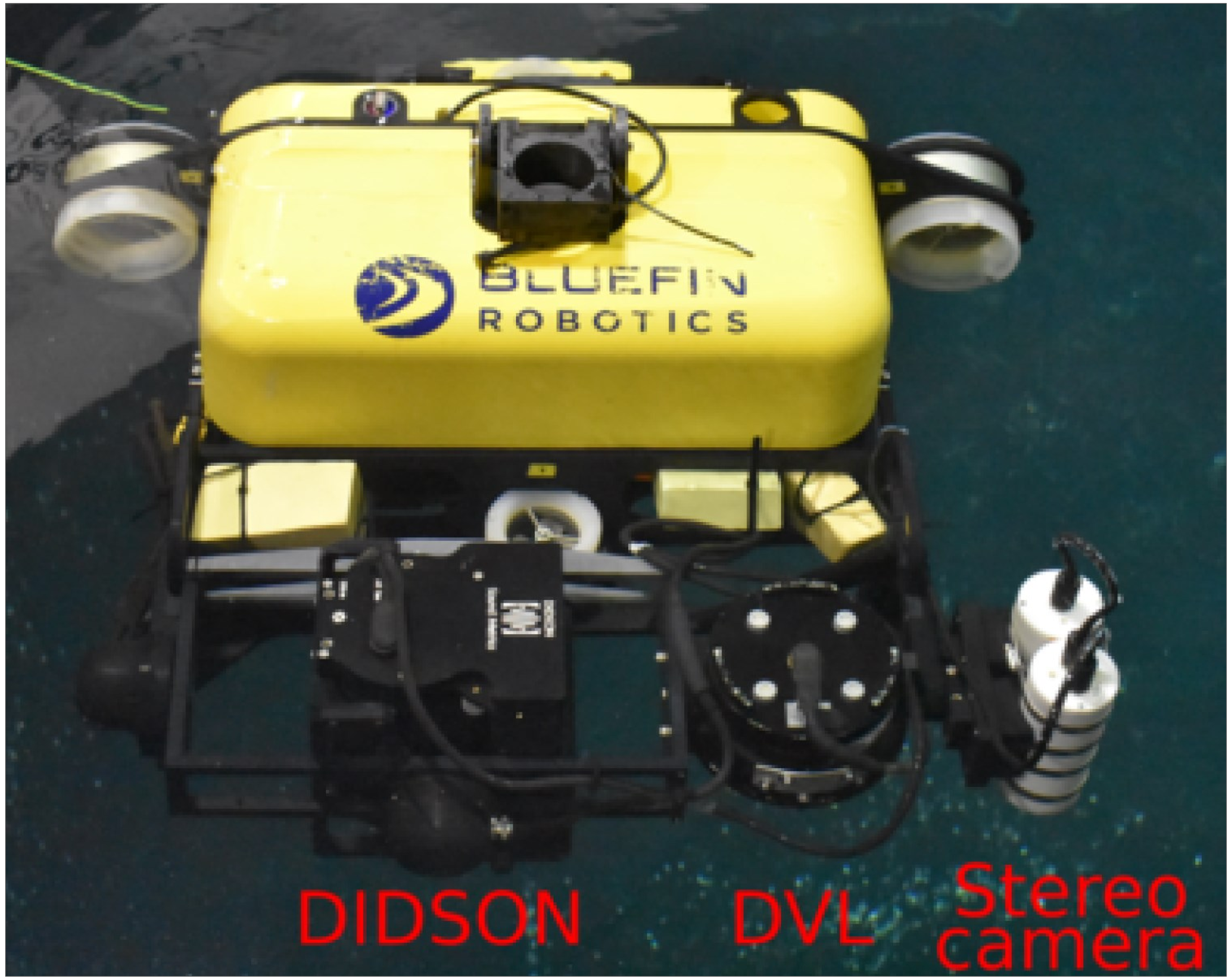

Underwater robot with sonar

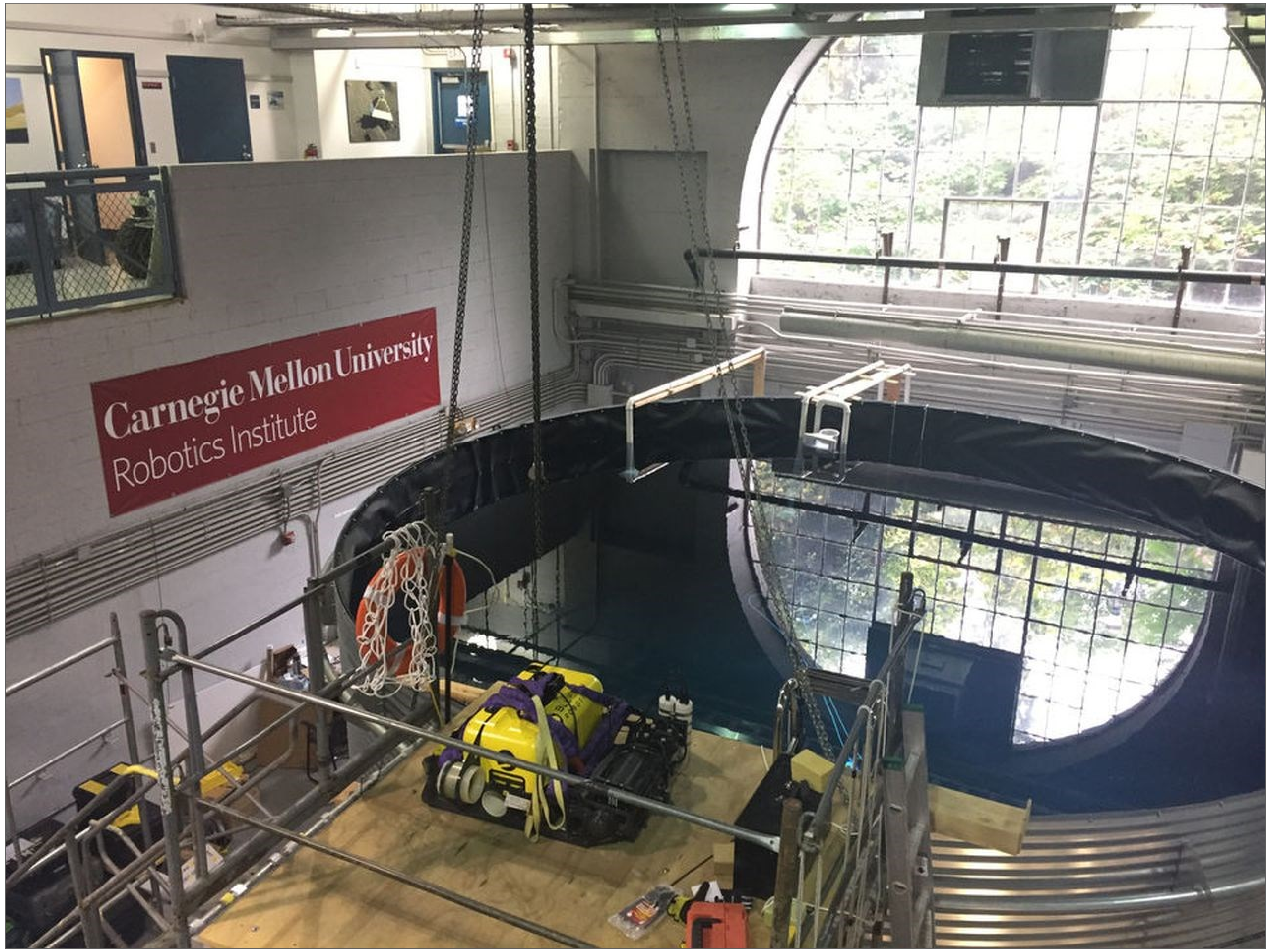

Robotics Institute High Bay

[Qadri et al., 2023]

Underwater 3D using imaging SONAR

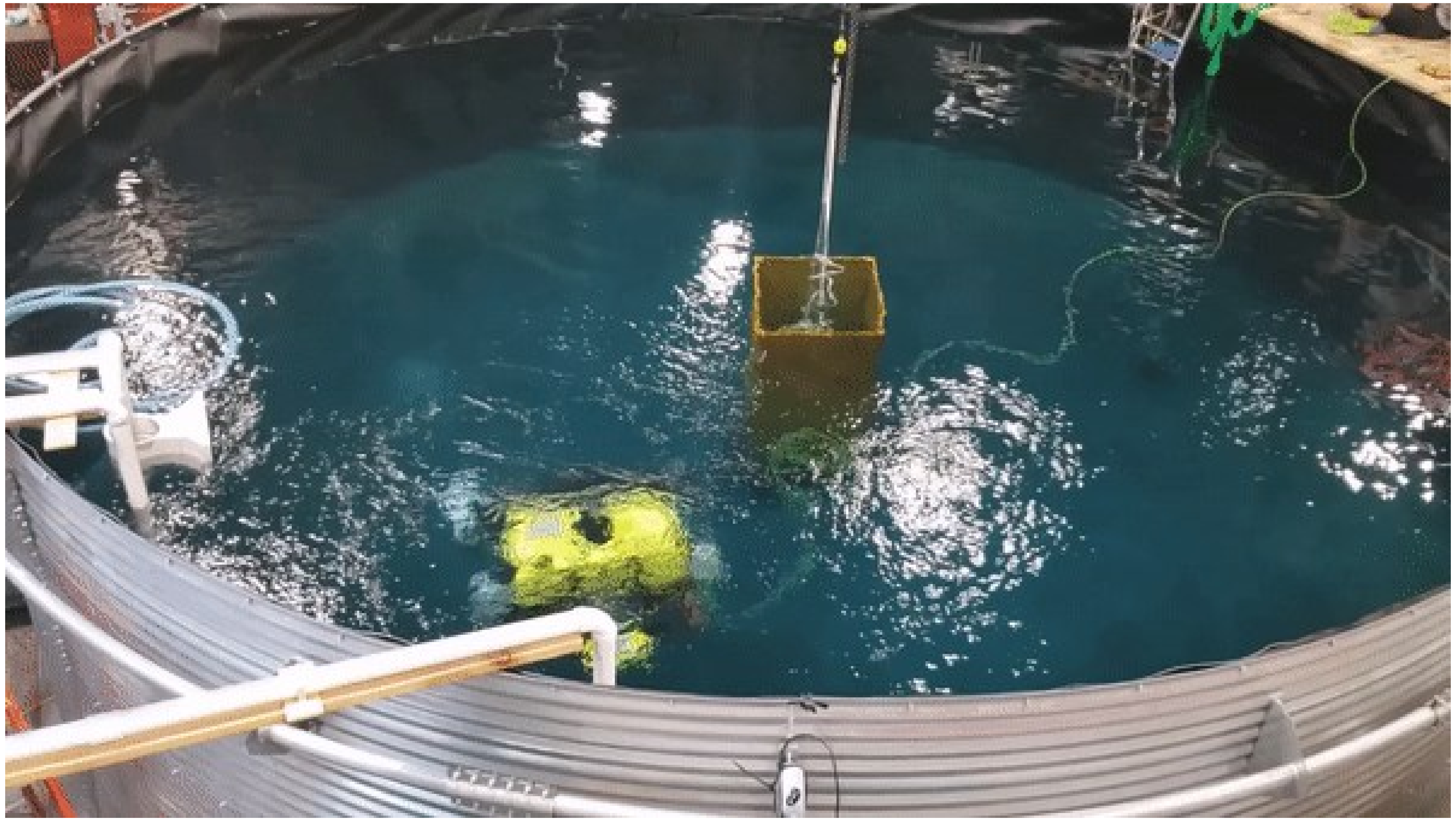

Test structure

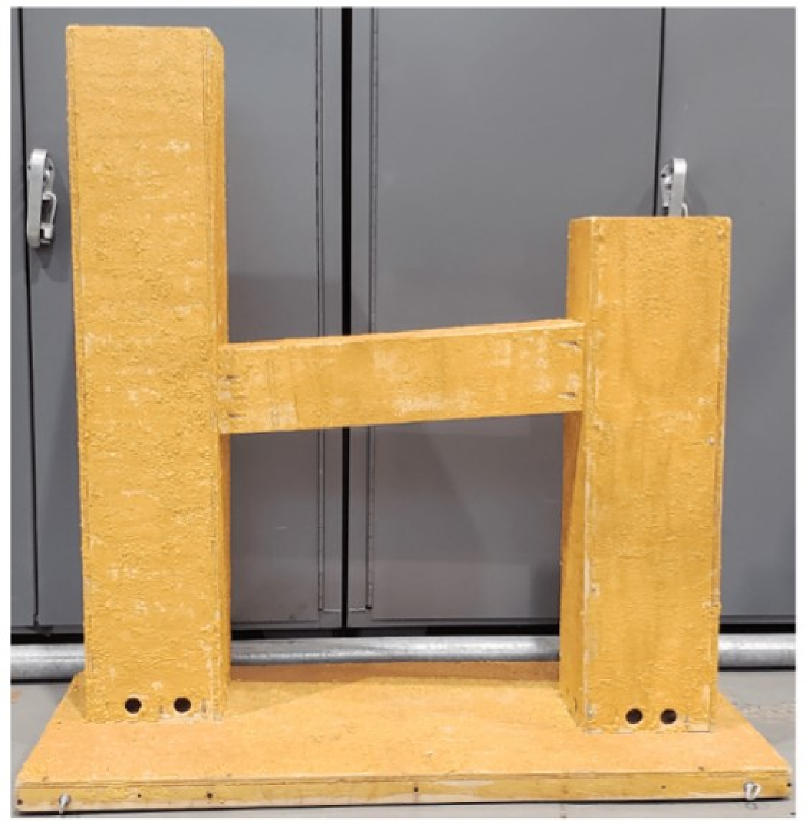

Ground truth mesh obtained using a laser scan

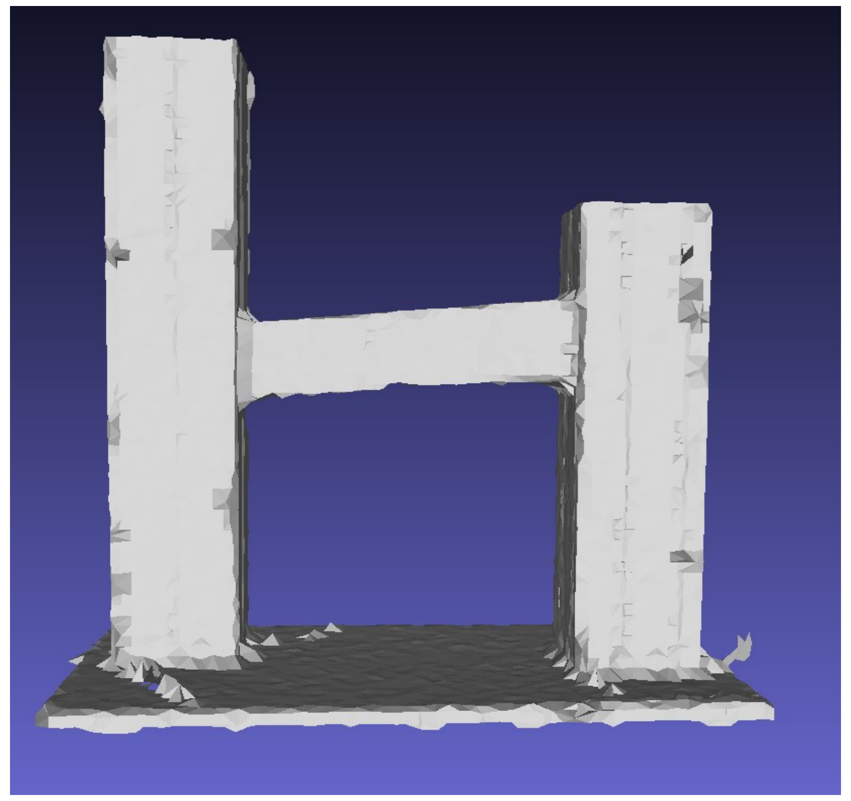

Sonar image collection points

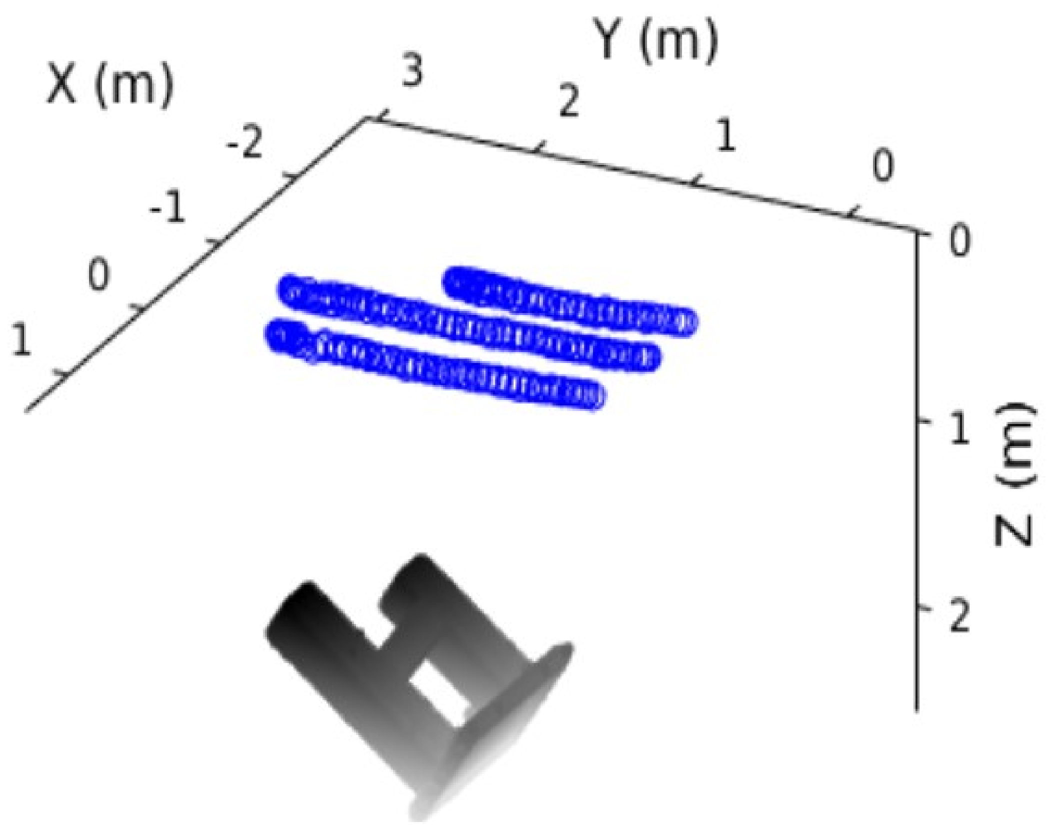

[Qadri et al., 2023]

Underwater 3D using imaging SONAR

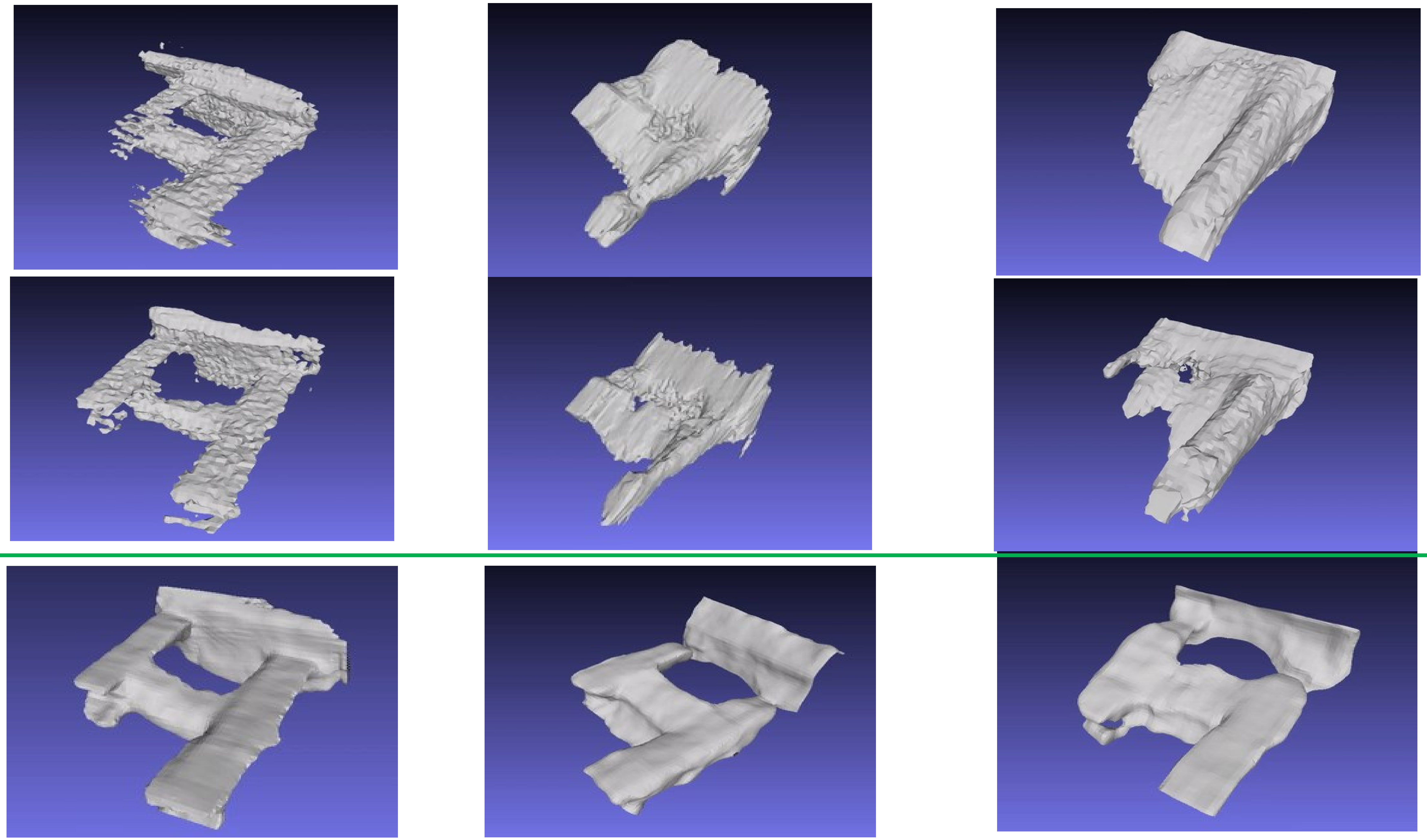

[Qadri et al., 2023]

Underwater 3D using imaging SONAR

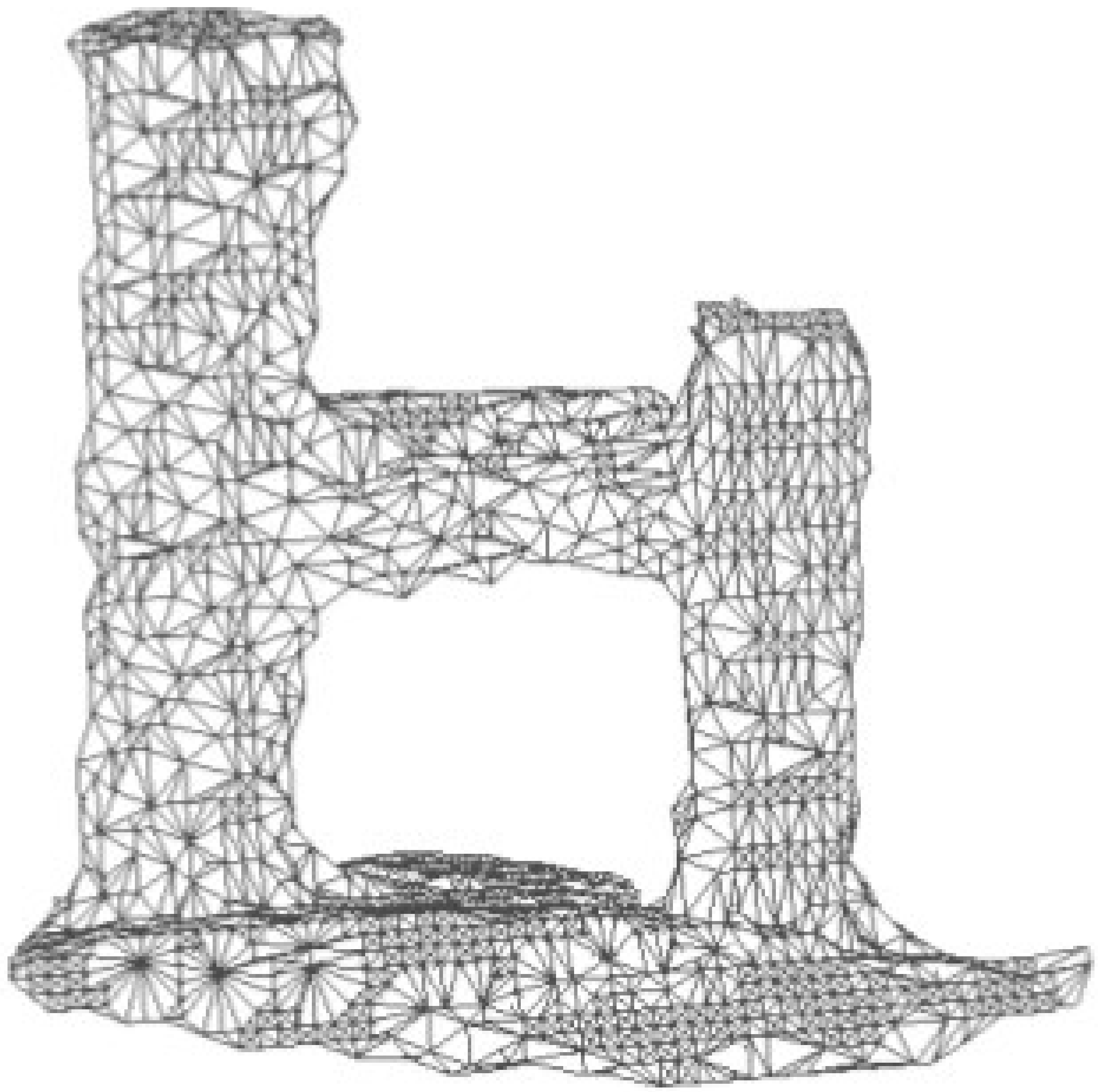

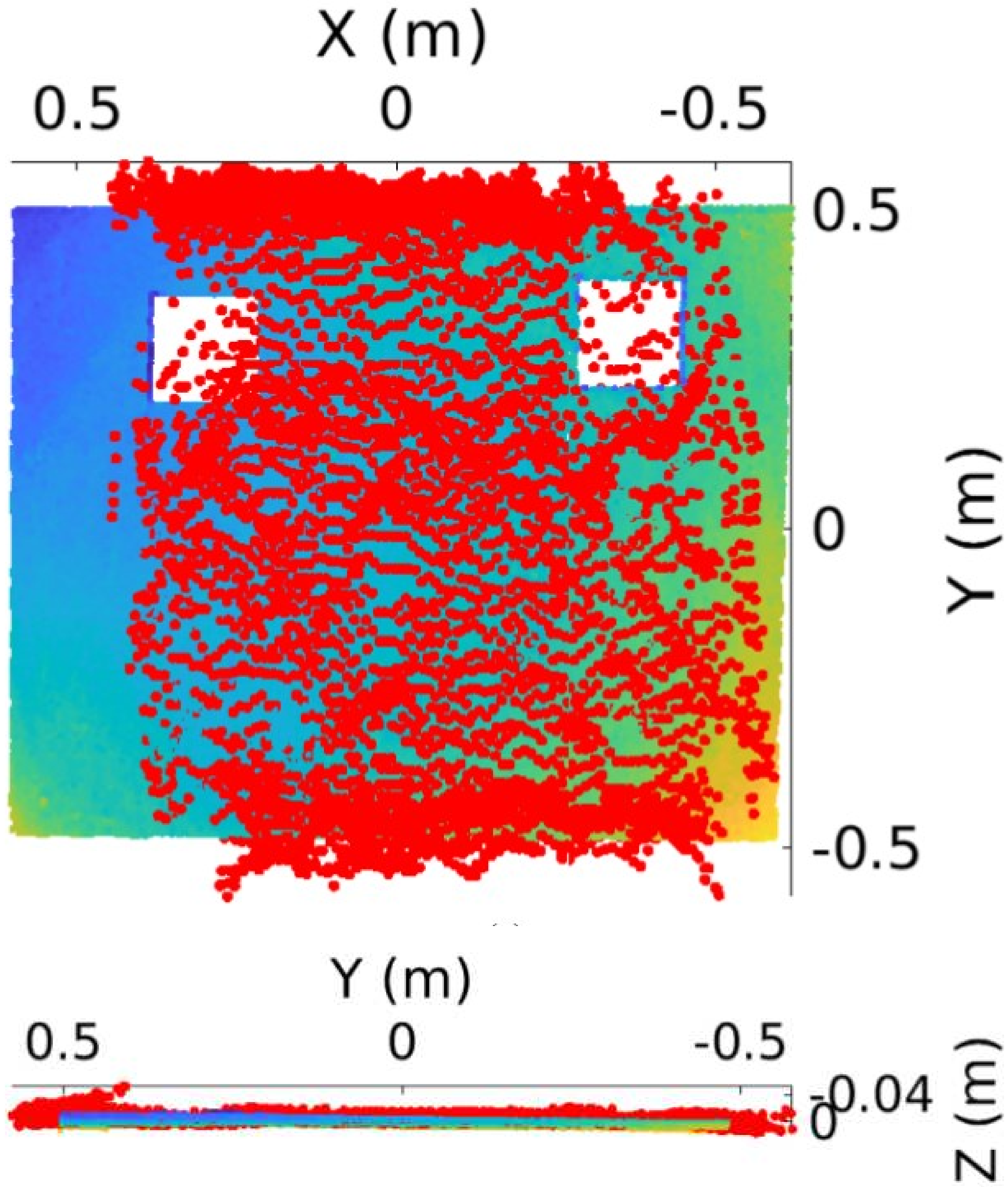

Millimeter-accuracy underwater 3D reconstructions using data captured with an acoustic sonar mounted on robot.

[Qadri et al., 2023]

Kaleidoscopic 3D scanning

kaleidoscopic system

[Ahn et al., CVPR 2023, Tuesday PM]

Kaleidoscopic 3D scanning

kaleidoscopic system

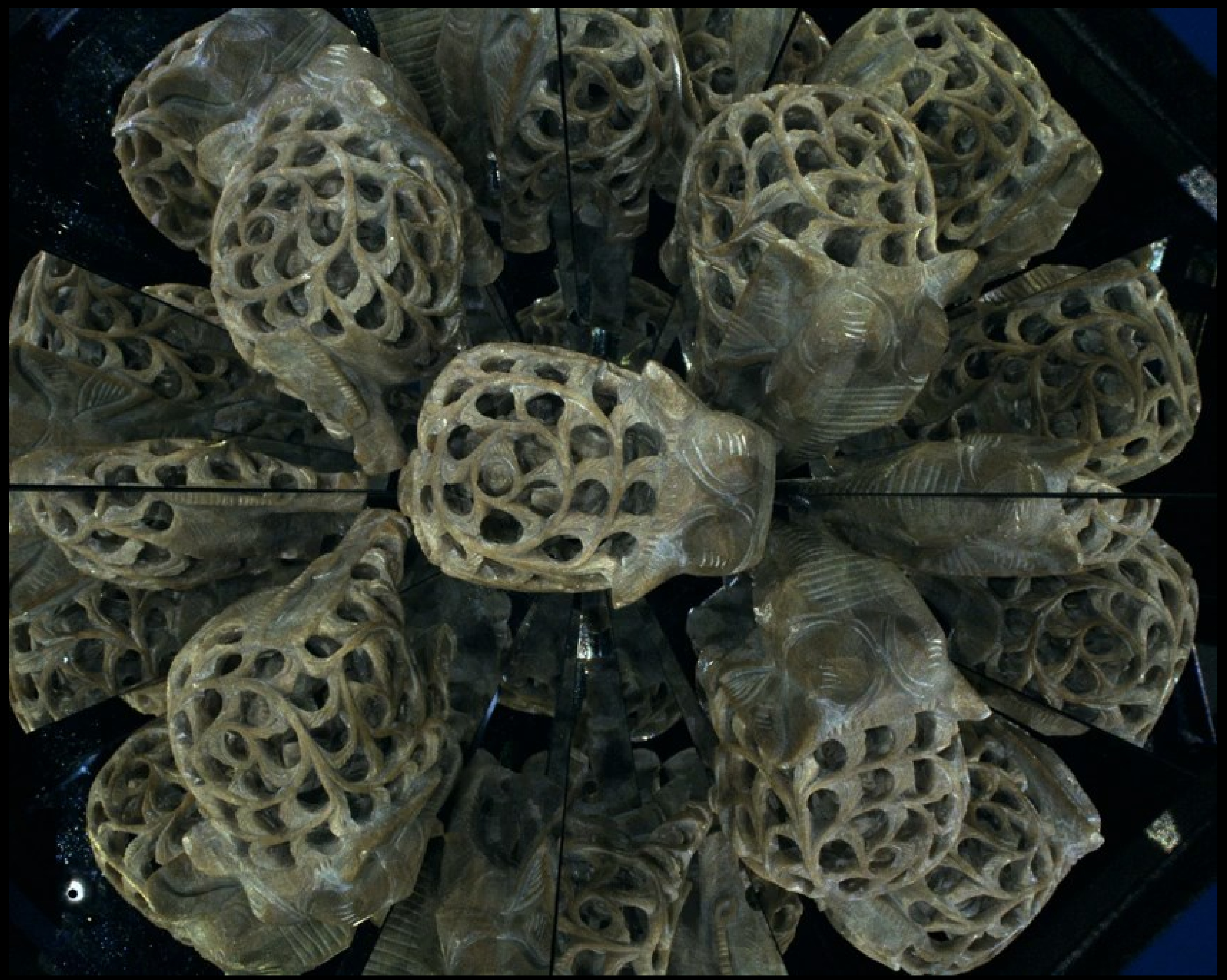

camera view

[Ahn et al., CVPR 2023, Tuesday PM]

Kaleidoscopic 3D scanning

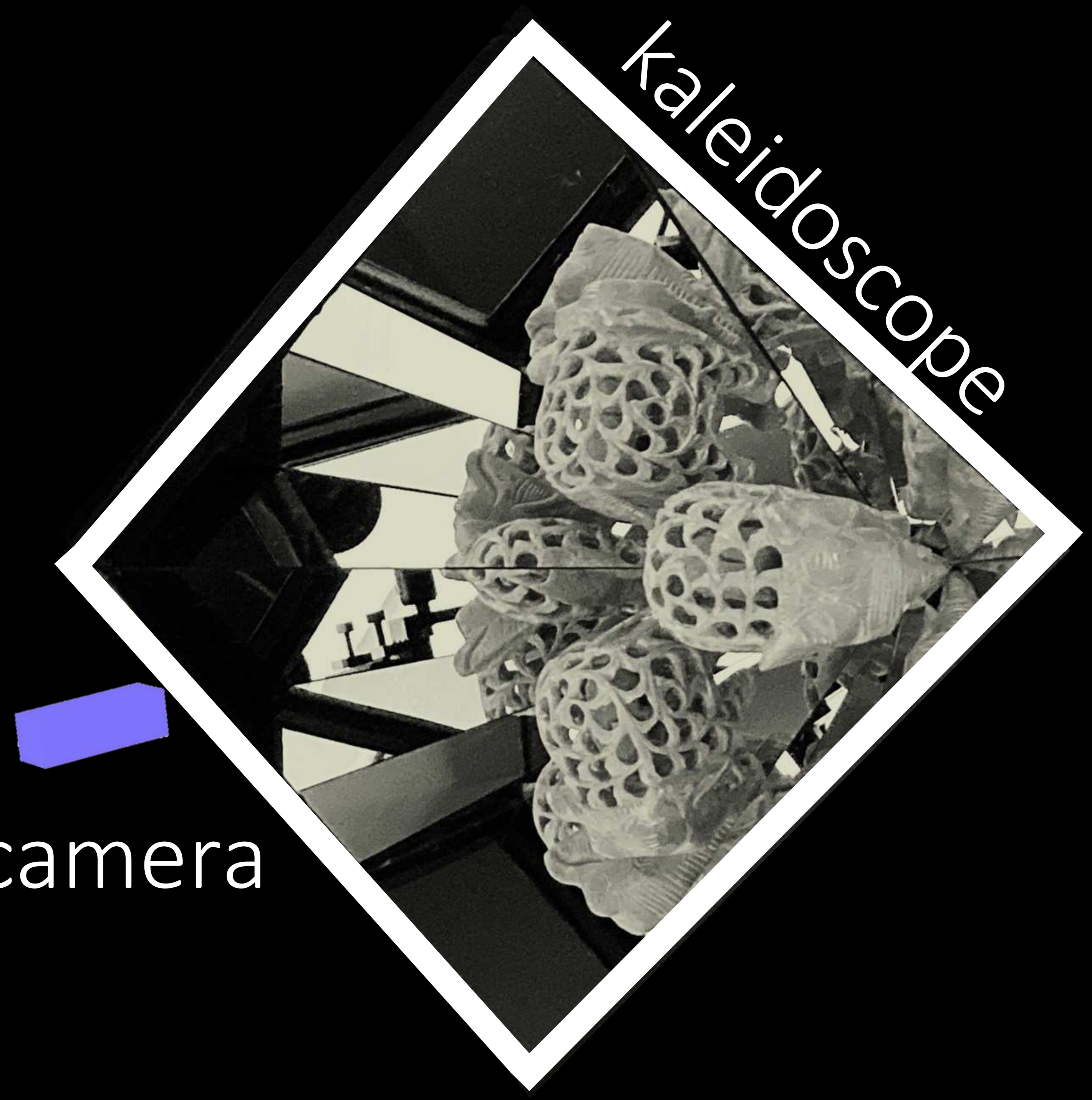

kaleidoscopic system

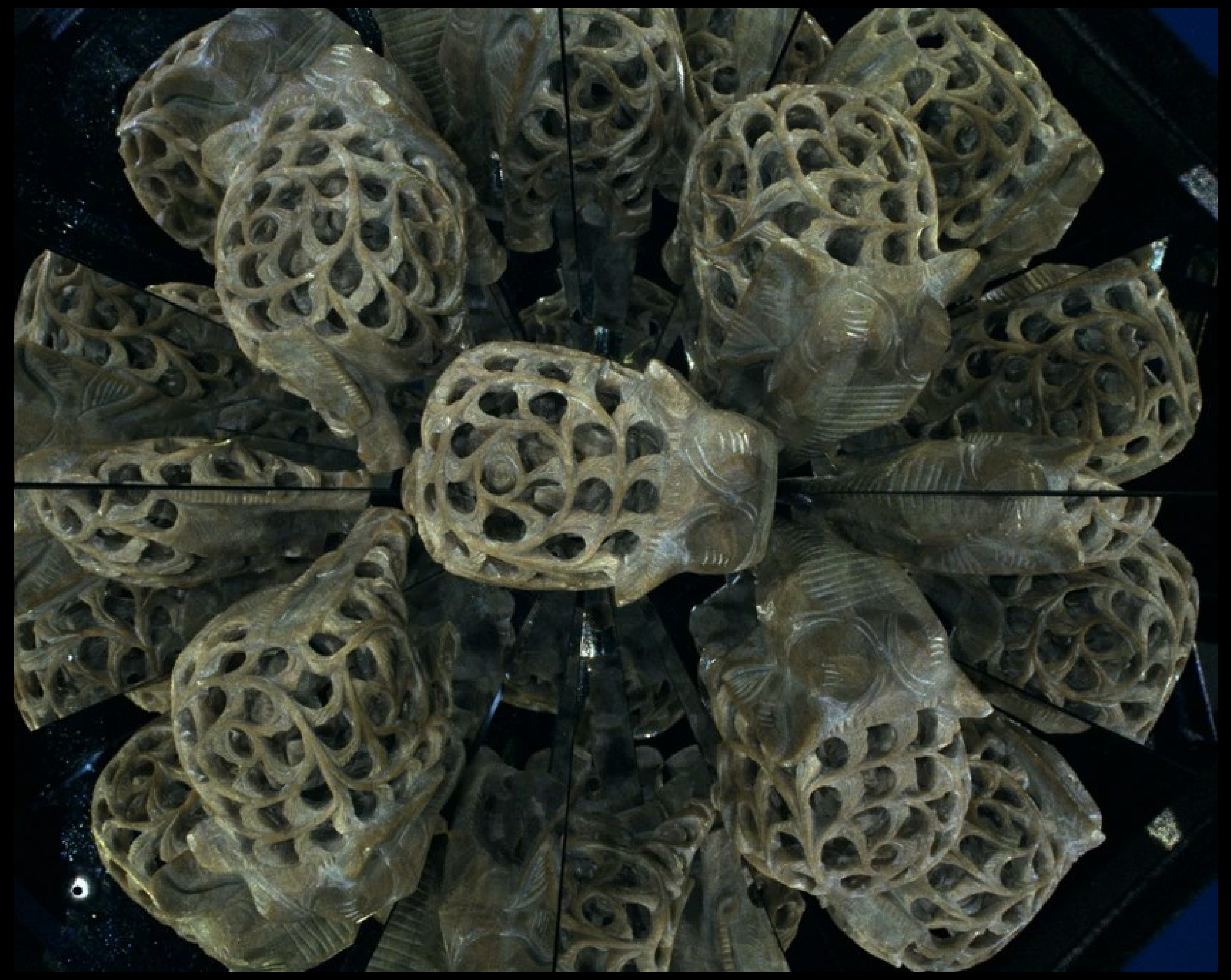

camera view

[Ahn et al., CVPR 2023, Tuesday PM]

Kaleidoscopic 3D scanning

kaleidoscopic system

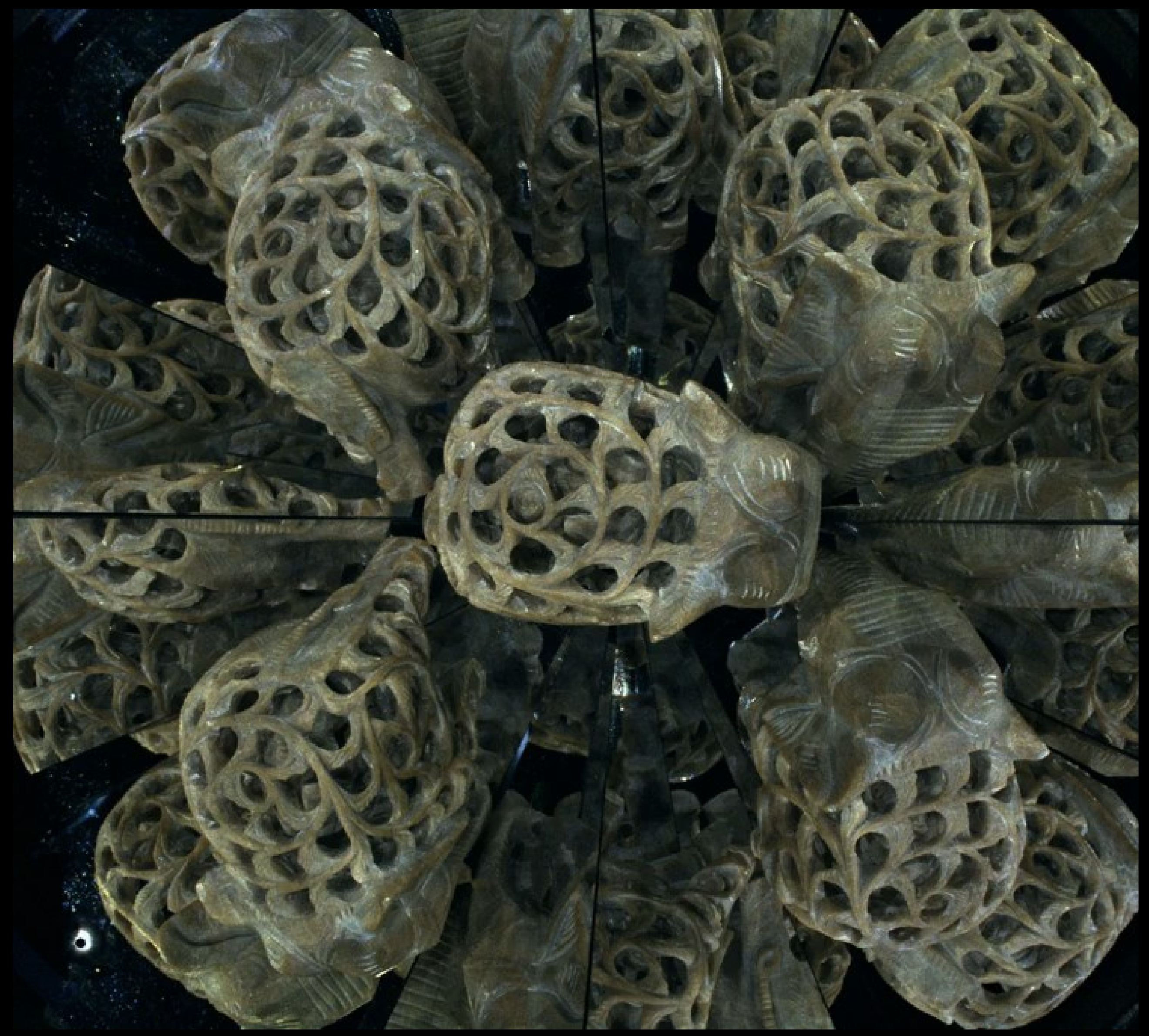

camera view

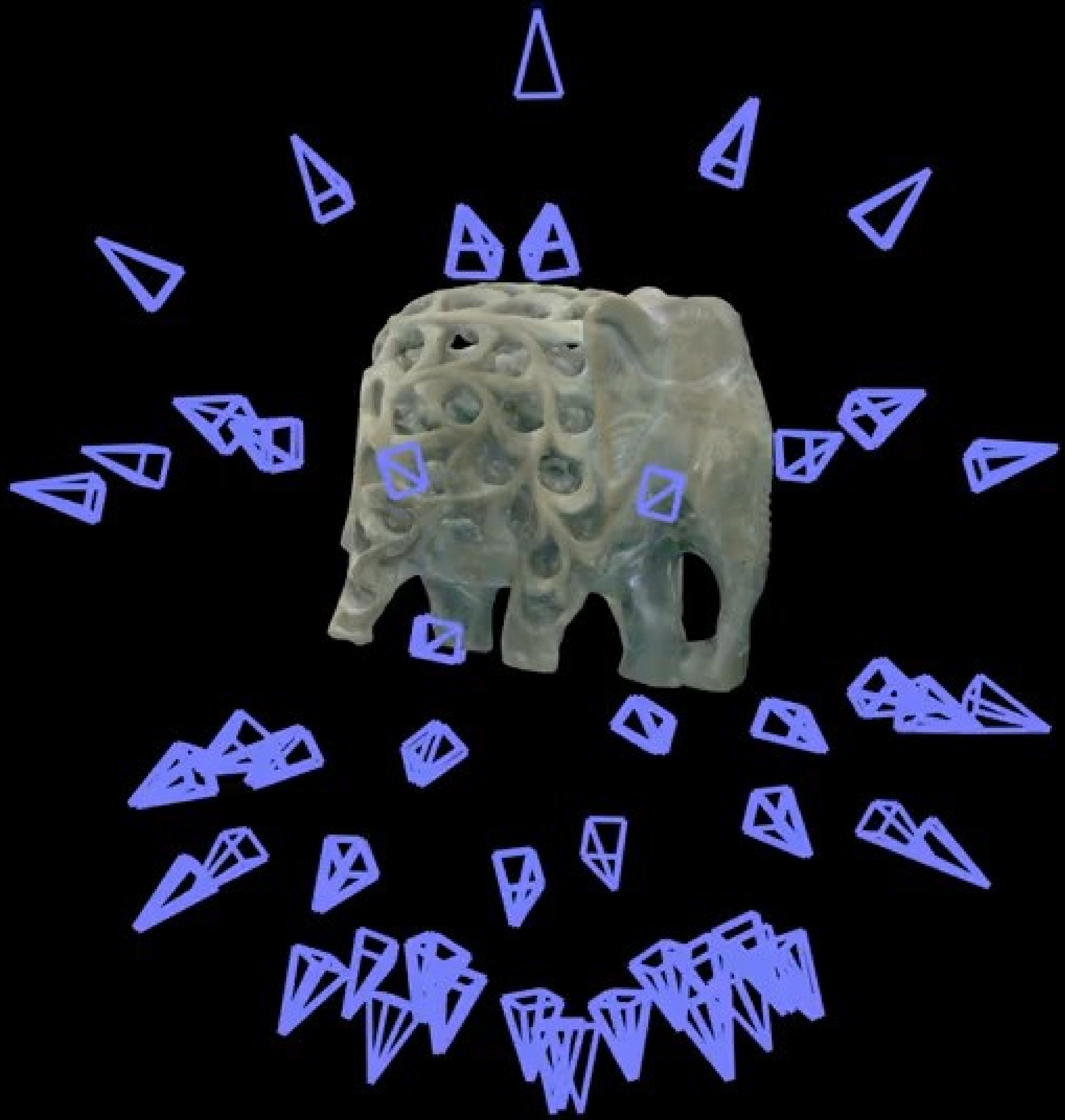

virtual cameras

[Ahn et al., CVPR 2023, Tuesday PM]

Kaleidoscopic 3D scanning

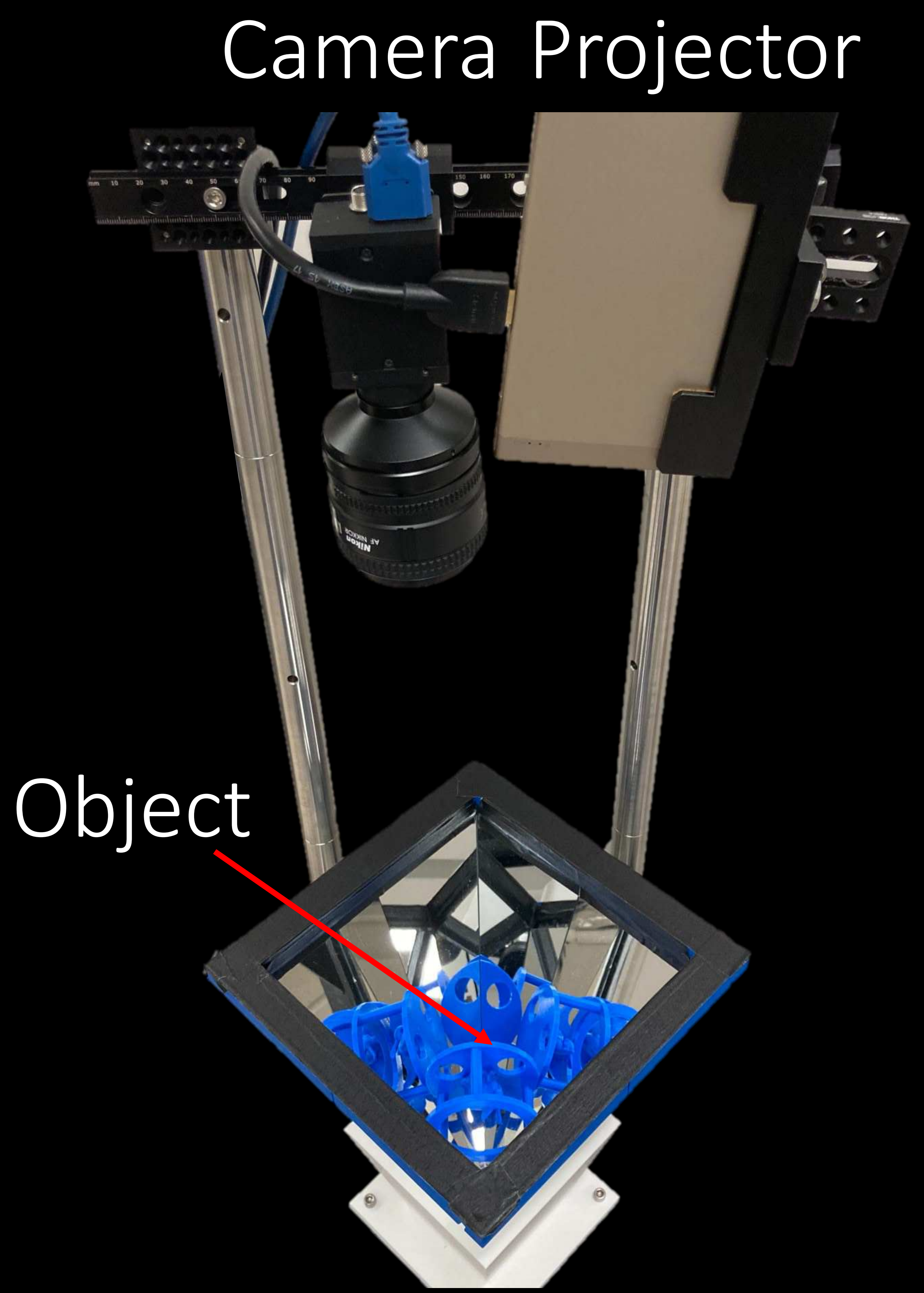

kaleidoscopic system

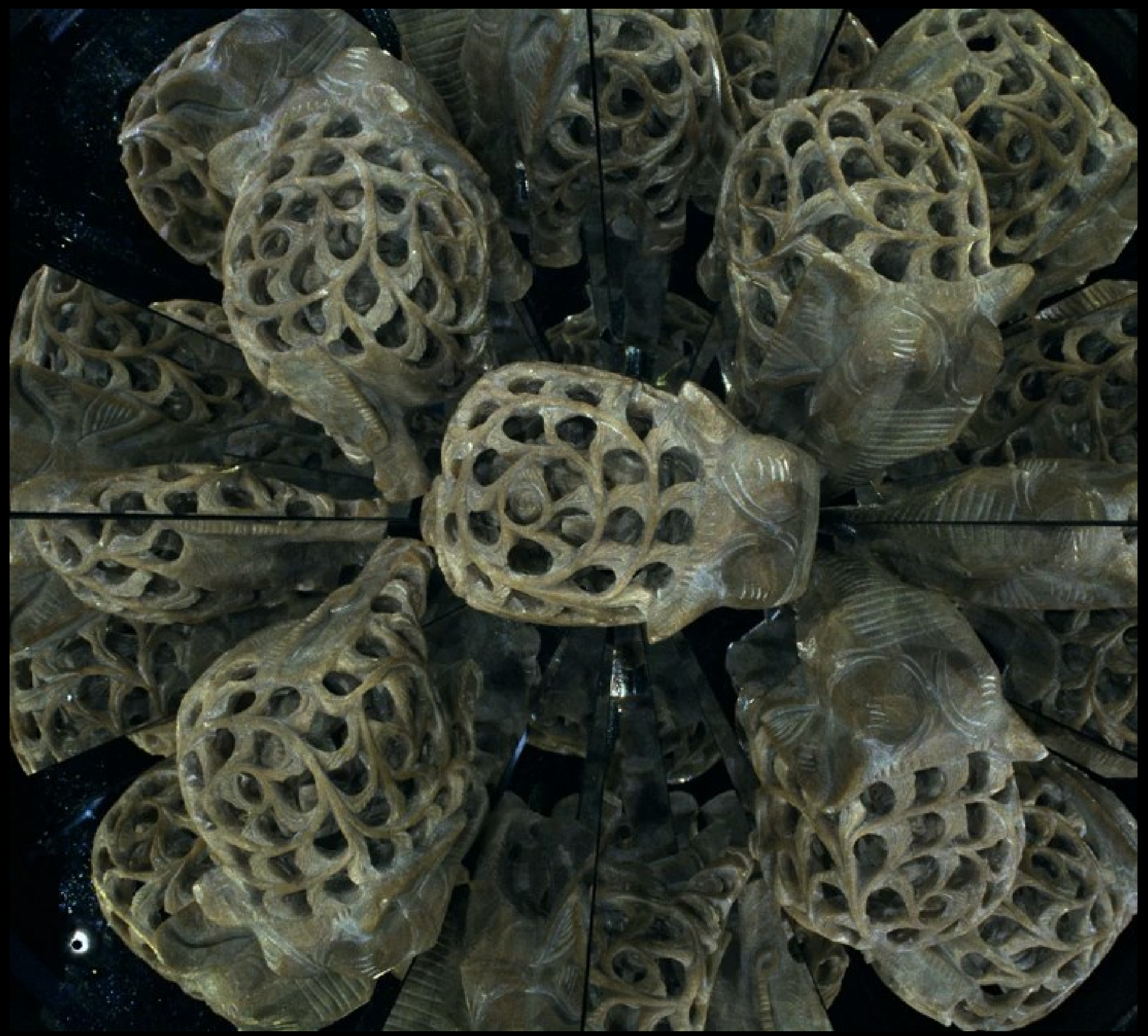

camera view

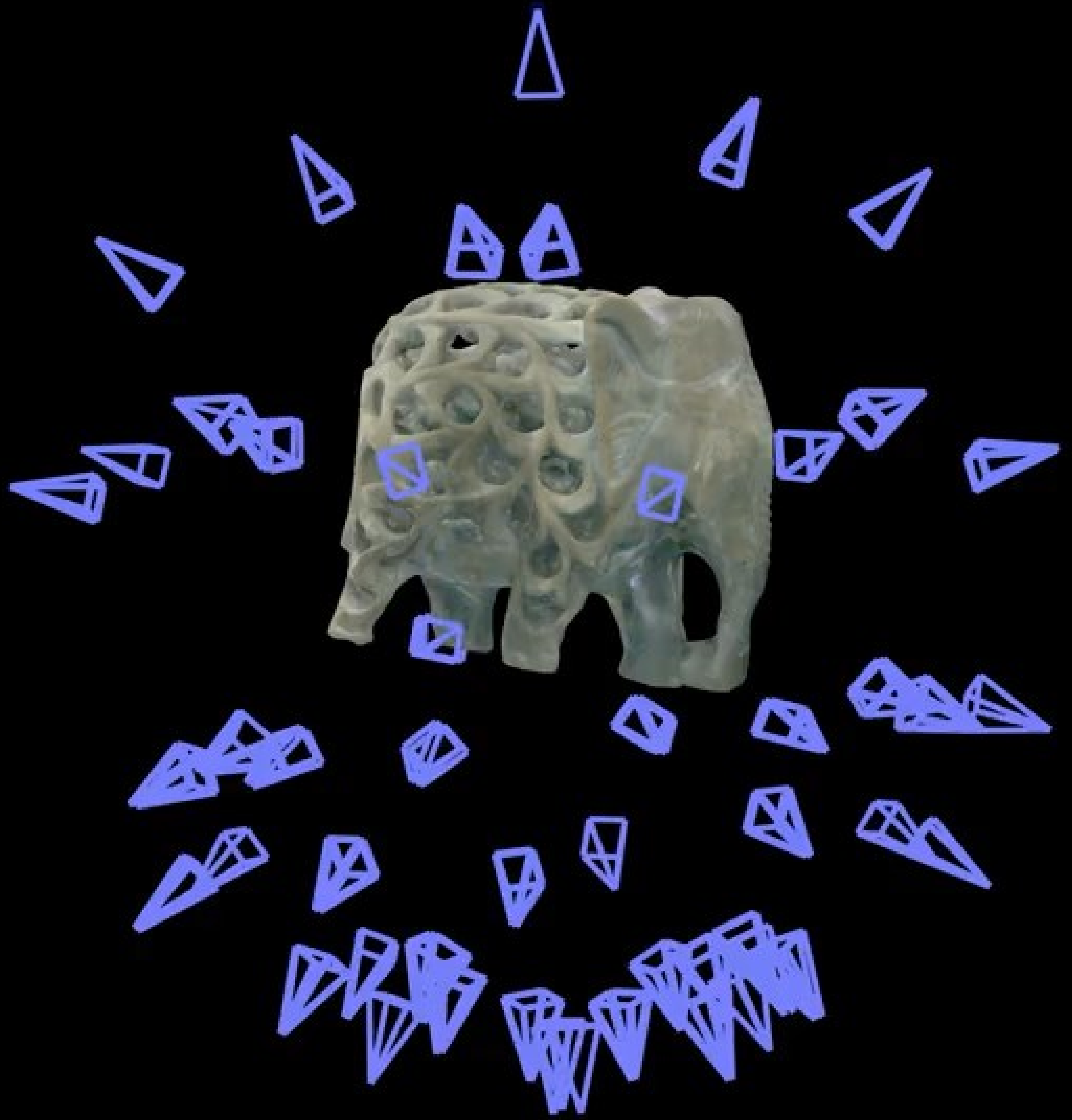

virtual cameras

[Ahn et al., CVPR 2023, Tuesday PM]

Example 3D scans

photograph

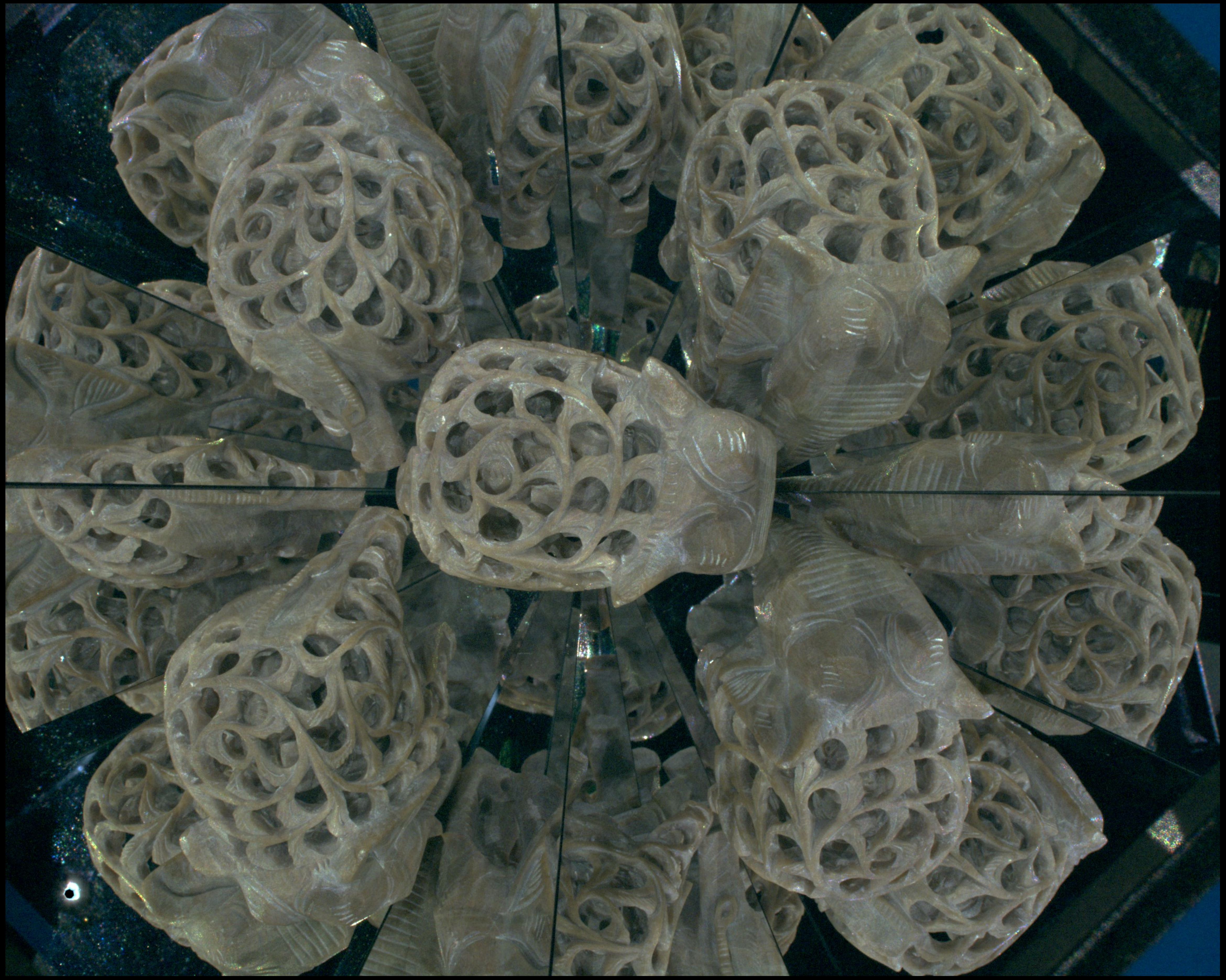

3D reconstruction

[Ahn et al., CVPR 2023, Tuesday PM]

Optimizing Gradient-Index (GRIN) Optics

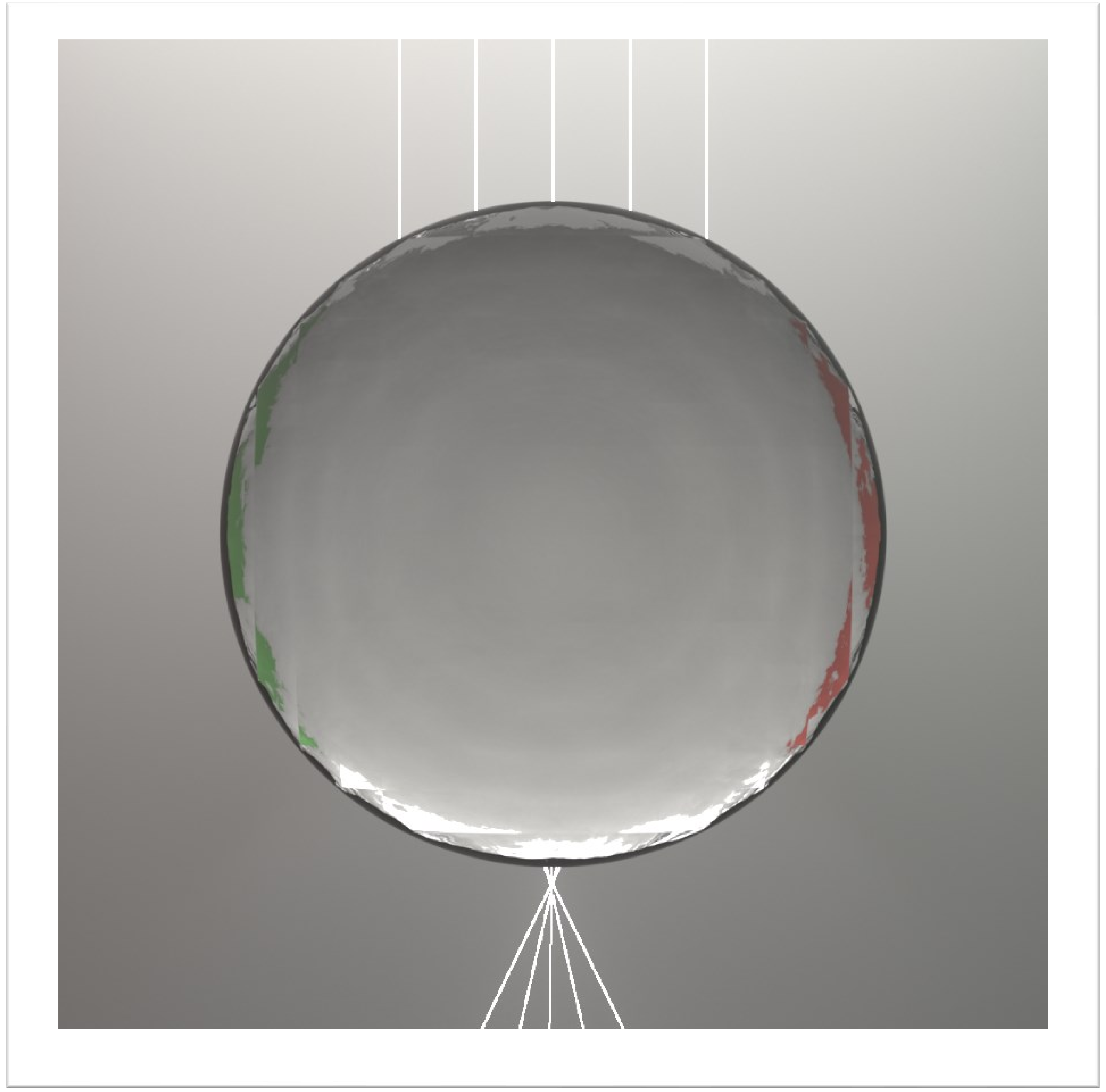

Luneburg Lens

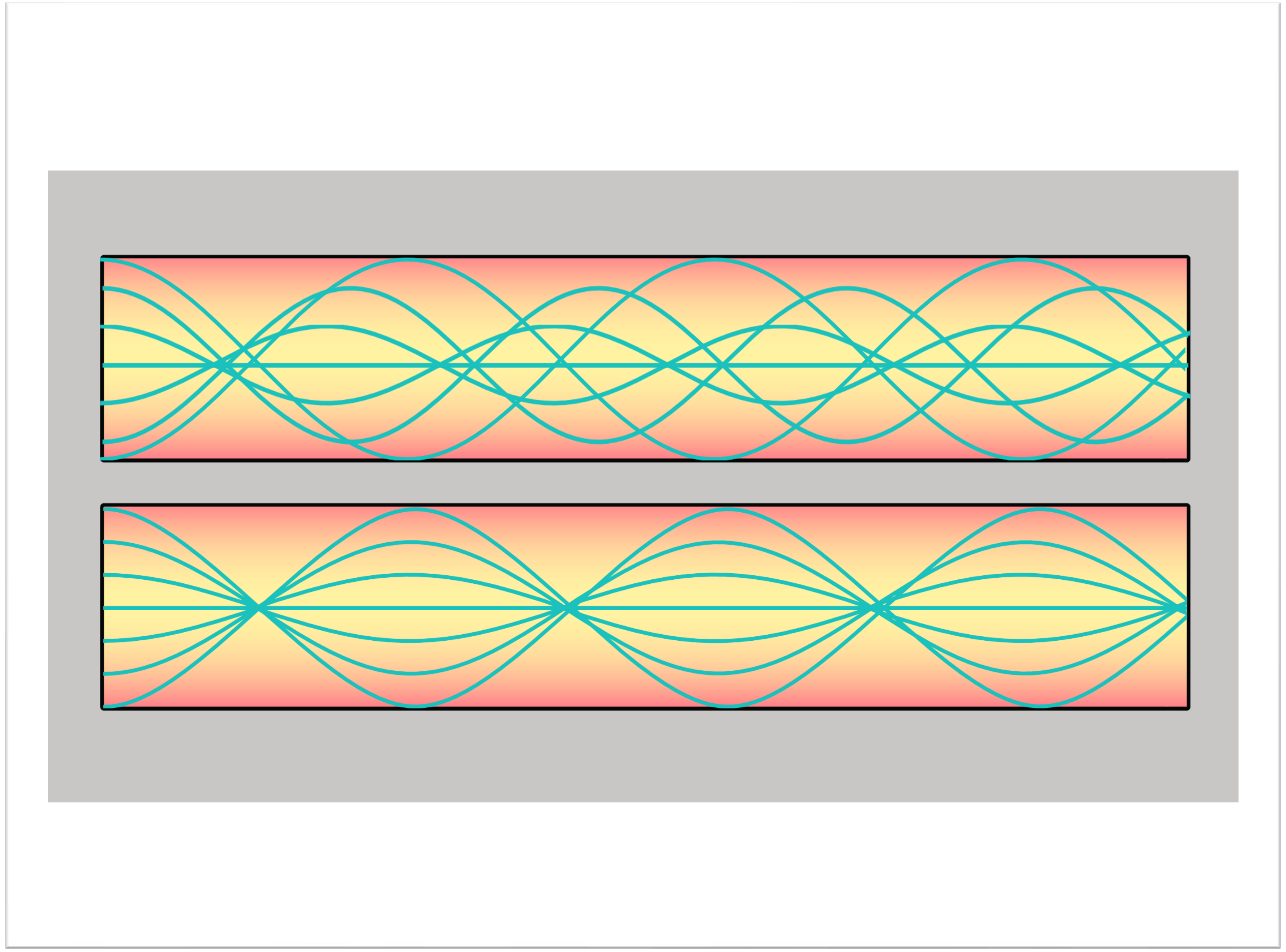

GRIN Fiber

[Teh et al., 2022]

Nonlinear Ray Tracing

$\eta(\mathbf{x})$: refractive index of the volume at location, $\mathbf{x}$

[Teh et al., 2022]

Nonlinear Ray Tracing

[Teh et al., 2022]

Nonlinear Ray Tracing

[Teh et al., 2022]

Nonlinear Ray Tracing

[Teh et al., 2022]

Nonlinear Ray Tracing

$$\frac{\mathrm{d}\mathbf{x}}{\mathrm{d}t} = \mathbf{v} \qquad \frac{\mathrm{d}\mathbf{v}}{\mathrm{d}t} = \eta \nabla \eta$$

[Teh et al., 2022]

Nonlinear Ray Tracing

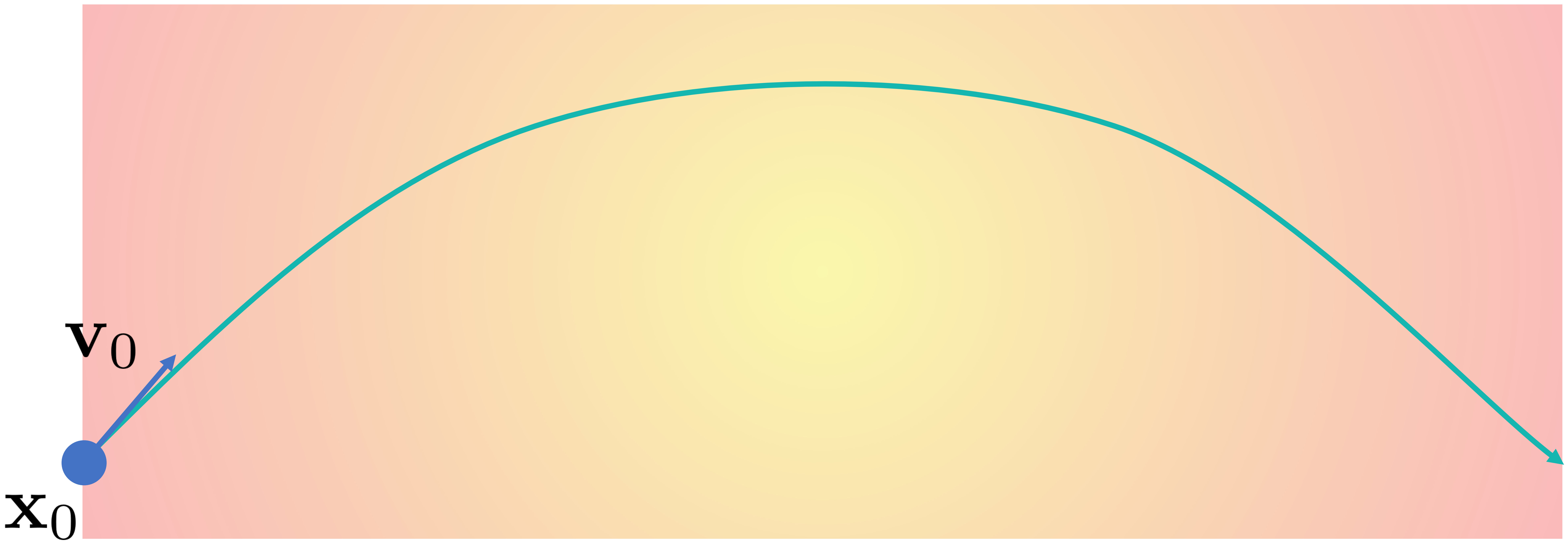

$$\frac{\mathrm{d}\mathbf{x}}{\mathrm{d}t} = \mathbf{v} \qquad \frac{\mathrm{d}\mathbf{v}}{\mathrm{d}t} = \eta \nabla \eta$$

[Teh et al., 2022]

Nonlinear Ray Tracing

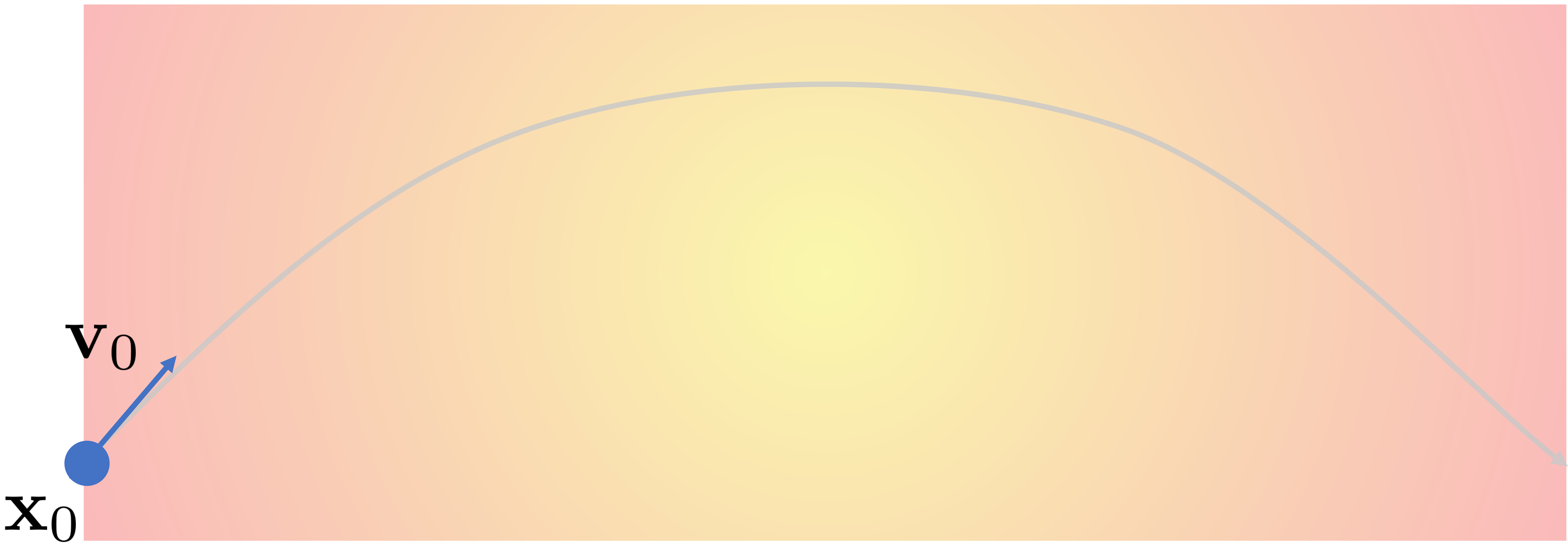

$$\mathbf{x}_i = \mathbf{x}_{i-1} + \mathbf{v}_i \Delta t \qquad \mathbf{v}_i = \mathbf{v}_{i-1} + \eta_{i-1} \nabla \eta_{i-1} \Delta t$$

[Teh et al., 2022]

Nonlinear Ray Tracing

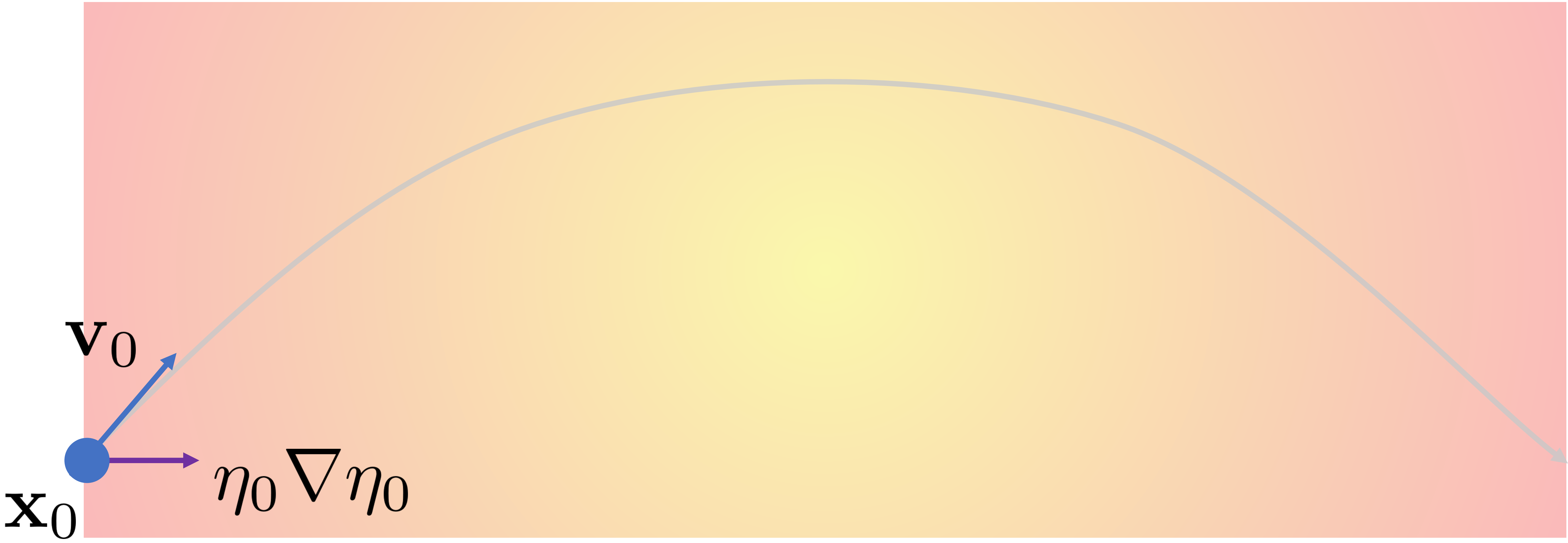

$$\mathbf{x}_i = \mathbf{x}_{i-1} + \mathbf{v}_i \Delta t \qquad \mathbf{v}_i = \mathbf{v}_{i-1} + \eta_{i-1} \nabla \eta_{i-1} \Delta t$$

[Teh et al., 2022]

Nonlinear Ray Tracing

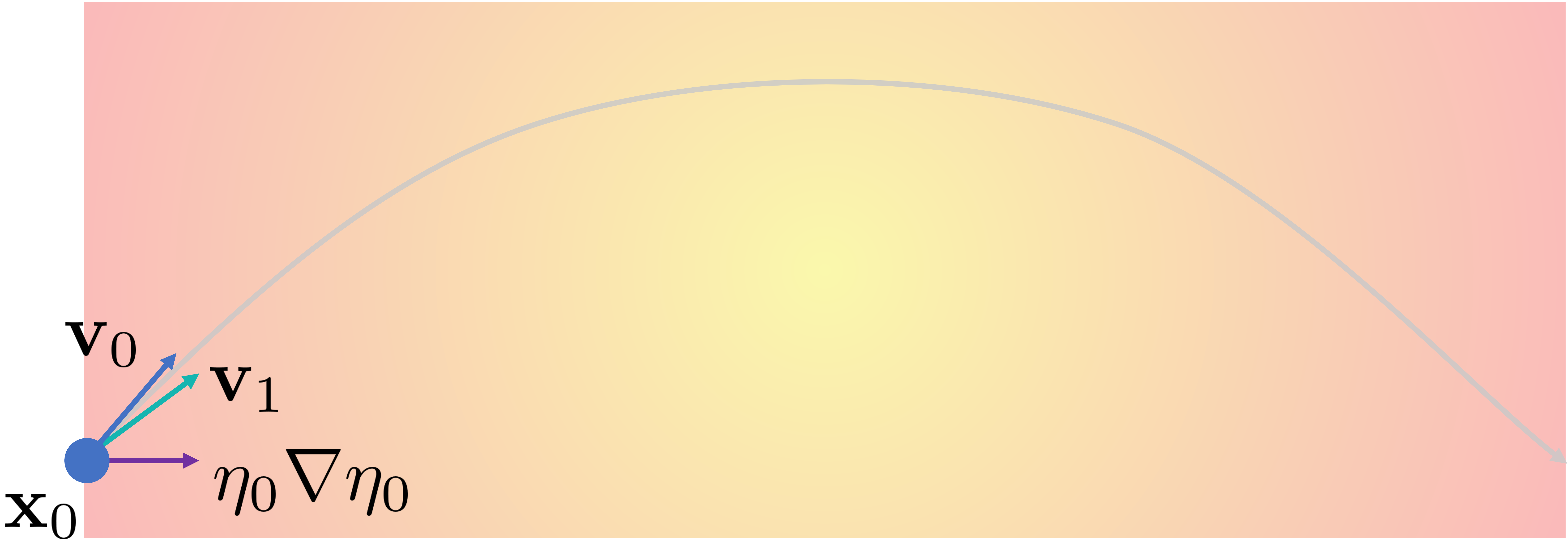

$$\mathbf{x}_i = \mathbf{x}_{i-1} + \mathbf{v}_i \Delta t$$

$$\boxed{\mathbf{v}_i = \mathbf{v}_{i-1} + \eta_{i-1} \nabla \eta_{i-1} \Delta t}$$

[Teh et al., 2022]

Nonlinear Ray Tracing

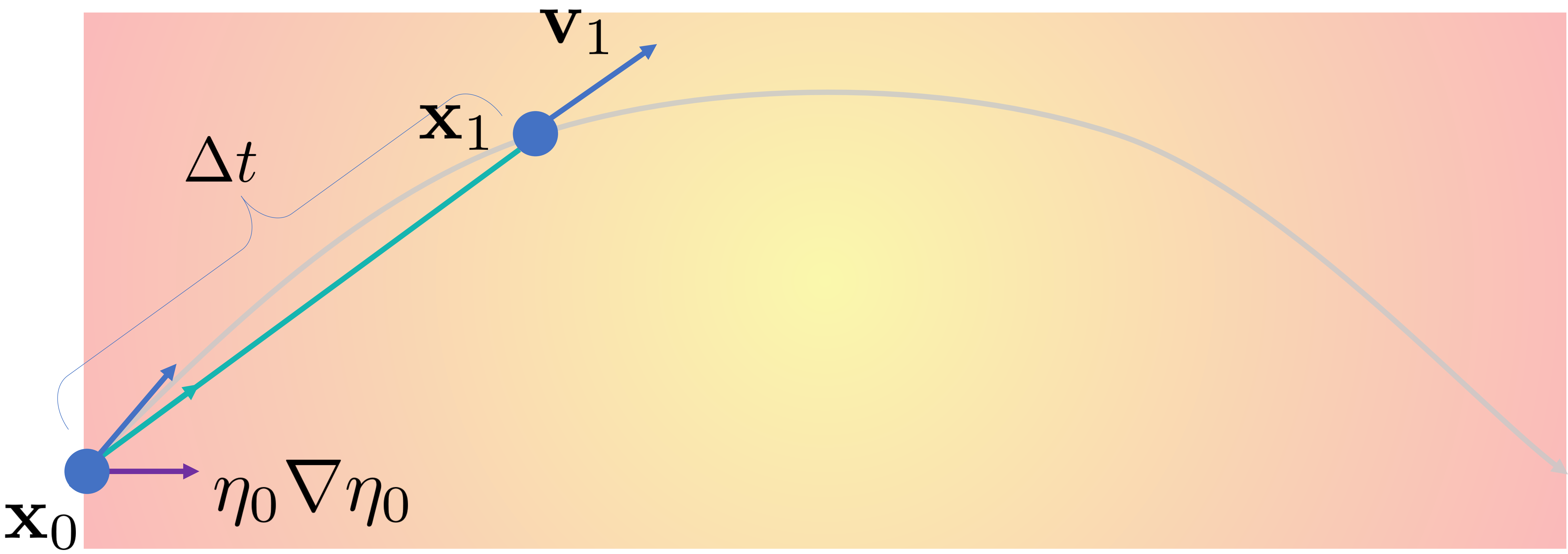

$$\boxed{\mathbf{x}_i = \mathbf{x}_{i-1} + \mathbf{v}_i \Delta t}$$

$$\mathbf{v}_i = \mathbf{v}_{i-1} + \eta_{i-1} \nabla \eta_{i-1} \Delta t$$

[Teh et al., 2022]

Nonlinear Ray Tracing

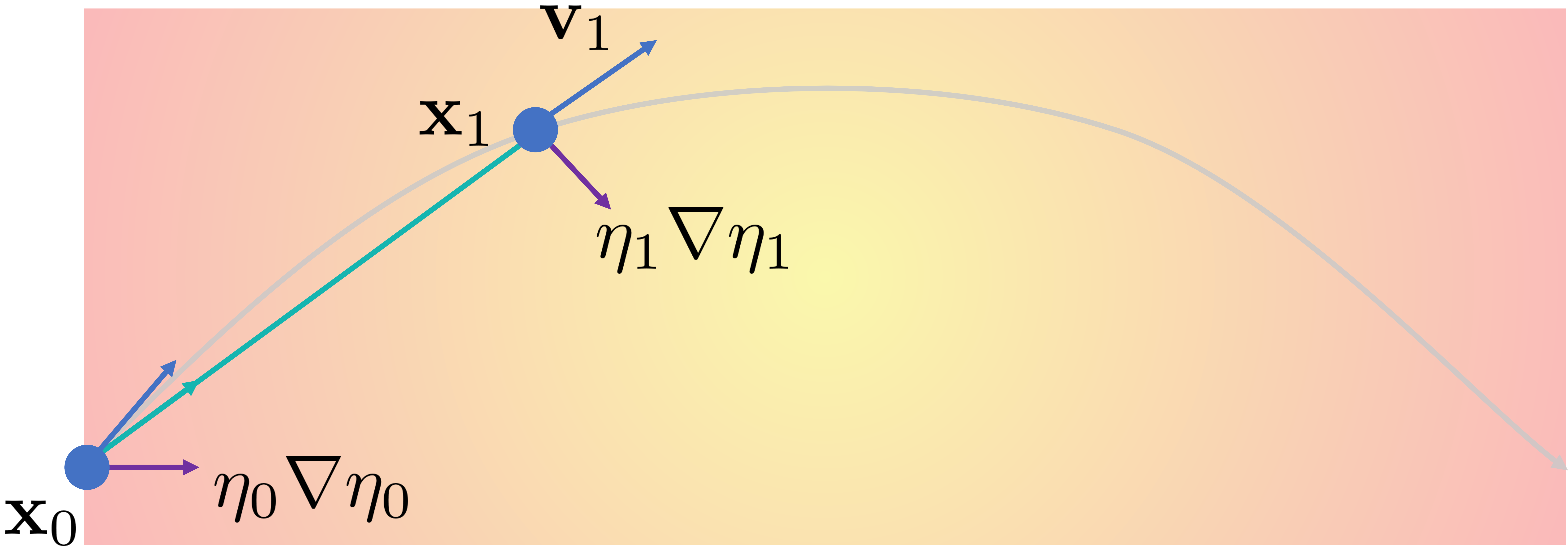

$$\boxed{\mathbf{x}_i = \mathbf{x}_{i-1} + \mathbf{v}_i \Delta t} \qquad \mathbf{v}_i = \mathbf{v}_{i-1} + \eta_{i-1} \nabla \eta_{i-1} \Delta t$$

[Teh et al., 2022]

Nonlinear Ray Tracing

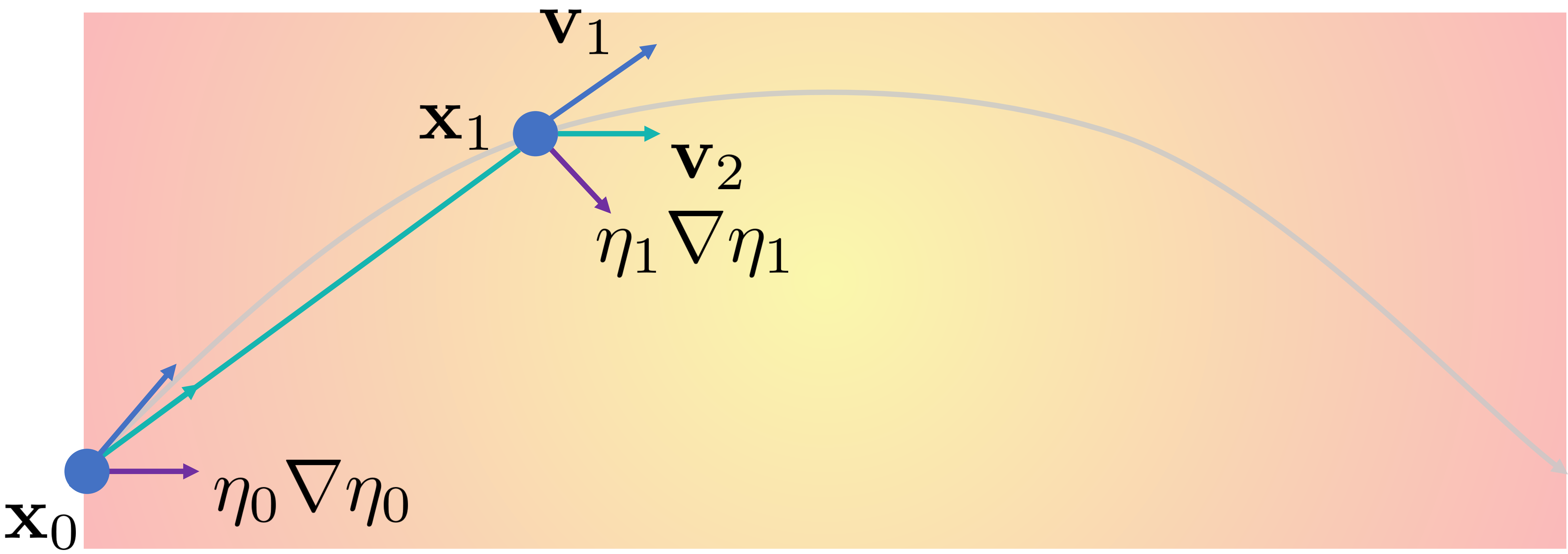

$$\mathbf{x}_i = \mathbf{x}_{i-1} + \mathbf{v}_i \Delta t \qquad \boxed{\mathbf{v}_i = \mathbf{v}_{i-1} + \eta_{i-1} \nabla \eta_{i-1} \Delta t}$$

[Teh et al., 2022]

Nonlinear Ray Tracing

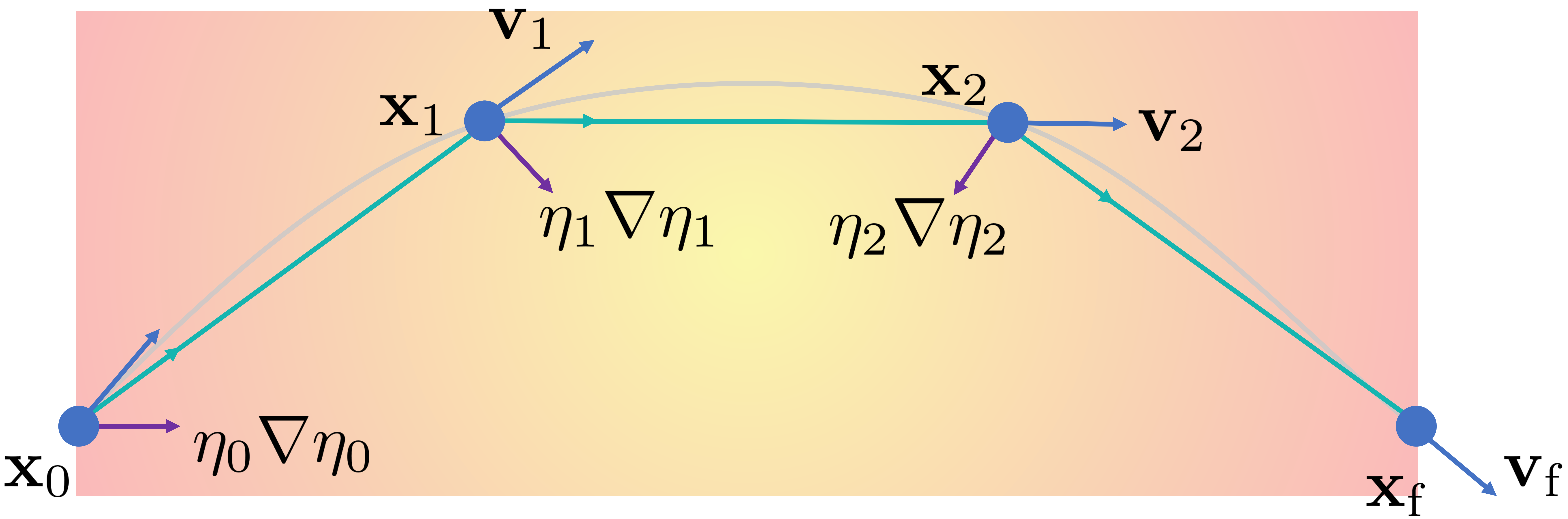

$$\mathbf{x}_i = \mathbf{x}_{i-1} + \mathbf{v}_i \Delta t \qquad \mathbf{v}_i = \mathbf{v}_{i-1} + \eta_{i-1} \nabla \eta_{i-1} \Delta t$$

[Teh et al., 2022]

Nonlinear Ray Tracing

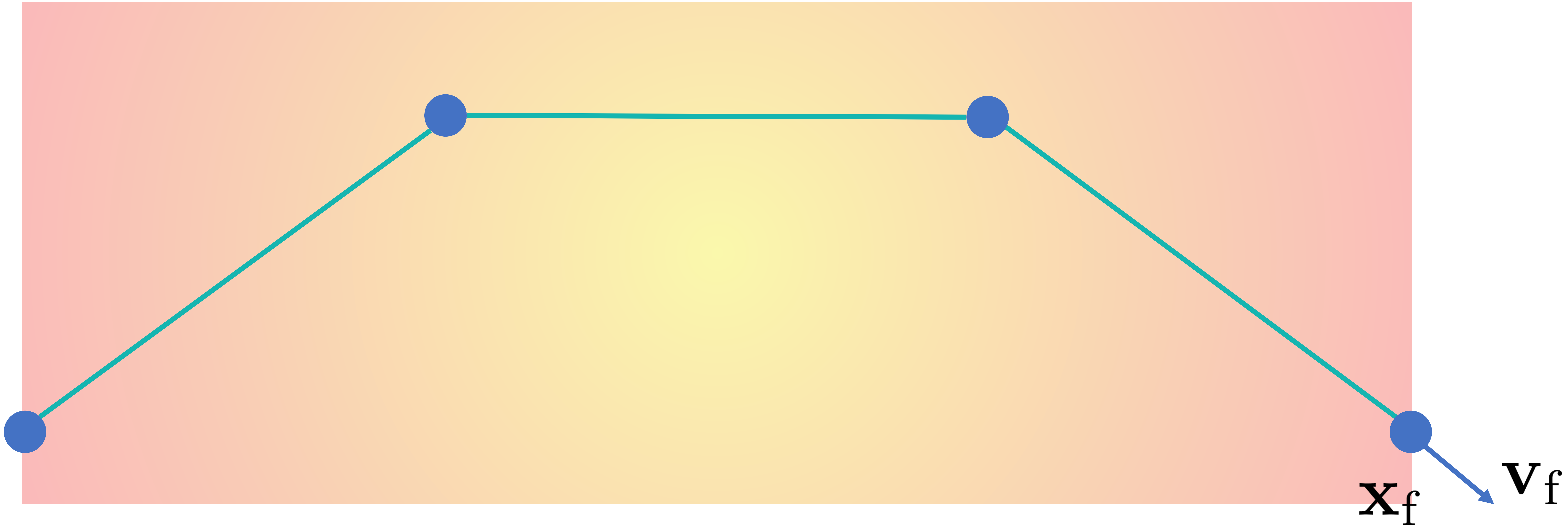

[Teh et al., 2022]

Nonlinear Ray Tracing

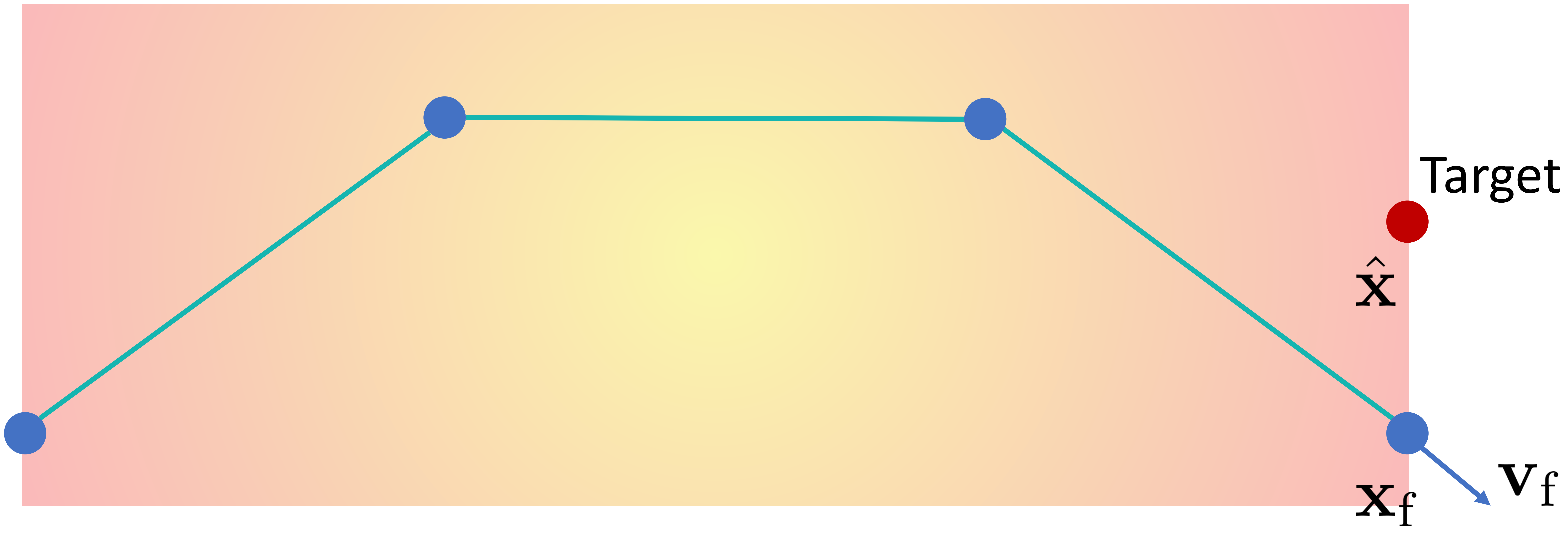

[Teh et al., 2022]

Nonlinear Ray Tracing

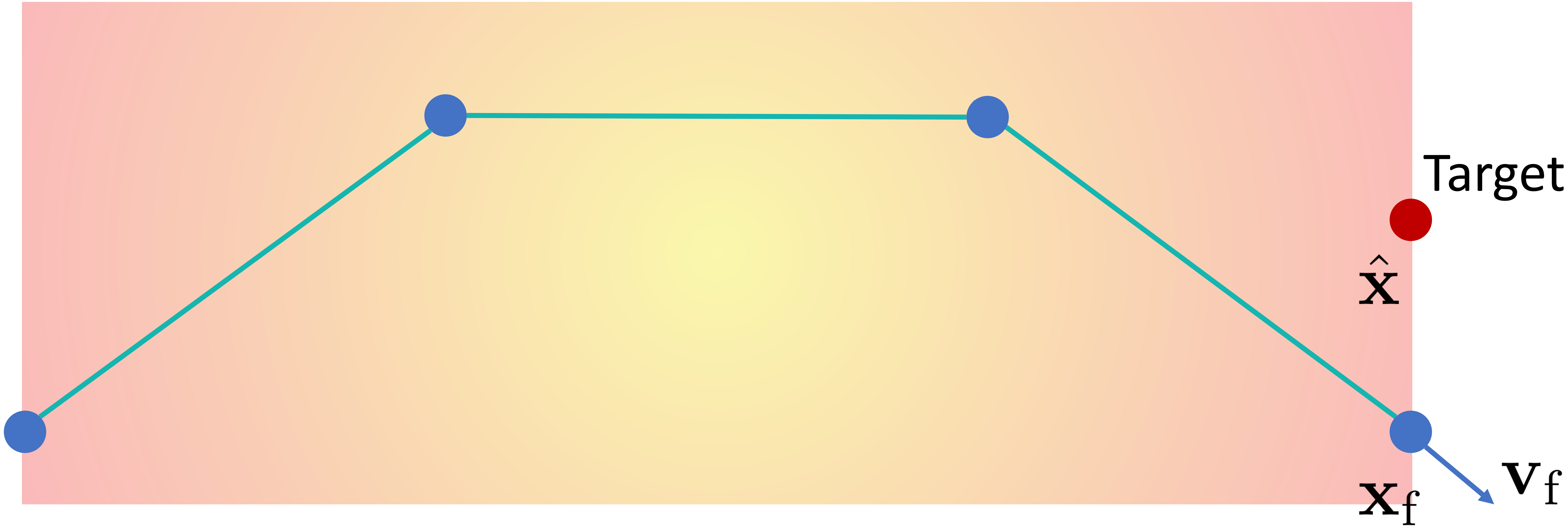

$$\min_{\eta} \left\| \hat{\mathbf{x}} - \mathbf{x}_\mathrm{f} \right\|^2$$

[Teh et al., 2022]

Nonlinear Ray Tracing

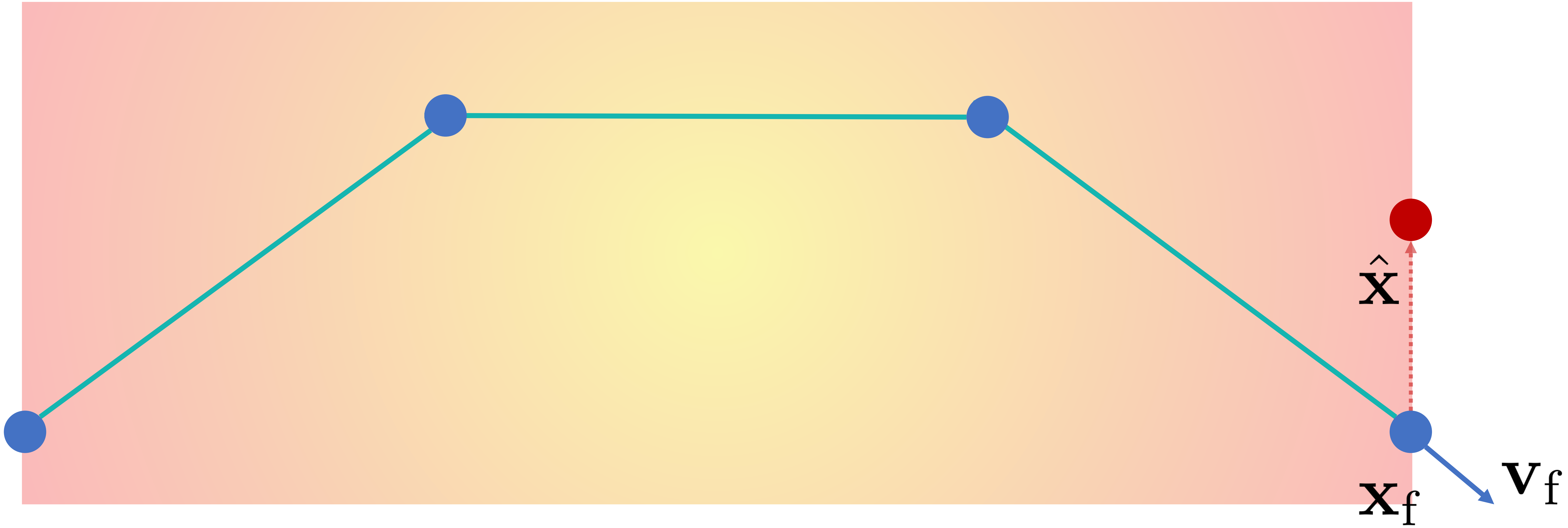

$$\frac{\mathrm{d}}{\mathrm{d}\eta}\|\hat{\mathbf{x}} - \mathbf{x}_\mathrm{f}\|^2$$

[Teh et al., 2022]

Nonlinear Ray Tracing in reverse

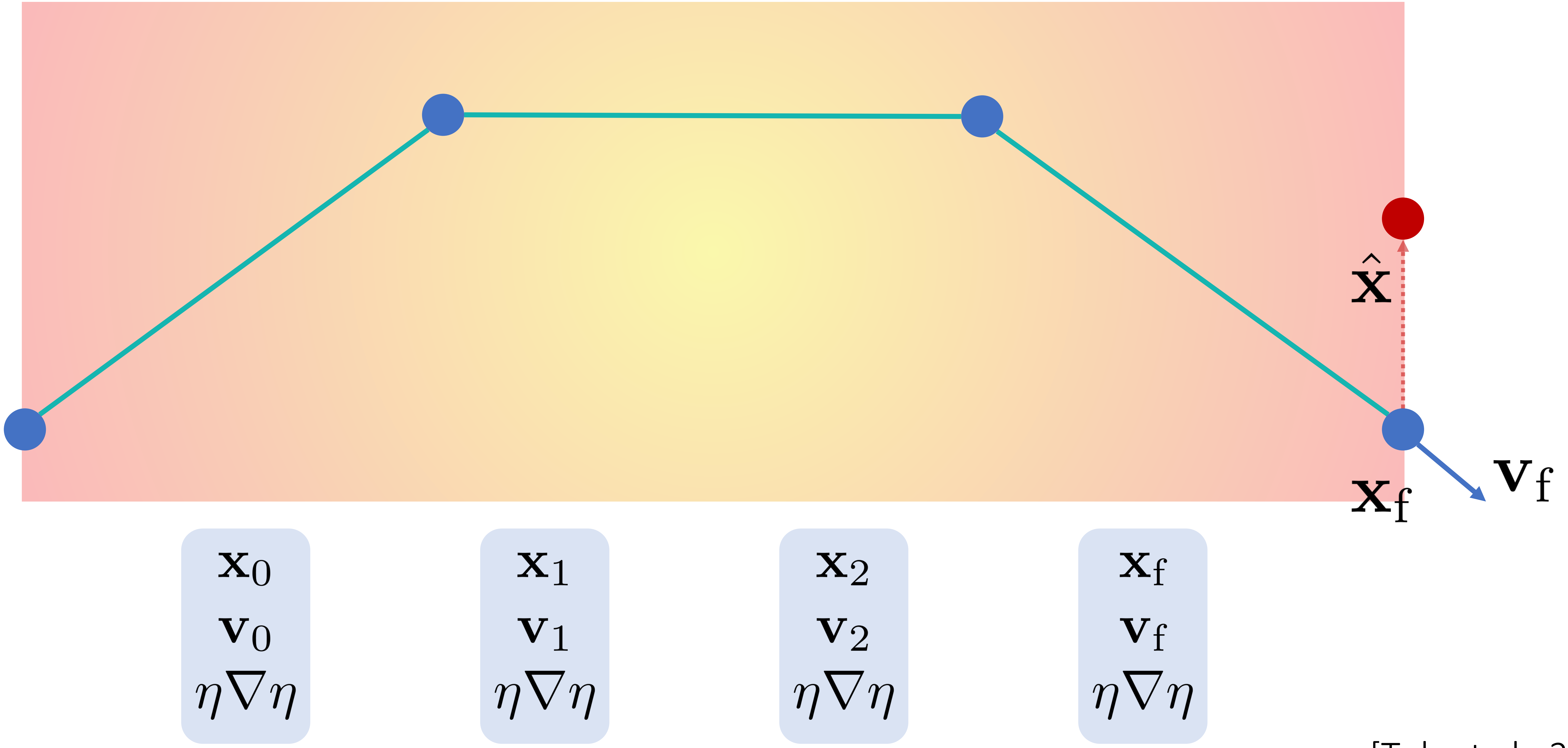

[Teh et al., 2022]

Nonlinear Ray Tracing in reverse

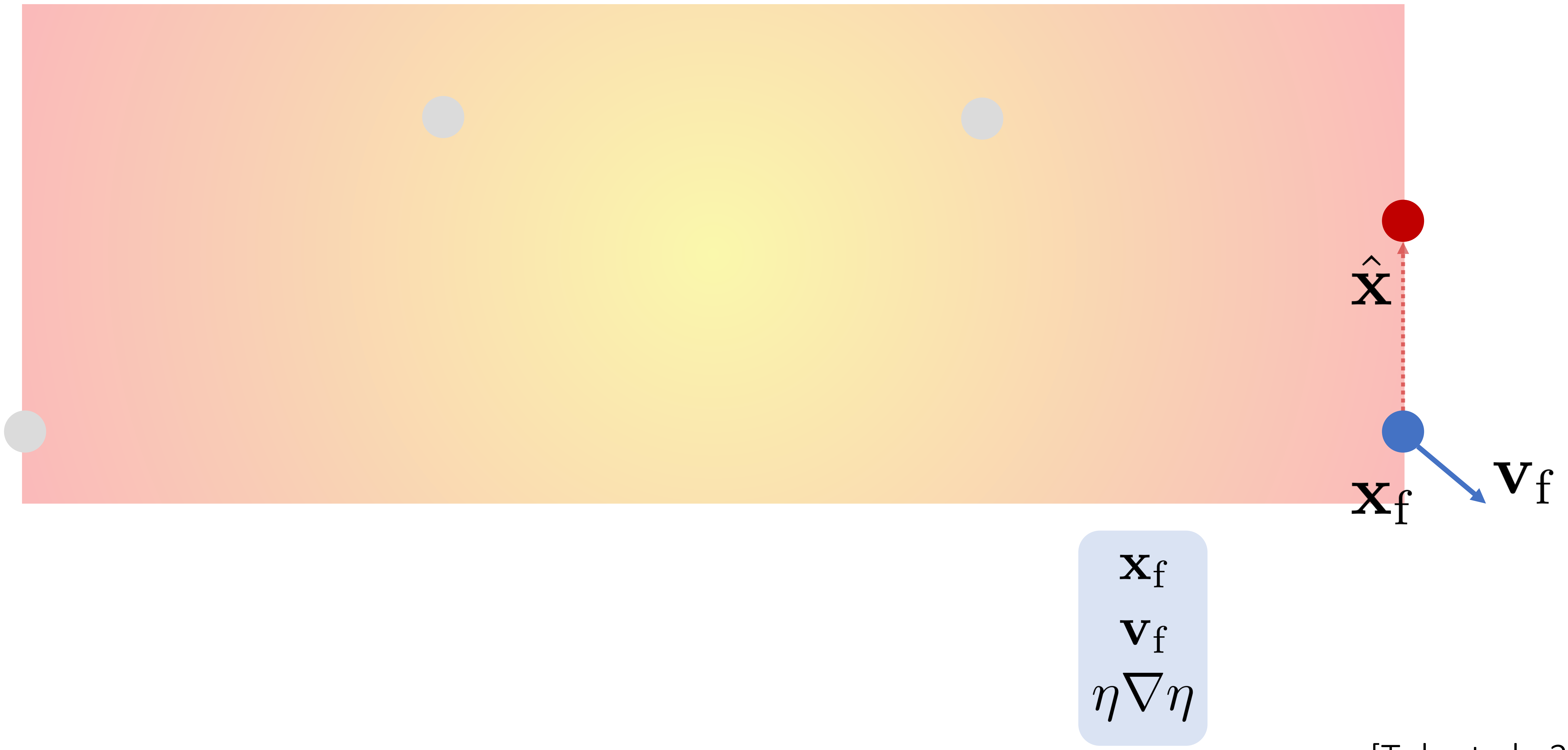

[Teh et al., 2022]

Nonlinear Ray Tracing in reverse

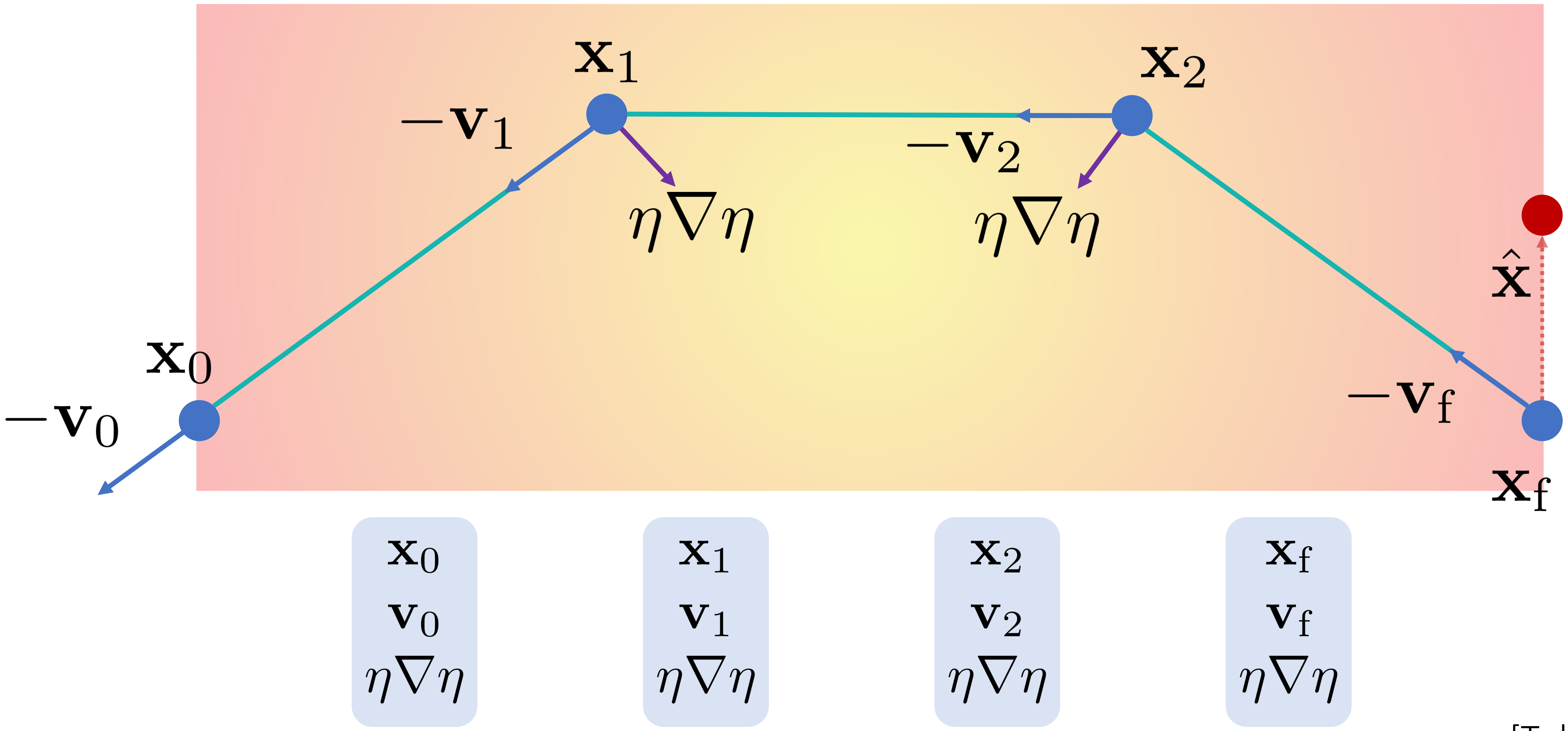

[Teh et al., 2022]

Nonlinear Ray Tracing in reverse

$$\min_{\eta} \sum_{i=1}^{N} \mathcal{F}_i \left[\iint_{(\mathbf{x}_0, \mathbf{v}_0) \in \Omega} C_i \left(\mathbf{x}\left(\sigma_f; \eta, \mathbf{x}_0, \mathbf{v}_0\right), \mathbf{v}\left(\sigma_f; \eta, \mathbf{x}_0, \mathbf{v}_0\right)\right) \, \mathrm{d}\mathbf{x}_0 \, \mathrm{d}\mathbf{v}_0 \right]$$
$$\text{s.t. } \dot{\mathbf{x}}\left(\sigma; \eta, \mathbf{x}_0, \mathbf{v}_0\right) = \mathbf{v}, \quad \forall \sigma \in \left[0, \sigma_f\right],$$
$$\dot{\mathbf{v}}\left(\sigma; \eta, \mathbf{x}_0, \mathbf{v}_0\right) = \eta \nabla \eta, \quad \forall \sigma \in \left[0, \sigma_f\right],$$
$$\mathbf{x}\left(0; \eta, \mathbf{x}_0, \mathbf{v}_0\right) = \mathbf{x}_0,$$
$$\mathbf{v}\left(0; \eta, \mathbf{x}_0, \mathbf{v}_0\right) = \mathbf{v}_0, \tag{15}$$

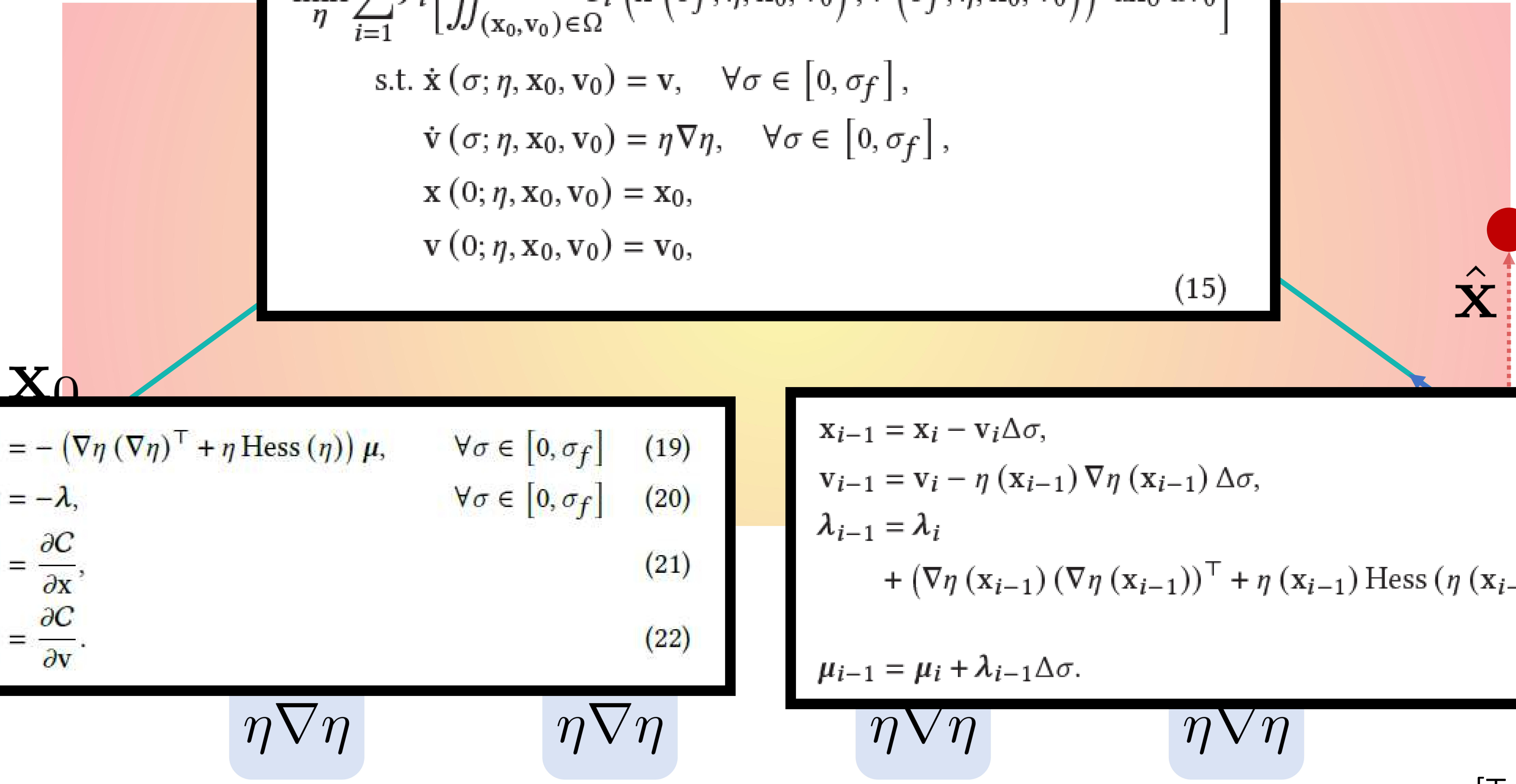

$$\dot{\boldsymbol{\lambda}} = -\left(\nabla\eta\left(\nabla\eta\right)^{\top} + \eta \,\mathrm{Hess}\left(\eta\right)\right)\boldsymbol{\mu}, \quad \forall \sigma \in \left[0, \sigma_f\right] \tag{19}$$
$$\dot{\boldsymbol{\mu}} = -\boldsymbol{\lambda}, \quad \forall \sigma \in \left[0, \sigma_f\right] \tag{20}$$
$$\boldsymbol{\lambda}\left(\sigma_f\right) = \frac{\partial C}{\partial \mathbf{x}}, \tag{21}$$
$$\boldsymbol{\mu}\left(\sigma_f\right) = \frac{\partial C}{\partial \mathbf{v}}. \tag{22}$$

$$\mathbf{x}_{i-1} = \mathbf{x}_i - \mathbf{v}_i \Delta\sigma, \tag{28}$$
$$\mathbf{v}_{i-1} = \mathbf{v}_i - \eta\left(\mathbf{x}_{i-1}\right)\nabla\eta\left(\mathbf{x}_{i-1}\right)\Delta\sigma, \tag{29}$$
$$\boldsymbol{\lambda}_{i-1} = \boldsymbol{\lambda}_i + \left(\nabla\eta\left(\mathbf{x}_{i-1}\right)\left(\nabla\eta\left(\mathbf{x}_{i-1}\right)\right)^{\top} + \eta\left(\mathbf{x}_{i-1}\right)\mathrm{Hess}\left(\eta\left(\mathbf{x}_{i-1}\right)\right)\right)\boldsymbol{\mu}_i \Delta\sigma, \tag{30}$$
$$\boldsymbol{\mu}_{i-1} = \boldsymbol{\mu}_i + \boldsymbol{\lambda}_{i-1}\Delta\sigma. \tag{31}$$

[Teh et al., 2022]

Optimizing Gradient-Index (GRIN) Optics

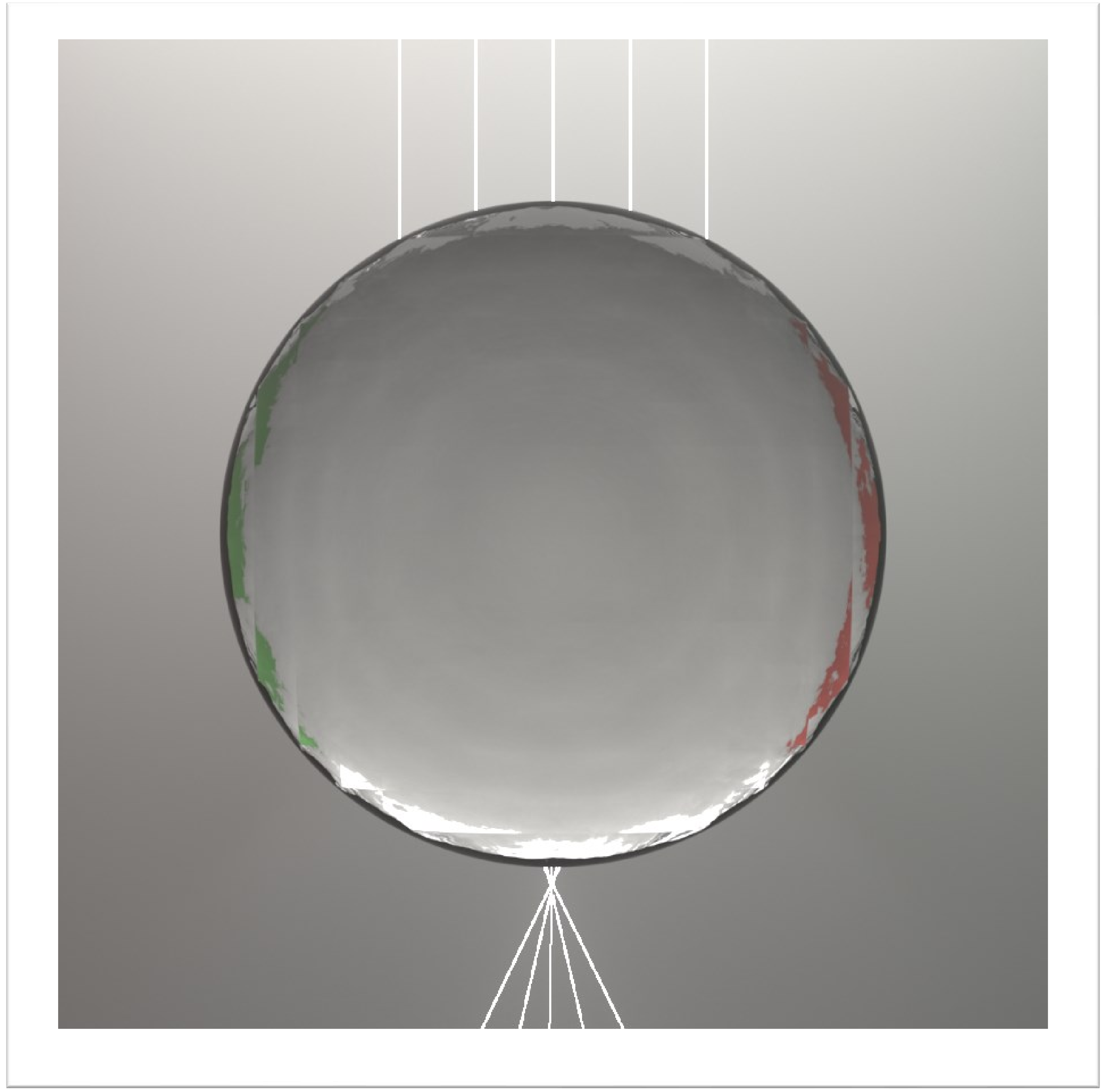

Luneburg Lens

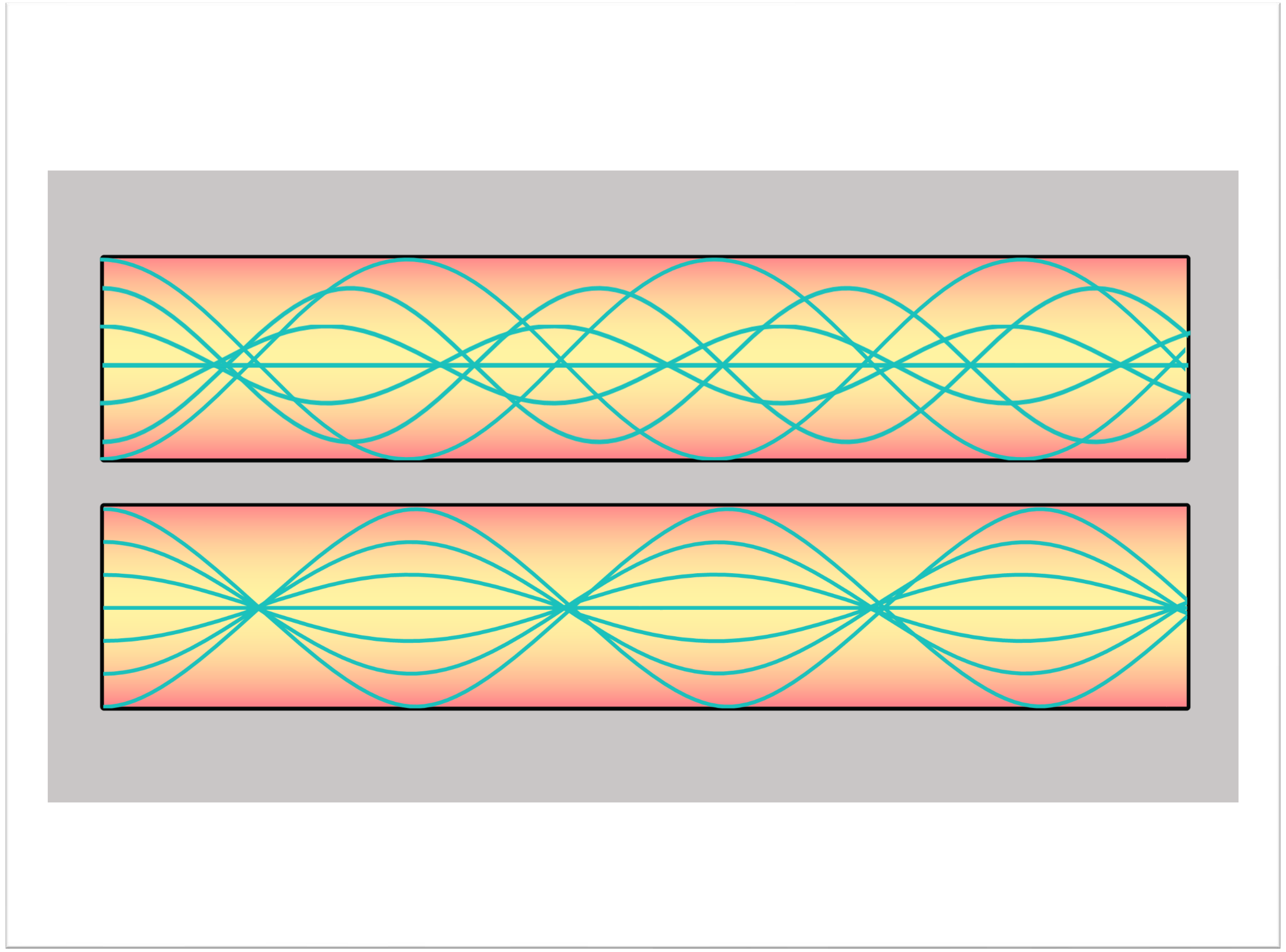

GRIN Fiber

[Teh et al., 2022]

Optimizing Gradient-Index (GRIN) Optics

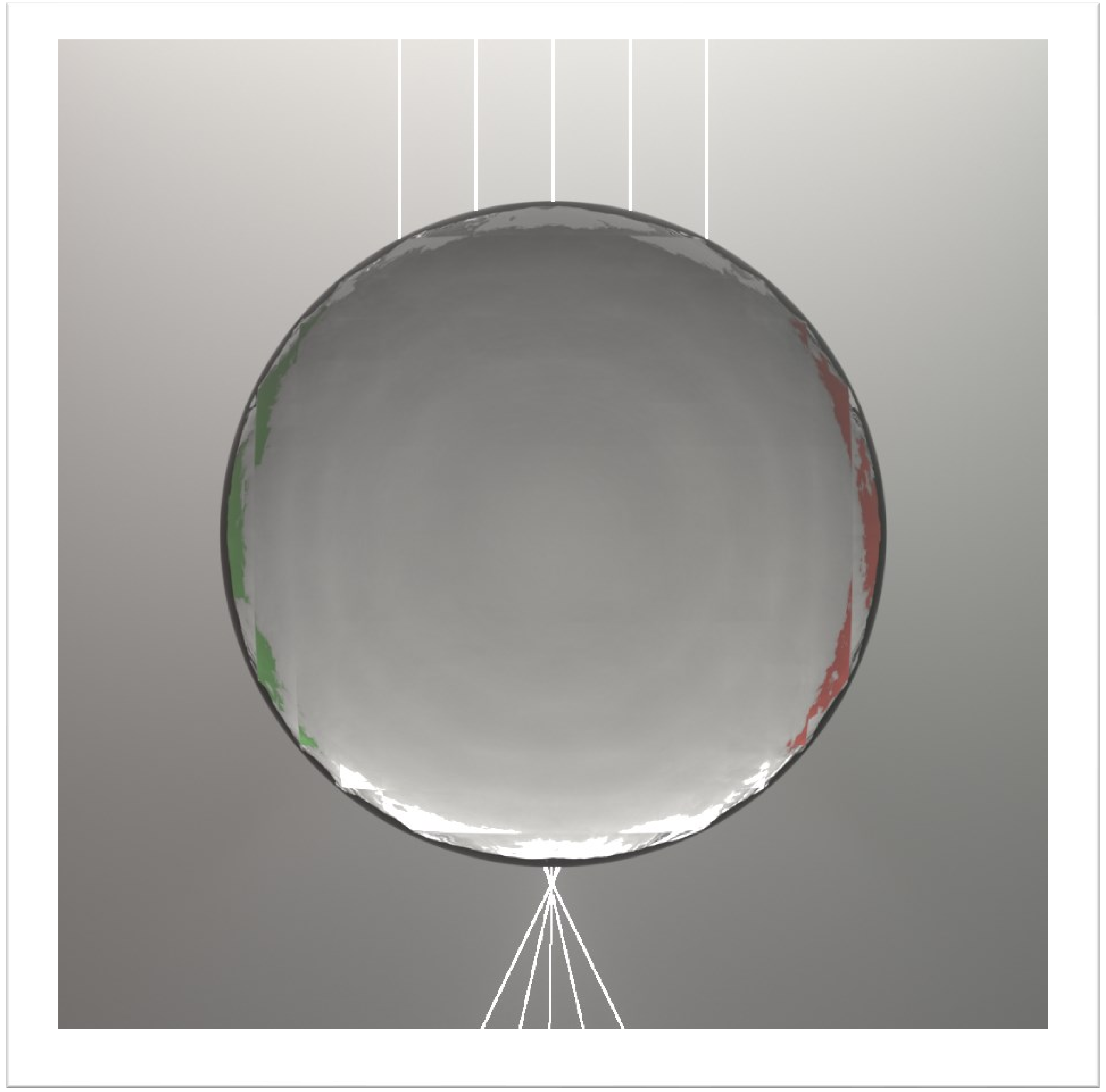

Luneburg Lens

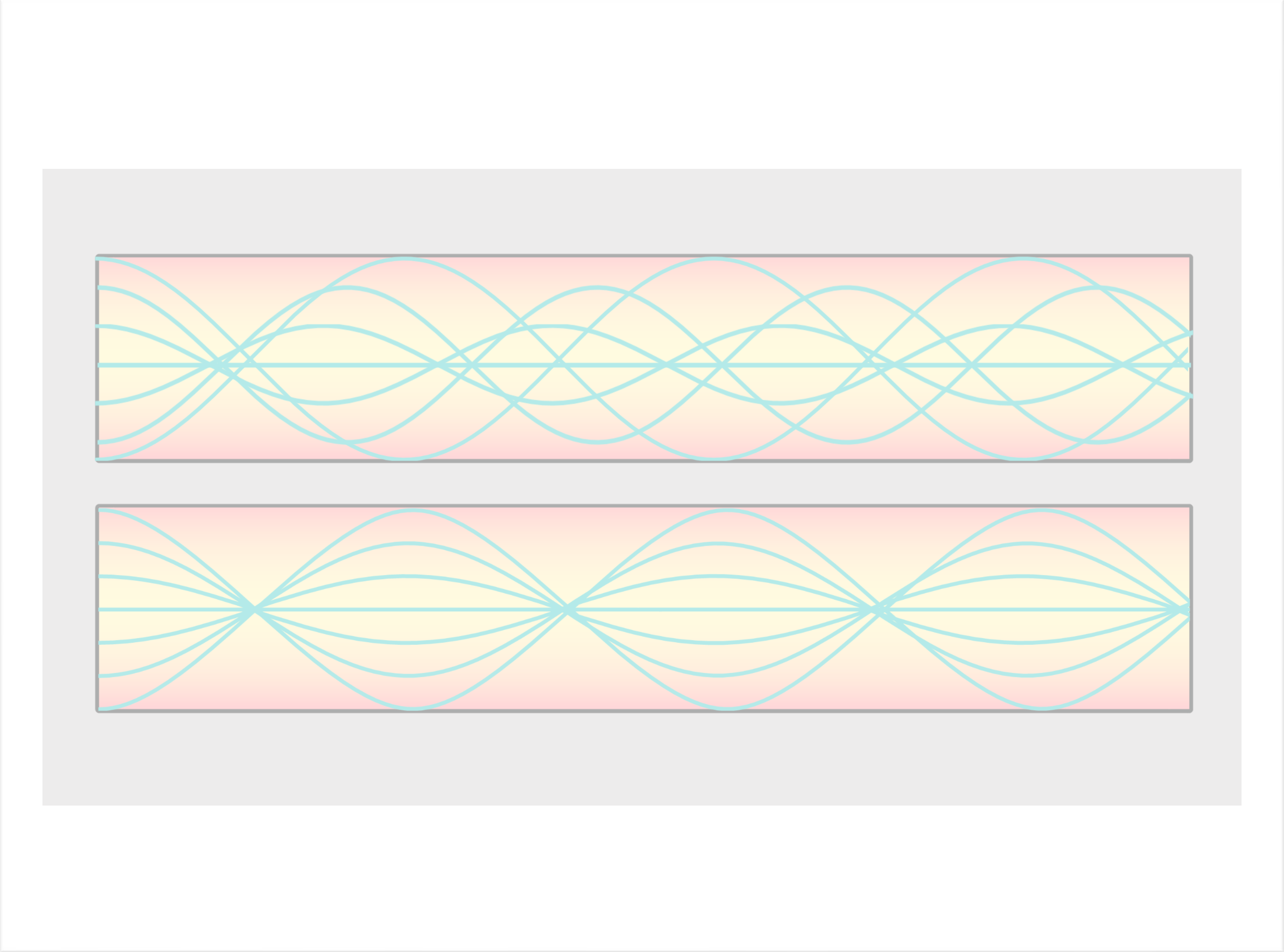

GRIN Fiber

[Teh et al., 2022]

Luneburg Lens

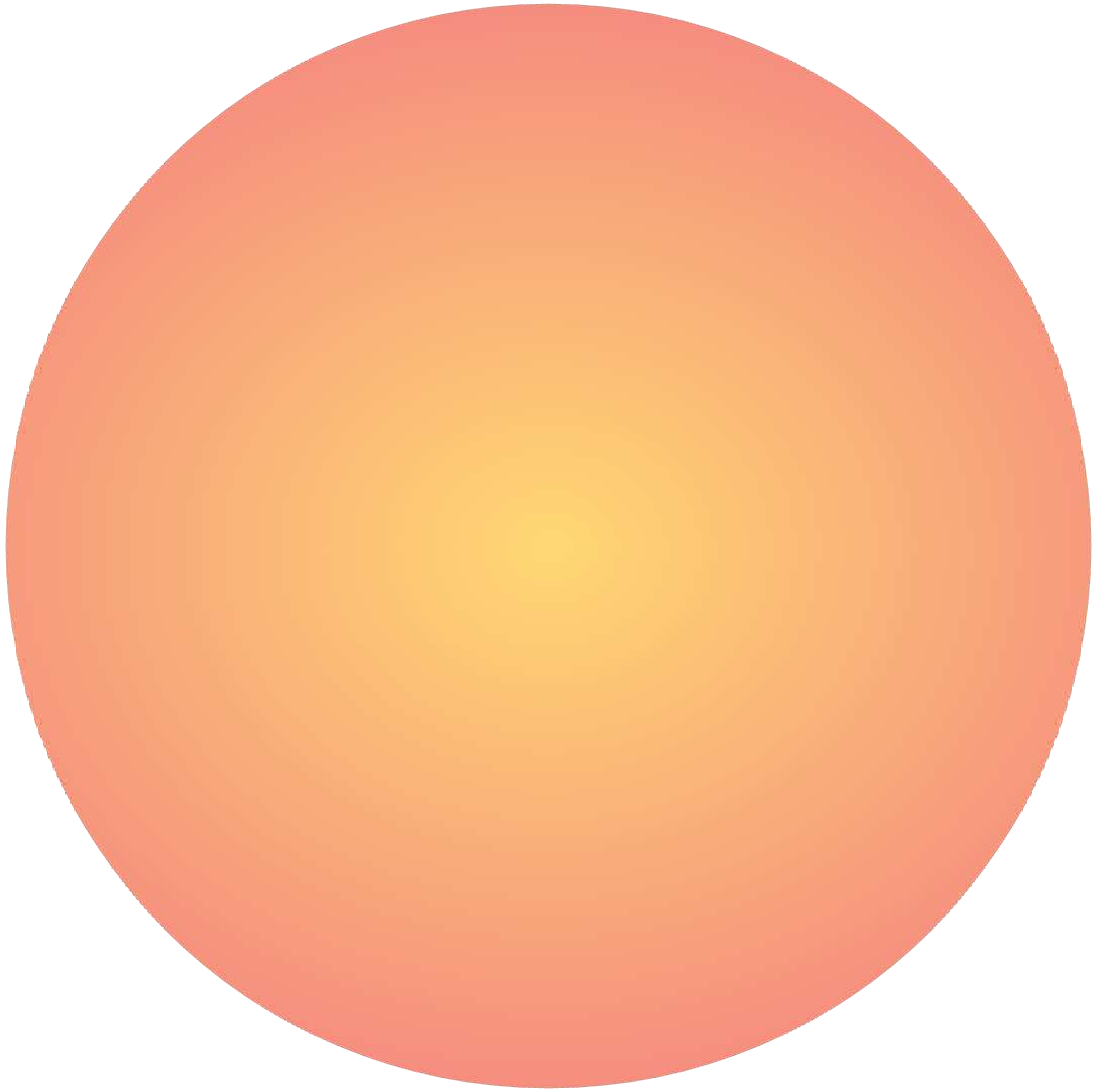

Luneburg Lens

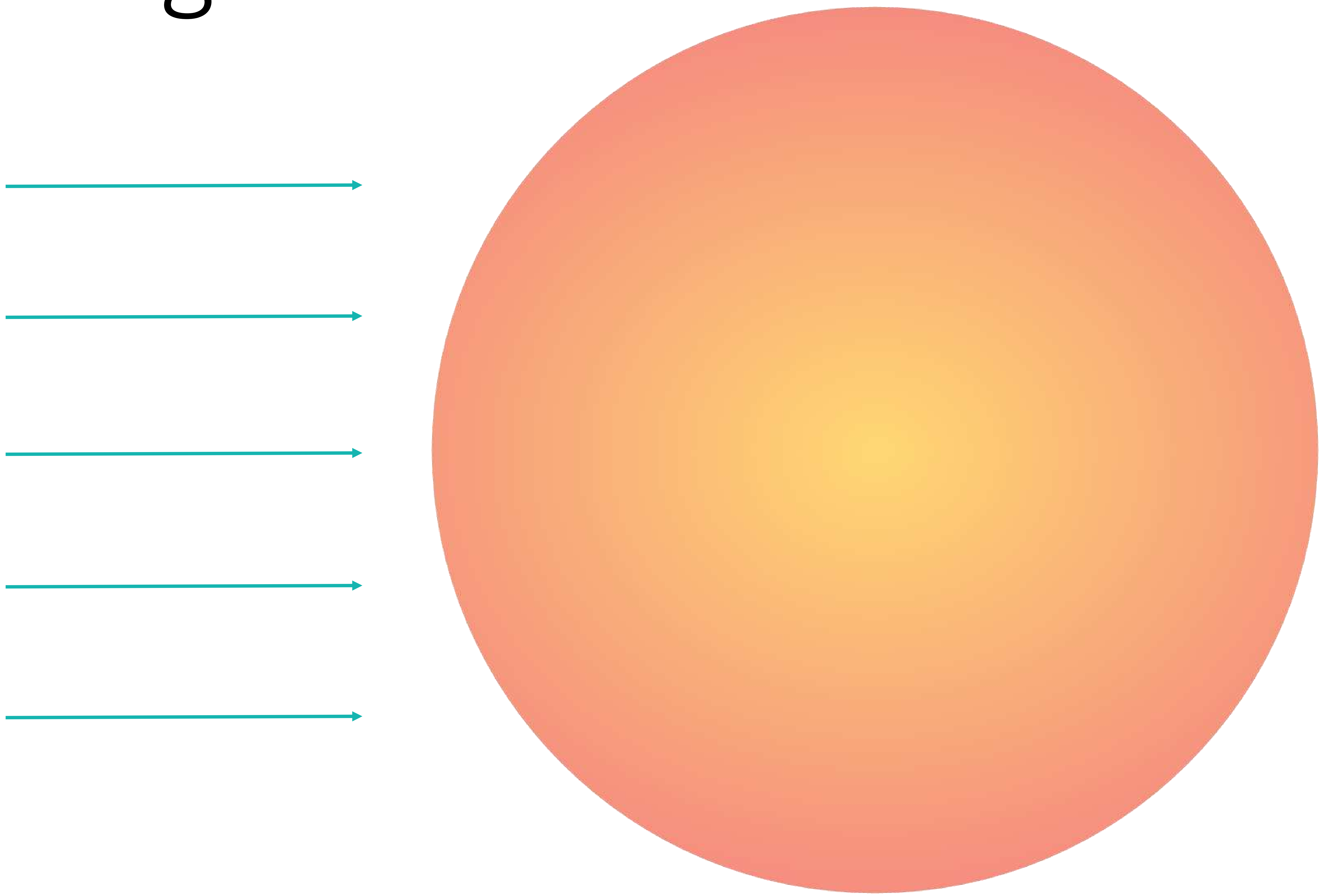

Luneburg Lens

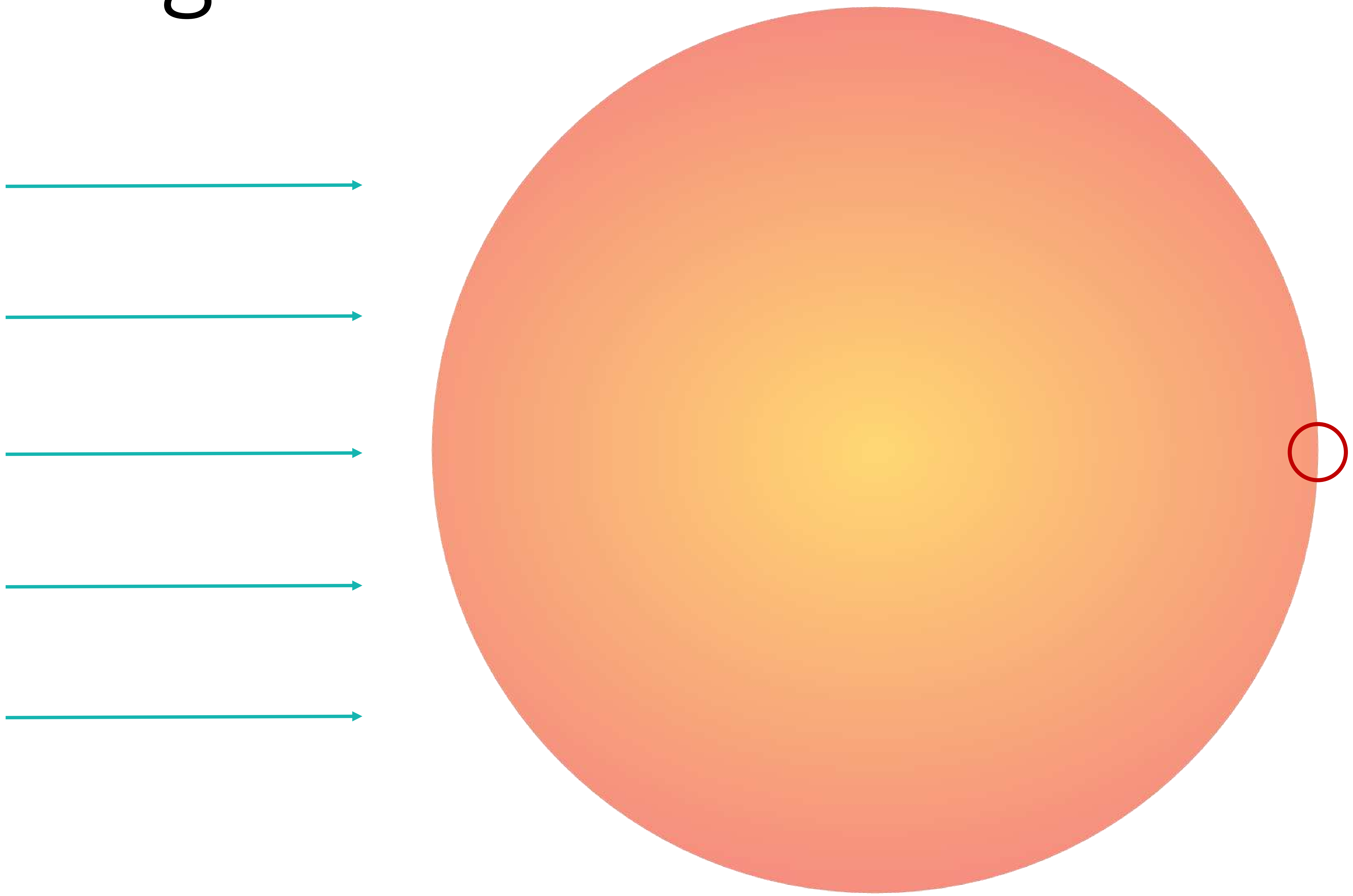

Luneburg Lens

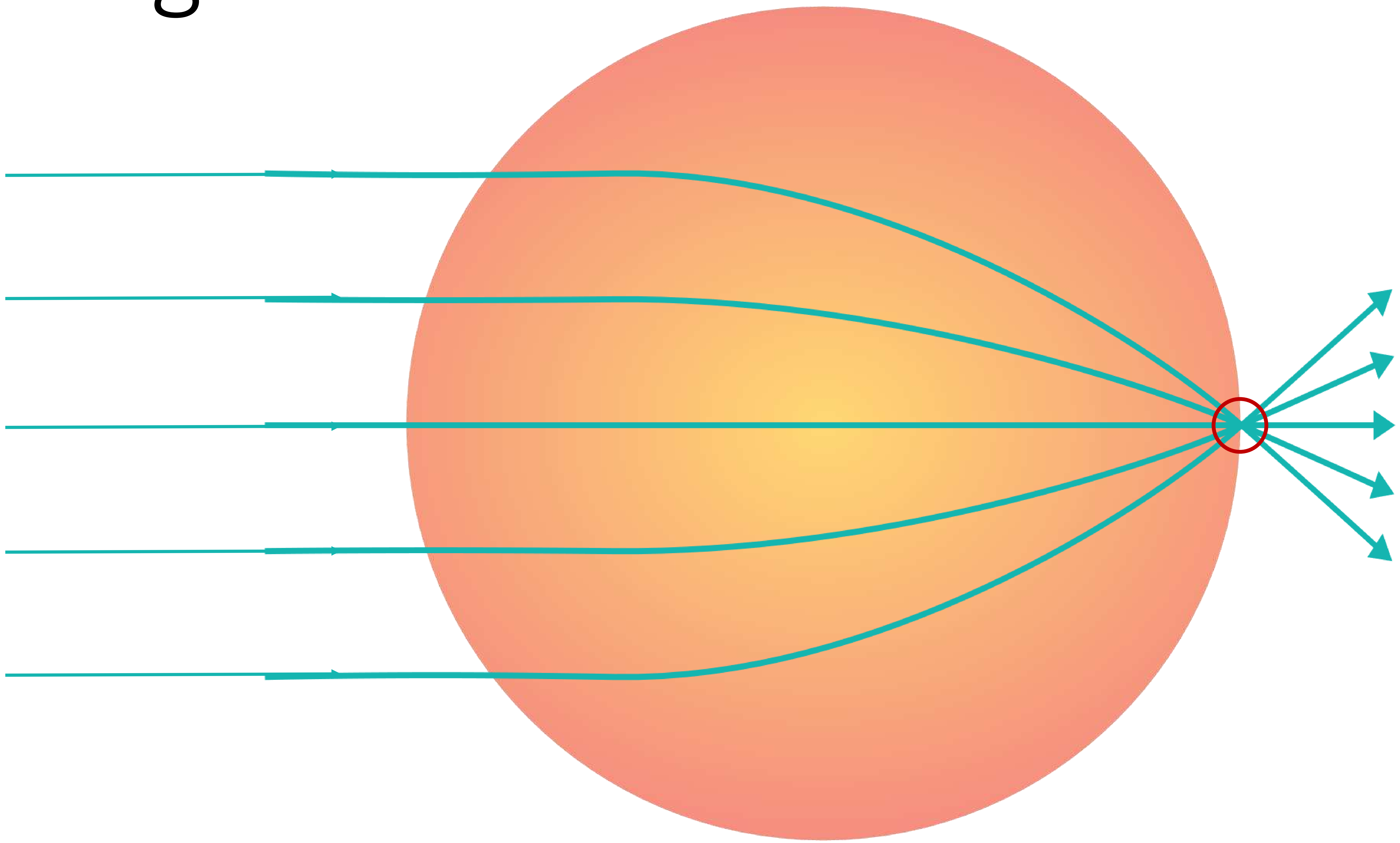

Luneburg Lens

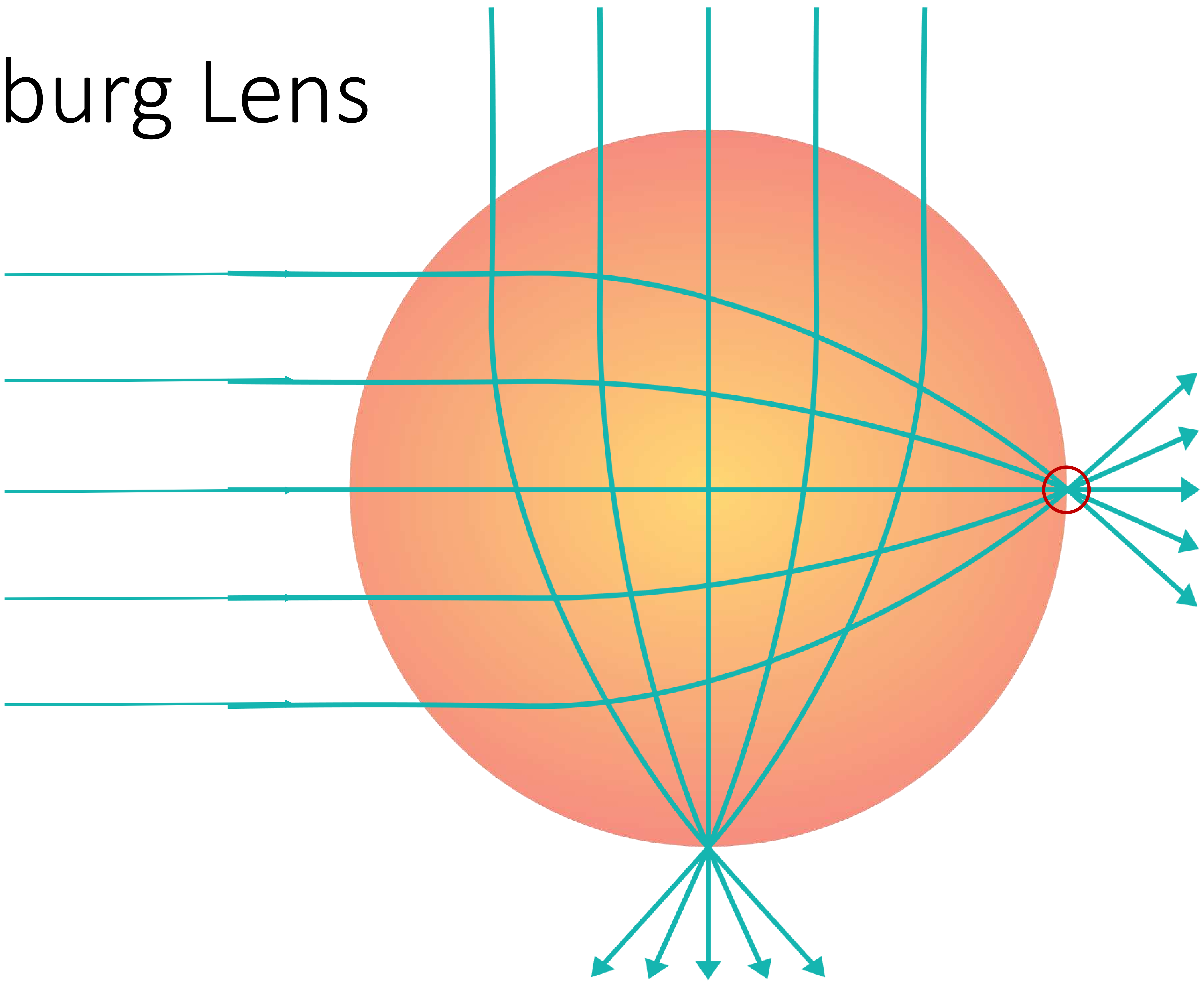

Luneburg Lens

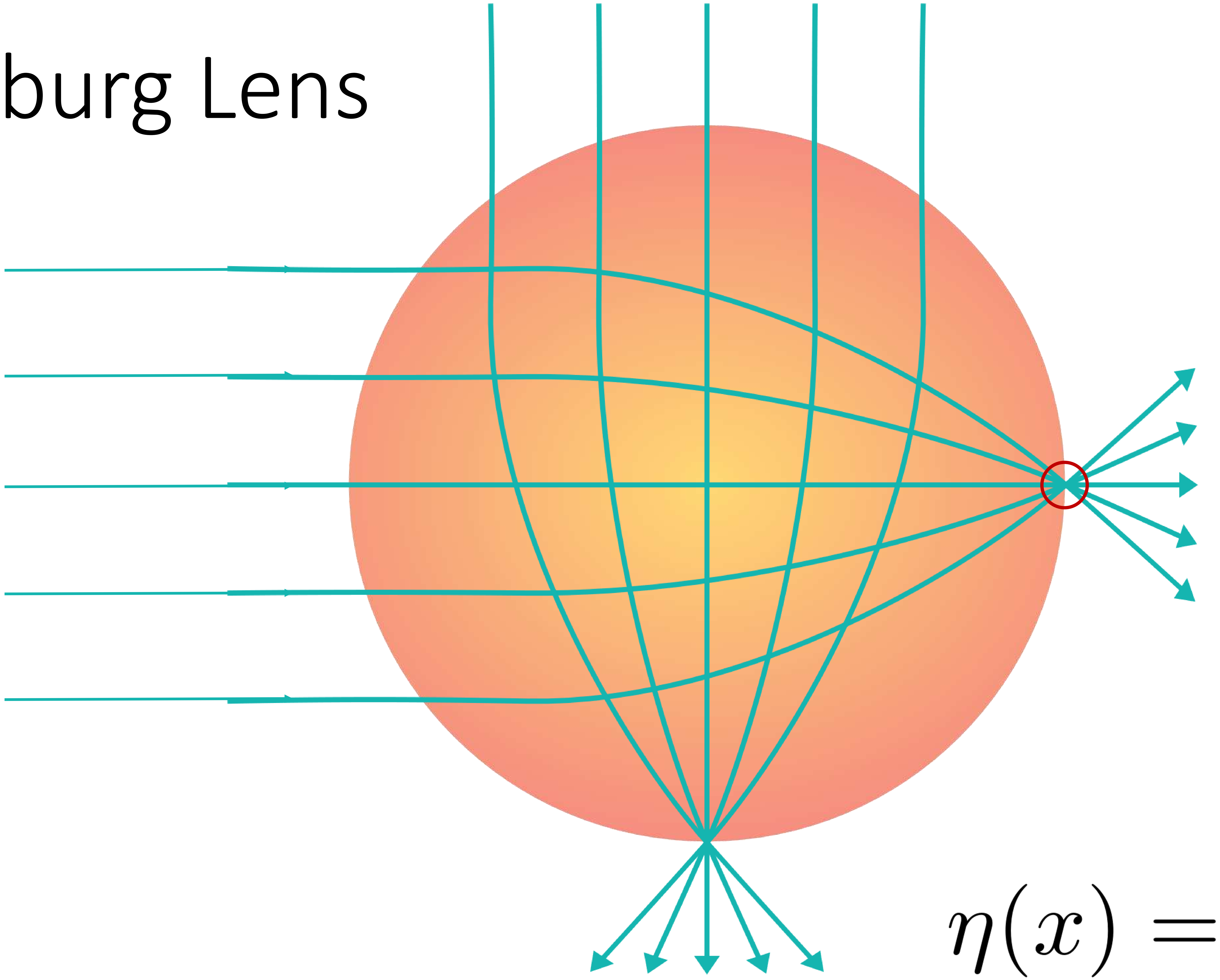

$$\eta(x) = \sqrt{2 - \|x\|^2}$$

[Luneburg, R. K. 1944]

Luneburg Lens

[Teh et al., 2022]

Luneburg Lens

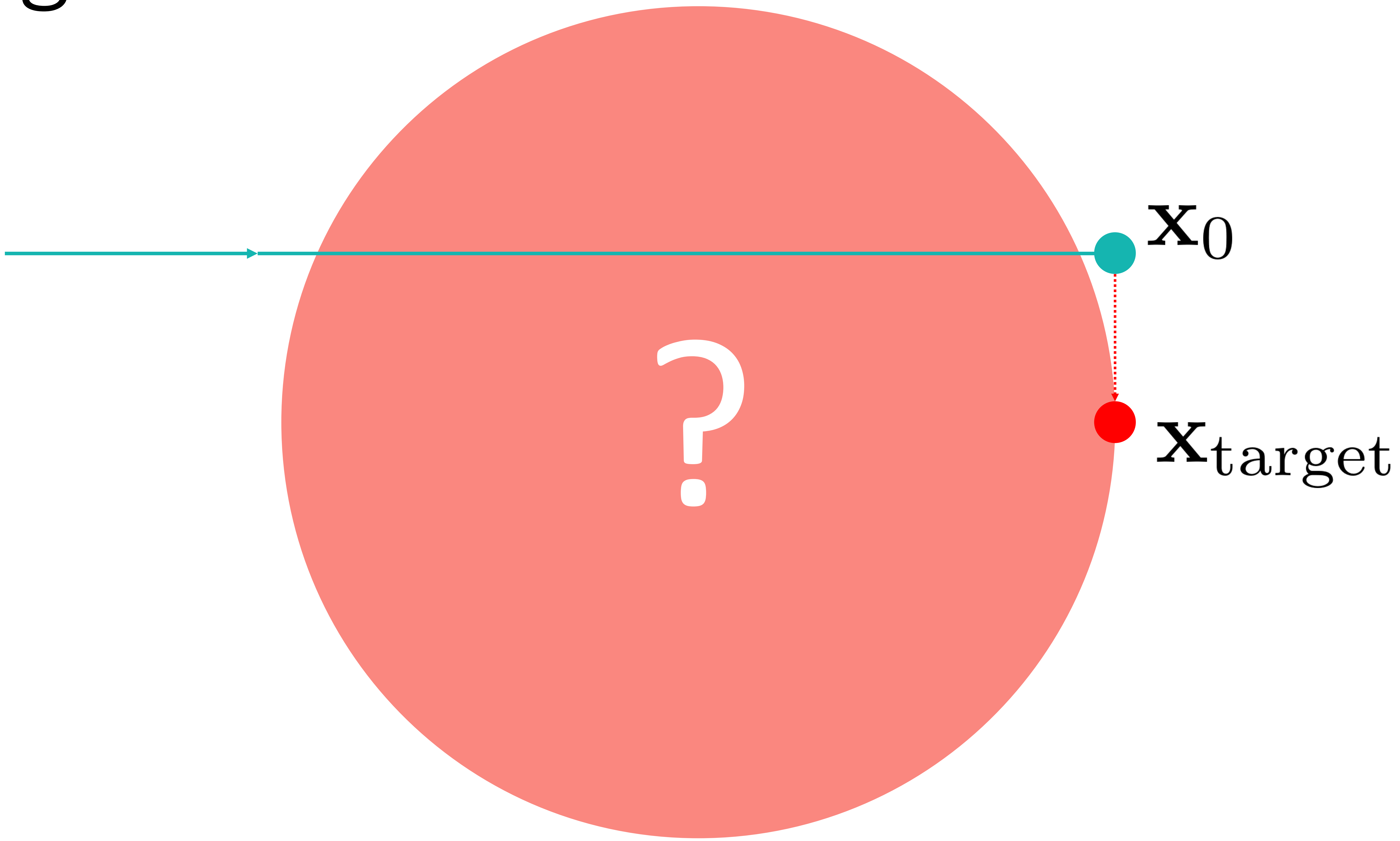

[Teh et al., 2022]

Luneburg Lens

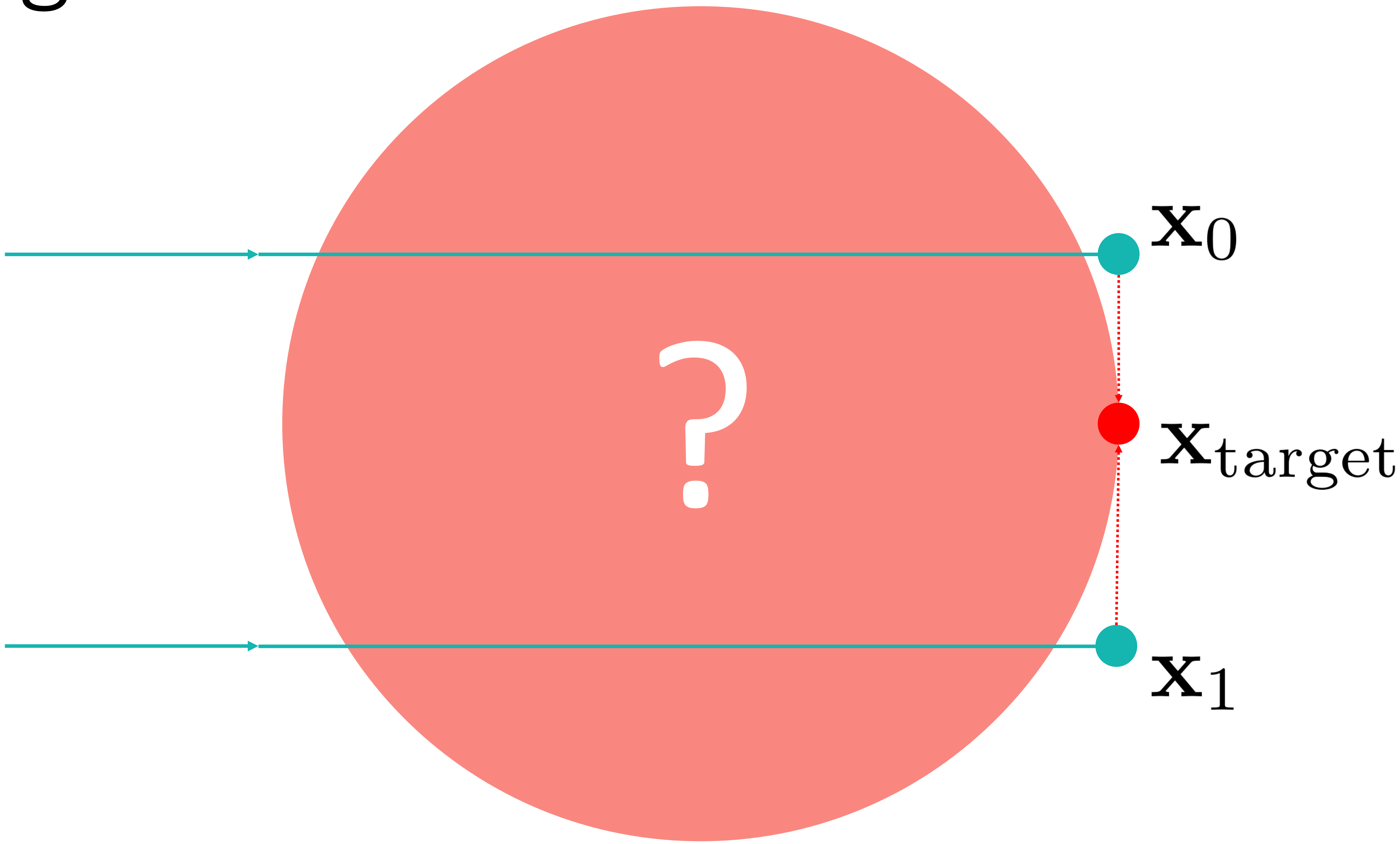

$$\min_{\eta} \sum_{i \in \text{rays}} \left\| \mathbf{x}_{\text{target}} - \mathbf{x}_{\text{i}} \right\|^2$$

[Teh et al., 2022]

Luneburg Lens

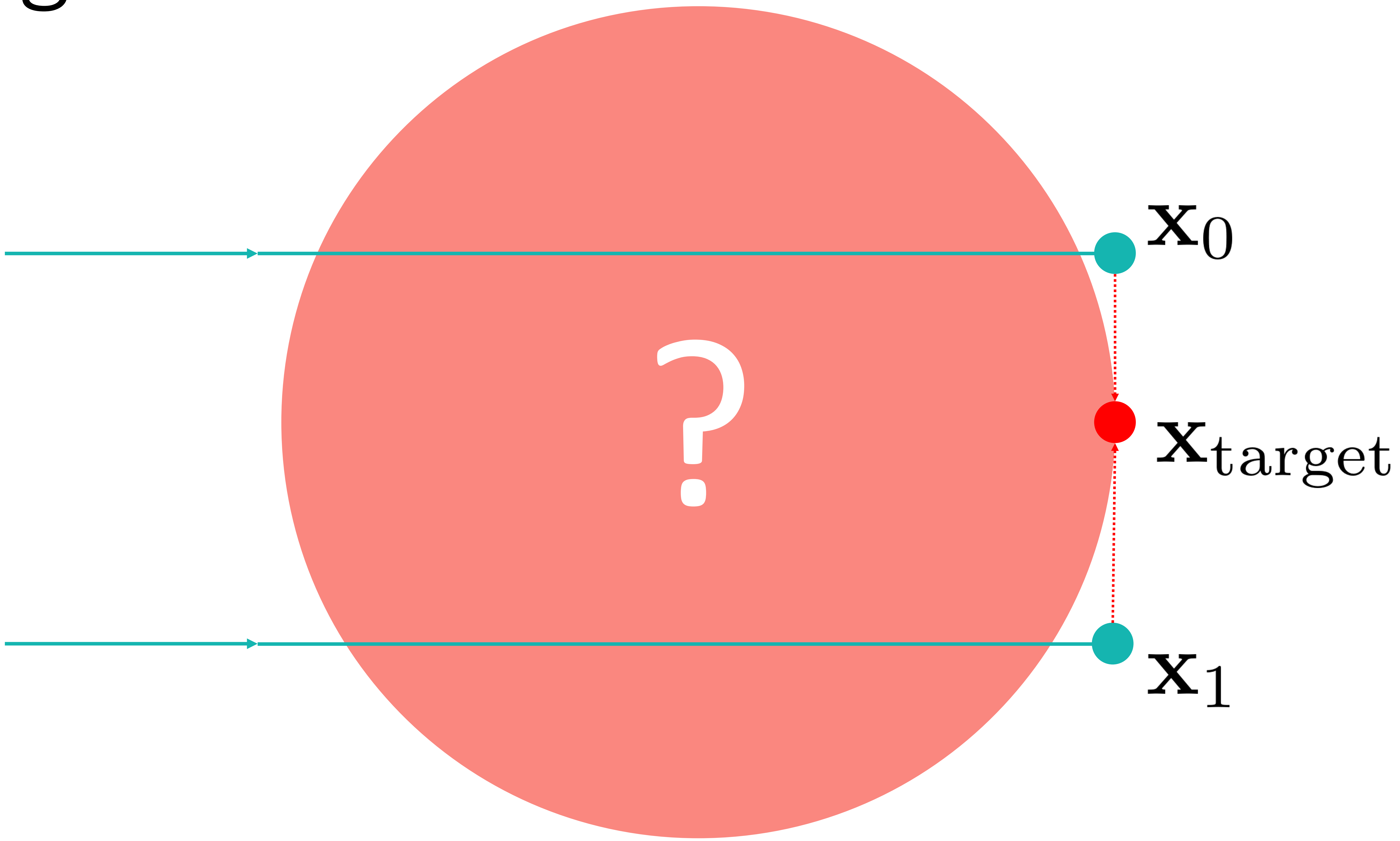

$$\min_{\eta} \sum_{i \in \text{rays}} \left\| \mathbf{x}_{\text{target}} - \mathbf{x}_{\text{i}} \right\|^2$$

[Teh et al., 2022]

Luneburg Lens

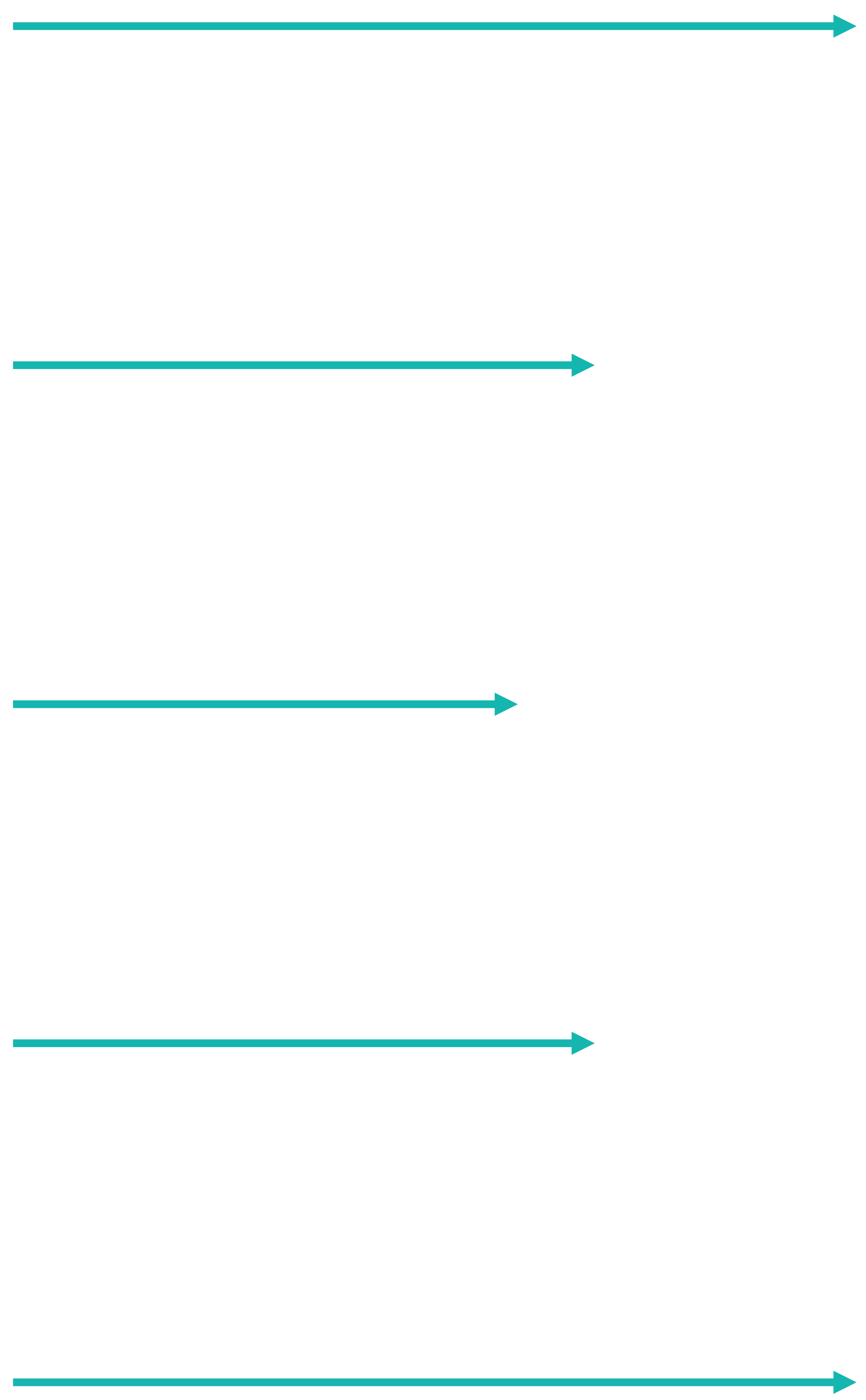

[Teh et al., 2022]

Luneburg Lens

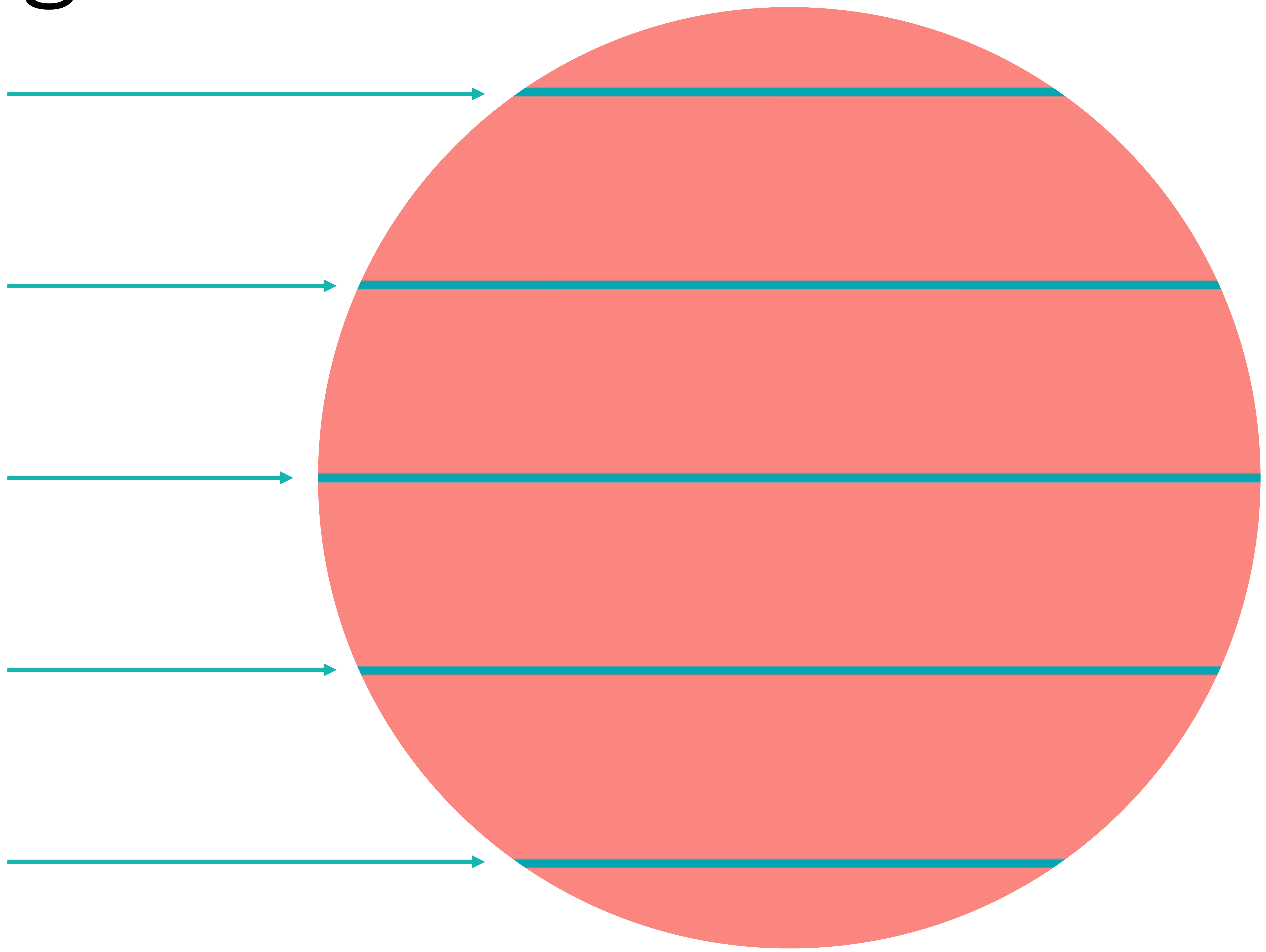

[Teh et al., 2022]

Luneburg Lens

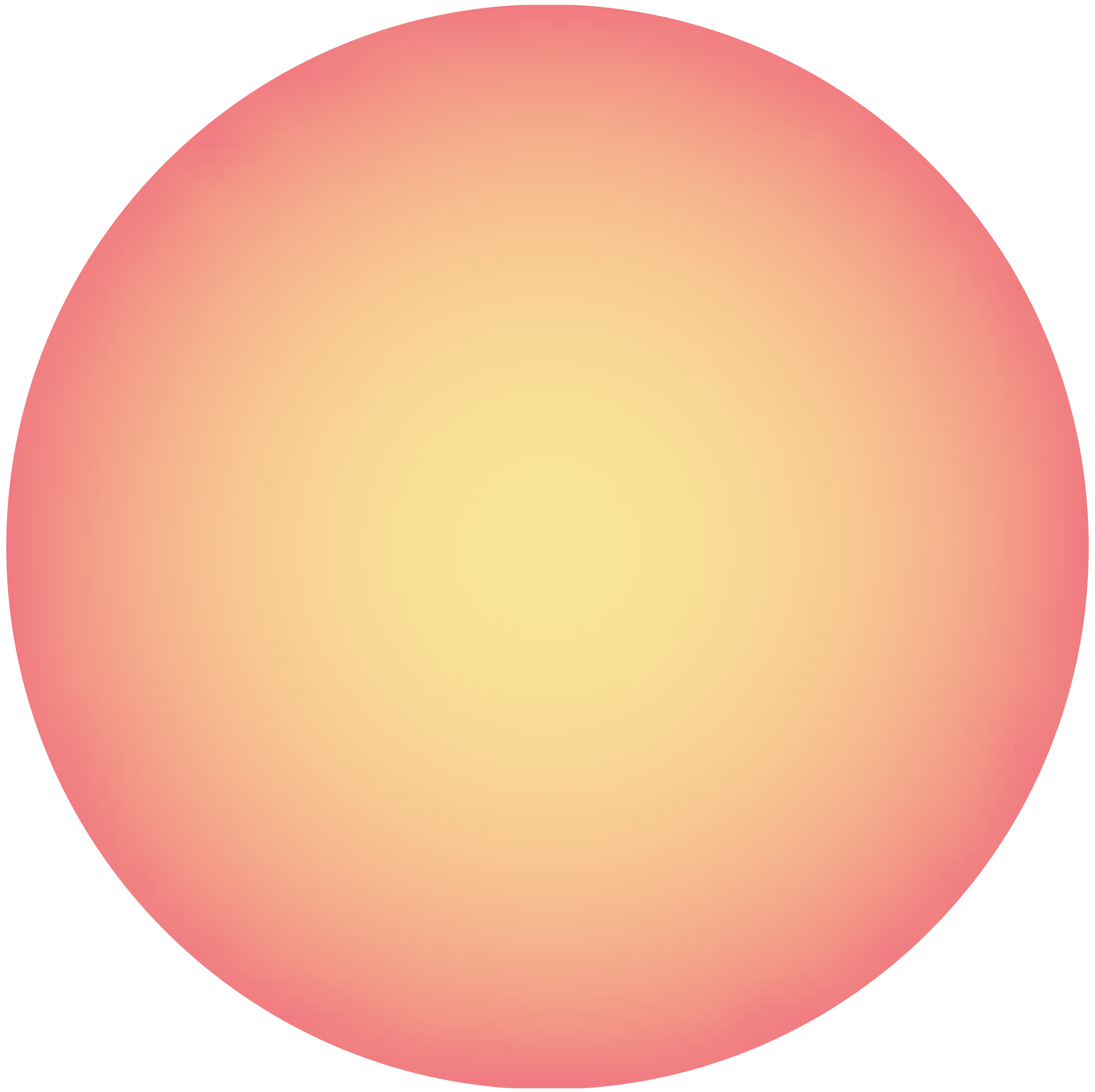

[Teh et al., 2022]

Luneburg Lens

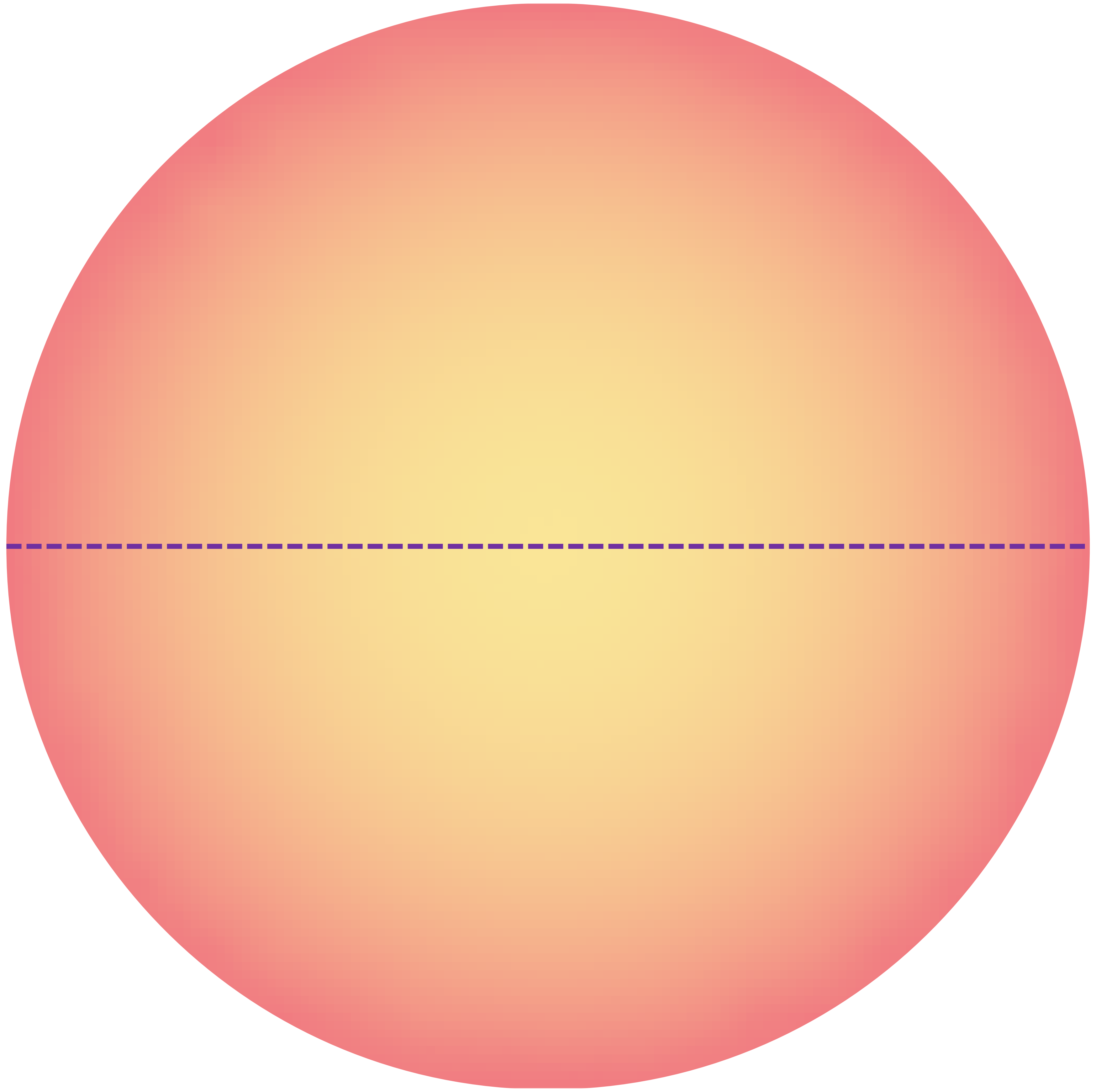

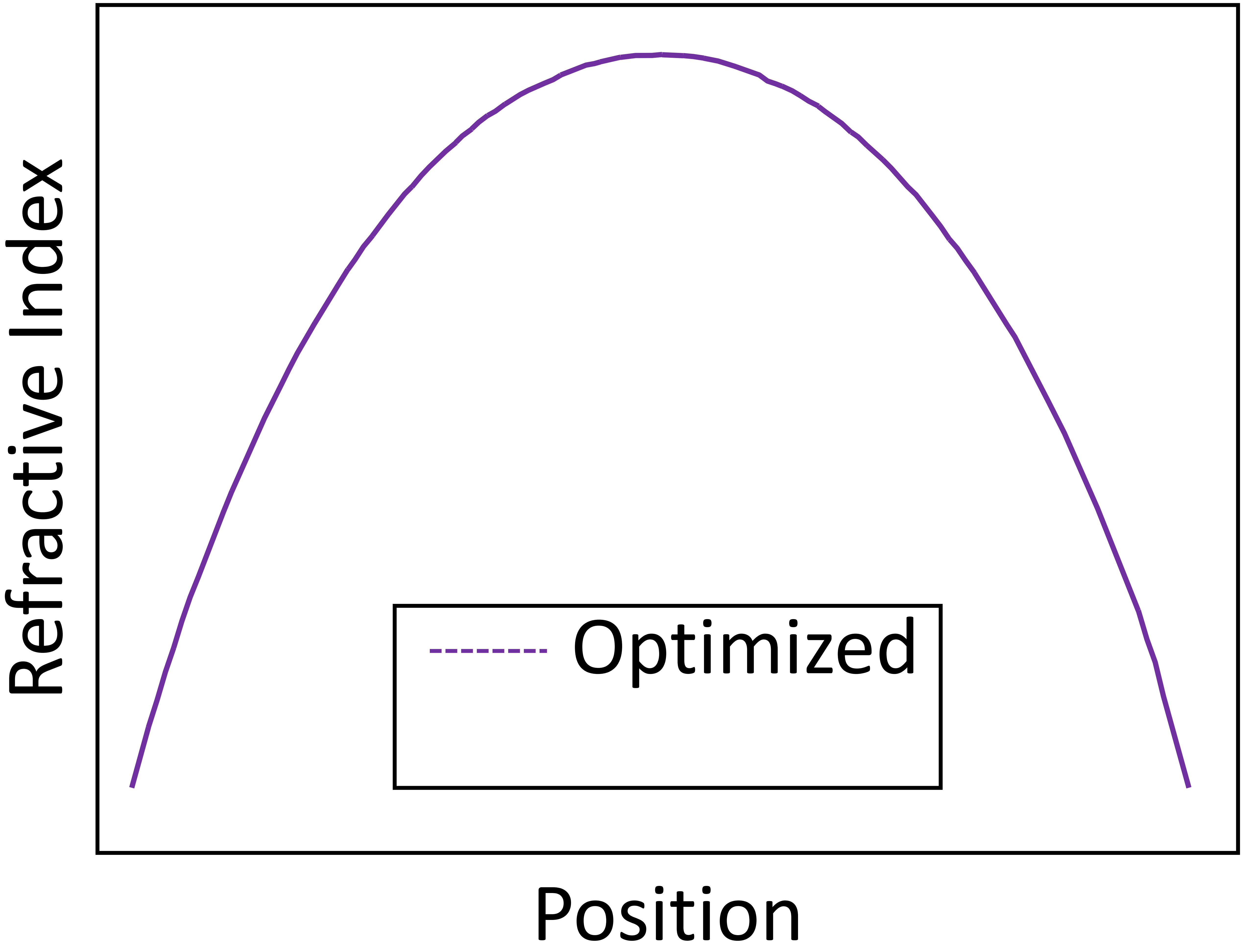

[Teh et al., 2022]

Luneburg Lens

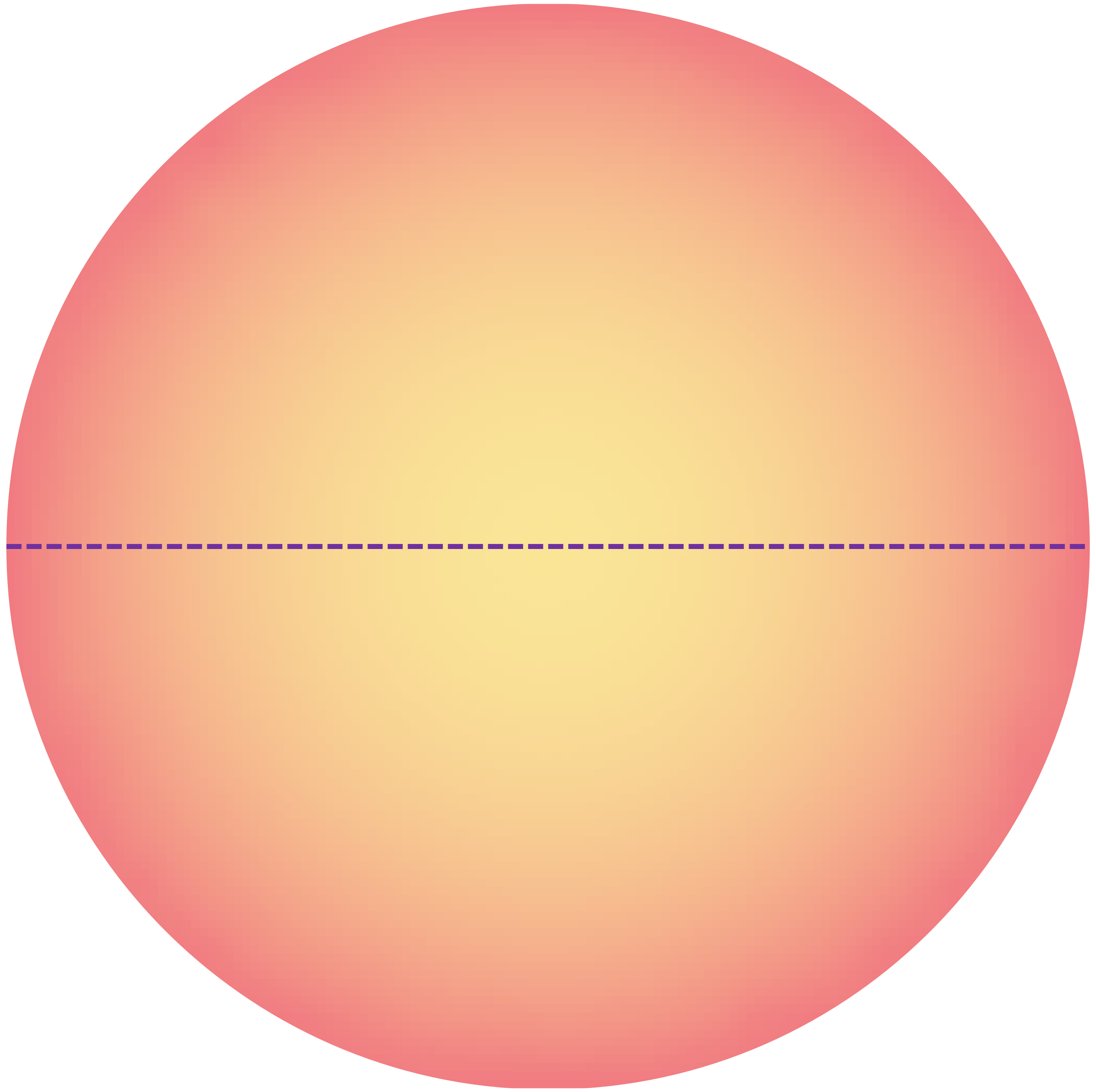

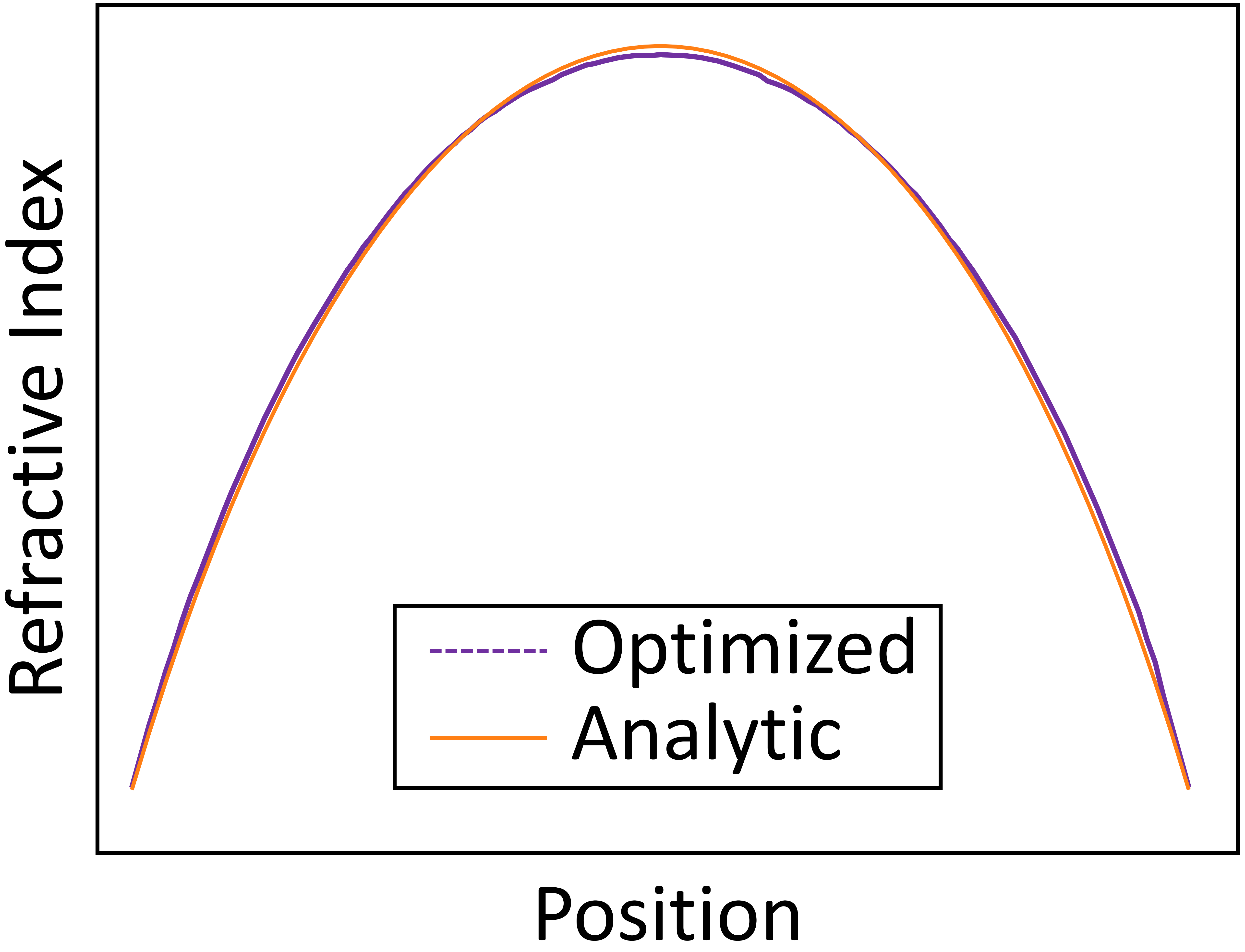

[Teh et al., 2022]

GRIN Fiber

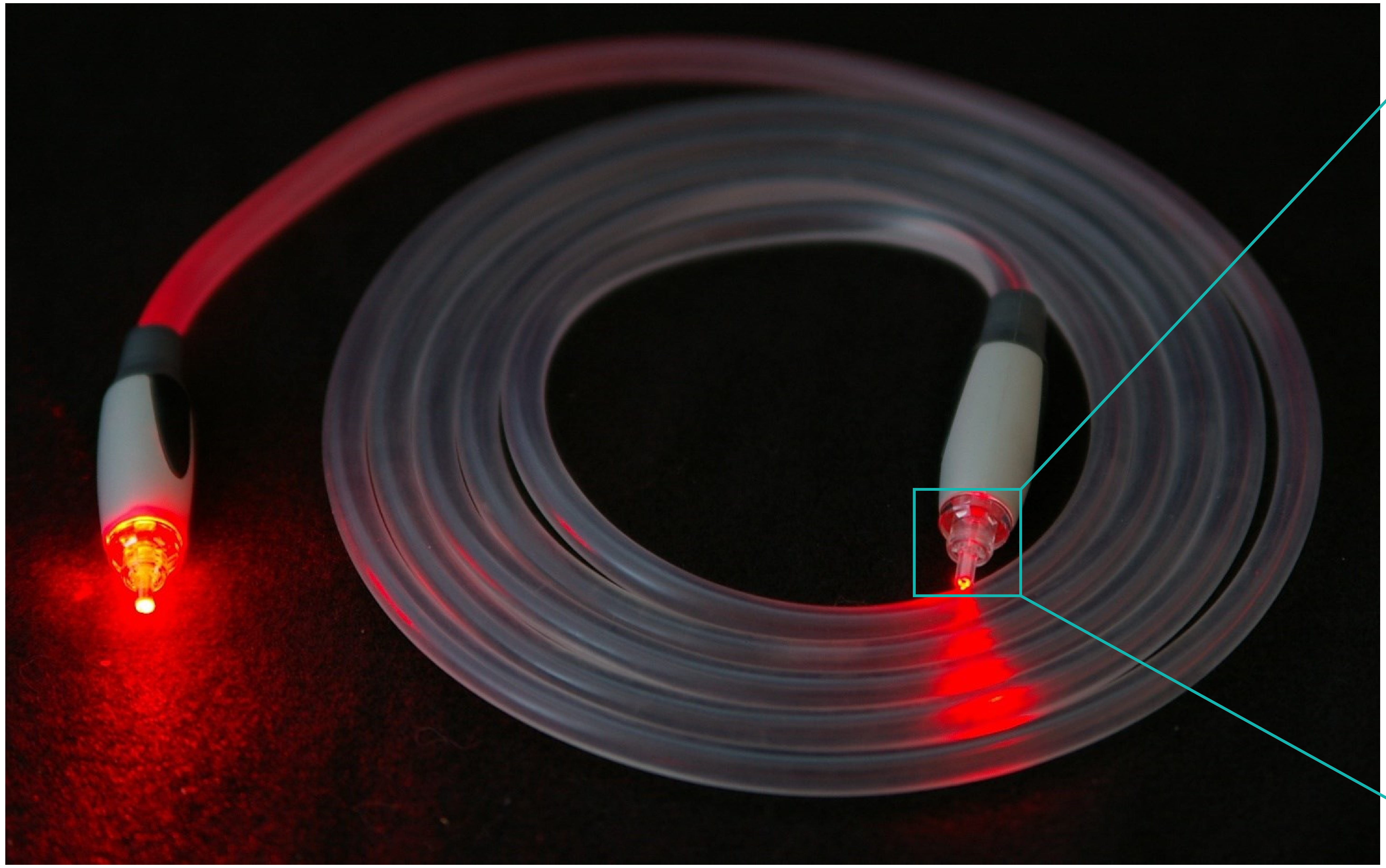

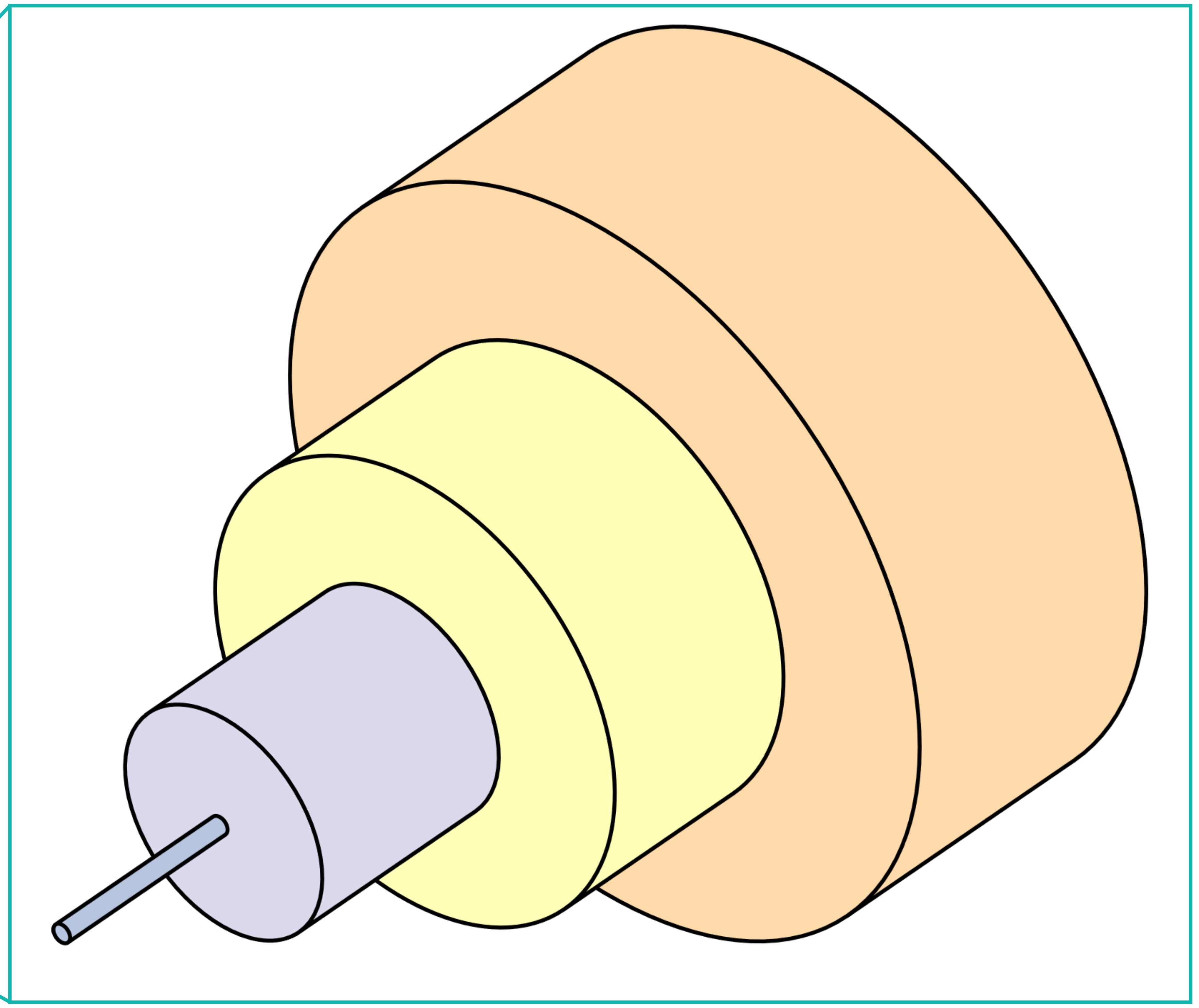

https://en.wikipedia.org/wiki/Optical_fiber

GRIN Fiber

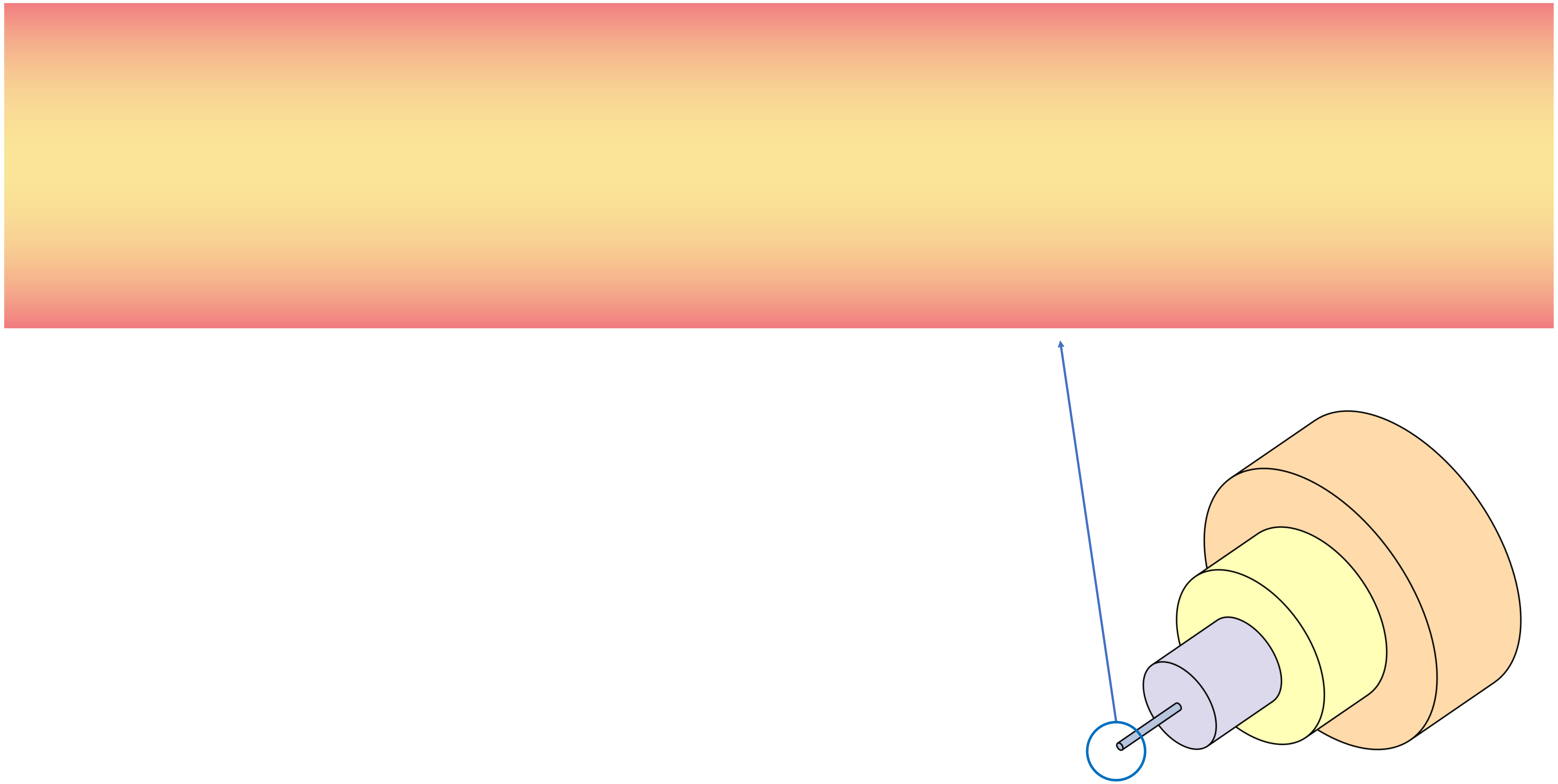

[Teh et al., 2022]

GRIN Fiber

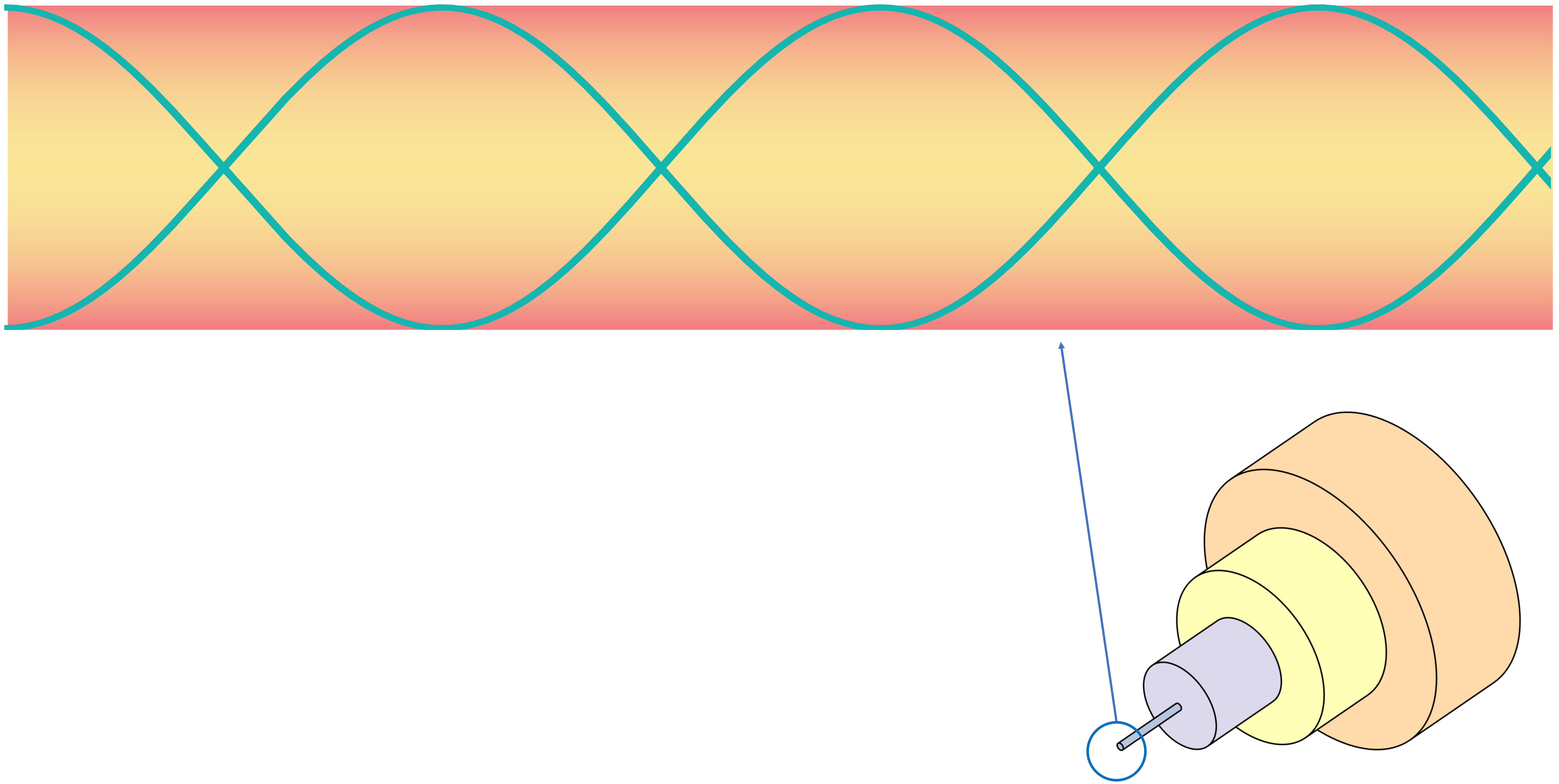

[Teh et al., 2022]

GRIN Fiber

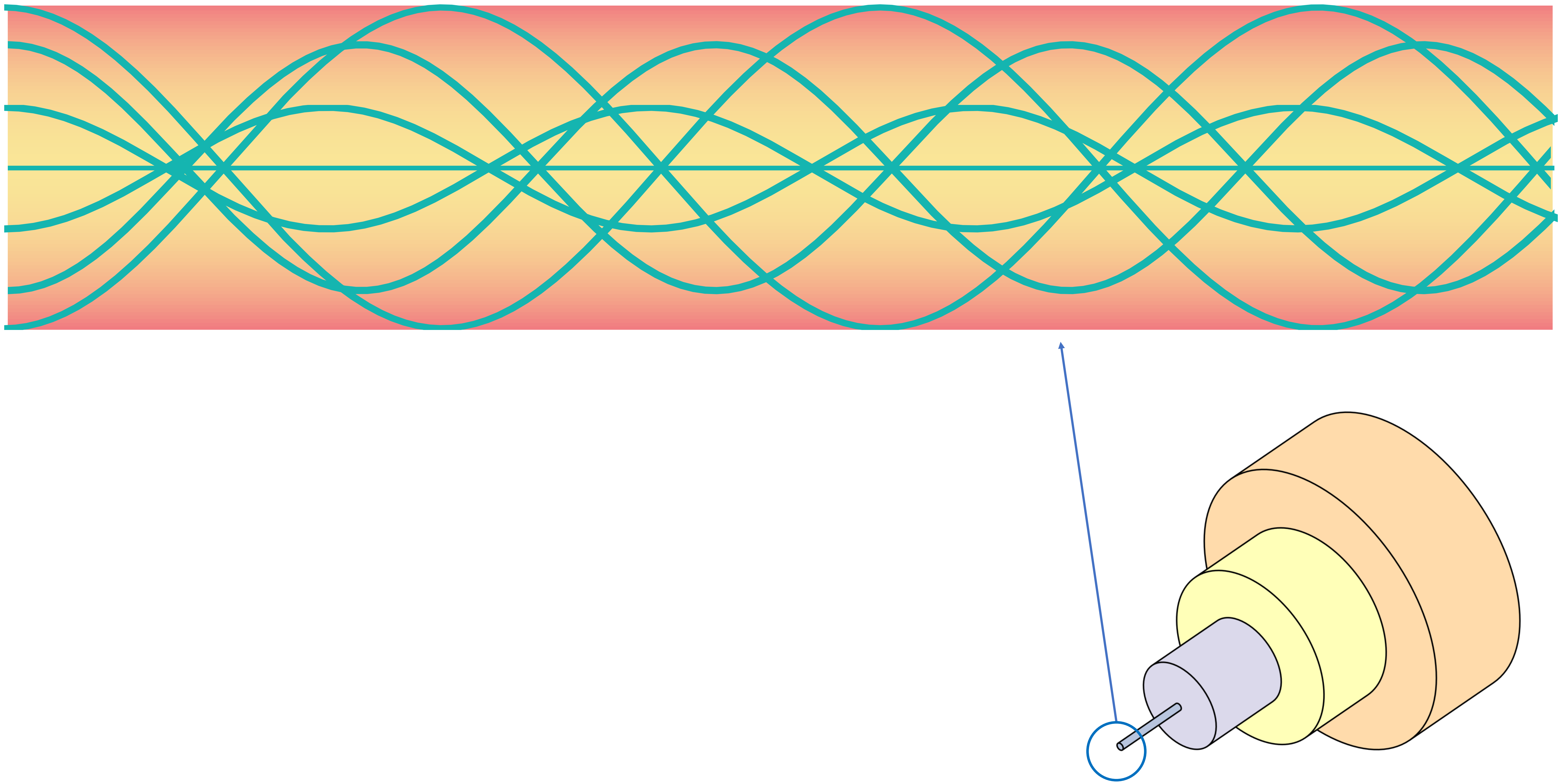

[Teh et al., 2022]

GRIN Fiber

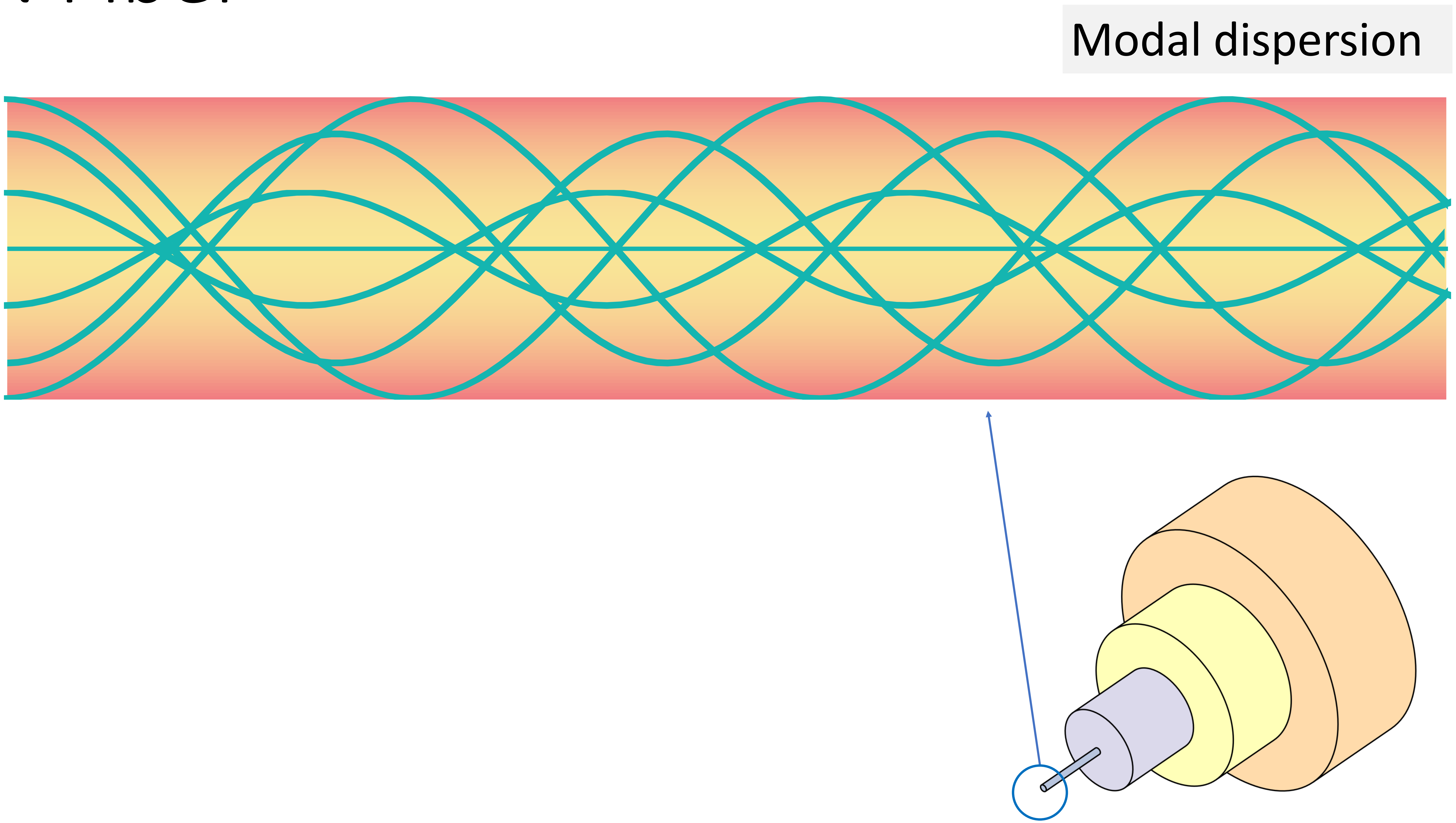

[Teh et al., 2022]

GRIN Fiber

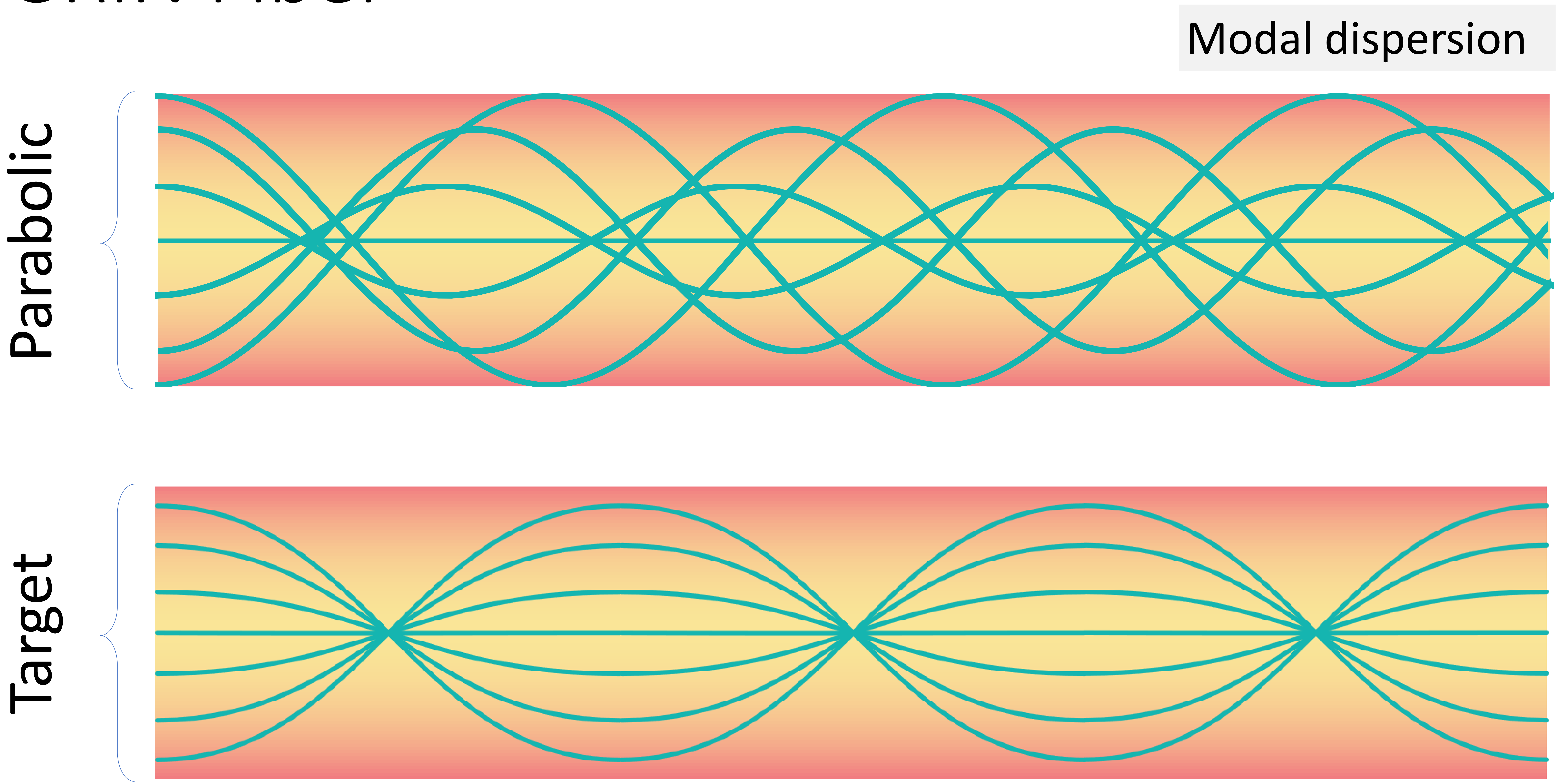

[Teh et al., 2022]

GRIN Fiber

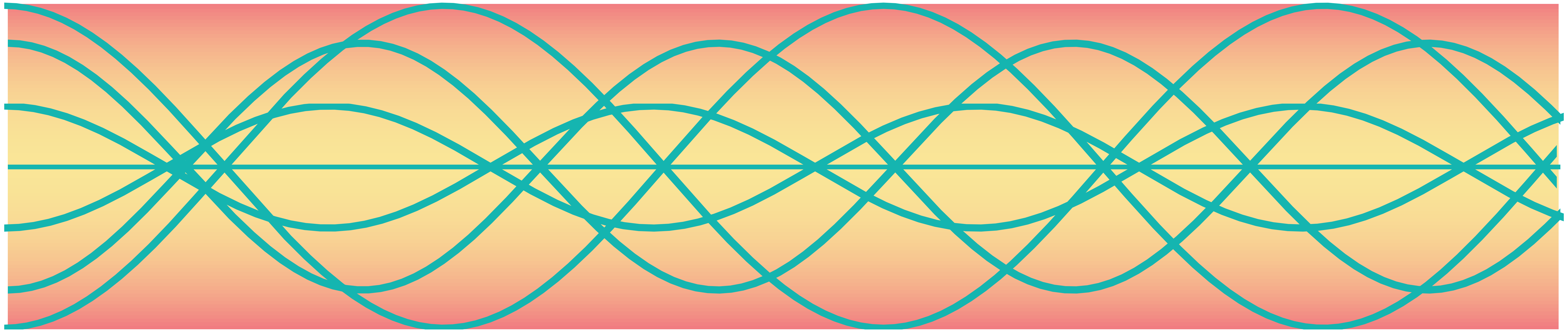

[Teh et al., 2022]

GRIN Fiber

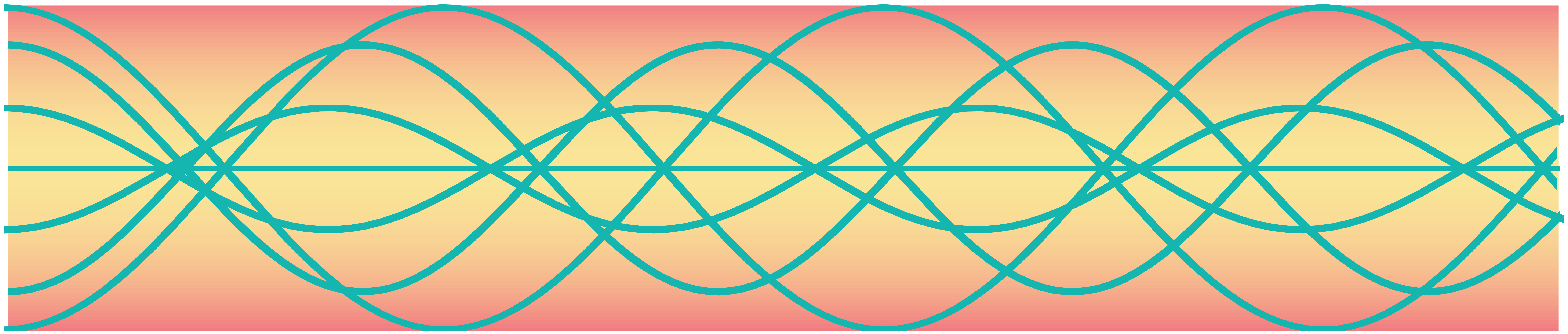

[Teh et al., 2022]

GRIN Fiber

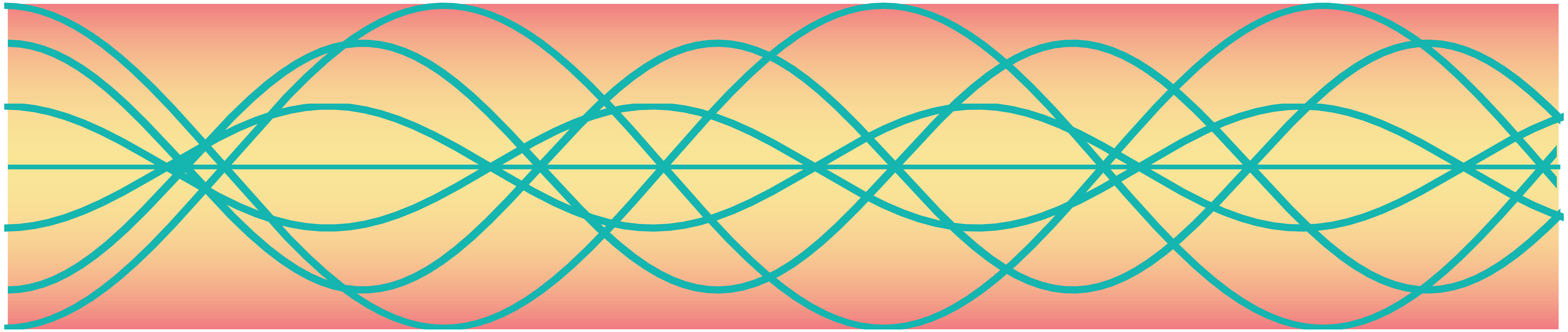

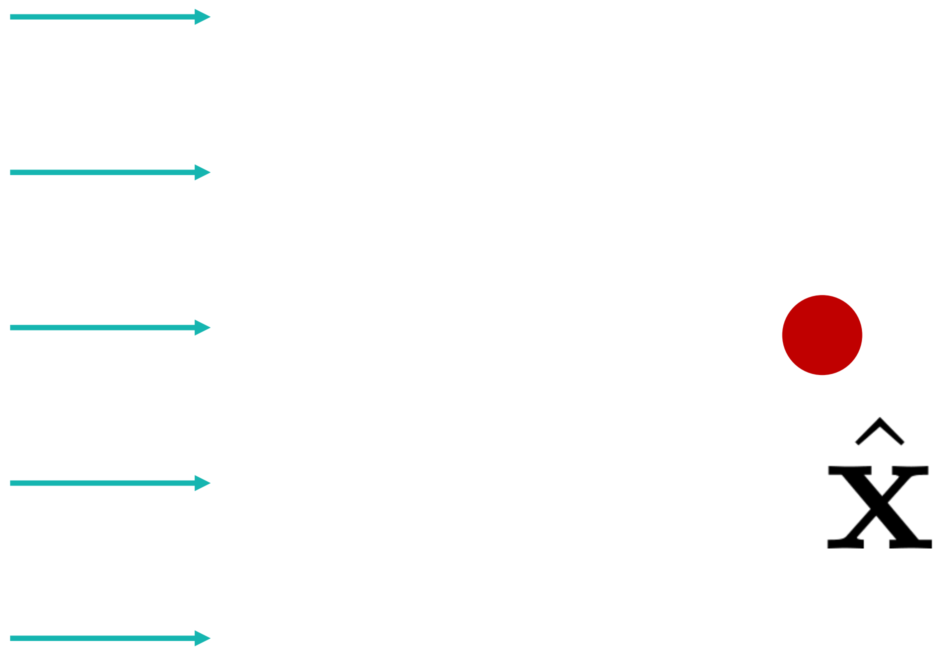

[Teh et al., 2022]

GRIN Fiber

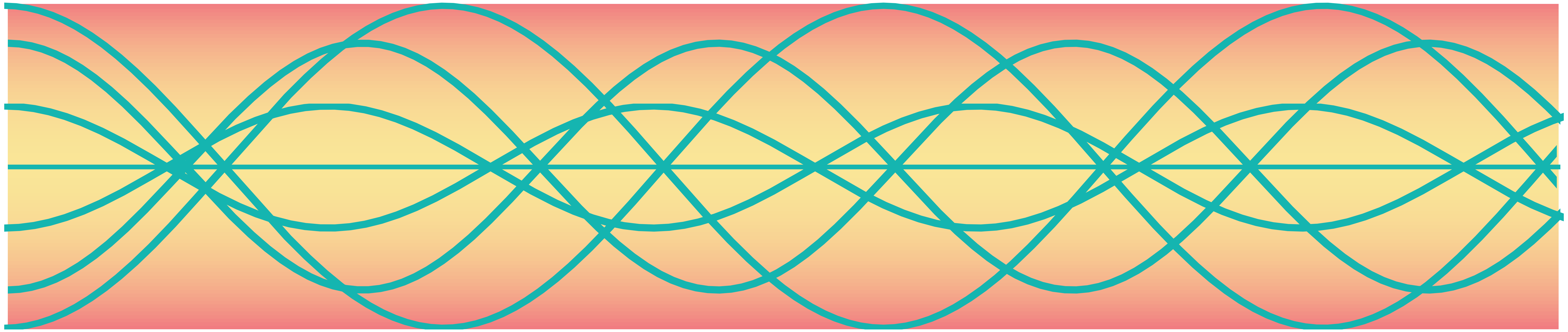

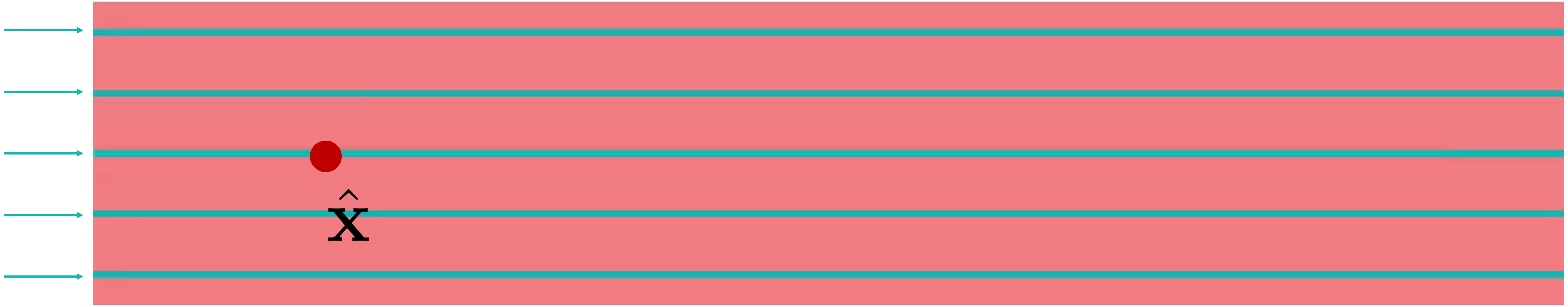

[Teh et al., 2022]

GRIN Fiber

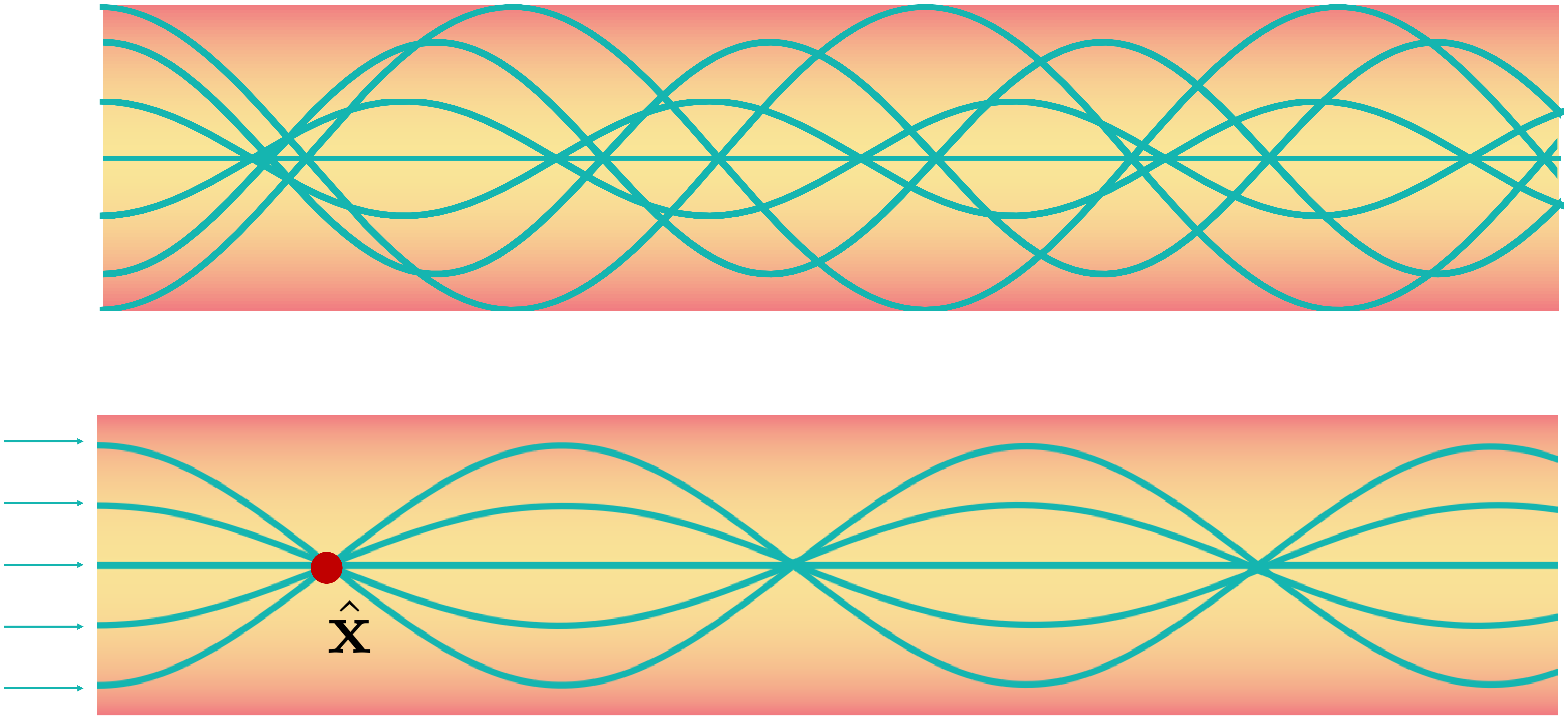

[Teh et al., 2022]

GRIN Fiber

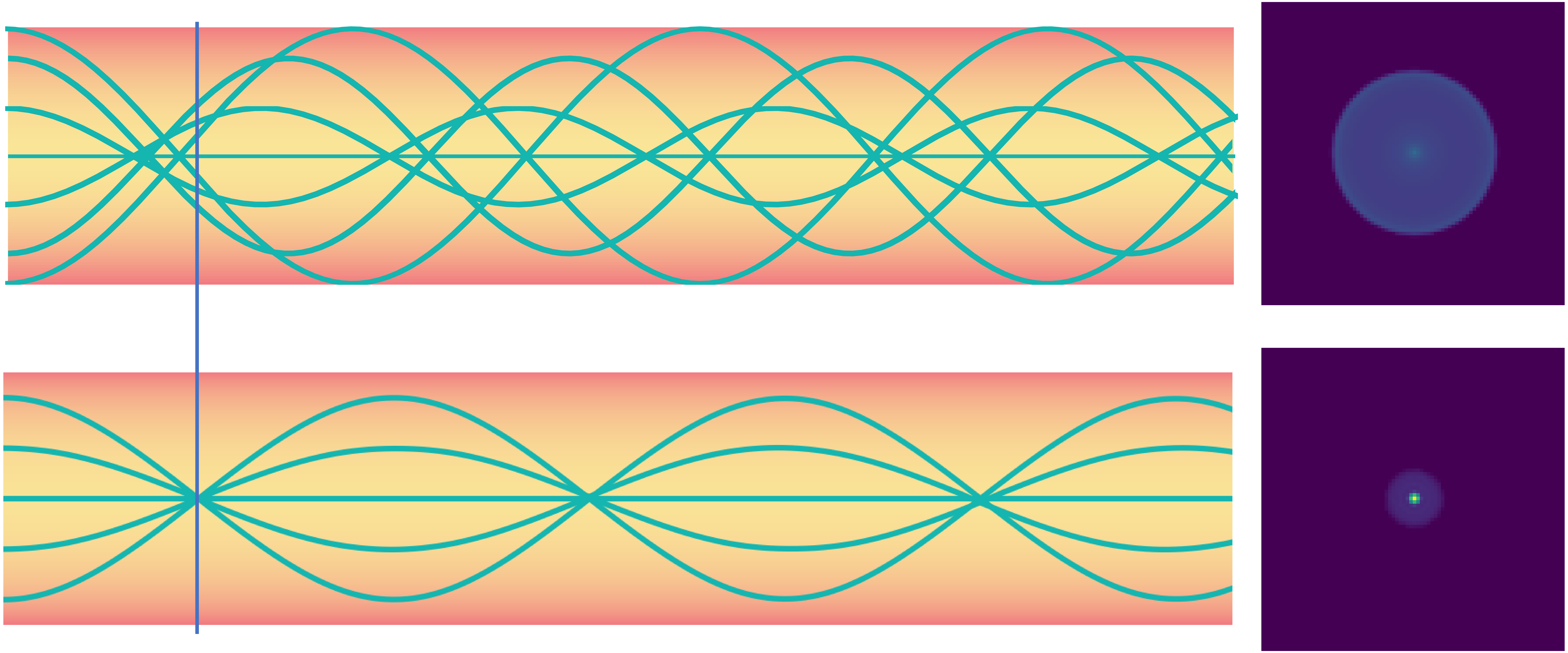

[Teh et al., 2022]

GRIN Fiber

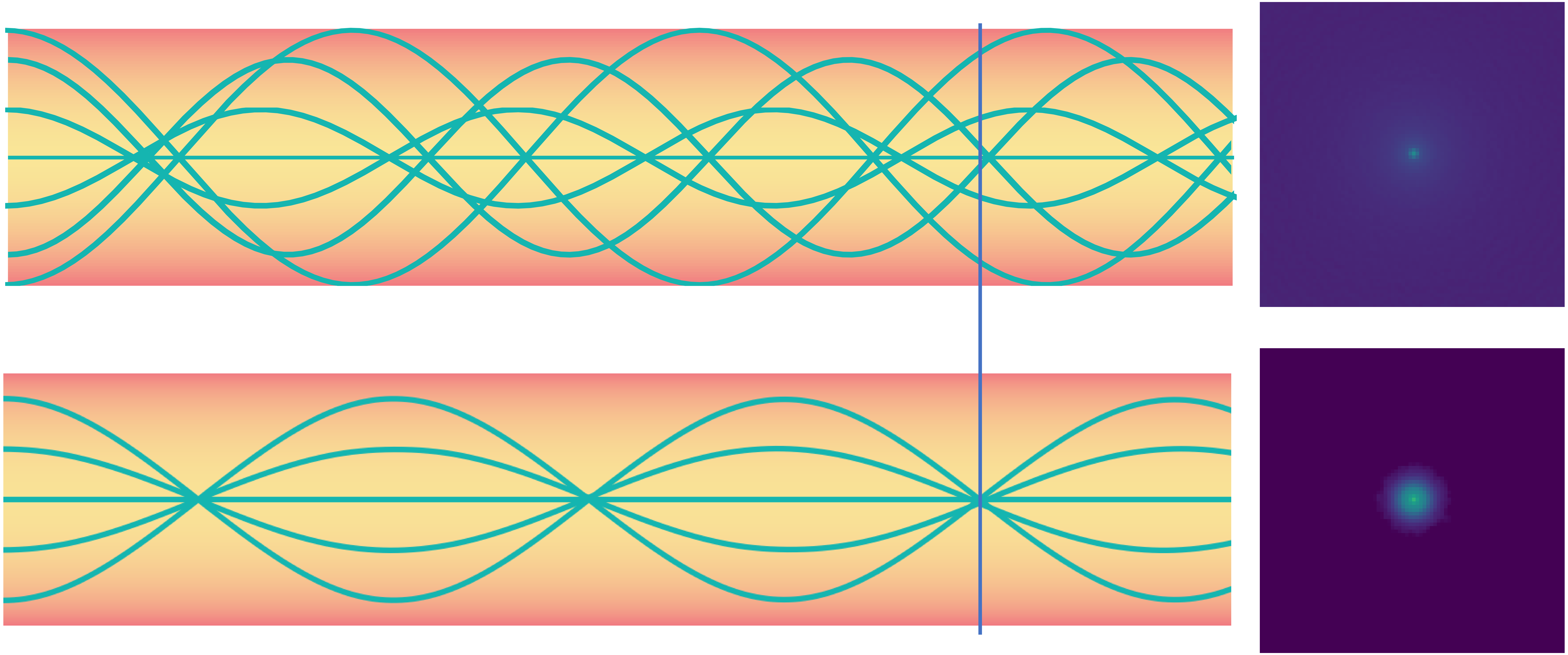

[Teh et al., 2022]

Multiview Display

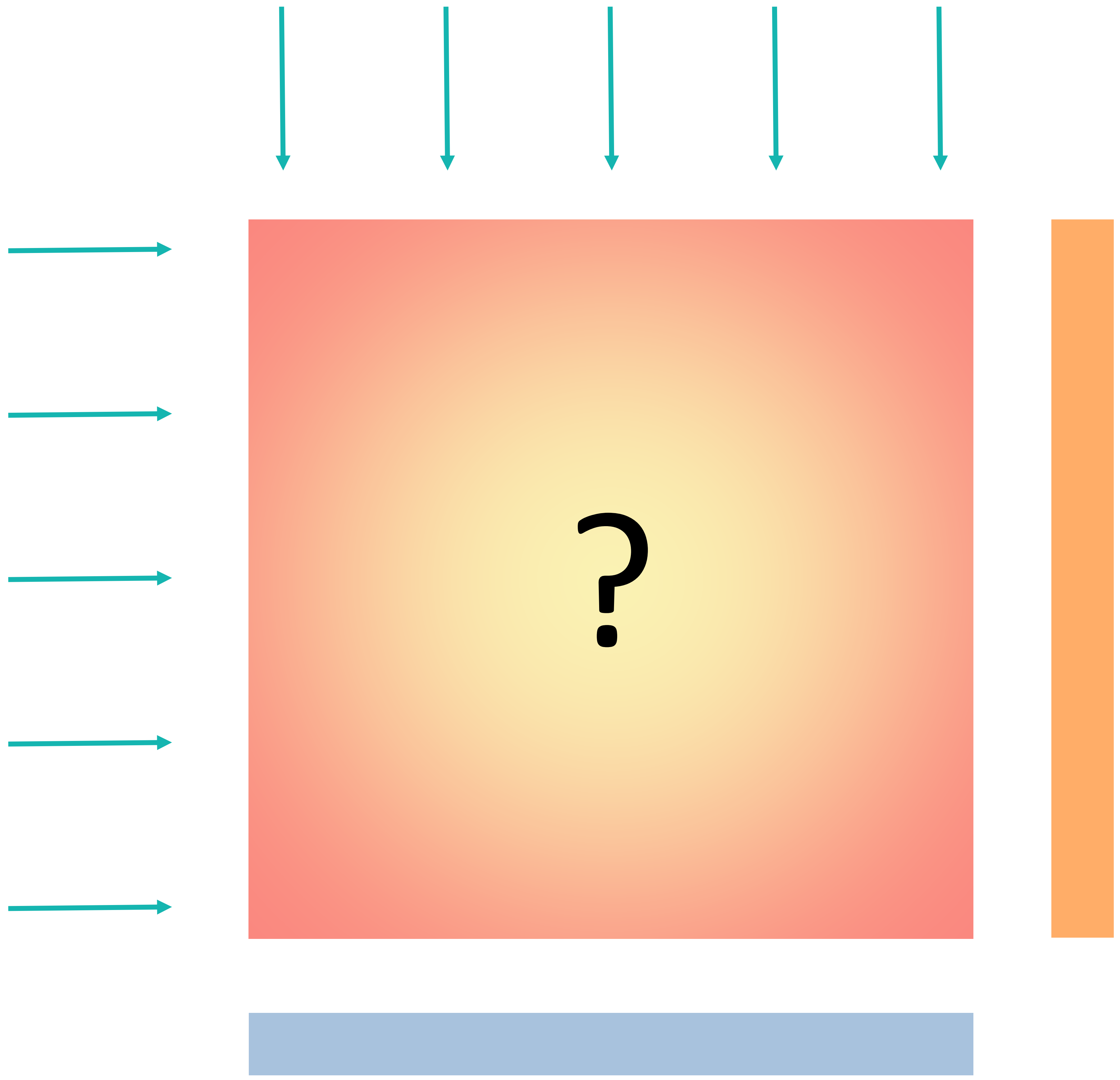

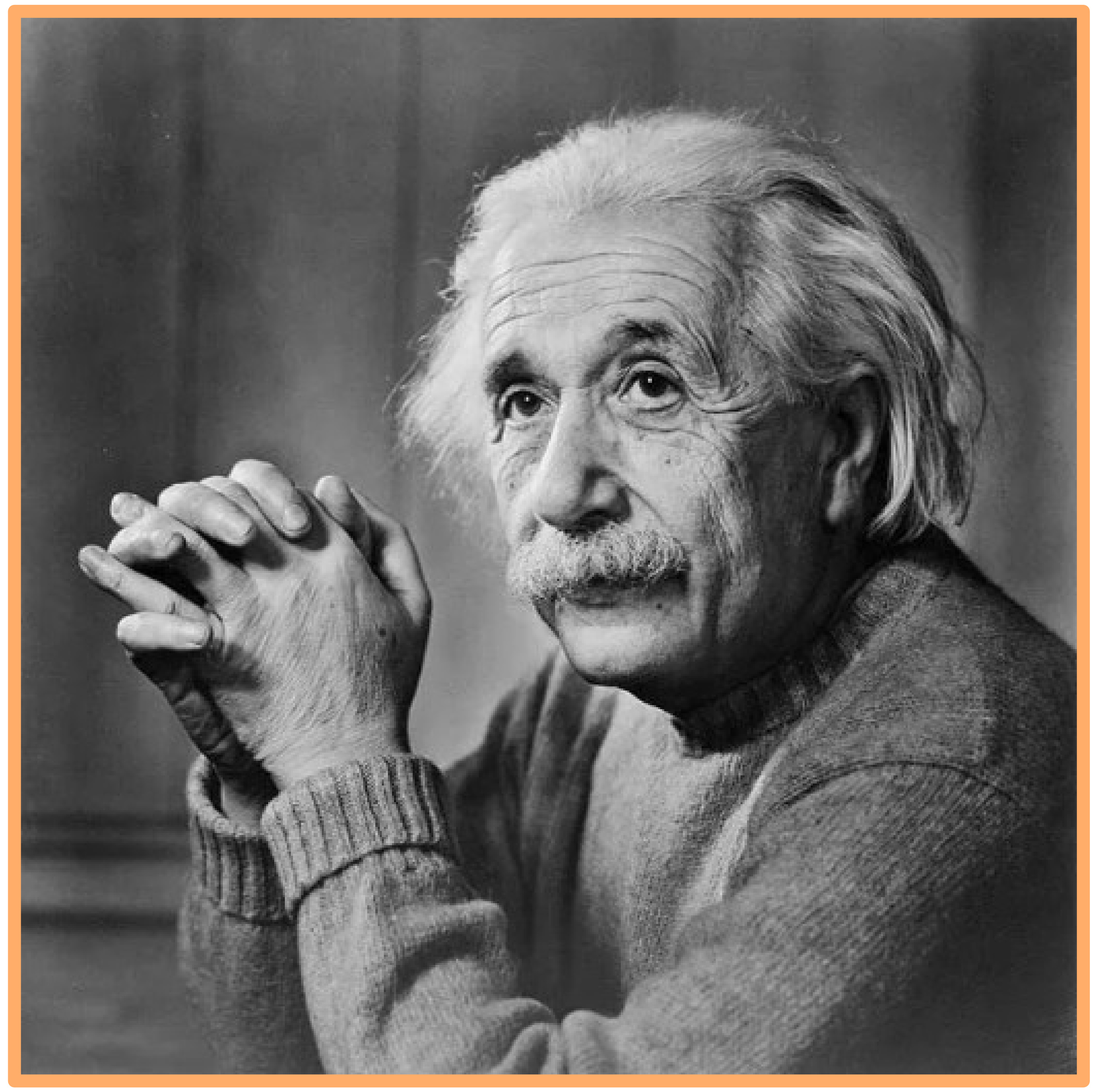

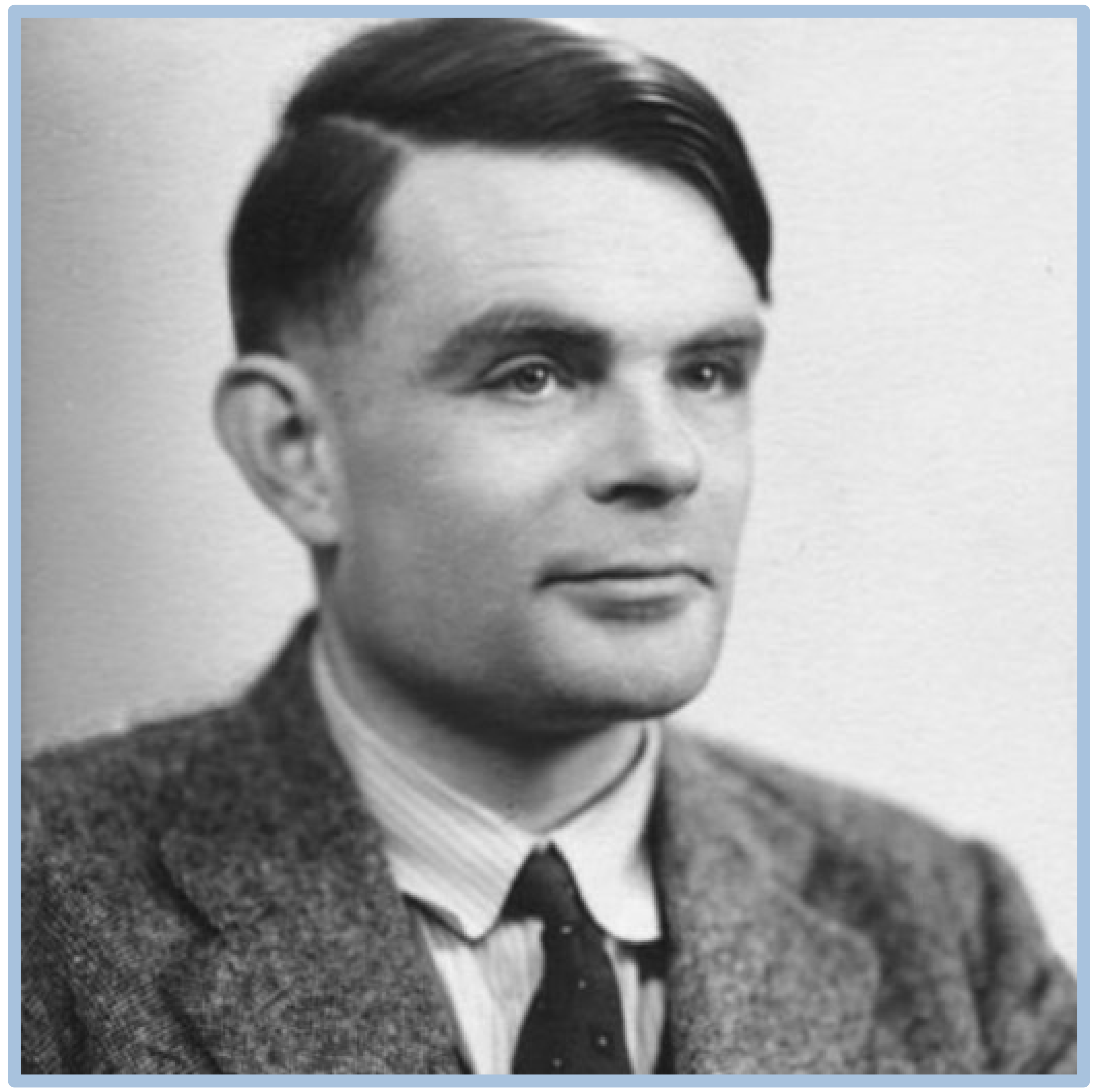

[Teh et al., 2022]

Multiview Display

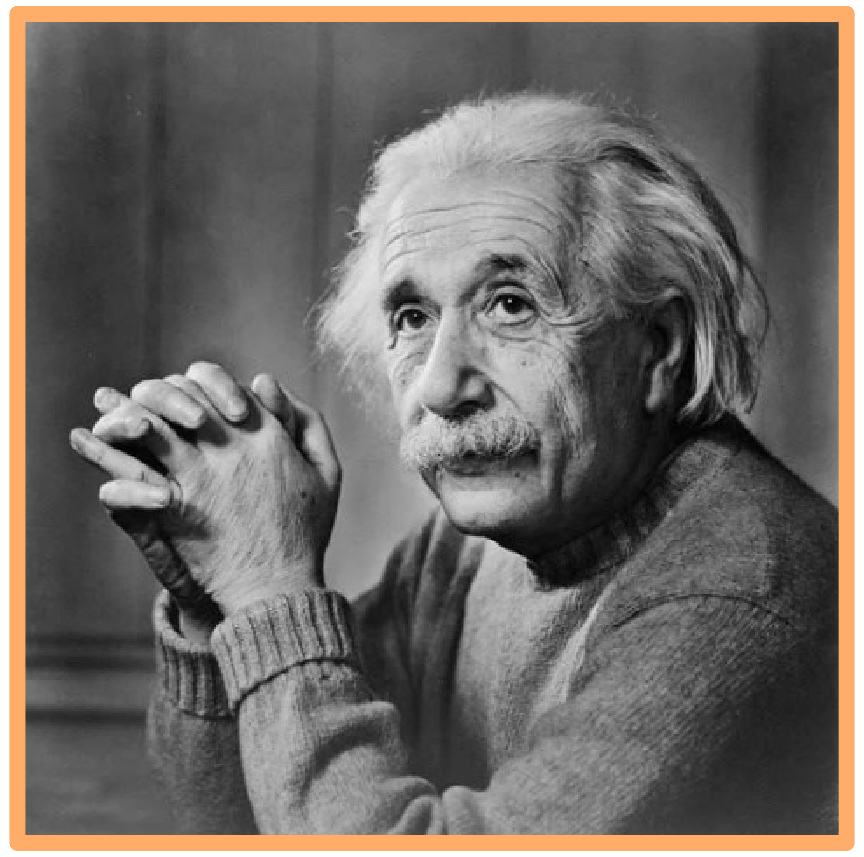

Target

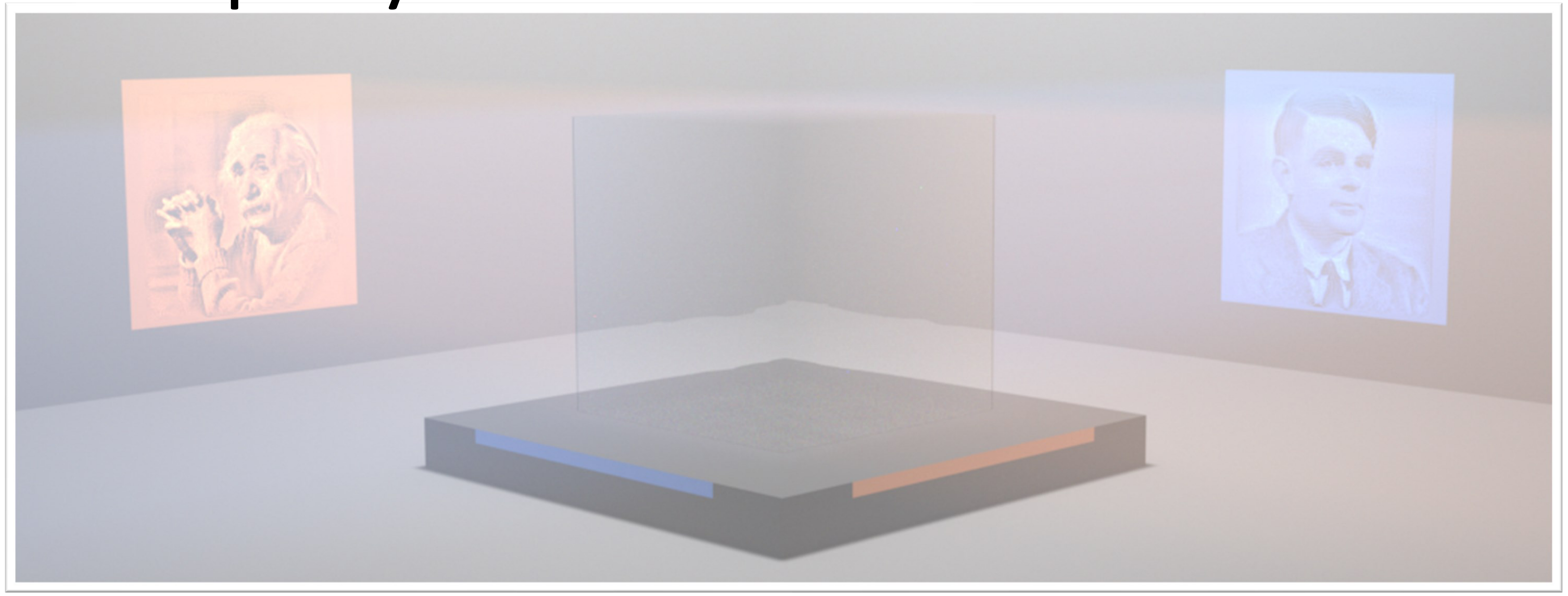

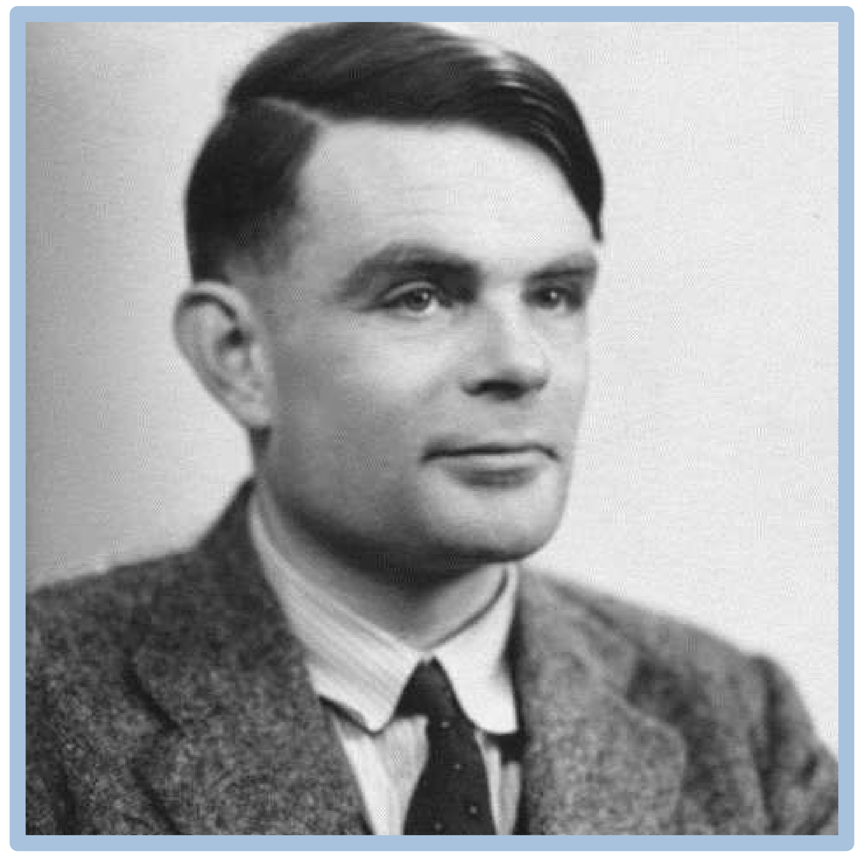

Target

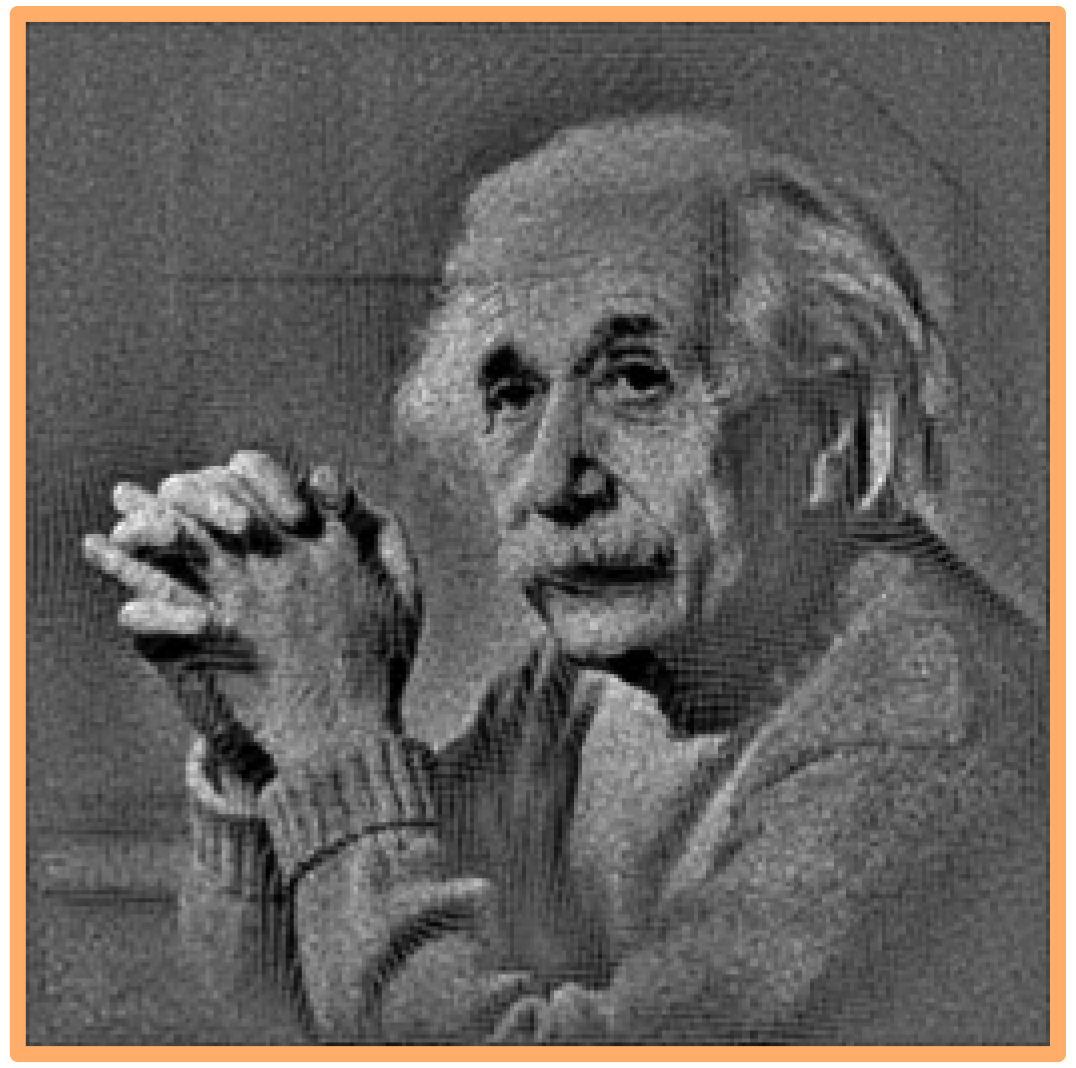

optimization results

[Teh et al., 2022]

Differentiable rendering for wildfire monitoring

[USDA NIFA project jointly with Sebastian Scherer and Katia Sycara]

What differentiable rendering does not give us

Inverse rendering (a.k.a. analysis by synthesis)

Analysis-by-synthesis optimization:

$$\min_{\substack{\text{scene} \\ \text{unknowns } \pi}} \text{loss}\left[\right.$$

$$\left., \text{render}\left(\begin{matrix}\text{scene} \\ \text{unknowns } \pi\end{matrix}\right)\right]$$

Inverse rendering (a.k.a. analysis by synthesis)

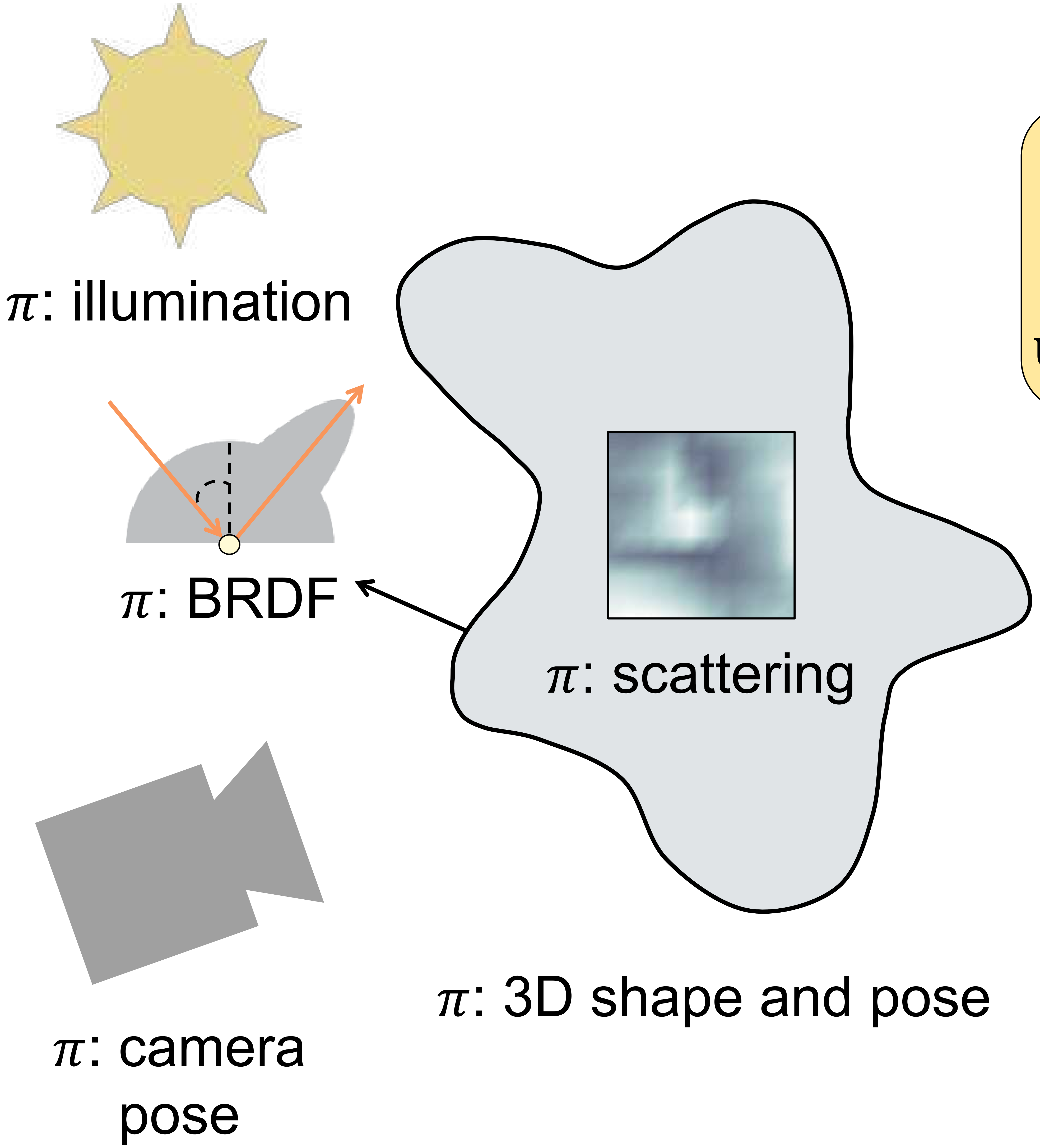

Analysis-by-synthesis optimization:

$$\min_{\substack{\text{scene}\\ \text{unknowns}\ \pi}} \ \text{loss}\Big[$$

$$,\ \text{render}\left(\substack{\text{scene}\\ \text{unknowns}\ \pi}\right)\Big]$$

Inverse rendering (a.k.a. analysis by synthesis)

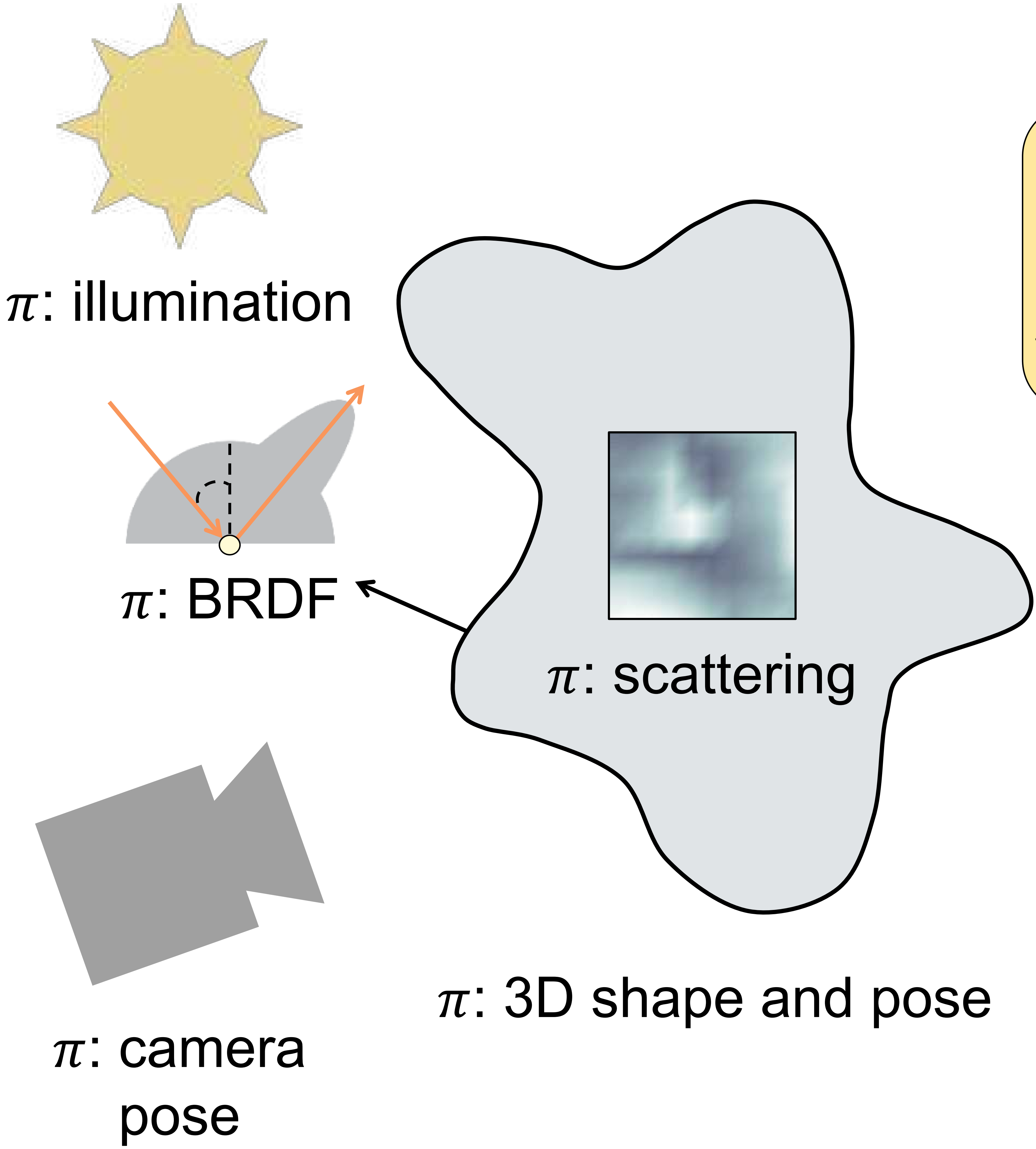

Analysis-by-synthesis optimization:

$$\min_{\substack{\text{scene} \\ \text{unknowns } \pi}} \ \text{loss}\Big[$$

$$, \ \text{render}\Big(\begin{matrix}\text{scene} \\ \text{unknowns } \pi\end{matrix}\Big)\Big]$$

Stochastic gradient descent (e.g., Adam):

initialize $\pi \leftarrow \pi_0$

while (not converged)

update $\pi \leftarrow \pi + \eta \cdot \frac{\mathrm{dloss}(\pi)}{\mathrm{d}\pi}$

Inverse rendering (a.k.a. analysis by synthesis)

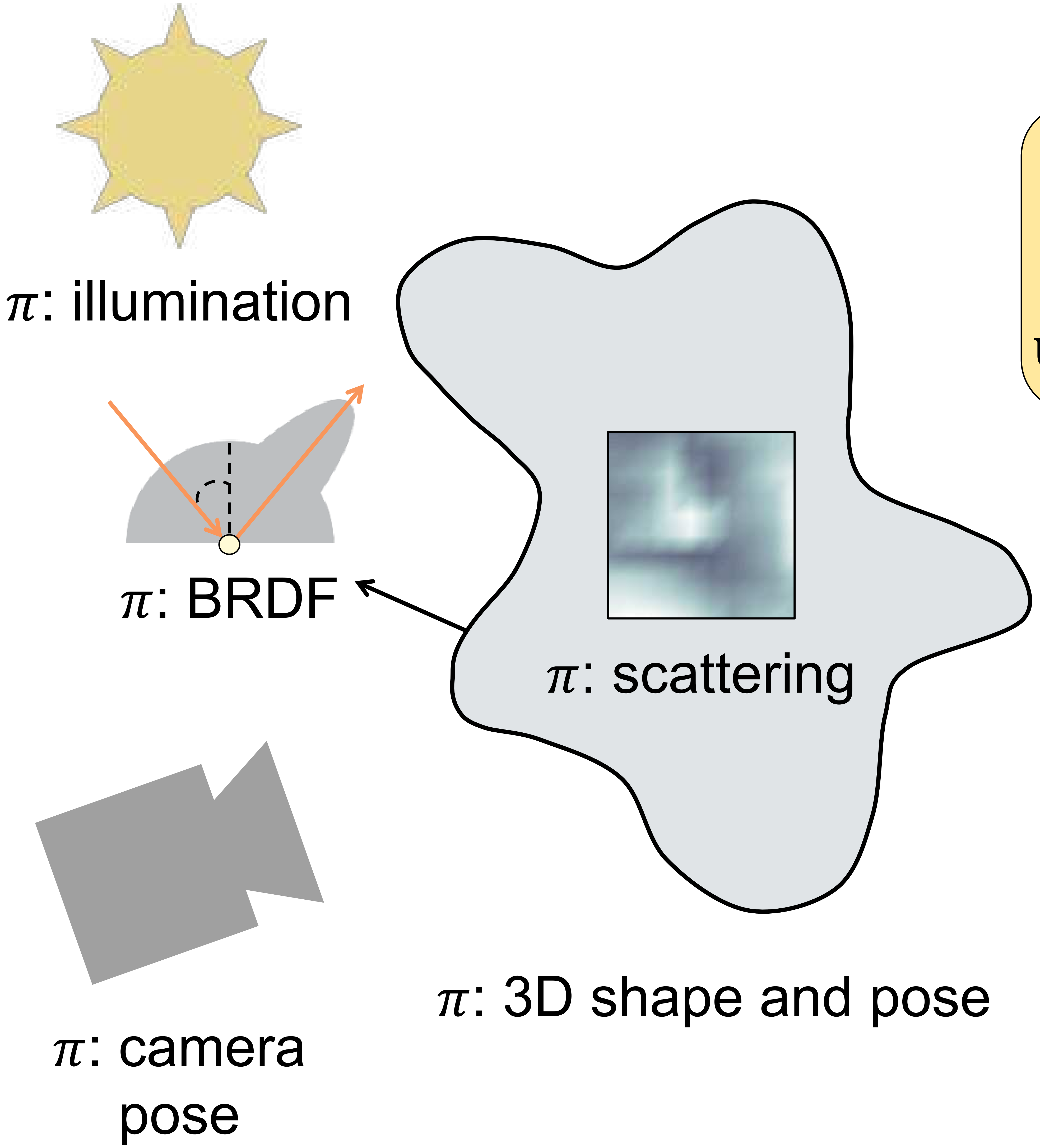

Analysis-by-synthesis optimization:

$$\min_{\text{scene unknowns } \pi} \; \text{loss}\left[\quad \right.$$

$$\left. , \text{render}\left(\text{scene unknowns } \pi\right)\right]$$

Stochastic gradient descent (e.g., Adam):

initialize $\pi \leftarrow \pi_0$

while (not converged)

update $\pi \leftarrow \pi + \eta \cdot \boxed{\frac{\mathrm{dloss}(\pi)}{\mathrm{d}\pi}}$

Differentiable rendering

Inverse rendering (a.k.a. analysis by synthesis)

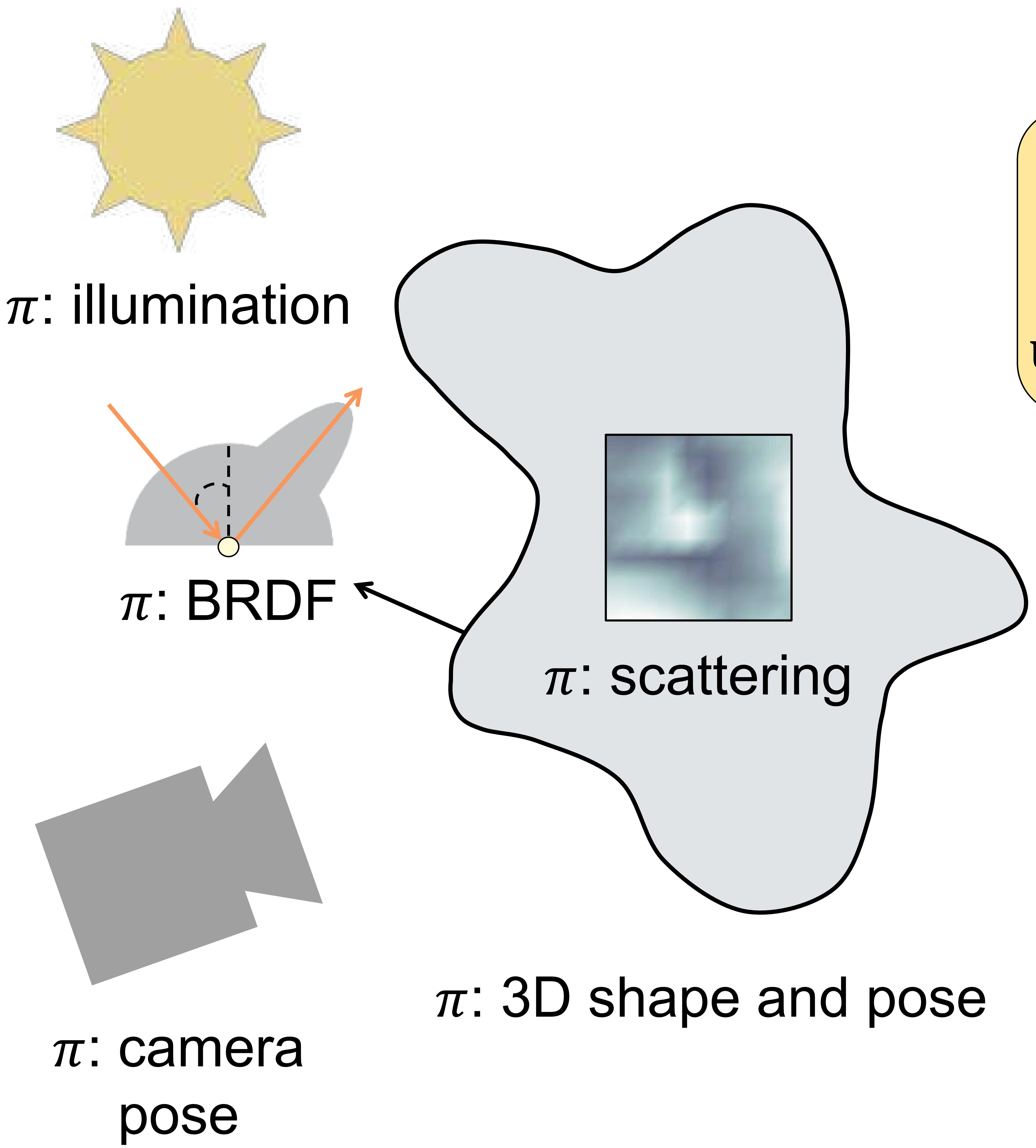

Analysis-by-synthesis optimization:

$$\min_{\text{scene unknowns } \pi} \text{loss}\left[\; \right.$$

$$\left. , \text{render}\left(\text{scene unknowns } \pi\right)\right]$$

Stochastic gradient descent (e.g., Adam):

$\boxed{\text{initialize } \pi \leftarrow \pi_0}$

while (not converged)

update $\pi \leftarrow \pi + \eta \cdot \boxed{\dfrac{\mathrm{d}\,\mathrm{loss}(\pi)}{\mathrm{d}\pi}}$

Differentiable rendering

Why we need good initializations

- Analysis-by-synthesis objectives are highly non-convex, non-linear
  - Multiple *local* minima

Why we need good initializations

- Analysis-by-synthesis objectives are highly non-convex, non-linear
  - Multiple *local* minima
- Ambiguities exist between different parameters
  - Multiple *global* minima

Why we need good initializations

- Analysis-by-synthesis objectives are highly non-convex, non-linear
  - Multiple *local* minima
- Ambiguities exist between different parameters
  - Multiple *global* minima

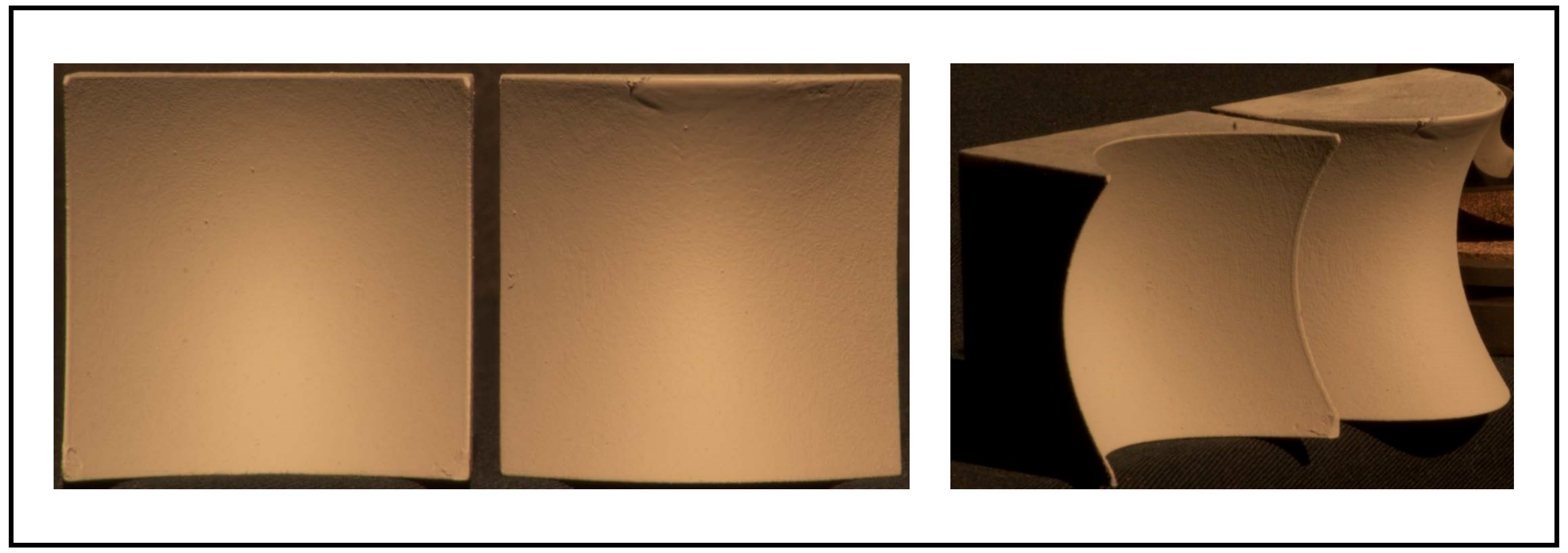

Ambiguities between shape and lighting [Xiong et al. 2015]

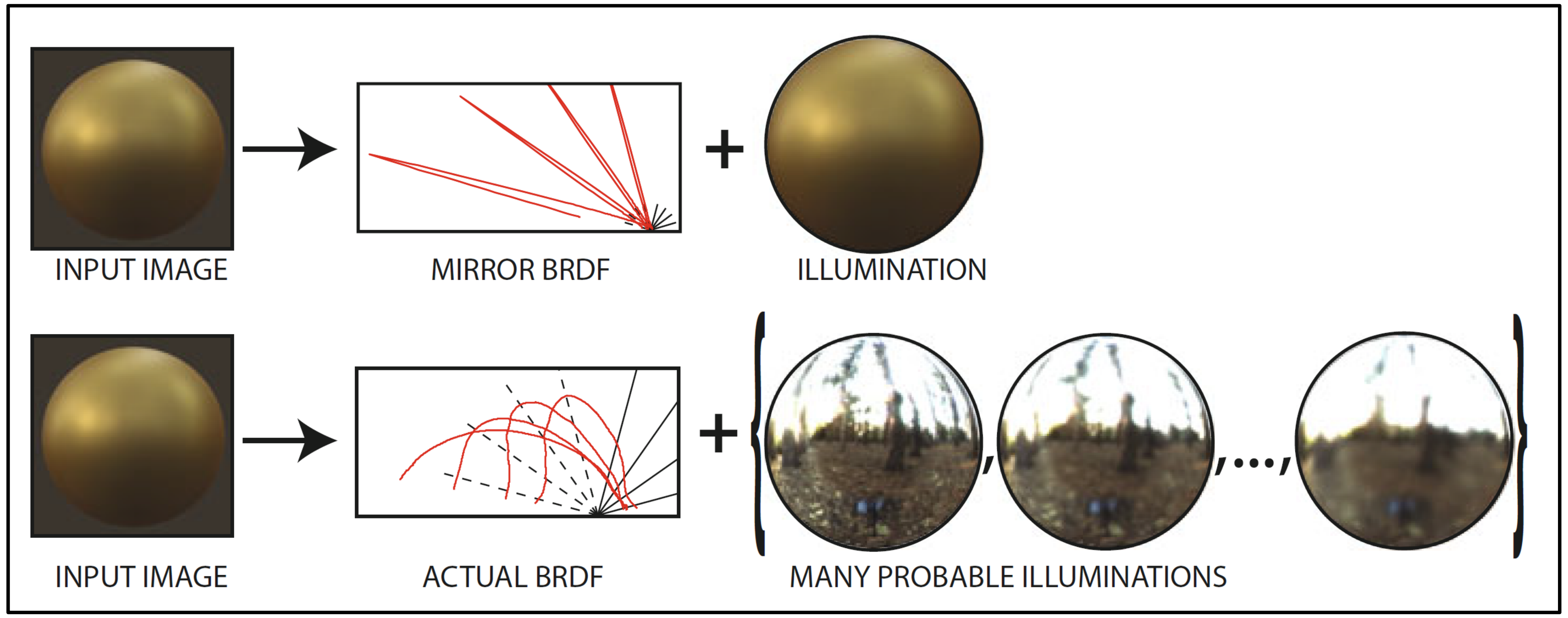

Ambiguities between BRDF and lighting [Romeiro and Zickler 2010]

Ambiguities between scattering parameters [Zhao et al. 2014]

Inverse rendering (a.k.a. analysis by synthesis)

Analysis-by-synthesis optimization:

$$\min_{\substack{\text{scene} \\ \text{unknowns } \pi}} \text{loss}\left[\right.$$  $$\left., \text{render}\left(\substack{\text{scene} \\ \text{unknowns } \pi}\right)\right]$$

Stochastic gradient descent (e.g., Adam):

initialize $\boxed{\pi \leftarrow \pi_0}$

while (not converged)

update $\pi \leftarrow \pi + \eta \cdot \boxed{\frac{\mathrm{dloss}(\pi)}{\mathrm{d}\pi}}$

Differentiable rendering

Inverse rendering (a.k.a. analysis by synthesis)

Analysis-by-synthesis optimization:

$$\min_{\substack{\text{scene}\\ \text{unknowns}\,\pi}} \ \text{loss}\Bigg[$$

$$,\ \text{render}\left(\substack{\text{scene}\\ \text{unknowns}\,\pi}\right)\Bigg]$$

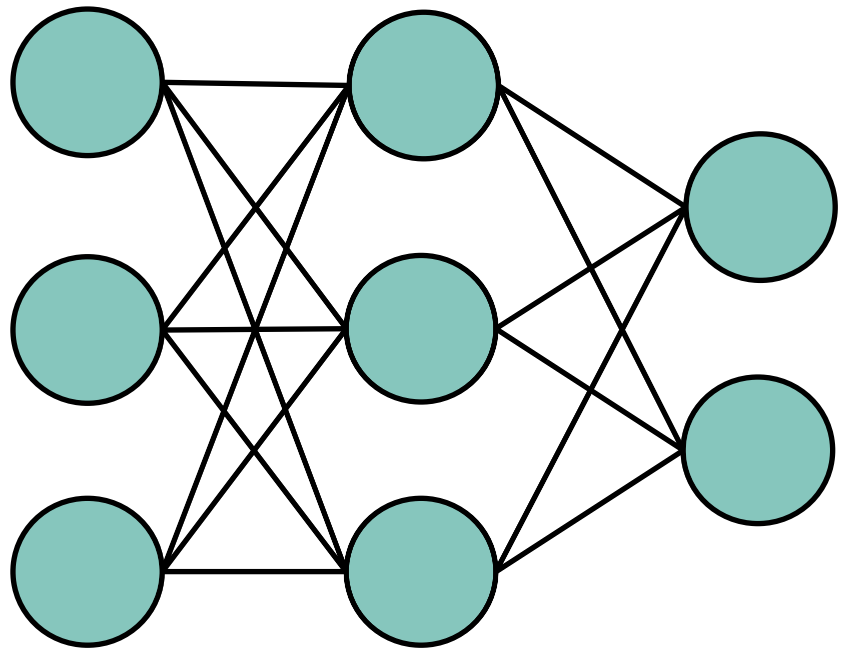

Neural network

Stochastic gradient descent (e.g., Adam):

$\boxed{\text{initialize } \pi \leftarrow \pi_0}$

while (not converged)

update $\pi \leftarrow \pi + \eta \cdot \boxed{\dfrac{\mathrm{dloss}(\pi)}{\mathrm{d}\pi}}$

Differentiable rendering

Inverse rendering (a.k.a. analysis by synthesis)

Analysis-by-synthesis optimization:

$\min_{\substack{\text{scene} \\ \text{unknowns } \pi}} \ \text{loss}\Big[$  $, \text{render}\big(\substack{\text{scene} \\ \text{unknowns } \pi}\big)\Big]$

Learned initializations help:

- avoid local minima
- accelerate convergence

 → 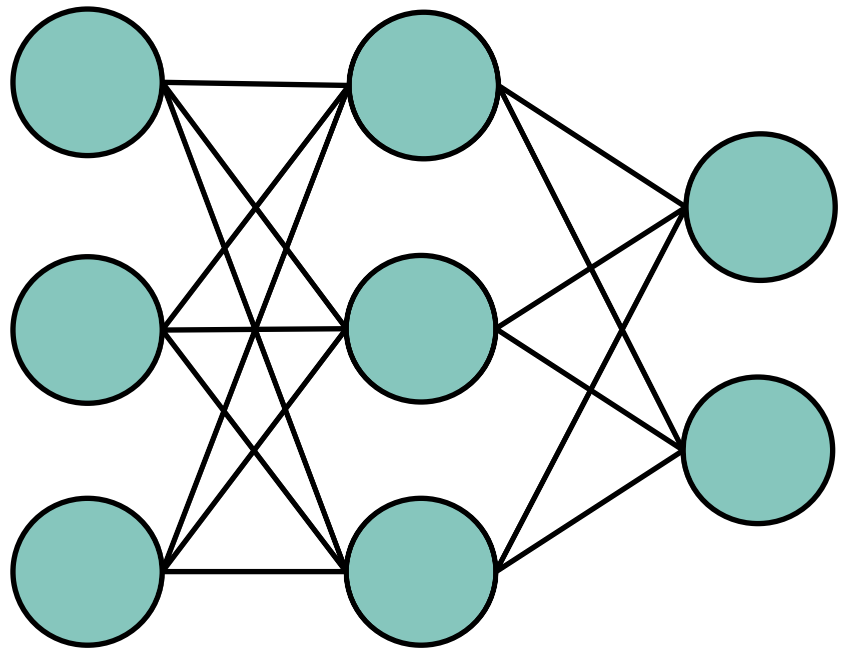 →

Neural network

Stochastic gradient descent (e.g., Adam):

$\boxed{\text{initialize } \pi \leftarrow \pi_0}$

while (not converged)

update $\pi \leftarrow \pi + \eta \cdot \boxed{\dfrac{\mathrm{dloss}(\pi)}{\mathrm{d}\pi}}$

Differentiable rendering

Inverse rendering (a.k.a. analysis by synthesis)

Analysis-by-synthesis optimization:

$\min_{\substack{\text{scene}\\ \text{unknowns } \pi}} \boxed{\text{loss}}\Big[$  $, \text{render}\left(\substack{\text{scene}\\ \text{unknowns } \pi}\right)\Big]$

Learned initializations help:

- avoid local minima
- accelerate convergence

 → 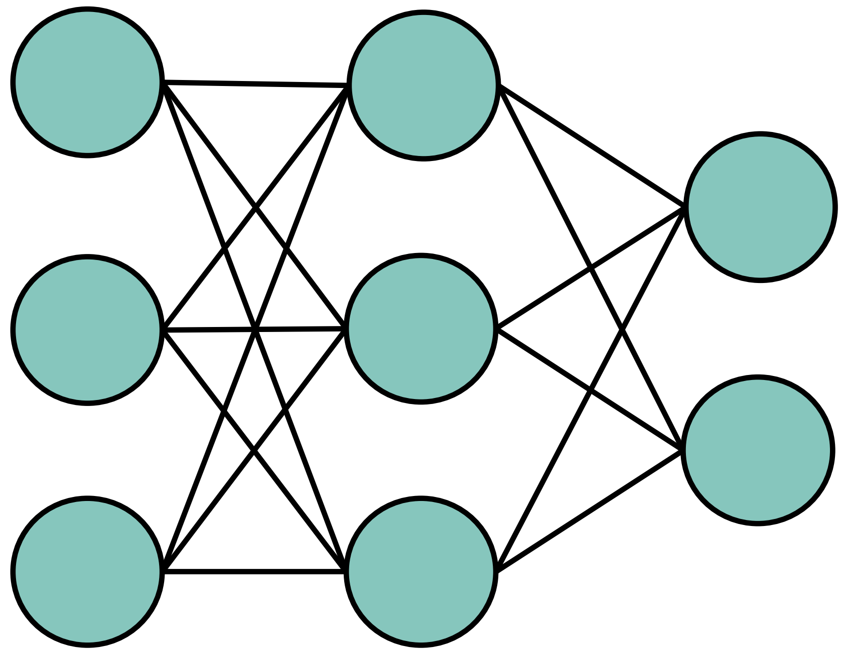 →

Neural network

Stochastic gradient descent (e.g., Adam):

$\boxed{\text{initialize } \pi \leftarrow \pi_0}$

while (not converged)

update $\pi \leftarrow \pi + \eta \cdot \boxed{\frac{\text{dloss}(\pi)}{\text{d}\pi}}$

Differentiable rendering

Why we need discriminative loss functions

- Well-designed loss functions can help reduce ambiguities
- Perceptual losses can help emphasize design aspects that matter
- Differentiable rendering can be combined with any loss function that can be backpropagated through

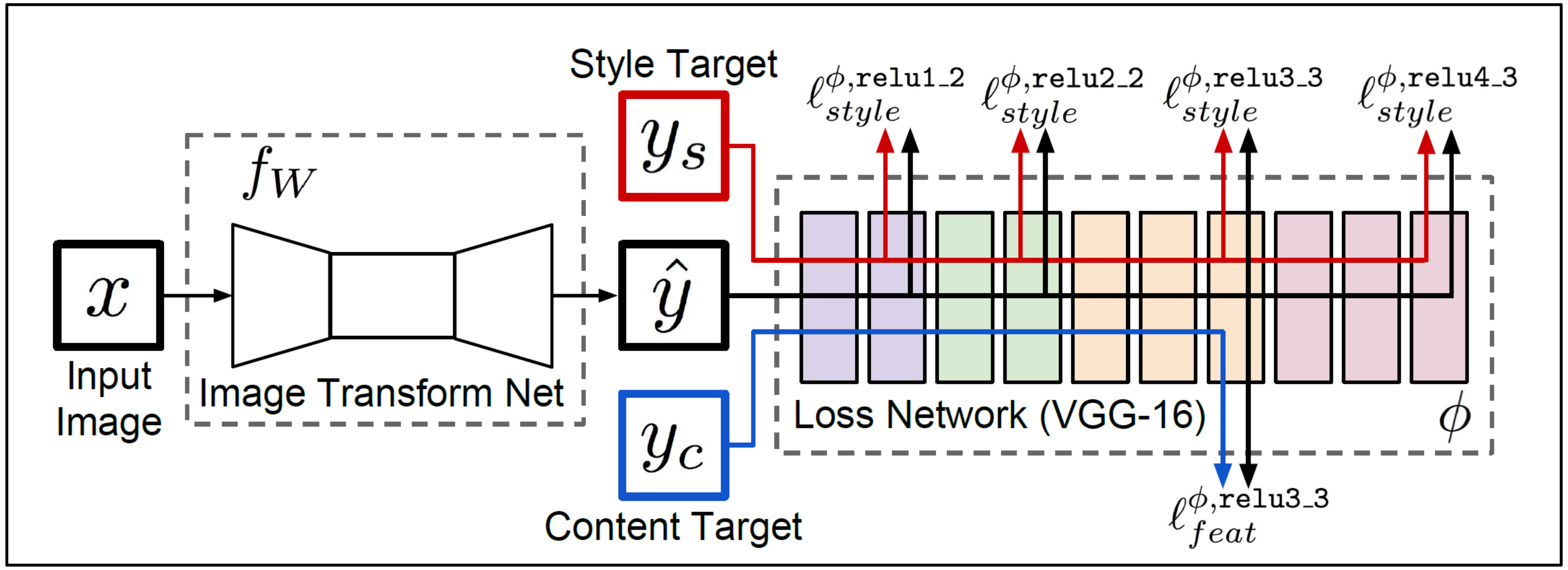

VGG-based *perceptual loss* [Johnson et al. 2016]

Inverse rendering (a.k.a. analysis by synthesis)

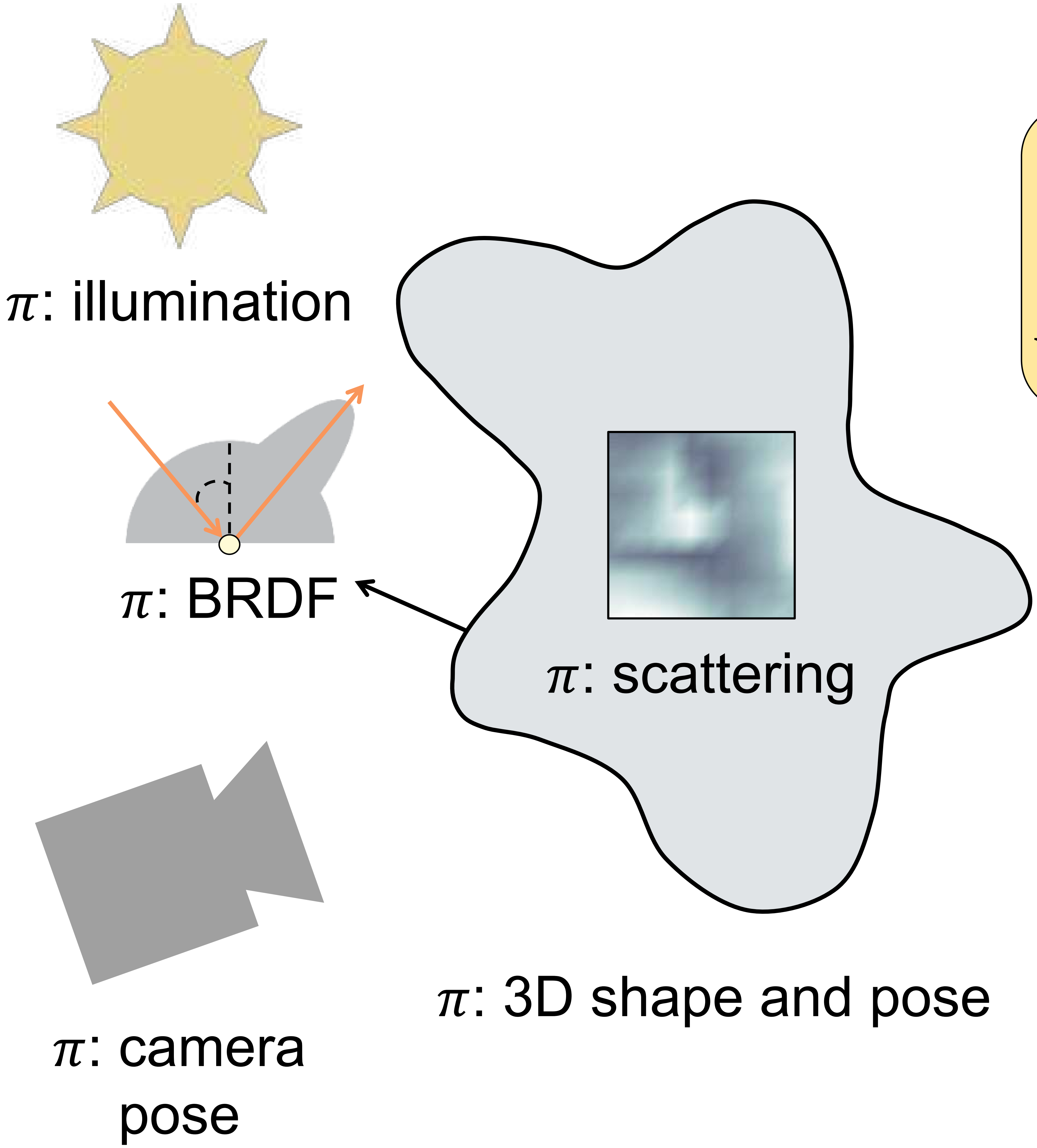

Analysis-by-synthesis optimization:

$$\min_{\text{scene unknowns } \pi} \boxed{\text{loss}}\left[\right.$$

$$\left. , \text{render}\left(\text{scene unknowns } \pi\right)\right]$$

Stochastic gradient descent (e.g., Adam):

$\boxed{\text{initialize } \pi \leftarrow \pi_0}$

while (not converged)

update $\pi \leftarrow \pi + \eta \cdot \boxed{\frac{\mathrm{dloss}(\pi)}{\mathrm{d}\pi}}$

Differentiable rendering

Inverse rendering (a.k.a. analysis by synthesis)

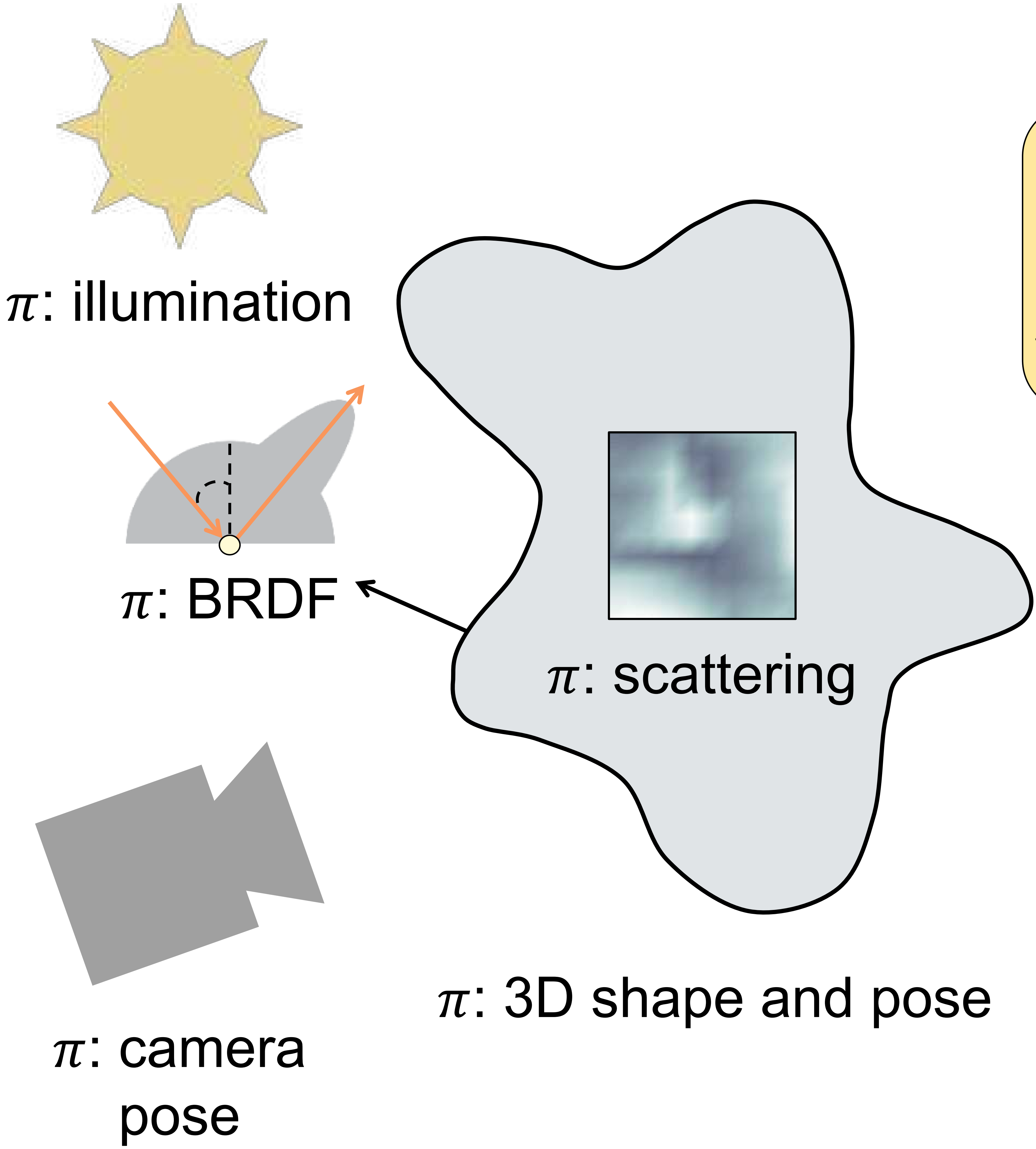

Analysis-by-synthesis optimization:

$$\min_{\substack{\text{scene}\\\text{unknowns }\pi}} \boxed{\text{loss}}\Big[$$

$$,\ \text{render}\left(\substack{\text{scene}\\\text{unknowns }\pi}\right)\Big]$$

Stochastic gradient descent (e.g., Adam):

$\boxed{\text{initialize } \pi \leftarrow \pi_0}$

while (not converged)

update $\pi \leftarrow \pi + \eta \cdot \boxed{\dfrac{\mathrm{dloss}(\pi)}{\mathrm{d}\pi}}$

Differentiable rendering

High signal-to-noise ratio is critical

- The extent to which we can improve upon an initialization strongly depends on the signal-to-noise ratio of our measurements

High signal-to-noise ratio is critical

- The extent to which we can improve upon an initialization strongly depends on the signal-to-noise ratio of our measurements

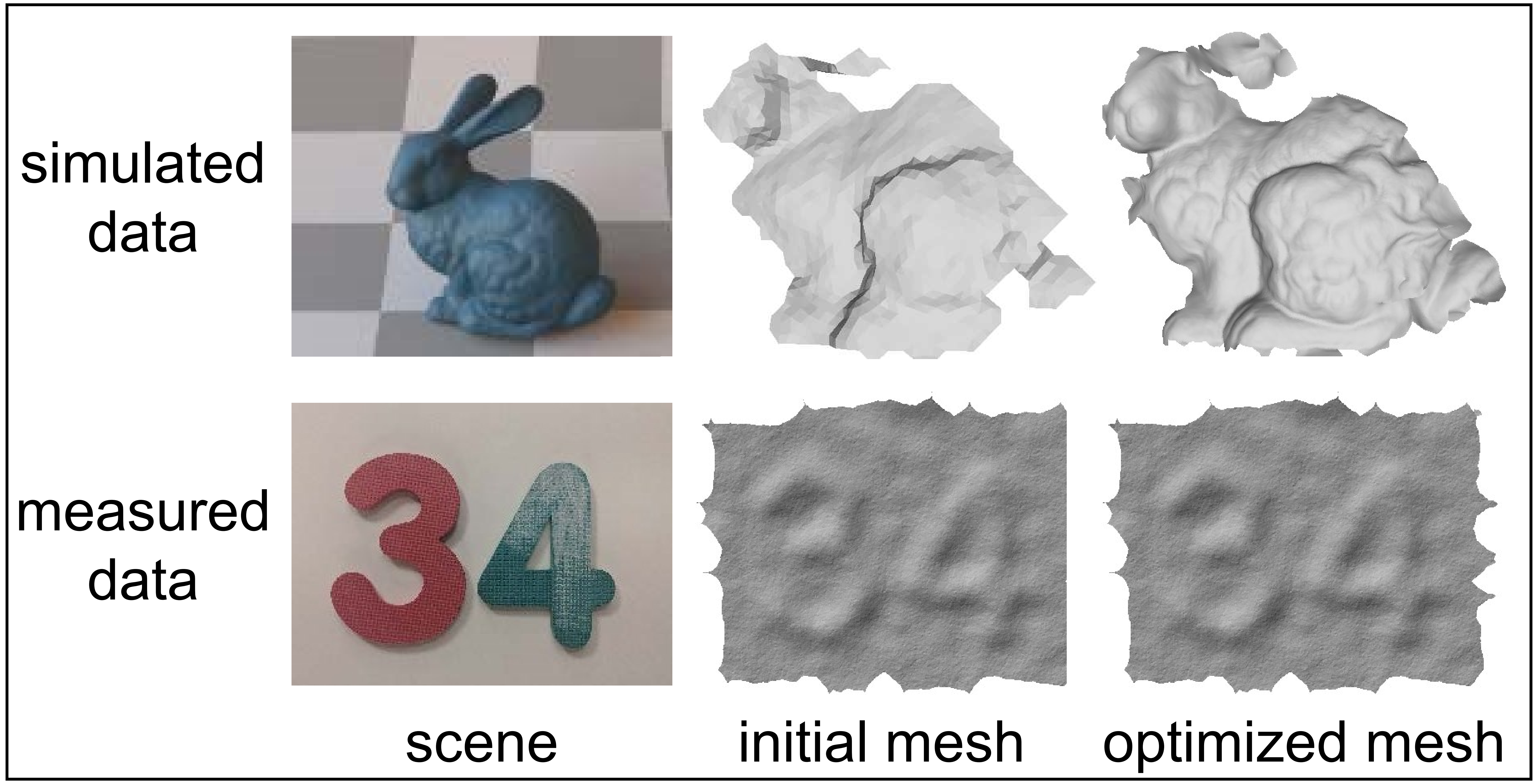

Non-line-of-sight imaging [Tsai et al. 2019]

High signal-to-noise ratio is critical

- The extent to which we can improve upon an initialization strongly depends on the signal-to-noise ratio of our measurements
- We need reliable camera models (noise, aberrations, other non-idealities)

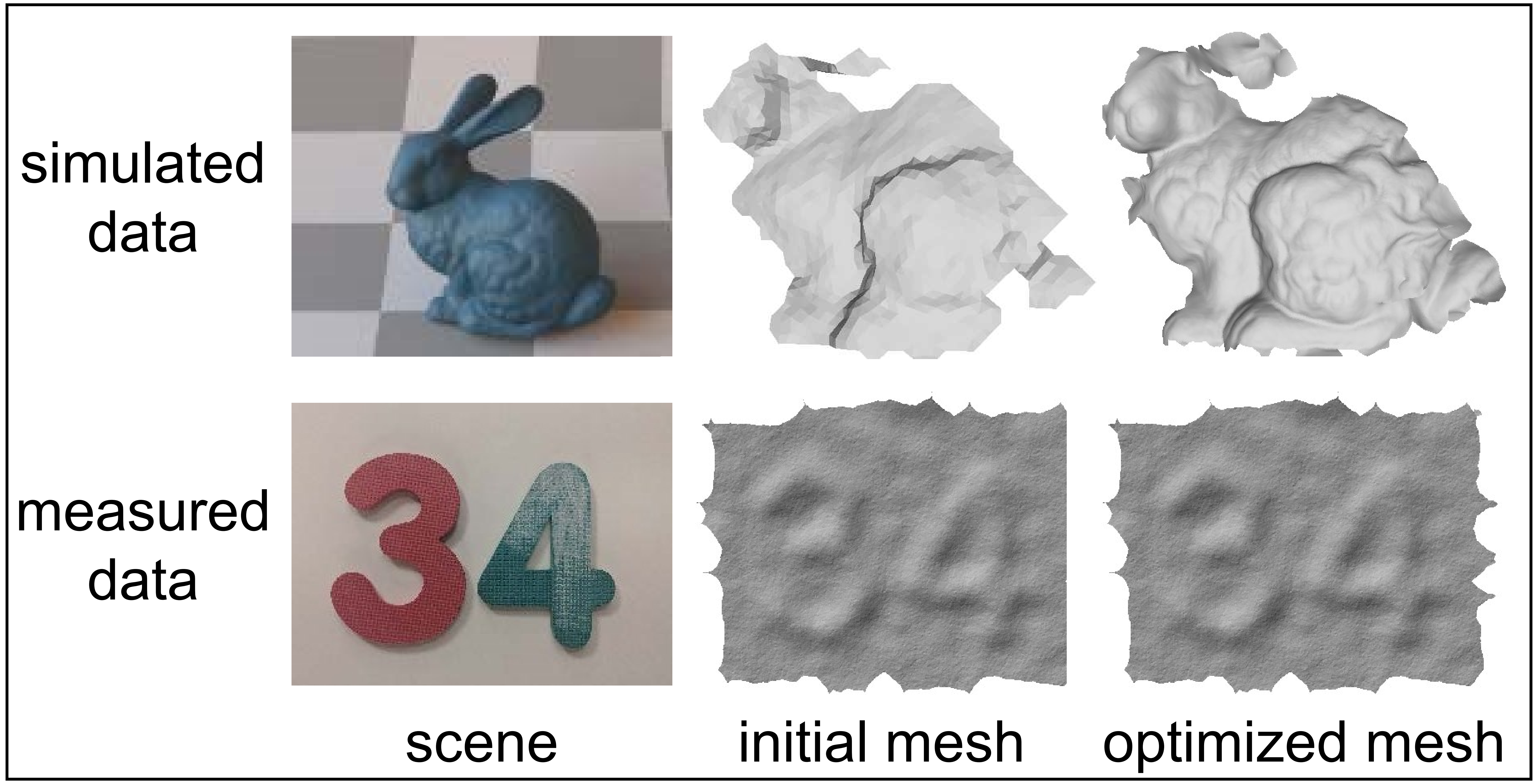

Non-line-of-sight imaging [Tsai et al. 2019]

High signal-to-noise ratio is critical

- The extent to which we can improve upon an initialization strongly depends on the signal-to-noise ratio of our measurements
- We need reliable camera models (noise, aberrations, other non-idealities)

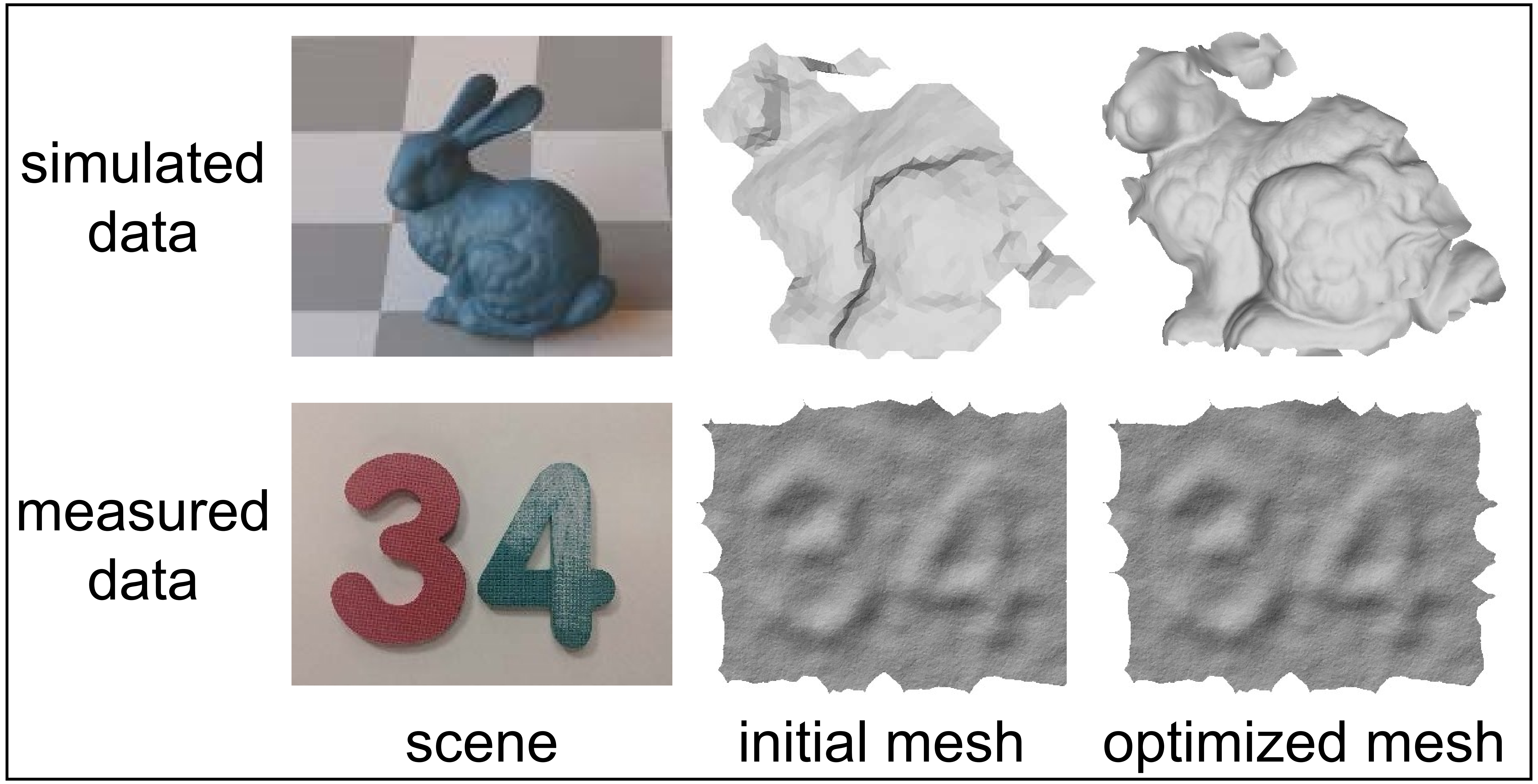

Non-line-of-sight imaging [Tsai et al. 2019]

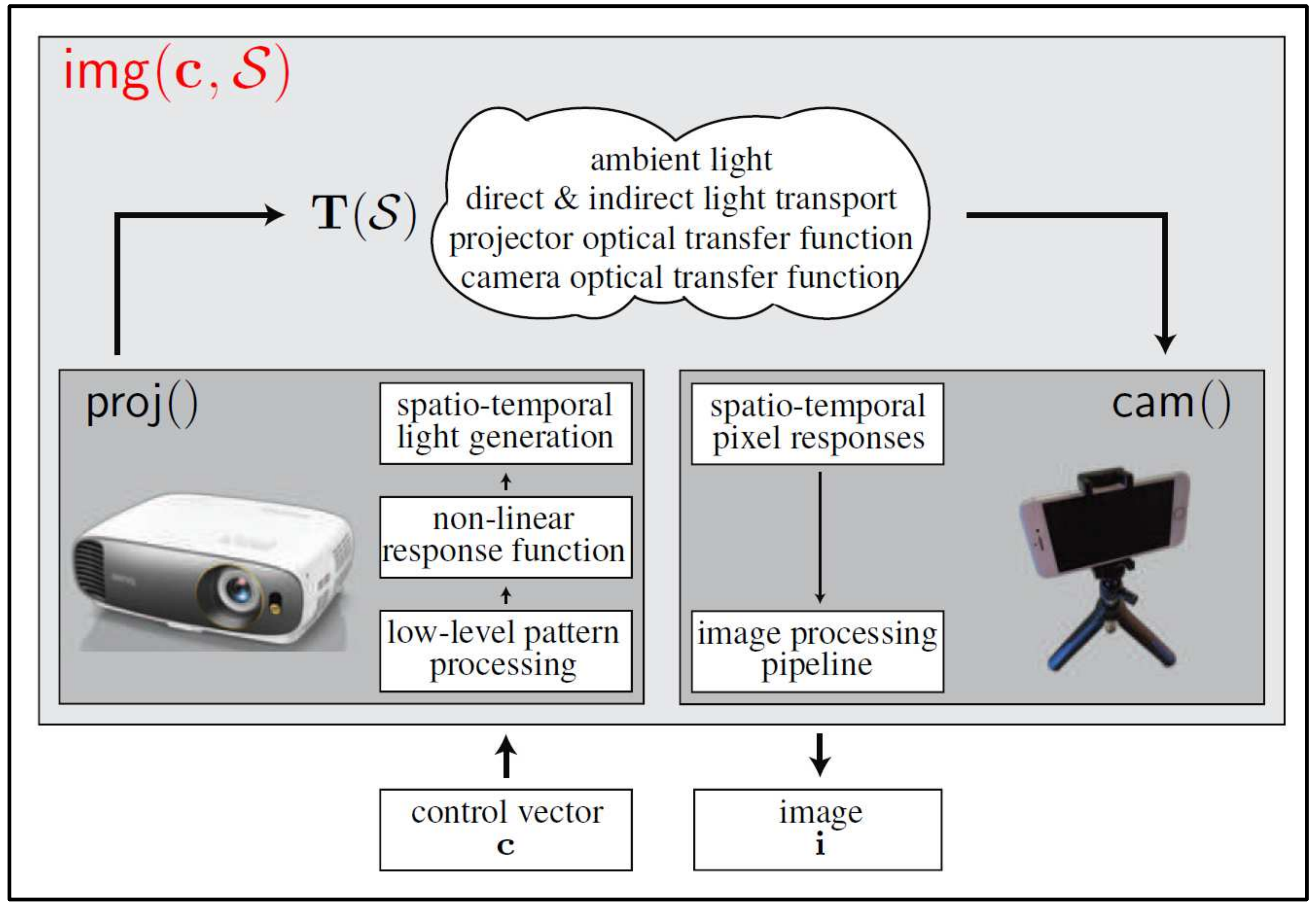

Optical gradient descent [Chen et al. 2020]

Physics-based rendering and its applications to computational imaging

forward rendering

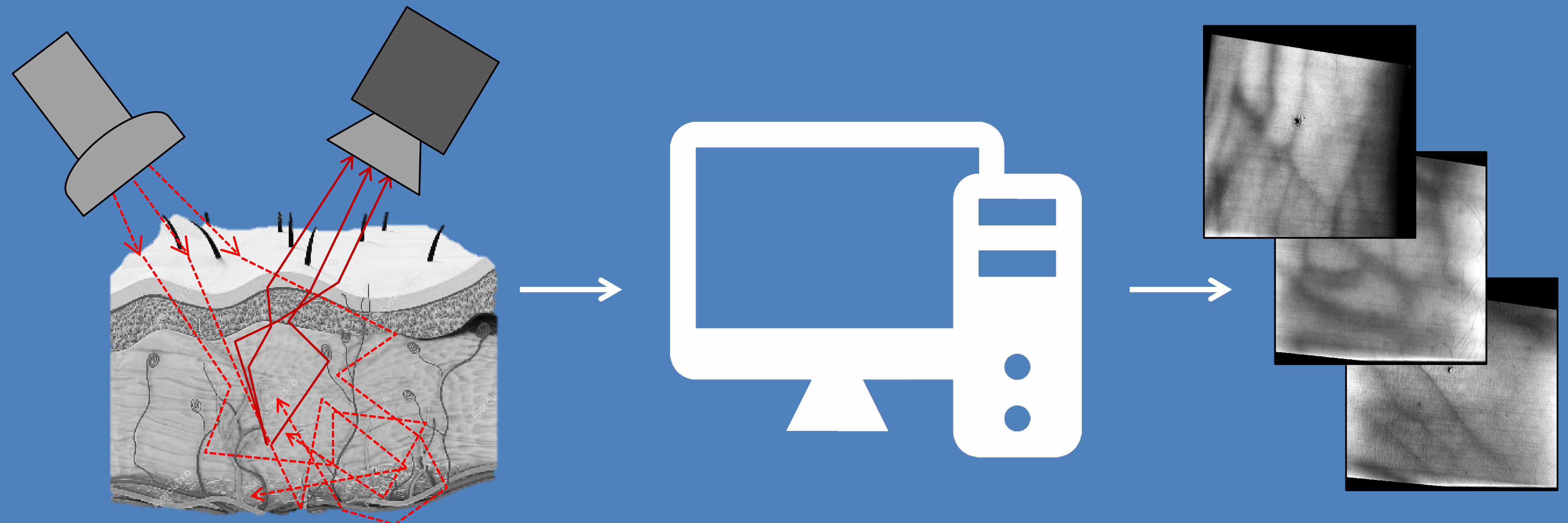

- accurate and efficient simulation
- virtually design sensors, optics, and algorithms

inverse rendering

- accurate and efficient differentiable simulation
- tractably solve general inverse problems

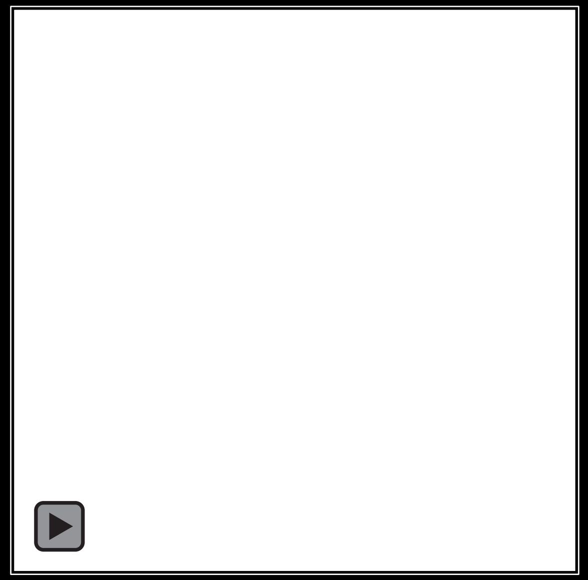

time-of-flight imaging

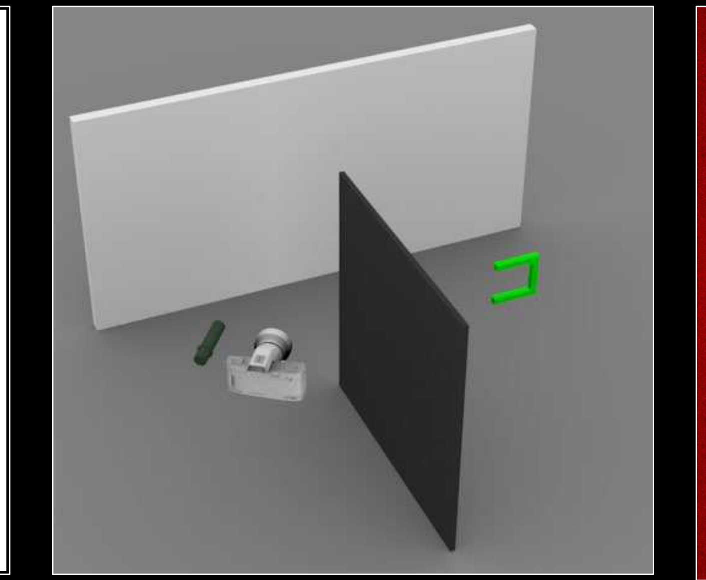

non-line-of-sight imaging

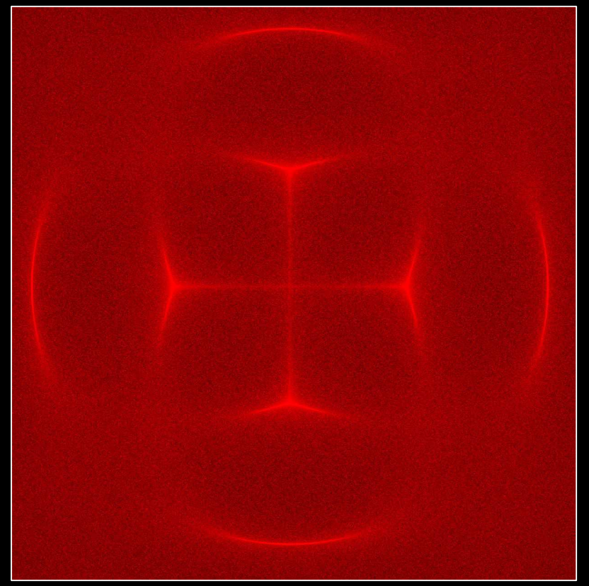

acousto-optic lensing

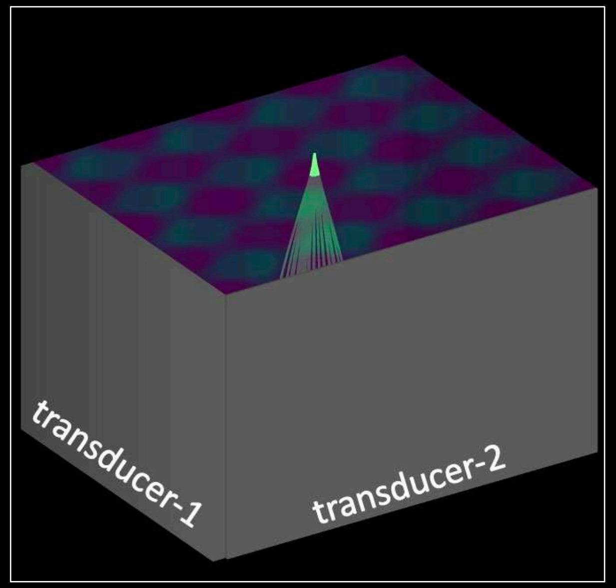

ultrafast light scanning

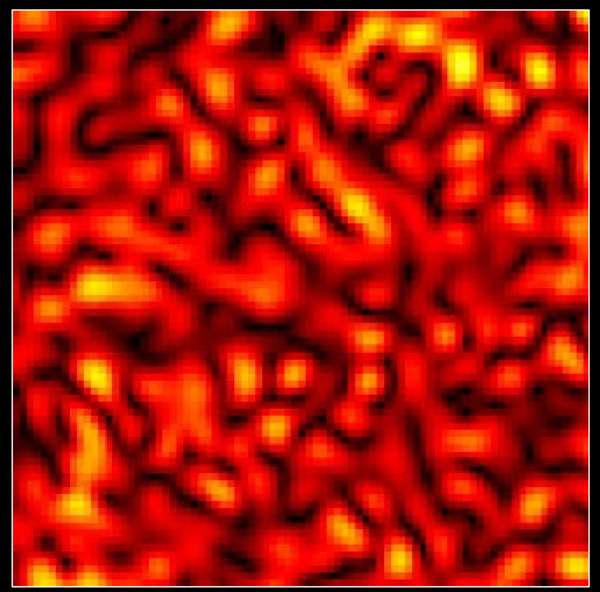

speckle imaging

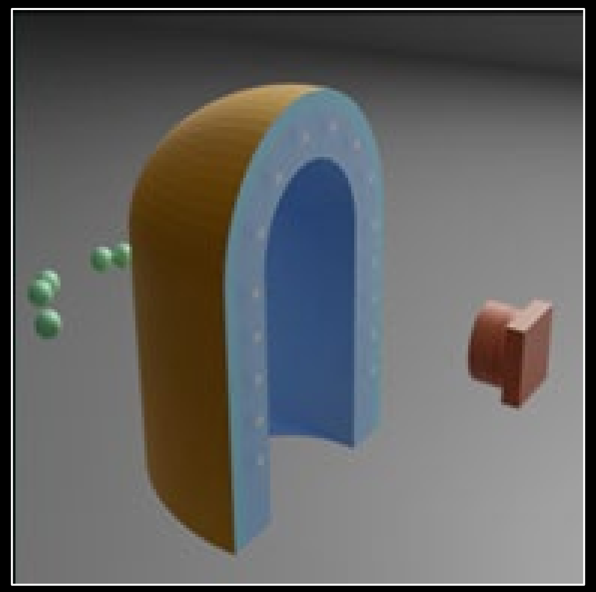

tactile sensor design

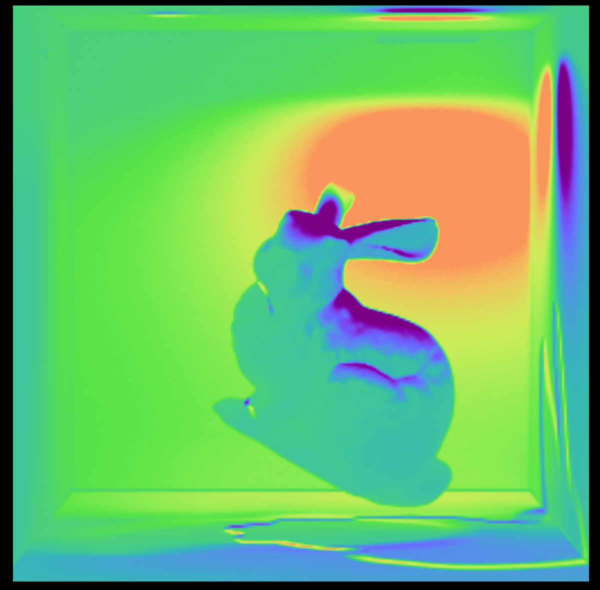

differentiable rendering

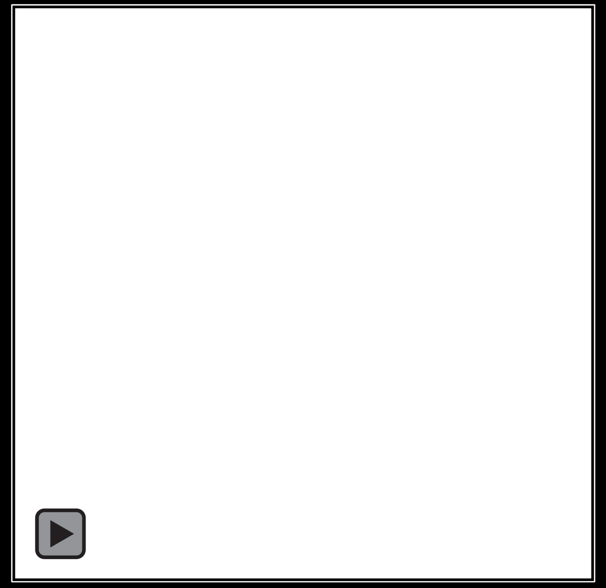

inverse problems

Take-Home Messages

- Great progress has been made in physics-based rendering
    - Capable of handling multiple types of imaging systems beyond RGB cameras (e.g., time-of-flight, sonar, tactile sensors).

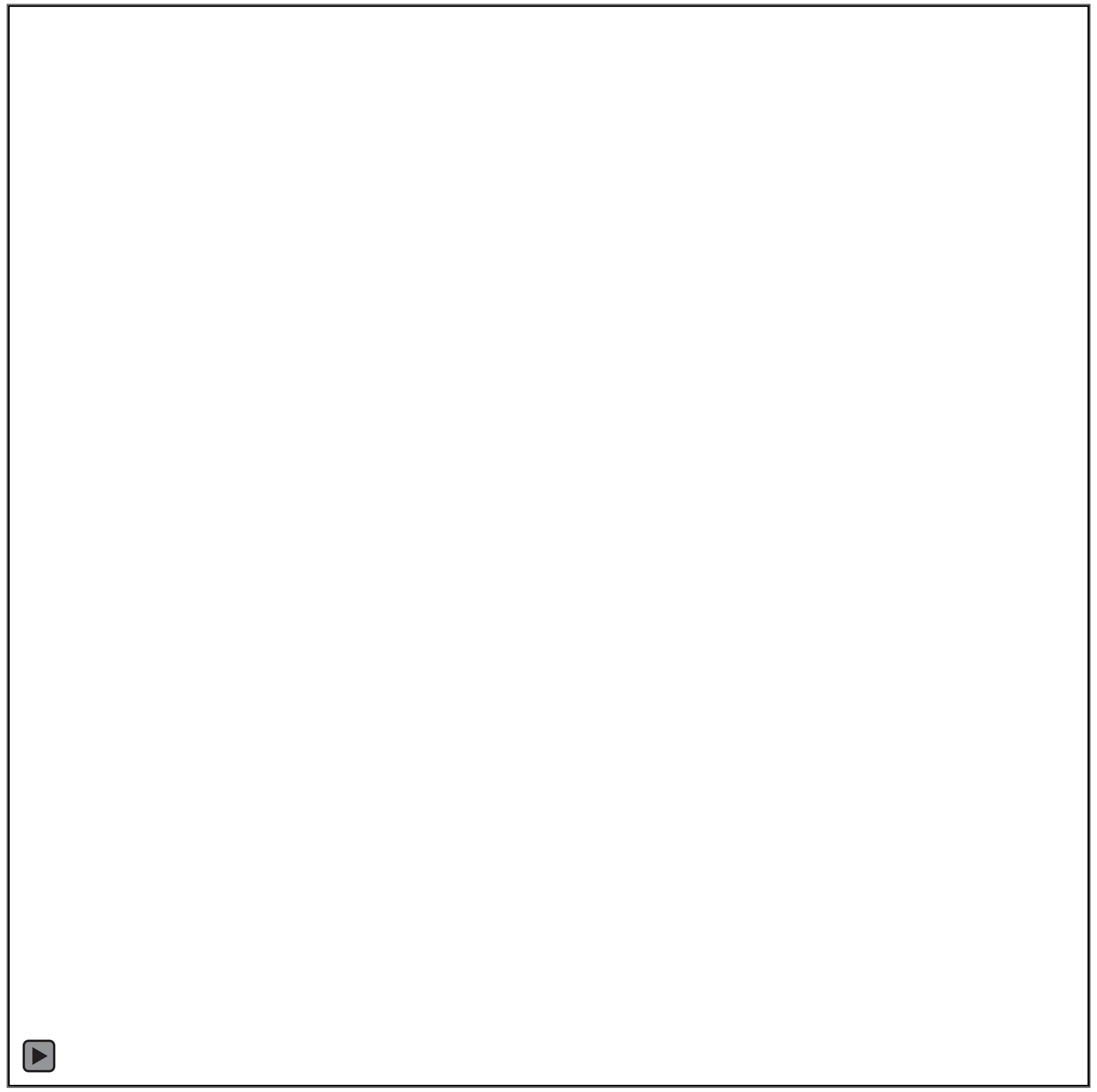

transient rendering of static scene

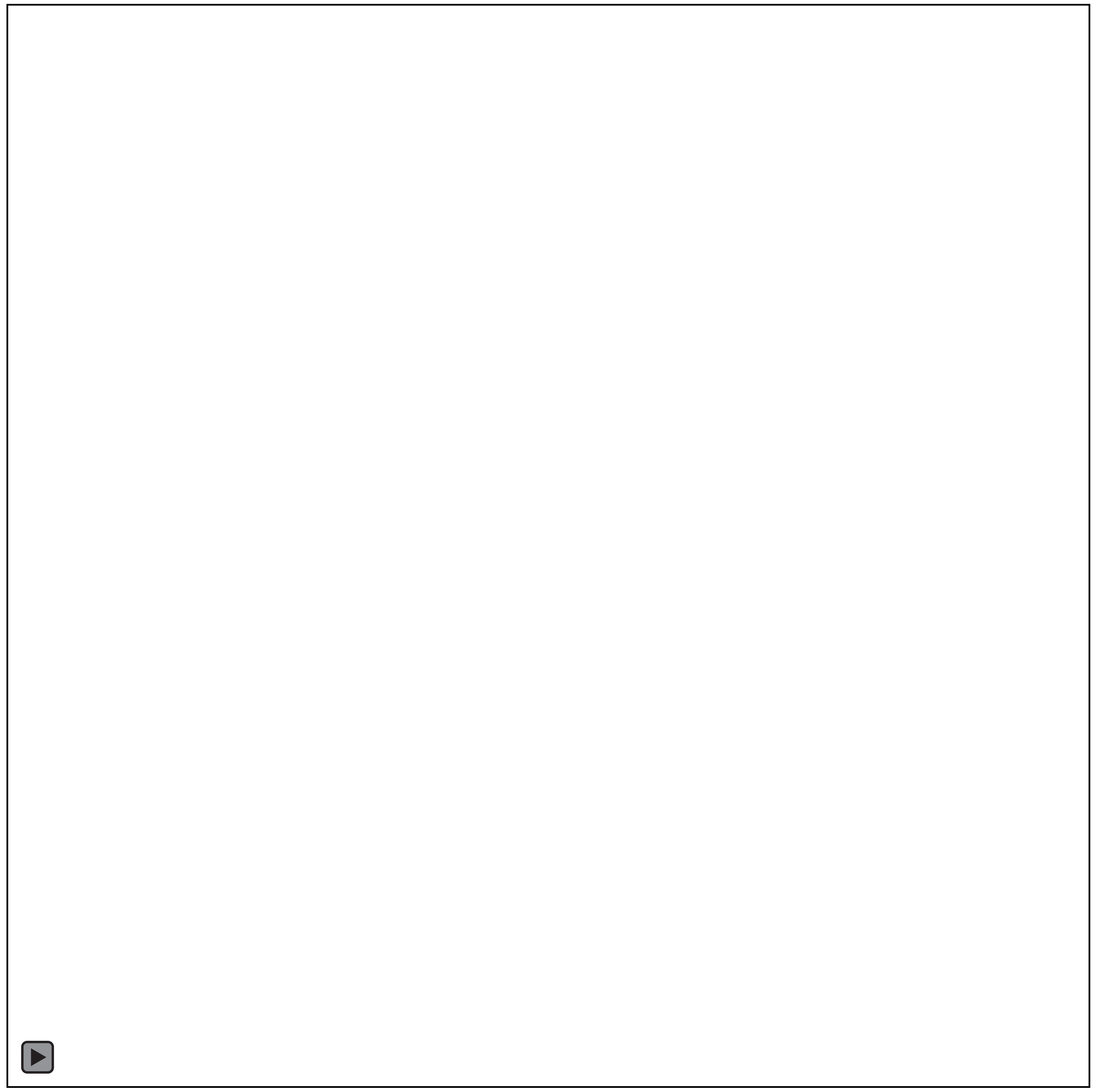

time-gated rendering of dynamic scene

Take-Home Messages

- Great progress has been made in physics-based rendering:
  - Capable of handling multiple types of imaging systems beyond RGB cameras (e.g., time-of-flight, sonar, tactile sensors).
  - Capable of handling more general scene models and light-matter interactions (e.g., speckle, continuous refraction and scattering).

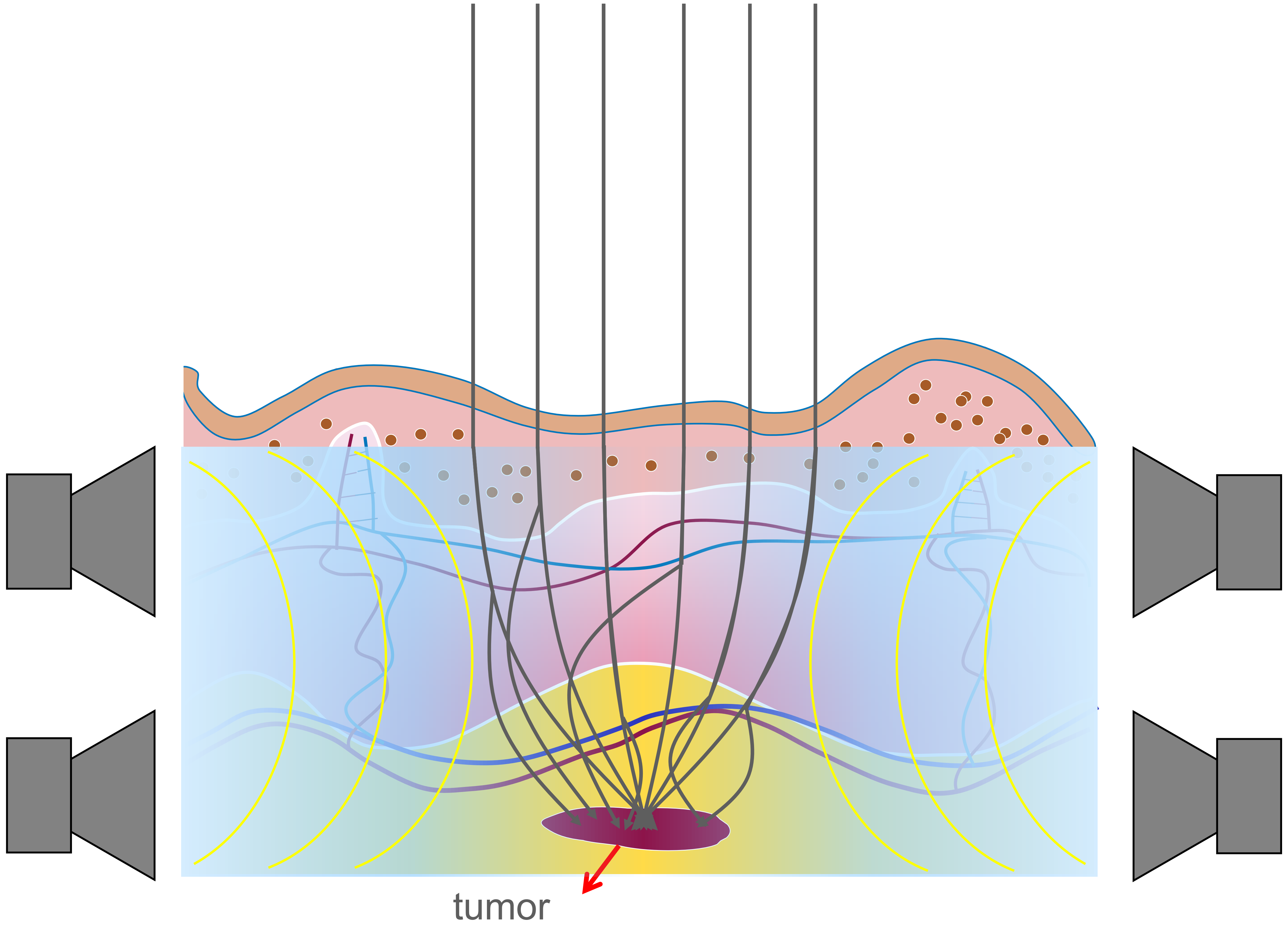

continuous refraction

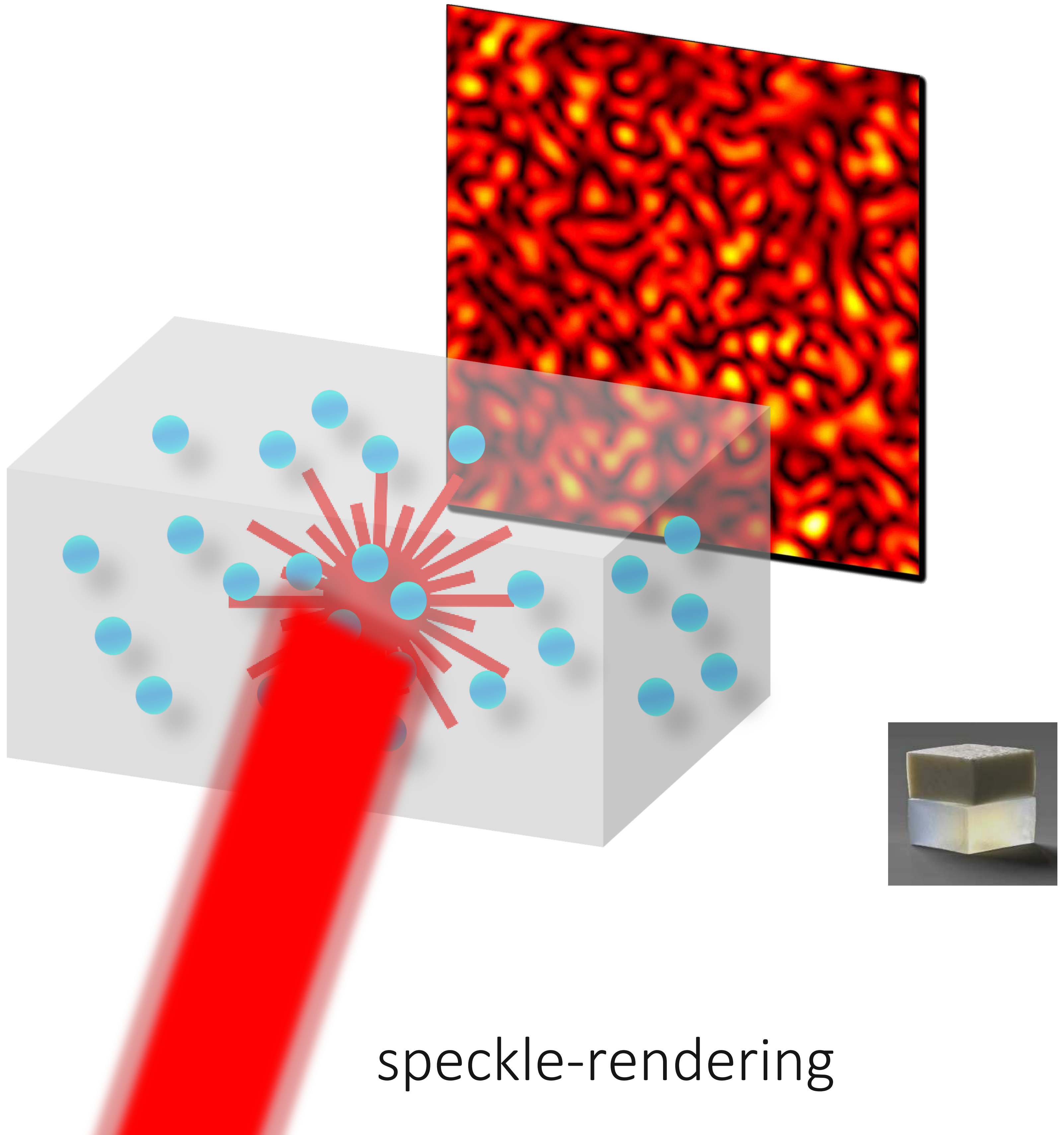

speckle-rendering

Take-Home Messages

- Great progress has been made in physics-based rendering
  - Capable of handling multiple types of imaging systems beyond RGB cameras (e.g., time-of-flight, sonar, tactile sensors).
  - Capable of handling more general scene models and light-matter interactions (e.g., speckle, continuous refraction and scattering).
  - Capable of acting as digital twins for scientific imaging applications.

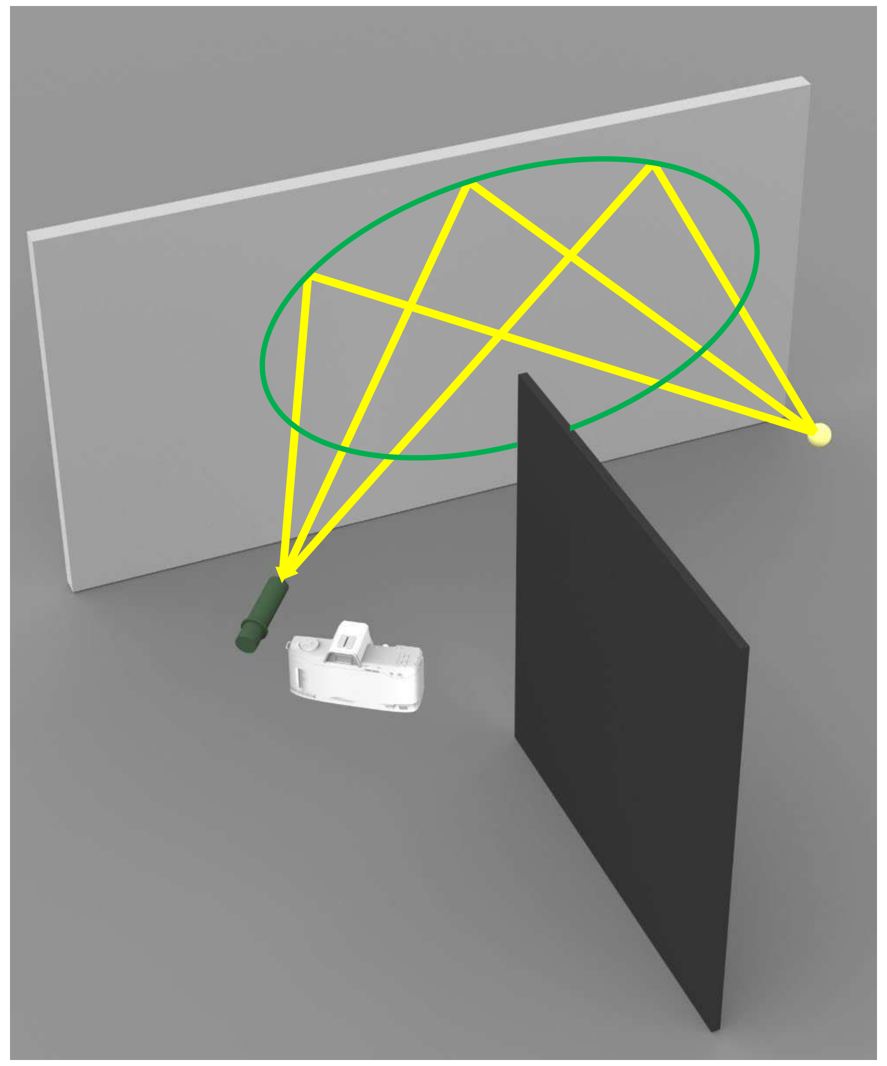

non-line-of-sight imaging

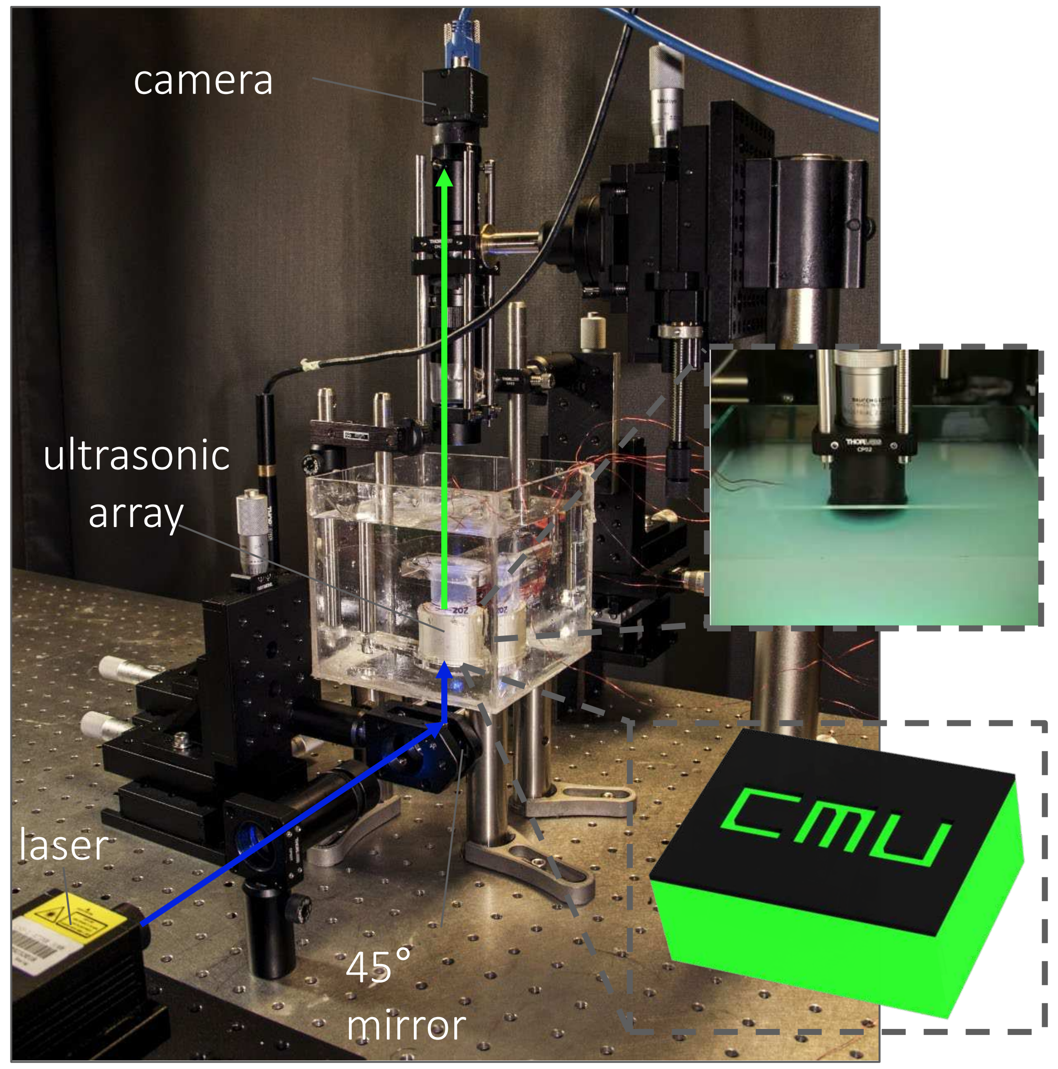

light throughput enhancement

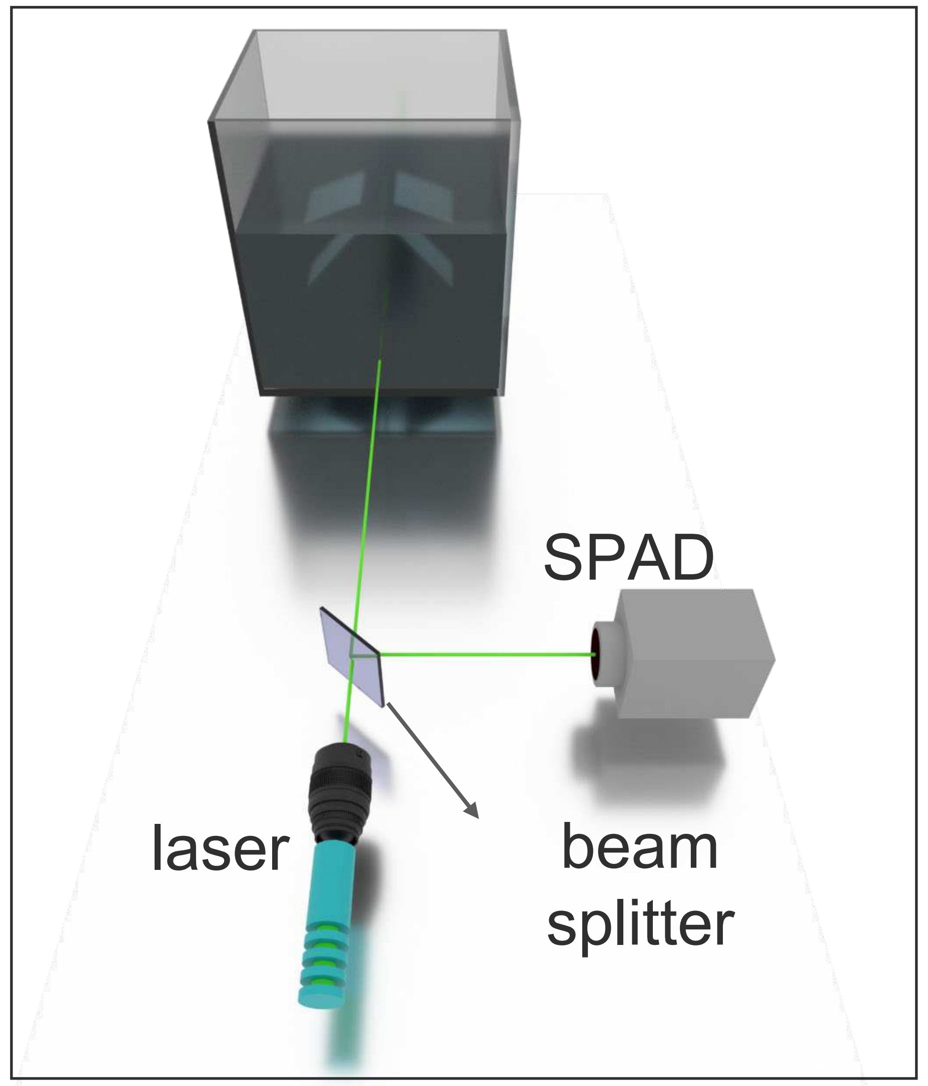

ultrafast light scanners

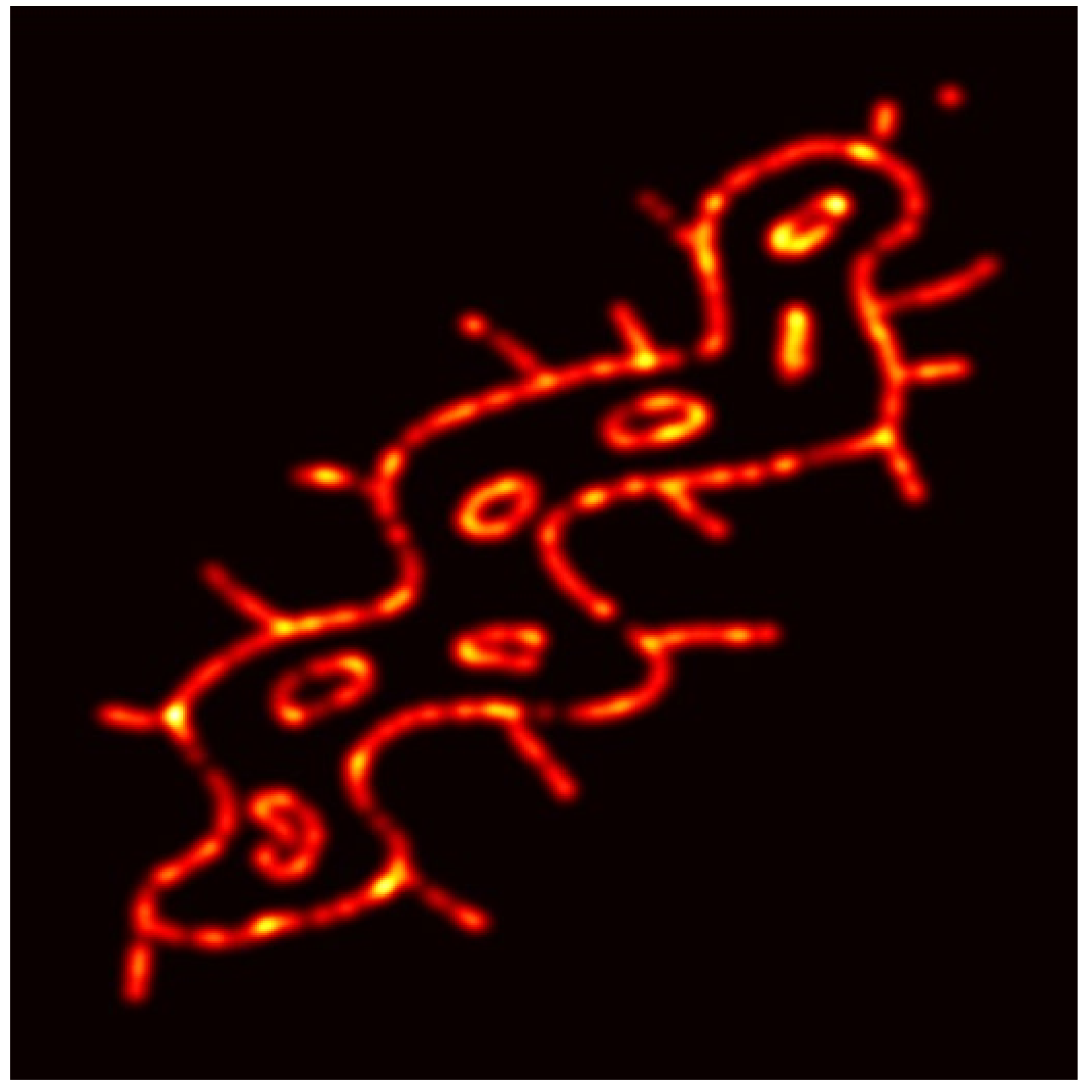

imaging through scattering media

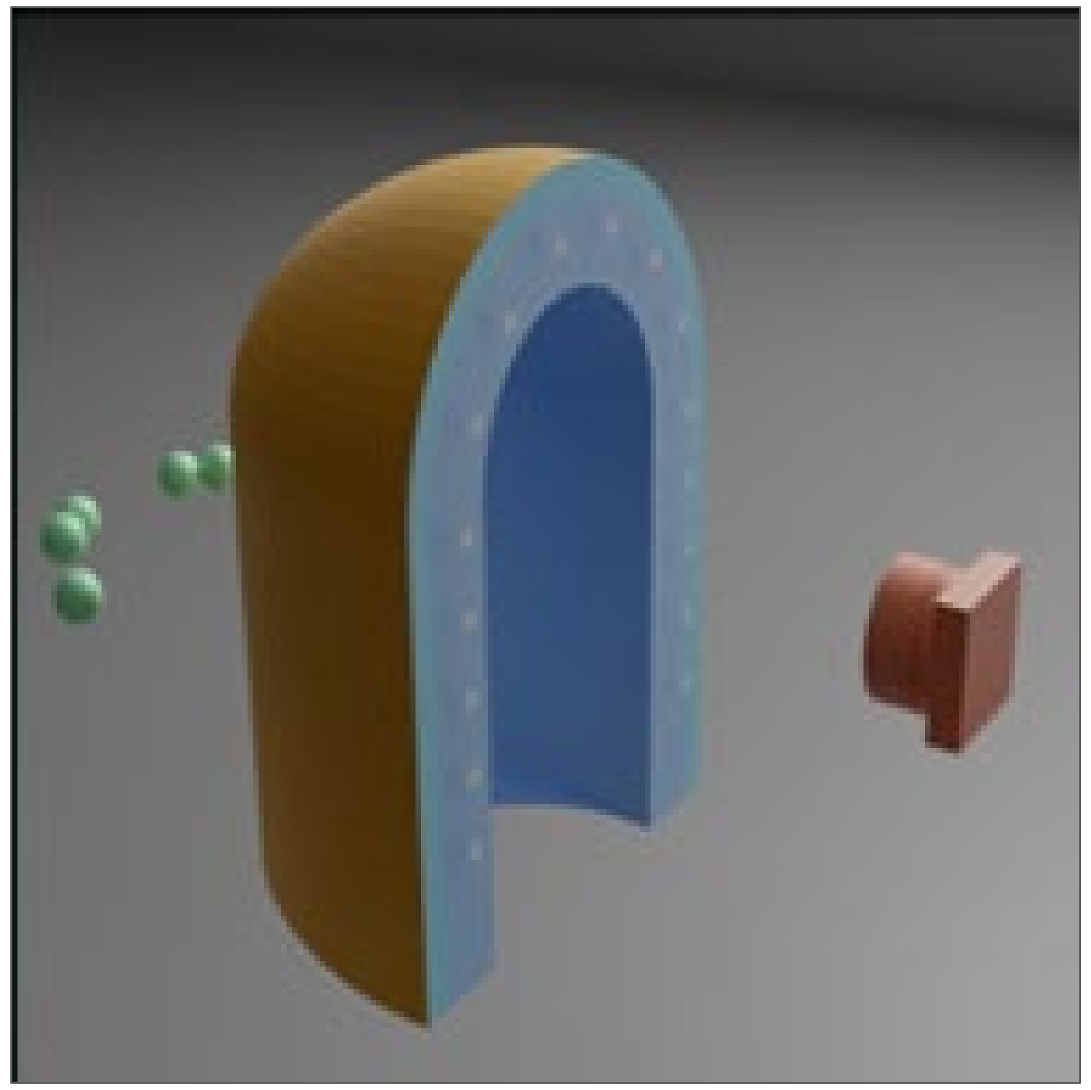

tactile sensor design

Take-Home Messages

- Great progress has been made in physics-based rendering
  - Capable of handling multiple types of imaging systems beyond RGB cameras (e.g., time-of-flight, sonar, tactile sensors).
  - Capable of handling more general scene models and light-matter interactions (e.g., speckle, continuous refraction and scattering).
  - Capable of acting as digital twins for scientific imaging applications.
  - Capable of differentiation for general inverse rendering problems.

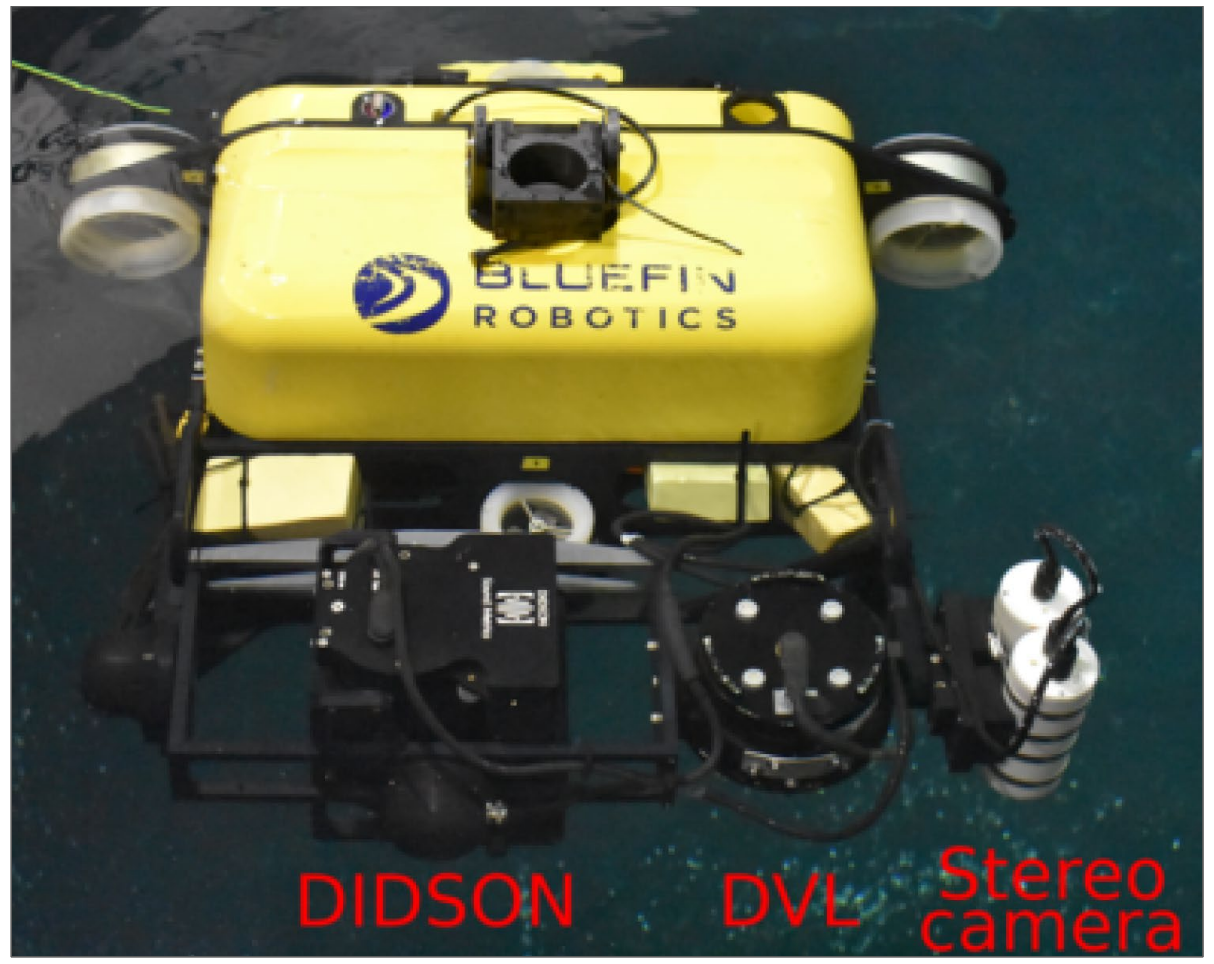

underwater sonar

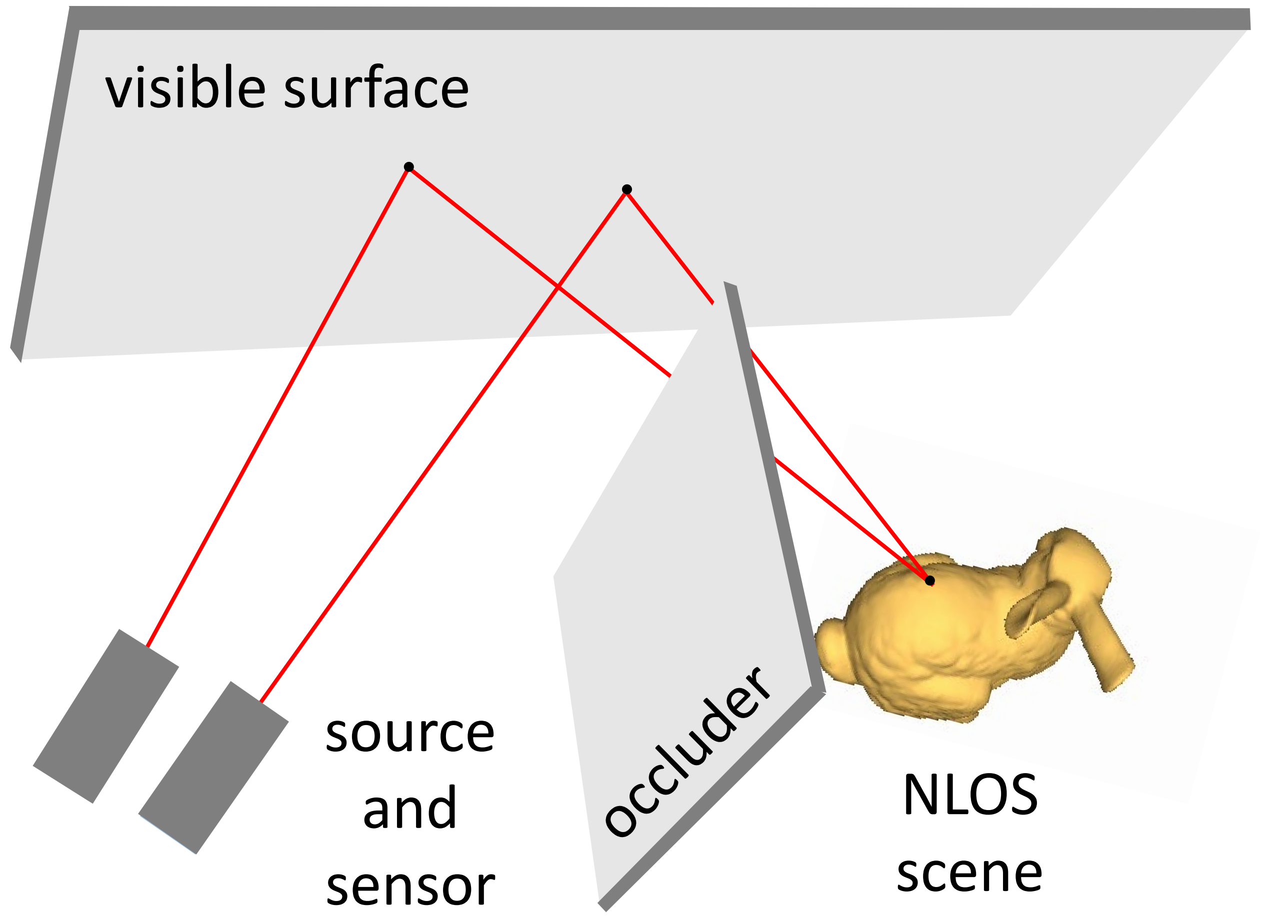

non-line-of-sight imaging

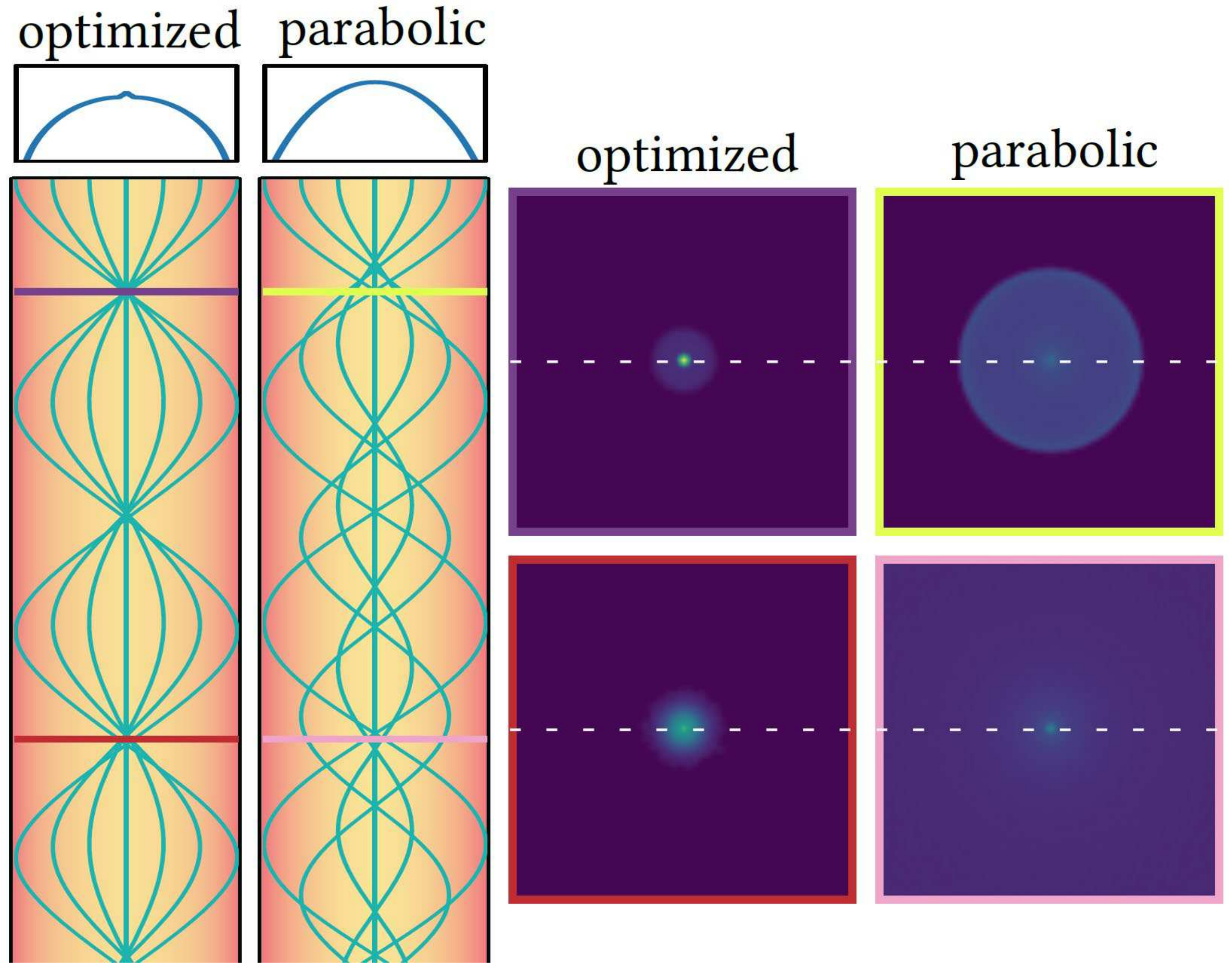

GRIN optic design

Monte Carlo rendering for more general physics and sensing

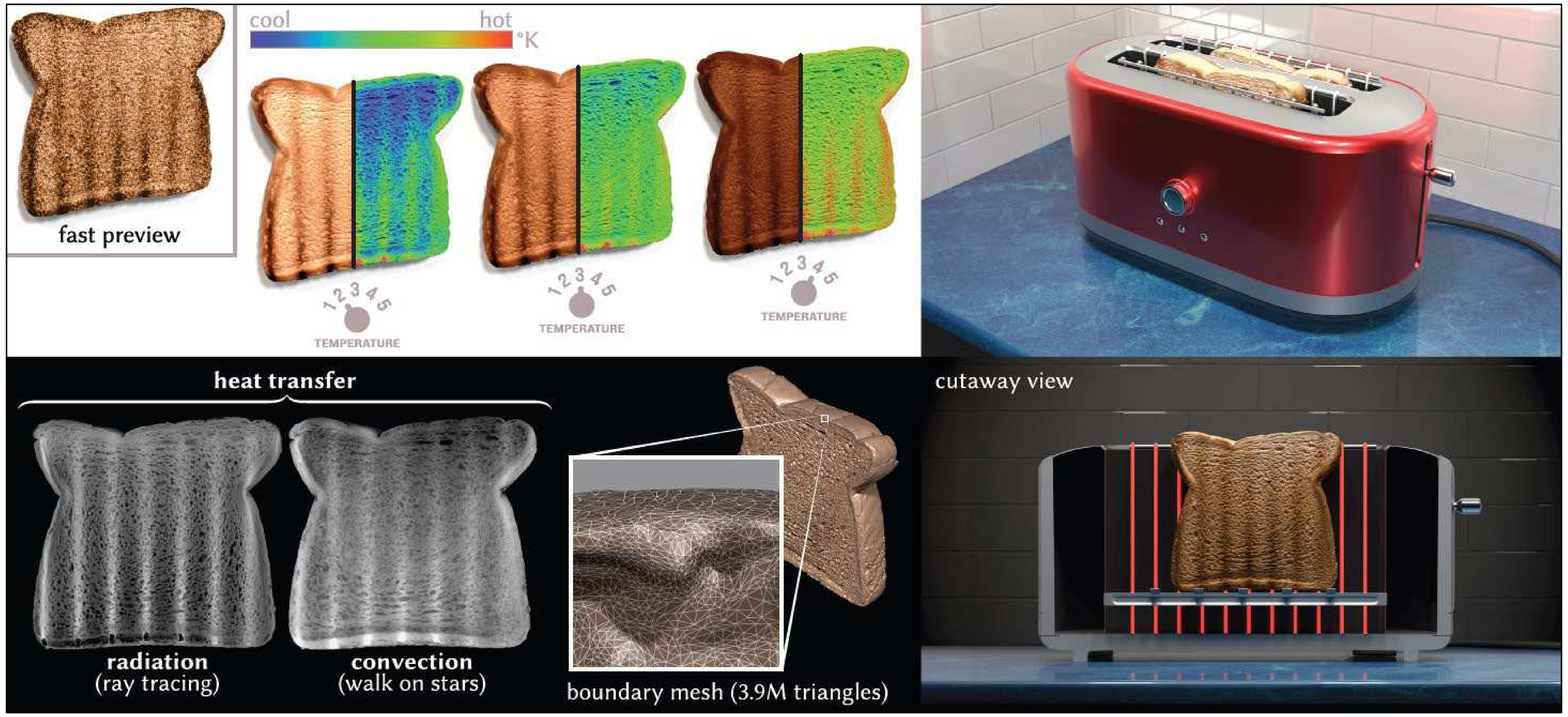

Simulation of general diffusion processes like heat transfer and oxygen flow

Joint work with
Rohan Sawhney, Bailey Miller, Keenan Crane
SIGGRAPH 2023

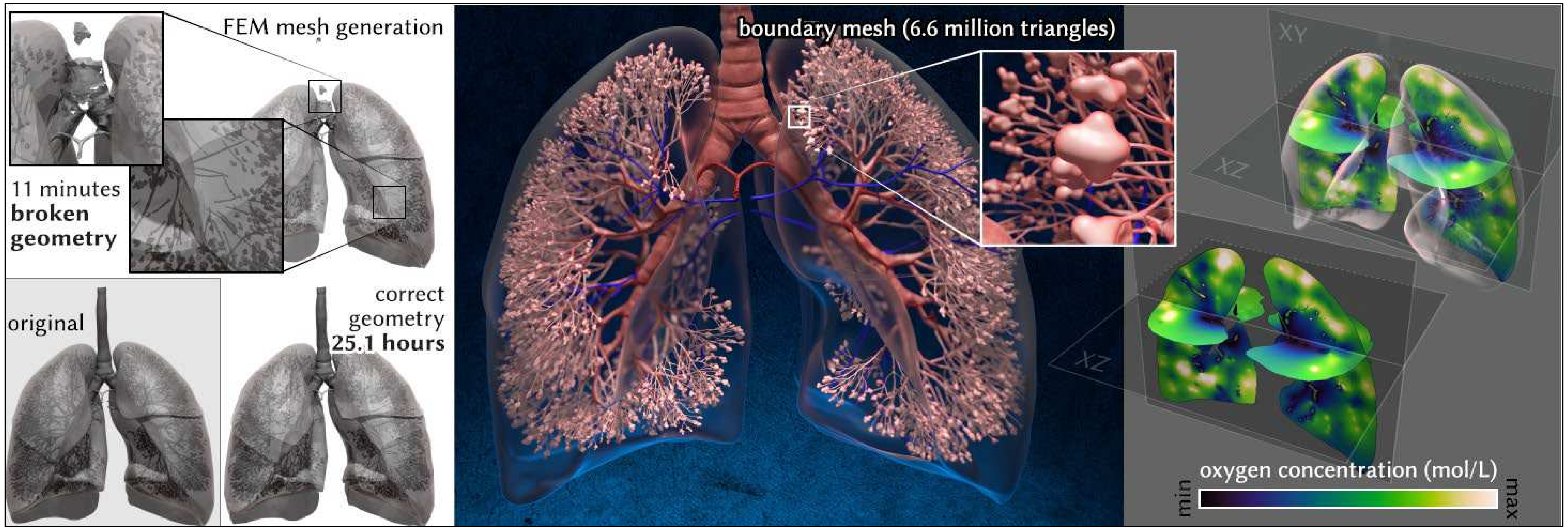


Many thanks to our collaborators

Many thanks to our sponsors

NSF

DARPA

Office of Naval Research
USN
ONR
Science & Technology

ALFRED P. SLOAN
FOUNDATION

aws

SEE BELOW THE SKIN

Physics-based rendering and its applications to computational imaging

forward rendering

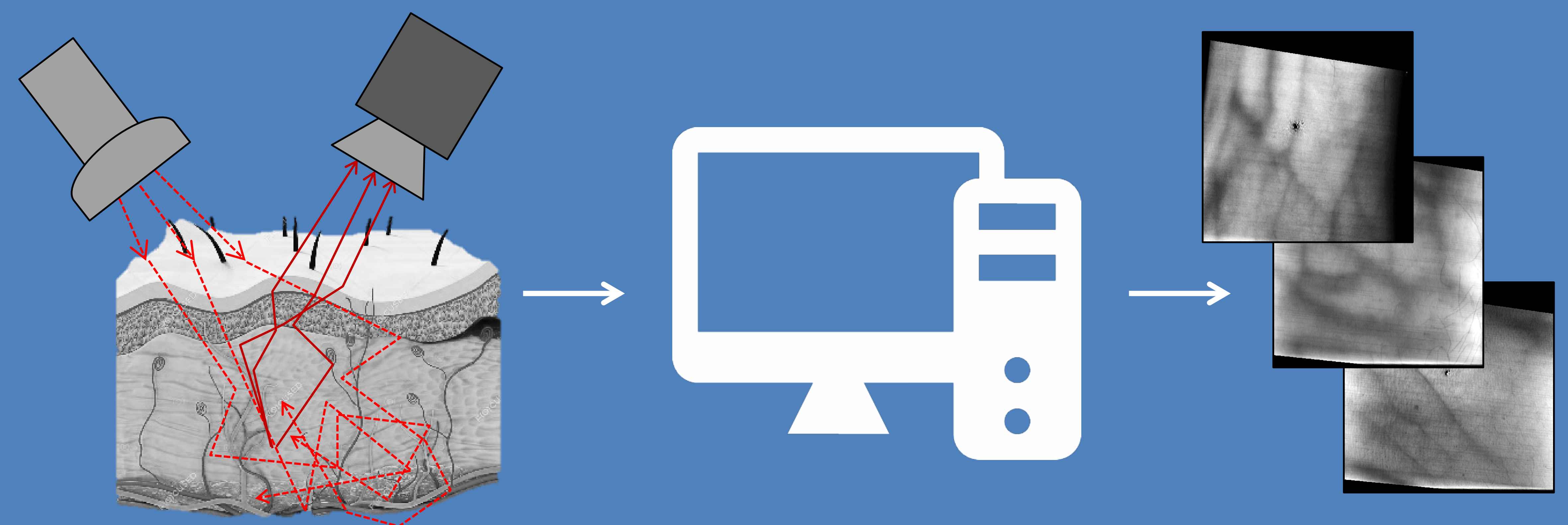

- accurate and efficient simulation
- virtually design sensors, optics, and algorithms

inverse rendering

- accurate and efficient differentiable simulation
- tractably solve general inverse problems

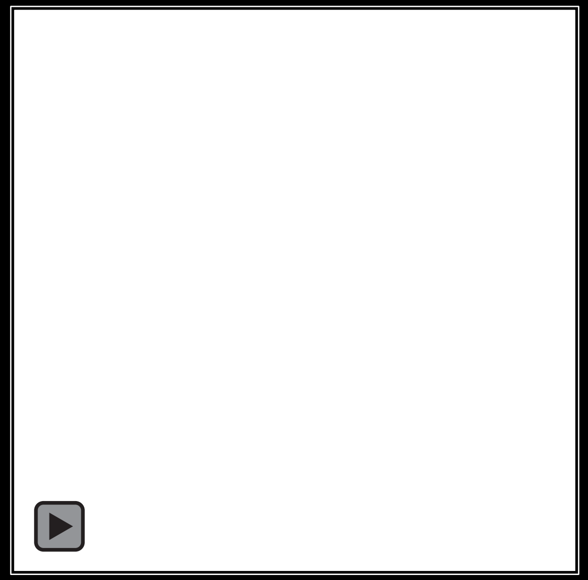

time-of-flight imaging

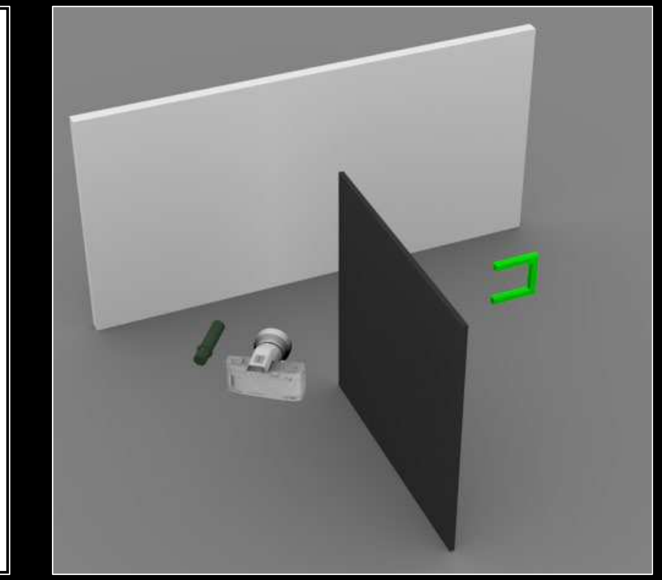

non-line-of-sight imaging

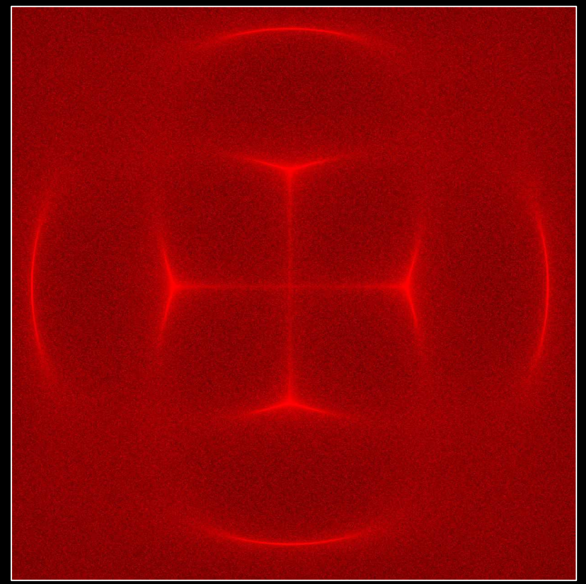

acousto-optic lensing

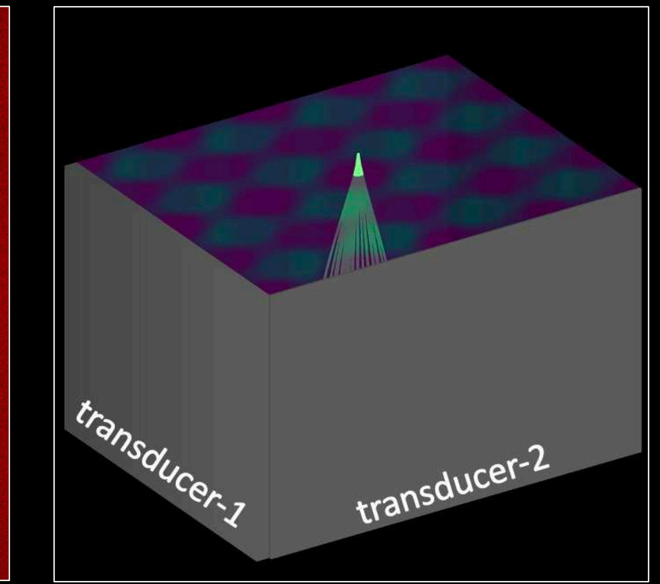

ultrafast light scanning

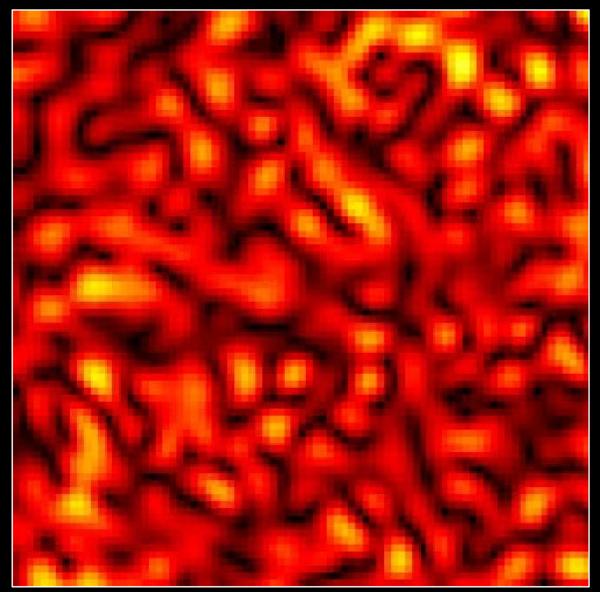

speckle imaging

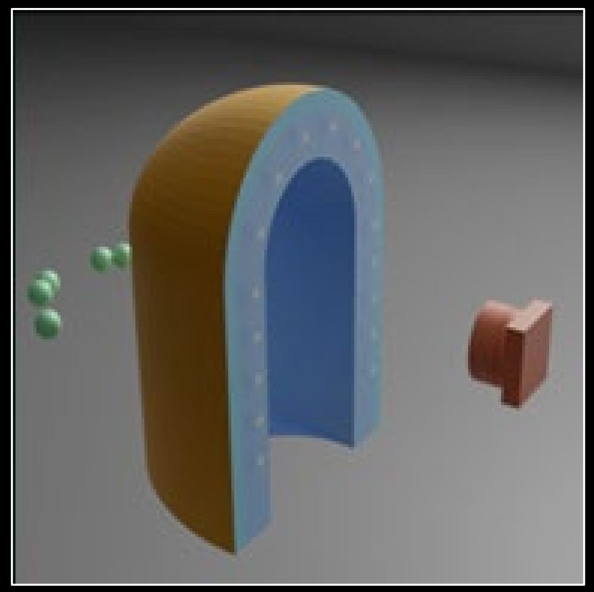

tactile sensor design

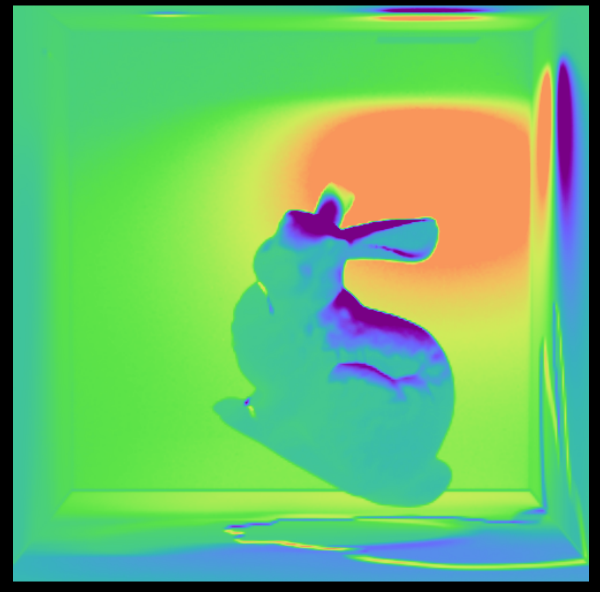

differentiable rendering

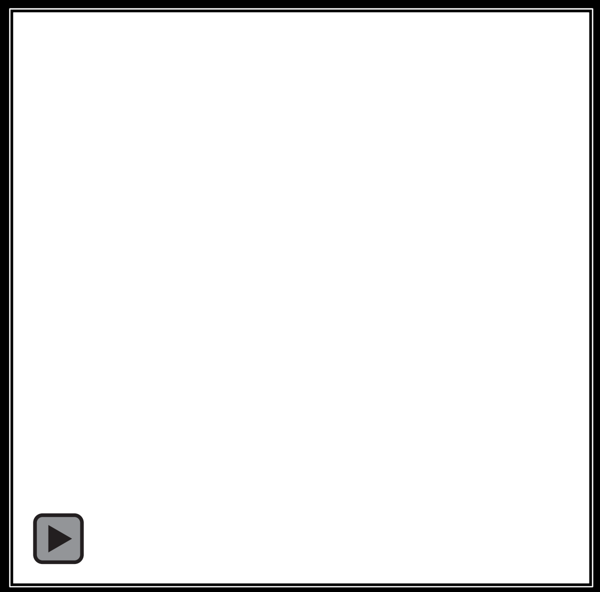

inverse problems